
*Proceedings of the
International
Solvent Extraction Conference*



TORONTO
SEPTEMBER
9th - 16th
1977

SPONSORED BY
CANADIAN INSTITUTE OF MINING AND METALLURGY
IN ASSOCIATION WITH
CANADIAN SOCIETY FOR CHEMICAL ENGINEERING and
SOCIETY OF CHEMICAL INDUSTRY

VOLUME 1

CIM SPECIAL VOLUME 21
1979
THE CANADIAN INSTITUTE OF MINING AND METALLURGY

Editors: B. H. Lucas
G. M. Ritcey
H. W. Smith
in close collaboration with Session Chairmen

Production Editors: D. E. Pickett
J. I. McGerrigle

COPYRIGHT (1979) BY THE CANADIAN INSTITUTE OF MINING AND METALLURGY
Suite 400, 1130 Sherbrooke Street, West
Montreal, Quebec, H3A 2M8.

2 Volumes

PRINTED BY HARPELL'S PRESS COOPERATIVE
Ste-Anne-de-Bellevue

G. M. Ritcey
*Conference
General Chairman
ISEC 77*



PREFACE

The International Solvent Extraction Conference was held in Canada for the first time, and took place at the Royal York Hotel, Toronto, from September 9-16, 1977. This was the opportunity for those involved in, or planning, solvent extraction technology to meet and exchange ideas.

These international conferences on solvent extraction have been held approximately every three years since the early 1960's. Although most areas of the technology were covered at this Conference, the major theme was directed to the mining and metallurgical industry. It was considered appropriate to emphasize this area which is of major importance in Canada. However, in order to achieve the end result — the useful application of solvent extraction in the production of a saleable commodity — we require technology transfer and active interfaces between the universities and the government and industrial organisations that are involved in the many aspects of solvent extraction technology.

The planning of ISEC 77 spanned over three years. It was decided in 1974 to hold the next conference, following the ISEC at Lyon, in Canada. Since it is absolutely necessary that a major international conference should be located where there are many people actively interested in the conference topic — in this case solvent extraction — the choice was Toronto. The Toronto area had the highest concentration of scientists involved in solvent extraction and is moreover easily accessible and has many attractions for conference delegates. The wisdom of this choice was well indicated by the successful development of the technical and social activities in the conference.

At this ISEC, we again had a truly international representation of session Co-chairman, speakers and delegates. A total of 445 delegates representing 33 countries were in attendance. Also, numerous organizations throughout the world were extremely kind and generous in the assistance they had provided ISEC 77.

ISEC 77 made several departures from previous international conferences on solvent extraction technology. Since the numbers of papers and technical sessions at previous ISEC meetings were becoming large, with many in competition with one another, we decided that ISEC 77 would have several Plenary Sessions which could be attended by delegates without conflict with other sessions. The General Sessions were usually run concurrently in groups of three. Also, Poster Sessions were introduced as a means of providing more intimate information exchange and proved to be most successful. Each session had been successfully built by its co-Chairmen around a major theme. We want to emphasize that the Poster Sessions are in no way inferior to the more formal sessions. Indeed, the informal presentation is gaining in popularity and will possibly be the favoured method within a few years.

In order to have these Proceedings ready for the Conference itself, completed papers would have had to be available several months in advance. We felt that much old work would therefore have been submitted and that it was desirable to have more recent information as well as a record of the main points discussed at the Conference. We hope that the additional time required to publish these papers has been worth the wait. Lastly, ISEC 77 had a fine display of technical exhibits which were on display for most of the week.

In addition to a good, balanced technical program, the Conference Committee believed that social activities were also important, but little time was allowed for sightseeing or technical visits in the five days on which sessions were held. However, we decided to follow the practice of the 1966 Goteborg Conference, and started the technical program just before a weekend, allowing ourselves a sightseeing trip to Niagara Falls on Sunday, and on Wednesday a choice of technical visits, the technical exhibits, sightseeing, shopping or just relaxing. So with a full and stimulating technical program, technical visits and social events, those who attended should remember ISEC 77. Additionally, many delegates were fortunate in their post conference tours to the uranium mines in Northern Ontario and the copper mines in Arizona.

I take this opportunity to thank the members of the Planning Committee, the session Co-chairmen, authors, technical exhibitors, delegates and the many friends of the Conference, for the realization of ISEC 77.

ISEC 77 marks another milestone in International Solvent Extraction Conferences and in the exchange of solvent extraction technology.

It has been an honour to serve your Conference as Chairman.

G.M. Ritcey



D. R. SPINK
*Technical Program
Chairman*

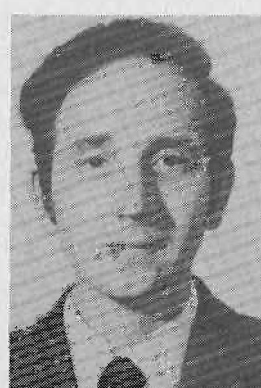
U.K. WORKING GROUP



C. HANSON



M. J. SLATER



A. NAYLOR

ORGANIZING COMMITTEE FOR ISEC 77



M. H. I. BAIRD
Secretary



I. J. ITZKOVITCH
Treasurer



M. M. HAFEZ
Associate Secretary



W. SOWA
Registration



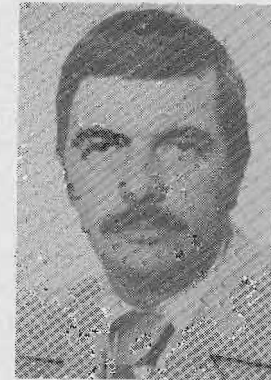
B. H. LUCAS
Proceedings



D. MACKAY
Exhibition



A. J. OLIVER
Visits and Tours



R. W. STANLEY
Publicity

SOCIAL PROGRAM



B. YAWNEY



R. Z. STODILKA



CHRISTINA STODILKA

POSTER SESSIONS



J. A. GOLDING



R. HATCH



S. A. BERKOVICH

FRIENDS OF ISEC 77

The following are the organizations who have so generously provided support to the International Solvent Extraction Conference in Toronto. The Conference Committee, the CIM, CSCChE and SCI wish to express their sincere gratitude.

Amax Nickel Division, Amax Inc. (USA)
Anamax Mining Company (USA)
Anglo American Corporation of South Africa Ltd. (S. Africa)
Arthur G. McKee & Co. of Canada Ltd. (Canada)
Ashland Oil Canada Ltd. (Canada)
Baker Perkins Inc. (USA)
Boliden Aktiebolag (Sweden)
Buffelfontein Gold Mining Company Ltd. (S. Africa)
Canadian Bechtel Limited (Canada)
Chem Pro Equipment Corporation (USA)
Conzinc Rio Tinto of Australia Ltd. (Sulphide Corp. Pty. Ltd.) (Australia)
Cyprus Bagdad Copper Company (USA)
Davy Power Gas Ltd. (U.K.)
Davy Power Gas, Inc. (USA)
Denison Mines Limited (Canada)
Dept. Energy, Mines and Resources (Canada)
Dow Chemical (Canada)
Eldorado Nuclear Limited (Canada)
Esso Chemical Canada Ltd. (Canada)
Falconbridge Nickel Mines Ltd. (Canada)
Fluor Utah, Inc. (USA)
General Mills, Inc. (USA)
General Mining and Finance Corp. Ltd. (S. Africa)
Government of the Province of Ontario (Canada)
Greey Mixing Equipment Ltd. (Canada)
Hatch Associates Ltd. (Canada)
Hoffman - La Roche Inc. (USA)
Holmes and Narver Inc. (USA)
Hudson Bay Mining and Smelting Company Ltd. (Canada)
Impala Platinum Ltd. (S. Africa)
INCO Limited (Canada)
Koninklijke/Shell Laboratorium, Shell Research B. V. (Netherlands)
McMaster University (Canada)
Metallurgie Hoboken-Overpelt (Belgium)
Noranda Mines Limited (Canada)
Noranda Research Centre (Canada)
Ontario Research Foundation (Canada)
Rio Algom Limited (Canada)
A. H. Ross & Associates (Canada)
Saskatchewan Mining Development Corp. (Canada)
Sherritt Gordon Mines Ltd. (Canada)
SNC — Geco Limited (Canada)
Stilfontein Gold Mining Company, Ltd. (S. Africa)
Texasgulf, Inc. (Canada)
Union Carbide Canada Ltd. (Canada)
University of Ottawa (Canada)
University of Toronto (Canada)
University of Waterloo (Canada)
West Rand Consolidated Mines Ltd. (S. Africa)
Wright Engineers Ltd. (Canada)

TABLE OF CONTENTS

Preface	iii
Organization Committee	iv
Friends of ISEC	vi
Welcoming Address	xv

VOLUME 1

CHAPTER 1 — EXTRACTANTS AND DILUENTS	1
--	---

Co-Chairmen: Dr. D.S. Flett, Warren Spring Laboratory, U.K.
 Prof. B.F. Myasoedov, Academy of Sciences, Moscow,
 USSR.

Session 1

a. Liquid Ion Exchange: Organic Molecules for Hydrometallurgy ● <i>R. Swanson*</i>	3
b. Strong Diluent Effects ● <i>R. Blumberg</i> and <i>J.F. Gai</i>	9
c. Ideas and Practice in Design of Solvent Extraction Reagents ● <i>A.J. van der Zeeuw</i> and <i>R. Kok</i>	17
d. Selective Solvent Extractants for the Refining of Platinum Metals ● <i>R.I. Edwards</i>	24

Session 3

a. Diluents in the Separation of Cobalt and Nickel ● <i>C.J. Bouboulis</i>	32
d. The Effect of Alkyl Phenols on the Copper Transfer Properties of the Extractant Acorga P-1 ● <i>R.F. Dalton</i>	40
e. Unified Approach to the Synthesis of Chelating Phase-Transfer Agents (C-PTA) ● <i>A. Warshawsky</i>	48
f. New Neutral Oxygen and Sulphur-Containing Metal Extractants Including Oil Sulphoxides and Sulphides ● <i>V.A. Mikhailov</i>	52

CHAPTER 2 — ORGANIC REAGENTS	61
------------------------------------	----

Co-Chairmen: Prof. A.S. Kertes, The Hebrew University, Jerusalem,
 Israel.
 Dr. W. Sowa, Ontario Research Foundation, Canada.

Session 5

a. The Significance of Surface Activity in Solvent Extraction Reagents ● <i>M. Cox</i> and <i>D.S. Flett</i>	63
b. Recent Developments and New Combinations of Extractants in Synergic Processes ● <i>G. Duyckaerts</i> and <i>J.F. Desreux</i>	73
c. Some Reagents Suitable for Metal Extraction from Sulphate Media: with Particular Emphasis on the Kinetics of Copper Extraction with Chelating Agents ● <i>L. Hummelstedt</i>	86
d. An Evaluation of Crown Compounds in Solvent Extraction of Metals ● <i>W.J. McDowell</i> and <i>R.R. Shoun</i>	95

Session 7

a. Bidentate Organophosphorous Compounds as Extractants from Acidic Waste Solutions: A Comparative and Systematic Study ● <i>R.R. Shoun</i> , <i>W.J. McDowell</i> and <i>B.S. Weaver</i>	101
e. Solvent Extraction Studies of Silver (1) by Tri-laurylamine in O-Xylene ● <i>D.H. Liem</i> and <i>M. Zangen</i>	107

Session 26	
a. Zolon Red as an Extracting Reagent • <i>A.N. Patel</i> and <i>A.M. Qureshi</i>	114
d. Study of the Complex Formation of Ytterbium (III) -di (2-ethylhexyl) Phosphoric Acid and Ytterbium (III) — Nitrate by Solvent Extraction • <i>S. Alegret</i> , <i>M. Aguilar</i> and <i>D.H. Liem</i>	116
CHAPTER 3 — CHEMISTRY OF SOLVENT EXTRACTION SYSTEMS	125
Co-Chairmen: Dr. A.W. Ashbrook, Eldorado Nuclear Ltd., Canada. Dr. B. Gaudernack, Institutt fur Atomenergi, Norway.	
Session 20	
a. Solvent Impregnated Resin — Bridging the Gap Between Liquid and Solid Extraction • <i>A. Warshawsky</i>	127
b. Selective Extraction of Alkali Halides by Crown Ethers • <i>L.E. Asher</i> and <i>Y. Marcus</i>	130
c. Potential Exploitation of Fundamental Properties of Multi-Component/Multi-Phase Systems for Achieving Less Common Separations in Inorganic Chemical Processing • <i>R. Blumberg</i>	134
CHAPTER 4 — PHYSICAL AND INORGANIC CHEMISTRY	141
Co-Chairmen: Dr. S.O.S. Andersson, MX-Processor, Sweden. Dr. A.J. Oliver, Inco, Canada.	
Session 11	
a. The Extraction of Anionic Metal Complexes from Aqueous Solutions by a Long-Chain Alkyl Ammonium Compound — Divalent Manganese, Iron, Cobalt, Nickel, Copper and Zinc-Thiocyanate Systems • <i>T. Sato</i> , <i>H. Watanabe</i> , <i>T. Kato</i> , <i>S. Kibuchi</i>	143
b. Thermodynamics of Partial Processes in the Solvent Extraction of Some Metal Acetylacetonates • <i>B. Allard</i> , <i>S. Johnson</i> , <i>R. Lundqvist</i> and <i>J. Narbutt</i>	150
f. Thermodynamics of Liquid-Liquid Distribution Reactions. Enthalpy and Entropy Controlled Extraction Processes • <i>Y. Marcus</i>	154
Session 28	
a. Electron Spin Resonance Spectral Studies of the Complexes Formed in the Extraction of Manganese (II), Copper (II) and Vanadium (IV) from Hydrochloric Acid Solutions by di(2-ethylhexyl) Phosphoric Acid • <i>T. Sato</i> , <i>T. Nakamura</i> and <i>M. Kawamura</i>	159
d. Four Parameter Correlation Equations for Calculation of Thermodynamic Parameters of Solvation-type Extraction Processes • <i>B.N. Laskorin</i> , <i>V.V. Yakshin</i> and <i>B.N. Sharapov</i>	164
e. Actinide Extraction with Chelating Agents Containing Phosphorus and Nitrogen • <i>D.I. Skorovarev</i> , <i>B.N. Laskorin</i> , <i>V.V. Yakshin</i> , <i>E.A. Filippov</i> and <i>V.V. Shatalov</i>	166
g. Extraction of Iron (III) and Gold (III) by a mixture of Isopropyl Ether and Benzene • <i>D. Maljkovic</i> and <i>M. Branica</i>	175
h. The Formation of a Third Phase in the Extraction of Pu(IV), U(IV) and Th(IV) Nitrates with Tributyl Phosphate in Alkane Diluents • <i>Z Kolarik</i>	178
CHAPTER 5 — MASS TRANSFER	184
Co-Chairmen: Dr. M.H.I. Baird, McMaster University, Hamilton, Canada. Mr. T.C. Lo, Hoffman-La Roche Inc., U.S.A.	

Session 4

- a. Aspects of the Kinetics and Mechanism of the Extraction of Copper with Hydroxyoximes • *R.J. Whewell*, M.A. Hughes and C. Hanson 185
- b. The Kinetics of the Extraction of Copper by LIX64N, and LIX63: Discussion of the Rate Law • *C.A. Fleming*, M.J. Nicol, R.D. Hancock and N.P. Finkelstein 193
- c. The Effect of Hydrodynamic Conditions on the Kinetics of Copper Extraction by LIX65N • *E. Susana Perez de Ortiz*, *M. Cox* and *D.S. Flett* 198
- d. Single Drop Kinetic Studies of the Solvent Extraction of Copper from Synthetic Leach Liquors • *H.Eccles*, G.J. Lawson and D.J. Rawlence 203
- e. Kinetics and Mechanism of Copper Extraction with 2-alkyl-5-hydroxyphenyl Alkyl Ketoximes • *A.J. Van der Zeeuw* and R. Kok 203

Session 9

- b. Mass Transfer Rate Across Liquid-Liquid Interfaces. Film Diffusion and Interfacial Chemical Reactions as Simultaneous Rate Determining Steps in the Liquid-Liquid Cation Exchange of Some Tervalent Cations • *R. Chiarizia* and *P.R. Danesi* 219
- c. Equilibrium and Mass Transfer for the Separation of Nickel and Cobalt in di(2 Ethyl Hexyl) Phosphoric Acid • *J.A. Golding*, *S. Fouda* and *V. Saleh* 227
- e. Electrostatic Extraction for Metals and Non-Metals • *P.J. Bailes* 233

Session 25

- a. On Axial Mixing and the Design of Packed Extraction Columns from First Principles • *H.R.C. Pratt* and W.J. Anderson 242
- c. Internal Sampling of Liquid-Liquid Spray Columns at Steady State. II. Application to Mass Transfer Experiments • *C.J. Lim*, *J.E. Henton*, *G. Bergeron* and *S.D. Cavers* 248
- d. The Retardation of Mass Transfer in a Modified Lewis Cell by Interfacially Active Copolymers • *B.J.R. Scholtens*, *S. Bruin* and *B.H. Bijsterbasch* 256
- e. Structural Mechanical Barriers in Extraction Systems. Effect on Mass Transfer and Coalescence • *G.A. Yagodin*, *V.V. Tarasov*, *A.V. Fomin* and *S.Y. Ivakhno* 260
- Panel Discussion* — Organic Reagents and Mass Transfer
Co-Chairmen: *Dr. M.H.I. Baird* and *Dr. A.S. Kertes* 265

CHAPTER 6 — MODELLING 271

Co-Chairmen: A.L. Mills, U.K. Atomic Energy Authority.
Dr. J. Liljenzin, Royal Institute of Technology,
Stockholm, Sweden.

Session 10

- b. Chemically Based Models to Predict Distribution Coefficients in the Pu(IV) and Np(IV) Nitrate — TBP Systems • *Ying-Chuh Hoh* and *R.G. Bautista* 273
- d. An Approximate Analytical Solution for Solvent Extraction Columns with Axial Dispersion • *M.A. Solemin* and *M.S. Medani* 279
- e. A Computational Algorithm for Three Component Equilibrium Staged Liquid Extraction Systems • *J.W. Tierney* 289
- f. Determination of Equilibrium Curves for Multicomponent Extraction Systems using the AKUFVE Equipment • *J.O. Liljenzin* 295

Session 13	
a. Modelling a Fluid Ion Exchange System • C.G. Brown, J.C. Agarwal, N. Beecher, W.C. Henderson, and G.L. Hubred	303
b. Automatic Control of a Multiple Mixer • C.R. McDonald and W.L. Wilkinson	309
d. Modelling of the IMI Mg Br ₂ - MgCl ₂ Process • J.F. Gai	316
CHAPTER 7 — EQUIPMENT	323
Session 6 — Peter Paige Memorial Session — Mixer Settlers	
Co-Chairmen: Dr. J. Palley, Holmes and Narver, Inc., USA. J.B. Scuffham, Davy Powergas Ltd., UK.	
a. Design of Mixer Settlers to Achieve Low Entrainment Losses and Reduce Capital Costs • I.E. Lewis	325
b. The Cities Service Company's Solvent Extraction and Electrowinning Plant at Miami, Arizona • A.D. Kennedy and C.L. Pfalzgraff	333
c. The Design of Mixer-Settlers for the Zambian Copper Industry • J.R. Orjans, C.W. Notebaart, J.C. Godfrey, C. Hanson and M.J. Slater	340
d. The Application of Basic Principles and Models for Liquid Mixing and Separation to Some Special and Complex Mixer-Settler Designs • E. Barnea	347
Session 8	
Co-Chairmen: Prof. J. Landau, University of New Brunswick, Canada. Dr. M.J. Slater, University of Bradford, U.K.	
a. Performance of a 36 in. Diameter Reciprocating Plate Extraction Column • A.E. Karr and T.C. Lo	355
b. Rapid Extractions with Centrifugal Extractors • G.R. Davies and D.B. Todd	362
c. Determinations of Actual Mass Transfer Rates in Extraction Columns • L. Steiner, M. Horvath and S. Hartland	366
e. The Effects of a Packed-Bed Diffuser-Precoalescer on the Capacity of Simple Gravity Settlers and Compact Settlers • E. Barnea and J. Mizrahi	374
CHAPTER 8 — DISPERSION AND COALESCENCE	385
Co-Chairmen: Dr. G.A. Davies, UMIST, Manchester, U.K. Prof. D.R. Woods, McMaster University, Hamilton, Canada.	
Session 12	
a. The Interaction of Droplets, Gas Bubbles and Solid Particles • E. Rushton, G.A. Davies and G. Rowden	387
b. The Relationship Between Batch and Continuous Phase-Disengagement • A.M.S. Vieler, D. Glasser, and W.A. Bryson	389
c. The Interpretation of Batch Separation Tests for Liquid Mixer Settler Design • J.C. Godfrey, D.K. Chang-Kakoti, M.J. Slater and S. Tharmalingan	406
d. Efficiency of Stabilized and Regenerated Fibrous Glass Coalescers • W.M. Langdon, V. Sampath and D.T. Wasan	413
e. Improving the Performance of Gravity Settlers with Vertical Baffles and Picket Fences • K. Lyne-Smith, J. Roberts and J. McGee	418
Session 29	
b. Study of Dispersion in a Pulsed Perforated-Plate Column • V. Khemanghorn, G. Muratet and H. Angelino	429

VOLUME 2

CHAPTER 9 — INORGANIC PROCESSES	437
Co-Chairmen: Dr. V. Lakshmanan, Eldorado Nuclear Ltd., Canada. Dr. V. Sefton, Sherritt Gordon Mines Ltd., Canada.	
Session 14	
a. The Recovery of Gallium from Bayer Process Aluminate Solutions by Liquid-Liquid Extraction • <i>A. Leveque</i> and <i>J. Helgorsky</i>	439
b. The Solvent Extraction of B ₂ O ₃ Carried by the Borax and Boric Acid Slurries • <i>M.S. Basol</i> and <i>S. Eren</i>	443
d. Solvent Extraction of Nickel, Cobalt and Copper from Laterite-Ammoniacal Leach Liquors • <i>S.C. Rhoads</i> and <i>R.E. Siemens</i>	446
<i>Panel Discussion</i>	453
Session 30	
b. Role of the Liquid-Liquid Partition of the Extractable Chelates in the Solvent Extraction of Divalent Transition Metal Ions with β -Diketones • <i>T. Sekine</i> and <i>R. Murai</i>	457
c. Extraction and Separation of Thorium (IV) and Protactinium (V) with 1-Phenyl-2-Methyl-3-Hydroxy-4-Pyridone • <i>M.J. Herak</i> , <i>I. Prpic</i> and <i>B. Tamhina</i>	462
d. Extraction of Ir(III), Ir(III, III, IV) and Ir(IV) Sulphate Complexes from Sulphuric-Acid Solutions with Nitrogen-Containing Extractants • <i>Yu. S. Shorikov</i> , <i>L.G. Anoshetchkina</i> , <i>Al. Ryzhov</i> , <i>N.M. Sinitsyn</i> , <i>A.M. Orlov</i> and <i>K.A. Bolshakov</i>	466
CHAPTER 10 — BASE METALS	473
Co-Chairmen: Dr. I.J. Itzkovitch, Ontario Research Foundation, Canada. Mr. A. Van Peteghem, Metallurgie Hoboken-Overpelt, Belgium.	
Session 16	
c. Possibilities for Use of Solvent Extraction in the Outokumpu Nickel Process • <i>R. Leimala</i> and <i>Bror G. Nyman</i>	475
e. Solvent Extraction of Base Metals Using In-situ Neutralization with Lime • <i>V.A. Ettel</i> , <i>J. Babjack</i> and <i>A.J. Oliver</i>	480
f. LIX34 — Continuous Pilot Plant Evaluations • <i>G. Kordosky</i>	486
Session 21	
a. Copper Extraction with an Alkylated 8-Hydroxyquinoline: Modifier Effects and Kinetics in Mixed Copper-Iron Solutions • <i>D.S. Flett</i> and <i>D.R. Spink</i>	496
b. Solvent Extraction of Vanadium (IV) with Di-(2-ethylhexyl) Phosphoric Acid and Tributylphosphate • <i>H. Ottertun</i> and <i>S. Strandell</i>	501
c. Liquid-Liquid Extraction of Nickel(II) by Dialkylphosphorodithionic Acids • <i>J.L. Sabot</i> and <i>D. Bauer</i>	509
d. The Complex Utilization of Red Mud or Low Grade Bauxite by Solvent Extraction • <i>V.G. Logomerac</i>	516
e. Recovery of Chromium and Vanadium from Alkaline Solutions Produced by an Alkaline Roast-Leach of Titaniferous Magnetite • <i>G.M. Ritcey</i> and <i>B.H. Lucas</i>	520

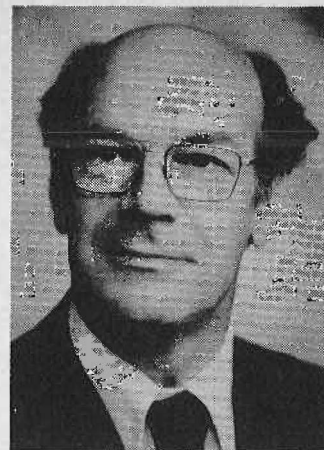
CHAPTER 11 — COPPER PROCESSING	523
Co-Chairmen: Dr. J.C. Agarwal, Kennecott Copper Corp., U.S.A. Mr. J. Dasher, Bechtel Corp., U.S.A.	
Session 23	
a. Synthesis, Structure and Hydrometallurgical Properties of LIX-34 ● <i>M.J. Virnig</i>	535
b. The ACORGA P-5000 Series in the Solvent Extraction of Copper. Performance Characteristics and Implications for Plant Economics ● J.A.J. Tumilty, <i>G.W. Seward</i> and J.P. Massam	542
c. Sensitivity of LIX Plant Costs to Variations of Process Parameters ● H.E. Barner, G.L. Hubred and <i>I.V. Klumpar</i>	552
<i>Panel Discussion on Operating Problems</i>	
Chairman: Mr. J. Dasher	565
CHAPTER 12 — URANIUM PROCESSING	565
Co-Chairmen: Dr. P.J.D. Lloyd, Chamber of Mines Research Organ- ization, South Africa. Mr. G.M. Ritcey, Energy Mines and Resources, Canada.	
Session 19	
a. A Review of Progress in the Application of Solvent Extraction for the Recovery of Uranium from Ores Treated by South African Gold Mining Industry ● <i>S.N. Finney</i>	567
b. Uranium Processing in South Africa <i>W.M. Craig</i>	577
c. Contribution to Paper 19a ● <i>W. Ruhmer</i>	580
<i>Panel Discussion on Practical Processing of Uranium</i>	
Chairman: G.M. Ritcey	
CHAPTER 13 — NUCLEAR PROCESSES	585
Co-Chairmen: Dr. K.B. Brown, Oak Ridge Nuclear Laboratories, U.S.A. Dr. P.M. Mouret, Commissariat à l'Énergie Atomique, France. Dr. P. Michel, COGEMA Groupe, C.E.A., France.	
Session 18	
a. Solvent Extraction of Enriched Uranium Fuels at the Savannah River Plant ● <i>M.C. Thompson</i>	587
b. Extraction and Selective Stripping of Uranium and Molybdenum in Sulfate Solution Using Amines ● E. Sialino, C. Mignot, <i>P. Michel</i> and J. Vial	592
d. A Solvent Extraction Flowsheet for a Large-Scale LWR Fuel Re- processing Plant ● F. Baumgärtner, <i>G. Koch</i> , W. Ochsenfeld, H. Schmeider and H.E. Goldacker	599
e. Experience with the Reprocessing of LWR, Pu Recycle and FBR Fuel in the MILLI Facility ● <i>W. Ochsenfeld</i> , F. Baumgärtner, V. Bauder, H.J. Bleyl, D. Ertel and G. Koch	605
Session 22	
a. Uranium, Neptunium and Plutonium Kinetics of Extraction by Tri- butylphosphate and Trilaurylamine in a Centrifugal Contactor ● P.L. Bergeonneau, C. Jaouen, <i>M. Germain</i> and A. Bathellier	612
c. Bidendate Organophosphorus Extractants: Purification Properties and Applications to Removal of Actinides from Acidic Waste Solutions ● <i>W.W. Schulz</i> and L.D. McIsaac	619

d. Extraction of Trivalent Transplutonium Elements by Alkalenedi-phosphine Dioxides • <i>B.F. Myasoedov</i> , M.K. Chmutova and T. Ya. Medved	630
e. Organic-Soluble Hydroquinones as Reducing Agents for Plutonium and Neptunium, and Utilization of Hydroxylamine Nitrate for the Stripping of Plutonium from Organic Solutions of Long-Chain Tertiary Amines • <i>G. Grossi</i>	634
Session 33	
a. Solvent Extraction of Plutonium with High Molecular Weight Neo-alkyl-Hydroxamic Acids • <i>G. Grossi</i> and G.M. Gasparini	640
b. Enhancement by Zirconium of Extraction of Lanthanides by Organophosphorus Acids • <i>G.A. Yagodin</i> O.A. Simegribova and N.A. Plesskaja	645
c. Reducing Reextraction of Plutonium in the Two-Phase System by Means of Various Reagents • M.F. Pushlekov, <i>N.S. Tikhanov</i> and N.N. Shchepetilnikov	648
d. The Tri-alkyl Aceto Hydroxamic Acids as Selective Extractants in the Reprocessing of Irradiated Nuclear Fuels • <i>G.M. Gasparini</i>	654
e. The Neo-tridecano-hydroxamic Acid as an Extractant of Long-lived Actinides from Purex-type-HAW Raffinates • <i>F. Mannone</i> , L. Cecille and D. Landat	661
CHAPTER 14 — ORGANIC PROCESSES	669
Co-Chairmen: Prof. C. Hanson, University of Bradford, U.K. Prof. Dr. U. Onken, Universitat Dortmund, Federal Republic of Germany.	
Session 15	
a. Separation of 2:3 and 2:6 Dichlorophenols by Dissociation Extraction with Monoethanolamine • <i>M.M. Anwar</i> , S.T.M. Cook, C. Hanson and M.W.T. Pratt	671
b. Extraction of Cyclohexanone-oxime and Cyclohexanone with Toluene in a Pulsed Packed Column • <i>A.J.F. Simons</i>	677
c. The Extraction and Separation at Near Critical Conditions of Components in Some Natural Products • F. Panzner, S.R.M. Ellis and <i>T.R. Bott</i>	685
d. Selectivity and Solvency Properties of Extraction Solvents and Their Mixtures • <i>A.B. van Aken</i> and J.M. Broersen	693
e. Performance of ARD Extractors in the Purification of Caprolactam T. Misek, <i>J. Marek</i> and J. Bergdorf	701
f. The Recovery of Pure Aromatics from Hydrocarbon Mixtures by Extraction Distillation and Liquid-liquid Extraction, using Morpholine Derivatives as Solvent • <i>G. Preusser</i> and J.E. Franzen ...	707
Session 31	
a. Solvent Extraction of Coal • <i>G.H. Beyer</i>	715
b. On a New Type of Extraction of Acids by Amine Salts through Addition • <i>V.S. Schmidt</i> and K.A. Rybakov	718
c. Dissociation Extraction — Economic Optimization of a Separation Process for Meta- and Para-Cresols • <i>M.W.T. Pratt</i> and J. Spokes	723

CHAPTER 15 — ANALYTICAL TOPICS	739
Co-Chairmen: Dr. A.W. Ashbrook, Eldorado Nuclear Ltd., Canada. Dr. H. Steiger, Energy Mines and Resources Canada.	
Session 17	
a. Applications of Chromatography in Investigation of Organic Losses in Solvent Extraction Processes for Copper and Uranium • A.W. Ashbrook, I.J. Itzkovitch and <i>W. Sowa</i>	741
b. Solvent Extraction Systems for Substoichiometric Separations in Neutron Activation Analysis • <i>J.W. Mitchell</i>	750
d. Control of a Solvent Extraction Process for Rare Earth Separation by Means of a Computer-based, On-stream XRF Analytical System • B. Gaudernack and <i>O.B. Michelsen</i>	754
e. Instrumentation and Control of the Solvent Extraction Section in the Falconbridge Matte Leach Process • <i>P.E. Vembe</i>	761
Session 32	
b. Protonation and Metal Complexation 1, 3, 4-Thiadiazolium-2-thiolate and 2, 3-Diaryl-2H-tetrazolium-5-thiolate Derivatives • <i>A.M. Kiwan</i> , <i>A.Y. Kassim</i> and <i>H.M. Marafie</i>	765
c. Solvent Extraction Studies by a Computer Controlled AKUFVE • <i>T. Wallin</i> , <i>D.H. Liem</i> and <i>K. Hogberg</i>	769
CHAPTER 16 — ENVIRONMENT	779
Co-Chairmen: Dr. Ruth Blumberg, IMI, Haifa, Israel. Mr. J.R. Hawley, Ministry of Environment (Ontario) Canada.	
Session 2	
a. Losses of Organic Compounds in Solvent Extraction Processes • A.W. Ashbrook, <i>I.J. Itzkovitch</i> and <i>W. Sowa</i>	781
b. The Applicability of Solvent Extraction to Waste Water Treatment • <i>D. Mackay</i> and <i>M. Medir</i>	791
c. MAR-Hydrometallurgical Recovery Processes • <i>S.O.S. Andersson</i> and <i>H. Reinhardt</i>	798
CONFERENCE SUMMARY AND CLOSING REMARKS	805
Conference Chairman: G.M. Ritcey.	
OFFICIAL DELEGATES LIST	I - 1
AUTHOR INDEX	I - 17
SUBJECT INDEX	I - 19

*Note: Italics indicates oral presentation.

A. W. Ashbrook
Co-Chairman
ISEC 77



WELCOMING ADDRESS

It is both a privilege and an honour for me to welcome you, on behalf of the Organising Committee, to Canada, to Toronto, and to the International Solvent Extraction Conference of 1977 — more affectionately known as ISEC 77. It is indeed a pleasure to see such a response from so many countries of the World. I am sure you will find Toronto a most interesting city, especially — or in spite of — it being known as “Toronto The Good”.

We also wish to extend a cordial welcome to the many Ladies and Children who are with us this week.

This is, I think, the 8th International Solvent Extraction Conference since the first one in the early 1960's, and the first to be held in Canada.

These ISEC's have, over the years, continued to attract a growing amount of attention World-wide, and this year is no exception as we again see a large attendance.

ISEC 77 presents several features not seen at previous conferences. First, the Plenary Sessions, which have as their objectives the assessment of the current — what I shall call if you will forgive me — the state-of-the-art in the solvent extraction field, plus some crystal-ball gazing into the future. To achieve maximum impact and discussion we have arranged no other sessions to conflict with the Plenary Sessions.

Another innovation is the Poster Session. The increasing popularity of this mode of information and knowledge transfer, with its more intimate character than the formal sessions will, we feel, provide a forum conducive to a free and uninhibited exchange of ideas. We hope you will take advantage of the Poster Sessions.

In addition, the regular sessions, together with the technical and social tours and events will, we trust, provide a challenging technical and a relaxing week. I am not sure whether these extremes are compatible but we shall, no doubt, find out.

In looking over the abstracts of the papers to be presented you will find, I think, a shift in overall emphasis of this year's ISEC — from the more basic aspects of SX in the recent ISEC's to a more applied content. This was one objective of this Committee, and we hope it proves to be appropriate.

One of the reasons for holding scientific conferences is to provide a meeting place — or *Katimavik* — where those working or involved in a particular discipline or field can meet, discuss, assess, argue, differ, predict, theorise, or indulge in other activities.

During the coming week YOU, representing the many facets of the field of solvent extraction, will undoubtedly do all these things. But most of all I think we need to assess the current situation from many directions, determine what the needs are, and where we should be going.

In viewing the three years since the last ISEC at Lyon, it appears to me that a plateau of activity was reached in this period. The impetus and stimulus experienced during the late 60's and early 70's appears to have run its course. The universal promise of the chelating reagent as a metal-specific extractant, for example, has not yet been fulfilled.

And while the number of papers in the SX field may have increased, I do not see any major breakthrough in this period. I wonder if we have not fallen in love with copper to the exclusion of other metals, and with oximes to the exclusion of other extractants.

Perhaps the exciting decade I referred to left us rather weak, as love affairs are apt to do, and some recuperation has been necessary. But on looking over the presentations which will be made to us this week, I do see areas where progress has been made, and many new ideas which will be advanced.

The attendance at this conference of some 450 delegates from 30 countries convinces me that the in-

terest and dedication in the SX field is alive and well. Undoubtedly we shall make considerable progress in the understanding and application of the solvent extraction technique. We must also endeavour to attract new people, provide a challenging environment, and integrate basic and applied knowledge to achieve our goals.

It is to this end that we are gathered together this week at ISEC 77. The Organising Committee has attempted to provide the environment, and it is now up

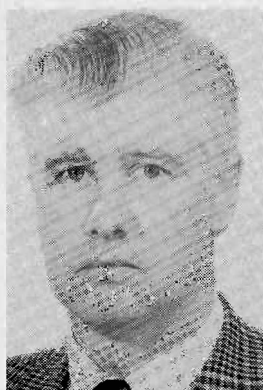
to *you*, the delegates, to determine the success of the conference in providing the stimulus and direction in the field of solvent extraction for the next three years, when the results can be reported at ISEC 80. It is hoped that the venue for ISEC 80 will be announced at the banquet.

Ladies and Gentleman, on behalf of the Organising Committee, it gives me great pleasure and, I must admit, some considerable relief, to declare ISEC 77 underway.

Chapter 1

Extractants and Diluents

Plenary Session 1
and
Session 3

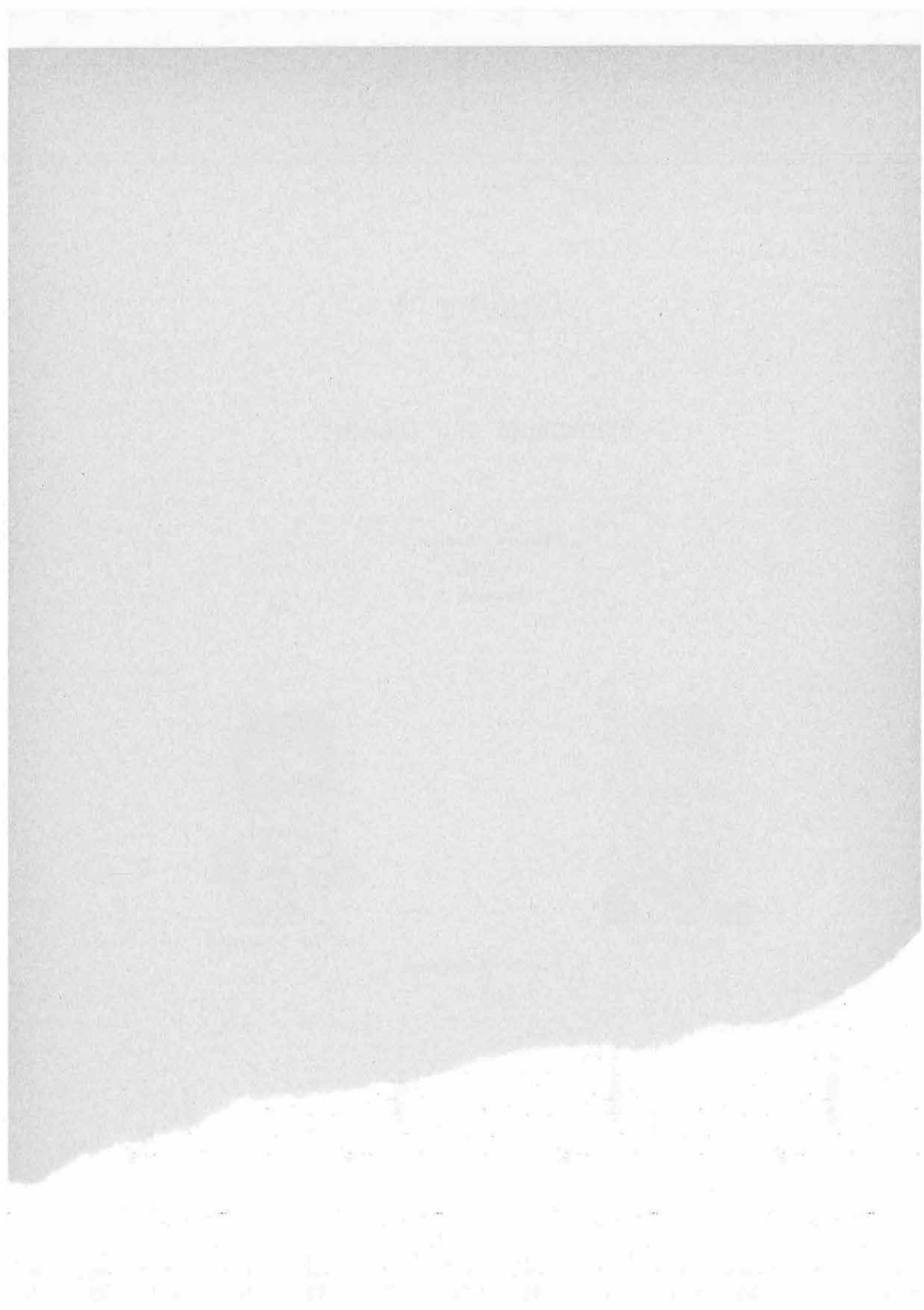


Dr. D.S. Flett



Prof. B.F. Myasoedov

Session Co-Chairmen



Liquid Ion Exchange: Organic Molecules for Hydrometallurgy

Ronald R. Swanson, Principal Scientist,
General Mills Chemicals, Inc.,
Minneapolis, Minnesota

ABSTRACT

Liquid ion exchange, a distinct subdivision of the liquid-liquid extraction operation family, was conceived only some twenty-five years ago. Starting with non-selective reagents, processes for recovering high-value metals were developed. With the advent of selective reagents, lower-value metals could be processed and have been to a greater degree each year.

Reagents used in liquid ion-exchange processes must meet certain criteria. Some of the more important characteristics are rates of reaction, phase separation and reagent stability. These characteristics are discussed, with particular attention to the hydroxyoxime reagents.

Introduction

LIQUID-LIQUID EXTRACTION or solvent extraction is one of the defined unit operations in which a solute is partitioned between two immiscible or partially immiscible phases. Liquid ion exchange or solvent ion exchange is a very similar operation in which ions are transferred between two immiscible phases. In liquid ion-exchange, reagents, other than the solvent molecules, are required which will exchange these ions across the interface.

Liquid-liquid extraction has been applied industrially for many years for the production of lubricating oils, pharmaceutical preparation, natural product isolation, etc. Liquid ion exchange, however, was not developed until the middle fifties when it was rapidly applied in the recovery of uranium from low-grade ore. Its use in copper production only started two years ago and large-scale use only in the last five.

Liquid ion exchange for metal recovery was made possible by the development of reagents which reversibly react with the appropriate metal to give complexes or salts which are soluble in organic solvents such as kerosene. Prior to the development of these compounds, liquid-liquid extraction had only limited applications such as in the purification of uranium.

The success of a liquid ion-exchange process is dependent principally on the reagent. It is in this area where the organic chemist has been able to develop reagents having properties that the metallurgist required. This interfacing between disciplines, organic chemistry and metallurgy, has led to rapid progress in hydrometallurgy in the last ten years.

Experimental Results and Discussion

Early Copper Recovery Methods

Primitive cultures obtained their copper-containing articles either from native copper deposits or from high-grade copper ores that were easily mined and smelted.

Until less than a century ago, only those deposits of copper which contained high concentrations of copper could be economically mined and processed. The only means of upgrading or concentrating an ore was by hand picking or crude gravity methods.

One chemical method of concentrating an ore was employed in 16th-century Spain. This consisted of piling the ore in large dumps and leaching with dilute sulfuric acid. The effluent from the dump was collected and run over scrap iron, where the copper precipitated and the iron dissolved. A high-grade cement copper was produced.

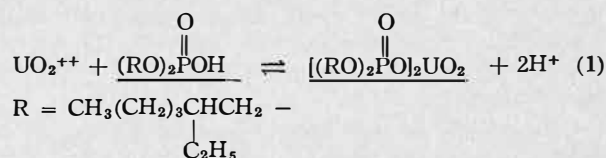
With the introduction of the flotation process, made possible by materials produced in the laboratory of the organic chemist and by the use of larger mining equipment, it became possible to mine and process increasingly poorer grades of copper ore economically. At the present time, it is economically feasible to mine and process ores containing approximately 0.3% copper.

If the rock contains less than approximately 0.3% Cu, then this material is trucked to large dumps where the copper is leached as described above and the metal is recovered by cementation over scrap iron (usually burned and shredded tin cans). The copper thus obtained is contaminated with other metals and must still be smelted and electro-refined before commercially pure copper is available for sale.

Early Development of Liquid Ion Exchange

An event of great importance to the copper industry occurred on a July morning in 1945 when the Manhattan Project reduced to practice a large-scale nuclear reaction. Subsequent developments dictated that large quantities of uranium would be required for both nuclear devices and peaceful uses of nuclear energy.

Uranium in the United States occurs predominantly in disseminated deposits, principally on the Colorado Plateau of the western U.S. A typical deposit contains ore grading 0.1% U₃O₈. Scientists of the USAEC were charged with the task of devising processes to recover the uranium from these deposits economically. They found that the uranium could be liberated from these ores by oxidative leaching with sulfuric acid to give a solution containing approximately 1 g of U₃O₈ per liter at pH 1-1.5. At first, the only means available to concentrate the uranium was by the use of solid ion-exchange resins. A cheaper and better process was required.



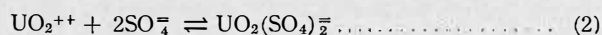
Underlined species are present in the organic (kerosene) phase.

Further research showed that by using a functional group reactive with the uranium species present in the solution, and modified properly to achieve solubility in kerosene, a liquid ion-exchange system would accomplish

this concentration. That is, by substituting kerosene for the polystyrene backbone of the resin and a high-molecular-weight, kerosene-soluble functionalized molecule for the reactive group, an all-liquid material capable of ion exchange could be produced.

The problem with the alkylphosphoric acid process is that Fe^{+3} is also extracted so that it must be reduced to the unextractable Fe^{+2} before the extracting process.

The USAEC also found that amines could also be used in the process because, as shown in equation 2, uranium can exist in sulfate solution in an anionic form.



The amines then extract the uranium as in equation 3.

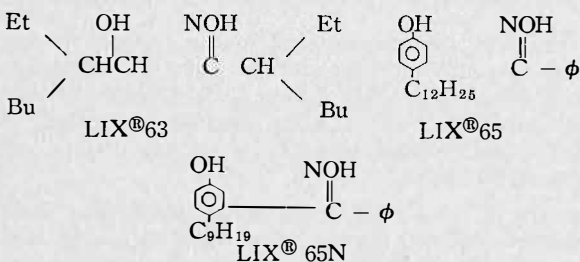


The problem of iron extraction is obviated because iron (either Fe^{+2} or Fe^{+3}) will not form an extractable sulfate complex.

This new system provided reagents which behaved as ion-exchange resins, but had all the advantages of a liquid-liquid system, i.e. simplified handling, reduced cost, etc. A number of mills were then built in the western U.S. to apply this new process. General Mills Chemicals Inc. became involved in this new technology, because it was one of our products (ALAMINE® 336, a tertiary amine containing C_8 and C_{10} alkyl groups) that was found to have optimal properties for this use.

LIX® 63/LIX® 64

It became apparent to scientists at GMCI, as they applied this new process to different metals and situations, that a major contribution to the copper industry could be made if the problem of extracting copper from dilute solutions could be solved. Three reagents were developed in searching for a solution: LIX®63, LIX®65 and LIX®65N.*



Although all three are hydroxy oximes, LIX®63 has an alcoholic hydroxyl versus phenolic hydroxyls for the other two and forms a 5-membered ring on chelation while LIX®65 and LIX®65N form 6-membered rings. The only difference between LIX®65 and LIX®65N is 3 carbons in the side chain. LIX®64N is LIX®65N with a catalytic amount of LIX®63 added.

Although the criteria that a reagent must meet are different for each metal and processing system, many of the criteria are similar. From our experience with uranium reagents and processing and what we learned in the development of copper reagents, the following list of criteria was developed:

1. It should exhibit good selectivity for copper over other metals in the solution.
2. It should extract the copper without pH adjustment and conserve acid values.

3. It should extract the copper rapidly.
4. The reaction should be reversible.
5. It should be compatible with readily available and inexpensive solvents.
6. It should be stable or have stability commensurate with costs of the operation.
7. It should not transfer anions.
8. It should have a very low degree of water solubility.
9. It should exhibit good phase separation characteristics.

10. Preferably it should be non-flammable or have a high flash point, be non-toxic (to man and beneficial bacteria), non-carcinogenic, etc.

11. Preferably it should be a one-component system (aside from solvent or diluent) so that properties do not change from changing composition.

Some of these criteria are obvious and are readily achieved; others present a continuum and present no black-and-white answer. Others are interdependent in that an improvement in one property can be achieved only at the sacrifice of another property.

Process Outline and Comparison to Cementation

Figure 1 gives an outline of a typical application of liquid-ion exchange for copper and a comparison with cementation. The figure shows that liquid-ion exchange is more complex than cementation, but two different products are produced. From cementation, a crude product is produced that must be smelted and electrorefined before it can be consumed by industry. With liquid ion exchange, pure cathode copper is obtained directly.

In the liquid ion-exchange process, the effluent from the leaching dump is contacted with a kerosene solution of LIX®64N and the copper extracted into the organic phase. Protons are exchanged for the copper so that we have regenerated the leach solution for recycle back to the dump. In the cementation process, the copper is exchanged for iron so that the aqueous solution becomes enriched in iron on each recycle. In addition, acid is not regenerated but rather consumed, so that acid must usually be added before recycle to the dump.

In cementation, the iron accumulated in the recycled leach solution tends to be precipitated in the dump, thereby plugging the dump so that percolation eventually becomes impossible. With the liquid ion-exchange system, no iron is added so this problem is eliminated. Data seem to indicate that copper recovery from a dump increases when solvent extraction is substituted for cementation.

Criterion 10 requires that the reagent or material in the organic system should be non-toxic to beneficial bacteria. This is because in most dump leaching bacteria are responsible for leaching of the copper. These bacteria utilize the copper and iron sulfides for energy in oxidizing the sulfide minerals to sulfate. If the reagent system contains materials toxic to these bacteria, reduced amounts of copper will be leached from the dump if these materials are allowed to reach it.

In cementation, once the copper has been precipitated it is washed from the iron, drained, dried and shipped to the smelter.

In liquid ion-exchange processing, the extraction of the copper into the organic phase is only part of the process. Once extracted, the copper must be stripped back into an aqueous phase for electrowinning. This is done by contacting the organic phase with aqueous sulfuric

*NOTE: The commercial products containing varying amounts of solvent to facilitate handling.

acid-copper sulfate solution from the electrowinning operation.

The reason liquid ion exchange is used in the recovery of copper from these solutions is two-fold: (1) purification and (2) concentration. LIX®64N is quite selective for copper, rejecting other materials to the raffinate. These non-extracted metals would make electrowinning difficult, if not impossible. Concentration is achieved by varying the concentration of active reagent in the organic phase and by varying the ratios of the organic and aqueous phases in both the extraction and stripping stages. Dump leach solutions typically contain approximately 1 g of Cu per liter and electrowinning solutions must contain 25-35 g of Cu per liter for efficient utilization of electrical energy. This degree of concentration is easily achieved by use of LIX 64N.

In the development of reagents for use in the process just described, a number of problems arose which required answers. Three such areas will be discussed in some detail: (1) rate of copper extraction, (2) reagent stability and (3) phase separation.

The Mixer: Rates of Reaction

Except for a few specialized applications, metallurgical operations utilize mixer-settlers for contacting and settling the organic and aqueous phases. The reasons for this are many: inexpensive, easy to fabricate, minimal control problems, readily cleaned of entrained solids, difficult to foul, easily scaled up and used in every previously built plant. Another advantage is that the mixing operation is independent of the settling operation, so that each unit may be sized as required by the system.

The phenomena occurring in a mixer are very complex. The rate at which a material will move from one phase to another is governed by a number of variables. Of a physical nature, we have such items as shape of the container, shape and position of baffles (if any), shape and position of the agitator, speed (power input) of the agitator, and location and size of inlet and outlet. The intrinsic properties of phases also greatly influence rates of reaction, such as viscosity of each phase, diffusion rates of reactants, and, of course, the temperature dependence of each of these properties. Although much work has been done to separate and understand the various aspects of reactions in mixers, it is still impossible to design a mixer from first principles. A number of semi-empirical correlations exist, however, that allow the scale-up of mixers once the relevant physical property data are available and a pilot unit has been operated.

From several standpoints, it is valuable to determine the rate of reaction for the transfer of copper from the aqueous phase to the organic phase. It was found very early in the development that LIX®65 did not extract copper at a rate consistent with a diffusion-controlled reaction. The reaction was considerably slower. It was also discovered that certain materials catalyzed this transfer reaction and, of course, the question of why this was so was raised. Two materials that catalyze the reaction are LIX®63 and D2EHPA.

In mixers one phase exists in a continuum and the other phase is dispersed as droplets. Because of the nature of a mixer as described above it would be difficult to ascertain the reasons for effects observed by the addition of various materials to a system. One could add LIX®63 to a LIX®65-copper sulfate system and find an increase in rate of reaction. However, is this due to changes in interfacial tension and hence drop size, density, viscosity, or catalytic effects? Independent, controlled experiments are the only means to a solution.

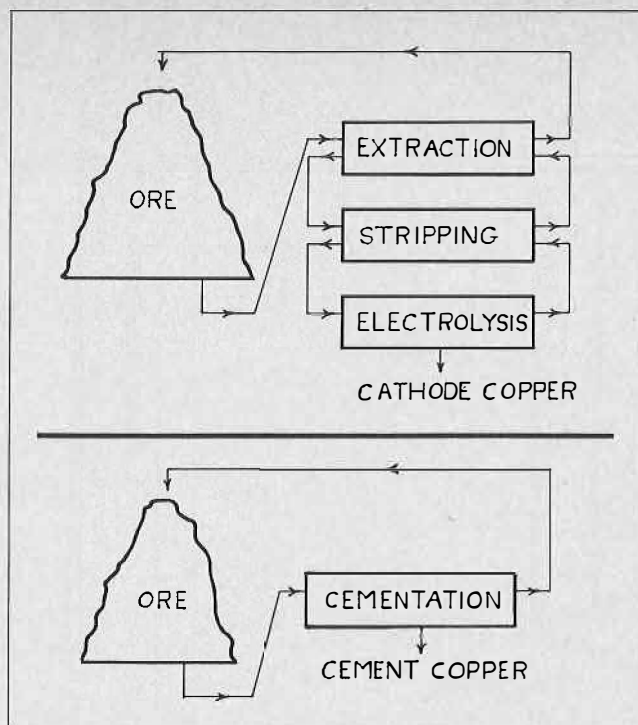


FIGURE 1.

To gain some insight into this problem, Prof. C. Geankoplis of Ohio State University investigated the rate of extraction of copper, with various modifiers, from dilute acidic copper solutions. This work was done using the apparatus shown in Figure 2.

The experiments were conducted by filling the extraction chamber with the organic solution and controlling the temperature at 28°C. Acidic copper sulfate solution was then introduced at the top of the column of liquid (but below the surface), allowed to fall as a droplet through the solution and collected at the bottom. The volume of solution added and the rate of fall of the drops were measured and from the known number of drops used, the droplet volume could be calculated. Concentration of copper in the solution was measured both before and after extraction.

In this type of experiment, extraction of copper will occur as the droplet is forming, as the droplet falls through the column of solution and when the droplet coalesces into the bulk aqueous. These end effects can be isolated and corrected for by using various lengths of columns. Methods for predicting the amount of extraction under each of these three regimes are available when only diffusion is occurring.

The apparatus, techniques and methods of calculation were checked for the acetic acid — methylisobutylketone — water system. The experimental and calculated values agreed very closely.

In Figure 3 are plotted the data obtained for kerosene solutions containing 5% by wt of 2-hydroxy-5-dodecylbenzophenone oxime with various amounts of 5,8-diethyl-7-hydroxy dodecan-6-oxime and di-2-ethylhexylphosphoric acid (D2EHPA). Also plotted is a line calculated for this system if mass transfer was the only limiting rate. The most obvious conclusion from the data is that actual transfer of copper is exceedingly slow compared to a mass-transfer limiting process.

It is also seen from the data that LIX®63 is very effective as a catalyst and that D2EHPA is even more effective.

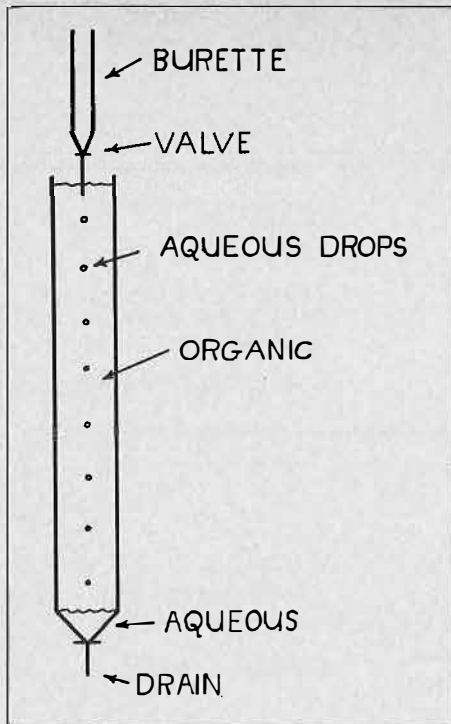


FIGURE 2.

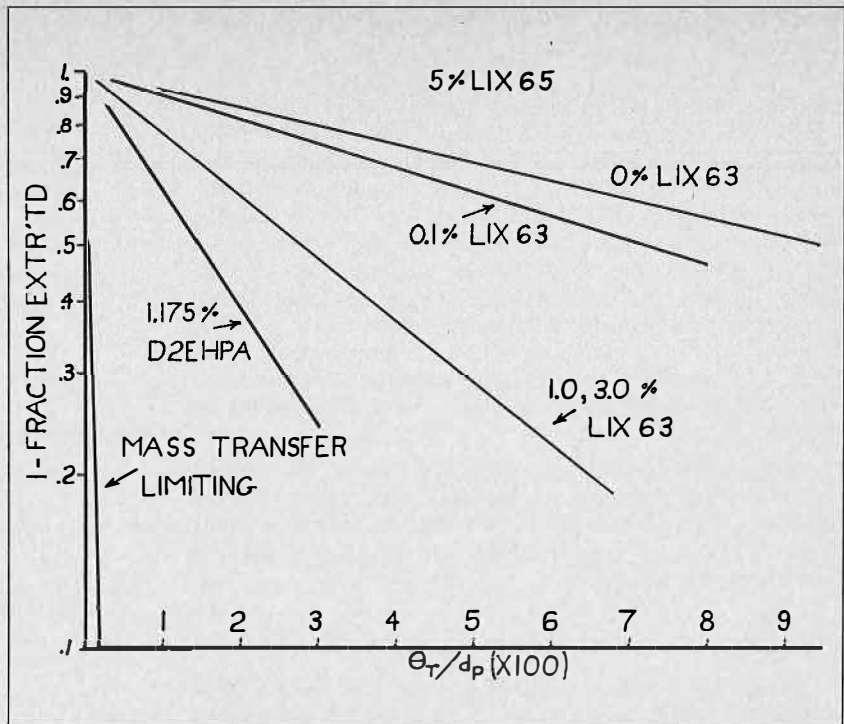


FIGURE 3.

Above a certain concentration of LIX®63, the rate is unaffected by any further increase in concentration.

Although a definitive answer has not been found for this catalytic behaviour, the following theory is advanced to explain it. Figure 4 shows a representation of an interface with mass transfer occurring. C_{MA} represents the concentration of copper in the bulk aqueous phase; C_{MO} is the concentration of copper in the bulk organic phase. C^*_{MA} and C^*_{MO} are the concentration of copper at the interface in the aqueous and organic layers respectively. In a system where copper is being transferred from the aqueous phase to the organic phase the concentration of the copper in the bulk aqueous phase will decrease as the interface is approached because it is at the interface that the copper is being removed. As the copper transfers across the interface, assuming microscopic reversibility, the concentration changes to C^*_{MO} where the ratio C^*_{MO}/C^*_{MA} is the distribution coefficient. The concentration then decreases to that of the bulk organic phase. Assuming that there is no chemical resistance at the interface, a rate of copper transfer can be calculated which was plotted in Figure 3. As the actual rate is considerably less than that theoretically possible, we must have some chemical resistance present.

To explain the accumulated experimental data and data in the literature, we have postulated the following mechanism for the catalytic activity of the LIX®63. The LIX®63 molecule, at first present in the bulk organic phase, first enters the interfacial region where the unshared pair of electrons of the oxime nitrogen bond to a hydrated cupric ion. The copper ion then attacks the oxygen of the α -hydroxy group with expulsion of a proton. Molecular motion then carries the half-formed complex, with its attendant counter ion, into the more organic-rich region of the interfacial region. At this point, reaction occurs with a LIX®65 molecule to complete the complex formation. The proton liberated in this reaction, the counter ion and the water of hydration initially present then diffuse to the bulk aqueous phase while the complex containing one atom of copper, one

molecule of LIX®63 and one molecule of LIX®65 diffuses to the bulk organic phase. In the bulk organic phase, the complex reacts with a molecule of LIX®65 with displacement of the LIX®63 and the cycle is then repeated.

The term, interfacial region, in our view, can best be described by stating what it isn't. The bulk organic phase is that region where the organic molecules are not perturbed by the presence of the bulk aqueous phase and vice versa. The interfacial region, then, is where both aqueous phase molecules and organic phase molecules are perturbed by each other. This interfacial region can be looked upon as a continuum between the two bulk phases possibly on the order of several molecular diameters in width, rather than a sharp discontinuity.

Solubility Losses

Reagent stability and solvent loss are problems of great importance to the mining industries' application of LIX®64N. Because of the high molecular weight of LIX®65N and the fact that two molecules of LIX®65N are required per atom of copper, 10.7 lb of LIX®65N are required to react with 1 lb of copper. At present prices, therefore, approximately \$70 worth of the reagent is required to react with 1 lb of copper worth \$0.74. Therefore, the reagent must be capable of being reused a number of times to make its use economically feasible. In fact, the reagent must be recycled 10,000 times to bring the cost down to 0.7¢.

It is interesting to note at this point that the USAEC commissioned a well-known organization in the 1950's to examine the liquid ion-exchange process and estimate its applicability to metals other than uranium. The results of this analysis indicated that liquid ion exchange could not be economically applied to metals valued at less than \$0.50/lb in 1955 dollars.

Because the solubility of LIX®64N is less than 1 ppm in aqueous solutions, losses on this account are minimal. What are termed solubility losses by the mining industry are not really solubility losses but rather physical entrain-

ment losses. This arises because, in a mixer, a Gaussian distribution of droplet sizes is produced, the smallest being a few microns in diameter, whereas others may be several millimeters in size. When this dispersion is allowed to settle, Stokes Law is followed. The large droplets settle rapidly and coalesce; the smallest may require many hours.

Because of the large flow rates encountered (in one plant they are greater than 12,000 gal/min), it is impractical to allow more than a few minutes for settling. These very fine droplets never do settle and are lost from the system. Well designed and operated plants will experience "solubility losses" of 50-100 ppm of organic phase.

While large numbers of very small droplets are produced in the mixers, the mechanism of coalescence in the settlers is also responsible for producing them. In the laboratory, we have obtained photographic evidence to illustrate this. Rather than immediate coalescence between the bulk organic and the droplet, the droplet rests on the interface for a period of time to allow the intermediate layer of aqueous solution to drain to the point at which collapse occurs between the two organic phases. As the kerosene rushes up due to the force of gravity, a new droplet is formed that is much smaller than the original. This new droplet then repeats the process, losing most of its kerosene to the bulk phase and, in turn, producing yet a smaller droplet. This process repeats itself an unknown number of times. In the laboratory we have observed up to four stages under the naked eye; magnification would undoubtedly reveal more. The importance of this coalescence phenomenon lies in the fact that as these droplets become smaller it requires less and less energy to displace them from the interface where they can coalesce. If turbulence occurs in the settler, then some of these droplets will be displaced and, in turn, some of them will be lost in the aqueous effluent from the settler.

Although the discussion so far has been concerned with kerosene drops in the aqueous phase, the same phenomena occur in the organic phase with droplets of the aqueous phase. Incomplete settling of these aqueous droplets can lead to what is termed "physical carryover". This is the transfer of aqueous phase from the extraction section to the stripping section or vice versa, leads to cross contamination and decreases the efficiency of the operation.

Stability

As mentioned above, the reagent must be recycled a large number of times if the cost of reagent is to be an insignificant item in the recovery of copper, or any metal. Some of the reagent is lost by "solubility losses". Some is lost by instability of the reagent and solvent by hydrolysis, oxidation, etc.

As the reagents we have been discussing utilize oxime groups as part of the copper functional moiety, the problem of both hydrolytic stability and possibly Beckman Rearrangement had to be dealt with. If the reagents were soluble in water then long-term stability would not be a problem, they would be unstable. However, in a liquid ion-exchange system the reagents are designed to be water insoluble and soluble in solvents such as kerosene. The reagents should certainly be more stable, because their contact with acid and water is greatly reduced. The reagents must reside in the interfacial region part of the time and it is in this region that hydrolytic attack most likely occurs.

The problem of measuring hydrolysis in a two-phase system is a most difficult one. Not only are variables

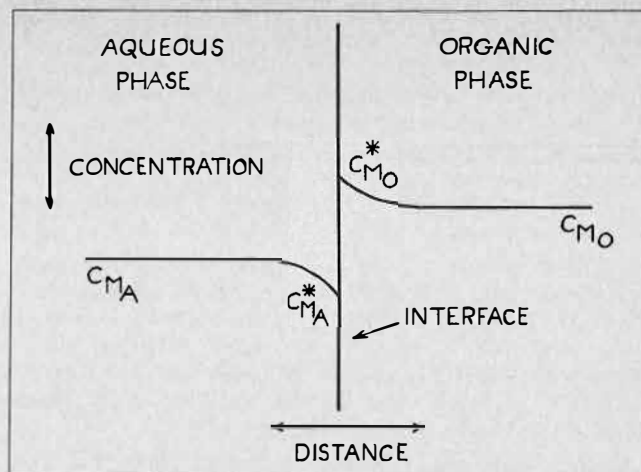


FIGURE 4.

such as temperature, concentrations of reagents, etc., important, but also physical variables such as interfacial area, turbulence in each phase, coalescence rates, mutual solubilities, etc. In addition, in an operating circuit the composition of each phase is continuously changing, i.e., the % of the reagent in the copper complex form, the concentration of acid in the aqueous phases, etc. It was decided that stability to hydrolytic attack would be determined with an aqueous phase approximating that found in the stripping section of a typical system. It was reasoned that these would be the conditions most likely to cause the most rapid change in the reagent.

The experiments were run by thermostating a round-bottom flask and agitating, under reproducible conditions, equal volumes of organic and aqueous phases. Samples were taken at various times (up to several years in some tests) and analyzed.

The analysis of the samples presented some problems. A number of changes in the system could and were followed. Among these changes were (1) the increase in ketone absorption by IR, (2) decrease in reagent concentration by GLC and (3) the decrease in capacity of copper ions to react with the organic. The last value was the one used in most of the tests, as it is the ability of the reagent to extract copper that is industrially important.

The experiments were conducted at 30°, 55° and 81°C. It was hoped that the rates of loss of copper extraction ability measured at the higher temperatures could be extrapolated to lower temperatures. This was desired because the ½ lives of some of the materials under test were longer than one year, even at the higher temperatures.

It was found, however, that extrapolation of data obtained at 81° and 55°C to 30° could not accurately predict ½ life at the lower temperature. This is undoubtedly due to the many factors which affect the rates of reaction in such a complex system.

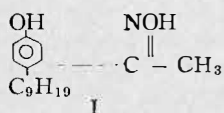
In a greatly accelerated test using an aqueous solution of 300 g/l of H₂SO₄, half lives of 10 days and 3 days were obtained for 2% LIX®63 in kerosene at 55°C and 81°C respectively. Extrapolation of this data to 30°C gives an estimated half life of 45 days, whereas the actually measured half life was 600 days. A very poor prediction. With LIX®65N, half lives of 560 days and 68 days were found at 55° and 81°C respectively.

Acid concentration of the aqueous phase is very important. When the concentration of H₂SO₄ was reduced from 300 to 150 g/l, the half life of LIX®63 was increased from 3 days to 35 days at 81°C and to 290 days at 55°C instead of 10 days.

From long experience with stability testing, it has been found that prediction of degradation rates is very difficult from one condition to another. However, when various reagents are compared under identical conditions, the differences found can be extrapolated to other conditions. For example, high-temperature data show that LIX®63 is less stable than LIX®65. This difference in stability has also been demonstrated in operating plants over the last 8 years.

In the discussion on the kinetics of copper transfer it was shown that D2EHPA was a better catalyst than LIX®63. The reason D2EHPA is not used as a catalyst is due to stability. Test work has shown that the combination with D2EHPA greatly decreases the half life of LIX®65N, probably due to the catalytic acid being present in the same phase as the LIX®65N.

So far, only the aliphatic oxime LIX®63 and the benzophenone type LIX®65 (or LIX®65N) have been discussed. Early in the development work reagents having an acetophenone-type structure, as contrasted with the benzophenone type, were examined. These compounds were discarded as having unsatisfactory properties in comparison with LIX®65. One of these properties is a very rapid rate of degradation in stability testing. It was found, for instance, that I



was degraded at a rate approximately 10 times that of LIX®65N and 2 or 3 times as fast as LIX®63 under the accelerated conditions. A possible explanation is that the oxime nitrogen is more easily protonated in I than in LIX®65 due to its greater basicity, but unlike LIX®63, which is even more basic, does not have the steric hindrance to reduce attack by water to complete the hydrolysis.

The last point to make on stability is that earlier the degradation of reagents was assumed to occur mainly in the stripping mixers. This is where the greatest interfacial area and the reagent are exposed to the highest acid concentrations. It could then with some justification be assumed that if in a given operation, the organic phase was present in the stripping mixers only 2% of the time, then the observed degradation rate would be one-fiftieth of that observed in the laboratory. This is a false extrapolation. Although it is very difficult to measure degradation rates in a plant, experience has shown the degradation rate in an operating system is of the same magnitude as measured in the laboratory, not one-fiftieth of the rate.

Conclusion

The criteria discussed above, along with those mentioned previously, have guided GMCI research for a number of years. Their application has produced LIX®65N, which is, at present, used world-wide to produce approximately one quarter of a million tons of copper annually. In addition, they have permitted development of new reagents of broader scope and application.

Without the organic chemist in the laboratory to synthesize the required reagents, this new pollution-free process for copper production would have been impossible.

DISCUSSION

K. Osso-Asare: Could you please comment on the effect of metal loading on the stability of LIX®63?

I. Itzkovitch: We have preliminary data which indicates that at 60°C, 150 g/l H₂SO₄, LIX®63 is more stable than when the same solution contains copper.

R. Swanson: We have not studied the system without copper being present, LIX®63 may decompose by a number of different routes other than simply by hydrolysis to the ketone. I would expect the hydrolysis reaction to be suppressed by the presence of copper, but other decomposition modes may be enhanced.

L. V. Gallacher: We have been doing considerable work with synergistic combinations of LIX®63 and dinonylnaphthalene sulfonic acid in selective extraction and have found that the stability of such combination in the presence of aqueous sulfuric acid is much greater than the reported stability of aromatic hydroxyoximes in similar mixtures. In view of the greater stability of the aromatic oximes alone in the presence of sulfuric acid, can you offer an explanation for this?

R. Swanson: No, I can not.

S. Andersson: Could you give information on the stability of LIX®63 and LIX®65N for copper extraction from solutions containing nitrates, in view of the interest for using nitric acid as an oxidant for leaching sulfidic copper ores?

R. Swanson: We have not examined this system and therefore couldn't give information on it. I do concur with Dr. van der Zeeuw's comment that both LIX®65 and SME-592 would be prone to nitration due to the activated ortho position and that the resultant complexes would be very difficult to strip. Our LIX®70 series of reagents does not have either ortho or para positions open for nitration and should give better results in this system.

Comment by A. J. van der Zeeuw on question by Andersson with respect to stability of hydroxyoximes in nitrate medium.

A. J. van der Zeeuw: Work done jointly by Shell and Brookside Metal Co. in Watford (UK) has shown that when pH drops below 1-1.5, the copper complexes of aromatic hydroxyoximes are nitrated in the ortho-position next to the OH. This holds for SME 529, and I am sure for LIX®65N too. The net effect is the generation of a complex that will not release its copper against an acceptable acid strength. This problem can be overcome by maintaining the pH above 1.5. Currently, Brookside are operating a proprietary process of extracting copper from a silver nitrate solution successfully with SME 529.

"Strong" Diluent Effects

R. Blumberg and J. E. Gai,
IMI — Institute for Research and Development
Haifa, Israel

ABSTRACT

An attempt has been made to indicate possibilities of influencing distributions in solvent extraction and liquid ion exchange systems by utilizing special diluent effects. Examples are presented of such effects in amine/acid, anion exchange, cation exchange and salt extraction systems, in the main relating to hydrogen bonding interactions.

Introduction

SOLVENT EXTRACTION is a complex concept and may mean different things to different persons; by definition however, the function of "mass transfer" must always be included. It has become customary in solvent extraction circles to regard the distribution coefficient, defined by the ratio of concentrations in each phase, as the measure of the overall equilibrium constant of the reversible transfer system. There are, of course, other constants which also express the overall transfer of material from one phase to another, e.g. the formation constant of the extracted species, or some overall dissociation constant. Fundamentally, therefore, it is of interest to attempt to influence these constants, since practically this will reflect on the "mass transfer" attained.

In a solvent extraction system the extractant may consist of a well defined single substance, or it may consist of a mixture of substances. Two decades ago it was the accepted practice to describe a mixed solvent phase as comprised of an "active" extractant or reagent and an "inert" diluent, assumed to be added for physical reasons, for example to change viscosity. Subsequently it was observed that the addition of a relatively small amount of a second "reagent" could influence the extraction quite out of proportion to the quantity added; this phenomenon was designated as "synergism", the explanation being that the composition of the extracted species was changed by incorporating the second reagent and this had a higher distribution coefficient; however only very limited advantage of synergistic effects has apparently been taken in practice.

In recent years it has been generally accepted that no "diluent" for any extractant is ever "inert" and increasing emphasis is being placed on diluent effects, particularly the effect of diluent polarity and polarizability. However, there seems to be relatively little work reported on diluents which provide specific interactions, namely hydrogen bonding to some component of the system, and even less on the application of such effects under that name.

The use of modifiers, especially alcohols, to prevent third phase formation in practical extraction systems is well known, but the nature of the interactions with the alcohol has not been fully evaluated, nor discussed as a diluent effect; very little, if any, attention has been paid to other modifiers even for the same purpose of "third phase suppression". More recently there is interest in the effect of additives on the state of the liquid-liquid interface and the effect of this on the kinetics of mass transfer.

However, the distribution coefficient as a function of diluent and modifier has hardly received attention.

The theme of the present paper has been described as "strong diluent effects", the term being fairly loosely interpreted. Our approach has been essentially practical, relying on basic concepts and on analogy, for attaining the aim.

Systems Considered

A. The first cases studied by the authors and their colleagues relate to the effect of protogenic diluents on tertiary amines as extractants. This work has been fairly extensive and has covered a variety of aspects, fundamental and practical. This is also the field within diluent-extractant interactions which has received most extensive attention, judging by the scientific literature, hence explanations of interactions are forthcoming. Perhaps the most striking fact is that notwithstanding all the basic studies, few real applications are described. This system will receive most attention in the present paper, an extension being made also to anion exchange systems using strong quaternary ammonium bases.

B. The second cases studied may be regarded as the reverse of the first, if acid/amine systems can be defined as "anion exchange" or anion extraction systems. Our interest in the effect of modifiers in cation/extractant systems has been derived mainly from the practical interest in bridging the extraction/stripping optimization gap in metal ion recovery systems. Compared to the work on amines, this study of diluent effects in cation exchange is cursory and preliminary in nature. It does, however, seem to be novel and significant. The authors are not aware of similar studies; even as recently as 1975 at a symposium on "Diluents in Solvent Extraction of Metals"⁽¹⁾, no attention was paid to non-hydrocarbons, and the effects sought were mainly physical.

C. The third practical case of interest presented, relates to the separation of metal values from sulphate ambients by amine extractants. The postulate which led to this study was that amine extractants as a class, because of the amine/anion/diluent interaction, should give wider possibilities for application than do specific or selective reagents. This can be regarded, therefore, as an extension of the study of interaction also to complexed metal cations.

D. Lastly, there are indications that salt extraction from brines can be markedly influenced by the extracting ambient. This is a field of solvent extraction which has received very little attention in general, notwithstanding the fact that selective separations from brines are fully feasible. Indicative results are presented here, mainly to stimulate interest in this field.

Amine/Acid Systems

Introduction

The influence of diluents on the extraction of acids by high molecular weight amines has been extensively examined, but the full range of possibilities has not yet been

exploited. A few general reviews of such extractions have appeared^(2,3,4,5), and attempts at correlating diluent effects have been made in terms of regular solution theory⁽⁶⁾, in the form of linear free energy correlations⁽⁷⁾, and in terms of empirical parameters of solvent polarity⁽⁸⁾.

Referring to tertiary amines, which seem to have been the most widely studied, acid extraction of the type



will be enhanced by any mechanism which reduces the free energy of the amine salt relative to that of the free amine, or, in other words, which provides more solvation to the amine salt. In order to effect comparisons, it is convenient to use K_{app} , the apparent formation constant, as defined by

$$K_{\text{app}} = \frac{(\overline{\text{AmHX}})}{(\overline{\text{Am}})a_{\text{H}^+} a_{\text{X}^-}} \dots \dots \dots (2)$$

For the cheaper and more common commercial hydrocarbon diluent, the range of K_{app} values available is about two orders of magnitude. For example, $\log K_{\text{app}}$ for trilaurylamine hydrochloride (TLA·HCl) is 3.1 in cyclohexane and 4.7 in benzene⁽⁹⁾. The former diluent represents the most inert type, supplying solvation by only relatively weak dispersion forces, while the aromatics are capable of much stronger polarization interaction with the highly polar amine salt.

Since the salts exist in these solutions as ion pairs, albeit highly aggregated and hydrated, a first type of strong diluent effect is achieved through dipole-dipole and ion-dipole interactions by using dipolar aprotic diluents having higher dielectric constants. Thus, with nitrobenzene the apparent formation constant of TLA·HCl is increased by two orders of magnitude, $\log K_{\text{app}}$ being 6.8⁽⁹⁾. This effect is general, although it is interesting to note the suggestion by Hyne⁽¹⁰⁾ that a specific form of added stabilization is possible by special geometric matching of dipoles (salt and diluent molecules) in an anti-parallel arrangement. This possibility is worthy of further investigation.

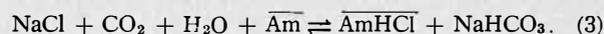
The other type of strong diluent effects is achieved by specific solvation. Specific solvation of the cation *only* is difficult to engineer in this case because of the shielding of the proton on the nitrogen atom due to steric hindrance. Although conjugation of the type $\overline{\text{AmH}^+ \text{B}}$ is known⁽¹¹⁾, B would have to be so basic as to itself be an extractant for the acid. With secondary and, particularly, primary amines this restriction disappears; it has been found that basic diluents such as anisole and tributyl phosphate (TBP) are quite effective in increasing the base strength of a primary amine⁽¹²⁾.

The best examples of specific solvation of anions are through hydrogen bonding to the anions; the smaller and/or more highly charged is the anion, the stronger is the interaction with the hydrogen bond donor. Thus, with chloroform as diluent⁽⁹⁾, $\log K_{\text{app}}$ for TLA·HCl rises to 6.9. Such solvation is accompanied by a marked decrease of water bound to the anion; this displacement of the water as a solvating agent for the anion has been discussed⁽¹³⁾.

Effect of Amphiprotic Diluents on Acid Extraction by Tertiary Amines

Amphiprotic diluents are capable of solvating both anions and cations, although specific solvation to the latter is probably only possible in solvent-separated ion pairs. Of these diluents, alcohols are the best known but have mostly been studied as additives to other, less effective, diluents. They were initially used as additives for prevent-

ing the formation of a third liquid phase, probably without understanding the mechanism involved. Their effect, however, is quite powerful, even with relatively small additions to a diluent which is otherwise inert. Thus, according to the correlations of Shmidt and Mezhev⁽⁷⁾, 0.1 mole fraction (10%) octanol in octane is enough to raise K_{app} by about 2 orders of magnitude. (For comparison, it may be noted that a mole fraction of 0.7 nitrobenzene added to octane was required to appreciably start influencing the extraction of H_2SO_4 by N-decylaniline⁽¹⁴⁾). Other more protogenic additives have been tested and have been found to have an even more marked influence; examples of these include oleic acid⁽¹⁴⁾ and dodecyl phenol⁽¹⁵⁾. In view of these striking effects of amphiprotic substances as additives, it is surprising that they have been so little studied as diluents in their own rights. Indeed, it transpires that alcohols can be very effective. In one very practical case⁽¹⁶⁾ it was desired to extract HCl at the level of acidity supplied by CO_2 according to the reaction



It was also desirable to stay at the level of basicity available from a tertiary amine but to "push" the base strength to the maximum. After studying many diluents, the one finally chosen was i-amyl alcohol which was found to permit significantly more extraction of HCl than did nitrobenzene or even a nitrobenzene-decanol mixture (see below). The amine used was Alamine 336* and $\log K_{\text{app}}$, as determined approximately by the method of half-titration $\text{pH}^{(12)}$, was⁽¹⁷⁾ 8.9.

A more detailed study has been made⁽¹⁸⁾ on decanol and nitrobenzene-decanol mixtures as diluents. Decanol alone is nearly as effective as nitrobenzene alone (Table 1) in enhancing the base strength of trioctylamine (TOA) and it was considered interesting to test whether mixtures of the two showed any non-additive (synergistic) effects. As can be seen from the table, there is such a non-additive effect which reaches its maximum at a diluent composition of about 80% nitrobenzene and 20% decanol, providing up to half an order of magnitude increase in K_{app} compared to that of nitrobenzene alone at the lower TOA concentrations.

It is worth also briefly mentioning a few of the main conclusions arrived at concerning some of these results. Decanol, when added to the nitrobenzene in small quantities, interacts strongly with the chloride ion. With increasing decanol concentration, there occurs increasing outer-sphere coordination to the ion. As the condition of pure decanol (as diluent) is approached, the specific solvation is not diminished, but the solvent becomes more structured and the presence of the amine salt only enhances this structuredness. Thus, it is mainly the entropy term which leads to an increase in the free energy (decrease in K_{app}) and not the want of solvation forces.

Anion Exchange by Tertiary Amines

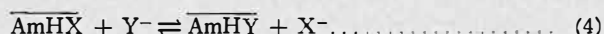
The effect of protogenic diluents on the solvation of anions can also be exploited to change the "normal" order of selectivity of liquid ion exchangers. The specific solvation supplied by such a diluent provides the possibility of increasing the selectivity to small anions, having high charge density instead of larger ones which might otherwise usually be preferred. If the exchanger is a tertiary amine the effect is enhanced because the cation itself forms very strong hydrogen bonds to suitable anions. Two examples will be used to demonstrate this.

*A C₈-C₁₂ tertiary amine, manufactured by General Mills Inc.

TABLE 1. Log K_{app} Values for the Formation of TOA.HCl in Nitrobenzene-Decanol Mixtures

Original TOA concn	1.0M	0.32M	0.10M	0.032M	0.01M
	% decanol in diluent				
0	6.60	6.66	6.71	6.75	6.64
20	6.47	7.02	7.23	7.26	7.28
40	6.44	7.03	7.16	7.21	7.16
60	6.35	6.82	6.97	7.05	6.96
80	6.26	6.60	6.76	6.74	6.71
100	6.05	6.24	6.38	6.42	6.48

Numerous studies have been made of the neutralization⁽¹⁾ in aprotic diluents. Choosing three acids of the many studied, it is known that the apparent formation constants of tertiary amine salts increases in the order Cl⁻ < NO₃⁻ < ClO₄⁻. This naturally leads to the expectation that in an anion exchange system, of the type



the exchanger will be selective to these ions in the same order. In at least one case⁽¹⁹⁾ the selectivity for nitrate over chloride was directly demonstrated in a system containing both ions. The first case presented here (Table 2) is a modest example of the effect of protogenic additives to a commercial aromatic hydrocarbon diluent (Paz Taro), on the exchange between chloride and perchlorate. In all three cases the initial solvent was a 0.55 N solution of the hydrochloride of Alamine 336 (prepared by extraction of HCl from aqueous solution), and it was contacted with a saturated solution of KClO₄ in the presence of excess solid KClO₄. Taking into account that on a molar basis the dodecyl phenol addition is only one fifth of the pentanol addition, the results of Table 2 not only clearly show the influence of the protogenic additives on this exchange, but also that the phenol has a much stronger effect than the alcohol.

The second example (Table 3) deals with Cl⁻-NO₃⁻ exchange, again using Alamine 336. The tests were of the "limiting conditions" type, i.e. a small solvent/aqueous ratio was taken so that the composition of the aqueous phase did not essentially change. The first two sets of results indicate the difference between an aprotic and a protic diluent. The former brings out the "normal" selectivity of nitrate over chloride, in which respect the higher chloride concentration in the aqueous phase should be noted. The alcohol completely changes the selectivity. Section B shows the expected effect of changes in proton donating capability with different alcohols, but it must be recognized that part of the effect is due to increasing water solubility in the lower alcohols. In this respect, it may be mentioned that investigators^(5,19,20) in the field of anion exchange by amine solvents have emphasized the correlation between increasing order of selectivity and decreasing free energy of dehydration of the ion involved. This implies that it is the interactions in the aqueous phase which are the important ones in determining the selectivity. This will be correct as long as the solvent has equally good (or, maybe, equally bad?) solvating capacity for the ions, but the position changes when there is a differentiating solvation mechanisms. In addition, the more the solvent becomes "water-like" in character, the easier it is to reverse the forementioned correlation.

Ion Exchange by a Quaternary Ammonium Salt

One other example of anion exchange will be cited, in connection with quaternary ammonium salts. These are

TABLE 2. Effect of Protopenic Additives on ClO₄⁻/Cl⁻ Exchange

Solvent : 25% Alamine 336 in Paz Taro (aromatic hydrocarbon), or in Paz Taro plus additive.
 Aqueous : Saturated KClO₄ solution plus excess solid KClO₄
 Org/Aq = 5/1

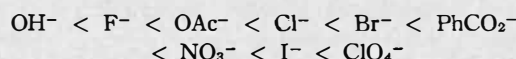
Diluent	Analyses of Equilibrium Phases, eq/l.		
	Aqueous	Organic	
	Cl ⁻	Cl ⁻	ClO ₄ ⁻
75% Paz Taro	1.68	0.20	0.34
60% Paz Taro + 15% i-AmOH	1.38	0.28	0.27
66% Paz Taro + 9% dodecyl phenol	1.32	0.30	0.26

TABLE 3. Diluent Effect on NO₃⁻/Cl⁻ Exchange

Aqueous Phase : 20.5% KCl + 6.4% KNO₃
 Solvent : A. Alamine 336 hydrochloride, prepared from a solution initially containing 50% amine.
 B. 50% Alamine 336 hydrochloride
 Org/Aq = 1/10

Diluent	Analyses of Organic Phases, eq/kg.		
	Cl ⁻	NO ₃ ⁻	Cl ⁻ /NO ₃ ⁻ ratio
A.			
Aromatic hydrocarbon	0.42	0.80	0.5
i-amyl alcohol	0.82	0.43	1.9
B.			
n-butanol	0.76	0.28	2.7
i-amyl alcohol	0.75	0.31	2.4
n-octanol	0.68	0.37	1.8

similar to tertiary amines in most cases in that the cations are not subject to specific solvation. They are different in that no hydrogen bonding is possible between the cation and anion. Another difference, relevant to the present example, is that quaternary ammonium hydroxides are well known, whereas hydroxides are generally unknown for tertiary amines*. In one ion exchange study⁽²⁰⁾, using tetraoctylamine compounds in toluene or dichloromethane, the order of increasing selectivity of the exchanger was



The hydroxide ion is small, has a high charge density on the oxygen atom, and in aqueous solution has a very strong specific interaction with water.

As a result, the equilibrium position for the reaction



lies very strongly to the left. Nevertheless, if the diluent is strongly protogenic, the equilibrium position can be significantly changed in the opposite direction. Thus, even

*However, it is interesting to note that this is not an impossibility. Conductometric and spectroscopic measurements⁽¹³⁾ on TOA solutions in nitrobenzene and in nitrobenzene-decanol mixtures, saturated with water, indicated that the following reaction occurs to a significant extent:

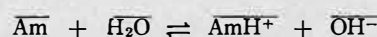


TABLE 4. Diluent-Reagent Interaction in Extraction of Cu(II) from Sulphate Systems, by LIX 64N 20% vol/vol, in diluent.

Single stage equi-volume extractions at 40°C
Feed: 5 g/l Cu, H⁺ 0.16 g/l (as free H₂SO₄)

Diluent	% Extraction
Xylene	41.0
Hexanol	nil 16%*
Di-isobutyl ketone	nil 22.6%*

*After pH adjustment of aqueous phase to 2.4, with NaOH.

TABLE 5. LIX 64N/Kerosene /Hexanol Systems for Cu(II) Extraction

Single stage equi-volume extraction at 40°C
LIX 64N 20% vol / vol in solvent
1st feed 1.17 g/l Cu, 2.1 g/l free H₂SO₄

Solvent Kerosene/hexanol volume ratio		Cu in Aq. phase g/l	% Extraction
100	0	0.19	83.8
95	5	0.32	72.6
80	20	0.89	24.0
50	50	1.02	12.8
0	100	0.98	16.2

2nd feed 1.24 g/l Cu, 0 free H₂SO₄

Solvent Kerosene/hexanol volume ratio		Cu in Aq. phase g/l	% Extraction
100	0	traces	100
95	5	0.16	87.1
80	20	0.51	58.9
50	50	0.54	56.5
0	100	0.67	46.0

TABLE 6. Stripping of Loaded Cu(II)/LIX 64N — 20% vol/vol in Kerosene, With and Without Dilution or Modification

Initial loaded LIX 64N — Cu 6.7 g/l.

	Loaded LIX ml	Additive ml	No. Stages	H ₂ SO ₄		% Stripping
				50 g/l	100 g/l	
1	40	—	1	10	30.7	50.4
				10	19.7	
2	40	—	1	10	31.0	56.4
				10	25.4	
3	20	20 K	1	10	24.2	47.1
				10	22.9	
4	20	20 K	1	10	84.4	96.0
				10	11.6	
5	30	10H	1	10	86.8	100
				10	13.2	
6	30	10 H	1	10	95.8	
7	20	20 H	1	10	100	

K = kerosene H = hexanol.

TABLE 7. Comparison of the Influence of Different Additives on Stripping of Cu(II) from Loaded LIX 64N

Additive	Dielectric constant	Donor Number	Aqueous strip	
			g/l Cu	g/l H ₂ SO ₄
Reference (No additive)			9.5	87
n-butanol	17		18.4	37
n-hexanol	13.3		15.9	56
MIBK*			11.5	77
i Pr ₂ O*	3.9	~19	10.6	79
Chloroform	4.8		10	85
Amylacetate	~ 5	~17	10	86

* MIBK = Methyl isobutyl ketone
i Pr₂O = isopropyl ether.

with a fairly strongly protic diluent such as i-amyl alcohol, after contacting a 31% Aliquat 336* solution (in chloride form) with a 5% NaOH aqueous solution, such that there was a five-fold excess of OH⁻ over Cl⁻, only 49% of the chloride was exchanged out of the solvent. However, with the solvent containing 46% dodecyl phenol and 23% i-amyl alcohol (instead of 69% alcohol only), all of the chloride was exchanged out. In fact, even with a Ca(OH)₂ slurry, with its much lower OH⁻ concentration, one contacting is enough to exchange 93% of the chloride initially present in the solvent. These effects are obviously due to the strong protonating power of the phenol.

Cation Exchange Systems

In the early 1960's high hopes were expressed in the scientific literature as regards the potential for solvent extraction technology in metal recovery, using cation exchange systems. Indeed, in the field of copper recovery from acidic leach liquors there has been a major breakthrough by the development and application of essentially specific reagents which can be applied in fully acidic systems. The natural drawback of such reagents has been the difficulty of bridging the optimization gap between "extraction" and "stripping", since reagents with favourable complex formation constants in acidic extraction media, require increasingly acidic media in the stripping cycle. Since work on polar modifiers in amine/diluent systems has indicated the possibility of formulating some acid/base reference scale as a function of composition of the solvent ambient, it was thought to do the same for cation exchange systems.

Tables 4, 5, 6, 7 all relate to hydroxyoxime/copper extraction systems. Various LIX reagents of General Mills Inc. were used in this work. In Table 4 the effect of making up the reagent in various diluents can be seen, while in Table 5 we see the result of progressively replacing hydrocarbon by an alcohol. Table 6 relates to stripping of copper from LIX 64N loaded extract by adding hexanol as modifier; in order to be sure that the effect was not due simply to dilution, comparative tests with kerosene addition are included. In Table 7 comparative data for various modifiers are given. Table 8 shows data using dinonyl naphthalene sulphonic acid (DNNSA) as the cation exchange reagent for extracting three different cations, Ni, Fe and Ca, from chloride solutions. In these tests n-butanol was the modifier selected.

Strong interactions of modifiers in the hydroxy oximes and also in the DNNSA express themselves in the fact that

*A C₈-C₁₂ quaternary ammonium salt, manufactured by General Mills Inc.

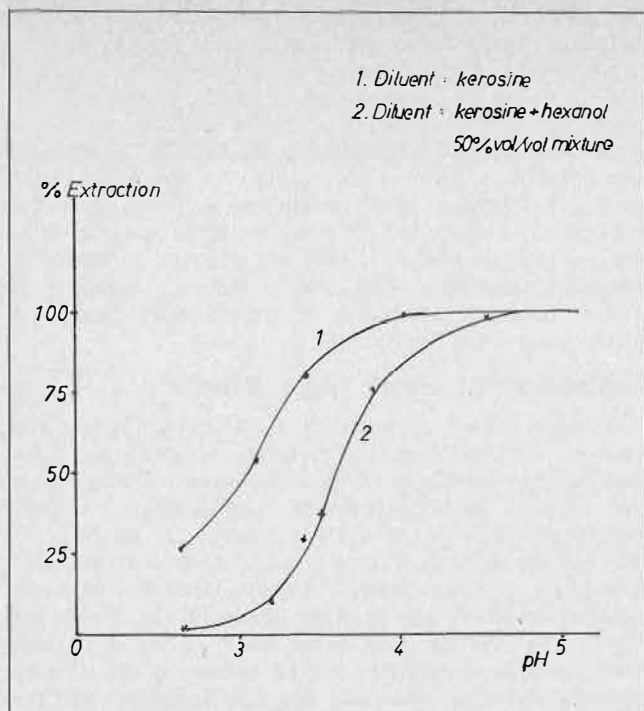


FIGURE 1 — Cu(II) Extraction by α bromo lauric acid.

the systems become more basic. These interactions seem to be quite general, for the effect, with a medium weak reagent such as α bromolauric acid, can be clearly seen in Figure 1. In general, if the overall "apparent" equilibrium constant, for example Cu^{++} extraction, is written as

$$K = \frac{(\overline{\text{CuR}}) (\text{H}^+)^2}{\text{Cu}^{++} (\overline{\text{HR}})^2} \quad (6)$$

it appears that solvation of H^+ in the system increases (HR) thus decreasing extraction. The overall effect of the modifier interaction, therefore, is in favour of stripping. This can, therefore, lead to bridging the extraction/stripping optimization gap. Thus a loaded extract of LIX 70 in kerosene 20% v/v, containing 5 g/l Cu(II) diluted with hexanol, can be stripped fully in one contact with 100 g/l sulphuric acid in contrast to the 350 g/l necessary to strip Cu(II) from LIX 70 without a modifier. A flow-sheet can be conceived, therefore, based on addition of an alcohol such as hexanol to loaded LIX 70 extract going into stripping, with subsequent separation of the alcohol again from the recycle solvent before extraction. This can make LIX 70 easier to strip at lower acidity and with fewer stages than currently used even with LIX 64N, while maintaining all the known extraction advantages of the former. Naturally an economic evaluation would have to be made in order to optimise such an approach.

A very preliminary IR study of Cu/LIX 64N/hydrocarbon systems with and without alcohol addition has been made. Some OH bands exhibited by LIX disappear when Cu(II) is added, but reappear on adding hexanol to the complex; hexanol itself does not display these bands.

Extraction of Metal Complexes in Amine Systems

A review of metal extraction processes described in the literature has led us to the postulate that "amine extractions should give wide possibilities for application, since extraction is possible from highly acidic solutions as

TABLE 8. Influence of n-Butanol on the Extraction of Ni, Fe or Ca from Neutral Chloride Solutions, using DNNSA.

Solvent A : DNNSA 0.3 eq/l in kerosene
7.2% water in solvent phase.

Solvent B : DNNSA 0.3 eq/l in kerosene plus 20% vol/vol n-butanol
5.6% water in solvent phase.

Equilibrium Systems equi-volume initial phases.

Solvent	Aqueous		Organic		D org/eq	Extraction %	
	Metal g/l	H ⁺	Metal g/l	H ₂ O %			
Ni	A	3.6	0.16	4.9	5.6	1.36	57.6
	B	3.8	0.13	4.7	5.8	1.74	55.4
	A	6.0	1.0	2.6	5.5	0.43	30.2
	B	6.6	1.0	2.0	4.8	0.30	23.2
Fe	A	2.2	0.18	4.0	4.9	1.82	64.5
	B	1.9	0.17	4.3	4.8	2.26	69.5
	A	4.1	1.07	2.0	5.1	0.49	32.8
	B	4.3	0.99	1.8	4.6	0.42	29.6
Ca	A	0.77	0.17	3.0	5.0	3.94	79.8
	B	1.3	0.11	2.5	5.7	1.92	65.8
	A	2.6	1.08	1.4	5.2	0.54	35.0
	B	3.3	1.07	0.7	4.4	0.18	17.5

TABLE 9. Cation/Amine/Diluent Interaction

	Aqueous Phase Compositions					
	Paz T		Xylene		n-Pentanol	
	Metal g/l	SO ₄ g/l	Metal g/l	SO ₄ g/l	Metal g/l	SO ₄ g/l
Feed (Fe)	5.8	29.4	5.8	29.4	5.8	29.4
n-Octylamine	2.1 ^(a)	12.6	1.8 ^(a)	12.1	4.6	13.4
Amberlite LA-1	2.4	8.5	2.4	7.7	6.2	14.4
Alamine 313	3.6	13.2	4.5	12.6	0.8 ^(b)	0.4
Feed (Al)	2.8	29.4	2.8	29.4	2.8	29.4
n-Octylamine	2.4 ^(a)	20.2	2.6 ^(a)	19.8	3.0	18.2
Amberlite LA-1	2.9	17.4	2.9	17.5	3.0	16.9
Alamine 313	2.9	19.7	2.9	17.6	2.9	20.2
Feed (Mn)	5.5	20.0	5.5	20.0	5.5	20.0
n-Octylamine	5.4 ^(a)	15.3	5.5 ^(a)	14.4	5.8	11.4
Amberlite LA-1	5.6	11.2	5.5	10.8	5.7	10.6
Alamine	5.6	12.9	5.5	12.0	5.7	12.7
Feed (Mn dil.)	0.32	1.1	0.32	1.1	0.32	1.1
n-Octylamine	0.32 ^(a)	1.1	0.32	0.8	0.32	1.0
Amberlite LA-1	0.33	0.82	0.32	0.7	0.32	0.6
Alamine	0.33	0.98	0.34	0.7	0.32	0.8

^(a) Solid organic phase at the interface

^(b) Precipitate at the bottom (inorganic)

Amberlite LA-1 = secondary branched chain, Rohm & Haas
Alamine 313 = tertiary branched chain, General Mills, Inc.

well as from slightly acidic solutions at higher salt concentration". As an initial step in studying this approach the limited target of extraction of the metal cations from aqueous sulphate solutions was examined. For this work a standard test was used to investigate three amines, primary, secondary and tertiary, and three diluents differing in polarity.

Sulphate solutions of Fe(III) Al(III) Mn(II) in diluted sulphuric acid were used, each at a concentration of 0.1 g ion/l. The sulphuric acid concentrations were taken in order to obtain the following ion ratios:

- a) For divalent metal –
Mn(II) – Me : H⁺ : SO₄ = 1 : 2 : 2
- b) For trivalent metal –
Al(III), Fe(III) – Me : H⁺ : SO₄ = 1 : 3 : 3

The amines were used as 0.5 m.mole/g solution in each of the diluents, quantities being taken so as to obtain 1 g.mole amine per 1 g.ion SO_4^{2-} .

Summarizing results are presented in Table 9. Extremes of behaviour were observed — thus the primary amine/non-polar diluent combination was very effective in extracting Fe(III) while the tertiary amine in polar diluent extracts only acid, to the point of causing a basic iron sulphate to precipitate. As was to be expected the branched-chain amine showed complexes of higher solubility than the straight-chain amine of equal total number of C-atoms.

Table 10 shows the basis, for the case of Al, of one of the more important correlations deduced, namely that extraction will be negligible below aqueous phase pH's corresponding to that required for precipitation of the metal (as oxide, hydroxide or basic sulphate, as the case may be)

Fe(III) 2.0-3.0 pH
Al(III) 4.5-6.0 pH
Mn(II) 8.0-10.0 pH

This condition imposes certain constraints on amine basicity and on amine/acid ratios in each case. Thus the secondary and tertiary amines, irrespective of the diluent

TABLE 10. Two Cross-Current Stage Extraction of Al(III)

	Initial aqueous		Equilibrium aqueous		
	Al g/l	SO_4	pH	Al g/l	SO_4
Primene JMT/Paz T	2.8 2.3	29.4 14.7	3.4 6.1	2.3 <0.005	14.7 2.6
Alamine 336/Paz T	2.8 2.9	29.4 17.8	1.9 2.9	2.9 2.9	17.8 16.8

Primene JMT = primary branched chain amine — Rohm & Haas
Alamine 336 = tertiary straight chain amine — General Mills, Inc.
Paz T = aliphatic hydrocarbon.

used, cannot reach the precipitation range of Mn(II), while the tertiary amines in a non-polar aliphatic hydrocarbon diluent (such as Paz T) cannot reach the range for Al(III) precipitation, hence also cannot extract Al(III). Furthermore, the amine must be in suitable salt form at the required pH, i.e. by using the suitable amine/acid ratio. Finally, the formation constant of the amine salt/metal salt complex must be high enough to cause the hydroxides to dissolve at the higher pH's, and the solubility of the complex in the diluent must be sufficient to prevent precipitation. The overall picture, therefore, is a very intricate interaction of diluent/amine/acid and salt, to achieve the desired aim.

Extraction of Salts from Brines

Within a broad program of work on separation and recovery of salts from halide brines, a study has been made of the distribution of salts and water between brines and various extractant/diluent combinations, namely amine hydrochloride — alcohol systems. A selection of data are presented in Tables 11 and 12. Two brines have been taken as representative, namely, Dead Sea Brine as such, which feeds the primary ponds of the Dead Sea Works Ltd. and the End Brine which leaves the ponds after carnallite precipitation⁽²¹⁾. Of interest is the transfer of water and salts, (primarily Mg (Ca) chlorides) and the way in which the diluent/modifier combinations change the ratio of the two. Extraction of hydrated salts has been reported to only a very limited extent in the scientific literature, and has hardly been used as a means of processing brines. However, extraction of salts can be an extremely efficient way of obtaining separations. In another paper⁽²²⁾ reference is made to such a process using a single solvent component. Now we see that interactions of mixed solvents are significant and should therefore be worth examining further. One interesting aspect is the almost constant ratio of salt to water extracted by a particular amine hydrochloride from the more dilute brine; another is the strongly dehydrating effect of the concentrated brine resulting in greater variability. No attempt has, however, been made thus far to quantify the interactions or to define the differences in the extracted species in the various cases.

TABLE 11. Salt Extraction by Primary Amine Hydrochlorides plus Alcohols

Dead Sea Brine containing 213 g/l $\text{MgCl}_2 + \text{CaCl}_2$ i.e. 2 m.mole/g unit water s.g. 1.22									
AmHCl	Diluent	Wt ratio Am/Dil.	Temp. °C	Equilibrium Organic phase					
				H_2O %	Ca + Mg m.mole/g.	$\text{MgCl}_2/\text{H}_2\text{O}$ wt-ratio	$\text{H}_2\text{O}/\text{Solv.}$ wt-ratio.	D org/aq. Ca+Mg*	
2EHA	t-butanol	1/0.14	RT	44.9	0.64	0.14	1.18	0.72	
"	"	1/0.46	"	37.1	0.46	0.12	0.78	0.62	
"	"	1/0.65	"	32.9	0.37	0.11	0.63	0.57	
t-octylamine	t-pentanol	1/0.85	RT	28.9	0.28	0.09	0.49	0.49	
"	"	1/2.5	"	17.7	0.12	0.06	0.22	0.34	
"	"	1/0.85	40°C	27.5	0.25	0.09	0.45	0.46	
"	"	1/2.5	"	16.5	0.09	0.05	0.22	0.27	
t-octylamine	n pentanol	1/0.85	RT	20.7	0.16	0.07	0.30	0.39	
"	"	1/2.5	"	12.0	0.06	0.05	0.15	0.25	
n-dodecyl amine	t-pentanol	1/2.0	RT	20.9	0.18	0.08	0.30	0.43	
2EHA	t-pentanol	1/0.14	RT	44.9	0.64	0.14	1.18	0.72	
"	nonyl phenol	"	"	40.1	0.54	0.13	0.93	0.68	
"	2-ethyl hexanol	"	"	39.2	0.51	0.12	0.89	0.66	
"	di-iso butyl carbinol	"	"	38.9	0.49	0.12	0.88	0.63	
"	2, 6, 8, -tri-methyl 4-nonanol	"	"	35.7	0.49	0.13	0.76	0.69	

2EHA = 2-ethyl hexyl amine D = distribution coefficient
*Concentration per unit of water.

TABLE 12. Salt Extraction by Primary Amine Hydrochlorides plus Alcohols

from End Brine containing 470 g/l MgCl ₂ + CaCl ₂ i.e. 4.9 m.mole/g unit water s.g. 1.35								
AmHCl	Diluent	Wt/ratio Am/dil	Temp. °C	Equilibrium Organic phase				
				H ₂ O %	Ca + Mg m.mole/g	MgCl ₂ /H ₂ O wt-ratio	H ₂ O/Solv. wt-ratio	D org/aq Ca + Mg*
2EHA	t-pentanol	1/0.14	RT	30.5	1.26	0.39	0.66	0.84
		1/0.46	"	24.0	0.94	0.37	0.43	0.80
		1/0.85	"	19.7	0.70	6.34	0.31	0.73
		1/0.65	40°C	21.4	0.80	0.36	0.36	0.76
t-octylamine	t-pentanol	1/0.85	40°C	21.2	0.15	0.07	0.31	0.14
		1/2.5	"	12.7	0.40	0.30	0.16	0.64
t-octylamine	n-pentanol	1/2.5	RT	13.7	0.63	0.44	0.18	0.94
n-dodecylamine	t-pentanol	1/2.0	RT	14.1	0.28	0.19	0.18	0.41

*Concentration per unit of water

Concluding Thoughts

The reader of this paper will immediately observe that much material relating to amine systems has been published and that the type of interactions between "diluent" / "modifier" / extractant and extracted species, is reasonably well postulated, if not always proven. Equally it is clear that this knowledge has not in general been utilized as a springboard for extending the study to other systems. This is indeed what the authors of this paper have tried to do, mainly by empirical tests, but using well-selected generalized examples. It is clear that much effort and thought would have to be expended to bring cation exchange to the same level of understanding as presently obtains in amine systems; even more so is the case in regard to extraction of salts. Nevertheless, with such striking effects as are displayed even by our limited work, one cannot but anticipate spectacular results from such studies.

Acknowledgement

The authors acknowledge the active participation of K. Hajdu and J. Moscovici in all the work connected with cation exchange and metal ion extraction, and of S. Newman in the work on extraction of hydrated salts and water from brines. Infrared interpretations were made by M. Ravey.

This paper is presented with the permission of the Managing Director of IMI.

References

1. Chem. and Ind., 6 March 1976, 170.
2. Marcus, Y. and Kertes, A. S., "Ion Exchange and Solvent Extraction of Metal Complexes", Wiley-Interscience, London, 1969, Chap. 10.
3. Schmidt, V. S., "Amine Extraction" (English translation), Israel Program for Scientific Translations, Jerusalem, 1971.
4. Schmidt, V. S., Shesterikov, V. N. and Mezkov, E. A., Russ. Chem. Revs. 1967, 36, 946.
5. Frolov, Yu.G., Ochkin, A. V. and Sergievsky, D. I., Atomic Energy Rev. 1969, 7, 138.
6. Kertes, A. S., J. Inorg. Nucl. Chem. 1964, 26, 1764; 1965, 27, 209.
7. Schmidt, V. S. and Mezhov, E. A., Soviet Radiochem. 1970, 12, 34.
8. Frolov, Yu G., Sergievskii, V. V. and Ryabov, V. P., Soviet Radiochem. 1971, 13, 650.
9. Muller, W. and Diamond, R. M., J. Phys. Chem. 1966, 70, 3469.
10. Hyne, J. B., J. Am. Chem. Soc. 1963, 85, 304.
11. Ralph, E. K. and Gilkerson, W. R., J. Am. Chem. Soc. 1964, 86, 4783.
12. Grinstead, R. R. and Davis, J. C., US Dep. of Interior, OSW, R and D Progress Report 320 (1968).
13. Diamond, R. M., in "Solvent Extraction Chemistry", Eds. D. Dyrssen, J.-O. Liljenzin and J. Rydberg, North Holland Publishing Co., 1967, p. 349.
14. Zvyagintsev, O. E., Frolov, Yu. G., Sergievskii V. V. and Huang Chung, Russ. J. Inorg. Chem. 1966, 11, 358.
15. Kreevoy, M. M. and Ditsch, L. T., (a) 139th ACS Meeting, St. Louis, 8M (March 1961), (b) Private communication, (c) US. Pat. 3,186,809, June 1, 1965.
16. Blumberg, R., Gai, J. E. and Hajdu, K., Proceedings ISEC 1974, 2789.
17. IMI internal reports.
18. Gai, J. E., D.Sc. Thesis, Technion, Haifa, 1971.
19. Kohara, H. and Saito, N., Bunseki Kagaku 1967, 16, 795; C. A. 1968, 68, 72854.
20. Ivanov, I. M., Gindin, L. M. and Chichagova, G. N., Izv. Sib. Otd. Nauk SSSR, Ser. Khim. Nauk 1967, 100; C. A. 1968, 69, 13377.
21. Epstein, J. A., Hydrometallurgy 1976, 2, 1.
22. Gai, J. E., "Modelling of the IMI MgBr₂ - MgCl₂ Process", Proceedings ISEC 1977.

DISCUSSION

D. H. Liem: I would like to comment that several years ago Prof. Dyrssen and I had studied the diluent effects on the extraction of Eu and Am by HDBP (cf Acta Chem Scand 1960). The results of our studies strongly indicate the interaction between the diluent and the extractant HDBP which resulted in the formation of different metal species and metal extraction behaviour. This kind of interaction may in part explain the results shown by Dr. Blumberg on the effects of diluent on metal extraction.

J. E. Gai: One of the theses put forward in the paper is that acid-base behaviour of cation exchange reagents, such as α -bromolauric acid, LIX 64N or DNNSA should be amenable to manipulation by suitable use of diluents in much the same way as is done for acid extraction by high molecular weight amines. In this sense some of the effects mentioned (e.g., Fig. 1) are due to diluent-reagent interaction as suggested by Dr. Liem. However, this is not always the case, especially if the cation is transferred as a hydrated species. If the diluent can solvate the hydrated species the effect may be

unexpected. Note for example, the different effects of butanol addition, shown in Table 8, on the extraction of Ni and Fe at low and at high acidities.

P. D. Mollère: Given that the co-extraction of contaminating species in the production of purified phosphoric acid may be related to the amount of water accompanying the P_2O_5 into the organic phase, have you investigated diluent effects from the standpoint of controlling the phase transfer of water in this extraction process or any other?

R. Blumberg: There are so many extracting systems for purifying phosphoric acid, that it does not seem justified to generalize in regard to the mechanism of transfer of impurities. On the other hand, it can indeed be stated that water distribution between phases may have a very real place in determining what transfers and how much. We have examined this particularly in relation to controlling direction of transfer and in separation among salts. This is dealt with in a general way in my paper 20c.

Y. Marcus: One may have a "diluent effect" even with neat, undiluted extractants, when they have side-chains built into the molecules. The length and shape, as well as the chemical nature of the side chain, affect the physical properties and the extraction effectiveness of the extractant. It is suggested that thought be given to choosing and synthetically modifying these built-in side chains in order to obtain the desired effects, without adding an extraneous diluent.

R. Blumberg: I fully agree that structures can be modified in order to attain certain pre-specified effects, which may also be obtainable by synthetic mixtures of reagents, diluents and modifiers. Thus extensive work has been done in our laboratories in regard to base strength of amines and the formation of amine salts as a function of such mixtures on the one hand, and by synthesizing amines to a pre-decided design, for steric effects,

resonance, etc. However, if, e.g., one wants to have the advantage in extraction and in stripping (as e.g. the case for LIX 70 referred to in the paper) then a synthetic mixture may have advantages as it can be separated into components and reconstituted as desired. Similarly, systems which give an extra liquid phase which then can be separated may also give advantage to synthetic mixtures as opposed to permanent built-in structures.

A. Warshawsky: (1) (Continued comment on Prof. Marcus's comment). We have taken this approach in modifying conventional side chain structure and incorporating side chains of various polarities, as will be demonstrated in the lecture this afternoon.

(2) Polar solvents for phosphoric acid, polymers containing oxyallylene chains, were prepared. The polyethers extract iron and other metals from phosphoric or mixed phosphoric-hydrochloric acids.

R. Blumberg: The answers given to the previous questions relate here also. Certainly, synthetics as a tool in tailor-making solvents cannot be over-emphasized, but the flexibility of mixture-compounding should not be overlooked.

A. S. Jassal: IMI has been a pioneer in solvent extraction technology for phosphoric acid from fertilizer acid. Does IMI technology employ diluents in the solvent for suppressing the ferric ions in particular, which usually complex with the solvents? Are there only diluents which would suppress the co-extraction of the cations and improve the distribution coefficient of P_2O_5 ?

R. Blumberg: The IMI phosphoric acid processes rely on systems which reject cations as compared to H^+ . Lime back-wash is the main expedient. However, solvent modification can indeed be utilized to advantage (cf, The Fertilizer Society Proceedings, Nov. 1975, London).

Ideas and Practice in the Design of Solvent Extraction Reagents

A. J. van der Zeeuw and R. Kok
Koninklijke/Shell-Laboratorium, Amsterdam
(Shell Research B.V.)
The Netherlands

ABSTRACT

The paper discusses the thinking behind our efforts to find new classes of accelerators for hydroxy oxime copper extractants. Examples of continuous mixer/settler experiments illustrating the effect of a chosen accelerator are given. The philosophy presented is also of use in attempts to find selective nickel extractants, and preliminary results illustrating this are provided.

Introduction

THE RAPID ADVANCE of the practical application of solvent extraction of metals to maturity, especially in the case of the chelating extraction of copper, has not been accompanied by an equally fast increase in the level of our knowledge of the reactions and mechanisms involved.

The present authors and their colleagues have always felt that obtaining theoretical information on kinetics, mechanisms, etc. should go side by side with reagent design in order for the maximum progress to be achieved in both.

The active cooperation of all colleagues in this rather broad field has resulted in considerable progress in improving the kinetics of copper extraction with hydroxy oximes. In addition, promising leads have been found that hopefully will result in the design of an attractive nickel extractant for acidic media.

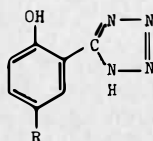
The present paper is devoted to the work done in the field of design of copper extraction accelerators and selective nickel extractants. A paper on mechanistic and kinetic aspects will be published elsewhere.

Practical Approaches to the Problem of Accelerator and Reagent Design

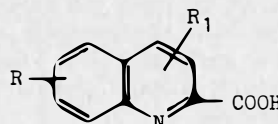
Survey of Currently Known Types of Accelerators

At a meeting of the Solvent Extraction and Ion Exchange Group of the Society of Chemical Industry in London, May 1976, Dr. Dalton (ICI) revealed that his colleagues and he had identified basically five types of accelerators for the extraction of copper with 2-hydroxyphenyl ketoxime extractants. Together with two types found in our work, the list of known accelerator types looks as follows:

- aliphatic α -hydroxy oxides
- hydroxyaryl tetrazoles



- alkalated hydroxyquinolines
- alkylquinaldic acid



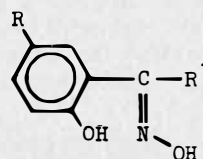
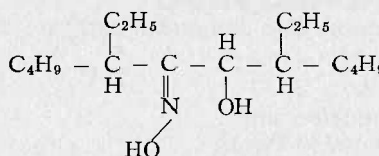
- alkylphosphoric acids
- sulfonic acids
- carboxylic acids

Working Hypotheses with Respect to the Mode of Action of Accelerators

The property common to classes a., b. and c. is their chelating power: they are copper-chelating reagents in their own right. Categories e., f. and g. are essentially acids, forming more or less normal salts. Class d. probably takes a position intermediate to the others, combining chelating and salt-forming properties.

The action of categories e. through g. is probably quite easy to explain: in the appropriate pH range they may form copper salts through a fast (ionic) mechanism, and in the organic phase the copper is transferred to the much stronger chelating agent. The above reasoning is backed by the behaviour of "VERSATIC". At pH 3 and higher, small amounts of "VERSATIC" have a spectacular accelerating effect on copper extraction with 2-hydroxyphenyl ketoximes. However, at pH 2 and lower, (the important range for copper extraction), amounts of up to 40% molar on oxime have no effect at all, except for ruining the iron rejection; at that pH the ability of "VERSATIC" to form copper salts has virtually disappeared. It would be interesting to know whether alkylphosphoric and sulfonic acids show similar behaviour below the pH values at which they are able to form copper salts.

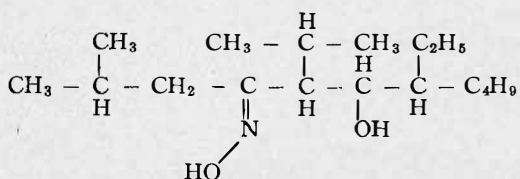
More intriguing, and also more useful from a practical point of view, would be to try and find a basic concept to define the action of chelating accelerators. To simplify the picture one might consider the only commercial one known so far, LIX®63, and compare it with the compound whose action it accelerates, the phenolic ketoximes:



One striking difference between the accelerator and the accelerated compound is that the former will form a five-membered ring when chelating copper, whereas the accelerated compound forms a six-membered ring with the metal; e.g.:



Since the competition for copper between the above accelerator and the accelerated compounds will thermodynamically go in favour of the latter, the obvious working hypothesis was that *kinetically* the formation of the five-membered ring with the accelerator is favoured. In this connection the behaviour of 7-ethyl-2-methyl-5-isopropyl-6-hydroxy-4-oximinoundecane



is interesting: the compound exerts no accelerating action at all. Copper-chelating capacity is totally absent. The high rate of reaction between, e.g., copper ions and the hydroxyquinoline reagents (Kelex®100 etc.) might also be explicable along these lines.

Another characteristic of the accelerator structure shown above is that the active groups are located in the middle of the chain. Experience with Shell copper extractants suggests⁽¹⁾ that this is not the most favourable position for good kinetics, and the logic of moving the active groups in the molecules to better (more exposed) locations was obvious.

Since in the open-chain accelerators of the hydroxy oxime type, all single bonds, including the C-C bond between the active groups, are in principle, freely rotating, at any moment in time only a part of all accelerator molecules might be in the right position to complex copper. This leads to a thermodynamically unfavourable influence on the equilibrium constant, and therefore to decreased copper/accelerator complex concentrations. Blocking the free rotation of the critical bond might therefore result in improved performance of the accelerator.

The three working hypotheses used as leads in our work may now be summarized as follows: in a search for new accelerating compounds one should look for copper chelating reagents proper, possessing one or more of these properties:

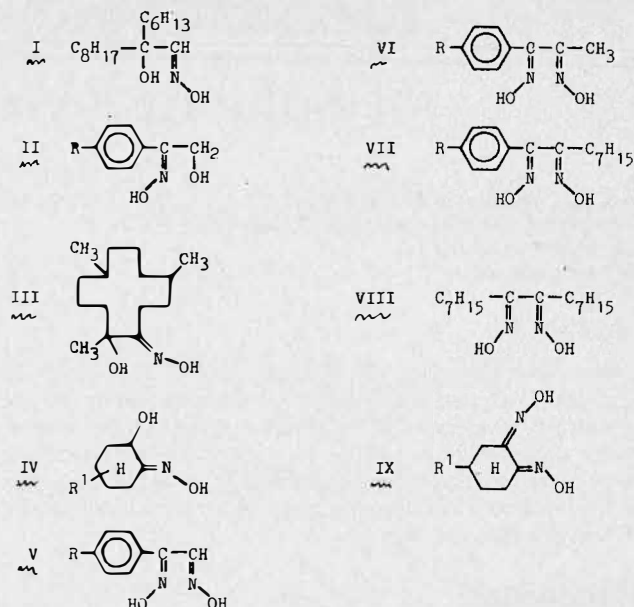
- ability to form five-membered rings with copper,
- active groups in easily accessible positions,
- fixation of the active groups in a favourable configuration.

New Accelerator Categories and Useful Variations of Known Types

The leads indicated above were successfully applied to the development of a previously unknown class of accelerators (vicinal dioximes) and to the design of new representatives of the already known hydroxy oxime class of accelerators.

Table 1 gives a survey of a number of these accelerators.

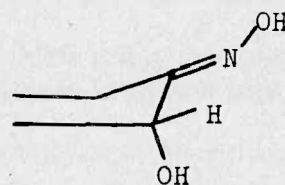
TABLE 1. Structures of New Hydroxy Oxime and Dioxime Accelerators



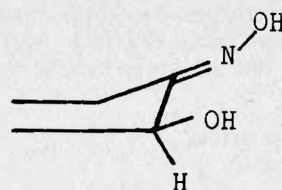
In Table 2 the effect of the above accelerators on the kinetic performance of a commercial sample of SME 529 is given, and compared with 5,8-diethyl-6-hydroxy-7-oximinododecane (DEHOD). The experiments were all done under the same set of standard conditions, which is comparable to that present in actual mixer/settler practice.

From this table, the accelerators tested can be ranked as follows: V = VI > VII > VIII > IX > II > I = III = DEHOD ≥ IV. It follows that the asymmetric open-chain hydroxy oximes from Table 1 have about the same activity as the known DEHOD, with the exception of compound II, which is clearly superior.

The performance of the hydroxycyclohexanone oxime IV is in fact surprisingly bad. Model studies show that, in the reagent as such, steric hindrance between the hydroxy and oximino groups is least when the former takes an axial position.



On the other hand, conditions for complex formation are better when the OH is in the equatorial position.



The situations are interchangeable through the boat ↔ chair transformation of the cyclohexane ring. The energy barrier will be at least of the same order as the rotational barrier in the open-chain hydroxy oximes, and possibly

TABLE 2. Absolute and Relative Effects of Accelerators from Table 1 on Commercial SME 529

Accelerator added	Quantity*, % mole on active matter in SME	Extraction in % a.t.e. after		Relative molar amounts of accelerators needed to achieve same performance
		30 s	60 s	
blank	—	43	65	—
DEHOD	5	67	82	1 (standard)
	10	82	92	
I	5		81	
	10		90	1
II	5		90	0.5
	10		97	
III	5		80	1
	10		90	
IV**	10		86	≥ 1
V***	0.5	84	94	0.05
VI****	0.1	65	80	0.05
	0.5	84	94	
	1.0	86	97	
VII***	0.5		81	0.1
	2.0		79	
VIII	0.5	62	79	0.2
	2.0	85	95	
IX*	2.0	66	82	0.4

*In cases where isomers are possible, the amount is quantity of active component needed

**Side chain R = ter-nonyl, derived from propylene trimer

***Side chain R = C₁₀₋₁₄ alkyl

****Side chain R = C₁₅₋₁₈ alkyl

higher. It is therefore understandable, that the performance of the hydroxycyclohexanone derivative is not impressive. Nevertheless, the fixation of active groups as a lead to more active reagents still has its value, as will be demonstrated later.

The open-chain vic. dioximes are extremely powerful accelerators. Theoretically, they may exist in four configurations, an anti, a syn and two amphi structures. (In symmetrical dioximes the two amphi structures are identical.) It was found that the anti configuration is by far the most active as an accelerator. (In addition, at least one of the other structures displays activity as a copper extractant proper, though on a lower level than the anti.) This backs our working hypothesis that the formation of a five-membered ring in the chelate is very important, if not essential, for the compound to act as an accelerator.

The cyclohexane dioxime IX is only moderately active. The anti form is an extremely potent copper extractant, able to extract copper from 2N H₂SO₄ at a very high rate. It is likely that for this reason the copper transfer equilibrium between the accelerator and SME 529 lies in favour of the former. Such a situation would also explain the low accelerating action of Kelex®100 on hydroxy oxime extractants. Only the relative abundance of the SME 529 over the accelerator remains to balance the net situation *quantitatively* in favour of the SME/copper complex.

Performance of a Dioxime Accelerator in Practice

To test the practical importance of the new category of dioxime accelerators, the performance of a standard batch

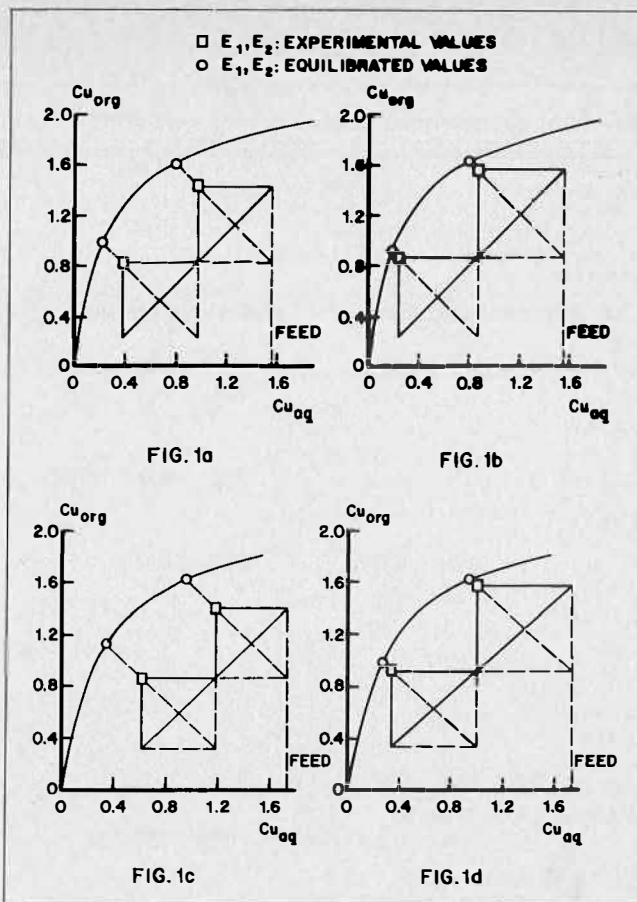


FIGURE 1 — Continuous mixer/settler run.
a. McCabe-Thiele construction of non-accelerated test, Table 3.
b. McCabe-Thiele construction of accelerated test, Table 3.
c. McCabe-Thiele construction of non-accelerated test, Table 3.
d. McCabe-Thiele construction of accelerated test, Table 3.

of SME 529 with and without a dioxime was compared. The accelerator chosen was No. VI from Table I, and it was added in an amount of 0.5 mole % (active anti-component on active reagent content) to an SME 529 solution in Shell diluent MSB 210 containing 35 g/l of SME (as supplied).

The (synthetic) leach solution contained approximately 1.65 g/l Cu²⁺, and 0.6 g/l Fe³⁺, both added as sulfates, and had a pH of 2.14. The strip solution contained 44.4 g/l Cu²⁺ and 106 g/l H₂SO₄.

The apparatus was a 2/2 stage Davy Powergas mixer/settler one-litre mixers). In all experiments the O/A phase ratio aimed at was 1/1 in extraction and 5/1 in the strip. In the strip mixers a local O/A of 1/1 was maintained by internal recycling. The experimental temperature was 25°C.

The aim was to test the extractant as severely as possible so that the accelerator would show the maximum influence. Therefore: a) the amount of aqueous copper offered slightly exceeded the loading capacity of the reagent; and b) in the second set of experiments the throughput rate was the maximum our experimental set-up would allow.

In the first set of experiments a residence time of 3 minutes in the mixers was applied. The results of the non-accelerated experiment are given in Table 3a and Figure 1a, those of the accelerated one in Table 3b and Figure 1b. In the second set of trials the throughput was pushed

TABLE 3. Influence of Dioxime Accelerator on the Performance of SME 529

3a. Non-accelerated test, normal residence time

Feed solution	: 1.56 g/l Cu, 0.57 g/l Fe ³⁺ ; pH 2.14						
Extractant solution	: 35 g/l SME 529 in MSB 210						
Strip solution	: 44.4 g/l Cu, 106 g/l H ₂ SO ₄						
Residence time, mixer	: 3 minutes						
Specific settler area	: 2.0 US gal./sq. ft./min						
Temperature	: 25°C						
Stg. eff., %	Metals in aqueous phase, g/l			Metals in organic phase, g/l			Stg. eff., %
	Fe	Cu _{eq}	Cu	Cu	Cu _{eq}	Fe	
77			1.56	1.44	1.62	0.0035	77
							
		0.79	0.97	0.83	0.98	0.0020	77
							80
		0.22	0.39	0.23	0.21		
			44.4				
							88
89	0.0012	45.3	45.2	0.38	0.28		88
							92
91	0.0132	50.9	50.4	1.44			92
Phase ratio: A/O extraction			: 1.03				
A/O stripping			: 0.207 (overall) (in mixers 1.0)				
Cu/Fe ratio: Loaded organic			: 420				
Advanced electrolyte			: 454				

3b. Accelerated test, normal residence time

Feed solution	: 1.56 g/l Cu, 0.57 g/l Fe ³⁺ ; pH 2.14						
Extractant solution	: 35 g/l SME 529 + 0.5 mole % accelerator VI in MSB 210						
Strip solution	: 44.4 g/l Cu, 106 g/l H ₂ SO ₄						
Residence time, mixer	: 3 minutes						
Specific settler area	: 2.0 US gal./sq. ft./min.						
Stg. eff., %	Metals in aqueous phase, g/l			Metals in organic phase, g/l			Stg. eff., %
	Fe	Cu _{eq}	Cu	Cu	Cu _{eq}	Fe	
			1.56	1.57	1.63	0.0038	93
							92
		0.82	0.87	0.87	0.92		93
							93
		0.20	0.25	0.23	0.21		
			0.44				
							87
88	0.0024	45.2	45.1	0.36	0.30		88
							95
95	0.014	51.4	51.1	1.57			95
Phase ratio: A/O extraction			: 1.02				
A/O stripping			: 0.201 (overall) (in mixers 1.0)				
Cu/Fe ratio: Loaded organic			: 413				
Advanced electrolyte			: 479				

3c. Non-accelerated test, short residence time

Feed solution	: 1.74 g/l Cu, 0.67 g/l Fe ³⁺ ; pH 2.14						
Extractant solution	: 35 g/l SME 529 in MSB 210						
Strip solution	: 48.0 g/l Cu, 106 g/l H ₂ SO ₄						
Residence time, mixer	: 1.5 minute						
Specific settler area	: 2.0 US gal./sq. ft./min						
Temperature	: 25°C						
Stg. eff., %	Metals in aqueous phase, g/l			Metals in organic phase, g/l			Stg. eff., %
	Fe	Cu _{eq}	Cu	Cu	Cu _{eq}	Fe	
			1.74	1.40	1.62	0.004	71
							71
		0.96	1.19	0.86	1.12	0.002	68
							68
		0.35	0.62	0.32	0.24		
			48.0				
							77
77	0.003	49.6	49.2	0.59	0.30		77
							74
73	0.015	54.1	52.8	1.40			74
Phase ratio: A/O extraction			: 0.96				
A/O stripping			: 0.23 (overall) (in mixers 1.0)				
Cu/Fe ratio: Loaded organic			: 350				
Advanced electrolyte			: 305				

3d. Accelerated test, short residence time

Feed solution	: 1.74 g/l Cu, 0.67 g/l Fe ³⁺ ; pH 2.14						
Extractant solution	: 35 g/l SME 529 + 0.5 mole % accelerator VI in MSB 210						
Strip solution	: 48.0 g/l Cu, 106 g/l H ₂ SO ₄						
Residence time, mixer	: 1.5 minute						
Specific settler area	: 2.0 US gal./sq. ft./min						
Temperature	: 25°C						
Stg. eff., %	Metals in aqueous phase, g/l			Metals in organic phase, g/l			Stg. eff., %
	Fe	Cu _{eq}	Cu	Cu	Cu _{eq}	Fe	
			1.74	1.57	1.63	0.003	92
							92
		0.95	1.01	0.92	0.98	0.002	90
							90
		0.27	0.34	0.33	0.25		
			48.0				
							74
71	0.002	49.4	49.0	0.56	0.30		71
							80
79	0.013	54.7	53.5	1.57			80
Phase ratio: A/O extraction			: 0.88				
A/O stripping			: 0.23 (overall) (in mixers 1.0)				
Cu/Fe ratio: Loaded organic			: 523				
Advanced electrolyte			: 423				

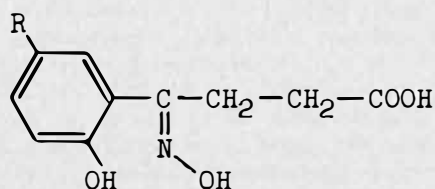
by applying a residence time of 1.5 minutes. Results are presented in Table 3c and Figure 1c for the non-accelerated tests, and in Table 3d and Figure 1d for the accelerated ones. Quite clearly the accelerator improves the overall copper extraction and the stage efficiencies greatly.

In spite of certain side-effects (e.g. slightly higher entrainment of aqueous in organic phase), indicating that further optimization of the preparation of the accelerators is necessary, the promise of the new category is clear.

Reagents with Built-in Accelerator Functions

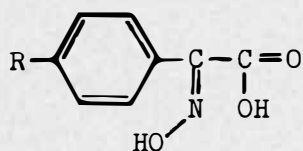
A logical consequence of the effect of physically mixing an extractant and an accelerator would be a combination of their functions chemically. Some of the various compounds synthesized and tested are interesting enough to be discussed briefly.

A compound combining the characteristic group of SME 529 with a carboxyl group as accelerator is 4-(2-hydroxy-5-nonylphenyl)-4-oximino-butanoic acid:



As expected, the kinetic performance of this compound was excellent. It is about twice as fast as chemically pure 2-hydroxy-5-nonylacetophenone oxime, and twenty times as fast as 2-hydroxy-5-nonylphenyl-n-propyl ketone oxime, with which it can be compared with respect to chain length. However, its pH_{50} for copper was found to be about 0.7 units higher, and its pH_{50} for Fe^{3+} about 1 unit lower, so that the separation factor Cu/Fe^{3+} was only 10. Both the good kinetics and the high iron extraction stem from the carboxylic group. The latter does not take part in any chelation, which can be seen from the behaviour of 4-oximinoundecanoic acid: this acts as a normal carboxylic acid towards metal ions, and shows no selectivity towards metals that otherwise easily take part in chelate formation.

In compounds of the class 1-(4-alkylphenyl)-1-oximinoacetic acid:



the chelating capacities of the combination carboxyl group/oxime, the rate-enhancing properties of the carboxyl group, and the possibility of five-membered chelate formation appear together. These compounds react extremely fast, as expected. For the 4-dodecylphenyl compound, pH_{50} for copper (for a 0.1 M reagent solution against 0.01 M Cu^{2+} in 0.5 M Na_2SO_4 background) was 0.25, whereas the pH_{50} for Fe^{3+} was 1.0. Obviously, this reagent is not very useful, but its behaviour backed our working hypotheses.

B. Trends in the Development of Extractants for Other Metals

Like copper, nickel is a potentially attractive metal to be won with the use of solvent extraction methods. Its price is relatively high, the quantities produced are substantial, and the future need for working ores that are less amenable to classical procedures is obvious.

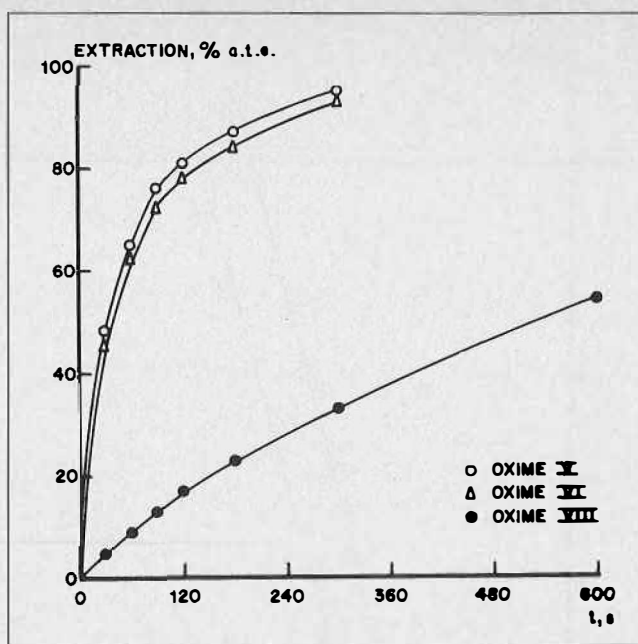


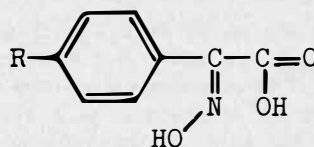
FIGURE 2 — Extraction rates for nickel with 0.005 M dioximes in toluene at 50°C. Aqueous phase: 2 g/l Ni^{2+} (as sulfate). pH 3.0. O/A=1. Baffled, turbine-stirred reactor

The most desirable properties for a good nickel extractant are the following:

- ability to extract nickel from moderately acidic medium,
- selectivity for nickel over iron (ferric and ferrous),
- rejection of associated cobalt, or alternatively the ability to release cobalt by some stripping method,
- attractive or at least acceptable rates of extraction and stripping,
- chemical stability under the conditions encountered in storage, extraction and stripping.

To date no reagents are known that show all these properties.

In our own research it is more or less standard to test any compound prepared as a potential extractant for copper and for nickel. The compounds belonging to the class of 1-(4-alkylphenyl)-1-oximinoacetic acids (already mentioned in Section A.5)



were found to have some virtues. They satisfy criteria a. and d. above. Cobalt is in fact co-extracted (separation factors Ni/Co 10-20), but can easily be stripped. A further disadvantage of these compounds is that, being carboxylic acids, they extract Fe^{3+} before nickel.

The most promising class of potential nickel extractants is that of the vicinal dioximes. Recently a very interesting paper⁽²⁾ described the properties of a number of symmetrical vic. dioximes, and one or two promising nickel reagents were identified. Major drawbacks found were the often extremely low extraction rates and the non-strippability of cobalt.

The useful experience with the influence of chain lengths in copper extraction⁽¹⁾ led to the investigation of asymmetrical, more exposed dioximes. Compounds V and

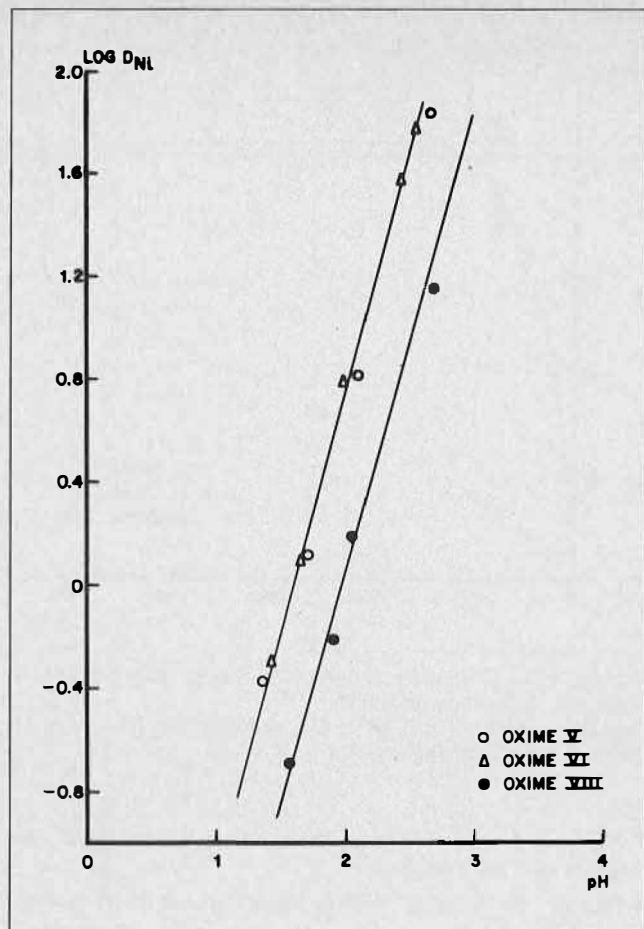
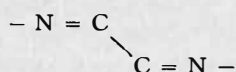


FIGURE 3 Log D/pH curves for 0.005 M dioximes in toluene at 50°C. Aqueous feed: 0.0005 M NiSO₄ in 0.5 M Na₂SO₄.

VI from Table 1 were a considerable improvement over those reported before⁽²⁾ in that times of equilibration could be measured in hours instead of days. Temperatures higher than ambient could increase the rates further to a level where they start to be attractive. Extraction rate curves at 50°C for compounds V, VI and VIII (representing the state of the art⁽²⁾) are presented in Figure 2: Log D/ pH plots (Figure 3) show that nickel extraction occurs in the attractive region. Iron is virtually not extracted in the pH range of interest.

Blytas⁽³⁾ has described the use of 4-alkyl-1,2-dioximino-cyclohexanes as extractants for nickel and other metals. Compound IX from Table 1 quantitatively extracts nickel from 2N H₂SO₄ at ambient temperature at a very fast rate. This result proves the value of the working hypothesis about fixation of the configuration of the active groups. Open-chain vic. dioximes probably have the trans-configuration in crystalline form and in solution⁽⁴⁾:



Molecular models show that the 4-alkyl-1,2-dioximino-cyclohexanes have the oxime groups fixed in a position extremely favourable for complex formation, which lowers the extraction pH values tremendously.

Although the leads indicated above certainly open up prospects, there are a number of serious difficulties still to be overcome. Firstly, all the compounds mentioned have only limited solubility in most organic diluents.

Secondly, only the anti-isomers are active nickel extractants, which necessitates optimization for anti production and, despite this, acceptance of (considerable amounts of) inactive isomers. Thirdly, in the case of the compounds of type IX, the extreme pH functionality leads to virtual non-strippability of the nickel.

Several ways of solving these problems have been found, and currently the desired structure is being optimized.

In an attempt to explain the often extremely low rates of reaction between nickel and open-chain dioximes of the type described before, it has been argued⁽²⁾ that a high activation energy barrier exists between the octahedral paramagnetic and the square-planar diamagnetic configuration, as a result of which the attainment of spin-pairing necessary to form the latter is hindered. Although this certainly could play a role, it is unlikely to be the only factor. Our results prove that acceptable and even high rates of extraction are possible. Moreover, the exchange of nickel between its "VERSATIC" acid salt (green, octahedral^(5a)) and hence probably paramagnetic^(5a,b) and oxime VIII from Table 1 (an extremely slow nickel extractant) in toluene is virtually instantaneous. This would suggest that a more important problem might be "peeling off" the aquo shell of the Ni²⁺ ion. Once in the organic solution either as an ion or as an easily ionizable species, the nickel reacts rapidly with the dioxime. The more favourable behaviour of the asymmetrical and especially of the cyclic dioximes may just be the result of the better orientation of the oxime groups.

REFERENCES

1. Van der Zeeuw, A. J., Inst. Chem. Eng. Symposium Series No. 42, 1975 p. 16.1
2. Burkin, A. R. and Preston, J. S., J. Inorg. Nucl. Chem. 1975, 37, 2187.
3. Blytas, G., US P.T. 3 703 573 of 21-11-1972 (to Shell Oil Co.).
4. a) Ungnade, H. E., Fritz, G. and Kissinger, L. W., Tetrahedron Suppl. 1963, 19, 235.
b) Borello, E. and Colombo, M., Gazz. Chim. Ital. 1957, 87, 615.
5. a) Ashbrook, A. W., J. Inorg. Nucl. Chem. 1972, 34, 3243.
b) Sacconi, L., in: Transition Metal Chemistry, Vol. 4, p. 216. Editor: R. L. Carlin, Marcel Dekker Inc., New York, 1968.

DISCUSSION

D. S. Flett: Have you examined the possibility of using accelerator compounds, in particular phase transfer agents such as dinonylnaphthalene sulfonic acid, to solve the problem of the slow rate of nickel extraction by dioximes?

A. J. van der Zeeuw: We are continuously looking into this problem. So far we have not identified a suitable compound. DEHPA works to some extent, but not sufficiently.

It is worthwhile to stress however, that the slowness of Ni-extraction by dioximes is inherent to the metal ion (Ni(H₂O)⁶2+), rather than to the extractant. It was recently found by two French workers that Ni-extraction by DEHPA is considerably slower than that of Zn, and they attributed this to a slow dehydration step. I tend to agree with this.

L. V. Gallacher: In connection with the preceding question on kinetic enhancement of nickel extraction, we have found a strong kinetic synergism in mixtures of LIX®63 and HDNNS in the selective extraction of Ni/Co mixtures. Working with Ni/Co feed solutions in sulfuric acid at pH 1.5, we found that equilibration with Ni requires approximately 2 hours when a 3:1 mole ratio of oxime to HDNNS is used. However, at ratios near 1:1, equilibration requires about 1 minute. The equilibrium Ni/Co selectivity is higher than 20:1 at the high mole ratio and is somewhat less at the 1:1 ratio. There appears to be an optimum intermediate ratio combining good selectivity with other desirable characteristics.

A. J. van der Zeeuw: I think Dr. Gallacher's remark opens interesting possibilities. We have never studied adding "accelerators" at such a high concentration. A complication I fear with the combination is, however, inducing hydrolysis of the hydroxyoxime like Drs. Ettel and Oliver reported sometime ago for the combination LIX®65 N/Dowfax 2AO, which is also a sulfonic acid. By extrapolation, such a risk would also exist for our dioximes in combination with strong organic-soluble acids and an aqueous phase.

R. Blumberg: Is it not likely that the accelerator effect of carboxylic acids is that these help the transfer of the metal ion to the organic phase and that then the complex formation takes place in the organic phase by a reversible redistribution

A. J. van der Zeeuw: It is a pity that because of lack of time I had to omit my survey of known accelerator systems. By the time the paper and the comments appear in print, Dr. Blumberg will have seen that I completely agree with her.

D. H. Liem: How do the accelerators you have investigated affect the selectivity of metal extraction? Have you any explanation on the mechanism of the effect of the accelerators?

A. J. van der Zeeuw: The selectivity is not influenced. The amounts needed are extremely small. Moreover the accelerator does not pick up iron itself, or (see comment by Dr. Hartlage) at least to a much smaller extent. One might think of an acceleration or iron pick-up by the reagent, but so far we have not observed this.

J. Hartlage: In our laboratory we have also studied dioximes as metal extractants. We have found that ferric iron is very slowly extracted, but the complex is extremely stable and results in poor stripping of the solvent. Have you also experienced this reagent poisoning by ferric iron?

A. J. van der Zeeuw: We have found a very slow pick-up of iron from ferric-containing solutions. It is to my mind not certain that this was in fact ferric pick-up. Dioximes are known to react with ferrous rather than ferric ions; perhaps small amounts of Fe³⁺ remaining in the aqueous, or formed therein, are being extracted. Stripping of the iron occurred quantitatively, though admittedly slow.

A. J. Monhemius: I was pleased to learn that the work on dioximes carried out in our group has been extended by Dr. van der Zeeuw at the Shell Laboratories. Firstly, a comment on the previous contribution to the discussion. Surely the importance of achieving selectivity of nickel over iron at the extraction stage lies in the fact that stripping of nickel from the dioxime extractants will require the use of strong acid solutions. The precipitation of iron from the strip liquor would require neutralisation of the acid and therefore presumably make the economics of the method somewhat un-economic.

Secondly, a question — has Dr. van der Zeeuw made any progress in the problem of stripping cobalt from the organic phase?

A. J. van der Zeeuw: The answer to your question is, No. I know of no other procedures to remove Co from chelating agents than are by now generally familiar. The best one still is H₂S precipitation, and it is messy. Other methods are no good either. With respect to the extension of the work at Imperial College may I comment that the work Dr. Blutas did with Shell Development Co. dates back as far as 1969. The patent is of 1972.

M. E. Kenney: You seem to have done a thorough job in examination of steric effects in the organic ligands. However, have you given any specific consideration to the ligand to metal bonding effects in designing your extraction reagents?

A. J. van der Zeeuw: The answer to your question is short... So far, No.

Selective Solvent Extractants for the Refining of Platinum Metals

R. I. Edwards, Chief Scientist,
National Institute for Metallurgy,
South Africa

ABSTRACT

A refining scheme based on solvent extraction and ion-exchange techniques has been developed for the platinum-group metals. The process is being operated on a commercial unit in South Africa.

In two of the separations involved, viz., the separation of platinum and palladium from the rest of the platinum-group metals and the separation of palladium, novel selective extractants are used. The structure, properties, mechanism of extraction, and plant performance of these solvents are described.

A new flowsheet is presented for the refining of platinum and palladium by use of the two solvents, and the possible advantages of this route compared with the conventional process are discussed.

Introduction

THE PLATINUM-GROUP METALS (PGM) are unrivalled by any other elements in the variety of complexes they form in aqueous media, which indicates that the refining of these metals could be efficiently accomplished by the techniques of selective solvent extraction or ion exchange. Many separations based on such techniques have been developed for analytical purposes^(1,2,3), but, until recently, application of these techniques to the commercial refining process has been rare indeed. Only one example has been published in the Western World, and this technique involves a peripheral separation⁽⁴⁾.

Undoubtedly, the fact that such separations are very much more involved than appears at first sight is the main reason for their rarity in commercial applications. However, the peculiar nature of the industry has also played a role in preventing the introduction of such techniques.

Since the refining of PGM is carried out on a small scale — the total annual production of refined metals is only a few hundred tons — the potential market for special solvents and resins for this application is very small. As a result, manufacturers of reagents have shown little interest in the field.

The industry is highly competitive and there is little or no technical cooperation between the various refiners. In fact, the tendency has been for refining technology to be kept as secret as possible. While it is known that many refiners have engaged in research on solvent extraction processes, very little of their work has been published and no common pool of knowledge has been established. Various processes have been patented recently^(5,6,7), but it is difficult to judge from these patents whether the process envisaged is really suitable for large-scale application.

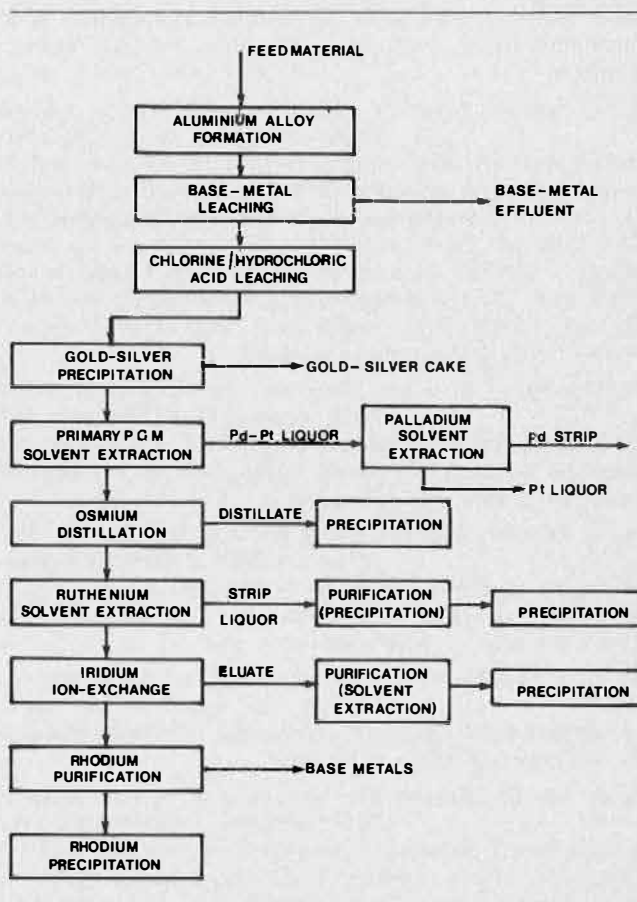


FIGURE 1 — The NIM process for refining of the platinum-group metals.

About five years ago, the National Institute for Metallurgy (NIM) first became involved in research into refining processes for the PGM. As a result of this research, which is still being carried out, a refining process based mainly on solvent extraction and ion exchange was developed, and has now been commissioned on a commercial unit at the premises of the Lonrho Refinery (S.A.) Ltd in South Africa.

During the development of the process, it became clear that, for certain separations, no commercially available solvent or resin was entirely suitable, and extractants specific to the particular separation were therefore developed at NIM. This paper describes the properties and functions of these extractants.

The Refining of 'Secondary PGM'

One version of the refining process, which is shown schematically in Figure 1, was developed especially for the treatment of materials rich in the 'secondary PGM' (rhodium, ruthenium, iridium, and osmium). This is the process (except for palladium separation) used at the Lonrho Refinery.

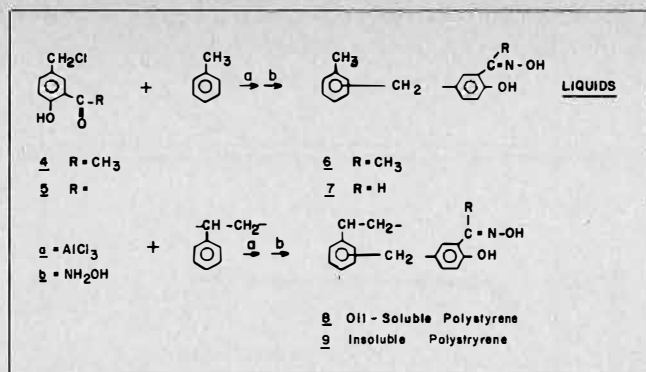


FIGURE 3. Synthesis of chelating agents of various physical forms.

ligands x. The other (y-S) contains the second ligand y attached to any neutral substrate S. In path (b) the chelating centre is assembled first in a single molecular precursor, and only then is the attachment of the hydrophobic region accomplished.

The main advantage of path (b) over path (a) is the fixation of the desired ligand-arrangement in one molecular species, and this leads to great synthetic versatility. Path (b) will be therefore referred to as a unified approach to the synthesis of C-PTA.

Practical examples for path (a) are numerous and the synthesis of LIX-64, P-5000 and SME reagents (see Figures 1 and 2) belong here. Practical examples for path (b) will be discussed in this paper.

Synthetic Considerations

For the practical implementation of approach (b), it is necessary to incorporate in the single molecular precursor an active site, and preferentially in a convenient and cheap method.

It was decided to use the chloromethylation of aromatic compounds as the key reaction⁽³⁰⁾ and the chloromethyl group therefore serves as the chemically active site.

The single molecular precursor containing ligands x and y in a pre-determined arrangement, is assembled as follows:



The chloromethyl group is exceptionally suitable for its role due to its high reactivity in various reactions, like Friedel-Crafts alkylations, nucleophilic substitution on nitrogen, oxygen or sulfur and also in free radical reactions.

Structure-Property Considerations

Building-in Metal Selectivity

The choice of the various type 2 compounds enables the determination of metal specificity and even selectivity. For example, when necessary to have a general transition metals extractant, then 2 will be 5-chloromethyl-8-hydroxyquinoline, i.e., 3.

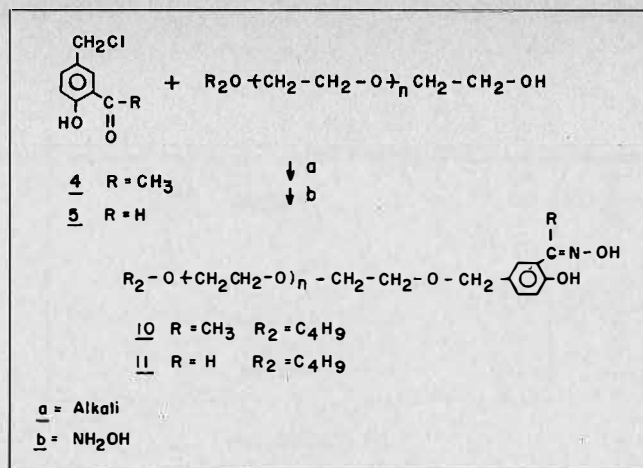
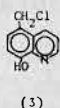


FIGURE 4. Synthesis of amphiphilic chelating agents.

However, if copper-selective reagents are desired, 4-chloromethyl salicylaldehydes (5), or 4-chloromethyl-2-hydroxyacetophenone (4) are used.



(4) R = CH₃

(5) R = H

Building in Phase and Physical Properties

Let us choose one reaction type in order to demonstrate this point. For example if 4 and 5 are reacted under Friedel-Crafts conditions with: (see Figure 3).

- toluene,
- low-molecular weight polystyrene,
- insoluble high molecular weight polystyrene.

The products will be: a hydrophobic liquid (case A), an oil-soluble polymer (case B) or an insoluble polymer (case C). If however 3, 4 and 5 are reacted with oligoalkylene derivative (see Figure 4); amphiphilic reagents with high surface activity are obtained.

Extraction Properties of Copper-Selective C-PTA

In this section we wish to present extraction data with particular emphasis on the principles discussed earlier, namely, how one single molecular precursor (4 or 5), containing the essential metal-binding ligands, will yield various reagents with different physical properties. Detailed and inclusive technical description of the reagents will be dealt with in a forthcoming paper.

Copper Specificity and Complex Structure

Chloromethylsalicylaldehyde (5) or 4-chloromethyl-2-hydroxyacetophenone (4), contain a copper-selective centre^(3,7,8). As expected, compounds 6, 7, 10, 11 form a 2:1 ligand-to-metal complex in the organic phase.

The extraction -pH profiles of reagents 6, 7, 11 in a 0.0315 molar concentration in toluene are given in Figure 5. Comparison between reagents 6 and 7 shows a steric effect in the oxime region. Comparison between compounds 6, 7 and 11 reveals the influence of the amphiphilic chain (due to a combination of polarity and buffering effects) on the pH 1/2 values.

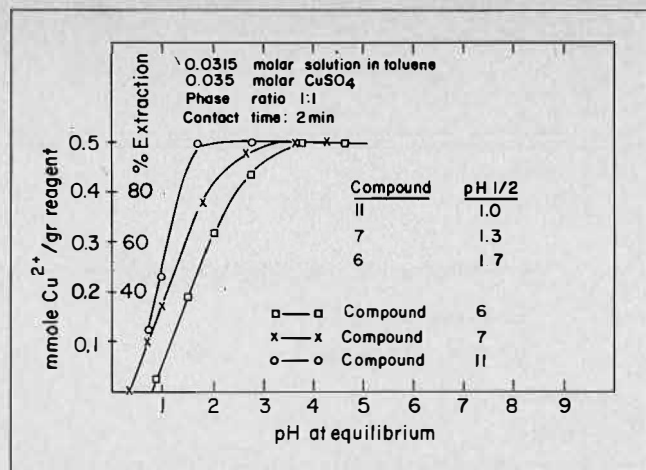


FIGURE 5. pH — extraction profile.

TABLE 1. Extraction of Divalent Cations.

(1) Zero extraction was determined by direct metal analysis, and by lack of change in pH of solution.
 (2) 0.0315M in toluene.

Cation	Conc. (gpl)	pH	Reagent	Contact Time (minutes)	% Extraction;
Ni	2	4	7	10	0
"	"	"	"	120	0
"	"	"	11	120	0
Zn	2.68	"	7	10	0
"	"	"	11	120	0

TABLE 2. Distribution Constant (D O/A) and Separation Factors (β Cu/Fe)

Reagent*	Cu (gp 1)	Fe (gp 1)	pH	Time (min)	D _{Cu}	D _{Fe}	β
6	4.0	4.0	2.0	15	2.06	910 ⁻³	310
7	4.6	4.0	1.4	15	4.51	310 ⁻³	671

*5% w/v solution in toluene.

TABLE 3. Reextraction with Sulphuric Acid*

Reagent	H ₂ SO ₄ (N)	% Reextraction
7	1	84
7	2	82
7	3	100
11	1	73
11	2	80
11	3	100

*Organic solvent: 0.0315M R, 0.015M Cu²⁺ in toluene;
 Phase Ratio = 1:1. Contact Time = 2 min.

TABLE 4. Acidity Values for Extraction and Reextraction

Reagent	pH _{1/2} (extraction)	[H ⁺] _{1/2} (reextraction)
7	1.3	0.4N
11	1.0	0.4N

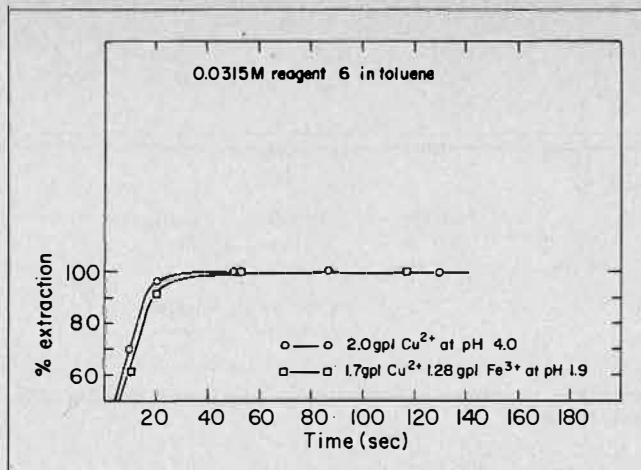


FIGURE 6. Rate of copper extraction.

The selectivity of the reagents for copper over the divalent transition metal cations seems to be very high, as the divalent cations are not extracted at all (see Table 1).

The selectivity of the reagents for copper over trivalent iron is of great practical interest. When solutions of reagents 7 and 11 were contacted with Fe(III) at pH 2.0, about 8 to 30 ppm of iron seemed to be extracted. However, this must be due to physical entrainment as that figure stays constant through changes of reagent concentration. Table 2 gives separation factors under specified conditions, indicating a high selectivity for copper over trivalent iron.

The information gathered so far, under various pH, copper concentrations and copper to ferric ratios, shows that, at even high reagent and ferric iron concentrations, separation factors can be as high as 1.5x10³.

5.2. Rate of Copper Extraction

Figure 6 shows rate of copper extraction from copper sulphate solution of pH 4, and from copper-iron solution of pH 1.9. Apparently, the presence of iron does not affect the rate of copper extraction. It is not necessary to emphasize that the good kinetics of the reagents has a significant practical value in the reduction of equipment size and retention times.

5.3. Metal Reextraction

Table 3 shows the effect of sulphuric acid strength on the reextraction (stripping) of the loaded organic solvent.

The results show that quantitative reextraction is achieved with 3N acid in one stage, and with 1N acid in 2-3 stages.

An interesting conclusion, regarding the role of the side chain, may be achieved by comparing acidity values for extraction (see Figure 5) and reextraction (see Table 3) given in Table No. 4.

This phenomenon is in contradiction to earlier reports that gains in pH_{1/2} values for extraction are upset by increases in [H⁺]_{1/2} values for reextraction⁽²⁷⁾. The reason for this exception is due probably to a kinetic effect exercised by the oxyethylene side chain of reagent 11.

In summary, it was shown that the unified synthetic approach to copper-selective C-PTA can have the following advantages:

- (1) Provide models for the study of property-structure relationship in chelating reagents.
- (2) Provide new and alternative ways to the synthesis of familiar and novel chelating extraction reagents.

Acknowledgement

The generous support of the Israeli National Council for Research and Development is gratefully acknowledged. The technical assistance of Miss Hedva Berckowitz is kindly acknowledged.

REFERENCES

- (1) Swanson, R. R. and Agers, D. W., 93rd AIME Meeting, N.Y. 1964.
- (2) Flett, D. S., Trans. Inst. Min. Metal 1974, C30.
- (3) Ashbrook, A. W., Coord. Chem. Revs. 1975, 16, 285.
- (4) Flett, D. S., Cox, M. and Heels, J. D., Int. Sol. Ex. Conf. Lyon, 1974, 2559.
- (5) Neelameggham, R., Ph.D. Thesis, Univ. of Utah, Salt Lake City, 1974.
- (6) Fleming, C. A., Inst. Min. Metal. 1976, 85, C211.
- (7) Van-der-Zeaw, A., in "Hydrometallurgy". In Chem. Eng. Sym. Series No. 42, 1975, Edits. G. A. Davies and J. B. Scuffham, paper No. 16.
- (8) Price, R. and Tumilty, T., in "Hydrometallurgy". In Chem. Eng. Symp. Series No. 42, 1975, Edits. G. A. Davies and J. B. Scuffham, paper No. 18.
- (9) Warshawsky, A., Kalir, R. and Patchornick, A., Proceed. Israel Chem. Soc. 43rd. Ann. Meet. Beer-Sheba 1975, 123.
- (10) Patchornick, A., Kalir, R., Fridkin, M. and Warshawsky, A., 1976, U.S. Patent 3,974, 110.
- (11) Warshawsky, A. and Patchornick, A., in "The Theory and Practice of Ion Exchange", Soc. Chem. Ind. Confer., Cambridge, 1976, paper No. 38.

DISCUSSION

D. S. Flett: You have indicated that the presence of iron does not affect the rate of copper extraction.

For LIX 65N it has been shown by Fleming of NIM, South Africa and by Lawson of Birmingham University, U.K. that ferric iron reduces the rate of copper extraction, in Fleming's work by about an order of magnitude. Work at Warren Spring Laboratory U.K. and the University of Waterloo, Ontario, Canada has also shown such an effect for copper extraction by Kelex 100. Would the author please comment on the difference between these data and his results with his hydroxyoximes?

A. Warshawsky: Our experiment was done in order to check for the iron retardation effect you have indicated. We were surprised not to measure any differences. This difference could result from the fact that our compounds are not mixtures of accelerators and extractants and so cannot be compared with SME 529 and P-1, P-17 and P-50.

K. Lewis: Did you investigate the complexation of nickel and zinc at $\text{pH} > 4$? What is the value of n in the polyester side chain of compound 11?

A. Warshawsky: Yes we tested Ni and Zn at $\text{pH} 5-6$. They are not extracted at all. n equals 2.

J. F. Urstad: What would one expect of chloride extraction in chloride systems on these reagents? In chloride systems, is there any degree of extraction of univalent copper where this ion is present?

A. Warshawsky: Chloride ions will be transferred into the organic phase under two conditions: (a) if the oxime is basic enough (and it seems that the oxime

nitrogen is not basic enough) and; (b) if an anionic complex is found; this is so when $[\text{Cl}^-] > 3\text{M}$. We did not study Cu^{+1} .

R. R. Grinstead: What are the solubility properties of oximino phenolic reagents in water?

A. Warshawsky: Their solubility is around 10-30 ppm in water from toluene.

C. Bouboulis: Would reagents with polyoxymethylene or polyoxyethylene chains form emulsion during the mixing of the two phases?

A. Warshawsky: Development products have sometimes shown emulsion problems. Now, the pure products separated under controlled reaction conditions do not show this. On the contrary, they yield very good separation times.

R. Taylor: What is the solubility of reagents 6 & 7 and their copper complexes under practical conditions, i.e., at concentrations up to 0.5M in diluents containing 20% aromatics max.?

What is the effect on extraction kinetics of operating under practical conditions where the amount of copper offered to the reagent is much less than the experiment described in this paper?

A. Warshawsky: The solubility in toluene is about 25-40% w/v for isomeric mixtures of oxime, and about 7% for pure reagents. Modifiers increase the solubility, and aliphatic-aromatic mixtures of 20:80 are possible. The extraction kinetics is subject to $[\text{Cu}]$ and rate expressions presented by Flett and others will hold true for this reagent.

New Neutral Oxygen and Sulphur-Containing Metal Extractants Including Oil Sulphoxides and Sulphides

V.A. Mikhailov. Department of Physical Chemistry, Institute of Inorganic Chemistry, Siberian Branch of Academy of Sciences, Kemerovo, U.S.S.R.

ABSTRACT

The paper is a survey of work, since the Hague Conference (1971), on the chemistry and applications of metal extraction by amine oxides, synthetic organic sulphides and sulphoxides and also oil sulphides and sulphoxides. Together with other problems, the production of oil sulphides and sulphoxides is considered. Special attention is paid to extraction of noble metals, non-cation-exchange synergistic extraction of uranyl sulphate by mixtures of D2EHPA with neutral donor extractants and to the evidence for the stability of extraction ability series while changing extracted metal and diluent.

Introduction

SUCH WELL-KNOWN and often used extractants as tertiary amines R_3N , ketones R_2CO and trialkylphosphine oxides R_3PO are only some examples of extractants of classes $R_nX(X=N,p,AS,S,Se,Te)$ and R_nXO . The most available and stable, and also the least toxic, among the new synthetic extractants of these two classes are without doubt dialkyl sulphides, R_2S , dialkyl sulphoxides, R_2SO , N-oxides of tertiary aliphatic amines, R_3NO , and substituted pyridines. The first systematic investigations of A.V. Nickolaev and co-workers on the extraction ability of organic sulphides and sulphoxides⁽¹⁻³⁾ and amine oxides^(2,4) with respect to a great number of metals in various media, as well as detailed studies of the extraction ability of different pyridine-N-oxides^(5,8), trioctylamine oxide⁽⁸⁻⁹⁾ and dioctyl sulphoxide^(8,10) with respect to uranyl nitrate as a classic example of co-ordination extraction, have shown that these extractants possess valuable properties and can find numerous applications in technology and analytical chemistry for problems which have been either impossible or difficult to solve using previously known extractants.

A survey of the extraction properties of N-oxides, dialkyl sulphoxides and dialkyl sulphides was made at ISEC-71⁽¹¹⁾. The present review discusses the main results of studies of the extraction ability of these new extractants and the stoichiometry of metal extraction with them which has been carried out over the last 6 years, and also work done on their practical uses. As well as synthetic extractants, the natural extractants, oil sulphides, and the products of their oxidation, oil sulphoxides are discussed. The results of work dealt with in previous reviews^(12,13) and in a recently published review⁽¹⁴⁾ on extraction by sulphoxides will be discussed only where necessary.

Dialkyl Sulphides

Dialkyl sulphides are easily available, very powerful and selective co-ordination extractants for Au, Pd and Ag. Nowadays they are widely used in analytical chemistry of these elements. Gold and palladium are extracted from various media^(3,11,15) in the form of complex non-electrolytes such as $[AuCl_3R_2S]$ or $[PdSO_4(R_2S)_2]$. The stoichiometry of the extraction of silver nitrate is characterized by the formation of $[AgNO_3(R_2S)_2]$ when the extractant is in excess⁽¹⁶⁾. When the concentration of $AgNO_3$ in the aqueous phase is increased, polynuclear complexes of the general formula $(AgNO_3)_{q+2}(R_2S)_{q+3}(q=0,1,2\dots)$ are formed, as was shown by detailed computer analysis of the distribution isotherms of silver nitrate between water and solutions of various dialkyl sulphides in a number of diluents⁽¹⁷⁾. Thus the ratio $AgNO_3:R_2S$ approaches 1:1 as the organic phase approaches saturation. The formation of polynuclear forms was confirmed by cryoscopic measurements of mean molecular masses of solutes in mixtures $AgNO_3-(C_8H_{17})_2S-C_6H_6$. In some systems it was also necessary to suppose the formation of dimers, $[AgNO_3(R_2S)_2]_2$, for consistency between the observed and the calculated extraction isotherms. Extraction of $AgNO_3$ from mixtures with $Cu(NO_3)$ and $Zn(NO_3)_2$ by solutions of $(C_8H_{17})_2S$ in $CHCl_3$ was studied by the method of extraction rays⁽¹⁸⁾, which were found to intersect at the point corresponding to anhydrous $AgNO_3$. It was shown also that the nitrates of Cu, Zn, Pb, Co, Ni, Cd, Ca are practically not extracted by sulphides. The extraction of Au, Pd, Pt, Ag from nitric or hydrochloric acid solutions by sulphides of various structures was studied by V.A. Pronin and co-workers^(19,20). $(Tert-C_4H_9)_2S$ proved to be the most effective extractant.

Apart from the above-named noble metals, dialkyl sulphides successfully extract Hg(II) from nitric or hydrochloric acid solutions^(1-3,11,13,21) as well as copper(I) chloride⁽²²⁾. The extraction of $HgCl_2$ by different dialkyl sulphides from aqueous solutions of $HgCl_2$ was studied in detail⁽²¹⁾. The computer analysis of extraction isotherms and cryoscopic measurements give evidence of the formation of $[HgCl_2R_2S]$, $[HgCl_2(R_2S)_2]$, $(HgCl_2R_2S)_2$ and possibly $(HgCl_2)_2R_2S_2$ in the organic phase. Copper(I) is extracted by dibutyl sulphide in the form of $[CuClR_2S]$ and a binuclear complex $2 CuCl \cdot 3R_2S$ ⁽²²⁾. The formation of polynuclear sulphide complexes while extracting $AgNO_3$, $HgCl_2$ and $CuCl$ makes it possible to assume that the stoichiometry of gold and palladium extraction is in reality also more complex and not confined to the formation of mononuclear species.

Pt(IV) is extracted by dialkyl sulphides from nitric or hydrochloric acid solutions much more poorly than Pd(II)^(1-3,12,19,20,23), but both metals can be extracted together from sulphuric acid solution⁽²³⁾. Other platinum metals, irrespective of oxidation states, are extracted very slowly with sulphides and in small amounts^(1-3,12,23) ap-

parently due to the kinetic inertness of their acido-complexes in reactions of substitution. In the presence of AgNO_3 in the organic phase, the extraction of chlorocomplexes of Pt(II), Pt(IV) and Rh(III) by dibutyl sulphide is greatly accelerated⁽²⁴⁾, and in a period of 1-4 hours the distribution coefficients reach values of 20-30 depending on the AgNO_3 concentration. In the absence of silver nitrate, Pt(II) is practically not extracted. The induced extractions of Pt(II), Pt(IV), Rh(III), Ir(III) are also observed in the presence of mercury compounds⁽²⁵⁾. Apart from Au, Pd, Ag, Hg and Pt(IV), dialkyl sulphides can also extract Tl(III) in form of $[\text{TlCl}_3(\text{R}_2\text{S})_2]$ under specially selected conditions (10 M H_2SO_4 -0.37 M NaCl)⁽¹²⁾. Nitrosoruthenium nitrate is not extracted by sulphides⁽²⁶⁾.

Almost immediately after discovering the ability of dialkyl sulphides to extract Au, Pd and Ag more effectively and selectively than was possible by use of previously known extractants, their intensive penetration into the analytical chemistry of noble metals began. The atomic absorption determination of gold in extracts, after its selective isolation with 0.01-0.02 M dibutyl sulphide solution in benzene or toluene, with simultaneous gold concentration, proved to be a very convenient method for the determination of small amounts of gold in rocks, ores and various technological products⁽²⁷⁻³³⁾. The best diluent for atomic absorption determination of gold using the technique of dispersion into the flame is toluene⁽³⁰⁾, the sensitivity of the method being near to $0.02 \mu\text{g}/\text{ml}$ ⁽³¹⁾. By another technique of atomization, the sensitivity can be increased up to $5.10^{-4}\text{g}/\text{t}(5.10^{-8}\%)$ with a limit of detection 5.10^{-9}g ⁽³²⁾, which provides the determination of Clark contents of gold (i.e. the mean contents in the earth's crust).

Extraction of gold by sulphides has greatly simplified its neutron activation determination in rocks⁽³⁴⁾. Palladium together with gold is transferred into the organic phase by extraction from hydrochloric acid solution. Both metals can be separately determined in the extract using modern techniques for the registration of nuclear radiations⁽³⁵⁾. For the isolation of gold from various solutions or natural waters, one can use partition chromatography with sulphide solution as the stationary phase⁽³⁶⁾. For gold determination in rocks and ores, the method of isotopic dilution can be used with substoichiometric extraction of gold by sulphide⁽³⁷⁾. Extraction with dialkyl sulphides as the method of gold separation has also been used for its polarographic determination in various materials^(38,39).

The high selectivity and effectiveness of gold extraction, together with the high capacity of the extractant, have made extraction with organic sulphides one of the most practical methods of matrix removal for the chemospectral analysis (i.e. the spectrum analysis after the preliminary chemical concentration and separation of the determined elements) of high purity gold⁽⁴⁰⁾. For suppressing the extraction of impurities by dibutyl sulphoxide resulting from the oxidation of the extractant by gold (III), it is advisable to use CHCl_3 as a diluent in this case. For extraction of gold by 1 M solution of $(\text{C}_4\text{H}_9)_2\text{S}$ in CHCl_3 , the degree of gold removal is 99.9995%. The method makes it possible to determine 26 elements in high-purity gold within the limits of detection of 2.10^{-5} to $2.10^{-8}\%$. This method has also been used for the neutron activation gamma-spectrometric determination of impurities in gold films⁽⁴¹⁾.

Dialkyl sulphides are no less useful for the precise separation and concentration of palladium and silver, the latter from nitric acid solutions. The methods of extraction and atomic absorption determination of palladium^(28,42) and silver⁽⁴³⁾, extraction and polarographic determination of silver in ores and technological products⁽⁴⁴⁾ and neutron activation determination of silver in rocks and minerals⁽⁴⁵⁾

have been developed. For determination of impurities in high-purity silver, after matrix removal with extraction by sulphides, one can use spectral⁽⁴⁶⁾, atomic absorption⁽⁴⁷⁾, neutron activation⁽⁴⁸⁾ or volt-amperometric⁽⁴⁹⁾ methods of analysis. For analysis of high-purity palladium the neutron activation gamma-spectrometric method has been developed⁽⁴¹⁾. Extraction by sulphides permits significant simplification of the simultaneous neutron activation determination of Pd, Au, Pt, Ir in natural materials^(50,51) and technological materials⁽⁵¹⁾. Some analytical uses of palladium extraction by dialkyl sulphides are discussed by Pitombo^(52,53).

At present organic sulphides seem to be used in the USSR for the separation and concentration of Au, Pd and Ag more often than any other extractant. At the last All-Union Conference on the chemistry, analysis and technology of noble metals⁽⁵⁴⁾, 15 reports dealt with the use of organic sulphides for these purposes. The possibility of using sulphide extraction in analytical chemistry of mercury merits investigation too.

Oil Sulphides as Natural Extractant

The ability of some unrefined oil products to extract Au, Pd and Ag has often been reported in the literature^(55,56). The last reports appeared quite recently⁽⁵⁷⁾. The active principle of unrefined oil products is the complex mixture of sulphur-organic (mainly heterocyclic) compounds which can be separated from sulphurous oils and used as an effective and selective natural extractant for Au, Pd, Ag, Hg^(12,13,58-60). Oil sulphides are potentially available in great amounts.

The present state of the problem of sulphur compounds in oil has been examined in monographs⁽⁶¹⁻⁶³⁾ and in review⁽⁶⁴⁾. In most of the oils studied, a major part of the sulphur is found to be in the form of mono- and bithiocycloalkanes, so they are⁽¹⁴⁾ the main components of concentrates of oil sulphides separated from oil distillates. Thiophenes are incapable of effective extraction of noble metals^(58,60) if concentrations in oil sulphides are not great^(14,65).

The methods of production of concentrates of oil sulphides from distillates of sulphurous oil by extraction with sulphuric acid (usually 86%) have been well developed^(62,65). Extraction by some organic solvents can also be used⁽⁶⁵⁾. A pilot plant for the production of oil sulphides was described⁽⁶⁶⁾. The processes used for the separation of oil sulphides also allows the refining of fuel from sulphurous compounds. A major part of the work on the separation of oil sulphides was made with fractions of oil from the Arlan deposit in Bashkirija.

The extraction ability of oil sulphides separated from straight-run kerosene — gas — oil fractions by means of extraction with sulphuric acid was studied in detail⁽⁵⁸⁾. The concentrate of oil sulphides was fractionated by distillation in the temperature range of 150-350°C into fractions boiling off at 40°C intervals. The total sulphur content in the fractions drops as the temperature of distillation increases, from 17.7% for the fraction 150-190°C to 10.4% for the fraction 310-350°C. At a sulphur concentration of 30g/l (the diluent being a mixture of polyalkylbenzenes) all the fractions extracted gold from hydrochloric acid solutions effectively and selectively. The distribution coefficients for small amounts of gold were virtually independent of the concentration of HCl in the aqueous phase in the range of 0.1-4.1 M and were about 400 for the fractions 190-230, 270-310, 310-360° and about 200 for the fractions 150-190, 230-270°C. The loading capacity of the sulphides with respect to gold was 140g/l. For extraction by $(\text{C}_4\text{H}_9)_2\text{S}$, the distribution coefficient of gold is close to 400 under comparable conditions.

The wide (190-350) fraction of sulphides effectively extracts palladium from hydrochloric acid solutions with distribution coefficients of 250-400, the total sulphur concentration being equal to 30g/l. The extraction of silver nitrate by oil sulphides obtained by various methods was also studied⁽⁶⁰⁾, their sulphide sulphur content being varied from 3.2 to 14.5%. Under comparable conditions (concentration of sulphide sulphur 0.1 M, the diluent-C₆H₆) almost all samples extracted silver much more effectively than did (C₈H₁₇)₂S. For practical use in technology, sulphides with the boiling temperature above 260°C are recommended. Their capacities with respect to silver, without the formation of third phases, approaches 120g/l (the concentration of sulphide sulphur 1.5 M, the diluent—kerosene). Mercury(II) and thallium(III) are also extracted by oil sulphides⁽¹³⁾. Oil sulphides are not inferior to dialkyl sulphides with respect to selectivity of the noble metals. Therefore, they are often used instead of dialkyl sulphides in the analytical applications of extraction by organic sulphides considered in the previous section.

Oil sulphides can find various uses in the hydro-metallurgy of gold, palladium and silver, in particular for silver refining⁽⁶⁷⁾. Their deficiencies are the gradual oxidation by gold(III)^(40,60), silver(I) (with light), nitric acid⁽⁴⁶⁾ and other oxidants to sulphoxides, and also the necessity of using complex-forming reactants at the stripping stage.

Synthetic and Oil Sulphoxides

Sulphoxides as extractants are in most cases the analogues of neutral extractants containing the phosphoryl group. The metals are extracted by them either in the form of complex non-electrolytes such as [UO₂(NO₃)₂(R₂SO)₂] (co-ordination extraction), or in the form of complex metaloacids such as HFeCl₄ (hydrate-solvate mechanism). The numerous data on extraction by sulphoxides have been systematized in reviews^(13,14). The stoichiometry of the co-ordination extraction by dialkyl sulphoxides and TBP is the same, but the extraction ability, quantitatively characterized by the value of the extraction constant, is for dialkyl sulphoxides always higher than that of TBP. The extraction of metals by cyclic sulphoxides has been investigated most completely in the works of A.M. Rozen, Yu.E. Nikitin and Yu.I. Myrinov. Dialkyl sulphoxides, in respect of extraction power, are inferior to phosphonates (RO)₂RPO, but cyclic sulphoxides are superior to phosphonates.

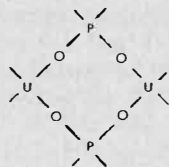
The continuous increase of interest in the extraction of metals by sulphoxides is caused, not only by their greater extraction ability in comparison with TBP, but also by prospects of the practical use of oil sulphoxides which are potentially available in great amounts. The oxidation of oil sulphides has been considered in detail in the monograph of E.N. Karaulova⁽⁶¹⁾ and in a review by G.D. Gal'pern⁽⁶⁴⁾. Oxidation of sulphides directly in oil distillates, followed by isolation of sulphoxides, for example by extraction with sulphuric acid⁽⁶⁵⁾, has been carried out by hydrogen peroxide in a foam-emulsion regime with foaming by air. However, it is preferable to separate a concentrate of oil sulphides and to oxidize that. Oxidation is carried out by hydrogen peroxide at 70-85°C with simultaneous evacuation to remove the water formed⁽⁶⁸⁾. In this way a large experimental batch of oil sulphoxides has been produced⁽⁶⁵⁾. Concentrates of sulphides produced by extraction with sulphuric acid or phenol can also be oxidized in a foam-emulsion regime⁽⁶⁹⁾. Macrokinetics of foam-emulsion oxidation of sulphides in oil distillates has been studied in detail⁽⁷⁰⁾. The pilot plant for production of sulphoxides from Arlan diesel cut with a distillation temperature of 190-360°C by its oxidation in the foam-emulsion regime, followed by extraction with 62% sulphuric acid, has been described⁽⁷¹⁾.

The extraction ability of oil sulphoxides is similar to that of synthetic cyclic sulphoxides and is essentially higher than that of TBP. Samples of sulphoxides, produced from Arlan Oil in various ways from corresponding sulphides with distillation temperatures of 270-350°C, differed only with respect to their sulphoxide sulphur contents (ranging from 2.6-10%), and the extraction ability of the sulphoxides contained in them was the same as deduced from extraction data for uranyl and thorium nitrates⁽¹³⁾. Examples of the possible technological use of oil sulphoxides are the extraction of uranium^(11,13,72), thorium^(11,13,73), zirconium and hafnium^(74,76) and rare earth metals⁽⁷⁷⁻⁸⁰⁾. Examples of detailed studies are the extraction and separation of niobium and tantalum from fluoride-sulphate media⁽⁸¹⁻⁸⁶⁾, the extraction of Mo and W from solutions obtained from hydrochloric acid dissolution of scheelite-powellite concentrate⁽⁸⁷⁾ and the extraction of tellurium from mixed hydrochloric and sulphuric acid solutions⁽⁸⁸⁾. The extraction of Fe, Cu, Cd, In, Ga, Tl, Zn by sulphoxides from hydrochloric acid solutions has been studied⁽⁸⁹⁾. The uses of oil sulphoxides in the technology and the analytical chemistry of noble metals are of great interest^(1-3,11-13,20,90,91). The co-ordination extraction of palladium(II) and probably gold(III) is due to co-ordination of sulphoxides to the metal through the sulphur atom. Therefore, palladium and gold are extracted by sulphoxides much more effectively than by TBP. Pt(II) and Ir(III) are not extracted by sulphoxides, but in the presence of Ce(IV) in the organic phase they can be extracted with simultaneous oxidation to [PtCl₄(R₂SO)₂] or H₂IrCl₆⁽⁹²⁾. Lewis and co-workers⁽⁹¹⁾ suggested a scheme for separation of rhodium, palladium, iridium and platinum, which is based on collective extraction of Pd(II), Pt(IV) and Ir(IV) but not Rh(III) from 6 M HCl with 1 M solution of di-n-heptyl sulphoxide in 1,1,2-trichloro-ethane; water stripping of Pt(IV) and Ir(IV) but not Pd(II) and subsequent separation of Pt(IV) and Ir(III) using the same extractant after iridium reduction. Pt(IV) and Ir(IV) are extracted from 6 M HCl as N₂MeCl₆. For the back-extraction of Pd(II) after water stripping, 10% aqueous dimethylamine solution is proposed. Similarly to derivatives of pyridine-N-oxide⁽⁷⁷⁾, and in contrast with TBP, sulphoxides are capable of extraction from low-acidity nitrate media of hydroxofoms of uranyl^(10,13), and also, of copper, iron, cobalt, nickel, bismuth(III), zirconium, hafnium^(93,95), and from chloride media-arsenic(III)⁽⁹⁶⁾.

The use of undiluted oil sulphoxides can be complicated by their high viscosity. The viscosity of sulphoxides with low aqueous solubilities separated from high-boiling fractions of oil distillates can be over 100 cst. Sulphoxides with a lesser molecular mass are less viscous, but more soluble in water. Thus, they seem to be usable only with high concentrations of non-extracted electrolytes in the aqueous phase, which act as salting-out agents. Using solutions of oil sulphoxides, the careful choice of diluent is often necessary in order to prevent third phase formation. The stability of sulphoxides to oxidation is sufficiently high.

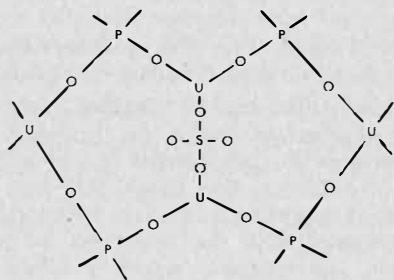
One of the possible fields of usage for oil sulphoxides is their application in synergistic extraction as donors which are more active than TBP. The extraction of trace quantities of rare earth elements^(97,98), uranium(VI)⁽⁹⁹⁻¹⁰¹⁾, iron(II) and of a series of non-ferrous metals⁽¹⁰²⁻¹⁰⁴⁾ by mixtures of B-diketones with dialkyl sulphoxides has been investigated in detail. A new type of synergistic extraction, in which sulphoxides as the donor additive are also more active than TBP, has recently been found in the non-cation-exchange extraction of uranyl sulphate from relatively concentrated aqueous solutions by mixtures of D2EHPA(HX), or its uranyl salt UO₂X₂, with a neutral donor extractant⁽¹⁰⁵⁻¹⁰⁶⁾. In the presence of the neutral

donor, the transfer to the organic phase of UO_2SO_4 , which is usually non-extractable, can take place. More than one molecule of UO_2SO_4 per formula unit of UO_2X_2 can be extracted, thus more than doubling the capacity of the extractant with respect to uranium. The mechanism of uranyl sulphate extraction is peculiar. UO_2X_2 in benzene solution exists as a linear polymer



(oxygen of uranyl are not shown).

The extraction of UO_2SO_4 results from co-ordinate unsaturation of uranyl in the polymeric chain, i.e. UO_2X_2 can be considered as an extractant possessing acceptor properties. According to the data of IR- and NMR-spectroscopy the molecule of UO_2SO_4 in the presence of a donor additive is connected to the links of U(IV) (further {U}) of the polymeric chain forming a bridged sulphate group as shown below:



The donor molecules solvate the binuclear grouping $\text{UO}_2\text{SO}_4\text{UO}_2$ and also some of the unloaded links {U}. At very high concentration of UO_2SO_4 in the aqueous phase, the formation in the extract of three-nuclear groups of $\text{UO}_2\text{SO}_4\text{UO}_2\text{SO}_4\text{UO}_2$ is possible. As a whole, the process, in that range of concentration of UO_2SO_4 in the aqueous phase in which the ratio $\text{UO}_2\text{SO}_4:\text{UO}_2\text{X}_2$ in the extract is not greater than 1, and assuming the independent behaviour of links, can be considered as the competitive adsorption of m molecules of the neutral extractant B, or groups $\text{UO}_2\text{SO}_4\cdot\text{MB}$ on the links {U} of the linear adsorbant, described by Langmuir's isotherm. Such an approach permits quantitative description of the observed extraction isotherms in a wide range of concentrations of UO_2X_2 and B in the organic and UO_2SO_4 in the aqueous phases. At concentrations of $(\text{C}_8\text{H}_{17})_2\text{SO}$ and TBP less than 0.5 M, $n=1$ and $m=0$, with formation constants for {U} $\text{SO}_4\text{UO}_2\text{B}$ being equal to 364 and 114⁽¹⁰⁷⁾. For a concentration range of TBP up to 2 M, it is necessary to take into account adsorption of TBP itself ($m=2$) and groups $\text{UO}_2\text{SO}_4\cdot n\text{TBP}$ with $n=1,2$. Corresponding to the experimental data^(107,108), isotherms of uranium extraction from UO_2SO_4 solutions by mixtures $\text{HX}+\text{B}$ and by HX itself are schematically represented in Figure 1. The range of the new synergistic effect (III) is preceded by well-known⁽¹⁰⁹⁾ ranges of weak antagonism (II) and the usual synergistic effect (I), explained by the formation of $\text{UO}_2(\text{HX})_2\cdot\text{B}$. On the whole, analogous phenomena for uranium extraction by mixtures HX with $(\text{C}_8\text{H}_{17})_2\text{SO}$ or TBP from aqueous solutions of UO_2Cl_2 or $\text{UO}_2(\text{NO}_3)_2$ were observed⁽¹⁰⁸⁾. Similar phenomena may be presumed to occur for extraction of other metals, while sulphates of copper, nickel, cadmium and vanadium by mixtures of HX with sulphoxides of TBP are not extracted.

In evaluating the perspectives for the usage of oil sulphoxides as extractants for metals which, in the final

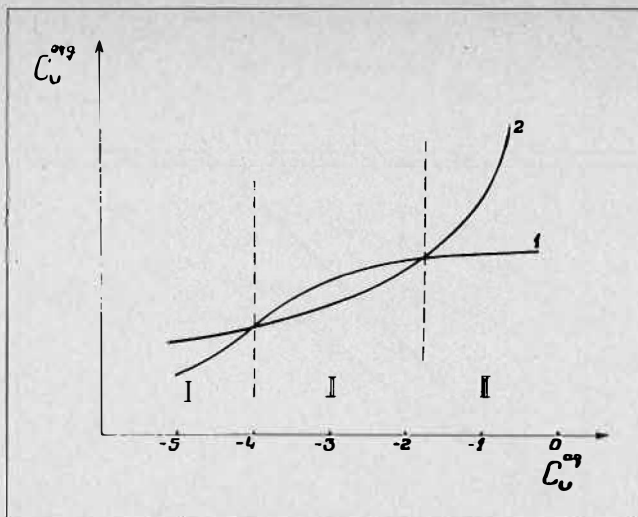


FIGURE 1. Isotherms of uranium extraction from UO_2SO_4 solutions by D2EHPA (1) and its mixture with donor additive (2) (schematically).

analysis, are determined by scales of their production, one should take into account, as well as other possible uses, the ability of oil sulphoxides to extract organic acids and phenols from industrial solutions and wastes⁽¹⁴⁾ and the application of both oil sulphides⁽¹¹⁰⁻¹¹²⁾ and sulphoxides^(114,113) as flotation reagents. In conclusion it should be emphasized that the extraction ability of organic sulphides contained in sulphurous oil of most of the world's deposits, and the oil sulphoxides which can be produced from them, has not yet been investigated.

Amine Oxides

N-oxides of substituted pyridines and tertiary amines have been proposed initially as extractants for uranium (VI)^(5-9,114-116). But the study of extraction by them of great number of elements from various media^(2,3,117-119) and subsequent more detailed investigations have shown that the sphere of their rational application is considerably wider than the initial suppositions. Pyridine-N-oxides (2-nonyl pyridine oxide and 4-(5-nonyl) pyridine oxide are mainly used) are typical co-ordination extractants lying with respect to their extraction ability, between $(\text{RO})_2\text{RPO}$ and RPR_2PO ⁽⁸⁾, and are also capable of the extraction of complex metalloacids by means of a hydrate-solvate mechanism. Amine oxides are much stronger bases and, according to A.M. Rozen and co-workers^(120,121), they react with HNO_3 in a manner similar to amines and R_3AsO with the transfer of the proton to give ion pairs $[\text{R}_3\text{NOH}][\text{NO}_3]$, in contrast with the majority of neutral extractants which form $\text{R}_n\text{XO} \cdots \text{HNO}_3$ by hydrogen bonding. Similarly amine oxides are easily protonated by other acids. So, the extraction by them of U(VI) ^(8,9,120-122), Pu(VI) ⁽¹²²⁾, W(VI) , Mo(VI) , Re(VII) ⁽¹¹⁹⁾, Co(II) ⁽¹²³⁾, Th(IV) ^(118,124), Zr(IV) , Ce(IV) , No(V) ⁽¹¹⁸⁾ at mild acidities is quite close to the extraction by amines themselves. But at low acidity when the extractant is weakly protonated, N-oxides of fatty amines extract U(VI) ^(8,9), Mo , W , Re ⁽¹¹⁹⁾, Co(II) ⁽¹²³⁾ and other metals much more effectively than amines.

Non ion-exchange extraction by amine oxides has often been complicated due to hydrolysis of the extracted salt in the aqueous phase and the transfer of hydrolysis products into the organic phase, so usually the stoichiometry of such processes is not known exactly. Cobalt(II) chloride is extracted by all neutral extractants L from TBP up to R_3NO and R_3AsO in the same form as tetrahedral $[\text{CoCl}_2\text{L}_2]$ ^(123,125,126). The extraction constant of CoCl_2 with solutions of trioctylamine oxide in $n\text{-C}_7\text{H}_{16}$, CCl_4 , C_6H_6

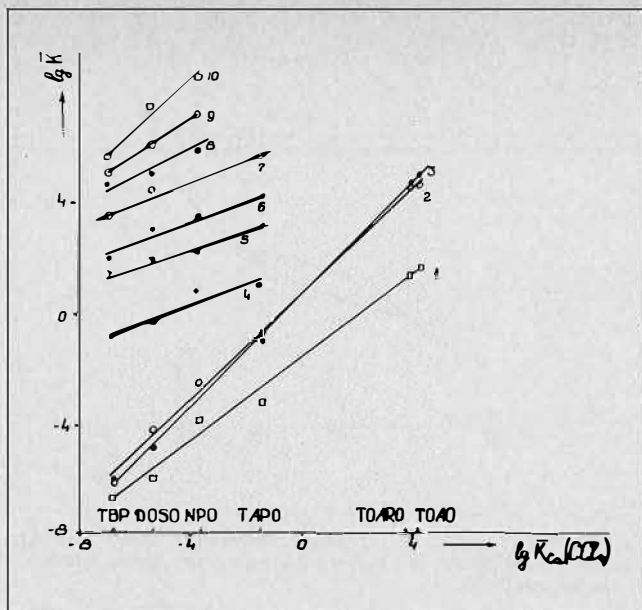


FIGURE 2. Linear correlations of extraction constants at 25°C.

1. $[\text{CoCl}_2\text{L}_2]$, CHCl_3 ;
2. $[\text{CoCl}_2\text{L}_2]$, C_6H_6 ;
3. $[\text{CoCl}_2\text{L}_2]$, $n\text{-C}_7\text{H}_{16}$;
4. $[\text{HNO}_3\text{L}]$, C_6H_6 ;
5. $[\text{HgCl}_2\text{L}]$, C_6H_6 ;
6. $[\text{HgCl}_2\text{L}_2]$, C_6H_6 ;
7. $[\text{HgCl}_2\text{L}_2]$, CCl_4 ;
8. $[\text{UO}_2(\text{NO}_3)_2\text{L}_2]$, CCl_4 ; (1g K + 3);
9. $[\text{UO}_2(\text{NO}_3)_2\text{L}_2]$, C_6H_6 ; (1gK + 3);
10. $[\text{Th}(\text{NO}_3)_4\text{L}_3]$, C_6H_6 ; (1gK + 3).

DOSO = di-n-octyl sulphoxide.

NPO = 2-nonyl pyridine-N-oxide.

TAPO = triisooamyl phosphine oxide.

TOARO = trioctylarsine oxide.

TOAO = trioctylamine oxide.

exceeds the appropriate constant for TBP by approximately 11 orders of magnitude. Thus, in those cases where the extraction is due to co-ordination, trioctylamine oxide, along with trioctylarsine oxide, proved to be the most effective extractants of the R_nXO type. With the use of $\text{R}_3\text{NO HCl}$, instead of N-oxide itself the extraction of CoCl_2 is abruptly reduced. In the absence of HCl in the aqueous phase the effectiveness of CoCl_2 extraction decreases in the series $\text{R}_3\text{NO R}_3\text{N.HCl R}_3\text{NO.HCl R}_3\text{N}^{(123)}$. NiCl_2 is practically not extracted by amine oxides.

Extraction of Fe(III), Ga(III), Ir(III), Au(III) from their solutions in hydrochloric acid by tri-n-laurylamine oxide was studied by Maksimovich et al.⁽¹²⁷⁾. A.I. Mikhailichenko and co-workers⁽⁷⁸⁾ have investigated the extraction of rare earth metals nitrates by a series of extractants R_nXO , including 2-nonyl pyridine and trioctylamine oxides. The co-ordination extraction of HgCl_2 from its aqueous solutions by 2-nonyl pyridine oxide has also been studied⁽¹²⁸⁾.

The ability of 2-nonyl pyridine oxide to extract Ta selectively without Nb from weak nitric acid solutions and Nb without Ta from strong nitric acid solutions is well known and finds numerous applications^(4,11). Extraction of Ta and Nb as well as Zr and many other fission products by 4-(5 nonyl) pyridine and trioctylamine oxides from solutions of nitric, hydrochloric and sulphuric acid had also been studied^(118,129). A procedure for the neutron activation determination of Nb and V in Li and LiOH using their selective extraction by 2-nonyl pyridine oxide has been developed⁽¹³⁰⁾. The selective extraction of V is carried out at pH 2.6-2.8.

Pt(IV) is extracted effectively and with sufficient selectivity from weak nitric or hydrochloric acid solutions by 2-nonyl pyridine oxide. The latter has been applied for matrix removal in the neutron activation determination of admixtures in $\text{Pt}^{(41)}$ and for the neutron activation determination of Pt in ores, minerals and technological products^(50,51).

Trioctylamine oxide effectively extracts W, Mo and Re in the pH ranges 1-6, 1-7 and 1-9 respectively⁽¹¹⁹⁾, i.e. from less acid solutions in comparison with trioctylamine. At 1.5 M HCl, the selective extraction of Re is possible with its separation from Mo and W. The simultaneous extraction of Mo, W, Re from 0.5-1 M HCl is possible using nonyl pyridine oxide. Trioctylamine oxide effectively extracts Mo, W, and Re from solutions which are formed by the dissolution of metals in hydrogen peroxide. The extraction by amine oxides has found an application in the atomic absorption determination of W, Mo and Re in complex technological solutions⁽¹³¹⁻¹³³⁾ and for the matrix removal in the chemicospectral analysis of high purity $\text{Re}^{(134,135)}$.

A great number of investigations on the extraction of trace quantities of uranium^(116,118), thorium^(118,124,136), tungsten^(118,137), niobium and tantalum^(118,129), zirconium^(118,138) and other elements from different media by amine oxides has been carried out by Ejaz. The conditions for extraction separation of many of these elements were found.

Trialkylamine oxides can be obtained easily by oxidation of the appropriate amines by hydrogen peroxide. Technical mixtures of trialkylamines can be also subjected to this type of oxidation. One should take into consideration the gradual degradation of these extractants, even at room temperatures, with the formation of N,N-dialkyl hydroxylamine and alkene-1, especially when stored as diluted dry solutions⁽¹²³⁾. Pyridines are easily oxidized to quite stable pyridine oxides by peracetic acid.

On the Series of Extraction Ability (EA) of Extractants

In this report, in common with most literature on extraction, the concept of a series of increasing EA has often been used. In doing so it was implicitly assumed that the sequence of extractants in the series of increasing EA does not change with changes of the extracted metal and/or the diluent. Such stability of EA series, especially with different reaction centres, under sufficiently wide variations either of extracted salts or diluents and extraction stoichiometry, is required both experimentally and theoretically. For a given extracted salt and a given diluent with an invariant extraction stoichiometry, the natural measure of EA is the effective extraction constant (e.g. for extraction $\text{UO}_2(\text{NO}_3)_2$ in the form of $[\text{UO}_2(\text{NO}_3)_2\text{L}_2]$, the effective extraction constant is determined as $K_4 = C_4 / 4(m^8)^3 C_L^2$, where C_4 and C_L are molar equilibrium concentrations of $\text{UO}_2(\text{NO}_3)_2$ and L in the organic phase). The values of K are only constant and only have a true thermodynamic meaning at low C_L . Experience has shown that the values of log K for different pairs of extracted salt-diluent combinations at invariable stoichiometry of extracted complex, not only form qualitatively the same sequences, but are connected with each other quantitatively by simple linear relationships. In Figure 2 the values of log K for the processes of co-ordination extraction forming $[\text{CoCl}_2\text{L}_2]$ (straight lines (1-3), $[\text{HNO}_3\text{L}]$ (4), $[\text{HgCl}_2\text{L}]$ (5), $[\text{HgCl}_2\text{L}_2]$ (6,7), $[\text{UO}_2(\text{NO}_3)_2\text{L}_2]$ (8,9), $[\text{Th}(\text{NO}_3)_4\text{L}_3]$ (10) in different diluents are plotted against log K for extraction of CoCl_2 in the form of $[\text{CoCl}_2\text{L}_2]$ with diluted solutions of different extractants in CCl_4 . In all cases, in accordance with the general principle of

linearity for free energy relationships, the values of $\log K$ are linearly tied with $\log K$ for the standard reaction. The values of K used for the construction of the plots are taken from (11, 21, 125, 126, 128, 138).

Thus, the EA of the extractants considered can be characterized by only one parameter and is independent of the extracted metal and diluent. In Figure 2 this parameter is $\log K$ for heterogeneous reaction of the formation of $[\text{CoCl}_2\text{L}_2]$ in CCl_4 . However, the linear correlations in Figure 2 can be seen to be due to a linear dependence of $\log K$ in each of the reaction series on some other parameter characterizing the donor strength of the extractants. Various possible parameters are the shift of frequency $\nu_{\text{sym}}(\text{OH})$ in the water molecule due to its interaction with the extractant in the medium of CCl_4 ^(125,126), the energy of the hydrogen bond $\text{XO} \cdots \text{HOH}$ ^(125,126), the basicity constant of the extractants^(120,121) or the donor number of Gutmann⁽¹⁴⁰⁾. The often-used linear correlations between $\log K$ and the sum of the constants of Taft cannot be used in this case owing to changes of reaction center. At the same time the linear correlations discussed are, naturally, applied also to the extractants distinguished merely by substituents at the same reaction center (e.g. $\equiv \text{PO}$):

At present, a rigorous theoretical basis for these linear correlations is absent. Supposing that the solvation energies of the extractant and the extracted complex can be estimated by running the solvation energies of the separate fragments of the molecules^(125,126), one can show that values of $\log K$ within each reaction series differ from $\log K$ for the corresponding reactions in vacuum by an almost con-

stant value. In other words, solvation effects which have a great influence on the values of $\log K$ for different diluents, result in the same alteration of $\log K$ for the whole of the reaction series as compared with values of $\log K$ in vacuum. This is confirmed by the similar slopes of the lines in Figure 2 for reaction series differing only with respect to the diluent (lines 2,3; 6,7 and 8,9). The lower slope of line 1 compared with lines 2,3 is due to the strong interaction of the reaction center and CHCl_3 with the formation of a hydrogen bond $\text{XO} \cdots \text{HCCl}_3$, the hydrogen bond energies increasing as the donor strength of the extractant increases. Thus it may be postulated that the values of $\log K$ for a series in a given diluent, which is incapable of strong interaction with the extractants, differ from $\log K$ for the same series in vacuum by a constant value which varies with its diluent. The most natural measure of the donor ability of the extractant therefore should be to characterize the extractant molecule in vacuum (more precisely, the oxygen atom in the free molecule of extractant).

The change of the nature of chemical bond in the extracted complex even at the same stoichiometry disturbs the linear correlation. So, the data^(120,121) about values of $\log K$ for HNO_3 extraction with solutions of trioctylamine and trioctylarsine oxides in C_6H_6 (10 gK \approx 6) do not lie on the straight line 4. The changes of extraction stoichiometry and simultaneous acid extraction can result in changes in the EA series. So, the distribution coefficients of thorium for extraction from 5.9N Al (NO_3)₃ at pH=1 are increased in the series trioctylamine oxide <TBP <di-n-octyl sulphoxide <2-nonyl pyridine oxide <triisooamylphosphine oxide⁽⁷⁹⁾. Pyridine oxides are often more effective than tertiary amine oxides for extractions from acid media.

REFERENCES

- (1) Nikolaev, A.V., Torgov, V.G., Gil'bert, E.N., Mikhailov, V.A., Pronin, V.A., Stadnikova, L.G., Kotljarevskii, I.L. *Izv. Sib. Otd. Akad. Nauk SSSR, ser. khim. nauk*, 1967, No. 14, vyp.6, 120.
- (2) Nikolaev, A.V., Torgov, V.G., Mikhailov, V.A., Gilbert, E.N., Kotljarevskii, I.L. In book "Metod izotopnykh indikatorov v nauchnykh issledovaniyakh i promyshlennom proizvodstve", Moskva, Atomizdat, 1971, p. 305.
- (3) Nikolaev, A.V., Torgov, V.G., Andrievskii, V.N., Gal'tsova, E.A., Gil'bert, E.N., Kotljarevskii, I.L., Mazalov, L.N., Mikhailov, V.A., Sadovskii, A.P., Cheremisina, I.M., Shatskaja, S.S. In book "Khimija protsessov ekstraktsii", Moskva, "Nauka", 1972, p. 75.
- (4) Gilbert, E.N., Torgov, V.G., Mikhailov, V.A., Artjukhin, P.I., Nikolaev, A.V., *Dokl. Akad. Nauk SSSR*, 1967, 174, 1329.
- (5) Nikolaev, A.V., Torgov, V.G., Mikhailov, V.A., Kotljarevskii, I.L. *Dokl. Akad. Nauk SSSR*, 1964, 156, 616.
- (6) Torgov, V.G., Nikolaev, A.V., Mikhailov, V.A., Korolenok, L.N., Stadnikova, L.G., Kotljarevskii, I.L., *Izv. Sib. Otd. Akad. Nauk SSSR, ser. khim. nauk*, 1964, No. 11, vyp. 3, 95.
- (7) Mikhailov, V.A., Torgov, V.G., *Zh. neorg. khim.*, 1965, 10, 2780.
- (8) Torgov, V.G., Mikhailov, V.A. In book "Ekstraktsija neorganicheskikh veshchestv", Nikolaev, A.V. (Ed.), Sib. Otd. izd-va "Nauka", Novosibirsk, 1970, p. 222.
- (9) Torgov, V.G., Mikhailov, V.A. Startseva, E.A. Nikolaev, A.V., *Dokl. Akad. Nauk SSSR*, 1966, 168, 836.
- (10) Torgov, V.G., Nikolaev, A.V., Mikhailov, V.A., Stadnikova, L.G., Kotljarevskii, I.L. *Zh. neorg. Khim.*, 1968, 13, 228.
- (11) Mikhailov, V.A., Torgov, V.G., Gil'bert, E.N., Mazalov, L.N., Nikolaev, A.V., *Proceedings Intern. Solvent Extraction Conference 1971, Society Chem. Ind., London*, 1971, 2, p. 1118.
- (12) Mikhailov, V.A., Torgov, V.G., chapter VI in book [62].
- (13) Mikhailov, V.A., Torgov, V.G., Nikolaev, A.V., *Izv. Sib. Otd. Akad. Nauk SSSR, ser. khim. nauk*, 1973, No. 7, vyp. 3, 3.
- (14) Nikitin, Ju. E., Murinov, Ju.E., Rozen, A.M. *Uspekhi khimii*, 1976, 45, 1395.
- (15) Nikolaev, A.V., Torgov, V.G., Mikhailov, V.A., Andrievskii, V.N., Bakovets, K.A., Bondarenko, M.F., Gil'bert, E.N., Kotljarevskii, I.L. Mardezova, G.N., Shatskaja, S.S. *Izv. Sib. Otd. Akad. Nauk SSSR, ser. khim. nauk*, 1970, No. 9, vyp. 4, 54.
- (16) Torgov, V.G., Shatskaja, S.S., Mikhailov, V.A., Gubenko, L.E., Andrievskii, V.N., *Izv. Sib. Otd. Akad. Nauk SSSR, ser. khim. nauk*, 1973, No. 7, vyp. 3, 70.
- (17) Mikhailov, V.A., Shatskaja, S.S., Bogdanova, D.D., Torgov, V.G., *Izv. Sib. Otd. Akad. Nauk SSSR, ser. khim. nauk*, 1976, No. 7, vyp. 3, 34.
- (18) Nikolaev, A.V., Mikhailova, M.P., *Izv. Sib. Otd. Akad. Nauk SSSR, ser. khim. nauk*, 1972, No. 12, vyp. 5, 74.
- (19) Pronin, V.A., Usol'tseva, M.V., Shastina, Z.N., Trofimov, B.A., Vjalykh, E.P. *Zh. neorg. khim.*, 1973, 18, 3037.
- (20) Pronin, V.A., Usol'tseva, M.V., Gusakova, N.K., Efremova, G.G., Amosova, S.V., Trofimov, V.A. *Zh. neorg. khim.*, 1977, 22, 171.
- (21) Mikhailov, V.A., Korol, H.A., Bogdanova, D.D. *Izv. Sib. Otd. Akad. Nauk SSSR, ser. khim. nauk*, 1975, No. 14, vyp. 6, 29.
- (22) Shelkovnikova, O.S., Nikolaev, A.V., Novosjолоv, R.I. *Izv. Sib. Otd. Akad. Nauk SSSR, ser. khim. nauk*, 1976, No. 7, vyp. 3, 44.
- (23) Torgov, V.G., Andrievskii, V.N., Gil'bert, E.N., Kotljarevskii, I.L., Mikhailov, V.A., Nikolaev, A.V., Pronin, V.A., Trotsenko, D.D. *Izv. Sib. Otd. Akad. Nauk SSSR, ser. khim. nauk*, 1969, No. 12, vyp. 5, 148.
- (24) Shelkovnikova, O.S., Nikolaev, A.V., Novosjолоv, R.I. *Izv. Sib. Otd. Akad. nauk SSSR, ser. khim. nauk*, 1975, No. 7, vyp. 3, 88.
- (25) Shelkovnikova, O.S., Nikolaev, A.V., Novosjолоv, R.I. *Izv. Sib. Otd. Akad. Nauk SSSR, ser. khim. nauk*, 1976, No. 7, vyp. 3, 98.
- (26) Sinitsyn, N.M., Travkin, V.F., Plotinskii, G.P., Popov, A.A., Mikhailov, V.A., *Izv. Sib. Otd. Akad. Nauk SSSR, ser. khim. nauk*, 1973, No. 7, vyp. 3, 64.
- (27) Judelevich, I.G., Zakharchuk, N.F., Vall, G.A., Torgov, V.G., Korda, T.N., Bikmatova, G.C., Neermolov, A.F. In book "Analiz i tekhnologija blagorodnykh metallov", "Metallurgija", Moskva, 1971, p. 272.
- (28) Gil'bert, E.N., Judelevich, I.G., Mikhailov, V.A., et al. *Orgaganicheskie reagenty v analiticheskoi khimii. Tezisy dokladov III Vsesojuznoi konf.*, Moskva, 1971, p. 219.
- (29) Judelevich, I.G., Vall, G.A., Torgov, V.G., Korda, T.N. *Zh. analit. khimii*, 1970, 25, 870.

- (30) Galanova, A.P., Pronin, V.A., Vall, G.A., Judelevich, I.G., Gil'bert, E.N., Zavodskaja Laboratorija, 1972, 38, 646.
- (31) Galanova, A.P., Kudrjavina, A.K., Pronin, V.A., Judelevich, I.G., Vall, G.A., Gil'bert, E.N., *Izv. Sib. Otd. Akad. Nauk SSSR, ser. khim. nauk*, 1973, No. 7, vyp. 3, 89.
- (32) Lanbina, T.V., Judelevich, I.G., Vasil'eva, A.A., Shelpakova, I.R., Khrapai, V.P., Provodenko, L.B. *Izv. Sib. Otd. Akad. Nauk SSSR, ser. khim. nauk*, 1973, No. 9, vyp. 4, 63.
- (33) Vall, G. A., Usol'tseva, M.V., Pronin, V.A., Shipitsyn, S.A., Skudaev, Ju.D., Judelevich, I.G. *Izv. Sib. Otd. Akad. Nauk SSSR, ser. khim. nauk*, 1974, No. 12, vyp. 5, 71.
- (34) Gil'bert, E.N., Glukhova, G.V., Glukhov, G.G., Mikhailov, V.A., Torgov, V.G., *J. Radioanal. Chem.*, 1971, 8, 39.
- (35) Gil'bert, E.N., Veriovin, G.V., Mikhailov, V.A., *Izv. Sib. Otd. Akad. Nauk SSSR, ser. khim. nauk*, 1975, No. 7, vyp. 3, 102.
- (36) Glukhov, G.G., Larionova, L.A., Gil'bert, E.N., *Izv. Sib. Otd. Akad. Nauk SSSR, ser. khim. nauk*, 1973, No. 7, vyp. 3, 87.
- (37) Gil'bert, E.N., Glukhov, G.G., Larionova, L.A., Mikhailov, V.A., *Izv. Sib. Otd. Akad. Nauk SSSR, ser. khim. nauk*, 1973, No. 7, vyp. 3, 85.
- (38) Zakharchuk, E.N., Bikmatova, G.S., Judelevich, I.G., *Zavodskaja Laboratorija*, 1971, 37, 530.
- (39) Gornostaeva, T.D., Pronin, V.A., *Zh. analit. khim.*, 1971, 26, 1736.
- (40) Nikolaev, A.V., Judelevich, I.G., Vall, G.A., Torgov, V.G. *Izv. Sib. Otd. Akad. Nauk SSSR, ser. khim. nauk*, 1974, No. 14, vyp. 6, 93.
- (41) Gil'bert, E.N., Veriovin, G.V., Semenov, V.I., Mikhailov, V.A. *Proceeding 1976 Intern. Conference "Modern Trends in Activation Analysis"*, 1976, Vol. II, München, p. 900.
- (42) Judelevich, I.G., Vall, G.A., Torgov, V.G., Korda, T.N. *Zh. analit. khim.*, 1971, 26, 1550.
- (43) Khlebnikova, A.A., Torgov, V.G. *Zh. analit. khim.*, 1976, 31, 1090.
- (44) Gornostaeva, T.D., Pronin, V.A., Mikhailov, V.A., *Izv. Sib. Otd. Akad. Nauk SSSR, ser. khim. nauk*, 1972, No. 4, vyp. 2, 89.
- (45) Gil'bert, E.N., Shatskaja, S.S., Mikhailov, V.A., Torgov, V.G., *J. Radioanal. Chem.*, 1973, 14, 279.
- (46) Vall, G.A., Shatskaja, S.S., Judelevich, I.G., Torgov, V.G., *Izv. Sib. Otd. Akad. Nauk SSSR, ser. khim. nauk*, 1973, No. 12, vyp. 5, 88.
- (47) Balandina, N.S., Judelevich, I.G., Khrapai, V.P., Abakumov, D.N., *Izv. Sib. Otd. Akad. Nauk SSSR, ser. khim. nauk*, 1973, No. 12, vyp. 5, 93.
- (48) Gil'bert, E.N., Veriovin, G.V., Bochkarev, B.N., Godovikov, A.A., Mikhailov, V.A., Zavoronkov, V.Ya., *J. Radioanal. Chem.*, 1975, 26, 253.
- (49) Gornostaeva, T.D., Pronin, V.A., *Zh. analit. khim.*, 1975, 30, 1139.
- (50) Gil'bert, E.N., Veriovin, G.V., Mikhailov, V.A., *J. Radioanal. Chem.*, 1976, 31, 365.
- (51) Gil'bert, E.N., Veriovin, G.V., Mikhailov, V.A., Antipov, N.I., Nikitin, V.N. *Proceedings 1976 Intern. Conf. "Modern Trends in Activation Analysis"*, München, 1976, Vol. II, p. 836.
- (52) L.R.M. Pitombo *Anal. Chem. Acta.*, 1969, 46, 158.
- (53) L.R.M. Pitombo *Anal. Chem. Acta.*, 1973, 62, 103.
- (54) *Vsesojuznoe soveshanie po khimii, analizu i tekhnologii blagorodnykh metallov. Tezisy dokladov. Part 2, Novosibirsk*, 1976.
- (55) Shvirin, G.N., Laskorin, B.N., Shvirina, E.M., Kuzmichjov, G.V., *Tsvetnye metally*, 1966, 7, 11.
- (56) Athavall, V.T., Kornik, N.V., et al, *Ind. J. Chem.*, 1967, 5, 585.
- (57) Chia-Lien Tseng. *Radiochem. and Radioanal. Letters*, 1976, 26, 165.
- (58) Nikolaev, A.V., Torgov, V.G., Mikhailov, V.A., Andrievskii, V.N., Bakovets, K.A., Bondarenko, M.F., Kotljarevskii, I.L., Mardezova, G.A., Shatskaja, S.S. *Izv. Sib. Otd. Akad. Nauk SSSR, ser. khim. nauk*, 1970, No. 9, vyp. 4, 54.
- (59) Chizhikov, D.M., Kreingauz, B.P., Denisova, G.M. *Izv. Sib. Otd. Akad. Nauk SSSR, ser. khim. nauk*, 1970, No. 9, vyp. 4, 120.
- (60) Torgov, V.G., Shatskaja, S.S., Mikhailov, V.A., Bondarenko, M.F., Pais, M.A., Nasonova, L.I. *Izv. Sib. Otd. Akad. Nauk SSSR, ser. khim. nauk*, 1973, No. 7, vyp. 3, 79.
- (61) Karaulova, E.N. *Khimija sul'fidov nefti*, "Nauka", Moskva, 1970.
- (62) Chertkov, Ja.B., Spirkin, V.G. *Sernistye i kislородnye soedinenija neftjanykh distillatov*, "Khimija", Moskva, 1971.
- (63) Rall, H.T., Thompson, C.J., Coleman, U.J., Hopkins, R.L. *Sulfur compounds in crude oil*. U.S. Bur Mines, Bull. 659, Washington, 1972.
- (64) Gal'pern, G.D. *Uspekhi khimii*, 1976, 45, 1395.
- (65) Bondarenko, M.V., Lapina, N.K., Nikitin, Ju.E., Sharipov, A.H., Zagretskaja, L.M., Nikitina, V.S., Pais, M.A., *Izv. Sib. Otd. Akad. Nauk SSSR, serija khim. nauk*, 1973, No. 7, vyp. 3, 16.
- (66) Parfjonova, M.A., Brodskii, E.S., Zimina, K.I., Lapina, N.K., Nikitina, V.S., Kakabekov, G.G., Simeonov, A.A., Kalamishvili, E.M. *Neftekhimija*, 1975, 15, 902.
- (67) Mikhailov, V.A., Shatskaja, S.S., Torgov, V.G., Antipov, I.I. In book "IX Vsesojuznoe soveshanie po khimii, analizu i tekhnologii blagorodnykh metallov. Tezisy dokladov", Krasnojarsk, 1973, p. 43.
- (68) Nikitin, Ju.E., Murinov, Ju.I., Ben'kovskii, V.G., Lapina, N.K., Antipov, N.I., Boldov, V.I., Vlasov, P.S., Ivanov, A.K., Bulantsev, V.V., Mikhailov, V.A. *Avtorskoe svidetel'stvo SSSR No. 397514; Bjull. izobr.*, 1974, 37, 55.
- (69) Zagretskaja, L.M., Masagutov, R.M., Sharipov, A.H., Bondarenko, M.F., Burmistrova, T.P., Latypov P.Sh., Khitrik, A.A., Kireeva, Z.A., *Neftekhimija*, 1974, 14, 765.
- (70) Khitrik, A.A., Latypov, R.Sh., Burmistrova, T.P., Gal'pern, G.D., Karaulova, E.N., Bardina, T.A., *Neftekhimija*, 1976, 16, 280.
- (71) Masagutov, R.M., Sharipov, A.H., Bondarenko, M.F., Burmistrova, T.P., Latypov, R.Sh., Khitrik, A.A., Zotov, A.D., Zemtsov, V.P., Smertin, G.I., Ismagilov, F.R. *Izv. Sib. Otd. Akad. Nauk SSSR, ser. khim. nauk*, 1973, No. 7, vyp. 3, 23.
- (72) Mohanty, S.R., Reddy, A.S., *J. inorg. nucl. Chem.*, 1975, 37, 1791.
- (73) Mohanty, S.R., Reddy, A.S., *J. inorg. nucl. Chem.*, 1975, 37, 1977.
- (74) Tsylov, Ju.A., Reznik, A.M., Shistenko, N.A., Vasil'eva, Z.S. *Izv. VUZ'ov. Khimija i khimicheskaja tekhnologija*, 1976, 19, 269.
- (75) Tsylov, Ju.A., Reznik, A.M., Turanov, A.N. *Zh. prikladn. khim.* 1976, 49, 201.
- (76) Tsylov, Ju.A., Reznik, A.M., Turanov, A.N. *Izv. VUZ'ov. Khimija i khimicheskaja tekhnologija*, 1976, 19, 1079.
- (77) Mikhailichenko, A.I., Sokolova, N.P., Sulaimankulova, S.K. *Zh. neorg. khim.*, 1973, 18, 2198.
- (78) Mikhailichenko, A.I., Kotliarov, R.V., Sokolova, N.P., Abramov, L.A., *Proc. Intern. Solvent Extraction Conf. 1974, Soc. Chem. Ind., London, 1974, Vol. 2, p. 1059*.
- (79) Mikhlin, E.B., Rozen, A.M., Norina, T.M., Nikonov, V.I., Afonina, T.A. *Zh. neorg. khim.*, 1976, 21, 1858.
- (80) Norina, T.M., Mikhlin, E.B., Nikonov, V.I., Afonina, T.A. *Nauchnye trudy Giredmeta, Moskva, "Metallurgija"*, 1976, 69, 40.
- (81) Nikolaev, A.I., Babkin, A.G., Mai'orov, V.G., Chistjakov, B.E., *Izv. Sib. Otd. Akad. Nauk SSSR, ser. khim. nauk*, 1973, No. 7, vyp. 3, 26.
- (82) Nikolaev, A.I., Babkin, A.G., Mai'orov, V.G., *ibid.*, p. 32.
- (83) Golovachova, T.S., Startsev, V.N., Novokshonova, V.D., Nikitin, Ju.E., Jankovskaja, N.V., *ibid.*, p. 36.
- (84) Chernjak, A.S., Smirnov, G.I., Bobrova, A.S., Mikhailov, V.A., Torgov, V.G., Druzhina, G.Ja., Kostromina, O.N., *ibid.*, p. 42.
- (85) Nikolaev, A.I., Il'in, E.G., Spivakov, M.N., Babkin, A.G., Zolotov, Ju.A., Scherbakova, M.N., *Zh. neorg. khim.*, 1975, 20, 194.
- (86) Nikolaev, A.I., Babkin, A.G., In book "Khimija i tekhnologija mineral'nogo syr'ja. Apatity", 1975, p. 60.
- (87) Mikhailov, V.A., Gil'bert, E.N., Torgov, V.G., Palant, A.A., Reznichenko, V.A., Shapiro, K.Ju., Rybakov, V.N., Penchalov, V.A. *Izv. Sib. Otd. Akad. Nauk SSSR, ser. khim. nauk*, 1973, No. 7, vyp. 3, 48.
- (88) Golovachova, T.S., Startseva, V.N., Judanova, N.V., Nikitin, Ju.E., *ibid.*, p. 55.
- (89) Nikitin, Ju.E., Mineeva, N.Z., Murinov, Ju.I., Rozen, A.M., *Zh. neorg. khimii*, 1976, 21, 3009.
- (90) Nikolaev, A.V., Torgov, V.G., Andrievskii, V.N., Gal'tsova, E.A., Gil'bert, E.N., Kotljarevskii, I.L., Masalov, L.L., Mikhailov, V.A., Cheremisina, I.M., *Zh. neorg. khim.*, 1970, 15, 1336.
- (91) Lewis, P.A., Movris, D.F.C., Short, E.L., *J. of the Less-Common Metals*, 1976, 45, 194.
- (92) Shelkovnikova, O.S., Nikolaev, A.V., Novosiolov, R.I., *Izvesija Sib. Otd. Akad. Nauk SSSR, ser. khim. nauk*, 1975, No. 12, vyp. 5, 50.

- (93) Nikitin, Ju.E., Murinov, Ju.I., Rozen, A.M., Abramova, A.A., *Izv. Sib. Otd.Akad.Nauk SSSR, ser.khim.nauk*, 1973, No. 7, vyp.3, 59.
- (94) Nikitin, Ju.E., Murinov, Ju.I., Rozen, A.M., Abramova, A.A., *Zh. neorg. khim.* 1973, 18, 765.
- (95) Nikitin, Ju.E., Afzaletdinova, N.G., Murinov, Ju.I., *Zh. neorg. khimii*, 1975, 20, 1950.
- (96) Nikitin, Ju.E., Kuvatov, Ju.G., *Zh. neorg.khim.*, 1976, 21, 2184.
- (97) Sekine, T., Dyrssen, D., *J. inorg. nucl. Chem.*, 1967, 29, 1481.
- (98) Augystson, J.H., Farbu, L., Alsted, J., *J.inorg.nucl. Chem.*, 1975, 37, 1243.
- (99) Subramanian, M.S., Viswanatha, A., *J.inorg.nucl.Chem.*, 1969, 31, 2575.
- (100) Subramanian, M.S., Pai, S.A., *J.inorg.nucl.Chem.*, 1970, 32, 3677.
- (101) Subramanian, M.S.; Pai, S.A., *Austr. J. of Chem.*, 1973, 26, 77.
- (102) Burgett, C.A., *Anal. Chem. Acta.*, 1973, 67, 325.
- (103) Burgett, C.A., *J. Chromatogr. Sci.*, 1973, 11, 611.
- (104) O'Laughlin, J.W., O'Brien, T.P., *Talanta*, 1975, 22, 587.
- (105) Mikhailov, V.A., Torgov, V.G., Us, T.V., *Dokl. Akad. Nauk SSSR*, 1974, 214, 1121.
- (106) Mikhailov, V.A., Torgov, V.G., Us, T.V., *Izv. Sib. Otd. Akad. Nauk SSSR, ser.khim.nauk*, 1974, No. 14, vyp. 6, 67.
- (107) Torgov, V.G., Us, T.V., Bogdanova, D.D., Mikhailov, V.A., *Izv. Sib.Otd.Akad.Nauk SSSR, ser.khim.nouk*, 1976, No. 9, vyp. 4, 74.
- (108) Torgov, V.G., Us, T.V., Mikhailov, V.A., Nikolaev, A.V., *Dokl. Akad. Nauk SSSR*, 1976, 227, 635.
- (109) Markus, Y., Kertes, A.S., *Ion Exchange and Solvent Extraction of Metal Complexes*, London, N.-Y.,-Sydney, Toronto. Wiley Interscience, 1969.
- (110) Chistjakov, B.E., Chapter VII in book [62].
- (111) Sokolova, E.S., Solozhenkin, P.M., *Izv. Sib. Otd. Akad. Nauk SSSR, ser. khim. nauk*, 1973, No. 7, vyp. 3, 96.
- (112) Chistjakov, B.E., Oleinikov, N.A., Chertkov, B.Ja., Spirkin, V.G., *ibid.*, p. 100.
- (113) Bocharov, V.A., Bagina, L.I., Ruchkin, I.I., Nikitin, Ju.E., Kapina, A.P., Sharipov, A.H., *ibid.*, p. 93.
- (114) Rusic, R.G., Maksimovic, Z.B., *Proc. Intern. Solvent Extraction Conf. 1971*, Soc. of Chem. Ind., London, 1971, vol. 2, p. 1180.
- (115) Maksimovic Z.B., Rusic R.G., *J. inorg nucl. Chem.*, 1972, 34, 1031.
- (116) Ejaz, M. *Separation Science*, 1975, 10, 425.
- (117) Leen, H.R., Vries, G.D., Brinkman, H.A.T. *J. Chromatogr.*, 1971, 57, 173.
- (118) Ejaz, M., Carswell, D.J., *J.inorg.nucl.Chem.*, 1975, 37, 233.
- (119) Torgov, V.G., Gil'bert, E.N., Mikhailov, V.A., Shaburova, V.P., *Izv. Sib.Otd.Akad.Nauk SSSR, ser.khim. nauk*, 1976, No. 9, vyp. 4, 69.
- (120) Rozen, A.M., Nikolotova, Z.I., Kartashova, N.A., *Dokl. Akad. Nauk SSSR*, 1973, 209, 1369.
- (121) Rozen, A.M., Denisov, D.A., *Radiokhimiya*, 1974, 16, 686.
- (122) Kennedy, J.K., Perkins, R., *J.inorg.nucl.Chem.*, 1964, 26, 1601.
- (123) Torgov, V.G., Bakovets, K.A., Mardezova, G.A., Drozdova, M.K., Mikhailov, V.A., *Izv.Sib.Otd.Akad.Nauk SSSR, ser.khim.nauk*, 1974, No. 7, vyp. 3, 70.
- (124) Ejaz, M., *Talanta*, 1976, 23, 193.
- (125) Torgov, V.G., Mikhailov, V.A., Drozdova, M.K., Mardezova, G.A., Gal'tsova, E.A., *Proc. Intern. Solvent Extraction Conf. 1974*, Vol. 1, Soc. Chem. Ind., London, 1974, p. 849.
- (126) Torgov, V.G., Drozdova, M.K., Mikhailov, V.A., Mardezova, G.A., Gal'tsova, E.A., Jumatov, V.D., *Izv. Sib. Otd. Akad. Nauk SSSR, ser. khim. nauk*, 1975, No. 7, vyp. 3, 78.
- (127) Maksimovic, Z.B., Ruvaras, A.Lj., Halasi, R., *Proc. Intern. Solvent extraction Conf. 1974*, Soc. of Chem. Ind., London, 1974, Vol. 2, p. 1937.
- (128) Mikhailov, V.A., Korol, H.A., Bogdanova, D.D., XII Vsesojuznoe Chugaevskoe soveshanie po khimii kompleksnykh soedinenii. Tezisy dokladov., Novosibirsk, 1975, Part 1, p. 104.
- (129) Ejaz, M., *Anal. Chem. Acta*, 1976, 81, 149.
- (130) Gil'bert, E.N., Glukhov, G.G., Mescherjakov, R.P., Mikhailov, V.A., Torgov, V.G., *Radiochem. Radioanal. Letters*, 1973, 15, 33.
- (131) Judelevich, I.G., Schabyrova, V.P., Torgov, V.G., *Vortrage der VII Hüttenmännischen Materialprufentagung, Balatonszeplek*, 1973, B II, S 35.
- (132) Judelevich, I.G., Schabyrova, V.P., Torgov, V.G., *Sib. Otd. Akad. Nauk SSSR, ser.khim.nauk*, 1973, No. 4, vyp. 2, 79.
- (133) Udelevich, I.G., Shaburova, V.P., *Chem. analit.*, 1974, 19, 941.
- (134) Shaburova, V.P., Judelevich, I.G., Torgov, V.G., Koljarevskii, I.L., *Zh. analit. khim.*, 1971, 26, 930.
- (135) Judelevich, I.G., Shaburova, V.P., Torgov, V.G., Scherbakova, O.I., *Zh. analit. khim.*, 1973, 28, 1049.
- (136) Ejaz, M., *Mikrochim. Acta*, 1976, 6, 643.
- (137) Ejaz, M., *Anal. Chem. Acta*, 1974, 71, 383.
- (138) Ejaz, M., *Anal. Chem.*, 1976, 48, 1158.
- (139) Mikhailov, V.A., Korol, N.A., Bogdanova, D.D., *Proc. Intern. Solvent Extraction Conf. 1974*, Vol. 3, Soc. Chem. Ind., London, 1974, p. 2745.
- (140) Gutmann, V., *Coordination Chemistry in Non-Aqueous Solutions*, Springer-Verlag, Wien, New York, 1968.

DISCUSSION

M. Elguindy: Please comment on the mechanism involved and the species extracted using sulphides and compared with sulphoxides.

V. Mikhailov: I think that it is more preferable to talk about extraction stoichiometry but not extraction mechanism when one deals with compositions of main species in organic phase. The sulphides and sulphoxides are co-ordination extractants and extract metals mainly in the form of non-electrolytic co-ordination compounds, though at high acidities sulphoxides can extract metallo-acids also. The species forming in the organic phase of sulphoxide extraction are similar to those with TBP. As for the sulphides, the most important species forming on extraction of gold (III), palladium (II) from hydrochloric acid media and silver (I) from nitric acid media or from silver nitrate aqueous-solutions are $[\text{AuCl}_3(\text{R}_2\text{S})_2]$, $[\text{PdCl}_2(\text{R}_2\text{S})_2]$ and $[\text{AgNO}_3(\text{R}_2\text{S})_2]$. At high metal concentrations a number of polymers can be formed in organic phases.

R.I. Edwards: We have found it possible to separate Au(III) and Pd(II) by kinetic effects. One way in which this can be done is to use a dialkyl sulphide with bulky alkyl groups. This slows down the rate of Pd

(II) extraction sufficiently so that a clean separation can be obtained by limiting contact time.

Are mercaptans removed from oil sulphides when they are used for commercial application in Au, Pd extraction?

With a complex mixture of sulphides: (a) is Pd(II) extraction slow or much faster than with a long-chain dialkyl sulphide (b) are such mixtures as selective for Pd(II) against Pt(II) as pure long-chain dialkyl sulphides?

V. Mikhailov: Special operations for mercaptan removal were not used but mercaptan concentration in Arlan oil is low. We did not study in detail the kinetics of palladium (II) extraction by oil sulphides and dialkyl sulphides. Our experience shows that in both cases first all the palladium is extracted in a few minutes but a true extraction equilibrium is not reached for days. We have not noticed a big difference in extraction rates and palladium (II) extraction selectivity between oil sulphides and pure dialkyl sulphides.

S. Dhara: Would you please tell me what is the number of carbon atoms in the alkyl radicals in dialkyl sulphides and dialkyl sulphoxides? As you mentioned in

your paper that those solvents are excellent in selective separation of Au, Pd, Ag, and Pt, would you please comment if it is possible for individual selective extraction from each other using these reagents? How is it possible to extract Ag from HCl acid using SX technique?

V. Mikhailov: Usually we employed dibutyl or dioctyl sulphide and dioctyl sulphoxide. The extraction properties of dialkyl sulphides and dialkyl sulphoxides with 4-8 carbon atoms in the alkyl radical are approximately the same but dibutyl sulphoxide is soluble in water in a noticeable quantity. Dialkyl sulphides and oil sulphides are powerful and selective extractants for the separation of Au(III) + Pd(II) from hydrochloric acid media or Au(III) + Pd(II) + Ag(I) from nitric acid media from all other metals. Platinum(IV) is extracted by them with small distribution coefficients and, very slowly though, from sulphuric acid media. It can be transferred into the organic phase together with Pd(II). As to the individual selective extraction of noble metals, dialkyl sulphides or oil sulphides extract from nitric acid media gold(III) and palladium(II) but not silver (I), so one can use sulphoxide extraction to separate Au and/or Pd from Ag. Sorry, but I have said nothing about silver extraction from hydrochloric acid media since sulphides and sulphoxides seem not to be useful for this purpose. Silver can be extracted from such media by amines, for example, and perhaps by N-oxides of amines.

T.K. Kim: What kind of selectivity is there for Nb, Ta, W, Mo, Re, Pt with N-oxides of tertiary aliphatic amines?

V. Mikhailov: The distribution coefficients of metal extraction by N-oxides of tertiary aliphatic amines are greatly influenced by acidity of aqueous phase and the nature of acid. For example, tri-octylamine oxide extracts Re from 1.5M HCl without Mo and W, but from sulphuric acid media all three metals are extracted together. But such separations can be made with amines themselves, since in more acid range, the extraction properties of amine and amine oxides are similar. Therefore, more important is the ability of amine oxides to extract W, Mo and Re from aqueous solutions with higher pH than it is possible using amines. As for Nb-Ta separation and Pt(IV) extraction, it seems to be better to use for this purpose, 2-nonyl pyridine oxide.

K. Lewis: For the extraction of uranium from acidic medium, how does the synergic effect of sulphoxide and di (2-ethylhexyl) phosphoric acid compare with the well known one of TOPO and di (2-ethylhexyl) phosphoric acid?

V. Mikhailov: Indeed, the synergistic effect of cation-exchange uranium extraction at the small uranium concentration in aqueous phase (field I in Figure 1) is well known. In this field sulphoxides are less active donor additives than TOPO. As to the discussed new synergistic effect which appeared as uranyl sulphate extraction in the field of high uranyl sulphate concentration in aqueous phase (field III in Figure 1), the quantitative comparison with TOPO is complicated by depolymerisation of UO_2X_2 in the presence of the latter and by a bigger yield in total uranyl sulphate concentration in the organic phase due to uranyl sulphate extraction by TOPO itself.

Chapter 2

Organic Reagents

Sessions
5, 7 and 26

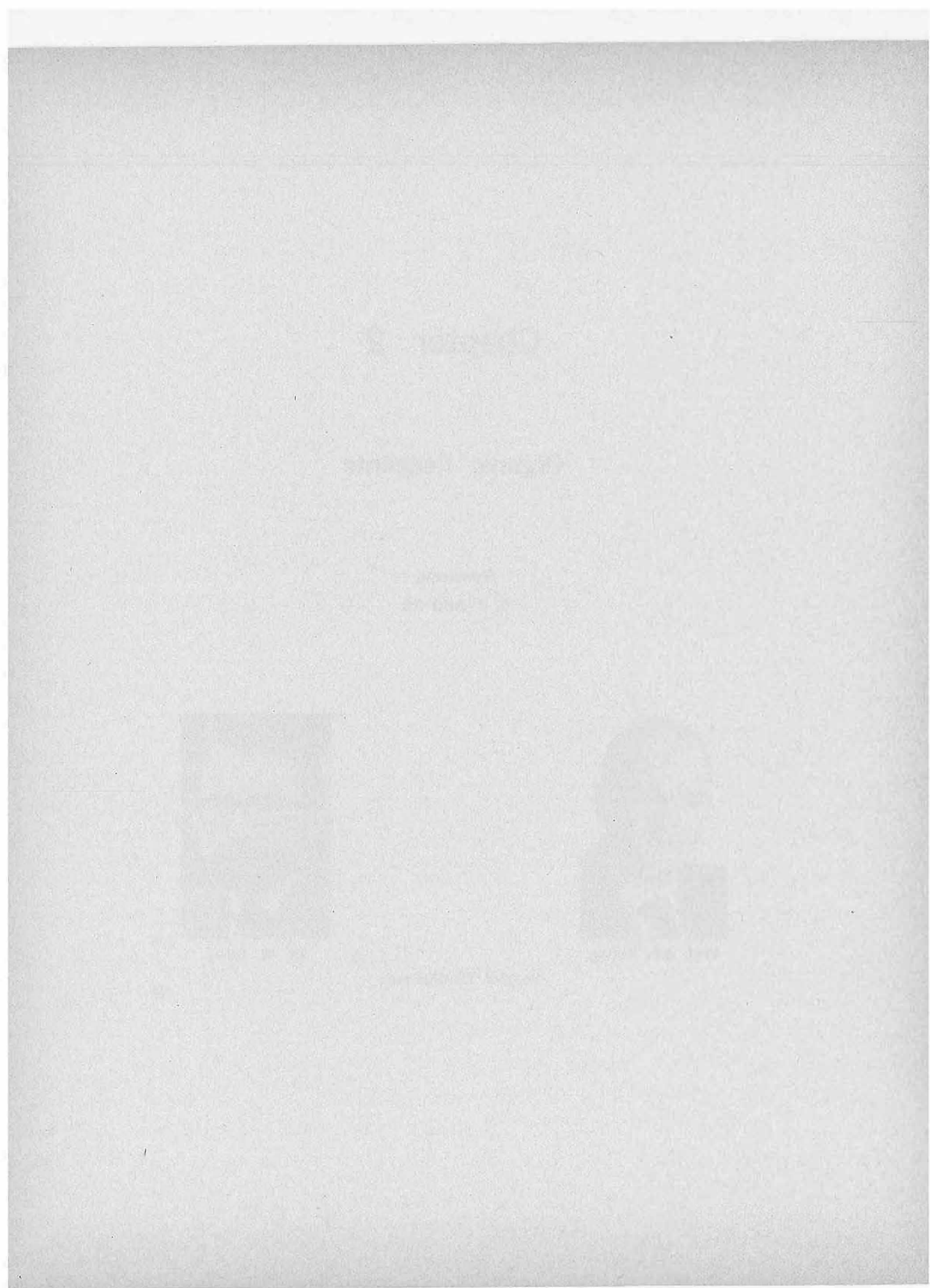


Prof. A.S. Kertes



Dr. W. Sowa

Session Co-Chairmen



The Significance of Surface Activity in Solvent Extraction Reagents

M. Cox, School of Natural Sciences, The Hatfield Polytechnic, Hatfield, Hertfordshire, U.K.

D.S. Flett, Warren Spring Laboratory, Stevenage, Hertfordshire, U.K.

SUMMARY

The interfacial activity of solvent extraction reagents for metal extraction has been reviewed in terms of interfacial tension, interfacial potential and interfacial viscosity. The main classes of extractants have been considered and the available data discussed and interpreted in terms of extraction kinetics, complex stoichiometry, interactions between extractants, diluent modifiers, diluent effects and interfacial pH. A combination of interfacial tension and potential measurements are concluded to be of major significance in the mechanistic understanding of the interfacial chemistry of such extraction systems but interfacial viscosity measurements seem to be of somewhat less value.

Introduction

SOLVENT EXTRACTION REAGENTS by their very nature will be molecules which possess both hydrophilic and hydrophobic properties. Their polar hydrophilic groupings are necessary to interact with the metal ions or complexes in the aqueous phase to give species which will be soluble in the organic or oil phase. The hydrophobic character provided by the organic part of the reagent molecule is required to maximise this solubility of the metal complex and also to reduce the aqueous solubility of the reagent itself thus minimising reagent losses to process raffinate. Such compounds will clearly exhibit interfacial activity at the oil-water interface and the addition of these extraction reagents to an oil-water system will therefore modify these interfacial properties, for example, lowering the interfacial tension and thereby facilitating the dispersion of these two phases. In addition, if appreciable adsorption of the reagent takes place at the interface then the interfacial concentration will exceed the bulk concentration of the reagent. The size of this interfacial excess concentration will depend on the interfacial activity of the reagent, its molecular geometry, the bulk concentration and the nature of the diluent. These properties are not totally independent in that the degree of solvency of the reagent by the diluent will influence the bulk concentration at which the interface will become saturated with a monolayer of reagent. It is too simplistic to envisage an interface as a plane surface so the interface in such systems might be defined as that interfacial volume wherein extractant molecules are preferentially adsorbed due to specific interaction with the aqueous phase which results in a preferred orientation of extractant molecules and wherein the population density of such molecules is influenced by their molecular geometry.

It is unlikely that interfacial properties of reagents will have a significant effect on the equilibrium parameters of an extraction process as they are dependent on bulk phase properties of the system. However, when rates of extraction processes are considered, these are dependent upon the concentration of species at or close to the reaction site.

Therefore, in solvent extraction systems, if bulk phase reactions are excluded or considered to be of minimal importance, then the reaction site must be the interface itself or a zone close to the interface in the aqueous or organic phase. In these regions there is a regime of concentration variation at a level greater or less than the bulk phase concentration depending on the reaction type and the species being considered. It is therefore expected that interfacial activity of reagents should correlate with extraction kinetics and it is important in the fundamental study of the mechanism of solvent extraction processes that the interfacial activity of the reagents used should be considered.

Interfacial activity can be demonstrated in several physico-chemical areas of which interfacial tension, interfacial potential and interfacial viscosity are the most common.

Interfacial Tension

Of these three parameters interfacial tension is the easiest to measure and thus provides most of the available data on solvent extraction systems. This phenomenon arises from the tendency of the interface formed between the two immiscible liquids to contract in a similar way to that observed in the surface tension at a air-liquid interface. Addition of a surface-active third component into the system, e.g. by dissolution into the oil phase, will cause the interfacial surface to be penetrated by any hydrophilic groups so that the contractile tendency of the interface will be reduced by the repulsion between these groups. The size of this reduction is a function of reagent type and concentration and may lead in particular cases ultimately to the formation of a single phase when the interfacial tension is reduced to zero. The criterion of immiscibility between the two phases is very important and it has been shown that even in the case of long-chain aliphatic hydrocarbons the water solubility produces a significant reduction in the equilibrium interfacial tension from the instantaneous reading⁽¹⁾. Thus in all measurements of interfacial tension the two phases should be mutually equilibrated.

Experimental Methods of Measuring Interfacial Tension

In principle all methods for measuring surface tension (air-liquid) are applicable to interfacial tension. In practice the assumption that the contact angle between the liquid-liquid-solid should be zero, i.e. $\cos \theta = 1$, is less likely to be true than in air-liquid-solid systems; thus, methods independent of contact angle are more preferable for interfacial tension. Because the viscosity of liquids is greater than that of gases, methods which involve movement of phases during the measurement are also less suitable for interfacial than surface tension. The most popular experimental methods are those involving the pendant drop, drop-weight or volume, du Nouy ring tensiometer and Wilhemy plate. All these techniques are simple to use but have inherent difficulties both in theory and practice.

Thus in the pendant drop method, which is based on the elongation of a drop hanging in the second liquid from an accurately ground capillary tip, difficulties arise in measurement of this elongation. It is recommended that recording is carried out photographically using a distortion-free optical system, which can be expensive. The very widely used drop weight or drop volume method has to be used with correction tables to adjust the volume/weight recorded to a true reading⁽²⁾. This is because if the liquid forming the drop wets the surface of the capillary tip the resulting drop on detachment is too large, and if the liquid does not wet the tip the drop is too small. Also the size of drop is a function of the time it takes to form. Thus in practice the drop is formed to 95% of its volume quickly and then completed very slowly so that the drop is at equilibrium when it detaches. It is also necessary to ensure that the surface of the drop is at equilibrium with its surroundings in that the adsorption of the surfactant is complete. In a recent study of the drop weight method for surface tension it was found that a 10 second drop time was appropriate for the measurement of carboxylic acids at air-water surface⁽³⁾. These methods using drops generate a new interface for each drop and this should be remembered if surface ageing effects or very slow attainment of surface equilibrium is suspected.

Methods in common use which employ an aged surface are the du Nouy ring tensiometer and Wilhemy plate. Both devices are often included in manufactured tensiometers and because they are relatively easy to operate are often used when a few results are required. However, in spite of the deceptively simple visible phenomena large errors can be involved, with, in particular, the du Nouy ring, when measuring surfactant solutions. One of the disadvantages of the ring is that the contact angles on the inside and outside of the ring may not be identical, and that as the ring is raised from the interface, surfactant may drain away from the ring as the interface is distorted. A modification replacing a straight single wire for the ring has been recommended to overcome the difficulty of varying contact angles⁽⁴⁾ when measuring surfactant solutions. Another problem concerns the rate of withdrawal of ring from the interface which will affect the magnitude of the measured interfacial tension. A rigorous theoretical treatment of the ring tensiometer together with correction tables for particular ring dimensions has been published⁽⁵⁾. However ring tensiometer data can have useful comparative value.

Some of these problems can be overcome by using the Wilhemy plate, where a thin plate is suspended from a balance through the interface. By suitable treatment the plate can be made to have a zero contact angle with either the water or oil phases. This apparatus relies on a true equilibrium system and so is favoured over the du Nouy ring, which ruptures the interface in cases where the surface is slow to reach or regain its equilibrium value⁽⁶⁾. Very good accounts of the various methods and their limitations are given by Bikerman⁽⁷⁾ and by Pugachevich⁽⁸⁾. The latter author recommends a maximum bubble pressure method as this does not involve any dependence on contact angle. He also draws attention to the difficulties which may arise with other methods when addition of another component may change a liquid from a non-wetting species to one which wets the test surface during the course of an experiment.

General Results

The interfacial tension of an oil-water system consisting of pure liquids is reduced by the addition of a surface-active material to one of the phases. The magnitude of

this reduction is a function of the bulk concentration of the surfactant and a smooth curve of interfacial tension, γ , against concentration is found. But in the presence of an inactive material no change of interfacial tension is found.

From these plots the interfacial concentrations of the adsorbed species, so important for interpretation of heterogeneous kinetics, can be determined by means of the Gibbs' adsorption isotherm, which has recently been verified for oil-water interfaces⁽⁹⁾. A full discussion of the derivation of this isotherm and its limitations can be found in standard texts^(7,10,11,12). For a single solute dissolved in a liquid-liquid system the Gibbs equation can be written as:

$$d\gamma = -\Gamma d\mu \dots \dots \dots (1)$$

where Γ = is interfacial excess concentration per unit area of the solute
 μ = is the chemical potential of the solute
 γ = is the interfacial tension

If γ_0 is the interfacial tension of the solute-free liquid-liquid system then the surface pressure caused by the addition of the solute:

$$\pi = \gamma_0 - \gamma$$

Substitution for μ under conditions of unit activity and rearranging equation 1 gives:

$$\Gamma = -\frac{c}{RT} \frac{d\gamma}{dc}$$

or as $c \frac{d\pi}{dc} = -c \frac{d\gamma}{dc}$

$$\Gamma = \frac{c}{RT} \frac{d\pi}{dc}$$

where c is bulk phase concentration of adsorbed species. From these expressions both the interfacial area per molecule of the adsorbed species and the interfacial concentration can be calculated^(10,11,12). It must be remembered, however, that the Gibbs' adsorption isotherm is a precise thermodynamic statement and should only be used in the above form when the reduction of the general equation to its single solute form can be justified. Also in situations where the adsorbed species may change in molecular complexity from that in the bulk phase the appropriate concentrations must be known. Thus caution should be taken in the application of the Gibbs' adsorption isotherm to produce quantitative data for adsorbed species in solvent extraction systems.

Even under the most suitable conditions the Gibbs' isotherm only permits indirect determination of the interfacial concentration and interfacial area of the adsorbed species; direct determination is very difficult for the oil-water interface. Adaptation of the Langmuir trough for such work has been reported^(13,14), but leakage past the barrier and maintenance of the appropriate contact angles prevent such adaptations from universal adoption for such studies. Of greater interest however is the work of Graham et al⁽⁹⁾ wherein use of isotopically labelled solutes emitting soft β -particles has permitted direct determination of the interfacial concentration of compounds like (cetyl - 1 -¹⁴C)- trimethyl ammonium bromide at a toluene-water interface. The limited detection range of these particles, while of obvious benefit in such direct measurement, requires the dissolution of a scintillating species in the organic phase for detection. The adsorption isotherm so obtained agreed well with that derived from the Gibbs' equation but extensive use of this method will be limited by the availability of suitably labelled compounds.

Use of Interfacial Tension Data

The significance of the interfacial tension data in the examination of interfacial behaviour of molecules will be demonstrated by considering different classes of compounds, members of which are used commercially as extractants.

Organic Acids

Of this group the carboxylic acids have been the most widely studied. All organic acids are interfacially active and so reduce the interfacial tension of the oil-water interface. This activity, as measured by interfacial pressure, increases with pH as the acid ionizes. The interfacial pressure also varies with concentration, rapidly approaching a limiting value at very low molar concentrations. The values of molecular areas determined for carboxylic acids at the benzene-water⁽¹⁵⁾ or heptane-water⁽¹⁶⁾ interface are all similar, and indicate that in these diluents the molecules are parallel to the interface in the dimeric hydrogen-bonded form. Different behaviour is found for the case of *n*-caprylic acid at a tetradecane-water interface⁽¹⁷⁾. With this long chain aliphatic solvent the acid adsorption is much greater and leads to a smaller interfacial area per molecule. Here the aliphatic chains of acid and solvent interact together in a side configuration in the interfacial region orientated perpendicular to the interface by the surface attraction of the polar carboxylic acid grouping. Such an alignment of solute and solvent might not be possible in the case of benzene where the π -electron cloud of the benzene ring is probably orientated parallel to the interface thereby encouraging parallel arrangement of dimeric molecules of carboxylic acids.

Another property which can be calculated from interfacial tension data is the critical micelle concentration, c.m.c. This can be indicated by a discontinuity in the interfacial tension versus concentration plot at the c.m.c. When a discontinuity does not occur, Danesi et al⁽¹⁸⁾ have shown that the c.m.c. for di-nonylnaphthalene sulphonic acid can be calculated from the concentration at which deviation of the interfacial tension (pressure) versus log concentration plots from linearity occurs; although from the Gibbs' equation such deviations merely show that the species adsorbed is not the same as exists in the bulk phase.

Carboxylic acids and their salts have also been extensively studied at the air-water surface and it is significant to note that in all cases replacing air by an oil phase increases the dimensions of the adsorbed film. This increase presumably occurs by a reduction of mutual interactions of the non-polar alkyl chains by solvation by the oil phase. Addition of inorganic salts to the aqueous phase causes a slight shift in the interfacial tension in addition to the change caused by pH. The variation is found to be more or less in the order of affinity of the metal ions for the carboxylic acid⁽¹⁹⁾, i.e. metal salts are more interfacially active than the parent acid although the magnitude of this effect is not large. The hiatus in the interfacial tension versus pH plot of lauric acid over nickel nitrate reported earlier⁽²⁰⁾ has not been substantiated in later work⁽²¹⁾ and thus nickel does not seem to behave in a different way from cobalt or copper.

The data on alkylphosphoric acids relates to the extraction of the uranyl cation, UO_2^{2+} , by di-(ethylhexyl) phosphoric acid, DEHPA. For this system interfacial tension measurements of the acid at a *n*-heptane-water interface increases from 3.9 dynes cm^{-1} to 12.7 dynes cm^{-1} (10^{-2} M uranyl ion) on formation of the metal complex⁽²²⁾. In this case therefore, the metal complex is less interfacially active than the extractant.

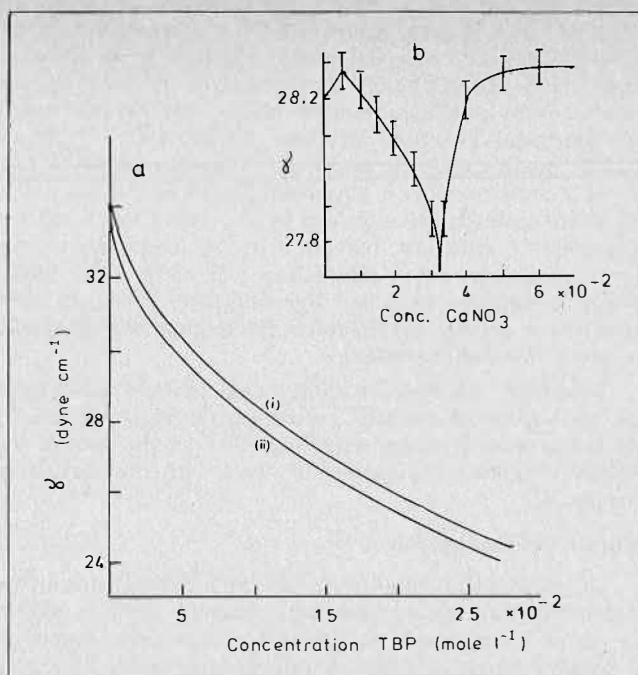


FIGURE 1. Variation of interfacial tension of System TBP — benzene — water — $\text{Ca}(\text{NO}_3)_2$ ⁽²⁷⁾
 (a) (i) TBP — Benzene — water
 (ii) TBP — benzene — water — $\text{Ca}(\text{NO}_3)_2$ at molar ratio TBP: $\text{Ca}(\text{NO}_3)_2$ 3:1
 (b) TBP — benzene — water — $\text{Ca}(\text{NO}_3)_2$ at fixed TBP concentration 0.1 Mole l^{-1} . (error bar as shown)

Amines

Another large class of compounds, several of which are used commercially as extraction reagents, are amines and quaternary amine salts. Here, in contrast to the acids, the interfacial activity of the amines increases with decreasing pH as protonation of the free base proceeds, so once again the ionic species is the more interfacially active. This has been confirmed recently by Tarasov et al⁽²³⁾ for the system tri-*n*-octylamine - toluene - water - perchloric acid. They found that as the concentration of perchloric acid was increased the interfacial tension decreased until a point where the 1:1 molecular complex was formed. Further increase in the perchloric acid concentration had no further effect. Again like the carboxylic acids, it has been shown that the nature of the counter-ion is important. Thus in the tri-*n*-octylamine - acid system the interfacial pressures were in the order $\text{Cl}^- > \text{NO}_3^- > \text{ClO}_4^-$, an order confirmed by extraction performance data. Similar results have been found for tetraheptyl-ammonium salts where interfacial pressures are in the order $\text{Cl}^- > \text{NO}_3^- > \text{ZnCl}_4^{2-}$ ⁽²⁴⁾. The effect seems to be much more pronounced than for carboxylic acids.

These data can be explained by consideration of the adsorbed species at the interface. The interface in this case is positively charged and the expansion of the interface is a function of the number of cations adsorbed per unit area. This electrostatic repulsion can be reduced by an interaction between the anions in the aqueous phase and the cations at the interface and thus a lowering of the interfacial pressure will result. Therefore a decrease in interfacial pressure can be correlated with an increasing interaction between the anions and cations. From electrostatic considerations alone it would be expected that the smallest anion would have the largest interaction with the monolayer. However in these cases the maximum interaction, lowest interfacial pressure, is found with perchlorate and tetrachlorozincate ions. This can be explained

on the basis that these ions cause the maximum disruption of the water structure and hence will tend to be rejected from the aqueous layer⁽²⁵⁾. In the case of the more water-soluble tetra-n-butylammonium halides the reverse order of interfacial pressures has been found, i.e., $I^- > Br^- > Cl^-$ ⁽²⁶⁾. In this case the positively charged monolayer can repel other cation-anion complexes forced out of the water structure towards the interface by the effect described by Diamond⁽²⁵⁾. However, reduction of the interfacial monolayer charge by anion interaction will allow these additional complexes to enter the interface. Thus in this situation a greater cation-anion interaction will promote a larger interfacial pressure.

Therefore, the observed interfacial tension parameters of amines and amine salts are dependent upon the nature of the counter-ion, the water-solubility of the species involved and their hydration or water structure-breaking properties.

Solvating Reagents

The most widely studied of this type of reagent is tri-n-butylphosphate. As expected the reagent itself is active at an oil-water interface; however, it has been found in a number of systems that the complex between TBP and ions in the aqueous phase is more interfacially active than the pure reagent. Thus by plotting the interfacial tension against the concentration of the aqueous ionic species at a constant TBP concentration it is possible to determine the stoichiometry of the interfacial complex from the minimum in the plot (Figure 1), although the figure shows that the change in γ associated with this is very small. Thus in a series of papers Chifu et al⁽²⁷⁻²⁹⁾

TABLE 1. Stoichiometry of Complexes Deduced from Interfacial Tension Studies on System tri-n-butylphosphate-benzene-water-MX

MX	Interfacial Complex	Reference
Ca(NO ₃) ₂	Ca(NO ₃) ₂ .3TBP	27
Sr(NO ₃) ₂	Sr(NO ₃) ₂ .3TBP	27
HNO ₃	HNO ₃ :TBP, 1:1, 1:2, 1:3, 1:4 (with 1:1 most interfacially active)	28
Cu(NO ₃) ₂	various plots give different complexes ranging (Cu(NO ₃) ₂ :TBP 1 : 2.6 - 3.7	29

TABLE 2. Interfacial Areas for o-hydroxyoximes

Oxime	R	Diluent	Conc. Range (M)	Area per molecule (Å ²)	Ref
R ¹	R				
C ⁴	C ₁	heptane	0.001 - 0.01	68.5	(33)
C ⁸	C ₁	"	0.001 - 0.1	82.7	(33)
C ⁹	C ₁	toluene	0.01 - 0.5	139.0	(33)
C ⁹	C ₁	heptane	0.001 - 0.1	78.1	(33)
C ⁸	C ₇	heptane	0.001 - 0.02	58.5	(33)
C ⁸	C ₇	toluene	0.05 - 0.1	105.3	(33)
C ₁	C ₇	heptane	0.002 - 0.05	91.7	(33)
C ₉	CH ₂ C ₆ H ₅	Escaid 100	0.001 - 0.01	90.5	(36)
C ₉	C ₆ H ₆	Escaid 200	0.001 - 0.01	118.0	(36)
		heptane	0.0001 - 0.01	83.4	(36)

note: values for t_{c8-c7} oxime are wrong

have determined the stoichiometry of a number of TBP complexes with metal salts and even nitric acid (Table 1), and these results confirm the stoichiometry obtained by other methods.

This technique is of course only applicable when the interfacial complex is more surface active than the pure reagent. In other cases the molecular complex would tend to be desorbed immediately on formation and diffuse away from the interface.

Starobinets et al have studied the interfacial tension of complexes formed between long-chain aliphatic alcohols and metal thiocyanates at heptane-water and toluene-water interfaces. They found a linear dependence for log D, distribution coefficient, and the interfacial tension for a series of metal thiocyanates⁽³⁰⁾ and also calculated the interfacial molecular area for the complex Zn(ROH)₃(NCS)₂⁽³¹⁾.

Chelating Reagents

The development of chelating reagents selective for particular metals has revolutionised the use of solvent extraction in hydrometallurgical flowsheets. The majority of data on this type of reagent has come from studies of the extraction of copper with two series of chelating reagents, which are derivatives of o-hydroxyoximes and 8-hydroxyquinoline. Of these two series of compounds more results are available for the hydroxyoximes reflecting the commercial importance of these compounds.

o-hydroxyoximes

Although these compounds do not spread at an air-water interface⁽³²⁾, and in an organic diluent have very little effect on the air-oil surface tension⁽³³⁾, when their solution is placed in contact with an aqueous phase a marked lowering of the interfacial tension is found. The hydroxyoxime molecule is thus adsorbed at the oil-water interface presumably with the polar groupings participating in a hydrogen-bonding interaction with the water molecules. Price and Tumilty⁽³⁴⁾, through the use of molecular models, suggest that the oxime is adsorbed at the interface as a dimer, similar to the carboxylic acids, and that the lone pair on the phenolic oxygen is then orientated to hydrogen bond with water molecules. This hypothesis was supported by consideration of molecular models at a planar interface with bulky substituents ortho to the phenolic group, or by using models of ketoximes rather than aldioximes, which showed that the complexing site in the dimer was now prevented from easily approaching the planar interface, and complex formation would be less favoured^(34,35). The metal complex too could not now rest conformably at the interface. Thus introduction of a 3-methyl substituent reduced both the rate of extraction and stripping when compared with the unsubstituted compound⁽³⁴⁾.

The interfacial area per molecule of hydroxyoximes has been shown to vary with molecular weight and diluent (Table 2). However the commercial compounds and indeed some laboratory-prepared model compounds are difficult to purify and thus great care is necessary in interpretation of interfacial tension data lest the presence of interfacially active impurities render the results and any interpretation therefrom meaningless. Thus it is now known⁽³⁷⁾ that the reported interfacial area for the C₈-C₇ hydroxyoxime (Table 2) is incorrect for this reason and some doubt must surround the other data, particularly as no correlation between molecular area and molecular weight appears to exist.

With regard to the diluent effect whereby the molecular areas are all larger for the aromatic diluent, this effect is probably due to penetration of the adsorbed layer by

diluent molecules if not by production of actual solvates as has been reported by Dalton et al⁽³⁵⁾ for toluene and P50, (Acorga Ltd) 5-nonylsalicylaldoxime. More problematical however is the interpretation of the actual areas in terms of molecular species adsorbed at the interface. Dalton⁽³⁵⁾ has calculated that the interfacial area per molecule of the boat conformation dimer of Price and Tumilty⁽³⁴⁾ would be 125 Å² for P50, against an end-on monomer configuration with a molecular area of 17 Å², with the experimental value somewhere in the middle. While it is well known now that, in anhydrous organic solvents, hydroxyoximes exist as dimers^(35,38) and that the degree of dimerisation varies with the degree of aromaticity of the diluent⁽³⁵⁾, no data exist for dimerisation constants in wet organic phases as would result in solvent extraction systems. Nor is it satisfactorily proved that dimers rather than monomers occupy the interface as competitive hydrogen-bonding could readily create energetic conditions more favourable for monomer adsorption than dimers. Thus, until these problems have been resolved, interpretation of interfacial tension data from hydroxyoxime systems should be treated with caution. However, it has been found that the variation in interfacial area of LIX 65N (General Mills Inc) with diluent type can be directly correlated with rate of copper extraction⁽³⁹⁾, i.e. higher molecular area gives lower extraction rate. A similar study by Whewell et al⁽⁴⁰⁾ has shown that the initial rate of copper extraction by LIX 64N (General Mills Inc) is dependent on the interfacial pressure of the system which is in agreement with the findings of Flett⁽³⁹⁾.

As expected from the very weakly acid nature of hydroxyoximes, no variation in interfacial tension with pH is found for the substituted salicylaldoximes at least up to pH 9^(19,41). The copper complex on the other hand is significantly less interfacially active than the parent hydroxyoxime^(19,36,41). In fact the preferential order of interfacial occupancy at pH5 has been shown by Fleming⁽⁴¹⁾ to be LIX 65N > LIX 63 > Cu(LIX63)₂ > Cu(LIX 65N)₂. From his interfacial studies Fleming also reported evidence for formation of an interfacial species consisting of two molecules of the copper complex, Cu(LIX 65N)₂, with one molecule of LIX 65N to which he attributes an interfacial blocking role in his interpretation of the slow kinetics associated with LIX 65N. Work at Warren Spring Laboratory however has not confirmed the finding⁽³⁰⁾ and further data are needed to resolve this problem.

8-hydroxyquinoline

No detailed work has been carried out on these compounds but individual interfacial tension measurements on 7-dodecyl-8-hydroxyquinoline (Kelex 100, Ashland Chemical Co) has shown this compound to be much more interfacially active than the hydroxyoxime reagents^(19,41,42). In this context it is of interest to note that the rate of copper extraction by Kelex 100 is over an order of magnitude faster than for LIX65N^(41,43).

Mixed Reagent Systems & Diluent Modifiers

While mixed reagent systems show a wealth of equilibrium and kinetic effects, the amount of interfacial tension data available is not large. However, sufficient data exist to demonstrate conclusively, in the authors' view, the importance of such data in the interpretation of the chemistry associated with these effects and to shed light on the role of diluent modifiers.

Synergistic Systems

Discussion of such systems will include equilibrium synergistic effects and kinetic accelerator compounds.

Equilibrium Synergistic effects

A typical equilibrium synergistic system is the extraction of the uranyl cation by di(2-ethylhexyl)phosphoric acid (DEHPA), tri-n-butylphosphate, (TBP), mixtures. Interfacial studies⁽²²⁾ have shown that addition of TBP to the DEHPA-UO₂²⁺ system increased the interfacial tension of the system and, while considerable enhancement in the distribution coefficient of UO₂²⁺ occurs⁽⁴⁴⁾, it has also been reported that the rate of UO₂²⁺ extraction is reduced by TBP addition⁽⁴⁵⁾.

Similarly, addition of carboxylic acids to hydroxyoxime and Kelex 100 systems causes considerable synergism in the extraction of copper, nickel and cobalt^(46,47,48). However, although considerable reduction in the rate of nickel extraction is found for all systems, interfacial tension measurements originally believed to show anomalous behaviour of the nickel system⁽²⁰⁾, have now been repeated and nothing untoward has been found for the LIX63 - lauric acid mixture⁽²¹⁾. A different result was obtained for Kelex 100-Versatic 9-11 (tertiary carboxylic acid, Shell Chemical Co) system where it was found that the interfacial tension increased with increasing Versatic 9-11 concentration⁽⁴²⁾. N.M.R. studies⁽⁴²⁾ showed evidence of a direct interaction between the Kelex 100 and the carboxylic acid and this result was used to explain the inhibition of cobalt oxidation on extraction by Kelex 100 in the presence of Versatic 9-11 reported by Lawson et al⁽⁴⁹⁾.

Thus synergism in the presence of mixed reagents appears to involve rate effects generally. Where interfacial tension studies show an increase in this parameter with addition of the synergistic agent to the primary extractant, this effect can be interpreted as a measure of the interaction between the synergist and the extractant, thus reducing the extractant activity within the interphase reaction zone with consequent reduction in extraction rate. The enhancement in degree of extraction, i.e. synergism, is thus caused by formation of an adduct, the free energy of formation of which is sufficient to overcome the reduction in activity of the extractant caused by interaction between the free extractant and the synergist.

Accelerator Compounds

Probably the best known commercial example of acceleration is that produced by the addition of LIX63 to LIX65N to yield the formulation marketed by General Mills Inc. as LIX64N. Here however, interfacial tension studies have shown that LIX63 is much less interfacially active than LIX65N, particularly in aliphatic diluents, and that mixed solutions of LIX63 and LIX65N yield interfacial tension data which reflect the LIX65N content only^(19,41,42). Thus for this system interfacial tension measurements do not seem to be particularly useful in an interpretive sense unless the hypothesis of Fleming⁽⁴¹⁾ is correct, whereby the presence of LIX63 prevents the formation of the interfacial blocking adduct formed between LIX65N and Cu(LIX65N)₂. In view of the known difference in activity of LIX63 and LIX65N, it is not clear just how LIX63 could prevent such adduct formation.

The use of carboxylic acids,⁽⁵⁰⁾ dialkylphosphoric acids⁽⁵¹⁾, alkyl/aryl sulphonic acids^(51,52), as accelerator compounds for copper extraction with hydroxyoximes has been reported. Addition of dinonylnaphthalene sulphonic acid, DNNSA, to the hydroxyoxime, or Kelex 100, carboxylic acid mixtures has also been reported to accelerate the extraction of nickel in this system⁽⁵³⁾. Interfacial tension studies with DNNSA in hydroxyoxime systems has shown that even the presence of small amounts of DNNSA totally displaces the hydroxyoxime from the interface⁽⁴⁸⁾. As DNNSA is fully ionised under the pH conditions

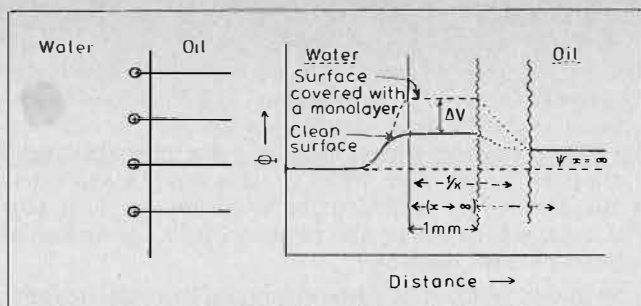


FIGURE 2. Distribution and interfacial potentials in polar (a) and non-polar oil (b)-water systems.

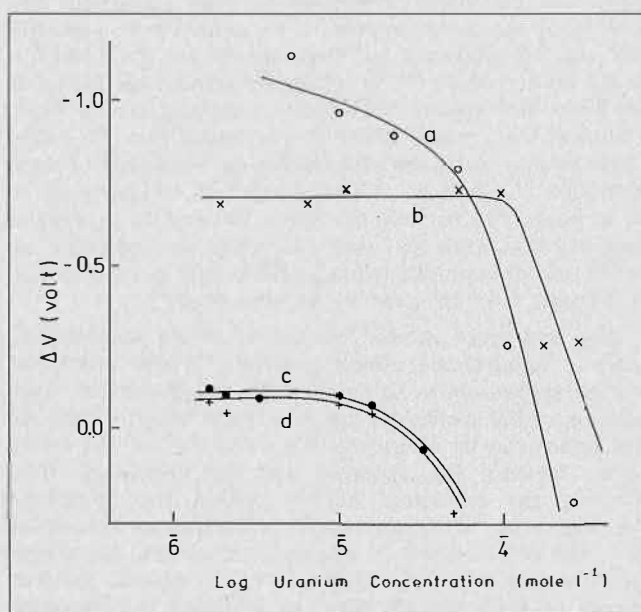


FIGURE 3. Variation of interfacial potential with uranium concentration for the system DEHPA — hexane — water — uranyl ion at pH 1.37⁽²²⁾

- (a) DEHPA (0.05M) alone
- (b) DEHPA (0.05M) + NaNO_3 (0.012M)
- (c) DEHPA (0.05M) + TBP (0.1M)
- (d) DEHPA (0.05M), TBP (0.1M), NaNO_3 (0.012M)

normally encountered during extraction of metal ions like copper and nickel⁽²¹⁾, there can be no doubt that in this system the DNNSA is acting as a phase transfer catalyst reagent for the metal ions followed by rapid ligand exchange reactions in the bulk organic phase. Thus it may be concluded that acceleration effects found for dialkyl-phosphoric and carboxylic acids should proceed by similar mechanisms, the degree of acceleration being dependent on the pK value for the acid.

Diluent Modifiers

Diluent modifiers tend to be used to inhibit third phase formation, improve compatibility between reagent and diluent and to improve phase break properties in solvent extraction systems. Examples of such compounds are long-chain alkyl and aryl alcohols. These have been shown to form a complete monolayer at a benzene-water interface and have a higher surface excess concentration than carboxylic acids⁽¹⁵⁾. Thus addition of such compounds as diluent modifiers to solvent extraction systems must be expected to modify the interfacial region, and interfacial tension studies should be rewarding in this area.

Interfacial tension data are only readily available for nonyl phenol with hydroxyoxime and Kelex 100 systems

related to copper extraction. Thus Hanson et al⁽⁵⁴⁾ has reported that the addition of nonyl phenol to the LIX64N system reduces both the rate and degree of copper extraction while Flett and Spink⁽⁵⁵⁾ have shown, for Kelex 100, nonyl phenol addition reduces extraction rate but enhances degree of extraction. While Hanson et al⁽⁵⁴⁾ report only that nonyl phenol is less interfacially active than LIX64N, Flett and Spink⁽⁵⁵⁾ have shown that the interfacial tension of Kelex 100 solutions are increased by addition of nonyl phenol and thus it can be concluded that nonyl phenol interacts with both hydroxyoximes and Kelex 100, reducing the interfacial activity of both compounds and hence reducing the extraction rate. Enhancement of the degree of extraction of copper by Kelex 100-nonyl phenol mixtures is construed as evidence for adduct formation between the Kelex 100 copper complex and nonyl phenol. The absence of such adduct formation in the case of the copper hydroxyoxime complexes causes depression in the degree of extraction through the reduced oxime activity. This effect has been put to commercial use in the development of the Acorga P5000 series of reagents as described by Tumilty et al.^(56,57)

Interfacial Potential^(10,12,52)

When interfacially active species are adsorbed at an oil-water interface the penetration of the hydrophilic part of the molecule will cause a short range disturbance of the aqueous phase adjacent to the monolayer. As this disturbance involves orientation of water molecule dipoles, and can involve ion pairs and similar species depending on the type of extractant, then a potential difference is created across the interphase volume. The magnitude of this potential difference will clearly depend directly upon the system and the value of such parameters as pH, temperature, ionic strength, etc. If the organic phase is polar enough to permit appreciable ionization of extracted complexes then a further distribution potential must be considered and added to the interfacial potential^(10,58). The non-polar nature of the diluents used in metal extraction systems reduces this additional potential to such low values that it may be disregarded. Under fixed conditions, therefore, measurement of interfacial potentials can yield information relating to molecular orientation of the extractant at the interface, the effect of diluent modifiers on it and the effect of interaction with the metal ion of interest. Such data are clearly complementary to interfacial tension data.

Measurement of Interfacial Potential

This is usually achieved by measuring the charging current of the capacitor formed between an electrode and the interface. Because an ionic double layer at a non-polar oil-water interface can extend up to several millimeters into the oil phase, measurements can be made by placing an electrode actually within the double layer^(10,58,59) (Figure 2). Indeed, in the non-polar condition usually encountered in solvent extraction of metals it has been found that zeta potential measurements correspond directly with interfacial potential measurements⁽⁶⁰⁾. With polar organic phases no such correspondence exists.

Results

Relatively few data are available from interfacial potential studies of relevance to solvent extraction systems. Data are available for the system $\text{UO}_2^{2+}/\text{DEHPA}/\text{TBP}$ ⁽²²⁾ which complement the interfacial tension data for this system discussed earlier. The values of the interfacial tension observed by Birch⁽²²⁾ are quite high, i.e. of the order of 0.1 - 1.0 V and his results are shown in Figure 3.

The figure shows that the interfacial potential becomes more negative on addition of TBP to DEHPA and at constant organic phase concentration increasing the uranium concentration in the aqueous phase changed the potential to more positive values. Increasing interfacial tension of this system with increasing TBP concentration has already been interpreted as indicating an interaction between TBP and DEHPA, thus reducing the bulk activity of DEHPA which in turn reduces the interfacial concentration. The variation in interfacial potential is therefore a further manifestation of this interaction. It was also found that the rate effect associated with this interaction would be reversed by the addition of sodium nitrate to the system. This salt addition however, although not materially affecting the interfacial tension values, did reduce the value of the interfacial potential at low uranium concentrations. Without more comprehensive data it is not possible to fully interpret the various changes observed in terms of interfacial molecular chemistry but it may be that the effect of sodium nitrate is to cause the TBP to act as a phase transfer reagent via $\text{UO}_2(\text{NO}_3)_2$ species followed by fast ligand exchange reaction in the bulk organic phase.

Fleming⁽⁴¹⁾ has recently measured the zeta potentials for LIX reagents at an octane-water interface. In the absence of copper ions the reagents did not change the zeta potential value from that of the octane-water system except at high (> 9) and low (< 4) pH values. Formation of the anionic, R^- , or protonated, RH_2^+ , species were invoked to explain these data. Studies in the presence of copper ions however, were carried out mostly over a pH range within which formation of copper hydroxide species occurred and the data therefore reflected strong adsorption of these species at the interface. It would have been more interesting if data over a pH range from 1.0 to 3.5 had been available. However, it is of interest to find that the variations of zeta potential of LIX 65N, LIX 64N and LIX 63 with pH are nearly identical, the difference in the variation being less than 10 mV over the pH range of 4 to 9.

It is worthwhile now to briefly consider some wider implications of interfacial potentials and their relationship with surface potential measurements of which considerably more data are available. Firstly, if precise information on molecular geometry at the interface is required, it is necessary to break down the interfacial potential into its individual dipole and electrostatic components. Such analyses have been carried out for surface potential measurements^(61,62) and some interfacial potential measurements where insoluble films are formed⁽⁶¹⁾. The algebraic relationship, interfacial models and their limitations have been fully discussed elsewhere^(10,58). The correlation of surface/interfacial potential with the molecular properties of the monolayer can be carried out in terms of the interfacial potential per adsorbed molecule. It is found for many films that this term is nearly constant, and can be expressed by:

$$\Delta V = 4\pi n\mu_{\perp}$$

where ΔV is the interfacial potential, n the number of molecules adsorbed at the surface, and μ_{\perp} the perpendicular component of the dipole moment. However this is recognised as an oversimplification because of the re-orientation of water molecules close to the interface. Thus the interfacial potential is related simply to the number of adsorbed species, but the relationship to standard dipole moments of molecules is unknown and probably complicated. Another important deduction arising from the concept of interfacial potentials is that the pH in the interphase volume will differ from that in the bulk aqueous phase. Thus if the interfacial tension of long chain car-

boxylic acids at a benzene-water interface is measured as a function of pH, the value of the interfacial tension indicative of half-ionization occurs at about three pH units to the alkaline side of the point at which these compounds are half-ionized in bulk aqueous solution⁽⁶³⁾. Similarly, amines at an interface are apparently half-ionized three to four units on the acid side when compared to bulk aqueous solution data. If it is assumed that the ionization properties of the head-group, (pK), does not alter from its bulk aqueous phase value, which is reasonable as the head-group remains immersed in an aqueous environment, then this indicates that the pH value near the interface must be different from the value in the bulk aqueous phase. Similar indications of pH changes at an interface can be observed by adsorption of indicator dyes. Thus adsorption of an acid dye at a benzene-water interface shows a colour change indicative of a more acid pH, while the opposite effect is noted for basic dyes⁽⁶⁰⁾.

A Boltzmann-type distribution of hydrogen ions in a potential field leads to:

$$c_{\text{H}^+} = ce^{-\frac{\epsilon\psi}{kT}}$$

which yields

$$\text{pH}_s = \text{pH}_b + \frac{\epsilon\psi}{2.303kT}$$

where pH_s is the interfacial pH and pH_b the bulk phase pH. Thus only when $\psi = 0$ will $\text{pH}_s = \text{pH}_b$ and if ψ is negative, then $\text{pH}_s < \text{pH}_b$. With a value of the interfacial potential ~ 200 mV, a change of three to four units in the pH range is obtained.

Recently Cante et al⁽⁶⁴⁾ have determined the interfacial pH of lauric acid-laurate soaps at a number of oil-water interfaces using zeta potential measurements and found that the interface pH was given by:

$$\text{pH}_s = \text{pH}_b - \xi/59$$

In this system the zeta potential is determined by the number of ionic charges at the interface while pH_b is governed by the distribution coefficient of the acid for the particular oil-water system. Thus it is difficult to use the value of pH_s to determine the nature and structure of the interfacial layer. A selection of their results are given in Table 3. In all cases the pH_s for chloroform is the most alkaline and n-hexadecane the most acidic. This can be explained by the inability of chloroform to support a lauric acid film at the interface, an explanation supported by interfacial tension measurement. Also it can be seen that the pH_s for a half neutralised solution is more acidic than one prepared by dilution without the addition of acid, indicating the attraction of the interfacial layer for protons.

Interfacial Viscosity⁽¹⁰⁾

Adsorption of a compound at a liquid-liquid interface will produce at surface saturation a coherent monolayer. This will behave in a similar fashion to the monolayers produced at the air-water interface by the spreading of, for example, fatty acids or other surfactants. However, the measurement of experimental parameters for these liquid-liquid adsorbed interfaces is much more difficult and hence the amount of data applicable to solvent extraction systems is very scarce. Thus as shown above, the measurement of interfacial area of adsorbed molecules is more easily derived from interfacial tension data than the more usual surface pressure vs. area curves as applied in the air-water system. However, in those systems which have been studied, it is found that the adsorbed monolayer at

TABLE 3. pH_s of Potassium Laureate-Lauric Acid Monolayers at an Oil-Water Interface

K Laurate	diluted				half neutralised		
	5×10^{-4}	2.5×10^{-3}	5×10^{-3}	1×10^{-2}	5×10^{-4}	5×10^{-3}	2×10^{-2}
Solvent							
CCl ₄					7.00		7.44
CHCl ₃	8.58	8.74	8.66	8.84	7.27	8.00	7.97
benzene					7.22		7.61
n. hexane					6.73		
cyclohexane	7.62	7.50	7.83	7.93	6.56	6.65	7.40
n. hexadecane	6.94	6.83	6.93	7.93	6.21	6.52	6.92

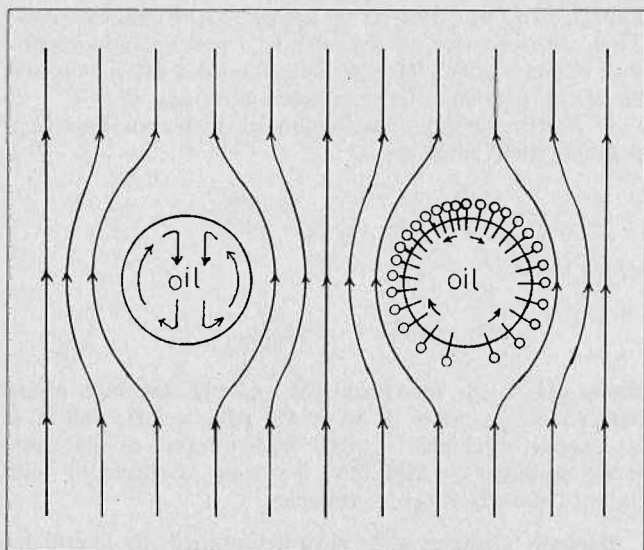


FIGURE 4. Circulation within a falling drop in the presence and absence of surface active species.

the oil-water surface is more expanded than a similar monolayer at the air-water surface. However, being coherent films these monolayers will be resistant to any shearing stresses in the plane of the surface and thus an interfacial viscosity will be experienced.

One of the most important consequences of this interfacial viscosity in a solvent extraction context is the effect it has on the bulk phases on each side of the monolayer. Because of the lack of slippage between the monolayer and the bulk liquid adjacent to it, when a monolayer flows along a liquid surface under the influence of a surface pressure gradient some of the underlying liquid is carried along with it. Conversely, if the lower phase is moving below a stationary uniformly spread monolayer, the molecules are carried along until the stress due to this viscous traction is balanced by the back-spreading pressure of the monolayer. This phenomena is found to reduce or prevent circulation with moving liquid drops and this is of paramount importance in the consideration of liquid-liquid extraction with surface active reagents (Figure 4). Therefore the measurement of interfacial viscosity could be of importance in the assessment of reagents.

However, the major difficulty arises from the construction of a suitably sensitive interfacial viscometer. There are usually modifications of surface, air-liquid viscometers, and work on the same principles of oscillating bobs, or viscous traction devices. Early work on films at the oil-water interface was carried out with an oscillating needle or disc placed at the interface. Measurement of the surface viscosity can then be achieved by displacement of the needle or disc in a horizontal plane and observing the damping of the oscillation, or, in a modification, the liquid

phases are rotated in bulk on a turn-table and the drag on the needle or disc measured. These methods however suffer from the disruption of the surface film by the indicating device and they have only a rather low sensitivity because of the inertial mass of the indicating needle or disc.

A modification of this viscous traction method, however, makes it suitable for liquid-liquid interfaces without reducing its inherent sensitivity of about 10^4 surface poise. The modification consists of replacing the knife-edge system of a surface viscometer with two concentric rings of thin stainless steel or platinum wire. These concentric rings form a canal which retards the motion of the interface when the vessel containing the two liquids is rotated. In a typical experimental situation an interface with an interfacial viscosity of 10^4 surface poise will produce a retardation over that observed for a clean interface of 10 seconds under a turntable speed of 1 revolution in 38 seconds. The overall equipment is quite versatile and by change of the canal width and speed of rotation, interfacial films of widely differing viscosities can be measured.

Difficulties arise with this equipment in the exact aligning of the rings concentric and also planar to the interface. A further problem is found in introducing a suitable marker into the canal to allow accurate timing. This should be light enough to be swept along with the film and talc seems to be most commonly used.

Results

The difficulties which arise in the measurement of interfacial viscosity and the little additional knowledge gained from these results probably account for the lack of data in this field. Surface viscosity, i.e. air-water, studies on the other hand are easier to obtain and are relevant to the stability of foams and emulsions⁽¹⁰⁾. In studies of compounds at an air-water and oil-water interface it is found that little change in viscosity occurs on addition of the oil, implying that the major contribution to the viscosity in both cases arises from the penetration of the head-groups of the adsorbed molecule into the water phase.

In the only known study of interfacial viscosity of a solvent extraction system Birch⁽²²⁾ found a wide scatter of results which probably arose from experimental difficulties. However in all his experiments on the DEHPA/TBP/Hexane/H₂O/UO₂²⁺ system the addition of nitrate ions to the aqueous phase lowered the interfacial viscosity (Figure 5). This he attributed to the nitrate ions disturbing the water structure in the interfacial region. As in all interfacial measurements, clean interfaces are essential as the presence of solid species at the interface will affect the observed results.

The extreme experimental difficulties in obtaining interfacial viscosity measurements, in the authors' opinion, are probably not justified in terms of the additional knowledge gained of the interfacial region. The combination of interfacial tension and interfacial potential measurements will give a better return for the effort involved in solvent

extraction systems. However the concept of interfacial viscosity is important and the consequences of this phenomenon on the solvent extraction process should be recognised.

Conclusion

This review has shown that interfacial physical chemical measurements are of considerable value in interpreting the chemistry, both equilibrium and kinetic, of the solvent extraction of metals. Interfacial tension measurements are found to be useful in determination of complex stoichiometry, in revealing interaction between mixed extractants, extractants and modifiers, and to, qualitatively at least, indicate diluent effects. Interfacial potential data are seen to be strongly related to interfacial tension variation and as such should always be taken together for interpretive purposes. Interfacial potential data should be useful in interpretation of molecular geometry and orientation at the interface and should yield useful information on the interaction between extractant and metal ion. The concept of interfacial pH is an important corollary of the theory of interfacial potentials. Interfacial viscosity, which should also yield data regarding the nature of the adsorbed film at the interface and variations therein with respect to changing parameters of the system, has been little studied due to inherent experimental difficulties. Development of a combined interfacial potential and tension approach to the interfacial equilibrium and kinetics should yield high dividends in terms of mechanistic understanding of the complex chemistry of the solvent extraction of metals.

REFERENCES

- (1) Aveyard, R. and Haydon, D.A., *Trans Farad Soc* 1965, 61, 2255.
- (2) Harkins, W.D. and Brown, F.E., *J Amer Chem Soc* 1919, 41, 499.
- (3) Pierson, F. W. and Whitaker, S., *J Colloid Interface Sci* 1976, 54, 203, 219.
- (4) Lenard, P., *Ann Physik* [4] 1924, 74, 381.
- (5) Huh, C. and Mason, S.G., *Colloid Polym Sci* 1975, 253, 566.
- (6) Padday, J.F. and Russell, D.R., *J Colloid Sci* 1960, 15, 503.
- (7) Bikerman, J.J., *Physical Surfaces*, Acad Press, NY, 1970.
- (8) Pugachevich, P.P., *Experimental Thermodynamics II*, IUPAC Butterworths, 1975, 991.
- (9) Graham, D.E., Chatergoon, L. and Phillips, M.C., *J Phys E* 1975, 8, 696.
- (10) Davies, J.T. and Rideal, E.K., *Interfacial Phenomena*, Acad Press, NY, 1963.
- (11) Defay, R., Prigogine, I., Bellemans, A. and Everett, D.H., *Surface Tension and Adsorption*, Longmans, 1966.
- (12) Adams, N.K., *The Physics and Chemistry of Surface*, Dover Pub Inc., 1968.
- (13) Askew, F.A. and Danielli, J.F., *Proc Roy Soc A* 1936, 155, 695.
- (14) idem, *Trans Farad Soc* 1940, 36, 785.
- (15) Hutchinson, E., *J Colloid Sci* 1948, 3, 219.
- (16) Seelich, F., *Monatsch* 1948, 79, 348.
- (17) Hutchison, E., *J Colloid Sci* 1948, 3, 235.
- (18) Chiarizia, R., Danesi, P.R., D'Alessandro, G. and Scuppa, B., *J Inorg Nucl Chem* 1976, 38, 1367.
- (19) Heels, J.D.G., PhD Thesis, Hatfield Polytechnic, 1976.
- (20) Flett, D.S., Cox, M. and Heels, J.D., *Proc ISEC 74*, Lyons, SCI London 1974, 3, 2559.
- (21) Flett, D.S., *Chemy Ind* 1977, (6), 223.
- (22) Birch, M.E.J., MSc Thesis, Loughborough Univ., 1969.
- (23) Tarasov, V.V., Yagodin, G.A., Yurtov, E.V. and Gritsko, I.N., *Tr Mosk Khim-Techol Inst* 1974, 81, 73.
- (24) Scibona, G., Danesi, P.R., Conte, A. and Scuppa, B., *J Colloid Interface Sci* 1971, 35, 631.
- (25) Diamond, R.M., *J Phys Chem* 1963, 67, 2513.
- (26) Tanaki, K., *Bull Chem Soc Japan* 1967, 40, 38.
- (27) Andrei, B. and Chifu, E., *Stud Univ Babes-Bolyai Ser Chem* 1976, 21, 10.
- (28) Chifu, E., Andrei, Z. and Tomoaia, M., *Ann Chim (Rome)* 1974, 64, 869.

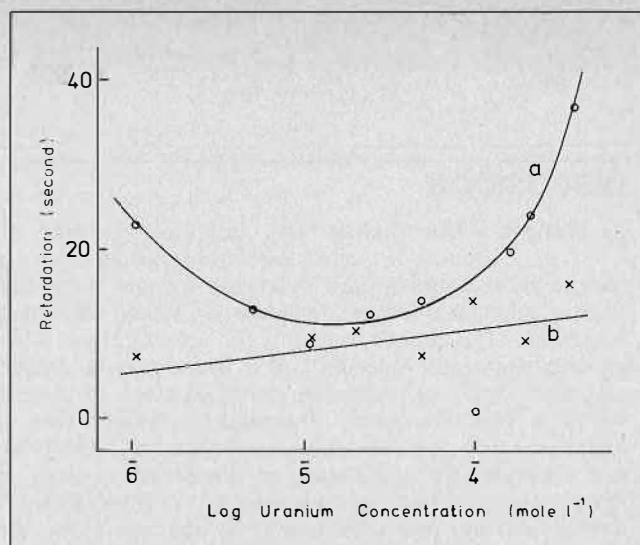


FIGURE 5. Variation of interfacial viscosity function, retardation in seconds versus uranium concentration for the system DEHPA — hexane — water — uranyl ion (a) in the absence of nitrate ions and (b) in the presence of nitrate ions.⁽²²⁾

- (29) Tomoaia, M., Andrei, Z. and Chifu, E., *Rev Roum Chim* 1973, 18, 1547.
- (30) Starobinets, G.L., Lomako, V.L. and Mazovka, E.R., *Dokl Acad Nauk B SSR* 1974, 18, 817.
- (31) Starobinets, G.L. and Lomako, V.L., *Vestsi Akad Navuk Belarus SSR Ser Khim Navuk* 1974, 94.
- (32) Hauxwell, F., Private communication.
- (33) Dobson, S. and van der Zeeuw, A.J., *Chemy Ind* 1976, (6), 175.
- (34) Price, R. and Tumilty, J.A., *Hydrometallurgy*, I Chem E Symp No. 42, London, 1975, paper 18.
- (35) Dalton, R.F., Hauxwell, F. and Tumilty, J.A., *Chemy Ind* 1976, (6), 181.
- (36) Melling, J. and Flett, D.S., Warren Spring Laboratory unpublished data.
- (37) Van der Zeeuw, A.J., private communication.
- (38) Laskorin, B.N., Yakshin, V.V., Ul'yanov, V.S. and Mirokhin, A.M., *Proc ISEC 74 Lyon*, SCI London, 1974, 2, 1775.
- (39) Flett, D.S., *Acc Chem Res* 1977, 10, 99.
- (40) Whewell, R.J., Hughes, M.A. and Hanson, C., *Adv in Extractive Metallurgy IMM London*, 1977, 21.
- (41) Fleming, C.A., National Institute for Metallurgy, Johannesburg 1976, Report No. 1793.
- (42) Flett, D.S., Cox, M. and Heels, J.D., *J Inorg Nucl Chem* 1975, 37, 2197.
- (43) Spink, D.R. and Okuhara, D.N., *Met Trans* 1974, 5, 1935.
- (44) Baes, C.F. (Jr.), *Nucl Sci Eng* 1963, 16, 405.
- (45) North, A.A., private communication cited in ref. 22.
- (46) Flett, D.S. and West, D.W., *Proc ISEC 71*, The Hague, SCI London, 1971, 214.
- (47) Nyman, B.G. and Hummelstedt, L., *Proc ISEC 74*, Lyon, SCI London, 1974, 1, 669.
- (48) Hummelstedt, L., Lund, H., Karjaluo, J., Berts, L.O. and Nyman, B.C., *Proc ISEC 74 Lyon*, SCI London, 1974, 1, 829.
- (49) Lakshmanan, V.I. and Lawson, G.J., *J Inorg Nucl Chem* 1973, 35, 4285.
- (50) Goren, M.B. and Coltrinari, E.L., *USP* 3, 927, 167.
- (51) Moore, R.H. and Partridge, J.A., Northwest Mining Assoc Meeting, Spokane, Washington, 1972.
- (52) Hazen, W.C. and Coltrinari, E.L., *USP* 3,872,209.
- (53) Morin, E.A. and Peterson, H.D., *USP* 3, 787, 286.
- (54) Hanson, C., Hughes, M.A., Preston, J.S. and Whewell, R.J., *J Inorg Nucl Chem* 1976, 38, 2306.
- (55) Flett, D.S. and Spink, D.R., *ISEC 77*, Toronto, paper 3f.
- (56) Tumilty, J.A., Dalton, R.F. and Massam, J.P., *Adv in Extractive Metallurgy*, IMM London, 1977, 123.
- (57) Tumilty, J.A. and Massam, J.P., *ISEC 77*, Toronto, paper 23b.
- (58) Llopis, J., *Modern Aspects of Electrochemistry* No 6, edited Bockris J O'M and Conway, B.E., Butterworth 1971, Chapter 2.
- (59) Kinlock, C.D. and McMullen, A.I., *J Sci Inst* 1959, 36, 347.

- (60) Hartley, G.S. and Roe, J.W., *Trans Farad Soc* 1940, 36, 101.
(61) Davies, J.T. and Rideal, E.K., *Can J Chem* 1955, 33, 947.

- (62) Davies, J.T., *Biochem Biophys Acta* 1953, 11, 165.
(63) Peters, R.A., *Proc Roy Soc A* 1931, 133, 147.
(64) Cante, C.J., McDermott, J.E., Saleed, F.Z. and Rosano, H.L., *J Colloid Interface Sci* 1975, 50, 1.

DISCUSSION

Y. Marcus: When dealing with interfaces between the phases in actual extraction systems, in contrast to those between pure water and solvent, it is necessary to take into account incipient or actual third-phase formation. The limited solubility of an extracted solute, or large aggregates (micelles?) of it which may be formed, may lead to the accumulation at the interface of material which is not molecularly dispersed. It should then be considered as a separate phase, and the simple Gibbs law and measurement techniques of interfacial tensions no longer apply. Often the quantity of a third phase is minute, and not detectable readily by the naked eye. (See our recent work on phosphoric acid — amine systems in *J. Inorg. Nucl. Chem.*). Have such effects been noted by the authors in their work?

M. Cox: We would like to thank Professor Marcus for his cautionary comments on third-phase formation. To date this has not been observed in our systems but we will certainly keep this problem in mind.

W.J. McDowell: About 15 years ago we measured the interfacial tension in a number of extraction systems and in general our results agree with your results indicating slower extraction with higher interfacial tension. This effect was also shown by systems in which we added "inert" surface active agents (inert as far as extraction of the metal is concerned). In our interfacial studies we obtained evidence which we interpreted as indicating the presence of an interfacial species, different from that existing in the bulk organic phase, and predominating when the interface was expanded by vigorous agitation. Have you seen in your work any evidence of such interfacial species?

M. Cox: We have not found evidence of the kind of interfacially active species you mention although it is quite likely that the interfacial species will differ from that of the bulk especially when aggregation of the extractant is possible. Some years ago I did study the uranium extraction with tri-octylamine sulphate and was able to confirm your observation of "anomalous extraction" but have not studied the interfacial properties of this system in our current programme.

A. Warshawsky: The hydroxyoximes incorporating oxalyl-kylene side chains were developed on arguments pertaining strongly to conclusions made in

this paper. In view of various unexplained difficulties in recovering copper from hydroxyoximes, what is the view of the authors in relationship to the influence of interfacial properties on this reaction, and what are their plans to study this reaction?

M. Cox: Some of these difficulties in recovering copper from loaded solutions containing specific chelating extractants could arise from the observation that the copper complex is interfacially less active than the extractant itself. Thus it is desorbed from the interface into the bulk solution. Perhaps the incorporation of other surface active constituents in the extractant molecule may aid the stripping process.

G.A. Yagodin: Do you not notice the change of the interface with time? Have you felt that the formation of the mechanical structural barrier is due to the film formation especially with the cations hydrolysed?

M. Cox: In certain cases we have noticed a dependency of the interfacial tension with time. In order to overcome problems concerned with presence of extraneous surface-active material we do clean the interface by suction several times to obtain reproducible results.

So far we have not experienced problems with hydrolysis of the metals. However, as was shown in the zeta-potential experiments of Fleming, these can strongly influence the results obtained. With other systems, e.g. carboxylic acid extractants, a solid film of the metal complex can be formed at the interface, but again we have not noticed any such behaviour in our work.

M.E. Keeney: Do your measurements on interfacial potential with the vibrating electrode actually measure the true zeta potential? If not, do these values compare favorably with true zeta potential measurements?

M. Cox: The vibrating plate electrode is used to measure the difference in potential between a clean interface and one with adsorbed species and therefore does not measure a zeta potential. However, it has been shown (ref. 60) that for non-polar media the interfacial potential and zeta potential do correspond.

Unfortunately very little work has been reported on solvent extraction systems, and to our knowledge nobody has yet compared both methods. So we do not know how comparable they are under these particular circumstances.

Recent Developments and New Combinations of Extractants in Synergic Processes

G. Duyckaerts and J.F. Desreux,† Analytical and Radiochemistry; University of Liège, Liège (Belgium).

ABSTRACT

It is the purpose of this paper to review the data on the synergic extraction of metal ions which have been reported since 1970. The properties of a variety of new systems of extractants are described with special emphasis on the β -diketones which are the most thoroughly investigated ligands. The mechanism of the synergic reactions is discussed. The influence of various factors such as nature and properties of the metal, the two extractants and the diluent are referred to whenever new data are available.

Introduction

THE EXTRAORDINARY SURGE of interest which has followed from the discovery by Cuninghame et al.⁽¹⁾ of a synergic effect in the extraction of rare earths attests to the importance of this area. In 1954, these authors reported that the extraction of Pr(III) and Nd(III) by mixtures of HTTA and TBP in kerosene was significantly larger than expected from the distribution ratios measured with either extractant alone. This phenomenon has been noticed as early as in 1879 by Vogel⁽²⁾ in the extraction of Co(II) thiocyanate by an equal mixture of ether and amylalcohol but synergism acquired its name only in 1958 when a group of workers from Oak Ridge⁽³⁾ investigated the extraction of U(VI) by combinations of organophosphorus extracting agents.

Since these pioneer works, several reviews dealing with the synergic effect have been published⁽⁴⁻¹⁰⁾; the two most recent of these are only concerned with 4f and 5f elements^(8,9). These reviews are mostly quoting scientific works carried out before 1970. Our concern in the present review is to give a presentation of the new developments in the field of synergic extraction. Owing to the diversity of extractant combinations for which synergism is observed, we shall adopt Healy's classification⁽⁹⁾ of the various synergic systems, namely:

- a) *acidic (anionic) plus neutral extractants*: the acidic extractant can be a β -diketone, another chelating agent such as salicylaldehyde or a phosphoric, carboxylic or sulfonic acid,
- b) *two acidic extractants*: most often two β -diketones or two organic acids,
- c) *two neutral extractants*: combinations of organophosphorus extractants, of sulfoxides or even of so-called inert diluents.
- d) *cationic plus neutral extractants*: essentially mixtures of amine salts and phosphorus derivatives,
- e) *cationic plus anionic extractants*: mixtures of amine salts and acidic compounds,
- f) *two cationic extractants*: such as two amine salts. This

system has not been investigated recently and will not be referred to any further.

The major part of the present review will be devoted to the first extractant system because it includes the β -diketones which are the most thoroughly investigated ligands as well as the most successful in promoting synergism.

Whenever the data are available, we shall attempt to correlate the synergic effect of each extractant system with the nature and properties of the metal, the two extractants and the diluent. Before dealing with these systems, it seems, however, appropriate to devote a separate section to the interpretation of distribution curves. The experimental method most frequently used consists in measuring the variation of the distribution ratio of a metal ion against the concentration of an extractant while keeping constant the concentration of the other extractant as well as factors such as pH and composition of the diluent. Despite the recent success of spectroscopic and calorimetric techniques, slope analysis remains the most widely used method to deduce the stoichiometry and stability of the new species formed in an organic phase.

Theory of the Synergic Effect

Generally speaking, the synergic coefficient (S.C.) as defined by Taube and Siekierski⁽¹¹⁾ may be described by:

$$\text{S.C.} = \log \frac{D_e^{(1,2)}}{D_e^{(1)} + D_e^{(2)}} \quad (1)$$

where $D_e^{(1)}$, $D_e^{(2)}$ and $D_e^{(1,2)}$ denote the distribution ratios of a metal ion between an aqueous and an organic phase, the latter containing respectively extractant (1), extractant (2) and a mixture of (1) and (2). A synergic enhancement of the extraction is reached whenever $\text{S.C.} > 0$. The cases where $\text{S.C.} < 0$ concern an *antagonistic* effect. It happens for some synergic systems that on increasing the concentration of one of the extractants, S.C. first increases and subsequently decreases; this decrease in synergism is called by some authors *antagonism* and more properly by others *destruction of synergism*⁽⁴⁾.

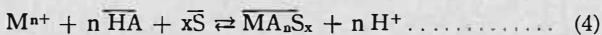
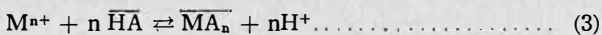
Most often the synergic effect is considered to arise from the formation of one or several new species which are more hydrophobic than the species involving one of the extractants alone. This is, for instance, the case if acidic and neutral extractants are used in combination. The next section is devoted to the theory of the synergic extraction by the β -diketones.

Slope Analysis

The synergic enhancement of the extraction of a metal ion (M^{n+}) by a mixture of a monoacidic chelating agent (HA) and a neutral donor ligand⁽⁵⁾ is due to the formation of one or several adduct complexes between the chelate MA_n and the donor ligand S in the organic phase. Thus, if X^- denotes an inorganic anion in the aqueous phase, at least three species, i.e. $MX_n S_p$, MA_n and $MA_n S_x$, can be assumed to be simultaneously present in the organic phase

†Chercheur qualifié F.N.R.S., Belgium.

and the various equilibria involved may be written as:



where bars refer to the organic phase. The distribution ratios of the metal in presence of S ($D_c(MX_nS_p)$) or HA ($D_c(MA_n)$) alone and in presence of the same concentrations of both extractants ($D_c(MA_nS_x)$) may be written as:

$$D_c(MX_nS_p) = K_{ex}(MX_nS_p) [X^-]^n [\bar{S}]^p \dots \dots \dots (5)$$

$$D_c(MA_n) = K_{ex}(MA_n) \frac{[\bar{HA}]^n}{[H^+]^n} \dots \dots \dots (6)$$

$$D_c(MA_nS_x) = D_c(MX_nS_x) + D_c(MA_n) + K_{ex}(MA_nS_x) \frac{[\bar{HA}]^n [\bar{S}]^x}{[H^+]^n} \dots \dots \dots (7)$$

where square brackets denote concentrations and where K_{ex} refers to the extraction constant of reactions [2], [3] or [4]. The above equations require the assumptions that polymerisation, hydrolysis or complexation by A^- in the aqueous phase occur only to a negligible extent.

The neutral ligand, S, is most often a very weak extractant by itself. If the further assumption is introduced that $D_c(MX_nS_p) \ll D_c(MA_n)$, then the synergic coefficient may be written:

$$S.C. = \log \frac{D_c(MA_nS_x)}{D_c(MA_n)} = \log \left(1 + \frac{K_{ex}(MA_nS_x)}{K_{ex}(MA_n)} [\bar{S}]^x \right) = \log (1 + \beta_{n,x} [\bar{S}]^x) \dots \dots \dots (8)$$

where $\beta_{n,x} = \frac{K_{ex}(MA_nS_x)}{K_{ex}(MA_n)}$ represents the stability constant of the synergic reaction in the organic phase:



If several adducts are formed equation [8] becomes:

$$S.C. = \log \left(1 + \sum_{i=1}^{i=x} \beta_{n,i} [\bar{S}]^i \right) \dots \dots \dots (10)$$

It follows from the above equations that the *synergic coefficient* is not influenced by side reactions in the aqueous phase between M^{n+} , X^- , OH^- and A^- , provided that $[A^-]$ is constant. Equations [8] and [10] remain valid if side reactions between HA and S occur in the organic phase, but then $[S^-]$ denotes the concentration of the free ligand S.

For analytical applications, the synergic effect is often related to the variation of $pH_{1/2}$ ($D_c = 1$) that arises from the addition of a neutral ligand. The above equations yield by substitution

$$S.C. = n(pH_{1/2} - pH_{1/2}^0) = n\Delta(pH_{1/2}) \dots \dots \dots (11)$$

where $pH_{1/2}^0$ and $pH_{1/2}$ refer to the pH of 50% extraction with and without the neutral ligand, S. Equation [11] is valid only if three assumptions are fulfilled, namely:

- the metal concentration is negligibly small when compared with the concentration of the chelating acid;
- the distribution of HA and S remains constant in the pH range investigated;
- the formation of hydroxocomplexes can be ignored in the same pH region.

With these same assumptions in mind, equation 6 gives, on taking logarithms to the base 10

$$\log (D_c(MA_nS_x) - D_c(MA_n)) = \log K_{ex}(MA_nS_x) + n \log [\bar{HA}] + x \log [\bar{S}] - n \log [H^+] \dots \dots \dots (12)$$

The stoichiometry numbers, n and x, are thus readily deduced from plots of $\log (D_c(MA_nS_x) - D_c(MA_n))$ against the log of *one* of the variables $[\bar{HA}]$, $[\bar{S}]$ or pH while keeping constant all others. The equilibrium constant, $K_{ex}(MA_nS_x)$, is calculated from equation [12] by introducing the experimental results. Radiotracers are most commonly used for distribution ratio measurements; the free concentrations, $[\bar{HA}]$ and $[\bar{S}]$, are then independent of the distribution ratio of the metal.

If the extraction proceeds via the formation of several simultaneous adducts, equation [12] has to be modified, thus:

$$\log (D_c(MA_nS_x) - D_c(MA_n)) = n \log [\bar{HA}] - n \log [H^+] + \log \sum_{i=1}^x K_{ex}(i) [\bar{S}]^i \dots \dots \dots (13)$$

or, if $[\bar{HA}]$ and $[H^+]$ are kept constant,

$$\log \frac{D_c(MA_nS_x)}{D_c(MA_n)} = \log \left(1 + \sum_{i=1}^x \beta_{n,i} [\bar{S}]^i \right) \dots \dots (14)$$

This equation can most often be solved for i and $\beta_{n,i}$ by curve-fitting methods and has been successfully applied by Sekine and Dyrssen⁽¹²⁾ to a large number of synergic equilibria involving β -diketones. Equations [1] — [14] can be modified if one has to consider synergic systems which do not include a β -diketone and a neutral extractant. However, the method of slope analysis does not allow a full understanding of all synergic systems quoted in the introduction. If a large number of species are formed successively when the concentration of one of the extractants is varied, the equilibria are so numerous that even a best curve-fitting with a large number of experimental data may not lead to a clear interpretation of the synergic effect. Such intricate situations have often been reported for systems of two extractants of the same type. Examples are afforded by the recent works of Mohanty and Reddy^(13,14) who investigated the extraction of U(VI) or Th(IV) by two neutral extractants, namely TBP and various sulfoxides. The stoichiometry of the adducts was unresolved and only trends in the relative solvating power of the extractants were deduced from slope analysis. Another example is discussed by Kolarik⁽¹⁵⁾ who reported on the synergic extraction of rare earths by two acidic agents. In some instances however, slope analysis has led to reliable determinations of the stoichiometry of such synergic adducts. Dolgashova and Fridman⁽¹⁶⁾ investigated the extraction of Cu(II) by mixtures of chelating agents and claimed that no change in the coordination number of the metal was involved; the number of extracted complexes was thus drastically reduced.

It is noteworthy that the slope analysis and other derived methods are subjected to various limitations even in the case of the β -diketones. These limitations can lead to erroneous interpretations and are the topic of the next section.

Limitations of the Method of Slope Analysis

It is interesting to note that many authors reported on applications of the synergic equation [12] with no comments on the fact that the experimental slopes are sometimes not even near to the expected theoretical values. The assumption is always made that activities may be replaced by concentrations as knowledge of the activity coefficients of the various species is usually lacking. This is a limitation of prime importance of the validity of the approach discussed above. Some other (or related) factors which might alter the quality of the results are worth mentioning.

(a) Side Reactions in the Aqueous Phase

These reactions between the metal ion and an extra ligand, Y^- , yielding species only soluble in the aqueous phase as well as hydrolysis lead to the following equation:

$$\log \frac{D_c(MA_nS_x)}{D_c(MA_n)} = \log \psi_o + \log K_{ex}(MA_nS_x) + n \log [HA] + x \log [S] - n \log [H^+], \dots \dots \dots (15)$$

where $\psi_o = \frac{[M^{n+}]}{[M^{n+}]_{tot}} = f(pH, [Y^-])$ is the distribution function for $[M^{n+}]$.

Slope analysis is thus still valid for plots against $\log [HA]$ or $\log [S]$ but not any more against pH.

(b) Side Reactions in the Organic Phase

Such reactions between HA or S and another reagent, L, such as an impurity lead to the conclusion that slope analysis remains valid as long as the concentration of L is constant and complexes with only one molecule of HA or S are formed.

(c) Side Reactions Involving Only the Synergic Extractants

Frequently A^- can form various complexes with the metal ion in the aqueous phase. For instance, the aqueous complexing of Np(IV) or Pu(IV) by HTTA has recently been reported⁽¹⁷⁾. Most often this additional complexation has been neglected. Provided no polynuclear species are formed in the aqueous phase, the expression for ψ_o may be written as:

$$\psi_o = \frac{1}{\sum_{i=0}^N \beta_i [A^-]^i} \dots \dots \dots (16)$$

where N denotes the maximum number of A^- in the aqueous complex MA_n . The slope of the log-log plot against $\log [HA]$ at constant $[S]$ and pH is now altered:

$$\log (D_c(MA_nS_x) - D_c(MA_n)) = \text{const} + \log \frac{[HA]_{tot}^n}{\sum_{i=0}^N \beta_i [HA]_{tot}^i} \dots \dots \dots (17)$$

Changing the pH at constant $[HA]$ and $[S]$ will yield a slope which is not necessarily n, while the slope with regard to $\log [S]$ leads to the correct value of x.

As HA is a weak acid and S a base, side reactions may occur by hydrogen bonding or by ion pair formation in the organic phase:



Furthermore, if S is strongly basic it may extract an inorganic acid HX from the aqueous phase:



Reactions [18] and [19] were reported to occur with aliphatic amines. The extraction of the metal is now related to the synergic systems. On the one hand, an adduct, MA_nS_x , is formed due to the synergic effect of the acidic component HA and of the neutral extractant, S. On the other hand, the extraction is now partially (or essentially) performed with a combination of a cationic extractant, the amine salt SHA and/or SHX, and an acidic extractant, HA. Table 1 presents some equilibrium constants which were recently reported for the formation of adducts between synergic extractants.

TABLE 1. Some Equilibrium Constants of Adducts Formed between Synergic Extractants

Equilibrium	Diluent	log K	Ref.
$\overline{HTTA.H_2O} + \overline{TBP} \rightleftharpoons \overline{HTTA.H_2O.TBP}$	Kerosene	0.54	(72)
$\overline{HBPHA} + \overline{TBP} \rightleftharpoons \overline{HBPHA.TBP}$	CCl_4	1.24	(148)
	benzene	1.11	(148)
$\overline{HBPHA} + \overline{TOPO} \rightleftharpoons \overline{HBPHA.TOPO}$	CCl_4	2.41	(148)
	benzene	2.32	(148)
$\overline{HDEHP} + \overline{TBP} \rightleftharpoons \overline{HDEHP.TBP}$	toluene	2.00	(106)
$\overline{HTTA} + \overline{TOA} \rightleftharpoons \overline{HTTA.TOA}$	benzene	3.15	(131)
$\overline{HTTA} + \overline{TOA} + H^+ + Cl^- \rightleftharpoons \overline{HTTA.TOA.HCl}$	benzene	5.32	(131)

Acidic Plus Neutral Extractants

Chelating Agent Plus Neutral Extractant Systems

This section is essentially devoted to β -diketones although other chelating agents such as salicylaldehyde are mentioned as well.

Distribution Studies

Correlations between the stability of neutral adducts and the nature of the metal, the extractants and the diluent have been extensively discussed by previous reviewers^(4,10). Tables 2, 3 and 4 present some recent data collected for actinides, lanthanides and transition metal ions. New facts summarized in the tables will now be discussed.

New Neutral Extractants

Just as in the past, the neutral extractants most frequently used in recent works are alkyl- or aryl- phosphates, phosphonates, phosphinates or phosphine oxides.

Several new measurements have confirmed earlier findings on the relative influence of the basicity and the sterical crowding of neutral extractants in synergic processes. Aromatic amines derived from pyridine, (P), were investigated by Irving⁽⁴⁾ in the synergic extraction of $Co(TTA)_2$ or of $Cu(II)$ chelates. New experimental data have now been collected on the extraction of $Ni(TTA)_2$ ⁽¹⁸⁾, $Co(PMBP)_2$ ⁽¹⁹⁾, $Ni(SAO)_2$ ⁽²⁰⁾, and $Zn(DPM)_2$ ⁽²¹⁾. The stability of the adducts decreases in the following order:

4 MP > 3 MP > P > 2,4 DMP > 2 MP > 2,6 DMP
pK 6.24 5.88 5.44 6.21 6.89

A correlation is obtained between the formation constants of the adducts and the pK values of the neutral extractants provided that the latter have no substituents in the ortho position. The abnormal behaviour of 2 MP and 2,6 MP is considered to arise from steric hindrance to coordination. The extraction of Zn (II) and Co (II) by HTTA and quinoline derivatives was also interpreted in terms of steric effects⁽²²⁾. It is interesting to note that a significant destruction of synergism was observed in the extraction of Ni (II) by salicylaldehyde⁽²⁰⁾ in presence of ortho substituted compounds.

Pyridine oxide, (PO), and its derivatives also promote the distribution of metal ions in the organic phase. The extraction of Co (PMBP)₂⁽¹⁹⁾ and $UO_2(TTA)_2$ ⁽²³⁾ was found to decrease in the sequence:

PO > 4 MPO > 3 MPO > 2 MPO > 2,6 DMPO (Co ₂ ⁺)
4 MPO > 3 MPO > 2 MPO > PO > 2,6 DMPO (UO ₂ ⁺)
pK 1.086 0.823 1.034 0.602 1.327

where the peculiar behaviour of PO should be noted. These neutral donors are expected to be less sterically crowded than pyridine derivatives because a bended M-O-N bond is formed between the metal and the neutral reagent. The synergic properties of amine oxides is however incompletely understood. Despite their lower basicity in terms of pK, pyridine oxides form more stable adducts than the corresponding pyridines when involved in the extraction of Co (PMBP)₂ and V (ACAC)₂⁽²⁵⁻²⁶⁾. On the other hand, spectrophotometric measurements⁽²⁵⁻²⁶⁾ in anhydrous CHCl₃, showed that Cu (TTA)₂ adducts with pyridines are more stable than with pyridine oxides:

	4 MP >	3 MP >	P >	2 MP >	2,6 DMP
log β _{2,1}	2.68	2.56	2.23	1.59	0.61
	4 MPO >	3 MPO >	2 MPO >	PO >	2,6 DMPO
log β _{2,1}	1.51	1.42	1.29	1.24	1.18

Synergic coefficients as high as 10⁶ were achieved by Kassierer and Kertes⁽²⁷⁻²⁸⁾ who reported the extraction of rare earths and transition metals by mixtures of HTTA and bidentate aromatic amines (o-phenanthroline or 2,2'-dipyridyl). The experimental data were interpreted in terms of 1:1 adducts with (Co²⁺, Cu²⁺, Zn²⁺) (TTA)₂ and of 1:1 and 1:2 adducts with lanthanide β-diketones. The extraction of UO₂²⁺ by HTTA is enhanced by o-phenanthroline⁽³⁰⁾.

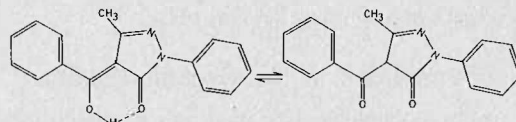
Subramanian and Pai⁽²⁹⁾ considered the effect exerted by sulfoxides on the extraction of UO₂²⁺ by various β-diketones. The authors found that the stability of the adduct complexes UO₂(TTA)₂S followed the trend:



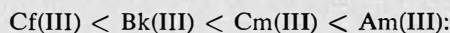
The basicity of the sulfoxides was estimated from the shift in wave number of the symmetric stretching band of the hydration water in CCl₄ and linear relationships were obtained between log β_{n,1} and the IR shifts.

New Chelating Agents

The data in Tables 2, 3 and 4 show that the β-diketone HTTA remains the most widely used chelating extractant. Recently, the study of synergic enhancement has been extended to several new β-diketones, namely 1,1,1,2,2,3,3,3-heptafluoro-7,7-dimethyl-4,6-octanedione (HFOD)⁽³¹⁾, 1,1,1,2,2,6,6,7,7,7 decafluoro-3,5-heptanedione (HFHD)⁽³¹⁾, 1,1,1,2,2,6,6,7,7,8,8,8 dodecafluoro-3,5-octanedione (HDDEFOD)⁽³¹⁾ and 2,2,6,6-tetramethyl-3,5-heptanedione (THD)⁽³²⁾. However, only one new β-diketone, 1-phenyl-3-methyl-4-benzoylpyrazolone-5 (HPMBP) has been under active consideration:



This β-diketone and some related derivatives were first synthesized by Jensen⁽³³⁾. HPMBP was found⁽¹⁰⁾ to be a more powerful extractant of rare earths and transition metals (such as Zn²⁺ or VO²⁺) than HTTA, thus allowing extraction from more acidic media. Furthermore, it is claimed to be less soluble in water, more stable on storage and easier to purify⁽¹⁰⁾. A large volume of work has been carried out in the U.S.S.R. on the synergic extraction of transplutonium elements by HPMBP⁽³⁴⁻³⁷⁾, Am (III) and Cm (III) were quantitatively extracted from 0.1 M HNO₃ solutions by mixtures of TOPO (0.01 M) and of HPMBP (0.05 M) in cyclohexane⁽³⁷⁾. The synergic coefficient increased in following the order⁽³⁴⁻³⁷⁾:



and the adducts MA₃ (TOPO)₂ and MA₂ (NO₃) (TOPO)₂ were reported whereas the only species extracted with TBP was MA₃ (TBP)₂. The synergic enhancement remains

TABLE 2. Some Equilibrium Constants of β-diketone Adducts of Actinides

Adduct	Neutral ligand S	Diluent	Aqueous phase	log K _{ex} (MA _n)	log ⁽¹⁾ K _{ex} (MA _n S _x)	log β _{n,1}	log β _{n,2}	Ref.	
Am(PMBP) ₃ S _x	MIBK	CHCl ₃	0.1M NH ₄ ClO ₄	-4.43	-3.47	0.59	0.96	(145)	
	TBP	"	"	"	-2.43	0.77	2.0	"	
	TBPO	"	"	"	-4.21	0.22	—	"	
	TOPO	"	"	"	"	(3.17)	(7.6)	"	
	TPPO	"	"	"	"	(10.57)	0.88	(15)	"
UO ₂ (TTA) ₂ S	DPSO	benzene	1.88M LiClO ₄			2.99	—	(29)	
	DBSO	"	"			3.42	—	"	
	DDCSO	"	"			3.86	—	"	
	DISPSO	"	"			3.91	—	"	
	DHSO	"	"			3.96	—	"	
UO ₂ (TTA) ₂ S	2,6 DMPO	CHCl ₃	pH=1.4 (HCl)	-2.77	-0.17	2.60	—	(23)	
	PO	"	"	-2.77	0.09	2.86	—	"	
	2MPO	"	"	-2.77	0.28	3.05	—	"	
	3MPO	"	"	-2.77	0.47	3.24	—	"	
	4MPO	"	"	-2.77	0.75	3.52	—	"	
	2,6DMPO	"	"	-2.71	-0.15	2.56	—	(24)	
UO ₂ (BTA) ₂ S	2,6DMPO	"	"	-3.19	-0.71	2.48	—	"	
UO ₂ (HAA) ₂ S	2,6DMPO	"	"	-1.41	1.79	3.20	—	"	
UO ₂ (BTA) ₂ S	DDSCO	benzene	1.88M LiClO ₄			3.58	—	(29)	
	UO ₂ (TTA) ₂ S	TBPO	CH ₂ Cl ₂	0.1M NaClO ₄	-2.50	4.50	7.00	—	(47)
		"	CHCl ₃	"	-2.93	4.09	7.02	—	"
		"	CHBr ₃	"	-2.80	4.38	7.18	—	"
		"	isopropylbenzene	"	-2.85	5.56	8.41	—	"
		"	chlorobenzene	"	-2.71	5.75	8.46	—	"
		"	benzene	"	-2.68	5.82	8.50	—	"
		"	o-dichlorobenzene	"	-2.70	5.82	8.52	—	"
		"	n-heptane	"	-2.91	5.72	8.63	—	"
		"	CCl ₄	"	-3.04	5.60	8.64	—	"
		"	n-hexane	"	-3.18	5.78	8.96	—	"
		"	cyclohexane	"	-2.86	6.32	9.18	—	"

(1) K_{ex}(MA_nS_x) refers throughout to the extraction constant of the highest adduct. (see equations |2| - |10|).

TABLE 3. Some Equilibrium Constants of β -diketone Adducts of Lanthanides

Adduct	Neutral ligand S	Diluent	Aqueous phase	log $K_{ex}(MA_n)$	log ⁽¹⁾ $K_{ex}(MA_nS_x)$	log $\beta_{n,1}$	log $\beta_{n,2}$	Ref.
La(TTA) ₃ S _x	DBuSO	CCl ₄	1M NaClO ₄	-10.50	-2.37	6.02	8.13	(62)
Ce(TTA) ₃ D _x	DBuSO	"	"	-9.99	-1.44	5.71	8.55	(62)
	TBP	"	"	-9.99	-1.16	6.10	8.83	(61)
Ce(PMPB) ₃ S _x	TBP	toluene	0.1M NaNO ₃	-2.28	0.60	1.76	2.88	(38)
	TOPO	"	"	-2.28	4.50	—	6.78	(38)
	TBPO	"	"	-2.28	4.86	—	7.14	"
Pr(TTA) ₃ S _x	DBuSO	CCl ₄	1M NaClO ₄	-9.53	-1.08	5.65	8.45	(62)
	TBP	"	1M NaClO ₄	-9.53	-0.59	5.79	8.94	(61)
	TOA	ChCl ₃	0.1M NaNO ₃	-8.92	-5.06	3.86	—	(48)
	TOA	benzene	"	-8.84	-4.25	4.59	—	"
	TOA	CCl ₄	"	-8.82	-3.75	5.07	—	"
Nd(TTA) ₃ S _x	DBuSO	CCl ₄	1M NaClO ₄	-9.35	-0.94	5.85	8.41	(62)
	TBP	"	"	-9.35	-0.55	5.90	8.80	(61)
	dipy	CHCl ₃	2M "	-10.12	-4.50	4.86	5.62	(27)
	"	benzene	"	-8.38	-1.67	5.21	6.71	(27)
	"	cyclohexane	"	-7.09	0.67	5.22	7.76	"
	"	CCl ₄	"	-8.85	-1.22	5.64	7.63	"
	phen	benzene	"	-8.38	0.65	6.36	9.03	"
Nd(HAA) ₃ S _x	TBP	cyclohexane	0.1M acetate	-6.15	4.35	—	10.50	(31)
Nd(FHD) ₃ S _x	"	"	"	-0.01	9.95	—	9.96	"
Pm(TTA) ₃ S _x	DBuSO	CCl ₄	1M NaClO ₄	-8.95	-0.73	5.82	8.22	(62)
	TBP	"	"	-8.95	-0.17	6.03	8.78	(61)
Sm(TTA) ₃ S _x	DBuSO	"	"	-8.68	-0.47	5.58	8.21	(62)
	TBP	"	"	-8.68	0.05	5.02	8.73	(61)
Eu(TTA) ₃ S _x	TBP	CH ₂ Cl ₂	0.1M NaClO ₄	—	—	3.32	5.24	(50)
	"	CHCl ₃	"	—	—	3.40	5.20	"
	"	CHBr ₃	"	—	—	3.66	5.62	"
	"	o-dichlorobenzene	"	—	—	4.30	7.20	"
	"	chlorobenzene	"	—	—	4.48	7.26	"
	"	benzene	"	—	—	4.70	8.50	"
	"	toluene	"	—	—	4.84	7.98	"
	"	isopropylbenzene	"	—	—	4.98	8.56	"
	"	CCl ₄	"	—	—	5.05	8.40	"
	TBP	n-hexane	"	—	—	5.87	10.78	"
	"	n-hexane	"	—	—	6.08	10.96	"
	"	n-heptane	"	—	—	6.27	11.14	"
Eu(HAA) ₃ S _x	TBP	cyclohexane	0.1M acetate	-5.79	5.05	—	10.84	(31)
Eu(FHD) ₃ S _x	TBP	cyclohexane	"	0.06	10.06	—	10.0	"
Eu(PMBP) ₃ S _x	Q	toluene	0.1M NaNO ₃	-4.87	-1.70	3.17	—	(40)
	TEHP	"	"	-4.87	1.61	—	6.48	"
	TBP	"	"	-4.87	1.69	—	6.56	"
	TOPO	"	"	-4.87	5.31	—	10.18	"
	TBPO	"	"	-4.87	5.83	—	10.70	"
Gd(TTA) ₃ S _x	DBuSO	CCl ₄	1M NaClO ₄	-8.40	-0.40	5.68	8.00	(62)
	TBP	"	"	-8.40	0.14	5.06	8.54	(61)
Tb(TTA) ₃ S _x	DBuSO	"	"	-8.22	-0.41	5.15	7.81	(62)
	TBP	"	"	-8.22	0.04	5.74	8.26	(61)
Dy(TTA) ₃ S _x	DBuSO	"	"	-7.98	-0.41	5.18	7.57	(62)
	TBP	"	"	-7.98	0.03	5.42	8.01	(61)
Ho(TTA) ₃ S _x	DBuSO	"	"	-7.87	-0.48	5.21	7.39	(62)
	TBP	"	"	-7.87	0.09	5.48	7.96	(61)
Er(TTA) ₃ S _x	DBuSO	CCl ₄	1M NaClO ₄	-7.76	-0.80	5.21	7.16	(62)
	TBP	"	"	-7.76	-0.16	5.53	7.60	(61)
Tm(TTA) ₃ S _x	DBuSO	"	"	-7.40	-0.61	5.05	6.79	(62)
	TBP	"	"	-7.40	-0.17	5.39	7.23	(61)
Tm(HAA) ₃ S _x	TBP	cyclohexane	0.1M acetate	-6.13	4.63	—	10.76	(31)
Tm(FHD) ₃ S _x	TBP	cyclohexane	0.1M acetate	0.27	10.47	—	10.20	"
Yb(TTA) ₃ S _x	DBuSO	CCl ₄	1M NaClO ₄	-7.14	-0.77	5.06	6.37	(62)
	TBP	"	"	-7.14	-0.33	5.35	6.81	(61)
Lu(TTA) ₄ S _x	DBuSO	"	"	-6.99	-1.09	5.06	5.90	(62)
	TBP	"	"	-6.99	-0.67	5.37	6.32	(61)

⁽¹⁾ $K_{ex}(MA_nS_x)$ refers throughout to the extraction constant of the highest adduct (see equations $|2| - |10|$).

sufficiently large to allow a quantitative extraction of Am(III) even if complex forming agents such as diethylenetriaminepentaacetic acid are added to the aqueous phase⁽⁶⁴⁾. Such additions are currently made in the TALSPEAK process to perform a separation of actinides and rare earths⁽⁶⁵⁾.

Separation factors for transplutonium element pairs are lowered in the synergic process. Myasoedov et al⁽³⁷⁾ de-

scribed a procedure to perform an effective americium-curium separation. It is based on the extraction of Cm(III) from weakly acidic solutions by HPMBP-TOPO mixtures. Am(III) is totally oxidized to Am(VI) by (NH₄)₂S₂O₈ prior to the extraction and is then reduced by contact with the HPMBP-TOPO mixtures to the non-extractable pentavalent state. After curium extraction, americium may be isolated from the aqueous phase by

hydroxide precipitation or by extraction after reduction to Am (III) by hydroxylamine. The method has been successfully used for almost quantitative isolation of radiochemically pure americium from highly radioactive solutions.

The synergic extraction of rare earths by combinations of HPMBP and various donor extractants was recently investigated by Navratil⁽³⁸⁻⁴⁰⁾. The author found that adducts of 1:1 and 1:2 stoichiometry were formed and that destruction of synergism sometimes occurred at very low concentrations of neutral extractants. Transition metals (Zn(II), Co(II)) are also extracted⁽⁴⁰⁻⁴²⁾ by HPMBP and TOPO or TBP. The stoichiometry of the adducts remains open to question: slope analysis led Zolotov et al.⁽⁴¹⁻⁴²⁾ to propose the formation of 1:1 adducts in various diluents whereas Navratil⁽⁴⁰⁾ interpreted extraction data in terms of 1:1 and 1:2 adducts in benzene.

Mention should also be made here of new thio- β -diketones. For instance, thiodibenzoylmethane and N-phenyl- β -mercaptocyanamide were proved to be valuable reagents for the synergic extraction of Ni(II) and Co(II) with pyridine⁽⁴³⁻⁴⁴⁾ bases and 1,1,1-trifluoro-4-(2-thienyl)-4-mercapto-3-butane-2-one (HSTTA) was used to extract a large number of transition metal ions in presence of TOPO⁽⁴⁵⁾.

The advent of new chelating extractants has brought about further discussions of a rule relating the stability of a metal chelate and the stability of its adducts. The validity of that rule was already questioned by Irving⁽⁴⁾ who wrote: "Can we generalize and say that the stronger the

complex, the smaller the tendency to form an adduct . . . and the smaller the synergic effect in solvent extraction?" A somewhat broadened version of the rule was proposed by Zolotov et al.⁽⁴²⁾ who stated that "the stronger a reagent is an acid; the more stable adducts it forms". The synergic extraction of UO_2^{2+} by sulfoxides and β -diketones is in keeping with the above rule: Subramanian et al.⁽²⁹⁾ found that synergism followed the order:

	HDBM <	HBA <	HBTA <	HTTA
pK	9.35	8.96	6.30	6.23

The extraction of rare earths by TBP and several fluorinated β -diketones⁽³¹⁾ is roughly accounted for by the same rule:

	HTTA <	HFOD <	HHAA <<	HFHD
pK	6.42	6.70	4.64	3.32

It is interesting to note the abnormal position of HFOD which could be attributed to the sterically demanding t-butyl group of this ligand. The rule is no more valid if one compares two β -diketones of widely different nature. Zolotov et al.⁽⁴¹⁾ pointed out that HPMBP (pK = 4.11) is a stronger acid than HTTA (pK = 6.23) but forms more stable Zn(II) β -diketonates which themselves form less stable synergic adducts with TOPO. It can be seen that the restricted form of the rule, as given by Irving⁽⁴⁾, can still be applied. New evidences for this applicability were afforded by a study carried out by Zolotov et al.⁽⁴⁶⁾ on the

TABLE 4. Some Equilibrium Constants of β -diketone Adducts of Alkali and Transition Metals

Adduct	Neutral ligand S	Diluent	Aqueous phase	log $K_{ex}(MA_n)$	log ⁽¹⁾ $K_{ex}(MA_nS_x)$	log β_{n1}	log β_{n2}	Ref.
Li (TTA) ₂ S _x	TBP	benzene	0.1M bicarbonate	-10.16	-4.20	—	5.96	(58)
	TBPO			-10.16	-2.20	—	7.96	"
Na (TTA) ₂ S _x	TBP	"	"	-11.16	-6.90	—	4.26	"
	TBPO			-11.16	-5.00	—	6.16	"
K (TTA) ₂ S _x	TBP	"	"	-11.16	-8.16	—	3.00	"
	TBPO			-11.16	-6.36	—	4.80	"
Cs (TTA) ₂ S _x	TBP	benzene	"	-10.20	-8.42	—	1.78	"
	TBPO	benzene	"	-10.20	-6.90	—	3.30	"
Sc (TTA) ₃ S _x	TBP	CHCl ₃	0.1M NaClO ₄			1.89	—	(54)
	"	CHBr ₃	"			2.16	—	"
	"	chlorobenzene	"			2.70	—	"
	"	o-dichlorobenzene	"			2.76	—	"
	"	benzene	"			2.92	—	"
	"	CH ₂ Cl ₂	"			2.94	—	"
	"	toluene	"			3.10	—	"
	"	CCl ₄	"			3.38	—	"
	"	n-heptane	"			4.42	—	"
	"	cyclohexane	"			4.52	—	"
"	n-hexane	"			4.61	—	"	
Fe (HAA) ₃ S _x	TBP	cyclohexane	0.1M acetate			-3.71	—	(146)
Co (PMBP) ₂ S _x	2,6 DMP	benzene	"	-8.1	-4.17	2.23	3.93	(19)
	2MP			-8.1	-3.87	2.69	4.23	"
	2,4DMP			-8.1	-3.64	2.77	4.46	"
	P			-8.1	-1.50	3.48	6.60	"
	3MP			-8.1	-1.40	3.52	6.70	"
4MP	-8.1	-1.31	3.57	6.79	"			
Co (BA) ₂ S _x	TOPO	CCl ₄	1M NaClO ₄	-13.05	-9.65	3.40	—	(147)
Co (PTA) ₂ S _x	"	"	"	-10.00	-1.51	5.02	8.48	"
Co (HAA) ₂ S _x	"	"	"	-3.90	6.68	5.19	10.58	"
Co (TAA) ₂ S _x	"	"	"	-8.34	-0.58	5.36	7.76	"
Co (FTA) ₂ S _x	"	"	"	-9.08	0.64	6.04	9.72	"
Co (TTA) ₂ S _x	"	"	"	-8.96	0.34	6.13	9.30	"
Co (BTA) ₂ S _x	"	"	"	-9.66	-0.32	6.15	9.34	"
Ni (TTA) ₂ S _x	2MP	benzene	0.1M acetate			—	5.4	(18)
	P					5.7	8.2	"
	3MP					6.5	9.2	"
	4MP					7.1	10.4	"

(1) $K_{ex}(MA_nS_x)$ refers throughout to the extraction constant of the highest adduct (see equations $|2| - |10|$).

synergic extraction of Zn(II) by TBP and widely different monoacidic chelating agents containing S-N S-S, O-O or N-O donor atoms. In agreement with Irving's rule⁽⁴⁾, thiodiketones (S-N and S-S) which form very stable complexes with Zn(II) because of π interactions exert no synergic effect on the extraction with TBP.

Diluent Influence on Synergism

Numerous investigators^(7,9) demonstrated that the synergic enhancement *strongly* depends on the diluent. As far as the so-called "inert" diluents are concerned, it has been shown for a large number of metals and extractants that synergism^(27,47-51) increases in the order (see Tables 1, 2 and 3):

cyclohexane > hexane > carbon tetrachloride > benzene > chloroform

Furthermore, diluent influence is very large for tetra- and trivalent metals and less pronounced for di- and mono valent metals. Several factors have already been advanced^(7,9) to interpret the diluent influence: dielectric constant of the organic phase, interactions of diluents (e.g. CHCl₃) with neutral donors or solubility of water in diluents. More recently, the regular solution theory⁽⁵²⁾ has been successfully used to account for the diluent effect on synergism. Akiba et al.⁽⁵³⁾ ascribed this effect to variations of the activity coefficients of the MA_n, S and MA_nS_x species from one diluent to the other. The thermodynamic equilibrium constant relative to the formation of the MA_nS adduct was written as:

$$\beta_{n,x}^{\circ} = \frac{(\overline{MA_n S_x})}{(\overline{MA_n})(\overline{S})^x} = \frac{[\overline{MA_n S_x}]}{[MA_n][S]^x} \cdot \frac{\gamma_{MA_n S_x}}{\gamma_{MA_n} \gamma_S^x}, \dots \dots \dots (20)$$

where parentheses denote activity and where γ represents an activity coefficient (the activity of the pure liquid is chosen as the standard state).

The authors investigated several synergic systems involving the same neutral ligand, TBP, for which the activity had been obtained experimentally. The coefficients γ_{MA_n} and $\gamma_{MA_n S}$ were calculated by the theory of the dilute regular solutions:

$$\ln \gamma = \ln \frac{V_A}{V_B} + \left(1 - \frac{V_A}{V_B}\right) + V_A (\delta_A - \delta_B)^2 / RT, \quad (21)$$

where A denotes the solute and B the diluent and where V is a molar volume and S a solubility parameter. Some assumptions had to be made in these calculations e.g., $V_{MA_n} = n V_{HA}$, $\delta_{MA_n} = \delta_{HA}$ or $V_{MA_n S} = V_{MA_n} + V_S$.

Furthermore, the unknown solubility parameters of the various adducts were estimated by empirical methods based on comparisons of data collected for different diluents. Equation [20] proved correct when a dozen diluents were considered and the calculated thermodynamic constants, $\beta_{n,x}^{\circ}$, are reported below:

	log $\beta_{n,1}^{\circ}$	log $\beta_{n,2}^{\circ}$	Reference
Zn(TTA) ₂ + TBP	4.05	—	(53)
UO ₂ (TTA) ₂ + TBP	5.77	—	(51)
Sc(TTA) ₃ + TBP	2.95	—	(54)
Eu(TTA) ₃ + TBP	4.39	7.37	(50)

The extraction data collected by Akiba et al.⁽⁵³⁾ for the system Zn(II)-HTTA-TBP were also interpreted by Tanaka⁽⁵⁵⁾ by the theory of the regular solutions. This author proposed a theoretical expression for the solubility parameter of the adduct MA_nS_x which was used to compute $\Delta \log K_{ex}$, the difference between the extraction constants in two diluents.

Nature of the Metal Ion

Synergic enhancements are expected only for metal complexes "coordinatively unsaturated". Metals with coordination number at least twice their charge were indeed reported⁽⁴⁻¹⁰⁾ to be involved in synergic extractions. No enhancement of the distribution has been reported, for example, for In(III)^(46,36) which is well known to form essentially tetrahedral complexes. Furthermore, if the ionic radius of the central metal ion is too small, the attachment of a new ligand may become impossible⁽⁶⁷⁾. For instance, no adducts of a variety of Zr(IV) or Hf(IV) β -diketonates with phosphorus derivatives could be synthesized whereas adducts with Th(IV) fluorinated β -diketonates were readily prepared. The ionic radii of Zr(IV) (0.79 Å) and Hf(IV) (0.78 Å) are around 0.2 Å smaller than the ionic radius of Th(IV) (0.99 Å).

A large increase of the synergic effect was noted by Healy⁽⁵⁸⁾ when the ionic radius of the alkali ions decreased. Most studies of the influence of the ionic size have been devoted to rare-earths. The formation constants of their adducts in the organic phase ($\beta_{n,x}$, |9|) tend to decrease with decreasing ionic radius⁽⁶¹⁻⁶²⁾, very often in an irregular manner. If the synergic effect (log K_{ex} (MA_nS_x) or log $\beta_{n,x}$) is plotted against Z, the lanthanide series can be divided into four tetrads and extraction data are plotted along four "smooth curves"⁽⁵⁹⁻⁶⁰⁾.

Number of electrons														
0	1	2	3	4	5	6	7	8	9	10	11	12	13	14
La	Ce	Pr	Nd	Pm	Sm	Eu	Gd	Tb	Dy	Ho	Er	Tm	Yb	Lu
-----				-----				-----				-----		
1st tetrad				2nd tetrad				3d tetrad				4d tetrad		

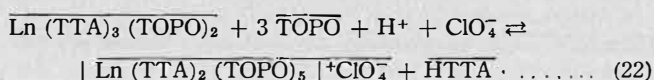
where Gd is common to the second and third tetrad. Excellent examples of the division in tetrads were recently reported by Alstad et al.⁽⁶¹⁻⁶²⁾ for the adduct formation constants $\beta_{3,1}$ and $\beta_{3,2}$ of rare earth TTA complexes with TBP or DBuSO. The division of the lanthanide series in four groups was first mentioned by Siekierski⁽⁶³⁾ in 1966 and was observed by Peppard et al.⁽⁶⁴⁾ in 1969 in the extraction of rare earths by organophosphorus acids. It was called tetrad effect by these authors. The same effect was called double-double effect by Siekierski⁽⁶⁵⁾ and was claimed to be observed⁽⁶⁶⁻⁶⁷⁾ in several properties of the rare earths such as cell-parameters, extraction constants or stability of complexes. The tetrad or double-double effect has been extensively discussed and was interpreted by Jørgensen⁽⁶⁸⁾ and Nuggent⁽⁶⁹⁾ in terms of variation of the Racah parameter E³. It has been recently reviewed by Sinha⁽⁷⁰⁾ who proposed another method, called the "inclined W hypothesis", for correlating properties of f elements.

Formation of Mixed Synergic Adducts

The formation of mixed synergic adducts has been reviewed by Marcus and Kertes⁽⁷⁾ and by Healy⁽⁹⁾. Some results on mixed adducts of f elements have been published recently. Zolotov et al.^(34,37) concluded that the synergic extraction of Am(III) and Eu(III) by HPMBP and TOPO in hexane or cyclohexane arises from the formation of MA₃(TOPO)₂ and MA₂(NO₃)(TOPO)₂. No mixed adduct was found with the less basic TBP at variance with Davis et al.^(71,73) who proposed that rare earths are extracted as M(TTA)₂(NO₃)(TBP)₂.

Spectrophotometry was successfully used by Taketatsu and Toriumi⁽⁷⁴⁾ to investigate the extraction of Er(III) or

Ho(III) from perchlorate solutions by mixtures of HTTA and TOPO. The authors presented spectroscopic evidence to support the prevalence of equilibrium [22]:



The mixed adduct is highly dissociated in polar diluents. The perchlorate ion can be replaced by other inorganic anions⁽⁷⁵⁾ but the overall equilibrium constant of [22] is then much lower:

	ClO_4^-	SCN^-	NO_3^-	Cl^-
$\overline{\text{Log K}_{\text{ex}}[22]}$	8.3	6.5	5.3	3.6

The extraction of mixed synergic complexes is not limited to the case of the actinides or the rare earths. The extraction of Sr(II) was reported⁽⁷⁶⁾ to proceed via the formation of Sr(TTA)(ClO₄)(TBP)₂. Aggett⁽⁷⁷⁾ studied the extraction of Fe(III) by acetylacetonate and TOPO from perchlorate solutions and concluded that the extracted species were FeA₃ and FeA₂ClO₄(TOPO)₂. The distribution of the latter compound involves the aqueous species FeA₂⁺ which is a major component of the aqueous phase. Furthermore, Takeda et al.⁽⁷⁸⁾ found that Fe(ACAC)₃ reacts with hydrogen halides, HX, in dichloromethane to yield Fe(ACAC)₂X, and Fe(ACAC)X₂H₂O.

The tendency to form mixed synergic complexes is probably enhanced by the basicity of the neutral ligand and by the weakness of the chelating agent, as indicated by the numerous mixed adducts reported for TOPO. The nature of the inorganic ligand is also of prime importance: NO₃⁻ ions which coordinate with metallic cations preferably to Cl⁻ or SO₄²⁻ ions, have a greater tendency to form mixed complexes. Moreover the relatively inert ClO₄⁻ ion also yields mixed synergic complexes, presumably by formation of ion pairs.

Structure of the Synergic Adducts and Mechanism of the Extraction

Much of the data on the synergic extraction by β-diketones is consistent with the view that one or several molecules of a neutral donor associate with a metal β-diketonate; the new adducts are more hydrophobic and thus better extracted⁽⁴⁻¹⁰⁾. The synergic reaction is usually considered to arise from the displacement of the hydration water of a complex by the donor extractant. Subramanian et al.⁽⁷⁹⁾ found that there is an inverse relationship between the amount of water extracted in the organic phase and the basicity of the donor. The influence of water appears, however, to be largely unresolved because Kassierer and Kertes⁽⁸⁰⁾ noted that the water content of an organic phase may drastically vary with the nature of the metal involved.

The structure of lanthanides and actinides synergic adducts and the mechanism of their formation has given rise to much controversy in the past⁽⁷⁾. Healy⁽⁸¹⁾ assumed that one or more chelate rings may open to allow the addition of donor molecules with no alteration of the coordination number of the central metal ion. On the other hand, Irving and Edgington⁽⁸²⁾ claimed that the coordination number of lanthanides and actinides may raise to eight and that ample room is available for the coordination of additional molecules without the opening of chelate rings. The latter assumption is now widely accepted. A coordination number as high as twelve was recently reported for a lanthanum compound⁽⁸³⁾ and a large number of rare earth complexes with a coordination number of eight are known. Solid state structures are, of course, no absolute proof of the conformational preference of species in solution but all X-ray structural analyses reported so far

are in agreement with Irving's assumption⁽⁸²⁾. Rare earths were found to be coordinated to six oxygen atoms of three chelating groups and to one or two donor atoms of a neutral extractant in various adducts such as Nd(TTA)₃(TPPO)₂⁽⁸⁴⁾, Eu(TTA)₃(phen)⁽⁸⁵⁾, Nd(TTA)₃(dipy)⁽⁸⁶⁾, Nd(TTA)₃(1,2-di-4-pyridyl)ethane⁽⁸⁷⁾. A similar structure was reported for Th(TTA)₄TOPO⁽⁸⁸⁾.

Further evidences to support a mechanism involving the direct coordination of the central metal ion by the donor extractant are afforded by NMR spectroscopy. The formation of lanthanide β-diketonate adducts has indeed given rise to a great deal of interest in a field of chemistry usually considered as not related to the synergic effect. Some paramagnetic β-diketonates, called lanthanide shift reagents, are extensively used to simplify the NMR spectra of a large number of donor organic substrates⁽⁸⁹⁾. Magnetic interactions between the unpaired spins of a rare earth ion and the resonating nuclei of the surrounding ligands lead to large paramagnetic shifts of the NMR peaks⁽⁸⁹⁻⁹⁰⁾. The modified spectra are often amenable to first order analysis.

There is a close analogy between the synergic effect and the properties of lanthanide shift reagents as the latter associate with an organic substrate, S, according to the reaction:



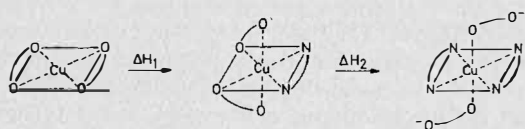
where A denotes sterically crowded β-diketones such as HTHD or HFOD. The paramagnetic shift is a function of the structure of the adduct *in solution* and the conformational preference of a lanthanide complex can be deduced from the NMR spectra^(39,91). The distances metal ion-organic substrate reported so far are in the range expected for the direct attachment of the donor atom of S to the central metal ion. It is noteworthy that rare earth TTA complexes can also behave as lanthanide shift reagents. Duyckaerts et al.⁽⁹²⁾ recently investigated by NMR the stoichiometry and stability of Eu(TTA)₃ adducts with MIBK, TPPO and 2 MP and studied some of the main features of the synergic effect such as the influence of the basicity of the donor extractant, of the presence of water or of an excess of HTTA.

In order to reach a better understanding of the synergic extraction of rare earths, several authors have carried out thermodynamic measurements either by direct titration calorimetry or by distribution experiments at different temperatures. Kertes and Kassierer^(27,93) studied the system Ln(TTA)₃.2H₂O-bipy-CHCl₃ and concluded that 1:1 and 1:2 adducts were formed. The authors obtained large exothermic enthalpy values and unfavourable entropy changes. The entropy data were interpreted in terms of a positive contribution due to the release of water and a larger negative contribution due to the binding of the neutral extractant. Similar trends were reported by Subramanian et al.⁽⁹⁴⁾ for the adducts Eu(TTA)₃(TOPO)_{1,2}, Eu(TTA)₃(DPSO)_{1,2} and Eu(TTA)₃(TBP)_{1,2}, by Choppin et al.⁽⁹⁵⁾ for Eu(TTA)₃(TBP)_{1,2} and Tm(TTA)₃(TBP) and by Dakternieks⁽⁹²⁾ for the adducts between lanthanide THD complexes and dipyrindyl or 1,8-naphthyridine (at variance with Kertes and Kassierer^(27,93) no evidence of 1:2 adducts was found).

The situation concerning the synergic extraction of transition metal ions requires some additional comments. Works on base adducts of divalent transition metal β-diketonates have been reviewed by Graddon⁽⁹⁶⁾. Relatively rigid five- and six-coordinated adducts are well known; the complexes usually show octahedral geometry eventually distorted by the Jahn-Teller effect as in the case of Cu(II) chelates. The donor molecules are directly complexed to the metal ion⁽⁹⁷⁻⁹⁸⁾ and no chelate ring is opened in the

synergic process in keeping with Irving's assumption⁽⁸³⁾. However, some most interesting data indicate that some neutral extractants can partially displace a β -diketone. If a strongly basic bidentate donor such as *N,N*-dimethylenediamine (DEMDA) is added to a highly fluorinated copper complex such as $\text{Cu}(\text{HAA})_2$, the resulting bis-adduct was shown by X-ray crystallography⁽⁹⁹⁾ to be octahedral with four short Cu-N distances in the equatorial plane and two long Cu-O bonds in the axial positions. The two remaining oxygen atoms of the β -diketone ligands are not coordinated to the metal ion but involved in intramolecular hydrogen bonds.

Additional information regarding these systems has been gained by calorimetric measurements. In agreement with the data collected for rare earths, the synergic extraction of transition metals was found to be exothermic with large negative entropy changes. Several thermodynamic measurements were carried out by Graddon et al.⁽¹⁰⁰⁻¹⁰³⁾, Choppin et al.⁽¹⁰⁴⁾ and Kertes et al.⁽²⁸⁾. The data provide evidences to support the influence of the basicity of the neutral extractant and of the acidity of the chelating agent. Furthermore, it seems that the increase of the formation constants observed for fluorinated β -diketonates is more a question of change in entropy than in enthalpy. Graddon et al.⁽¹⁰¹⁾ also interpreted the enthalpy changes for the formation of $\text{Cu}(\text{II})$ adducts with diamines:



The same authors reported on calorimetric studies of adducts of thio- β -diketonates⁽¹⁰⁶⁾.

Non-chelating Acid Plus Neutral Extractant Systems

Mixtures of phosphoric or carboxylic acids and of neutral extractants are known to promote the extraction of metal ions⁽⁴⁻¹⁰⁾. Several important differences with similar systems involving β -diketonates should be pointed out. The synergic effect is usually markedly lower and often followed by destruction of synergism; it is observed with fewer metal ions. Phosphoric and carboxylic acids dimerize⁽⁷⁾ in non-polar diluents; they extract metals by formation of solvated complexes $\text{MA}_n(\text{HA})_p$. Moreover, they strongly interact with neutral extractants by hydrogen bonding whereas such interactions are relatively weak in the case of the β -diketonates. An excellent example of the need to consider all interactions with an organophosphoric acid is afforded by a recent study of the association between HDEHP and TBP. Liem⁽¹⁰⁶⁾ found that the acidic extractant dimerizes in both the aqueous and the organic (toluene) phases and forms a 1:1 complex with TBP. The presence of various $(\text{HA})_n(\text{S})_p$ complexes is widely regarded as the main reason for the extraction inefficiency of acid-donor combinations and for the destruction of synergism. The mechanism of the synergic effect was attributed either to a direct complexation of the metal ion by S or to a partial substitution of the acid groups by the neutral extractant⁽⁴⁻¹⁰⁾. The former mechanism is now favored by many authors.

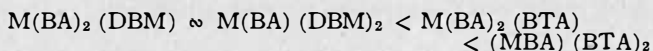
Relatively few works were devoted in the past to the present systems and even less papers have been published on the subject in recent years. Combinations of phosphoric acids and neutral phosphorus derivatives remain the most popular synergic mixtures. Nash and Choppin⁽¹⁰⁴⁾ compared the extraction of $\text{Zn}(\text{II})$ by TBP and HTTA or HDEHP and found that the latter compound exerted no synergic effect. Bykhovtsov et al.⁽¹⁰⁷⁻¹⁰⁹⁾ referred to the

influence of the inorganic anion in the aqueous phase on the extraction of $\text{U}(\text{VI})$ by HDEHP-TBP mixtures. The extraction of macroscopic quantities of uranium from sulfate solutions was enhanced by the addition of nitric acid. The extracted species was claimed to be $\text{UO}_2\text{A}_2\cdot\text{UO}_2(\text{NO}_3)_2(\text{TBP})_2$. Similar results were obtained⁽¹⁶⁰⁾ for $\text{Th}(\text{IV})$ which was extracted as $\text{Th}(\text{NO}_3)_3\cdot\text{Th}(\text{NO}_3)_4(\text{TBP})_3$. Calorimetric measurements performed by Marcus and Kolarik⁽¹¹¹⁾ on the UO_2^{2+} -TBP-HDEHP system indicated that the formation of the adduct $\text{UO}_2(\text{HA})_2\text{S}$ in dodecane was exothermic. To interpret the enthalpy variations with the concentration of TBP or UO_2^{2+} , the authors had to take into account the association reactions in the organic phase. Liems and Sinegribova⁽¹¹²⁾ studied by curve fitting the synergic extraction of $\text{Hf}(\text{IV})$ by combinations of HDBP and TOPO in hexane. They gave evidences to support the formation of mixed species with SO_4^{2-} or ClO_4^- ions, for example, $\text{Hf}(\text{ClO}_4)_3\text{As}_3$ and $\text{Hf}(\text{ClO}_4)_2\text{A}_2\text{S}_2$. The extraction of Cs^+ or Rb^+ by HDEHP and 2-phenylphenol was investigated by Smelov and Lanin⁽¹¹³⁾ who found weak synergic effects attributed to the presence of MAS_2 species.

Some recent data have been collected on the extraction with carboxylic acids. Mention should be made here of the extraction of $\text{U}(\text{VI})$ by aromatic carboxylic acids⁽¹¹⁴⁾ and TOPO. A synergic enhancement was noticed at high pH ($\text{pH} > 2.0$) whereas a destruction of synergism occurred at low pH where aromatic acids are non-dissociated and are hydrogen-bonded with TOPO. A new aliphatic carboxylic acid with an additional $\text{P}=\text{O}$ group, (carboxy-2-ethyl) diphenylphosphine oxide was used by Rocca and Porthault⁽¹¹⁵⁾ who quantitatively extracted $\text{Co}(\text{II})$ as $\text{CoA}_3\cdot\text{HA}\cdot\text{S}_3$ in the presence of 4-(3-phenylpropyl)pyridine.

Acidic Plus Acidic Extractants

A few examples of synergic enhancement due to two acidic extractants have been quoted recently. Most of these are related to the extraction of metals by two β -diketonates (*HA* and *HB*) and the synergic process may involve the stepwise formation of several complexes. For instance, the extraction of a trivalent metal may proceed via the formation of MA_3 , MA_2B , MAB_2 and MB_3 and also of adducts MA_3HA or MB_3HB as noted by Sekine and Dyrssen⁽¹²⁾. Shigematsu and Honjyo⁽¹¹⁶⁾ studied the extraction of $\text{Lu}(\text{III})$ by mixtures of HBA and HDBM or of HBA and HBTA. The authors determined by curve fitting the extraction constants K_{ex} relative to all the complexes of the MA_nB_m type. They achieved a good agreement between experimental and statistically calculated values of K_{ex} for the system HBA-HDBM but found some discrepancies for the system HBA-HBTA. The addition of a neutral extractant, TOPO, brought about significant synergic effects increasing in the order:



which reflects the Lewis acidity of the β -diketonates. Like previous investigators⁽¹¹⁷⁾, Woo et al.⁽¹¹⁸⁻¹¹⁹⁾ reported on the synergic extraction of rare earths by mixtures of HTTA and HACAC. A maximum enhancement was achieved when HACAC was also the diluent and the authors concluded that the species $\text{M}(\text{TTA})_3(\text{HACAC})$ was formed. Combinations of HTTA and HACAC in various diluents were also used to extract $\text{Cu}(\text{II})$ whose distribution was well accounted for by a statistical model⁽¹²⁰⁾.

Mixtures of β -diketonates with other acids have been investigated as well. Kolarik⁽¹⁵⁾ studied the extraction of rare earths by HPMBP and *n*-octyl hydrogen *n*-octylphosphonic acid and ascribed the synergic effect to the forma-

tion of several intermediate complexes. A simpler system was described by Dolgashova and Fridman⁽¹⁶⁾: the extraction of Cu(II) by HACAC and hydroxyquinoline involves only the complex MAB which give rise to an antagonistic effect. Nikolaeva et al.⁽²¹⁾ reported a limited enhancement of the extraction of V(V) by the HPMBP and palmitic acid and Hala et al.⁽¹²²⁻¹²⁴⁾ used mixtures of the acidic extractant, N-benzoyl-N-phenyl-hydroxylamine, (HA) and of phenols⁽¹²²⁾, nitrophenols⁽¹²³⁾ or halogenacetic acids⁽¹²⁴⁾, (HB) to extract Hf(IV). In the latter case, a substitution mechanism was favoured by the authors who found from the slope analysis that the synergism was due to the complex HfA₃B. Phenols and their derivatives were assumed to be involved in adducts HfA₄.HB by hydrogen bonding⁽²³⁻¹²⁴⁾.

A final point of interest is that two chelating agents of the hydroxyoxime type have been used together in the extraction of Cu(II). The kinetics and mechanism of the distribution have been very recently reviewed by Flett⁽¹²⁵⁾.

Neutral-plus-Neutral Extractants

Combinations of two neutral extractants, usually oxygen-containing donors, can lead to small synergic effects. No clear understanding of the intricate mechanism of the extraction has yet been reached. Recent data related to the extraction of U(VI) or Th(IV) by mixtures of two sulfoxides (S₁ and S₂) or of TBF and a sulfoxide were reported by Mohanty and Reddy⁽¹³⁻¹⁴⁾. The synergic effect was attributed to the formation of mixed complexes UO₂Cl₂(S₁)_n(S₂)_m or ThCl₄(S₁)_n(S₂)_m whose stoichiometry could not be deduced from the slope analysis. The extent of the competition between the neutral donors was however estimated. It was found that DPSO solvated UO₂Cl₂ better than TBP although the SO group is less basic than the PO group.

Irving and Lewis⁽¹²⁶⁾ carried out an extensive study of the extraction of InCl₃ by mixtures of "inert" diluents. Large enhancement of the extraction were noted for mixtures of nitrobenzene with various donor diluents. The synergic effect was observed at high acidity of the aqueous phase and was always followed by a destruction of synergism. The mechanism of the extraction is probably dependent on the nature of the donor diluent used. For instance, distribution experiments performed with nitrobenzene-*n*-hexanol mixtures involved the extraction of large amounts of water and HCl as (H₂O)₄HCl. As a consequence, a solvated acido-complex species (H₉O₄)⁺(S)_mInCl₄⁻ was probably extracted in the organic phase. On the other hand, the extraction of water and acid by nitrobenzene-ethyl ether mixtures was relatively low and several factors were suggested by the authors to account for the synergic effect. The most important factor could be the high solubility of the ether in the aqueous phase. Similar measurements were also reported for Zn(II).

Cationic-plus-Neutral Extractants

Weak synergic effects (factors of 10 or less) were recently reported for mixtures of tertiary or quarternary ammonium salts and of neutral phosphorus derivatives. Zolotov et al.^(34,127,128) considered the extraction of Am(III), Cm(III), Cf(III) and Eu(III) by combinations of TOAHNO₃ and TBP, TBPO or TOPO. No synergic enhancement was observed with MIBK. The synergic coefficient *S.C.* was barely influenced by the nature of the diluent but was increased by the addition of a salting-out agent such as LiNO₃. The authors presumed that the enhanced extraction was due to the formation of mixed anionic complexes, the central metal ion being directly

coordinated to NO₃⁻ anions and to TBP molecules: M(NO₃⁻)_{3+p}(TBP)_n(TOAH⁺)_p. Smaller synergic effects were measured with TOPO. The formation of mixed anionic complexes was also suggested by Khopkar and Narayanankutty⁽¹²⁹⁾ who investigated the extraction of Am(III) and Eu(III) by Aliquat thiocyanate (tricaprylmethylammonium thiocyanate) and phosphorus derivatives. The synergic effect was found to decrease in the order TBP > TBPO > TOPO, i.e. when the basicity of the neutral donor was increased. The authors presumed that neutral extractant molecules coordinated in the species M(SCN)₃(S)_x are gradually replaced by R₄N⁺SCN⁻. This substitution would be easier for less basic donors and would yield complexes such as |Am(SCN)₄(TOPO)₃|⁻ R₄N⁺ or |Am(SCN)₅(TBP)₂|²⁻ |(R₄N₂)²⁺. The extraction of Mo(VI) by TOAHCl and TBP⁽¹³⁰⁾ was also accounted for by the formation of mixed anionic species |MoO₂Cl₃TBP|⁻ TAOH⁺.

Cationic-plus-Anionic Extractants

Very extensive studies of the large synergic effect ($\approx 10^3$) observed in the extraction of Am(III) and Ce(III) by mixtures of TOA and HTTA from hydrochloric acid solutions were performed by Newman and Klotz⁽¹³¹⁻¹³²⁾. The authors had previously investigated the interactions between the extractants and reported on the formation of TOAHCl, TOAHTTA and TOAHClHTTA. The extraction measurements were carried out in such conditions that no free amine was available for complexation. The three organic species mentioned above were found to have the same extractive power and to yield the complexes M(TTA)₃TOAHCl, M(TTA)₃TOAHTTA and M(TTA)₃TOAHClHTTA. Genov et al.^(48,49,133) arrived at similar conclusions in an investigation of the extraction of Pr(III), Gd(III) and Yb(III) from nitrate solutions but in later works, these authors interpreted the synergic effect caused by aliphatic amines in terms of the adduct M(TTA)₃S (see table 2) and neglected the formation of the TOAHTTA and TOAHNO₃ species.

Pyridine and its methylated derivatives⁽¹³⁴⁻¹³⁵⁾ as well as piperidine and 2-aminopyridine⁽¹³⁶⁾ also enhance the extraction of rare earths. Genov et al.⁽¹³⁴⁻¹³⁵⁾ and Kononenko et al.⁽¹³⁶⁾ proposed that the extraction proceeds via the formation of M(TTA)₄HS species. The synergic effect increased in the order:



which does not reflect the steric hindrance mentioned above.

The complexes M(TTA)₄HS, where S denotes an aliphatic or aromatic amine, are probably ion pairs with the central metal ion surrounded by four β -diketone groups and the ammonium cation hydrogen-bonded to some of the oxygen atoms of the anion. Such structures were examined by X-ray spectrometry by Leipoldt et al.⁽¹³⁷⁾ and by Aslanov et al.⁽¹³⁸⁻¹⁴⁰⁾. The latter authors found that in the solid state, M(TTA)₄HS can exist in two forms: an hydrogen-bonded ion pair or an acidic tetrakis β -diketonate co-crystallized with non-stoichiometric quantities of bases such as diethylamine or piperidine. NMR spectroscopy of paramagnetic lanthanides allows⁽⁹²⁾ to study the formation of Eu(TTA)₄⁻(H₂MP)⁺ *in solution*. The calculated stability constant was found to be much higher than the formation constants of the mono- and bis-adducts Eu(TTA)₃S_{1,2}. The interaction of Eu(TTA)₃ with a quaternary ammonium salt (trilaurylmethylammonium chloride) was also investigated⁽⁹²⁾ by NMR.

Other cationic reagents have been used. Rahaman and Finston⁽¹⁴¹⁾ considered the extraction of Co(II) by HTTA

and tetraphenylarsonium chloride from acetate solutions. From the slope analysis, the authors concluded that Co(II) was extracted as $[\text{Co}(\text{TTA})_2 \text{CH}_3\text{CO}_2]^- | (\text{C}_6\text{H}_5)_4\text{As}^+$.

It is noteworthy that organophosphoric or carboxylic acids can be involved in similar synergic processes. Dep-tula⁽¹⁴²⁾ reported a synergic effect followed by a destruction of synergism for the system UO_2^{2+} -mono-*n*-butyl-phosphoric acid (H_2A)-TOA- H_2SO_4 which was due to the formation of $[\text{UO}_2\text{SO}_4\text{HA}]^- | \text{TOAH}^+$. Liem and Sinegribova⁽¹¹²⁾ observed an antagonistic effect in the extraction of Hf(IV) by mixtures of HDEHP and TOA which was attributed to a strong interaction between the extractants. The extraction of Mn(II) by naphthenic acid⁽¹⁴³⁾ and TOA and of Ca(II) or Mg(II) by commercial carboxylic acids (versatic) and water soluble amine-alcohols⁽¹⁴⁴⁾ has also been investigated.

Acknowledgments

We gratefully acknowledge research support from the Fonds National de la Recherche Scientifique of Belgium.

ABBREVIATIONS

ACAC(H)	= acetylacetone
BA(H)	= benzoylacetone
BP(A)(H)	= N-benzoyl-N-phenylhydroxylamine
BTA(H)	= benzoyltrifluoroacetone
DBM(H)	= dibenzoylmethane
DBSO	= dibenzylsulfoxide
DBuSO	= dibutylsulfoxide
DDCSO	= didecylsulfoxide
DEHP (H)	= di-2-ethyl hexyl phosphoric acid
DHSO	= dihexylsulfoxide
dipy	= 2,2'-dipyridyl
DISPSO	= diisopentylsulfoxide
x, y DMP	= pyridine substituted by methyl groups in positions x and y
x, y DMPO	= pyridine oxide substituted by methyl groups in positions x and y
DPSO	= diphenylsulfoxide
FHD (H)	= 1,1,1,2,2,6,6,7,7,7-decafluoro-3,5-heptanedione
FOD (H)	= 1,1,1,2,2,3,3-heptafluoro-7,7-dimethyl-4,6-octanedione
FTA (H)	= 2-fluorotriethylacetone
HAA (H)	= hexafluoroacetylacetone
MIBK	= methyl isobutyl ketone
xMP	= pyridine substituted by a methyl group in position x
xMPO	= pyridine oxide substituted by a methyl group in position x
P	= pyridine
phen	= 1,10-phenanthroline
PMBP (H)	= 1-phenyl-3-methyl-4-benzolpyrazolone-5
PO	= pyridine oxide
PTA (H)	= pivaloyltrifluoroacetone
Q	= quinoline
SAO (H)	= salicylaldehyde
TAA (H)	= trifluoroacetylacetone
TBP	= tributylphosphate
TBPO	= tributylphosphine oxide
TEHP	= triethylhexylphosphate
THD (H)	= dipivaloylmethane; 2,2,6,6-tetramethyl-3,5-heptanedione
x, y, zTMP	= pyridine substituted by methyl groups in positions x, y and z
TOA	= trioctylamine
TOPO	= trioctylphosphine oxide
TPPO	= triphenylphosphine oxide
TTA (H)	= thenoyltrifluoroacetone

REFERENCES

- (1) Cuninghame, J.G., Scargill, B. and Willis, H.M., UK AERE Rept. C/M 215, 1956.
- (2) Vogel, H., Ber. Chem. Ges. 1879, 12, 2313.
- (3) Blake, C.A., Baes, C.F., Brown, K.B., Coleman, C.F. and White, J.C. in Proc. Intern. Conf. on the Peaceful Uses of Atomic Energy, Geneva, 1958, vol. 28, IAEA, Vienna, 1959, p. 289.

- (4) Irving, H.M.N.H., in Solvent Extraction Chemistry (Edited by Dyrssen, D., Liljenzin, J.O. and Rydberg, J.) North Holland, Amsterdam, 1967, p. 91.
- (5) Peppard, D.F., in Advances in Inorganic Chemistry and Radiochemistry (Edited by Emeleus, H.J. and Sharpe, A.G.) Academic Press, New York, 1966, vol. 9, p. 1.
- (6) Healy, T.V., in Solvent Extraction Research (Edited by Kertes, A.S. and Marcus, Y.), Wiley, New York, 1969, p. 257.
- (7) Marcus, Y. and Kertes, A.S., Ion Exchange and Solvent Extraction of Metal Complexes, Wiley, New York, 1969, p. 815.
- (8) Weaver, B., in Ion Exchange and Solvent Extraction, (Edited by Marinsky, J.A. and Marcus, Y.), M. Dekker, New York, 1974, vol. 6, p. 189.
- (9) Healy, T.V., in Gmelin Handbuch, Band 21, Teil D2, no. 21, Springer Verlag, Berlin, 1975, p. 360.
- (10) Zolotov, Y.A., Extraction of Chelate Compounds, Ann Arbor Humphrey Sciences Publ., London, 1970.
- (11) Taube, M. and Siekierski, S., Nukleonika, 1961, 6, 489.
- (12) Sekine, T. and Dyrssen, D., J. Inorg. Nucl. Chem. 1967, 29, 1457, 1475, 1481 and 1489.
- (13) Mohanty, S.R. and Reddy, A.S., J. Inorg. Nucl. Chem. 1975, 37, 1791.
- (14) Mohanty, S.R. and Reddy, A.S., J. Inorg. Nucl. Chem. 1975, 37, 1977.
- (15) Kolarik, Z., J. Inorg. Nucl. Chem. 1971, 33, 1135.
- (16) Dolgashova, N.V. and Fridman, Y.D., Zh. Anal. Khim. 1972, 27, 1453.
- (17) Bagawde, S.V., Ramakrishna, V.V. and Patil, S.K., J. Inorg. Nucl. Chem. 1976, 38, 2085.
- (18) Kawamoto, H. and Akaiwa, H., J. Inorg. Nucl. Chem. 1969, 31, 1141.
- (19) Al-Niimi, N.S., Al-Karaghoul, A.R. and Aliwi, S.M., J. Inorg. Nucl. Chem. 1973, 35, 577.
- (20) Rao, A.P. and Dubey, S.P., J. Inorg. Nucl. Chem. 34, 2041.
- (21) Ueda, K., Aoki, T., Matsui, M., Shigematsu, T., Bull. Inst. Chem. Res. Kyoto Univ. 1972, 50, 653.
- (22) Shigematsu, T., Honjyo, T., Tabushi, M. and Matsui, M., Bull. Chem. Soc. Jap. 1970, 43, 793.
- (23) Manchanda, V.K., Shukla, J.P. and Subramanian, M.S., J. Inorg. Nucl. Chem. 1974, 36, 2595.
- (24) Manchanda, V.K., Shukla, J.P. and Subramanian, M.S., J. Radioanal. Chem. 1976, 29, 69.
- (25) Al-Niimi, N.S. and Rasoul, H.A.A., J. Inorg. Nucl. Chem. 1974, 36, 2051.
- (26) Al-Niimi, N.S., Al-Karaghoul, A.R., Aliwi, S.M. and Jalhoom, M.G. J. Inorg. Nucl. Chem. 1974, 36, 283.
- (27) Kassierer, E.F. and Kertes, A.S., J. Inorg. Nucl. Chem. 1972, 34, 3221.
- (28) Kassierer, E.F. and Kertes, A.S., J. Inorg. Nucl. Chem. 1972, 34, 3209.
- (29) Subramanian, M.S. and Pai, S.A., Aust. J. Chem. 1973, 26, 77.
- (30) Kononenko, L.I., Burtenko, L.M. and Vitkun, R.A., Radiokhimiya 1971, 13, 556.
- (31) Mitchell, J.W. and Banks, C.V., Talanta 1972, 19, 1157.
- (32) Dakternieks, D.R., J. Inorg. Nucl. Chem. 1976, 38, 141.
- (33) Jensen, B.S., Acta Chem. Scand. 1959, 13, 1668 and 1891.
- (34) Chmutova, M.K., Myasoedov, B.F., Kochetkova, N.E., Spivakov, B.Y. and Zolotov, Y.A., Radiokhimiya 1974, 16, 702.
- (35) Myasoedov, B.F., Kochetkova, N.E. and Chmutova, M.K., Zh. Anal. Khim. 1973, 28, 1723.
- (36) Chmutova, M.K., Pribylova, G.A. and Myasoedov, B.F., Zh. Anal. Khim. 1973, 28, 2340.
- (37) Myasoedov, B.F., Chmutova, M.K. and Lebedev, I.A., Proc. Int. Conf. Solv. Extr. Conf. 1971, Soc. Chem. Ind., London 1971, vol. I, p. 815.
- (38) Navratil, O. and Mikulec, Z., Collect. Czech. Chem. Commun. 1973, 38, 2430.
- (39) Navratil, O., Collect. Czech. Chem. Commun. 1974, 39, 2019.
- (40) Navratil, O., Proc. Int. Conf. Solv. Extr. 1974, Soc. Chem. Ind., London, 1974, vol. III, p. 2585.
- (41) Zolotov, Y.A. and Gavrilo, L.G., Radiokhimiya 1969, 11, 389.
- (42) Zolotov, Y.A. and Gavrilo, L.G., J. Inorg. Nucl. Chem. 1969, 31, 3613.
- (43) Chikuma, M., Yokoyama, A. and Tanaka, H., J. Inorg. Nucl. Chem. 1974, 36, 1243.
- (44) Chikuma, M., Yokoyama, A. and Tanaka, H., J. Inorg. Nucl. Chem. 1975, 37, 199.
- (45) Honjo, T., Yashima, S. and Kiba, T., Bull. Chem. Soc. Jap. 1973, 46, 3772.
- (46) Zolotov, Y.A., Petrukhin, O.M. and Gavrilo, L.G., J. Inorg. Nucl. Chem. 1970, 32, 1679.

- (47) Akiba, K., *J. Inorg. Nucl. Chem.* 1973, **35**, 3323.
- (48) Genov, L. and Dukov, I., *Monatsh. Chem.* 1973, **104**, 750.
- (49) Genov, L. and Dukov, I., *Z. Chem.* 1974, **14**, 446.
- (50) Akiba, K., *J. Inorg. Nucl. Chem.* 1973, **35**, 2525.
- (51) Akiba, K. and Suzuki, N., *Bull. Chem. Soc. Jap.* 1971, **44**, 1043.
- (52) Hildebrand, J.H. and Scott, R.L., "Solubility of non-electrolytes", Dover Publ., New York, 1957.
- (53) Akiba, K., Suzuki, N. and Kanno, T., *Bull. Chem. Soc. Jap.* 1969, **42**, 2537.
- (54) Akiba, K., Ishikawa, T. and Suzuki, N., *J. Inorg. Nucl. Chem.* 1971, **33**, 4161.
- (55) Tanaka, M., *Proc. Int. Solv. Extr. Conf.* 1971, Soc. Chem. Ind., London, 1971, vol. I, p. 18.
- (56) Zolotov, Y.A. and Gavrilova, L.G., *Zh. Anal. Khim.* 1970, **25**, 813.
- (57) Bok, L.D.C., Wessels, G.F.S. and Leipoldt, J.G., *Z. Anorg. Allg. Chem.* 1974, **404**, 76.
- (58) Healy, T.V., *J. Inorg. Nucl. Chem.* 1968, **30**, 1025.
- (59) Peppard, D.F., Mason, G.W. and Lewey, S., in *Solvent Extraction Research*, (Edited by Kertes, A.S. and Marcus, Y.), Wiley, New York, 1969, p. 49.
- (60) Peppard, D.F., Bloomquist, C.A.A., Horwitz, E.P., Lewey, L. and Mason, C.W., *J. Inorg. Nucl. Chem.* 1970, **32**, 339.
- (61) Farbu, L. Alstad, J. and Auguston, J.H., *J. Inorg. Nucl. Chem.* 1974, **36**, 2091.
- (62) Auguston, J.H., Farbu, L. and Alstad, J., *J. Inorg. Nucl. Chem.* 1975, **37**, 1243.
- (63) Fidelis, I. and Siekierski, S., *J. Inorg. Nucl. Chem.* 1966, **28**, 185.
- (64) Peppard, D.F., Mason, G.W. and Lewey, S., *J. Inorg. Nucl. Chem.* 1969, **31**, 2271.
- (65) Siekierski, S. and Fidelis, I., *J. Inorg. Nucl. Chem.* 1972, **34**, 2225.
- (66) Siekierski, S., *J. Inorg. Nucl. Chem.* 1971, **33**, 377.
- (67) Fidelis, I. and Siekierski, S., *J. Inorg. Nucl. Chem.* 1971, **33**, 3191.
- (68) Jørgensen, C.K., *J. Inorg. Nucl. Chem.* 1970, **32**, 3127.
- (69) Nugent, L.J., *J. Inorg. Nucl. Chem.* 1970, **32**, 3485.
- (70) Sinha, S.P., *Structure and Bonding* 1976, vol. 30, p. 1.
- (71) Tournier, R.A. and Davis, M.W., Jr., *Separ. Sci.* 1972, **7**, 159.
- (72) Cox, E.C., Jr. and Davis, M.W., Jr., *Separ. Sci.* 1973, **8**, 205.
- (73) Hayden, J.G., Gerow, I.H. and Davis, M.W., *Separ. Sci.* 1974, **9**, 337.
- (74) Taketatsu, T. and Toriumi, N., *J. Inorg. Nucl. Chem.* 1969, **31**, 2235.
- (75) Taketatsu, T. and Ohkura, N., *Bull. Chem. Soc. Jap.* 1971, **44**, 2430.
- (76) Sekine, T. and Hasegawa, Y., in *Solvent Extraction Research* (Edited by Kertes, A.S. and Marcus, Y.), Wiley, New York, 1968, p. 289.
- (77) Aggett, J., *Inorg. Nucl. Chem.* 1970, **32**, 2767.
- (78) Takeda, K., Isobe, K., Nakamura, Y. and Kawaguchi, S., *Bull. Chem. Soc. Jap.* 1976, **49**, 1010.
- (79) Subramanian, M.S., Khopkar, P.K., Shukla, J.P. and Pai, S.A., *J. Inorg. Nucl. Chem.* 1974, **36**, 3862.
- (80) Kassierer, E.F. and Kertes, A.S., *J. Inorg. Nucl. Chem.* 1972, **34**, 778.
- (81) Ferraro, J.R. and Healy, T.V., *J. Inorg. Nucl. Chem.* 1962, **24**, 1463.
- (82) Irving, H. and Edgington, D.N., *J. Inorg. Nucl. Chem.* 1960, **15**, 158.
- (83) Harman, M.E., Hart, F.A., Hurtshouse, M.B., Moss, G.P. and Raithby, P.R., *J. Chem. Soc., Chem. Commun.* 1976, 396.
- (84) Leipoldt, J.G., Bok, L.D.C., Laubscher, A.E. and Basson, S.S., *J. Inorg. Nucl. Chem.* 1975, **37**, 2477.
- (85) Watson, W.H., Williams, R.J. and Stemple, N.R., *J. Inorg. Nucl. Chem.* 1972, **34**, 501.
- (86) Leipoldt, J.G., Bok, L.D.C., Basson, S.S. and Laubscher, A.E., *J. Inorg. Nucl. Chem.* 1976, **38**, 1477.
- (87) Leipoldt, J.G., Bok, L.D.C., Basson, S.S., van Vollenhoven, J.S. and Laubscher, A.E., *J. Inorg. Nucl. Chem.* 1976, **38**, 2241.
- (88) Leipoldt, J.G., Wessels, G.F.S. and Bok, L.D.C., *J. Inorg. Nucl. Chem.* 1975, **37**, 2487.
- (89) Horrocks, W.D., in *NMR of Paramagnetic Molecules* (Edited by La Mar, G.N., Horrocks, W.D. and Holm, R.M.) Academic Press, New York, 1973, p. 479.
- (90) Desreux, J.F. and Reilley, C.N., *J. Amer. Chem. Soc.* 1976, **98**, 2105.
- (91) Reilley, C.N., Good, B.W. and Desreux, J.F., *Anal. Chem.* 1975, **47**, 2110.
- (92) Desreux, J.F., Massaux, J. and Duyckaerts, G., *J. Inorg. Nucl. Chem.*, in press.
- (93) Kertes, A.S. and Kassierer, E.F., *Inorg. Chem.* 1972, **11**, 2108.
- (94) Mathur, J.N., Pai, S.A., Khopkar, P.K. and Subramanian, M.S., *J. Inorg. Nucl. Chem.* 1977, **39**, 653.
- (95) Kandil, A.T., Aly, H.F., Raieh, M. and Choppin, G.R., *J. Inorg. Nucl. Chem.* 1975, **37**, 229.
- (96) Graddon, D.P., *Coord. Chem. Rev.* 1969, **4**, 1.
- (97) Pradilla-Sorrano, J. and Fackler, J.P., *Inorg. Chem.* 1973, **12**, 1174.
- (98) Pretorius, J.A. and Boeyens, J.C.A., *J. Cryst. Mol. Struct.* 1976, **6**, 169.
- (99) Bush, M.A. and Fenton, D.E., *J. Chem. Soc. A* 1971, 2446.
- (100) Graddon, D.P. and Ong, W.K., *Aust. J. Chem.* 1974, **27**, 741.
- (101) Graddon, D.P. and Ong, W.K., *J. Inorg. Nucl. Chem.* 1975, **37**, 469.
- (102) Graddon, D.P. and Heng, K.B., *Aust. J. Chem.* 1971, **24**, 1781.
- (103) Dakternieks, D.R. and Graddon, D.P., *Aust. J. Chem.* 1973, **26**, 2537.
- (104) Nash, K.L. and Choppin, G.R., *J. Inorg. Nucl. Chem.* 1977, **39**, 131.
- (105) Dakternieks, D.R. and Graddon, D.P., *Aust. J. Chem.* 1974, **27**, 1351.
- (106) Liem, D.M., *Acta Chem. Scand.* 1972, **26**, 191.
- (107) Bykhovtsov, V.L. and Melikhova, G.N., *Radiokhimiya* 1969, **11**, 619.
- (108) Bykhovtsov, V.L., *Radiokhimiya* 1970, **12**, 412.
- (109) Bykhovtsov, V.L. and Zimia, T.Y., *Radiokhimiya* 1970, **12**, 686.
- (110) Bykhovtsov, V.L., *Radiokhimiya* 1970, **12**, 539.
- (111) Marcus, Y. and Kolarik, Z., *Inorg. Nucl. Chem. Lett.* 1974, **10**, 275.
- (112) Liem, D.H. and Sinegribova, O., *Acta Chem. Scand.* 1971, **25**, 301.
- (113) Smelov, V.S. and Lanin, V.P., *Radiokhimiya* 1974, **16**, 180.
- (114) Mareva, S., Jordanov, N. and Konstantinova, M., *Anal. Chim. Acta* 1972, **59**, 319.
- (115) Rocca, J.L. and Porthault, M., *Anal. Chim. Acta* 1972, **61**, 457.
- (116) Shigematsu, T. and Honjyo, T., *Bull. Chem. Soc. Jap.* 1970, **43**, 796.
- (117) Newman, L. and Klotz, P., in *Solvent Extraction Chemistry* (Edited by Dryssen, D., Liljenzin, J.O. and Rydberg, J.) North-Holland, Amsterdam, 1967, p. 128.
- (118) Woo, C., Wagner, W.F. and Sands, D.E., *J. Inorg. Nucl. Chem.* 1972, **34**, 307.
- (119) Woo, C., Wagner, W.F. and Sands, D.E., *J. Inorg. Nucl. Chem.* 1971, **33**, 2661.
- (120) Hasegawa, Y., *Bull. Chem. Soc. Jap.* 1969, **42**, 3425.
- (121) Nikolaeva, S.A., Mel'chakova, N.V. and Peshkova, V.M., *Zh. Anal. Khim.* 1974, **29**, 2055.
- (122) Hala, J., *J. Less Common Met.* 1972, **26**, 117.
- (123) Hala, J. and Smola, J., *Collect. Czech. Chem. Commun.* 1973, **38**, 2588.
- (124) Hala, J., *Collect. Czech. Chem. Commun.* 1974, **39**, 3475.
- (125) Flett, D.S., *Accounts Chem. Res.* 1977, **10**, 99.
- (126) Irving, H.M.N.H. and Lewis, D., *Chem. Scr.* 1974, **5**, 202 and 208.
- (127) Chmutova, M.K., Myasoedov, B.F., Spivakov, B.Y., Kochetkova, N.E. and Zolotov, Y.A., *J. Inorg. Nucl. Chem.* 1973, **35**, 1317.
- (128) Spivakov, B.Y., Zolotov, Y.A., Myasoedov, B.F., Chmutova, M.K. and Kochetkova, N.E., *Zh. Neorg. Khim.* 1972, **17**, 3334.
- (129) Khopkar, P.K. and Narayanankutty, P., *J. Inorg. Nucl. Chem.* 1972, **34**, 3233.
- (130) Shmidt, V.S., Mezhev, E.A., Tsevtkova, Z.N. and Shesterikov, V.N., *Radiokhimiya* 1973, **15**, 126.
- (131) Newman, L. and Klotz, P., *Inorg. Chem.* 1972, **11**, 2150.
- (132) Newman, L. and Klotz, P., *Inorg. Chem.* 1966, **5**, 461.
- (133) Genov, L. and Georgiev, G., *Monatsh. Chem.* 1969, **100**, 1892.
- (134) Kuznik, B., Genov, L. and Georgiev, G., *Monatsh. Chem.* 1974, **105**, 1190.
- (135) Kuznik, B., Genov, L. and Georgiev, G., *Monatsh. Chem.* 1975, **106**, 1543.
- (136) Kononenko, L.I. and Vitkun, R.A., *Zh. Neorg. Khim.* 1970, **15**, 1345.
- (137) Leipoldt, J.G., Bok, L.D.C., Basson, S.S., Laubscher, A.E. and van Vollenhoven, J.S., *J. Inorg. Nucl. Chem.* 1977, **39**, 301.
- (138) Butman, L.A., Aslanov, L.A. and Porai-Koshits, M.A., *Zh. Strukt. Khim.* 1970, **11**, 46.

- (139) Il-Inskii, A.L., Porai-Koshits, M.A. Aslanov, L.A. and Lazarev, P.I., *Zh. Strukt. Khim.* 1972, 13, 277.
 (140) Aslanov, L.A. and Porai-Koshits, M.A., *Zh. Strukt. Khim.* 1974, 17, 836.
 (141) Rahaman, M.S. and Finston, H.L., *Anal. Chem.* 1969, 41, 2023.
 (142) Deptula, C., *J. Inorg. Nucl. Chem.* 1970, 32, 277.
 (143) Kremenskaya, I.N., Goncharov, E.V. and Balanevskaya, T.S., *Zh. Neorg. Khim.* 1972, 17, 201.
 (144) De, A.K. and Ray, S., *Sep. Sci.* 1974, 9, 261.
 (145) Bacher, W. and Keller, C., *J. Inorg. Nucl. Chem.* 1973, 35, 2945.
 (136) Tomazic, B.B. and O'Laughlin, J.W., *Anal. Chem.* 1973, 45, 1519.
 (147) Sekine, T., Murai, R., Niitsu, M. and Ihara, N., *J. Inorg. Nucl. Chem.* 1974, 36, 2569.
 (148) Le Roux, H.J. and Fouché, K.F., *J. Inorg. Nucl. Chem.* 1972, 34, 747.

DISCUSSION

R. Blumberg: This is rather a comment, relevant to both papers (a) and (b)). The importance of water as an active contributor to the extraction mechanism should not be underestimated. Hence, synergetic reagents may actually, in part, change the hydration of the extracted species. Similarly, the composition of the species at the interface may be considerably different from the bulk species and water may have a very important role in such cases.

L.V. Gallacher: I would like to add to Dr. Blumberg's comments on the likely importance of water in synergic extractant combinations. Several years ago Van Dalen and his coworkers found that the addition of di(2-ethylhexyl) phosphoric acid to solutions of dinonylnaphthalene sulfonic acid (HDNNS) in hydrocarbon solvents caused the rejection of water from the sulfonic acid micelles. Combinations of these two reagents were found to exhibit enhanced extraction of trivalent cations. We found in our own work that the addition of the aliphatic hydroxy oxime LIX 63 to HDNNS solutions in kerosene also results in the rejection of water. Mixtures of HDNNS and LIX 63 show selective extraction of Cu^{+2} in the presence of Fe^{+3} , and Ni^{+2} in the presence of Co^{+2} . These phenomena suggest that the formation of the synergic HDNNS/reagent complex involves the displacement of water of hydration from HDNNS in the organic phase.

J.F. Desreux: The role of water in synergic extraction is briefly discussed in the present review. Recent works (ref. 79-80) amply demonstrate the importance of this factor. We have recently investigated by NMR the association of paramagnetic rare earth TTA complexes with neutral donors in anhydrous and hydrated solutions. Water was found to impede the formation of the synergic adducts (ref. 92).

V.A. Mikhailov: All systems which were reviewed in your paper are systems with trace metal concentration. But our experience (a-e) of investigation of uranium synergistic extraction by mixtures of D2EHPA with TBP or dioctyl sulphoxide shows that many very interesting and important things occur in the field of high metal concentration though such systems are much more difficult for quantitative description. What is known now about synergistic effects in systems with high metal concentration?

(a) Mikhailov, V.A., Torgov, V.G., *Us T.V. Dokl. Acad. Nauk SSSR*, 1974, 214, 1121; (b) Mikhailov, V.A., Torgov, V.G., *Us T.V. Izv. Sib. Otd. Akad. Nauk SSR*, ser. khim. nauk, 1974, No. 14, vpp. 6, 67; (c) Torgov, V.G., *Us T.V., Bogdarova, D.D., Mikhailov, V.A., Izv. Sib. Otd. Akad. Nauk SSSR*, ser khim. nauk, 1976, No. 9, vpp. 474; (d) Torgov, V.G., *Us T.V., Mikhailov, V.A., Nikoloev, A.V., Dokl. Akad. Nauk SSSR*, 1976, 227, 635; (e) Mikhailov, V.A., paper on this conference.

Y. Marcus: To the point raised by Dr. Mikhailov: In work published a couple of years ago by Dr. Kolarik and myself on extraction by alkylphosphoric acid - TBP mixtures of uranium and lanthanides, we definitely found dependence of both distribution and enthalpy data on metal loading. This was ascribed to polymerization of the extracted species and its disaggregation by the synergistic agent.

J.F. Desreux: Most studies of synergic extraction out so far are concerned with tracer quantities of metal. The use of higher metal concentrations is expected to lead to significant alterations of the distribution equilibria. For instance, Dolgashova and Fridman (ref. 16) reported on the influence of metal loading on the extraction of Cu(II) by two acidic agents, namely acetylacetone and hydroxyquinoline. This extraction system exhibits an antagonistic effect at low concentrations and a synergic effect at high concentrations. Marcus and Kolarik's paper is referred to as ref. 111.

B.F. Myasoedov: What could you say about the influence of synergistic effect on separation factors of metals?

J.F. Desreux: The main drawback of synergic extraction remains its lack of selectivity. Most often, an increase in the separation factors has been achieved only if the oxidation state of one of the metals to be separated was changed before proceeding to the extraction.

M. Elguindy: From your experience and work, are there systematic or scientific steps or suggestions to follow in the choice of practical systems to affect a synergic effect causing a dramatic increase in distribution of metal without detrimentally affecting stripping?

J.F. Desreux: For metal ions that have a strong tendency to increase their coordination sphere, the highest synergic coefficients are usually observed with combinations of acidic and neutral extractants. The acidic extractant should form relatively weak complexes while the neutral extractant should be a strong donor. Furthermore, inert diluents such as aliphatic hydrocarbons must be preferred. Stripping is readily performed by changing the pH.

If the metal exhibits a low coordination number, one may resort to other synergic systems such as two neutral or two acidic extractants although relatively little information is available for such extraction systems.

A. Warshwasky: As the authors have completed a review on synergistic extraction, I would like to pose a challenging practical question. Works presented at this ISEC '77 Conference show that this subject has been split into such terms as accelerated effect, divalent effect, interfacial properties, etc. Will the authors recommend, in view of their knowledge of recent literature and in view of complexibility and high cost of synergistic reagent, concentrating on studies of the more practical commercial-type extractants?

J.F. Desreux: More studies of commercial extractants are certainly needed. The present review does not concentrate on practical aspects as some of these were recently discussed by D.S. Flett in a review on the mechanisms of extraction by LIX reagents (ref. 125).

D.S. Flett: It is worth commenting that, in the synergistic system of hydroxyoxime/carboxylic acid,

hydroxyoxime/sulphonic acid and alkylated and hydroxy quinoline/carboxylic acid mixtures, the equilibrium effects are also accompanied by kinetic effects. There is also ample evidence that the composition of the interface is materially changed in these systems. I believe, when such systems are to be studied, that both equilibrium chemistry and kinetics should be examined so that a complete understanding of the extraction systems may be developed.

ORGANIC REAGENTS

Some Reagents Suitable for Metal Extraction from Sulphate Media - with Particular Emphasis on the Kinetics of Copper Extraction with Chelating Agents

L. Hummelstedt, Institute of Industrial Chemistry, ÅBO AKADEMI, 20500 Åbo 50, Finland

ABSTRACT

The review concerns primarily chelating liquid cation exchangers which are most generally useful for metal extraction from sulfate media. After discussing new commercial reagents and studies of the purification and properties of some hydroxyoximes a critical review is presented of the kinetic studies of copper extraction using LIX 64 N from General Mills Chemicals, Inc. The single drop technique is shown to yield unreliable rate data at $\text{pH} > 2$, which explains conflicting results concerning the pH dependence of the extraction rate. Consideration of aggregation phenomena leads to a new rate equation explaining observed fractional reaction orders as well as the effect of the diluent on the activation energy. Further topics considered in the review are some new applications of LIX reagents, fundamental studies of Kelex reagents from Ashland Chemical Company and a few applications of reagents not belonging to the chelating extractants.

Introduction

BECAUSE OF THE RELATIVELY weak complexing tendency of the sulfate ion, most of the extraction reagents employed for extraction of metal ions from sulfate media are liquid cation exchangers, among which the chelating extractants form a particularly important group. They will therefore be discussed separately. Quite comprehensive literature reviews on the liquid-liquid extraction of metals have recently been published^(1,2) and the following presentation is therefore limited to some of the latest developments.

Chelating Extractants

New Commercial Reagents

Kordosky et al.⁽³⁾ have discussed LIX 34, a new copper extractant developed by General Mills Chemicals, Inc. The

chemical nature of this reagent has not yet been disclosed, but it is stated to belong to a totally new class of metal extractants. Its copper extraction properties are similar to those of LIX 64 N and it may therefore be assumed to be a chelating agent. According to the manufacturer⁽³⁾ the area of most immediate application appears to be the treatment of low-copper leach solutions where high copper recovery and excellent iron rejection must be realized in a minimum number of stages. LIX 34 also extracts other metals such as zinc, cadmium, lead, mercury and silver, its behavior toward cobalt and nickel being particularly interesting. The loading and stripping of Ni(II) is stated to be quite slow compared to the loading and stripping of Co(II). It is therefore suggested that a combination of kinetically selective extraction and stripping stages might yield a good separation of Co(II) and Ni(II) although the extraction equilibrium is more favorable for Ni(II). The air oxidation of Co(II) in the organic phase to a non-strippable Co (III) complex is claimed to be much slower than the corresponding reaction when LIX 64 N is used as extractant.

Stability testing in progress is stated to indicate that LIX 34 is extremely stable under a wide variety of conditions. This appears to be a major advantage over the hydroxy oximes which now dominate the extractant market.

General Mills Chemicals, Inc. has also recently introduced LIX 54, another new metal extractant of unknown structure. According to the manufacturer this reagent is intended for extraction of copper, nickel and zinc from ammoniacal solutions, showing in many cases a better performance than LIX 64 N and LIX 65 N. Its main advantages are high metal transfer ability (with copper the maximum loading is 40 g/l), very low ammonia uptake and rapid phase separation even when the reagent is used at 100% concentration. The selectivity for copper over zinc and nickel has been improved and the H_2SO_4 content of the stripping acid may be as low as 25 g/l for copper and 1-3 g/l for nickel and zinc. The loading capacity for nickel increases strongly with the aromatics content of the diluent. Cobalt(II) is extracted and stripped very rapidly

while cobalt(III) is believed to be unextractable. In the organic phase cobalt(II) will oxidize to the cobalt(III) complex which is extremely difficult to strip. The manufacturer therefore advises caution in using LIX 54 with aqueous solutions containing cobalt.

New information has been published concerning the copper extractants recently introduced by Acorga Ltd^(4,6) and Shell⁽⁷⁻⁹⁾. The former company offers extractants based on 5-nonyl-salicylaldoxime (Acorga P-50) or 2-hydroxy-5-nonylphenyl benzyl ketoxime (Acorga P-17) while the Shell Metal Extractant 529 (SME 529) contains 2-hydroxy-5-nonylaceto-phenone oxime as the active component. These extractants are thus similar in structure to LIX 65 N (2-hydroxy-5-nonyl benzophenone oxime) of General Mills Chemicals, Inc. Acorga P-50 extracts copper much faster than Acorga P-17^(5,6) while Flett⁽⁹⁾ considers SME 529 and Acorga P-17 to have about equal extraction rates, both being considerably faster than LIX 65 N. Vernon⁽¹⁰⁾ reports a technical comparison of LIX 65 N, Acorga P-17 and SME 529 in which all three reagents met the requirements of a projected plant equally well. He concludes that considerations of price and hydrolytic stability become important in such a situation. The stability of the extractants was still under investigation, no data being reported.

It appears that faster kinetics is the main advantage of the Acorga and Shell extractants in comparison with LIX 65 N. This in turn is slower than the most widely used copper extractant LIX 64 N, which in addition to LIX 65 N contains a small amount of LIX 63 (5,8-diethyl-7-hydroxy-6-dodecanone oxime).

There is still not enough information available to allow a reliable comparison of the various copper extractants but the increasing competition in this area certainly indicates that the commercial importance of copper extraction is expected to grow considerably.

Research and Development

Purification and Properties of LIX Reagents

Ashbrook^(11,12) has published comprehensive studies on the purification and properties of commercial 2-hydroxyoximes (LIX reagents of General Mills, Inc.). Thin-layer chromatography⁽¹¹⁾ showed the aromatic hydroxyoximes LIX 64, 64 N, 65 N, 70, 71 and 73 to contain inactive *syn* and active *anti* isomers while LIX 64, 64 N, 70 and 73 also contained a minor amount of the aliphatic component LIX 63, for which no isomers were reported. Very recently Tammi⁽¹³⁾ has shown that LIX 63 exhibits the same type of isomerism. He has also developed two different methods for separating the isomers. Infrared and n.m.r. spectra^(12,13) indicate that the *syn* isomers form intramolecular hydrogen bonds to a larger extent than the *anti* isomers, for which the intermolecular type of hydrogen bonding is predominant. Figure 1 shows that this difference between the two isomers of LIX 63 is also reflected in the mean aggregation numbers, which were measured on iso-octane solutions using vapor pressure osmometry.

Ashbrook⁽¹²⁾ also reports u.v.-visible spectra and proton-ligand stability constants for the *syn* and *anti* isomers of the aromatic LIX reagents. The *syn* isomers are considerably more acidic than the corresponding *anti* isomers. The copper extraction rate of the *syn* isomers increases with pH, being very fast in ammoniacal solutions⁽¹¹⁾. According to Tammi⁽¹³⁾ this is not true for the *syn* isomer of LIX 63, which is unreactive toward copper in ammoniacal solutions of pH 10.

Hanson et al.⁽¹⁴⁾ have reported that LIX 64 N and LIX 65 N (as well as SME 529, Acorga P-17 and Acorga P-50) contain considerable amounts of a weakly acid impurity,

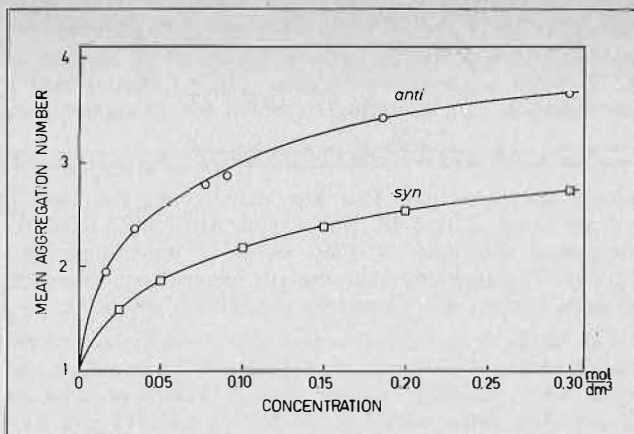


FIGURE 1⁽¹³⁾. The concentration dependence of the mean aggregation number at 25°C for the two isolated isomers of LIX 63 dissolved in iso-octane.

incapable of extracting copper at pH values <4. The impurity appears to be nonylphenol, a starting material in the synthesis of these extractants. Nonylphenol was found to decrease the rate of extraction of copper with LIX 65 N. When present in large concentrations it also had a deleterious effect on the extraction equilibrium.

Kinetics of Copper Extraction with LIX 64 N.

All except one of the commercial copper solvent extraction plants now operating use LIX 64 N as extractant⁽¹⁾ and it is therefore natural that the kinetic performance of this reagent has become the subject of intensive research. LIX 64 N is a mixture containing the aromatic hydroxyoxime LIX 65 N as main component and only about one percent of the aliphatic hydroxyoxime LIX 63, which has been found to improve the kinetics of copper extraction⁽¹⁵⁾.

Neelameggham⁽¹⁶⁾ studied the rate of extraction of copper with LIX 64 N, which he apparently believed to be a mixture of similar hydroxyoximes. He used kerosene as diluent and performed his experiments partly in a stirred cell with quiescent interface, partly in a dispersion cell with unknown interfacial area. For the extraction rate N_{Cu} Neelameggham proposed an equation which may be written in the following form, where a bar indicates species in the organic phase:

$$N_{Cu} = k [Cu^{2+}] [\overline{LIX\ 64\ N}]^{0.5} [H^+]^{-1} \dots \dots \dots (1)$$

Flett et al.⁽¹⁷⁾ and Spink and Okuhara⁽¹⁸⁾ studied the catalytic effect of LIX 63 on the extraction of copper with LIX 65 N using an AKUFVE apparatus^(18,22) and toluene as diluent. Their radiotracer technique permitted rate studies close to the equilibrium position under practically zero mass transfer conditions. For mixtures of LIX 65 N and LIX 63 rate equation (2) was obtained:

$$N_{Cu} = k [(Cu^{2+}) [\overline{LIX\ 65N}] [\overline{LIX\ 63}]^{0.5} [H^+]^{-1} \dots \dots \dots (2)$$

Studies using the mixed reagent LIX 64 N yielded a reaction order close to 1.5, as may be deduced from equation (2).

In reviewing the extraction mechanisms proposed by Neelameggham⁽¹⁶⁾ and Flett et al.⁽¹⁷⁾ Ashbrook⁽²⁾ has pointed out that these authors used commercially produced reagents without considering the possible effects of isomers or impurities. The same is true for Atwood et al.⁽²³⁾ who performed rate studies with LIX 64 N, LIX 65 N and LIX 63 in xylene using the single drop technique. In contrast to the previous investigators Atwood et al. worked with a nitrate instead of a sulfate medium in order to permit

easy calculation of the copper transfer from the pH changes when drops of aqueous phase were allowed to fall through a continuous organic phase. They reported rate equation (3), according to which the extraction rate

$$N_{Cu} = k [Cu^{2+}] [\overline{LIX\ 63}]^{0.5} [\overline{LIX\ 65\ N}]^{0.5} \dots \dots \dots (3)$$

is independent of pH. This was stated to be the case in the pH range 2.21-4.98. Miller and Atwood⁽²⁴⁾ have re-interpreted the data of Flett et al.⁽¹⁷⁾ and Spink and Okuhara⁽¹⁸⁾ suggesting that the pH dependence observed by these authors was caused by the reverse reaction.

The single drop technique was also employed in recent studies at the University of Bradford⁽²⁵⁻²⁷⁾, in which the about 85% aliphatic solvent Escaid 100 was used as diluent. The extractants LIX 64 N^(25,26), LIX 63 and LIX 65 N⁽²⁷⁾ were used without purification, the presence of nonylphenol in the aromatic extractants being discovered during the experiments⁽¹⁴⁾. In reporting this impurity Hanson et al.⁽¹⁴⁾ concluded that comparisons of reagents as delivered are not likely to yield definite evidence on the mechanism of extraction. Rate equations similar to (2) were considered invalid⁽²⁷⁾, one objection being the ability of LIX 65 N to extract copper in the absence of LIX 63. No reaction orders were reported but the initial extraction rate with LIX 64 N was found to be directly proportional to the concentration ratio of total copper to free protons in the aqueous phase as long as the ratio was lower than about four⁽²⁵⁾. The experiments were performed at pH values < 2, mostly using drops of organic phase rising through a continuous aqueous phase containing copper sulfate and sulphuric acid. In a separate paper⁽²⁸⁾ the interpretation of pH measurements in such media was discussed.

Studies of the rate of stripping of copper from extract phases containing LIX 64 N⁽²⁵⁾ or different mixtures of LIX 63 and LIX 65 N⁽²⁷⁾ were also performed at the University of Bradford. The results indicate that the stripping reaction is first order in organic copper and aqueous free proton⁽²⁵⁾ and show a considerable catalytic effect of LIX 63⁽²⁷⁾.

The kinetic study by Fleming⁽²⁹⁾ is the first one employing extractants purified by isolation and recrystallization of the solid copper complexes. In this case the experiments were performed far from equilibrium in a stirred cell with quiescent interface using aqueous sulfate solutions and organic phases containing chloroform as diluent. The copper transfer was calculated from the pH change, applying corrections for the sulfate-bisulfate equilibrium. Extraction mechanisms and rate equations are proposed for LIX 63 and LIX 65 N alone as well as for mixtures of both reagents. For the mixtures, rate equation (4) is reported,

$$N_{Cu} = k [Cu^{2+}] [\overline{LIX\ 63}]^{(0.5-1.0)} [\overline{LIX\ 65\ N}] [H^+]^{-1} \dots (4)$$

the fractional order for LIX 63 being ascribed to dimerization of the reagent. This equation is quite similar to equation (2) but the proposed catalytic mechanism differs from that suggested by Flett et al.⁽¹⁷⁾.

The results of all the previously mentioned investigations have been critically examined in a very recent study at the Institute of Industrial Chemistry at Åbo Akademi⁽³⁰⁾. This examination of the literature revealed diverging opinions primarily regarding the reaction order for the hydrogen ion, the cause of fractional reaction orders for extractants and the magnitude of the activation energy of the extraction reaction. There is also a large variation in the absolute values of the reaction orders for the extractants, as exemplified by the orders 0.5 and 1.5 for LIX 64 N reported by Neelameggham⁽¹⁶⁾ and Flett et al.⁽¹⁷⁾, respectively.

Most investigators have found the copper extraction rate inversely proportional to the hydrogen ion concentration, a reaction order of zero being reported only by Atwood et al.⁽²³⁾. Their result is probably due to the fact that they used the single drop technique at relatively high pH values (2.21-4.98). Under such circumstances the hydrogen ions liberated from the organic phase may make the hydrogen ion concentration considerably higher at the interface than in the bulk of the aqueous phase. This means that the interfacial pH, which affects the rate of extraction, may become relatively independent of the bulk pH, indicating a reaction order close to zero for the hydrogen ion. The relative difference between the interface and bulk hydrogen ion concentrations decreases with increasing bulk acidity and the single drop technique may therefore be expected to yield more reliable rate data at low pH. This explains why the single drop experiments of Whewell et al.⁽²⁵⁾ at pH < 2 indicate a reaction order of -1 for H⁺ at low ratios between total copper and free protons.

These conclusions may be supported by calculations of aqueous-phase mass transfer coefficients using equations found in the literature⁽³¹⁾. Since Atwood et al.⁽²³⁾ used a dispersed aqueous phase the maximum value of the aqueous mass transfer coefficient may be calculated using equation (5)⁽³²⁾, which is valid for drops with turbulent circulation when the mass transfer resistance in the continuous phase is negligible:

$$(k_a)_{k_c \rightarrow \infty} = \frac{2.87 u_t}{768 (1 + \mu_a/\mu_c)} \dots \dots \dots (5)$$

For the terminal drop velocity, u_t , Atwood et al.⁽²³⁾ report 10.84 cm/s and for the viscosities, μ_c and μ_a , 0.0075 poise and 0.01 poise, respectively, for a given set of experimental conditions. Substitution of these figures in equation (5) yields $(k_a)_{k_c \rightarrow \infty} = 0.0174$ cm/s. Under the reported conditions the experimental copper extraction rate varied between 1.20×10^{-8} mol/cm²s and 6.06×10^{-10} mol/cm²s depending on the aqueous copper concentration, corresponding to hydrogen ion liberation rates between 2.40×10^{-8} mol/cm²s and 1.21×10^{-9} mol/cm²s. Using the higher figure the difference ($[H^+]_i - [H^+]$) between the H⁺ concentrations at the interface and in the bulk of the aqueous phase is obtained:

$$[H^+]_i - [H^+] = \frac{2.40 \cdot 10^{-8} \text{ mol/cm}^2\text{s}}{0.0174 \text{ cm/s}} = 1.38 \times 10^{-3} \text{ mol/dm}^3$$

Clearly $[H^+]_i$ would be relatively independent of the bulk value $[H^+]$ in the pH range 3-5, and even at pH 2 $[H^+]_i$ would be more than 10% greater than $[H^+]$. For lower extraction rates the errors would be smaller, but it should be remembered that the highest possible value has been used for the aqueous mass transfer coefficient in the calculation above.

In the single drop experiments performed at the University of Bradford⁽²⁵⁻²⁷⁾ the organic phase was dispersed and the aqueous phase continuous. A reasonable maximum value for the aqueous mass transfer coefficient, k_c , might in this case be calculated using equation (6), which has been proposed by Garner and Tayeban⁽³³⁾:

$$Sh = 0.6 Re^{0.5} Sc^{0.5} \dots \dots \dots (6)$$

In equation (6), which is stated to be valid for $Re < 200$, the dimensionless groups are

$$Sh = \frac{k_c d}{D} \quad Sc = \frac{\mu_c}{\rho_c \cdot D}$$

$$Re = \frac{d u_t \rho_c}{\mu_c}$$

TABLE 1⁽³⁰⁾. Initial Copper Extraction Rates with Rising Drop Technique Using Anti Isomers of LIX 65 N (0.1 mol/dm³) and LIX 63 (0.03 mol/dm³) in Benzene and Continuous Aqueous Phases Containing 1.57 · 10⁻² mol/dm³ of Copper Sulfate

pH	Initial rate
	mol/m ² s
2.0	5.8 · 10 ⁻⁵
2.5	8.1 · 10 ⁻⁵
3.0	9.5 · 10 ⁻⁵
3.5	12.2 · 10 ⁻⁵
4.0	14.0 · 10 ⁻⁵

Unfortunately the papers⁽²⁵⁻²⁷⁾ do not contain sufficient information for a calculation of k_c . There is also considerable uncertainty regarding the proper value of the diffusion coefficient, D , for the hydrogen ion in solutions containing more than one electrolyte⁽³⁴⁾.

In the study at Åbo Akademi⁽³⁰⁾ some single drop experiments were performed in the pH range 2-4 using an apparatus similar to that described by Whewell et al.⁽²⁵⁾, the organic phase being dispersed. Aqueous sulfate solution containing 1.57 x 10⁻² mol/dm³ of copper were contacted with a benzene solution containing 0.1 mol/dm³ of the *anti* isomer of LIX 65 N and 0.03 mol/dm³ of the *anti* isomer of LIX 63. The isomers were isolated from the commercial reagents as copper and nickel complexes, respectively, using methods developed by Tammi^(35,18). The initial extraction rates as defined by Whewell et al.⁽²⁵⁾ are collected in Table 1⁽³⁰⁾, which shows a very slow increase of the extraction rate with pH in the range 2-4, suggesting a much smaller change of the interfacial pH value. In these experiments the drop diameter was 0.195 cm and the drop velocity 9.98 cm/s. Assuming a value of 6 × 10⁻⁵ cm²/s for the diffusion coefficient of H⁺ in these electrolyte solutions, equation (6) yields a value of 0.033 cm/s for the mass transfer coefficient on the aqueous side⁽³¹⁾. At pH 4.0, where the experimental rate of hydrogen ion liberation was 2 · 14.0 · 10⁻⁵ mol/m²s, this mass transfer coefficient yields an interfacial pH very close to 3.0. A more detailed analysis of the data in Table 1 suggests that the true mass transfer coefficient may be about 0.01 cm/s⁽³¹⁾.

It is concluded that the single drop technique yields unreliable rate data at least at pH values > 2 because of unsatisfactory control of the hydrogen ion concentration at the interface.

In comparison with the single drop apparatus the rate of mass transfer is greatly enhanced in the AKUFVE⁽¹⁹⁻²²⁾ where vigorous mixing occurs both in the mixer and in the centrifuge. The unknown and possibly varying interfacial area is a drawback in rate studies, but the AKUFVE appears to yield a correct pH dependence for the copper extraction rate even at pH values > 4^(17,18). The criticism expressed by Miller and Atwood⁽²⁴⁾ concerning the pH dependence was discussed and found to be invalid⁽³⁰⁾.

It should be pointed out that Spink and Okuhara⁽¹⁸⁾ observed a reaction order of -0.54 for the hydrogen ion when extracting copper with LIX 64 N dissolved in the recommended diluent Napoleum 470, which gives a higher extraction rate than toluene. This finding suggests that considerable differences in acidity between the interface and the bulk of the aqueous phase may occur in the AKUFVE also.

The stirred cells used by Neelameggham⁽¹⁶⁾ and Fleming⁽²⁹⁾ represent intermediate cases of stirring intensity. It is interesting to note that the experimental reaction

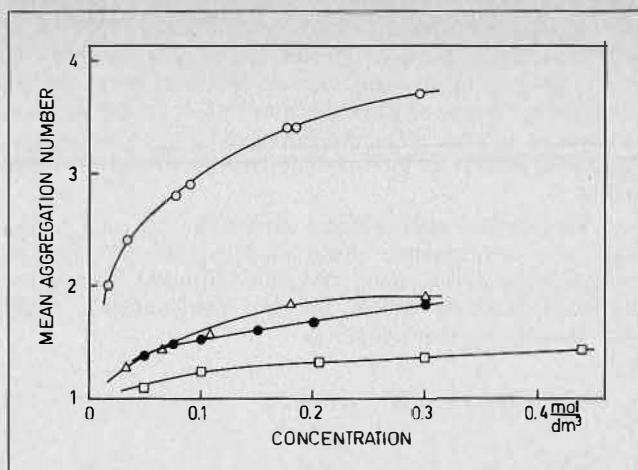


FIGURE 2⁽³⁰⁾. Mean aggregation number of the *anti* isomer of LIX 63N in different solvents at 25°C., (o) iso-octane, (●) benzene, (Δ) toluene, (□) chloroform. Concentration calculated as monomer.

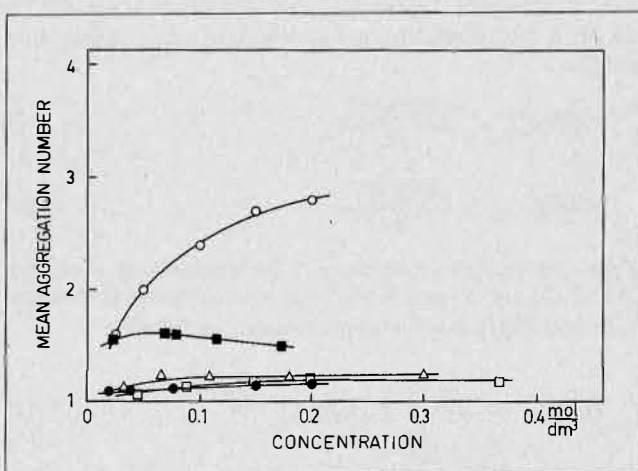


FIGURE 3⁽³⁰⁾. Mean aggregation number of the *anti* isomer of LIX 65N in different solvents at 25°C., (o) iso-octane, (●) benzene, (Δ) toluene, (■) xylene, (□) chloroform. Concentration calculated as monomer.

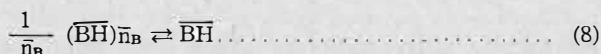
orders for H⁺ found by Neelameggham were -0.5 to -0.75 while Fleming observed approximately zero-order dependence on H⁺ at high pH values and orders close to -1 at low pH values in each series of experiments with different concentration levels of the extractant. Fleming considered the near-zero order at the start of the reaction to be an artifact of the experimental method, being due to the fast rate of change of pH at high pH values. However, difficulties in the experimental measurements would be expected to produce scatter rather than systematic deviations.

In conclusion it may be stated that -1 appears to be the most probable reaction order for the hydrogen ion in the copper extraction reaction.

Neelameggham⁽¹⁶⁾ and Fleming⁽²⁹⁾ have ascribed observed fractional reaction orders to aggregation of the extractants in the organic phase while other investigators have suggested partial interface coverage⁽¹⁷⁾ or interface protonation of LIX 63 by LIX 65 N^(23,24) as the cause of this phenomenon. The first explanation is strongly supported by Figures 2 and 3⁽³⁰⁾ which show osmometrically determined mean aggregation numbers for the *anti* isomers of LIX 63 and LIX 65 N, respectively, in different solvents. The extensive aggregation of LIX 63 in iso-octane supports data by Fleming⁽²⁹⁾ which are based on

the freezing point depression in cyclohexane. LIX 65 N shows a similar picture but the aggregation tendency of this reagent is lower than that of LIX 63. For both extractants the mean aggregation numbers are relatively low in benzene, toluene and chloroform and high in iso-octane. Xylene represents an intermediate type of solvent as shown in Fig. 3.

A very simple mathematical model can be used to explain why investigators using different solvents and/or concentration levels have obtained different and often fractional reaction orders for the extractants⁽³⁰⁾. Consider the dissociation equilibria



where n_R and n_B are the mean aggregation numbers of RH (= LIX 65 N) and BH (= LIX 63), respectively. The concentrations of the aggregates may be roughly approximated by the calculated monomeric concentrations $[\overline{LIX\ 65\ N}]$ and $[\overline{LIX\ 63}]$ divided by the appropriate mean aggregation number:

$$[\overline{RH}]_{\bar{n}_R} \approx \frac{[\overline{LIX\ 65\ N}]}{\bar{n}_R} \dots \dots \dots (9)$$

$$[\overline{BH}]_{\bar{n}_B} \approx \frac{[\overline{LIX\ 63}]}{\bar{n}_B} \dots \dots \dots (10)$$

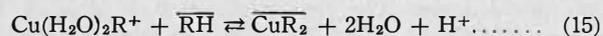
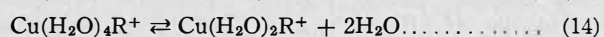
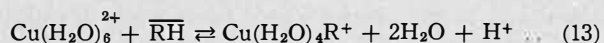
If the concentration constants of the dissociation equilibria (7) and (8) are K_7 and K_8 the real monomer concentrations $[\overline{RH}]$ and $[\overline{BH}]$ may be approximated as follows:

$$[\overline{RH}] \approx \frac{K_7}{(\bar{n}_R)} \frac{[\overline{LIX\ 65\ N}]}{\bar{n}_R} \dots \dots \dots (11)$$

$$[\overline{BH}] \approx \frac{K_8}{(\bar{n}_B)} \frac{[\overline{LIX\ 63}]}{\bar{n}_B} \dots \dots \dots (12)$$

Osmometric studies with mixtures of LIX 63 and LIX 65 N⁽³⁰⁾ indicate that the mean aggregation numbers are mutually increased in such a way that the n values in Figures 2 and 3 should be read at concentrations corresponding to the total oxime concentration $[\overline{LIX\ 63}] + [\overline{LIX\ 65\ N}]$. An important consequence of this is that the mean aggregation number of LIX 63 in a mixture may be considerably higher than would be expected from the concentration of LIX 63 alone. This effect may help to explain the puzzling rate data obtained by Whewell et al.⁽²⁷⁾ for mixtures with constant $[\overline{LIX\ 63}]$ but different $[\overline{LIX\ 65\ N}]$.

The extraction of copper with LIX 65 N alone was considered to occur according to the scheme suggested by Neelameggham⁽¹⁶⁾ where the dehydration of the first complex is the rate-limiting step:



The same mechanism has been proposed by McClellan and Freiser⁽³⁷⁾ for the extraction of zinc, nickel, cobalt and cadmium with dithizones. If reaction (14) is the slow step, the rate equation becomes

$$N_{Cu} = k_{14} \frac{K_{13} K_7 [Cu^{2+}] [\overline{LIX\ 65\ N}]}{(\bar{n}_R) \frac{1}{\bar{n}_R} \cdot [H^+]} \dots \dots \dots (16)$$

Here k_{14} is the forward rate constant of reaction (14) while K_{13} and K_7 are the equilibrium constants of the corresponding reactions.

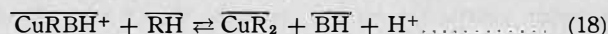
For LIX 65 N alone, reaction orders in the range 1.01-1.27 have been reported in toluene^(17,18) and chloroform⁽²⁹⁾, where \bar{n}_R is only slightly greater than one (Figure 3). This suggests that reaction (15) is not very much faster than (14).

Flett et al.⁽¹⁷⁾ and Fleming⁽²⁹⁾ have assumed the formation of the 1:2 complex CuR_2 to be rate-limiting, which should give a reaction order for LIX 65 N of about 2 in toluene and chloroform. Flett et al. ascribe the low order actually observed to surface saturation with LIX 65 N, but it seems that this phenomenon should then also be felt in extracting with mixtures of LIX 65 N and LIX 63. Fleming suggests that the interface is largely blocked by a surface active complex $(CuR_2)_2RH$ and proposes that LIX 63 catalyzes the extraction by preventing the formation of this complex. However, LIX 63 is found to be less surface active than LIX 65 N^(29,27) and it therefore seems somewhat unlikely that LIX 63 would be able to displace $(CuR_2)_2RH$ from the interface.

In the study at Åbo Akademi⁽³⁰⁾ the first step in the catalytic mechanism is proposed to be a reaction with LIX 65 N according to reaction (13) which maintains equilibrium. LIX 63 then catalyzes the slow dehydration step by forming a mixed complex, probably without liberating a proton because of the low pH (< 2) in industrial extraction processes:



This rate-limiting step is followed by the fast reaction



Essentially the same mechanism was suggested by Flett et al.⁽¹⁷⁾ who did not, however, discuss the importance of the dehydration step. Fleming⁽²⁹⁾ considers a reaction of CuB^+ with RH to form $CuBR$ to be the rate-limiting step. In a very recent reply to the criticism by Miller and Atwood⁽²⁴⁾ Flett et al.⁽³⁸⁾ also consider it likely that LIX 63 participates in the first rather than in the second reaction step, a proposal originally made by Ashbrook⁽²⁾. The conclusion is based on the greater interfacial activity of LIX 65 N. This interpretation may be correct but it requires that a proton be dissociated from the LIX 63 molecule at pH values < 2, a reaction considered improbable by Whewell et al.⁽²⁷⁾.

Since the extraction rate with LIX 65 N alone is not very much lower than with the mixture LIX 64 N⁽²⁷⁾ the uncatalyzed parallel reaction should also be taken into account in the rate equation. This leads to the following expression for the total extraction rate with mixtures of LIX 65 N and LIX 63:

$$N_{Cu} = \frac{K_{13} K_7 [Cu^{2+}] [\overline{LIX\ 65\ N}]}{(\bar{n}_R) \frac{1}{\bar{n}_R} \cdot [H^+]} \cdot \left(k_{14} + k_{17} \frac{K_8}{(\bar{n}_B) \frac{1}{\bar{n}_B}} [\overline{LIX\ 63}] \right) \dots \dots \dots (19)$$

Investigators using solvents with a high aliphatic content^(16,25-27) have found very low reaction orders, indicating high mean aggregation numbers \bar{n}_R and \bar{n}_B . In fact the aggregation in such solvents should be similar to that in isoctane (Figures 2 and 3).

Even if some of the literature data must be considered uncertain due to the use of the single drop technique it seems clear that the apparent activation energy of copper extraction with mixtures of LIX63 and LIX65N increases with the degree of aggregation of the extractants in the solvents used. Flett et al.⁽¹⁷⁾ report a value of 15 kJ/mol in toluene, Fleming⁽²⁹⁾ 19.4 kJ/mol in chloroform, Atwood et al.⁽²³⁾ 25.0 kJ/mol in xylene, Neelameggham⁽¹⁶⁾ 45.0 ± 15.0 kJ/mol in kerosene and Whewell et al.⁽²⁵⁾ and Hughes et al.⁽²⁶⁾ about 45 kJ/mol in Escaid 100. This is readily understandable from equation (19) since a temperature increase will increase the dissociation constants K_7 and K_8 and decrease the mean aggregation numbers. It thus appears that the activation energies reported are largely due to aggregation phenomena and not to the reaction itself. The existence of parallel catalyzed and uncatalyzed reactions makes the measurement of activation energies even more difficult.

Since the hydroxyoximes are assumed to react in the monomeric form, the results presented do not support the hypothesis of Price and Tumilty⁽⁵⁾ and Dalton et al.⁽⁶⁾ according to which complex formation would occur via the dimeric form of the reagent. It seems probable that considerable dissociation of extractant aggregates occurs at the interface against a water solution and the interfacial monomer concentration may therefore be relatively high although the reaction order is determined by the form in which the extractant exists in the bulk of the organic phase. The osmometrically obtainable mean aggregation number appears to give very useful information regarding the bulk species. It is interesting to note that the hydroxyoximes have very little effect on the surface tension against air while they decrease the interfacial tension at a water/organic phase boundary⁽⁸⁾. This behavior suggests that vapor-pressure osmometry should give reliable information about the whole organic phase while interfacial tension measurements against water reflect only the properties of the interface. Dobson and van der Zeeuw⁽⁸⁾ have also shown that the interfacial population density of hydroxyoximes against a water solution is higher in n-heptane than in toluene. This may explain why aliphatic diluents generally give faster copper extraction than aromatic ones. However, the authors also give an example of the opposite behavior and conclude that no direct relation exists between interfacial population density and molecular size, or between interfacial population density and extraction rates.

Fleming⁽²⁹⁾ considers the addition of the second ligand to be rate-limiting step in the extraction of copper with LIX63 alone, the experimental reaction order being 1.45. If this figure is interpreted as $2/\bar{n}_B$, one obtains the mean aggregation number 1.38 which agrees well with the curve for chloroform in Figure 2.

In the study at Åbo Akademi⁽³⁰⁾ it was clearly demonstrated that LIX63 reacts with copper in at least three different ways depending on the pH. At high pH a polymerized 1:1 complex is formed in a reaction where LIX 63 loses two protons. This complex has recently been discussed by Preston⁽³⁹⁾. At intermediate pH values the normal 1:2 complex is formed in a reaction where LIX63 loses one proton, and at the lowest pH values (down to 0.5), no protons seem to be split off. In this case sulfate and bisulfate ions are transferred to the organic phase, as shown by chemical analysis. The existence of different

copper complexes in different pH regions is evident from the absorption spectra of the extract phase.

It therefore seems that the catalytic action of LIX63 is quite possible without dissociation of the molecule, as suggested in reaction (17). The behavior of LIX63 at low pH is not yet well known, although Sudderth and Jensen⁽⁴⁰⁾ have discussed the extraction of sulfate and bisulfate together with copper in strongly acidic solutions, pointing out that the extraction is very fast under such conditions. More recently Christie et al.⁽⁴¹⁾ have reported that LIX63 extracts copper as a neutral chloro-complex at low pH values.

Some predictions regarding rate equations for the stripping of copper have been presented^(30,38) on the basis of thermodynamic arguments. The expression for extracts containing mixtures of LIX63 and LIX65N has already in part been experimentally confirmed by Whewell et al.^(25,27).

New Applications of LIX Reagents

de Schepper⁽⁴²⁾ has described a process for extracting germanium selectively with LIX63 from sulphuric acid solutions (≈ 90 g H_2SO_4/dm^3), hydrochloric acid solutions (≈ 50 g HCl/dm^3) or their mixtures, anions being transferred to the organic phase. The extract is scrubbed with water and stripped with a sodium hydroxide solution. An industrial plant using this method for recovery of germanium from waste water was started at Metallurgie Hoboken-Overpelt in April 1975 and is reported to work very satisfactorily⁽⁴³⁾.

LIX70 mixed with carboxylic acid (Versatic 911) and a small amount of dinonylnaphthalene sulphonic acid (DNNS) has been used for the selective extraction of Ni(II) from acidic sulfate solutions containing Ni(II) and Co(II)^(44,45). The carboxylic acid helps to prevent oxidation of co-extracted Co(II) in the organic phase but at the same time it makes the extraction impractically slow unless a low concentration of the surface active liquid cation exchanger DNNS (or a similar sulphonic acid) is added. Oliver and Ettl⁽⁴⁶⁾ have recently reported that LIX65N is slowly decomposed if kept in contact with Dowfax-2A0 or other sulphonic acids such as DNNS. Nyman⁽⁴⁷⁾ has studied the stability of a mixed extractant containing LIX70, Versatic 911 and DNNS over a period of 810 days. The extracting capacity did decrease to some extent during the first month but remained practically constant after that, suggesting that no irreversible decomposition reaction was taking place. Of course, the decomposition rate may well be different in an extraction circuit, particularly if operated at elevated temperature. Unfortunately we still have no experience from large-scale operation of this process, which offers a separation factor $S_{Ni,Co} > 100$.

Studies of Kelex Reagents

The Kelex reagents of Ashland Chemicals Co. have been investigated by Ashbrook^(48,49), who reports on their purification and properties. Kinetic studies^(29,18,50) of Kelex 100 have given different reaction orders for the extractant but all the investigators consider the addition of the second ligand to be rate-limiting. It seems difficult to explain why Fleming⁽²⁹⁾, using a stirred cell, has observed the expected reaction order around two while the AKUFVE experiments^(18,50) yield a reaction order close to one for Kelex 100, which would not be expected to form aggregates in either one of the solvents used (chloroform and toluene, respectively).

Mixtures of Kelex 100 with Versatic 911 have been employed for the separation of Ni(II) and Co(II)⁽⁵¹⁾. The carboxylic acid was shown to form mixed complexes with

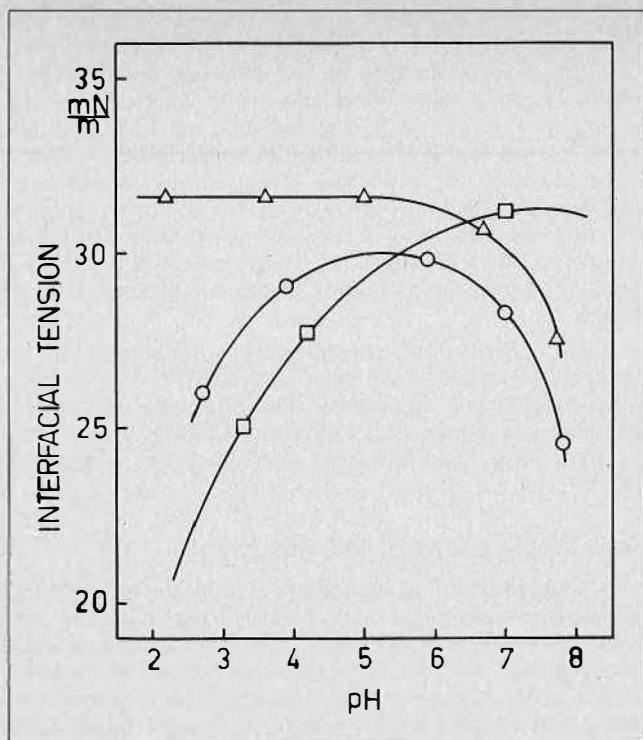


FIGURE 4⁽⁵³⁾. Interfacial tension as a function of pH for (Δ) 0.1 mol/dm³ Versatic 9-11 in toluene over water, (\square) 0.01 mol/dm³ Kelex 100 in toluene over water, (o) 0.01 mol/dm³ Kelex 100 and 0.1 mol/dm³ Versatic 9-11 in toluene over water.

the metal chelates, apparently thereby decreasing the tendency of Co(II) to be oxidized to a non-strippable trivalent complex. Flett et al.⁽⁵²⁾ consider the oxidation of Co(II) to be an interfacial reaction and suggest that the addition of Versatic 911 prevents the oxidation by removing the Kelex molecules from the interface in the form of a hydrogen bonded complex. The arguments are largely based on measurements of the interfacial tension between toluene solutions and aqueous solutions of different pH values. Solutions of Kelex 100, Versatic 911 and their mixtures all gave decreasing interfacial tension with increasing pH⁽⁵²⁾. In a study of the same systems using a highly automated ring balance Sandström⁽⁵³⁾ recently obtained curves of quite different shapes, as exemplified by Figure 4⁽⁵³⁾. It seems reasonable to expect the beginning protonation at low pH to decrease the interfacial tension of the Kelex-solution while Versatic 911 should show a corresponding effect at high pH due to the dissociation of the carboxylic acid. A mixture would then be expected to produce a curve with a maximum at an intermediate pH. Sandström found no evidence of an interaction between Kelex 100 and Versatic 911 in benzene, toluene or isooctane, this conclusion also being supported by osmometric data in the same solvents. It therefore appears more probable that Versatic 911 counteracts the oxidation of Co(II) by occupying coordination positions around the metal ion, as suggested previously⁽⁵¹⁾.

Bauer and Chapman⁽⁵⁴⁾ have recently presented a compact mathematical model correlating experimental equilibrium data for the extraction of copper from acid sulfate solutions by Kelex 100 in xylene. The model is useful in process design and simulation calculations on digital computers.

Other Extractants

The use of carboxylic acids in mixtures with chelating extractants has already been mentioned repeatedly. Car-

boxylic acids have also been used alone for many separations⁽⁵⁵⁾ but this important reagent group will not be discussed further in the present paper since it is covered by a separate review paper⁽⁵⁶⁾ at ISEC 77.

Several examples of useful extractants may be found in a recent paper by Rice and Smith⁽⁵⁶⁾ who review the extraction of zinc, cadmium and mercury(II) from sulfate and chloride media using solvating extractants, liquid anion exchangers and liquid cation exchangers. The solvating extractants discussed include tri-n-butyl phosphate (TBP) and tri-n-octyl phosphine oxide (TOPO) while long chain primary, secondary and tertiary alkyl amines, quaternary ammonium salts and sulphonium salts are considered among the liquid anion exchangers. The cation exchangers include LIX and Kelex reagents as well as carboxylic acids and di(2-thylhexyl) phosphoric acid (DEHPA). Traces of Hg(II) are readily extracted from strongly acidic sulfate media by amines, apparently in the form of anionic sulfato complexes. Somewhat surprisingly DEHPA also extracts Hg(II) under such conditions and it is suggested that DEHPA acts as a solvating extractant for neutral Hg(HSO₄)₂.

A process for selective extraction of ferric iron from trivalent chromium⁽⁵⁷⁾ represents an interesting new application of DEHPA. According to this method the Fe(III) concentration in a Cr(III) solution containing 100 g H₂SO₄/dm³ (or even more) may be decreased from 30 g/dm³ to less than 5 mg/dm³ by extracting with a kerosene solution of DEHPA in the temperature range 50-70°C. Hydrochloric acid is used as stripping agent. No chromium is transferred to the organic phase and a very sharp separation of Fe(III) and Cr(III) is thus possible.

NOTATION

BH	= symbol for undissociated LIX 63
d	= drop diameter
D	= diffusion coefficient
D _{Ni}	= distribution ratio of nickel
k	= reaction rate constant
k _c	= mass transfer coefficient in continuous phase
k _d	= mass transfer coefficient in dispersed phase
K	= equilibrium concentration constant
N _{Cu}	= extraction rate for copper
\bar{n}	= mean aggregation number
Re	= Reynolds number
RH	= symbol for undissociated LIX 65 N
S _{Ni, Co}	= separation factor = D _{Ni} /D _{Co}
Sc	= Schmidt number
Sh	= Sherwood number
u _t	= terminal drop velocity
μ_c	= viscosity of continuous phase
μ_d	= viscosity of dispersed phase
ρ_c	= density of continuous phase

REFERENCES

- (1) Flett, D.S. and Spink, D.R., *Hydrometallurgy* 1976, 1, 207.
- (2) Ashbrook, A.W., *Coord. Chem. Rev.* 1975, 16, 285.
- (3) Kordosky, G.A., MacKay, K.D. and Virnig, M.J., Paper presented at the AIME Annual Meeting, Las Vegas, Nevada, February 22-26, 1976.
- (4) Birch, C., *Proceedings of International Solvent Extraction Conference 1974*, Vol. 3, 2837 (Society of Chemical Industry, London 1974).
- (5) Price, R. and Tumilty, J.A., *Symposium on hydrometallurgy of the Institution of Chemical Engineers, Manchester, April 2-4, 1975*. Institution of Chemical Engineers Symposium Series No. 42, p. 18.1.
- (6) Dalton, R.F., Hauxwell, F. and Tumilty, J.A., *Chem. and Ind.* 1976, 181.
- (7) van der Zeeuw, A.J., *Symposium on hydrometallurgy of the Institution of Chemical Engineers, Manchester, April 2-4, 1975*. Institution of Chemical Engineers Symposium Series No. 42, p. 16.1.
- (8) Dobson, S. and van der Zeeuw, A.J., *Chem. and Ind.* 1976, 175.

- (9) Flett, D.S., *Mineral Processing and Extractive Metallurgy* 1975, 84, C 60.
- (10) Vernon, P.N., *Mineral Processing and Extractive Metallurgy* 1975, 84, C 62.
- (11) Ashbrook, A.W., *J. Chromatography* 1975, 105, 141.
- (12) Ashbrook, A.W., *Hydrometallurgy* 1975, 1, 5.
- (13) Tammi, T.T., *Hydrometallurgy*, in press.
- (14) Hanson, C., Hughes, M.A., Preston, J.S. and Whewell, R.J., *J. inorg. nucl. Chem.* 1976, 38, 2306.
- (15) Swanson, R.R., Phenolic oximes. U.S. Pat. 3, 925, 472 (to General Mills Chemicals, Inc.).
- (16) Neelameggham, R., Solvent extraction studies with hydroximes and alkylphosphoric acid. Ph.D. thesis, University of Utah, Salt Lake City, 1972.
- (17) Flett, D.S., Okuhara, D.N. and Spink, D.R., *J. inorg. nucl. Chem.* 1973, 35, 2471.
- (18) Spink, D.R. and Okuhara, D.N., *Met. Trans. AIME* 1974, 5, 1935.
- (19) Rydberg, J., *Acta Chem. Scand.* 1969, 23, 647.
- (20) Andersson, C., Andersson, S.O., Liljenzin, J.O., Reinhardt, H. and Rydberg, J., *Acta Chem. Scand.* 1969, 23, 2781.
- (21) Johansson, H. and Rydberg, J., *Acta Chem. Scand.* 1969, 23, 2797.
- (22) Reinhardt, H. and Rydberg, J., *Chem. Ind.* 1970, 50, 488.
- (23) Atwood, R.L., Thatcher, D.N. and Miller, J.D., *Met. Trans. B AIME* 1975, 6 B, 465.
- (24) Miller, J.D. and Atwood, R.L., *J. inorg. nucl. Chem.* 1975, 37, 2539.
- (25) Whewell, R.J., Hughes, M.A. and Hanson, C., *J. inorg. nucl. Chem.* 1975, 37, 2303.
- (26) Hughes, M.A., Preston, J.S. and Whewell, R.J., *J. inorg. nucl. Chem.* 1976, 38, 2067.
- (27) Whewell, R.J., Hughes, M.A. and Hanson, C., *J. inorg. nucl. Chem.* 1976, 38, 2071.
- (28) Whewell, R.J. and Hughes, M.A., *J. inorg. nucl. Chem.* 1976, 38, 180.
- (29) Fleming, C.A., The kinetics and mechanism of solvent extraction of copper by LIX 64 N and Kelex 100, National Institute for Metallurgy, Johannesburg, South Africa, Report No. 1793 (26th March, 1976).
- (30) Hummelstedt, L., Tammi, T., Paatero, E., Andresén, H. and Karjaluoto, J., 4th International Congress in Scandinavia on Chemical Engineering, Copenhagen 18th - 20th April 1977, Metallurgical Processes 123-144.
- (31) Paatero, E., private communication.
- (32) Heertjes, P.M. and de Nie, L.H., Mass Transfer to Drops, Chapter 10, p. 388 in *Recent Advances in Liquid-Liquid Extraction*, ed. C. Hanson, Pergamon Press 1971.
- (33) Garner, F.H. and Tayeban, M., *An. R. Soc. esp. Fis. Quim.* 1960, 56B, 479.
- (34) Danckwerts, P.V., *Gas-Liquid Reactions*, McGraw-Hill Book Company 1970, p. 141.
- (35) Tammi, T.T., Extraktion av nickel och kobolt med extraktionsmedel innehållande hydroxioximer, Tech. Lic. Thesis, Åbo Akademi, Åbo, Finland (1975).
- (36) Tammi, T.T., private communication.
- (37) McClellan, B.E. and Freiser, H., *Anal. Chem.* 1964, 36, 2262.
- (38) Flett, D.S., Melling, J. and Spink, D.R., *J. inorg. nucl. Chem.* 1977, 39, 700.
- (39) Preston, J.S., *J. inorg. nucl. Chem.* 1975, 37, 1235.
- (40) Sudderth, R.B. and Jensen, W.H., Paper presented at the 76th General Meeting of Canadian Inst. of Mining and Metallurgy, Montreal, Canada, April 1974.
- (41) Christie, P.G., Lakshmanan, V.J. and Lawson, G.J., *Hydrometallurgy* 1976, 2, 105.
- (42) de Schepper, A., *Hydrometallurgy* 1976, 1, 291.
- (43) Feneau, C. and Ancion, M., private communication.
- (44) Nyman, B.G. and Hummelstedt, L., Proceedings of International Solvent Extraction Conference 1974, Vol. 1, 669 (Society of Chemical Industry, London 1974).
- (45) Hummelstedt, L.E.L., Nyman, B.G. and Leimala, R.J., Extraction agent composition. Can. Pat. 993662 (to Outokumpu Oy, Finland).
- (46) Oliver, A.J., and Ettel, V.A., Paper presented at the C.I.M. 14th Annual Conference of Metallurgists, Edmonton, Canada, August 24-27, 1975.
- (47) Nyman, B.G., private communication.
- (48) Ashbrook, A.W., *J. Chromatography* 1975, 105, 151.
- (49) Ashbrook, A.W., *Hydrometallurgy* 1975, 1, 93.
- (50) Flett, D.S., Hartlage, J.A., Spink, D.R. and Okuhara, D.N., *J. inorg. nucl. Chem.* 1975, 37, 1967.
- (51) Hummelstedt, L., Sund, H.-E., Karjaluoto, J. Berts, L. and Nyman, B.G., Proceedings of International Solvent Extraction Conference 1974, Vol. 1, 829 (Society of Chemical Industry, London 1974).
- (52) Flett, D.S., Cox, M. and Heels, J.D., *J. inorg. nucl. Chem.* 1975, 37, 2197.
- (53) Sandström, G. Undersökning av växelverkan mellan Kelex 100 och Versatic 9-11, M.Sc. Thesis, Åbo, Finland (1976).
- (54) Bauer, G.L. and Chapman, T.W., *Met. Trans. B AIME* 1976, 7B, 519.
- (55) Ashbrook, A.W., *Miner. Sci. Eng.* 1973, 5, 169.
- (56) Rice, N.M. and Smith, M.R., *J. appl. Chem. Biotechnol.* 1975, 25, 379.
- (57) Nyman, B.G. and Hultholm, S.-E., Process for selective extraction of ferric iron from trivalent chromium. U.S. Pat. 3, 875,285 (to Outokumpu Oy, Finland).

DISCUSSION

R. Blumberg: In determining transfer rates across interfaces it seems there should be significance in the nature of the dispersion, whether transfer takes place into or out of a drop. In particular, this may be important in regard also to the nature of the complex populating the interface, because of limitation imposed by the physical drop and diffusion to or from the bulk.

L. Hummelstedt: It is true that the type of dispersion should be taken into account when discussing mass transfer rates across interfaces. In our treatment of results obtained with the single drop technique we have used an equation given by Heertjes and de Nie (ref. 32 in the paper) for dispersed aqueous phases and an equation proposed by Garner and Tayeban (ref. 33) for the opposite type of dispersion. In single drop experiments the composition of the drops may change considerably while the composition of the continuous phase remains practically constant.

M. Cox: We agree with Professor Hummelstedt that our interfacial tension studies reported in *J. Inorg. Nucl. Chem.* for the Kelex 100 Versatic 911 system are incorrect; indeed we have repeated this work and agree with the shape of the curves given in this paper. However, we do still consider that some intermolecular hydrogen bonding does exist between the two components as was

shown in the above paper by our p.m.r. studies. Commenting on the lack of such evidence of complex formation arising from molecular weight studies, is the technique sensitive enough to distinguish between the hydrogen bonding of the acid itself and any intermolecular hydrogen bonding between the acid and Kelex 100?

L. Hummelstedt: I agree that the lack of asymmetric evidence does not exclude the existence of some intermolecular hydrogen bonding between Kelex 100 and Versatic 911. However, it indicates that this interaction must be rather weak compared to the dimerization of the carboxylic acid. We therefore believe that the formation of mixed ligand complexes of Co(II) is the main factor responsible for the stabilization of divalent cobalt in the presence of Versatic 911.

C.A. Fleming: In proposing the existence of such a species at the interface, can you give us any reasons why you believe the mixed ligand (copper-LIX65N-LIX63) complex will be preferred to the copper (LIX65N)₂ complex, which forms in the absence of LIX 63?

L. Hummelstedt: The mixed ligand complex postulated is a positively charged interfacial species containing an undissociated LIX 63 molecule. This inter-

mediate is assumed to react rapidly with a second LIX 65N molecule and its concentration at the interface may therefore be quite low. One reason for the increased extraction rate of LIX 65N in the presence of LIX 63 may be the ability of LIX 63 to extract copper at low pH without liberating protons (ref. 30 in the paper). In a paper before the Extractants and Diluents Session of this Conference, van der Zeeuw and Kok have suggested another working hypothesis, according to which the five-membered rings formed with the metal by LIX 63 and similar accelerators are kinetically preferred although they are less favourable thermodynamically than the six-membered rings formed by LIX 65N and similar extractants.

L.V. Gallacher: In your paper and in subsequent discussion with Professor Danesi, it was suggested that synergic complexes of two reagents in the organic phase would not be stable at the organic/aqueous interface in the presence of water. We have evidence which suggests that LIX 63: HDNNS complexes with an oxime: sulfonic acid mole ratio of 2 or 3 to 1 are quite stable at the interface. The extraction of Ni^{+2} with such mixtures requires 2 hours for equilibration. Yet, when a 1:1 oxime: sulfonic acid mole ratio is used, equilibration occurs in 1 minute. (Note: The solutions were prepared by combining 10% LIX 63 solution and 10% HDNNS solution, both in Escaid 200, to obtain various mole ratios.) These results suggest that free sulfonic acid is present at the interface only when there is excess sulfonic acid present beyond the requirements of the oxime: HDNNS complex, and therefore that the complex is stable at the interface. The same phenomena are observed with didodecyl-naphthalene sulfonic acid. Can you comment on these observations?

L. Hummelstedt: I was referring to a study by Oliver and Ettl (ref. 46 in the paper) according to which LIX 65N is slowly decomposed in the presence of sulfonic acids such as dinonylnaphthalene sulfonic acid (DNNS). In the selective extraction of nickel (ref. 44 in the paper) the extractant mixture contained LIX 70 and Versatic 911 as main components and only about 0.01 mol/dm³ of DNNS. According to your very interesting

observations, the sulfonic acid may partly have reacted with the small amount of LIX 63 present in LIX 70, but judging from the greatly enhanced extraction rate there must have been sufficiently free DNNS left. Your concentrations of LIX 63 and DNNS certainly appear to have been very much higher than ours.

G.A. Yagodin: It is clear nowadays that in many extraction systems reaction takes place at the interphase. We do not know the activities and even the concentrations at the interface. Are there any ideas how to estimate the aggregation of the extracted salts and extractants in this particular field?

L. Hummelstedt: At present there does not seem to be any experimental technique giving fully unambiguous information about the state of the various species at the interface. Some progress may be made by using combinations of different methods such as tensiometry and vapor pressure osmometry, but much of our evidence will probably continue to be circumstantial rather than direct.

A.S. Kertes: Based on our experience (Surface and Colloid Science, Vol. 8, pp. 194-295, Wiley & Sons, New York, 1976), the correlation between the extraction capacity of an extractant and the average aggregation number of the extracted salt or complex is frequently misleading. We were more successful in that and similar correlations when expressing the mass-action law equilibria in terms of a set of specific aggregates predominating in solution, rather than using the mean aggregation number either of the extractant or the extracted salt, or both. Did you attempt such a correlation and if yes, with what results?

L. Hummelstedt: Our treatment is based on our own osmometric data for the extractants and on kinetic copper extraction data from the literature. The information available did not appear sufficient to justify a more detailed and realistic aggregation model containing specific aggregates, and we have not yet attempted to use such a model. However, it appears that even our simple model is able to provide a qualitative explanation for most experimental observations reported in the literature.

An Evaluation of Crown Compounds in Solvent Extraction of Metals*

W.J. McDowell and R.R. Shoun, Chemical Technology Division, Oak Ridge National Laboratory, Oak Ridge, Tennessee 37830

or phenol increased extraction of KCl. Alcohol system results indicated an adduct of one crown ether and one or two alcohol molecules per KCl.

ABSTRACT

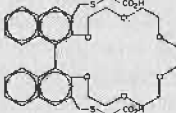
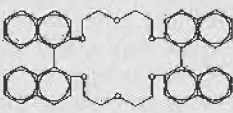
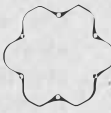
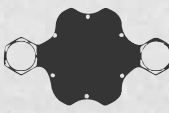
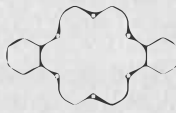
Unexpectedly low results were obtained for extraction of chlorides, perchlorates, nitrates, and thiocyanates of alkalis, alkaline earths, and actinides from aqueous solutions by water-immiscible solutions of crown ethers. The expected preference for ions matching the crown ether hole-size was not seen here or in solubilizing dry alkali chlorides. Addition of an organic-soluble acid increased alkali extraction, with preference for the ion sized to fit the crown ether. Addition of an organic-soluble alcohol

Introduction

IT HAS BEEN AMPLY DEMONSTRATED that crown ethers such as those shown in Table 1 are able to form adducts with alkali metal salts and, under some conditions, to solubilize these salts into organic solvents where it would normally be impossible to dissolve the salt.^(1,2) Evidence

*Research sponsored by Energy Research and Development Administration under contract with the Union Carbide Corporation.

TABLE 1. Screening Tests with Crown Ether Solutions.

		ORGANIC SOLUTION					
		<p>DICARBOXY DINAPHTHYL 18-CROWN-6 (CDN18-C-6)</p> 	<p>BIS DINAPHTHYL 18-CROWN-6 (BISDN18-C-6)</p> 	<p>18-CROWN-6 (18-C-6)</p> 	<p>DIBENZO 18-CROWN-6 (DB18-C-6)</p> 	<p>DICYCLOHEXYL- 18-CROWN-6 (DC18-C-6)</p> 	<p>15-CROWN-5 (15-C-5)</p> 
AQUEOUS SOLUTION ^a		0.01 M in CHCl ₃	0.01 M in CHCl ₃	0.1 M in benzene	0.01 M in benzene	0.1 M in benzene	0.1 M in benzene
		DISTRIBUTION COEFFICIENTS, $D_M = [M]_{org} / [M]_{aq}$					
0.1 M HNO ₃ ^b	<p>Sr } < 10⁻⁴ Ce } Am } Cs 0.007</p>					Am < 10 ⁻⁴	
2 M HNO ₃ ^b	<p>Sr } < 10⁻⁴ Ce } Am } Cs 0.035</p>					Am < 10 ⁻⁴	
NEUTRAL NITRATE	<p>Ca < 10⁻⁴ K 0.22</p>	<p>K } < 10⁻⁴ Ca }</p>				K < 10 ⁻⁴	
HYDROXIDE	<p>Na 0.95 K 2.58 Ca 1.86 Sr 2.65 Ba 2.05</p>	<p>Na } < 10⁻⁴ K } Ba } Ca 0.1 Sr 0.001</p>	<p>Na } < 10⁻⁴ K } Sr } Ba }</p>	<p>Na } < 10⁻⁴ K } Sr } Ba }</p>		K } < 10 ⁻⁴ Ba }	
NEUTRAL CHLORIDE	<p>Ca < 10⁻⁴ K 0.21</p>	<p>K } < 10⁻⁴ Ca }</p>				K < 10 ⁻⁴	
4 M LiClO ₄ ^b						<p>Zn } < 10⁻⁴ Eu } Ca 0.13 Am 0.0007</p>	
THIOCYANATE, 2 M ^c						<p>Li 0.020 Na 0.023 K 0.035 Ca 0.049</p>	<p>Li 0.014 Na 0.0066 K 0.014 Ca 0.0056 Ba 0.0097</p>

ABBREVIATIONS:  = ETHYLENE;  = METHYLENE;  = CYCLOHEXYLENE;  = B5N70;  = NAPHTHALENE.

TOPO = TRI-N-OCTYLPHOSPHINE OXIDE

^a0.01 to 0.1 M EXCEPT AS OTHERWISE NOTED.

^bTEST CATIONS AT TRACER LEVELS.

^cDC18-C-6 LOADINGS FROM 38 TO 94%, AND 15-C-5 LOADINGS FROM 11 TO 28% FROM THIOCYANATE SOLUTIONS.

has been presented indicating that the alkali metal ion in these adducts is situated in the hole in the crown ether ring and that the stability of the adduct formed depends on the correspondence between the size of the ion and the size of the hole in the crown ether⁽¹¹⁾.

Although most of the early work with crown ether complex formation used homogeneous alcohol-water systems, a number of more recent studies of relative binding of alkali metal ions have involved extraction of metal salts from aqueous phases into water-immiscible solutions of the crown ethers. The anion most commonly used in these studies was picrate^(9,8). In addition, dicyclohexyl-18-crown-6 has been used as the extractant in a countercurrent liquid-liquid distribution system for the separation of calcium isotopes as calcium chloride⁽⁹⁾. These facts suggest that crown ethers could be useful specific reagents for two-phase solvent extraction systems. Therefore, consistent with our present interests, most of the work reported here (both that of others and our own) will be concerned with the applicability of crown ethers to liquid-liquid extraction systems.

Special anions such as picrate would not be desirable in the kind of extraction system we want to consider. Chloride or some other mineral acid would be more suitable. Further requirements of a suitable extraction system would include: (1) adequate solubility in a solvent of high flash point (and preferably of low toxicity), such as dodecane or diethylbenzene, (2) very low distribution to the aqueous phase (e.g., $\leq 10^{-6} M$), and (3) ability to extract the compound or compounds of interest with a distribution coefficient greater than 1, preferably greater than 10. The purpose of this work was to examine the available crown ethers for applicability, within such criteria, to liquid-liquid extraction systems of interest in hydrometallurgical and related applications.

Experimental

Dicarboxydinaphthyl-18-crown-6 and bis dinaphthyl-18-crown-6 were supplied by D. J. Cram*. Dicyclohexyl-18-crown-6, dibenzo-18-crown-6, 18-crown-6, and 15-crown-5 were obtained from the Aldrich Chemical Company and the Parish Chemical Company. All these compounds were used as received. Dicyclohexyl-18-crown-6 from more than one source was used in this work. However, in each set of experiments for determining a specific effect (e.g., reagent dependence, order of extraction) only one batch of reagent was used so that results are internally consistent, although cross-comparison of extraction coefficients under the same conditions shows more scatter than would be expected from considering individual studies. Di(2-ethylhexyl) phosphoric acid was obtained from the Virginia-Carolina Chemical Company and was purified by a copper precipitation method prior to use⁽¹⁰⁾. Other chemicals used were of the usual reagent grade quality.

Equilibrations were done in small separatory funnels and vials. The equilibrated phases were analyzed by radiochemical and atomic absorption methods.

*Department of Chemistry, UCLA.

Results and Discussion

General Screening Tests

The crown ethers used in this study and their approximate solubilities in benzene or chloroform are listed in Table 1. Each compound is shown structurally and is identified both by name and by an abbreviated form, which is used throughout the remainder of this paper. Two solvents, benzene and chloroform, were used here as in previous survey work because they avoid some solubility limitations and thus facilitate intercomparison of reagents; however, neither of them meets our requirements for practical process applications. Table 1 also shows the distribution of several metal salts from aqueous solutions to the crown ether solutions. Although the distribution coefficients ($D = [M]_{org}/[M]_{aq}$) are uniformly and disappointingly low, the results do suggest some specific effects. Compound CDN18-C-6 extracted salts from hydroxide systems essentially as would be expected because of its carboxylic acid groups; on the other hand, the reversal in order of extractability of sodium and potassium from that expected for a carboxylic acid alone⁽¹¹⁾ seems to imply that the structure of the crown ether has an effect. A similar reversal in the expected order of extractability of potassium and calcium⁽¹²⁾ observed in neutral chloride and nitrate systems provides further evidence of such an effect. High selectivity for strontium over barium and potassium has been noted by Helgeson, Timko, and Cram for a similar compound with a carboxy functional group⁽¹³⁾.

Compounds BisDN18-C-6, 18-C-6, DB18-C-6, and 15-C-5 extracted so little of the alkalis and alkaline earths from dilute aqueous solutions that work with them was suspended. The subsequent systematic investigation used primarily DC18-C-6.

As an adjunct to the liquid-liquid extraction investigation, the relative solubilization of the alkali and alkaline earth chlorides was tested in the presence of minimum amounts of water; that is, the nominally dry salts were contacted with an organic crown ether solution. The results are shown in Table 2. The expected size relationship that has been reported for other systems^(1,2) does not seem to have any discernible effect on the order of solubilization of these chloride salts under these conditions. Maximum loadings obtained in the tests with 0.1 M DC18-C-6 in benzene were 50% when the group I elements were mixed, 30% when the group II elements were mixed, and 10% and 35% for lithium and calcium, respectively, when tested separately. This can be compared with potassium permanganate, which is reported to solubilize in DC18-C-6 in a 1:1 mole ratio⁽¹⁴⁾. The only case in our tests in which loading approached a 1:1 mole ratio was the calcium extraction from 2 M calcium thiocyanate solution.

Prompted by the apparent difficulty of solvating the mineral acid anions into the organic phase, experiments were designed in which an organic-phase-soluble anion was present. Di(2-ethylhexyl) phosphoric acid (HDEHP) is known to extract the alkali metals (although with low distribution coefficients) in the order $Li > Na > K > Rb > Cs$ ⁽¹⁵⁾. Solutions containing 0.1 M HDEHP and 0.4 M

TABLE 2. Relative Solubilization of Chloride Salts by Crown Ether Solutions

Organic Phase	Conc. Order in Organic	Solids Phase
0.1 M DC18-C-6 in C ₆ H ₆	Ca >> Li > Sr > Na > K > Ba > Mg > Rb > Cs	Individual salts
0.1 M 15-C-5 in C ₆ H ₆	Na > Li > K > Rb > Ba > Ca > Cs > Sr >> Mg	Individual salts
0.01 M BisDN18-C-6 in CHCl ₃	K ≈ Na > Li > Rb > Cs and Ca > Mg > Sr >> Ba	Mixed within groups
0.1 M 18-C-6 in C ₆ H ₆	Rb > Li > Cs > K > Na and Ca > Mg > Sr > Ba	Mixed within groups
0.1 M DB18-C-6 in C ₆ H ₆	Na > K ≈ Li > Rb >> Cs and Ca > Mg > Sr > Ba	Mixed within groups
0.1 M DC18-C-6 in C ₆ H ₆	Li > K ≈ Rb > Cs > Na and Ca > Sr > Mg > Ba	Mixed within groups
0.1 M DC18-C-6 in C ₆ H ₆	Li > Sr > Ca > Rb > K > Na > Cs > Ba > Mg	All mixed

TABLE 3. Effect of Crown Ether on Order of Extraction of Alkali Metals by HDEHP

Alkali Metal	Extraction relative to Cs		Extraction Coefficient With Crown ether ^b
	Without Crown Ether ^a	With Crown Ether ^b	
Li	8.2	0.46	0.023
Na	2.6	0.40	0.020
K	1.2	7.2	0.36
Rb	0.87	3.2	0.16
Cs	1.0	1.0	0.05

^aSee Ref 14; organic phase was 65% in the salt form.

^b0.1 M HDEHP, 0.4 M DC18-C-6; total alkali ion concentration in aqueous phase, 0.5 M.

DC18-C-6 were equilibrated at pH 4.8 (HDEHP 50% in the salt form) with a solution that was 0.1 M in each of the alkali metal nitrates. In these tests the order of extraction was found to be $K > Rb > Cs > Li > Na$ (Table 3).

Perhaps the most pertinent observation to be made from the above tests is that anions such as nitrate, chloride, perchlorate, and hydroxide are very difficult to solvate into crown ether solutions in the diluents chosen. Thiocyanate, being a large anion, is somewhat easier to solvate, and we can conclude from the work of others that permanganate and picrate are even more readily solvated. It is reasonable to expect large anions of an organic character such as picrate to be easily solvated into organic phases. Thus, in order to utilize crown ethers as extractants, either an organophilic anion must be supplied for the metal ion or provisions must be made for solvating the inorganic anion into the organic phase.

Alcohols as Anion Solubilizers

In the early work with the crown ethers, complexes with alkali metal salts were frequently formed in mixtures of alcohol and water in which both the salt and the crown ether were soluble. Further, it was noted by Pedersen and Frensdorff⁽¹⁾ that the addition of small amounts of methanol greatly increased the amount of salts solvated by crown ether solutions. Thus, they hypothesized that alcohol or some analogous compound might take part in the complex, possibly serving to complete the solvation sphere of the cation or solvate the anion. Some of our early experiments in which 10% butanol was added to a benzene solution of crown ether produced a two-to three-fold increase in potassium extraction from 0.01 M KCl, suggesting that a water-immiscible alcohol in the organic phase might effectively promote the extraction of alkali salts of the mineral acids by crown ether solutions. This opinion was subsequently reinforced by information obtained from Y. Marcus⁽¹⁶⁾, in which he reported significant enhancement of salt solubilization by crown ethers using a number of alcohols and other hydrogen bonding compounds. These pieces of information led us to examine a mixed alcohol-crown ether system in some detail.

The 2-Ethylhexanol — DC18-C-6 System

Figure 1 shows the effect of varying the 2-ethylhexanol content of the benzene diluent on potassium extraction from 2 M MgCl₂-0.01 M KCl by 0.1 M DC18-C-6. In this figure, log D_K ($D_K = [K]_{org}/[K]_{aq}$) is plotted vs log volume percent of alcohol (proportional to molarity). The average slope is 1.5, approaching slope 1.0 at low alcohol concentration, and approaching 2.0 at the higher alcohol

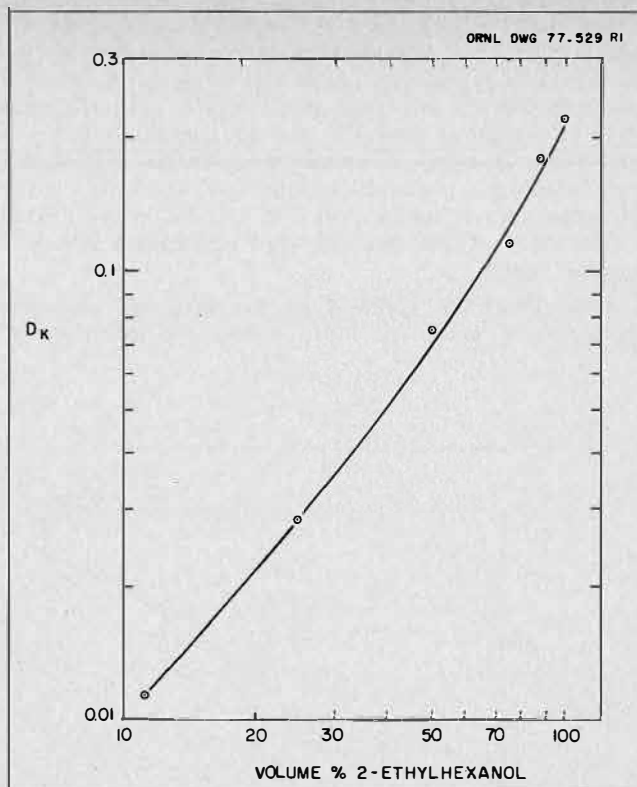


FIGURE 1. Potassium extraction from 2.0 M MgCl₂ by 0.1 M DC18-C-6 in benzene — 2-ethylhexanol as a function of the volume percent of alcohol.

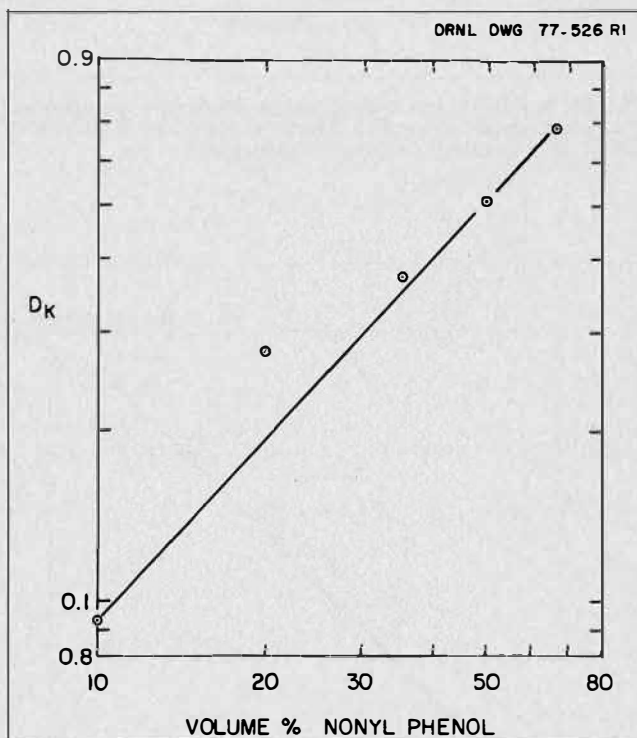


FIGURE 2. Potassium extraction from 2.0 M MgCl₂ by 0.1 M DC18-C-6 in benzene-nonylphenol as a function of the volume percent of phenol.

concentration. The effect of nonylphenol on potassium extraction is similar (Figure 2), the slope of a comparable plot being about 1.0; however, higher concentrations were not tested because of the viscosity of the nonylphenol.

These data indicate that the alcohol and phenol are similarly and strongly involved in the formation of the KCl-crown ether adduct in the organic phase and suggest the formation of an organic-phase species containing one mole of alcohol or phenol at low concentrations and possibly more at higher concentrations. Analyses show that very little $MgCl_2$ is extracted in this system; only 2.7×10^{-4} M magnesium is found in 0.1 M DC18-C-6 in 75% 2-ethylhexanol — 25% benzene when equilibrated with 2 M aqueous $MgCl_2$.

Since DC18-C-6 contains no ion exchange sites, the extraction of potassium must involve the extraction of

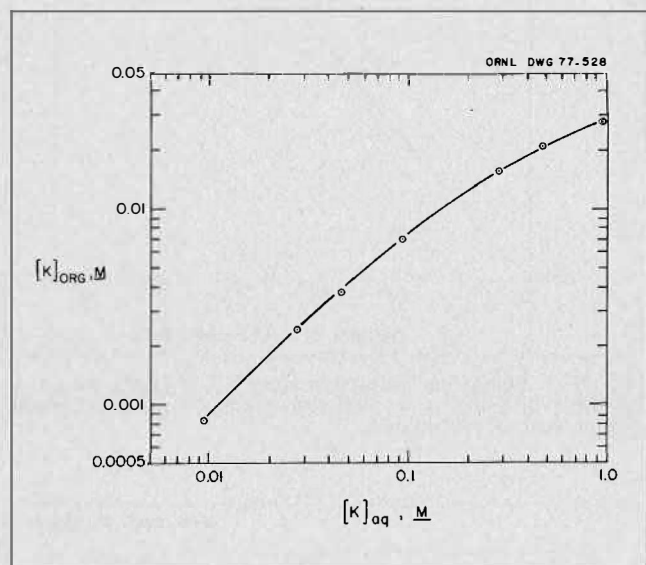


FIGURE 3. Equilibrium organic-phase potassium vs aqueous-phase potassium. Extraction was from $MgCl_2$ by 0.1 M DC18-C-6 in 25% benzene — 75% 2-ethylhexanol.

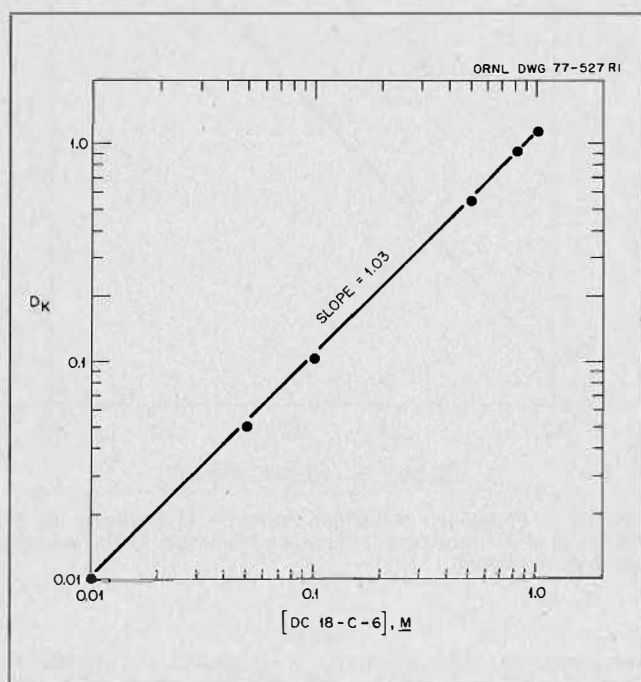
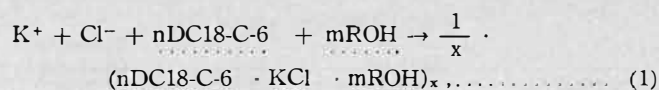


FIGURE 4. Potassium extraction as a function of DC18-C-6 concentration in 25% benzene — 75% 2-ethylhexanol. Aqueous phase was 2 M $MgCl_2$.

chloride, and a general equation for this extraction could be:



in which dotted underlines indicate an organic-phase species, ROH represents the alcohol, and possible association of the organic-phase adduct into an x-fold aggregate is provided for. Figure 3 shows a plot of $\log [K]_{org}$ vs $\log [K]_{aq}$ in a system where the aqueous phase is 2 M $MgCl_2$ and the organic phase is 0.1 M DC18-C-6 in 75% 2-ethylhexanol — 25% benzene. The initial slope of this curve is 1.0, which indicates that, if potassium is unassociated in the aqueous phase, then the complex is also unassociated in the organic phase and the value of x is 1.

The dependence of potassium extraction from 2 M $MgCl_2$ on the concentration of DC18-C-6 in 25% benzene — 75% 2-ethylhexanol is shown in Figure 4. These data yield a slope of almost exactly 1.0, indicating (since polynuclear complexes are ruled out) the association of one mole of potassium (as KCl) with one mole of DC18-C-6 in this system over the concentration range used here. This is in agreement with reported data indicating a one-to-one association in similar crown ether adducts^(1,2).

Figures 5 and 6 show acid dependence and ionic strength dependence, respectively, of KCl extraction by 0.1 M DC18-C-6 in 25% benzene — 75% 2-ethylhexanol. In both cases, however, the aqueous-phase chloride concentration increases along with the ionic strength variable since we knew of no "inert" anion to substitute for chloride. Thus, Figure 5 suggests that the acid dependence, if any, is slight. The nature of the extractant does not lead one to expect an increased extraction due to increased acid concentration; therefore, we suspect that what appears to be a small positive acid dependence may be related to the small chloride concentration increase. However, plotting $\log D_K$ vs $\log [Cl^-]$ from these data yields a slope greater than the expected value of 1, suggesting that changes in the medium, or activity effects, may also be contributing to the observed increase in D_K . Figure 6 likewise probably reflects primarily the change in chloride concentration or activity.

Conclusions

Although crown ethers form complexes with alkali and alkaline earth compounds in homogeneous alcohol-water systems and extract the picrate salts of these elements in two-phase systems, they extract the common mineral-acid salts very poorly and not in the order expected from the size of the ion relative to the size of the crown ether hole. Solubilization of the anion appears to be critical in the extraction of salts by crown ethers; i.e., providing a means

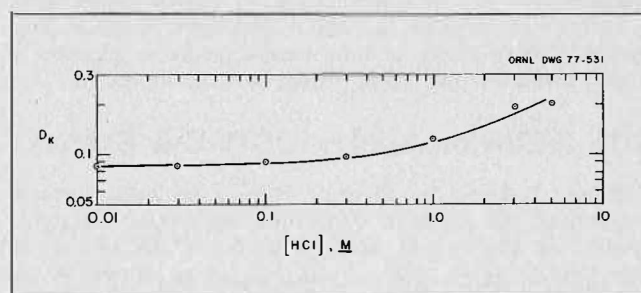
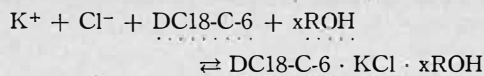


FIGURE 5. Acid dependence of potassium extraction by DC18-C-6 in 25% benzene — 75% 2-ethylhexanol at ionic strength of 6.

of solubilizing the anion appears to be necessary. The latter can be accomplished by using an alcohol as the main component of the organic diluent. A study of KCl extraction from $MgCl_2$ solutions by DC18-C-6 in 75% 2-ethylhexanol — 25% benzene suggests a reaction such as:



where x is 1 or 2.

Acknowledgment

The authors wish to acknowledge the excellent atomic absorption work of Marion Ferguson and the cooperation of the ORNL Analytical Chemistry Division and the excellent technical assistance of G. N. Case in this work.

NOTATION LIST

BisDN18-C-6	= bis dinaphthyl-18-crown-6
CDN18-C-6	= dicarboxydinaphthyl-18-crown-6
DB18-C-6	= dibenzo-18-crown-6
DC18C-6	= dicyclohexyl-18-crown-6
D_K	= distribution coefficient for potassium
D_m	= $\frac{[K]_{org}/[K]_{aq}}{[m]_{org}/[M]_{aq}}$ = distribution coefficient for the metal, M
15-C-5	= 15-crown-5
18-C-16	= 18-crown-6
HDEHP	= di(2-ethylhexyl)phosphoric acid

REFERENCES

- (1) Pedersen, C.J. and Frensdorff, H.K., *Angew.Chem. Intern.Ed.Engl.* 1972, 11, 16.
- (2) Lehn, J.M., *Structure and Bonding* 1973, Vol. 16, 1-70, Springer-Verlag, New York.
- (3) Frensdorff, H.K., *J.Am.Chem.Soc.* 1971, 93, 4684.
- (4) Pedersen, C.J., *Fed.Proc.* 1968, 27, 1305.
- (5) Sadakane, A., Iwachido, T. and Toei, K., *Bull.Chem.Soc. Jpn.* 1975, 48, 60.
- (6) Danesi, P.R., Meider-Gorican, H., Chiarizia, R. and Scibona, G., *J.Inorg.Nucl.Chem.* 1975, 37, 1479.

Discussion

K.D. MacKay: Do you have information on the toxicity of the crown ethers?

W.J. McDowell: We have no specific information. It is my impression that they are not very toxic. Does Dr. Marcus have any information on this?

Y. Marcus: A Japanese firm provides toxicity data sheets. It appears that the more water-soluble crown ethers, like 18-crown-6, have fairly high toxicity; but the water-insoluble ones, like DBC, have rather low toxicity, not being readily absorbable (their oil-solubility is not high either).

A. Warshawsky: On toxicity of polyethers, recent work unpublished at our department, shows that dibenzyl-18-crown, etc., can effectively solubilize amino acids; care should be taken.

K.M. Lewis: The Aldrich Catalog lists 15-crown-5 as a 'Cancer Suspect Agent' and 18-Crown-6 as an irritant. An article in *Chemical and Engineering News*, Sept. 1976 referred to an explosion hazard in the synthesis of 18-crown-6. That explosion was apparently caused by peroxide formation in the dioxane solvent used.

G. Grossi: Could you give us some information about the loading capacity of the crown compounds ex-

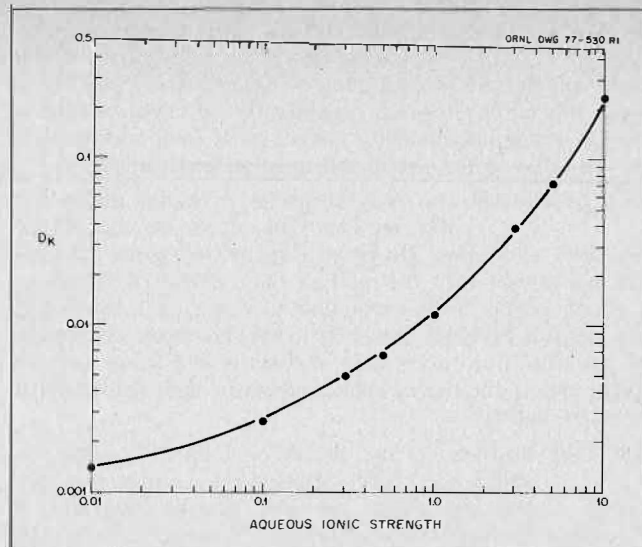


FIGURE 6. Potassium extraction by DC18-C-6 in 25% benzene — 75% 2-ethylhexanol as a function of aqueous ionic strength. $MgCl_2$ concentration was 0.03 to 3.3 M.

- (7) Rais, J. and Selvcky, P., Czech. Patent No. 149403, July 15, 1973.
- (8) Rais, J., Kyrs, M. and Kadlecova, L., in *Proceedings of International Solvent Extraction Conference 1974*, Vol. 2, 1705-15.
- (9) Jepson, B.E. and DeWitt, R., *J.Inorg.Nucl.Chem.* 1976, 38, 1175.
- (10) McDowell, W.J., Perdue, P.T. and Case, G.N., *J.Inorg. Nucl.Chem.* 1976, 38, 2127.
- (11) Nikolaev, A.V. et al., *Izv. Sib.Otd.Akad.Nauk. SSSR* 1972, 5, 52.
- (12) McDowell, W.J. and Harmon, H.D., *J.Inorg.Nucl.Chem.* 1969, 31, 1473.
- (13) Helgeson, R.C., Timko, J.M. and Cram, D.J., *J.Am. Chem.Soc.* 1973, 93, 3023.
- (14) Sam, D.J. and Simmons, J.F., *J.Am.Chem.Soc.* 1972, 94, 4024.
- (15) McDowell, W.J., *J.Inorg.Nucl.Chem.* 1971, 33, 1067.
- (16) Marcus, Y., Personal communication, 1976.

tracting systems with respect to the ions to be extracted? What is the solubility of the metal ion — crown ether compounds in organic solvents?

W.J. McDowell: We have observed loading as high as 1 salt molecule per crown ether molecule with thiocyanates. This is the stoichiometry usually reported in the literature although some one-metal-to-two-crown ether sandwich complexes have been reported. High loadings are usually difficult to achieve, however, because of low extraction coefficients. As to the solubility of the complex, it has been our experience that the solubility of the crown ether itself, is limiting. If the crown ether is soluble, the metal complexes are also.

P.D. Mollère: Have you investigated the use of other cyclic polyfunctional analogs of the crown ethers, e.g. cyclic polysiloxanes or polythio- or selenoethers — which might exhibit differences in solubility and/or hole size?

W.J. McDowell: We have looked only at two or three substituted porphyrins and they did not extract chloride salts. However, they were tested under conditions where crown ethers did not extract, i.e. without a means of solubilizing or substituting the anion.

A.J. Monhemius: Can the author give any information on the effect of the addition of crown ethers on the pH of extraction of the metals by D2EHPA? Does the author see any application of crown ethers to the extraction of transition metals, or is their use likely to be restricted to the alkali and alkaline earth metals?

W.J. McDowell: Our measurements were not made in a way to show the effect on the pH of, say, 50% extraction. However, since extraction at the same pH was greater with the mixture than with HDEHP alone, I would expect 50% extraction to occur at a lower pH. We feel it is probably too early to say, however, since many of the transition metal ions are nearly the same size, we might expect the use of crown ethers in their extraction to be more limited.

J.E. Gai: Reports in the literature indicate complexing ability for alkali metal ions by non-cyclic polyethers containing polar terminal groups (capable of "closing" the ring by coordination). In view of the present high cost of crown ethers and possibly lower cost of synthesizing non-cyclic ethers, these latter compounds should be interesting. Does the author have any information on the non-cyclic polyethers?

W.J. McDowell: We have not done any work with the linear polyethers. I believe they are not as selective as the cyclic polyethers. Perhaps Dr. Marcus could add something to this.

Y. Marcus: Linear polyethers, such as the polyglymes, are fairly strong complexing agents for the alkali cations. As extractants they suffer from higher aqueous solubilities, and considerably lower selectivities, compared with the cyclic crown ethers. The pre-formed hole in the later discriminates much better between ions of different sizes.

A. Warshawsky: Commenting on the use of linear polyethers, we have prepared pseudo-crown structures by binding linear polyoxyalkylene in polymeric matrices, showing however anion exchanger properties, of considerable interest for separation in chloride media.

R. Edwards: Is there a large measure of flexibility in designing the crown ether for selectivity for a particular metal ion?

W.J. McDowell: Yes, ring sizes of 12 units (12-crown-4) up to more than 30 units can be made.

R. Blumberg: In our paper 1(b) we give data on the solubility of chloride salts in amine hydrochloride/alcohol mixtures and alcohols alone. It would seem that crown ethers added for selectivity to systems which do dissolve chlorides may be interesting.

W.J. McDowell: We agree. I believe that crown ethers, in combination with any organic soluble substance that solubilizes the inorganic anion or substitutes (by cation exchange) an organic anion, offer possibilities for useful solvent extraction systems.

Y. Marcus: On my paper at this conference on Friday (20b) I will give chemical details on the extraction of alkali halides with crown ethers, and show the necessity of employing anion — solvating solvents together with the crown ethers for effective and selective extraction.

Here I will try to help answer some of the questions that have been raised.

The cost of the crown ethers is high, as long as the demand is low. I have a quotation from a Japanese firm for DBC (dibenzo-18-crown-6) for Can. \$3000/kg for 1 g quantities, reducing to \$600/kg for kg quantities or Can. \$200/kg for a 25 kg lot. The cost of production in quantity of commercial grade DBC need not be greater than \$10/kg starting from catechol and chloroethyl ether.

Bidentate Organophosphorus Compounds as Extractants from Acidic Waste Solutions: A Comparative and Systematic Study*

R.R. Shoun, W.J. McDowell, and Boyd Weaver,
Chemical Technology Division, Oak Ridge National
Laboratory, Oak Ridge, Tennessee 37830 USA

ABSTRACT

A comparative study has been made of several bidentate organophosphorus compounds. Tetraalkyl carbamoylmethylphosphonates and tetraalkylalkyl diphosphonates were tested for their ability to extract americium from nitric acid. Aromatic, aliphatic, and mixed diluents were compared as to the effect on extraction behavior, aqueous-phase solubility, and organic-phase solubility. Reagent and acid dependences are presented for selected compounds.

Introduction

IN THE EARLY 1960's, Siddall demonstrated that the dialkyl [(dialkyl-carbamoyl)methyl]phosphonates would extract trivalent lanthanides and actinides from strong nitric acid solutions^(1,2). He later patented the use of these bidentate compounds for the removal of trivalent americium and curium from highly acid (2-6 M HNO₃) Purex waste streams⁽³⁾. These compounds are superior to monodentate extractants, such as tributyl-phosphate (TBP) or dibutyl butylphosphonate (DBBP), for extraction from such solutions. The monodentate extractants require highly salted solutions at lower acid concentrations.

More recently, workers including Schulz at Atlantic Richfield Hanford Company, Richland, Washington, and McIsaac at Allied Chemical Corporation, Idaho Falls, Idaho, have studied the use of organophosphorus bidentate extractants for the removal of alpha-emitting nuclides from acidic radioactive wastes at their respective locations^(4,5). Wastes at both Hanford and Idaho Falls are highly salted. A typical composition can be seen in Table 1. Three extraction cycles of a simulated waste of this type using 30 vol % (0.9 M) dibutyl [(diethylcarbamoyl)methyl]phosphonate (DBDECMP) reduced the plutonium content of the waste by a factor of greater than 5000 and the americium content by a factor of 600⁽⁵⁾. The chemical and radio-chemical character of waste varies with the site, depending upon the type of material processed. Since many wastes with which we will be required to deal at ORNL are acid solutions containing minimum amounts of salt, our study of the bidentate extractants has been concerned with obtaining and testing compounds that would extract from acid solutions containing little or no salts with a minimum loss of the reagent to the aqueous phase.

One of the problems associated with the use of the tetraalkyl carbamoyl-methylphosphonates is the presence, in most preparations, of some impurity that extracts trivalent actinides at low acidities and retains them when

TABLE 1. Typical Composition of Hanford and ICPP Actinide Wastes*

Hanford CAW Solution		ICPP First-Cycle Waste ^b	
Component	Concentration (M) ^a	Component	Concentration (M) ^a
NO ₃	5.0	F	3.2
H	2.2	NO ₃	2.4
Al	0.8	H	1.6
Na	0.5	Al	0.6
F	0.3	Zr	0.5
Fe	0.009	B	0.2
Si	0.002	Hg	0.04
Ca	0.001	CrO ₃	0.01
Ce	0.007	Na	0.01
Mg	0.0006	Sn	0.003
Ni	0.0003	Pu	2200 ^d
Pu	0.002-0.01 ^e	U	~1000 ^d
241 _{AM}	0.002-0.01 ^e	Am	40 ^d
		Np	10 ^d

*Data taken from Schulz, Wallace W., and McIsaac, Lyle D., Removal of Actinides from Nuclear Solutions with Bidentate Organophosphorus Extractants. ERDA Report AHR-SA-217, Atlantic Richfield Hanford Company, Richland, Washington (August 1975).

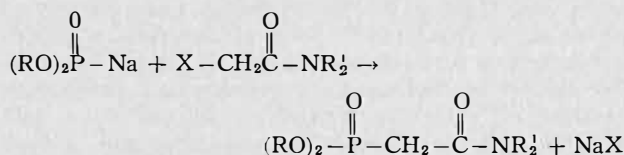
^aExcept where noted.

^bFrom co-processing of Zr-clad and Al-clad fuels.

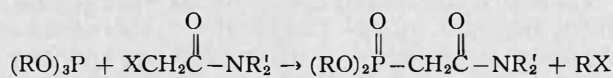
^cConcentration in g/liter.

^dConcentration in µg/liter.

normally used water stripping is attempted. These compounds may be prepared by the Michaelis reaction:



or by the Arbuzov rearrangement:



where R and R' are normal or branched chain alkanes and X is chlorine or bromine^(1,2). With the larger, branched R groups of interest, the Arbuzov rearrangement takes place only at temperatures of 200°C or higher and significant product loss is encountered by the formation of impurities requiring removal from the primary product.

One or more of the principal impurities present in the technical-grade tetraalkyl carbamoylmethylphosphonates (CMPs) is believed to be an acidic material since it creates a serious problem in stripping the trivalent actinides from the CMP solution by water or low concentrations of nitric

*Research sponsored by Energy Research and Development Administration under contract with the Union Carbide Corporation.

TABLE 2. Elemental Analyses of Molecularly Distilled CMPs

Compound ^a	% Carbon ^b		% Hydrogen ^b		% Nitrogen ^b	
	Theor.	Found	Theor.	Found	Theor.	Found
DHDECMP	59.50	59.48	10.47	10.51	3.86	3.74
DBDECMP	54.72	54.88	9.77	9.83	4.56	4.51
EHDI BCMP	65.68	65.81	11.37	11.22	2.95	2.87
DHDI BCMP	63.01	62.96	10.98	11.07	3.34	3.19
DBD BCMP	59.50	59.49	10.47	10.64	3.86	3.86
DEHDEC P	62.22	62.30	10.86	11.02	3.46	3.29
DEHDECMP	63.01	63.05	10.98	11.06	3.34	3.21

^aExtractant Compounds:
 DHDECMP = dihexyl [(diethylcarbamoyl)methyl] phosphonate
 DBDECMP = dibutyl [(diethylcarbamoyl)methyl]phosphonate
 EHDI BCMP = di(2-ethylhexyl) [(diisobutylcarbamoyl)methyl]phosphonate
 DHDI BCMP = dihexyl [(diisobutylcarbamoyl)methyl] phosphonate
 DBD BCMP = dibutyl [(dibutylcarbamoyl)methyl] phosphate
 DEHDEC P = di(2-ethylhexyl) (diethylcarbamoyl)phosphate
 DEHDECMP = di(2-ethylhexyl) [(diethylcarbamoyl)methyl]phosphonate

^bCarbon, hydrogen, and nitrogen analyses by Galbraith Laboratories, Knoxville, Tennessee.

acid. The impurities present in these commercial preparations have been studied by workers at Battelle-Pacific Northwest Laboratory, Rocky Flats, and Oak Ridge National Laboratory.^(6,7,8) Methods of studying the impurities have varied. Martin at Battelle examined both technical-grade and purified material by GC-MS, NMR, and IR⁽⁷⁾. Thin layer and column chromatography combined with radiotracer testing, elemental analysis, and IR were used by Bahner at ORNL to investigate an enhanced source of impurities, i.e., the pot residue from molecular distillation of technical-grade CMPs. Martin and Bahner have concluded that the principal offending impurity is alkyl [(dialkylcarbamol)methyl]phosphonic acid⁽⁸⁾.

Various methods have been used to purify the technical-grade CMPs. Schulz prepared satisfactorily pure reagent for his applications using Siddall's method of acid hydrolysis and alkaline wash⁽⁴⁾. More recently, at the same installation, purifications have been carried out by washing a dihexyl [(diethylcarbamoyl)methyl]phosphonate (DHDECMP) solution with ethylene glycol and then passing the material through a macroporous, strong base (Rohm and Haas A-26) ion exchange resin column to remove acidic impurities⁽⁹⁾. Kilogram amounts of CMPs for bench-scale research are purified at ORNL by molecular distillation. McIsaac has recently used a purification consisting of molecular distillation followed by a pass through a silica gel column. Gas chromatographic analysis of this purified material indicates a very pure product⁽¹⁰⁾.

The choice of a suitable compound for study and use at Idaho Falls was initially DBDECMP⁽⁵⁾. This compound is as good an extractant as DHDECMP and appeared to be more easily purified; however, a significant aqueous-phase solubility hindered its practical use in a continuous solvent extraction system. The choice made by workers at Hanford and Idaho Falls is now DHDECMP. This compound has adequate actinide extraction power and low aqueous-phase solubility (similar to that of TBP in water).

This research is addressed to the problems of selecting and testing bidentate organophosphorus extractants having low aqueous-phase solubility, high organic-phase solubility, and adequate extractant power. We are studying new compounds in which the R groups on the end (or both ends) of the molecule are made larger and/or branched with the objective of decreasing the aqueous-phase solubility and making the compound more compatible with straight-chain aliphatic diluents.

Experimental

The tetraalkyl carbamoylmethylphosphonates were obtained as technical-grade material from the Wateree Chemical Company, Lugoff, South Carolina. They were purified for this study by molecular distillation at a pressure of $\sim 1 \mu$ and a temperature of 55 to 105°C (depending upon alkyl chain lengths and branching). The distilled products were checked for the absence of acidic extractants by testing their ability to extract americium from 0.01 M HNO₃. Elemental analyses of the molecularly distilled compounds were done by Galbraith Laboratories, Inc., Knoxville, Tennessee.

Diluents for the extractants were reagent- or commercial-grade quality and used without further purification. Aqueous acid solutions were prepared from reagent-grade concentrated acid.

Radioactive tracers were obtained from ORNL, ICN, or New England Nuclear.

Equilibrations were performed by shaking 5 ml of each phase for at least 15 min in cylindrical separatory funnels equipped with Teflon stop-cocks. Previous experiments indicated that equilibrium was reached in <1 min. After phase separation, 1-ml samples of each phase were taken for gamma counting. The distribution coefficient, D, was then calculated from the ratio of the count rate in the organic phase to that in the aqueous phase.

The organic phases containing the extractant were pre-equilibrated twice with acid of the concentration to be used in the experiment to ensure the desired equilibrium concentration of acid during the extraction.

Results and Discussion

Comparison of Carbamoylmethylphosphonates

Seven compounds were tested using, in each case, molecularly distilled fractions. Elemental analyses of these compounds (Table 2) are in excellent agreement with the theoretical values. In addition, tests of americium extraction at low acid concentrations assured us that the acidic compounds that prevent low acid stripping of americium were not present. Extraction coefficients in the presence of 0.01 M HNO₃ were typically <0.1 for all the purified compounds.

Table 3 shows the comparative capabilities of the seven compounds to extract americium. The effect of reagent structure on extraction can be seen in the results in diethylbenzene (DEB) and dodecane where, in general, the smaller (but more aqueous-soluble) compounds are better extractants. Although more of the compounds are soluble in DEB without third-phase formation (a third phase consists of the nitric acid adduct of the CMP that separates from the bulk of the organic phase after the CMP solution is contacted with HNO₃), distribution coefficients are higher in dodecane. It is clear that the type of diluent, aliphatic or aromatic, as well as the structure of the extractant, is important in determining the extraction behavior of these compounds.

Choice of Diluent

Aliphatic diluents have the advantage of providing a higher americium distribution coefficient than do aromatic diluents; however, if one desires to use an aliphatic diluent, those compounds with straight alkyl chains on either end (e.g., hexyl and ethyl or butyl and ethyl) should be avoided. Such compounds extract nitric acid (about 2 moles of acid per mole of CMP), and the nitric acid adduct separates into a third phase. An aromatic diluent such as DEB successfully circumvents the third-phase problem but depresses

TABLE 3. Extraction of Americium from 6 M HNO₃ by Carbamoylmethylphosphonates

Compound ^a	Concentration (vol %) (M)		D _{Am} in indicated diluent						
			KERMAC 470B	KERMAC 627	DEB ^b	Dodecane	PMH ^c	DIBP ^d	MIBK ^e
DHDECMP	30	0.5	*	*	4.5	9.2 ^f		4.7	
	50	0.8	*	*	23				
DBDECMP	30	0.5	*	*	6.3	*			
		0.9	*	*					
DEHDECMP	30	0.5	3.3	4.1	1.5	*			
	50	0.7	8.3		9.5		11	17	
DEHDIBCMP	30	0.5	0.3	0.4	0.3	0.7			
	50	0.6	*			2.7			
DHDIBCMP	30	0.5	2.0	*	0.6	*	5.7		
		0.7	5.7						
DBDBCMP	30	0.5	*	*	1.0	*	*		
		0.8							
DEHDECMP	30	0.5	0.36	0.36	0.82	0.67			
	50	0.7				1.0			
	50	1.2							

*Third-phase formation on contact with 6 M HNO₃.

^aExtractant compounds:

DHDECMP = dihexyl [(diethylcarbamoyl)methyl]phosphonate
 DBDECMP = dibutyl [(diethylcarbamoyl)methyl] phosphonate
 DEHDECMP = di(2-ethylhexyl) [(diethylcarbamoyl)methyl]phosphonate
 DEHDIBCMP = di(2-ethylhexyl) [(diisobutylcarbamoyl)methyl] phosphonate
 DHDIBCMP = dihexyl [(diisobutylcarbamoyl)methyl]phosphonate
 DBDBCMP = dibutyl [(dibutylcarbamoyl)methyl]phosphonate
 DEHDECMP = di(2-ethylhexyl) (diethylcarbamoyl)phosphonate

^bDEB = diethylbenzene

^cPMH = pentamethylheptane

^dDIBP = diisopropylbenzene

^eMIBK = methylisobutylketone

^fWith 15 vol % tridecanol added. Third phase in unmodified dodecane.

distribution coefficients by a factor of 2 or more. An organic-soluble — aqueous-insoluble modifier such as tridecanol (TDA) may also be added to prevent third-phase formation. Fifteen percent by volume (vol %) TDA was necessary to prevent third-phase formation in a 30 vol % (0.8 M) solution of DHDECMP in dodecane when contacted with 6 M HNO₃. The americium distribution coefficient (D_{Am}) in this system is 9.2, as compared with 4.5 in the system with DEB as a diluent. Several diluents were tested with di(2-ethylhexyl) [(diethylcarbamoyl)methyl]phosphonate (DEHDECMP) in the extraction of americium from 6 M HNO₃. These comparisons may be seen in Table 3.

Figure 1 shows the effect of the aliphatic-aromatic content of the diluent on the extraction of americium from 6 M HNO₃ by 0.5 M DEHDECMP. In these tests the xylene concentration in dodecane was varied from 100 vol % to 5 vol %. It was possible to obtain extraction data down to 10% xylene; third-phase formation occurred at 7.5% xylene. The D_{Am} increased rapidly until the aromatic content of the mixture dropped to about 15 vol %. These results suggest that an aromatic content of 10 to 15% would be an optimum diluent composition.

The significant effect of the diluent type, both on extraction power and solubility, prompted a study of two commercial diluents that are prepared for the solvent extraction industry, KERMAC 470B and KERMAC 627⁽¹¹⁾. KERMAC 470B is reported to contain about 50% naphthenes, with smaller amounts of paraffins and aromatics, while KERMAC 627 is reported to contain primarily paraffins with the remainder being naphthenes and aromatics. Neither compound is said to contain olefins. Comparisons of extractants and diluents may be seen in Table 3. The effect is apparent for dihexyl [(diisobutylcarbamoyl)methyl]phosphonate (DHDIBCMP) and DEHDECMP in KERMAC 470B. Neither compound is com-

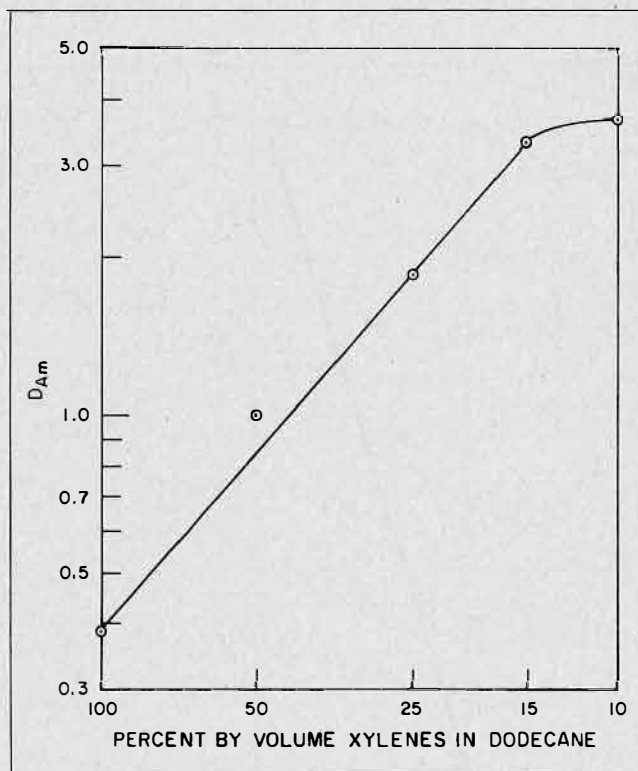


FIGURE 1. Optimization of americium extraction by variation of the xylene concentration in dodecane.

patible with dodecane upon contact with 6 M HNO₃; however, each remains in solution at 0.7 M in KERMAC 470B and exhibits an adequate distribution coefficient for americium when used in the mixed diluent.

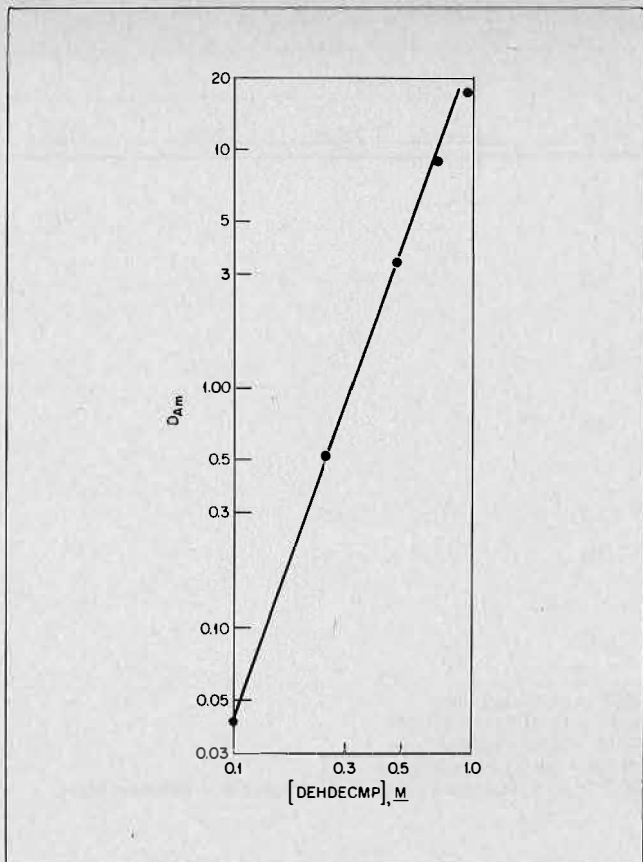


FIGURE 2. Americium extraction dependence on reagent concentration for the system 6 M HNO₃ vs DEHDECMP in KERMAC 470B.

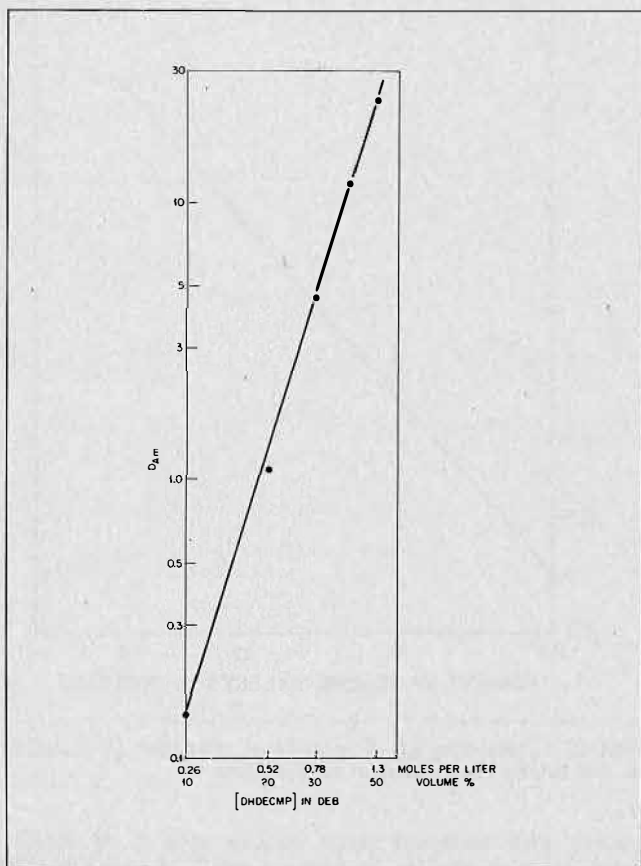


FIGURE 3. Americium extraction dependence on reagent concentration for the system 6 M HNO₃ vs DHDECMP in DEB.

Systematic Studies of DEDECMP and DEHDECMP

The compounds DEHDECMP and DHDECMP were chosen for more extensive descriptive studies because DHDECMP is being used or planned for use (along with either chlorinated or aromatic diluents) at both Hanford and Idaho Falls and DEHDECMP appears to offer the advantages of lower aqueous-phase distribution of the extractant and higher organic-phase solubility. When used in a mixed aromatic-aliphatic diluent, DEHDECMP has a very low aqueous-phase solubility (about 3% that of DHDECMP) and shows no evidence of third-phase formation upon acid contact up to 8 M HNO₃. At a concentration of 1 M (extracting from 6 M HNO₃), it gives an americium distribution coefficient of 17.5 (see Fig. 2). Equilibration of this organic with fresh 6 M HNO₃ gave an americium distribution coefficient within experimental error, indicating the equilibrium value may be approached from either direction. Some limitations exist in the capacity of this extractant mixture for metal adduct. Attempts to load a 0.5 M DEHDECMP solution in a mixed diluent (KERMAC 470B) with europium from 6 M HNO₃ produced a third phase when the europium concentration was 0.02 M in the aqueous phase and 0.01 M in the organic phase.

The dependence of americium extraction on reagent concentration for DHDECMP in DEB is seen in Figure 3. A least-squares fit of these data indicates that the americium distribution coefficient is proportional to the 3.2 power of the reagent concentration, suggesting that the average number of extractant molecules associated with each americium is about 3. Figure 2 shows that the reagent

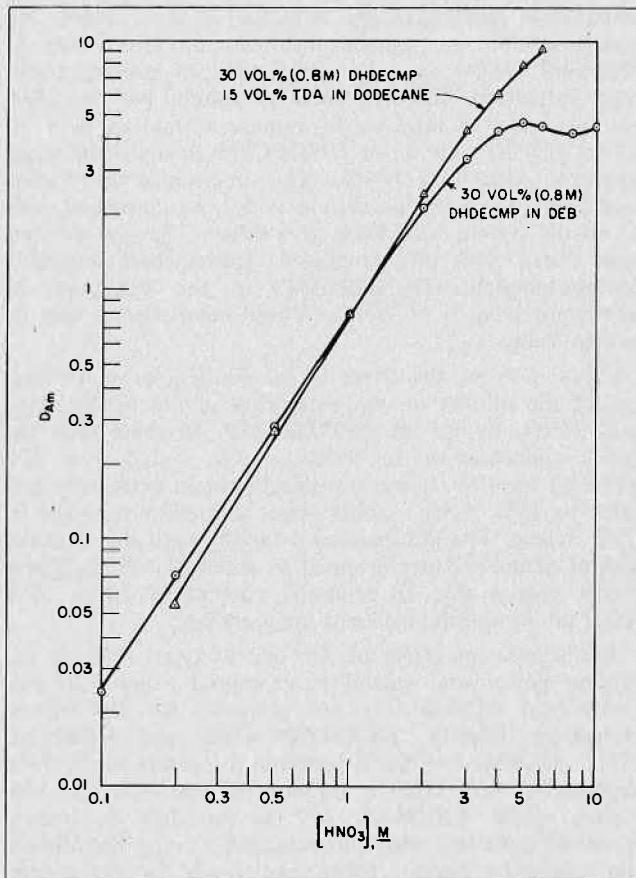


FIGURE 4. Americium extraction dependence on nitric acid concentration for the systems 0.1 — 10 M HNO₃ vs 30 vol % (0.8M) DHDECMP in 15 vol% TDA — dodecane, and 30 vol % (0.8M) DHDECMP in DEB.

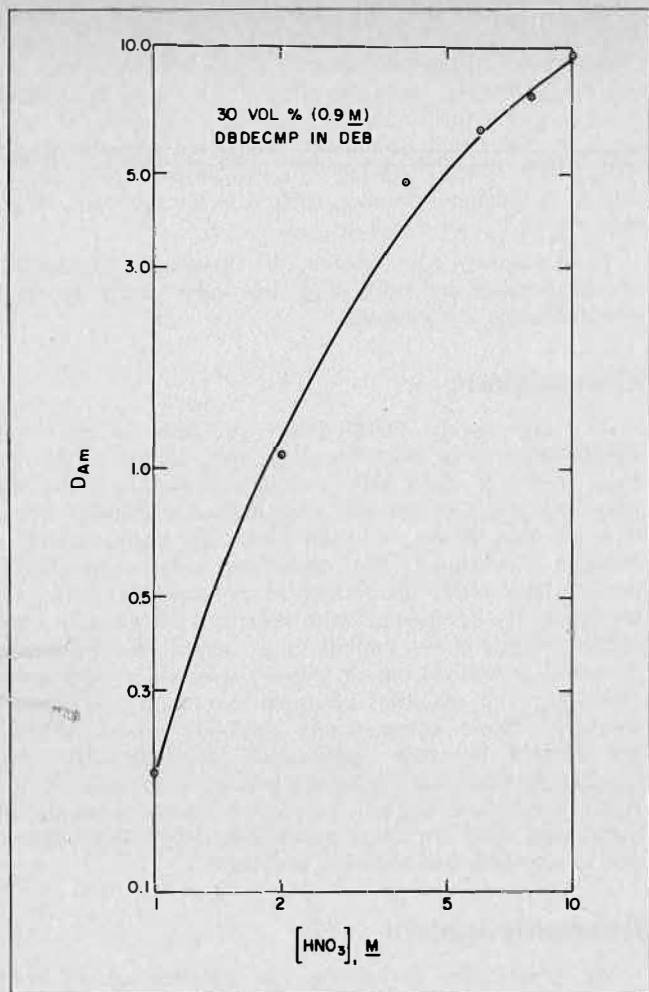


FIGURE 5. Americium extraction dependence on nitric acid concentration for the system 1 — 10 M HNO_3 vs 30 vol % (0.9 M) DBDECMP in DEB.

concentration dependence for DEHDECMP in KERMAC 470B is 2.5 power, suggesting either that the branching on the extractant molecule may be causing some steric hindrance or that nonspecific solvent-solute interaction in the organic phase at higher extractant concentrations may be involved.

Curves illustrating the dependence of americium extraction on acid concentration are shown in Figure 4. The curve for 30 vol % (0.8 M) DHDECMP in dodecane modified with 15 vol % TDA is somewhat steeper than that for the same concentration of the compound in DEB. For the latter system, the curve forms a straight line up to about 2 M HNO_3 , and then decreases in slope to become nearly flat between 4 and 10 M HNO_3 . The dependence of americium extraction on acid concentration over the straight portion of each curve is about 1.5 power.

Figure 5 shows the dependence of americium extraction on aqueous acid concentration for DBDECMP in DEB. This dependence appears to be greater than that for the other compounds at lower acidities; however, the curve does not form a straight line, possibly reflecting the significant aqueous-phase solubility of this extractant at the higher acid concentrations.

The dependence of americium extraction on aqueous acid concentration for DEHDECMP at 30 vol % (0.7 M) and 50 vol % (1.1 M) in DEB is shown in Figure 6 and for 0.5 M DEHDECMP in both KERMAC 470B and KERMAC 627 in Figure 7. The dependence appears to be less than second power for the extractant in DEB and

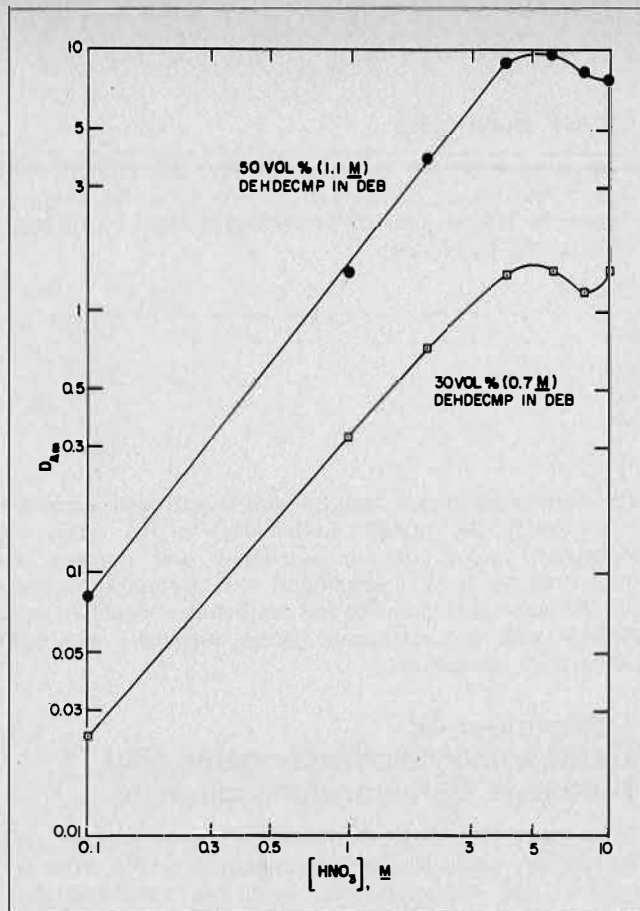


FIGURE 6. Americium extraction dependence on nitric acid concentration for the systems 0.1 — 10 M HNO_3 vs 50 vol % (1.1 M) and 30 vol % (0.7 M) DEHDECMP in DEB.

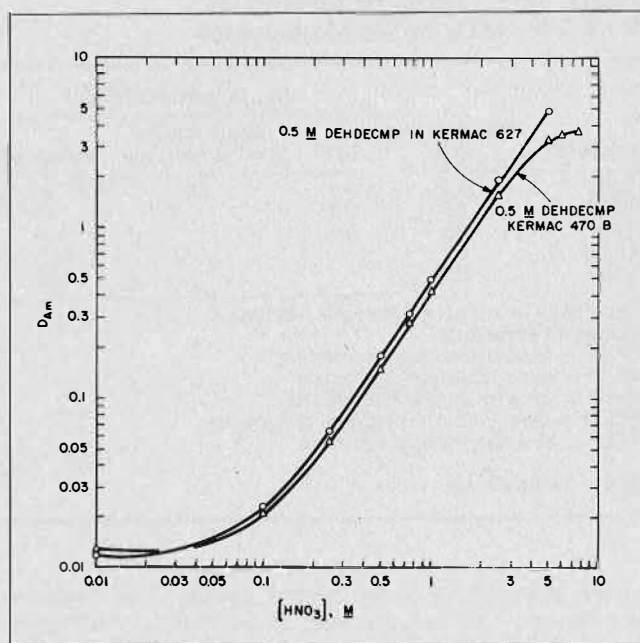


FIGURE 7. Americium extraction dependence on nitric acid concentration for the systems 0.01 — 7.5 M HNO_3 vs 0.5 M DEHDECMP in KERMAC 627 and KERMAC 470B.

about second power for the extractant in the mixed diluents in the straight-line portion of these plots. A third phase was formed in the KERMAC 627 in those experiments

equilibrated with HNO₃ at concentrations higher than 5 M. This is probably due to the lower aromatic content of KERMAC 627.

Other Elements

As a part of the systematic study, distribution coefficients have been determined for the following elements from 6 M HNO₃ with 0.5 M DEHDECMP in KERMAC 470B as the extractant:

Element	D
Cs	3.3×10^{-4}
Sr	2.6×10^{-3}
Co	2.6×10^{-3}
Ag	7.1×10^{-3}
Eu	2.13
Tm	0.63
Am	3.4

The separation factor between americium and europium (representing the middle lanthanides) is 1.6, while the separation factor between americium and thulium (representing the heavy lanthanides) is 6. Intergroup separation between the actinides and lanthanides would be very difficult with this extractant system, especially with light and middle lanthanides.

Comparison of Tetraalkylalkyldiphosphonates and Tetraalkyl Carbamoylphosphonate

The tetraalkylalkyldiphosphonates are structurally similar to the carbamoylmethylphosphonates. We have examined five diphosphonates and one carbamoylphosphonate. Results of tests for americium extraction from 6 M HNO₃ are shown in Table 4. In the first three compounds, the distance between phosphonate groups was

TABLE 4. Extraction of Americium from 6 M HNO₃ by Diphosphonates

Compound ^a	Concentration (M)	D _{Am} in Indicated Diluent		
		DEB ^b	50 vol % DEB; 50 vol % dodecane	Dodecane
TBMDP	0.75	4.6	6.8	*
TBEDP	0.5	0.17		*
TBPDP	0.5	0.5		*
TEHEDP	0.5			0.12
TOEDP	0.5			0.46

*Third-phase formation on contact with 6 M HNO₃.

^aExtractant compounds:

TBMDP = tetrabutylmethanediphosphonate
 TBEDP = tetrabutylethanediphosphonate
 TBPDP = tetrabutylpropanediphosphonate
 TEHEDP = tetra(2-ethylhexyl)ethanediphosphonate
 TOEDP = tetraoctylethanediphosphonate

^bDEB = diethylbenzene.

varied from one to three methyl groups. This comparison shows a marked decrease in americium distribution as the distance between the coordinating oxygens is increased. A comparison of two compounds with two-carbon midchains, one having normal and the other having branched end groups, shows that the compound with normal alkyl groups gives an americium distribution coefficient about four times that of the branched compound. This suggests that branching sterically interferes with formation of the metal salt adduct. The di(2-ethylhexyl)-(diethylcarbamoyl)phosphonate (DEHDECMP), which differs

from the DEHDECMP only in the absence of the mid-CH₂ group, has an americium distribution coefficient under identical conditions of about 13 times less than that for the DEHDECMP when the diluent is a mixed KERMAC diluent. From this and the results of varying the P = O spacing in the diphosphonates, it appears that the single-CH₂-group spacing (giving a six-membered ring in the adduct if bidentate bonding occurs) is the optimum structure for this class of compounds.

High viscosity and apparent low loading capacities for the diphosphonates have kept descriptive study of these compounds at a minimum.

Conclusions

The compounds, DHDECMP (presently in use) and DEHDECMP (an attractive alternate), appear to be the most useful of the CMPs presently available. While the lower-molecular-weight and normal-alkyl-substituted members of this group of compounds are more effective actinide extractants, the higher-molecular-weight compounds have lower distribution to the aqueous phase. Of the latter, the compounds with branched substituents have higher organic-phase solubilities in normal hydrocarbons. A mixed aliphatic-aromatic diluent is useful to maximize extraction and maintain adequate extractant and adduct solubility. Some commercially available mixed diluents are suitable for such applications. A single-CH₂-group spacing between the coordinating groups is optimum for adduct formation. Tetraalkyl-diphosphonates are less useful extractants than tetraalkyl carbamoylmethyl-phosphonates due to solubility and viscosity problems.

Acknowledgment

We would like to express our appreciation to both W. W. Schulz and L. D. McIsaac for samples of two organophosphorus bidentate compounds, to Kerr McGee Refining Corporation for samples of KERMAC diluents, and to S. E. Dorris for excellent technical assistance.

NOTATION LIST

CMP	= carbamoylmethylphosphonate
D	= distribution coefficient (ratio of count rate in organic phase to that in aqueous phase)
D _{AM}	= distribution coefficient of americium
DBBP	= dibutyl butylphosphonate
DBDBCMP	= dibutyl [(dibutylcarbamoyl)methyl phosphonate]
DBDECMP	= dibutyl [(diethylcarbamoyl)methyl] phosphonate
DEB	= diethylbenzene
DEHDECMP	= di(2-ethylhexyl) [(diethylcarbamoyl)methyl] phosphonate
DEHDECMP	= di(2-ethylhexyl) (diethylcarbamoyl) phosphonate
DEHDIBCMP	= di(2-ethylhexyl) [diisobutylcarbamoyl] methyl phosphonate
DHDECMP	= dihexyl [(diethylcarbamoyl)methyl] phosphonate
DHDIBCMP	= dihexyl [(diisobutylcarbamoyl)methyl] phosphonate
DIPB	= diisopropylbenzene
GC-MS	= gas chromatography-mass spectrometry
IR	= infrared spectrometry
KERMAC 470B	= a commercial mixed diluent
KERMAC 627	= a commercial mixed diluent
MIBK	= methylisobutylketone
NMR	= nuclear magnetic resonance
PMH	= pentamethylheptane
TBEDP	= tetrabutylethanediphosphonate
TBMDP	= tetrabutylmethanediphosphonate
TBP	= tributylphosphate
TBPDP	= tetrabutylpropyldiphosphonate
TDA	= tridecanol
TEHEDP	= tetra(2-ethylhexyl)ethanediphosphonate
TOEDP	= tetraoctylethanediphosphonate

REFERENCES

- (1) Siddall, T.H., *J.Inorg.Nucl.Chem.* 1963, 25, 883.
- (2) Siddall, T.H., *J.Inorg.Nucl.Chem.* 1964, 26, 1991.
- (3) Siddall, T.H., U.S. Patent 3,243,254 (1966).
- (4) Schulz, W.W. and McIsaac, L.D., August 1975, ERDA Report AHR-SA-217 or CONF-750913-13.
- (5) McIsaac, L.D., Baker, J.D. and Tkachyk, J.W., August 1975, ERDA Report ICP-1080.
- (6) Navratil, J.D., Personal Communication, May 1976.
- (7) Martin, E.C., Personal Communication, June 1976.
- (8) Bahner, C.T., Shoun, R.R. and McDowell, W.J., 1977, ERDA Report ORN/TM-5878.
- (9) Schulz, W.W., Personal Communication, March 1977.
- (10) McIsaac, L.D., Personal Communication, March 1977.
- (11) Products of the Kerr-McGee Refining Corporation.

DISCUSSION

G. Grossi: What is the chemical and radiation stability of these carbamoylmethyl phosphonates, namely: radiolytic behaviour with alpha particles; hydrolysis with nitric acid (3M or more); behaviour in the presence of nitrous acid.

R.R. Shoun: Much of the actual process development has been by Schultz and co-workers at Hanford, and McIsaac and co-workers at Idaho Falls. Alpha radiolysis studies by McIsaac and co-workers at Idaho Falls indicate that the stability of the carbamoylmethylphosphonates is at least as good as the radiation stability of TBP.

We find no indication of hydrolysis of these compounds with 2M nitric acid but studies now underway do show hydrolysis with both 4M and 6M nitric acid. We will next study the effect of 3M nitric acid.

I believe that McIsaac has found little or no effect of nitrous acid on extraction behaviour.

B.F. Myasoedov: Would you comment on the mechanism of extraction with bidentate organophosphoric compounds and selectivity with respect to iron (Fe) extraction?

R.R. Shoun: We have not yet determined extraction mechanisms but plan to work toward that end. Iron extraction by the bidentates is virtually nil according to work reported by McIsaac at Idaho Falls.

F. Kolarik: Did you study the selectivity of your extractants with respect to Pu(IV) and lanthanides?

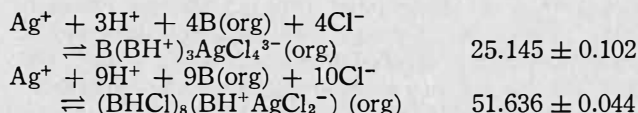
R.R. Shoun: We find little selectivity with respect to the trivalent lanthanides and actinides — all are extracted by these compounds.

Lyle McIsaac and co-workers at Idaho Falls have found that Pu(IV) is extracted much more strongly than are the trivalent actinides under identical conditions.

ORGANIC REAGENTS

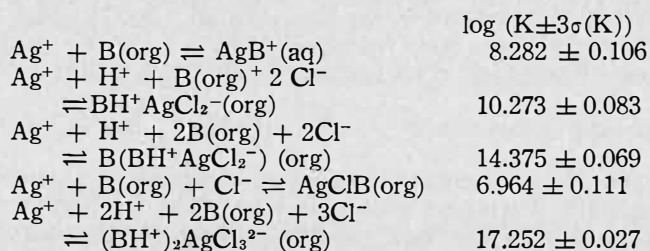
Solvent Extraction Studies of Silver (I) by Trilaurylamine in O-Xylene

Djiet Hay Liem and Mendel Zangen*
Department of Inorganic Chemistry,
Royal Institute of Technology (KTH)
S-100 44, Stockholm 70, Sweden



ABSTRACT

The complex formation between Ag(I) and trilaurylamine (TLA) (=B) in the two-phase system o-xylene/1.0 M (H, Li)Cl has been studied from the distribution of Ag(I) between the two phases as a function of the TLA concentration in o-xylene and [H⁺] in the aqueous phase. The distribution of Ag(I) has been studied using AKUFVE equipment and the radioactive Ag-110m as a tracer. The distribution data have been analyzed using the LETA-GROP DISTR program and the formation of the following Ag(I)-TLA complexes were indicated:



Introduction

LONG-CHAIN AMINE EXTRACTANTS, e.g. trioctylamine(TOA) or trilaurylamine(TLA), have been successfully used for the extraction of metal ions.^(1,2) In recent years the complex formation properties of these extractants with respect to inorganic acids in the organic/aqueous two-phase systems have been extensively studied by several authors.^(2,3) These studies have given strong indications of the formation of amine acid aggregates in the organic phase. In order to understand the equilibria of the metal extraction when long-chain amines are used as extractants a detailed knowledge of these amine aggregation equilibria is of great importance. In the present work we report studies of the extraction of silver(I) from 1.0 M (H, Li)Cl aqueous medium by trilaurylamine (TLA) into o-xylene. The two-phase system, 1.0 M (H, Li)Cl/o-xylene was chosen for this study, since for this system the distribution

*Present address: Radiochemistry Department, Soreq Nuclear Research Center Israel Atomic Energy Commission, Yavna, Israel.

equilibria of TLA-HCl species have been studied previously.^(3,4) The use of long-chain amine extractants is known to be effective for anion-forming metal complexes, e.g., $ZnCl_4^{2-}$ and $FeCl_4^-$ species², by the formation of extractable amine salts. Silver ions which were found to form strong anionic chloride complexes, $AgCl_n^{-(n-1)}$, $n = 2$ to 4, in aqueous chloride solutions⁽⁵⁾ may thus be expected to form extractable Ag(I)-TLA species. The distribution data of Ag(I) as a function of C_{TLA} and $\log(H^+)$ were analyzed graphically as well as numerically using the LETAGROP-DISTR program.⁽⁶⁾ The use of long-chain amines for the extraction of silver(I) seems to have been reported previously mainly for melt salt systems at high temperatures.⁽²⁾ In the present work the studies have mainly been carried out using the AKUFVE equipment, which has been shown to be a powerful device for solvent extraction studies.⁽⁷⁾

Experimental

Reagents

o-Xylene (Fluka, puriss) was purified by washing it with dilute NaOH solution, distilled water, dilute HCl solution and finally several times with distilled water.

TLA and $TLAH^+Cl^-(s)$, kindly supplied by Dr. Mamoun Muhammed, have been purified as described previously.³

LiCl(p.a. Kebo), HCl(p.a. Merck, Darmstadt) were used without further purification.

Radioactive Ag-110m was supplied by AB Atomenergi, Sweden, in the form of silver metal. It was dissolved in concentrated HNO_3 , evaporated to dryness and afterwards dissolved in 1.0 M HCl solution. The Ag-110m isotope was checked by gamma-spectrometry and was found to be radioactive pure.

Distribution Experiments

A general description of AKUFVE and its use for solvent extraction studies have been reported previously.⁽⁷⁾ In the present work the organic and aqueous phases from the centrifuge were circulated to the detectors using glass tubes instead of teflon tubes. The scintillation detectors consist of two hole-through NaI crystals (Teledyne) in conjunction with a Tracerlab Spectro/Matic scaler. The $\log(H^+)$ of the aqueous solution was either calculated from the amount of acid added for $\log(H^+) > 2$ or measured potentiometrically using a combined glass electrode (Radiometer Gk2351C) in conjunction with a digital voltmeter (DM2022, Dynamco Instruments, England). The E_0 and the correction for liquid junction potential were determined in a separate E_0 titration and (H^+) calculated from the relationship:

$$E = E_0 + 59.16 \log(H^+) + j(H^+) \text{ mV.}$$

The solutions in the AKUFVE were thermostated via the heat exchangers and the temperature kept constant at $25.0 \pm 0.5^\circ C$ by an external circulating thermostated water-alcohol mixture. The distribution ratio of Ag-110m was determined from the ratio of number of counts per unit time for the two detectors corrected for by the background and a counting ratio factor. This correction factor includes correction for volume ratio and crystal efficiency and was determined by comparison of a given distribution ratio, D , from an AKUFVE measurement with the value obtained from an off-line measurement using an external detector (Tracerlab SC-70 Compu/Matic V). For each run of experiment the counting ratio was found to be practically constant.

Chemical Model

The Ag(I) is assumed to exist as the species $(H^+)_p(Ag^+)_qB_r(Cl^-)_s(org)$ and $(H^+)_k(Ag^+)_lB_m(Cl^-)_n(aq)$ and a given species may be denoted by giving the appropriate values of $(p, q, r, s)(org)$ or $(k, l, m, n)(aq)$. The species $(0, 1, 0, 2)(aq)$ thus correspond to the ionic complex $AgCl_2^-(aq)$ and e.g., the species $(BHCl)_2AgCl(org)$ may be denoted by $(2, 1, 2, 3)(org)$. We make the reasonable assumption that any Ag(I) species extracted in the organic phase is uncharged, i.e. $p+q=s$. Application of the mass-action law gives the following relationships:

$$K_{pqrs}^{org} = [(H^+)_p(Ag^+)_qB_r(Cl^-)_s]_{org} (H^+)^{-p}(Ag^+)^{-q}(B)_{org}^{-r}(Cl^-)^{-s} \quad (1)$$

$$K_{klmn}^{aq} = [(H^+)_k(Ag^+)_lB_m(Cl^-)_n] (H^+)^{-k}(Ag^+)^{-l}(B)_{org}^{-m}(Cl^-)^{-n} \quad (2)$$

The distribution ratio, D_{calc} , for Ag(I) between the two phases may thus be expressed by the equation:

$$D_{calc} = \frac{(\sum q[(H^+)_p(Ag^+)_qB_r(Cl^-)_s]_{org}) / \sum l[(H^+)_k(Ag^+)_lB_m(Cl^-)_n]}{\sum q K_{pqrs}^{org} (H^+)^p (Ag^+)^q (B)_{org}^{-r} (Cl^-)^{-s} / (\sum l K_{klmn}^{aq} (H^+)^k (Ag^+)^l (B)_{org}^{-m} (Cl^-)^{-n})} \quad (3)$$

The mass-balance for Ag(I), B and $Cl(-)$ may be expressed by the following relationships:

$$C_{Ag} = \sum (Ag) + V_f \sum (Ag)_{org} = \sum l K_{klmn}^{aq} (H^+)^k (Ag^+)^l (B)_{org}^{-m} (Cl^-)^{-n} + V_f \sum q K_{pqrs}^{org} (H^+)^p (Ag^+)^q (B)_{org}^{-r} (Cl^-)^{-s} \quad (4)$$

$$C_{Cl} = \sum (Cl) + V_f \sum (Cl)_{org} = \sum n K_{klmn}^{aq} (H^+)^k (Ag^+)^l (B)_{org}^{-m} (Cl^-)^{-n} + V_f \sum s K_{pqrs}^{org} (H^+)^p (Ag^+)^q (B)_{org}^{-r} (Cl^-)^{-s} \quad (5)$$

$$C_B = \sum (B) + V_f \sum (B)_{org} = \sum m K_{klmn}^{aq} (H^+)^k (Ag^+)^l (B)_{org}^{-m} (Cl^-)^{-n} + V_f \sum r K_{pqrs}^{org} (H^+)^p (Ag^+)^q (B)_{org}^{-r} (Cl^-)^{-s} \quad (6)$$

Here $V_f = V_{org} V_{aq}^{-1}$ denotes the volume ratio of the organic to the aqueous phase and $C_i = n_i V_{aq}^{-1}$ moles/l where n_i is the total number of moles of component i in the two-phase system. Given the values of C_{Ag} , C_B , C_{Cl} , $[H^+]$ and K_{pqrs}^{org} , K_{klmn}^{aq} we may calculate $[Ag^+]$, $[B]_{org}$ and $[Cl^-]$ from (4), (5) and (6). Given the values of these parameters we may calculate D_{calc} from equation (3). In the Letagrop-DISTR program used for the analysis of the data these calculations are carried out in a procedure called BDTV.⁽⁹⁾ In the present work we furthermore may assume that Ag(I) predominantly exist as mononuclear species since the total concentration, C_{Ag} , was kept below 2.5×10^{-4} M. This assumption was supported by a set of experiments showing that the distribution of Ag(I) to be unaffected by a variation of C_{Ag} as required by (3) when $q = l = 1$.

Computer Analysis of the Data

The distribution data given as $\log[H^+]$, C_{Ag} , C_B , C_{Cl} , D_{exp} and V_f were analysed by the computer program LETAGROP-DISTR⁽⁸⁾. In this program, for a given chemical model, a set of constants K_1, K_2, \dots, K_N for the formation of Ag(I)-TLA species is sought which minimizes

$$\text{the error-square sum } U = \sum_1^{N_p} (\log D_{calc} - \log D_{exp})^2,$$

where N_p represents the number of experimental points available. The model which gives the lowest U_{min} will be assumed to be the "best" model out of the models tried.

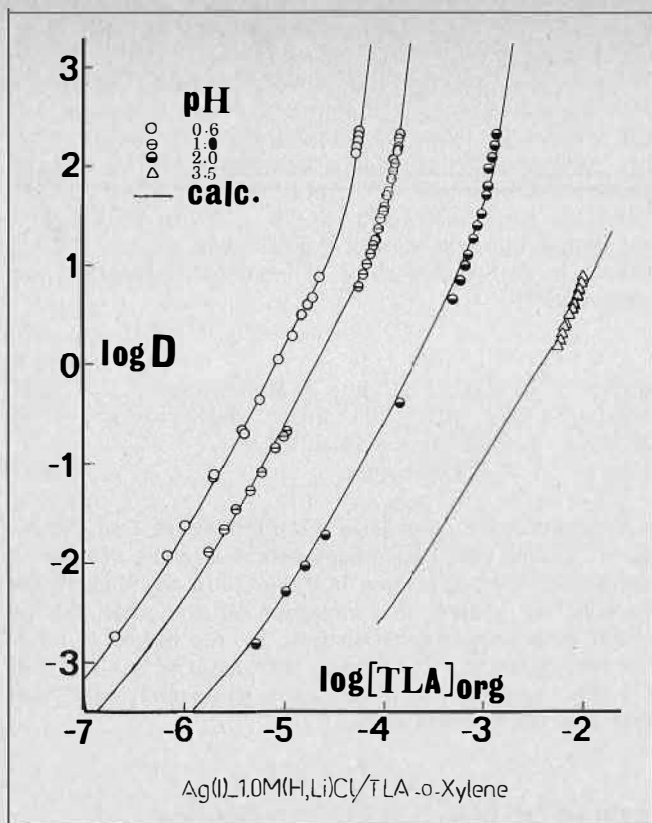


FIGURE 1. The distribution of Ag (I) in the two-phase system 1.0 M (H,Li)Cl/o-xylene as a function of the equilibrium concentration of TLA in the organic phase for various constant values of $-\log(\text{H}^+) = 0.6(\text{O})$, $1.0(\ominus)$, $2.0(\bullet)$ and $3.5(\Delta)$. The drawn lines have been calculated assuming the formation of the $(\text{H}^+)_x(\text{Ag}^+)_y(\text{TLA})_z(\text{Cl}^-)_s$ species with the equilibrium constants given in Table 1, Model 1.

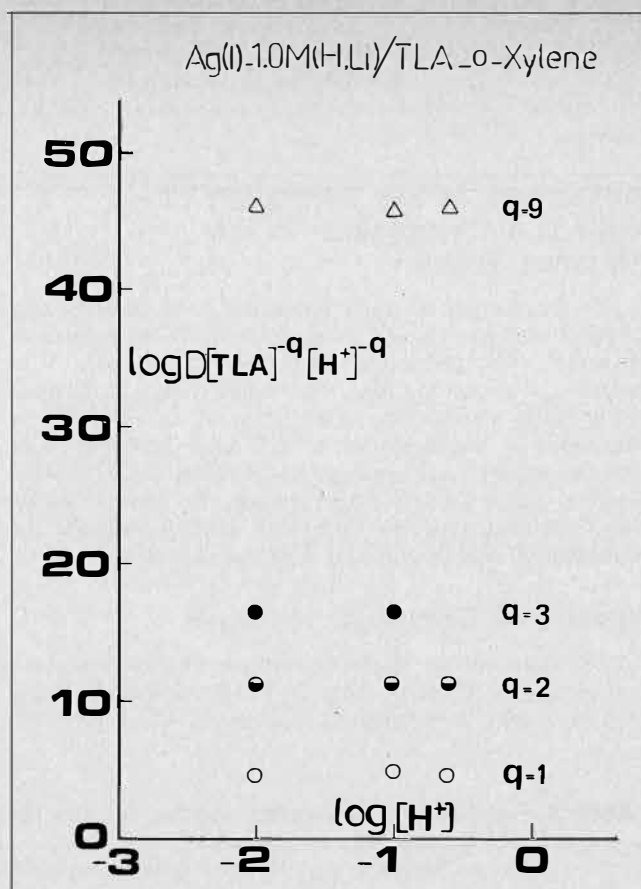


FIGURE 2. The distribution of Ag(I) in the two-phase system 1.0 M (Li,H)Cl/o-xylene for selected set of points in Figure 1 which lie on lines with various constant values of slope $q = 1(\text{O})$, $2(\ominus)$, $3(\bullet)$ and $9(\Delta)$.

In DISTR one may also minimize the following additional error-square sums:

$$U = \sum_1^{N_p} (D_{\text{exp}} D_{\text{calc}}^{-1} - 1)^2 \text{ and } U = \sum_1^{N_p} (D_{\text{calc}} D_{\text{exp}}^{-1} - 1)^2$$

For more detailed informations on the computer program the reader is referred to References 6, 8 and 9.

Results

The data for the distribution of Ag(I) in the two-phase system 1.0 M (H,Li) Cl/TLA were recorded as: $-\log(\text{H}^+)$, $\log D_{\text{exp}}$, and $\log(\text{TLA})_{\text{org}}$. $(\text{TLA})_{\text{org}}$ was calculated from the initial total concentration, C_{TLA} , assuming the formation of (TLAHCl) , $(\text{TLAHCl})_3$ and $(\text{TLAHCl})_{50}$ in the organic phase with the equilibrium constants given by Hogfeldt et al.²⁴. C_{Ag} was less than 2.5×10^{-4} M.

The complete table of distribution data, comprising 234 points is available from the authors. Typical of this data are the following excerpts:

$-\log[\text{H}^+]$	$\log D_{\text{exp}}$	$\log[\text{TLA}]_{\text{org}}$
0.600	-0.688	-5.404
1.000	-1.950	-5.766
2.036	1.798	-2.930
3.906	-0.934	-2.712
3.251	2.019	-1.707
7.218	-1.205	-0.782

The distribution of Ag(I) was studied as a function of C_{TLA} for different constant values of $\log(\text{H}^+)$ as well as a

function of $\log(\text{H}^+)$ for constant values of C_{TLA} . Figure 1 shows part of the available data given as $\log D$ versus $\log(\text{TLA})_{\text{org}}$ for various constant values of (H^+) . The plot gives distribution curves which are practically parallel for the range of TLA concentrations studied and the slope of each curve seems to vary from 1 to 3 with increasing $\log(\text{TLA})_{\text{org}}$.

This clearly indicates the formation of Ag(I)-TLA species in the organic phase which may generally be represented by the formula $(\text{H}^+)_x(\text{Ag}^+)(\text{TLA})_q(\text{Cl}^-)_x$ with $q = 1, 2$ and 3 . The sub-index x for H^+ and Cl^- indicates that the corresponding coefficients are constant but undetermined, since (H^+) and Cl^- have been kept constant during these sets of experiment. Furthermore, Figure 1 shows that for $\log(\text{TLA})_{\text{org}}$ greater than a given value, e.g. $\log(\text{TLA})_{\text{org}} > -4$ for $\text{pH}=1.0$, the distribution curves give a greater slope than 3 which thus indicate the formation of Ag(I)-TLA species in the organic phase with values of q greater than 3 (approximately 8 to 9).

A more detailed analysis of this part of the distribution curve was done using the computer and will be discussed later. In Figure 2 we plot $\log D(\text{TLA})_{\text{org}}^{-q}(\text{H}^+)^{-q}$, $q = 1, 2, 3, 9$ as a function of $\log(\text{H}^+)$ for set of points in Figure 1 which show different constant values of slope corresponding to 1, 2, 3, 9. As was discussed previously, the values of the slope in Figure 1 indicate the formation of $(\text{H}^+)_x(\text{Ag}^+)(\text{TLA})_q(\text{Cl}^-)_x$ species in the organic phase with values of $q = 1, 2, 3, 9$. The plots in Figure 2 are seen to give slopes equal to zero for the lines $\log D(\text{TLA})_{\text{org}}^{-q}(\text{H}^+)^{-q}$ versus $\log(\text{H}^+)$ for values of $q = 1, 2, 3$ and 9 . From Figures 1 and 2 we may thus draw the conclusions that

the distribution data strongly indicate the extraction of Ag(I)-TLA species with the chemical formula (BHCl)_qAgCl with q = 1, 2, 3, 9. This conclusion from graphical analysis will be used as the starting model in the computer analysis.

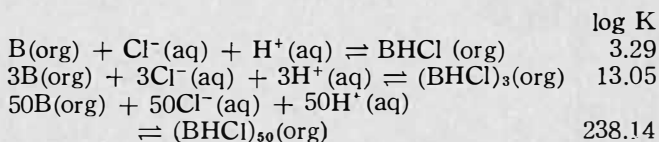
Indications of the Formation of Ag(I)-TLA Complexes in the Aqueous Phase

The distribution of Ag(I) between 1.0 M (H,Li)Cl and o-xylene was also studied using TLA in the base form as extractant. The distribution data, given in Figure 3 as logD(B)_{org}⁻¹ versus log (B)_{org} for -log(H⁺) = 6 to 7, practically fall in a single line with a slope of -1. This may be interpreted as the formation of 1:1 Ag(I)-TLA species in both the aqueous and organic phases which are (H⁺) independent within the pH range studied. As will be shown later, the results of the computer analysis indicate the formation of AgClB(org) and AgB⁺(aq) species.

Results of Computer Analysis

The results of the computer analysis of 234 points are summarized in Table 1 where the different models which have been tried are compared. The model which gives the

lowest value of U_{min} will be considered as the "best" model out of the models tried. An additional criterion of the analysis is to describe the experimental data within the experimental errors by as simple a model as possible. In this analysis we made the assumptions of the formation of the following silver(I)-chloro complexes in the aqueous phase found previously^(5,10): AgCl₂⁻ (logβ₂ = 5.34), AgCl₃²⁻ (logβ₃ = 5.65) and AgCl₄³⁻ (logβ₄ = 5.23). Furthermore we assume the formation of the following TLA(= B)-HCl species in the organic phase as reported by Högfeltd and coworkers^(3,4):



In Table 2 we summarize the different (H⁺)_p(Ag⁺)_q(TLA)_r(Cl⁻)_s species which have been included in the analysis of the different models given in Table 1. In the start of the analysis we assume the formation of the main species found from the graphical analysis, i.e. the species (1,1,1,2) (= BH⁺AgCl₂⁻), (2,1,2,3) (= (BH⁺)₂AgCl₃²⁻), (3,1,3,4) (= (BH⁺)₃AgCl₄³⁻) in the organic phase and AgB⁺ and AgB₂⁺ in the aqueous phase.

TABLE 1. Equilibrium Constants ^alogβ_{p,q,r,s} for the Formation of (H⁺)_p(Ag⁺)_q(TLA)_r(Cl⁻)_s Species.

Ag(I) - 1.0 M (Li, H)Cl/TLA-o-Xylene for various assumptions of chemical models which minimize the error-square sum				
System	U = ∑ _{i=1} ^{Np} (log D _{calc} - log D _{exp}) ² with Np = 234 points.			
Model	(H ⁺) _p (Ag ⁺) _q (TLA) _r (Cl ⁻) _s (aq)	(H ⁺) _p (Ag ⁺) _q (TLA) _r (Cl ⁻) _s (org)	U _{min}	σ(logD)
I	(0,1,1,0)8.28 ± 0.09	(0,1,1,1)6.97 ± 0.09; (1,1,1,2)10.27 ± 0.08; (1,1,2,2)14.38 ± 0.06; (2,1,2,3)17.25 ± 0.03; (3,1,4,4)25.14 ± 0.09; (9,1,9,10)51.54 ± 0.04	0.513	0.048
II	(0,1,1,0)8.53 ± 0.26	(0,1,1,1)7.18 ± 0.23; (1,1,1,2)9.75, max. 10.13 (1,1,2,2)14.46 ± 0.19; (2,1,2,3)17.43 ± 0.06 (3,1,4,4)25.40 ± 0.26	4.005	0.133
III		(0,1,1,1)5.50, max. = 5.94; (1,1,1,2)10.45 ± 0.17; (1,1,2,2)14.05 ± 0.11; (2,1,2,3)17.26 ± 0.07; (3,1,4,4)23.96, max. = 24.17; (9,1,9,10)51.64 ± 0.11	4.527	0.141
IV	(0,1,1,0)8.09 ± 0.24	(0,1,1,1)7.21 ± 0.22; (1,1,1,2)10.26; max. = 10.51 (2,1,2,3)17.38 ± 0.09; (3,1,4,4)25.10 ± 0.22; (9,1,9,10)51.52 ± 0.19	6.345	0.167
V	(0,1,1,0)9.51 ± 0.21	(0,1,1,1)7.87 ± 0.26; (1,1,1,2)10.87 ± 0.10; (1,1,2,2)15.22 ± 0.23; (3,1,4,4)26.38 ± 0.20; (9,1,9,10)51.70 ± 0.25;	10.201	0.212
VI	(0,1,1,0)8.09 ± 0.05	(1,1,1,2)10.29 ± 0.16; (1,1,2,2)14.52 ± 0.05; (2,1,2,3)17.25 ± 0.05; (3,1,4,4)24.89 ± 0.07; (9,1,9,10)51.66 ± 0.09	2.918	0.112
VII	(0,1,1,0)8.37 ± 0.14	(0,1,1,1)7.07 ± 0.13; (1,1,2,2)14.43 ± 0.092; (2,1,2,3)17.53 ± 0.03; (3,1,4,4)25.21 ± 0.14; (9,1,9,10)51.57 ± 0.08	1.391	0.078
VIII	(0,1,1,0)8.47 ± 0.02	(0,1,1,1)7.10 ± 0.06; (0,1,3,1)7.89, max. = 8.35; (1,1,1,2)10.26 ± 0.07; (1,1,2,2)14.48 ± 0.03; (2,1,2,3)17.25 ± 0.02; (3,1,4,4)25.33 ± 0.02; (9,1,9,10)51.63 ± 0.04	0.618	0.052
IX	(0,1,1,0)7.45 ± 0.11	(0,1,1,1)6.00, max. = 6.32; (1,1,2,2)14.42 ± 0.06; (1,1,1,2)10.29 ± 0.19; (2,1,2,3)17.26 ± 0.06; (9,1,9,10)51.77 ± 0.09	4.124	0.133
X	(0,1,1,0)8.04 ± 0.18 (0,1,2,0)9.51, max. = 9.72	(0,1,1,1)7.00 ± 0.08; (0,1,3,1)9.07, max. = 9.33; (1,1,1,2)10.29 ± 0.07; (1,2,2,2)14.27 ± 0.08; (2,1,2,3)17.25 ± 0.03; (3,1,4,4)25.09 ± 0.09; (9,1,9,10)51.63 ± 0.04	0.442	0.044

^aThe equilibrium constant β_{p,q,r,s} = [(H⁺)_p(Ag⁺)_q(TLA)_r(Cl⁻)_s]_i / [H⁺]_i^p [Ag⁺]_i^q [TLA]_i^r [Cl⁻]_i^s, where the sub-index i refers to the organic or aqueous phase as given in the reaction. The limits given correspond approximately to log (β ± 3σ(β)) and if σ(β) > 0.2β the maximum value log (β + 3σ) is given.

^bThe best model assumed.

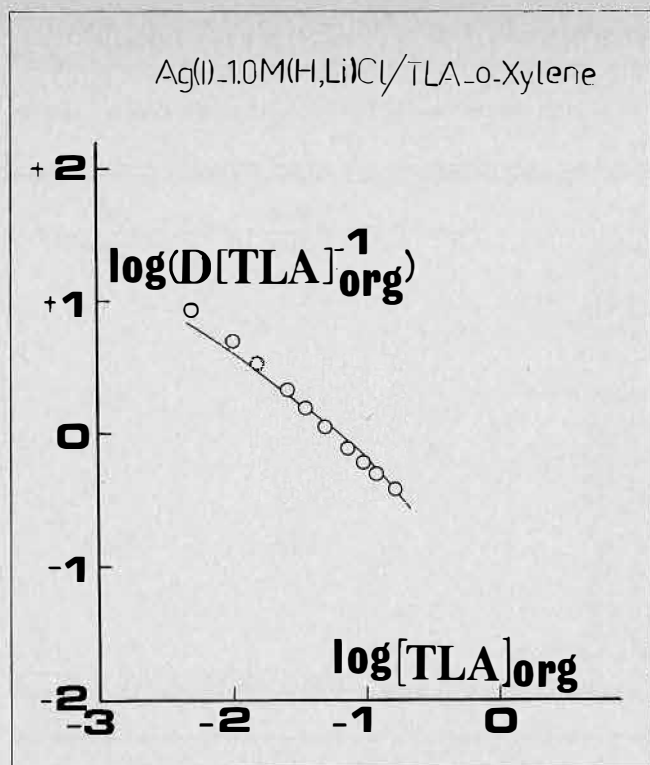


FIGURE 3. The distribution of Ag(I) in the two-phase system 1.0 M (Li,H)Cl/TLA-o-xylene for values of $-\log(\text{H}^+) = 6$ to 7. The drawn line has a slope of 1 and has been calculated assuming the formation of Ag(I)-TLA species and equilibrium constants given in Table 1, Model I.

Using the species selector available in the Letagrop program (Rurik = 17)⁹, with $F\sigma = 1.0$, i.e., only species which $\sigma(y) \leq K$ are accepted, we finally concluded the main Ag(I)-TLA species formed in the system is as given in Table 1. From Table 1 one can see that the lowest $U_{\min} (= 0.513)$ with $\sigma(\log D) = 0.048$ is found for Model I where the following species are assumed to be formed: $\text{AgB}^+(\text{aq}) (= 0,1,1,0)(\text{aq})$ and in the organic phase $\text{AgClB}(\text{org}) (= 0,1,1,1)$, $(\text{BH}^+)(\text{AgCl}_2^-)(\text{org}) (= 1,1,1,2)$, $(\text{BH}^+ \text{AgCl}_2^-) \text{B}(\text{org}) (= 1,1,2,2)$, $(\text{BH}^+)_2(\text{AgCl}_3^{2-})(= 2,1,2,3)$, $\text{B}(\text{BH}^+)_3\text{AgCl}_4^{3-}(\text{org})(= 3,1,4,4)$ and $(\text{BHCl})_8(\text{BH}^+ \text{AgCl}_2^-)(\text{org})(= 9,1,9,10)$.

Significantly bigger values of U_{\min} and $\sigma(\log D)$ were found, (cf. Models II-VII, IX), if from Model I the formation of any one species was neglected, e.g. in Model II the formation of the species $(9,1,9,10) (= \text{BHCl})_8(\text{BH}^+ \text{AgCl}_2^-)$ in the organic phase was neglected and for this model we found $U_{\min} = 4.005$ and $\sigma(\log D) = 0.133$, while neglecting the formation of $(\text{BH}^+)_2\text{AgCl}_3^{2-}(\text{org}) (= 2,1,2,3)$ in Model V it was found that $U_{\min} = 10.201$ and $\sigma(\log D) = 0.212$. Assuming the additional formation of the species $(0,1,3,1) (= \text{AgClB}_3)(\text{org})$ to Model I (cf. Model IX) gave no improvement to the error-square sum minimized, $U_{\min} = 0.618$ and $\sigma(\log D) = 0.052$, indicating no significant formation of the species $\text{AgClB}_3(\text{org})$. When to Model I the additional formation of $\text{AgB}_2^+(\text{aq})$ and $\text{AgClB}_3(\text{org})$ are assumed (Model X) we find a slight improvement of $U_{\min} (= 0.442)$ and $\sigma(\log D) (= 0.044)$. However, within the experimental errors the data are satisfactorily described by assuming the formation of the species in Model I with the equilibrium constants given in Table 3. In Figure 4 the error-function $(\log D_{\text{calc}} - \log D_{\text{exp}})$ is plotted versus $\log(\text{TLA})_{\text{org}}$ and as can be seen the error seems to be randomly distributed.

TABLE 2. Summary of the Different $(\text{H}^+)_p(\text{Ag}^+)_q(\text{B})_r(\text{Cl}^-)_s$ Species Included in the Letagrop Analysis of the Distribution Data of Ag(I) in the Two Phase System 1.0 M-(H, Li)Cl/TLA-o-xylene.

Aqueous phase	Organic phase
$(\text{AgCl}_2^-; \text{AgCl}_3^{2-}; \text{AgCl}_4^{3-})^a$ $\text{AgB}^{2+}; \text{AgB}_2^+$	$(\text{BHCl}; (\text{BHCl})_3; (\text{BHCl})_{5,9})^a$ $\text{AgClB}^b; \text{AgClB}_2; \text{AgClB}_3; \text{AgClB}_4$ $\text{BH}^+ \text{AgCl}_2^-; \text{B}(\text{BHAgCl}_2)^b; \text{B}_2(\text{BHAgCl}_2);$ $\text{B}_3(\text{BHAgCl}_2); (\text{BH}^+)_2\text{AgCl}_3^{2-b};$ $\text{B}(\text{BH})_2\text{AgCl}_3;$ $\text{B}_2(\text{BH})_2\text{AgCl}_3; (\text{BH}^+)_3\text{AgCl}_4^{3-b};$ $\text{B}(\text{BH})_3\text{AgCl}_4^b;$ $\text{B}_2(\text{BH})_3\text{AgCl}_4; (\text{BHCl})_4\text{BAgCl};$ $(\text{BHCl})_5\text{AgCl};$ $(\text{BHCl})_6\text{AgCl}; (\text{BHCl})_8\text{AgCl}; (\text{BHCl})_9\text{AgCl}^b;$ $(\text{BHCl})_{10}\text{AgCl}; (\text{BHCl})_{5,9}\text{AgCl}.$

^aThe value of the equilibrium constant (cf. Ref. 5,10 and 3,4) is not varied during the computer calculations.

^bAg(I)-TLA species assumed to be formed with equilibrium constants given in Table 3 which give the best fit to the distribution data (cf. Table 1, model I).

TABLE 3. The Extraction of Ag(I) by Trilaurylamine into o-xylene from 1.0 M (Li, H)Cl Medium.

Equilibrium constants for the formation of set of Ag(I)-HS-TLA-Cl⁻ species which were found to give the minimum error-square sum

$$U = \sum_1^{234} (\log D_{\text{calc}} - \log D_{\text{exp}})^2$$

$\text{Ag}^+ + \text{B}(\text{org}) \rightleftharpoons \text{AgB}^+(\text{aq})$	8.282 ± 0.106	$\log(\beta + 3\sigma(\beta))$
$\text{Ag}^+ + \text{H}^+ + \text{B}(\text{org}) + 2 \text{Cl}^- \rightleftharpoons \text{BH}^+ \text{AgCl}_2^-(\text{org})$	10.273 ± 0.083	
$\text{Ag}^+ + \text{H}^+ + 2 \text{B}(\text{org}) + 2 \text{Cl}^- \rightleftharpoons \text{B}(\text{BH}^+ \text{AgCl}_2^-)(\text{org})$	14.375 ± 0.069	
$\text{Ag}^+ + \text{B}(\text{org}) + \text{Cl}^- \rightleftharpoons \text{AgClB}(\text{org})$	6.964 ± 0.111	
$\text{Ag}^+ + 2 \text{H}^+ + 2 \text{B}(\text{org}) + 3 \text{Cl}^- \rightleftharpoons (\text{BH}^+)_2\text{AgCl}_3^{2-}(\text{org})$	17.252 ± 0.027	
$\text{Ag}^+ + 3 \text{H}^+ + 4 \text{B}(\text{org}) + 4 \text{Cl}^- \rightleftharpoons \text{B}(\text{BH}^+)_3\text{AgCl}_4^{3-}(\text{org})$	25.145 ± 0.102	
$\text{Ag}^+ + 9 \text{H}^+ + 9 \text{B}(\text{org}) + 10 \text{Cl}^- \rightleftharpoons (\text{BHCl})_8(\text{BH}^+ \text{AgCl}_2^-)(\text{org})$	51.636 ± 0.044	

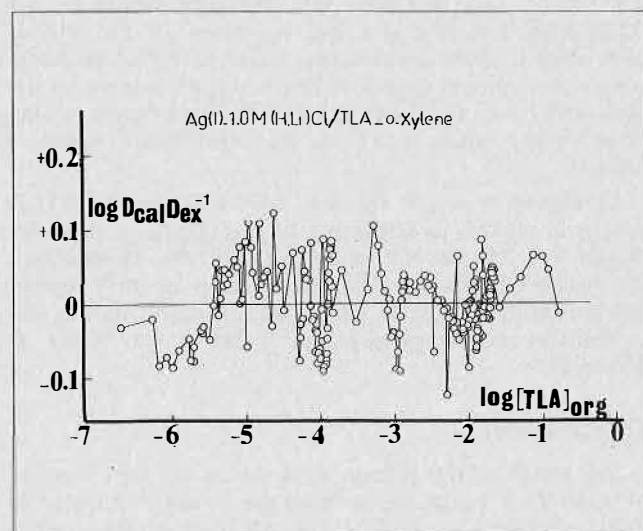


FIGURE 4. The error $(\log D_{\text{calc}} - \log D_{\text{exp}})$ as a function of $\log(\text{TLA})_{\text{org}}$ for the two-phase system Ag(I)-1.0M (H,Li)Cl/TLA-o-xylene assuming the formation of $(\text{H}^+)_p(\text{Ag}^+)_q(\text{TLA})_r(\text{Cl}^-)_s$ species and equilibrium constants which minimized the

error-square sum $U = \sum_1^{234} (\log D_{\text{calc}} - \log D_{\text{exp}})^2$ (cf. Table 1, Model I).

TABLE 4. The Equilibrium Constants ${}^a\log\beta_{pqrs}$ for the Formation of $(H^+)_p(Ag^+)_q(TLA)_r(Cl^-)_s$ Species.

System. Ag(I)—1.0 M (H,Li)Cl/trilaurylamine (= TLA)-o-xylene which minimize different error-square sums $U = \sum_1^{234} (fel(i))^2$. The computer analysis is based on the assumptions of the formation of the species given in Table 3 (cf. Table 1 Model I)

Minimized error fel(i)	(p,q,r,s)log β_{pqrs} Aqueous Phase	Organic Phase	U _{min}	$\sigma(\gamma)$
$\log(D_{calc}D_{exp}^{-1})$	(0,1,1,0)8.28 ± 0.09	(0,1,1,1)6.97 ± 0.09 (1,1,1,2)10.27 ± 0.08 (1,1,2,2)14.38 ± 0.06 (2,1,2,3)17.25 ± 0.03 (3,1,4,4)25.14 ± 0.09 (9,1,9,10)51.64 ± 0.04	0.513	0.048
$D_{exp}D_{calc}^{-1} - 1$	(0,1,1,0)8.28 ± 0.09	(0,1,1,1)6.99 ± 0.08 (1,1,1,2)10.28 ± 0.08 (1,1,2,2)14.38 ± 0.06 (2,1,2,3)17.27 ± 0.03 (3,1,4,4)25.14 ± 0.09 (9,1,9,10)51.65 ± 0.05	2.672	0.109
$D_{calc}D_{exp}^{-1} - 1$	(0,1,1,0)8.27 ± 0.09	(0,1,1,1)6.95 ± 0.09 (1,1,1,2)10.27 ± 0.08 (1,1,2,2)14.37 ± 0.05 (2,1,2,3)17.24 ± 0.03 (3,1,4,4)25.13 ± 0.09 (9,1,9,10)51.63 ± 0.04	2.680	0.109

${}^a\beta_{pqrs} = [(H^+)_p(Ag^+)_q(TLA)_r(Cl^-)_s][H^+]^{-p}[Ag^+]^{-q}[TLA]_{org}^{-r}[Cl^-]^{-s}$, where the sub-index t indicates the phase referred to in the reaction. The limits given correspond approximately to $\log(\beta \pm 3\sigma(\beta))$.

In Table 4 we compare the results of Letagrop calculations assuming the formation of $(H^+)_p(Ag^+)_q(TLA)_r(Cl^-)_s$ species in Table 1, Model I and minimizing the following three different types of error-square sum:

$$U_1 = \sum_1^{N_p} (\log D_{calc} - \log D_{exp})^2$$

$$U_2 = \sum_1^{N_p} (D_{exp}D_{calc}^{-1} - 1)^2; \text{ and}$$

$$U_3 = \sum_1^{N_p} (D_{calc}D_{exp}^{-1} - 1)^2$$

The results show that practically the same values for the equilibrium constants for the formation of the species were found. Since minimizing different types of error-square sum means giving different weight factors to the data, the result thus indicate that the assumption of the same weight factor ($w=1$) to the experimental points is justified.

In Figures 5 and 6 the distribution of the Ag(I)-TLA species in mole% as a function of $\log(TLA)_{org}$ is given for $-\log(H^+) = 2.0$ and 3.30 and $C_{Ag} = 10^{-4}$ M. These curves are calculated using the HALTAFALL program⁽¹²⁾ assuming the formation of $(H^+)_p(Ag^+)_q(TLA)_r(Cl^-)_s$ species and equilibrium constants given in Table 3 (cf. Table 1, Model I).

Discussion

The results of this present work thus show the formation of Ag(I)-TLA complexes in both the aqueous and organic phases. Indications for the formation of Hg(II)-trioctylamine(TOA) complexes in chloride aqueous solution were reported by Caban and Chapman.⁽¹¹⁾ Our results that Ag(I) are extracted as different Ag(I)-TLA complexes are surprising but may in part be understood considering that, under the extraction conditions studied, the anionic species $AgCl_2^-$, $AgCl_3^{2-}$ and $AgCl_4^{3-}$ are expected to be present in the solution in comparable concentrations, namely for

$(Cl^-) = 1$ M we have the ratio $(AgCl_2^-):(AgCl_3^{2-}):(AgCl_4^{3-}) = \beta_2:\beta_3:\beta_4 = 1:2:0.8$. The conclusion for the formation of the species $(BHCl)_s(BH^+AgCl_2^-)$ should, in this stage, only be considered as a formal description for the formation of Ag(I)-TLA complexes with consumption $n_{Ag} n_{TLA}$ greater than 4. The present work shows the need of a detailed knowledge of the two-phase distribution equilibria of the extractant used in order to obtain a deeper understanding of the metal extraction equilibria involved.

Acknowledgments

The authors gratefully acknowledge the financial support by the Swedish National Science Research Council, the Swedish Board for Technical Development and Axel Jonsson Stiftelsen. Dr. Mamoun Muhammed has kindly supplied the purified TLA. The authors thank Prof. Ingemar Grenthe for valuable discussions.

SYMBOLS AND ABBREVIATIONS

- TLA or B = trilaurylamine (= tri-n-dodecylamine), $(n-C_{12}H_{25})_3N$
 = equilibrium concentration in the aqueous phase
 = equilibrium concentration in the organic phase
 n_i = number of moles of reagent i
 V_{aq} = volume of aqueous phase
 V_{org} = volume of organic phase
 V_t = $V_{org}V_{aq}^{-1}$, volume ratio of organic phase to aqueous phase
 C_i = $n_iV_{aq}^{-1}$, initial total concentration of reagent i in the two-phase system with respect to the aqueous phase in moles/l
 I_{aq}, I_{org} = — activity in cpm of Ag-110m in the aqueous and organic phase corrected for background, difference in sample volume and crystal efficiency in the two detectors used.
 D_{exp} = $(\sum [Ag(I)]_{org}) / (\sum [Ag(I)]_{aq}) = I_{org}I_{aq}^{-1}$, experimental net distribution ratio of Ag(I)
 D_{calc} = net distribution ratio of Ag(I) calculated for given extraction conditions, assuming the formation of the set of species $(H^+)_p(Ag^+)_qB_r(Cl^-)_s$ and $(H^+)_k(Ag^+)_lB_m(Cl^-)_n$ in the organic and aqueous phase with a given set of equilibrium constants K_{pqrs}^{org} and K_{klmn}^{aq} (cf. equations (1) and (2))

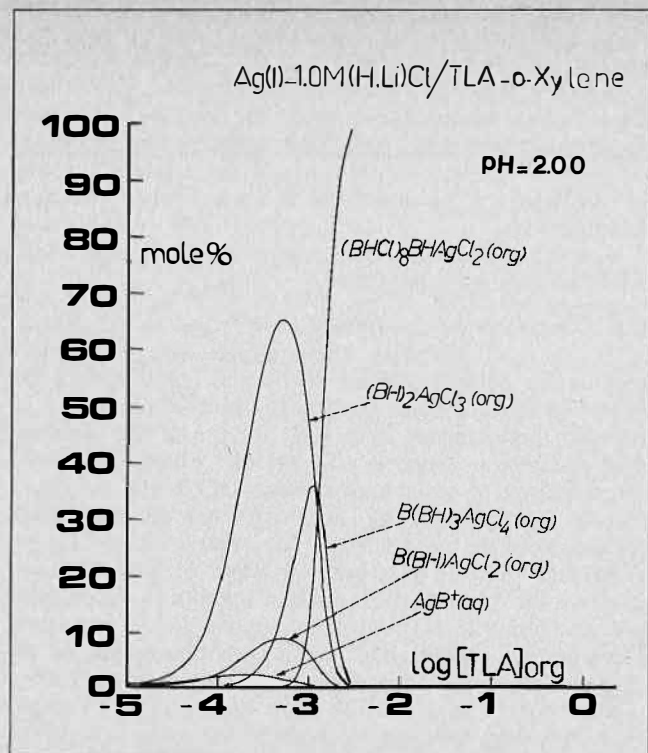


FIGURE 5. The distribution of Ag(I)-TLA species in mole % as a function of $\log[TLA]_{org}$ in the two-phase system Ag(I)-1.0M (M,Li)Cl/TLA-o-xylene for pH=2.0 and $C_{Ag} = 10^{-4}$ M. The curves have been calculated using the HALTAFALL program¹² assuming the formation of Ag(I)-TLA-HCl species and equilibrium constants given in Table 1, Model I.

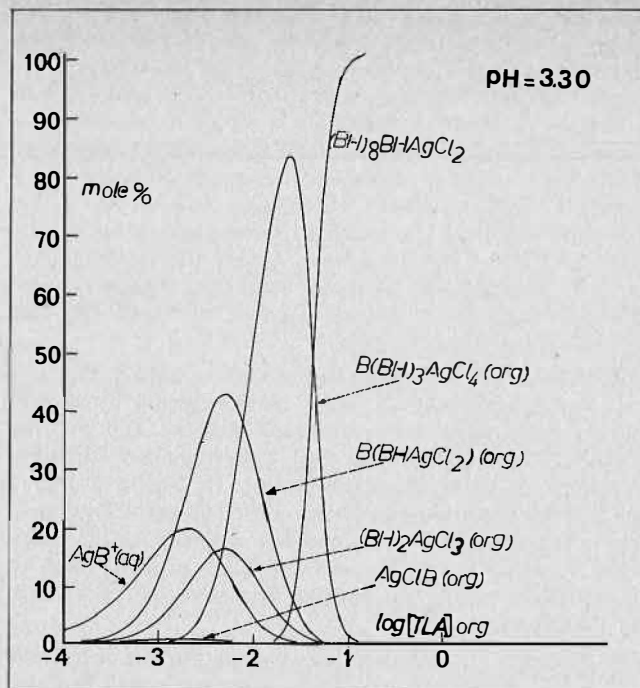


FIGURE 6. The distribution of Ag(I)-TLA species in the system Ag(I)-1.0 M (H,Li)Cl/TLA-o-xylene for pH = 3.3 and $C_{Ag} = 10^{-4}$ M. The curves have been calculated assuming the formation of $(H^+)_n(Ag^+)_m(TLA)_n(Cl^-)_s$ species with the equilibrium constants given in Table 1, Model I.

U_{min} = minimised error-square sum, e.g. $\sum_1^{N_p} (\log(D_{ca}) - D_{exp}^{-1})^2$ for val = 1 in DISTR⁶, where N_p represents the number of experimental points.
 $\sigma(y)$ = standard deviation of the minimized error y , e.g. $y = \log D$ for val = 1 (cf. Ref.)⁸.

REFERENCES

- (1) Marcus, Y. and Kertes, A.S., Ion Exchange and Solvent Extraction of Metal Complexes, Wiley-Interscience 1969.
- (2) Marcus, Y., Kertes, A.S. and Yanir, E., Equilibrium Constants of Liquid-Liquid Distribution Reactions, International Union of Pure and Applied Chemistry, 1974, Butterworths, London.
- (3) Högfeltd, E., Proceedings ISEC Jerusalem, 1968, 57.
- (4) Högfeltd, E. and Tavares, M. de Jesus, Trans. Roy. Inst. Technol. 1964, No. 227.
- (5) Sillén, L.G. and Martell, A.E., Stability Constants of Metal-ion Complexes 1964, Spec. Publ. No. 17, The Chemical Society, London.
- (6) Liem, D.H., Acta Chem. Scand. 1971, 25, 1521.
- (7) Rydberg, J., Acta Chem. Scand. 1969, 23, 647; Reinhardt, H. and Rydberg, J., Acta Chem. Scand. 1969, 23, 2781.
- (8) Ingri, N. and Sillén, L.G., Ark. Kemi 1964, 23, 97.
- (9) Sillén, L.G. and Warnqvist, B., Ark. Kemi 1969, 31, 315, 341; Arnek, R., Sillén, L.G. and Wahlberg, O., Ark. Kemi 1969, 31, 353.
- (10) Forbes, G.S. and Cole, H.I., J. Am. Chem. Soc. 1921, 43, 1154; Kratochvil, J., Tezah, B. and Vouh, V.B., Archiv Kem 1954, 26, 191.
- (11) Caban, R. and Chapman, T.W., AIChE Journal 1972, Vol. 18, No. 5, 904.
- (12) Ingri, N., Kakolowicz, W., Sillén, L.G. and Warnqvist, B., Talanta 1967, 14, 1261.

DISCUSSION

J.E. Gai: In view of the low solubility of Ag(I) in aqueous solutions, it is hardly likely that the data could be of use in any industrial process.

I always have an uneasy feeling with computer analyses which may or may not have a bearing on actual chemical reality. These analyses are limited to certain definite species according to the choice of the analyst, and cannot include species which he may have overlooked. Are there any confirmatory measurements by an independent method, for the existence of the proposed species?

D.H. Liem: The solubility of Ag(I) is dependent on the chloride concentration in the solution due to the formation of the $AgCl_n^{-(n-1)}$ species with $n = 2, 3$ and 4. Assuming the equilibrium constants given in the paper for the formation of $AgCl_2^-$, $AgCl_3^{2-}$ and $AgCl_4^{3-}$ and the solubility product for $AgCl(s)$ $K_{so} = 10^{-9.74} M^2$ (cf. Ref. 5), we may, e.g., calculate for 1M Cl^- medium the solubility of Ag(I) to be $C_{Ag} = 0.45$ mM = 48.2 mg/l. The use of TLA for the extraction of Ag(I) may thus be of practical use in the case where silver is found as by-product or impurity in a process.

The chemical model, assumed to be the one which gives the best description to the experimental data, was chosen from a number of models which are considered as reasonable from a chemical point of view. As was shown in the paper, the formation of the main species was also indicated from the graphical analysis of part of the data. One of the advantages of computer analysis is the possibility to compare objectively which of several reasonable chemical models gives the best description, i.e. the lowest minimized error-square sum, to the experimental data. To our knowledge there is yet no other study reported on the extraction of Ag(I) by TLA from chloride medium.

A.S. Kertes: I hope you will not be surprised for my expressing scepticism concerning the reality of aqueous phase complexes such as AgCl_3^{2-} and AgCl_4^{3-} in view of their stability constants being so close to that of AgCl_2 . However, to build up a set of mass-action law equilibria in order to explain the extraction behaviour of silver from chloride media on these questionable complexes, I think, is rather speculative. Could you please estimate from your log values of the organic phase species $(\text{BH}^+)_2\text{AgCl}_3^{2-}$, $\text{B}(\text{BH}^+)_3\text{AgCl}_4^{3-}$ and $(\text{BHCl})_8(\text{BH}^+\text{AgCl}_2^-)$ the contribution of these, somewhat strange-stoichiometry complexes to the total silver extracted into the triaurylamine/o-xylene phase?

D.H. Liem: The formation of the species AgCl_2^- , AgCl_3^{2-} and AgCl_4^{3-} have been reported by several authors from work using different methods and may be considered as unquestionable. (Cf. Reference 5, Stability Constants of Metal Ion Complexes). In Figure 5 and 6 one can see from the calculated curves the contribution in Ag(I) extracted of the species $(\text{BH}^+)_2\text{AgCl}_3^{2-}(\text{org})$, $\text{B}(\text{BH}^+)_3\text{AgCl}_4^{3-}(\text{org})$ and $(\text{BHCl})_8(\text{BH}^+\text{AgCl}_2^-)(\text{org})$ to be dependent on the pH and the concentration of TLA in the organic phase.

V.S. Shmidt: The method of calculation of constants which is applied in your work may be valid only at conditions assuring the constancy of these constants in all the range of component concentrations studied. As the dielectric constant of organic media is much changed

with changing of amine salt concentration, the assumption about the constancy of constants is probably not fully correct. This fact causes much doubt about the validity of the applied method. The calculations by the method may result in conclusions about formation of complexes which do not exist in reality. This result must be asserted by an independent method. Have you any independent evidence of formation of the described complexes other than type calculations?

In which phase was the constant ionic strength maintained in your experiments?

D.H. Liem: As was mentioned in the paper in the analysis of the data, these effects were taken into account by considering the distribution equilibria of the TLA-HCl species which have been reported previously by Högfeldt and Taxares from EMI Studies of the same extraction system. Since in the present studies the initial concentration of silver ion has been kept below 10^{-4}M , it may be expected that Ag^+ ions extracted will not significantly affect the properties of the organic phase. To my knowledge there is at present no other method available to study the formation of Ag-7LA species in the organic phase at tracer level of silver as was studied in our work. The proposed model gives the simplest description of the data available within the experimental errors expected.

The activity factor of the ionic species in the aqueous phase was kept constant by keeping the ionic strength of the aqueous solution constant at 1.0 M (Li, HCl).

ORGANIC REAGENTS

Zolon Red as an Extracting Reagent

A. N. Patel and A. M. Qureshi,
Department of Chemistry,
University of Nigeria,
Nsukka, Nigeria

ABSTRACT

Zolon red, an organic dye, acidic in nature, which exists in enolic form, forms a deep blue silver compound with silver ion in which H^+ ion of the hydroxyl group in zolon red is replaced by Ag^+ ion. A possible use of the reagent is demonstrated for recovery of silver from silver chloride laboratory waste.

ZOLON RED, an organic dye, forms coloured precipitates with silver, gold, mercuric and cuprous ions,^(1,3) but no work has been attempted on zolon red for its possible use as a solvent extraction reagent.

The blue dye, which is given the name of zolon blue (Structure I, Figure 1) is a keto form of the reaction product of 3-methyl-1-phenylpyrazol-5-one and glutamic aldehyde whereas zolon red (Structure II) is an enol form of the same product as shown by infrared spectra and elemental analysis. Zolon red had IR adsorption band at 3350 cm^{-1} for $-\text{OH}$ stretching frequency whereas zolon blue had no $-\text{OH}$ band in its infrared spectrum. Further, it was also observed that the dilute solution of the blue dye changed to red on long standing indicating slow conversion of the keto form (structure I) to the enol form (Structure II). Also zolon red was observed to exist in dimeric form

in methanol, perhaps through hydrogen bonding as indicated by its molecular weight determined in methanol. Zolon red's molecular weight was found to be 820.20 which is twice that calculated from the Structure II.

Zolon red (HZR) is a weak acid with a single dissociable proton. It is sparingly soluble in water but dissolves in most organic solvents. The saturated ethanolic solution of 10^{-3} M concentration of HZR of orange colour gave coloured precipitates with Ag^+ (deep blue), Au^{+++} (red purple), Pd^{++} (purple), Hg^+ (red), Hg^{++} (red) and Cu^+ (deep blue).

Aqueous solution of silver nitrate in the presence of sodium acetate buffer forms a deep blue silver compound with HZR in the ratio of 1:1. Quantitative analysis of dry solid silver zolon red (AgZR) confirmed the 1:1 ratio of Ag^+ and ZR^- ions. The quantitative precipitation of Ag^+ ions from aqueous solutions of $10^{-3} - 10^{-2}\text{ M}$ silver nitrate was obtained in the presence of sodium acetate buffer using 10^{-3} M ethanolic solution of HZR. This method was successfully tried for gravimetric estimation of silver within 0.35% limit with samples of low silver concentration.

The infrared spectra of solid HZR and AgZR in nujol were identical except that HZR had an absorption band at 3350 cm^{-1} due to $-\text{OH}$ stretching frequency which disappeared in the case of AgZR signifying replacement of the hydroxyl hydrogen in HZR by Ag^+ . The ethanolic solutions of both compounds showed a strong maximum absorption at 510 nm further supporting the formation of AgZR by ion association.

TABLE 1. Distribution of Ag Ions Between 10^{-3} M HZR in Benzyl Alcohol and Aqueous Silver Nitrate Solutions.

Initial conc. of Ag^+ ions in aqueous phase, M	pH of aq. phase	Volume phase ratio of org.: aq.	Distribution Coefficient $D = [\text{Ag}^+]_{\text{org.}}/[\text{Ag}^+]_{\text{aq.}}$
0.10	5.00	1:1	5.42
0.10	6.00	1:1	8.57
0.10	7.00	1:1	11.50
0.10	7.50	1:1	19.50
0.15	7.00	1:1	21.85
0.20	7.00	1:1	21.50
0.15	7.00	0.6:1	16.68
0.15	7.00	1.2:1	31.89

The distribution data determined for extraction of silver from aqueous solutions of silver nitrate with saturated solution of HZR in benzyl alcohol are summarised in Table 1.

The distribution coefficient increases with increasing Ag^+ ion concentration in the aqueous phase up to a limit where HZR in the organic phase is used up completely in the formation of AgZR . The distribution coefficient increased at higher pH values. This trend is obvious in view of the fact that H^+ ions liberated from HZR are removed easily by a buffer whereby the formation of AgZR is favoured. The volume phase ratio also affects the distribution coefficient.

AgZR is soluble in acids and aqueous cyanide solution. However, the HZR regenerated is destroyed in acids whereas it remains stable in aqueous cyanide solution, silver forming the cyanocomplex according to



Thus, silver can be recovered quantitatively as the cyanocomplex by stripping the organic phase with aqueous cyanide solution. The regenerated HZR remains in the organic phase and can be subsequently reused for further extraction, though its extracting power is reduced by repeated regeneration. The method, successfully applied for recovery of silver from silver chloride residue (laboratory waste), involves first dissolving silver chloride residue in dilute ammonia solution, followed by equilibration with 10^{-3} M HZR in benzyl alcohol until the aqueous phase gives a negative test for Ag^+ ions. The extract organic phase is then stripped with 0.2M sodium cyanide solution. The aqueous phase containing a cyanocomplex of silver is evaporated with 5M HNO_3 and the residue after dissolving

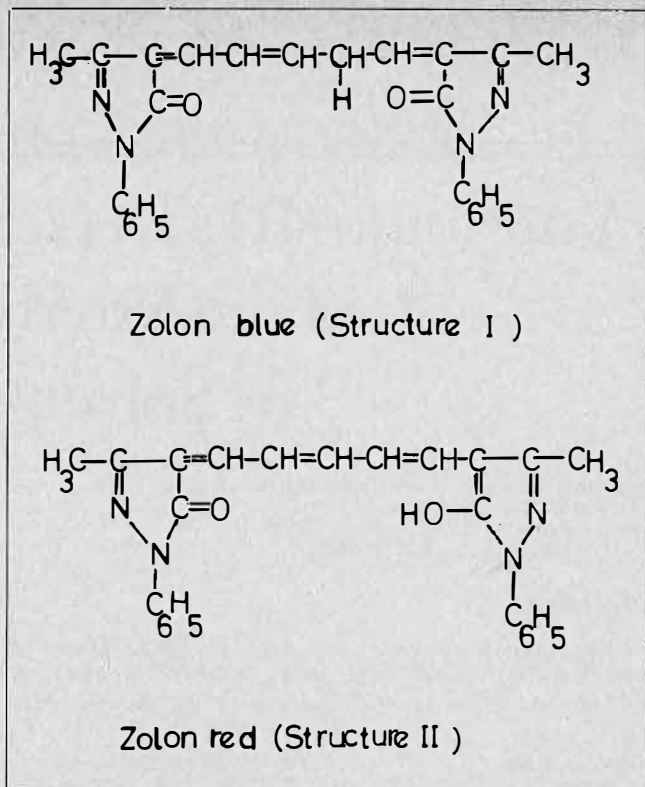


FIGURE 1. Structures of Zolon Blue and Red.

in water is treated with a saturated solution of sodium carbonate. Silver carbonate so formed is separated by filtration, washed well with water and dissolved in 5M HNO_3 . The solution is concentrated by evaporation and, on cooling, crystals of silver nitrate are separated. The organic phase containing regenerated HZR can be reused. It has also been observed that the presence of nickel, lead, zinc, tin, antimony and copper(II) have no significant effect on the distribution coefficient of silver. The effects of gold and copper (I) ions, which tend to depress the distribution coefficient of silver, are under study.

REFERENCES

- (1) Ebstein, J., Anal. Chem. 1947, 19, 272.
- (2) Kruse, J.M. and Million, M.G., Anal. Chem. 1953, 25, 1188.
- (3) Gehauf, B. and Goldenson, J., Anal. Chem. 1955, 27, 420.

Study of the Complex Formation of Ytterbium (III)-Di (2-Ethylhexyl) Phosphoric Acid and Ytterbium (III)-Nitrate by Solvent Extraction

Salvador Alegret^a, Manuel Aguilar^b and D. Hay Liem^c,
Department of Inorganic Chemistry,
Royal Institute of Technology (KTH)
S-100 44 Stockholm 70, Sweden.

ABSTRACT

The complex formation between ytterbium(III) and di(2-ethylhexyl) phosphoric acid (HDEHP) (= HA) or nitrate ions in the two-phase system X M (H, Na) (NO₃,

ClO₄)/HDEHP-toluene (X = 0.10 or 1.0) has been studied from the distribution of Yb(III) between the two phases as a function of the concentration of HDEHP in the organic phase, C_{HDEHP}, and of the concentration of NO₃⁻ in the aqueous phase as well as of -log(H⁺). The distribution data have been analyzed graphically as well as numerically using the computer program LETAGROP-DISTR. The results of the analysis show the formation of the following ytterbium(III) species:

Aqueous phase	Equilibrium reaction	log (-K ± 3σ)
0.10 M (H, Na)ClO ₄	Yb(III) + 3H ₂ A ₂ (org) ⇌ YbA ₃ (HA) ₃ (org) + 3H ⁺	3.119 ± 0.036
	Yb(III) + 5/2 H ₂ A ₂ (org) ⇌ YbA ₃ (HA) ₂ (org) + 3H ⁺	1.357 ± 0.107
1.00 M (H, Na)ClO ₄	Yb(III) + 3H ₂ A ₂ (org) ⇌ YbA ₃ (HA) ₂ (org) + 3H ⁺	2.826 ± 0.063
	Yb(III) + 5/2 H ₂ A ₂ (org) ⇌ YbA ₃ (HA) ₂ (org) + 3H ⁺	1.008 (log (K + 3σ) = 1.246)
0.10 M (H, Na) NO ₃	Yb(III) + 3H ₂ A ₂ (org) ⇌ YbA ₃ (HA) ₃ (org) + 3H ⁺	3.209 ± 0.055
	Yb(III) + 5/2 H ₂ A ₂ (org) ⇌ YbA ₃ (HA) ₂ (org) + 3H ⁺	1.252 (log (K + 3σ) = 1.481)
0.10 M H(NO ₃ , ClO ₄)	Yb(III) + NO ₃ ⁻ ⇌ YbNO ₃ ²⁺	0.45 ± 0.07
1.00 M (H, Na) (NO ₃ , ClO ₄)	Yb(III) + NO ₃ ⁻ ⇌ YbNO ₃ ²⁺	- 0.17 ± 0.09

Introduction

NUMEROUS STUDIES have been reported⁽¹⁻³⁾ on the use of di(2-ethylhexyl) phosphoric acid, HDEHP (= HA), for the extraction and fractionation of metals in general and lanthanoid/actinoid elements in particular. The great interest in the use of HDEHP for metal extraction is in part because HDEHP can function as a liquid ion exchanger and is found to be effective even at low pH regions. Using di(2-ethylhexyl) phosphoric acid as extractant, it has been shown that metal complex formation in both the organic and aqueous phases can successfully be studied.⁽⁴⁾ However, a detailed equilibrium analysis of the metal extraction processes requires preliminary studies of the distribution of HDEHP itself in the two-phases system studied, since HDEHP is found to form dimers and even higher aggregates in nonpolar solvents. In a previous paper⁽⁵⁾ we reported studies on the extraction of europium(III) by HDEHP from 0.10 M (H,Na)ClO₄ into toluene, and found that europium(III) was mainly extracted as the species EuA₃(HA)₃(org). This conclusion is in agreement with the results found by other authors.⁽⁵⁾ However, the formation of other species MA_N(HA)_x with values of x < N (= ionic charge of metal ion M) have also been reported.^(4,6) In this present work we report the

extraction of ytterbium(III) by HDEHP into toluene from X M (Na,H)ClO₄ or (Na,H)(NO₃,ClO₄), with X = 0.10 or 1.00. The studies are part of a series of investigations on the use of dialkyl-phosphoric acid as extractant for lanthanoid and actinoid elements as well as for non-nuclear metals. The main purpose of the study is to determine, with a higher degree of accuracy than is now reported, which ytterbium species are formed as well as the equilibrium constant for the formation of these ytterbium species in the organic and aqueous phases. For this purpose a preliminary determination has been made on the distribution, dimerization and dissociation equilibria of di(2-ethylhexyl)phosphoric acid in the two-phase system toluene/0.10 M (Na,H)ClO₄ (cf. Ref. 7). Furthermore, a detailed analysis of the data is made using the computer program LETAGROP-DISTR.⁽⁸⁾

Experimental

Reagents

HDEHP, di(2-ethylhexyl)phosphoric acid, (C₈H₁₇O)₂P(O)H, Albright and Wilson, was purified as described previously.⁽⁷⁾ NaClO₄, HClO₄ and toluene were of *pro analysis* quality (Merck, Darmstadt). They were prepared and purified as described previously.⁽⁷⁾ NaNO₃ (Merck, *pro analysis*) was twice recrystallized from double-distilled water and dried at 120°C. HNO₃, (Merck, p.a.) was used without further purification. The radioactive Yb-169 was obtained in the form of ¹⁶⁹YbCl₃ in 0.1 M HCl solution with less than 1% ¹⁷⁵YbCl₃ from the Radiochemical Center, Amersham, England. Solutions of ¹⁶⁹Yb(III) in 0.1 M, 1.0 M HClO₄ or 0.1 M HNO₃ were prepared by evaporat-

^aPresent address: Departamento de Química Analítica, Facultad de Ciencias, Universidad Autónoma de Barcelona, Bellaterra (Barcelona), Spain.

^bPresent address: Departamento de Química Analítica, Facultad de Ciencias, Universidad de Bilbao, Apartado 644, Bilbao, Spain.

^cTo whom all correspondence should be addressed.

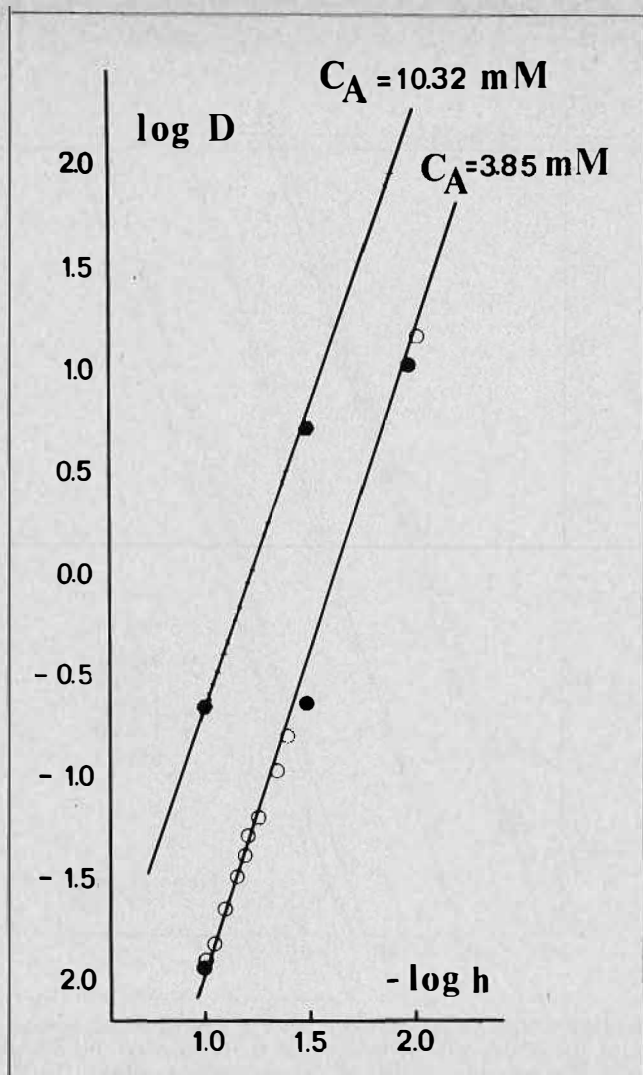


FIGURE 2. The distribution of Yb(III) between HDEHP-toluene and 0.10 M (Na,H) ClO₄ as a function of $-\log h$ for two constant values of $C_A = 3.85 \times 10^{-3}$ M (O, ●) and 10.32×10^{-3} M. The curves have been calculated assuming the formation of Yb(III)-HDEHP species with the equilibrium constants given in Tables 3 and 2, Model III.

K_{pqrs}^{org} , K_{lmno}^{aq} and other experimental parameters such as the concentrations of the chemical components chosen. In the DISTR program one may, e.g., minimize the following error-square sums:

$$U_1 = \sum_1^{N_p} (\log(D_{calc} D_{exp}^{-1}))^2; U_2 = \sum_1^{N_p} ((D_{exp} D_{calc}^{-1}) - 1)^2$$

$$\text{and } U_3 = \sum_1^{N_p} ((D_{calc} D_{exp}^{-1}) - 1)^2,$$

where N_p represents the number of experimental points used for the calculation. The dominant species in the system and their constants of formation may usually be found from graphical analysis. These values can be used as starting values in the computer analysis of the data. During the computer calculations we assume the formation of the species HA(org), H₂A₂(org), HA(aq), A⁻(aq) and H₂A₂(aq) with the equilibrium constants found previously.⁽⁷⁾ These values were not varied during the calculations. The model which, within the experimental errors, gives the lowest value of the minimized error-square sum, U_{min} , will be assumed as the "best" model out of the other models tried.

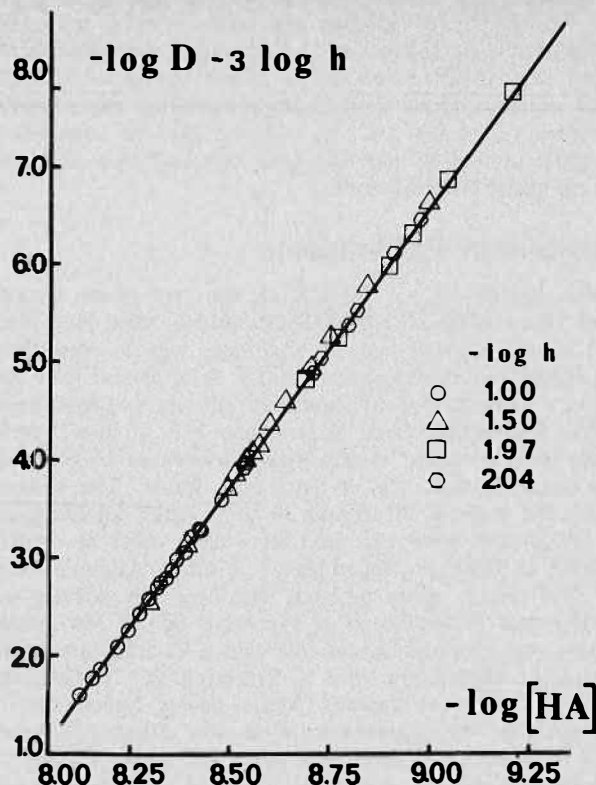


FIGURE 3. The distribution of Yb(III) in the two-phase system 0.10 M (Na,H)ClO₄/HDEHP-toluene given as a $\log Dh^3$ versus $\log (HA)$ for various constant values of $-\log h = 1.000$ (O), 1.500 (Δ), 1.973 (\square) and 2.043. The (HA) was calculated assuming the formation of HDEHP species with the equilibrium constants given in Table 3. The drawn line has been calculated assuming the formation of Yb(III)-HDEHP species with the equilibrium constants given in Table 2, Model III.

Results

The System Yb(III)-0.10 M (Na,H)ClO₄/HDEHP-toluene

The distribution data are given in Table 1. In Figure 1 the distribution of Yb(III) between the two phases, 0.10 M (Na,H)ClO₄ and HDEHP-toluene, is given as $\log D$ versus $\log(\frac{1}{2} C_A)$ for different constant values of $-\log(H^+) = 1.00, 1.50, 1.973$ and 2.043 . The experimental points are seen to fall on straight lines with slope approximately equal to +3. Since, in the extraction conditions used, the di(2-ethylhexyl)phosphoric acid, HDEHP (= HA), is found previously (cf. Ref. 7) to be predominantly in dimeric form, we use the relationship:

$$C_A = (HA)_{org} + 2(H_2A_2)_{org} + (HA) + (A^-) + 2(H_2A_2) \approx 2(H_2A_2)_{org} \dots \dots \dots (5)$$

These lines in Figure 1 thus strongly indicate the predominant formation of extractable $(H^+)_p(Yb^{3+})_q(H_2A_2)_3$ species. In Figure 2 the distribution of Yb(III) is given for constant values of $C_A = 3.85 \times 10^{-3}$ and 10.3×10^{-3} M as a function of $-\log(H^+)$. In the pH range studied it is seen that the experimental points follow straight lines with slope of approximately +3, which thus indicate the predominant formation of $(H^+)_{-3}(Yb^{3+})_p(H_2A_2)_3$ (org) species. This conclusion is further supported from the plot $\log D(H^+)^3$ versus $\log(HA)$ in Figure 3 for different constant values of $-\log(H^+)$ given previously which gives a straight line with a slope of +6. These results, as shown by the

TABLE 1. The Distribution of $^{169,175}\text{Yb(III)}$ Between Solutions of di(2-ethylhexyl) Phosphoric Acid and 0.10 M (H,Na)ClO₄ at 25°C.

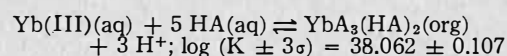
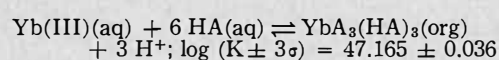
For different constant values of $\log(\text{H}^+)$. Initial concentration of Yb(III) in the aqueous phase $< 10^{-5}$ M. Volume ratio constant (= 1.0). Values of $\log(\text{HA})$ and $\log(D_{\text{calc}} D_{\text{exp}}^{-1})$ calculated assuming the formation of the $(\text{H}^+)_p(\text{Yb}^{3+})_q(\text{HA})_r$ species with the equilibrium constants given in Table 3 and Table 2, Model No. III.

$\log(\text{H}^+) = -1.000$ $C_A M$	$\log D_{\text{exp}}$	$\log(\text{HA})$	$\log(D_{\text{calc}} D_{\text{exp}}^{-1})$	$C_A M$	$\log D_{\text{exp}}$	$\log(\text{HA})$	$\log(D_{\text{calc}} D_{\text{exp}}^{-1})$
8.30×10^{-3}	-0.9797	-8.540	0.008	5.16×10^{-3}	-0.1126	-8.646	+0.033
1.08×10^{-2}	-0.5890	-8.483	-0.049	6.19×10^{-3}	+0.1216	-8.606	+0.028
1.10×10^{-2}	-0.5937	-8.479	-0.021	7.23×10^{-3}	+0.3342	-8.572	+0.012
1.38×10^{-2}	-0.2732	-8.429	-0.053	8.26×10^{-3}	+0.4919	-8.543	+0.024
1.43×10^{-2}	-0.2845	-8.421	+0.004	8.31×10^{-3}	+0.5094	-8.541	+0.014
1.52×10^{-2}	-0.2189	-8.408	+0.016	9.29×10^{-3}	+0.6306	-8.517	+0.035
1.65×10^{-2}	-0.0530	-8.390	-0.045	1.03×10^{-2}	+0.7843	-8.494	+0.015
1.79×10^{-2}	+0.0571	-8.372	-0.051	1.66×10^{-2}	+1.3855	-8.389	+0.024
1.79×10^{-2}	+0.0135	-8.372	-0.008	2.494×10^{-2}	+1.9046	-8.300	+0.025
1.93×10^{-2}	+0.1136	-8.356	-0.012				
2.07×10^{-2}	+0.2235	-8.341	-0.032	$\log(\text{H}^+) = -2.043$			
2.14×10^{-2}	+0.2479	-8.333	-0.014	1.15×10^{-3}	-0.3291	-8.981	-0.017
2.21×10^{-2}	+0.2844	-8.326	-0.009	1.54×10^{-3}	+0.0240	-8.916	-0.011
2.48×10^{-2}	+0.4374	-8.301	-0.014	2.31×10^{-3}	+0.5844	-8.826	-0.064
2.50×10^{-2}	+0.4411	-8.299	-0.008	2.69×10^{-3}	+0.7706	-8.792	-0.058
2.76×10^{-2}	+0.5961	-8.278	-0.009	3.46×10^{-3}	+1.0998	-8.736	-0.068
2.86×10^{-2}	+0.5679	-8.270	+0.038	3.85×10^{-3}	+1.2378	-8.712	-0.070
3.22×10^{-2}	+0.7382	-8.244	+0.020	8.31×10^{-3}	+2.2128	-8.542	-0.062
3.57×10^{-2}	+0.8928	-8.221	-0.002				
4.29×10^{-2}	+1.1185	-8.181	+0.009	$\log(\text{H}^+) = -1.973$			
4.65×10^{-2}	+1.2192	-8.164	+0.012	4.10×10^{-4}	-1.8716	-9.210	+0.052
5.00×10^{-2}	+1.3021	-8.148	+0.022	8.30×10^{-4}	-0.9772	-9.052	+0.026
5.35×10^{-2}	+1.4058	-8.133	+0.008	1.25×10^{-3}	-0.4168	-8.961	-0.031
				1.66×10^{-3}	-0.0576	-8.899	-0.041
$\log(\text{H}^+) = -1.500$				2.08×10^{-3}	+0.2212	-8.849	-0.039
1.03×10^{-3}	-2.1512	-9.002	+0.057	2.49×10^{-3}	+0.4525	-8.809	-0.045
2.06×10^{-3}	-1.2913	-8.848	+0.061	2.91×10^{-3}	+0.6405	-8.775	-0.037
3.10×10^{-3}	-0.7723	-8.758	+0.053	3.33×10^{-3}	+0.8298	-8.745	-0.055
4.13×10^{-3}	-0.4120	-8.695	+0.052	3.74×10^{-3}	+0.9631	-8.719	-0.041
				4.16×10^{-3}	+1.1145	-8.695	-0.057

relationships given in Figure 1, 2 and 3, thus indicate the predominant formation of $\text{YbA}_3(\text{HA})_3$ in the organic phase, assuming that only mononuclear ytterbium species are being formed. This last assumption is reasonable since in the experiment the initial total concentration of Yb(III), C_{Yb} , is always less than 10^{-6} M and variation of C_{Yb} seems not to affect the distribution of Yb(III).

These results of the graphical analysis are further refined by a computer analysis using the LETAGROP-DISTR program. In Table 2 we summarize the results of the computer analysis for the extraction system Yb(III)-0.10 M (Na,H)ClO₄/HDEHP-toluene for $N_p = 72$ points. Model I in which the formation of $\text{YbA}_3(\text{HA})_3(\text{org})$ is assumed, gives a significantly lower value of the minimized error-square sum $U_{\text{min}} (= 0.3535)$ and $\sigma(\log D) (= 0.071)$ compared with Model II, where we assume the extraction of the species $\text{YbA}_3(\text{HA})_2(\text{org})$ ($U_{\text{min}} = 2.299$ and $\sigma(\log D) = 0.180$). Assuming the formation of both $\text{YbA}_3(\text{HA})_3(\text{org})$ and $\text{YbA}_3(\text{HA})_2(\text{org})$ in Model III, a significant improvement of $U_{\text{min}} (= 0.1011)$ and $\sigma(\log D) (= 0.038)$ is found compared with Model I.

No improvements of U are found when to Model III additional species as $\text{YbA}_2^{2+}(\text{aq})$ and $\text{YbA}_2^+(\text{aq})$ are assumed to be formed, since the value of their formation constant β is reduced to zero. We may thus conclude that the "best" description of the data available is given by Model III by assuming the formation of the following Yb(III) species:



or, using the dimeric species $\text{H}_2\text{A}_2(\text{org})$ as the reacting component, we may express the extraction process by the equilibrium reactions

TABLE 1A. The Distribution of 169,175-Yb(III) Between Solutions of Di(2-ethylhexyl) phosphoric Acid and 0.10 M (Na,H)ClO₄ as a Function of $\log[\text{H}^+]$ at Constant Values of $C_A = 3.850 \times 10^{-3}$ M and 1.032×10^{-2} M

Initial concentration of Yb(III) in the aqueous phase $< 10^{-5}$ M. Volume ratio 1.0. $\log(D_{\text{calc}} D_{\text{exp}}^{-1})$ calculated assuming the formation of HDEHP species and Yb(III)-HDEHP species with the equilibrium constants given in Table 3 and Table 2, Model III.

$C_A = 3.850 \times 10^{-3}$ M - $\log(\text{H}^+)$	$\log D_{\text{exp}}$	$\log(D_{\text{calc}} D_{\text{exp}}^{-1})$
1.000	-1.9114	-0.032
1.046	-1.8215	+0.016
1.097	-1.6524	-0.000
1.155	-1.4943	+0.016
1.187	-1.3978	+0.015
1.222	-1.2928	+0.015
1.260	-1.2073	+0.043
1.301	-1.0912	+0.050
1.347	-0.9779	+0.074
1.398	-0.8254	+0.074
2.024	+1.1509	-0.040

$C_A = 1.032 \times 10^{-2}$ M - $\log(\text{H}^+)$	$\log D_{\text{exp}}$	$\log(C_{\text{calc}} D_{\text{exp}}^{-1})$
1.012	-0.6343	-0.025
1.057	-0.5205	-0.005
1.108	-0.3696	-0.003
1.165	-0.2156	+0.013
1.231	-0.0254	+0.020
1.308	+0.2016	+0.024
1.403	+0.4587	+0.054
1.891	+1.9008	+0.071

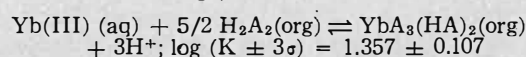
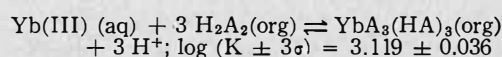


TABLE 2. Equilibrium Constants $\log \beta_{pqr}$ for the Formation of $(H^+)_p(Yb^{3+})_q(HA)_r$ in the Two-phase System Yb(III)-0.10 M (Na,H)ClO₄/HDEHP-toluene which Minimize the Error-square sum

$$U = \sum_1^{72} (\log D_{calc} - \log D_{exp})^2$$

Model No.	(p,q,r)log β _{pqr}	U _{min}	σ(log D)
I	(-3, 1, 6) 47.289 ± 0.025	0.3535	0.071
II	(-3, 1, 5) 38.715 ± 0.064	2.299	0.180
^b III	(-3, 1, 5) 38.062 ± 0.107	0.1011	0.038
	(-3, 1, 6) 47.166 ± 0.036		

^aThe limits of β_{pqr} ($= [(H^+)_p(Yb^{3+})_q(HA)_r]_{org} [H^+]^{-p} [Yb^{3+}]^{-q} [HA]^{-r}$) given correspond to $\log(\beta \pm 3\sigma(\beta))$.

^bThe best model assumed.

TABLE 3. Equilibrium Constants for the Formation of HDEHP Species in the Two-phases System X M (H,Na) (NO₃,ClO₄)/HDEHP-toluene, (X = 0.10 or 1.0) used in the Present Work for Computer Calculations of Yb(III) Extraction Data. (Cf. Ref. 7 & 10)

HA(aq) ⇌ HA(org)	K ₁ = 6.157 × 10 ⁴
2 HA(aq) ⇌ H ₂ A ₂ (org)	K ₂ = 4.809 × 10 ¹⁴ M ⁻¹
HA(aq) ⇌ H ⁺ + A ⁻	K _a = 0.3394 M (= 0.7127 for X = 1.0)
2 HA(aq) ⇌ H ₂ A ₂ (aq)	K _{2aq} = 8.0 × 10 ¹² M ⁻¹

TABLE 4. The Distribution of 169,175-Yb(III) Between Solutions of Di(2-ethylhexyl) phosphoric Acid and 1.0 M (H,Na)ClO₄ at 25°C

Initial concentration of Yb(III) in the aqueous phase < 10⁻⁵ M. Volume ratio kept constant (= 1.0). Log (HA) and log (D_{calc} D_{exp}⁻¹) calculated assuming the formation of the (H⁺)_p(Yb³⁺)_q(HA)_r species with the equilibrium constants given in Table 3 and Table 5, Model No. III.

log(H ⁺) = -0.968		C _A = 4.318 × 10 ⁻³ M				
C _A M	log D _{exp}	log (HA)	log (D _{calc} D _{exp} ⁻¹)	log(H ⁻)	log D _{exp}	log ⁻¹ (D _{calc} D _{exp})
3.670 × 10 ⁻²	+0.5087	-8.215	+0.024	-1.014	-1.9663	-0.098
3.308 × 10 ⁻²	+0.4756	-8.238	-0.077	-1.065	-1.8793	-0.032
2.941 × 10 ⁻²	+0.2298	-8.263	+0.018	-1.123	-1.7048	-0.033
2.817 × 10 ⁻²	+0.1767	-8.273	+0.015	-1.190	-1.5150	-0.022
2.573 × 10 ⁻²	+0.0606	-8.293	+0.015	-1.315	-1.2072	+0.045
2.209 × 10 ⁻²	-0.0605	-8.326	-0.060	-1.366	-1.0511	+0.042
2.206 × 10 ⁻²	-0.1386	-8.326	+0.017	-1.424	-0.8547	+0.020
1.838 × 10 ⁻²	-0.3685	-8.366	+0.012	-1.491	-0.6404	+0.006
1.657 × 10 ⁻²	-0.5061	-8.389	+0.017	-1.570	-0.4459	+0.049
1.708 × 10 ⁻²	-0.4614	-8.382	+0.011	-1.667	+0.2028	-0.005
1.537 × 10 ⁻²	-0.5596	-8.405	-0.026	-1.792	+0.2028	+0.065
1.452 × 10 ⁻²	-0.6846	-8.418	+0.027			
1.367 × 10 ⁻²	-0.7522	-8.431	+0.017			
1.281 × 10 ⁻²	-0.8129	-8.445	-0.006			
1.196 × 10 ⁻²	-0.9404	-8.460	+0.034			
1.110 × 10 ⁻²	-1.0012	-8.477	-0.000			
1.032 × 10 ⁻²	-1.0872	-8.493	-0.007			
9.292 × 10 ⁻³	-1.2090	-8.516	-0.0193			

The System Yb(III)-1.0 M (Na,H)ClO₄/HDEHP-toluene

The distribution data are given in Table 4 and in Figure 1 the distribution of Yb(III) between 1.0 M (Na,H) ClO₄ and HDEHP-toluene as log D versus log (½ C_A) for a constant level of -log(H⁺) = 1.00. The data are seen to fall on a straight line with a slope of approximately 3 which thus corresponds to the results found for the extraction of Yb(III) from 0.10 M ClO₄⁻ medium. These results thus agree with those found previously for the

TABLE 5. Equilibrium Constants $\log \beta_{pqr}$ for the Formation of $(H^+)_p(Yb^{3+})_q(HA)_r$ in the Two-phase System Yb(III)-1.0 M (Na,H)ClO₄/HDEHP-toluene which Minimize the Error-square Sum

$$U = \sum_1^{29} (\log D_{calc} - \log D_{exp})^2$$

Model No.	(p, q, r) log β _{pqr}	U _{min}	σ(logD)
I	(-3, 1, 5) 38.470 ± 0.081	0.5830	0.1443
II	(-3, 1, 6) 46.961 ± 0.026	0.0673	0.0490
^b III	(-3, 1, 5) 37.713, max. = 37.950	0.0410	0.0390
	(-3, 1, 6) 46.872 ± 0.074		

^aThe limits of β_{pqr} ($= [(H^+)_p(Yb^{3+})_q(HA)_r]_{org} [H^+]^{-p} [Yb^{3+}]^{-q} [HA]^{-r}$) given correspond to $\log(\beta \pm 3\sigma(\beta))$ and if $\sigma(\beta) > 0.2\beta$, the maximum value $\log(\beta + 3\sigma)$ is given.

^bThe best model assumed.

TABLE 6. The Distribution of 169,175-Yb(III) Between Solutions of Di(2-ethylhexyl) phosphoric Acid and 0.10 M (H,Na)NO₃ at 25°C

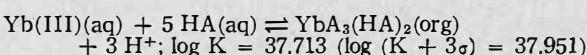
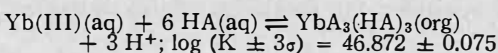
Initial Concentration of Yb(III) in the aqueous phase was less than 10⁻⁵ M. The volume ratio was kept constant (= 1.0) and the values of log (HA) and log (D_{calc} D_{exp}⁻¹) were calculated assuming the formation of the (H⁺)_p(Yb³⁺)_q(HA)_r species with the equilibrium constants given in Table 3 and Table 7, Model No. III.

log(H ⁺) = -0.983		C _A = 4.270 × 10 ⁻³ M				
C _A M	log D _{exp}	log (HA)	log (D _{calc} D _{exp} ⁻¹)	log(H ⁺)	log D _{exp}	log (D _{calc} D _{exp} ⁻¹)
1.708 × 10 ⁻²	-0.1518	-8.282	+0.005	-1.205	-1.2415	-0.020
1.623 × 10 ⁻²	-0.2231	-8.393	+0.010	-1.284	-0.9965	-0.028
1.537 × 10 ⁻²	-0.2980	-8.405	+0.015	-1.381	-0.7529	+0.019
1.452 × 10 ⁻²	-0.3470	-8.418	-0.010	-1.501	-0.3657	-0.008
1.367 × 10 ⁻²	-0.4438	-8.431	+0.010	-1.578	-0.1229	-0.020
1.281 × 10 ⁻²	-0.5271	-8.445	+0.009	-1.673	+0.1268	+0.015
1.196 × 10 ⁻²	-0.6024	-8.460	-0.004	-1.811	+0.3657	+0.010
1.110 × 10 ⁻²	-0.6945	-8.477	-0.008	-1.964	+0.9639	+0.050
1.025 × 10 ⁻²	-0.7959	-8.494	-0.009			
9.400 × 10 ⁻³	-0.9187	-8.513	+0.003			
2.761 × 10 ⁻²	+0.4665	-8.277	+0.006			
1.032 × 10 ⁻²	-0.7528	-8.493	-0.043			

extraction of Yb(III) from 0.10 M (Na,H)ClO₄ medium and indicate the predominant formation of YbA₃(HA)₃ (org).

The data consisting of 29 points have been computer analyzed and the results summarized in Table 5. In agreement with the results for the system Yb(III)-0.10 M (Na, H) ClO₄/HDEHP-toluene, Model III, in which the formation of both YbA₃(HA) and YbA₃(HA)₃ in the organic phase is assumed, gives a lower U_{min} (= 0.041) and σ(logD) (= 0.0390) than the assumption of either YbA₃(HA)₂(org), (Model I, U_{min} = 0.5830 and σ(logD) = 0.1443) or YbA₃(HA)₃(org) alone (cf. Model II, U_{min} = 0.0673, σ(logD) = 0.0490).

From the available data, the best description of the system is thus the assumption of the formation of the extractable species YbA₃(HA)₂ and YbA₃(HA)₃ with the following equilibrium constants:



The System Yb(III)-0.10 M (H,Na)NO₃/HDEHP-toluene

The distribution data are given in Table 6 and plotted in Figure 4 as log D versus log(½ C_A) for log(H⁺) =

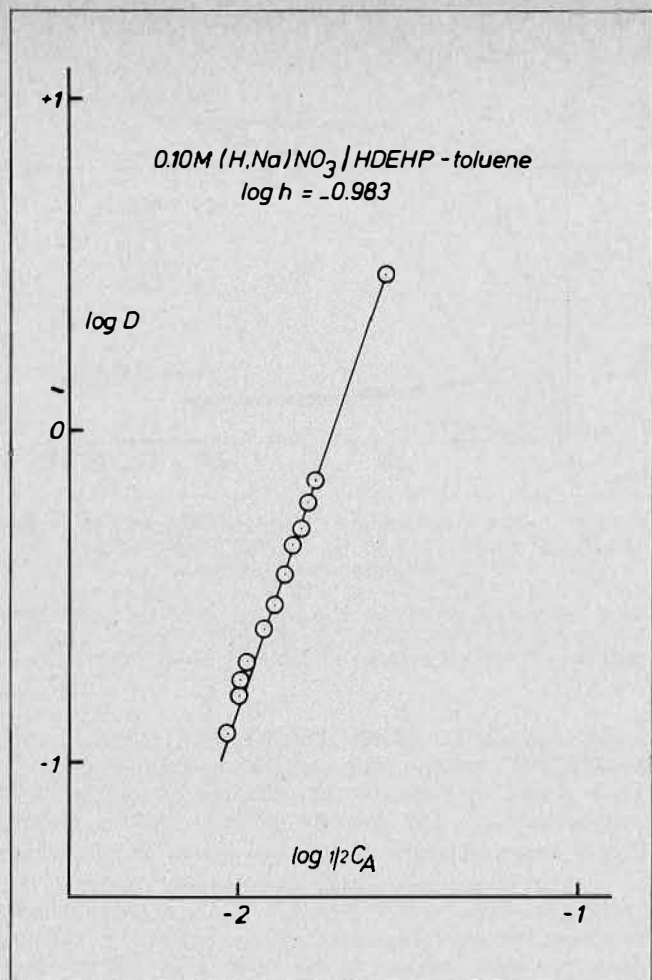
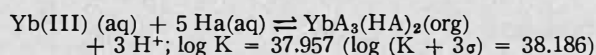
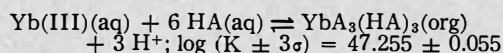


FIGURE 4. The distribution of Yb(III) in the two-phase system 0.10 M (Na,H)NO₃/HDEHP-toluene as a function of C_A for a constant value of -log h = 0.983. The drawn line has been calculated assuming the formation of Yb(III)-HDEHP species with the equilibrium constants given in Table 7, Model III.

-0.983, and in Figure 5 as log D versus log(H⁺) for C_A = 0.427 × 10⁻³ M. The experimental points in both figures fall along straight lines with slope of +3, thus indicating the predominant extraction of the species YbA₃(HA)₃. This agrees with the results found previously for the extraction of Yb(III) from perchlorate medium. The data (N_p = 20 points) are subjected to Letagroup analysis and the results are summarized in Table 7. Assuming the formation of the extractable species YbA₃(HA)₂ and YbA₃(HA)₃ (Model III, U_{min} = 0.0075, σ(logD) = 0.0204), gives a better fit to the data than the assumption of either YbA₃(HA)₂, (Model I, U_{min} = 0.2636, σ(logD) = 0.118) or YbA₃(HA)₃ alone (Model II, U_{min} = 0.0154, σ(logD) = 0.0285). We thus conclude that out of the three models tried the "best" description for the system is given by the assumption of the formation of the following extractable Yb(III) species:



or can also be given by:

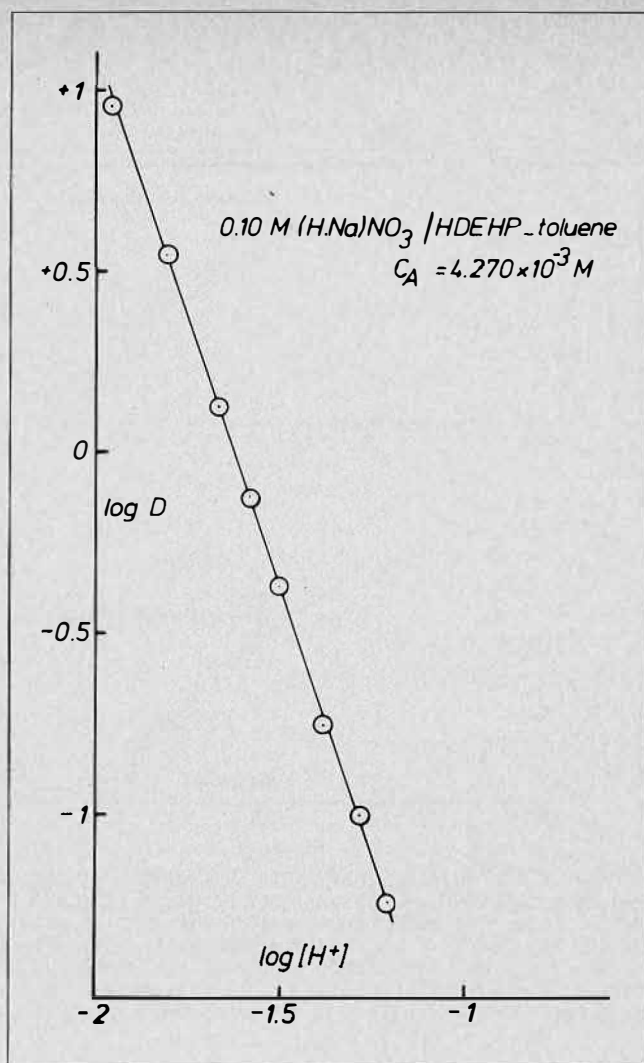
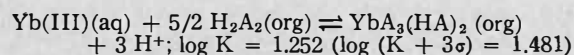
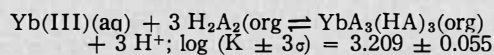


FIGURE 5. The distribution of Yb(III) in the two-phase system 0.10 M (Na,H)NO₃/4.270 × 10⁻³ M HDEHP-toluene as a function of log(H⁺). The drawn line has been calculated assuming the formation of Yb(III)-HDEHP species with the equilibrium constants given in Table 7, Model III.

TABLE 7. Equilibrium Constants ^a log β_{pqr} for the Formation of (H⁺)_p(Yb³⁺)_q(HA)_r in the Two-phase System Yb(III)-0.10 M (Na,H)NO₃/HDEHP-toluene which minimize the Error-square Sum

$$U = \sum_{i=1}^{20} (\log D_{\text{calc}} - \log D_{\text{exp}})^2$$

Model No.	(p, q, r) log β _{pqr}	U _{min}	σ(logD)
I	(-3, 1, 5) 38.685 ± 0.077	0.2636	0.1178
II	(-3, 1, 6) 47.218 ± 0.019	0.0154	0.0285
^b III	(-3, 1, 5) 37.850, max. = 38.078	0.0075	0.0204
	(-3, 1, 6) 47.147 ± 0.055		

^aThe limits of β_{pqr} (= [(H⁺)_p(Yb³⁺)_q(HA)_r]_{org} / (H⁺)^{-p}(Yb³⁺)^{-q}(HA)^{-r} given correspond to log(β ± 3σ(β)) and if σ(β) > 0.2β, the maximum value log(β + 3σ) is given.

^bThe best model assumed.

The Formation of Yb(III)-NO₃⁻ Complex

The complex formation between Yb(III) and nitrate ions was studied from the variation of the distribution of Yb(III) as a function of the nitrate concentration, C_{NO₃} in the two-phase system Yb(III)-0.10 M (Na, H) (ClO₄, NO₃)/4.271 × 10⁻² M HDEHP-toluene as well as in the

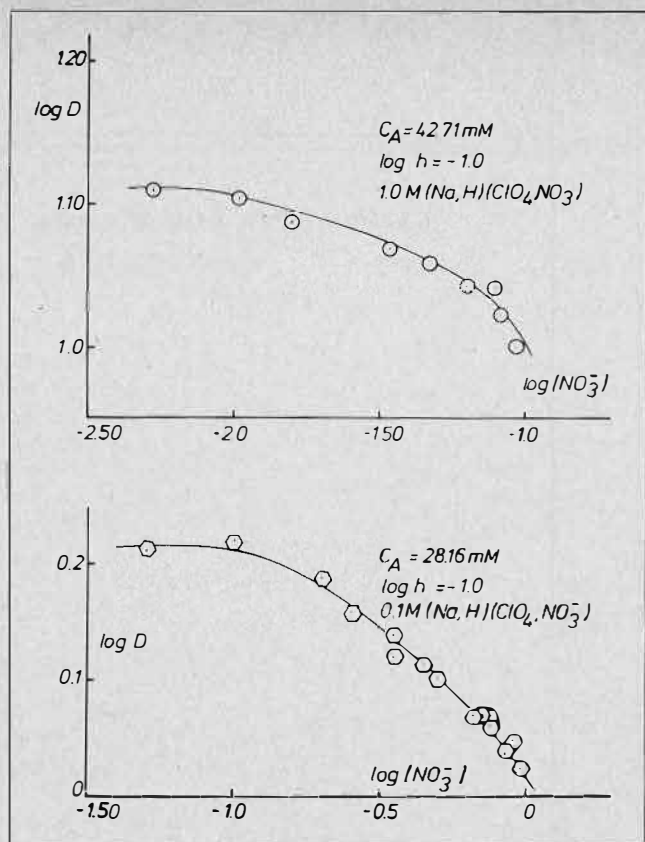


FIGURE 6. The distribution of Yb(III) as a function of (NO_3^-) between the two-phases systems: 1.0 M (Na,H) $(\text{ClO}_4, \text{NO}_3)/42.71 \times 10^{-3}$ M HDEHP-toluene (\odot) and 0.10 M (Na,H) $(\text{ClO}_4, \text{NO}_3)/28.16 \times 10^{-3}$ M DHEHP-toluene. The drawn curves have been calculated assuming the formation of YbNO_3^{2+} (aq) and Yb(III)-HDEHP species with the equilibrium constants given in Tables 3, 10 (Model I) and 9 (Model I).

TABLE 8. Distribution Data of 169,175-Yb(III) for the Two-phases System X M (Na,H) $(\text{ClO}_4, \text{NO}_3)/\text{HDEHP-toluene}$, $(X=0.10 \text{ or } 1.0)$ and $\log(\text{H}^+) = -1.000$, at 25°C

Initial concentration of Yb(III) in the aqueous phase $< 10^{-5}$ M. Volume ratio kept constant (= 1.0). Value of the error $\log(D_{\text{calc}}/D_{\text{exp}}^{-1})$ calculated assuming the formation of the $(\text{H}^+)_p(\text{Yb}^{3+})_q(\text{HA})_r(\text{NO}_3^-)_s$ species with the equilibrium constants given in Table 3 and Table 9 Model I.

0.10 M $(\text{HClO}_4, \text{NO}_3)/4.271 \times 10^{-2}$ M HDEHP-toluene			1.00 M (Na, H) $(\text{ClO}_4, \text{NO}_3)/2.816 \times 10^{-2}$ M HDEHP-toluene		
$C_{\text{NO}_3^-}$ M	$\log D_{\text{exp}}$	$\log(D_{\text{calc}}/D_{\text{exp}}^{-1})$	$C_{\text{NO}_3^-}$ M	$\log D_{\text{exp}}$	$\log(D_{\text{calc}}/D_{\text{exp}}^{-1})$
3.12×10^{-3}	+1.0871	+0.030	0	+0.2855	-0.052
5.20×10^{-3}	+1.1096	+0.005	4.99×10^{-2}	+0.2081	+0.011
1.04×10^{-2}	+1.1062	+0.003	0.100	+0.2264	-0.021
1.56×10^{-2}	+1.0942	+0.008	0.200	+0.1469	+0.032
3.64×10^{-2}	+1.0716	+0.007	0.250	+0.1371	+0.029
4.16×10^{-2}	+1.0881	-0.015	0.300	+0.1395	+0.015
4.68×10^{-2}	+1.0608	+0.007	0.350	+0.1193	+0.023
5.72×10^{-2}	+1.0656	-0.009	0.400	+0.1582	-0.028
6.24×10^{-2}	+1.0453	+0.006	0.450	+0.1166	+0.003
6.76×10^{-2}	+1.0540	-0.008	0.500	+0.0976	+0.011
7.28×10^{-2}	+1.0631	-0.023	0.550	+0.1670	-0.070
7.80×10^{-2}	+1.0448	-0.010	0.600	+0.0671	+0.020
8.32×10^{-2}	+1.0231	+0.007	0.650	+0.0078	+0.069
8.84×10^{-2}	+1.0235	+0.001	0.700	+0.0724	-0.006
9.36×10^{-2}	+1.0056	+0.014	0.750	+0.0681	-0.011
9.88×10^{-2}	+1.0045	+0.010	0.810	-0.0003	+0.046
			0.850	+0.0360	+0.002
			0.900	+0.0489	+0.020
			0.950	+0.0228	-0.003
			1.000	+0.0640	-0.053

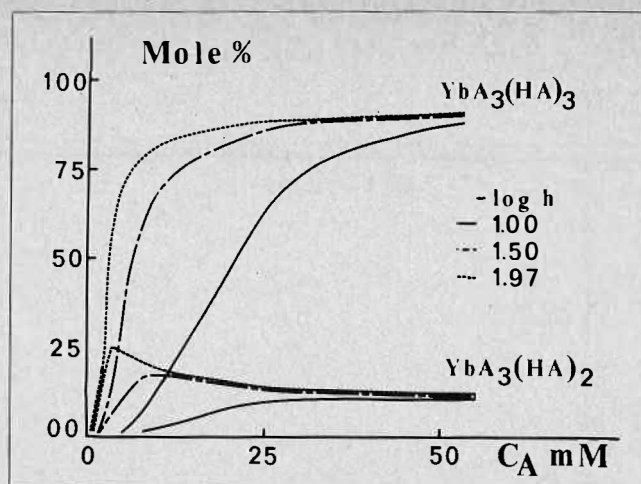
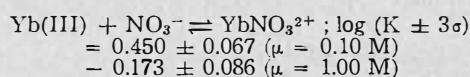


FIGURE 7. The distribution of Yb(III)-HDEHP species in the two-phase system 0.10 M (H, Na) $\text{ClO}_4/\text{HDEHP-toluene}$ as a function of C_A for different constant values of $-\log h = 1.000$ (—), 1.500 (- - -), 1.970 (- · - ·). The curves have been calculated using the HALTAFALL program¹⁹ assuming the formation of $(\text{H}^+)_p(\text{Yb}^{3+})_q$ (HDEHP)_r species with the equilibrium constants given in Tables 3 and 2 (Model III).

system Yb(III)-1.0 M (Na,H) $(\text{ClO}_4, \text{NO}_3)/2.816 \times 10^{-2}$ M HDEHP-toluene. The distribution data are given in Table 8 and in Figure 6 the data are plotted as $\log D$ versus $\log C_{\text{NO}_3^-}$. The decrease of $\log D$ with increasing $C_{\text{NO}_3^-}$ is seen to follow a straight line with a limiting slope of -1 in both cases, which thus strongly indicate the formation of the species YbNO_3^{2+} in the aqueous phase. In the extraction ranges studied, the pH of the aqueous phase was kept constant at the value 1.00, and no other Yb(III) aqueous species are expected to be formed. The data were computer analyzed and the results summarised in Tables 9 and 10. During the calculations we assumed the formation of $\text{YbA}_3(\text{HA})_3$ and $\text{YbA}_3(\text{HA})_2$ species in the organic phase with the equilibrium constants found previously for the systems Yb(III)-0.10 M (Na, H) $\text{ClO}_4/\text{HDEHP-toluene}$ and Yb(III)-1.00 M (Na, H) $\text{ClO}_4/\text{HDEHP-toluene}$. From Tables 9 and 10 it is seen that in both cases the assumption of the formation of $\text{Yb}(\text{NO}_3)_2^{2+}$ (aq) species (Model I) gives a lower value of U_{min} and $\sigma(\log D)$ compared with Model II where the formation of $\text{Yb}(\text{NO}_3)_2^+$ (aq) was assumed. Assuming the formation of both $\text{Yb}(\text{NO}_3)_2^{2+}$ and $\text{Yb}(\text{NO}_3)_2^+$ in the aqueous phase (cf. Model III, Tables 9 and 10) we found no significant improvement in the minimized error-square sum U_{min} compared with Model I where only YbNO_3^{2+} (aq) was assumed to be formed. In Model III for 1.0 M (Na, H) $(\text{ClO}_4, \text{NO}_3)$ (cf. Table 10) the formation of the species $\text{Yb}(\text{NO}_3)_2^+$ (aq) was even rejected during the calculations as seen from the value found for its constant of formation $K(=O)$. From these results we may thus conclude that the best fit to the available data is the assumption of the formation of YbNO_3^{2+} in the aqueous phase with the following equilibrium constant:



Discussion

Our results thus show the predominant formation of the species $\text{YbA}_3(\text{HA})_3(\text{org})$ and $\text{YbA}_3(\text{HA})_2(\text{org})$ from both perchlorate and nitrate medium. The $\text{YbA}_3(\text{HA})_2$ species formed are proportionally minor as compared with the $\text{YbA}_3(\text{HA})_3$ species which, e.g., can be seen in Figure 7, calculated using the HALTAFALL program (cf. Ref.

TABLE 9. Equilibrium Constants $^a \log \beta_{pqrs}$ for the Formation of the Species $(H^+)_p(Yb^{3+})_q(HA)_r(NO_3^-)_s$ in the Two-phases System Yb(III)-0.10 M $H(ClO_4, NO_3)/4.271 \times 10^{-2}$ M HDEHP-toluene which Minimize the Error-square sum $U = \sum_1^{16} (\log D_{calc} - \log D_{exp})^2$

Model No.	(p, q, r, s) (aq) $\log \beta_{pqrs}$	(p, q, r, s) (org) $\log \beta_{pqrs}$	U_{min}	$\sigma(\log D)$
I ^b	(0, 1, 0, 1) 0.450 ± 0.067	^{nv} (-3, 1, 5, 0) 38.062 ^{nv} (-3, 1, 6, 0) 47.166	2.502×10^{-3}	0.013
II	(0, 1, 0, 2) 1.546 ± 0.096	- " -	4.770×10^{-3}	0.018
III	(0, 1, 0, 1) 0.372, max. = 0.632 (0, 1, 0, 2) 0.774, max. = 1.481	- " -	2.401×10^{-3}	0.013

^aThe limits of $\beta_{pqrs} (= [(H^+)_p(Yb^{3+})_q(HA)_r(NO_3^-)_s]_{org} / [H^+]^p [Yb^{3+}]^q [HA]^r [NO_3^-]^s)$ given correspond approximately to $\log(\beta \pm 3\sigma(\beta))$ and if $\sigma(\beta) > 0.2\beta$, the maximum value $\log(\beta + 3\sigma)$ is given.

^{nv}The value of the constant is not varied during the calculations.

^bThe best model assumed.

TABLE 10. Equilibrium Constants $^a \log \beta_{pqrs}$ for the Formation of the Species $(H^+)_p(Yb^{3+})_q(HA)_r(NO_3^-)_s$ in the Two-phases System Yb(III)-1.0 M (Na,H) $(ClO_4, NO_3)/2.816 \times 10^{-2}$ M HDEHP-toluene which Minimize the Error-square Sum $U = \sum_1^{20} (\log D_{calc} - \log D_{exp})^2$

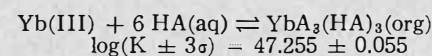
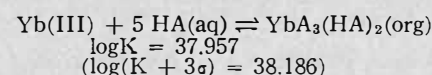
Model No.	(p, q, r, s) (aq) $\log \beta_{pqrs}$	(p, q, r, s) (org) $\log \beta_{pqrs}$	U_{min}	$\sigma(\log D)$
I ^b	(0, 1, 0, 1) - 0.173 ± 0.086	^{nv} (-3, 1, 6, 0) 46.871	2.229×10^{-2}	0.034
II	(0, 1, 0, 2) - 0.070 ± 0.146	- " -	5.533×10^{-2}	0.054
III	(0, 1, 0, 1) - 0.173 ± 0.090 (0, 1, 0, 2) = 0, max. = - 0.197	- " -	2.224×10^{-2}	0.035

^aThe limits of $\beta_{pqrs} (= [(H^+)_p(Yb^{3+})_q(HA)_r(NO_3^-)_s]_{org} / [H^+]^p [Yb^{3+}]^q [HA]^r [NO_3^-]^s)$ given correspond approximately to $\log(\beta \pm 3\sigma(\beta))$ and if $\sigma(\beta) > 0.2\beta$, the maximum value $\log(\beta + 3\sigma)$ is given.

^{nv}The value of the constant is not varied during the computer calculations.

^bThe best model assumed.

19), where the distribution of the different Yb(III) species is given as a function of C_A . The distribution data for the systems Yb(III)-1.0 M (Na,H) $ClO_4/HDEHP$ -toluene and Yb(III)-0.10 M (Na,H) $NO_3/HDEHP$ -toluene may in fact be explained satisfactorily by only assuming the formation of $YbA_3(HA)_3(org)$ only, as can be seen from the obtained values of the U_{min} and $\sigma(\log D)$. However, since the data for the system Yb(III)-0.10 M (Na,H) $ClO_4/HDEHP$ -toluene clearly show the formation of both $YbA_3(HA)_3$ and $YbA_3(HA)_2$ in the organic phase, it seems reasonable to assume that these species are being formed also and in case Yb(III) are extracted from 1.0 M ClO_4^- or 0.10 M NO_3^- aqueous media. The significant improvement of U_{min} and $\sigma(\log D)$ for the model in which the formation of both $YbA_3(HA)_3(org)$ and $YbA_3(HA)_2(org)$ is assumed, compared with the model where only $YbA_3(HA)_3(org)$ is assumed to be formed, seems to support the conclusion, (cf. Tables 5&7). Assuming the formation of $YbNO_3^{2+}$ with the equilibrium constant $K = 10^{0.45} M^{-1}$ found previously, we may recalculate the data for the system Yb(III)-0.10 M (Na,H) $NO_3/HDEHP$ -toluene. We found the following values for the equilibrium constant for the formation of the species, $YbA_3(HA)_2(org)$ and $YbA_3(HA)_3(org)$, which minimize the error-square sum U , ($U_{min} = 0.0075$, $\sigma(\log D) = 0.020$ for $N_p = 20$ points):



These values are comparable with the values found for the system Yb(III) 0.10 M (Na,H) ClO_4 for the formation of $YbA_3(HA)_2(org)$ and $YbA_3(HA)_3(org)$ (cf. Table 2, Model III).

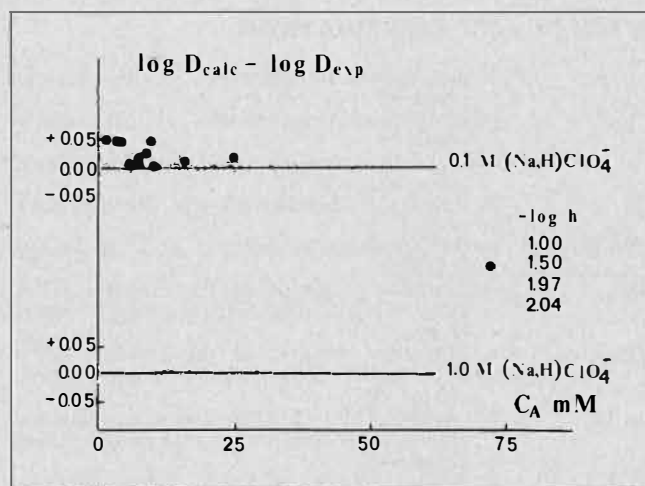


FIGURE 8. Error function, $\log(D_{calc} D_{exp}^{-1})$ as a function of C_A for systems: 0.1 and 1.0 M (H,Na) $ClO_4/HDEHP$ -toluene.

In Figure 8 we plot the error function, $\log(D_{calc} D_{exp}^{-1})$, as a function of C_A for the two-phase system, 0.10 M (H,Na) $ClO_4/HDEHP$ -toluene and 1.0 M (H,Na) $ClO_4/HDEHP$ -toluene, assuming the formation of $YbA_3(HA)_2(org)$ and $YbA_3(org)$ with the equilibrium constants found previously (cf. Table 2, Model III and Table 5, Model III). In Table 11 we found for the system, 0.10 M (H,Na) $ClO_4/HDEHP$ -toluene, that minimizing the following different error-square sums gives practically the same values for $\log K$ for $YbA_3(HA)_2(org)$ and $YbA_3(HA)_3(org)$. This means that the results of the analysis are practically independent of the choice of weight factor given to the points. In this present work the weight factor has been given the value $w = 1$.

TABLE 11. Comparison of Equilibrium Constants $\log \beta_{pqr}$ for the Formation of $(H^+)_p(Yb^{3+})_q(HA)_r$ Species in the System Yb(III)-0.10 M $(Na,H)ClO_4/HDEHP$ -toluene which Minimize Different Error-square Sums $U = \sum_1^{72} (fel(i))^2$

The computer calculations are based on the assumption of the formation of the species $YbA_3(HA)_2 (= -3, 1, 5)$ and $YbA_3(HA)_3 (= -3, 1, 6)$ in the organic phase (cf. Table 2, model III).

Minimized Error fel(i)	(p, q, r) (org) $\log \beta_{pqr}$	U_{min}	$\sigma(y)$
fel(1) = $\log(D_{calc} D_{exp}^{-1})$	(-3, 1, 5) 38.062 ± 0.107	0.1011	0.038
	(-3, 1, 6) 47.166 ± 0.036		
fel(2) = $D_{exp} D_{calc}^{-1} - 1$	(-3, 1, 5) 38.083 ± 0.108	0.5321	0.087
	(-3, 1, 6) 47.165 ± 0.038		
fel(3) = $D_{calc} D_{exp}^{-1} - 1$	(-3, 1, 5) 38.042 ± 0.108	0.5289	0.087
	(-3, 1, 6) 47.165 ± 0.035		

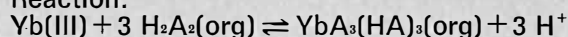
^aThe limits of β_{pqr} ($= [(H^+)_p(Yb^{3+})_q(HA)_r]_{org} [H^+]^{-p} [Yb^{3+}]^{-q} [HA]^{-r}$) given correspond approximately to $\log(\beta \pm 3\sigma(\beta))$.

In Table 12 we summarize the equilibrium constant for the formation of $YbA_3(HA)_3(org)$ for a different two-phase system: aqueous solution/dialkylphosphoric acid-toluene. The values of the constant for the formation of $YbNO_3^{2+}(aq)$ found in this work, $K = 10^{0.450}$ ($\mu = 0.10$ M) and $10^{0.173}$ ($\mu = 1.00$ M), are comparable with those reported by Kriss and Sheka^(16,17), $K = 10^{0.45}$ (3.26 H ClO_4) and $10^{0.57}$ (3 M H(ClO_4)), and by Peppard et al.⁽¹⁵⁾, $K = 10^{-0.22}$ (1.0 M (Na,H) (NO_3, ClO_4)).

SYMBOLS AND ABBREVIATIONS

[]	= equilibrium concentration in the aqueous phase, M
[] _{org}	= equilibrium concentration in the organic phase, M
C_A	= initial total concentration of di(2-ethylhexyl) phosphoric acid, M
C_i	= initial total concentration of chemical component i, M
HDEHP, HA	= di(2-ethylhexyl)phosphoric acid, $(C_8H_{17}O)_2 P(OH)O$
K_{pqr}^{org}	= formation constant of the complex $(H^+)_p(Yb^{3+})_q(HA)_r(NO_3)_s$ in the organic phase, cf. eqn. (2)
K_{lmno}^{aq}	= formation constant of the complex $(H^+)_l(Yb^{3+})_m(HA)_n(NO_3)_o$ in the aqueous phase, cf. eqn. (3)
I_{aq}, I_{org}	= γ -activity of ¹⁶⁹ Yb(III) in the aqueous and organic phase, given in cpm for equal volumes of samples.
D	= $\sum(Yb)_{org} / \sum(Yb) = I_{org} / I_{aq}$, net distribution of Yb(III)
D_{exp}, D_{calc}	= the experimental and calculated distribution ratio of Yb(III); D_{calc} is calculated for a given extraction condition and set of $(H^+)_p(Yb^{3+})_q(HA)_r(NO_3)_s$ species in the aqueous and organic phases with the set of equilibrium K_{pqr} , which minimize an error-square sum, U.
U_{min}	= the minimized error-square sum, U, e.g., for $val = 1$ the program minimizes $U = \sum_1^{Np} (\log(D_{calc} D_{exp}^{-1}))^2$, where Np represents the number of experimental points (cf. Ref. 8)
$\sigma(y)$	= standard deviation of the minimized error, y, e.g. $y = \log D$ for $val = 1$ (cf. Ref. 9)

TABLE 12. Equilibrium Constant $\log K$ for the Reaction:



Two-phases System Aqueous Phase/Dialkylphosphoric Acid-toluene at 25°C if not Otherwise Stated.

Two-phase System	log K	Ref.
1.0 M (Na, H) ClO_4 /HDBP-toluene	5.00	18
1.0 M (Na, H) NO_3 /HDBP-toluene	4.80	"
1.0 M (Na, H) ClO_4 /HDAP-toluene	4.91	"
1.0 M (Na, H) NO_3 /HDAP-toluene	4.71	"
1.0 M (Na, H) ClO_4 /HDIAP-toluene	4.73	"
1.0 M (Na, H) NO_3 /HDIAP-toluene	4.53	"
1.0 M (Na, H) ClO_4 /HDOP-toluene	4.96	"
1.0 M (Na, H) NO_3 /HDOP-toluene	4.76	"
1.0 M (Na, H) ClO_4 /HDEHP-toluene	2.97	"
1.0 M (Na, H) ClO_4 /HDEHP-toluene	2.826	This work
0.1 M (Na, H) ClO_4 /HDEHP-toluene	3.119	"
1.0 M (Na, H) NO_3 /HDEHP-toluene	2.77	18
0.1 M (Na, H) NO_3 /HDEHP-toluene	3.209	This work
0.5 M (Na, H) Cl /HDEHP-toluene	2.58 ^a	11, 12
1.0 M (Na, H) ClO_4 /HDEHP-toluene	2.48	13, 14

Temperature 22 °C.

Acknowledgments

The authors gratefully acknowledge the financial support by the Swedish National Science Research Council and the Swedish Board for Technical Development. One of us (S.A.) extends his thanks to the *Patronato de la Universidad Autónoma de Barcelona* for the opportunity given to him to work in Sweden.

REFERENCES

- (1) Marcus, Y., Kertes, A.S. and Yanir, E., *Equilibrium Constants of Liquid-Liquid Distribution Reactions Part 1*, Int. Union Pure and Appl. Chem., Butterworths, London 1974.
- (2) Marcus, Y. and Kertes, A.S., *Ion Exchange and Solvent Extraction of Metal Complexes*, Wiley-Interscience, London 1967.
- (3) Peppard, D.F., *Advances in Inorg. and Radiochem.*, vol. 9, 1, (edited by Emeleus H.J. and Sharpe, A.G.) Acad. Press, N.Y. 1968.
- (4) Liem, D.H., *Inaug. Diss. Stockholm 1971*, (Available on request).
- (5) Aguilar, M. and Liem, D.H., *Acta Chem. Scand.* 1976, A30, 313.
- (6) Mason, G.W., Schofer, N.L. and Peppard, D.F., *J. Inorg. Nucl. Chem.* 1970, 32, 3899.
- (7) Liem, D.H., *Acta Chem. Scand.* 1972, 26, 191.
- (8) Liem, D.H., *Acta Chem. Scand.* 1971, 25, 1521.
- (9) Ingri, N. and Sillén, L.G., *Ark. Kemi* 1964, 23, 97; Sillén, L.G. and Warnqvist, B., *Ark. Kemi* 1969, 31, 315; Sillén, L.G. and Warnqvist, B., *Ark. Kemi* 1969, 31, 341; Arnek, R., Sillén, L.G. and Wahlberg, O., *Ark. Kemi* 1969, 31, 353.
- (10) Kielland, J., *J. Am. Chem. Soc.* 1937, 2, 1675.
- (11) Baes, C.F., *J. Inorg. Nucl. Chem.* 1962, 24, 707.
- (12) Peppard, D.F., Mason, G.W., Maier, J.L. and Driscoll, W.J., *J. Inorg. Nucl. Chem.* 1957, 4, 334.
- (13) Stary, J., *Talanta*, 1966, 13, 421.
- (14) Pierce, T.B. and Peck, P.F., *Analyst* 1963, 88, 217.
- (15) Peppard, D.F., Mason, G.W. and Hucher, I., *J. Inorg. Nucl. Chem.* 1963, 24, 881.
- (16) Kriss, E.E. and Sheka, Z.A., *Radiokhimiya* 1962, 4, 312.
- (17) Sheka, Z.A. and Kriss, E.E., *Radiokhimiya* 1962, 4, 720.
- (18) Kolarik, Z. and Pankova, H., *J. Inorg. Nucl. Chem.* 1966, 28, 2325.
- (19) Ingri, N., Kakolowicz, W., Sillén, L.G. and Warnqvist, B., *Talanta* 1967, 14, 1261.

Chapter 3

Chemistry of Solvent Extraction Systems

Session 20

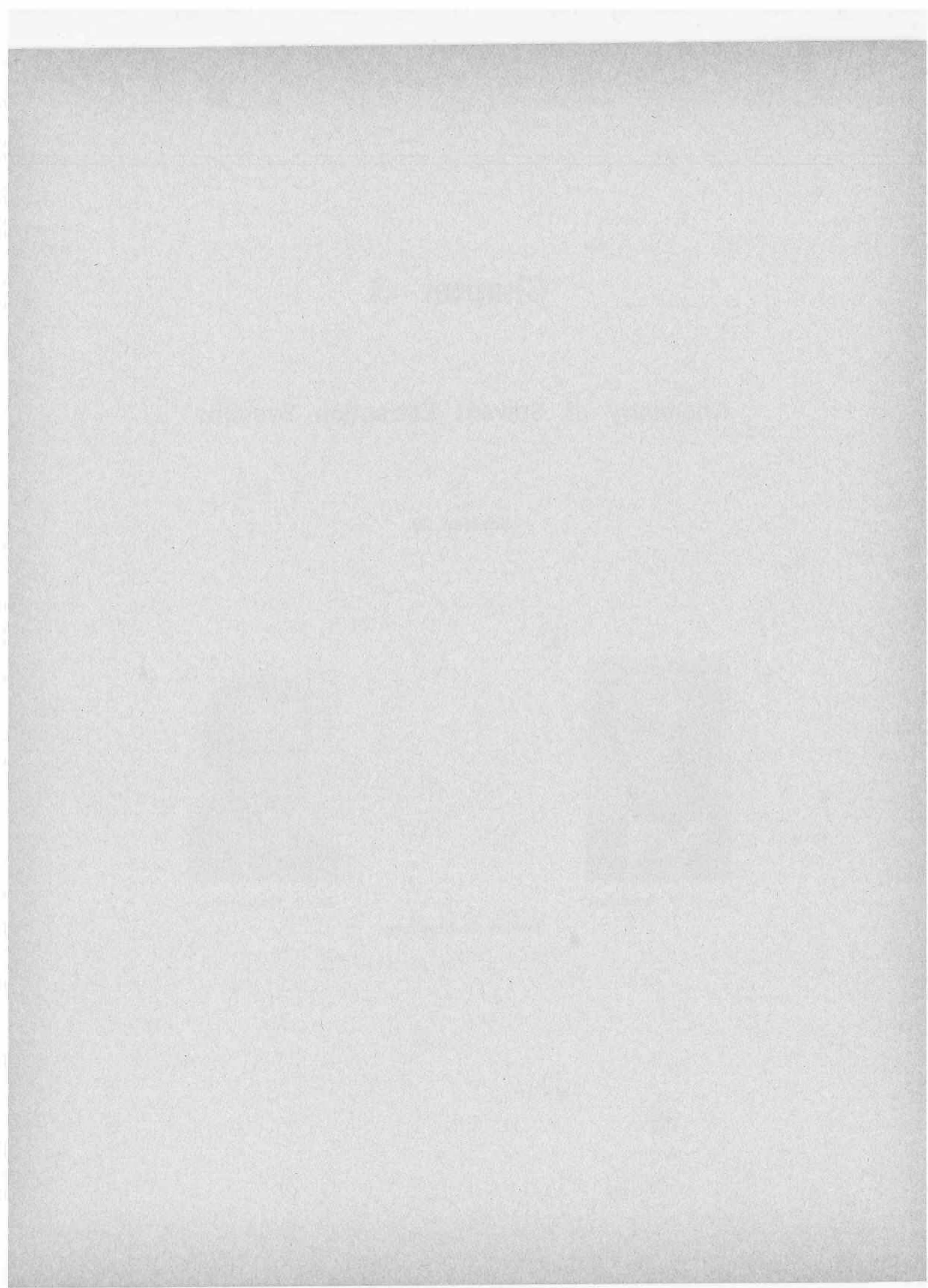


Dr. A.W. Ashbrook



Dr. B. Gaudernack

Session Co-Chairmen



Solvent Impregnated Resin: Bridging the Gap Between Liquid and Solid Extraction

A. Warshawsky,
The Weizmann Institute of Science,
Rehovot, Israel

ABSTRACT

Solvent-impregnated resins (SIR), incorporating hydroxyaryloxime reagents I-A and I-B and an analogous chelating resin I-C, are discussed in terms of ligand mobility, complex-resinate structures and kinetic phenomena. The comparison indicates that SIR resins show greater ligand mobility, and a higher degree of metal complexation, as well as better mass transfer rates than resin I-C therefore closely resembling the behaviour of such reagents in solvent extraction processes. However, reagent losses are expected to be lower as the reagents can be recovered when passed through fresh resin columns.

Introduction

PHASE TRANSFER OF METAL SPECIES from an aqueous phase to an organic phase is utilized for purification purposes in two forms of hydrometallurgical processes:

- (1) Liquid-liquid extraction (solvent extraction, SX),
- (2) Solid-liquid extraction (resin ion-exchange, IX).

Liquid extraction shows advantages in mass transfer rates and offers economic superiority in size of equipment and process time. However, it is riddled with problems such as phase disengagement difficulties and reagent losses. Solid extraction shows lower mass transfer rates and needs large size equipment and longer process time. However, the equipment is simple, easy to operate, and there are basically no problems of phase disengagement and reagent losses.

The great advance in recent years in the development of selective liquid extraction reagents, particularly for copper/iron separation⁽¹⁾, has called for similar developments in ion exchange resins. Solvent impregnated resins^(2,3) and Levextrel polymers⁽⁴⁾ were introduced to fill this gap.

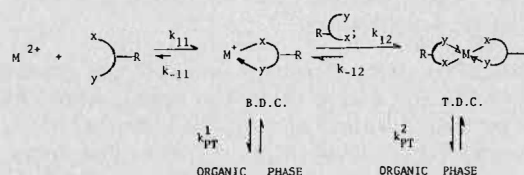
Chelating Liquids and Resins

In order to understand the basic differences between a solvent extraction and an ion exchange process, let us examine the various stages involved in the extraction of a divalent ion, most commonly Cu^{2+} , by the hydroxyaryloxime type of reagents⁽¹⁾ as represented in Scheme No. 1.

Under thermodynamic equilibrium conditions, the tetradentate complex (T.D.C.) has a much higher stability constant than the bidentate complex (B.D.C.). However, due to entropy effects, more time will be needed to form the T.D.C. That means, that under practical operation conditions, such as short contact times in mixer-settler units or in ion exchange columns, the B.D.C. may have an important role.

Scheme No. 1

Formation of M^{2+} -chelate* complexes and the transfer into organic or resin phase.



In SX processes^(5,6,7), in general, the complex formation rate constants k_{11} and k_{12} are of same order of magnitude as the phase-transfer constants k_{PT}^1 and k_{PT}^2 . That means, that in SX systems the most stable complex is formed and extracted and ion selection is therefore performed under thermodynamic equilibrium conditions. In some cases, however, commercial extractants are able to select copper due to kinetic preference⁽⁸⁾.

In IX processes a different situation exists. The metal-resinate formation constants, k_{11} and k_{12} , are much smaller in comparison to those for SX, since diffusion into macromolecular beads is involved. In addition, $k_{11} \gg k_{12}$ because the formation of B.D.C. in the resin phase is a bimolecular reaction involving a free ion M^{2+} and a chelating site on the polymer backbone, whereas the formation of T.D.C. is a bimolecular reaction involving two very inflexible polymeric chelating sites. This means that in many cases under practical operation, formation of T.D.C. is not achieved. As a result the metal-resinate chelates are not of the highest order of stability, implying also that lower selectivity factors are to be expected in comparison to analogous systems in solution. In a more general sense, it can be concluded that incorporation of a chelating functional group in a polymer matrix does not necessarily lead to the transformation of all the properties of the liquid chelate into a solid form.

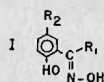
Copper-Selective SIR Resins

Solvent-impregnated resins (SIR) were conceived as a result of a compromise between the need for chelating resins, their shortcomings, and the advantages of SX reagents. An "ideal" SIR resin should, as a result, combine the best properties of solvents and polymers as follows:

- (a) High mobility of the reagent in the resin phase,
- (b) High mass transfer rates,
- (c) High selectivity factors,
- (d) Low reagent losses,
- (e) Good phase separation properties and
- (f) High chemical and physical stability.

*For hydroxyaryloximes: $x = \text{OH}$, $y = > \text{C} = \text{N-OH}$

Chelating resins incorporating hydroxyaryloxime groups⁹ (I-C) and SIR resins incorporating similar reagents¹⁰ (I-A and I-B) were prepared and compared with an emphasis on properties a-f discussed above.



I-A $R_1 = \text{CH}_3$ $R_2 = \text{---CH}_2\text{---C}_6\text{H}_4\text{CH}_3\text{---ON}$ XAD-2, XAD-4, XE-305-PEG-600

I-B $R_1 = \text{H}$ $R_2 = \text{---CH}_2\text{---C}_6\text{H}_4\text{CH}_3\text{---ON}$ XAD-2, XAD-4

I-C $R_1 = \text{CH}_3$ $R_2 = \text{---CH}_2\text{---NH---}$ Polystyrene

Copper Complexation Dependence on Ligand Mobility

The mobility of the ligand in resin I-B was investigated by correlating the degree of copper complexation, expressed as the concentration of copper on the polymer, with the reagent concentration in the polymer. The linear relationship obtained, (see Figure 1) with a slope of 0.5, indicates complete and free mobility of the ligand for the concentration range studied.

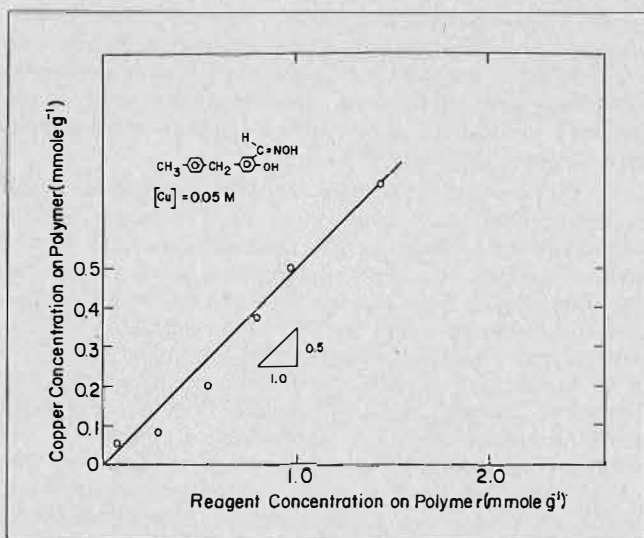


FIGURE 1. Copper complexation vs. reagent I-B concentration on XAD-4.

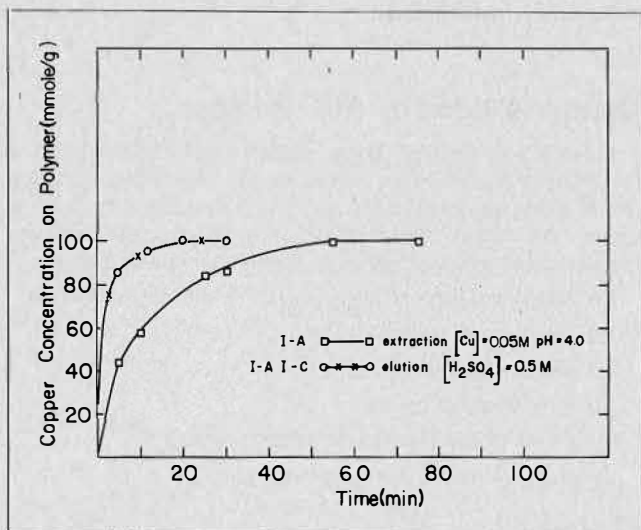


FIGURE 2. Extraction rates — I-A and I-C.

Comparison between SIR resins I-A and I-B (1.0 mmole reagent per gram polymer) and resin I-C (2.1 mmole reagent per gram polymer) shows that the SIR resins complex 0.5 mmole of copper per gram resin at pH 4 (100% complexation) whereas under the same conditions, resin I-C complexes only 0.38 mmole of copper per gram (36% complexation) indicating the restricted mobility of resin I-C. (see Figure 2).

Mass Transfer rates

In ion exchange resins⁽¹¹⁾, the rate-controlling step for mass transfer is either film diffusion (FD) or particle diffusion (PD). Half-life times ($t_{1/2}$) for the two processes are given in Equation 1 for film diffusion control (F.D.C.) and Equation 2 for particle diffusion control (P.D.C.):

$$t_{1/2} = 0.23 \frac{\bar{r} \delta \bar{c}}{Dc} \text{ (F.D.C.)} \dots \dots \dots (1)$$

$$t_{1/2} = 0.030 \frac{\bar{r}^2}{D} \text{ (P.D.C.)} \dots \dots \dots (2)$$

where

\bar{r} = bead radius.

\bar{D} = diffusion coefficient in bead.

\bar{c} = concentration of functional groups in bead.

D = diffusion coefficient in solution.

c = concentration of metal ion in aqueous phase.

δ = film thickness.

At solution concentrations above 0.1 M, the ratio $\bar{D}/D < 10^{-2}$ and the rate determining step is particle diffusion. This implies that in an ion-exchange resin, usually mass transfer depends on bead parameters alone and not on concentration (see Equation 2).

In SX processes, mass transfer is dependent on many factors, such as interfacial surface, agitation, and concentrations in both aqueous and organic phases. Recent studies on the extraction of copper with LIX-64N show^(5,6,7) that the rate expression has a first order dependency on copper aqueous concentration. The dependence of the extraction rate into I-A on copper concentration in the aqueous phase (see Figure 4) suggests great resemblance to the SX process.

For F.D.C. processes, calculations⁽¹¹⁾ show that for a typical ion exchanger, setting $\bar{r} = 0.1$ cm, $\bar{c} = 2$ M, $\delta = 5 \times 10^{-3}$ cm and $D = 10^{-5}$ cm²/sec, the following $t_{1/2}$ values are obtained:

when

$$[M^{2+}] = 5 \times 10^{-3} \text{ M} : t_{1/2} = 40 \text{ min.}$$

$$[M^{2+}] = 5 \times 10^{-4} \text{ M} : t_{1/2} = 400 \text{ min.}$$

In comparison, for SIR resin I-A (see Figure 2)

when

$$[Cu^{2+}] = 0.24 \text{ M} : t_{1/2} = 2 \text{ min.}$$

$$[Cu^{2+}] = 0.01 \text{ M} : t_{1/2} = 7.5 \text{ min.}$$

In comparison, for resin I-C ($\bar{c} = 2.1$ M and $c = 0.05$ M), $t_{1/2} = 11$ min. (see Figure 2). This result implies that an ordinary type of chelating resin, having double the concentration of functional groups, shows a much smaller rate of mass transfer due to decreased ligand mobility. Finally, comparison between rates of copper extraction and elution (Figure 4) reveals that the elution reaction is much faster than the extraction reaction for both types of resins, namely for both I-A and I-C. The reason for this is

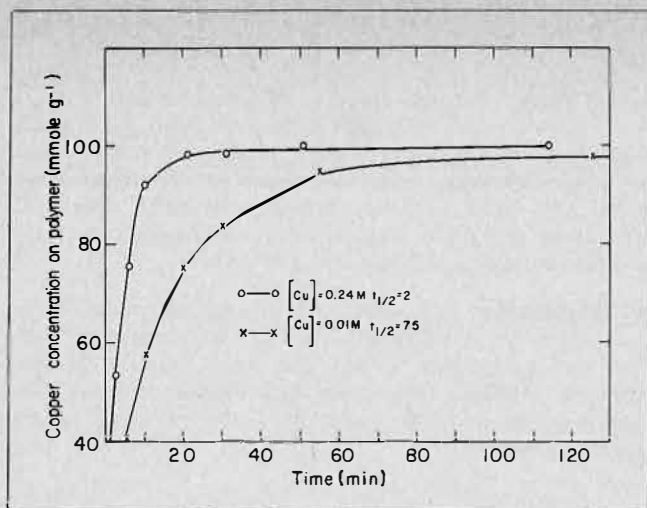


FIGURE 3. Extraction rate vs. concentration in solution 1-A on XE-305-PEG-600 = [1M] pH = 4.0.

probably the high ion-concentration during elution (0.5M) compared with 0.01-0.05M concentration of copper ions in the extraction stage.

Selectivity Factors

Selectivity factors for copper/iron for resins I-A and I-B are in the range of 500 depending on conditions, and the resins do not show any capacity for iron in the absence of copper. Resin I-C on the other hand has a considerable capacity (0.37 mmole Fe/g) for Fe^{3+} . Resins I-A and I-B do not extract other divalent ions, such as Zn, Ni and Co.

Phase-Separation, Physical Stability and Reagent Losses

Solvent-impregnated resins behave as ordinary resins; they are easy to handle, pack readily into columns and offer the ordinary advantages of resins. The problem of most concern is reagent losses by solubility. The solubility data presented in Table 1 are based on U.V. measurements and could vary in comparison to other methods.

The conclusion is that distribution coefficients are usually higher for polymers than for liquids. More significantly, when an organic-aqueous suspension representing a possible leakage mixture was passed through a fresh polymer, the reagent was recovered (see Table 2).

When solutions containing 10-15 ppm reagent were passed through columns XAD-2, XAD-4, or XE-305-PEG-600, the outgoing effluent was free of reagent.

In summary, the comparison between solvent impregnated resins I-A and I-B, and chelating resin I-C, are in favour of the SIR resins in most aspects such as metal-binding capacity, rate of metal binding, and selectivity over other ions. SIR resins compare favourably with solvent extraction reagents as they have high metal capacities, selectivity for copper over iron, and good rates of mass transfer.

REFERENCES

- (1) Ashbrook, A.W., *Coord. Chem. Revs.* 1975, 16, 285.
- (2) Warshawsky, A., *Trans. Inst. Min. Metal* 1974, 83, C101.
- (3) Warshawsky, A. and Patchornick, A., *The Theory and Practice of Ion Exchange*, S.C.I. Conference, Cambridge, 1976. M. Streat Ed., Paper No. 38.
- (4) Kroebe, R. and Meyer, A., *Proc. I.S.E.C. 1974*, SCI, London 1974, Vol. 3, 2025.

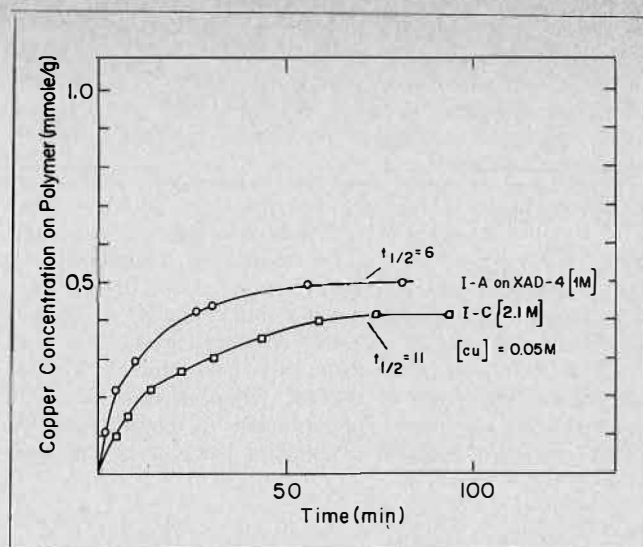


FIGURE 4. Rate of extraction/elution on XAD-4.

TABLE 1. Distribution Coefficients for Reagents I-B and LIX-64N.

Reagent (R)	Polymer (P) or solvent	[R/P]	Aqueous Solubility of Reagent $\times 10^{-3}$ [M]	Distribution Coeff. Do/A
I-B	XAD-4	1	0.02-0.1	$2 \times 10^2 - 5 \times 10^4$
I-B	toluene	0.03	0.16	2×10^2
LIX-64N	XAD-4	1	0.014	7×10^4
LIX-64N	toluene	1	0.014	7×10^4

TABLE 2. Recovery of Entrained Reagent on Fresh XAD-4.

Initial Reagent Concentration: 155 ppm of (3-aldoxime-4-hydroxy-4'-methyl) diphenylmethane in toluene-saturated water.
Volume: 30 ml Polymer: 1 g of XAD 4

Time of Contact (min)	Final Reagent Concentration (ppm)
5	146
15	54
70	24
80	15

- (5) Neelameggham, R., Ph.D. Thesis, Univ. of Utah, Salt Lake City, 1972.
- (6) Flett, D.S., Cox, M., and Heels, J.D., *Proc. I.S.E.C. 1974*, SCI, London 1974, Vol. 3, 2559.
- (7) Fleming, D.S., *Nat. Inst. Metal Report No. 1793*, 1976.
- (8) Flett, D.S., *Trans. Inst. Min. Metal* 1974, 83, C30.
- (9) Warshawsky, A., Patchornick, A. and Kalir, R., *South-African Patent 75/0641*.
- (10) Warshawsky, A., *Israel Patent Appl. 50120 (25.7.1976)*.
- (11) Helfferich, F., *Ion Exchange*, McGraw-Hill, N.Y. 1962, pp 255-277.

DISCUSSION

R.R. Grinstead: I agree that solvent-impregnated (SI) resins may offer the advantage of better kinetics of absorption over solid IX resins. I disagree that they are clearly better than solid IX in: 1. the *kinetics of stripping*; 2. the *reversibility*, or 3. the *selectivity*. Dow Chemical now offers two such copper-selective IX resins, which absorb Cu, Ni, Co and other ions quite reversibly, and can be stripped rapidly and easily with mineral acid or ammonia. The functional group is also quite selective

for copper over iron in forming the 1:1 complex. The observed selectivity is somewhat lower because iron is absorbed by an anion exchange mechanism. This problem can be and is being corrected, and resins with considerably better copper-to-iron selectivity should become available in the near future.

A. Warshawsky: Comparing with the paper by R.R. Grinstead et al, "New selective ion exchange resins for copper and nickel extractive metallurgy of copper", AIMM and Petroleum Engineers 1976), it is obvious that the resins reported, XF 4195 and XF 4196 are not thermodynamically selective for Cu^{2+} as Fe^{3+} is also absorbed, but is stripped prior to copper elution. This is due to the formation of the 1:1 complex since in rigid resins the 1:2 complex is possible due to ligand mobility. Unfortunately it is hard to compare rates since the data

in the article is not comparable, but values for elution in the order of 0.5-1 minute are hard to surpass.

K.S. Chung: I am interested in knowing whether some of your solvent-impregnated resin is miscible with water. If so, in my opinion, such resin may be used as a homogeneous resin to extract (or pre-concentrate) metal ions from aqueous solution with better specificity and simplicity than conventional, heterogeneous resin. Would you please elaborate on this respect?

A. Warshawsky: The resins are not miscible with water. Therefore, they are to be used as ordinary ion exchangers except that an adsorption column must be attached to recover lost organic reagent. The specificity of the "SIR" resins for Cu^{2+} ions is by far the highest measured.

CHEMISTRY OF SOLVENT EXTRACTION SYSTEMS

Selective Extraction of Alkali Halides by Crown Ethers

L. E. Asher and V. Marcus,
Department of Inorganic and Analytical Chemistry,
The Hebrew University, Jerusalem, Israel

ABSTRACT

*The alkali halides may be extracted from their aqueous solutions, or from brines containing alkaline earth halides, in a cyclic process in which no chemicals are consumed, with cyclic polyethers (crown compounds) in suitable anion-solvating solvents. This combination can act as a liquid membrane between a concentrated aqueous brine and water, so that only potassium chloride is transferred, the driving force being its high chemical potential in the brine. Results obtained for dibenzo-18-crown-6 in *m*-cresol for the extraction of sodium and potassium chloride, fluoride, bromide and iodide lead to conditional equilibrium constants. A computer program yields equilibrium concentrations for competitive extraction employing these constants, the initial concentrations and the volume ratio. It was applied to brines containing sodium, potassium, magnesium and calcium chlorides, as for instance brines connected with the Dead Sea processes. Factors governing the loss of the components to the aqueous phase and the extraction efficiency have been determined, and correlated with molecular properties.*

Introduction

THE REMOVAL OF THE ALKALI CATIONS from aqueous solutions by the use of crown compounds in non-polar solvents has been reported in the previous International Solvent Extraction Conference.⁽¹⁾ However, it was necessary to employ large anions, such as picrate or diphenylaminatate, in order to effect extraction. The halides would not extract under these conditions, and the aqueous phase is modified by the addition of the electrolytes providing the large anions.

Alkali halides can be removed from aqueous solutions by double exchange, with a cation exchanger in the hydrogen form and an anion exchanger in the hydroxide form. Nothing is added in this process to the aqueous solution, but for a cyclic process, the exchangers must be regenerated, and chemicals are consumed. Extraction processes can be based on this, with liquid ion exchangers, some of which are capable of exchanging hydrogen ions for alkali metal ions (e.g. dipicrylamine for potassium ions) and then removing the hydrogen halide formed with a long-chain amine. Again, for regenerating the reagents, chemicals are consumed in quantities at least equivalent to the alkali halides extracted. To avoid this, a solvating solvent should be used, which can solvate both ions as effectively as water does. This is possible for lithium salts at high concentrations, using long-chain alcohols⁽²⁾, but the heavier halides cannot be removed in this way. On the other hand, if iodine is added to cesium iodide the cesium triiodide formed may be extracted into a solvent like nitrobenzene (and removed therefrom with water), but this leaves excess iodine in the aqueous phase, and again, chemicals are consumed. The extraction of, say, sodium or potassium chloride in a cyclic process which does not leave any excess chemicals in the aqueous phase and in which no chemicals are consumed seems hopeless.

However, with the advent⁽²⁾ of cyclic polyethers (crown compounds), which selectively complex the alkali metals, in particular also sodium and potassium, new prospects emerged. These were realized by finding⁽³⁾ that with an anion-solvating solvent, such as an alcohol, the combination of crown ether/solvent can take care of the solvating requirements of both cation and anion, and remove both from the aqueous phase. It remained to look into the quantitative aspects of this extraction, and find out any regularities, which would permit the a priori selection of the best combination of crown ether/solvent for a given situation.

TABLE 1. Effect of Time of Shaking Together the Phases on Degree of Saturation of the Organic Phase (0.10M DBC/m-cresol, 0.10M KCl aq., 25°C).

Time, min.:	1	2	10	30	50	1100
Degree of saturation, %:	43.2	42.7	41.8	42.4	42.2	41.3

Experimental

Materials. Crown ethers were obtained from the Aldrich and Fluka companies, in addition to gifts from Dr. Frensdorff⁴. Icosahydrodibenzohexaoxacyclooctadecin (dicyclohexyl-18-crown-6, DCC) consisted of a mixture of isomers which was not resolved. Octahydrodibenzohexaoxacyclooctadecin (dibenzo-18-crown-6) DBC) was recrystallized from acetone, unless noted otherwise.

Procedures. The solvents and water were mutually pre-equilibrated prior to extractions, in order to avoid large volume changes. Known volumes of organic and aqueous solutions were shaken together in a thermostatic bath at 15.0, 25.0 and 40.0°C, allowed to settle in the bath and sampled. Survey equilibrations were made at room temperature (20±2°C) by vortexing solutions in test tubes, for 2-3 minutes. Sodium and potassium were determined by flame photometry (organic solutions were diluted with methanol) and the precision was within 2%, as found on duplicate samples and determinations generally made.

Results

The rate of reaching equilibrium was found to be rapid, and times of shaking together the phases of from 1 min. to 24 hr. were found not to affect the results. For instance, extraction of potassium chloride from its 0.10M aqueous solution with 0.10M DBC in m-cresol at 25°C gave the results in Table 1.

From the expected analytical error of up to 2% relative, the expected deviation of the degrees of saturation is ±0.8% from the mean 42.3, so that no significant effect can be detected in the results shown in Table 1.

Discrimination Against Extraction of Alkaline Earths

The combination DBC/m-cresol was found to be very effective for extracting sodium and in particular potassium chlorides from aqueous solutions (see below). It was tested, therefore, for its power to discriminate against the alkaline earths, magnesium and calcium. The solvent, m-cresol, extracts 0.002M salt from 4M magnesium chloride, and 0.0006M salt from 2M calcium chloride. In the presence of 0.10M DBC, the same amount of magnesium and 0.002M calcium chlorides are extracted. Successive application of a solution of 0.25M DBC/m-cresol to fresh samples of synthetic Dead Sea brines (0.19M KCl, 1.70M NaCl, 0.42M CaCl₂ and 1.70M MgCl₂) led to organic phases which did not contain more than 0.004M of the alkaline earths. In the following, therefore, extraction of calcium and magnesium chlorides is disregarded, since tests with other systems such as DBC/ benzyl alcohol or DCC/2-ethylhexanol, gave similar results.

Extraction of Potassium and Sodium Chlorides

The extraction of sodium and potassium chlorides with DBC dissolved in different solvents was measured over a range of aqueous concentrations up to near saturation. The results for the range below 0.36M (equilibrium con-

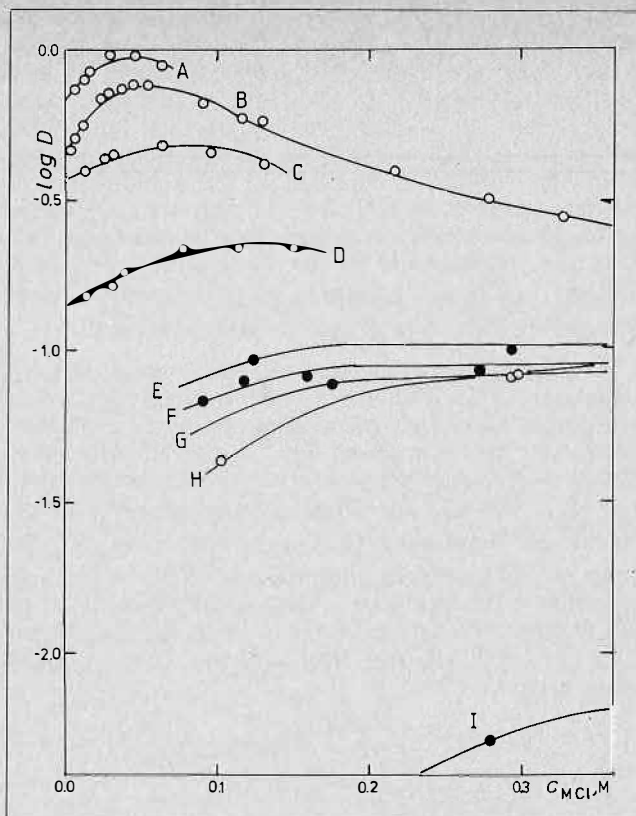
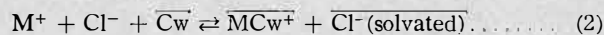


FIGURE 1. Log \underline{D} for KCl or NaCl between 0.10M DBC and aqueous solutions. KCl/m-cresol: A-15°, B-25°, C-40°; KCl/benzyl alcohol: D-25°; NaCl/m-cresol: E-15°, F-25°, G-40°; p-nonylphenol at 40°: H-KCl; I-NaCl. The curves are calculated from eqs. (1) and (5).

centrations) are shown in Figure 1. These and the results for higher concentrations conform to the equation⁽⁶⁾

$$\underline{D} = \underline{a}_{\pm} [M^+]^{-1} [\overline{Cw}] (K_1' [\overline{Cw}]^{-1/2} + K_2' \underline{a}_{\pm}) \dots \dots \dots (1)$$

where \underline{D} is the distribution ratio, \underline{a}_{\pm} the mean activity of the salt in the aqueous solution, square brackets the molar concentration, M^+ the metal cation, \overline{Cw} the crown ether, a bar over the symbol, the organic phase, and K_1' and K_2' are two conditional equilibrium constants. They pertain to the extraction reactions,



for extraction as separated ions, and



for extraction as ion pairs, respectively. The free crown ether concentration is obtained by difference at low saturations,

$$[\overline{Cw}] = \overline{c}_{Cw} - \overline{c}_M = \overline{c}_{Cw} - \underline{D}[M^+] \dots \dots \dots (4)$$

where c is the total molar concentration, and from

$$[\overline{Cw}] = \{ [(K_1' \underline{a}_{\pm})^2 + 4\overline{c}_{Cw} (1 + K_2' \underline{a}_{\pm}^2)]^{1/2} - K_1' \underline{a}_{\pm} \} / 4(1 + K_2' \underline{a}_{\pm}^2) \dots \dots \dots (5)$$

generally at any saturation. The conditional constants are obtained from,

$$\underline{D}[M^+] \underline{a}_{\pm}^{-1} (\overline{c}_{Cw} - \underline{D}[M^+])^{-1/2} = \frac{K_1' + K_2' \underline{a}_{\pm} (\overline{c}_{Cw} - \underline{D}[M^+])^{1/2}}{K_1' + K_2' \underline{a}_{\pm} (\overline{c}_{Cw} - \underline{D}[M^+])^{1/2}} \dots \dots \dots (6)$$

employing the results at low saturations of the organic phase. The results, expressed as the conditional constants, are shown in Table 2.

Curves calculated from these constants and eqs. (1) and (5) agree well with the data. The solvent p-nonyl phenol is too viscous at 25°C to permit its use, but it could be employed either at 40°C or diluted to 75% by volume, with toluene. Both raising the temperature and dilution reduce the extractive power, but the selectivity for potassium over sodium is maintained. The temperature dependence leads⁽⁵⁾ to enthalpy and entropy of extraction values for the extraction as separate ions and as ion pairs described, respectively, by the conditional constants K'_1 and K'_2 , which are consistent with those obtained for complexing the cations in homogeneous solutions⁽⁶⁾.

A computer program was written⁽⁷⁾, permitting the calculation of the equilibrium concentrations when sodium and potassium are co-extracted from brines containing, eventually, also magnesium and calcium chlorides. As input data, it is necessary to insert the initial concentrations c_{Na}^0 , c_{K}^0 , c_{Cl}^0 and c_{Cw}^0 , the phase volume ratio V , and the conditional constants $K'_{i,M}$ ($i = 1, 2; M = Na, K$). The program includes general information on the activity coefficients of the four salts in aqueous solutions, alone and in mixtures, required for calculating a_{\pm} appearing in eqs. (1), (5) and (6). The program then calculates iteratively,

$$D_M = \frac{K'_{M1} y_{\pm MCl} c_{MCl}^0 X Y A^{-1/2} + K'_{M2} y_{\pm MCl} c_{MCl}^0 X^2 Y^2}{\dots} \quad (7)$$

$$X = \frac{[(AY^2 + 4Vc_{Cw}^0(1 + BY^2))^{1/2} - \frac{A^{1/2}Y}{2(1 + BY^2)}]}{\dots} \quad (8)$$

$$Y = (c_{Cl}^0 - X^2 - Vc_{Cw}^0)^{1/2} \quad (9)$$

$$A = \frac{K'_{K1} y_{\pm KCl} c_{KCl}^0 (1 + D_{KV})^{-1} + K'_{Na1} y_{\pm NaCl} c_{NaCl}^0 (1 + D_{NaV})^{-1}}{\dots} \quad (10)$$

$$B = \frac{K'_{K2} y_{\pm KCl} c_{KCl}^0 (1 + D_{KV})^{-1} + K'_{Na2} y_{\pm NaCl} c_{NaCl}^0 (1 + D_{NaV})^{-1}}{\dots} \quad (11)$$

Table 2. Conditional Constants K'_1 and K'_2 for Extraction of Sodium and Potassium Chlorides with DBC.

Salt	Solvent	Temp. °C	$K'_1, M^{-1/2}$	K'_2, M^{-2}
KCl	m-cresol	15	2.0	324
KCl	m-cresol	25	1.40	223
KCl	m-cresol	40	1.25	70
KCl	benzyl alcohol	25	0.46	24.5
KCl	p-nonyl phenol (75%)	25	<0.1	3
KCl	p-nonyl phenol	40	0.11	3.6
NaCl	m-cresol	15	0.28	4.4
NaCl	m-cresol	25	0.23	3.8
NaCl	m-cresol	40	0.26	2.8
NaCl	p-nonyl phenol	40	<0.01	0.36
KF	m-cresol	25	4.1	915
KBr	m-cresol	25	1.3	246
KI	m-cresol	25	1.6	376

TABLE 3. Comparison of Calculated and Observed Distribution Ratios for Coextraction of Potassium and Sodium Chlorides from a Magnesium Chloride Brine by DBC/m-cresol at 25°C.

C_{MgCl_2}, M	C_{KCl}, M	C_{NaCl}, M	$D_{KCl}(obs.)$	$D_{KCl}(calc)$	$D_{NaCl}(obs.)$	$D_{NaCl}(calc)$
0.50	0.0046	0.049	8.0	8.0	66	33
	0.0162		4.0	3.9		
	0.056		1.51	1.40		
1.00	0.0035	1.25×10^{-3}	13.5	15.1	66	33
	0.0203		3.9	4.5		
	0.110		0.83	0.93		
4.4	0.0067	1.32×10^{-4}	9.0	9.0	66	33
	1.32×10^{-4}		480	450		

$$y_{\pm MCl} = \gamma_{\pm MCl} (1 - 0.015 c_M^0)^{1/2} (1 + D_M V)^{-1/2} + 0.001 \frac{M_{MCl} c_M^0}{c_M^0} (1 + D_M V)^{-1} \quad (12)$$

$$\ln \gamma_{\pm MCl} = \ln \gamma_{\pm MCl}^0 + (1/2) \sum_i (I_i/I) [z_i^{-1} \ln \gamma_{\pm MCl} - \ln \gamma_{\pm}] \quad (13)$$

$$\ln \gamma_{\pm MCl}^0 = -S I^{1/2} (1 + a_M I^{1/2})^{-1} + 2b_M I + (3/2) c_M I^2 + (4/3) d_M I^3 \quad (14)$$

$$I = [3(c_{Cl}^0 - (c_{K}^0 + c_{Na}^0)) + Y^2] / (1 - 0.15 \sum_M c_{MCl}^{1/2} + 0.001 \sum_M M_{MCl} c_{MCl}) \quad (15)$$

In these equations, A , B , X and Y are auxiliary functions, y_{\pm} the activity coefficient on the molar scale, γ_{\pm} that on the molal scale (in mixtures of ionic strength I) and γ_{\pm}^0 for pure solutions (of the same ionic strength), and S , a_M , b_M , c_M and d_M known⁽⁸⁾ coefficients. The final results are D_M ($M = Na$ and K), the equilibrium aqueous concentrations c_{NaCl} and c_{KCl} , and an enrichment factor $\alpha_{K/Na} = (c_{KCl}/c_{NaCl}) / (c_{KCl}^0/c_{NaCl}^0)$. A comparison of some calculated results with experimental data is shown in Table 3.

In other coextraction experiments, from synthetic Dead Sea brines, enrichment factors $\alpha_{K/Na}$ of above 17 were obtained from the second successive extraction on fresh aqueous samples, the organic concentration of potassium chloride building up to more than that initially in the aqueous feed, the 0.25M DBC/m-cresol becoming saturated by the alkali chlorides.

Extraction of Potassium Salts Other than Chloride

Distribution ratios were obtained for the extraction of potassium sulfate, chloride, bromide, iodide, nitrate, acetate and fluoride from their 0.10M aqueous solutions into 0.10M DBC in m-cresol at 25°C. The distribution ratios increase in the order given above.

Detailed data for the bromide, iodide and fluoride salts, along with those for the chloride, are shown in Figure 2. The conditional extraction constants obtained from these constants are included in Table 2. The extractability of the chloride, bromide and iodide correlate with the decreasing difficulty of removing these anions from their hydration environments, measured by their Gibbs free energies of hydration. The extraordinary good extractability of fluoride, on the contrary, must be connected by its high ability to hydrogen-bond to the rather acidic phenolic hydrogen of the m-cresol^(5,9).

Choice of Crown Compound

The following crown compounds were tested for their selective extraction of potassium and sodium chlorides (all

TABLE 4. Efficiencies of Solvents for Extraction of Potassium Chloride with 0.10M DBC at 20°C. Also given are the DBC Solubilities in the Solvents.

Solvent	$\log K'_2$ for 0.10M KCl	$\log K'_2$ for 1.00M KCl	solubility of DBC, M	$\Sigma\pi$ of solvent
nitrobenzene		-1.10	0.194	
benzonitrile		-0.97	0.120	1.56
acetophenone		-0.90**	0.072	1.58
benzaldehyde		-0.16**	0.073	1.48
aniline	0.80	0.66	0.222	0.90
benzyl alcohol	1.14**		0.075	1.10
m-cresol	2.35	2.20	0.314	2.06
o-chlorophenol	2.37			2.16
2,4-xyleneol	4.35*			2.23

*Approximate value, estimated from that for DCC by subtracting 0.15 (the mean difference shown by m-cresol and o-chlorophenol).

**Supersaturated solutions.

being of the 18-crown-6 type); unsubstituted 18-crown-6 (C), cyclohexyl-18-crown-6 (CC), dicyclohexyl-18-crown-6 (isomer mixture DCC), dibenzo-18-crown-6 (DBC), bis(tertiarybutylbenzo)-18-crown-6 (BTBC) and dibromobenzo-18-crown-6 (DBrBC). The compounds C and CC are unsuitable for extraction, because of their excessive water solubility, and therefore loss from the organic phase. The others show small to negligible losses. The loss was found to depend on the solvent; it was greater from 2-ethylhexanol than from benzylalcohol solvents. For DBC in the latter it was 0.005%, for the even less aqueous-soluble BTBC from the former it was 0.07%. For DCC in either solvent the loss was somewhat greater, although precise values are not available. (Indirect measurement had to be resorted to, via extractability of picrate to chloroform from the aqueous phase, containing the lost DCC). It is evident that DBC and, even more, its substitution products BTBC and DBrBC would show entirely negligible losses through solubility in the aqueous phase, and that any losses in a process would be mechanical entrainment only.

More detailed comparisons of extraction efficiencies were conducted on DBC and DCC. For the following solvents, in which both are soluble: methylene chloride, chloroform, nitrobenzene, benzonitrile, acetophenone, benzaldehyde, aniline and benzy alcohol, a constant difference of 0.93 ± 0.16 in $\log K'_2$ (reaction 3) in favor of DCC was found for the extraction of potassium chloride. This difference is comparable with the difference between the homogeneous complexing constants of potassium with these two solvating ligands⁽⁶⁾. This shows that the solvent plays a role in the reaction⁽³⁾ which has nothing to do with the crown ether or the cation side of the ion pair. However, for the more acidic solvents, m-cresol and o-chlorophenol, the difference in $\log K'_2$ is reduced to 0.15 only, because the solvent solvates the oxygens of the crown ether by hydrogen bonding, and exerts a regulating effect through this.

Choice of Solvent

It was found⁽⁵⁾ that a good correlation exists between the solvent efficiency, measured through $\log K'_2$ for situations where ion-pair extraction predominates, and the Gibbs free energy of transfer of chloride ions from water to the solvent, $\Delta G_{tr}^\circ(\text{Cl}^-, \text{H}_2\text{O} \rightarrow \text{S})$. This quantity is available for few solvents directly, but can be estimated from other properties, such as the E_T index for betaine absorbance⁽¹⁰⁾. Table 4 lists the better solvents and the values of $\log K'_2$ obtained from extraction with 0.10M DBC in the solvent at 25°C from 1.00 or 0.10M aqueous potassium chloride. Only aromatic solvents were found to give sufficient solubil-

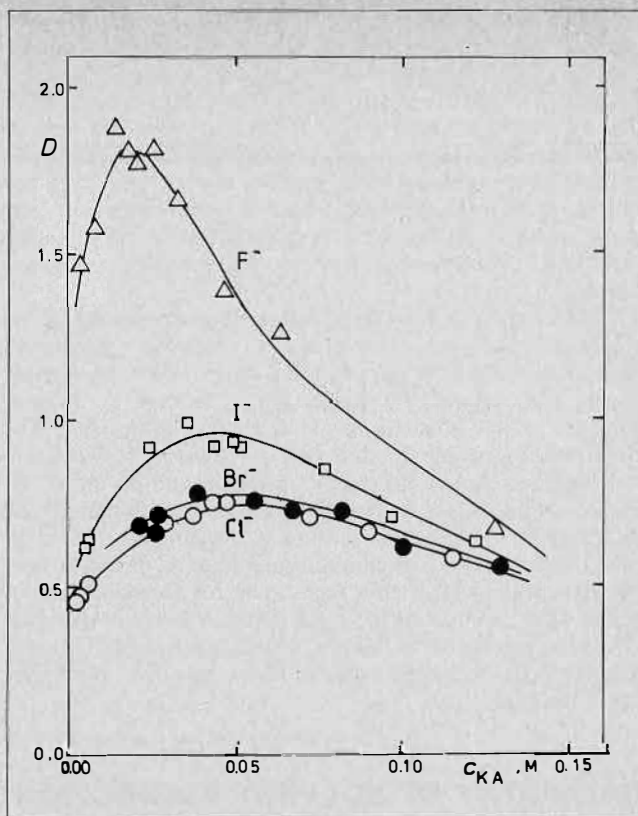


FIGURE 2. D for potassium halides between 0.10M DBC/m-cresol and aqueous solutions at 25°. The curves are calculated from eqs. (1) and (5).

ity for DBC to permit extraction with 0.10M solutions (see Table 4). Many more solvents are suitable for use with DCC: pentanoic acid, hexanoic acid, hexanol, 1-octanol, 1-decanol, cyclohexanone, 2-ethyl hexanol, 2-octanol, 2-ethylhexanoic acid show $\log K'_2$ values decreasing from 1.95 to -0.14 in the order given. However, the loss of DCC to the aqueous phase might be appreciably larger than that of DBC. The solubilities of the crown ethers in the solvents and in water may be estimated approximately⁽⁵⁾, using the solubility parameter, 11.0 for DBC, and the tabulated values for the solvents, and from hydrophobic group contributions $\pi^{(11)}$, wherefrom $\Delta(\Sigma\pi)$ for DCC and DBC is 2.0, the latter being the more hydrophobic. Solubilities of the solvents in water are also available, and when not, again $\Sigma\pi$ values⁽¹¹⁾ may be resorted to. These would be approximate indices to solvent losses from aqueous solubility, the loss decreasing the higher $\Sigma\pi$.

Conclusion

The rapid and efficient extraction of the alkali chlorides from their aqueous solutions with suitable crown ether/solvent combinations has been demonstrated. Attention was focused on the extraction of sodium and potassium chloride, particularly the latter, but extraction of the bromide, iodide and especially of the fluoride was found to be even more effective. The extraction is governed, obviously, by the crown compound concentration $[C_w]$ in eq. (1), so a high solubility is desirable, and the relationships furthering this have been determined. It is governed also by a high activity of the alkali halide, a_{\pm} in eq. (1), and this can be provided by the less extractable salt, say NaCl, in the extraction of KCl from NaCl + KCl mixtures, or by alkaline earths in the extraction from some natural and industrial brines, such as Dead Sea water. If no foreign salt is present, then the a_{\pm} provided by the sodium chloride or

the potassium chloride alone is sufficient for efficient extraction by a suitable crown compound/solvent combination. It is this combination which leads to high values of K'_1 and particularly K'_2 in eq. (1), and data for choosing the appropriate crown ether (from the point of view of solubility, loss to aqueous phase, selectivity for K versus Na and cation complexing ability) and of the solvent (from the points of view of solubility, loss to aqueous phase, and anion solvating ability) have been provided. A combination can thus be tailor-made for any alkali halide extraction problem.

A process⁽³⁾ can thus be based on these properties of the crown-ether/solvent combination, whereby potassium chloride is selectively removed from brines into the organic phase, and stripped by water, the difference in thermodynamic activities, $a_{\pm KCl}$, providing the driving force. The crown-ether/solvent combination is recycled between the two aqueous phases of feed and product, and no chemicals are consumed. The crown-ether/solvent combination can therefore be incorporated into a liquid membrane by established technology. A preliminary experiment demonstrated the effectiveness of such a membrane for Dead Sea water. Other applications, such as purification of a magnesium chloride solution from alkalis which are harmful for the magnesia produced therefrom, or in selective electrodes come to mind.

REFERENCES

- (1) Danesi, P.R., Tusek, L., and Scibona, G., Proc. ISEC 1974, 2, 1761; Rais, J., Krys, M. and Kadlecova, L., Proc. ISEC 1974, 2, 1705.
- (2) Marcus, Y., J. Chem. Eng. Data, 1975, 20, 141; J. Phys. Chem., 1976, 80, 2451.
- (3) Pedersen, C.J., J. Amer. Chem. Soc., 1967, 89, 7017.
- (4) Asher, L.E. and Marcus, Y., Proc. 25th IUPAC Congress, Jerusalem, July 1975; Israel Pat. Appl. No. 47198, April 1975.
- (4a) Dr. H.K. Frensdorff, of DuPont, Inc., is thanked for these gifts.
- (5) Marcus, Y., and Asher, L.E., submitted for publication, 1977.
- (6) Izatt, R.M., Eatough, D.J. and Christensen, J.J., Structure and Bonding, 1973, 16, 161.
- (7) Dr. Z. Kolarik, Kernforschungszentrum Karlsruhe. is thanked for help with the program.
- (8) Lietzke, M.H., and Stoughton, R.W. J. Phys. Chem., 1962, 66, 508; J. Soln. Chem., 1972, 1, 299.
- (9) Taylor, R.P., and Kuntz, I.D., Jr., J. Am. Chem. Soc., 1972, 94, 7963; Kenjo, T., Brown, S., Held, E., and Diamond, R.M., J. Phys. Chem., 1972, 76, 1775.
- (10) Krygowski, T.M., and Fawcett, W.R., J. Am. Chem. Soc., 1975, 97, 2143; Dimroth, K., Reichert, Ch., Srepmann, T., and Bohlmann, Ann. Chem., 1963, 661, 1.
- (11) Hansch, C., Quinlan, J.H., and Lawrence, G.L., J. Org. Chem., 1968, 33, 347.

CHEMISTRY OF SOLVENT EXTRACTION SYSTEMS

Potential Exploitation of Fundamental Properties of Multi-Component/Multi-Phase Systems, for Achieving Less Common Separations in Inorganic Chemical Processing

Ruth Blumberg,
IMI — Institute for Research and Development,
Haifa, Israel.

ABSTRACT

Current work in solvent extraction is self-restricting when it comes to extending the scope of its application in inorganic chemical processing.

A means of broadening the approach to the field is presented, based primarily on the concept of invariant systems as inherent in the Gibbs phase rule. This is illustrated with examples of water transfer, salt and acid extractions, where solute-solute, solute-water, solute-solvent interactions need be considered.

Introductory

IN INORGANIC CHEMICAL PROCESSING, solvent extraction applications have been classified either according to the object, e.g. copper extraction, phosphoric acid purification, or according to the operation, e.g., ion exchange, metathetic salt/acid reactions, separations of

metal values, etc. As the field of solvent extraction has matured, with the successful implementation of solvent extraction processes, there is an increasing tendency to stay within the framework of proven fields and only to expand by making second order changes to achieve specific objectives. The leading question asked now is not "what can one do by solvent extraction?" but rather "can one separate A from B, or recover C, by a solvent extraction technology?"

Solvent extraction research has become essentially "intensive" in character, rather than "extensive"; as a result, the study of solvents and their potential seems to have decreased, and considerable effort goes instead into studies which have little general applicability. Analogies are sought only infrequently, and the lessons learned and the approaches developed in one field of solvent extraction seem to be applied only to a very limited extent to other fields. Individual limitations of scope and interest seem also to restrict the possibilities of cross fertilisation by using analogies from essentially different fields.

Even though the range of solvent candidates is large, the types of organic compounds actually used as bulk

solvents are relatively limited. This lack of exploitation of solvent potential is surprising, even when taking into account the constraints of commercial availability and costs. All in all, the solvent types which have found practical application are very few. Groups of polar compounds seem to have been overlooked. Thus, while the significance of solvent polarity in solvent extraction is well accepted, its exploitation in practice, for inorganic processing and separations, is very limited. In a few specific cases the skills of the synthetic organic chemist have been successfully applied in modifying selected extractants towards optimisation, or in tailoring compounds to test certain postulates; this symbiosis of solvent extraction expertise with synthetic finesse and skill is, however, the exception rather than the rule.

In its broadest sense, solvent extraction can be classified together with volatilisation and precipitation as a separation technique entailing mass transfer across a phase boundary. Since it is essentially a reversible transfer system at equilibrium, any phase can be selected to describe the system as a whole. By definition, solvent extraction requires that two liquid phases be present, but there is no other limit a priori on the number of phases; a limitation is placed, however, by the Gibbs phase rule. The rigorous definition of a multi-phase/multi-component system in liquid/liquid extraction is always difficult and often quite impracticable. Fortunately, however, such systems can usually be manipulated towards specific aims without the need for rigorous and detailed characterisation. In the final instance, if the system at equilibrium is invariant within the meaning of the phase rule, any single liquid phase defines the system completely. In the same vein it is possible to make a system invariant by pre-selecting the levels of the appropriate number of specific parameters. Then, by inspection one liquid phase can be chosen to characterise the whole system. It seems, therefore, that a more generalized approach to systems involving solvents and multi-phase/multi-component solvent extraction is possible which is less dependent upon extensive equilibrium data.

Once we accept the premise that liquid/liquid extraction is a separation technique based on transfer across a phase boundary, it follows logically that all expedients for favouring such transfer are legitimate, provided that technological and economic feasibility are not sacrificed in the final instance. This also leads logically to the inspection of systems to identify controlling parameters for exploitation in mass transfer.

Water Transfer

For our purposes we can say that in inorganic processing all liquid/liquid extractions have in common the fact that an aqueous solution constitutes one of the phases, and that the second liquid phase consists of, or contains, an organic component which is loosely defined as the solvent or extractant. Since water is such an effective solvent for ions and polar molecules, the degree to which water itself distributes between the phases may be of considerable significance in defining the characteristics of transfer, and in determining the separation that can be attained. Thus the activity of water may be not less important a parameter than the concentration of the solutes nominally being separated in the specific extraction process. In the appropriate cases water can be regarded as essential in the mechanism of transfer between the phases.

One measure of the extent to which water can be transferred to or from a system, is the partial pressure of water in the system; this also defines the thermodynamic activity of water in that system. A very elegant and original exposé of this has been presented within the

TABLE 1. Vapour Pressure of Water as a Measure of Water in Solvent⁽⁴⁾

Systems:		K ₂ CO ₃ /H ₂ O/Cyclohexanol	
Temperature:		40°C	
Aqueous Solution wt % solute	Vapour Pressure H ₂ O mm Hg	Solvent Phase wt % water	cations meq/g
K ₂ CO ₃			
zero	55.3	11.7	—
30.8	47.6	6.1	—
42.4	38.3	4.1	—
51.8	27.6	2.3	0.005
MgCl ₂ *			
23.5	42.0	5.1	0.03
34.2	25.0	6.3	0.54

*The measurements were made with natural brines containing also CaCl₂ as a secondary component.

framework of utilising liquid/liquid extraction as a means of concentrating brines without evaporation⁽¹⁾. Essentially, this was also the factor exploited in the studies on water desalination by solvent extraction⁽²⁾. In both cases the relative quantity of water transferred goes down as the salinity of the aqueous phase goes up. The interaction between solute and water thus becomes significant and may express itself either in the fact that the solute holds back the water from transferring, or that the solute and water are co-transferred.

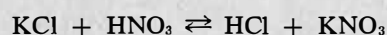
In Table 1, two cases are presented spanning similar ranges of vapour pressure. The levels of hydration in conjugate solvent phases are comparable provided solute does not transfer. At high magnesium chloride concentration there is considerable salt transfer; this is not the case with potassium carbonate, hence in the former case the water content of the solvent goes through a minimum as the aqueous phase concentration increases.

When there is no special bonding between the solute and solvent, i.e. only water transfers across the boundary, then the water levels in various solvents reflect the ionic strength of the aqueous phase and can be used as a measure of the partial water vapour pressure in brines⁽¹⁾. When there is a specific interaction between solute and solvent, the water activity alone no longer suffices for defining the equilibrium system, H₂O/solute/solvent, as a whole. At the same time, the distribution coefficient of the solute which relates to its concentration in the conjugate phases also does not define the system. In a labile interacting system of a multiple number of components and phases, the distribution coefficient may lose its practical usefulness unless some auxiliary device is applied for defining the state of the system.

Here the phase rule, with its definition of degrees of freedom and invariant compositions, can be utilised to great advantage. Even in the simplest system, as described in relation to water transfer, the invariant aqueous solution in the presence of its solid phase defines a real limit of transfer, and this provides a basis for comparison, either among solvents or among aqueous phases. This can be seen in Table 2 where hydration levels for three solvents are compared.

Invariant Systems

The concept of mass transfer at invariant composition is readily utilized also for defining more complex systems. The metathetic reaction:



for converting potassium chloride into potassium nitrate by employing a solvent for separation of acids from salts⁽³⁾ is a case in point. When both solids and a saturated brine are present along with the conjugate organic phase, there are three degrees of freedom according to the phase rule; by fixing the temperature, pressure and acidity in one phase, the system becomes invariant. This provides a valid reference state for comparing and evaluating solvents for the purpose of this conversion.⁽⁴⁾ A number of solvents is compared in Table 3; the effect of temperature and acidity is shown in Table 4.

Metathetic reactions of this type, with polyvalent acids which can produce acid salts, e.g. H_2SO_4 or H_3PO_4 , would be extremely difficult to evaluate were it not possible to select invariant points. In this connection it is clear that the aqueous phase can be uniquely determining; hence by inspection of the solubility data, fixed points suitable for

TABLE 2. Water Content of Butanone, Butanol-1, Butanol-2, in Equilibrium with Saturated Solution of Salts⁽¹⁾ -30°C

Solute	Vapour Pressure mm Hg	Butanone	Butanol-1 gH ₂ O/100g solvent	Butanol-2
None	31.8	14.2	26.0	53.6
K ₂ SO ₄	30.8	13.3	20.7	34.8
CuSO ₄ · nH ₂ O		13.4	20.3	33.8
KNO ₃	29.2	8.5	15.5	21.7
KCl	26.6	6.3	10.4	11.2
NH ₄ Cl	24.5	4.9	9.3	10.6
NaCl	23.9	4.1	7.4	8.7
NaBr	19.7	2.4	5.7	5.3
Ca(NO ₃) ₂	14.9	2.6	8.9	7.2
MgCl ₂	10.3	1.4	26.9	10.4
Solubilities: equivalents solute/litre solvent phase				
Ca(NO ₃) ₂		—	1.0	0.23
MgCl ₂		—	2.2	0.75

TABLE 3. Solvent Screening under Invariant Conditions for the Metathetic Reaction:⁽⁴⁾

NaCl + HNO₃ ⇌ HCl + NaNO₃
Both Solids Present, Fixed H⁺ level in aqueous phase, Fixed temperature

Solvent Mixture 1 : 1 vol. ratio	Aqueous H ⁺ wt %	H ₂ O	Organic H ⁺ wt %	Cl ⁻	D _{H⁺} org. aq.	Equi- valent Ratio Cl ⁻ /H ⁺
i-amyl alcohol	0.07	8.0	0.17	1.3	2.5	0.22
" + 1,5-pentanediol	0.07	11.5	0.19	1.8	2.7	0.27
" + tetrahydrofuran	0.07	9.9	0.22	0.85	3.1	0.11
" + methylethylketone	0.06	9.6	0.17	1.0	2.8	0.16
" + dibutyl sulfoxide	0.06	7.0	0.19	>0.2	3.4	very low

TABLE 4. Effect of Temperature and Acidity on Conjugate Phase Compositions⁽⁴⁾

System: K⁺ H⁺ NO₃⁻ Cl⁻ H₂O/n-Pentanol [Invariant, in presence of 2 solids: KNO₃ and KCl at fixed acidity level in aqueous phase and selected temperatures.

Temp. °C	Aqueous wt %					Solvent wt %				
	H	K	Cl	NO ₃	H ₂ O	H	Cl	NO ₃	H ₂ O	Pentanol
7	0.15	9.0	10.2	5.7	75	0.08	1.9	1.5	10.6	86
	0.29	5.3	12.1	5.5	77	0.16	3.9	2.9	13.7	79
20	0.14	11.7	10.9	7.9	69	0.09	1.8	1.6	9.7	87
	0.27	8.0	12.1	8.1	71	0.16	3.2	4.2	12.4	80
30	0.12	14.6	11.0	11.5	68	0.09	1.8	2.7	9.4	86
	0.25	10.4	11.9	11.2	66	0.17	3.0	5.2	11.7	80

comparison of solvents can be selected. This is seen from the two examples in Table 5, (a) and (b).

The utilisation of invariant compositions deriving from a multiplicity of solid species in multi-component/multi-phase systems with only one liquid phase (and that an aqueous brine) is truly classic, e.g. as presented by D'Ans⁽⁶⁾ for salts of the oceans, or as utilised in recovering salts from brines of the Dead Sea⁽⁷⁾. This has been extended, above, to the case with two liquid phases, where an additional component (solvent) has been added and an additional phase is present, thus maintaining the invariance of the system. A similar approach to systems with multiplicity of liquid phases only has hardly been considered.

Systems in which one aqueous and two solvent phases are present become invariant if the degrees of freedom are reduced by fixing selected parameters such as significant concentrations and temperature. Table 6(a) and (b) shows a selection of such cases previously published⁽⁸⁾. Table 6(a) shows acid-water-ether systems which are truly invariant when a second organic phase appears. At fixed temperature and pressure, the overall compositions given fall just outside or just inside the three phase regions. In Table 6(b) the aqueous phase is essentially specified, being a saturated solution; hence at fixed temperature and pressure and preselected diluent-amine ratio, the system becomes invariant when two organic phases appear, namely an amine hydrochloride-rich and an amine-rich phase, respectively.

The separation of a second solvent phase constitutes a second liquid/liquid interface for mass transfer, hence, by definition, it provides a more sophisticated separation system. This opens up a whole field for study, since "the when and the where" of second organic phase formation, let alone "the why and the how", are only partially understood.

Salt Extraction

The extraction of salts by polar solvents has received very little attention. Starting with the direct solubility of anhydrous or hydrated species in specific solvents, and going on from there to consider the distribution of salts between solvent and aqueous phases, can give useful indications of separation possibilities. Such data, however, will by no means give the whole picture, nor can conclusions be derived directly from them. The distribution of salts between brines and organic solvents frequently shows unexpected trends because of the strong interactions among the species involved. It has been shown, with alcoholic solvents, that utilization of the separation factors between magnesium and calcium and between bromide and chloride permits obtaining separate streams of MgCl₂ and MgBr₂ from a multicomponent halide brine⁽⁹⁾. In

TABLE 5. Invariant Systems

(a) $KCl + H_3PO_4 \rightleftharpoons KH_2PO_4 + HCl$ ^{5a)}, 2 solid phases ($KH_2PO_4 \cdot H_3PO_4 + KCl$), 2 liquid phases (aqueous, solvent), ambient temperature

Solvent	Organic Phase Compositions		
	H ₃ PO ₄	HCl wt %	H ₃ PO ₄ /HCl Molar Ratios
Dibutyl carbitol	48	3.5	7.4
Dibutyl ether	10	0.7	5.5
n-Butanol	46	3.8	9.0
Cyclohexanol	39	3.6	3.6
i-Amyl alcohol	38	3.9	2.8
n-Octanol	29	3.5	0.05

(b) $KCl + H_2SO_4 \rightleftharpoons K_2SO_4 + HCl$ ^{5b)} Acidity level determines solid phases present. ambient temperature

Solid Phases	Aqueous		Solvent pentanol		
	H ⁺ meqs/g	Cl ⁻ meqs/g	H ⁺ meqs/g	Cl ⁻ meqs/g	H ₂ O wt %
KCl + KH ₂ SO ₄	4.82	3.02	1.78	1.57	13
KCl + KH ₂ SO ₄ + K ₂ SO ₄	2.67	2.4	0.75	0.71	11
KCl + K ₂ SO ₄	1.8	2.7	0.41	0.48	10

TABLE 6. Two and Three Liquid Phase Systems ⁽⁶⁾

a) Acid-Water/Ethers, Temperature — 30°C, all compositions as weight per cent

System Overall Composition	Phase	Aqueous		Organic	
		Bottom		Middle	Top
		H ₃ PO ₄	56	69	
H ₂ O	22	29		0.5	
i-propyl ether	22	2		95.0	
H ₃ PO ₄	58	70	45	5.0	
H ₂ O	20	28	8	0.5	
n-propyl ether	22	2	47	94.5	
H ₂ SO ₄	50	63		3	
H ₂ O	27	33		—	
n-butyl ether	23	4		97	
H ₂ SO ₄	51	63	36	4	
H ₂ O	24	32.5	10	—	
n-butyl ether	25	4.5	54	96	

b) NaCl — HCl — H₂O/tertiary amine

tri-lauryl amine	Saturated with NaCl	25	
tri-lauryl amine . HCl		25	
n-Pentanol		50	
tri-lauryl amine	Saturated with NaCl	12	85.5
tri-lauryl amine . HCl		37	1.5
n-Pentanol		51	13

addition, the strong interaction of chloride on bromide in the system leads to the eventual concentration of the bromide many-fold. Table 7 shows a comparison of distributions of single salts for a number of alcohols, while Table 8 shows the strong interaction between chloride and bromide. In Table 9 comparative distribution data are given for sodium, calcium and magnesium chlorides using butyl lactate as the solvent.

The existence of solvent-ion interactions is well recognized, e.g. Na and K are rarely extracted, while Ca and Mg are readily extracted. What is perhaps less accepted is that in specific cases the order of extraction may be altered by virtue of the interaction. Tables 7, 8 and 9 taken together exemplify a whole range of interactions in salt transfer. Apart from alkali and alkaline earth chlorides which are among the salts most prevalent in natural brines, polar solvents can extract various other salts from aqueous halide media. Table 10 presents a selection of distribution

TABLE 7. Partition Coefficients of Pure Halides between Alcoholic Solvents and Water ⁽⁴⁾

Aqueous Solutions Conjugate conc. eqs/l	CaCl ₂ 9.86	CaBr ₂ 9.55	MgCl ₂ 6.8
Solvents	Distribution Coefficients of Salts $\frac{D_{org}}{aq}$		
n-butanol	0.14	0.39	0.53
i-amyl alcohol	0.03	0.24	0.10
benzyl alcohol	0.02	0.19	0.05

TABLE 8. Chloride-Bromide Interactions in the System MgCl₂-MgBr₂-H₂O/n-Butanol ⁽⁴⁾

Conjugate Phase Compositions at Ambient Temperature					
n-Butanol Phase			Aqueous Phase		
Br g/l	Cl	H ₂ O wt %	Br g/l	Cl	
4.0	nil		98	nil	
4.0	0.2	16.8	98	14	
11.0	nil		169	nil	
12.8	69.1	17.6	21	284	
19.2	nil		216	nil	
17.0	2.5	14.6	178	43	
17.5	52.0	17.3	34	366	
37.2	nil		274	nil	
34.1	8.5	16.6	152	146	
36.2	29.3	16.8	93	203	

TABLE 9. Distributions in Ca — Mg — Na — Cl — H₂O/Butyl Lactate Systems ⁽⁴⁾

Conjugate Phases					Distribution Coefficient $\frac{D_{org}}{aq}$	
Aqueous			Organic			
Ca	Na wt %	Mg	Ca	Na Mg wt %	Ca	Na Mg
5.5	—	—	0.10	— —	8.4	0.02 — —
5.9	2.7	—	0.25	0.16 —	6.4	0.04 0.06 —
5.6	4.6	—	0.83	0.32 —	8.8	0.15 0.07 —
4.9	—	5.0	4.5	— 1.1	21.5	0.92 — 0.22

TABLE 10. N, N-Dimethyl Caprylamide/Chloride Salt/Water Systems ⁽⁴⁾

Cation	Aqueous Solution wt % Salt	Distribution Coefficient $\frac{D_{org}}{aq}$	Water in Organic Phase wt %
Mn(II)	15.8	0.10	9
Co(II)	15.5	0.25	11
Zn(II)	16.5	0.47	12
Mg	9.0	0.50	33
Ca	15.6	0.62	29
Fe(III)	16.5	0.85	3

coefficients for salts utilizing N,N-dimethyl caprylamide as the solvent. It is interesting to note that the water transferred varies by more than an order of magnitude, depending upon the cation in the system.

While the data presented here are interesting in their own right, more important is the fact that they point to a whole area which is essentially unexplored and unexploited, and this is the extraction of hydrated salt species

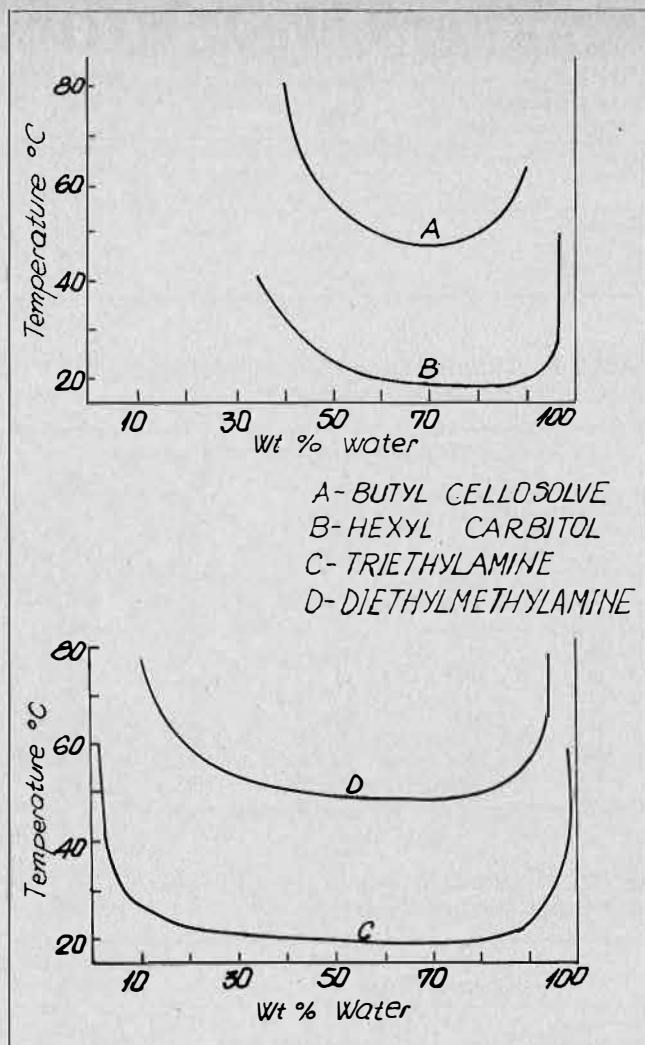


FIGURE 1. Reciprocal solubilities.

by hydrogen-bonding solvents. The degree of structuredness in the aqueous phase may be a significant factor in determining the behaviour of a specific system.

Solvent Classes

In looking at classes of solvents one can order them in very many ways, e.g. according to dielectric constant, donor number, acidity, basicity, tendency to hydrogen bonding, oligomer formation, and so on. Several of these classifications are pragmatic, using scales of reference wholly related to the particular purpose for which the solvent is to be utilised. One such pragmatic scale can be related to the solvent's capacity to dissolve water; this extends the continuity of properties of solvents from pure water at one end through to neat polar solvents at the other.

One property of the solvent which changes in the same sense as its ability to dissolve water, is its tendency to solvate polar molecules and ions. Thus, there is a continuous change in the nature of the species in the solvent, from hydrated species, through hydrated-solvated species, to essentially solvated species, depending upon the species and on the solvating power of the solvent relative to water. This makes the solvent phase contiguous with water as the ambient for reactions, and also as the tool for separations after or during such reactions.

TABLE 11. N-Substituted Amides as Acid Extractants⁽⁴⁾

Aqueous system: H_3PO_4 150 g/l $CaCl_2$ 344 g/l HCl 4 g/l
 Ambient temperature

Solvent	Conjugate Solvent Phase Composition		
	H ⁺	Cl ⁻ moles / l	PO ₄
n-butanol (reference case)	2.20	1.4	0.8
N-n-butylacetamide	4.07	3.1	0.9
N-n-butylcaproamide	2.28	1.8	0.5
N-n-propylcaproamide	2.48	1.8	0.6
N,N-di-butylacetamide	4.0	2.1	1.9
N,N-di-methylcaproamide	3.9	2.4	1.6

Clearly, the characteristics of a solvent are modified by the quantity of water dissolved; similarly, as an extension to this, it is to be expected that an essentially aqueous ambient is modified by having an organic solvent dissolved in it. Studies have appeared in the literature on the effect of homogeneous mixed solvents in reactions with solid ion exchangers, but the use of mixed solvents has hardly been extended to other areas. However, it is not always clear where one is to seek for data on solvating, polar solvents; whole classes of polar solvents seem to have been ignored, while a few types are well accepted and are utilised in many contexts. Among the latter are neutral phosphate esters, alcohols, amines, and more recently ethers. On the other hand, glycol ethers, for example, though commercially available, have essentially not been considered in liquid/liquid extraction. Their properties, however, as bulk solvating solvents, are no less interesting than those of accepted types. Thus, their mutual miscibility with water, as a function of temperature, changes in the same way as that of the amines proposed for use in water desalination. This is clearly seen in Figure 1 where mutual miscibility is plotted as a function of temperature. N-substituted fatty acid amides, too, have similar characteristics in relation to water miscibility and temperature dependence. This brings us, then, to a somewhat different approach to solvent extraction separations, namely the utilisation of the effect of small temperature changes on mutual miscibility to effect transfer of hydrated species to and from the solvent. In general, solvents which extract water will also extract acids. Table 11 shows data for a number of N-substituted amides.

Concluding Comments

The study of solvent extraction as an abstract, academic theme unrelated to applications and industrial implementation is unacceptable. On the other hand, success must lean first and foremost on chemistry and then on technology. It is clear a priori that chemical research in solvent extraction is an interdisciplinary activity which would draw on various other fields for its basic data and understanding. These contiguous fields include coordination chemistry, analytical chemistry, thermodynamics, synthetic organic chemistry and stereochemistry, among others. Of these, at least coordination chemistry should be the hand-maiden of solvent extraction, so that those who desire to separate specific elements by solvent extraction should scan the vast literature on coordination compounds. The same can be said in regard to the considerable work which has been done on reactions in non-aqueous solutions; what is now required is to integrate all these fields with the aim of attaining technological success.

However, lest one misjudge the field, it is in place to recount some of the successes. Metal extraction needs no stress; in particular the success of copper recovery reflects

the symbiosis of organic synthesis with careful technological evaluation and development. Similarly, the process utilising an invariant solvent extraction system for the metathetic conversion of potassium chloride to potassium nitrate can be regarded as a classic of its kind⁽¹⁰⁾. By its nature, an invariant system implies a single-stage equilibrium and indeed in these cases countercurrent multi-stage contacting becomes redundant.

Another process utilising the concept of invariant systems but in conjunction with the temperature effect on water and acid distribution, aims at cleaning wet process phosphoric acid⁽¹¹⁾. In fact one of the fields in which there is currently great activity involving solvent extraction technology is the upgrading of wet process phosphoric acid.

Multi-phase systems have required originality in developing and designing separation equipment, be this a decanter-thickener for separating two liquid and one solid phase, or a settler for separating and delivering three liquid phases⁽¹²⁾.

Solute-solute interactions and solute-solvent interactions have been exploited to the full in a process for obtaining separate streams of magnesium chloride and magnesium bromide from the brines of the Dead Sea which are essentially chloride brines of sodium, potassium, calcium and magnesium⁽⁹⁾. The interaction between chloride and bromide is so strong in this system that bromide can be concentrated ten to twentyfold by virtue of the solvation effects only.

When a start is made to utilize fully and to understand all the information available, we shall be justified in claiming that no separation is impossible by solvent extraction.

Acknowledgments

In the course of developing inorganic chemical processes I have personally come to know solvent extraction as a very powerful separation tool. Our successes, however, have always been group successes. Accordingly, sincere acknowledgment is due to my IMI colleagues, past and

present, who participated through the years in all aspects of our solvent extraction projects. First and foremost, I extend sincere thanks to Dr. A. Baniel whose clear foresight induced us to enter this field. Without his originality and intellectual stimulus much of this broad programme would probably never have been undertaken.

Thanks are due to Dr. Stephen Garnett for constructive criticism and help during the preparation of this paper, which is published with the permission of the management of IMI.

REFERENCES

- (1) Baniel, A., *J. Appl. Chem.* 1958, 8, 611.
Idem 1959, 9, 521.
- (2) Texas A & M Research Foundation 1960 Prog. Rep. No. 35 Development of the Solvent Demineralisation of Saline Water.
- (3) Baniel, A. and Blumberg, R., 1959, U.S. Pat. 2902341.
Idem 1959, U.S. Pat. 2894813.
- (4) IMI unpublished data.
- (5a) Hajdu, K., Process design for preparation of mono-potassium phosphate by means of an organic solvent. Chem. E. Diploma Thesis, 1966, Technion-Israel Institute of Technology, Haifa, Israel.
- (5b) Cejtlin, J., Preparation of potassium sulphate from potassium chloride and sulphuric acid by extraction with an organic solvent. D.Sc. Thesis, 1959, Technion-Israel Institute of Technology, Haifa, Israel.
- (6) D'Ans, J., Die Lösungsgleichgewichte der Systeme der Salze ozeanischer Salzablagerungen. Kali-Forschungs-Anstalt GmbH, Berlin, 1933, Verlagsgesellschaft für Ackrbau, M.B.H.
- (7) Novomeysky, M.A., *Trans. Inst. Chem. Eng.* 1936, 14, 60.
- (8) Blumberg, R., *Israel Chem. Eng.* 1973, 2, 23.
- (9) Baniel, A. and Blumberg, R., 1965 Israel Pat. 23760.
1973 Israel Pat. of add. 41225.
- (10) Araten, Y., Baniel, A. and Blumberg, R., *The Fertiliser Society*, London 1967, Proceedings No. 99.
- (11) Baniel, A. and Blumberg, R., 1968 U.K. Pat. 1,112,033.
Idem 1970 U.K. Pat. 1,209,272.
- (12) Meyer, D., Application of a Mixer Settler for the Separation of Three Liquid Phases, IMI Staff Report. 12th Congress of the Israel Institute of Chemical Engineers 1976, April.

DISCUSSION

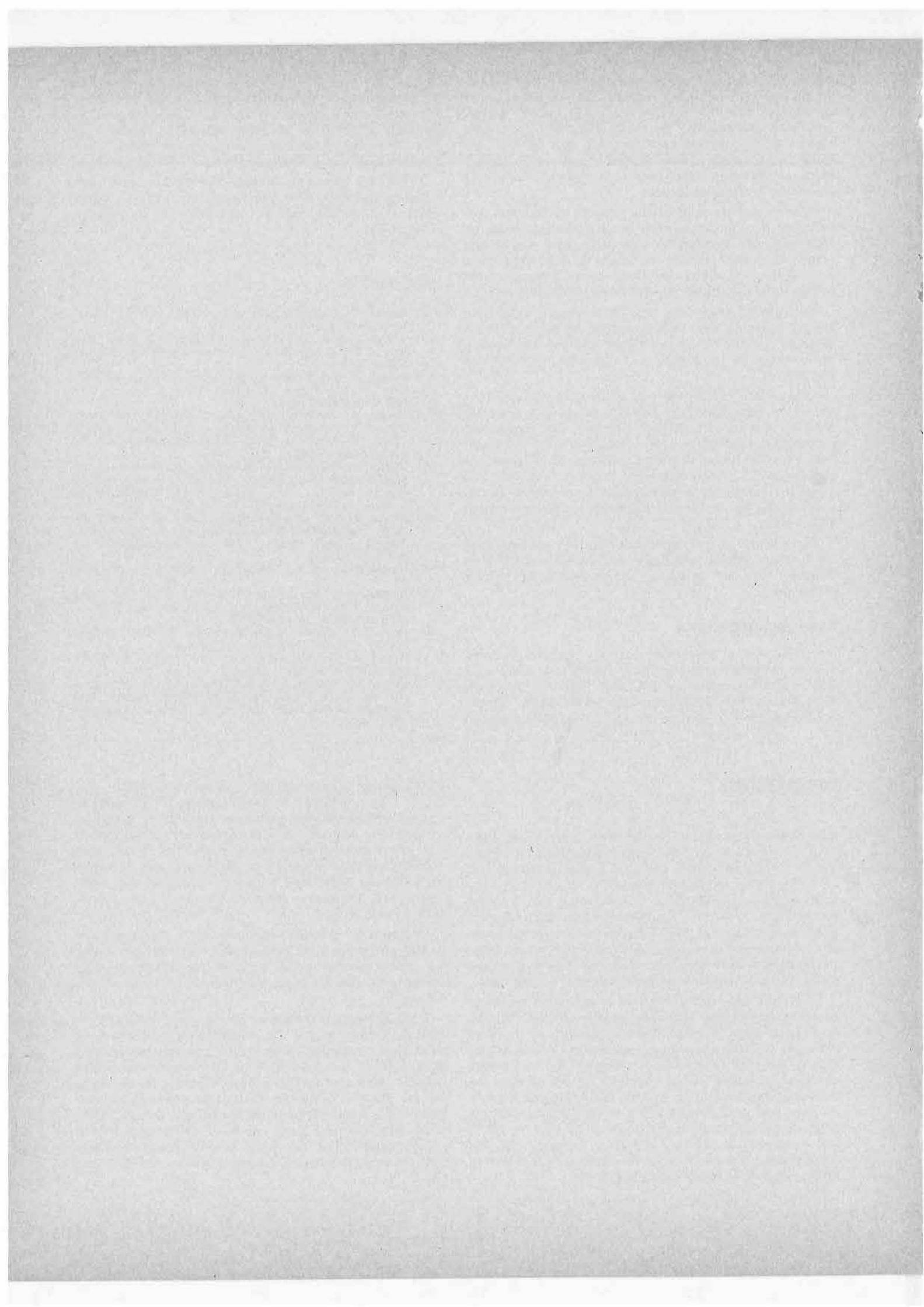
A.S. Kertes: Third-phase formation has been noted many years ago, the earliest originating from Oak Ridge in the mid 1950's. We have reviewed the topic at an earlier ISEC meeting in Harwell, 1965, ("Solvent Extraction Chemistry of Metals", MacMillan Co., London, pp. 377-401, 1966) for organo-phosphorus and amine extraction systems, and have offered an interpretation in terms of specific chemical interactions. Since, several other interpretations have been advanced, and even at this Conference several papers have been presented on the topic.

I have my own doubts whether a separation technique based on third phase formation can be utilized. Namely, one has to bear in mind that the stability of the third phase, its formation and disappearance, are extremely susceptible to small temperature changes, not to mention chemical parameters. For example, in the systems described at this Conference by Drs. Maljkovic and Branica, on iron and gold extraction by isopropyl ether-benzene mixtures, a temperature difference of as little as 0.5°C will cause a third phase to appear or disappear. Do you really believe that a separation flowsheet with that kind of limitations can be technologically feasible?

R. Blumberg: It was certainly not my intention to give anyone the impression that I thought we had discovered the phenomenon of third phase formation — quite the contrary; as Prof. Kertes very rightly points out, this phenomenon was observed over two decades ago. I have tried now to point out the significance of having an additional phase in a solvent extraction system, when one regards the system broadly as a specific case of the Gibbs Phase Rule.

Undoubtedly tentative explanations of the appearance of the third phase have been offered, but I believe we are far from knowing how to anticipate or induce the third phase; even less have we known how to use it to our advantage.

Notwithstanding Professor Kertes' reservations, it is indeed possible to put the temperature dependence of third phase formation to very good use; this has recently been done on industrial scale in the inorganic processing industry, with considerable success. There is no reason to assume that this cannot or will not be extended to other cases in the future. Thus instead of being a nuisance technologically, the third phase can be of considerable help in process control since the system becomes pseudo-invariant and the compositions of conjugate phases are therefore fixed.



Chapter 4

Physical and Inorganic Chemistry

Sessions 11 and 28

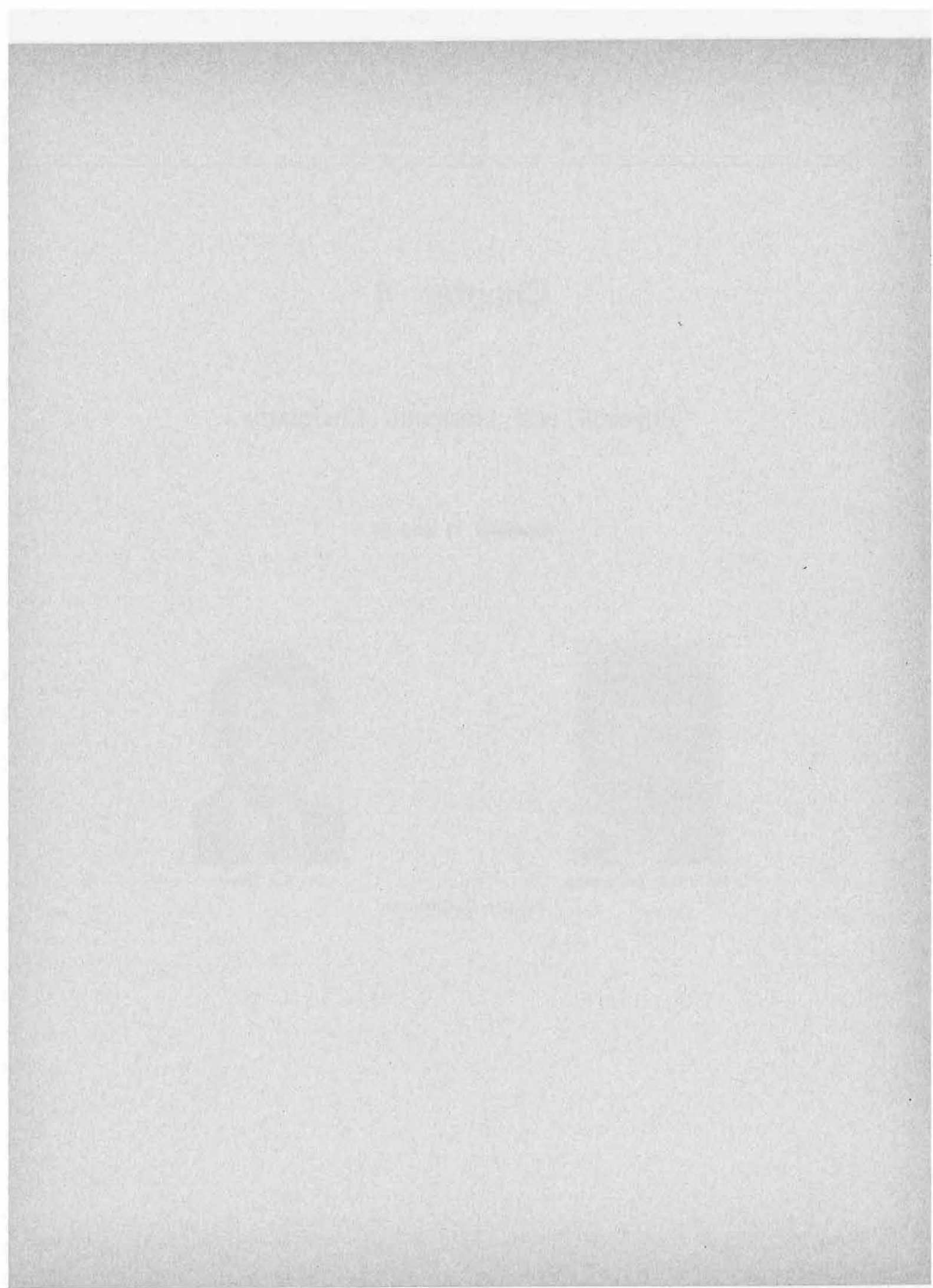


Dr. S.O.S. Andersson



Dr. A.J. Oliver

Session Co-Chairmen



The Extraction of Anionic Metal Complexes from Aqueous Solutions by a Long-Chain Alkyl Ammonium Compound — Divalent Manganese, Iron, Cobalt, Nickel, Copper and Zinc-Thiocyanate Systems

Taichi Sato, Hiroshi Watanabe and Tadaski Kato,
Department of Applied Chemistry,
Faculty of Engineering,
Shizuoka University, Hamamatsu, Japan

ABSTRACT

The extraction of anionic divalent manganese, iron, cobalt, nickel, copper and zinc-thiocyanato anionic species from aqueous solutions by tricaprylmethylammonium chloride in benzene has been investigated under different concentrations. Both the aqueous and organic phases have been examined spectrophotometrically. The infrared spectrophotometry and the measurements of water content, apparent molecular weight and magnetic moment have been applied to the organic extracts, and the electron spin resonance experiment to the organic manganese(II)- and copper (II)-complexes. The mechanism of the extractions and the structures of the extracted species are discussed on the basis of the results obtained.

Introduction

TRICAPRYLMETHYLAMMONIUM THIOCYANATE has been utilized as a selective agent in the spectrophotometric determination of cobalt(II)⁽¹⁾. We have also investigated extractions of thorium(IV)⁽²⁾, uranium(VI)⁽³⁾, titanium(IV)⁽⁴⁾, vanadium(IV)⁽⁴⁾ and zirconium(IV)⁽⁵⁾ from aqueous solutions containing hydrochloric acid in the presence of potassium thiocyanate by quaternary compounds. The present paper extends the work to the extraction of divalent manganese, iron, cobalt, nickel, copper and zinc.

Experimental Reagents

Tricaprylmethylammonium chloride (General Mills; Aliquat-336; $R_3R'NCl$), used as the quaternary compound, was purified by washing several times with aqueous sodium chloride solution and n-hexane⁽⁶⁾, and was diluted with benzene. The stock solutions of divalent manganese, iron, cobalt, nickel, copper and zinc were prepared by dissolving their chlorides ($MnCl_2 \cdot 4H_2O$, $FeCl_2 \cdot 4H_2O$, $CoCl_2 \cdot 6H_2O$, $NiCl_2 \cdot 6H_2O$, $CuCl_2 \cdot 2H_2O$ and $ZnCl_2$) in hydrochloric acid solutions of the required concentrations. The other chemicals were analytical reagent grade.

Extraction and Analytical Procedures

The procedure for obtaining distribution coefficients (the ratio of the equilibrium concentration of divalent metals in the organic phase to that in the aqueous phase) was as follows: equal volumes (15 ml) of Aliquat-336 in benzene and the aqueous metal chloride solutions containing hydrochloric acid in the presence of potassium thiocyanate were shaken for 10 min in a stoppered 50 ml conical flask in a water-bath thermostated at the required temperature (preliminary experiments showed that equilibrium for each metal is complete in 10 min.); the organic phases centrifuged from the aqueous phases were stripped with 1-2 M hydrochloric acid, and then the distribution coefficients were determined.

Divalent metals were determined by EDTA titration using Erio T (eriochrome black T) for manganese⁽⁶⁾, MTB (methylthymol blue) for iron⁽⁷⁾, PAN(1-(2-pyridylazo)-2-naphthol) for copper⁽⁸⁾, and XO(xylenol orange) for cobalt, nickel and zinc^(9,10) as indicators. The concentrations of chloride and thiocyanate in the organic phase were determined as follows: the precipitate from the organic solution with silver nitrate was decomposed by boiling for 1 hr in the presence of concentrated nitric acid, and residue was weighed as silver chloride⁽¹¹⁾; accordingly the loss in weight from the initial precipitate was equivalent to the concentration of thiocyanate. The water content of the organic phase was determined by Karl-Fischer titration.

The complexes free from benzene were prepared by drying the metal-saturated organic phases.

Spectrophotometry and ESR Spectral Measurement

The absorption spectra were obtained on a Shimadzu Model QV-50 spectrophotometer, using matched 1.00 cm fused silica cells. The infrared spectra of the samples prepared by evaporation of diluent in the organic phases were determined on a Japan Spectroscopic Co. Ltd. spectrometer Model IR-S, equipped with potassium chloride prisms, and a Model IR-A1 grating infrared spectrophotometer for measurement at 4000-650 cm^{-1} , and a Model IR-F, a grating model for measurement at 700-200 cm^{-1} , as a capillary film between thallium halide plates or polyethylene films, respectively.

Electron spin resonance (ESR) spectra of the organic extracts for manganese and copper were determined on a

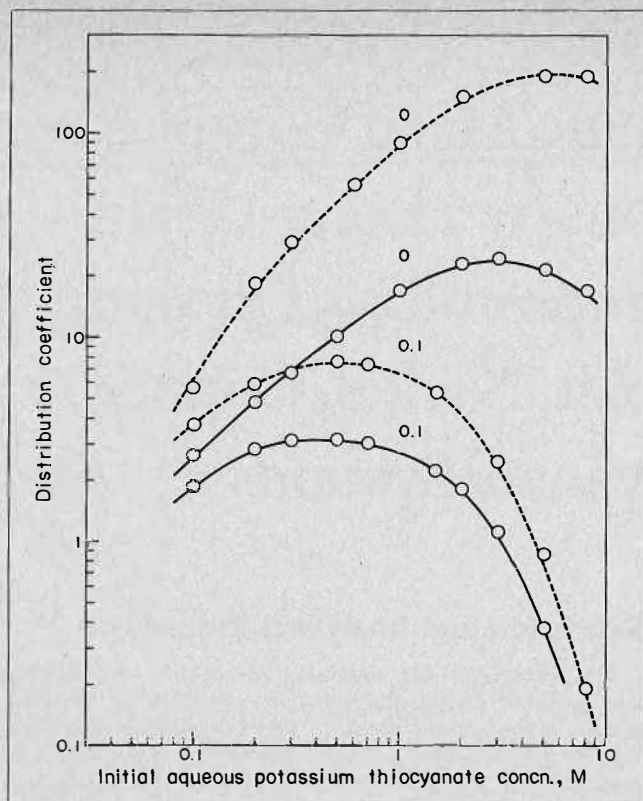


FIGURE 1. Extraction of manganese(II)-thiocyanato complex from hydrochloric acid solutions in the presence of potassium thiocyanate at different concentrations by Aliquat-336 in benzene. Continuous and broken lines represent extractions with 0.02 and 0.03 M Aliquat-336, respectively; numerals on curves are initial aqueous hydrochloric acid concentrations, M.

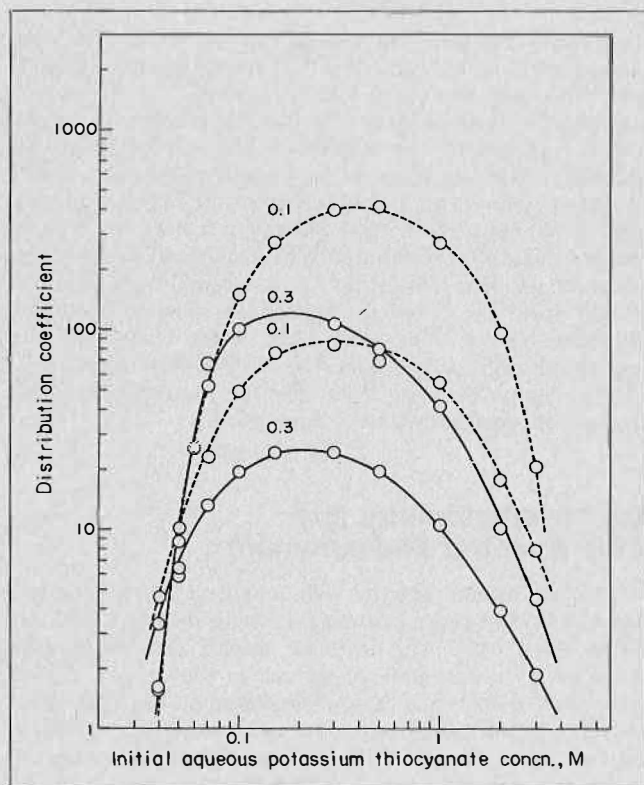


FIGURE 2. Extraction of iron(II)-thiocyanato complex from hydrochloric acid solutions in the presence of potassium thiocyanate at different concentrations by Aliquat-336 in benzene. Continuous and broken lines represent extraction with 0.02 and 0.03 M Aliquat-336, respectively; numerals on curves are initial aqueous hydrochloric acid concentrations, M.

high-sensitivity ESR spectrometer; designed in the Research Institute of Electronics, Shizuoka University^(12,13). The calculation of ESR derivative line shape of samples was made using a FACOM 230-45S computer.

Measurement of Apparent Molecular Weight and Magnetic Moment

The apparent molecular weight was determined in benzene on a Hitachi Model 115 isothermal molecular weight apparatus, and the magnetic moment was measured by a Gouy method⁽¹²⁾.

Results and Discussion

Extraction Isotherms

The extraction of divalent manganese, iron, cobalt, nickel, copper and zinc from their solutions (0.007 M for all metals except copper in 0.0035 M) containing hydrochloric acid in the presence of potassium thiocyanate at different concentrations by Aliquat-336 in benzene at 20°C gave the results shown in Figures 1-6. These show that the extraction efficiency follows the order $Zn > Co > Cu > Fe > Mn > Ni$, and falls with increasing the initial aqueous hydrochloric acid concentration. The distribution coefficients for divalent metals first rise with aqueous thiocyanate concentration, and pass through maxima and then fall again. The variation of the distribution coefficients may be attributed to the formation of the metal ion-thiocyanato complex for the rise in the curve,

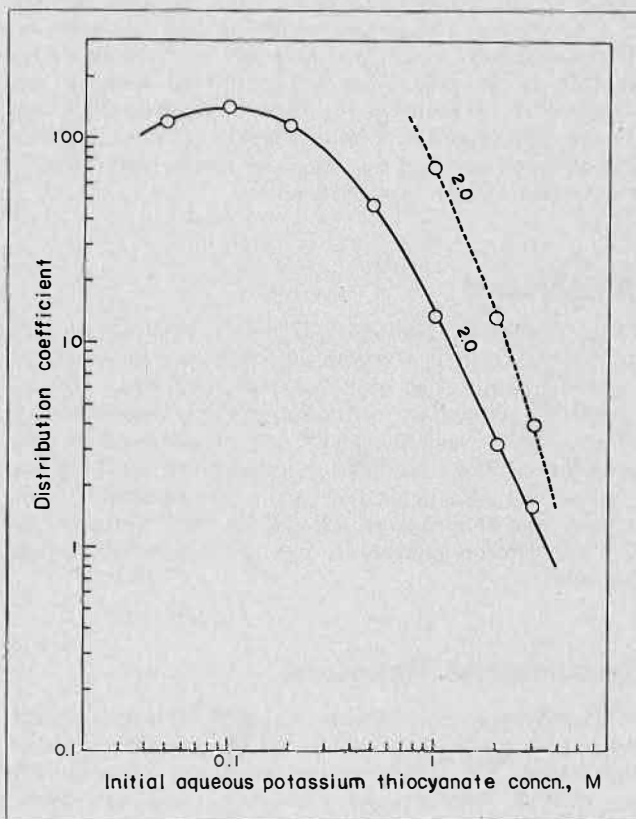


FIGURE 3. Extraction of cobalt(II)-thiocyanato complex from hydrochloric acid solutions in the presence of potassium thiocyanate at different concentrations by Aliquat-336 in benzene. Continuous and broken lines represent extraction with 0.02 and 0.03 M Aliquat-336, respectively; numerals on curves are initial aqueous hydrochloric acid concentrations, M.

and to the competition between metal ion and thiocyanate or hydrochloric acid for association with the quaternary compound for a check on this rise. In the extraction of divalent metal chloride solutions (0.007 M for all metals except copper in 0.0035 M) containing hydrochloric acid (0.05 M for manganese, iron and nickel, 0.2 M for cobalt and copper, and 1.0 M for zinc) and lithium chloride at various concentrations in the presence of potassium thiocyanate (1.0 M for manganese and copper, 2.0 M for iron, nickel and zinc, and 3.0 M for cobalt) by Aliquat-336 (0.01 M for copper, 0.02 M for iron, cobalt, nickel and zinc, and 0.03 M for manganese) in benzene at 20°C, however, the distribution coefficients are not appreciably influenced by chloride concentration, except in the case of zinc. For the extraction of aqueous solutions containing zinc chloride, the gradual decrease in the distribution coefficient with increasing the chloride concentration may be explained as being due to the presence of $ZnCl^{+14}$, on the assumption that the extracted species contains no chloride. Additionally, the values of log (distribution coefficient) decrease linearly with log (initial aqueous hydrochloric acid concentration) at a fixed total chloride concentration ($[HCl] + [LiCl] = 0.5$ M for iron and nickel, 1.0 M for manganese, and 2.0 M for cobalt and copper), analogously to the curve for hydrochloric acid alone. It is thus presumed that the species containing chloride ion is not extractable; when the hydrochloric acid in the aqueous phase is partly replaced by lithium chloride, the decrease in the distribution coefficient is checked, owing to the removal of the competition for metal-thiocyanato complex between hydrochloric acid and quaternary salt.

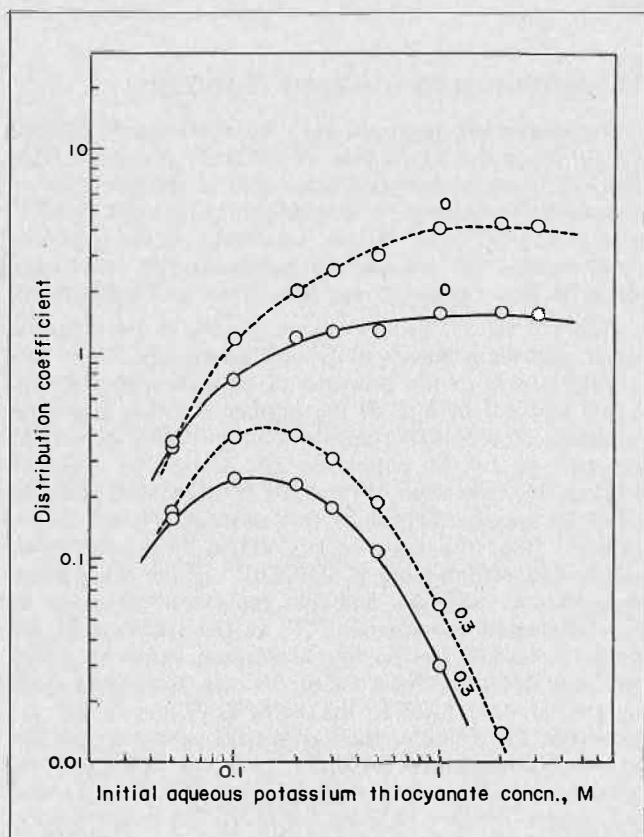


FIGURE 4. Extraction of nickel(II)-thiocyanato complex from hydrochloric acid solutions in the presence of potassium thiocyanate at different concentrations by Aliquat-336 in benzene. Continuous and broken lines represent extractions with 0.02 and 0.03 M Aliquat-336, respectively; numerals on curves are initial aqueous hydrochloric acid concentrations, M.

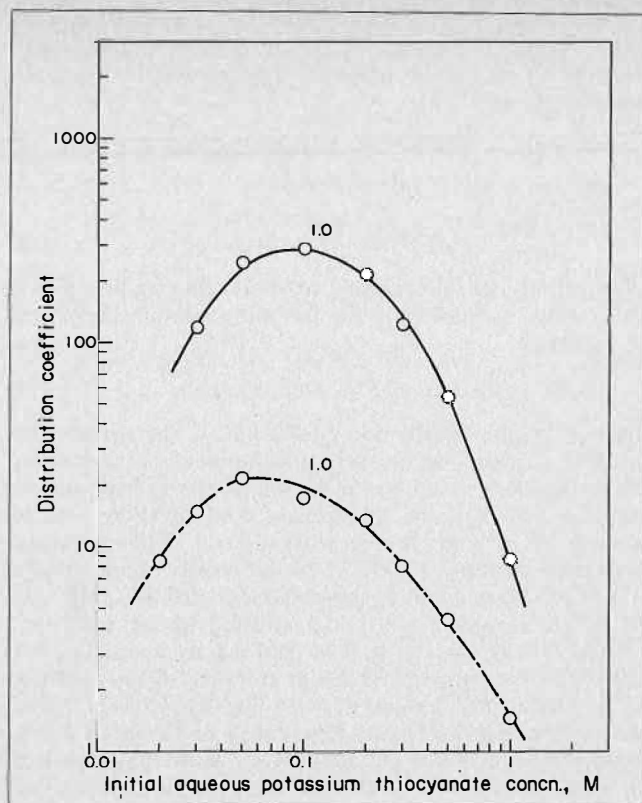


FIGURE 5. Extraction of copper(II)-thiocyanato complex from hydrochloric acid solutions in the presence of potassium thiocyanate at different concentrations by Aliquat-336 in benzene. Continuous and chain lines represent extractions with 0.02 and 0.01 M Aliquat-336, respectively; numerals on curves are initial aqueous hydrochloric acid concentrations, M.

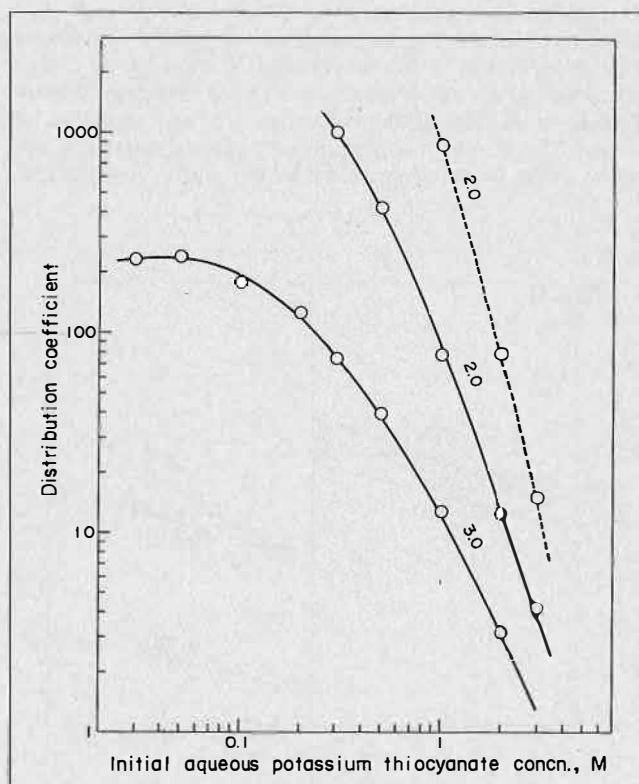
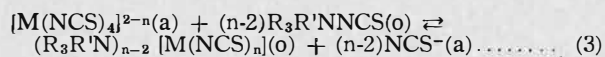
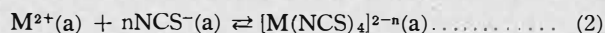
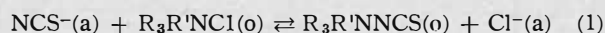


FIGURE 6. Extraction of zinc(II)-thiocyanato complex from hydrochloric acid solutions in the presence of potassium thiocyanate at different concentrations by Aliquat-336 in benzene. Continuous and broken lines represent extractions with 0.02 and 0.03 M Aliquat-336, respectively; numerals on curves are initial aqueous hydrochloric acid concentrations, M.

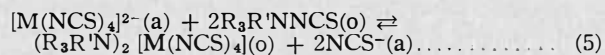
The extraction of divalent metal from aqueous solutions in the presence of thiocyanate by Aliquat-336 probably depends on an ion-exchange reaction similar to those for other instances^(2,4), viz.



in which (a) and (o) represent aqueous and organic phases, respectively. Accordingly, the following relationship would be expected:

$$\log E_a = \log K + m \log (C_A - mC_M) / C_{\text{NCS}} \dots \dots \dots (4)$$

where E is the distribution coefficient, K the equilibrium constant, C_A the total quaternary compound concentration, C_M the divalent metal concentration of the organic phase, and C_{NCS} the aqueous thiocyanate concentration, and in addition m = n-2. In the extraction of divalent metals from their solutions (0.007 M for all metals except copper in 0.0035 M) containing hydrochloric acid (0, 0.05 and 0.1 M for manganese, 0.1, 0.2 and 0.3 M for iron, 0.7, 1.0 and 2.0 M for cobalt, 0.05 and 0.1 m for nickel, 0.5 and 1.0 M for copper, and 2.0 M for zinc) in the presence of potassium thiocyanate (1.0 M for manganese, nickel and copper, and 3.0 M for iron, cobalt and zinc) at 20°C, log-log plots of E vs. (C_A-mC_M)/C_{NCS} show that Equation (4) is satisfied for m = 2. It is therefore considered that divalent metal-thiocyanato complex ion is associated with two molecules of quaternary compound, and accordingly n-2 in Equation (3) is expressed by 2, i.e.



This is supported by the following fact: in the extraction of divalent manganese, iron, cobalt, nickel and zinc chloride solutions in the presence of 2.0 M potassium thiocyanate by 0.02 M Aliquat-336 in benzene at 20°C, the molar ratios of divalent metal and thiocyanate concentrations in the organic phase to the concentration of Aliquat-336 as a function of initial aqueous metal concentration attain the limiting values of 0.5 and 2, respectively,

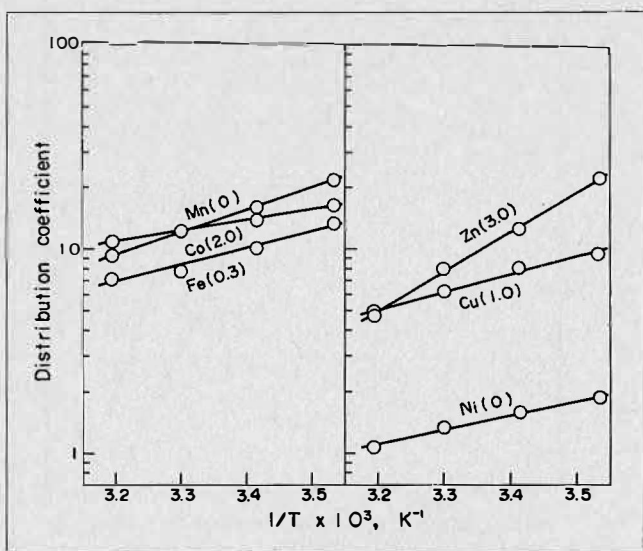


FIGURE 7. Temperature-dependence of distribution coefficient for the extraction of divalent metals-thiocyanato complexes from hydrochloric acid solutions in the presence of potassium thiocyanate at 1.0 M by 0.02 M Aliquat-336 in benzene. Figures in parentheses are initial aqueous hydrochloric acid concentrations, M.

at 0.01 M initial aqueous metal concentration, except in the case of nickel, implying that the complex formed in the organic phase contains divalent metal/thiocyanate/Aliquat-336 in the molar ratio 1 : 4 : 2, indicating the stoichiometry (R₃R'₂N)₂[M(NCS)₄] as expressed in Equation (5). In the extraction of nickel, those molar ratios do not yet attain the limiting value at 0.01 M initial aqueous nickel concentration, but they decrease gradually above this concentration and approach the limiting values of 0.5 and 2, respectively. A similar experiment for the water content of the organic phase gives the result that the water content of the organic phase steeply decreases with increasing the initial aqueous metal concentration for all divalent metals except for nickel, in which its decrease becomes gradual. This suggests that the complexes of divalent metals except nickel have no coordinated water.

Temperature Effect

The extraction of divalent manganese, iron, cobalt, nickel, copper and zinc from their solutions (0.007 M for all metals except copper in 0.0035 M) containing hydrochloric acid (0 M for manganese and nickel, 0.3 M for iron, 1.0 M for copper, 2.0 M for cobalt, 3.0 M for zinc) in the presence of 1.0 M potassium thiocyanate by 0.02 M Aliquat-336 in benzene at temperature 10 and 50°C gave the results indicated in Figure 7. This shows that the distribution coefficient increases with rising temperature. This dependence on temperature is contrary to those found for thorium(IV)⁽²⁾, titanium(IV)⁽⁴⁾ and vanadium(IV)⁽⁴⁾, but agrees with that for zirconium(IV)⁽⁴⁾. The heats of reaction (change in enthalpy, kcal/mol) for Equation (5) were estimated to be 4.95, 3.69, 2.42, 3.44, 3.85 and 9.06 for manganese, iron, cobalt, nickel, copper and zinc.

Absorption and Infrared Spectra

The absorption spectra of both the aqueous and organic phases from the extraction of divalent metal chloride solutions containing hydrochloric acid in the presence of potassium thiocyanate by Aliquat-336 in benzene at 20°C were examined under various conditions. Some representative results, the spectra for manganese(II), cobalt(II), nickel(II) and copper(II) are illustrated in Figures 8-10.

Figure 8 shows the absorption spectra of the aqueous cobalt chloride solutions (0.007 M) containing 0.9 M hydrochloric acid in the presence of potassium thiocyanate at 1.0 and 3.0 M and of the organic solution from the extraction of cobalt(II) chloride solution (0.007 M) in the presence of 1.0 M potassium thiocyanate by 0.02 M Aliquat-336 in benzene. From this it is deduced that the cobalt(II) species formed in the aqueous solution transforms⁽¹⁵⁾ from the aquo ion [Co(H₂O)₆]²⁺ to the four-coordinated complex ion [Co(NCS)₄]²⁻ as the thiocyanate concentration increases, and that the extracted species is in a tetrahedral coordination^(16,17). In the spectrum of the organic cobalt(II) species, the absorption bands at 16000 cm⁻¹ and 7900 cm⁻¹ are assigned to the transitions from the ground state A₂(F) to the states⁴T₁(P) and ⁴T₁(F), respectively. The value of the ligand field parameter for the cobalt (II)-thiocyanato complex may be calculated by using the elements of the materials determined by Tanabe and Sugano⁽¹⁸⁾: B = 663 cm⁻¹ and 10 Dq = 4650 cm⁻¹, in which B represents the Racah parameter for electron repulsion. Accordingly it is considered that the value of 10 Dq in the cobalt(II)-thiocyanato complex is close to the value (4100 cm⁻¹) which is four-ninths times the value of 10 Dq (9300 cm⁻¹) in the hexaquo cobalt(II) ion. Further, the factor β in the nephelauxetic species^(19,20), the ratio

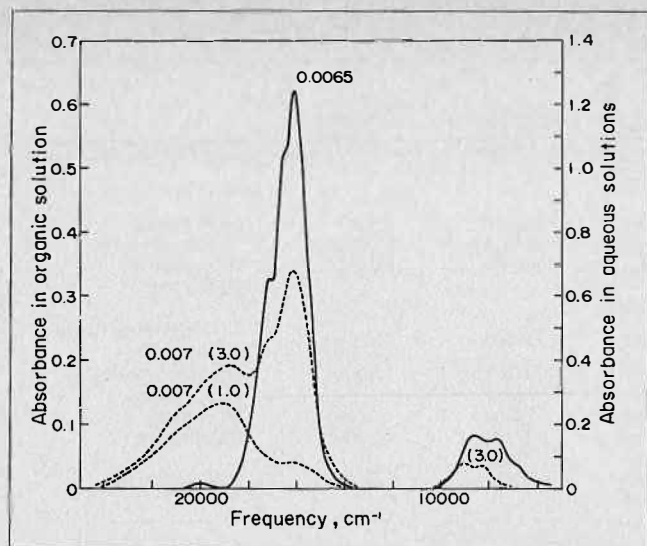


FIGURE 8. Absorption spectra of the aqueous cobalt chloride solutions containing 0.9 M hydrochloric acid in the presence of potassium thiocyanate and of the organic solution from the extraction of cobalt(II) chloride solution in the presence of 1.0 M potassium thiocyanate by 0.02 M Aliquat-336 in benzene. Continuous and broken lines represent organic and aqueous solutions, respectively; numerals on curves and in parentheses are the concentrations of cobalt and initial aqueous potassium thiocyanate, respectively, M.

between the value of representative parameter of inter-electronic repulsion in the complex and in the corresponding free ion, is estimated to 0.59, implying that the nephelauxetic effect caused by bond formation is relatively large. Figure 9 gives the absorption spectra of the organic extracts from aqueous manganese(II) and copper(II) chloride solutions in the presence of thiocyanate by Aliquat-336 in benzene. The absorption bands at 25000, 22700, 21700 and 20200 cm^{-1} , due to the transitions from the ground state ${}^6A_1(S)$ to the states ${}^4T_1(G)$, ${}^4T_2(G)$, 4E and ${}^4A_1(G)$ and ${}^4T_2(D)$, are observed in the spectrum of the organic manganese(II) extract. It is thus expected that the manganese(II)-thiocyanate complex is in a tetrahedral coordination. In addition, the value of the ligand field parameter is determined on the basis of the energy diagram⁽¹⁸⁾: $B = 690 \text{ cm}^{-1}$ and $10 Dq = 4090 \text{ cm}^{-1}$. As the nephelauxetic ratio β is estimated to be 0.72, it is thought that the extent to which covalent bond formation occurs in the manganese(II) complex is less than that in the cobalt(II) complex. For the organic extract of copper(II), the value of $10 Dq = 11900 \text{ cm}^{-1}$ is obtained from the spectrum, but it is difficult to predict whether the species is either octahedral or square-planar since the spectrum consists of a broad band.

In Figure 10, the absorption spectra of the organic solutions from the extraction of nickel(II) chloride solutions (0.0021, 0.21 and 0.8 M) in the presence of 3.0 M potassium thiocyanate by 0.02 M Aliquat-336 in benzene are given in comparison with that of aqueous nickel chloride solution (0.07 M) in presence of 1.0 M potassium thiocyanate. The spectrum of the aqueous solution of nickel(II) chloride reveals the characteristic feature of octahedral species⁽¹⁵⁾, showing the absorption bands at 25300, 15200 and 9200 cm^{-1} ascribed to three spin-allowed transitions ${}^3A_{2g}(F) \rightarrow {}^3T_{1g}(P)$, ${}^3A_{2g}(F) \rightarrow {}^3T_{1g}(F)$ and ${}^3A_{2g}(F) \rightarrow {}^3T_{2g}(F)$, respectively. In contrast, the spectrum of the high nickel loading organic solution exhibits the absorption bands of the tetrahedral species^(21,23); the transitions from the ground state ${}^3T_1(F)$ to the states ${}^3T_1(P)$ and ${}^3A_2(F)$ appear at 16900 (and/or 15900) and 8000

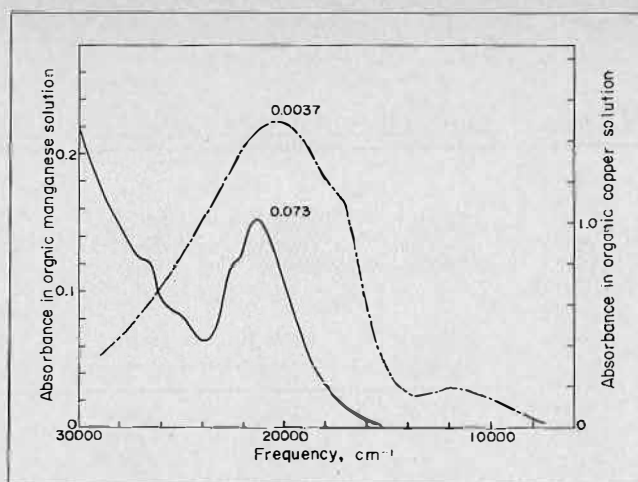


FIGURE 9. Absorption spectra of the organic extracts from aqueous manganese(II) and copper(II) chloride solutions in the presence of potassium thiocyanate by Aliquat-336 in benzene. Continuous and chain lines represent organic solutions of manganese and copper, respectively; numerals on curves are metal concentrations, M.

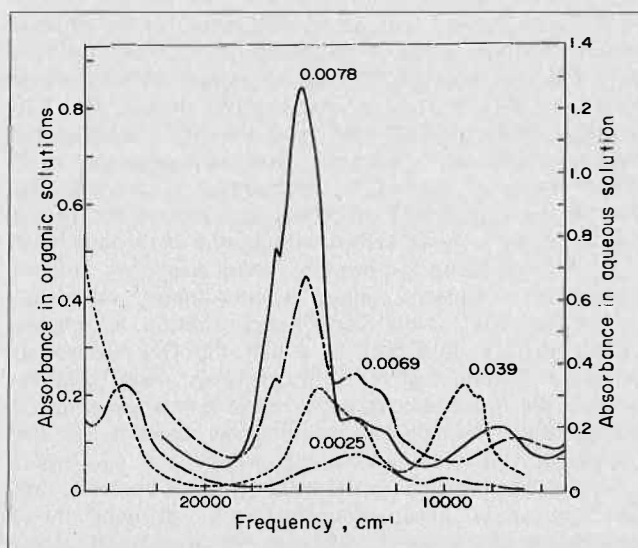


FIGURE 10. Absorption spectra of the organic solutions from the extraction of nickel(II) chloride solutions in the presence of 3.0 M potassium thiocyanate by 0.02 M Aliquat-336 in benzene. Continuous (and/or chain) and broken lines represent organic and aqueous solutions, respectively; numerals on curves are nickel concentrations, M.

cm^{-1} , respectively. The ligand field parameter is thus obtained as $B = 980 \text{ cm}^{-1}$ and $10 Dq = 4350 \text{ cm}^{-1}$. Since the factor $\beta = 0.91$, it seems that the covalency of the nickel(II) complex is very low. From the absorption spectral results, it is inferred that with increasing the concentration of nickel extracted in the organic phase the extracted species transforms from hexa- to tetra-coordination, indicating the formation of the complexes of $(R_3R'N)_2[Ni(NCS)_4(H_2O)_2]$ in an octahedral O_h symmetry and $(R_3R'N)_2[Ni(NCS)_4]$ in a tetrahedral T_d symmetry at low and higher nickel concentrations, respectively. This corresponds to the result that the water content of the organic phase diminishes gradually with increasing the initial aqueous nickel concentration.

The organic extracts from manganese(II), iron(II), cobalt(II), nickel(II), copper(II) and zinc(II) chloride solutions containing hydrochloric acid in the presence of potassium thiocyanate by Aliquat-336 in benzene at 20°C were

TABLE 1. Infrared Spectral Data for Divalent Metal-thiocyanato Complexes with Aliquat-336

Frequency, cm ⁻¹							Probable assignment
R ₃ R' ⁿ NNCS·H ₂ O	(R ₃ R' ⁿ N ₂) ₂ [Mn(NCS) ₄]	(R ₃ R' ⁿ N ₂) ₂ [Fe(NCS) ₄]	(R ₃ R' ⁿ N ₂) ₂ [Co(NCS) ₄]	(R ₃ R' ⁿ N ₂) ₂ [Ni(NCS) ₄]	(R ₃ R' ⁿ N ₂) ₂ [Cu(NCS) ₄]	(R ₃ R' ⁿ N ₂) ₂ [Zn(NCS) ₄]	
3400(wb)* 3200(sh) 2920(s) 2860(ms) 2092(s) 1710(vw) 1620(vw)				3440(vw)			OH stretching CH stretching (sym. and asym.) CN stretching OH bending
1465(m) 1375(w)	2920(s) 7820(ms) 2050(s)	2920(s) 2820(ms) 2050(s)	2920(s) 2820(ms) 2070(s)	2920(s) 2820(ms) 2090(s)	2920(s) 2820(ms) 2070(s)	2920(s) 2820(ms) 2070(s)	
720(w) 468(w)	1465(m) 1375(w)	1465(m) 1375(w)	1465(m) 1375(w)	1465(m) 1375(w)	1465(m) 1375(w) 798(w)	1465(m) 1375(w)	CH ₃ degenerate bending CH ₂ scissoring CH ₃ sym. bending CS stretching CH ₂ rocking NCS bending
	720(w) 479(m) 280(sb)	720(w) 479(m) 304(sh) 280(sb)	720(w) 479(m) 307(sb) 282(m)	720(w) 479(m) 307(sb) 280(sh) 255(sb)	720(w) 473(s) 310(sb) 300(sh)	720(w) 479(s) 280(sb)	

*s = strong, ms = medium strong, m = medium, w = weak, vw = very weak, b = broad, sh = shoulder

examined by infrared spectroscopy. The frequencies and probable band assignments for the complexes prepared by drying the organic solutions saturated with divalent metals are given in Table 1, compared with those for the organic extract from the aqueous potassium thiocyanate solution only. The spectrum of the organic extract without metal shows the OH stretching and bending bands, the CN stretching band at 2092 cm⁻¹ and the NCS bending frequency at 468 cm⁻¹, implying that the compound R₃R'ⁿNNCS·H₂O²³ is formed by exchanging completely the chloride ion in R₃R'ⁿNCl according to Equation (1). In the spectra of the organic metal extracts, the absorptions due to the OH stretching and bending modes disappear, indicating that the complexes contain no coordinated water supporting the result of the Karl-Fischer titration, except the organic extract of nickel in which the OH absorption bands are slightly observed. This probably arises from the fact that the nickel species extracted at low aqueous nickel concentration displays a coordination number of six, associated with four thiocyanate groups and two water molecules. Simultaneously the infrared result confirms that the thiocyanate group coordinates to divalent metal through nitrogen atom⁽²⁴⁾, although the thiocyanate group bonded to a metal forms either the M-N or M-S bond, depending on the nature of metals.

Structure of Complexes

The magnetic moment of the complexes and their probable structure are given in Table 2. As the observed values of the magnetic moment are analogous to the spin-only values for their metals, it is expected that the contribution of the orbital angular momentum by ligand field is completely quenched for the complexes. This corresponds to

TABLE 2. Magnetic Moment and Probable Structure of Divalent Metalthiocyanato Complexes with Aliquat-336

3d ⁿ	Complex	Structure	Obs. μ _{eff} , B.M.	S.O.* μ _{eff} , B.M.
5	(R ₃ R' ⁿ) ₂ [Mn(NCS) ₄]	Tetrahedral, T _d	6.09	5.92
6	(R ₃ R' ⁿ) ₂ [Fe(NCS) ₄]	Tetrahedral, T _d	5.12	4.90
7	(R ₃ R' ⁿ) ₂ [Co(NCS) ₄]	Tetrahedral, T _d	4.05	3.87
8	(R ₃ R' ⁿ) ₂ [Ni(NCS) ₄]	Tetrahedral, T _d	2.97	2.83
9	(R ₃ R' ⁿ) ₂ [Cu(NCS) ₄]	Distorted Tetrahedral, D _{2d}	1.76	1.73
10	(R ₃ R' ⁿ) ₂ [Zn(NCS) ₄]	Tetrahedral, T _d	0	—

*This is the value of spin-only magnetic moment

the data for the apparent molecular weights indicating that the complexes exist as monomer. Hence, those experimental results also support the structure of the complexes deduced from the spectral studies.

The ESR spectra of manganese(II) and copper(II) complexes are shown in Figures 11-12, compared with the calculated spectra based on the line shapes arising from randomly oriented samples in the tetrahedral and distorted tetrahedral symmetries, T_d and D_{2d}, respectively^(13,25,26). The experimental spectra show the hyperfine structures consistent with the calculated curves. The spectrum of manganese(II) complex exhibits the isotropic six-hyperfine line shape (Figure 11), and the calculated g value is g = 1.996. In contrast, the spectrum of copper(II) complex indicates the typical feature due to a distorted tetrahedral symmetry, and the calculated g values are g_{||} = 2.265 and g_⊥ = 2.053.

It is concluded that the extracted species of manganese(II), iron(II), cobalt(II), nickel(II) and zinc(II) give a tetrahedral T_d symmetry, although the copper(II) species is in a distorted tetrahedron (point group D_{2d} symmetry). However, species of nickel(II) extracted at low aqueous concentration exists as a complex (R₃R'ⁿ)₂-[Ni(NCS)₄(H₂O)₂] in an octahedral O_h symmetry.

Acknowledgment

We wish to thank Dr. K. Watanabe of the Research Institute of Electronics, Shizuoka University, for the ESR spectral measurement, and Messrs. T. Nakamura, T. Kato, S. Ishiguro and S. Kotani for assistance with part of the experimental work.

REFERENCES

- (1) Wilson, A.W. and McFarland, O.K., *Anal. Chem.* 1963, 35, 302.
- (2) Sato, T., Kotani, S. and Good, M.L., *J. Inorg. Nucl. Chem.* 1973, 35, 2547.
- (3) Sato, T., Kotani, S. and Good, M.L., *J. Inorg. Nucl. Chem.* 1974, 36, 451.
- (4) Sato, T., Watanabe, H., Kotani, S. and Yamamoto, M., *Anal. Chim. Acta* 1976, 84, 397.
- (5) Sato, T. and Watanabe, H., *Anal. Chim. Acta* 1970, 49, 463.
- (6) Flaschka, H., *Chemist-Analyst* 1953, 42, 56.
- (7) Koros, E., *Acta Pharm. Hung.* 1957, 27, 10.
- (8) Cheng, K.L., *Anal. Chem.* 1958, 30, 243; Cheng, K.L. and Bray, R.H., *ibid.* 1955, 27, 782.

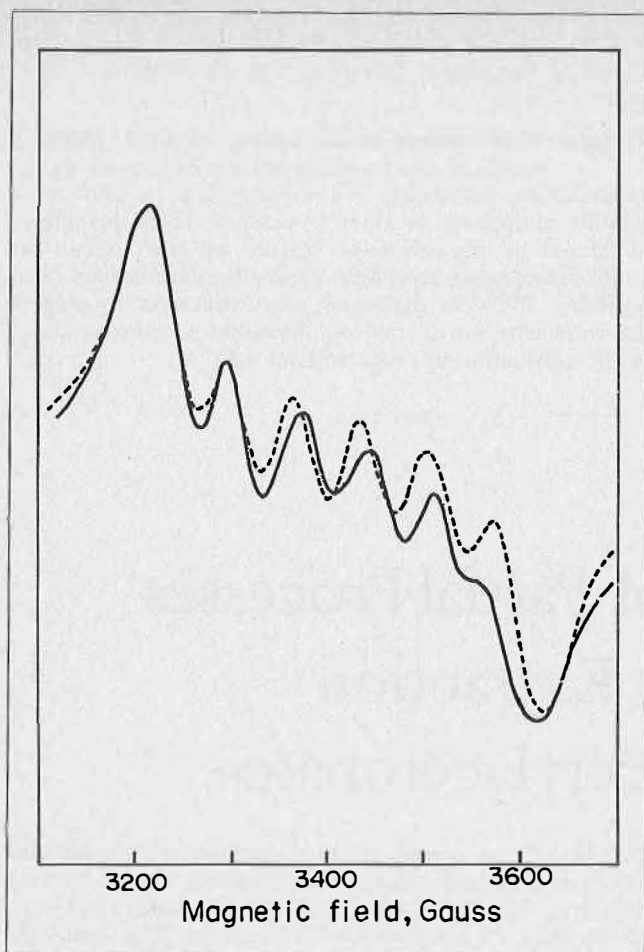


FIGURE 11. ESR spectrum of manganese(II)-thiocyanato complex. Continuous and broken lines are observed and calculated spectra, respectively.

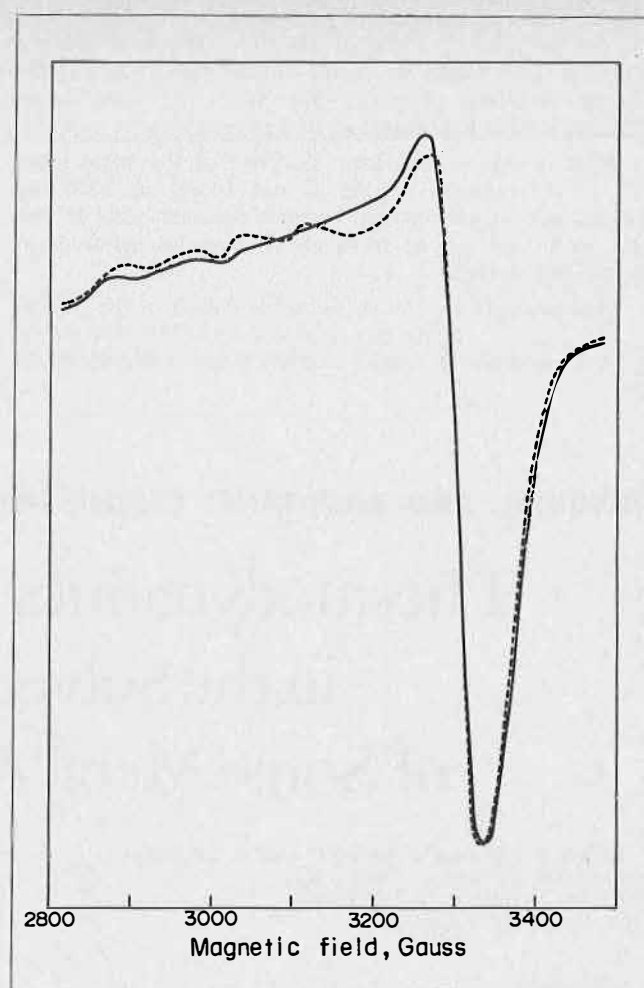


FIGURE 12. ESR spectrum of copper(II)-thiocyanato complex. Continuous and broken lines are observed and calculated spectra, respectively.

- (9) Kinunnunen, J. and Wennerstrand, B., *Chemist-Analyst* 1957, 46, 92.
- (10) Korble, J. and Pribil, R., *Chemist-Analyst* 1956, 45, 102.
- (11) de Sousa, A., *Talanta* 1961, 8, 782.
- (12) Sato, T. and Nakamura, T., *J. Inorg. Nucl. Chem.* 1972, 34, 3721.
- (13) Sato, T., Nakamura, T. and Terao, O., *J. Inorg. Nucl. Chem.* 1977, 39, 401.
- (14) Sato, T. and Kato, T., *J. Inorg. Nucl. Chem.* (in press).
- (15) Gill, N.S. and Nyholm, R.S., *J. Chem. Soc.* 1959, p. 3977.
- (16) Sato, T. and Nakamura, T., *J. Inorg. Nucl. Chem.* 1972, 34, 3721.
- (17) Sato, T. and Ueda, M., "Proc. Int. Solvent Extraction Conf., Lyon, 1974", Vol. 1, p. 871, Soc. Chem. Ind., London (1974).
- (18) Tanabe, Y. and Sugano, S., *J. Phys. Soc. Japan* 1954, 9, 753, 766.
- (19) Jorgensen, C.J., "Absorption Spectra and Chemical Bonding in Complexes", p. 134, Pergamon Press, Oxford (1962).
- (20) Dunn, T.M., "Modern Coordination Chemistry" (Edited by Lewis, J. and Wilkins, R.G.), p. 267, Interscience, New York (1960).
- (21) Venanzi, L.M., *J. Chem. Soc.* 1958, p. 719.
- (22) Cotton, F.A., O.D. and Goodgame, D.M.L., *J. Am. Chem. Soc.* 1961, 83, 344.
- (23) Cotton, F.A. and Goodgame, D.M.L., *J. Am. Chem. Soc.* 1960, 82, 5771, 5774.
- (24) Nakamoto, K., "Infrared Spectra of Inorganic and Coordination Compounds", 2nd Edn., p. 152, Interscience, New York (1970).
- (25) Kneubüher, F.K., *J. Chem. Phys.* 1960, 33, 1074.
- (26) Vänngård, T. and Aasa, R., "Proc. the 1st Int. Conf. on Paramagnetic Resonance, Jerusalem, 1962" (Edited by Low, W.), Vol. 2, p. 509, Academic Press, New York (1963).

DISCUSSION

Y. Marcus: I am worried by the possibility of oxidation in your amine thiocyanate systems, particularly in the presence of acid, by air. This would be shown most readily in the iron(II) systems you described, but also in others, where catalytic oxidation could occur. I have no experience with quaternary amine systems, but some work we did with tertiary amines showed serious problems with oxidation in acid thiocyanate systems, producing coloured, unstable organic phases.

T. Sato: As pointed out, there is the possibility of oxidation in the amine thiocyanate system. Accordingly, all possible care is taken to avoid the oxidation reaction in the selection of the experimental conditions: the extractions are carried out from the aqueous solutions of Mn(II), Fe(II), Co(II), Ni(II) and Zn(II) in 0.007M and of Cu(II) in 0.0035M since the concentration of Cu(II) in 0.007M occurs in the formation of precipitate and in addition, the concentration of acid contained in their aqueous solutions to prevent the hydrolysis is as low as possible. Therefore we have no trouble in the formation of amine thiocyanato complexes with the oxidation in the presence of thiocyanate, except for the oxidation of ferrous species to ferric. In the extraction of iron, however, the absorption spectra of the species in the organic phase are not much different from that of ferrous ion, although the organic colour is slightly changed from green to brown.

A.J. Oliver: Further to Dr. Marcus's comments I would like to add that we have observed that the cupric ion also seems to slowly oxidize thiocyanate (CIM Bulletin). I would appreciate Dr. Sato's comments as to whether he also has observed this phenomenon.

T. Sato: In our experiments, evidence of the coexistence of cuprous species is not found in both the organic and aqueous phases because the extraction is carried out by the use of fresh cupric aqueous solutions in the present system.

A. Warshawsky: Our work on noble metals in the thiocyanate has indicated to us that the stability of thiocyanate in acidic solution is low and sulphur or

sulphur compounds precipitate out at pH values lower than 2. This will complicate work at the acid range presented in this paper. This remark is an addition to Prof. Marcus's report.

T. Sato: With relation to the answer to Prof. Marcus's comment, the experimental conditions are chosen to avoid the formation of the precipitate in sulphur or sulphur compounds as much as possible. If the precipitate is formed in this extraction system, we can't obtain the amine thiocyanato complexes indicating their normal compositions. Thus, in particular, the extractions to prepare the complexes are carried out from the aqueous solutions in the concentration range without acid.

PHYSICAL AND INORGANIC CHEMISTRY

Thermodynamics of Partial Processes in the Solvent Extraction of Some Metal Acetylacetonates

B. Allard, S. Johnson, J. Narbutt* and R. Lundqvist
Department of Nuclear Chemistry,
Chalmers University of Technology,
Fack, Göteborg 5, Sweden

ABSTRACT

Partial processes of the overall partition of chelate complexes in liquid two-phase systems have been proposed. Measured thermodynamic data for the partition of some metal acetylacetonates (with Be, Cu, Zn, Ce, Hf, Th, U and Np) have been compared with estimated data for contributions from various partial processes such as mixing and water structuring, inner- and outer-sphere dehydration and interactions with the organic diluent.

Introduction

WHILE THE PRACTICAL IMPORTANCE of solvent extraction as a separation method is increasing, the prediction of extraction behaviour of metals in quantitative terms can only be accomplished for some very simple systems. The application of the theory of regular solutions became successful in predicting the effect of inert diluents on distribution ratios⁽¹⁾. However, in order to allow a quantitative interpretation and prediction of thermodynamic partition data and the influence of chemical and physical system parameters on a two-phase equilibrium, a division of the partition process into partial processes is required⁽²⁾. Despite the fact that the major part of the free energy change for the overall partition process is usually due to the processes in the aqueous phase, a quantitative estimation of these effects can rarely be accomplished. Only recently, attempts have been made to estimate the contributions from the processes in the aqueous phase, e.g. based on semi-empirical data for the solubility of hydrocarbons in water⁽³⁾. In the present investigation a

division of the overall partition process into partial processes is proposed and the corresponding thermodynamic functions are estimated empirically, especially for complexes between acetylacetonate (denoted by HA) and some divalent (Be, Cu, Zn, HfO, UO₂) and tetravalent (Ce, Th, U, Np) ions.

Partial Processes in Two-phase Equilibria

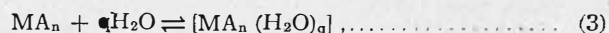
The complex formation-partition model can be used to describe the extraction of a metal ion, Mⁿ⁺, with a chelating agent, e.g. acetylacetonate, HA, which forms extractable complexes⁽³⁾:



where (org) denotes species in the organic phase (species in the aqueous phase without denotation). (In the present systems only monomeric complexes are formed).

For the complex formation, according to (1), a positive contribution to both the enthalpy and the entropy can be expected due to the destruction of the hydration layer around the metal ion; while the formation of an MA_n⁻ species will be accompanied by large negative enthalpy and entropy changes. For the total reaction, a negative enthalpy change and a positive entropy change will usually be obtained. The complex formation process according to (1) will not be discussed any further in this paper since only the partial processes of the partition of the uncharged complex according to (2) will be considered.

A hydration in the inner coordination sphere of species in the aqueous phase, according to



may sometimes be expected. A necessary requirement for the formation of an inner-sphere hydrated species is coordinative unsaturation which means that the number of ligand atoms is less than the maximal coordination num-

*On leave from the Department of Radiochemistry, Institute of Nuclear Research, Warsaw, Poland.

ber. This may be the only requirement for complexes between hard metals and complexing agents with oxygen ligand atoms. In these cases the coordination polyhedron is largely determined by the geometry of the ligand and the metal-ligand bond distances are largely determined by electrostatic interactions. The probability of inner-sphere hydration is increasing when the radius of the central ion is increasing for complexes with similar stoichiometric composition.

For complexes with soft metals, however, the geometry of the coordination polyhedron may be influenced by the shape of the orbitals. Although the size of the coordination polyhedron allows an increase of the number of coordinated ligand atoms, the entering of water may be prevented, in certain directions due to the existence of non-bonding orbitals.

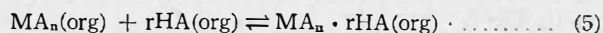
Many metal chelates, e.g. metal acetylacetonates, are hydrated to some extent in the outer coordination sphere (ligand hydration) in aqueous solutions⁽⁴⁾, as given by



The extent of outer-sphere or ligand hydration is of course largely dependent on the properties of the ligand, such as polarity and electron density, presence of donor atoms, bonding, geometry, etc. A simultaneous hydrogen formation with the ligand atom and ion-dipole interaction with the central atom is not sterically impossible. The thermodynamic functions of the outer-sphere hydration should be related to the number of ligands and be less dependent on the central atom. This gives a rather constant contribution to the functions for the overall process in a series of similar complexes of different metals, unless differences in the geometry of the coordination polyhedron result in steric hindrances for hydration.

Besides the specific hydration according to (3) and (4), a water structuring effect can be expected in the vicinity of the hydrophobic surface of a complex having large organic ligands. This hydrophobic structuring is well known for hydrocarbons dissolved in aqueous solutions⁽⁵⁾. Due to the non-polar surface of the organic ligands, the number of tetracoordinated water molecules is increased which is accompanied by a substantial decrease in entropy, since the water molecules have less freedom for random movements.

In some systems an adduct formation with the chelating agent itself can occur in the organic phase:



For diluents with donor atoms or atoms capable of forming hydrogen bonds, a solvation in the organic phase may be accomplished, preferably in the outer coordination sphere. The solvation will cause an entropy decrease due to the loss of the degree of freedom for random movements of the diluent molecules and the ordering around the complex species in the organic phase. On the other hand, the disordering of the original solvent structure will give a positive entropy contribution. The net change will, however, always be negative. Moreover, there is always a mixing (hole formation) process in both phases, which contributes to the thermodynamic functions for the overall process. Generally, this process gives positive enthalpy and entropy changes in both phases⁽⁶⁾.

Expected Thermodynamic Values for the Partition Process

For the actual partition process, the overall measured thermodynamic parameters Δh^P and Δs^P could be divided into

$$\Delta h^P = \Delta h^M + \Delta h^H + \Delta h^W + \Delta h^{\text{Int}} \dots (6a)$$

$$\Delta s^P = \Delta s^M + \Delta s^H + \Delta s^W + \Delta s^{\text{Int}} \dots (6b)$$

where P denotes partition, M mixing, H hydration, W water structuring and Int specific interactions in the organic phase.

Assuming regular and dilute solutions, but with an athermal entropy of mixing⁽⁶⁾, the partition constant K_p^s (in molar fractions) for a species A in a liquid two-phase system can be described by

$$-RT \ln K_p^s = v_A[(\delta_A - \delta_o)^2 - (\delta_A - \delta_{aq})^2] + RT \left[\ln \frac{v_{aq}}{v_o} + v_A \left(\frac{1}{v_{aq}} - \frac{1}{v_o} \right) \right] \dots (7)$$

where v is the molar volume and δ the solubility parameter, and o and aq denote species in the organic and aqueous phase, respectively. From eqn (7) the terms corresponding to the enthalpy and entropy changes Δh^M and Δs^M can formally be evaluated⁽⁷⁾. This division into enthalpy and entropy terms should, however, not be done as a rule. Deviations from the requirements stated for regular systems will cause errors in the enthalpy and entropy terms which, fortuitously, largely cancel when comparing free energy values. In this investigation, using very similar systems, the values corresponding to the mixing process have not been estimated. Instead the measured values have been directly compared (see below).

The changes in the thermodynamic functions due to outer-sphere hydration may be estimated by comparison of thermodynamic parameters for the solubility in water of polar (with oxygen) and non-polar homomorphic hydrocarbons⁽⁴⁾, e.g. alcohols with alkanes⁽⁸⁻¹⁴⁾. In the molar volume range 80-160 cm³/mole, values for the standard enthalpy of solution are rather constant, about $\Delta h_{so1}^o = 2 \pm 2$ kJ/mole for straight-chain alkanes or aromates like benzene, toluene and xylene. The corresponding standard entropy values show a linear dependence of the molar volume, with values of $T \Delta s_{so1}^o = -27 \pm 3$ kJ/mole for the alkanes, and $T \Delta s_{so1}^o = -17 \pm 3$ kJ/mole for the aromates, assuming $v = 90$ cm³/mole, which is approximately the molar volume of one ligand in acetylacetonates. For alcohols a slight increase of the standard enthalpy of solution with increased volume can be noticed. For cyclic and straight chained 1-alcohols as well as for 1,4-dioxan the standard enthalpy values are $\Delta h_{so1}^o = -10 \pm 3$ kJ/mole, and for 2- and 3-alcohols, $\Delta h_{so1}^o = -13 \pm 3$ kJ/mole. The corresponding standard entropy values are $T \Delta s_{so1}^o = -19 \pm 3$ kJ/mole for both 1-, 2-, 3- and cyclic alcohols and $T \Delta s_{so1}^o = -14$ kJ/mole for 1,4-dioxan. Thus an outer-sphere or ligand hydration involving a water molecule from the hydrophobic layer seems to cause enthalpy and entropy changes of about $\Delta h^H = -12 \pm 5$ kJ/mole and $T \Delta s^H = 8 \pm 6$ kJ/mole for aliphatic compounds and $T \Delta s^H = 3 \pm 6$ kJ/mole for aromatics. The numerical difference in entropy between alcohols, with hydrogen bonded water, and alkanes, with hydrophobic structured water only, is very small which indicates that the formation of a hydrogen bonded water merely involves a stronger interaction with a water molecule that already has a certain orientation in the vicinity of the ligand.

Enthalpy values of hydrogen bonding are normally $-\Delta h^H = 15-25$ kJ/mole⁽¹⁵⁾. From other chelate systems the entropy change caused by the bonding of one hydrate water has been estimated to be $-T \Delta s^H = 15-17$ kJ/mole⁽¹⁶⁾. The enthalpy and entropy changes of ion-dipole interaction between the metal ion and an oxygen atom in a water molecule (inner-sphere hydration) would probably be of the same order.

For hydrogen-bonding diluents in the organic phase a $-\Delta^{int}$ -value of about 15-25 kJ/mole (e.g. 25 kJ/mole for chloroform)⁽¹⁷⁾ and a corresponding negative $T\Delta s^{int}$ -value numerically smaller will be expected. Solvation in the outer-sphere by dipol-dipol interaction is likely to give numerically smaller values for Δh^{int} . In Table 1, predicted signs of the standard enthalpy and entropy are given according to the discussion above. The influence of parameters such as the molar volumes, the ionic strength of the aqueous phase, etc. are summarised in Table 2.

Experimental

Distribution Measurements

The distribution of metal acetylacetonates was measured as previously described.⁽⁷⁾ Aqueous phases were 0.1 and 1.0 M (Na,H)ClO₄ and as organic diluents, n-hexane and benzene were used. The measurements on Be, Cu, Zn and Np were carried out by using the AKUFVE technique, while the other systems were performed by a batch technique.

Chemicals

Sodium perchlorate and acetylacetone were prepared and purified according to conventional methods. All other chemicals were of p.a. quality and used without further purification.

TABLE 1. Predicted Signs for the Partial Processes of the Partition of Acetylacetonates Between Organic Diluents and Water.

Phase	Partial process	Δh	Sign* and $T\Delta s$
Aq	Mixing	-	-
	Water restructuring		+
	Outer-sph. dehydration	+	+(¹)
	Inner-sph. dehydration	+	+
Org	Mixing	+	+
	Adduct formation	-	-
	Solvation	-	-

(¹)Hydration involving water from the hydrophobic water layer will give a slight negative value.
*The signs refer to the reaction $A \rightarrow A(org)$

Results

Measured values for the partition of acetylacetonates with Be, Cu, Zn, Ce, Hf, Th, U and Np between inert organic diluents and aqueous NaClO₄⁻ solutions are given in Table 3.

Discussion

The values in Table 4 indicate a hydration of CuA₂ corresponding to one molecule of water in outer-sphere position ($\Delta h^H \approx 10$ kJ/mole), and possibly three outer-sphere water molecules for ZnA₂, in comparison with BeA₂. The values of ZnA₂ could also be explained by assuming one water molecule in the outer-sphere and one in the inner-sphere (with $\Delta h^H \approx 25$ kJ/mole) which is probable (see below). Distribution measurements at various ionic strengths (0.5 M NaClO₄) indicate, however, that BeA₂ must have at least one hydrated water molecule at zero ionic strength⁽¹⁹⁾. Thus, CuA₂ would have about two water molecules in outer-sphere position, while ZnA₂ would have two in the outer-sphere and one in the inner-sphere. The values for ThA₄, UA₄ and NpA₄ indicate an outer-sphere hydration of about one water molecule per ligand. A specific interaction in the organic phase indicating an adduct formation with acetylacetone, with a corresponding decrease of the number of hydrated water molecules, can explain the data for CeA₄. Evidently, HfOA₂ is strongly hydrated both in outer- and inner-sphere position, while for UO₂A₂ the water is partly replaced by acetylacetone.

These conclusions are supported by complementary experiments. By evaporation of water containing organic solutions of BeA₂ and CuA₂, only non-solvated species will be formed. Solid hydrates of CuA₂ can not be obtained even from solutions with a very high water content⁽¹⁹⁾. For ZnA₂, however, a species with a coordination number higher than four is always obtained, either ZnA₂·H₂O or (ZnA₂)₃, and the existence of ZnA₂·2H₂O and ZnA₃⁻ has also been suggested^(27,28). The formation of a hydrate that is extractable, e.g. ZnA₂·H₂O, can not directly be indicated. Such a species would, however, have a slightly higher solubility parameter value which would give a larger Δh^M value. Such small changes of a overall enthalpy change can not be detected, according to Table 4, since the errors of the other contributions probably are much larger.

TABLE 2. Predicted Changes of the Thermodynamic Functions for the Partial Partition Processes Due to Variations of Parameters of the Extraction System.

Symbols (plus or minus) denote the numerical changes, "0" denotes very small changes and "no" denotes that the thermodynamical functions of the partial process should be independent of the parameter.

Phase	$v_A^{(1)}$		CN ⁽²⁾		$n^{(3)}$		I ⁽⁴⁾		$\delta^{(5)}$		
	Δh	$T\Delta s$	Δh	ΔTs	Δh	$T\Delta s$	Δh	$T\Delta s$	Δh	$T\Delta s$	
Aq	Water restruct.	0	+	0	0	0	+	-	-	no	no
	+ mixing										
	Outer-sph. dehydr.	0	0	0	0	+	+	-	-	no	no
	Inner-sph. dehydr.	0	0	+	+ ⁽⁶⁾	0	0	-	-	no	no
Org	Mixing	+	+	0	0	+	+	no	no	+	0
	Solvation	0	0	+	+ ⁽⁶⁾	+	+	no	no	+	+

(¹)Increased volume but with constant stoichiometry and coordination number (coordinative saturation)

(²)Possibility for increased coordination number but otherwise constant molecular volume (change from coordinative unsaturation to saturation)

(³)Increased volume giving increased number of ligands and changed stoichiometry

(⁴)Increased ionic strength (decreased water activity)

(⁵)Increased solubility parameter

(⁶)Assuming that hydration respective adduct formation occurs

TABLE 3. Measured Partition Constants (in molar fractions) and Standard Enthalpy and Entropy Changes for the Partition Process of Acetylacetonates between Inert Organic Diluents and Aqueous Solutions of Various Ionic Strength

Complex	Diluent	I	logk ₅	Δh ^P	TΔs ^P	Ref.
BeA ₂	n-hexane	0.1	1.38	25	33	18
		1.0	1.50	22	30	18
CuA ₂	n-hexane	0.1	0.18	35	36	19
		1.0	0.27	32	34	19
CuA ₂	benzene	0.1	1.54	33	42	19
		1.0	1.72	26	36	19
ZnA ₂	n-hexane	0.1	-0.90	60	55	19
		1.0	-0.45	51	48	19
ZnA ₂	benzene	0.1	0.16	57	58	19
		1.0	0.48	47	50	19
CeA ₄	n-hexane	1.0	0.02	40	40	20
ThA ₄	n-hexane	1.0	1.49	68	76	20
UA ₄	n-hexane	1.0	1.51	65	74	20
NpA ₄	n-hexane	1.0	1.39	72	80	21
HfOA ₂	benzene	0.1	2.04	65	76	22
		1.0	2.12	58	70	22
UO ₂ A ₂	benzene	0.01	1.24	8	15	22
		1.0	1.32	4	11	22

For CeA₄, an adduct formation with HA has in fact been found, but not for ThA₄, UA₄ or NpA₄^(30,31). An adduct formation with UO₂A₂ is also indicated from the distribution measurements⁽²²⁾, and both UO₂A₂·H₂O and UO₂A₂·HA can be isolated as solids.

For most of the complexes crystallographic data are available⁽²³⁻²⁶⁾. Divalent acetylacetonates may form 4-coordinated tetrahedral or square planar complexes as seen in Figure 1. For a planar or distorted tetrahedral configuration, a 5th atom might be coordinated perpendicular to the square face, giving a 5-coordinated tetragonal pyramidal configuration, or eventually, at the addition of a 6th atom, a 6-coordinated octahedral configuration. For the tetravalent 8-coordinated species, a 9th atom might enter perpendicular to one of the square faces of the antiprism or of the corresponding distorted dodecahedron.

For BeA₂ the intermolecular distances of the coordination polyhedron prevent the formation of an inner-sphere hydrated species. For most acetylacetonate complexes, a simultaneous ion-dipole interaction and hydrogen bond formation with hydrate water is possible (see above). For an undistorted planar structure like the coordination polyhedron for CuA₂, however, the hydrogen bond distance will be too large (> 2.84 Å) for simultaneous interaction with the metal, giving very weak H - O - H-interactions, if any. Moreover, it is well known that Cu in solution, e.g. water, tend to be 4-coordinated with a square planar configuration and with two additional coordinated molecules at a substantially larger distance from the central atom on the axis perpendicular to the square plane⁽³¹⁾. The presence of an unpaired d-electron may explain this configuration. For Zn, however, with a filled d-shell, both

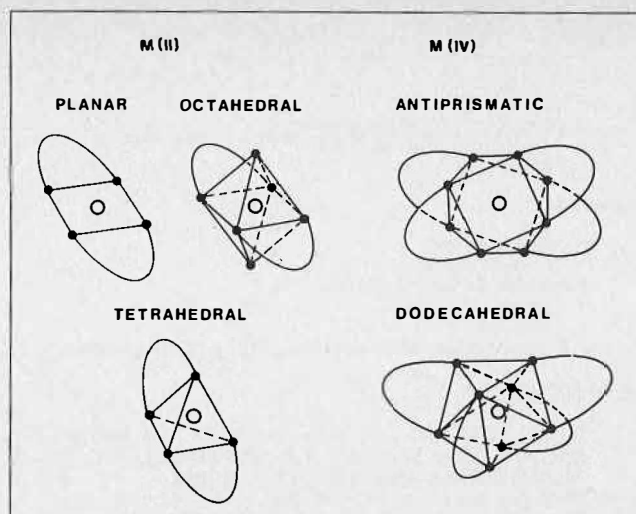


FIGURE 1. Coordination polyhedra for di- and tetravalent metal acetylacetonates.

TABLE 4. Measured Thermodynamic Functions Compared with the Values for BeA₂ at the Ionic Strength 0.1 M (1.0 M for MA₄)

Complex	Diluent	Δh _{rel} ¹⁾	TΔs _{rel} ¹⁾
BeA ₂	n-hexane	0	0
CuA ₂	n-hexane	10	3
	benzene	8	9
ZnA ₂	n-hexane	35	22
	benzene	32	25
CeA ₄	n-hexane	-4	-20
ThA ₄	n-hexane	24	16
UA ₄	n-hexane	21	14
NpA ₄	n-hexane	28	20
HfOA ₂	benzene	40	43
UO ₂ A ₂	benzene	-17	-18

$$^1)\Delta h_{rel} = \Delta h^P - x \cdot \Delta h^P_{BeA_2}$$

$$\Delta s_{rel} = \Delta s^P - x \cdot \Delta s^P_{BeA_2}$$

x = 1 for CuA₂, ZnA₂, HfOA₂, and UO₂A₂; x = 2 for MA₄.

tetrahedral and octahedral species are known and also intermediates between them.

Despite all simplifications, the general picture given in Tables 1, 2 and 4 concerning the partial processes may give some qualitative and semi-quantitative description of the actual processes. It should, however, be pointed out that since many parameters have been used, it is always possible to establish acceptable fits between measured and calculated data just by a suitable combination of the contributions from the different processes,

Acknowledgments

The valuable comments and suggestions by Prof. J. Rydberg, Dr. S. Wingefors and Docent J.O. Liljenzin are gratefully acknowledged.

Parts of this work have been supported by the Swedish Atomic Research Council and the Swedish Natural Science Research Council.

NOTATION

Δh	= enthalpy change [kJ/mole, at 25°C]
Δs	= entropy change [kJ/mole°]
K ₅	= partition constant [molar fractions, at 25°]
δ	= solubility parameter [(J/cm ³) ^{1/2}]
I	= ionic strength [M]
v	= molar volume [cm ³ /mole]

Superscript

- P = partition
M = mixing
W = water structuring
Int = interaction (organic phase)
H = hydration (aqueous phase)
° = standard function

Superscript

- o = organic phase
aq = aqueous phase
A = solute (metal complex)
n = number of ligands
sol = solubility
rel = relative value in comparison with a reference system

REFERENCES

- (1) Irving, H.M.N.H., in "Ion Exchange and Solvent Extraction" (Eds. Marinsky, J.A. and Marcus, Y.), Vol. 6, Marcel Dekker, New York 1974, p. 140.
- (2) Rydberg, J., J. Ind. Chem. Soc. 1974, 51, 15.
- (3) Siekierski, S., Radioanal. Chem. 1976, 31, 335.
- (4) Narbutt, J., to be published.
- (5) Frank, H.S. and Evans, M.W., J. Chem. Phys. 1945, 13, 507.
- (6) Hildebrand, J.H., Prausnitz, J.M. and Scott, R.L., "Regular and Related Solutions", Van Nostrand/Reinhold, New York 1970.
- (7) Allard, B., Johnson, S. and Rydberg, J., Proc. Int. Solvent Extraction Conf., Lyon 1974, p. 1419.
- (8) Nemethy, G. and Scheraga, H.A., J. Chem. Phys. 1962, 36, 3461.
- (9) Hill, D.J.T., Thesis, Univ. of Queensland, 1965.
- (10) Nelson, A.D. and DeLigny, C.L., Rec. Trav. Chim. Pays-Bas, 1968, 87, 528.
- (11) Reid, D.S., Quickenden, M.A.J. and Franks, F., Nature 1969, 224, 1293.
- (12) Franks, F. (ed.), "Water: A Comprehensive Treatment", Vol. 2, Plenum Press, New York-London, 1973.
- (13) Avegard, R. and Heselden, R., J. Chem. Soc. Faraday Trans. 1974, 70, 1953.
- (14) Gill, S.J., Nichols, N.T. and Wadsö, I., J. Chem. Thermodynamics 1976, 8, 445.
- (15) Kandil, A.T., Aly, H.F., Raieh, M. and Choppin, G., J. Inorg. Nucl. Chem. 1975, 37, 229.
- (16) Choppin, G., Proc. 13. Int. Conf. Coordination Chem., Poland 1970.
- (17) Irving, R.J. and Schultz, R.A., J. Chem. Soc. Dalton Trans. 1973, 22, 2414.
- (18) Johnson, S., to be published.
- (19) Johnson, S., Narbutt, J. and Allard, B., to be published.
- (20) Allard, B., J. Inorg. Nucl. Chem. 1977, 39, 694.
- (21) Liljenzin, J.O. and Stary, J., J. Inorg. Nucl. Chem. 1970, 32, 1357.
- (22) Lundqvist, R., to be published.
- (23) Amirthaligam, V., Padmanabhan, V.M. and Shankar, J., Acta Cryst. 1960, 13, 201.
- (24) Piper, T.S. and Belford, R.L., Mol. Phys. 1962, 5, 169.
- (25) Montgomery, H. and Lingafelter, E.C., Acta Cryst. 1963, 16, 748.
- (26) Allard, B., J. Inorg. Nucl. Chem. 1976, 38, 2109.
- (27) Lippert, E.L. and Truter, M., J. Chem. Soc. 1960, 4996.
- (28) Rudolph, G. and Hemy, M.C., Inorg. Chem. 1964, 3, 1317.
- (29) Suzuki, N. and Oki, S., Bull. Chem. Soc. Jap. 1962, 35, 237.
- (30) Rydberg, J., Sv. Kem. Tidskr. 1955, 67, 499.
- (31) Graddon, D.P., Coord. Chem. Rev. 1969, 4, 1.

PHYSICAL AND INORGANIC CHEMISTRY

Thermodynamics of Liquid-Liquid Distribution Reactions. V. Enthalpy - and Entropy-Controlled Extraction Processes

Y. Marcus,

Department of Inorganic & Analytical Chemistry,
The Hebrew University of Jerusalem,
Jerusalem, Israel.

ABSTRACT

Solvent extraction equilibria have been shown to be determined essentially by either enthalpic or entropic contributions. A discussion of the interactions occurring in the systems must not be based on data which are obscured by extraneous effects, like enthalpy changes obtained from the temperature dependence of the distribution ratios. Calorimetric data on two-phase heats of transfer, properly corrected for dilution and mixing, decide whether an extraction system is enthalpy- or entropy-controlled, as manifested by the relative size of ΔH and of $T\Delta S$ for the overall transfer process for defined standard states. The extraction of uranyl nitrate by TBP in dodecane is controlled by a balance between the dehydration enthalpy balanced by the ion-association (80%) and the bonding with the extractant (20%) enthalpies. The extraction of lithium bromide is governed by the entropy barrier, created by removal of the structure-breaking bromide

anion from its aqueous environment, and loss of translational entropy on ion-pairing.

Introduction

PRACTICING EXTRACTION CHEMISTS and technologists are interested in the position of the distribution equilibrium under various conditions of temperature and the concentrations of the components of the system. They are also interested in the possibility of improving the selectivity of distribution systems, and in being able to control the extraction and back extraction equilibria, by manipulating well understood variables, rather than by empirically varying all the variables of the systems. To this end, a thorough thermodynamic analysis of the situation should prove very helpful, since it should be able to tell which are the main interactions involved, which of these are adjustable by proper choice of reagents and their concentrations, or of the temperature, and where to put the main effort of development.

The position of the equilibrium in the system is customarily described in terms of a conditional equilibrium constant K' . This quantity, although independent of the concentrations of the reactants and products, depends on the

concentrations of all the other components in both phases, and, of course, on the temperature. This equilibrium constant K' can be expressed also as a Gibbs free energy change for the extraction equilibrium.

$$\Delta G' = -RT \ln K' \quad (1)$$

In order, however, to relate this quantity to the interactions occurring in the system, it is necessary to define appropriate standard states for the two phases and find the standard Gibbs free energy change ΔG^* , and the corresponding standard enthalpy and entropy changes

$$\Delta G^* = \Delta H^* - T\Delta S^* \quad (2)$$

This is not a trivial, textbook-thermodynamics requirement, since an injudicious choice here may obscure the whole issue. Furthermore, it is necessary at this stage to realize that ΔG^* and ΔS^* depend on the concentration scale employed, and again, wrong conclusions may be drawn if this point is not carefully considered. In order to avoid the arbitrariness involved in choosing the molal scale (dependence on the often irrelevant molar mass of the solvent), and the complications involved with temperature and pressure sensitive volumes involved in the molar scale, it is advantageous to consider the unitary⁽¹⁾ parts of the Gibbs free energy $\Delta G^*_{(x)}$ and of the entropy $\Delta S^*_{(x)}$, i.e. to employ the mole fraction scale. A choice of the standard state is often not as straightforward as it seems. The two phases at equilibrium usually exhibit some mutual miscibility, so that the state of infinite dilution of all solutes in each of the two separate solvents (water and the organic solvent) is not identical with the state of infinite dilution of all solutes in the mutually saturated solvents, which applies in the present context. Sometimes, therefore, literature data on the behavior of a solute in a solvent must be modified for the presence of the second solvent, arising from the other phase. Furthermore, in systems involving a liquid extractant and a diluent, each of them may be legitimately considered as a standard state, and a transfer of the solute (the distribuend) between the two may become of interest⁽²⁾. On the other hand, if high concentrations of the solute are necessary to effect measurable extraction, there is a point in considering the saturated, rather than the infinite dilute, solution as the standard state^(3,4). The choice among these possibilities depends on the availability of auxiliary data, such as solubilities and activity coefficients, heats of dilution and of mixing, the mutual solubility of the two solvents and its temperature dependency, etc.

The determination of the unitary standard Gibbs free energy change $\Delta G^*_{(x)}$ from the conditional equilibrium constant K' is generally straightforward. Usually, it is sufficient to set

$$\Delta G^*_{(x)} = RT \left[\lim_{\text{Mall solutes} \rightarrow 0} - \ln K'_{(m)} - r \ln(\text{mols H}_2\text{O/kg}) + p \ln(\text{mols solvent/kg}) \right] \quad (3)$$

where r is the sum of the stoichiometric coefficients of the reactants (assumed to be all in the aqueous phase), p the corresponding sum for the products (assumed all in the solvent phase), and $K'_{(m)}$ is the equilibrium constant on the molal scale. In eq. (3), the pure organic solvent is the standard state for the organic phase. If the equilibrium constant is in the molar scale $-\ln v$ should replace $\ln(\text{mols/kg})$, where v is the molar volume expressed in liters. If not all the reactants and products are in the above designated phases (as in an exchange reaction⁽⁵⁾, or one involving an organic extractant explicitly⁽²⁾), r and p must be suitably modified.

The determination of the standard enthalpy change H^* is more troublesome. Since, usually, the temperature dependence of the activity coefficients is unknown, the temper-

ature dependence of the conditional equilibrium constant, $d \ln K'/d \ln (1/T)$, is an unreliable measure of this enthalpy change. Contrary to the relative insensitivity of the free energy change to undetermined activity coefficients or their ratios, included in K' , the enthalpy change can be very sensitive. Cases have been found⁽⁵⁾ where the heats of dilution and mixing, which would manifest themselves in the temperature dependence of the activity coefficient term, are larger than the proper heat of extraction, expressible as $d \ln K^*/d \ln (1/T)$. The only valid way to obtain the enthalpy change is, therefore, to measure it calorimetrically. The two-phase calorimetric heat of transfer of the distribuend measured on the system must be (a) corrected for accompanying heats of dilution, heats of reconcentration, heats of mixing of the excess reagents at their changing concentrations, etc., and (b) corrected to give the value for the standard state. The former corrections may be an appreciable part of the measured ΔH (see above⁽⁵⁾), typically⁽²⁾, say, 20%, and the latter may often be conveniently made by extrapolation to zero solute concentration, if this, indeed, is the standard state. Otherwise, the corrections under item (a) above can be made directly to the standard state by including the proper limits in the integrals for the heats of solution, mixing, etc.^(5,6), to give ΔH^* .

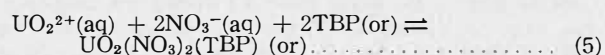
Once the standard unitary Gibbs free energy change $\Delta G^*_{(x)}$ and the standard enthalpy change H^* have been obtained per mole of the specific extraction equilibrium, the standard unitary entropy change must be obtained by difference

$$\Delta S^*_{(x)} = (\Delta H^* - \Delta G^*_{(x)})/T \quad (4)$$

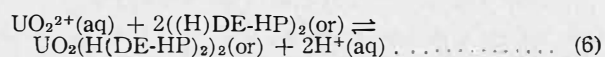
Inspection of the magnitudes of the quantities obtained now decides whether $|\Delta H^*| > |T\Delta S^*_{(x)}|$, so that the extraction equilibrium is enthalpy controlled, or whether the reverse relationship applies between the absolute values, i.e. $|T\Delta S^*_{(x)}| > |\Delta H^*|$, and then the equilibrium is entropy controlled.

Enthalpy Controlled Extraction

It is often implied by authors that the considerable and selective extraction of a distribuend with a given extractant is due to the large energy of the bond formed between them. This may be true, but is very seldom substantiated by the evidence presented. There are, however, cases where the enthalpy control of the extraction has been well documented, according to the concepts presented above. This is the case for the extraction of dioxo-uranium(VI) nitrate with tri-*n*-butylphosphate (TBP) in dodecane⁽²⁾



and for the extraction of the dioxo-uranium(VI) cation with (dimeric) bis(2-ethyl-hexyl) phosphoric acid (H)DE-HP in dodecane from dilute nitric acid in exchange for hydrogen ions⁽⁵⁾



The data for reaction (5) lead to $\Delta H^*_{(5)} = -54.5 \pm 1.5 \text{ kJ mol}^{-1}$, compared with $T\Delta S^*_{(5)} = -9.0 \pm 1.5 \text{ kJ mol}^{-1}$, so that the reaction is clearly enthalpy controlled. The data for reaction (6) lead to less precise values (due to complications inherent in the exchange reaction, and to polymerization side reactions) $\Delta H^*_{(6)} = -30 \pm 3 \text{ kJ mol}^{-1}$, compared with $T\Delta S^*_{(6)} = +2 \pm 6 \text{ kJ mol}^{-1}$, but again the enthalpy control is clear. Although the entropy changes involved in these reactions are interesting⁽⁷⁾, here consideration will be given only to the enthalpy changes, and only for the former reaction, (5), where the data are more precise.

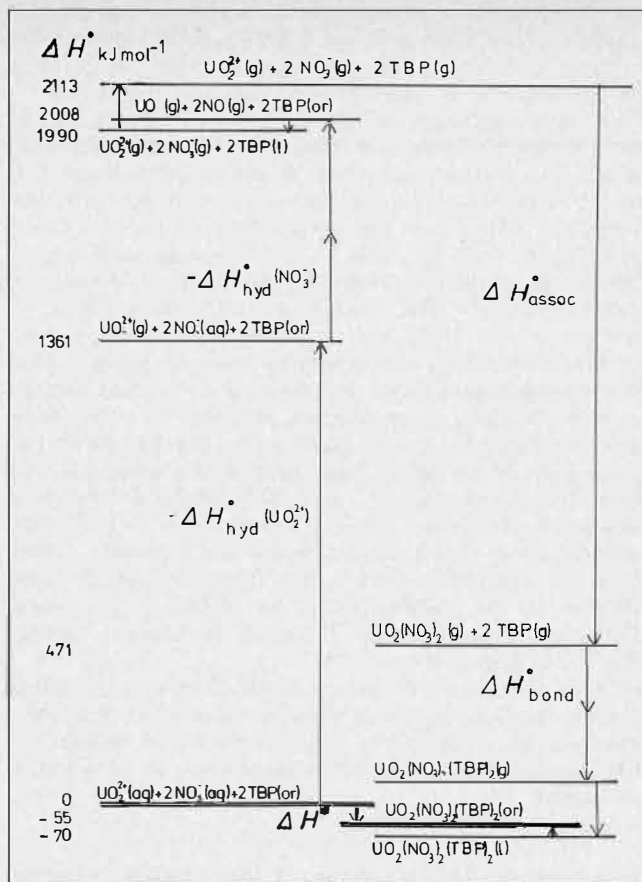


FIGURE 1. The enthalpy level diagram for extraction of uranyl nitrate from aqueous solutions into TBP in dodecane, based on infinite dilution standard states.

The relationships involved here are best shown in an enthalpy diagram⁽⁷⁾ (Figure 1). It is seen that two interactions dominate the diagram by their size: the heat of hydration of the uranyl (dioxouranium(VI)) cation $\Delta H_h(\text{UO}_2^{2+}) = -1361 \pm 23 \text{ kJ mol}^{-1}$, the negative of which must be invested in order to remove the uranyl cation from its aqueous environment, and the heat of electrostatic association $\Delta H_{\text{assoc}}(\text{UO}_2^{2+} + 2\text{NO}_3^-) = -1642 \pm 3 \text{ kJ mol}^{-1}$, which is returned on formation of the species in the organic phase. To these must be added the negatives of the heat of hydration of the two nitrate anions $2\Delta H_h(\text{NO}_3^-) = 2(323.5 \pm 6) = -647 \pm 6 \text{ kJ mol}^{-1}$, to give three large blocks of enthalpy, which have nothing to do with the particular extractant employed, describing the hypothetical reaction



for which the net standard enthalpy change is endothermic: $\Delta H^*_{(7)} = +366 \text{ kJ mol}^{-1}$. It is the gap between this value, and the observed exothermic enthalpy change, $\Delta H^*_{(5)} = -54.5 \text{ kJ mol}^{-1}$, which is covered by interactions with the extractant and the diluent, where judicious choices can make meaningful improvements. This gap of $-420.5 \text{ kJ mol}^{-1}$ constitutes only 21% of the total hydration enthalpy which must be invested for the extraction to proceed. Once the reagent employed, TBP, has been decided on, the two new bonds between the uranium atom and the two phosphoryl oxygen atoms contribute most of the remaining gap $2\Delta H_{\text{bond}}(\text{U} \cdots \text{O}-\text{P}) = 2(-201.5 \pm 11.0) = -403 \pm 22 \text{ kJ mol}^{-1}$. This leaves only 17.5 kJ mol^{-1} for any diluent effects, provided in this case by the choice of

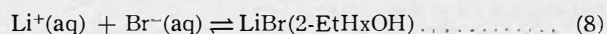
dodecane. This small quantity is the balance between the removal of two TBP molecules from their infinite dilution state in dodecane⁽⁸⁾ to the gas state, and their replacement by a molecule of the adduct $\text{UO}_2(\text{NO}_3)_2(\text{TBP})_2$, again at infinite dilution.

In the light of this analysis, the profound effect that salting-out agents, in particular non-extractable nitrates, have on the extraction can be understood, for instance. By providing nitrate anions in the aqueous phase, which effectively ion-pair with the uranyl cation to produce at least $\text{UO}_2\text{NO}_3^+(\text{aq})$ (if not altogether $\text{UO}_2(\text{NO}_3)_2(\text{aq})$), which is considerably less hydrated than the dipositive UO_2^{2+} cation, they reduce the amount of enthalpy which has to be invested for extraction to occur. They effectively decrease the enthalpy barrier which must be overcome, both absolutely (since also the enthalpy regained by electrostatic association on the other side is reduced) and by starting, as it were, from an initially higher level. Thus, for the overall process, which, as we know, is enthalpy controlled, much more is seen to be gained by manipulations in the aqueous phase, than by changing the diluent, for instance.

Entropy Controlled Extraction

It is seldom realized that there are extraction systems where the moving force for the distribuend to leave the aqueous phase and enter the organic phase is not due to better bonding energetics that it may find there but rather a higher entropy. This may be the case for a water-structure-enforced ion pair which is extracted into a dissociating solvent. For instance, tetraphenylarsonium bromide would have⁽⁹⁾ an endothermic enthalpy barrier of $\Delta H_{\text{tr}} = +2.5 \text{ kJ mol}^{-1}$ for transfer from water to propylene carbonate, but a positive entropy change $T\Delta S_{\text{tr}} = +5.4 \text{ kJ mol}^{-1}$ would push it over it (assuming the values⁽⁹⁾ for pure water and propylene carbonate to hold for the mutually saturated solvents, the experiment not having ever been made). The entropy control exerted in this case is small, however.

On the other hand, only recently has it been found^(4,6) that cases exist where the entropy control provides a barrier which has to be overcome, and extraction remains inefficient unless it is sufficiently lowered. In the case of the extraction of lithium bromide from aqueous solutions into 2-ethylhexanol



from relatively dilute solutions, the standard enthalpy change is⁽⁶⁾ $\Delta H^*_{(8)} = -7.7 \pm 0.2 \text{ kJ mol}^{-1}$ and the entropy term⁽⁴⁾ is $T\Delta S^*_{(x)(8)} = 38.0 \pm 0.6 \text{ kJ mol}^{-1}$, so that the extraction is clearly entropy controlled, that is opposed by the negative entropy change, hence inefficient. The standard state in this case, designated by prime and asterisk, is infinite dilution in both the aqueous and the organic phases, but with the proviso⁽⁴⁾ that in the organic phase the salt is completely ion-paired. This is a hypothetical state, where the ions are paired, but no further solute-solute interactions occur. However, it is readily defined operationally, through the chemical potential

$$\mu^*_{(m)}(\text{or}) = \lim_{m_{\text{LiBr}} \rightarrow 0} (\mu_{(m)}(\text{or}) - RT \ln m_{\text{LiBr}}(\text{or})) \quad (9)$$

Nevertheless, extraction does take place, and is improved as the concentrations increase, until, at saturation, the extraction is naturally neither enthalpy nor entropy controlled, both contributions being necessarily equal, making $\Delta G^s_{(x)(8)} = \Delta H^s_{(8)} - T\Delta S^s_{(x)(8)} = 0$ (superscript s designating the saturated standard state). For this state, then, $\Delta H^s_{(8)} = T\Delta S^s_{(x)(8)} = -27.9 \pm 0.8 \text{ kJ mol}^{-1}$, the barrier being 27% lower than in dilute solutions.

The interactions leading to these values are summarized in Figure 2, where an entropy barrier is a downward pointing arrow, signifying a decrease in entropy. It is seen that a very large barrier is provided by the entropy of transfer of the two ions, in the separated form, from water to the alcohol (lowest level in the diagram). This is estimated⁽⁴⁾, via the experimental $\Delta S^{*(x)}$ and the entropy change for ion pairing $\Delta S'_{ip}$, obtained from the ion pairing theories of Bjerrum or of Fuoss. Thus, it does not provide an independent estimate of $\Delta S^{*(x)}$, since the alternative, of estimating ΔS_{sol} , for the solvation of the gaseous ions by the alcohol, from the Born equation leads to impossibly large negative values, due to the notorious failure of the Born equation for such estimations. However, the estimation from the ion-pairing theory is sufficiently reliable to affirm a large negative magnitude to this ΔS_{tr} for the separated ions.

A more effective analysis can be made through a hypothetical transfer via the gaseous state, as was done with the enthalpy in the case of uranyl nitrate extraction⁽⁷⁾ discussed above. However, contrary to that case, the entropy balance does not include quantities dominating the diagram, but is made up rather delicately from relatively small contributions. The loss of entropy on transfer, contributing to the entropy barrier, is made up as follows:

(a) Loss of translational entropy on ion pairing in the gas phase of $-131.3 \text{ JK}^{-1}\text{mol}^{-1}$; this overshoots ΔS_{ip} in the diagram, because of a gain of rotational entropy of $76.1 \text{ JK}^{-1}\text{mol}^{-1}$, so that the net loss is $-55.2 \text{ JK}^{-1}\text{mol}^{-1}$.

(b) Hindered rotation of the ion-pair in the alcohol, so that not all of the $76.1 \text{ JK}^{-1}\text{mol}^{-1}$ is regained; this is included in $\Delta S'_{sol}$.

(c) Immobilization of alcohol (and of water saturating the alcohol) by solvating the ion-pair, making up the balance of $\Delta S'_{sol}$, which is altogether $-206.1 \text{ JK}^{-1}\text{mol}^{-1}$. The total barrier is thus $-261.3 \text{ JK}^{-1}\text{mol}^{-1}$, which is only partly overcome by positive entropy contributions: release of oriented hydration water molecules when the lithium and bromide ions leave the aqueous phase. The net effect here is $-\Delta S_{hyd} = +133.9 \text{ JK}^{-1}\text{mol}^{-1}$, which is rather small because of effect (d).

(d) Structure is reestablished when the structure-breaking bromide ion leaves the aqueous phase.

(The electrostatic effect of dehydration, according to the Born equation, should have led to $-\Delta S_{hyd}(\text{Born}) = +231.4 \text{ JK}^{-1}\text{mol}^{-1}$, the difference due to structure reestablishment being, therefore $-97.5 \text{ JK}^{-1}\text{mol}^{-1}$.) The entropy barrier is thus made up by effects; (a) loss of translational entropy on ion pairing, (b) hindered rotation of ion pair, (c) solvation and hydration of ion pair and (d) water structure reestablishment after bromide ions transfer, and is compensated partly by rotational entropy gained on ion pairing and release of hydration water after lithium ions transfer.

The lowering of the entropy barrier on going to saturated solutions can be ascribed⁽⁴⁾ to the disappearance of contribution (d) from the barrier. In concentrated solutions water molecules are immobilized by the lithium ions to such an extent that no more structured free water exists in the solution, so that no structure can be reestablished if a bromide ion leaves. Furthermore, incipient ion pairing in the aqueous phase lowers some of the contribution a) to the barrier, since less translational entropy is lost.

Conclusions

Many authors have previously published series of papers with titles such as "thermodynamics of solvent extrac-

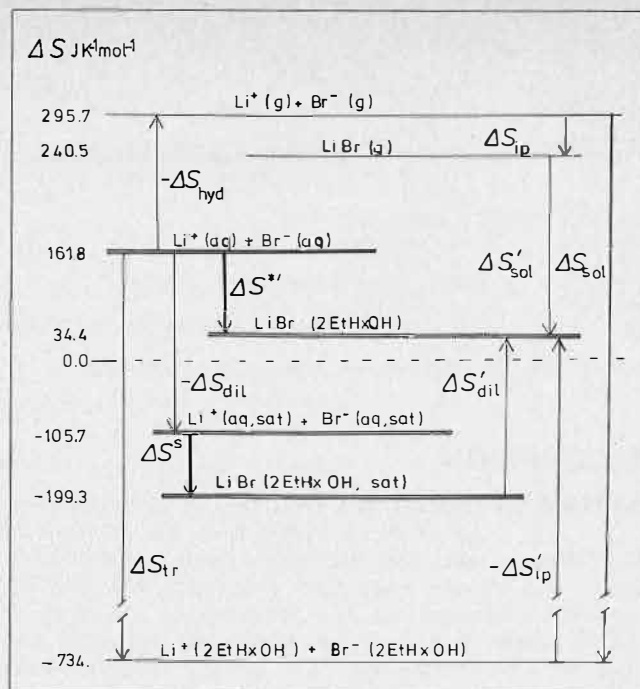


FIGURE 2. The entropy level (third law absolute values) diagram for extraction of lithium bromide from aqueous solutions into 2-ethylhexanol, based on infinite dilution (modified for ion-pairing in the organic phase) and on saturated solution standard states.

tion," in which they tried to analyze enthalpies and entropies in terms of interactions. Much of this work has missed the truth, since it was based on experimental information which was wrong, due to disregard of proper standard states, heats of dilution and of mixing, correction for critical terms⁽¹⁾ in the Gibbs free energy and entropy, etc., detailed in the critique in the introduction to the present paper. Comparison with independent data, experimental or derived, for partial processes has therefore suffered from incompatibility of standard states, disregard of a communal entropy on transfer between gas and liquid phases, and of changes in the states of reagents present in excess, when one mole of the extraction reaction occurs. In the papers summarized here^(2,4-7) these pitfalls have been avoided as far as could be discerned. It is therefore believed that the analysis in terms of interactions made on the basis of the experimental data is valid. It is also believed that enthalpy control, and entropy control, first demonstrated in this series, are manifested in many systems additional to those used here for the purpose of illustration. It is further believed that a rational approach to design and improvement of extraction systems has to tackle the major contributions which, in the end, determine from their balance the Gibbs free energy, hence the equilibrium constant, and finally the position of extraction equilibrium under given conditions.

LIST OF SYMBOLS

G	= Gibbs free energy
H	= enthalpy
K	= equilibrium constant for distribution reaction
M	= molality
p	= sum of stoichiometric coefficients of products
r	= sum of stoichiometric coefficients of reactants
S	= entropy
T	= temperature (absolute)
v	= molar volume

μ	= chemical potential
(aq)	= in the aqueous phase
(or)	= in the organic phase
2-Et-HxOH	= 2-ethylhexanol
(H)DE-HP	= di(2-ethylhexyl)phosphoric acid
TBP	= tri-n-butyl phosphate
'	= related to conditional equilibrium constant
° or *	= related to changes between defined standard states
ass.	= of association
h or hyd	= of hydration
ip	= of ion pairing
(m)	= on the molal concentration scale
sol	= of solvation
tr	= of transfer from the aqueous to the organic phase
(x)	= on the mole fraction concentration scale

REFERENCES

- (1) Gurney, R., "Ionic Processes in Solution," McGraw-Hill, New York, 1953.
- (2) Marcus, Y. and Kolarik, Z., J. Chem. Eng. Data 1973, 18, 155.
- (3) Milicevic, B., Helv. Chim. Acta 1963, 46, 1466.
- (4) Marcus, Y., J. Phys. Chem. 1976, 80, 2451.
- (5) Marcus, Y. and Kolarik, Z., J. Inorg. Nucl. Chem. 1976, 38, 1069.
- (6) Marcus, Y., J. Chem. Eng. Data 1975, 20, 141.
- (7) Marcus, Y., J. Inorg. Nucl. Chem. 1975, 37, 493.
- (8) Marcus, Y. and Kolarik, Z., J. Soln. Chem. 1977, 6, 39
- (9) Cox, B.G., Hedwig, G.R., Parker, A.J. and Watts, D.W., Austr. J. Chem. 1974, 27, 477.

DISCUSSION

R. Blumberg: I should like Prof. Marcus to comment on the place of hydration in his calculations. Prof. Marcus mentioned that LiBr cannot be dissolved in the 2-ethyl-hexanol when fully anhydrous. My own experience with chlorides and bromides of a variety of cations shows that hydrated species are extracted and that the solvent therefore may contain ion-pair bound water and solvent-bound water. One would expect this to be reflected in thermodynamic values obtained if it has not been taken into account.

Y. Marcus. Anhydrous lithium bromide *can* be dissolved in 2-ethyl-hexanol, but its dissolution is too slow to yield accurate calorimetric data for the heat of solution. The saturated solution is very viscous, and covers the undissolved material with a paste which dissolves very

slowly in excess solvent. The value quoted for the heat of solution for the hydrate pertains to water-saturated solvent, where dissolution is rapid (Y. Marcus, J. Chem. Eng. Data, 20, 141 (1975)). Under such conditions, the ions are both hydrated and solvated, and this effect was taken into account when the entropy contribution to the free energy of transfer were considered (Y. Marcus, J. Phys. Chem. 80 2455 (1976)). For transfer between the saturated solution standard states, however, the simplification was noted that the alcoholic solution contained practically no water (< 10% of the lithium bromide content, on a mole basis), so that the transfer occurs between essentially binary solutions of lithium bromide in water and lithium bromide in 2-ethyl-hexanol. Whether this is generally so for saturated solutions in lithium halides in other alcohols is not known.

Electron Spin Resonance Spectral Studies of the Complexes Formed in the Extraction of Manganese (II), Copper (II) and Vanadium (IV) from Hydrochloric Acid Solutions by Di-(2-ethylhexyl)-Phosphoric Acid

Taichi Sato, Takato Nakamura and Masanori Kawamura,
Department of Applied Chemistry,
Faculty of Engineering,
Shizuoka University,
Hamamatsu, Japan.

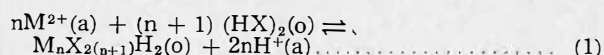
formed in the extraction of manganese(II), copper(II) and vanadium(IV) from hydrochloric acid solutions by DEHPA are investigated by ESR spectroscopy, to obtain further information on the extraction mechanism in those systems.

ABSTRACT

The distribution of manganese(II), copper(II) and vanadium(IV) between hydrochloric acid solutions and solutions of di-(2-ethyl-hexyl)-phosphoric acid (DEHPA; HX) in organic solvent has been investigated under different conditions. The formed complexes have been examined by the electron spin resonance (ESR) spectroscopy, spectrophotometry and the measurement of magnetic moment. As a result, it is found that the monomeric species $Mn(X_2H)_2$, $Cu(X_2H)_2$ and $VO(X_2H)_2$ which give the structure types of point group symmetries of T_d , D_{4h} and C_{4v} , respectively, are formed in the extraction under the general condition where DEHPA is present in excess, although an increase in the metal concentration of the organic phase leads to the formation of a polymeric species.

Introduction

IN THE PREVIOUS PAPERS^(1,2), the following equilibrium equation, expressed as an ion-exchange reaction governed by the formation of polymeric species, has been given for the extraction of divalent metals from sulphuric and hydrochloric acid solutions by di-(2-ethyl-hexyl)-phosphoric acid (DEHPA) as the basis of investigating the composition of the metal complexes formed in these extraction systems:



where $n \geq 1$, X is the anion $(C_8H_{17}O)_2PO_2^-$, $(HX)_2$ the dimeric solvent⁽³⁾, (a) and (o) are the aqueous and organic phases, respectively. Additionally, one of the present authors has reported that the extraction of vanadium(IV) by DEHPA from sulphuric acid solutions also follows Equation (1) in which M is displaced by VO⁽³⁾. In contrast, its extraction from hydrochloric acid solutions has been examined by Rigg et al⁽⁴⁾, but there are few observations on the extraction mechanism and the structure of the complex formed in the extraction process. Recently, however, we have carried out the electron spin resonance (ESR) spectral studies on the vanadyl complexes formed in the extraction of vanadium(IV) from hydrochloric acid solutions by tri-n-octylamine (TOA) and tricaprilmethylammonium chloride (Aliquat-336)⁽⁵⁾. In this work, therefore, the metal-ligand bonding character in the complexes

Experimental

The DEHPA (Union Carbide Corp. and Daihachi Chemical Industry Co., Ltd.) was purified by the usual method^(6,7), and diluted with kerosene or n-hexane. Aqueous solutions of manganese(II), copper(II) and vanadium(IV) were prepared by dissolving their chlorides ($MnCl_2 \cdot 4H_2O$, $CuCl_2 \cdot 2H_2O$ and $VOCl_2$) in hydrochloric acid solutions of the required concentrations. Other chemicals were of analytical reagent grade.

Procedures for obtaining the distribution coefficients were as described for uranium(VI) extraction⁽⁶⁾, except that metals in the organic phases were stripped with 1 M hydrochloric acid (preliminary experiments showed that equilibrium between the phases for the extraction of each metal was complete in 10 min). The concentrations of metals were determined by EDTA titration using Xylenol Orange⁽⁸⁾ (except Eriochrome Black T for manganese⁽⁹⁾) as indicator. The water content and chloride concentration of the organic phase were determined by Karl-Fischer titration and Vorhard titration using nitro-benzene, respectively. However, since the divalent metals are not sufficiently strongly extracted into DEHPA, it is rather difficult to get the organic phases saturated with their metals⁽¹⁰⁾. Thus the complexes saturated with manganese(II) and copper(II) were prepared as follows^(1,2): a solution of 0.1 M DEHPA in n-hexane was contacted with the aqueous solution of divalent manganese and copper chlorides at 20 g/l, and then 0.5 M sodium hydroxide solution was added drop-wise; the complexes were freed from n-hexane by drying the metal-saturated organic phases in vacuo. In contrast, the complex was prepared by drying the organic phase saturated with vanadium from the extraction of vanadyl chloride solution with a solution of DEHPA in n-hexane.

For the organic extracts so prepared or the organic phases themselves, the ESR spectra were determined on a high-sensitivity spectrometer, designed in the Research Institute of Electronics, Shizuoka University^(1,5). The calculation for the ESR spectra were made using a FACOM 230-45S computer. Electronic spectra were obtained on a Shimadzu Model QV-50 spectrometer⁽¹⁾. The magnetic susceptibility was measured by the Gouy method at room temperature^(1,11).

Results and Discussion

Extraction Isotherm

The results for the extraction of aqueous solutions containing 1 g/l each of manganese(II), cupric and vanadyl chlorides in mixtures of hydrochloric acid and lithium chloride with 0.1 M DEHPA in kerosene at 20°C are indicated in Figures 1-3, compared with those for the extraction from hydrochloric acid solutions of varying acidity with the solutions of DEHPA in kerosene. As the distribution coefficients diminish uniformly on increasing the aqueous acidities, it is considered that the extractions

are principally dominated by the ion-exchange reaction in which hydrogen is liberated. In the extraction of manganese(II) and copper(II) (Figures 1-2), however, the diminution in the distribution coefficient becomes gradual at low acidity. This probably results from the formation of the hydrolyzed species, as observed in the extraction of thorium(IV)⁽¹²⁾ also. The extraction of all metals from mixed hydrochloric acid and lithium chloride solutions shows that the distribution coefficients are not appreciably influenced by the chloride ion concentration, but decrease with increasing hydrogen ion concentration. Accordingly, it is inferred that the species containing chloride ion are inextractable, as supported by the chemical analytical result, and that the chloride ion concentration in the organic phase is not much influenced by the amount of metals extracted.

If we assume that the extraction progresses according to Equation (1), the distribution coefficient should be inversely second-power dependent upon the hydrogen ion concentration. In the extraction of vanadium(IV) (Figure 3), the slopes of log-log plots of the distribution coefficient vs. the aqueous chloride ion concentration seem to approach a limiting value of -2. For the extraction of manganese(II) and copper(II) (Figures 1-2), the plots are not always observed to approach a limiting value of -2, but log-log plots of the distribution coefficient vs. the aqueous equilibrated pH value give the slope of ~ -2. In addition, as Equation (1) for $n = 1$ leads to the relationship

$$\log 4E_s = \log K + 2\log (C_s - 4C_M)/C_H \dots \dots \dots (2)$$

where E is the distribution coefficient, K the equilibrium constant, C_s the total DEHPA concentration, C_M the

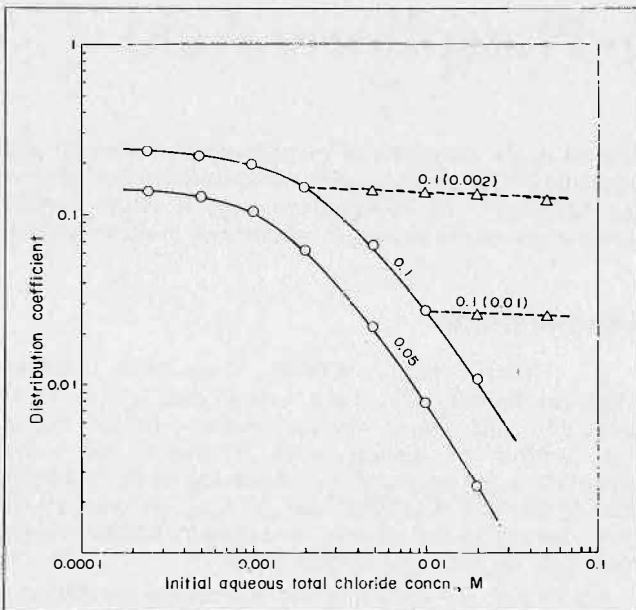


FIGURE 1. Extraction of manganese(II) from hydrochloric acid solutions by DEHPA in kerosene. Numerals on curves are DEHPA concentrations, M; figures in parentheses indicate initial aqueous hydrochloric acid concentrations, M; continuous and broken lines represent the extraction from HCl solutions and mixed HCl/LiCl solutions, respectively.

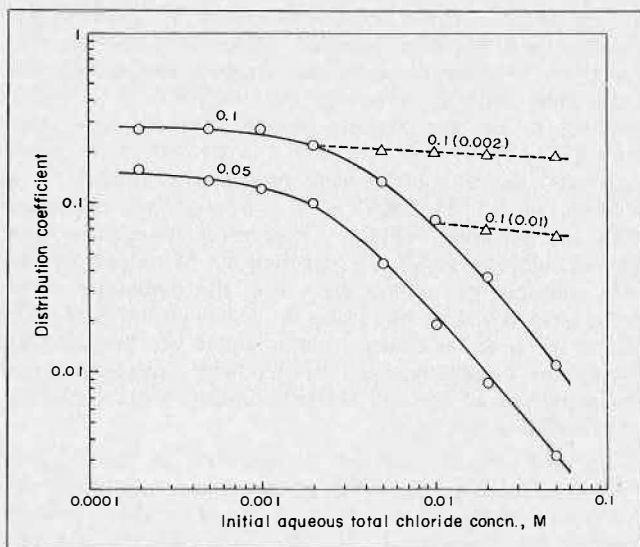


FIGURE 2. Extraction of copper(II) from hydrochloric acid solutions by DEHPA in kerosene. Numerals on curves are DEHPA concentrations, M; figures in parentheses indicate initial aqueous hydrochloric acid concentrations, M; continuous and broken lines represent the extraction from HCl solutions and mixed HCl/LiCl solutions, respectively.

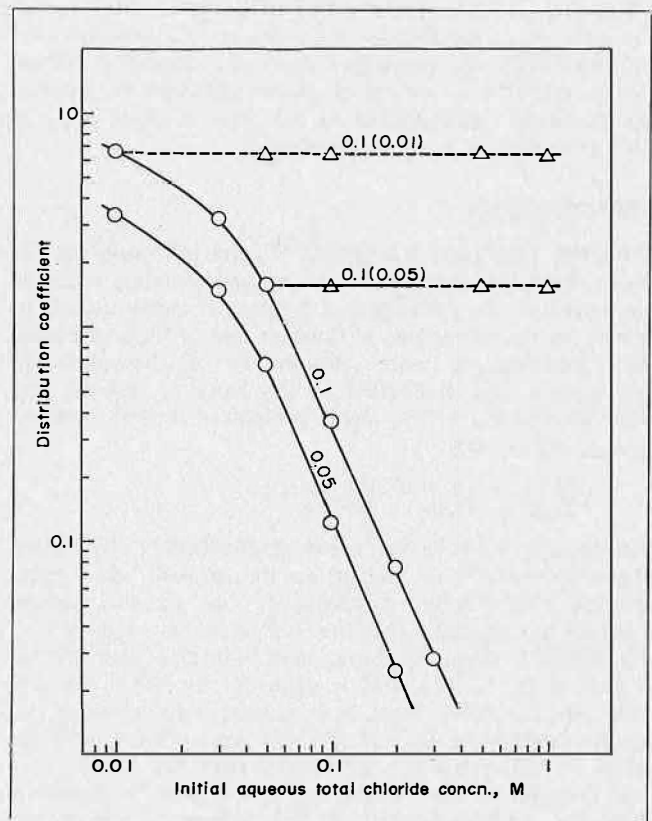


FIGURE 3. Extraction of vanadium(IV) from hydrochloric acid solutions by DEHPA in kerosene. Numerals on curves are DEHPA concentrations, M; figures in parentheses indicate initial aqueous hydrochloric acid concentrations M; continuous and broken lines represent the extraction from HCl solutions and mixed HCl/LiCl solutions, respectively.

TABLE 1. Variation of the Molar Ratio of [DEHPA] to [Mn] or [Cu] in the Organic phase as a Function of Initial Aqueous Metal Chloride Concentration for the Extraction of Aqueous Solution Containing the Chlorides of Manganese(II) and Copper(II) with 0.1M DEHPA in n-hexane at 20°C

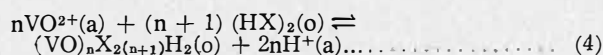
Initial Aqueous MCl ₂ Conc., g/l*	[DEHPA]/[Mn] _{org}	[DEHPA]/[Cu] _{org}
1	44.4	62.1
2.5	33.9	46.9
10	29.8	31.6
25	20.0	26.5
50	17.4	23.9
100	16.1	20.7

*M = Mn or Cu, and aqueous solution contains 0.0002M hydrochloric acid.

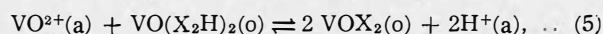
metal concentration in the organic phase and C_H the aqueous acidity, the values of $\log E$ are plotted against $\log (C_S - 4C_M)/C_H$ at constant hydrochloric acid concentration. Consequently it is found that Equation (2) is satisfied at $[HCl] = 0.0002-0.02$ M for manganese(II) and copper(II), and at $[HCl] 0.05$ M for vanadium(IV). Hence the extractions under these conditions are expressed by the reaction forming the monomeric species. However, since the extraction of vanadium(IV) at $[HCl] = 0.05$ M is postulated to involve the formation of a polymeric species, the following relationship must hold:

$$\log 4E_s = \log K_1 + 2\log (C_S - 2C_M)/C_H \dots \dots \dots (3)$$

where K_1 is a constant. A log-log plot of E vs. $(C_S - 2C_M)$ shows that Equation (3) is satisfied at hydrochloric acid concentrations below 0.05 M. We thus presume that although the monomeric species is formed when DEHPA is present in excess, the increase in the vanadium concentration in the organic phase involves the formation of a polymeric vanadium(IV)-DEHPA complex. Accordingly, the following general equilibrium expression describes the extraction of vanadium(IV) from hydrochloric acid solutions:



Rigg et al⁽⁴⁾ have postulated an equilibrium such as



but this equation is not satisfied under the experimental conditions of this investigation.

Composition of DEHPA Complexes

In the extraction of aqueous solutions containing the chlorides of manganese(II), copper(II) and vanadium(IV) at various concentrations with the solutions of DEHPA (0.1 M for Mn(II) and Cu(II), 0.05 M for V(IV)) in n-hexane at 20°C, the molar ratios of [DEHPA] to [Mn] [Cu] and [V] in the organic phases gradually decrease with increasing the initial aqueous metal chloride concentrations as shown in Table 1-2. In addition, the water contents of the organic phases decrease with increasing the metal concentrations, indicating that the formed complexes have no water. In the extraction of manganese(II) and copper(II) (Table 1), since $[DEHPA] \gg 4[Mn]_{org}$ or $4[Cu]_{org}$, it seems that the organic phases are not saturated with metals under this experimental condition. In Table 2, however, the molar ratio $[DEHPA]/[V]_{org}$ is less than four at initial aqueous vanadyl chloride of 5 g/l, and its ratio approaches a limiting value of two above this vanadyl chloride concentration. Therefore, we presume

TABLE 2. Variation of the Molar Ratio of [DEHPA] to [VO] in the Organic Phase as a Function of Initial Aqueous Vanadyl Chloride Concentration for the Extraction of Aqueous Solutions Containing Vanadyl Chloride with 0.05M DEHPA in n-hexane at 20°C.

Initial aqueous VOCl ₂ conc., g/l*	[DEHPA]/[VO] _{org}
1	7.14
2	5.75
5	3.81
12.5	2.59

*Aqueous solution contains 0.01M hydrochloric acid.

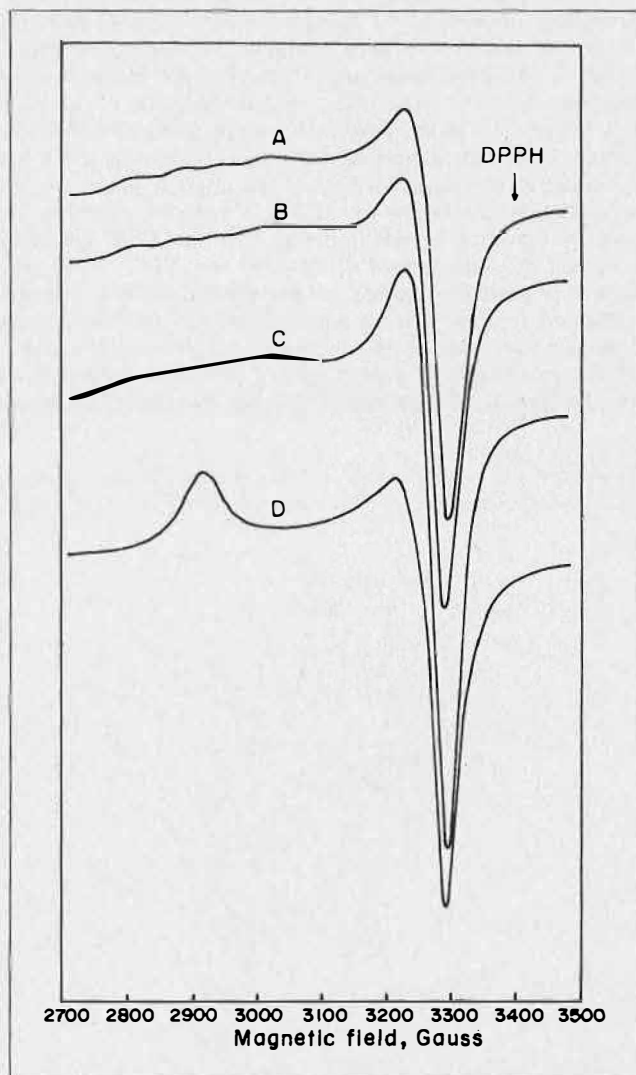


FIGURE 4. ESR spectra of organic extracts from aqueous solutions containing cupric chloride with 0.1 M DEHPA in n-hexane. A, B and C, cupric chloride solutions at 2.5, 10 and 50 g/l, respectively; D, copper(II)-saturated organic extract.

that the monomeric species $Mn(X_2H)_2$ or $Cu(X_2H)_2$ is predominantly formed in the extraction under the general condition; in the extraction of vanadium(IV), the monomeric species $VO(X_2H)_2$ is formed when DEHPA is present in excess, and an increase in vanadium concentration of the organic phase leads to the formation of a polymeric species.

These facts are supported by the ESR spectral results for the organic extracts of copper(II) and vanadium(IV)

and the organic solutions of manganese(II), copper(II) and vanadium(IV), shown in Figures 4-6. The ESR line shapes for the monomeric species of copper(II) (Figure 4) exhibit almost the same spectral behaviour, indicating that only one kind of species is formed in the organic phase, and in addition their spectra reveal the different pattern in comparison with that of the complex saturated with copper^(1,2) which does not give the hyperfine structure ascribed to the formation of polymeric species. Similar trend is also observed in the spectra of manganese(II) species (Figure 5): the monomeric species shows the isotropic six-hyperfine line shape exhibiting only the change in the intensity of those lines at the same resonance potential. In this case, the resonance potential in the spectra of the organic extracts freed from n-hexane is little different from those of the organic solutions in n-hexane. In the copper(II) complexes, however, the former in solid state is different from the latter in organic solution, as indicated previously⁽¹⁾. The ESR line shapes of the organic extracts from aqueous solutions containing vanadyl chloride of 1 and 5 g/l (Figure 6) show almost the same spectral behaviour which gives the hyperfine structure, suggesting that the monomeric species is formed in the organic phase. At an aqueous concentration of 12.5 g/l vanadyl chloride, its pattern becomes broad, implying that the ESR spectrum contains the line shapes of coupled ion VO²⁺. This tendency is strongly marked in the spectrum of a vanadyl saturated organic extract which does not give the hyperfine structure, due to the formation of polymeric species. If the extraction of vanadium(IV) proceeds according to the formation of monomeric species, the hyperfine struc-

ture should be observed in the ESR spectrum of the organic extract because of the presence of isolated ion VO²⁺. It is therefore considered that the polymeric species is formed by substituting the hydrogen ion of the species VO(X₂H)₂ for vanadyl ion in the aqueous phase which contains coupled ion VO²⁺. From these results, Equation (4) also holds for the extraction of vanadium(IV) from hydrochloric acid solutions by DEHPA.

Structure and Bonding Character of DEHPA Complexes

The electronic spectrum of the species Cu(X₂H)₂ in n-hexane shows a broad band at 12270 cm⁻¹, interpreted as arising from the transition ²E_g to ²T_{2g} in a field of octahedral symmetry, although it is difficult to predict whether the species is either octahedral or square planar. Thus the magnetic moment for this complex is theoretically expected to be 1.96 B.M. if metal-ligand bonding is ionic, but the experimental value of 1.80 B.M. is obtained at 298 K. We assume that the discrepancy of these values may be ascribed to bonding effect. However, since the value of 10 Dq is determined as 21000 cm⁻¹ from the electronic spectrum of the manganese(II)-DEHPA complex, it is found that the agreement between the calculated

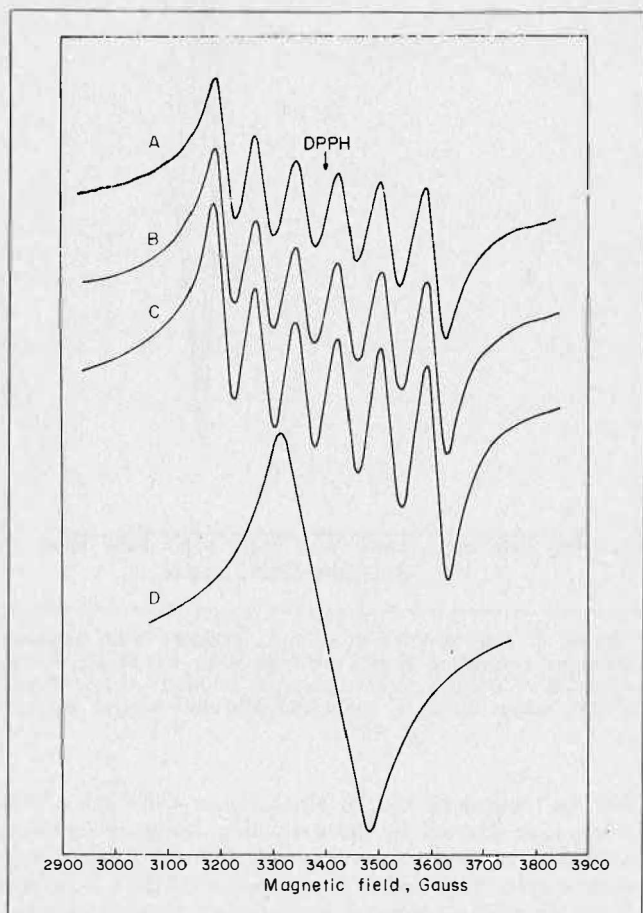


FIGURE 5. ESR spectra of organic solutions from the extraction of aqueous solutions containing manganese(II) chloride with 0.1 M DEHPA in n-hexane. A, B and C, manganese chloride solutions at 2.5, 10 and 25 g/l, respectively; D, manganese(II)-saturated organic solution.

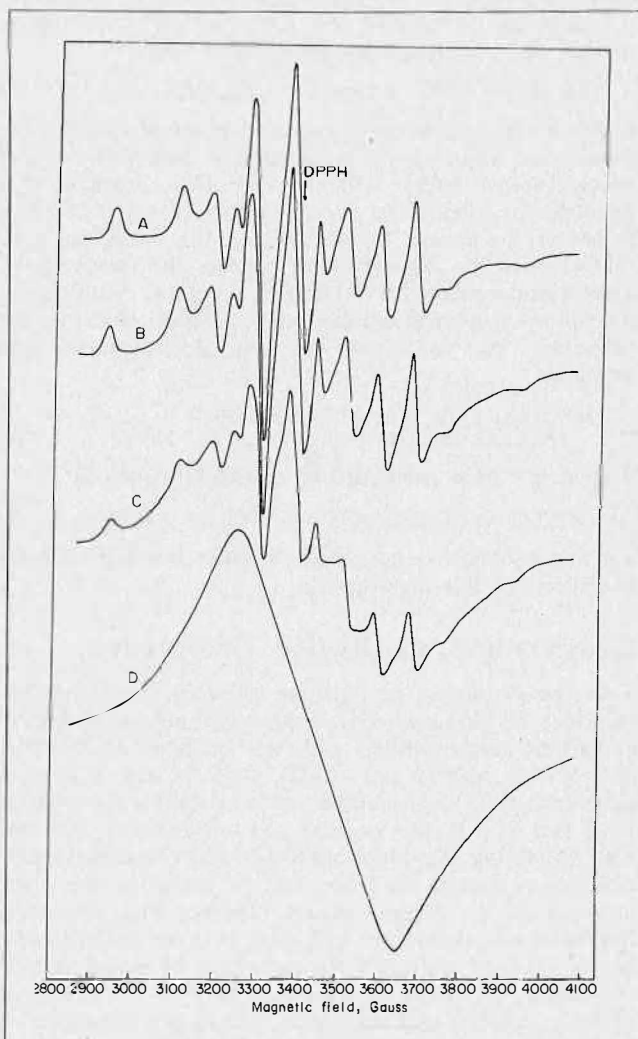


FIGURE 6. ESR spectra of organic extracts from aqueous solutions containing vanadyl chloride with 0.05 M DEHPA in n-hexane [A, B and C, vanadyl chloride solutions at 1, 5 and 12.5 g/l, respectively; D, vanadyl-saturated organic extract.

value (5.92 B.M.), obtained by using the spin-orbit coupling constant of the free ion and the 10 Dq value, and the experimental result (5.93 B.M. at 298 K) supports the structure in a tetrahedral symmetry, deduced from the spectral study. For the vanadium(IV)-DEHPA complex, as the observed value of the magnetic moment (1.65 B.M. at 283 K) is analogous to the spin-only value for vanadium(IV) (1.73 B.M.), it is expected that the complex possesses little of the spin-spin interaction in vanadyl ions, different from the complexes with TOA and Aliquat-336⁽¹⁵⁾.

The structure of two dimeric HX_2 groups being chelated to the central cupric ion which displays a coordination number of four through the oxygen atoms occupying the corner of square is given for the monomeric species of copper(II). It is thus deduced that the copper(II) complex with DEHPA is approximately in a square planar symmetry, D_{4h} . As regards the structure of the manganese(II)-DEHPA complex, we propose that the manganese displays a coordination number of four in a tetrahedral symmetry, T_d , being chelated to two HX_2 groups in the monomeric species. For the constitution of the vanadium(IV)-DEHPA complex, it is considered that vanadium displays a coordination number of five in a point group C_{4v} symmetry, being chelated to two HX_2 groups in the monomeric species, and forming a polymer chain for its polymeric species. Further, the probable assignments⁽¹³⁾ for the electronic spectra of the vanadyl complex with DEHPA are shown in Table 3.

The ESR parameters of the species $Cu(X_2H)_2$, $Mn(X_2H)_2$ and $VO(X_2H)_2$, determined by the computer simulation method^(6,14), are given in Table 4. Accordingly if we take 12270 cm^{-1} as the value of Δ_{\perp} and Δ_{\parallel} in a field of octahedral symmetry with tetragonal distortion, coefficients for the wave functions of copper ion, α^2 , β^2 and β_1^2 are obtained as 0.62, 0.98 and 0.93, respectively, according to the following relationship⁽¹⁵⁾:

$$g_{\parallel} = 2.0023 - 8\lambda_{Cu}\alpha^2\beta^2/\Delta_{\parallel} \dots\dots\dots (6)$$

$$g_{\perp} = 2.0023 - 2\lambda_{Cu}\alpha^2\beta_1^2/\Delta_{\perp} \dots\dots\dots (7)$$

where Δ_{\perp} and Δ_{\parallel} are the energy differences ΔE_{xy} and $\Delta E_{yz, xz}$, respectively, in the transition from the state B_{1g} to the excited state E_g , and λ_{Cu} the spin-orbital coupling constant for the free cupric ion (-828 cm^{-1}). In this case the values of $\alpha^2\beta^2$ and $\alpha^2\beta_1^2$ represent the parameters on the degree of covalency for metal-ligand bondings parallel and perpendicular to molecular z-axis, respectively. As the value of $\alpha^2\beta^2$ and $\alpha^2\beta_1^2$ are almost equal, it is inferred that the σ -bond plays an important role for the species $Cu(X_2H)_2$, i.e. the bonding in the b_1 orbital is covalent, while the in-plane σ -bonding is covalent, and in-plane and out-of-plane π -bondings are ionic. In the vanadyl complex with DEHPA, if the b_2 orbital is considered as non-bonding orbital, the molecular orbital coefficients⁽¹⁶⁻¹⁸⁾ are obtained by

$$g_{\parallel} = 2.0023 - 8\lambda_v\beta_1^{*2}/\Delta_{\parallel} \dots\dots\dots (8)$$

$$g_{\perp} = 2.0023 - 2\lambda_v\epsilon_{\pi}^{*2}/\Delta_{\perp} \dots\dots\dots (9)$$

where β_1^{*2} and ϵ_{π}^{*2} are the fractional contributions of the wave functions in the orbitals $d_{x^2-y^2}$ and $d_{xz, yz}$, respectively, of the vanadyl ion, λ_v the spin-orbital coupling constant for the free ion of vanadium, and $\Delta_{\parallel} = \Delta E$ in the transition ${}^2B_2 \rightarrow {}^2B_1$ and $\Delta_{\perp} = \Delta E$ in the transition ${}^2B_2 \rightarrow E(1)$. The molecular parameters of β_1^{*2} and ϵ_{π}^{*2} are obtained as 0.78 and 0.93, respectively. These values indicate that the b_1 orbital is covalent, and that the e orbital in the out-of-plane π -bonding is ionic.

On the basis of the results obtained, it is presumed that the monomeric species formed in the extraction of manganese(II), copper(II) and vanadium(IV) from hydrochloric acid solutions by DEHPA give the point group

TABLE 3. Electronic Spectra of the Species $VO(X_2H)_2$

ν, cm^{-1}	ϵ	Assignment
35700	1000	${}^2B_2 \rightarrow {}^2E(11)$
29400	100	${}^2B_2 \rightarrow {}^2A_1$
14700	52	${}^2B_2 \rightarrow {}^2B_1$
12050	65	${}^2B_2 \rightarrow {}^2E(1)$
9530	48	Forbidden

TABLE 4 ESR parameters of the species $Cu(X_2H)_2$, $Mn(X_2H)_2$ and $VO(X_2H)_2$

ESR Parameter	$Cu(X_2H)_2$	$Mn(X_2H)_2$	$VO(X_2H)_2$
g_{\parallel}	2.333	1.996 ^{*a})	1.930
g_{\perp}	2.076		1.976
$ A $	72.2 gauss (78.6×10^{-4} cm^{-1})	77.0 gauss ^{*b})	163.7 gauss (147.5×10^{-4} cm^{-1})
$ B $	8 gauss (7.8×10^{-4} cm^{-1})	(71.8×10^{-4} cm^{-1})	73.2 gauss (67.3×10^{-4} cm^{-1})
ΔH	45 gauss	55 gauss	—

*a) This denotes g-value.

*b) This is indicated by $|A_{av}|$ of average value.

symmetries of T_d , D_{4h} and C_{4v} with the composition $Mn(X_2H)_2$, $Cu(X_2H)_2$ and $VO(X_2H)_2$, respectively, and they possess little of the interaction of central ion with the π -bonding of coordinated oxygen atoms in DEHPA.

Acknowledgment

We wish to thank Dr. K. Watanabe of the Research Institute of Electronics, Shizuoka University for the ESR spectral measurement, and the Daihachi Chemical Industry Co., Ltd. for sample of DEHPA.

REFERENCES

- (1) Sato, T. and Nakamura, T., *J. Inorg. Nucl. Chem.* 1972, **34**, 3721.
- (2) Sato, T. and Ueda, M., "Proc. Int. Solvent Extraction Conf., Lyon, 1974", Vol. 1, p. 871, Soc. Chem. Ind., London (1974).
- (3) Sato, T. and Takeda, T., *J. Inorg. Nucl. Chem.* 1970, **32**, 3387.
- (4) Rigg, T. and Garner, J.O., *J. Inorg. Nucl. Chem.* 1967, **29**, 2019.
- (5) (a) Sato, T., Nakamura, T. and Terao, O., *J. Inorg. Nucl. Chem.* 1977, **39**, 401; (b) Sato, T., Ikoma, S. and Nakamura, T., *ibid.* 1977, **39**, 395.
- (6) Sato, T., *J. Inorg. Nucl. Chem.* 1962, **24**, 699.
- (7) Sato, T., *J. Inorg. Nucl. Chem.* 1965, **27**, 1853.
- (8) Kinnunen, J. and Wennerstrand, B., *Chemist-Analyst* 1957, **46**, 92.
- (9) Flaschka, H., *Chemist-Analyst* 1953, **42**, 56.
- (10) Baes, C.F., Jr., *J. Inorg. Nucl. Chem.* 1962, **24**, 707.
- (11) Gray, T.F., "Chemistry of the Solid State" (Edited by Garmer, W.E.), p. 147, Butterworths, London (1955).
- (12) Sato, T., *Z. anorg. allg. Chem.* 1968, **358**, 296.
- (13) Ballhausen, C.J. and Gray, H.B., *Inorg. Chem.* 1962, **1**, 111.
- (14) Vanngard, T. and Aasa, R., "Proc. the 1st Int. Conf. on Paramagnetic Resonance, Jerusalem, 1962" (Edited by Low, W.), Vol. 2, p. 509, Academic Press, New York (1963).
- (15) McGarvey, B.R., *J. Phys. Chem.* 1967, **71**, 51.
- (16) Kivelson, D. and Lee, S.K., *J. Chem. Phys.* 1964, **41**, 1896.
- (17) Kivelson, D. and Neiman, R., *J. Chem Phys.* 1961, **35**, 149.
- (18) Maki, H. and McGarvey, B.R., *J. Chem. Phys.* 1958, **29**, 31.

Four-parameter Correlation Equations for Calculation of Thermodynamic Parameters of Solvation-type Extraction Processes

B. N. Laskorin, V. V. Yakshin, B. N. Sharapov,
Institute of Chemical Technology,
Moscow, USSR.

ABSTRACT

The isoentropic pattern of the extraction processes occurring via the donor-acceptor mechanism enables the use of the Drago-Wayland type equations for describing the complexing agent — ligand interaction and computing both enthalpy and the free energy:

$$-\Delta X = C_{K,\Delta X} C_B + E_{K,\Delta X} E_B \dots \dots \dots (1)$$

where ΔX is the enthalpy ΔH or free energy ΔG of the extraction process, kcal/mole; the $C_{K,\Delta X}$, $E_{K,\Delta X}$ are contributions of complexing agent (extracted compound) to the thermodynamical characteristics ΔX ; and C_B , E_B are the extracting agents factors similar to the parameters of Drago-Wayland.

Introduction

MOST OF THE DEPENDENCES relating the extraction capacity of compounds to their structure assume the decisive role of chelating agent — ligand interaction in solvation-type extraction processes that determines the reduction of free energy of the reacting system. Recently it has been shown that donor-acceptor interactions are well described by the intermolecular hydrogen bond model⁽¹⁾, the thermodynamic characteristics of which may be used to calculate extraction constants⁽²⁻⁴⁾. The use of the entire apparatus of semi-empirical description of H-bonds based on vast experimental material should considerably extend the practical results obtained.

Equations

Thus, the established isoentropicity of extraction processes proceeding according to the donor-acceptor mechanism^(5,6) makes it possible to apply Drago-Wayland equations⁽⁷⁾ for calculation of free energy as well as the enthalpy of chelating agent — ligand interactions:

$$-\Delta X = C_{K,\Delta X} \cdot C_B + E_{K,\Delta X} \cdot E_B \dots \dots \dots (1)$$

where ΔX is the enthalpy (ΔH) or free energy (ΔG) of the extraction process, kcal/mole; $C_{K,\Delta X}$, $E_{K,\Delta X}$ are the contributions of the chelating agent (compound to be extracted) into the thermodynamic characteristic ΔX ; and C_B , E_B are extractant factors, identical to those in Ref⁽⁷⁾.

Parameters C_B and E_B may be calculated from the thermodynamic characteristics of H-bonds of neutral organophosphorus compounds (NOPC) with phenol⁽⁸⁾ and water⁽⁹⁾. Independent results of hydration energy determination for a sufficiently representative number of compounds⁽¹⁾, the C_B and E_B values for which are known⁽¹⁰⁾,

were used to determine the unknown C_A and E_A values for water that should be substituted into (1) instead of $C_{K,\Delta X}$ and $E_{K,\Delta X}$ respectively. Averaging solutions of sets of two equations (1) (45 such sets were solved in Ref⁽¹¹⁾) we obtain:

$$C_A(H_2O) = 0.442 \pm 0.172 \text{ and } E_A(H_2O) = 2.09 \pm 0.54.$$

Combined solution of (1) for each of the studied NOPC^(8,9) (where ΔX is the enthalpy of interaction with H_2O and C_6H_5OH) gives the values of C_B and E_B (Table 1).

TABLE 1. Factors C_B and E_B for Neutral Organophosphorus Compounds

Compound	C_B	E_B	C_B/E_B
$(CH_3O)_3PO$	4.40	0.98	4.480
$(C_4H_9O)_3PO$	3.55	1.12	3.170
$(i-C_4H_9O)_3PO$	2.90	1.20	2.417
$(i-C_6H_{11}O)_3PO$	3.77	1.12	3.366
$(C_4H_9S)_3PO$	2.44	1.20	2.033
$(CH_3O)_2P(O)CH_3$	3.77	1.12	3.366
$(C_4H_9O)_2P(O)C_4H_9$	4.03	1.20	3.358
$CH_3OP(O)(CH_3)_2$	5.79	1.09	5.411
$C_4H_9OP(O)(C_4H_9)_2$	5.18	1.25	4.144
$(CH_3)_3PO$	6.49	1.12	5.795
$(C_4H_9)_3PO$	5.87	1.29	4.550
$(CH_3O)_2P(O)N(CH_3)_2$	4.01	1.16	3.457
$(C_4H_9O)_2P(O)N(C_4H_9)_2$	3.80	1.20	3.167
$(C_4H_9O)_2P(O)N(i-C_4H_9)_2$	3.35	1.20	2.792
$(C_4H_9O)_2P(O)N(sec-C_4H_9)_2$	3.55	1.12	3.170
$(C_4H_9O)_2P(O)(cyclo-C_6H_{11})$	5.08	0.98	5.184
$CH_3OP(O)[N(CH_3)_2]_2$	4.06	1.29	3.147
$C_4H_9OP(O)[N(C_4H_9)_2]_2$	4.28	1.29	3.318
$(CH_3)_2P(O)N(CH_3)_2$	5.82	1.16	5.017
$(C_4H_9)_2P(O)N(C_4H_9)_2$	5.40	1.25	4.320
$CH_3P(O)[N(CH_3)_2]_2$	4.53	1.34	3.380
$C_4H_9P(O)[N(C_4H_9)_2]_2$	4.95	1.25	3.960
$[N(CH_3)_2]_3PO$	8.90	0.89	10.000
$[N(C_4H_9)_2]_3PO$	5.79	1.07	5.411
$[N(C_6H_{13})_2]_3PO$	4.07	1.34	3.037
$CH_3 \begin{matrix} \diagup \\ \diagdown \end{matrix} \begin{matrix} P(O)N(CH_3)_2 \\ P(O)N(C_4H_9)_2 \end{matrix}$	3.59	1.25	2.872
$C_4H_9 \begin{matrix} \diagup \\ \diagdown \end{matrix} \begin{matrix} P(O)N(CH_3)_2 \\ P(O)N(C_4H_9)_2 \end{matrix}$	5.37	1.07	4.990
$C_4H_9O \begin{matrix} \diagup \\ \diagdown \end{matrix} \begin{matrix} P(O)NHC_4H_9 \\ P(O)NHC_4H_9 \end{matrix}$	2.38	1.70	1.400
$(C_4H_9O)_2P(O)NHC_4H_9$	3.91	1.52	2.572
$C_4H_9P(O)(NHC_4H_9)_2$	7.21	1.25	5.768
$(NHC_4H_9)_3PO$	2.81	1.61	1.745
$C_4H_9OP(O)(NHC_4H_9)_2$	2.81	1.61	1.745
$(C_4H_9O)_2P(O)NH_2$	5.08	0.98	5.184
$(C_4H_9O)_2P(O)NHCH_3$	3.56	1.16	3.069
$(C_4H_9O)_2P(O)NHC_3H_7$	3.58	1.20	2.983
$(C_4H_9O)_2P(O)NHC_4H_9$	3.56	1.16	3.069
$(C_4H_9O)_2P(O)NHC_4H_9-sec$	4.84	0.94	5.149
$(C_4H_9O)_2P(O)NHC_4H_9-tert$	5.05	0.89	5.674
$(C_4H_9O)_2P(O)NHC_6H_{11-cyclo}$	4.86	0.98	4.959
$(C_4H_9O)_2P(O)NHC_{12}H_{25}$	5.54	0.98	5.653
$(C_6H_{13}O)_2P(O)NHC_4H_9$	4.01	1.16	3.457
$(C_8H_{17}O)_2P(O)NHC_4H_9$	4.01	1.16	3.457
$(C_8H_{17}O-sec)_2P(O)NHC_4H_9$	4.42	1.03	4.291
$(2EG)_2P(O)NHC_4H_9^*$	4.04	1.25	3.232

*2EG = $C_4H_9-CH(C_2H_5)-CH_2O-$

TABLE 2. Parameters C_K and E_K .

Compound	Parameter calcd	$C_{K, \Delta x} \pm \sigma$	$E_{K, \Delta x} \pm \sigma$	$-C/E$	n	Solvent
$UO_2(NO_3)_2$	ΔH	2.56 ± 0.82	-3.41 ± 3.52	0.751	5	CCl_4
$UO_2(NO_3)_2$	ΔH	2.79 ± 0.47	-3.87 ± 1.94	0.721	3	kerosene
HNO_3	ΔH	1.16 ± 0.59	-4.44 ± 2.55	0.261	5	CCl_4
HNO_3	ΔH	0.42 ± 0.17	-0.55 ± 0.98	0.764	2	kerosene
$UO_2(NO_3)_2$	ΔG_{298}°	2.66 ± 0.70	-7.95 ± 3.06	0.334	9	$CHCl_3$
HNO_3	ΔG_{298}°	0.61 ± 0.20	-3.09 ± 0.79	0.197	5	$CHCl_3$
$UO_2(NO_3)_2$	ΔG_{298}°	4.02 ± 0.83	-9.79 ± 3.51	0.411	5	C_6H_6
$UO_2(NO_3)_2$	ΔG_{298}°	2.99 ± 0.88	-6.81 ± 3.73	0.439	5	CCl_4
HTICl ₄	ΔG_{298}°	1.68 ± 0.42	-3.38 ± 2.05	0.497	5	CCl_4
$UO_2(NO_3)_2$	ΔG_{298}°	2.70 ± 0.83	-5.88 ± 2.55	0.459	2	kerosene
HNO_3	ΔG_{298}°	1.35 ± 0.97	-4.87 ± 3.22	0.277	2	kerosene

n is the number of sets of equations (1)

TABLE 3. Equation $y = A_0 + A_1x$ Relating Experimental and Calculated Values of Thermodynamic Characteristics of Extraction

Compound	x exp	y calcd	A ₀	A ₁	r	s	Solvent
$UO_2(NO_3)_2$	$-\Delta H$	$-\Delta H$	1.08	0.86	0.96	0.88	CCl_4
$UO_2(NO_3)_2$	$-\Delta H$	$-\Delta H$	0.56	0.93	0.99	0.43	kerosene
HNO_3	$-\Delta H$	$-\Delta H$	-0.16	0.71	0.93	0.32	CCl_4
HNO_3	$-\Delta H$	$-\Delta H$	0.35	0.69	0.91	0.22	kerosene
$UO_2(NO_3)_2$	$-\Delta G_{298}^\circ$	$-\Delta G_{298}^\circ$	0.00	0.98	0.99	0.68	C_6H_6
HNO_3	$-\Delta G_{298}^\circ$	$-\Delta G_{298}^\circ$	0.13	1.03	0.98	0.15	$CHCl_3$
$UO_2(NO_3)_2$	$-\Delta G_{298}^\circ$	$-\Delta G_{298}^\circ$	0.32	0.86	0.97	0.77	$CHCl_3$
$UO_2(NO_3)_2$	$-\Delta G_{298}^\circ$	$-\Delta G_{298}^\circ$	0.24	0.93	0.97	0.77	CCl_4
HTICl ₄	$-\Delta G_{298}^\circ$	$-\Delta G_{298}^\circ$	0.44	0.90	0.98	0.56	CCl_4
$UO_2(NO_3)_2$	$-\Delta G_{298}^\circ$	$-\Delta G_{298}^\circ$	0.45	0.90	0.98	0.56	kerosene
HNO_3	$-\Delta G_{298}^\circ$	$-\Delta G_{298}^\circ$	0.32	1.45	0.95	0.37	kerosene

r is the correlation coefficient; s is standard deviation.

Results

Experimental^(10,11) and calculated values of enthalpies of donor-acceptor complexes have been compared. Complexes of $(C_4H_9O)_3PO$ with I_2 , $[(CH_3)_2N]_3PO$ with FC_6H_4OH , CF_3CH_2OH , $(CF_3)_2CHOH$, $(CH_3)_3SnCl$ and with $CHCl_3$ were obtained in CCl_4 solutions; complexes of $Al(CH_3)_3$ with $(CH_3O)_3PO$, $(CH_3)_3PO$ and with $[(CH_3)_2N]_3PO$ in C_6H_6 solutions; and $(CH_3O)_3PO \dots SbCl_5$ in CH_2Cl_2 . Bearing in mind the different solvation capacities of the solvents, the agreement between ΔH_{exp} and ΔH_{calc} is quite satisfactory. If the G_B/E_B ratio characterizes the "hardness" of compounds, the most soft base (in Table 1) is $[N(CH_3)_2]_3PO$ (the highest C_B/E_B value), while water ($C_A/E_A = 0.212$) is a "softer" acid than phenol.

Solutions of equation (1) for extraction of HNO_3 with NOPC (in CCl_4 ⁽⁶⁾, chloroform⁽¹²⁾, kerosene⁽⁶⁾); of $UO_2(NO_3)_2$ (in CCl_4 ⁽⁶⁾, benzene⁽¹³⁾, chloroform⁽¹²⁾, kerosene⁽⁶⁾); and of HTICl₄ in CCl_4 ⁽¹⁴⁾ are given in Table 2. Correlation parameters of equations relating experimental and calculated using $C_{K, \Delta x}$, $E_{K, \Delta x}$, C_B and E_B values of enthalpy and free energy are satisfactory and confirm the possibility of using (1) for quantitative description of extraction equilibria (Table 3).

The introduced quantities, $C_{K, \Delta x}$, $E_{K, \Delta x}$, should be considered as effective values that characterise the compound extracted as the result of all interactions that accompany the extraction process (i.e. interactions: chelating agent — ligand, chelating agent — solvent, chelating agent — water, ligand — solvent, ligand — water, etc.).

Solvent Effect

Naturally, the values of $C_{K, \Delta x}$ and $E_{K, \Delta x}$ are determined by the nature of the solvent. Without going into the

problem of the effect of solvent on donor-acceptor reactions and on properties of the forming complexes, it should be noted that the difficulties encountered at present are of theoretical rather than experimental character. Even the most successful theory of Onsager about the reactive field acting on a molecule and created by its polarized neighbours, despite considerable improvements, still uses empirical parameters for explaining the IR spectra of species with H-bonds when passing from gaseous medium to solutions. Until the general problem of determining the mechanism of interaction of the solvent and the dissolved compound is solved, results of empirical description should be applied. The reduction of uranyl nitrate hardness ($C_{K, \Delta x}/E_{K, \Delta x}$) on extraction with various solvents, in the order: kerosene, carbon tetrachloride, benzene, chloroform, should be included among such results.

Conclusion

Using the values of C_B and E_B for the most important organophosphorus extractants, various unknown thermodynamic parameters of extraction of acids and metal salts may be calculated.

REFERENCES

- (1) Laskorin, B. N., Yakshin, V. V. and Sharapov, B. N., Dokl. AN SSSR, 1976, 227, 666.
- (2) Karyakin, A. V. and Kriventsov, G. A., "State of water in organic and inorganic compounds", Moscow, Nauka, 1973.
- (3) Laskorin, B. N., Sharapov, B. N. and Yakshin, V. V., Proc. Intern. Solvent Extraction Conf., 1, Lyon 1974, p. 63.
- (4) Torgov, V. G. and Mikhailov, A. V., Proc. Intern. Solvent Extraction Conf., 1, Lyon 1974, p. 849.
- (5) Buchikhin, E. P., Klyshevich, R. P. and Zarubin, A. I., Radiokhimiya, 1975, 17, 38.

- (6) Komarov, E. V. and Shpunt, L. B., sb. "Chemistry and thermodynamics of solutions", vyp. 3, Leningrad, LGU, 1973.
- (7) Drago, R. S. and Wayland, B. B., J. Am. Chem. Soc. 1965, 87, 3571.
- (8) Laskorin, B. N., Yakshin, V. V. and Sharapov, B. N., DAN SSSR, 1974, 218, 871.
- (9) Laskorin, B. N., Yakshin, V. V. and Sharapov, B. N., DAN SSSR, 1974, 218, 1140.
- (10) Drago, R. S., Vogel, G. G. and Needham, T. E., J. Am. Chem. Soc. 1971, 93, 6014.
- (11) Guryanova, E. N. and Goldshtein, I. P., Romm I. P., "Donor-acceptor bonds", Moscow, Khimiya, 1973.
- (12) Laskorin, B. N., Yakshin, V. V., Buchikhin, E. P., Sokalskaya, L. I. and Medvedev, V. I., Conference on the study of the structure of organic compounds by physical methods, Kazan, 1971.
- (13) Nikolaev, A. V. (Ed.), "Extraction of inorganic substances", Novosibirsk, Nauka, 1970.
- (14) Khranenko, S. P. and Chuchalin, L. K., Izv. Sibirskogo otd. AN SSSR, Ser. Khim. Nauk, 1972, 14, 3.

DISCUSSION

V. S. Shmidt: The method of prediction of free energy values for different extraction reactions is very interesting and promising. You showed the validity of the method for various organo-phosphorus compounds. Can you apply the method for calculations comprising extraction with amines and amine salts?

V. V. Lakshin: The method is entirely applicable to amine systems. You must previously calculate C_B and E_B for the extractant of interest using any reaction of an amine salt, the constant of which equilibrium may be determined experimentally, e.g. reaction of Amine HCl with alcohol, leading to formation of adduct amine HCl·HOR. After determination of values C_B and E_B , further calculation causes no problems.

PHYSICAL AND INORGANIC CHEMISTRY

Actinide Extraction with Chelating Agents Containing Phosphorus and Nitrogen

D. I. Skorovarov, B. N. Laskorin, V. V. Yakshin, E. A. Filippov and V. V. Shatalov, Institute of Chemical Technology, Moscow, USSR.

ABSTRACT

Electron-donor properties of organophosphorus derivatives, (XYZ)P = L (X, Y, Z = OR, R, NR₂; L = O, S, Se, Te), in processes of H-bond formation, hydration and extraction increase with introduction of alkylamide groups. On the basis of quantum-chemical calculations this is explained by conjugation of the unshared nitrogen pair with higher 3d-orbitals of phosphorus.

Several examples of uranium, plutonium and neptunium extraction with phosphorus-nitrogen-containing extractants with different radicals at the heteroatoms are described. The properties of these extractants are found to be determined by the spatial and electronic structure of substituents at phosphorus and nitrogen.

Introduction

ONE OF THE MAIN METHODS of perfecting processes of actinide extraction is the use of new chelating agents with improved physical and chemical properties. Higher extraction constants and increased selectivity in relation to the metals to be extracted are among the most important of such characteristics. This stimulates continuous search for new extractants among various classes of organoelemental compounds. Organophosphorus compounds still provide most of the effective extractants and, in our opinion, the possibilities of this class are far from being exhausted. For instance, the reactivity of phosphoric acid amides and imides at extraction equilibria have been studied considerably less than esters, although preliminary results of their application are encouraging. The aim of the present work is to extend our knowledge about the structure and reactivity of phosphorus-nitrogen organic derivatives and their application in processes of extraction and purification of uranium and actinide elements.

Organophosphorous Compounds as Extractants

The search for effective chelating agents may be assisted by considering some general regularities that relate the structure and extraction capacity of organophosphorus compounds (OPC). It is quite obvious that the variety of OPC and of the metal derivatives extracted renders the description of all extraction processes by one model practically impossible. In this paper we shall study extraction equilibria of the donor-acceptor or solvating type in extraction of heavy metal salts (Lewis acids) from aqueous solutions with neutral organophosphorus compounds (NOPC). We chose these processes because their mechanisms have been extensively studied and they may be described within the donor-acceptor model.

The most complete and consistent solution of the stated problem may be obtained by non-empirical quantum-chemical calculation of the reacting systems. Since such calculations require impractically large amounts of computer time, empirical and semi-empirical dependences between the structure and reactivity are usually used. Al-

TABLE 1. Effective Charges and Overlap Integrals of X-P Bonds

	X	P	Z _X *	Z _P *	S _{ij}	S _{P-X}
O	2s	3s	5.95	5.85	0.114	0.402
	2s	3p	5.95	4.80	0.257	
	2p	3s	4.55	5.85	0.176	
	2p	3p	4.55	4.80	0.242	
C	2s	3s	3.95	5.85	0.180	0.561
	2s	3p	3.95	4.80	0.342	
	2p	3s	3.25	5.85	0.281	
	2p	3p	3.25	4.80	0.329	
N	2s	3s	4.95	5.85	0.147	0.617
	2s	3p	4.95	4.80	0.291	
	2p	3s	3.90	5.85	0.222	
	2p	3p	3.90	4.80	0.285	
	2p	3d	1.40	2.77	0.137	

TABLE 2. Experimental and Calculated Thermodynamic Characteristics of Donor-acceptor Reactions Involving NOPC

X	Y	Z	$\sum S_i$ i = X,Y,Z	(XYZ) P = O						P = S	P = Si	P = Ti		
				$\sum \sigma_i^+$	$-\lg \bar{\kappa}$ (HNO ₃)	$\lg \bar{\kappa}$ /UO ₂ (NO ₃) ₂	pKa	$-\Delta G_{293}$ (H ₂ O)	$-\Delta G_{298}$ (C ₆ H ₅ OH)	$-\Delta H$ (H ₂ O)	$-\Delta H$ (C ₆ H ₅ OH)	$-\Delta H$ (C ₆ H ₅ OH)		
RO	RO	RO	1.206	0.36	-1.06	-0.30	—	0.2	2.8	4.0	5.4	4.5	4.6	—
				(0.37)	(-1.06)	(-0.01)	(3.87)	(0.1)	(2.8)	(3.8)	(5.2)	(4.5)	(4.7)	(4.4)
RO	RO	R	1.365	1.20	-0.86	1.54	—	0.6	3.2	4.0	5.4	—	—	—
				(1.19)	(-0.77)	(1.36)	(5.21)	(0.5)	(3.2)	(4.1)	(6.0)	(4.8)	(4.9)	(4.7)
RO	R	R	1.524	2.04	-0.35	2.80	6.19	0.8	3.4	4.8	7.5	5.1	5.2	—
				(2.01)	(-0.48)	(2.73)	(6.53)	(0.9)	(3.6)	(4.5)	(6.8)	(5.2)	(5.0)	(5.0)
R	R	R	1.683	2.88	—	4.60	8.44	1.9	4.5	5.2	7.7	5.8	—	—
				(2.83)	(-0.18)	(4.10)	(1.87)	(1.4)	(4.0)	(4.9)	(7.6)	(5.6)	(5.4)	(5.3)
RO	RO	NR ₂	1.422	1.46	—	—	—	0.7	3.3	4.2	6.6	—	5.1	—
				(1.48)	(-0.66)	(1.85)	(5.68)	(0.7)	(3.4)	(4.3)	(6.3)	(5.0)	(5.0)	(4.8)
RO	NR ₂	NR ₂	1.635	2.56	—	—	7.55	1.3	3.9	4.5	7.2	—	5.4	—
				(2.58)	(-0.27)	(3.69)	(7.46)	(1.2)	(3.9)	(4.8)	(7.4)	(5.5)	(5.4)	(5.2)
NR ₂	NR ₂	NR ₂	1.851	3.66	0.08	5.12	8.97	1.9	4.5	5.8	9.0	5.9	6.6	5.6
				(3.69)	(0.12)	(5.55)	(9.27)	(1.8)	(4.5)	(5.3)	(8.5)	(6.0)	(5.7)	(5.6)
R	R	NR ₂	1.740	3.14	—	—	—	1.2	3.8	5.0	7.8	—	—	5.4
				(3.12)	(-0.08)	(4.60)	(8.25)	(1.5)	(4.2)	(5.0)	(7.9)	(5.7)	(5.5)	(5.4)
R	NR ₂	NR ₂	1.794	3.40	—	—	—	1.8	4.4	4.8	7.8	—	—	—
				(3.40)	(0.02)	(5.06)	(8.60)	(1.7)	(4.3)	(5.2)	(8.2)	(5.8)	(5.6)	(5.5)
R	RO	NR ₂	1.581	2.30	—	—	—	0.6	3.9	4.2	6.5	—	—	—
				(2.30)	(-0.37)	(3.22)	(7.01)	(1.1)	(3.8)	(4.6)	(7.1)	(5.3)	(5.3)	(5.1)

though describing only a particular series of similar compounds, they may be used to predict properties of extractants and to explain experimental results.

Reactivity of Extractants

It is well known that extraction processes are accompanied by various chemical and physical conversions. However, in most cases, the reaction of complex formation involving the extractant and the complex to be extracted is the limiting step. This simple but very constructive approach simplifies the model of extraction equilibria, in particular for solvation-type processes that proceed without rupture or formation of chemical bonds in the initial compound. The constant of extraction equilibrium is then determined by the electron-releasing properties of the metal to be extracted and by the electron-attracting capacity of the extractant. Both may be determined or calculated⁽²⁾.

In the present study the electron-donor properties of (XYZ)P = L compounds (X,Y,Z = OR, R, NR₂; L = O, S, Se, Te) are estimated on the basis of overlap integrals (S_i) of atomic orbitals for P-X, P-Y and P-Z bonds. Assuming that the chelating capacity of NOPC is determined by the electron density of the P = L moiety, the donor capacity should increase with $\sum S_i$ (i = X,Y,Z), all other conditions being equal. The following hybridizations of atomic orbitals were taken for calculations⁽³⁾: P (sp³), C (sp³), O (sp²), N (sp²). Following the data obtained in Ref. (4) we assumed that additional p_π-d_σ conjugation of X,Y and Z with P should be taken into account only for the P-N bond. Such interaction is due to the capacity of the ligand force field to lower the 5-fold degeneration of the 3d-orbitals of phosphorus so that combined but independent overlap with these and 2p_π oxygen orbitals is possible at L = O. It is realized for point group C_{3v} and C_s symmetry of NOPC molecules.

Interatomic distances were assumed equal to the sums of covalent radii of atoms. Effective charges (Z*) and overlap integrals of atomic orbitals corresponding to the so-called pure bonds (S_{ij}) (Table 1) were calculated as described in Ref.⁽⁵⁾.

Overlap integrals of hybrid orbitals of P and X σ-bonds (X = O, C and N) were calculated as

$$S_{P-X} = \sum q_i^+ q_j^+ S_{ij} \dots \dots \dots (1)$$

TABLE 3. Correlation Equations, $y = a_0 + a_1 S_i$

a ₀	a ₁	n	r	S	y	P = L
-5.84	5.15	10	0.999	0.028	$-\sum \sigma_i^+$	P = L
0.88	2.39	10	0.998	0.34	$-\Delta H_{H_2O}$	P = O
-0.94	5.08	10	0.998	0.48	$-\Delta H_{C_6H_5OH}$	P = O
-3.14	2.68	10	0.928	0.30	$-\Delta G_{H_2O}$	P = O
-0.46	2.68	10	0.998	0.23	$-\Delta G_{C_6H_5OH}$	P = O
-3.28	1.84	4	0.984	0.11	$\lg K_{HNO_3}$	P = O
-10.42	8.63	5	0.986	0.43	$\lg K_{UO_2(NO_3)_2}$	P = O
2.85	1.53	5	0.977	0.089	$-\Delta H_{C_6H_5OH}$	P = S
1.68	2.32	4	0.974	0.18	$-\Delta H_{C_6H_5OH}$	P = Se
2.30	1.78	2	—	—	$-\Delta H_{C_6H_5OH}$	P = Te
6.22	8.37	4	0.937	—	pKa	P = O

where q_i and q_j are the contributions of the s- and p-orbitals into hybrid te and tr orbitals.

The sums of overlap integrals for heteroatom-substituent bonds, $\sum S_i$ (i = X,Y,Z), are in good agreement with the thermodynamic characteristics of donor-acceptor reactions (Tables 2 and 3). The free energies (ΔG) and enthalpies (ΔH) of (XYZ)P = O complex formation with phenol⁽⁶⁾ and water⁽⁷⁾ and enthalpies (ΔH) of (XYZ)P = S⁽⁸⁾, (XYZ)P = Se and (XYZ)P = Te⁽⁹⁾ complex formation with phenol were measured by the method of IR spectrometry in CCl₄ solutions; pKa of the conjugated acids was determined by potentiometric titration with perchloric acid in nitromethane^(10,11); extraction was carried out by derivatives with R = C₆H₅ in chloroform solutions^(12,13); sums of Kabachnik constants were calculated according to Ref.⁽¹⁴⁾. The previously established empirical correlations^(15,16) between extraction properties and intermolecular hydrogen bonds are supported by the data presented in Tables 2 and 3.

Note the high correlation coefficient (r = 0.999) for the linear dependence between the sum of total constants of substituents at phosphorus, $\sum \sigma_i^+$ (i = X,Y,Z) and the sum of overlap integrals $\sum S_i$ (i = X,Y,Z):

$$-\sum \sigma_i^+ = -5.84 + 5.15 \sum S_i \dots \dots \dots (2)$$

n = 10, r = 0.999 and S = 0.028, where n is the number of compounds studied, r is the correlation coefficient and S is the standard deviation.

The value of r suggests that introduction of σ^* constants is justified from the quantum-chemical point of view and that the entire range of organophosphorus reactions that obey the rule of linear free energy dependences (LFE) may be described by ΣS_i . This supports the use of calculated overlap integrals of substituents with phosphorus in organophosphorus molecules for the quantitative description of reactivity, at least for donor-acceptor processes.

Therefore, introduction of P-N bonds into molecules of organophosphorus extractants which possess the highest overlap integral among the compounds studied (Table 1), should increase the reactivity of extractants. This should be particularly noticeable in molecules with C_{3v} and C_s symmetry groups, the value of $S_{ppr} - 3d\pi$ being appreciable in this case. The electronic and spatial structure of the substituents (R) at the phosphorus and nitrogen atoms may considerably affect the $p_\pi - d_\pi$ conjugation of substituents with phosphorus and the electron-releasing capacity of the molecules. Since there are no methods of calculating this effect at present, empirical dependences obtained directly from experimental data are used for establishing the optimal structure of extractants. In the following sections of this paper we shall demonstrate the advantages of extractants containing phosphorus and nitrogen for extraction from aqueous nitrate solutions of actinide salts.

Experimental

The initial aqueous solution contained amounts of ^{233}U , ^{239}Pu and ^{237}Np sufficient to provide 10^4 - 10^6 counts per min per ml. Radiochemically pure ^{233}U and ^{239}Pu , free of ^{232}Th and ^{241}Am were obtained by extraction into ether and sorption purification on VP-1AP.

Plutonium and neptunium were converted to various oxidation states by standard techniques⁽¹⁷⁾. Pu(III) was prepared by reduction of 0.01 g-atom/l of Pu(IV) in 1M nitric acid with 0.2-0.3M excess of hydrazine nitrate solution for 30 min at 70-80°. Pu(IV) was stabilized in a sodium nitrate solution. Pu(VI) was prepared by oxidation of Pu(IV) with $\text{K}_2\text{B}_2\text{O}_7$ (0.1M) for an hour at 80-90°.

Np(IV) was prepared by heating a solution of 10^{-4} - 10^{-5} g-atom/l of ^{237}Np in 1M nitric acid in the presence of 0.2-0.3M hydrazine nitrate for 30 min at 80-90°. After adding 0.01M Fe(II) sulphate to the cooled solution it was diluted to required activity. Np(V) was stabilized in sodium nitrate solution (0.01M) at 50-60° for 15-20 min. Np(VI) was prepared by adding several drops of 0.1 mg/ml potassium permanganate until colouring of the solution and subsequent heating for 15 min at 50-60°.

In several cases Pu and Np were quantitatively converted to the extreme oxidation states electrochemically

TABLE 4. Distribution of Nitric Acid Between Aqueous and Organic Phases Depending on Extractant Concentration in Octane*

N	Extractant	E, M			Solvation Number n	K \pm G (mole $^{-1}$) $^{-1}$
		0.1	0.05	0.025		
I	$\text{CH}_3\text{NHP(O)}(\text{OC}_8\text{H}_{17})_2$	0.0379	0.0194	0.0093	1	0.40 ± 0.03
II	$\text{C}_4\text{H}_9\text{NHP(O)}(\text{OC}_8\text{H}_{17})_2$	0.0290	0.0118	0.00573	1	0.66 ± 0.03
III	$(\text{C}_6\text{H}_{13})_2\text{NP(O)}(\text{OC}_4\text{H}_9)$	0.0240	0.0097	0.0046	1	0.27 ± 0.04
IV	$(\text{C}_4\text{H}_9\text{NH})_2\text{P(O)}(\text{OC}_8\text{H}_{17})$	0.0350	0.0165	0.0083	1	0.51 ± 0.11
V	$(\text{C}_4\text{H}_9\text{NH})_3\text{P(O)}$	0.0630	0.0330	0.0165	1	2.00 ± 0.06
VI	$(\text{C}_4\text{H}_9)_2\text{N}_3\text{P(O)}$	0.054	0.0284	0.0139	1	1.20 ± 0.1

*Ratio of organic to aqueous phases 1:1; period of phase contact — 10 min; HNO_3 concentration — 1M.

in an anion-exchange membrane electro-dialyzer (stainless steel cathode, platinum anode, current density - 300 A/m² at 20-30°). The completeness of actinide oxidation or reduction was verified spectrophotometrically. The obtained solutions were then diluted to the required activity and acidity.

The structure and purity of the organic reagents and diluents were checked by ^{14}N , ^{31}P , ^{14}N NMR and IR spectrometry, potentiometric titration and by elemental analysis. Study of extraction equilibria was carried out at $22 \pm 2^\circ\text{C}$ in glass and fluoroplastic separatory funnels with mechanical agitation.

Prior to extraction, organic solutions were brought into contact with nitric acid solutions of appropriate concentrations. The samples were analyzed radiometrically on a PST-100 instrument with a side counter. At low distribution coefficients (< 0.001), activity of the organic phase was measured by adding an aliquot to a weighed sample of B-3e ZnS(Ag) phosphor in the corresponding diluent. Samples dried under an IR lamp gave values that satisfactorily agreed (5-10%) with distribution coefficients determined from the aqueous phase, even at very low extractant concentrations.

The equilibrium concentration of nitric acid in the organic phase was determined by potentiometric titration using a pH-340 instrument equipped with a glass-calomel electrode system and a standard salt bridge. The equilibrium constant of nitric acid extraction was calculated according to equation

$$K = \frac{[\text{H}^+]_{(w)} + \text{NO}_3^-_{(w)} + n \cdot S_0 \rightleftharpoons n \cdot S \cdot \text{HNO}_3_{(o)}}{\frac{[\text{H}^+]_{(w)} [\text{NO}_3^-]_{(w)} [\text{S}]^n}{Y_{\text{H}}} = \frac{Y_{\text{H}}}{X_{\text{H}} [\text{NO}_3^-]_{(w)} [\text{S}]}} \quad (3)$$

where Y_{H} and X_{H} are the equilibrium concentrations of nitric acid in organic and aqueous phases respectively, $[\text{S}]$ is the concentration of free extractant. At $n = 1$, $S = S_0 - Y_{\text{H}}$ (S_0 is the initial extractant concentration).

Results

The distribution of nitric acid between aqueous phase and solutions of organophosphorus chelating agents at different extractant concentrations is shown in Table 4. The dependence of the distribution coefficient of nitric acid (D) on the free extractant concentration in organic phase is always linear with the slope and solvation number equal to unity. On account of this it is possible to calculate the extraction constants of nitric acid for all studied chelating agents.

TABLE 5. Dependence of Distribution Coefficients on Extractant Concentration in Octane*

N	Extractant, E	E	D	E	D	E	D	n**
I	$\text{CH}_3\text{NHP(O)}(\text{OC}_8\text{H}_{17})_2$	0.01	27.2	0.003	3.0	0.001	0.3	2
III	$(\text{C}_6\text{H}_{13})_2\text{NP(O)}$	0.05	13.0	0.02	2.3	0.01	0.55	2
IV	$(\text{C}_4\text{H}_9\text{NH})_2\text{P(O)}$	0.01	19.6	0.003	1.8	0.001	0.20	2
V	$(\text{C}_4\text{H}_9\text{NH})_3\text{P(O)}$ ***	0.005	7.95	0.0025	2.30	0.001	0.34	2
VI	$(\text{C}_4\text{H}_9)_2\text{N}_3\text{P(O)}$ ***	0.005	19.6	0.0025	6.25	0.0006	0.45	2

*Initial ^{233}U concentration — 50-80 counts/sec per 0.1 ml; $\mu = 1$; D — distribution coefficient.

**n — Solvation number (tgd).

***In benzene

TABLE 6. Dependence of Plutonium (III, IV, VI) Distribution Coefficients on Extractant Concentration in Octane

N	Extractant, E	Plutonium oxidation state								
		III			IV			VI		
		E	D	n	E	D	n	E	D	n
I	CH ₃ NHP(O)(OC ₈ H ₁₇) ₂	0.005	100	2.82	0.001	22.4	2.09	0.005	34.6	2.0
		0.0025	12.8		0.0005	5.5		0.0025	8.65	
		0.0016	3.64		0.00025	1.36		0.001	1.37	
II	C ₄ H ₉ NHP(O)(OC ₈ H ₁₇) ₂	0.005	55	3.0	0.0005	14.4	2.1	0.005	89.5	1.93
		0.0025	7.32		0.00025	3.6		0.0025	23.2	
		0.001	0.55		0.0001	0.72		0.001	4.12	
III	(C ₆ H ₁₃) ₂ N—P(O)(OC ₄ H ₉) ₂	0.1	1.43	3.1	0.005	2.7	1.92	0.01	1.52	2.0
		0.07	0.35		0.0025	0.72		0.005	0.33	
		0.05	0.15		0.001	0.11		0.0025	0.104	
IV	(C ₄ H ₉ NH) ₂ P(O)OC ₈ H ₁₇	0.005	36.7	2.86	0.0005	11.3	2.0	0.005	7.97	1.94
		0.003	7.9		0.00025	2.5		0.0025	2.0	
		0.001	0.32		0.0001	0.5		0.001	0.36	
V	(C ₄ H ₉ NH) ₃ P(O)*	0.05	3.33	3.0	0.0025	7.5	2.28	0.01	11.02	1.93
		0.025	0.44		0.00125	1.83		0.005	2.92	
		0.016	0.132		0.0005	0.185		0.0025	0.71	
VI	[(C ₄ H ₉) ₂ N] ₃ P(O)*	0.01	40.8	2.0	0.0005	40.0	2.0	0.001	2.27	2.0
		0.005	9.0		0.00025	12.5		0.0005	0.59	
		0.0025	2.23		0.000125	2.5		0.00025	0.15	
VII	C ₁₂ H ₂₅ NHP(O)(OC ₈ H ₁₇) ₂	0.001	0.0036	—	0.001	0.077	2.0	0.001	0.059	2.0
					0.0005	0.017		0.0005	0.014	
					0.0001	0.0007		0.00025	0.0032	

*in benzene

As can be seen, gradual introduction of alkylamide radicals into organophosphorus molecules leads to an increase of nitric acid extraction constants. For instance, introduction of butylamide fragments in the series II < IV < V leads to a 3-fold increase of the constant and trisamides of phosphoric acid are effective extractants of nitric acid. Similar results have been obtained for nitric acid extraction with phosphoric acid amides in chloroform⁽¹⁸⁾; trisamides turned out to be more effective extractants than trioctylphosphin oxide.

Phosphoric Acid Amides

On the basis of the linear dependences between nitric acid extraction constants and those of uranium and actinide nitrates, $\lg K_i = a \lg K_{\text{HNO}_3} + b_i$ (Ref.⁽¹⁹⁾), it may be assumed that phosphoric acid amides should be effective chelating agents of transuranium elements. To verify this assumption we studied the distribution of tracer quantities of ²³³U, ²³⁹Pu and ²³⁷Np between aqueous nitrate solutions and extractant solutions in octane (Tables 5, 6 and 7). Preliminary experiments established that at constant ionic strength of the aqueous solution, $\mu = 1$ (HClO₄ + HNO₃), NO₃ distribution coefficients are independent of concentration in the range of 0.1-1 mole/l. It follows from data presented in Tables 5-7 that Pu(III) is extracted in the form of a trisolvate (n = 3), Np(V) as a monosolvate, while all other compounds form disolvates (n = 2). The calculated concentrational constants (\tilde{K}) of actinoid extraction reactions are given in Table 8.

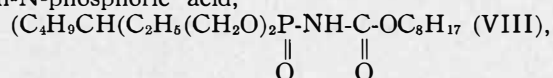
As can be seen from the data presented in Table 8, even a simple increase of the length of hydrocarbon radical at the nitrogen atom from methyl to dodecyl in dioctylphosphoric acid monoalkylamide, (RNHP(O)(OC₈H₁₇)₂), in the series I < II < VII considerably reduces (by two orders of magnitude) extraction constants of all studied actinide. A similar reduction of K occurs when passing from secondary (I,II,V,VII) to tertiary amides (III,VI) of

phosphoric acid. Increase of the number of alkylamide substituents at phosphorus atom in series II < IV < V increases \tilde{K} for U(VI) and Np(IV) and Np(VI), while for Pu(III,IV,VI) a reversed dependence is observed.

It should be noted that for all studied phosphoric acid amides the extraction constants are very high and these derivatives belong to "superstrong" extractants ($K > 10^6$) of uranium and transuranium elements from nitrate solutions.

Another group of phosphorus-nitrogen containing extractants are phosphoric acid amides, the amide nitrogen atom of which has a substituent with a (RO)₂P(O)NHR' π -electron system (R' = C(O)R'', C(O)OR'', C(O)NR''₂, P(O)(OR''), SO₂R'', etc.). In this case the nitrogen atom will conjugate both with the P atom and with the adjacent π -electron system, leading to redistribution of the electron density in the molecule and to alteration of its electron-releasing properties.

For instance, in the di(2-ethylhexyl) ether of octylurethan-N-phosphoric acid,



nitrogen of the amide group may conjugate either with the phosphoryl or carbonyl or with both groups. The monotonic increase of nitric acid distribution coefficient with increase of acidity of the aqueous phase from 0.1 to 10 mole/l during extraction with a 0.1M benzene solution renders determination of the extraction constant impossible. In the limiting case, VIII extracts 2M nitric acid, suggesting formation of a 1:2 complex, presumably involving both reaction centers (carbonyl and phosphoryl groups).

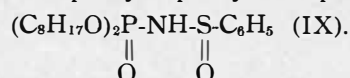
Distribution coefficients of U(VI) in the given system are inversely proportional to hydrogen-ion concentration in the power of one, are independent of nitrate-ion concentration and decrease with nitric acid concentration in

the aqueous phase^(20,21). The bilogarithmic dependences of U(VI) distribution coefficients on extractant and nitric acid concentrations are linear with tg close to unity in the 0.1-0.001M range of extractant concentration and in the 0.1-1M range of ionic strength of the aqueous phase. This distinguishes VIII from monofunctional organophosphorus and carbonyl compounds for which the solvation number tends to 2 in these conditions and confirms the bifunctional nature of VIII. The U(VI) extraction constant, calculated for these conditions, is $(2.35 \pm 0.4) \cdot 10^4$ (mole \cdot l)⁻¹.

Pu(IV) extraction probably proceeds similarly, although the distribution coefficient is independent of nitrate-ion concentration in the aqueous phase and the solvation number is 0.5 (Table 9). The extraction maximum for plutonium is observed at 2M nitric acid and the extraction constant is $(3.4 \pm 0.2) \cdot 10^3$ (mole \cdot l)⁻¹.

Np(IV) extraction differs from that of U(VI) and Pu(IV). The distribution coefficient is independent of hydrogen-ion concentration in a wide range and depends on nitrate-ion concentration in the power of three. The solvation number approaches unity (Fig. 4); extraction maximum is observed at 6M nitric acid; extraction is $(1.1 \pm 0.2) \cdot 10^3$.

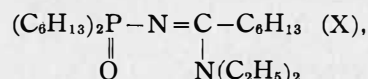
Another example of a conjugated amide system is the dioctyl ether of N-phenylsulphonylamidophosphoric acid,



This compound extracts nitric acid in the form of a monosolvate in the concentration range of 0.1-4M. In the case of U(VI) and Pu(IV) extraction with benzene solution of IX, the distribution coefficients decrease with increase of nitric acid concentration and are independent of nitric-ion concentration in the aqueous phase. The solvation number in both cases is $n = 1$ (Table 9). Np(IV) forms a 2:1 complex in these conditions.

Both examples described above show that introduction into extractants containing phosphorus and nitrogen of substituents capable of conjugation with nitrogen considerably alters the capacity to extract uranium and transuranium elements. The fact that not only the dentativity of the extractant, but also the extraction mechanism changes, may be used for separation of elements with similar properties.

Phosphoric acid imides, such as diethylamide of N-dihexylphosphorylimidoenanthic acid,



constitute yet another group of promising extractants. The sp^2 hybridization of the nitrogen atom determines the nature of interaction with the higher vacant phosphorus orbitals. The P atom may additionally conjugate with the double C=N bond in α -position to the phosphoryl group.

The fact that nitric acid concentration in the organic phase monotonically increases with the concentration in the aqueous phase during extraction by 0.1M benzene solution of X hinders determination of the extractant constant. Maximal saturation is reached at 1.75M of acid per 1M of extractant at 10M acid concentration in the aqueous phase. The amount of actinide extracted increases with acid concentration in the aqueous phase up to 2M in the case of U(VI) and to 6M in the case of Pu(IV) and Np(IV). Variation of hydrogen-ion concentration from 0.1M to 1M at constant ionic strength of the solution, $\mu = 1$ (lithium nitrate), does not affect distribution coefficients of all three metals. In contrast, variation of nitrate-ion concentration affects only the Pu(IV) distribution coefficient, while for the other two metals a linear dependence is observed with $tg = 1.0$ for U(VI) and $tg = 2.0$ for Np(IV). At $\mu = 1$ the solvation number for U(VI) is 2.0, for Pu(IV) $n = 1.1$ and for Np(IV) $n = 1.5$. Con-

TABLE 7. Dependence of Neptunium (IV, V, VI) Distribution Coefficients on Extractant Concentration in Octane

N	Extractant, E	Neptunium oxidation state								
		IV			V			VI		
		E	D	n	E	D	n	E	D	n
I	CH ₃ NHP(O)(OC ₈ H ₁₇) ₂	0.005	16.9	2.1	0.1	6.05	1	0.005	1.15	2.0
		0.0025	3.29		0.01	0.58		0.0025	0.33	
		0.001	0.5		0.001	0.058		0.001	0.056	
II	C ₄ H ₉ NHP(O)(OC ₈ H ₁₇) ₂	0.005	11.8	2.02	0.001	0.425	1	0.01	3.56	2.1
		0.0011	0.43		0.0005	0.153		0.005	0.9	
		0.0005	0.117		0.0001	0.024		0.0025	0.195	
III	(C ₆ H ₁₃) ₂ NP(O)(OC ₄ H ₉) ₂	0.01	1.38	1.95	0.1	1.08	0.3	0.05	4.18	1.94
		0.005	0.40		0.01	0.55		0.025	0.96	
		0.001	0.018		0.001	0.29		0.010	0.16	
IV	(C ₄ H ₉ NH) ₂ P(O)OC ₈ H ₁₇	0.01	25	2.1	0.1	2.2	0.5	0.01	3.85	2.0
		0.0025	1.33		0.01	0.71		0.005	0.975	
		0.001	0.22		0.001	0.25		0.0025	0.245	
V	(C ₄ H ₉ NH) ₃ P(O)*	0.05	12.6	2.0	0.1	0.4	—	0.005	1.92	2.07
		0.0025	3.2	—	—	—	—	0.0025	0.47	—
		0.001	0.618	—	—	—	—	0.001	0.077	—
VI	[(C ₄ H ₉) ₂ N] ₃ P(O)*	0.005	2.2	1.9	0.1	1.49	—	0.01	3.31	2.0
		0.0025	0.70		0.01	0.67		0.005	0.85	
		0.001	0.115		—	—		0.001	0.035	
VII	C ₁₂ H ₂₅ NHP(O)(OC ₈ H ₁₇)	0.001	0.111	2.0	0.001	0.14	—	0.001	0.0034	2.03
		0.00075	0.055		0.0005	0.032		0.00075	0.0014	
		0.0005	0.028		—	—		0.0005	0.0007	

*in benzene

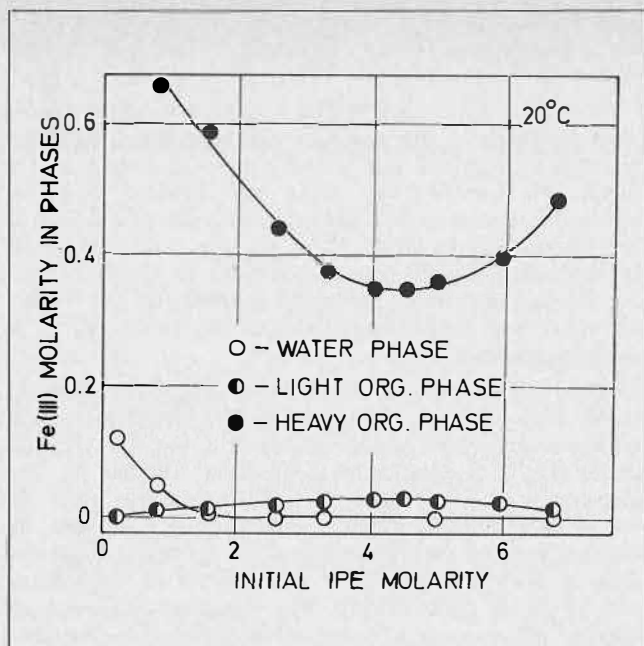


FIGURE 4. Iron (III) molarity in phases in extraction with diluted IPE concentration in initial organic solvent. Initial concentrations of components: $c_{Fe}^i = 0.14$ M, $c_{HCl}^i = 9.3$ M and phase ratio $r^i = 1.0$.

increase of the initial concentration of IPE and HCl. This change in phase volumes is caused by the increase of ether transition from the organic into the aqueous phase due to the solvation of the acid.

After the addition of iron(III) into the mentioned system, under the given conditions, three liquid phases appear. The third phase is observed in such a wide concentration range as 0.08 – 0.41 M $FeCl_3$, 6.6 – 9.3 M HCl and 0.4–7.1 M IPE. A change of IPE content in the system is accompanied by a significant phase volume change (Figure 2). The heavy organic phase most probably contains a hydrosolvate of tetrachloroferrate(III) acid having low solubility in both the aqueous and organic phase. The volume of the heavy organic phase reaches maximum when the system contains sufficient IPE for the solvation of the metallic complex species. Simultaneously, the volume of the light organic phase is at minimum. A decrease in the volume of the light organic phase is caused mostly by the decrease of the amount of benzene in the initial mixed solvent. The disappearance of the light organic phase occurs under given conditions (Figure 2) and shows that benzene is present also in the heavy organic phase. This fact explains the decrease in the volume of the heavy organic phase at high concentrations of IPE.

The results obtained by the analyses of the heavy organic phase show that the decrease of its volume is not followed by a corresponding decrease in metal content (Figure 3). The total quantity of iron(III) in the heavy organic phase is practically independent of the initial IPE concentration (above 2 M). On the other hand, the concentration of iron(III) in the heavy organic phase passes through the minimum at the given initial IPE concentration (Figure 4). The concentration of other components, H_2O and HCl, in the heavy organic phase show similar dependence on the initial concentration of IPE. As a consequence, the partial distribution ratio between the heavy organic phase and the light organic phase $(D_e)^{HL}$ passes through the minimum at an initial concentration of about 4.5 M IPE, while the corresponding partial extraction factor $(D_m)^{HL}$ attains an approximately constant value (Figure 5).

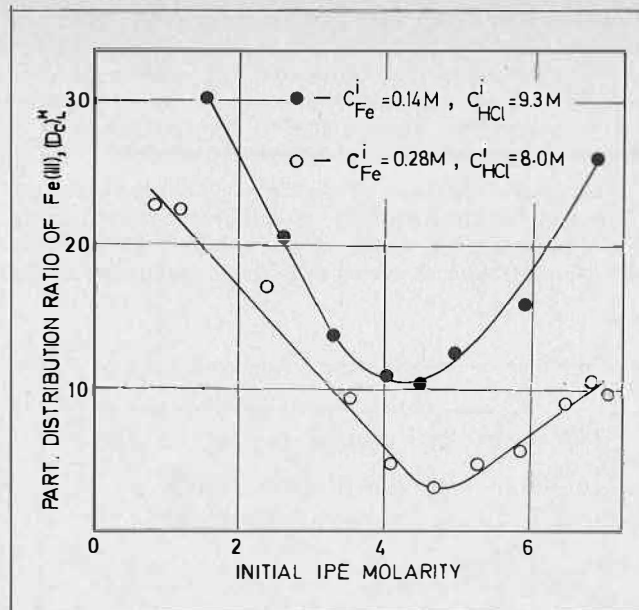


FIGURE 5. Partial distribution ratio heavy organic phase/light organic phase of iron (III) as a function of IPE concentration in initial organic solvent. Initial phase ratio $r^i = 1.0$.

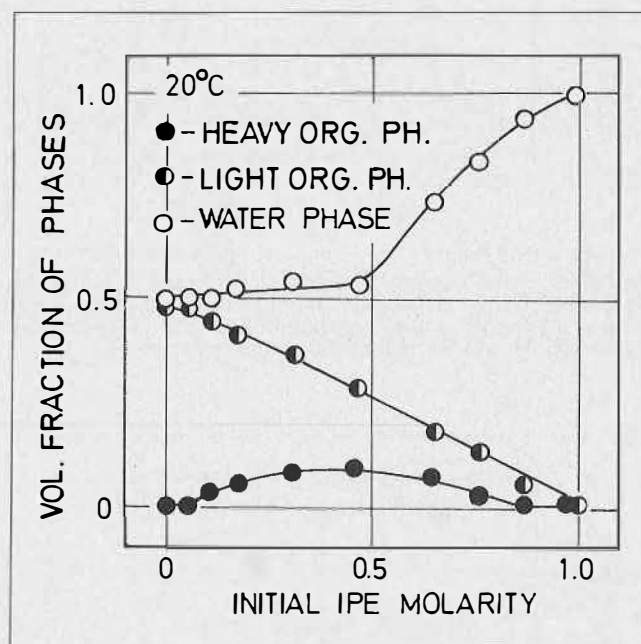


FIGURE 6. Volume changes of phases in the system: $AuCl_3$ -HCl-Water-IPE-Benzene, as a function of IPE concentration in initial organic solvent. Initial concentrations of components: $c_{Au}^i = 0.09$ M, $c_{HCl}^i = 11.8$ M and phase ratio $r^i = 1.0$.

The extraction behaviour of the $AuCl_3 - HCl - H_2O - IPE - benzene$ system differs considerably from the previously described $FeCl_3 - HCl - H_2O - IPE - benzene$ system. Contrary to the system with iron(III) chloride, the heavy organic phase formed by gold(III) chloride is "resistant" to the increase of the water content. An increase of water does not contribute, in this case, to the similarity of phases (heavy organic and aqueous) and they remain separate. After an increase of IPE content in the system the phase volumes markedly change (Figure 6). The third phase is also observed in a wide concentration range (0.09 – 1.14 M $AuCl_3$, 7.7 – 11.8 M HCl and 1.2 – 7.1 M IPE).

The volume of the heavy organic phase attains a maximum and the volume of aqueous phase increases. High initial HCl concentration (11.8 M) causes the transfer of available IPE in the aqueous phase. An increase of mutual solubility increases the similarity in the characteristics of the phases and they become completely miscible.

The results obtained by the analyses of phase content show that the total quantity of gold(III) extracted in the heavy organic phase is the largest at about 4.0 M initial IPE concentration. It seems that in this region the diluted

solvent contains a sufficient quantity of the active extractant accompanied by a relatively high IPE activity (Figure 7).

Compared with the iron(III) system, the concentration of components in the gold(III) system changes quite differently in direction and extent with the change in the initial IPE concentration. In a wide range (1-5 M) of initial IPE concentration, the concentration of gold(III) in the heavy organic phase varies slightly, while the water concentration rapidly increases (Figure 8). This indicates an increase of water molecule number in the hydro-solvate of tetrachloroaurate(III) acid due to the change in solvent composition.

The distribution ratio is strongly dependent upon the initial IPE molarity, while the partial distribution ratio between the heavy organic phase and the light organic phase (D_c)^H is practically independent (Figure 9). The distribution ratio is also strongly dependent upon the initial HCl molarity. These results strongly indicate the enhancement of the extraction in the investigated system. This is probably caused by an increase of the solvent activity in the inert diluent. The direction and extent of diluent influence, as in some other systems, is connected with any of the parameters of the system examined.

The main differences between the iron(III) and the gold(III) extraction from the aqueous solution of hydrochloric acid by diluted IPE are particularly expressed in the characteristics of the heavy organic phase. The extraction by diluted IPE has some advantages over undiluted IPE. For instance, the AuCl₃ - HCl - H₂O - IPE system is homogenous at a high acid concentration while the AuCl₃ - HCl - H₂O - IPE - benzene system is heterogeneous making a good separation possible.

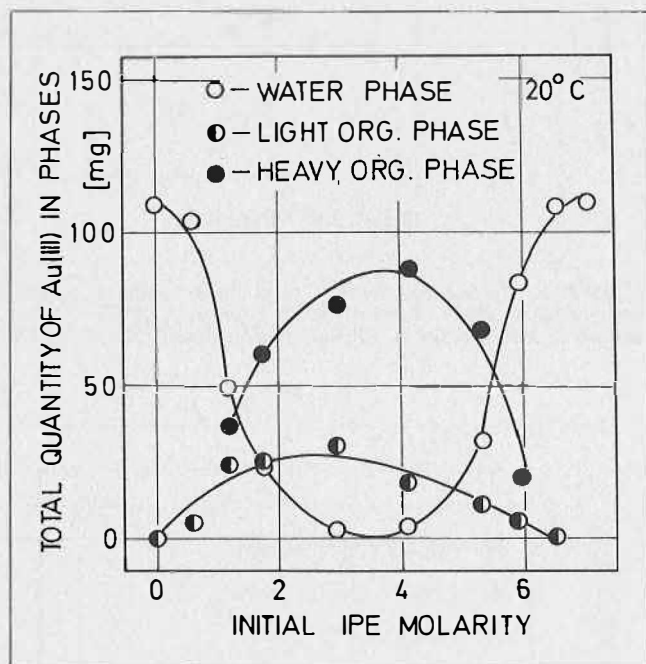


FIGURE 7. Total quantity of gold (III) in phases in extraction by diluted IPE as a function of IPE concentration in initial organic solvent. Initial concentrations of components: $c_{Au}^i = 0.09$ M, $c_{HCl}^i = 11.8$ M and phase ratio $r^i = 1.0$.

Acknowledgment

The authors would like to express their gratitude to the Self-management Council for Scientific Research of S.R. Croatia for its financial support.

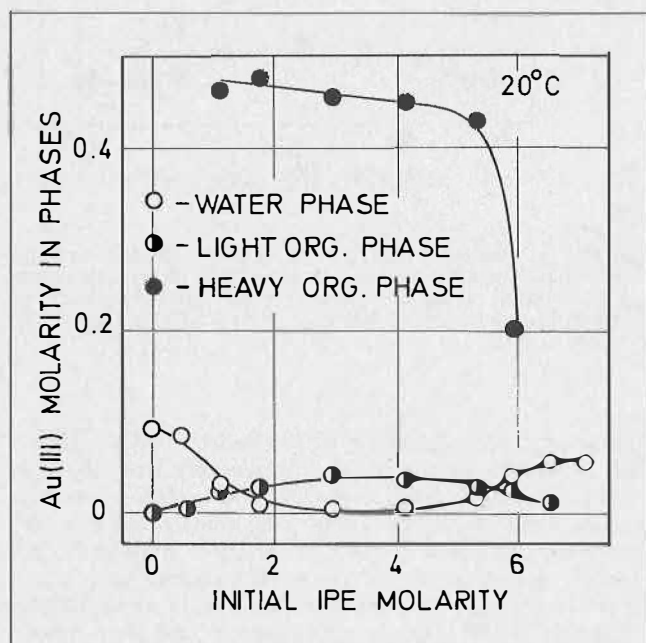


FIGURE 8. Gold(III) molarity in phases in extraction by diluted IPE concentration in initial organic solvent. Initial concentrations of components: $c_{Au}^i = 0.09$ M, $c_{HCl}^i = 11.8$ M and phase ratio $r^i = 1.0$.

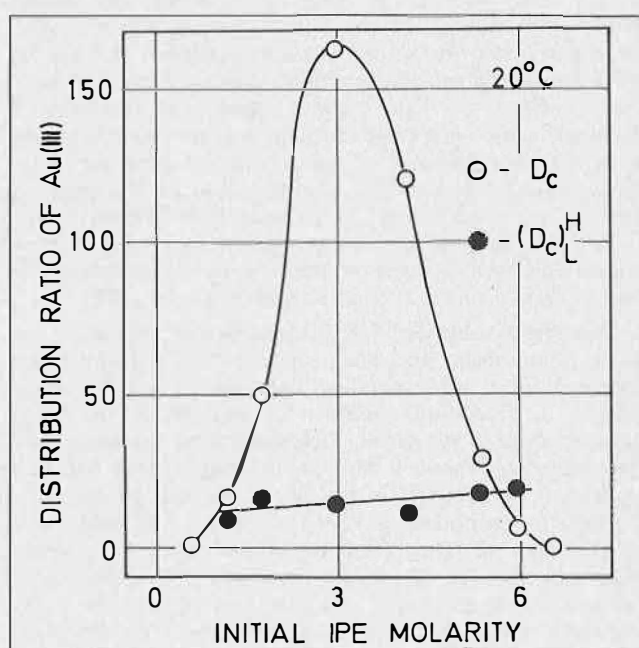


FIGURE 9. Distribution ratio and partial distribution ratio heavy organic phase/light organic phase of gold (III) as a function of IPE concentration in initial organic solvent. Initial concentrations of components: $c_{Au}^i = 0.09$ M, $c_{HCl}^i = 11.8$ M and phase ratio $r^i = 1.0$.

REFERENCES

- (1) D. Maljkovic, M.Sc. Thesis, Univ. Zagreb, 1965.
- (2) D. Maljkovic and M. Branica, *Croat. Chem. Acta*, **38** (1966) 65.
- (3) D. Maljkovic and M. Branica, *Ibid.* **38** (1966) 193.
- (4) D. Maljkovic, Ph.D. Thesis, Univ. Zagreb, 1976.
- (5) A.P. Bobylev and L.N. Komissarova, *Zh. Fiz. Khim.* **48** (1974) 145.
- (6) R.L. Erickson and R.L. McDonald, *J. Amer. Chem. Soc.* **88** (1966) 2099.
- (7) V.V. Fomin and A.F. Morgunov, *Zh. Neorg. Khim.* **5** (1960) 233.
- (8) H.N. Nachtrieb, G.J. Conway, *J. Amer. Chem. Soc.* **70** (1948) 3547.
- (9) C.G. Hass, *Extraction of Gold Chloride by Isopropyl Ether*, Dissertation, Part II, University of Chicago, Chicago, 1951.
- (10) E.D. Metzler, R.J. Myers, *J. Amer. Chem. Soc.* **72** (1950) 3776.
- (11) G. Schwarzenbach, H. Flaschka, *Complexometric Titrations*, Methuen, London, 1969.
- (12) H.A. Laurence, *Anal. Chem.* **24** (1952) 1496.

DISCUSSION

M. El Guindy: Have you examined the dependency of the Au system extraction upon free HCl? Would other ions such as Al³⁺, Rh³⁺ behave similarly to gold? Three-phase formation is most likely affected by HCl and metal ion activity – comment please.

D. Maljkovic: Our experiments confirm that the extraction and especially the appearance of the phases strongly depend on the initial concentration of HCl. This dependence varies by the changing of concentration of other components in the system, but it is not the object of this paper. Al³⁺ doesn't behave similarly to gold(III), and on Rh³⁺ we have no evidence. Three-phase formation in the discussed system is probably due to changes occurring in the composition of the hydro-solvated chlorometallic acid when parameters such as activities of hydrochloric acid and metal ion are varied. Activity of the solvent is also a very important parameter.

V. A. Mikhailov: The behaviour of iron (III) in system H₂O – HCl-diisopropyl ether-benzene is quite different from that of gold(III). How can one explain such a difference?

D. Maljkovic: Iron (III) and gold (III) at given conditions in the discussed system form a third phase, and their different behaviour is caused by the nature of the chlorometallic complex and their hydration and solvation properties.

A. S. Kertes: Offhand one would expect that ferric and gold chloride behave quite similarly in ether extraction systems. I understand that this is not the case in the complex systems you have been looking at. It has been noted in the literature that temperature is the single most important physical parameter governing the formation of a third liquid phase. I hope you will agree with that. My question is now, do you have any, even fragmentary, experimental information which could suggest that the difference in the phase behaviour between iron and gold-containing systems is essentially a temperature effect? What I would expect is, for example, that the ferric chloride system becomes, as you say, resistant to the increase in the water content the way the gold chloride system behaves, but at a slightly higher temperature.

D. Maljkovic: In addition to the results presented, we have some experimental data (D. Maljkovic, Ph.D. Thesis, Univ. of Zagreb, 1975) which show that both systems are uncommonly sensitive to temperature variations especially in the room temperature region. It can explain why the poor reproducibility of experiments sometimes is noticed. Because of very complex behaviour it is not possible to confirm that the difference in the phase behaviour of gold and iron systems is dependent on the above mentioned, as well as other similar systems, to clarify the temperature effect on formation of liquid phases in ether extraction systems.

REFERENCES

- (1) D. Maljkovic, M.Sc. Thesis, Univ. Zagreb, 1965.
- (2) D. Maljkovic and M. Branica, *Croat. Chem. Acta*, **38** (1966) 65.
- (3) D. Maljkovic and M. Branica, *Ibid.* **38** (1966) 193.
- (4) D. Maljkovic, Ph.D. Thesis, Univ. Zagreb, 1976.
- (5) A.P. Bobylev and L.N. Komissarova, *Zh. Fiz. Khim.* **48** (1974) 145.
- (6) R.L. Erickson and R.L. McDonald, *J. Amer. Chem. Soc.* **88** (1966) 2099.
- (7) V.V. Fomin and A.F. Morgunov, *Zh. Neorg. Khim.* **5** (1960) 233.
- (8) H.N. Nachtrieb, G.J. Conway, *J. Amer. Chem. Soc.* **70** (1948) 3547.
- (9) C.G. Hass, *Extraction of Gold Chloride by Isopropyl Ether*, Dissertation, Part II, University of Chicago, Chicago, 1951.
- (10) E.D. Metzler, R.J. Myers, *J. Amer. Chem. Soc.* **72** (1950) 3776.
- (11) G. Schwarzenbach, H. Flaschka, *Complexometric Titrations*, Methuen, London, 1969.
- (12) H.A. Laurence, *Anal. Chem.* **24** (1952) 1496.

DISCUSSION

M. El Guindy: Have you examined the dependency of the Au system extraction upon free HCl? Would other ions such as Al³, Rh³ behave similarly to gold? Three-phase formation is most likely affected by HCl and metal ion activity – comment please.

D. Maljkovic: Our experiments confirm that the extraction and especially the appearance of the phases strongly depend on the initial concentration of HCl. This dependence varies by the changing of concentration of other components in the system, but it is not the object of this paper. Al³ doesn't behave similarly to gold(III), and on Rh³ we have no evidence. Three-phase formation in the discussed system is probably due to changes occurring in the composition of the hydro-solvated chlorometallic acid when parameters such as activities of hydrochloric acid and metal ion are varied. Activity of the solvent is also a very important parameter.

V. A. Mikhailov: The behaviour of iron (III) in system H₂O – HCl-diisopropyl ether-benzene is quite different from that of gold(III). How can one explain such a difference?

D. Maljkovic: Iron (III) and gold (III) at given conditions in the discussed system form a third phase, and their different behaviour is caused by the nature of the chlorometallic complex and their hydration and solvation properties.

A. S. Kertes: Offhand one would expect that ferric and gold chloride behave quite similarly in ether extraction systems. I understand that this is not the case in the complex systems you have been looking at. It has been noted in the literature that temperature is the single most important physical parameter governing the formation of a third liquid phase. I hope you will agree with that. My question is now, do you have any, even fragmentary, experimental information which could suggest that the difference in the phase behaviour between iron and gold-containing systems is essentially a temperature effect? What I would expect is, for example, that the ferric chloride system becomes, as you say, resistant to the increase in the water content the way the gold chloride system behaves, but at a slightly higher temperature.

D. Maljkovic: In addition to the results presented, we have some experimental data (D. Maljkovic, Ph.D. Thesis, Univ. of Zagreb, 1975) which show that both systems are uncommonly sensitive to temperature variations especially in the room temperature region. It can explain why the poor reproducibility of experiments sometimes is noticed. Because of very complex behaviour it is not possible to confirm that the difference in the phase behaviour of gold and iron systems is dependent on the above mentioned, as well as other similar systems, to clarify the temperature effect on formation of liquid phases in ether extraction systems.

The Formation of a Third Phase in the Extraction of Pu(IV), U(IV) and Th(IV) Nitrates with Tributyl Phosphate in Alkane Diluents

Z. Kolarik,
Institute of Hot Chemistry,
Nuclear Research Centre,
Karlsruhe, Federal Republic of Germany

ABSTRACT

The formation of a third phase was studied in the system Pu(IV), U(IV) or Th(IV) nitrate - nitric acid - water - TBP - alkane diluent. The composition and density of the third phase were determined at various starting aqueous concentrations of the metal nitrate and nitric acid. The maximum concentration of Pu(IV), U(IV) or Th(IV) in the equilibrium organic phase at which still no third phase is formed was measured as a function of the nitric acid concentration in the equilibrium aqueous phase, the temperature, the molecular size and structure of the diluent, the equilibrium uranium(VI) concentration in the organic phase, the analytical concentration of TBP and the ageing of the third phase.

Introduction

NITRATES OF TETRAVALENT ELEMENTS are extracted by TBP in the form of solvates of the type $M(NO_3)_4 \cdot xTBP$, where $x = 2$ with $M = U(IV)^{(1)}$ and $Pu(IV)^{(2)}$ and may be 2, 3 or 4 with $M = Th^{(3-5)}$. The solvates exhibit a limited solubility in aliphatic hydrocarbons and separate at higher metal loadings as a second heavier organic phase. The appearance of a third phase in an extraction system would cause serious difficulties in a nuclear process and thus detailed information is desirable on the conditions under which an organic phase loaded with $M(IV)$ could split. Rather numerous papers deal with systems involving $Th(IV)^{(3,5-16)}$, but little is known about the formation of a third phase in systems with $Pu(IV)^{(2,8,10,17)}$ and no data are available in the current literature on systems with $U(IV)$. So the main aim of this work was to clarify the effect of important process variables like the nitric acid concentration, temperature, diluent composition, etc. on the formation of the $Pu(IV)$ and $U(IV)$ -containing third phase; some data on $Th(IV)$ were gained for comparison.

Experimental

An aqueous solution containing nitric acid and a $M(IV)$ nitrate was shaken with a TBP solution in a thermostated vessel for 10 - 15 min. ($Pu(IV)$ was in some cases present initially in the organic phase). The amount of $M(IV)$ was chosen so that a third phase was formed. If the properties of the third phase were to be studied, samples of all three phases were taken. If the maximum attainable concentration of $M(IV)$ in the organic phase was to be measured, a fresh TBP solution was added in 0.1 to 0.2 ml portions until the third phase disappeared. The shaking time between the addition of two successive portions of the TBP solution was 5 to 10 min. Samples of both phases were

then taken. The experiments with $U(IV)$ were performed in nitrogen atmospheres.

$U(IV)$, $Pu(IV)$ and $Th(IV)$ were determined by complexometric titration with xylenol orange as an indicator. Aqueous samples were diluted with water, acidified to pH 1 - 2 with nitric acid and titrated. Samples of the organic phase were pipetted into methanol and the metal was transferred, in a short stirring period, into the alcohol phase; then nitric acid was added to a concentration of $\sim 0.2M$, the solution was diluted five to six times with water and $M(IV)$ was titrated. Free nitric acid was determined by potentiometric alkalimetric titration after masking $M(IV)$ with a mixture of fluorides and oxalates.

Samples of the organic phase loaded with $U(IV)$ were analyzed immediately after the phase separation. A spectrophotometric measurement showed that $< 2\%$ $U(IV)$ is oxidized by nitric acid during 30 min even at an organic concentration of HNO_3 as high as $0.75M$. Mass balance of $U(IV)$ was made in each experiment and 94 - 100% of the $U(IV)$ amount taken was found.

A stock solution of uranium(IV) nitrate was prepared by electrolytic reduction of uranyl nitrate. The solution contained $0.2M$ hydrazinium nitrate and practically no free nitric acid and was stored in a dark bottle at $\sim 5^\circ C$. The concentration of $U(IV)$ decreased during several weeks from $1.54M$ to $1.51M$.

A stock solution of plutonium(IV) nitrate was provided by the experimental reprocessing plant WAK at Karlsruhe, Germany, and contained $0.85M$ $Pu(IV)$ and $6.5M$ nitric acid; the fraction of $Pu(VI)$ was $\sim 2\%$.

All chemicals were reagent grade with the exception of some diluents. Octomethyl butane (Rhone Poulenc) contained $\sim 90\%$ basic substance and $\sim 10\%$ other branched hydrocarbons; no appreciable content of oxygenated impurities or olefines was found by gas chromatographic and mass spectroscopic analyses.

Results and Discussion

Properties of the Third Phase

Two factors can influence the composition and density of the third phase, namely the equilibrium nitric acid concentration in the aqueous phase, C_H , and the number of the TBP moles per g-atom $M(IV)$ added to the system, r . Table 1 shows that only the value of r influences significantly the composition of the $Pu(IV)$ -containing third phase. Plots of the $Pu(IV)$ concentration in the third phase, \bar{C}'_{Pu} and the density of the phase vs. r imply that limiting values of $\bar{C}'_{Pu} = 1.13 M$ and $d = 1.315 g/cm^3$ would be reached at high r . This would correspond to the contents of $\sim 91 wt\%$ $Pu(IV)$ solvate, $\sim 1.6 wt\%$ nitric acid and 7 to 8 wt% water plus dodecane in the plutonium-saturated third phase. The actual composition was found to vary between 48 wt% $Pu(IV)$ solvate, 3 wt% HNO_3 and 49 wt% $H_2O +$ dodecane at $r = 0.22$ and 86 wt%

TABLE 1. The Concentrations of M(IV) (\bar{C}_M^I) and Nitric Acid (\bar{C}_H^I) in the Third Phase and its Density as Functions of the Equilibrium Aqueous HNO₃ Concentration, C_H , and the Number of TBP Moles Per One g-atom M(IV) in the Whole System, r , at 25.0°C.

M(IV)	C_H (M)	r	\bar{C}_M^I (M)	\bar{C}_H^I (M)	d (g/cm ³)	Diluent
Pu (IV)	31.4	0.39	0.820	0.58	1.249	<i>n</i> -Dodecane
	4.40	0.39	0.825	0.64	1.227	"
	4.65	0.39	0.835	0.80	1.202	"
	7.46	0.39	0.800	0.77	1.202	"
	2.62	0.068	0.214	—	—	<i>n</i> -Tetradecane
	1.71	0.22	0.498	0.53	1.062	<i>n</i> -Dodecane
	3.37	0.35	0.612	0.72	1.123	"
	4.77	0.54	0.997	0.74	1.252	"
	6.64	0.78	1.116	0.34	1.317	"
	0.85	0.30	0.514	0.31	1.110	"
U(IV)	1.45	0.30	0.586	0.36	1.163	"
	2.13	0.30	0.617	0.42	1.154	"
	3.40	0.30	0.686	0.65	1.204	"
	1.56	0.41	0.693	0.29	1.197	"
	1.56	0.59	0.752	0.26	1.234	"
	1.64	0.83	0.808	0.21	1.265	"

TABLE 2 The Concentrations of Th(IV) (\bar{C}_{Th}) and Nitric Acid (\bar{C}_H^I) in the Third Phase as Functions of the Equilibrium Aqueous HNO₃ Concentration, C_H , and the Number of TBP Moles per One g-atom Th in the Whole System, r , at 25.0°C. Diluent: a Mixture of *n*-alkanes (C_{10} to C_{13}).

C_H (M)	r	\bar{C}_{Th} (M)	\bar{C}_H^I (M)
0.96	0.68	0.619	0.20
1.95	0.68	0.686	0.36
2.90	0.68	0.706	0.49
4.60	0.68	0.784	0.68
0.94	0.52	0.423	0.21
0.93	0.55	0.435	0.21
0.85	0.62	0.531	0.20
4.42	0.27	0.382	0.76
4.49	0.34	0.493	0.78
4.57	0.48	0.617	0.72

Pu(IV) solvate, 1.6 wt% HNO₃ and ~12 wt% H₂O + dodecane at $r = 0.78$. It should be noticed that no extreme r value is needed for the formation of a third phase which has a higher density than the aqueous phase.

Both C_H and r play an important role in the formation of the U(IV) and Th(IV)-containing third phases (Tables 1 and 2). The plots of \bar{C}_U^I and the density of the U(IV)-containing third phase vs. r appear to tend to certain saturation values at high r , but they can be only very roughly estimated by extrapolation. The estimated \bar{C}_U^I and density at high r suggest that the U(IV) saturated third phase would contain only ~70 wt% U(IV) solvate. The actual composition of the U(IV)-containing third phase changes from 51 wt% U(IV) solvate, 2 wt% HNO₃ and 47 wt% H₂O + dodecane at $r = 0.30$ to 65 wt% U(IV) solvate, 1 wt% HNO₃ and 34 wt% H₂O + dodecane at $r = 0.83$, both at $C_H = (1.56 \pm 0.1)M$.

An attempt was made to obtain information on the Pu(IV) and U(IV) species in the third phase by spectroscopic measurements. The Pu(IV)-containing third phase exhibits a very high absorbance and its spectrum could properly be measured in the lower absorbance region only. The positions of the peaks seem to be the same and the positions of the minima clearly are the same as in the spectrum of an alkane solution of TBP moderately loaded

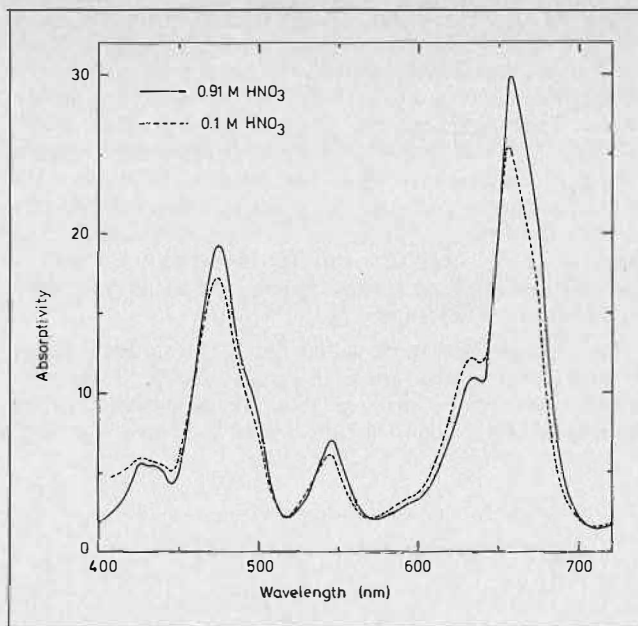


FIGURE 1. Absorption spectra of the U(IV)-containing third phase at two nitric acid concentrations.

with Pu(IV). No difference can be seen between the spectra of third phases formed at $C_H = 2M$ and $6M$. Our spectra of the third phase are practically identical with those of regular organic phase published earlier and ascribed to the solvate $Pu(NO_3)_4 \cdot 2TBP^{(8)}$. There is an absence of the 600 and 683 nm peaks assigned to Pu(IV) hexanitrate species⁽⁸⁾ as well as the 831 nm peak of Pu(IV). Spectra of two U(IV)-containing third phases differing in nitric acid concentration are shown in Figure 1. A variation of the acidity causes only minor changes of the U(IV) solvate spectrum. The shape of the spectrum and the influence of the nitric acid concentration on it are the same as in a regular organic phase moderately loaded with U(IV). Spectra of U(IV) in 20% TBP/kerosene published by Smirnov-Averin et al.⁽¹¹⁾ seem to be appreciably affected by the presence of U(VI) at < 500 nm.

The Solubility of M(IV) Solvates as a Function of the Aqueous Concentration of Nitric Acid and the Temperature

The main attention was paid in this work to the influence of different variables on the maximum attainable Pu(IV), U(IV) and Th(IV) organic concentrations, at which still no third phase is formed (henceforth called solubility of solvates and denoted S_M). The effect of nitric acid is shown in Figures 2 to 4 in the form of the dependences of $S_M = f(C_H)$ measured at different temperatures. We could confirm the fundamental difference between the course of the $S_{Pu} = f(C_H)$ and $S_{Th} = f(C_H)$ curves, which has been reported earlier⁽¹⁷⁾. However, we did not find any maximum on the S_{Pu} vs. C_H curve in our system with 30% TBP, while Mills and Logan⁽¹⁷⁾ have observed a maximum at 6 to 7 M nitric acid in a system with 20% TBP. The minima on the S_{Pu} vs. C_H curves at 1 to 2 M nitric acid have not yet been reported in the current literature. At organic concentrations of $< 0.2M$ (corresponding to $C_H < 2M$), nitric acid obviously salts the Pu(IV) solvate out of the organic phase. The increase of S_{Pu} with the nitric acid concentration at $C_H > 2M$ could imply specific interactions between the Pu(IV) solvate and nitric acid in the organic phase. However,

formation of Pu(IV) nitrate species other than a tetranitrate has been shown not to occur in 20% TBP/kerosene at an organic concentration of nitric acid up to 0.9M (corresponding to $C_H = 12.5M$)⁽⁸⁾ and this was corroborated by our spectrophotometric measurements in 30% TBP/dodecane. Thus if there is any specific interaction between the Pu(IV) solvate and nitric acid, it must be weak, of a molecular nature and does not influence the configuration of the coordination sphere of Pu^{4+} in the solvate. The increase of S_{Pu} with C_H can be observed also with a strongly branched dodecane diluent and at varying concentrations of TBP (Figure 5).

The thorium solvate is salted out of the organic phase by nitric acid in the whole C_H range studied (Figure 3). It may also play a role in that, at increasing C_H , the fraction of TBP bound to nitric acid increases, the con-

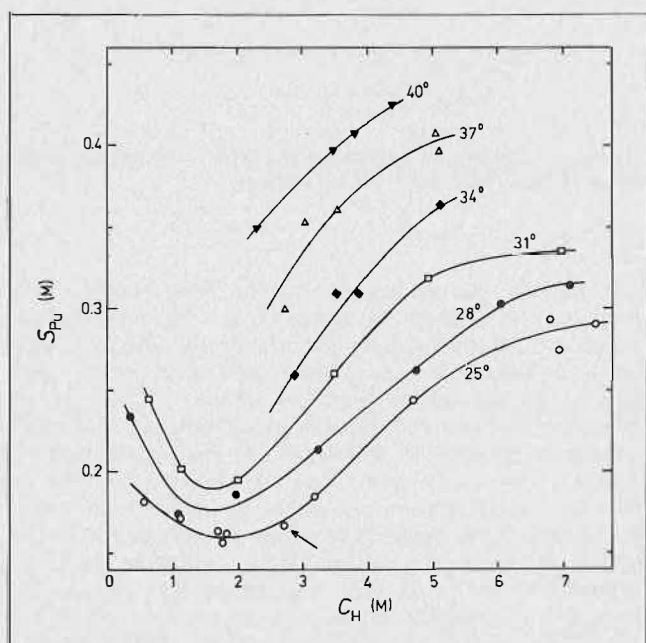


FIGURE 2. The solubility of the Pu(IV) solvate in the organic phase as a function of the aqueous equilibrium HNO_3 concentration at various temperatures. Starting organic phase 30% TBP in *n*-dodecane. Point with arrow: the third phase was aged for four days before redissolving.

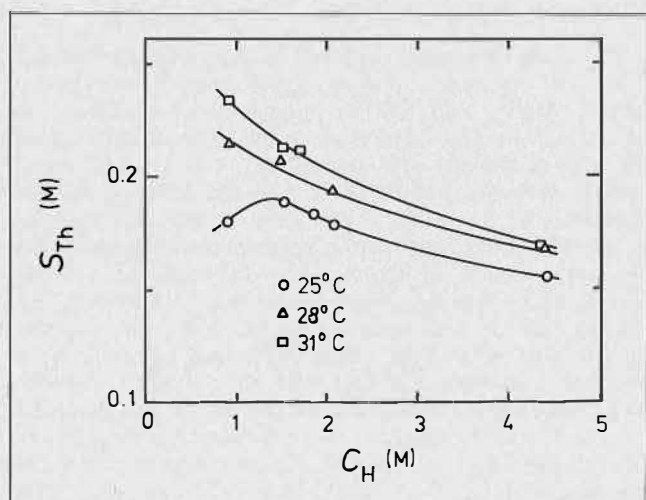


FIGURE 3. The solubility of the Th(IV) solvate in the organic phase as a function of the aqueous equilibrium concentration of HNO_3 at various temperatures. Starting organic phase 30% TBP in a mixture of *n*-alkanes (C_{10} to C_{13}).

centration of free TBP decreases and the solvate number x in $Th(NO_3)_4 \cdot xTBP$ is lowered. The solubility behaviour of the U(IV) solvate represents an intermediate between those of the Pu(IV) and Th(IV) solvates (Figure 4). The slight increase of the solubility with the nitric acid concentration at $C_H > 3M$ cannot be due to partial oxidation of U(IV) to U(VI) in the organic phase, because only U(V) and not U(VI) is determined by the complexometric titration.

The effect of temperature variations on the solubility of the solvates is also demonstrated in Figures 2 to 4. As shown in Figure 6, the $\log S_M$ vs. $1/T$ dependences are linear. It would not be justified to calculate the enthalpy change of the solution from the slopes of the lines, because they may include variations of activity coefficients, the free TBP concentration, etc. Nevertheless, a semi-quantitative evaluation of the temperature effect should be possible and it can be shown that the Gibbs free energy of the solution of the solvates in dodecane plays a subordinate role. For example the contribution of the entropy factor to the enthalpy of the solution of the Pu(IV) solvate in dodecane at 25°C appears to be as high as ~90% with concentrations expressed on the molar scale and ~80% on the mole fraction scale. The entropy must be highly positive ($> 100 J K^{-1} mole^{-1}$) and a considerable disorder must be produced in the structure of the long straight chain dodecane diluent.

The solubility of the Pu(IV) solvate is so strongly enhanced by a temperature increase that at 45°C the third phase was found under no conditions in a single equilibration of our stock Pu(IV) solution with 30% TBP in dodecane.

The Effect of Diluent on the Solubility of the Solvates

The very pronounced effect of the molecular size of *n*-alkane diluents on the solubility of the solvates is demonstrated in Figure 7. The sensitivity of the solvates toward diluent variations decreases in the same order as the sensitivity toward temperature changes, namely $Pu(IV) > U(IV) > Th(IV)$. An isomerization of the diluent molecule strongly influences the solubility of the Pu(IV) solvate, (compare the corresponding S_{Pu} vs. C_H curves for

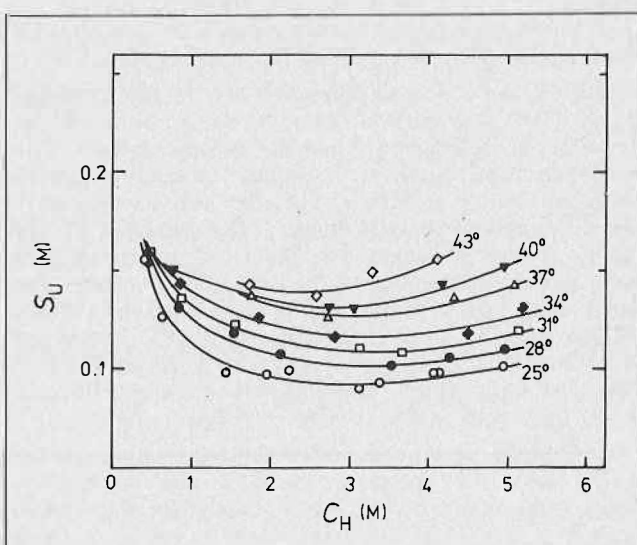


FIGURE 4. The solubility of the U(IV) solvate in the organic phase as a function of the aqueous equilibrium HNO_3 concentration at various temperatures. Starting organic phase 30% TBP in *n*-dodecane.

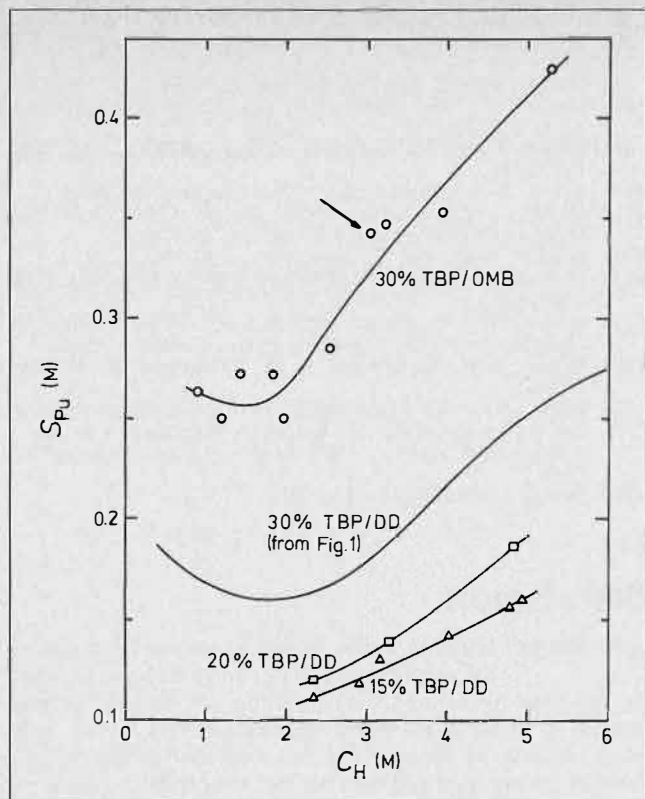


FIGURE 5. The solubility of the Pu(IV) solvate at 25.0°C in various starting organic phases as a function of the aqueous equilibrium HNO_3 concentration; DD — *n*-dodecane; OMB — octamethyl butane ("tripropylene"). Point with arrow: the third phase was aged three days before redissolving.

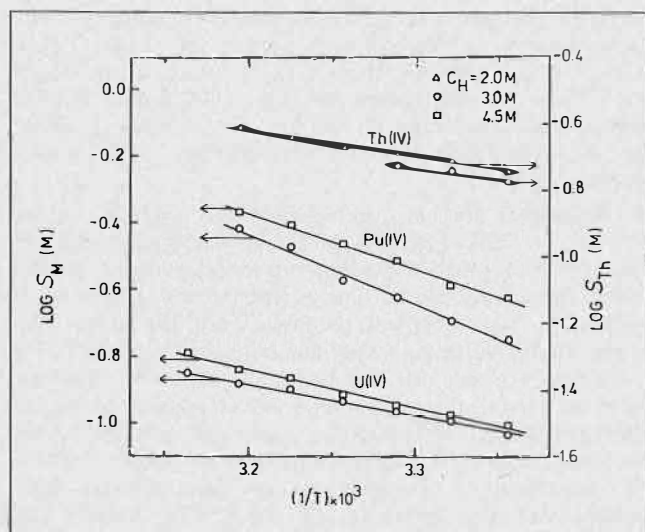


FIGURE 6. The $\log S_M$ vs. $1/T$ dependences at various aqueous equilibrium HNO_3 concentrations.

n-dodecane and highly branched octamethyl butane diluents in Figures 2 and 5). On the other hand, there is a moderate difference only between the S_{Th} value measured with 2,2,4-trimethyl pentane diluent and the S_{Th} value read for *n*-octane diluent on the corresponding line in Figure 7; and no difference was found between the S_{Th} values obtained with *n*-heptane and 3-methyl hexane diluents.

It is quite obvious that data on the third phase formation taken from different sources can be compared only

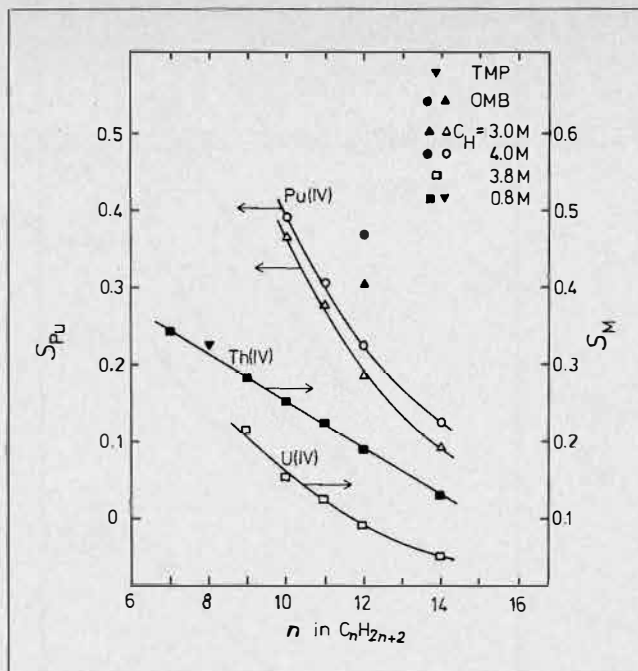


FIGURE 7. The solubility of the solvates in the organic phase as a function of the molecular size of *n*-alkane diluents. 25.0°C, 30% TBP. Points for 2,2,4-trimethyl pentane (TMP) and octamethyl butane (OMB) diluents are given for comparison.

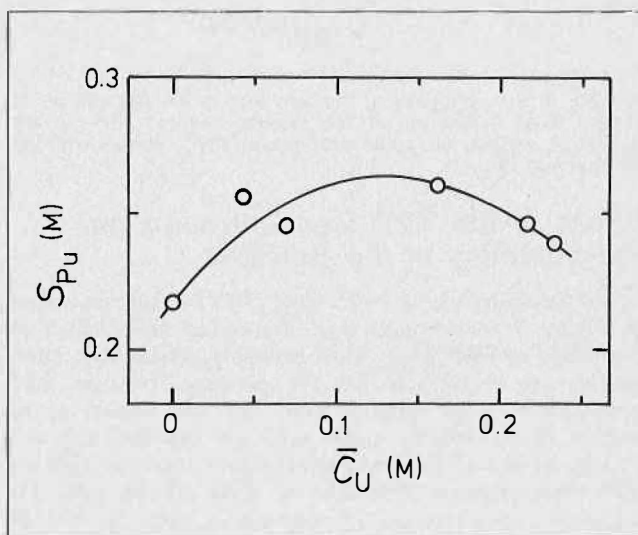


FIGURE 8. The solubility of the Pu(IV) solvate in the organic phase at 25.0°C as a function of the organic equilibrium U(VI) concentration. Aqueous equilibrium HNO_3 concentration 3 M. Starting organic phase 30% TBP in *n*-dodecane.

if they have been obtained with defined diluents. Results gained, e.g. with kerosene diluents of different composition, cannot be fully compared.

Effect of U(VI) on the Solubility of the Pu(IV) Solvate

The dependence of S_{Pu} on the organic uranium(VI) concentration has a maximum (Figure 8) and shows that the S_{Pu} value can be increased up to 1.2 times in extracting Pu(IV) with 30% TBP in dodecane from 4M nitric acid together with U(VI).

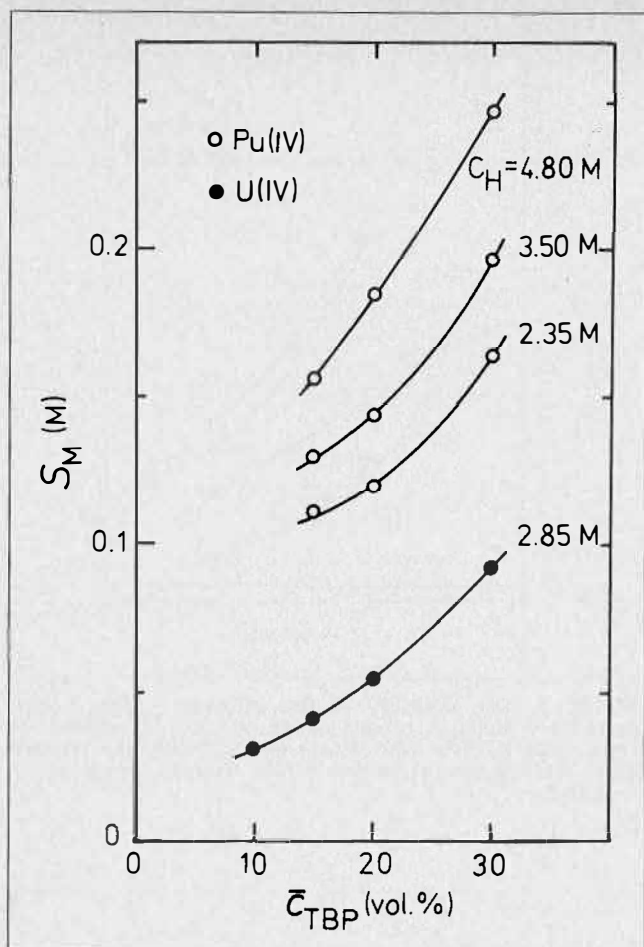


FIGURE 9. The solubility of the solvates in the organic phase at 25.0°C as a function of the starting organic TBP concentration at various aqueous equilibrium HNO_3 concentrations. n-Dodecane diluent.

Effect of the TBP Concentration on the Solubility of the Solvates

The solubility of the Pu(IV) and U(IV) solvates is shown in Figure 9 to decrease with decreasing analytical concentration of TBP, \bar{C}_{TBP} . Most probably, nonspecific interactions are responsible for the decrease, because third phases formed in systems with TBP are known to be soluble in moderately polar solvents and the effective polarity of the TBP/alkane solvent must increase with the TBP concentration. The S_{Pu} vs. \bar{C}_{TBP} curves valid for different C_{H} tend to reach a common S_{Pu} value of $\sim 0.1\text{M}$ at zero concentration of TBP, at which the organic concentration of nitric acid is very low at any C_{H} .

Effect of the Ageing of the Third Phase on its Solubility

Three to four days of ageing does not change the solubility of the Pu(IV)-containing third phase in the systems with n-dodecane and octamethyl butane (see points marked with an arrow in Figures 2 and 5).

REFERENCES

- (1) Smirnov-Averin, A.P., Kovalenko, G.S. and Krot, N.N., *Russ. J. Inorg. Chem.* 1963, 8, 1257.
- (2) Best, G.F., McKay, H.A.C. and Woodgate, P.R., *J. Inorg. Nucl. Chem.* 1957, 4, 315.
- (3) Hesford, E., McKay, H.A.C. and Scargill, D., *J. Inorg. Nucl. Chem.* 1957, 4, 321.
- (4) Madigan, D.C. and Catrall, R.W., *J. Inorg. Nucl. Chem.* 1961, 21, 334.

- (5) Savolainen, J.E., CF-52-2-113, 1952.
- (6) Ewing, R.A., Kiehl, S.J., Jr. and Bearse, A.E., BMI-955, 1954.
- (7) Chesne, A. and Regnaut, P., *Transl. AAEC/K-200*, 1958.
- (8) Healy, T.V. and McKay, H.A.C., *Trans. Faraday Soc.* 1956, 52, 633.
- (9) Siddall, T.H., III, *Ind. Eng. Chem.* 1959, 51, 41; DP-181, 1956.
- (10) Farell, M.S. and Goldrick, J.D., *AAEC/E 26*, 958.
- (11) Gresky, A.T., Bennett, M.R., Brandt, S.S., McDuffee, W.T. and Savolainen, J.E., ORNL-1367, 1952.
- (12) Schultz, W.W. and Voiland, E.E., HW-32417, 1954.
- (13) McKay, H.A.C., Naish, G.N. and Scargill, D., *AERE-C/R 1168*, 1953.
- (14) McKay, H.A.C., *Progr. Nucl. Energy, Series III, Process Chemistry, 1*, 122. Pergamon Press, London (1956).
- (15) Rozen, A.M., *Ekstratsiya 1*, 52. Gosatomizdat, Moscow (1962).
- (16) Mills, A.L. and Logan, W.R., *Proc. Int. Conf. Solvent Extraction Chemistry, Gothenburg, Sweden, 27 August - 1 September, 1966*, p. 322, North Holland, Amsterdam (1967).
- (17) Horner, D.E., ORNL-4724, 1971.

DISCUSSION

A.S. Kertes: Looking at the family of curves representing the solubility of U(IV) solvates as a function of aqueous nitric acid concentration at various temperatures, I think it is rather significant that at an acid concentration of about 0.4M the solubility of the solvate remains practically constant in the temperature range investigated, 25-43°C. This certainly is a quite unusual phenomenon, and I would like to have your interpretation. Doesn't that piece of evidence contradict your fundamental concept that third-phase formation is essentially due to nonspecific interactions? I should admit that some fifteen years ago we advocated the concept that third-phase formation is likely to be due to specific interactions in solvent extraction systems, leading to the formation of complex solvates which exhibit limited solubility in non-polar-diluents (*J. Inorg. Nucl. Chem.*, 25, 1531 (1963); *Can. J. Chem.*, 42, 878 (1964); *Third Intern. Conf. Peaceful Uses of Atomic Energy*, Vol. 10, p. 392, 1964; "Solvent Extraction Chemistry of Metals", MacMillan, London, pp. 377-401, 1966). We have not done any work on such systems since.

Z. Kolarik: I am not sure whether the solubility of the U(IV) solvate at $C_{\text{H}} = 0.4\text{M}$ can really be considered as practically temperature-independent. At this particular acidity of the aqueous phase, the curves of S_{U} vs. C_{H} are rather steep and the precision of the S_{U} measurement, attainable in our experimental procedure, makes the temperature effect difficult to be characterized. Anyway, at 0.4M HNO_3 , the temperature effect appears to be less pronounced than at higher C_{H} values and I regret having no interpretation for this phenomenon. As for the question of interactions, I of course, do not deny specific interactions like the formation of the U(IV); Pu(IV) and Th(IV) solvates in the system studied. Speaking about nonspecific interactions, I mean those between the solvates and the diluent, which are the reason for the limited solvate solubility.

G.M. Ritcey: In the system TBP-Zr- HNO_3 for treating high concentrated HNO_3 (8-10 m) for recovery and separation of Zr-Hf, would you consider the third phase found at saturation to be similar to the results you obtained with U,Pu,Th?

Z. Kolarik: Only qualitative data are available on the formation of a Zr-containing third phase and it is difficult to predict whether Zr behaves like Pu(IV), U(IV), or Th(IV).

Chapter 5

Mass Transfer

Sessions 4, 9 and 25
Panel Discussion



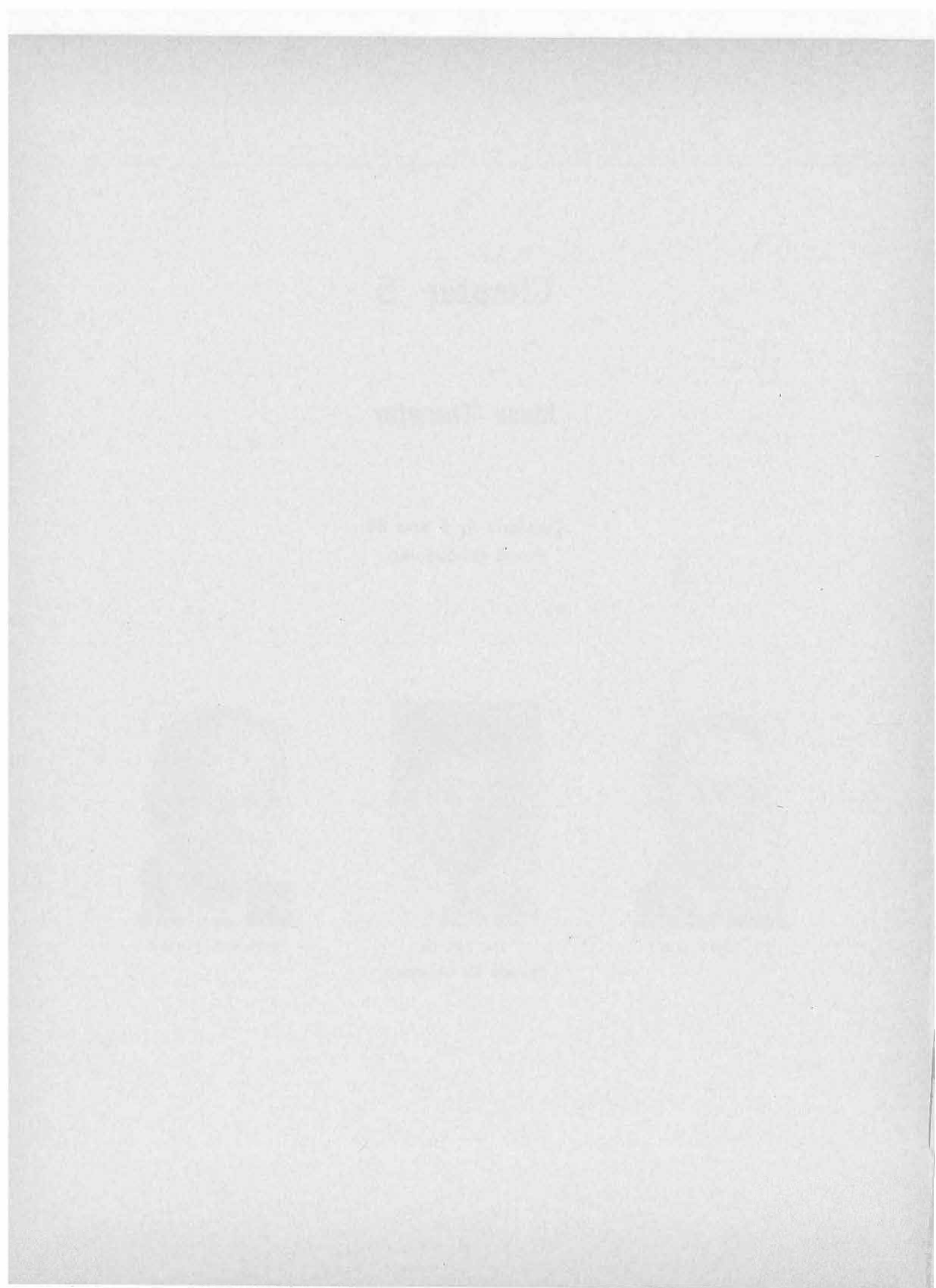
Dr. M.H.I. Baird



Dr. T.C. Lo
Session Co-Chairmen



Prof. A.S. Kertes



Aspects of the Kinetics and Mechanism of the Extraction of Copper with Hydroxyoximes

R. J. Whewell, M. A. Hughes and C. Hanson,
Schools of Chemical Engineering,
University of Bradford, UK

ABSTRACT

The importance of the organic phase concentration of oxime monomers, rather than the total oxime concentration, enables the differences between the results of various workers on the copper-oxime solvent extraction system to be reconciled. Study of the partition of oxime between organic and aqueous phases allows a reaction model to be established in which a rate-determining chemical reaction step is considered along with the diffusion behaviour in a narrow aqueous zone adjacent to the interface. The apparent dependence of the observed rate of extraction on the apparatus in which the rate is measured is explained through the diffusion processes in the organic phase close to the interface.

Introduction

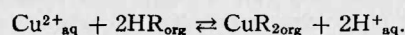
THE COMMERCIAL APPLICATION of solvent extraction to the recovery of metals has encouraged fundamental research on the equilibria and the kinetics of extraction reactions. Whereas the equilibria are readily measured and may be interpreted through the chemistry and the stoichiometry of the system, a study of reaction kinetics encompasses many problems to be solved before a clear picture emerges. Our particular interest is the reaction between hydroxyoximes in an organic diluent and the copper species in acidic aqueous phases.

Mass transfer, with reaction between two "immiscible" liquid phases has been studied in non-metal systems, such as the nitration and sulphonation of hydrocarbons^(1,2) and the hydrolysis of esters⁽³⁾. Although the interface must be important in such reactions, it has nevertheless been proved in these cases that reaction occurs in the bulk aqueous phase in a film adjacent to the organic phase. The properties of such an aqueous film cannot necessarily be assumed to be identical with those of the bulk phase. A dependence of rate on interfacial area cannot be held to prove a truly interfacial mechanism for the reaction, as the volume of a finite homogeneous interphase zone will similarly be dependent on interfacial area.

For the extraction of a metal by a chelating reaction, a series of steps can be envisaged:

1. diffusion of metal species from the aqueous phase to the interfacial region;
2. diffusion of extractant species from the organic phase to the interfacial region;
3. chemical reaction;
4. diffusion of the metal complex to the bulk organic phase; and
5. diffusion of any counterion, formerly attached to the extractant into the aqueous phase.

A trivial stoichiometric equation for such a reaction sequence involving copper and a weakly acidic hydroxyoxime reagent (HR) can be written:



The rate-controlling step in the kinetics might be any one (or more?) of the stages (1) to (5), and indeed might change during the course of an extraction or be dictated by the type of experiment chosen to investigate the kinetics.

As long ago as 1904, Nernst⁽⁴⁾ recognized that molecular diffusion of reacting molecules might be rate-controlling in a heterogeneous reaction. More recently, for the extraction of copper with 8-hydroxyquinoline, Rod⁽⁵⁾ reports that the kinetics are controlled by diffusion of reactant species to an aqueous zone close to the interface when concentrations of copper and extractant are very low in a constant interface cell of the Prochazka⁽⁶⁾ type.

A number of interpretations⁽⁷⁻¹⁰⁾ of the kinetics of two-phase metal chelation reactions have been proposed in terms of chemical rate equations originally developed for reactions in truly homogeneous media. However, any success of such analyses does not prove that the reaction occurs under homogeneous conditions. Indeed, many of these workers fail to consider the area of the interface separating the phases, shown by our early work⁽¹¹⁾ to be an important parameter in determining kinetics.

Our kinetic studies in Bradford have so far been concerned principally with the initial part of the extraction (i.e. into unloaded phases) and of stripping (i.e. into aqueous phases containing only sulphuric acid) and it is natural that our discussion should be restricted to these regimes.

Chemical Problems in the Study of Kinetics

Much of our research work on the copper-hydroxyoxime systems has been carried out under conditions as closely related as possible to those encountered on an operating solvent extraction plant. Since the extractants "as delivered" are impure chemicals, these studies show only the "trends" in system behaviour.

We have succeeded in preparing samples of purified oximes^(12,13) from commercial reagents LIX65N⁽¹⁴⁾, LIX-63⁽¹⁴⁾, SME529⁽¹⁵⁾, P17⁽¹⁶⁾ and P50⁽¹⁶⁾ with purities between 97% and 101% total oxime, based on nominal formula weights for the oximes. Some variations in purity from 100% might be expected in view of the existence of a distribution of side-chain lengths in some of the commercial reagents. It is evident, however, that the presence of impurities, even at low concentrations, can upset studies of interfacial behaviour; while our purification procedures may still be inadequate, there is no doubt that some samples previously produced by simple methods (such as column chromatography alone) are quite unsatisfactory in purity for close physico-chemical study.

Three particular chemical problems have become clear: (a) *Nonylphenol*⁽¹⁷⁾. The presence of an alkyl phenol impurity in all of the extractants as delivered was postulated to account for discrepancies between the results of different analytical methods applied to the reagents. Alkyl phenols are very difficult to separate from the hydroxyoximes but are somewhat more readily separated from the copper complexes.

The effect of nonylphenol on the initial rate of extraction of copper is shown by the single-drop experiment results in Figure 1. The range of concentration of nonylphenol covered is comparable with the range of contaminant concentrations in the reagents as delivered. Since varying concentrations of nonylphenol in the reagents give rise to varying degrees of kinetic depression, it is not possible to comment on the ordering of the oxime chemicals when nonylphenol is present in the experimental organic phases. There is undoubted interaction between nonylphenol and the oxime molecules and it is to be expected that interfacial properties will also be affected.

(b) *Oxime Isomerism*. Two isomers are known for the LIX65N oxime, of which the *syn* does not extract copper under acidic conditions. The *anti* and *syn* isomers have differing protonation constants and so can be differentiated in an analytical titration (unlike the *anti* isomer and nonylphenol). The results of single-drop experiments at a constant concentration of *anti* isomer and varying concentrations of *syn* isomer are shown in Figure 2; very

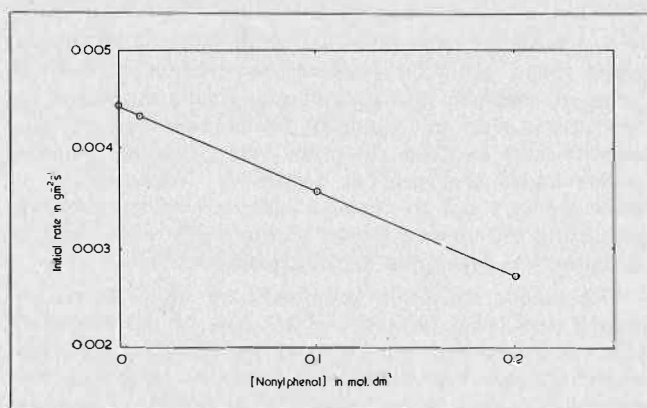


FIGURE 1. Effect of added nonylphenol on rate of extraction of copper from 2.64 g dm⁻³ copper sulphate, 1.76 g dm⁻³ sulphuric acid by 0.1 mol dm⁻³ purified LIX65N *anti* (with 0.0072 mol dm⁻³ LIX65N *syn*) in n-heptane at 28°C.

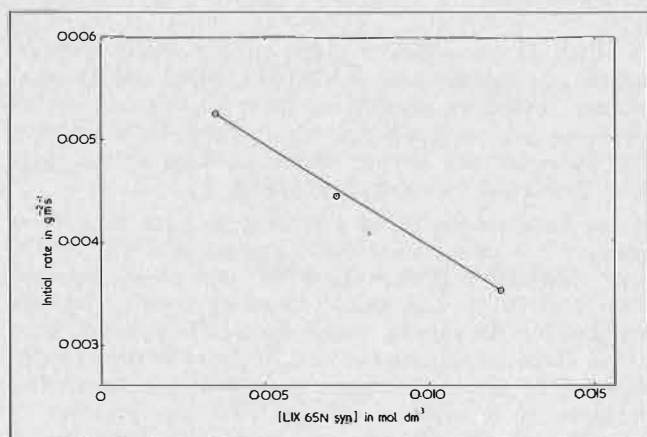


FIGURE 2. Effect of LIX65N *syn* isomer concentration on the rate of extraction of copper from 2.64 g dm⁻³ copper sulphate, 1.76 g dm⁻³ sulphuric acid by 0.1 mol dm⁻³ purified LIX65N *anti* in n-heptane at 28°C. The *syn* content of the commercial sample corresponds to about 0.015 mol dm⁻³ on this graph.

significant dependence of rate on "inactive" isomer content is found. We have shown that the *syn:anti* isomer ratio is unchanged over a period of many days at room temperature, even when the oxime is in dilute solution, but any changes in this ratio between samples can interfere with comparative testing.

(c) *Kerosene*. The presence of kerosene and of the above contaminants makes it difficult to establish a true scale of molarity for the extractant during use. We have found ultimate loading⁽¹⁸⁾ to be of most practical use in determining oxime concentrations but application of the results necessarily includes the assumption of a certain stoichiometry for the copper complex. Further, the presence in the reagent as delivered of kerosene, often of unspecified origin, interferes with studies such as that of the effect of the diluent on extraction equilibria and kinetics⁽¹⁹⁾.

The Species in Solution

The Aqueous Phase

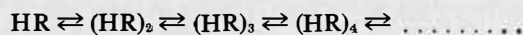
The aqueous phases used in our studies are mixtures of copper sulphate and sulphuric acid and so contain Cu²⁺, SO₄²⁻ and H⁺ ions, together with substantial concentrations of HSO₄⁻ and CuSO₄ complexes or ion pairs²⁰. Solutions used for stripping are more complicated.

The Organic Phase — Aggregation Properties of Purified Oximes

One author has suggested that the oxime extractants are principally dimeric in organic solution⁽²¹⁾, and another that no aggregation at all is detectable⁽²²⁾. We have carried out experiments on solutions of purified oximes in dry n-heptane, measuring changes in vapour pressure at 28°C with a Knauer osmometer, using naphthalene as calibrant.

The results are shown in Table 1; measured values of molecular weights at low (< 0.01 mol dm⁻³) concentrations of oxime were close to the nominal values quoted. The mean aggregation numbers are ratios of measured to nominal molecular weight. It is clear that aggregates larger than dimers are formed.

Measurements of mean aggregation numbers do not permit the calculation of oxime monomer concentrations without the assumption of the stoichiometry of the other species present. The results in Table I would support the use of only one parameter in any model relating mean aggregation number to concentration for each oxime. Models restricted to dimers and trimers are unsuccessful in modelling the results and higher species must be included. The best single parameter model is based on a mathematically infinite (but in practice restricted) series of complexes (HR)_n:



related by a single constant:

$$K_n = \frac{[(HR)_n]}{[(HR)_{n-1}][HR]}$$

Values of K_n and of the calculated monomer concentrations are shown in Table 2. In order to reinforce the point that these monomer concentrations are calculated on the basis of a feasible but not necessarily true hypothesis, the results of an alternative calculation, nearly as satisfactory, are also shown for comparison. This second calculation is based on a single monomer/tetramer equilibrium, with:

$$K_4 = \frac{[(HR)_4]}{[HR]^4}$$

TABLE 1. Vapour Phase Osmometry of Purified Oximes in Dry n-heptane

Purified Oxime	Nominal Mol. wt.	Temp. °C	Mean aggregation number at oxime concentrations (mol dm ⁻³)			
			0.05	0.10	0.15	0.20
LIX65N*	339.5	28	1.70	2.09	2.35	2.68
P17	353.5	28	1.58	1.87	2.13	2.36
SME529	277.4	28	1.46	1.69	1.85	2.04
P50	263.4	28	1.24	1.49	1.72	1.91
LIX65N	339.5	38*	1.41	1.79	2.10	2.38
P17	353.5	38*	1.40	1.65	1.86	2.08
P50	263.4	38*	1.11	1.34	1.53	1.72

*concentrations 0.0536, 0.1072, 0.1608, 0.2144 mol dm⁻³ including syn isomer content

†effective concentrations 1.6% lower than at 28°C owing to volume expansion

It is, however, unlikely in practice that tetramers will be formed without the intervening dimers and trimers.

Both methods of calculation clearly demonstrate that aggregation occurs in the order:



Effect of Temperature on Aggregation

Some values of mean aggregation numbers measured for oximes in n-heptane at 38°C are shown in Table 1. Significantly less aggregation than at 28°C is noted and the consequent increases in monomer concentration can be calculated.

Effect of the Diluent on Aggregation

The relationship between the "hydrogen bonding" capabilities of various diluents and the degree of extraction of copper from aqueous phases has been established⁽¹⁹⁾. In a later paper this dependence of copper equilibria on diluent will be quantified in terms of the influence of oxime solvation in reducing the favourability of both aggregation and copper extraction. The decrease in aggregation when hydrogen-bonding diluents are substituted for n-heptane is shown in Table 3; ethanol is a diluent of particularly high hydrogen-bonding ability and aggregation is seen to diminish practically.

Aggregation in Practical Solutions

Direct vapour phase measurements of commercial extractants in kerosene are not possible but the trends noted above can be used to infer likely interactions. Thus:

(i) Diluent molecules are in competition with other oxime molecules for oxime molecule bonding sites (Table 3). With both of these interactions through hydrogen bonding, the oxime aggregate in heptane will be bonded through the N or O donor atoms of the oxime, the donor ability of the unionised β -hydroxyoxime being small⁽¹³⁾. Commercial kerosenes such as Escaid 100⁽²³⁾ have components of greater hydrogen-bonding ability than heptane and will therefore reduce the extent of aggregation in the systems.

(ii) Nonylphenol has a very considerable hydrogen-bonding ability⁽¹⁹⁾ and by solvation-type interaction with oxime will further reduce aggregation. Thus some early VPO results obtained at 30°C in dry heptane with a partially purified LIX65N sample (containing nonylphenol) give $K_s \approx 13$, cf 21 on Table 2.

(iii) The copper complex, written simply as CuR_2 , exists at this stoichiometry under forcing conditions of copper extraction. There is to date no evidence on interactions which could give rise to species such as $\text{CuR}_2\cdot\text{HA}$ at low organic copper concentrations.

TABLE 2. Estimation of Monomer Concentrations at 28°C from Vapour Phase Osmometry Using Models

Oxime	K_s	Series Model Monomer concn. at total oxime concns. (mol dm ⁻³)			K_4	Tetramer Model Monomer concn. at total oxime concns. (mol dm ⁻³)		
		0.05	0.10	0.20		0.05	0.10	0.20
LIX65N	21	0.0186	0.0242	0.0294	20000	0.0239	0.0305	0.0378
P17	16	0.0215	0.0289	0.0360	7500	0.0289	0.0279	0.0475
SME529	11	0.0257	0.0362	0.0469	2500	0.0350	0.0478	0.0611
P50	8	0.0293	0.0430	0.0578	1100	0.0394	0.0562	0.0733

TABLE 3. Vapour Phase Osmometry of Purified LIX65N at 38°C in Varying Dry Diluents

Diluent	Mean aggregation no. at oxime concns.				K_s	K_4
	0.0528	0.1057	0.1585	0.2114		
n-heptane	1.41	1.79	2.10	2.38	14.5	5500
toluene	1.08	1.15	1.22	1.28	1.7	50
ethanol	1.03	1.08	1.11	1.13	0.7	10

TABLE 4. Interfacial Tension and Monomer Concentration from the Gibbs Plot (Wet n-heptane Diluent). Concentrations in mol dm⁻³.

Total P50 concn.	Interfacial tension in mN m ⁻¹	P50 monomer concns. calculated from			
		Line A	$K_4 = 1100$	Line B	$K_s = 8$
0.025	25.3	—	0.0236	0.0188	0.0182
0.05	22.0	0.0427	0.0394	0.0324	0.0293
0.10	19.9	0.0631	0.0562	0.0457	0.0430
0.20	18.6	0.0803	0.0733	0.0575	0.0578
0.40	17.7	0.0933	0.0915	0.0653	0.0720
0.80	16.8	0.1096	0.1118	0.0759	0.0844

(iv) The proton acceptor capability of LIX63⁽¹³⁾ makes likely some rather strong hydrogen bonding (with possible charge separation) between LIX 63 and other oxime molecules. We have also found evidence of marked self-aggregation of purified LIX63 in n-heptane even at 0.01 mol dm⁻³ oxime.

(v) At an aqueous interface, water molecules can form strong hydrogen bonds with oximes and effectively prevent aggregation of the type outlined above. Indeed, if in a bulk aqueous phase the oximes were to form micelles, then these micelles would be clusters with the hydrophilic groups of the oxime on the periphery, in contrast to the organic phase aggregates. It is therefore likely that in an interfacial reaction zone, the oxime will be present as a monomer, at a concentration in equilibrium with the organic bulk phase oxime monomer concentration.

Confirmation of Oxime Aggregation

It is useful to have confirmation that the monomer concentrations quoted in Table 2 are realistic. Gibbs plots have been reported by us⁽¹²⁾ and by others⁽²⁴⁾ to relate interfacial tension to oxime concentration; following Danesi⁽²⁵⁾ we have used the deviation of the Gibbs plot from linearity above 0.01 mol dm⁻³ oxime to estimate oxime monomer concentrations in solution. A typical plot (for purified P50 in n-heptane) is shown in Figure 3; the two lines A and B represent the limits of possible fit. Monomer concentrations (Table 4) calculated from the lines A and B correspond with the results from the tetramer model and series model respectively.

Partition of the Oximes Between Organic and Aqueous Phases

Studies of the solubility of purified oximes in aqueous phases using a turbidometric titration technique have been reported earlier⁽²⁶⁾; the values in $\mu\text{mol dm}^{-3}$ at pH 2 are P50 (6.8) > SME529 (3.0) > P17 (1.02) > LIX65N (0.97). These values are the aqueous oxime concentrations in equilibrium with precipitated pure oxime. Of greater interest are values of partition coefficients of oximes between the phases, which give concentrations of aqueous oxime at equilibrium with real organic solutions.

The results of a partition experiment with purified P50 in n-heptane at 25°C and an aqueous phase of ionic strength 0.1 mol dm⁻³ at pH are shown in Figure 4.

When aqueous phase P50 concentrations were plotted against total organic P50 concentration, a curve was obtained. However, Figure 4 shows a straight line relationship between aqueous oxime concentration and the organic monomer concentration, whether calculated from K_4 or K_s (Table 2). The partition coefficient P_{HR} is given by:

$$P_{HR} = [\text{P50 monomer}]_{\text{org}} [\text{P50}]_{\text{aq}}^{-1} = 1.08 \times 10^4 \text{ (series)} \text{ or } 1.38 \times 10^4 \text{ (tetramer)}$$

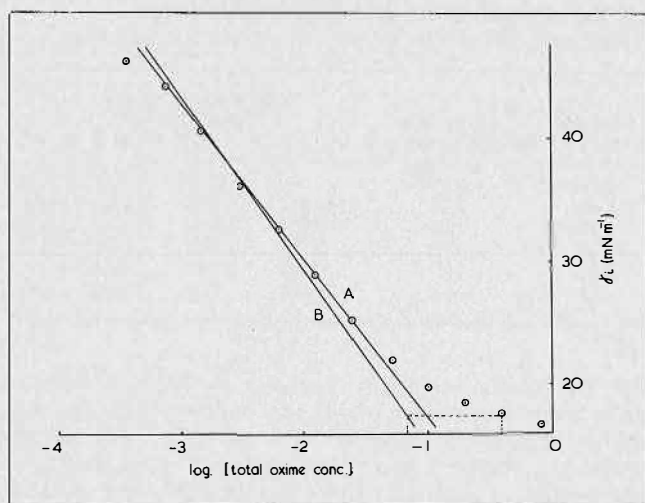


FIGURE 3. The Gibbs plot for purified P50 in n-heptane. The aqueous phase contained 1.75 g dm⁻³ sulphuric acid.

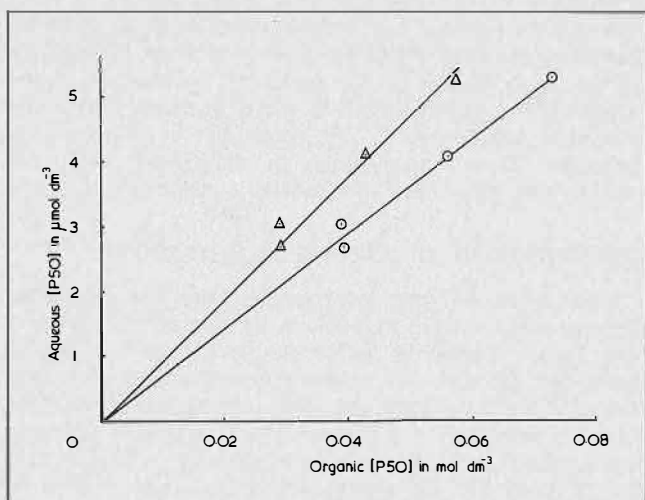


FIGURE 4. Measured aqueous concentration of P50 as a function of calculated organic P50 monomer concentration, using (○) $K_4 = 1100$, or (△) $K_s = 8$. Isotherms obtained at 25°C after 15 prewashes.

Unfortunately, the above method could be applied only to P50, for which the aqueous solubility is greatest. It is not expected that the series of oximes will have partition coefficients differing markedly from 10⁴, particularly since the trend of aqueous solubility is the reverse of that of aggregation.

It follows from Figure 4 that the oxime species present in the aqueous phase is the monomer, at least up to 80% of the maximum solubility of P50. It is therefore likely that for all of the oxime reagents an oxime monomer will be the important species in an aqueous environment.

Other Implications of Aggregation

Dependence of Rate of Extraction on Organic Extractant Concentration

Among the studies of extraction kinetics carried out, there is some disagreement on the dependence of rate on the bulk organic phase extractant concentration. Table 5 summarises the results as apparent "orders of reaction", rate = $k[\text{LIX65N}]^n$. This disagreement can now be explained qualitatively in terms of aggregation properties, on the basis that the oxime monomer is the reactive species.

High degrees of aggregation go with high concentrations of oxime and diluents of low hydrogen bonding ability. Increase in the total concentration of oxime has the least effect on monomer concentration (also on rate) when the degree of aggregation is greatest. Thus our studies⁽¹⁸⁾ were carried out at high (10-100 vol %) oxime concentrations in a diluent (Escaid 100) of the lowest hydrogen bonding ability of those on Table 5; the order of reaction with respect to total LIX65N concentration is apparently 0.5 and the increase in monomer concentration consequent upon an increase in total oxime concentration is small. On the other hand, studies in chloroform⁽²²⁾, a diluent of considerable hydrogen bonding ability⁽²⁹⁾, reflect the very low degree of aggregation and so show a greater apparent order of reaction. Table 5 as a whole suggests a true "order of reaction" of at least 1.5 for the oxime monomer but, unfortunately, this cannot be verified more quantitatively since aggregation parameters for unpurified oximes are unknown.

We have also found a linear dependence of initial rate on the total SME529 (as delivered) concentration in Escaid 100, under the same conditions as for the LIX65N experiments (Table 5); aggregation occurs in SME529 to an extent lower than in LIX65N (Table 2), and indeed the apparent order of the extraction reaction is higher.

Activation Energies

Table 5 also shows apparent activation energies determined from changes in rate of extraction with temperature. Provided that the studies are carried out in plant diluents, the apparent activation energy⁽²⁸⁾ will be the value useful for design purposes. However, decreases in the degree of aggregation with temperature increase (Table 1) result in increases in the effective monomer concentration. To determine a true activation energy, it is necessary to compare extraction by solutions of the same monomer concentration at different temperatures.

Again, our experiments⁽²⁸⁾ have the greatest dependence of monomer concentration on temperature and so give the greatest apparent activation energy. Other experiments^(9,22), under conditions leading to very little aggregation, will have a very slight dependence of monomer concentration on temperature and the activation energies are indeed lower. Since the low values are those most representative of the monomer reaction, the activation energies of dif-

TABLE 5. Dependence of Rate of Extraction on Total Oxime Concentration and on Temperature. Activation Energy in kJ mol^{-1} .

Ref.	Diluent	Oxime concn.	Apparent order (LIX65N)	Activation energy (LIX64N)
22	chloroform	low and comml.	1.0 - 1.3	19
9	toluene	low	1.0 - 1.3	15
27	xylene	intermediate	0.5	25
18, 28	Escaid 100	commercial	0.5	45

fusion (16 kJ mol^{-1} in aqueous and Escaid 100 media⁽²⁸⁾) are very similar to that of the extraction reaction.

Two single-drop experiments were carried out with purified LIX65N in n-heptane (Table 6). The second organic solution ($0.0535 \text{ mol dm}^{-3}$ LIX65N) was calculated to give at 38°C the same monomer concentration as 0.10 mol dm^{-3} LIX65N at 28°C ; the value 0.0535 is an average of 0.0495 and 0.0574 , being the concentrations calculated from the tetramer and series models respectively. An activation energy of 25 kJ mol^{-1} (of low precision) was obtained.

The activation energy of stripping is expected to be uncomplicated by the influence of temperature on the species distribution. In two sets of experiments using copper-preloaded solutions of LIX64N (as delivered) in Escaid, trends in the results (Table 7) show activation energies of 16 and 15 kJ mol^{-1} for phases C and D respectively. It is therefore certain that diffusion plays an important role in stripping as well as in extraction.

A Diffusion-Controlled Reaction

The combination of chemical rate dependences with a low activation energy in the copper-oxime system suggests that a mass-transfer-with-chemical-reaction model will be the most appropriate. Such models are frequently based on a reaction zone, adjacent to (rather than at) the interface. As a result, reaction-zone concentrations are generally defined by partition relationships rather than by surface chemical isotherms. The choice for the copper-oxime system is between an interfacial reaction and an aqueous reaction zone and no evidence so far presented enables the precise location of the reaction to be established. We have, however, shown that oximes can exist at finite concentrations in aqueous phases. Organic species will thus certainly penetrate the aqueous phase during the two-phase reaction, forming *de facto* an aqueous reaction zone; the depth of the zone represents a balance between the rate of reaction and the rate of transfer of the species concerned.

In the development below, we therefore use partition coefficients in order to obtain estimates of reaction-zone concentrations. It is clear that the environment in the reaction zone will be more akin to the aqueous bulk phase than to the organic phase but our treatment of the zone as a truly aqueous zone is undoubtedly a simplification. Charge effects at the interface have an influence on ionic concentrations close to the interface. A lack of other information, however, precludes any calculations other than those based on a wholly aqueous environment.

Attempts to deduce interfacial concentrations by surface chemical models, such as the Gibbs isotherm^(24,12), have not so far correlated rate phenomena. Our studies of purified oximes in hexane, for example, show the saturation of the interface with a monolayer of oxime at bulk oxime concentrations above $0.0005 \text{ mol dm}^{-3}$ and it is not clear how the dependence of rate on oxime concentration can be thus accommodated.

TABLE 6. Rising Drop Experiments with Purified LIX65N in n-heptane; Aqueous Phase 2.64 g dm^{-3} Copper, 1.76 g dm^{-3} Sulphuric Acid.

Oxime concn. (mol dm^{-3})	Temperature	Initial rate in $\text{g m}^{-2} \text{ s}^{-1}$
0.1000	28	0.0045
0.0535	38	0.0062

TABLE 7. Falling Drop Experiments with 2.53 ml dm^{-3} Sulphuric Acid and $20 \text{ vol. } \%$ LIX64N (as delivered) in Escaid 100, Preloaded with Copper

Temperature ($^\circ\text{C}$)	Initial rate in $\text{g m}^{-2} \text{ s}^{-1}$	
	Organic phase C	Organic phase D
18	0.0013	0.0017
28	0.0016	0.0020
38	0.0018	0.0025

The Rate-Determining Diffusional Process

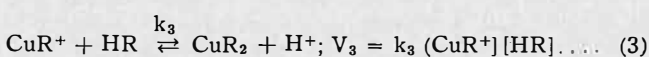
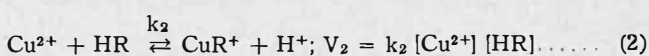
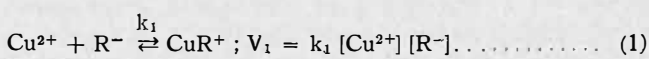
Diffusion processes may limit the supply of aqueous copper or of extractant, or may inhibit the removal of proton or of organic copper. The diffusivity of copper in aqueous phases has been studied⁽³⁰⁾, giving acid concentration-dependent values of around $D_{\text{Cu,aq}} = 0.5 \times 10^{-5} \text{ cm}^2 \text{ s}^{-1}$. Since $D_{\text{Cu,org}} \lesssim D_{\text{Cu,aq}}$, and since the presence of counter-diffusing protons would be expected to accelerate the diffusion of copper⁽³¹⁾, it seems unlikely that the diffusion of copper in the aqueous phase (or of the more rapidly diffusing proton) could be rate-determining.

Confirmation of the importance of organic-phase diffusion comes from observations made during the commissioning of our Prochazka⁽⁶⁾ cell with the copper-LIX64N system. Initial rates were about one-tenth of those in rising drop experiments and after 10-20 minutes a black band of copper complex (up to 1 mm thick) could be seen at the interface. As the band became visible, the rate of extraction continued to reduce, and it was evident that an organic phase diffusion process was limiting the rate.

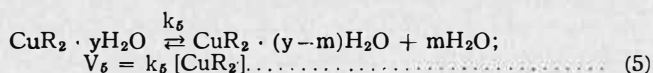
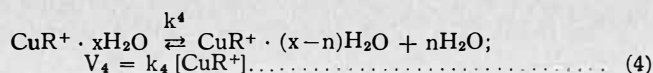
It is tempting to infer that it is the CuR_2 species (or an aggregated species including copper) that diffuses slowly. The nature of the species is unimportant, however, as the rate of transfer of copper from the reaction zone must be just half the rate of transfer of oxime to the zone and the nature of the diffusion process determines only the effective value of the diffusivity D to be inserted into a rate equation.

The Rate-Determining Reaction Step

There are three possible rate-determining reaction steps taking place in the zone, expressed in their simplest form as:



In addition, loss of water from complex species could be of importance:



In the above equations, HR represents the oxime extractant, k_1, k_2, k_3 are second order rate constants for forward reactions, k_4 and k_5 are first order rate constants for forward reactions and V_1 to V_5 are reaction velocities in $\text{mol dm}^{-3}\text{s}^{-1}$. The expected dependences of the initial rate from our work^(11,18) are:

$$\text{Initial rate} = k ([\text{Cu}^{2+}]/[\text{H}^+]^a)_{\text{aq}} [\text{HR monomer}]_{\text{org}}^b \dots \dots \dots (6)$$

with $a < 1$ and $b \geq 1.5$. Equation (2) can be dismissed immediately as rate determining since no inverse proton dependence would result.

Identification of the Rate Limiting Step

Comparing equations (1) and (2):

$$V_2/V_1 = k_2[\text{HR}]_{\text{aq}} [\text{R}^-]_{\text{aq}}^{-1} k_1^{-1} = [\text{H}^+]K_1^{\text{H}} k_2k_1^{-1} \dots \dots \dots (7)$$

where $K_1^{\text{H}} = [\text{HR}]_{\text{aq}} [\text{H}^+]_{\text{aq}}^{-1} [\text{R}^-]_{\text{aq}}^{-1} \approx 10^{9.7}$ from ref. 13 or $\approx 10^8$ under interfacial conditions⁽¹²⁾. At $[\text{H}^+] = 0.01 \text{ mol dm}^{-3}$ it is therefore necessary to suggest that $k_1 > 10^6 k_2$ if (1) is to be of major importance. This difference is unlikely; a study of the nickel-8-hydroxyquinoline system⁽¹⁰⁾ shows that $k_1 = 150k_2$ (provided that the authors' explanation is correct) and that both reactions (1) and (2) proceed simultaneously. If both reactions proceed in the copper-oxime systems, route (1) will be of minor importance in extractions from acidic liquors but may assume a more important role in ammoniacal systems.

Comparing equations (2) and (3):

$$V_3/V_2 = [\text{CuR}^+]_{\text{aq}} [\text{Cu}^{2+}]^{-1} = [\text{R}^-]_{\text{aq}} K_1 \dots \dots \dots (8)$$

where $K_1 = [\text{CuA}^+]_{\text{aq}} [\text{Cu}^{2+}]_{\text{aq}}^{-1} [\text{R}^-]_{\text{aq}}^{-1}$, and $k_2 \approx k_3 \approx 10^8$, the value being intermediate between that of 2×10^7 for copper-phenanthroline⁽³²⁾ at the lower temperature of 11°C and the diffusion limit⁽³³⁾ calculated for species of diffusivity $0.5 \times 10^{-5} \text{ cm}^2\text{s}^{-1}$ as $9 \times 10^9 \text{ dm}^3\text{mol}^{-1}\text{s}^{-1}$. As discussed later, $[\text{CuR}^+] \ll [\text{Cu}^{2+}]$ and $V_3 < V_2$ for the copper-oxime system.

The dehydration reactions (4) and (5) can be assigned values of k_4 and k_5 equal⁽³²⁾ to that quoted⁽³⁴⁾ as $2 \times 10^8 \text{ s}^{-1}$ for the hexaquo-copper(II) ion. With $k_3/k_4 = 0.5$, we therefore obtain:

$$V_3/V_4 = 0.5 [\text{HR}]_{\text{aq}} \dots \dots \dots (9)$$

and since the aqueous solubilities of the oximes are close to $10^{-6} \text{ mol dm}^{-3}$, it is clear that the dehydration reaction (4) is very much faster than the reaction step (3). Reaction (4) has nevertheless been suggested by others to be rate-determining in copper-oxime systems.

It remains to consider reaction (5). With $k_3/k_5 = 0.5$:

$$V_3/V_5 = 0.5 [\text{CuR}^+]_{\text{aq}} [\text{HR}]_{\text{aq}} [\text{CuR}_2]_{\text{aq}}^{-1} \dots \dots \dots (10)$$

Estimation of the right hand side of (10), from species concentrations discussed in the next section, shows that V_5 is at least $1000V_3$ and that this dehydration reaction is also fast.

It is therefore concluded that the rate-determining step is equation (3); in choosing (3) we concur with Fleming⁽²²⁾ but not necessarily with his suggested interfacial complex. The chosen rate equation is therefore:

$$\text{Rate} = k_3 [\text{CuR}^+]_{\text{aq}} [\text{HR}]_{\text{aq}} = k [\text{Cu}^{2+}] [\text{HR}]_{\text{aq}}^2 [\text{H}^+]^{-1} \dots \dots (11)$$

Influences on the Rate-Determining Step

The basis of equation (11) is that the ratio V_3/V_2 (equation 8) is small. For a metal M and an extractant HA:

$$\frac{[\text{MA}^+]_{\text{aq}}}{[\text{M}^{2+}]_{\text{aq}}} = [\text{A}^-]_{\text{aq}} K_1 = \frac{[\text{HA}]_{\text{org}} K_1}{[\text{H}^+]_{\text{aq}} k_1^{\text{H}} P_{\text{HA}}}$$

where $P_{\text{HA}} = [\text{HA}]_{\text{org}} [\text{HA}]_{\text{aq}}^{-1}$ and $[\text{HA}]_{\text{org}}$ refers to the organic monomer concentration. In the case of the copper-oxime systems, assuming equilibrium conditions with $[\text{HA}]_{\text{org}} = 0.03 \text{ mol dm}^{-3}$, $[\text{H}^+] = 0.01 \text{ mol dm}^{-3}$ and $P_{\text{HA}} \approx 10^4$, $K_1^{\text{H}} = 10^{9.7}$:

$$\text{ratio } \frac{V_3}{V_2} = \frac{0.03 \times K_1}{0.01 \times 10^{9.7} \times 10^4} = 10^{-13.2} K_1 \ll 1$$

The value of V_3/V_2 expresses the relative importance of reactions (2) and (3) in determining the rate; low values of V_3/V_2 are given by low aqueous solubility of the extractant (high P_{HA}), low aqueous pH value (high $[\text{H}^+]$) and low values of k_1/k_1^{H} (low preference of extractant for metal over proton). Thus extractants of greater solubility than the oximes, such as 8-hydroxyquinoline⁽⁵⁾ and dithizone^(8,35) may show increased influence of rate-determining steps associated with the formation of the first complex rather than the second.

When extraction by the various commercially available hydroxyoxime reagents is compared, however, it is not in the value of $P_{\text{HA}}K_1^{\text{H}}$ that the reason for the variations lies. These differences (particularly between P50 and the other oximes) can be ascribed to (a) differences in the degree of aggregation, resulting in different values of HR_{org} for given total oxime concentrations, and (b) differences in the diffusivity values appropriate to the region close to the interface.

A "Maximum" Chemical Rate

If one could achieve a situation in which diffusion were unimportant, then the "maximum" rate could be estimated from the above chemistry. It is assumed that the reactions are sufficiently fast for the concentrations of reagents in the reaction zone to be close to their equilibrium values. Since the maximum aqueous solubility of the CuR_2 complex⁽²⁶⁾ is $0.13 \mu\text{mol dm}^{-3}$, this sets an upper limit of aqueous $[\text{CuR}_2]$ beyond which copper would be transferred to the organic phase. If the reaction zone were to contain CuR_2 at this limiting concentration, then the concentration of CuR^+ will be about $216 \mu\text{mol dm}^{-3}$, for a total aqueous copper ion concentration of 0.04 mol dm^{-3} and $K_1 = 9K_2$ ($K_n = [\text{CuR}_n]_{\text{aq}} [\text{CuR}_{n-1}]_{\text{aq}}^{-1} [\text{R}^-]^{-1}$). The ratio $K_1/K_2 = 9$ is based on values for other copper complex systems, notably copper 8-hydroxyquinolate⁽³⁰⁾. If the oxime monomer (maximum solubility $0.97 \mu\text{mol dm}^{-3}$ for LIX65N) is present at a partition equilibrium value of, say, $0.5 \mu\text{mol dm}^{-3}$, then the chemical rate (equation 11) would be approximately: rate = $10^8 \times 216 \times 10^{-6} \times 0.5 \times 10^{-6} = 1.08 \times 10^{-2} \text{ mol dm}^{-3}\text{s}^{-1}$.

If the "maximum" rate for our standard phases were $10^{-4} \text{ mol m}^{-2}\text{s}^{-1}$, then this would be compatible with the reaction occurring in a zone of depth $10 \mu\text{m}$ extending into the aqueous phase from the interface. Such a zone depth is not unrealistic by comparison with the expected magnitude of the stagnant layer surrounding a drop.

Mass Transfer with Chemical Reaction

The limiting rate estimated above cannot truly represent the events in a system partially governed by the diffusion of extractant species. As a first step, the reaction in the

zone can be treated by Astarita's equation⁽³⁷⁾:

$$\bar{R}_A = [2D_A \int_{[A]_b}^{[A]_i} r(A) d[A]]^{0.5} \dots \dots \dots (12)$$

The preliminary application of this equation to the extraction of metals has been outlined⁽³⁸⁾; for the purposes of this paper, \bar{R}_A is the rate of mass transfer per unit interfacial area of the HR monomer, D_A is the effective diffusivity of the monomer in the aqueous reaction zone, $r(A)$ is the rate equation (11), and $[A]_i$, $[A]_b$ are the interfacial and bulk aqueous concentrations of HR.

Following the derivation in ref. 38, but neglecting from the start the reverse reaction (as we are concerned with initial rates):

$$\bar{R}_{HR} = [2D_{HR} \int_{[HR]_b}^{[HR]_i} \frac{k}{[HR]} [Cu^{2+}] [HR]_{aq}^2 [H^+]^{-1} d[HR]]^{0.5}$$

$$[2D_{HR} k [Cu^{2+}] [H^+]^{-1} ([HR]_i^3 - [HR]_b^3) / 3]^{0.5},$$

or, with $[HR]_b^3 \approx 0$, and the limiting aqueous concentration of HR close to the interface, $[HR]_i$, related to $[HR]_{org}$ (the organic monomer concentration) by a partition coefficient P_{HR} :

$$\bar{R}_{HR} = ([HR]_{org} / P_{HR})^{1.5} ([Cu^{2+}] / [H^+])^{0.5} (2D_{HR} k / 3)^{0.5} \dots \dots (13)$$

Equation (13) may be compared with equation (6), and "orders of reaction" $a = 0.5$, $b = 1.5$ are seen to be reasonable in the light of the experimental findings. Predicted rates of mass transfer are correct to an order of magnitude.

Organic Phase Diffusion

Equation (13) above describes the main features of the extraction of copper, and shows how rates obtained by a single experimental method (the rising drop experiment) may be related to bulk phase concentrations. In particular, the equation shows how the orders of reaction in the simple chemical equation (6) are modified by the influence of diffusion on a fast reaction in an aqueous zone. Equation (13) does not, however, account for differences observed when the rates of extraction are obtained by different experimental methods and does not predict the build-up of organic phase copper complex near to the interface during a Prochazka cell experiment.

The appropriate modification to equation (13) is the replacement of the term $[HR]_{org} / P_{HR}$. It was assumed above that this ratio gives the limiting zone concentration of HR close to the interface but if the organic interfacial concentration of HR cannot be equated to the bulk concentration, then the ratio is more properly expressed as $[HR]_{org,int} / P_{HR}$. The concentrations $[HR]_{org}$ and $[HR]_{org,int}$ can be related by simple diffusion expressions such as:

$$Flux_{HR} (= \bar{R}_{HZ}) = \frac{D_{HR,org}}{\delta} ([HR]_{org} - [HR]_{org,int}) \dots \dots (14)$$

$$Flux_{CuR_2} = \frac{D_{CuR_2,org}}{\delta} ([CuR_2]_{org,int} - [CuR_2]_{org}) \dots \dots (15)$$

where $D_{HR,org}$ and $D_{CuR_2,org}$ are effective molecular + eddy diffusivities in the organic phase region considered (unlike D_{HR} above, which refers to an aqueous environment) and δ is the distance over which diffusion takes place. It is clear that good mixing in the organic phase gives low values of δ and results in a small difference between $[HR]_{org}$ and $[HR]_{org,int}$. As mixing becomes poorer, so δ increases and D decreases, $[HR]_{org,int}$ falls below $[HR]_{org}$ and the rate of extraction decreases.

Discussion

The model contains three major factors:

$[HR]_{org,int} / P_{HR}$; depends on oxime, diluent and apparatus.
 $[Cu^{2+}] / [H^+]$; depends only on the aqueous phase concentrations.

$2D_{HR} k / 3$; depends only on the oxime in use.

The first factor is of the greatest interest; the dependence on the method chosen to study kinetics can be illustrated:

(i) The batch stirred tank. Calculation of the interfacial area generated, based on rising drop rates of extraction, gives estimates which do not correlate with the variations of drop size with agitation. A high value of $D_{HR,org}$ and a low value of δ would be given by the considerable turbulence in the tank; drop coalescence and redispersion may also effectively reduce δ .

(ii) With rising drop experiments, there is sufficient internal circulation in the organic drop to provide stirring and to keep δ low. There is a small reduction in rate when the phases are inverted⁽¹¹⁾.

(iii) For a stirred cell in which a magnetic stirrer bar is supported close to the interface to ensure gentle agitation of the organic interfacial region, rates of mass transfer of half the rising drop values have been achieved. The rate is determined in part by the stirring speed but stirring as effective as internal circulation in the single drops cannot be achieved without the creation of unwanted dispersion.

(iv) In our Prochazka⁽⁶⁾ cell, initial rates one-tenth of the rising drop rates were obtained. Stirring is here removed to some distance from the interface and concentration of organic copper close to the interface is noted. As this localised organic copper concentration builds up, so the rate of extraction decreases, showing the effect of bulky and possibly interacting CuR_2 molecules on the diffusivity and the concentration gradient of the oxime.

(v) In the Hahn static cell⁽³⁹⁾, the conditions are set to ensure only molecular diffusion, and the several days required to achieve satisfactory concentration gradients indicate the extreme slowness of the reaction.

We note with interest that the rates of mass transfer measured by Fleming⁽²²⁾ in a Lewis-type cell are (allowing for the change in diluent) an order of magnitude lower than our single drop measurements, in accordance with the comments in (iv) above. The experiments (ii)-(v) are all diffusion-controlled, at least in part, and there is no reason to suggest that (i) is not also treatable by a mass transfer with chemical reaction model. Equation (13) is unlikely to describe experiment (v) in which diffusion will be the sole factor.

During the final drafting of this paper, a publication by Hummelstedt *et al.*⁽⁴⁰⁾ has come to our notice, in which the aggregation properties of the LIX65N *anti* isomer are studied and equation (4) is said to be rate-determining. In our treatment above we have given fuller consideration to aggregation, including estimation of actual monomer concentrations and the demonstration that the monomer concentrations cannot be assumed to be small by comparison with the aggregate concentrations. Our discussion shows why we are currently unable to accept (4) as rate-determining and highlights the importance of diffusion processes in the mechanism.

Acknowledgments

The authors wish to thank Nchanga Consolidated Copper Mines of Zambia for the financial support of the work described in this paper, and their co-workers, in particular

Dr. J.S. Preston who is now at Murdoch University, Western Australia.

LIST OF SYMBOLS

Symbols are defined in detail in the text.

D	= Diffusivity
k_n	= First or second order rate constants
K_1^H	= Proton association constant
K_1, K_2	= Stepwise copper complex equilibrium constants
K_a, K_b	= Organic phase oxime aggregation constants
P	= Partition coefficient
\bar{r}	= Rate of mass transfer per unit interfacial area
V_a	= Notional reaction velocities
γ_i	= Interfacial tension

REFERENCES

- (1) Hanson, C., Marsland, J.G. and Wilson, G., Chem. Eng. Sci. 1971, 26, 1513. Giles, G.W., Hanson, C. and Ismail, H.A.M. in "Advances in Industrial Nitration Chemistry." ed. Albright, L.F. and Hanson, C.: Symposium Series, American Chemical Society, 1976, ch. 12.
- (2) Chaudhry, M.S.K., MSc thesis, University of Bradford, 1970.
- (3) Viallard, A., Chem. Eng. Sci. 1961, 14, 183.
- (4) Nernst, W., Z. Phys. Chem. 1904, 47, 52.
- (5) Rod, V. and Rychnovsky, L., Proc. 5th CHISA Congress, Prague, 1975, paper I 1.7.
- (6) Prochazka, J. and Bulicka, J., Proc. Int. Solvent Extraction Conf. (ISEC '71), Society of Chemical Industry, London, 1971, vol. II, 823.
- (7) Irving, H., Rossotti, F.J.C. and Williams, R.J.P., J. Chem. Soc. 1955, 1906.
- (8) McClellan, B.E. and Freiser, H., Analyt. Chem. 1964, 36, 2262.
- (9) Flett, D.S., Okuhara, D.N. and Spink, D.R., J. Inorg. Nucl. Chem. 1973, 35, 2471.
- (10) Yamada, K., Nakagawa, K., Haraguchi, K. and Ito, S., Nippon Kagaku Kaishiz, 1975, 294.
- (11) Whewell, R.J., Hughes, M.A. and Hanson, C., J. Inorg. Nucl. Chem. 1975, 37, 2303.
- (12) Al Diwan, T.A.B., Hughes, M.A. and Whewell, R.J., J. Inorg. Nucl. Chem. 1977, 39, 0000.
- (13) Preston, J.S. and Whewell, R.J., J. Inorg. Nucl. Chem. 1977, 39, 0000.
- (14) General Mills Inc.
- (15) Shell Chemicals Ltd.
- (16) Acorga Ltd.
- (17) Hanson, C., Hughes, M.A., Preston, J.S. and Whewell, R.J., J. Inorg. Nucl. Chem. 1976, 38, 2306.
- (18) Whewell, R.J., Hughes, M.A. and Hanson, C., J. Inorg. Nucl. Chem. 1976, 38, 2071.
- (19) Whewell, R.J., Hughes, M.A. and Hanson, C. in "Advances in Extractive Metallurgy 1977". Ed. Jones, M.J., Institution of Mining and Metallurgy, London, 1977, p. 21.
- (20) Whewell, R.J. and Hughes, M.A., J. Inorg. Nucl. Chem. 1976, 38, 180.
- (21) Price, R. and Tumilty, J.A., IChemE Symp Ser. 42, 1975, paper 18.
- (22) Fleming, C.A., National Institute for Metallurgy Report 1793, Johannesburg, 1976.
- (23) Essochem Europe Inc.
- (24) Dobson, S. and van der Zeeuw, A.J., Chem. Ind. 1976, 175.
- (25) Chiarizia, R., Danesi, P.R., D'Alessandro, G. and Scuppa, B., J. Inorg. Nucl. Chem. 1976, 38, 1367.
- (26) Hughes, M.A., Preston, J.S. and Whewell, R.J., submitted to Anal. Chim. Acta.
- (27) Atwood, R.L., Thatcher, D.N. and Miller, J.D., Met. Trans. (AIME) 1975, 6B, 465.
- (28) Hughes, M.A., Preston, J.S. and Whewell, R.J., J. Inorg. Nucl. Chem. 1976, 38, 2067.
- (29) Hansen, C. and Beerbower, A. in "Kirk-Othmer's Encyclopaedia of Chemical Technology." 971, supp. vol. p. 889.
- (30) Hughes, M.A., Middlebrook, P.D. and Whewell, R.J., J. Inorg. Nucl. Chem. 1977, 39, 0000.
- (31) Vinograd, J.R. and McBain, J.W., J. Amer. Chem. Soc. 1941, 63, 2008.
- (32) Mark, H.B. and Rechnitz, G.A., "Kinetics in Analytical Chemistry." Interscience, New York, 1968.
- (33) Laidler, K.J., "Chemical Kinetics." McGraw-Hill, New York, 1965.
- (34) Eigen, M., Pure Appl. Chem. 1963, 6, 97.
- (35) Hönaker, C.B. and Freiser, H., J. Phys. Chem. 1962, 66, 127.
- (36) "Stability Constants of Metal Ion Complexes." Spec. publ. no. 17, The Chemical Society, London, 1964.
- (37) Astarita, G., "Mass Transfer with Chemical Reaction." Elsevier, 1967.
- (38) Hanson, C., Hughes, M.A. and Marsland, J.G., Proc. Int. Conf. Solvent Extraction (ISEC '74), Society of Chemical Industry, London, 1974, III, 2401.
- (39) Hahn, H.T., USAEC Report HW-32626, 1954.
- (40) Hummelstedt, L., Tammi, T., Paatero, E., Andresen, H. and Karjaluo, J., 4th Int. Congress in Scandinavia in Chem. Engng., 1977, p. 123.

DISCUSSION

M.E. Kenney: After purification of the oxime reagents, what experimental methods were used to characterize the products?

R.J. Whewell: We subjected our purified reagents to an "ultimate loading" test with copper (see J. Inorg. Nucl. Chem. 1976, 38, 2071). The results were verified by non-aqueous and semi-aqueous titrations (J. Inorg. Nucl. Chem. in press). Non-aqueous titration is a useful technique for estimating the *syn*-isomer content of L1X 65N. The concentrations of nonylphenol and related compounds were measured by thin-layer chromatography.

G.A. Yagodin: Were the activation energies for reversible or direct processes? How far were you from equilibrium? What is the difference in rates in the Lewis cell and those in the turbulent regime? What can be said about film formation at the interface?

R.J. Whewell: Our studies of activation energy were based on initial rate data, in which the reverse reaction can be shown not to interfere. The extent of approach to equilibrium was not more than 5% and was generally lower. Initial rates in our Prochazka (ISEC '71) cell are around one tenth of rising drop rates; in a constant interface cell with gentle agitation close to the interface, rates increase to 0.4 - 0.5 of the rising drop rate. Inversion of the phases in the single-drop experiment from aqueous continuous to organic continuous results in a decrease in rate of 15-20%. Since we have not yet completed our work on the estimation of interfacial area generated in stirred tank tests, I am not able to comment quantitatively on the reaction rates in tank and single drop experiments. We have not seen an interfacial film in the copper oxime systems of the sort described for Nickel - D2EHPA (Met. Trans. 8B, 169 (March 1977) but under diffusion-controlled conditions in the Prochazka cell experiments, a black band of copper complex on the organic side of the interface becomes clearly visible. Experiments to study and to simulate this band are of considerable current interest to us.

The Kinetics of the Extraction of Copper by LIX65N and LIX63: Discussion of the Rate Law

C. A. Fleming, M. J. Nicol, R. D. Hancock and
N. P. Finkelstein,
National Institute for Metallurgy,
Johannesburg

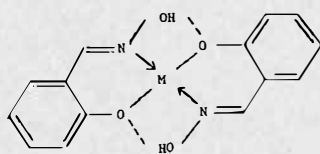
ABSTRACT

Data are presented for the kinetics of the extraction of copper from aqueous nitrate solutions across a quiescent interface by solutions of LIX65N, LIX63, and mixtures of the two solutions in chloroform. The data are consistent with a kinetic model in which the rate is controlled by mass transport to and from the interfacial zones. On the basis of this model, the various rate laws for this process that have appeared in the literature are discussed and rationalized.

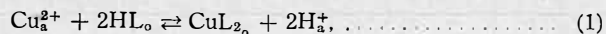
Introduction

IN RECENT YEARS considerable interest has centred on the development of chelating compounds that will selectively extract copper from dilute acid leach liquors in the presence of ferric ions. One such reagent that has found commercial application is LIX64N[†], a mixture of a β -hydroxy aromatic oxime (LIX65N) and an α -hydroxy aliphatic oxime (LIX63). The major component (LIX65N), which achieves the desired selectivity, exhibits slow reaction kinetics when used alone; small amounts of LIX63 act as a catalyst in the mixture.

The elementary chemistry of LIX - type reagents has been adequately described elsewhere.⁽¹⁻⁷⁾ Briefly, simple β -hydroxy aromatic oximes react with most divalent base metals to form complexes of the type:



The stoichiometry of the overall reaction can be represented by the equation



where the subscripts a and o refer to the aqueous and organic phases respectively, and HL represents the reagent molecule.

Although the literature contains contradictory views on the location of chelate formation in solvent extraction, the current body of opinion favours interaction at the phase boundary⁽⁹⁻¹⁵⁾ rather than homogeneous reaction in the aqueous phase.^(16,17) Moreover, the available evidence suggests that chemical reaction at the interface,^(4,8,13) rather than mass transport to, from, or across the interface,

controls the reaction kinetics. However, in the work published to date, there has been little agreement on either an empirical rate expression or on the mechanism of extraction. It is possible that these differences of opinion are partly due to the vastly different conditions employed in the various studies. In this paper, attempts are made to resolve these differences and a rate law and mechanism are presented.

Experimental

Solutions and Materials

Analar-grade copper nitrate was used, and the solutions were prepared in triply-distilled water. LIX65N and LIX63 were purified by the following method. The solid copper complex of the reagent was prepared at room temperature by the reaction of ethanolic solutions of cupric nitrate and the reagent. The complex was purified by recrystallization from hot ethanol, and washed in distilled water. The copper was then stripped by dissolution of the complex in diethyl ether and shaking the solution with a 20 per cent solution of sulphuric acid. Three to four stripping treatments were necessary to remove all the copper. Evaporation of the ether at low vacuum and room temperature yielded the isometrically pure reagent.

Reagent solutions were prepared in Analar-grade chloroform.

Kinetic Measurements

The quiescent-interface apparatus that was employed in this study was developed by Lewis⁽¹⁸⁾ and has been described by Pratt.⁽¹⁹⁾ The surface area of contact (80 cm²) between the two phases was measured as the cross-sectional area of the reaction vessel, minor corrections being made for the shaft of the impeller and for the vortex formed at high stirring speeds. An impeller (of which there were two on a single shaft) was centrally located in each phase. The impellers were driven at a constant velocity by a motor of variable speed. The copper solution and an equal volume of chloroform were stirred until a steady pH was obtained, at which point a specific volume of a concentrated solution of the ligand in the chloroform was injected into the organic phase with a Mettler D.V. 10 automatic titrator. As the reaction proceeded, changes in the concentration of protons in the aqueous phase were monitored with a glass electrode and a Radiometer PHM64 Research pH meter, which measured changes in pH correct to 0.001 units. Equation 1 shows that Cu²⁺ is related to H⁺, and it is therefore possible for the change in copper concentration with time to be measured.

Mass-transfer Characteristics of the Cell

As will be demonstrated, the rate of extraction is dependent on the agitation in the cell, and it was therefore considered necessary for the mass transfer to and from the

[†] LIX64N, LIX65N, and LIX63 are registered products of General Mills, Inc.

interface to be characterized. A convenient method was found to be the study of the rate of transfer of 8-hydroxyquinoline between chloroform and water. Spectrophotometric measurements were used to monitor changes in the concentration of 8-hydroxyquinoline when either a dilute ($2.5 \times 10^{-3} \text{M}$) aqueous solution was contacted with pure chloroform or a concentrated (0.1M) solution in chloroform was presented with pure water. In the first case, the rate is governed by transport of the 8-hydroxyquinoline in the interface, and, in the second case, it is limited by transport from the aqueous interface. When the diffusion coefficient of 8-hydroxyquinoline in water was assumed to be $1.5 \times 10^{-5} \text{ cm}^2 \text{ s}^{-1}$, the thickness of the aqueous diffusion layers, calculated from the rates of transfer at 60 $\text{r} \cdot \text{min}^{-1}$, were found to be 0.012 cm in the first and 0.013 cm in the second case. (A simple Nernst diffusion-layer model was assumed.) For all mass-transfer calculations in this paper, a thickness of 0.012 cm at 60 $\text{r} \cdot \text{min}^{-1}$ is used for the diffusion layers of both the aqueous and organic phases.

TABLE 1. Effects of Variations of the Interfacial Area and the Aqueous Volume on the Rate of Extraction of Copper by LIX64N

Interfacial area cm^2	Aqueous volume cm^3	Rate, R $10^9 \text{ mol} \cdot \text{cm}^{-2} \cdot \text{s}^{-1}$
79.7	250	2.90
79.7	400	2.90
124.6	350	2.90
124.6	500	2.88
283.5	600	2.90
283.5	900	2.89

$[\text{Cu}^{2+}] = 2.0 \times 10^{-5} \text{ mol} \cdot \text{cm}^{-3}$, $[\text{LIX64N}] = 5 \times 10^{-5} \text{ mol} \cdot \text{cm}^{-3}$,
 $\text{pH} = 4.00$, stirring speed = 60 $\text{r} \cdot \text{min}^{-1}$.

Results

The kinetic data are reported as the rate of change in the concentration of hydrogen ions in the bulk aqueous phase, and were obtained from the following expression:

$$R = \frac{V}{A} \frac{[\text{H}^+]_2 - [\text{H}^+]_1}{t_2 - t_1} \text{ mol} \cdot \text{cm}^{-2} \cdot \text{s}^{-1}, \dots \dots \dots (2)$$

where R is twice the rate of transfer of copper to the organic phase (c.f. Equation 1).

Kletenik and Navrotskaya⁽⁹⁾ observed a linear relationship between the reaction rate and the factor A/V (in equation 2) for the extraction of iron (III) by di-isopentyl hydrogen phosphate. On the basis of this relationship, these authors proposed that the reaction at the interface controlled the kinetics of the reaction. The results presented in Table 1 suggest that the same relation holds good for the copper-LIX64N reaction. In these experiments, interfacial areas were varied by use of reaction vessels of different cross-sectional areas.

In experiments designed to show whether the reaction is controlled by mass transport, the concentrations of copper ions, LIX65N and LIX63 were held at an excess that was approximately constant in relation to the protons, and the rate was measured as a function of stirring speed as the pH value of the aqueous phase decreased from 4.2 to about 3.0. The results for a number of stirring speeds between 20 and 150 $\text{r} \cdot \text{min}^{-1}$, are presented in Figure 1. It was found that the rate has a similar dependence on stirring speed for the reactions of copper with LIX63, LIX65N, and KELEX100^{††}, but these results are not included here. So that mass-transport control in the organic phase could be distinguished from that in the aqueous phase, experiments were carried out in which the rate was

^{††}KELEX100 is a registered product of Ashland Chemicals Co.

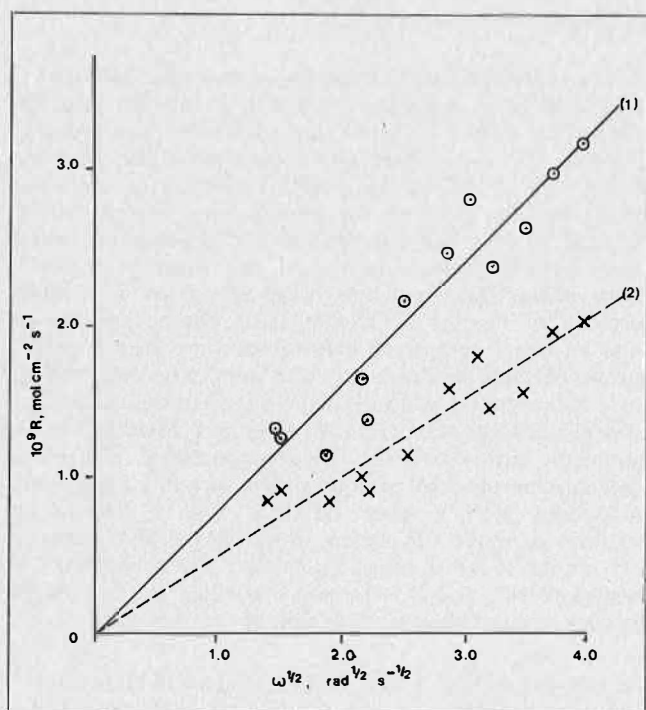


FIGURE 1. The effect of stirring speed on the rate of extraction of copper ($7.5 \times 10^{-5} \text{ mol} \cdot \text{cm}^{-3}$) by a mixture of LIX65N ($6.7 \times 10^{-6} \text{ mol} \cdot \text{cm}^{-3}$) and LIX63 ($6.0 \times 10^{-6} \text{ mol} \cdot \text{cm}^{-3}$) at (1) pH 4 and (2) pH 3.

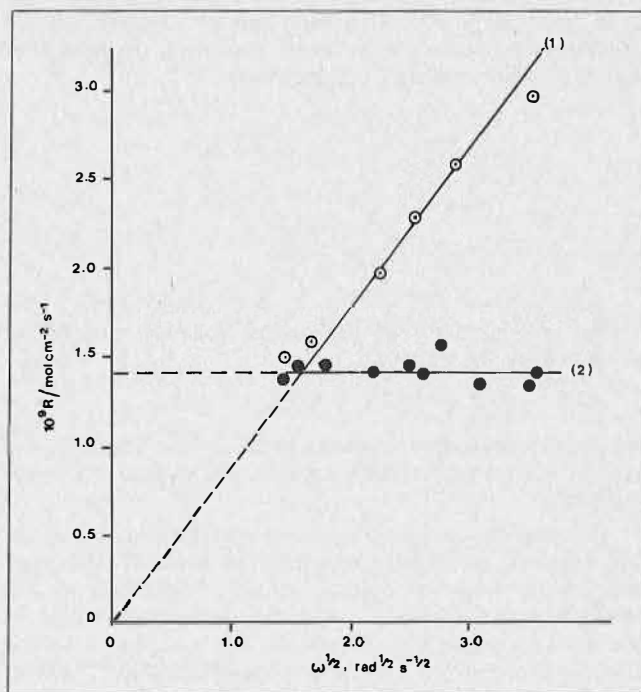


FIGURE 2. The effect of stirring speed on the rate of extraction of copper ($7.5 \times 10^{-5} \text{ mol} \cdot \text{cm}^{-3}$) by a mixture of LIX65N ($6.0 \times 10^{-6} \text{ mol} \cdot \text{cm}^{-3}$) and LIX63 ($6.7 \times 10^{-6} \text{ mol} \cdot \text{cm}^{-3}$) at pH 4 in which (1) organic phase only stirred and (2) aqueous phase only stirred.

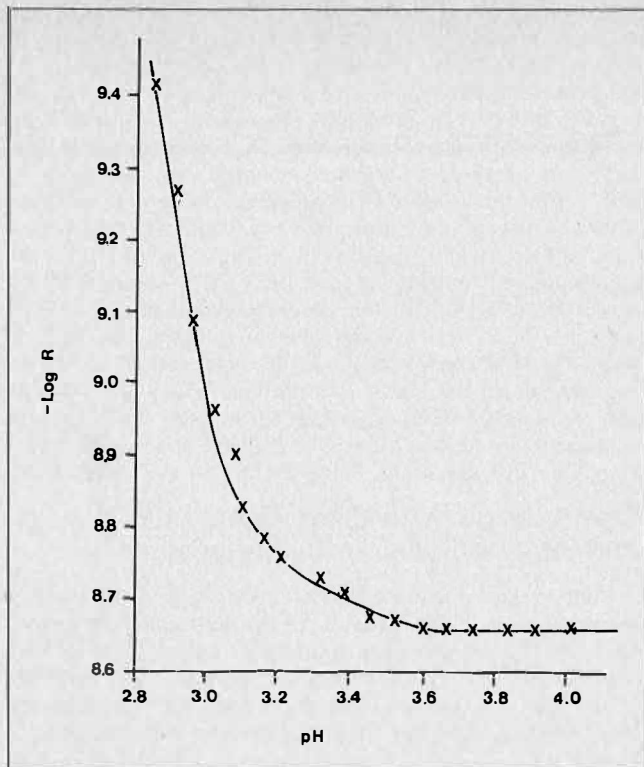


FIGURE 3. The effect of pH on the rate of extraction of copper (7.5×10^{-6} mol. cm^{-3}) by a mixture of LIX65N (6.7×10^{-6} mol. cm^{-3}) and LIX63 (6.0×10^{-6} mol. cm^{-3}) at a stirring speed of 60 r. min^{-1} .

measured as a function of stirring speed with the impeller in only one phase. The results are presented in Figure 2, and suggest that, under these conditions, the rate is controlled by diffusion in the organic phase. Comparison of curves (1) in both Figures 1 and 2 shows that the rate is essentially the same whether only the organic phase or both phases are stirred.

The results presented in Figures 3 show the effect of decreasing pH during a kinetic run on the rate of extraction. Similar curves were obtained in all experiments. The dependence of the rate on pH is fairly complex, with apparent independence of the rate on the bulk proton concentration at high pH values and a non-linear inverse dependence at lower pH values. As will be demonstrated in Discussion (below), simple quantitative interpretation of the data is possible only in the region where the rate is independent of pH, and most of the results will therefore be confined to those obtained in this region.

The effect of variations in the concentration of copper ions on the rate of extraction by a mixture of LIX65N and LIX63 at a pH value of 4 is shown in Figure 4. Similar curves were obtained with LIX65N and LIX63 alone. It is apparent that the rate increases with increasing copper concentration at low concentrations but becomes independent of the copper concentration at high (i.e., greater than about 0.05 M) concentrations.

Similar treatment of data on the effect of variations in the concentrations of LIX65N yields the results shown in Figure 5. As can be seen, a reasonable linear relation between the rate and the concentration of the extractant is obtained. In Table 2 a list is given of the results of experiments in which various amounts of the copper-LIX65N complex were added to the organic phase. It is apparent that the rate is noticeably reduced only at high concentrations of the complex.

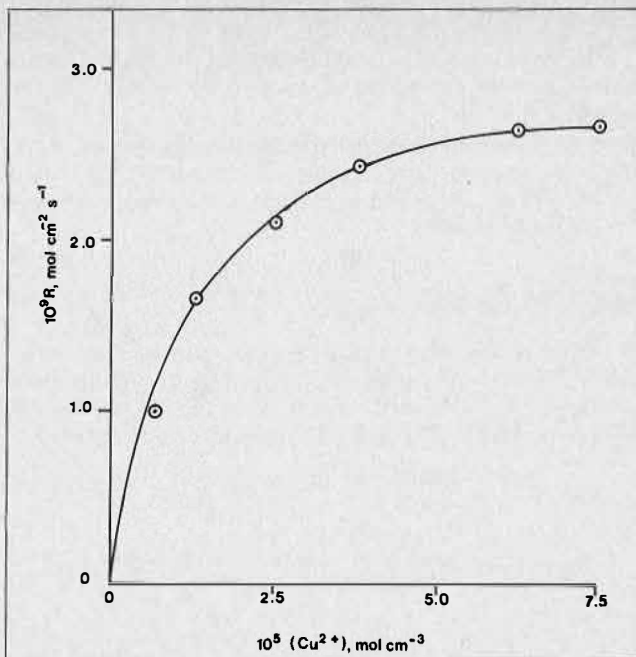


FIGURE 4. The effect of the concentration of copper on the rate of extraction by a mixture of LIX65N (6.7×10^{-6} mol. cm^{-3}) and LIX63 (6.0×10^{-6} mol. cm^{-3}) at pH 4 and a stirring speed of 60 r. min^{-1} .

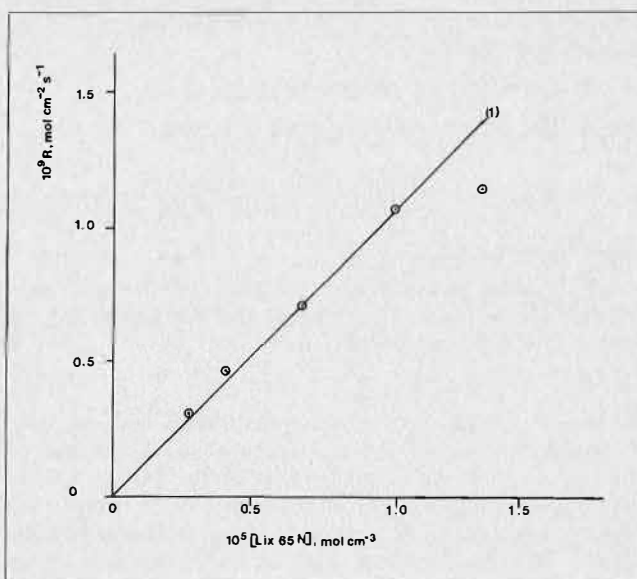


FIGURE 5. The effect of the concentration of LIX65N on the rate of extraction of copper (7.5×10^{-5} mol. cm^{-3}) at pH 4.

TABLE 2. The Effect on the Rate of the Concentration of the Copper Complex of LIX65N in the Organic Phase

$[\text{Cu}(\text{LIX65N})_2]$ 10^6 mol. cm^{-3}	Rate R 10^9 mol cm^{-2} s^{-1}
0.85	2.41
1.70	2.37
3.15	2.45
4.55	2.40
9.00	2.19
17.00	1.49

$[\text{Cu}^{2+}]_0 = 7.50 \times 10^{-5}$ mol. cm^{-3}
 $\text{LIX65N} = 6.67 \times 10^{-6}$ mol. cm^{-3} , $\text{LIX63} \approx 6.0 \times 10^{-6}$ mol. cm^{-3}
 pH = 4.00, stirring speed = 60 r. min^{-1} .

Discussion

The main emphasis in the following discussion on the kinetics of the extraction of copper by various LIX reagents will be on

- (i) a mass-transport model for the process and
- (ii) a comparison with, and rationalization of, the various rate expressions and mechanisms that have appeared in the literature.

Mass-transport Model

Under steady-state conditions, the rates of mass transport of the various reactants and products to and from the interface (or interfacial zones) must be equal. On the basis of a simple Nernst-type diffusion model, therefore,

$$\frac{D_{H^+} \{ [H^+]_i - [H^+]_a \}}{\delta_a} = \frac{2D_{Cu^{2+}} \{ [Cu^{2+}]_a - [Cu^{2+}]_i \}}{\delta_a}$$

$$= \frac{D_{HL} \{ [HL]_o - [HL]_i \}}{\delta_o} = \frac{2D_{CuL_2} \{ [CuL_2]_i - [CuL_2]_o \}}{\delta_o}$$

If (i) $[CuL_2]_o \ll [CuL_2]_i$, i.e., in the absence of appreciable amounts of added complex and for short reaction times, and

$$(ii) D_{Cu^{2+}} \approx D_{HL} \approx D_{CuL_2} \approx D_{H^+}/10 = D, \text{ (Ref 20)}$$

the interfacial concentrations of all species can be expressed in terms of $[CuL_2]_i$ and the bulk concentrations. Also, if the extraction reaction is assumed to be at equilibrium at the interface (or in the interfacial zones), then the equilibrium constant

$$K = [CuL_2]_i [H^+]_i^2 / [Cu^{2+}]_i [HL]_i^2$$

can be expressed in terms of $[CuL_2]_i$ to yield

$$K = \frac{[CuL_2]_i \{ [H^+]_a + \alpha [CuL_2]_i \}^2}{\{ [Cu^{2+}]_a - 5\alpha [CuL_2]_i \} \cdot \{ [HL]_o - 2[CuL_2]_i \}^2} \quad (3)$$

where $\alpha = 0.2 \delta_a/\delta_o$.

On the basis of the Nernst diffusion model, and assuming the above inequality is valid, the expression for the rate of reaction may be written

$$R = 2D[CuL_2]_i/\delta_o \quad (4)$$

In theory, combination of this relationship with equation 3 should yield an expression describing the dependence of the rate on the bulk concentrations of the various species and the agitation. Unfortunately, no general, simple analytical solution can be obtained, and correlation with the kinetic data can therefore best be illustrated only under certain limiting conditions.

Thus, for $[Cu^{2+}]_a \gg [HL]_o \gg [H^+]_a$, Equation 3 can be simplified and written in the form

$$K = \frac{\alpha^2 [CuL_2]_i^3}{[Cu^{2+}]_a \{ [HL]_o - 2[CuL_2]_i \}^2}$$

which may be re-arranged to give

$$[CuL_2]_i = \frac{[HL]_o}{4} + \frac{[CuL_2]_i^2}{[HL]_o} \left\{ 1 - \frac{\alpha^2}{4K} \frac{[CuL_2]_i}{[Cu^{2+}]_a} \right\}$$

Since $K = 0.45$ under the conditions of these experiments, the second term in the brackets is small relative to 1 for reasonable values of α and high $[Cu^{2+}]_a$. Under these conditions,

$[CuL_2]_i = [HL]_o/2$ and substituting in (4) gives

$$R = D[HL]_o/\delta_o \quad (5)$$

i.e., the rate is governed by the mass transport of the

product CuL_2 from the interface. Under these conditions, the rate should be independent of the concentrations of protons and copper, first order in the concentration of the extractant, and dependent on the agitation only in the organic phase. The results in Figures 2, 3, 4, and 5 are consistent with these predictions. A comparison can also be made of the limiting rate at high concentrations of Cu^{2+} (Figure 4) with that predicted from this relation. Thus, by use of the value of $\delta_o = 0.012$ cm (see above) and an acceptable estimate (5×10^{-6} cm² s⁻¹) for D , the calculated limiting rate of 5.2×10^{-9} mol. cm⁻² s⁻¹ agrees fairly well with the observed value of 2.7×10^{-9} mol. cm⁻² s⁻¹. It should also be pointed out that, in terms of this model, addition of complex CuL_2 to the organic phase will have a noticeable effect on the rate only at concentrations approaching those of the interfacial concentration ($[HL]_o/2$) of CuL_2 in the absence of added complex. The results in Table 2 confirm this prediction.

Comparison with Rate Expressions and Mechanisms in the Literature

Flett *et al.*⁽⁸⁾, using a tracer method in a Akufve apparatus, studied the kinetics of the extraction of copper by LIX65N and mixtures of LIX65N and LIX63. In their experiments, the concentration of the Cu^{2+} was normally lower than that of the extractant, and, for pH value less than about 3, also less than that for the bulk protons.

Under these conditions, equation 3 can be simplified and written

$$K = \frac{[CuL_2]_i [H^+]_a^2}{\{ [Cu^{2+}]_a - 5\alpha [CuL_2]_i \} [HL]_o^2} \quad (6)$$

and substituting for

$$R = \frac{2D[CuL_2]_i}{\delta_o} \quad (4)$$

yields an expression for the rate

$$R = \frac{2DK}{\delta_o} \frac{[Cu^{2+}]_a [HL]_o^2}{5\alpha K [HL]_o^2 + [H^+]_a^2}$$

This expression is generally consistent with the results published by Flett *et al.*, who found the rate to be first order in the concentration of Cu^{2+} , between 1.01 and 1.27 order with respect to LIX65N, and between -0.85 and -1.22 order with respect to the proton. This equation predicts orders of 1.0 for Cu^{2+} and, depending on the concentrations of HL and H^+ , between 0 and 2.0 for LIX65N and between 0 and -2.0 for the proton. The inverse one-half to three-quarter order with respect to the proton concentration reported by Neelameggham¹⁶ can also be accommodated by this model.

Atwood *et al.*⁽¹³⁾, in a study of the extraction of copper by LIX64N in a single-drop reaction cell, reported somewhat different results, since they observed a zero-order dependence on the proton concentration even at low pH values. However, as pointed out by Flett *et al.*⁽²¹⁾, the pH value in the cell was not constant during a run, and the results could best be interpreted in terms of an inverse proton dependence. Atwood *et al.* also found a first-order dependence on the copper concentration even at high concentrations of copper, contrary to the findings of this investigation. However, they used concentrations of

†The calculated value was obtained by using the sum of the concentrations of LIX65N and LIX63. Use of the concentration of LIX65N only gives a calculated limiting rate of 2.6×10^{-9} mol cm⁻² s⁻¹. In view of the uncertainty of the mechanistic role of LIX63, it is not possible at this stage to assess its contribution to the rate in terms of a mass-transport model.

LIX64N in excess of 0.1M, and, under these conditions, the simplified expression 5 is not valid, hence zero-order dependence on the concentration of Cu^{2+} is not expected. On the basis of calculations of the mass transport to a falling drop, they excluded mass transport in the continuous (organic) phase as limiting the rate. This is to be expected, since, under the conditions of their experiments, the mass transport of protons from the interface within the falling aqueous drop is likely to be rate controlling.

Acknowledgment

This paper is published by permission of the Director General of the National Institute for Metallurgy.

NOTATION

$[M]_a$:	= Concentration of species M in the aqueous phase (mol cm^{-3})
$[M]_o$:	= Concentration of species M in the organic phase (mol cm^{-3})
$[M]_i$:	= Concentration of species M in the interfacial zone (mol cm^{-3})
$[\text{H}^+]_1, [\text{H}^+]_2$:	= Concentrations of protons in the aqueous phase after t_1 and t_2 seconds respectively (mol cm^{-3})
V:	= Vol. of aqueous phase (cm^3)
A:	= Interfacial area (cm^2)
D_m :	= Diffusion coefficient of species M ($\text{cm}^2 \text{s}^{-1}$)
δ_a :	= Thickness of the Nernst diffusion layer in the aqueous phase (cm)
δ_o :	= Thickness of the Nernst diffusion layer in the organic phase (cm)

DISCUSSION

L. Hummelstedt: Would LIX63 have any effect on the extraction rate under the conditions you have just described?

C.A. Fleming: While stressing that the mechanism of LIX63 catalysis is still not clear — and in fact this model does not readily permit a mechanism to be assigned to it — I must add that LIX63 certainly does catalyse the extraction of copper by LIX65N under the conditions described. Tentatively, at this stage, I will suggest that this could be associated with the formation of a mixed ligand complex similar to that proposed by Flett et al.⁽¹⁾. On the basis of our model, this species (at the interface) would have a greater thermodynamic stability than the analogous complex of copper and two molecules of LIX65N.

S.D. Cavers: The authors assumed that the reaction takes place at the physical interface. Is this necessarily so?

REFERENCES

- (1) Flett, D.S., *Trans. Inst. Min. Metall.*, 1974, C30.
- (2) Laskorin, B.N., Yaksin, V.V., Ul'yanov, V.S. and Mirokhin, A.M., Paper presented to ISEC 74, Lyon, France, 1974, 1775.
- (3) Ashbrook, A.W., *J. Chromatogr.* 1975, 105, 141.
- (4) Ashbrook, A.W., *Coord. Chem. Revs.* 1975, 16, 285.
- (5) Wheeler, R.J., Hughes, M.A. and Hanson, C., *J. Inorg. Nucl. Chem.* 1975, 37, 2303.
- (6) Van der Zeeuw, A.J., *Int. Chem. Eng. Symposium Series*, 1975, 42, 16.1.
- (7) Flett, D.S. and Spink, D.R., *Hydrometall.* 1976, 1, 207.
- (8) Flett, D.S., Okuhara, D.N. and Spink, D.R., *J. Inorg. Nucl. Chem.* 1973, 35, 2471.
- (9) Kletenik, Yu B. and Navrotskaya, V.A., *Russian J. Inorg. Chem.*, 1967, 12(11), 1648.
- (10) Navrotskaya, V.A. and Kletenik, Yu B., *Russian J. Inorg. Chem.*, 1969, 14(7), 997.
- (11) Alimarin, J.P., Zolotov, Yu A. and Boduya, V.A., *Pure Appl. Chem.*, 1971, 25.4, 667.
- (12) Roddy, J.W., Coleman, C.F. and Arai, S., *J. Inorg. Nucl. Chem.* 1971, 33, 1099.
- (13) Atwood, R.L., Thatcher, D.N., and Miller, J.D., *Metall. Trans. B*, 1975, 6B, 465.
- (14) Flett, D.S., Hartlage, J.A., Spink, D.R., and Okuhara, D.N., *J. Inorg. Nucl. Chem.*, 1975, 37, 1967.
- (15) Price, R., and Tumilty, J.A., *Int. Chem. Eng. Symposium Series*, 1975, 42, 18.1.
- (16) Neelameggham, R., Ph.D. Thesis, University of Utah, 1972.
- (17) Hanson, C., Hughes, M.A., and Marsland, J.G., Paper presented to ISEC 74, Lyon, France, 1974. 2401.
- (18) Lewis, J.B., *Chem. Eng. Sci.*, 1954, 3, 248, 260.
- (19) Pratt, H.R.C., *Ind. Chem.*, 1955, 63.
- (20) Adams, R.N., *Electrochemistry at Solid Electrodes*, Dekker, 1969, pp. 220-222.
- (21) Flett, D.S., Melling, J., and Spink, D.R., *J. Inorg. Nucl. Chem.*, 1977, 39, 700.

C.A. Fleming: No. In proposing an interfacial reaction mechanism one assumes that the ligand is located in the interface, i.e., the hydrophilic functional groups of the ligand are in the aqueous phase while (nominally) the hydrophobic alkyl chain is in the organic phase. It is suggested that this is the major pathway — but not the only one. In fact, it can be shown theoretically⁽²⁾ that a homogeneous aqueous phase mechanism can compete with the interfacial mechanism — provided that the aqueous phase reaction zone is confined to a region very close to the interface.

REFERENCES

- (1) D.S. Flett, D.N. Okuhara and D.R. Spink, *J. Inorg. Nucl. Chem.* 35, 2471 (1973).
- (2) C.A. Fleming and J.J. Nicol, Unpublished.

The Effect of Hydrodynamic Conditions on the Kinetics of Copper Extraction by LIX65N

E. Susana Perez de Ortiz,
Dept. Chem. Eng., Imperial College, London, UK
M. Cox, Hatfield Polytechnic, Herts, UK
D. S. Flett,
Warren Spring Laboratory, Stevenage, Herts, UK

SUMMARY

A mixed kinetic model incorporating both chemical reaction and mass transfer parameters has been developed to describe the extraction of copper by hydroxyoxime extractants. Using estimated parameters for a variety of hydrodynamic conditions, the model gives trends similar to those observed in single drop, Lewis cell and AKUFVE studies. The computed data showed that the discrepancies in reaction orders obtained for the reactants are directly attributable to the neglect of the mass transfer contributions in the development of the various chemical reaction mechanisms. It is concluded that this type of model should be employed to explore the relationship between chemical reaction and mass transfer rates in such studies over the concentration ranges of interest so as to avoid unnecessary difficulties in data interpretation and development of extraction mechanisms.

Introduction

LATELY, CONSIDERABLE EFFORT has been devoted to the study of the mechanism of extraction of copper by hydroxyoximes. These studies have been particularly concerned with 5-nonyl 2 hydroxy benzophenone oxime (LIX65N*) by itself or together with an aliphatic α hydroxyoxime (LIX63*) which acts as an accelerator compound. This mixture is marketed under the trademark LIX®64N* and both LIX65N and LIX64N are used commercially in copper hydrometallurgy across the world. Thus, elucidation of the extraction mechanism is of commercial importance in terms of optimization of contactor design and reagent design generally and the results of such studies are also of direct relevance to the other hydroxyoxime compounds available commercially, i.e. SME 529 (Shell Chemicals) and the Acorga Ltd P5000 series of extractants.

To date there have been four main kinetic investigations⁽¹⁻⁴⁾ all of which have concluded that the rate of extraction is controlled by a slow interfacial reaction of first order with respect to the copper concentration in the aqueous phase. However, further agreement as to the order of reaction with respect to the other system variables, i.e. extractant concentration and pH, is lacking. Three different experimental techniques have been used and Table 1 shows the apparent reaction orders obtained for the system variables together with the experimental method employed. For a full description of the various experimental techniques the original papers should be consulted. However, as each method employs quite different hydrodynamic conditions, it is possible that this

Table 1. Summary of Apparent Orders of Reaction for Copper Extraction with Hydroxyoximes

Reference	Extractant	Experimental Method	Order of Reaction		
			[H ⁺]	[RH]	[Cu ²⁺]
1	LIX65N	AKUFVE	-0.9	1.01	1
2	LIX65N	Lewis Cell	-0.6	1.10	1
6	LIX65N	Single Drop	ND	0.5 ^(a)	1
1	LIX64N	AKUFVE	-1.0	1.59 ^(b)	1
3	LIX64N	Single Drop	0	0.5 ^(c)	1
4	LIX65N	Single Drop	-1.0 ^(d)	- ^(e)	1

N.D = not determined

(a) Average value from published data (ref. 6)

(b) Value obtained from varying LIX64N concentration (Ref 1)

(c) Value obtained by varying LIX65N concentration at constant LIX63 concentration (Ref 3)

(d) Only below a rate of 0.1 m mol m⁻² s⁻¹ (Ref. 4)

(e) No chemical order ascribable to (RH) concentration dependence

could account for the differences in reaction orders found in the four studies. Thus the AKUFVE⁽¹⁾ employs a highly turbulent regime with a large but unknown interfacial area. The Lewis cell⁽²⁾ technique employs a known interfacial area with an upper limit of bulk phase turbulence set so as to prevent interfacial distortion. The single drop technique⁽³⁾ provides the least turbulent bulk conditions of all under fixed interfacial area conditions.

In the study of rate processes in a heterogeneous system, the hydrodynamic conditions within the system are of major importance. While for rate processes in a homogeneous system the effect of the concentration of the reactants on the reaction rate can be determined directly, in a heterogeneous system the site of the reaction has first to be established and the effect of the rate of transport of the reactants and products has to be known before conclusions regarding the reaction mechanism can be drawn. For example, only when the rate of extraction for a given interfacial area per unit volume is independent of the rate of mass transport of reactants and products, i.e. the degree of turbulence of the phases, can it be concluded that the extraction rate is controlled by chemical reaction. If the extraction is studied in a transition regime, i.e. when the rate of mass transport still affects the extraction rate, a mixed kinetic mechanism applies and interpretation of rate data by chemical reaction rate criteria alone will yield erroneous reaction orders and result in development of incorrect kinetic schemes.

To date, two significant developments have taken place with regard to models of the extraction mechanism. Chapman et al⁽⁷⁾ have developed a mass transfer model for a system with fast interfacial chemical reactions. Application of this model to the rate of copper extraction by Kelex 100 (dodecyl 8 hydroxy quinoline, Ashland Chemical Co) shows that in some ranges of process conditions the extraction rate can be as low as 0.02 times the predicted mass transfer rate and thus any model must therefore accommodate not only mass transfer as related to the hydrodynamics of the system but also the chemical

*(General Mills Inc.)

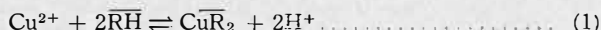
kinetic requirements as given by the chemistry of the extraction process.

Danesi and coworkers^(8,9) have developed models to account for both hydrodynamic and kinetic factors in the study of the rate of extraction of europium III by dinonyl naphthalene sulphonic acid under steady state⁽⁸⁾ and non steady state conditions⁽⁹⁾. The models have been successfully applied to data determined for both conditions using a Lewis cell technique.

In the present study a model similar to that of Danesi et al^(8,9) has been developed contemporaneously. However, while Danesi et al have applied their model solely to their own experimental data, the purpose of the present exercise has been to apply the model to the extraction of copper by LIX65N and LIX64N to show the relative effects of the system hydrodynamics and interfacial chemical reaction rates when the three very different experimental techniques are used. For this purpose three of the studies cited above^(1,2,3) have been selected as being representative of each technique. This paper describes the development of the model and its application in the three studies selected.

A Model for the Study of Interfacial Reaction Kinetics

The overall extraction reaction for copper is given by:



where RH is the hydroxyoxime, CuR₂ is the organic soluble copper complex and the bars denote organic phase species.

The rate equations reported in the literature all describe the initial rate (i.e. the rate far from equilibrium) in the following form.

$$r = k \frac{[\text{Cu}^{2+}]^1 [\text{RH}]^m}{[\text{H}^+]^n} \quad (2)$$

where k is the reaction rate constant and [] denotes bulk phase concentrations, and 1, m and n are the reaction orders.

If the chemical reactions take place at the interface then the rate of reaction will be proportional to the interfacial area per unit volume of aqueous phase and the interfacial concentrations of reactants, rather than the bulk phase concentrations, should be used in the rate expression, i.e.

$$r' = k' \frac{[\text{Cu}^{2+}]_i^1 [\text{RH}]_i^m}{[\text{H}^+]_i^n} \quad (3)$$

where the subscript i indicates interfacial values.

The interfacial and bulk phase concentrations are related by the equations of mass transfer. In order to simplify the mathematical analysis the following assumptions are made:

- (i) the system is in steady state;
- (ii) both bulk phases are well mixed and thus bulk phase concentrations are uniform;
- (iii) concentration changes between the bulk phases and the interface are confined to the two stagnant films formed at each side of the interface;
- (iv) the copper complex and the chelating agent are insoluble in the aqueous phase and copper and hydrogen ions are insoluble in the organic phase.

From condition (iv) it follows that copper transfer from the aqueous to the organic phase can only take place via chemical reaction. Therefore, the rate of mass transfer of

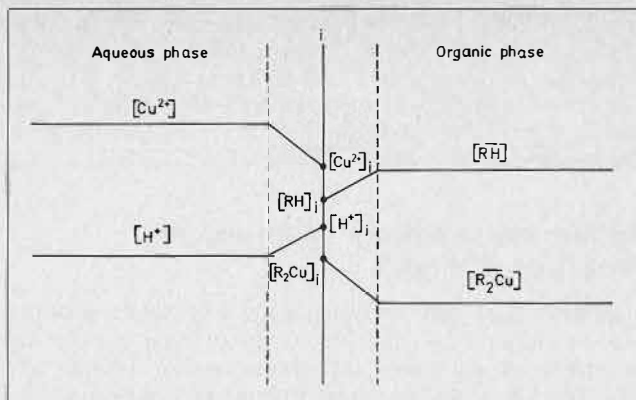


FIGURE 1. Concentration profiles at the organic-aqueous boundary.

copper from the bulk aqueous phase to the interface is equal to the rate of chemical reaction and the rates of transfer of the other species are linked to the transfer of copper by the stoichiometry reaction (1). Thus

$$N = r' = K_{\text{Cu}} ([\text{Cu}] - [\text{Cu}]_i) = -\frac{1}{2} K_{\text{H}} ([\text{H}] - [\text{H}]_i) = \frac{1}{2} K_{\text{RH}} ([\overline{\text{RH}}] - [\text{RH}]_i) = -K_{\text{CuR}_2} ([\overline{\text{CuR}_2}] - [\text{CuR}_2]_i) \quad (4)$$

where N is the number of moles per unit area per unit time and K_{Cu}, etc, are the mass transfer coefficients of the respective species. For convenience the charges on the copper and hydrogen ions have been dropped.

The concentration profiles of reactants and products as defined by the model are shown in Figure 1. Rearrangement of equation (4) and substitution in equation (3) yields

$$r' = \frac{k' \left\{ [\text{Cu}] - \frac{r'}{K_{\text{Cu}}} \right\}^1 \left\{ [\overline{\text{RH}}] - \frac{2r'}{K_{\text{RH}}} \right\}^m}{\left\{ [\text{H}] + \frac{2r'}{K_{\text{H}}} \right\}^n} \quad (5)$$

Further rearrangement yields

$$r' = k' \frac{[\text{Cu}]^1 [\overline{\text{RH}}]^m}{[\text{H}]^n} \cdot F \quad (6)$$

where

$$F = \frac{\left\{ 1 - \frac{r'}{K_{\text{Cu}} [\text{Cu}]} \right\}^1 \left\{ 1 - \frac{2r'}{K_{\text{RH}} [\overline{\text{RH}}]} \right\}^m}{\left\{ 1 + \frac{2r'}{K_{\text{H}} [\text{H}]} \right\}^n}$$

Thus from equation (6) the kinetic expression for a heterogeneous reaction differs from that for a homogeneous reaction by the factor F. This factor describes the hydrodynamic conditions of the system via the mass transfer coefficients of the species involved in the reaction.

The ratio $\frac{r'}{K_j [j]}$ represents the ratio between the rate of chemical reaction and the maximum rate of mass transfer possible for the species j, at concentration [j], i.e. when the interfacial concentration is zero for the given mass transfer coefficient. Therefore, in general, F is affected not only by the hydrodynamic conditions of the system but also by the concentration of the reactants and the rate of extraction itself. Thus, when the values of the reaction orders 1, m and n are determined from experimental rate data obtained by varying the reactant concentrations, the values obtained will also depend on the concentration of the reactants and the hydrodynamic conditions of the system unless the value of F is known for each data point.

Thus, when the value of F differs from unity, the values of l , m and n obtained from equation (2) will only be apparent reaction orders and different values will arise for different conditions of turbulence and ranges of concentration. When the value of F is unity, then equation (2) and (6) are equivalent.

Numerical Analysis of Interfacial Reaction Kinetics

A numerical study of equation (6) will yield a quantitative measure of the effect of the rate of mass transfer and reactant concentrations on the extraction kinetics. To facilitate this study, equation (6) must be rearranged, i.e.

$$\frac{k' [Cu]^{1+m-n-1} [1-y]^l [x_1 - 2ay]^m}{K_{Cu} y [x_2 + 2by]^n} = 1 \dots \dots \dots (7)$$

where

$$y = \frac{r^1}{K_{Cu} [Cu]} ; x_1 = \frac{[RH]}{[Cu]} ; x_2 = \frac{[H]}{[Cu]} ;$$

$$a = K_{RH}/K_{Cu}$$

and

$$b = K_H/K_{Cu}$$

Now the ratio of the mass transfer coefficients of two species is known⁽¹⁰⁾ to be proportional to the square root

of the ratio of the molecular diffusivities of the species, i.e.

$$\frac{K_{RH}}{K_{Cu}} \propto \sqrt{\frac{D_{RH}}{D_{Cu}}} \dots \dots \dots (8)$$

where D denotes molecular diffusivity. Values of the diffusion coefficients of the various species have been chosen such that the values of a and b in equation (7) are unity as the values of these parameters are not critical with respect to the calculated data. A similar procedure has been followed by Danesi et al^(8,9). Also, for the purposes of the calculations, the values of the reaction order parameters l , m and n have been set at unity as concluded by Flett et al⁽¹⁾ since the AKUFVE studies, being the most turbulent, must most closely represent conditions under which F will be close to unity.

The degree of turbulence in each experimental method is characterised in equation (7) by the mass transfer coefficient. Atwood, Thatcher and Miller⁽³⁾ have assumed that the rate of extraction for their falling drop method is about ten times slower than the rate of diffusion without chemical reaction. Thus, although the rate of pure diffusion may be slower than their estimates, a mass transfer coefficient ten times greater than the reaction rate constant k' is chosen for the calculations relevant to the falling drop technique i.e. $k'/K_{Cu} = 0.1$. For the Lewis cell the single phase mass transfer coefficients measured by Austin and Sawistowski⁽¹¹⁾ gave mass transfer rates of the order of a hundred times greater than the reaction rates reported by Fleming⁽²⁾, and consequently the value $k'/K_{Cu} = 0.01$ was chosen for this experimental method. Finally, for the AKUFVE studies an arbitrary value of k'/K_{Cu} of 0.001 has been chosen. Equation (7) may now be solved numerically for each experimental technique. For computational purposes x_1 has been varied between 0.5 and 5000 while x_2 has been varied between 0.015 and 10. These ranges of concentration ratio values cover a much wider range than those covered in the three experimental investigations.

Results and Discussion

The results of the computations are shown graphically as $\log \left(\frac{[Cu^{2+}] - [Cu^{2+}]_e}{[Cu^{2+}]} \right)$ versus $\log \left(\frac{[RH]}{[Cu^{2+}]} \right)$ or versus $\log \left(\frac{[H^+]}{[Cu^{2+}]} \right)$ plots in Figures 2-3 for the falling single drop studies, Figures 5-6 for the Lewis

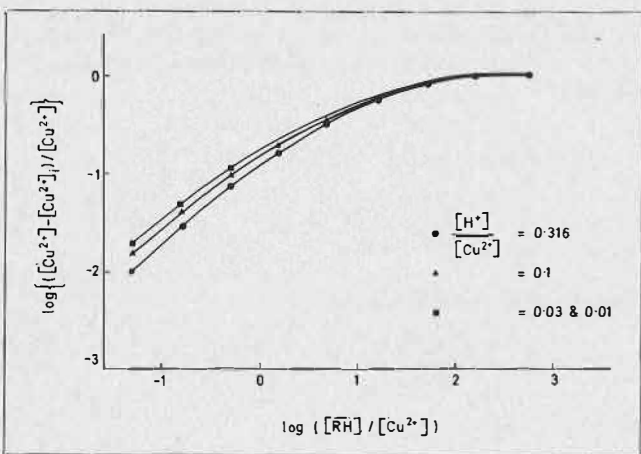


FIGURE 2. Computed rate of extraction as a function of extractant concentration for $k'/K_{Cu} = 0.1$, experimental conditions of Atwood et al $[H^+]/[Cu^{2+}] = 0.06$; $\log([RH]/[Cu^{2+}])$ from 0.5 to 1.5.

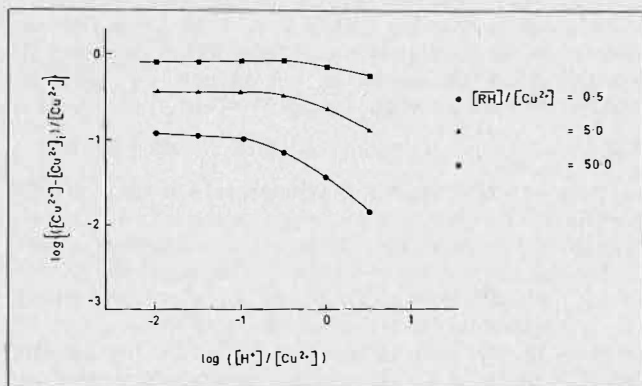


FIGURE 3. Computed rate of extraction as a function of pH for $k'/K_{Cu} = 0.1$, experimental conditions of Atwood et al $[RH]/[Cu^{2+}]$ from 3 to 30, $\log([H^+]/[Cu^{2+}])$ from -0.25 to -3.0.

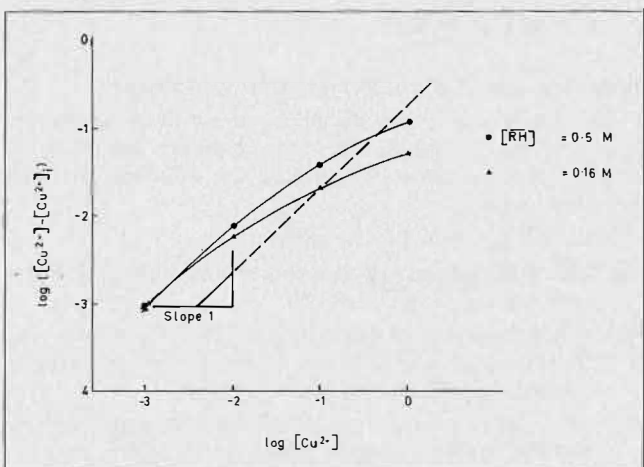


FIGURE 4. Computed variation of the rate of transfer with aqueous copper concentration for $k'/K_{Cu} = 0.1$, experimental conditions of Atwood et al $[RH] = 0.05 M$, $\log[Cu^{2+}]$ from -1 to -2.5.

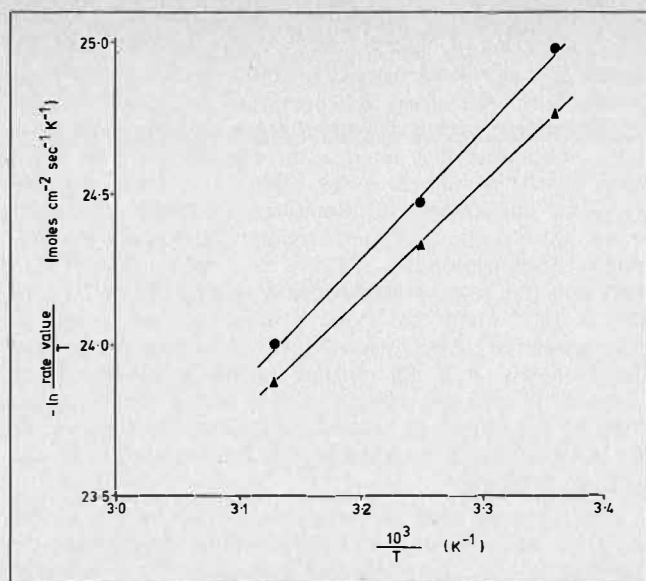


FIGURE 3. Eyring plot for extraction of copper from copper-acid aqueous system.

● — low loading of copper (first cycle),
○ — high loading of copper (fourth cycle) in organic phase.

3.25g l⁻¹ sulphuric acid was regarded as the 'standard' aqueous system. Further studies were carried out with this solution but at higher temperatures, 35.0 and 46.5 ± 0.3°C. The copper transfer rate values, moles Cu per cm² phase interface per sec obtained at the three temperatures and at various residence times, are shown in Table 4. Eyring⁽¹¹⁾ plots from the results of the first and fourth cycles of the organic phase at the three temperatures were constructed and are shown in Figure 3. The activation energy for the extraction of copper with 20% v/v LIX 64N in kerosene, containing 0.2 to 0.5g l⁻¹ copper in the organic phase, was calculated to be 41.4kJ mole⁻¹ (9.9 kcal mole⁻¹), while for a copper loading of 0.7 to 1.9g l⁻¹ in the organic phase, the value was 33.3kJ mole⁻¹ (8.0 kcal mole⁻¹). The higher value is in good agreement with the results reported by Hughes *et al.*⁽⁹⁾ and Atwood and co-workers⁽¹¹⁾, but the lower value of 33.3kJ mole⁻¹ is considerably higher than Flett's⁽¹¹⁾ value of 15kJ mole⁻¹. However, the maximum loading of copper for a 20% v/v solution of LIX 64N in kerosene in contact with an aqueous phase at pH 1.5 is about 6 g l⁻¹, and for the system under study the loading achieved represents less than 50% approach to chemical equilibrium. Consequently, a significant difference between the present lower value and that of Flett is to be expected. Although about 30% of maximum loading was achieved, the rate controlling process could not be diffusional because the activation energy is greater than 21kJ mole⁻¹ (5 kcal mole⁻¹). The mass transfer values reported in Table 2 indicate that the presence of gangue metals in aqueous solution can significantly affect the rate of transfer of copper into a 20% v/v solution of LIX 64N in kerosene. However, it is emphasised that the gangue metal-copper systems were not of constant sulphate concentration, although they were of equivalent pH value. The gangue metal concentrations employed during these investigations were regarded as being comparable with those that would be obtained on acid leaching of a Kansanshi (Zambia)-type ore. It was also assumed that the lowest pH value of a leach liquor presented for extraction would be in the region of 1.5. The pH value is the controlling parameter in acid leaching and the concentration of sulphate ions contributed by either gangue metal sulphates or sulphuric acid could not

TABLE 4. Variation of Transfer Rate Value with Temperature and Copper Concentration in the Organic Phase. Aqueous Phase: 4.0 g l⁻¹ Copper, 3.25g l⁻¹ H₂SO₄, pH 1.51.

	Organic cycle number	Temperature (°C ± 0.3)		
		25.0	35.0	46.5
Total residence time of drops in column (secs)	1	27.2	26.4	26.2
	2	53.8	52.7	52.4
	3	80.8	79.1	78.5
	4	107.6	105.3	104.3
Copper concentration in organic phase (g l ⁻¹)	1	0.182	0.328	0.536
	2	0.356	0.610	1.00
	3	0.520	0.900	1.44
	4	0.680	1.180	1.88
Rate value × 10 ⁹ (mole cm ⁻² sec ⁻¹)	1	4.53	8.67	14.27
	2	4.62	8.08	13.31
	3	4.49	7.94	12.78
	4	4.41	7.82	12.57

TABLE 5. Variation of Transfer Rate Value with Concentration of Ferric Iron in the Aqueous Phase. Temperature 25 ± 0.3°C.

Copper concn. (g l ⁻¹)	Aqueous System Ferric concn. (g l ⁻¹)	H ₂ SO ₄ concn. (g l ⁻¹)	pH	Mean rate value × 10 ⁹ (mole cm ⁻² sec ⁻¹)
3.94	4.0	2.23	1.54	5.67
3.97	8.0	0.85	1.54	4.70
4.13	12.0	0.0	1.52	4.56

be maintained at a constant value without affecting the pH⁽¹⁹⁾.

Earlier experiments⁽¹⁵⁾ on the effects that gangue metals may have on the rate of extraction of copper indicated that ferric iron could have a deleterious effect, whilst magnesium slightly improved the rate and aluminium had a significant accelerating effect, when the aqueous phase contained a constant acid concentration. If, however, the pH is maintained constant with sulphuric acid, the effects of gangue metals on the rate are not nearly as large. The rate of extraction of copper from the standard copper sulphate-sulphuric acid solution was 4.34 × 10⁻⁹ moles cm⁻² sec⁻¹, whereas when iron(III) or magnesium or aluminium was present in the aqueous phase, the values obtained were respectively 6.74, 3.63 and 6.00 × 10⁻⁹ moles cm⁻² sec⁻¹. Hence the presence of iron or aluminium appears to increase the rate whilst magnesium reduces it. The concentration of a gangue metal, particularly a metal which might co-extract with copper into the organic phase, may have a significant effect on the rate of transfer.

Fleming⁽¹⁴⁾ reported a considerable decrease in rate constants due to the effect of small amounts of ferric ions on the kinetics of copper extraction by LIX 64N, and the effect of ferric ion concentration on the rate of extraction of copper in the single drop column was, therefore, investigated. Transfer rate values were calculated from the gradients of the mass transfer vs. residence time lines shown in Figure 1, and are reported in Table 5. Increasing the ferric iron concentration from 4g l⁻¹ to 12g l⁻¹ reduced the rate value only slightly, from 5.7 to 4.6 × 10⁻⁹ moles cm⁻² sec⁻¹, unlike the magnitude of reduction reported by Fleming (10² sec⁻¹)⁽¹⁴⁾. However, Fleming used purified reagents and, probably more significant, chloroform as diluent. Although the effect of ferric iron on the rate of

extraction of copper appears to reach a maximum in the range 0 to 4gl⁻¹ ferric ion, all the ferric-copper systems studied under the conditions of this investigation had rate values greater than that for the standard copper-acid system.

The nature and concentration of the gangue metal ion is not necessarily the principal factor that influences the kinetics of extraction, and the various systems studied also differed in sulphate ion concentration. The effects of increasing the sulphate anion concentration in the aqueous phase using sodium sulphate are shown in Figure 4. Increasing the sulphate concentration from 9.0gl⁻¹ to 111.8gl⁻¹, whilst maintaining a constant pH value of 1.5, reduces the extraction rate value from 4.34 to 2.11 x 10⁻⁹ mole cm⁻² sec⁻¹, and it is concluded that the rate of transfer of copper from the aqueous into the organic phase is more significantly affected by sulphate ion concentration than by the presence of gangue metals. The

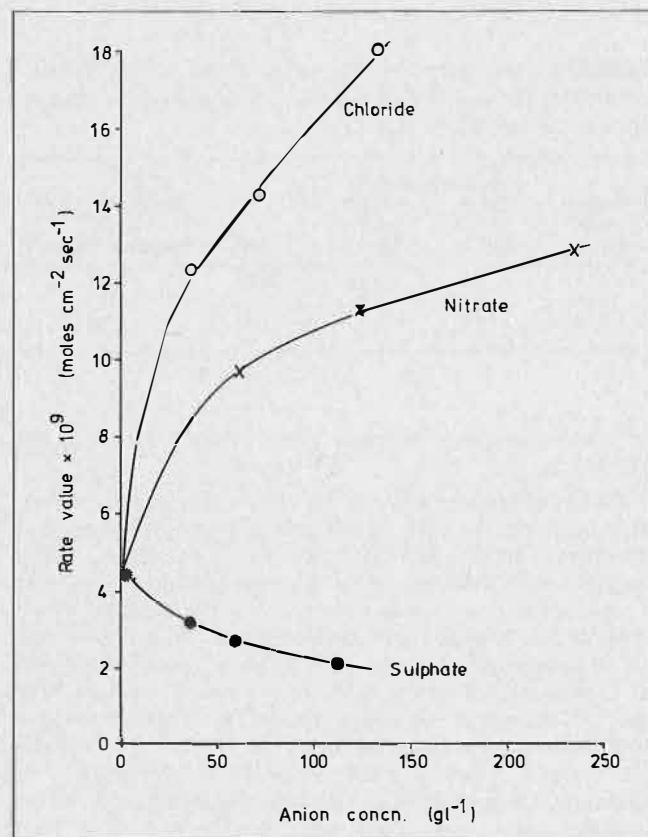


FIGURE 4. Effect of nature and concentration of anions on rate of extraction of copper with 20% v/v LIX 64N in kerosene. Aqueous copper concentration 4gl⁻¹, temperature 25.0 ± 0.3°C.

influence of anions on the transfer rate is even more pronounced when the anionic matrix consists predominantly of chloride or nitrate ions (Figure 4). The present investigation confirmed the previous observation⁽¹⁵⁾ that the rate of extraction of copper from chloride solution is more rapid than that from a corresponding nitrate solution, which in turn is more rapid than from sulphate solutions. The addition of significant quantities of nitrate anion (60gl⁻¹) to a sulphate solution having a total sulphate concentration of 112gl⁻¹ at a pH value of 1.5 increased the rate of extraction of copper from 2.11 to 3.93 x 10⁻⁹ moles cm⁻² sec⁻¹. This increase would be even greater if chloride ions were substituted for nitrate. Unfortunately, it is not possible to decide whether these increases in rate are entirely due to some specific properties of the nitrate or chloride anions or alternatively, to the accompanying increase in the ionic strength of the aqueous solution.

The increased rate of extraction of copper due to the presence of chloride or nitrate anions appears to be common to all copper selective extractants⁽²⁰⁾. It is likely, therefore, that differences in activity of the copper ions in the various aqueous solutions may make a major contribution to the differences in extraction rate, and it is possible also, that if protonation of the extractant molecules occurs in the acid environment, the presence of the various extractant salts will lead to different concentrations of extractant molecules at the phase interface.

The effects of temperature on the rate of extraction of copper from copper sulphate-sulphuric acid and copper-ferric sulphate-sulphuric acid solutions are illustrated in Figure 5 and Table 6. The Eyring plot (Figure 6) was constructed from the natural logarithms of the mean rate values at each temperature, which were obtained from the gradients of the lines in Figure 5. The activation enthalpies calculated for the copper-acid and copper-iron(III)-acid solutions were respectively, 29.7 and 26.3kJ mole⁻¹ (7.1 and 6.3kcal mole⁻¹). These values are in good agreement with that reported by Atwood *et al.*⁽¹¹⁾ and suggest a chemically controlled reaction. It would appear that the presence of a significant quantity of iron(III) in solution does not appreciably affect the activation energy of the extraction of copper.

During this present investigation only the forward reaction, i.e., extraction, was considered; no allowances were made for the reverse reaction, back extraction, since it was not intended to advance a rate equation for the extraction of copper with 20% v/v LIX 64N in kerosene.

Conclusion

The extraction of copper from aqueous solutions containing various gangue metals appears not to be a first order reaction. This finding contrasts with previously

TABLE 6 Effect of Temperature on the Rate of Extraction of Copper from Copper-acid and Copper-iron(III)-acid Solutions.

Aqueous system	Temp. (°C ± 0.3)	Total residence time of drops in column (secs)	Total copper concn. in organic phase (gl ⁻¹)	Mean rate value × 10 ⁹ (mole cm ⁻² sec ⁻¹)
4.0gl ⁻¹ Cu.....	25.0	107.6	0.680	4.22
3.25gl ⁻¹ H ₂ SO ₄	35.0	105.3	1.180	7.28
pH 1.51.....	46.5	104.3	1.88	12.11
3.94gl ⁻¹ Cu.....	25.0	106.0	0.870	5.26
4.0gl ⁻¹ Fe(III).....	35.0	104.4	1.44	8.21
2.23 gl ⁻¹ H ₂ SO ₄	46.5	102.4	2.10	13.49
pH 1.54.....				

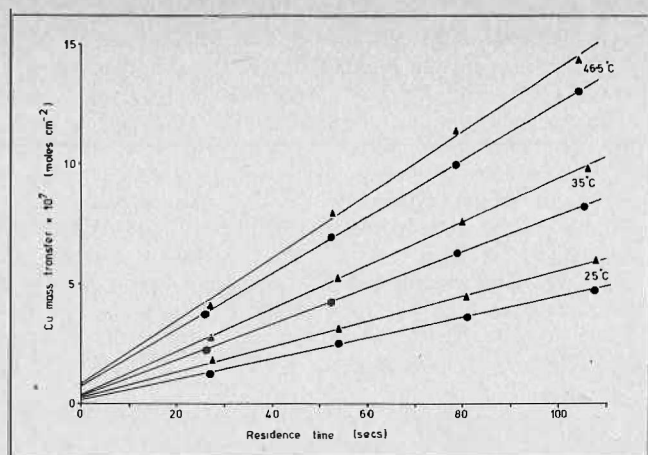


FIGURE 5. Effect of temperature and ferric ions on mass transfer of copper.

Aqueous solutions; ● — 4.0gl^{-1} Cu, 3.25gl^{-1} H_2SO_4 ,
▲ — 3.94gl^{-1} Cu, 4.0gl^{-1} Fe (III),
 2.23gl^{-1} H_2SO_4

published data derived from the single drop technique, but the difference could possibly be explained by the longer residence times of the organic drops in the continuous aqueous phase achieved during the present investigation. The results presented demonstrate that there could be a gradual change of mechanism as the two phases approach equilibrium; a significant decrease in the activation energy, from 41 to 33 kJ mole^{-1} , was measured as the copper content of the organic phase increased to 2gl^{-1} , suggesting a change in the reaction mechanism.

Considering the effects of anions on the rate of extraction of copper from an aqueous phase having a constant pH value, sulphate anions appear to reduce the rate of extraction while nitrate and in particular chloride anions tend to increase it. It was not possible, however, to determine whether ionic strength has a significant effect on the transfer rate, as it is impossible to differentiate between a contribution which is due to an increase in ionic strength and that due to the presence of an anion added when increasing the ionic strength.

The presence of gangue metals does appear to have a small but significant effect on the rate of extraction of copper from aqueous sulphate solutions. The activation energy for the extraction of copper with 20% v/v LIX 64N in kerosene was calculated and found to be 29.7 kJ mole^{-1} for a copper- H_2SO_4 solution and 26.3 kJ mole^{-1} for a 4gl^{-1} ferric ion-copper- H_2SO_4 solution. Increasing the concentration of ferric ion from 4gl^{-1} to 12gl^{-1} reduced the rate of extraction of copper by approximately 18%.

Acknowledgments

Grateful acknowledgment is made to Professor N.A. Warner, Head of the Department of Minerals Engineering, for his interest and encouragement; to N.C.C.M. (Zambia) for financial support and for permission to publish this paper; and to Dr. R.J. Whewell of the University of Bradford and Messrs. B. Hail and R. Sutton of the University of Birmingham for their advice and assistance in the construction of the single drop apparatus.

REFERENCES

- (1) Flett, D.S., Okuhara, D.N. and Spink, D.R., *J. Inorg. Nucl. Chem.* 1973, 35, 2471.
- (2) Whewell, R.J., Hughes, M.A. and Hanson, C. *ibid.* 1975, 37, 2303.

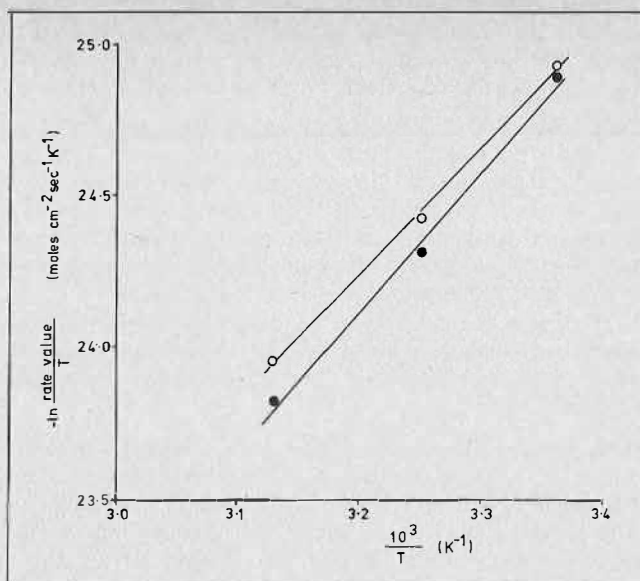


FIGURE 6. Arrhenius plot for extraction of copper from copper-acid and copper-iron(III)-acid solutions.

● — 4.0gl^{-1} Cu, 3.25gl^{-1} H_2SO_4
▲ — 3.94gl^{-1} Cu, 4.0gl^{-1} Fe(III), 2.23gl^{-1} H_2SO_4

- (3) Spink, D.R. and Okuhara, D.N., *Metall. Trans.* 1974, 5, 1935.
- (4) Flett, D.S., Hartlage, J.A., Okuhara, D.N. and Spink, D.R., *J. Inorg. Nucl. Chem.* 1975, 37, 1967.
- (5) Spink, D.R. and Okuhara, D.N., *Proc. Internat. Solvent Extn. Conf. ISEC 74*, Society of Chemical Industry, London, 1974, 3, 2527.
- (6) Baumgartner, F. and Finsterwalder, L., *J. Phys. Chem.* 1970, 74, 108.
- (7) McKay, H.A.C. and Rees, D., *AERE-C/R-1199*, Harwell, 1953.
- (8) Knock, W. and Lindner, R., *Z. Elektrochem.* 1960, 64, 1020.
- (9) Hughes, M.A., Preston, J.S. and Whewell, R.J., *J. Inorg. Nucl. Chem.* 1976, 38, 2067.
- (10) Whewell, R.J., Hughes, M.A. and Hanson, C., *J. Inorg. Nucl. Chem.* 1976, 38, 2071.
- (11) Atwood, R.L., Thatcher, D.N. and Miller, J.D., *Metall. Trans.* 1975, 6B, 465.
- (12) Brisk, M.L. and McManamey, W.J., *I. Chem. E. Symposium Series No. 26*, p. 21. Instn. Chem. Engrs. London, 1967.
- (13) Brisk, M.L. and McManamey, W.J., *J. Appl. Chem.* 1969, 19, 109.
- (14) Fleming, C.A., Report No. 1793, National Institute for Metallurgy, Johannesburg, 1976.
- (15) Eccles, H., Lawson, G.J. and Rawlence, D.J., *Hydrometallurgy* (in press).
- (16) Farbu, L., McKay, H.A.C. and Wain, A.G., *Proc. Internat. Solvent Extn. Conf. ISEC 74*, Society of Chemical Industry, London, 1974, 3, 2427.
- (17) Nitsch, W., *Dechema Monograph*, 1965, 55, 143.
- (18) Vogel, A.I., "A Textbook of Quantitative Inorganic Analysis". Longmans, London 1962, p. 343.
- (19) Eccles, H., Lawson, G.J. and Rawlence, D.J., *Hydrometallurgy* (in press).
- (20) Ellender, P.S. and Lawson, G.J., *Chem. and Ind.* (in press).

DISCUSSION

M.H.I. Baird: Did you compare your measured extraction rates with values predicted from correlations for diffusional mass transfer?

H. Eccles: No we did not. I agree this may be a useful study if we intend to propose a reaction mechanism or equation.

Y.A. Yagodin: How did you treat the drops; as rigid or oscillating ones? What was the dispersion from experiment to experiment under the same conditions? Can anything be said about the place of limiting reaction?

H. Eccles: The drops were treated as rigid spheres when calculating the droplet radius. We did calculate the percentage circulation of the drop and found this to be of the order of 25%. The dispersion of the drops, and I assume you mean the droplet rate of formation, was always within the range 65 to 68 drops per min for all our investigations.

It is possible to suggest a place of limiting reaction from our studies, but the present theories proposed by other workers suggest it is an interfacial controlled reaction.

G.A. Davies: In your presentation you showed data for drop formation rates over the range 63-68 drops/min and stated that this parameter was investigated. This range would not be significant to draw this conclusion. The drop formation rate will certainly have a significant influence on the overall mass transfer achieved, particularly for short columns. Have you considered this? Did you consider using short columns, in addition to present equipment, to investigate the mechanism of mass transfer?

H. Eccles: Drop rates from 20 to 120 drops per minute have been studied on previous occasions. The

mass transfer of copper from the aqueous to the organic phase is dependent upon the rate of injection of organic droplets through the continuous phase. However we observed that above 40 drops min^{-1} the mass transfer was relatively constant, i.e., approximately with a 5% error and therefore independent of drop rate. We have now commenced studying the mass transfer of copper using a technique which effectively reduces the length of the column. It was not our original intention to investigate the mechanism of mass transfer as I explained during the presentation. We were initially concerned with comparing mass transfer data obtained with aqueous solutions that could possibly be obtained if the leaching agent for the ores (copper) was changed.

W.C. Cooper: How do you explain the effect of the Cl^- , NO_3^- and SO_4^{2-} anions on the rate of extraction?

H. Eccles: The increased rate of extraction of copper due to the presence of chloride or nitrate anions appears to be common to all copper-selective extractants. We believe therefore, that the differences in the activity of copper ions in the various aqueous solutions may make a major contribution to the differences in extraction rate, and it is possible also that if protonation of the extractant molecules occurs in the acid environment, the presence of the various extractant salts will lead to different concentrations of extractant molecules at the interface.

MASS TRANSFER

Kinetics and Mechanism of Copper Extraction with 5-alkyl-2-hydroxyphenyl Alkyl Ketoximes

A. J. van der Zeeuw and R. Kok,
Koninklijke/Shell-Laboratorium,
Amsterdam (Shell Research B.V.),
The Netherlands.

ABSTRACT

The paper involves work done to elucidate the kinetics and mechanism of the copper-chelating reaction with hydroxy oximes. The kinetics of the forward and backward reaction were measured independently; from the results, together with theoretical considerations, it is concluded that the mechanism very likely involves the dimer of the reagent. The work shows that both accelerators and retardants can be classified as compounds showing a higher interfacial activity than the reagents proper. The actual involvement of the accelerators in the mechanism still remains unclear. Some fresh views are put forward on the influence of diluents and modifiers.

Experimental

Kinetic Measurements

Solutions, Preparation of Chemicals

THE AQUEOUS SOLUTIONS were made up from analytically pure chemicals and contained an ionic background of 0.5 M Na_2SO_4 .

The organic solutions were made up in analytically pure diluents. Oximes of the (5-alkyl-2-hydroxyphenyl)-n-alkyl ketoxime type were prepared by subjecting the 4-alkylphenyl esters to a Fries rearrangement, distilling the ketones formed, oximating them and recrystallizing the oximes various times, in most cases from pentane or heptane.

Syn-2-hydroxy-5-nonylbenzophenone oxime (syn-HNBPO) was prepared by boiling diluent-free commercial LIX® 65 N with 4N aqueous/alcoholic NaOH for 12 hours. After working-up and isolation, the syn-HNBPO had a melting point of 114-115°C.

Anti-HNBPO was prepared by separating the isomers of diluent-free commercial LIX® 65 N through column chromatography on activated silica. Thin-layer chromatographic analysis showed that each of the isomers was free of the other.

"Diluent-free 5,8-diethyl-6-hydroxy-7-oximinododecane (DEHOD) was prepared by dissolving commercial LIX® 63 in methanol, adding slowly under stirring a methanol solution of $\text{Cu}(\text{CH}_3\text{COO})_2 \cdot \text{H}_2\text{O}$, filtering off the olive-green crystalline precipitate, washing the latter repeatedly with acetone, and drying it in the air. Then the crystalline copper complex was dissolved in heptane and treated three times with excess of 2 N H_2SO_4 . Because even then some copper remained in the organic layer, the latter was washed once more with 0.5 N HNO_3 . The colourless

TABLE 1. Survey of Kinetic Experiments Under Relaxation Conditions

Experiments reported in this table were done in toluene unless stated otherwise. All concentrations are in mmoles/l.

Exp.	Initial conditions		Equilibrium, conditions				
	[RH] _{o/a}	[Cu]	[RH] _{f/a}	[Cu]	[Cu]	D _{Cu}	pH
A	20	11.7	17.8	1.1	10.6	0.106	1.53
B	20	2.2	18	1.0	1.2	0.83	2.00
C	20	1.18	18	1.05	0.12	8.86	2.52
D	20	0.99	18	0.97	0.02	43.9	2.98
E	20	11.1	18.1	0.93	10.2	0.091	1.50
F	20	1.9	18.4	0.79	1.13	0.69	1.92
G	20	1.6	17.3	1.35	0.20	6.82	2.51
H	6	3.6	5.9	0.25	3.37	0.075	2.00
I	10	2.3	9.3	0.38	1.89	0.20	2.00
K	60	3.4	53	3.0	0.47	6.23	2.00
L	= H						
M	= B						
N	= K						
} but with tracer copper added to the organic phase instead of the aqueous phase							
2. Experiments with anti-2-hydroxy-5-nonylbenzophenone oxime (anti-HNBPO)							
P	20	2.0	18.2	0.80	1.20	0.67	2.00
3. Experiments with HOPHO in heptane							
Q	20	1.85	18.0	0.98	0.88	1.11	1.50
R	20	1.06	18.1	0.96	0.09	10.2	2.00
S	= Q						
T	= R						
} but with tracer copper added to the organic phase instead of the aqueous phase							

organic layer was then dried over Na₂SO₄ and the diluent evaporated to leave a white crystalline material with melting point 40-41 °C.”

Apparatus, Operating Conditions, Procedure, and Reliability

A cylindrical double-walled glass vessel (capacity 250 ml, internal diameter 70 mm) was used, equipped with four baffles (width 70 mm), a bottom sampling cock (no dead space), a quickfit flange lid with the necessary inlet and outlet tubes, and a six-bladed turbine stirrer (tip-to-tip diameter 28 mm). In all experiments the position of the stirrer was 5 mm below the interface.

In all experiments the organic phase was held as the continuous phase. The organic/aqueous (O/A) phase ratio was 1/1, 100 ml of each phase being present at the start of each experiment. The stirrer speed throughout was 2000 ± 20 rev/min. The temperature was maintained at 25 ± 0.2 °C by means of a thermostat bath connected to the double wall of the vessel.

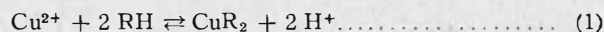
The kinetic experiments were carried out using the relaxation technique⁽¹⁾. After equilibration of the phases with respect to copper distribution and temperature, the layers were separated and one of the phases was seeded with radio-active copper. The actual experiment was then started by rapidly adding the aqueous phase to the organic phase under stirring. This was timed to take 3 seconds. End of addition was set as time zero. Dispersion time in this reactor is less than 1 second.

Sampling was done from the bottom cock. The absence of dead space meant that homogeneous sampling was ensured. The size of the samples was ± 6 ml. After phase disengagement, which took 7 seconds, the layers were separated and analysed.

The fact that mixing and disengagement of the phases normally takes time might be a reason to question the reliability of the method used. However, the total uncertainty (approx. 11 seconds) was only 6% on the fastest run reported, and less than 3% on most. We therefore neglected the time effect. The good reproducibility of the measurements shows that this was justified.

The Kinetics of the Forward and Backward Reactions

In its simplest form the reaction between a copper ion and a single chelating reagent can be presented as:



This equation, which fully disregards any aspects of mechanism, polymerization of the reagent, etc., indicates which dependences one has to establish in order to devise a suitable rate equation.

The forward reaction will at least be dependent on the Cu²⁺ concentration at the site of the reaction, and on a free (i.e. not copper-bound) reagent concentration. Other factors, like hydrogen ion concentration, or complex concentration, might be reflected in the rate of the forward reaction if they play a role in the mechanism. The backward reaction will show dependences on hydrogen ion concentration and complex concentration, and again on any factors that might creep into the mechanism.

Under conditions of equilibrium, Flett et al.⁽¹⁾ have carried out tracer experiments and interpreted the results on the basis of

$$k_f t = \frac{[Cu]_o - [Cu]_{eq}}{[Cu]_o} \ln \frac{[Cu]_o - [Cu]_{eq}}{[Cu]_t - [Cu]_{eq}} \dots \dots \dots (2)$$

Let us consider the differentiated rate equation of a process as in equation (1), and also take into account possible complications as indicated. The rate of disappearance of Cu²⁺ from the aqueous phase will be given by:

$$-\frac{dCu}{dt} = k_f [RH]_{free}^w [X]^x [Y]^y [Z]^z [Cu] - k_r [P]^p [Q]^q [R]^r [H]^m [CuR_2] \dots \dots \dots (3)$$

provided the reactions are first order in copper ions and in complex. [X]^x, [Y]^y etc. indicate any additional factor that might influence the kinetics apart from the obvious one. It can easily be seen that when one looks for the dependency on copper concentration and all other factors are constant (that is, at conditions of equilibrium as in Flett's tracer studies) this equation reduces to:

$$-\frac{dCu}{dt} = k_f [Cu] - k_r [CuR_2] \dots \dots \dots (4)$$

Simple mathematical treatment easily leads to equation (2), as illustrated in Ref. 2.

The fact that this relation produces a straight line with the experimental data through a considerable range of conversions supports the hypothesis of a first order dependence on aqueous and organic copper concentrations.

A survey of the most important data relevant to the kinetic experiments done by us is given in Table 1. The letter references used in figures relate to this table as well.

1. The Influence of the Hydrogen Ion Concentration

Flett et al. have found that in the extraction of Cu^{2+} with LIX 64 N the rate of disappearance of Cu^{2+} from the aqueous phase is inversely proportional to the hydrogen ion concentration, all other factors being kept constant. Thus, in the symbols of equation (2):

$$k_f' = k_f'' [\text{H}^+]^{-1} \quad (5)$$

Miller and Atwood⁽²⁾, however, argued that, in fact, the apparent inverse first-order relation found resulted from a direct first-order relation between the rate of the *backward reaction* and the hydrogen ion concentration, or, in terms of equation (4):

$$k_r' = k_r'' [\text{H}^+]^{+1} \quad (6)$$

One may put the conditions given in equations (5) and (6) in a more general form, and assume that the forward rate depends on the m^{th} power of the hydrogen ion concentration, and the reverse on the n^{th} power of that same concentration. Or in formulae:

$$k_f' = k_f'' [\text{H}^+]^m \quad (5')$$

$$k_r' = k_r'' [\text{H}^+]^n \quad (6')$$

Now the following reasoning can be set up:

$$k' = k_f' \frac{[\text{Cu}]_{\text{eq}}}{[\text{Cu}]_{\text{aq}}} \quad (7)$$

Substitution of (5') and (6') into (7) then yields:

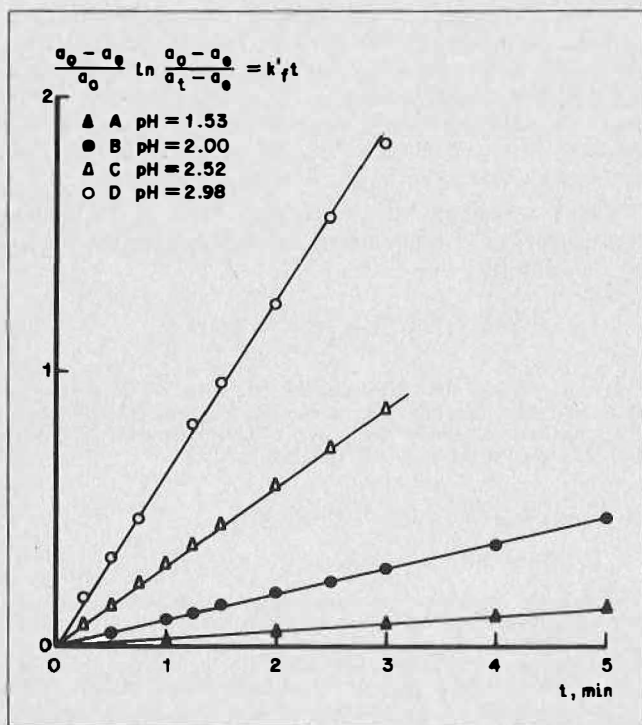


FIGURE 1. The rate expression as a function of time at different pH. Forward reaction, HOPHO in toluene. Tracer copper added to aqueous phase.

$$k_f' [\text{H}^+]^n = k_f'' [\text{H}^+]^m \frac{[\text{Cu}]_{\text{eq}}}{[\text{Cu}]_{\text{aq}}}, \text{ or}$$

$$k_f' = k_f'' [\text{H}^+]^{n-m} \frac{[\text{Cu}]_{\text{eq}}}{[\text{Cu}]_{\text{aq}}} \quad (8)$$

Now the equilibrium constant K_{eq} derived from equation (1) is*:

$$K_{\text{eq}} = \frac{[\text{CuR}_2]}{[\text{Cu}] [\text{RH}]^2}, \text{ or} \quad (9)$$

$$\frac{[\text{Cu}]_{\text{eq}}}{[\text{Cu}]_{\text{aq}}} = K_{\text{eq}} \frac{[\text{RH}]^2}{[\text{H}^+]^2} \quad (10)$$

By combining (8) and (10) it follows that

$$k_f' = k_f'' K_{\text{eq}} [\text{RH}]^2 \times [\text{H}^+]^{n-m-2} \quad (11)$$

and, since k_f' is now by definition no longer a function of H^+ :

$$n - m - 2 = 0 \quad (12)$$

The experimental result of Flett et al.⁽¹⁾ being that $m = -1$, it follows of necessity that n must be $+1$. If, as Miller and Atwood⁽²⁾ suggest, $m = 0$, the consequence is that n must be 2.

*This part of the derivation depends on the assumption that the overall correctness of equation (2) is satisfactorily demonstrated by the relations found by various authors between D_{Cu} and pH and between D_{Cu} and reagent concentration. We feel that this is in fact true.

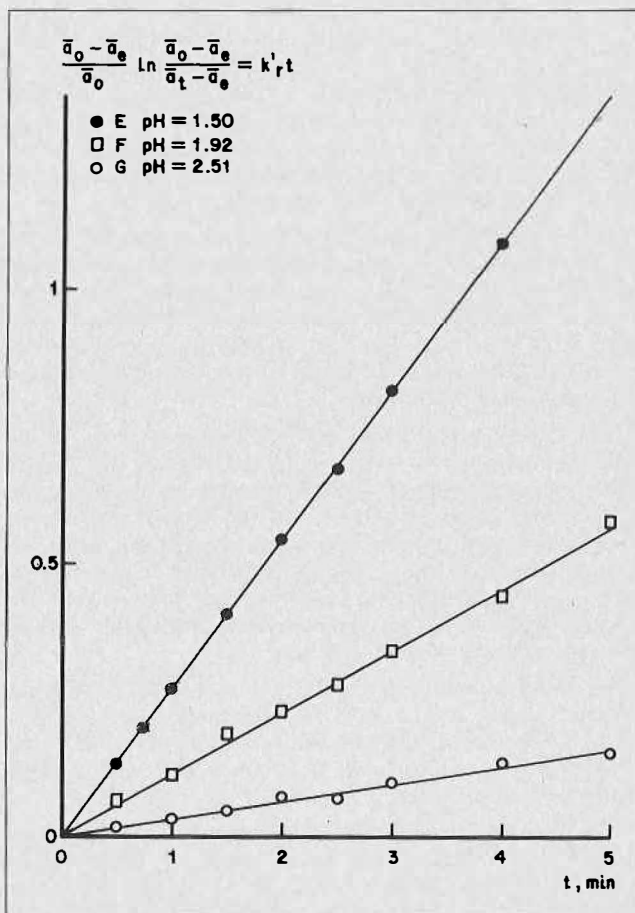


FIGURE 2. The rate expression as a function of time at different pH. Backward reaction, HOPHO in toluene. Tracer copper added to organic phase.

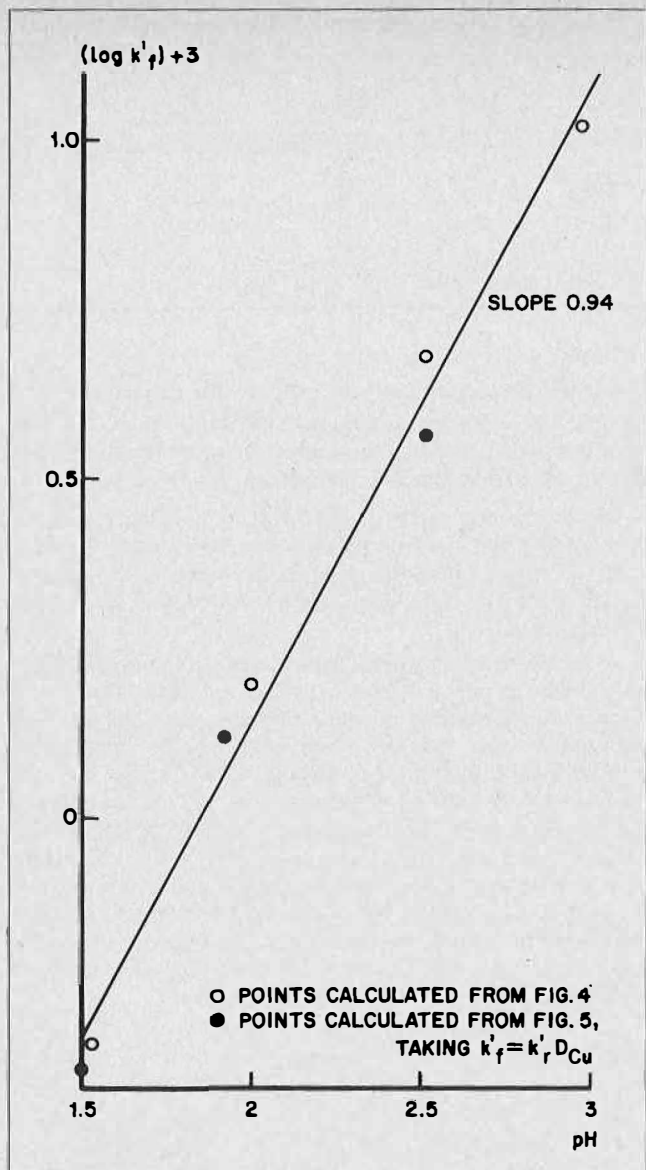


FIGURE 3. Relation between k'_f and pH. HOPHO in toluene.

Figures 1-4 present the results of a series of experiments with chemically pure (2-hydroxy-5-tert-octylphenyl)-n-heptyl ketoxime (HOPHO) in toluene as a function of pH. The rates were followed under relaxation conditions with tracer copper distribution. Care was taken that both the free organic reagent concentration and the copper complex concentration were kept equal in all experiments, so that the property under investigation could be properly isolated.

The rate of the forward reaction was followed by adding tracer copper to the aqueous phase (Figure 1) and that of the backward reaction by adding tracer copper to the organic phase (Figure 2).

Figure 3 shows the relation between the forward rate constant and pH*. Both the constants measured directly from Figure 1 and those derived from the measured values of Figure 2 via formula (7) are given. Similarly, Figure 4 gives the relation between the backward rate constant and pH. The slopes of the plots are 0.94 and -0.90, respectively, close enough to unity to substantiate the view that

*It must be realized that the rate constants discussed throughout this work are still a function of the interfacial area.

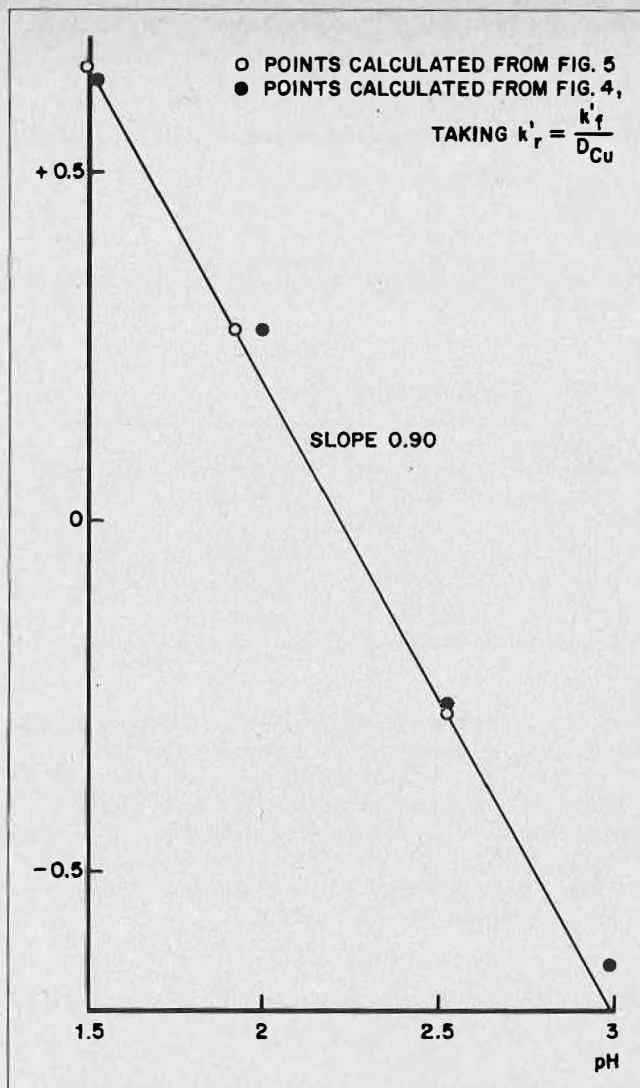


FIGURE 4. Relation between k'_r and pH. HOPHO in toluene.

in equation (12) $n = 1$ and $m = -1$. In other words, the forward reaction is inversely proportional, and the backward reaction directly proportional, to the hydrogen ion concentration.

2. The Influence of the Free Reagent Concentration

A reasoning similar to that given for the pH dependence leads to the conclusion that, in terms of equation (3):

$$w - p - 2 = 0 \dots\dots\dots (13)$$

if [P] is the free monomeric reagent influencing the backward reaction, and p its exponent in the rate equation.

In interpreting the results of experiments designed to find the relation between rate and reagent concentration, one faces a fundamental problem: to decide whether the reagent concentration should be expressed in terms of free (that is not bound to copper) analytical concentration, $[RH]_{t,a}$, free monomeric reagent, $[RH]_{t,m}$, or free dimeric reagent, $[(RH)_2]_t$. In the context of this paper we shall (for reasons which will become clear) express the relation to be found in terms of both free monomeric reagent, $[RH]_{t,m}$, and free dimeric reagent $[(RH)_2]_t$.

It is now generally accepted that the reaction between copper and the chelating reagent is an interfacial one. Our

TABLE 2. Data on Dimerization of Some Oximes in 0.01 – 0.04 M Solutions in Toluene and Isooctane

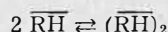
Oxime	MW	Toluene			Isooctane		
		MW _{app}	α*	K _{eq} *	MW _{app}	α*	K _{eq} *
2-Hydroxy-5-tert-octyl acetophenoxime	263	301	0.25	8.9	372	0.59	70
HOPHO	347	378	0.17	5.0	486	0.57	62
2-Hydroxy-5-methylphenyl-n-heptyl ketoxime	248	281	0.23	7.8	340	0.54	51
anti-HNBPO	339	368	0.16	4.5	439	0.46	32
syn-HNBPO	339	385	0.24	8.3		insoluble	
DEHOD	271	304			374		

*These values for α and K_{eq} were calculated using 0.025 as the average concentration in the range measured.

TABLE 3. Concentration Data.

Original oxime conc. [RH] _{0,a} ' M	Free oxime conc. [RH] _{fr,a} ' M	Free monomer conc. [RH] _{f,m} ' M	Free dimer conc. [(RH) ₂] _f ' M
0.006	0.0058	0.00552	0.00014
0.01	0.0093	0.00863	0.00034
0.02	0.018	0.0158	0.001
0.06	0.053	0.039	0.007
0.1	0.088	0.058	0.015

work concerning interfacial tensions and interfacial population densities of hydroxy oximes⁽³⁾ leads us to believe that the reagent will collect at the interface predominantly as a monomer. On the other hand it has been suggested^(4,5) that in the bulk phase, hydroxy oximes occur at least partly as dimers. Table 2 presents a few data on apparent molecular weights, degree of dimerization α and equilibrium constants K_{eq} for the reaction



for some chemically pure oximes in toluene and isooctane.

In the interpretation of our experiments carried out with HOPHO in toluene we calculated $[\overline{RH}]_{f,m}$ from the free stoichiometric reagent concentration using the value 5.0 for K_{eq} and assuming 2/1 complexation with copper.

The values for $[\overline{RH}]_{f,m}$ and $[(\overline{RH})_2]_f$ used in Figures 5 and 6 and some other useful data are presented in Table 3.

It can be seen that especially in the higher concentration range a considerable part of the oxime will be in the dimeric state.

A series of experiments with chemically pure HOPHO in toluene at pH 2.0 under relaxation conditions (tracer copper added to the aqueous system) gave the relation between k'_f and the free monomeric reagent concentration illustrated in Figure 5. It may be concluded that the dependency is close to a second-order one. Alternatively, the figures may be plotted against $[(\overline{RH})_2]_f$, in which case a neat first-order plot is obtained (Figure 6). When one plots the forward rate constants against the free analytical reagent concentration, the slope is 1.76, which deviates considerably from 2. In retrospect this may be seen as a justification for not choosing the free analytical reagent concentration as the variable in the plotting.

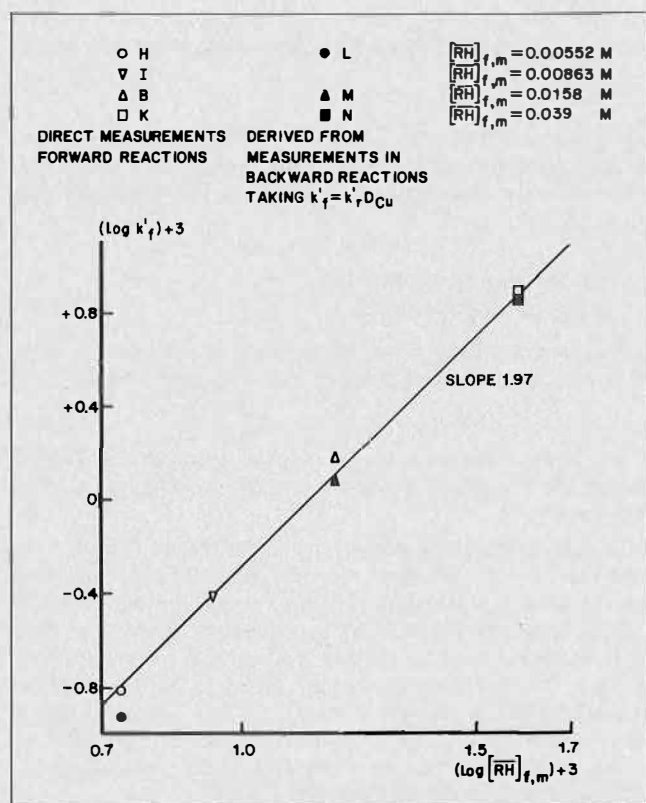


FIGURE 5. Relation between k'_f and free monomeric reagent concentration at pH 2.00. HOPHO in toluene.

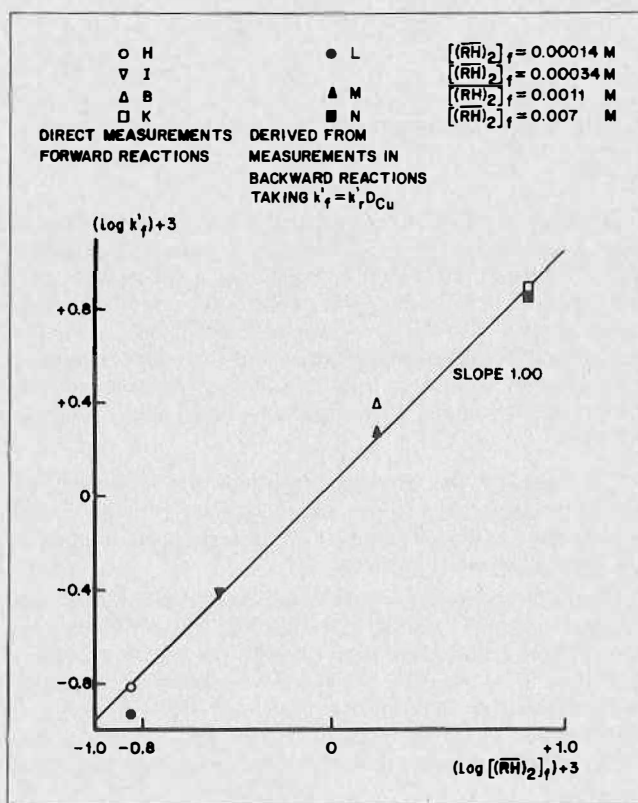


FIGURE 6. Relation between k'_f and free dimeric reagent concentration at pH 2.00. HOPHO in toluene.

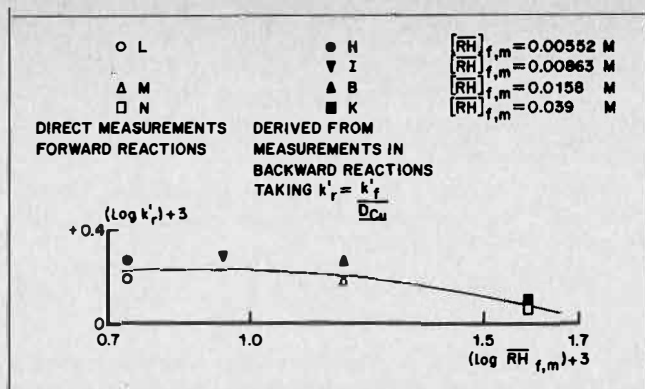


FIGURE 7. Relation between k'_r and free monomeric reagent concentration at pH 2.00. HOPHO in toluene.

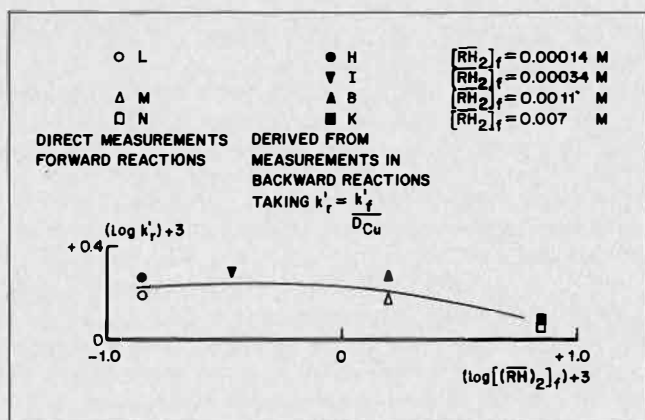


FIGURE 8. Relation between k'_r and free dimeric reagent concentration at pH 2.00. HOPHO in toluene.

The results for the stripping reaction presented in Figures 7 and 8, are less easy to interpret. In the low concentration range the dependency of k'_r on both the free monomeric and dimeric reagent concentrations is obviously zero order. At higher concentrations the picture becomes somewhat complicated, because the plot acquires a slope. The slope is however slight, and might easily be caused by increasing deviation of the organic phase from the ideal state. This would undoubtedly come out more strongly in the stripping reaction than in the extraction, since in the former, one has to consider the behaviour of the copper complex. It would appear justified to describe the back reaction as basically zero order in free reagent concentration.

3. The Influence of the Diluent

In general terms, the change from an aromatic to an aliphatic diluent is known to result in better pH functionality of the reagent and in higher extraction rates.

In experiments using n-heptane as the diluent a serious difficulty is the limited time available. The useful period for measurements in toluence can easily be 10 minutes or longer, whereas the reactions in heptane are over within 2-3 minutes. In our experimental process this causes problems in timing of samples; it also means that the time needed for combining the phases and for phase disengagement after sampling can no longer be neglected.

Keeping in mind the above reservations, the measurements carried out and shown in Figures 9 and 10 appear very reasonable.

Table 4 compares the rate constants shown in Figures 9 and 10 with those measured in toluene under comparable conditions.

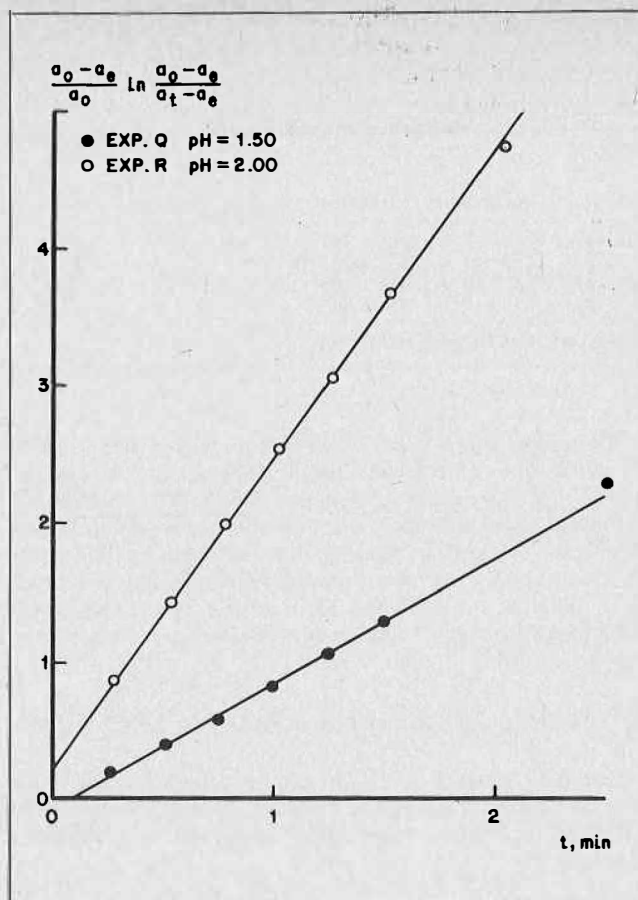


FIGURE 9. The rate expression as a function of time at different pH. Forward reaction, HOPHO in heptane. Tracer copper added to aqueous phase.

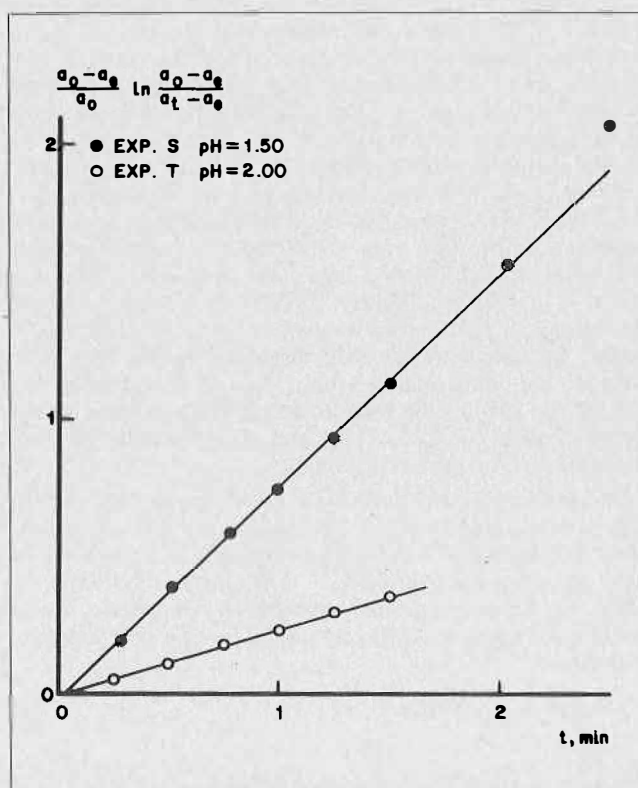


FIGURE 10. The rate expression as a function of time at different pH. Backward reaction, HOPHO in heptane. Tracer copper added to organic phase.

TABLE 4. Reaction Rate Constants of Copper Extraction and Stripping with HOPHO in Toluene and Heptane at 25°C

Initial concentration 0.02 M						
pH		Heptane	Toluene*	Ratio	D _{Cu}	
					Heptane	Toluene*
1.50	k _f '	14.6 × 10 ⁻³	0.46 × 10 ⁻³	31.7	1.15	0.1
	k _r '	12.7 × 10 ⁻³	4.70 × 10 ⁻³	2.7		
2.00	k _f '	40.8 × 10 ⁻³	1.41 × 10 ⁻³	28.9	10.2	0.82
	k _r '	4.0 × 10 ⁻³	1.58 × 10 ⁻³	2.5		

*Values extracted from Figures 3 and 4.

Two conclusions can be drawn from above data. Firstly, as in the case of toluene, the dependencies of k_f' and k_r' on [H⁺] are again minus first and first order, respectively. Secondly, both the forward and the backward reactions are faster in heptane than in toluene, but the difference is much greater for the forward reaction. The net result is in practice found in the form of the known better pH functionality (higher distribution coefficient at equal pH) for the aliphatic diluent.

4. The Rate Equation and a Possible Mechanism

From Sections 1 and 2 it can now be concluded that the rate equation for the reaction of copper ions with HOPHO in toluene may have either of the following forms:

$$-\frac{dCu}{dt} = k_f' [\overline{RH}]_{i,m}^2 [H^+]^{-1} [Cu] - k_r' [H^+] [\overline{Cu}] \dots (15a)$$

$$-\frac{dCu}{dt} = k_f' [(\overline{RH})_2]_f [H^+]^{-1} [Cu] - k_r' [H^+] [\overline{Cu}] \dots (15b)$$

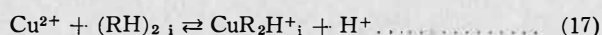
In attempts to find a mechanism fitting these equations one has to take into consideration that at least the initial reaction is assumed to take place at the interface. In the concentration range studied the interfacial population density of "an" oxime species in HOPHO/toluene solutions is virtually constant, as can be seen from the slope of the σ₁/log C plot in Figure 11. Although these measurements refer to a static system, it is reasonable that the conclusion also holds for a dynamic (extracting) one: because of the high rate of diffusion of fresh reagent molecules to the interface, the latter will still maintain a constant population density. This in fact means that, if the species populating the interface creeps into the mechanism, its concentration will disappear in the rate constant(s). The consequence now is that, if one accepts that one of the species (HOPHO)₂ or HOPHO collects at the interface, rate equations (15a) and (15b) must result from the influence of "the other one".

It has been argued in Section 2 that the species collecting at the interface will probably be the monomer, HOPHO. Because of the high degree of satisfaction of its need for hydrogen bridging⁽⁵⁾ the dimer, (HOPHO)₂ is likely to behave neutrally towards the interface, or it might even show a slight preference for the bulk organic. In formula:

$$[(\overline{RH})_2]_i = a [(\overline{RH})_2] \dots (16)$$

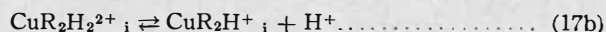
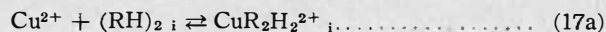
$$a \leq 1$$

We now propose the following mechanism:



Equations (16) through (19) lead to rate equation (15b), if (18) is rate determining. Because of the fixed relation through the dimerization constant between [(RH)₂]_f and [RH]_{f,m} equation (15a) will also hold.

It should be stated that, by splitting equation (17) into two parts, one obtains a mechanism similar to that proposed by Price and Tumilty⁽⁴⁾, e.g.:



The only difference is that the present authors suggest a two-step dissociation of the complex CuR₂H₂²⁺ in order to account for the rate dependencies.

Apart from fitting the rate equations, the mechanism also qualitatively explains the difference in behaviour found between toluene and heptane as diluents (Section 3). In the more polar toluene the dimer concentration is lower, which leads to a decrease in the overall forward rate constant. The influence on the backward rate constant (which is independent of the reagent concentration) is much less pronounced. In the extreme case of solutions in ethers or ketones one would estimate that there was very little dimer present. Ether solutions of hydroxy oximes do not extract copper from acidic medium, only from ammoniacal medium.

Side by side with the effect of diluents on dimer concentration goes their influence on interfacial concentration (or concentration close to the interface) of any reagent species. The mutual imponderability of these effects is still an obstacle to a more quantitative explanation.

In some cases modifiers are added to a chelating reagent, usually to improve the general level of its performance or handlability. The modifiers are often oxygen-containing polar compounds, like higher phenols or alcohols, or tributyl phosphate. They are usually added in considerable quantities, e.g. 10-40% on total diluent volume, and sometimes more, and one frequently finds that the "modified" reagent has a lesser pH functionality than the pure one⁽⁶⁾. As stated in 3, such a decreased pH functionality does in fact mean that k_f' is more strongly negatively influenced than k_r'. It might well be that this effect of modifiers belongs to the same category as the diluent effect.

5. The Influence of Accelerators and Retardants

The role of accelerators in the extraction of copper with hydroxy oxime extractants is far from clear. With respect to the one case which has been investigated to some depth, i.e. the combination LIX® 65N + LIX® 63, it has been found⁽¹⁾ that the latter appears in the rate equation of the forward reaction to an approximate 0.5 order, and a mechanism was proposed to account for that dependency.

On the basis of the same work⁽¹⁾, however, other authors⁽²⁻⁷⁾ proposed mechanisms that differed markedly from the first one, as well as from each other, and it was rightly stated⁽⁷⁾ that the role of the accelerator is still unknown.

When adopting the view that the primary reaction between copper ions and the chelating reagent takes place at the interface, a possible mental step is to assume that the accelerator interferes with the mechanism at that same interface⁽⁷⁾. A consequence of that idea would be that a category of retardants can also exist: strongly polar, non-chelating compounds that may successfully compete with the extractant for space at the interface. Ultimately one may then conceive that the accelerator may exert one or

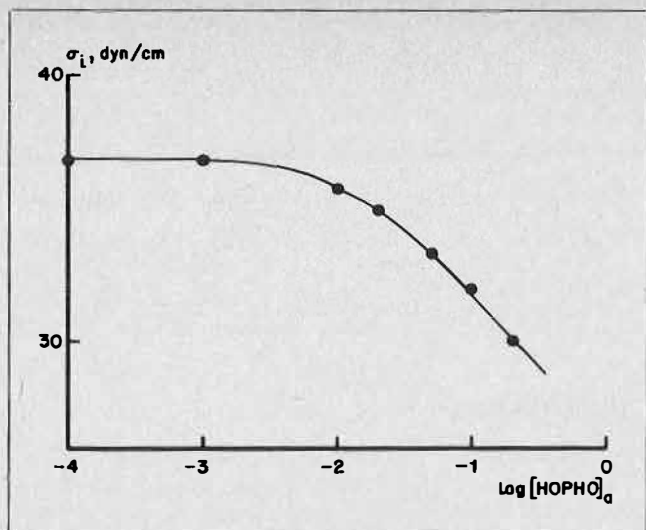


FIGURE 11. Interfacial tension of HOPHO in toluene at 25°C with 0.5 M Na₂SO₄ at pH 2.0.

TABLE 5. The Influence of Accelerators and Retardants on k' :

Oxime	Standard exp.	Compound added	mmole/l	mole % on oxime	$k' \times 10^{-3}, s^{-1}$
HOPHO	B	—	—	—	1.55
	B	DEHOD	0.20	1.00	1.38
	B	DEHOD	0.27	1.35	1.13
	B	DEHOD	0.68	3.4	2.53
	B	DEHOD	2.0	10.0	3.58
	B	tert-octylphenol	2.0	10.0	1.52
	B	tert-octylphenol	4.0	20.0	1.46
	anti-HNBPO	P	—	—	—
	P	DEHOD	0.68	3.4	4.1
	P	syn-HNBPO	2.0	10.0	4.9

both of the following functions:

1. act as an accelerator proper, because of its assumed high rate of reaction with the copper, or (and)
2. compete with retardants for space at the interface.

Table 5 shows the influence of some accelerating and retarding compounds on the forward reaction rate of two oximes with copper ions, measured under relaxation conditions. The initial and equilibrium conditions of the standard (blank) experiments are given in Table 1 under letter B for HOPHO and P for anti-HNBPO.

The highly surprising conclusion to be drawn from Table 5 is that DEHOD, a well-known accelerating molecule, starts to work as an accelerator only at quite a high concentration, and that below that it even is a retardant.

A very marked retarding effect is also shown by syn-HNBPO. The latter starts to display extracting action at high pH values, and to all intents and purposes may be considered here to be non-chelating. Tertoctylphenol shows little activity as a retardant, and it is only expected to influence reaction rates strongly at high concentrations, which is in line with literature findings⁽⁶⁾.

The interfacial population density of a solute in a two-phase system can be calculated from the slope of a plot of the interfacial tension σ_i against the logarithm of the concentration of that solute⁽³⁾. The numerical value obtained, however, is indicative of the space a molecule needs at the interface, rather than of the tendency for such a molecule to collect at the interface.

This tendency is expressed more appropriately in the solute concentration at which a decrease in the interfacial tension becomes observable. A direct visualization of this

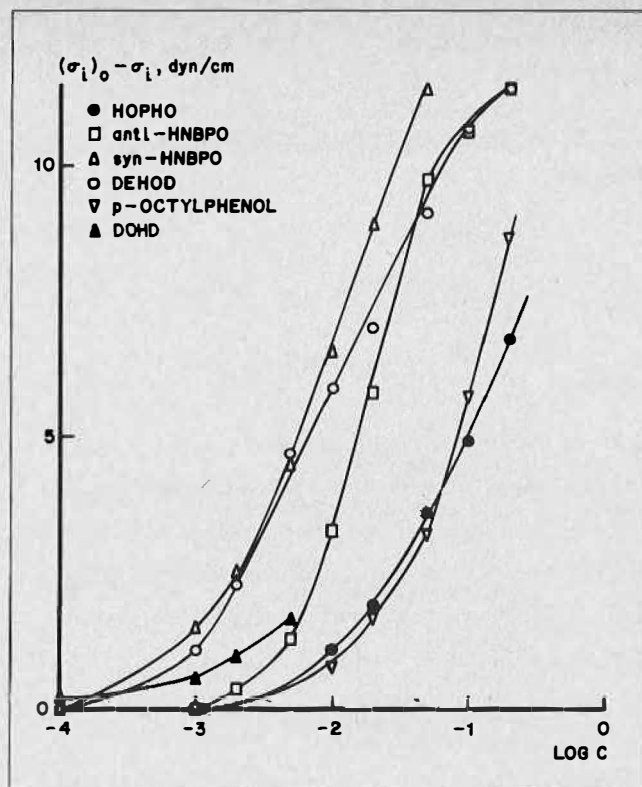


FIGURE 12. Interface pressures of extractants, accelerators and retardants at 25°C with 0.5 M Na₂SO₄ at pH 2.0.

tendency is obtained when the interface pressure, $(\sigma_i)_0 - \sigma_i^*$ (in which $(\sigma_i)_0^*$ is the interfacial tension of the pure diluent in the system), is plotted against the logarithm of the concentration of the solute, $\log C$. This has been done in Figure 12 for a few extractants, accelerators and retardants.

In comparing the curves of HOPHO and p-octylphenol one sees that neither of the two shows a marked preference over the other to collect at the interface. This would explain why the phenol at low to moderate concentrations hardly influences the rate of the reaction: behaving almost as HOPHO, it barely decreases the concentration of $(\text{HOPHO})_2$ at or close to the interface. Of course at higher concentrations the phenol starts to act as a modifier.

Syn-HNBPO, DEHOD and 8.9-dioximinohexadecane (DOHD) display a more pronounced tendency towards interface orientation than anti-HNBPO and HOPHO. Syn-HNBPO is a distinct retardant for anti-HNBPO. It seems possible that in its obviously very effective competition for space at the interface, it suppresses the interfacial concentration of the dimers of the active component; in other words the syn-HNBPO decreases the factor a in equation (16). The net result is a decrease in reaction rate.

Qualitatively the effect of the accelerators DEHOD and DOHD also finds a basis in their clear preference for the interface. Attempts to find a reasonable mechanism for the accelerated reactions (in which of course by definition the accelerators have to play a role) are however seriously impeded by the peculiar retarding action of DEHOD at low concentrations. At present we are inclined to believe that the DEHOD (isolated from a commercial product) might contain one or more impurities that could act as powerful retardants. Only relatively large amounts of DEHOD may then be able to overcome this initial unfavourable influence. Work is going on to clarify this point.

* $(\sigma_i)_0 - \sigma_i$ and $(\sigma_i)_0$ are given in dyn/cm. 1 dyn/cm = 1 mN/m.

NOTATION

Concentration

- [X] = Concentration of X in the aqueous phase
[X] = Concentration of X in the organic phase

Subscripts

- a = Analytical
eq = Equilibrium
f = Free
i = At the interface
m = Monomeric
o = Initial
t = At time t

General

- A = Aqueous
a.t.e. = Approach to equilibrium
D = Distribution coefficients
DEHOD = 5,8-Diethyl-6-hydroxy-7-oximinododecane
DOHD = 8,9-Dioximinohexadecane
HNBPO = 2-Hydroxy-5-nonylbenzophenone oxime (syn and anti)
HOPHO = 2-Hydroxy-5-tert-octylphenylheptyl ketoxime
K_{eq} = Equilibrium constants
k_f, k_r = Forward and backward reaction rate constant, in s⁻¹
MW = Molecular weight
O = Organic
Stg. eff. = Stage efficiency
α = Degree of dimerization
σ_i = Interfacial tension

Subscripts

- app = Apparent
aq = Aqueous
eq = Equilibrated
i = At the interface
org = Organic

REFERENCES

- (1) Flett, D.S., Okuhara, D.N. and Spink, D.R., *J. Inorg Nucl. Chem.* 1973, 35, 2471.
- (2) Miller, J.D. and Atwood, R.L., *J. Inorg. Nucl. Chem.* 1975, 37, 2539.
- (3) Dobson, S. and Van der Zeeuw, A.J., *Chem. & Ind.* 1976, 5, 175.
- (4) Price, R. and Tumilty, J.A., *Inst. Chem. Eng. Symposium Series No. 42*, 1975, p. 18.1.
- (5) Laskorin, B.N. *et al.*, *Proc International Solvent Extraction Conference 1974*, p. 1775. Society of Chemical Industry, London.
- (6) Ritcey, G.M., *C.I.M. Bulletin*, April 1973, p. 75.
- (7) Ashbrook, A.W., *Coord. Chem. Rev.* 1975, 16, 285.

DISCUSSION

L. Hummelstedt: I wish to congratulate you on an excellent paper containing very interesting data. As for the strange retarding effect of the accelerator at low concentrations, could it possibly be due to experimental errors? If there are two parallel reactions, one catalytic and one uncatalyzed, the accelerator effect may be rather small at low concentrations.

A.J. Van der Zeeuw: Apart from the possibility we mentioned in the paper (impurity), your suggestion cannot be ruled out. The lack of experimental data is precisely the reason why we do not (at this moment) wish to draw any conclusion as to the mode of action of the accelerators. Only more experiments with thoroughly purified material in the concentration range of interest (see my paper) can possibly show whether the effect is "real". Only then is it justified to start thinking about the reaction path.

Mass Transfer Rate Across Liquid-Liquid Interfaces. Film Diffusion and Interfacial Chemical Reactions as Simultaneous Rate Determining Steps in the Liquid-Liquid Cation Exchange of Some Tervalent Cations

Pier Roberto Danesi and Renato Chiarizia,
C.N.E.N., CSN-Casaccia,
Laboratorio Chimica Fisica,
Rome, Italy.

ABSTRACT

Mass transfer rate studies of some trivalent cations, i.e. Fe^{+3} , Eu^{+3} , Ce^{+3} , Tm^{+3} and Gd^{+3} , from aqueous perchloric acid solutions into toluene solutions of the liquid cation exchanger dinonylnaphthalene sulfonic acid, HD, performed as function of both the hydrodynamics of the system (cell geometry and stirring speed) and the chemical composition of the solutions by using a constant interfacial area cell, are reviewed. A set of interfacial chemical reactions has been proposed as the main rate determining processes of the mass transfer kinetics in the region where this is independent of the stirring speed of the phases, assuming negligible diffusional resistance. This set of reactions consists of:

- formation of an interfacial complex between the interfacially adsorbed molecules of the ion-exchanger and the bulk metal containing species; and
- replacement at the interface of the interfacial complex by bulk organic molecules of the ion-exchanger.

By applying the stationary condition to the interfacial complex, its concentration has been evaluated and a rate expression derived which has allowed calculation of the rate constants of the chemical reactions. Further, it has been shown that the proposed mechanism does not change as long as the extraction goes to equilibrium. Moreover, when the stirring speed of the phases was reduced, a diffusional contribution to the overall extraction rate (through the stationary layers adjacent to both sides of the interface) was considered to superimpose upon the contribution due to the interfacial chemical reactions. In this case a simplified model coupling diffusion and the previously determined chemical reactions has been found to explain the experimental transfer rate data well.

Introduction

THE MASS TRANSFER RATE of metal cations in liquid-liquid extraction systems depends in the most general case on both the kinetics of the chemical reactions taking place in the system and the rates of diffusion of the transferring species in the two liquid phases. When constant interfacial area cells and extracting compounds exhibiting surface active behaviour are used in transfer rate experiments (this is the case with all the so-called

liquid ion exchangers and with most other extractants) the role of interfacial processes (both film diffusion and interfacial chemical reactions) can be expected to predominate over rate processes occurring in the bulk phases.

In this paper, kinetic studies of liquid ion exchange of Fe^{+3} , Eu^{+3} , Ce^{+3} , Tm^{+3} and Gd^{+3} from aqueous perchloric acid solutions into toluene solutions of the liquid cation exchanger dinonylnaphthalene sulfonic acid (from now on called HD), performed in our laboratory using constant interfacial area cells, are reviewed⁽¹⁻³⁾. An alternative reaction mechanism, more consistent with equilibrium distribution data, is also proposed.

The very strong surface active behaviour of HD at the water-organic interface previously reported⁽⁴⁾, the existence of a region where the rate of mass transfer is independent of stirring, as well as the linear relationship between the mass transfer rate and the specific area (interfacial area/volume), always met in our experimental systems, have been taken as a strong indication that interfacial processes can be the predominant effect in determining the liquid ion exchange kinetics. By assuming as negligible the diffusional resistance, a set of interfacial chemical reactions has been proposed as the main rate determining process of mass transfer in the region where the rate is independent from the stirring of the phases.

Moreover the decrease of the rate of mass transfer observed when the stirring rate is reduced has indicated that film diffusion processes also have to be taken properly into account together with interfacial chemical reactions. Therefore, a general model coupling together film diffusion processes and interfacial chemical reactions has been elaborated. With this model it has been possible to explain the dependence of the mass transfer rate on both hydrodynamics (stirring rate, interfacial area, volume of the phases) and chemical parameters (concentration of the extractant, concentration of the extractable cation and acidity).

Experimental

The experimental procedures for the kinetics measurement are reported in references⁽¹⁻³⁾. The hydrodynamic and geometrical conditions under which the experiments have been conducted are described in detail in references⁽¹⁻³⁾. Figure 1 schematically shows a typical constant-interfacial-area cell used in the experiments. The initial rate of disappearance of the metal cation from the aqueous phase, i.e. at time zero, $-d[M^{+3}]/dt = \vec{V}$, or from

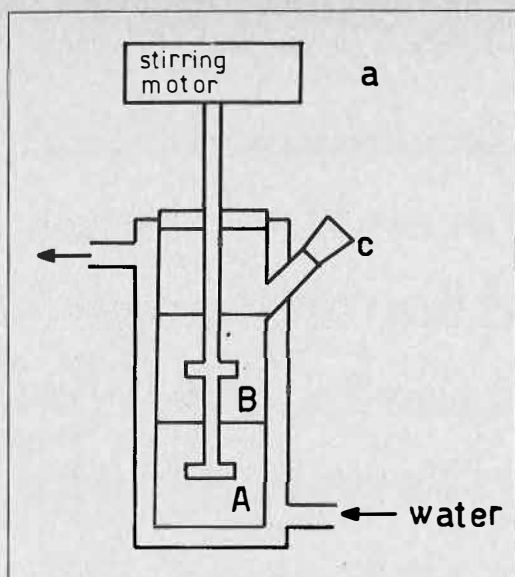


FIGURE 1. Constant interfacial area cell used for the kinetics experiments. A: aqueous phase, B = organic phase. Interface area = 12.6 cm². Stirrer blades = 20 × 5 × 2 mm; distance between stirrer blades = 20 mm; volume of aqueous phase = 30 cm³.

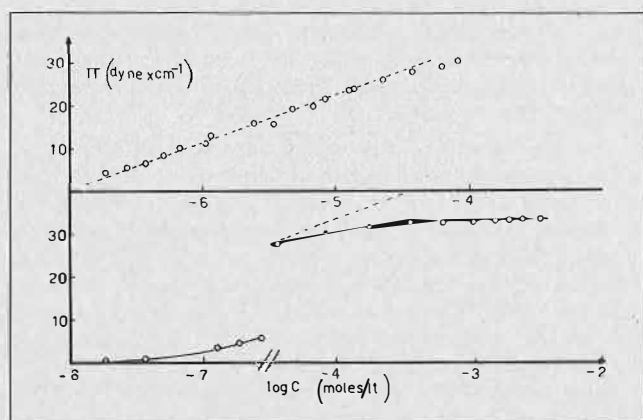


FIGURE 2. Interfacial pressure, π , vs logarithm of analytical concentration of HD in toluene, $\log C$. Uncertainty of π values = ± 0.2 dyne/cm. Aqueous phase: $[\text{HClO}_4] = 0.102 \text{ M}$; $T = 25.0 \pm 0.1^\circ\text{C}$.

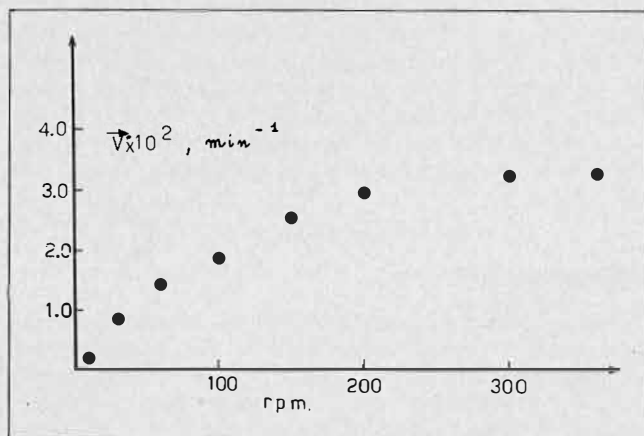


FIGURE 3. \vec{V}^* vs. stirring speed of the phases (expressed in rpm.). The composition of the system was the following: $[\text{Eu}^{+3}] = 1.58 \cdot 10^{-6} \text{ M}$, $\bar{C}_{\text{HD}}^0 = 0.01 \text{ M}$; $[\text{HClO}_4] = 0.545 \text{ M}$.

the organic phase $-\frac{d[\bar{M}]}{dt} = \bar{V}$, with $[\text{M}^{+3}]$ and $[\bar{M}]$ molar concentrations of the metal in the aqueous and organic phase, respectively, and t = time in minutes, has been determined either by electrochemical monitoring or by radioanalytical techniques. Experimental details of the interfacial pressure measurements are reported in reference⁽⁴⁾.

Results and Discussion

Interfacial Measurements

HD is a very strongly surface-active compound. Figure 2 shows how its interfacial pressure, π , varies with the logarithm of the analytical concentration of HD in toluene. The increase of interfacial pressure can be ascribed to the formation at the interface of an adsorbed monolayer of HD molecules. The occurrence of a completely saturated water-organic interface is indicated by the constant slope of the π vs. $\log C$ curve according to the Gibbs equation $d\pi/d\ln C = n_i kT$, where n_i is the number of adsorbed molecules at the interface per unit area. As can be seen, saturation of the interfacial plane is obtained at a bulk toluene concentration of HD as low as $6 \times 10^{-7} \text{ M}$. It follows then that in the concentration range used in the kinetics experiments the interface is always completely saturated with HD molecules.

Dependence of the Initial Mass Transfer Rate on the Stirring Rate, Volume of the Aqueous Phase and Interfacial Area.

In order to determine the dependence of the initial mass transfer rate (at time = 0) on the stirring speed of the phases the quantity $\vec{V}^* = \vec{V}/a_{\text{M}^{+3}}$, i.e. the mass transfer at time zero, $\vec{V} = -d[\text{M}^{+3}]/dt$, divided by the initial trivalent metal ($\text{M} = \text{Fe}, \text{Eu}, \text{Ce}, \text{Gd}, \text{Tm}$) activity

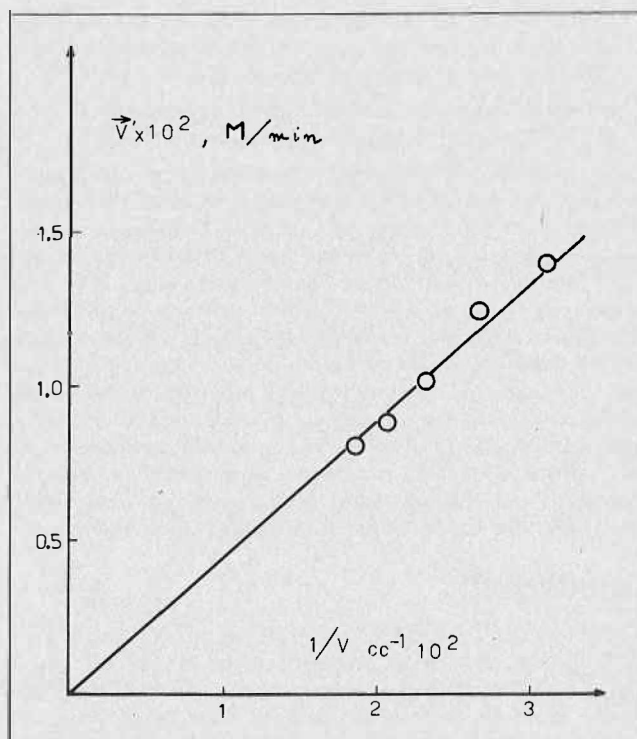


FIGURE 4. $\vec{V}^* = \vec{V} / [\text{Fe}^{+3}]$ vs. $1/V$ (aqueous volume) plot; V is the volume of the aqueous phase; $[\text{Fe}^{+3}] = 6.87 \cdot 10^{-4} \text{ M}$, $\bar{C}_{\text{HD}}^0 = 0.020 \text{ M}$, $[\text{HClO}_4] = 0.451 \text{ M}$, interface area 18.9 cm².

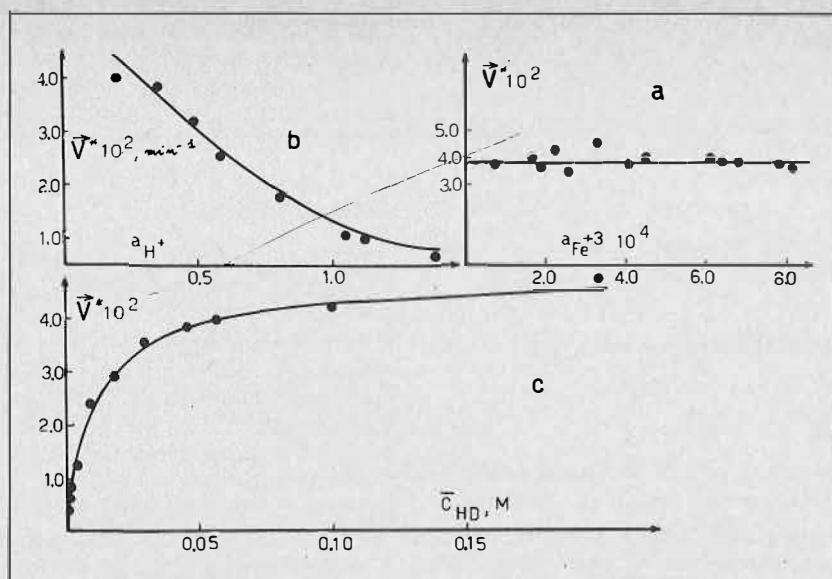


FIGURE 5. \vec{V}^* vs. concentration (or activity) plots; (a) \vec{V}^* vs $a_{Fe^{+3}}$ ($\bar{C}_{HD}^0 = 0.046$ M, $[HClO_4] = 0.451$ M), (b) \vec{V}^* vs. a_{H^+} ($\bar{C}_{HD}^0 = 0.046$ M, $[Fe^{+3}] = 6.87 \times 10^{-4}$ M), (c) \vec{V}^* vs. \bar{C}_{HD}^0 ($[HClO_4] = 0.451$ M, $[Fe^{+3}] = 6.87 \times 10^{-4}$ M); interface area = 18.9 cm², aqueous and organic volumes = 43 cm³; full points = experimental values; continuous lines calculated through eq. 3 with $K_1 = 4.80 \times 10^{-2}$ and $K_3 = 1.16 \times 10^{-1}$, $\nu = 2$.

($a_M + 3$), for a given chemical composition of the system, has been measured. The mean molar activity in the aqueous phase has been computed as the product of the molar metal ion concentration and the mean activity coefficient of the M(III) perchlorate. This activity coefficient, y_M , has been obtained by the Davies equation assuming that the ionic strength was only determined by the perchloric acid. The experimental \vec{V}^* values, plotted as function of the stirring speed have shown that, with the cell and stirring system used by us, the rates become independent of the stirring speed in the stirring region 200-350 rpm. This can be taken as an indication that in our experimental conditions the thickness of the diffusion films, δ , becomes either constant or small enough not to influence any longer the mass transfer rate.

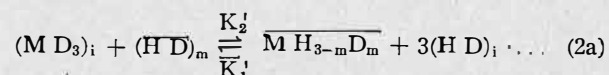
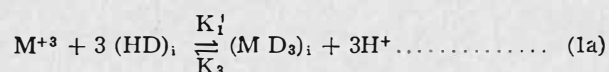
Figure 3 shows a typical \vec{V}^* vs. rpm plot obtained in the case of Eu^{+3} . Similar behaviour has been also found for the other M^{+3} cations. When \vec{V}^* was determined as function of the interfacial area, A , or the inverse volume of the aqueous phase, $1/V$, a linear relationship was always obtained. Figure 4 shows a typical \vec{V} vs. $1/V$ plot. These facts indicate that the rate determining processes are taking place near the interface (either interfacial reactions or diffusion processes in the interfacial liquid films).

Forward and Reverse Mass Transfer Rates. Equilibrium Law.

The initial mass transfer rates ($t = 0$) as function of the chemical composition of the system ($[HClO_4]$, $\bar{C}_{HD}^0 =$ analytical concentration of HD in toluene and $[M^{+3}]$) have been determined for the Fe^{+3} forward and reverse extraction. The results, plotted in the form of normalized velocities, $\vec{V}^* = \vec{V}/a_{M^{+3}}$ or $\vec{V}^* = \vec{V}/[M]$, are shown in Figures 5 and 6. The mean molar activity of H^+ in the aqueous perchloric acid, a_{H^+} , has been calculated as the product of the mean molar activity coefficient, y_{HClO_4} , and the molarity of the solution. In the case of the reverse initial mass transfer rates, ideal behaviour of the metal containing organic species has been assumed. In the case of Eu^{+3} ,

Ce^{+3} , Tm^{+3} and Gd^{+3} , only the initial forward mass transfer rates have been obtained. Figure 7 (full and empty circles and empty squares) shows the results obtained for Eu^{+3} extraction. The data of Figures 5, 6, 7 refer to stirring speeds in the plateau region of Figure 3.

By assuming that in these stirring conditions film diffusion processes are negligible, the results can be explained according to a reaction mechanism based on interfacial chemical reactions between the bulk metal species and the interfacially adsorbed monolayer of HD molecules. Interfacial chemical reactions as rate determining steps have been similarly proposed for several other solvent extraction systems studied from the kinetics point of view⁽⁵⁻¹¹⁾. The following set of interfacial chemical reactions has been found to agree with the experimental data:



(The bar indicates organic species, i indicates interfacial species and hydration molecules have been omitted.)

By assuming that a steady state condition is instantaneously established ($t = 0$) for the interfacial complex $(MD_3)_i$ the following rate laws follow:

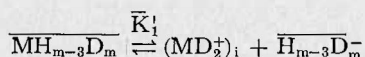
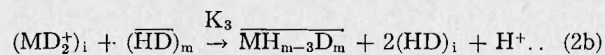
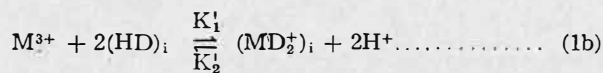
$$\vec{V}(\text{direct transfer at } t = 0) = \frac{K_1' \bar{C}_{(HD)_m} y_M C_M^0}{\bar{C}_{(HD)_m} + K_R' a_{H^+}^{\nu}} \dots \dots \dots (3)$$

$$\overleftarrow{V}(\text{reverse transfer at } t = 0) = \frac{\bar{K}_1' K_R' a_{H^+}^{\nu} \bar{C}_M^0}{\bar{C}_{(HD)_m} + K_R' a_{H^+}^{\nu}} \dots \dots \dots (4)$$

$$\vec{V}(\text{overall transfer = at } t \neq 0) = \frac{K_1 y_M \bar{C}_{(HD)_m} C_M^0 - K_R' \bar{K}_1' a_{H^+}^{\nu} \bar{C}_M^0}{\bar{C}_{(HD)_m} + K_R' a_{H^+}^{\nu}} \dots \dots \dots (5)$$

with $m = 7$ (degree of polymerization of HD in toluene), $K_1 = K_1' [HD]_i$ (the interfacial concentration of HD is a constant), $\bar{K}_1 = \bar{K}_1' [HD]_i$, $K_2 = K_2'/m$, $K_R = K_3 / K_2$, $K_R' = K_R/m$, $y =$ activity coefficient, $C_M^0 =$ bulk aqueous

metal cation concentration, $\overline{C}_M^o = \overline{MH_{3-m}D_m} =$ bulk organic metal concentration, $\overline{C}_{HD}^o = m\overline{C}_{(HD)_m}^o$ (the analytical concentration of HD is m times the polymer concentration since HD is practically completely polymerized in our experimental conditions) and $\nu = 3$. It should be mentioned that in reference⁽¹⁻³⁾ a different set of interfacial chemical reactions was proposed, i.e.:



(followed by the fast readjustment of the freed polymerized HD), leading to the same rate laws 3,4,5, with $\nu = 2$.

Although the previously proposed mechanism better explained the kinetics experimental data obtained with Fe^{+3} , rates 3, 4, 5 with $\nu = 3$ are in better agreement with the equilibrium distribution law which can be derived by setting eq. 5 equal to zero, i.e.:

$$E = \frac{\overline{C}_M^o}{C_M^o} \left(\text{at equilibrium} \right) = \frac{K_1 \overline{C}_{HD}^o y_M}{K_1 K_R a_{H^+}^{\nu}} \dots \dots \dots (6)$$

In fact $\log E$ vs. $\log [H^+]$ plots of distribution data⁽¹²⁾ yield straight lines with slope values closer to -3 than to -2 . This is particularly true for the lanthanides trivalent cations. Moreover the experimental distribution data⁽¹²⁾ of Eu^{+3} , Ce^{+3} , Tm^{+3} and Gd^{+3} better agree with the ones calculated through eq. 6 when ν is set equal to 3. Further, according to mechanisms 1a and 2a, the direct and reverse reactions are the opposite of each other while this is not true with mechanisms 1b and 2b. The solid lines reported in Figures 5, 6, 7, have been calculated from equations 3 and 4 with $\nu = 2$ for Fe^{+3} and $\nu = 3$ for Eu^{+3} and the K_1 , \overline{K}_1 and K_R values reported in the figures. These parameters have been obtained by best fitting the experimental points with equations 3 and 4. As mentioned above in the

case of Fe^{+3} the curves calculated with $\nu = 3$ and the corresponding rate constants (see Table 1) gave a slightly poorer fit to the experimental points. They have not been reported in the figures, since except for the curve of Figure 6b where a difference has been observed, they practically coincide with the curves calculated with $\nu = 2$.

Rate Constants

The rate constants K_1 , \overline{K}_1 and K_R for Fe^{+3} and K_1 and K_R for Eu^{+3} , evaluated by best fitting of the experimental points, are reported in Table 1. In the case of Eu^{+3} , where reverse mass transfer rates have not been experimentally obtained \overline{K}_1 has been evaluated from eq. 6 inserting the experimental K_1 and K_R rate constants and the E values of reference⁽¹²⁾. For Ce^{+3} , Tm^{+3} , and Gd^{+3} , where not enough initial mass transfer rate experiments have been performed, the rate constants have been evaluated by extrapolating the reaction mechanism 1a, 2a and assuming that K_1 and \overline{K}_1 had the same numerical value as for Eu^{+3} . A support to the validity of this extrapolation can be found in the similar external structure that the various lanthanide cations are likely to have both in water and in the organic phase. In fact, in water all lanthanide ions are present as highly hydrated cations with very close values of the solvated radii. It is therefore likely that rate constants for the interaction between such hydrated cations and the interfacially adsorbed HD molecules would be the same. Similarly in the organic phase the polymerized $\overline{MH_{m-3}D_m}$ species can be described as a large polymerized micelle containing inside a relatively small hydrated metal cation. In this case also it is therefore plausible that the rate constant relative to the dissociation of such a polymeric molecule would be the same for all the trivalent lanthanide cations. The difference between the kinetic behaviour of the trivalent cations can then be entirely attributed to the different K_R values. Once this hypothesis on the constancy of K_1 and \overline{K}_1 for all the trivalent lanthanide cations has been formulated, K_R values for Ce^{+3} , Gd^{+3} and Tm^{+3} can be calculated through eq. 6 using the E values of ref.⁽¹²⁾. Table 1 summarizes the numerical values of the rate constants.

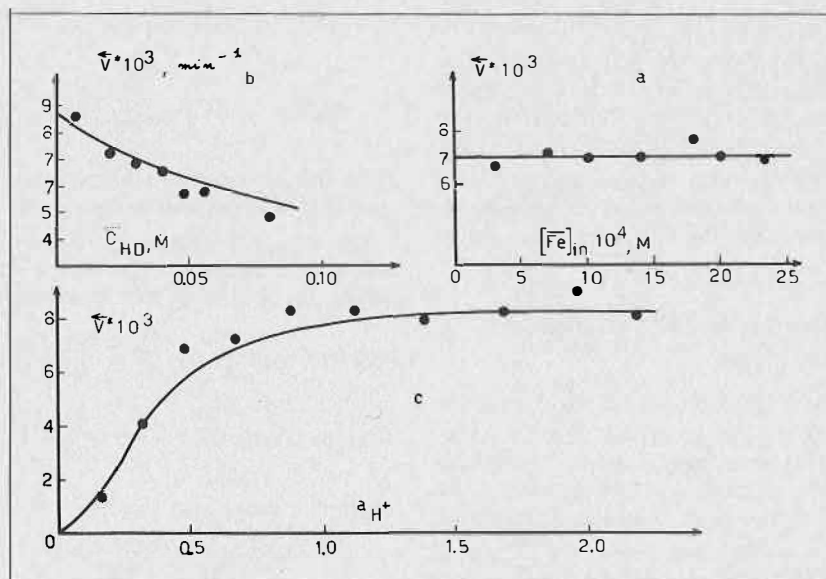


FIGURE 6. \overline{V}^* vs. concentration (or activity) plots; (a) \overline{V}^* vs. $[Fe]$ ($\overline{C}_{HD}^o = 0.025$ M, $[HClO_4] = 1.11$ M), (b) \overline{V}^* vs. \overline{C}_{HD}^o ($[HClO_4] = 1.18$ M, $[Fe] = 7.01 \times 10^{-4}$ M), (c) \overline{V}^* vs. a_{H^+} ($\overline{C}_{HD}^o = 0.0125$ M, $[Fe] = 1.16 \times 10^{-3}$ M); interface area = 18.9 cm², aqueous and organic volumes = 40 cm³; full points = experimental values; continuous lines calculated through eq. 4 with $\overline{K}_1 = 8.27 \times 10^{-3}$ and $K_R = 1.16 \times 10^{-1}$, $\nu = 2$.

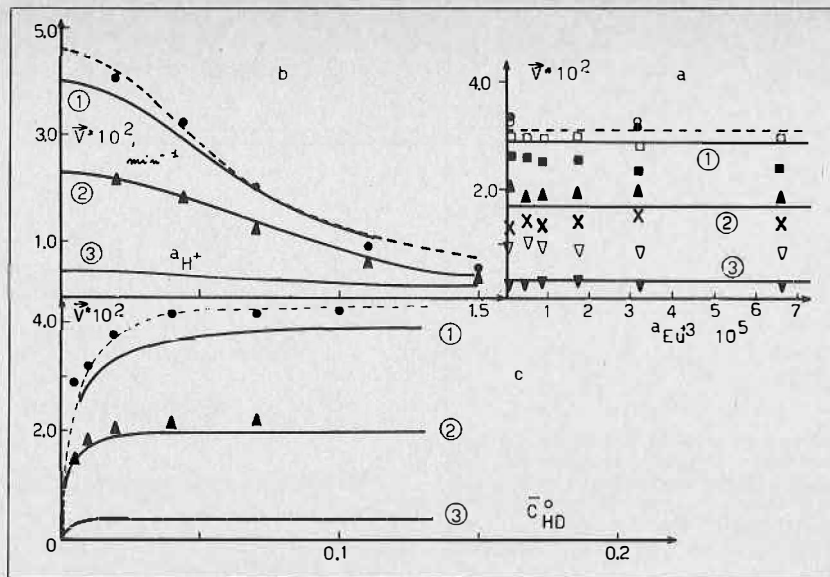


FIGURE 7. \vec{V}^* vs. activity (or concentration) plots. Different symbols refer to experimental points obtained at different stirring speeds of the phases: ○, 360 rpm; ●, 280 rpm; □, 200 rpm; ■, 150 rpm; ×, 60 rpm; ▽, 30 rpm; ▼, 10 rpm (a) \vec{V}^* vs. $a_{Eu^{+3}}$ ($\bar{C}_{HD}^0 = 0.01$ M; $[HClO_4] = 0.545$ M), (b) \vec{V}^* vs. a_{H^+} ($\bar{C}_{HD}^0 = 0.01$ M; $[Eu^{+3}] = 1.58 \times 10^{-6}$ M), (c) \vec{V}^* vs. \bar{C}_{HD}^0 ($[HClO_4] = 0.545$ M; $[Eu^{+3}] = 1.58 \times 10^{-6}$ M). Dashed lines calculated through eq. 3. Solid lines calculated through eq. 12 with (1) $\delta = 10^{-3}$ cm; (2) $\delta = 10^{-2}$ cm; (3) $\delta = 10^{-1}$ cm. The following values have been used in the calculations: $K_1 = 4.6 \times 10^{-2} \text{ min}^{-1}$; $K_R = 3.0 \times 10^{-2} (\text{moles} \times \text{L}^{-1})^{-2}$; $D_{(HD)m} = D_{Eu^{+3}} = 3 \times 10^{-4} \text{ cm}^2 \times \text{min}^{-1}$; $A = 12.6 \text{ cm}^{-2}$; $V = 0.0301$. The activity coefficients have been calculated as reported in the text. The solid lines calculated with $\delta = 10^{-4}$ and 10^{-5} cm practically coincide with the dashed lines. The lines calculated with $\delta = 1$ cm practically coincide with abscissa axis.

TABLE 1. Rate Constants of Some Tervalent Metal Cations Normalized to a Specific Interfacial Area $A/V = 0.42 \text{ cm}^{-1}$

Ion	K_1^a (min^{-1})	\bar{K}_1^a (min^{-1}) $v=2$	\bar{K}_1^a (min^{-1}) $v=3$	K_R (mole/l^{-1}) $v=2$	K_R (mole/l^{-1}) $v=3$
Fe ⁺³	$(4.3 \pm 0.1) \cdot 10^{-2c,e}$	$(7.7 \pm 0.5) \cdot 10^{-3c}$	$(7.7 \pm 0.5) \cdot 10^{-3e}$	$(1.16 \pm 0.1) \cdot 10^{-1c}$	$(1.7 \pm 0.5) \cdot 10^{-1e}$
Eu ⁺³	$(4.6 \pm 0.2) \cdot 10^{-2c,e}$	$(7.3 \pm 0.5) \cdot 10^{-3f}$	$(1.4 \pm 0.5) \cdot 10^{-2g}$	$(2.5 \pm 0.5) \cdot 10^{-2c}$	$(3.0 \pm 0.5) \cdot 10^{-2e}$
Ce ⁺³	4.6×10^{-2b}	$7.3 \times 10^{-3b,f}$	$1.4 \times 10^{-2b,g}$	$1.9 \times 10^{-2b,f}$	$2.4 \cdot 10^{-2b,g}$
Gd ⁺³	4.6×10^{-2b}	$7.3 \times 10^{-3b,f}$	$1.4 \times 10^{-2b,g}$	$2.4 \times 10^{-2b,f}$	$3.2 \cdot 10^{-2b,g}$
Tm ⁺³	4.6×10^{-2b}	$7.3 \times 10^{-3b,f}$	$1.4 \times 10^{-2b,g}$	$3.7 \times 10^{-2b,f}$	$4.7 \cdot 10^{-2b,g}$

- a) These rate constants are dependent on the A/V ratio since they have been evaluated by curve fitting of rates defined as $\vec{V}^* = -d[M]/dt$; ($\vec{V} = \vec{N} A/V$; $\vec{N} =$ flux through the interface). Rate constants K_1^+ and K_1^- independent from A/V can then be obtained through the relationship $K_1^+ = K_1 (V/A)$.
 b) Evaluated through the assumptions reported in the text.
 c) By best fitting the experimental points with eq. 3 or 4 with $v = 2$.
 e) By best fitting the experimental points with eq. 3 or 4 with $v = 3$.
 f) From eq. 6 with $v = 2$;
 g) From eq. 6 with $v = 3$.

Chemical Reaction and Diffusion Processes as Simultaneous Rate Determining Processes.

The full triangles of Figure 7b, c, representing the dependence of \vec{V}^* on a_{H^+} and \bar{C}_{HD}^0 at a stirring speed of 100 rpm, as well as the various sets of points of Figure 7a, indicate that diffusion processes become rate determining in our experimental apparatus at the lower stirring speeds. In order to interpret the decrease of the initial ($t = 0$) mass transfer rate with the decrease of the stirring speed of the two phases, a model has been elaborated where the previously reported chemical reactions have been coupled with the diffusion processes of the reacting species, Figure 8 gives a pictorial representation of the model. To deal with the problem of the mass transfer of ions between two liquid phases in presence of chemical reactions the diffusion law⁽¹³⁾

$$\vec{N}_A = X_A (\vec{N}_A + \vec{N}_B) - CD_{AB} - \nabla X_A \dots \dots \dots (7)$$

holding for two components, has been used. Here \vec{N} is the molar flux, $C = C_A + C_B$ the molar density of the solution, X the mole fraction and D_{AB} the diffusivity. Since the previously described chemical reactions take place at the interface they will not appear in the differential equation obtained from a shell mass balance but only in the boundary conditions necessary to get a solution. In order to simplify the use of eq. 7 for our five component system (M^{+3} , H^+ , HD, water, toluene), the following considerations have been taken into account:

1. The diffusion of the diluents, water and toluene, can be neglected.
2. The mole fractions of the three diffusing species, $X_{M^{+3}}$, X_{H^+} , X_{HD} are small numbers.
3. The following correlations hold between the fluxes $\vec{N} = \vec{N}_{M^{+3}} = -1/3 \vec{N}_{H^+} - \vec{N}_{(HD)m}$.

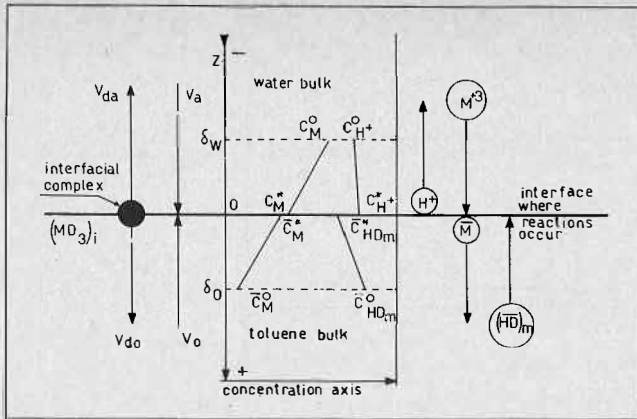


FIGURE 8. Schematic representation of the diffusion processes in presence of interfacial chemical reactions. δ_w and δ_o represent the thickness (in water and organic phase respectively) of the diffusion films. C^o and C^* are bulk and near the interface concentrations. The movement of the species to and from the interface as well as the interfacial reactions are also shown.

- Only diffusion along the vertical Z axis has to be considered.
- The diffusivities $D_{M^{+3}}$, D_{H^+} , $D_{(HD)_m}$, will be treated as independent coefficients.

The following three differential equations have to be solved

$$\vec{N}_{M^{+3}} = -D_{M^{+3}} \frac{d[M^{+3}]}{dz} \quad (8a)$$

$$\vec{N}_{H^+} = -D_{H^+} \frac{d[H^+]}{dz} \quad (8b)$$

$$\vec{N}_{(HD)_m} = -D_{(HD)_m} \frac{d[(HD)_m]}{dz} \quad (8c)$$

where square brackets represent concentrations. By using eqns. (8a, b, c) at the steady state (which in our case is assumed to be reached instantaneously, that is at $t = 0$), $d\vec{N}/dz = 0$, and by integrating twice with respect to z we get (for M^{+3}) $[M^{+3}] = c_1 z + c_2$, (c_1 and c_2 integration constants). The two boundary conditions:

B.C.1 $z = \delta_w$ $[M^{+3}] = C_{M^{+3}}^o$, B.C.2 $z = \delta_o$ $[M^{+3}] = C_{M^{+3}}^*$, are easily deduced from Figure 8 (C^* and C^o indicate concentrations near the interface and bulk concentrations respectively). They can be used to obtain

$$\vec{N}_{M^{+3}} = \frac{D_{M^{+3}}}{\delta_w} (C_M^o - C_M^*) \quad (9)$$

A linear concentration profile through the diffusion film is therefore assumed. It is worth noticing that B.C. 2 takes into account the chemical kinetics of the system by considering that the rate of disappearance of M^{+3} at the interface (i.e. the flux $\vec{N}_{M^{+3}}$ at $z = 0$) occurs according to the mechanism represented by eqns. 1a and 2a. Therefore it follows

$$\vec{N}_{M^{+3}} (z = 0) = \frac{K_1^+ y_M C_M^* C_{(HD)}^*}{C_{(HD)_m}^* + K_R y_{H^+}^3 C_{H^+}^{*3}} \quad (10)$$

Similarly to eq. 9, two other equations are obtained:

$$\vec{N}_{H^+} = \frac{D_{H^+}}{\delta_w} (C_{H^+}^o - C_{H^+}^*) = \frac{D_{(HD)_m}}{\delta_o} \left(\frac{C_{HD}^o}{7} - C_{(HD)_m}^* \right) \quad (11)$$

where C_{HD}^o is the bulk analytical concentration of HD in toluene and 7 is its degree of polymerization. Since eqns 9-11 hold simultaneously they can be solved with respect to \vec{N} :

$$\vec{N} \frac{A}{V} = \frac{K_1 y_M \left(C_M^o - \frac{\vec{N} \delta_w}{D_{M^{+3}}} 10^3 \right) \left(\frac{C_{HD}^o}{7} - \frac{\vec{N} \delta_o}{D_{(HD)_m}} \right)}{\left(\frac{C_{HD}^o}{7} - \frac{\vec{N} \delta_o}{D_{(HD)_m}} 10^3 \right) + \frac{K_R}{7} y_{H^+}^3 \left(C_{H^+}^o + \frac{3\vec{N} \delta_w}{D_{H^+}} 10^3 \right)^3} = \vec{V} \quad (12)$$

Equation 12 is dimensionally consistent when the following units are used: \vec{N} (mole \times min $^{-1}$ \times cm $^{-2}$), A (cm 2), V (l), C^o (mole \times l $^{-1}$), K_1 (min $^{-1}$), K_R (mole \times l $^{-1}$) $^{-2}$, δ (cm), D (cm 2 \times min $^{-1}$). In this case the initial reaction rate \vec{V} will be expressed in (mole \times l $^{-1}$ \times min $^{-1}$) since $\vec{V} = \vec{N}(A/V)$. Equation 12 can be simplified by considering that in our experimental conditions it is always $K_R y_{H^+}^3 (C_{H^+}^o + 3\vec{N} \delta_w / D_{H^+})^3 = K_R a_{H^+}^3$ (values of $\delta_w = 10^{-3}$ cm and $D_{H^+} \approx 3 \times 10^{-4}$ cm 2 \times min $^{-1}$ have been considered).

It follows then, after some algebra, that

with

$$a\vec{N}^2 + b\vec{N} + c = 0 \quad (13)$$

$$a = \frac{\delta_o}{D_{(HD)_m}} 10^3 \left(\frac{K_1^+ \delta_w 10^3}{D_{M^{+3}}} + \frac{A}{V} \right) \quad (14)$$

$$-b = \frac{A}{7V} (C_{HD}^o + K_R a_{H^+}^3) + K_1^+ 10^3$$

$$\left(\frac{\delta_o C_M^o}{D_{(HD)_m}} + \frac{\delta_w C_{HD}^o}{7D_{M^{+3}}} \right) \quad (15)$$

$$c = \frac{K_1^+}{7} C_M^o C_{HD}^o (K_1^* = K_1 y_M); \left(K_1 = K_1^+ \frac{A}{V} \right)$$

It is worth noticing that while K_R is independent of the interfacial area, A , and the volume of the phases, V , K_1 is not. In fact K_1 has been obtained through \vec{V}^* which is related to the flux \vec{N}^* by the relationship $\vec{N}^* (A/V) = \vec{V}^*$. It follows then $K_1 = K_1^+ (A/V)$ where K_1^+ is this time independent of A/V . In the limiting case of zero thickness of the diffusion film ($\delta_w = \delta_o = 0$), eq. 12 reduces to eq. 3. Further it is easy to show that when diffusion is the pre-dominant rate determining process, $\vec{N}_{M^{+3}} = (D_{M^{+3}} / \delta_w) C_M^o$, that is Fick's first law of diffusion. Equation 12 represents the experimental data well as shown by the calculated solid curves of Figures. 7a-c. To perform the calculations it has been assumed that $D_{M^{+3}} = D_{(HD)_m} = 3 \times 10^{-4}$ cm 2 \times min $^{-1}$. Further, since only qualitative information was searched for, it has been assumed $\delta_w = \delta_o = \delta$. The solid curves of Figures. 7a-c have been obtained for different δ values ranging from 10^{-5} to 10^{-1} cm. This means that they can be associated to different stirring speeds of the phases since by increasing the stirring δ is decreased according to a law which depends on the hydrodynamic characteristics of the system.

The set of calculated curves indicates that:

— The shape of the curves obtained in absence of diffusion ($\delta = 0$) is not altered by the simultaneous presence

of both diffusion and chemical reactions ($\delta \neq 0$); consequently, unless the contribution of diffusion is excluded by other considerations, the simultaneous presence of both diffusion and chemical reactions as rate determining processes cannot be ruled out.

— Within the limit of uncertainty associated with the experimental determinations, the model elaborated does not allow one to distinguish between the absence of diffusion and a rather small thickness of the diffusion film ($10^{-5} \text{ cm} < \delta < 10^{-4} \text{ cm}$).

— within the limits of validity of the approximations used, the experimental points obtained at a stirring speed of 100 rpm can be explained by an increase of the thickness of the diffusion film to about $7 \times 10^{-3} \text{ cm}$.

Concentration vs. Time Equation.

The situation at the interface, where the chemical reactions take place, for $t \neq 0$, is schematically shown in Figure 8. By assuming that the interfacial steady state condition is valid all through the time when the mass transfer takes place, it follows that the reaction rate at the interface will then be given by

$$\vec{N}_{M^{+3}}/s=0 \frac{A}{V} = \frac{(K_1 y_M \bar{C}_M^* \bar{C}_{(HD)m}^* - (K_R/m) \bar{K}_1 a_{H^+}^3 \bar{C}_M^*)}{\bar{C}_{(HD)m}^* + (K_R/m) a_{H^+}^3} = \vec{V}$$

Since the reacting species have to diffuse to and from the interface, the interfacial concentrations (C^*) can be expressed in terms of bulk concentrations (C^0) by following the same reasoning reported above. The following equation is then obtained for the flux \vec{N} of the trivalent metal cation:

$$\vec{N} \frac{A}{V} = \frac{K_1 y_M \left(C_M^0 - \frac{\vec{N} \delta_w}{D_M} 10^3 \right) \left(\frac{\bar{C}_{HD}^0}{7} - \frac{\vec{N} \delta_o}{D_{(HD)m}} 10^3 \right) - \frac{K_R}{7} \bar{K}_1 a_{H^+}^3 \left(C_M^0 + \frac{\vec{N} \delta_o}{D_M} 10^3 \right)}{\left(\frac{\bar{C}_{HD}^0}{7} - \frac{\vec{N} \delta_o}{D_{(HD)m}} 10^3 \right) + \frac{K_R}{7} a_{H^+}^3} \quad (16)$$

Also to obtain eq. 16 the simplification $a_{H^+}^* = a_{H^+}^0$ has been introduced. \bar{C}_M^0 represents the metal concentration in the organic phase and D_M its diffusion coefficient. If H^+ and \bar{C}_{HD}^0 are constant and much larger than the total metal concentration, $C_{M \text{ total}} = C_M^0 + \bar{C}_M^0$, they can be considered as time independent and eq. 16 can be integrated to get a C_M^0 vs time function. By setting

$$\begin{aligned} \alpha &= \frac{\delta_o}{D_{(HD)m}} 10^3 \left(K_1 y_M \frac{\delta_w}{D_M} 10^3 + \frac{A}{V} \right) \\ -\beta &= \frac{A}{7V} (\bar{C}_{HD}^0 + K_R a_{H^+}^3) + K_1 y_M \bar{C}_{HD}^0 \\ \frac{\delta_w}{7D_M} 10^3 + \frac{K_R}{7} \bar{K}_1 a_{H^+}^3 + \frac{\delta_o}{D_M} 10^3 \\ -\gamma &= K_1 y_M \frac{\delta_o}{D_{(HD)m}} 10^3 \\ \nu &= K_1 y_M \frac{\bar{C}_{HD}^0}{7} + \frac{\bar{K}_R}{7} \bar{K}_1 a_{H^+}^3 \end{aligned}$$

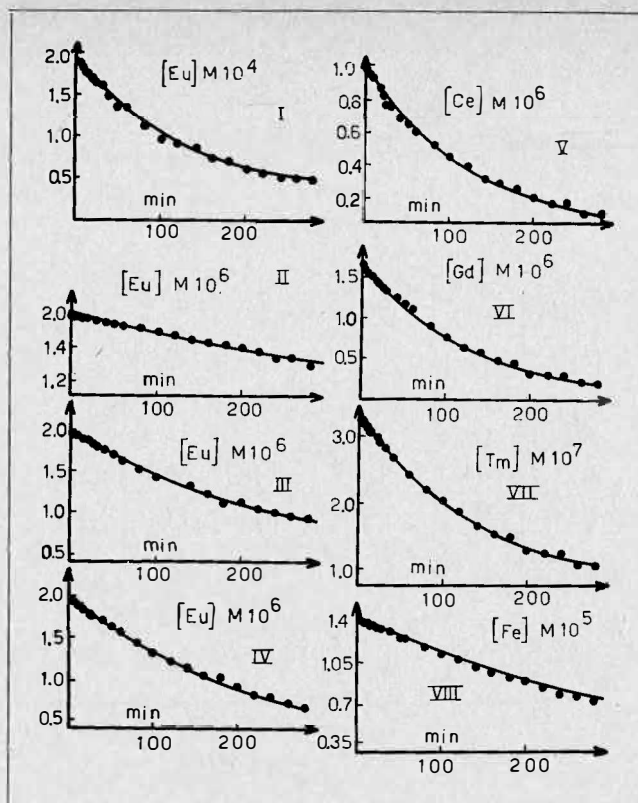


FIGURE 9. Concentration (molarity) vs. time (min) data (full points) for M^{+3} transfer. Solid lines calculated through eq. 17. $\bar{C}_{HD}^0 = 0.01 \text{ M}$.

- (I) $C_{Eu \text{ total}} = 1.98 \times 10^{-4} \text{ M}$, $[\text{HClO}_4] = 0.500 \text{ M}$, rpm = 110, $\delta/D = 17 \text{ min/cm}$.
- (II) $C_{Eu \text{ total}} = 2.00 \times 10^{-6} \text{ M}$, $[\text{HClO}_4] = 0.118 \text{ M}$, rpm = 10, $\delta/D = 333 \text{ min/cm}$.
- (III) $C_{Eu \text{ total}} = 1.98 \times 10^{-6} \text{ M}$, $[\text{HClO}_4] = 0.118 \text{ M}$, rpm = 30, $\delta/D = 117 \text{ min/cm}$.
- (IV) $C_{Eu \text{ total}} = 1.94 \times 10^{-6} \text{ M}$, $[\text{HClO}_4] = 0.118 \text{ M}$, rpm = 60, $\delta/D = 83 \text{ min/cm}$.
- (V) $C_{Eu \text{ total}} = 1.00 \times 10^{-6} \text{ M}$, $[\text{HClO}_4] = 0.118 \text{ M}$, rpm = 100, $\delta/D = 30 \text{ min/cm}$.
- (VI) $C_{Gd \text{ total}} = 1.62 \times 10^{-6} \text{ M}$, $[\text{HClO}_4] = 0.118 \text{ M}$, rpm = 100, $\delta/D = 30 \text{ min/cm}$.
- (VII) $C_{Tm \text{ total}} = 3.31 \times 10^{-7} \text{ M}$, $[\text{HClO}_4] = 0.500 \text{ M}$, rpm = 100, $\delta/D = 23 \text{ min/cm}$.
- (VIII) $C_{Fe \text{ total}} = 1.40 \times 10^{-5} \text{ M}$, $[\text{HClO}_4] = 0.118 \text{ M}$, rpm = 30, $\delta/D = 150 \text{ min/cm}$.

$$-\epsilon = \frac{K_R}{7} \bar{K}_1 a_{H^+}^3 C_{M \text{ total}}$$

and recalling that $\vec{N}(A/V) = -(dC_M^0/dt) = \vec{V}$, it follows

$$-\int_{C_{M \text{ total}}^0}^{C_M^0} \frac{2\alpha(V/A)dC_M^0}{-(\beta + \gamma C_M^0) - ((\beta + \gamma C_M^0)^2 - 4\alpha(\nu C_M^0 + \epsilon))^{1/2}} = t \quad (17)$$

since for $C_M^0 = C_{M \text{ total}}$, $-f = t = 0$

Figure 9 shows examples of concentration vs. time data, covering a time interval ranging from a few minutes to several hours, for the transfer of some trivalent lanthanide cations (Eu, Tm, Gd, Ce) and Fe(III) from aqueous perchloric acid solutions to toluene solutions of HD obtained for experimental conditions where chemical reactions and diffusion are both rate determining. Equation 17 represents the experimental data well as shown by the calculated solid curves. To perform the calculation a numerical integration of eq. 17 has been performed through a suitable computer program. To perform the calculation the rough approximation:

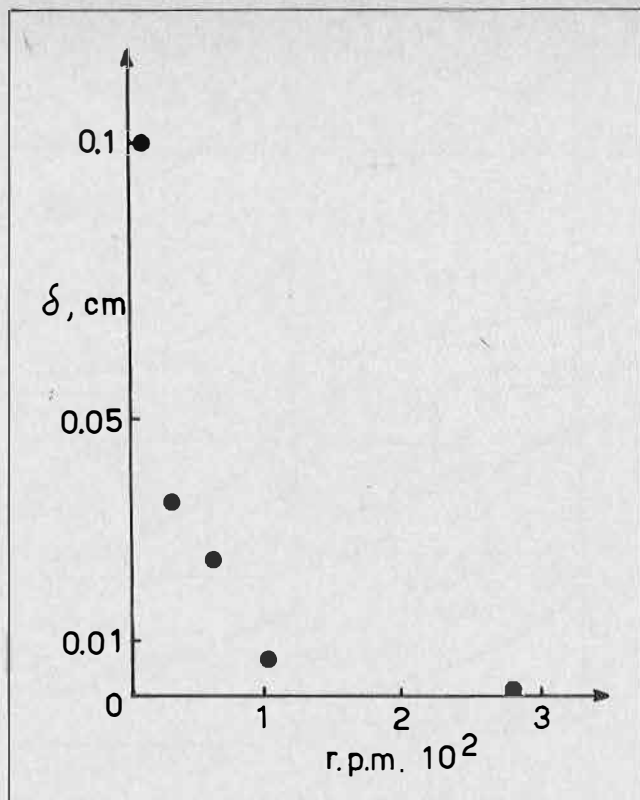


FIGURE 10. Stirring speed (rpm) vs. thickness of the diffusion film (δ) plot for the experimental conditions used in this work. The δ values have been obtained from the δ/D values reported in Figure 9 assuming $D = 3 \times 10^{-4} \text{ cm}^2/\text{min}$. The point referring to 280 rpm has been taken from Figure 7.

$$\frac{\delta_w}{D_M} = \frac{\delta_o}{D_M} = \frac{\delta_o}{D_{(HD)_m}} \text{ has been introduced.}$$

A and V are the interfacial area (12.6 cm^2) and the volume of the phases (0.03 l) used in all the experiments. The K_1 , \bar{K}_1 , K_R values reported in Table 1 have been used. $C_{M \text{ total}}$, $\bar{C}^{\circ}_{HD}[\text{HClO}_4]$ for each concentration - time curve and the best δ/D values fitting the experimental data are also reported in the figures. For all the lanthanide ions these values lie in the range 17-30 min/cm when the stirring speed is 100 rpm. If an average D value equal to $3 \times 10^{-4} \text{ cm}^2/\text{min}$ is assumed for all the lanthanide ions, it follows that a thickness of the diffusion film $\delta = (7 \pm 2) \times 10^{-3} \text{ cm}$ can explain all the experimental data. This value is in good agreement with the δ value at 100 rpm stirring speed evaluated from the forward initial mass transfer data.

As far as the concentration vs. time curves obtained at 60, 30, 10 rpm stirring speeds are concerned, the following δ/D values have been found to fit the experimental data: 83 min/cm (60 rpm), 117 min/cm (30 rpm), 333 min/cm (10 rpm). If the same D value previously reported is assumed, it follows the relationship rpm vs δ reported in Figure 10. The good agreement between calculated and experimental concentration vs time curves seems to indicate that, within the limits of validity of the approximations introduced to perform the calculation, (a) the assumptions formulated on the steady state hold also at $t \neq 0$, (b) the identified reaction mechanism does not change with time, (c) the indirect way of evaluating K_R and the assumption about the constancy of K_1 , and \bar{K}_1 for all lanthanide cations are reasonable.

NOTATION

\vec{V}	= $-d[M^{+3}]/dt$ = forward mass transfer rate
\overleftarrow{V}	= $-d[M]/dt$ = reverse mass transfer rate
$[M^{+3}]$	= aqueous metal concentration
$[M]$	= organic metal concentration
\vec{V}^*	= $\vec{V}/[M^{+3}]$, $\overleftarrow{V}^* = \overleftarrow{V}/[M]$ = normalized mass transfer rates
V	= volume of the aqueous or organic phase
A	= interfacial area
$\vec{N} = \vec{V}(V/A)$	= mass transfer flux
C^* and C°	= molar concentrations near the interface and in the bulks
γ	= activity coefficient, a = activity
δ	= thickness or diffusion film
D	= diffusivity
K_1	= rate constants
E	= distribution ratio
π	= interfacial pressure

REFERENCES

- (1) Danesi, P.R., Chiarizia, R., and Saltelli, A., *J. Inorg. Nucl. Chem.* 1976, 38, 1687.
- (2) Danesi, P.R., Chiarizia, R., and Sanad, W.A.A., *J. Inorg. Nucl. Chem.* 1977, 39, 519.
- (3) Chiarizia, R., and Danesi, P.R., *J. Inorg. Nucl. Chem.* 1977, 39, 525.
- (4) Chiarizia, R., Danesi, P.R., D'Alessandro, G., and Scuppa, B., *J. Inorg. Nucl. Chem.* 1976, 38, 1367.
- (5) Danesi, P.R., Muhamed, M., and Chiarizia, R., submitted for publication on *J. Inorg. Nucl. Chem.*
- (6) Flett, D.S., O-Kuhara, D.N., and Spink, D.R., *J. Inorg. Nucl. Chem.* 1973, 37, 2471.
- (7) Flett, D.S., Cox, M., and Heels, J.D., *J. Inorg. Nucl. Chem.* 1975, 37, 2533.
- (8) McDowell, W.J., and Coleman, C.F., *J. Inorg. Nucl. Chem.* 1967, 29, 1325.
- (9) Roddy, J.W., Coleman, C.F., and Arai, S., *J. Inorg. Nucl. Chem.* 1971, 33, 1099.
- (10) Baumgärtner, F., and Finsterwalder, L., *J. Phys. Chem.* 1970, 74, 108.
- (11) Vandegriff, G.F., and Horwitz, E.P., *J. Inorg. Nucl. Chem.*, in press.
- (12) Chiarizia, R., Danesi, P.R., Raich, M.A., and Scibona, G., *J. Inorg. Nucl. Chem.* 1975, 37, 1495.
- (13) Bird, R. Byron, Stewart, W.E., and Lightfoot, E.N., *Transport Phenomena*, 1960, Wiley, Tokyo.

DISCUSSION

A.J. Monhemius: There is a certain amount of controversy about whether activities or concentrations of species should be used in rate expressions. Activity is a bulk property of a solute whereas the rate expression is concerned with processes on a molecular level. I notice that Dr. Danesi has used ionic activities in his rate expressions and I would like to hear his comments about this.

P.R. Danesi: The rate of process should depend on the number of collisions between the reacting species. The rate of reaction should then depend on the concentrations since the number of collisions is directly correlated to concentrations. Nevertheless this fact is not experimentally verified and, especially when ions are involved, a corrective *kinetic factor* has to be introduced to explain the dependence has been found to coincide with the ratio of the activity coefficients. Moreover, when the rate constant is derived from the theory of absolute reaction rates it follows that

$$K_r = \frac{KT}{h} \cdot K_o^\ddagger \frac{a_A a_B}{a^\ddagger} \text{ where the term}$$

$\frac{KT}{h} \cdot K_o^\ddagger$ is the rate constant for an ideal system and a_A , a_B , and a^\ddagger are activities.

It follows then that activities have to be used instead of concentrations. In conclusion, the use of activities for reactions occurring in solution seems to be both theoretically and experimentally justified.

C.A. Fleming: (1) In the two series of experiments in which (a) Diffusion contribution to the rate was minimized, (b) Chemical contribution to the rate was minimized, did the order of reaction with respect to the concentration of the various species vary?

(2) To what do you attribute the independence of the rate on reagent concentration at high concentrations of reagent? Is the formation of micelle 3 envisaged in this region?

P.R. Danesi: (1) As I have shown, the apparent order of reaction is a complex function of the molecularity of the various reaction steps present in the extraction mechanism. Therefore, as the equations have clearly shown, even a rather simple reaction mechanism

will produce variable reaction order. The zero order of reaction at high extractant concentration is an example of this effect.

(2) The formation of micelles is in this case a fast step which also occurs at very low extractant concentrations in the order of 10^{-5} molar.

W. Nitsch: What are your arguments for excluding the effect of the hydrodynamics of the cell in the plateau region?

P.R. Danesi: The plateau of the curve rate versus stirring speed is of course dependent on both the hydrodynamics of our experiments as well as the chemical nature of the system we have investigated. It is therefore expected that by altering the hydrodynamics features of the cell the plateau could fall either in a different position or even disappear (if the stirring efficiency becomes extremely poor). The problem is then to find operating conditions where a good plateau can be found.

MASS TRANSFER

Equilibrium and Mass Transfer for the Separation of Nickel and Cobalt in di (2 Ethyl Hexyl) Phosphoric Acid

J. A. Golding, S. A. Fouda and V. Saleh
Chemical Engineering Department,
University of Ottawa,
Ottawa, Ontario.

ABSTRACT

Binary equilibrium data have been obtained for the extraction of cobalt and nickel in di(2-ethyl-hexyl)phosphoric acid. The data showed that metal uptake of one component was greatly influenced by the presence of the other metal. The separation factor was estimated from the equilibrium data at 25°C. It was also found that metal uptake by D2EHPA decreased with increase in temperature. Mass transfer coefficients were obtained for co-extraction, scrubbing and stripping, using a Lewis type unit cell. Mass transfer coefficients for extraction were found to be higher than those obtained in scrubbing and stripping. Extraction mass transfer coefficients lay in the 1.92×10^{-3} to 7.70×10^{-3} cm/s range; they were observed to increase with increase in Reynolds number. Comparison of mass transfer coefficient values with values obtained for the extraction of acetic acid into benzene suggests that mass transfer rates were diffusion-controlled.

Equilibrium Studies

Introduction

THE APPLICATION OF LIQUID - LIQUID extraction as a means of recovering and separating metals has made great progress over recent years. Initial uses were directed towards the recovery of rare earths and radio-active material. However, in recent years liquid - liquid extraction has been used in the recovery of copper and other 3 d-type transition metals such as cobalt and nickel⁽¹⁾. Much

research effort has been devoted to the problem of separating cobalt and nickel, with high separation factors being obtained when using a mixture of Kelex 100 and Versatic 911. These extractants were reported to exhibit a synergistic effect⁽²⁾. Kinetic synergism was also successfully used for the separation of these two metals in acid sulphate systems using a mixture of hydroxyoxime and tertiary carboxylic acid⁽³⁾. Cobalt and nickel can also be extracted from aqueous solution by di(2-ethyl-hexyl) phosphoric acid (D2EHPA)⁽⁴⁾ and this is the basis of a proposed process for the separation of these two metals^(4,6). In this process nickel and cobalt were first co-extracted at a pH of 5.0-5.5. The loaded solvent was then scrubbed with an aqueous cobalt solution, up to 20 g/l. The cobalt was then extracted into the organic phase, the nickel being recovered in the raffinate solution. A dilute mineral acid was used to recover the cobalt but was not as efficient as scrubbing with the aqueous cobalt solutions.

Because of the interest in separation of cobalt and nickel (using D2EHPA), it was felt that a fundamental study of the equilibrium of binary solutions of cobalt and nickel and D2EHPA would be of great assistance in determining the mechanism of this process. Examination of the pure metal extraction isotherms⁽⁵⁾ for cobalt and nickel indicated that a 10% D2EHPA solution in kerosene could be a very efficient solvent. A study was therefore undertaken to obtain equilibrium and mass transfer data for this system.

Experimental

Standard solutions containing varying amounts of cobalt and nickel were prepared, the pH of these solutions being adjusted to 4.0. The organic solvent comprised 10%

D2EHPA and 5% tri-butyl phosphate in kerosene (Shell-Sol LX154) and was treated with ammonium hydroxide to form the ammonium salt. The ammonia was added in 5% excess of the stoichiometric amount several hours before the equilibrium runs were carried out. In carrying out runs, the solutions were shaken for ten minutes and allowed to stand overnight. The two phases were then separated. It appears that the equilibrium is rapidly achieved since in preliminary shake-out tests it was found that equilibrium was reached in less than two minutes which was the minimum practical time required to shake the two solutions, separate the phases and sample for analysis.

After the phases were separated, the pH of the aqueous phase was measured and an aqueous phase sample taken for analysis. Analysis of the aqueous phase was carried out directly using an atomic absorption spectrophotometer. In case of the organic phase, random samples were stripped with three portions of equal volumes of 10% sulphuric acid and then analysed. Material balances were found to be within 6%. The organic concentrations of the remaining samples were calculated from the initial and final aqueous phase concentrations. In carrying out these runs both phases were found to remain clear and no

precipitation or emulsion formation was observed over the concentration range studied⁽⁷⁾.

Results and Discussion

Equilibrium data were obtained for a synthetic sulphate solution with the initial aqueous metal ion concentration maintained at 10.0 ± 0.73 g/l. The initial nickel ion concentration was varied from 0 - 10.73 g/l and the cobalt from 0 - 9.4 g/l. The initial pH was constant at 4.0 and the temperature maintained at 25°C. The equilibration of the solvent with NH_4OH maintained the equilibrium pH in the range 4.85-5.7 with the higher pH values being observed at low aqueous to organic volumetric ratio. This range of equilibrium pH was recommended to produce higher extraction coefficients for both metals⁽⁸⁾. The equilibrium data for pure cobalt, pure nickel and binary mixtures are shown in Tables 1 and 2. Extraction isotherms for the pure metal solutions and the binary solutions are shown in Figures 1 and 2. A family of extraction isotherms for each metal is shown at various equilibrium aqueous concentration ranges of the other metal. Figures 1 and 2 show clearly that the presence of one metal in the aqueous phase suppresses the extraction of the other metal. In comparing the extraction isotherms for both metals, it is seen that cobalt is slightly more favourably extracted than nickel as could be expected from the data in the literature⁽¹⁾. It can also be seen that while the stoichiometric extraction corresponded to a maximum molar ratio of metal to extractant of 0.5:1⁽⁸⁾,

TABLE 1. Equilibrium Data for the Extraction of Cobalt and Nickel in 10% Di(2-Ethyl-Hexyl) Phosphoric Acid, Single Component Equilibrium

Aqueous Phase Concentration g/l		Organic Phase Concentration g/l		Equilibrium Aqueous pH (1)
Nickel	Cobalt	Nickel	Cobalt	
—	0.06	—	2.34	5.70
—	0.50	—	4.45	5.65
—	3.20	—	6.20	5.35
—	5.40	—	8.00	5.15
—	7.50	—	9.50	5.00
—	8.44	—	9.60	4.95
1.11	—	4.81	—	5.5
3.46	—	6.97	—	5.15
6.64	—	8.18	—	5.10
8.96	—	8.85	—	4.98
9.83	—	8.80	—	4.95

(1) Initial pH = 4 in all cases.

TABLE 2. Equilibrium Data for the Extraction of Cobalt and Nickel in 10% Di(2-Ethyl-Hexyl) Phosphoric Acid. Binary Equilibrium

Aqueous Phase Concentration g/l		Organic Phase Concentration g/l		Equilibrium Aqueous pH	Separation Factor $K_{\text{Ni}}^{\text{Co}}$
Nickel	Cobalt	Nickel	Cobalt		
0.01	0.05	0.28	2.10	5.85	1.05
0.06	0.63	0.53	3.89	5.42	0.69
0.52	3.20	0.60	5.20	5.27	1.41
0.80	5.20	0.64	6.40	5.15	1.45
0.87	7.08	1.19	6.60	5.10	0.68
0.20	0.55	0.95	3.45	5.65	1.33
1.05	3.07	1.05	4.38	5.30	1.43
1.60	4.93	1.00	5.05	5.18	1.64
1.90	6.39	1.00	5.30	5.00	1.57
2.00	6.87	1.00	5.80	5.00	1.69
0.34	0.32	1.98	2.63	5.65	0.97
1.84	1.80	2.44	3.79	5.29	1.62
3.00	3.71	2.58	3.76	5.05	1.18
4.02	5.14	2.70	4.50	4.92	1.30
0.05	0.02	1.33	1.16	5.98	2.25
0.55	0.38	2.40	2.14	5.72	1.31
2.55	1.55	2.81	3.10	5.50	1.82
3.90	2.90	2.90	3.51	5.25	1.62
4.70	3.93	3.28	3.60	5.15	1.38
0.59	0.23	2.88	1.76	5.68	1.59
2.62	1.00	3.73	2.75	5.20	1.93
4.27	2.20	4.16	3.10	5.10	1.45
5.51	3.11	4.20	3.20	5.02	1.35
5.93	3.41	4.20	3.40	4.94	1.41
0.03	0.06	0.81	1.62	5.90	0.94
0.25	0.41	1.50	3.07	5.68	1.24
1.60	2.18	1.65	4.36	5.40	1.93
2.50	4.34	1.50	4.40	5.12	1.64
2.90	5.58	1.75	4.70	5.1	1.43
0.95	0.12	3.76	0.89	5.65	1.84
3.90	0.58	4.59	1.32	5.25	1.97
6.12	1.07	4.71	1.66	5.12	2.08
7.50	1.48	4.85	2.10	4.89	2.37
7.92	1.67	5.50	2.30	4.85	2.27
0.10	0.02	2.38	0.24	5.85	0.65
1.25	0.08	4.18	0.44	5.2	1.64
4.50	0.48	4.90	0.49	5.09	0.88
6.80	0.66	5.70	0.48	4.95	1.10
8.40	0.80	6.00	0.80	4.85	1.33

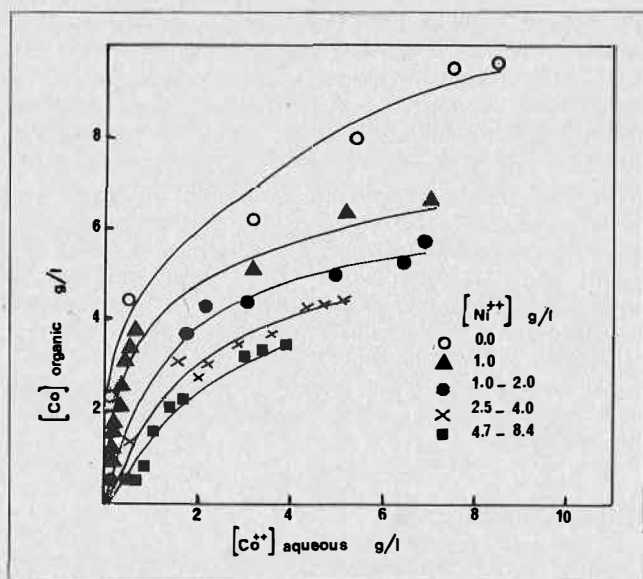


FIGURE 2. Effect of cobalt on the extraction of nickel in 10% D2EHPA.

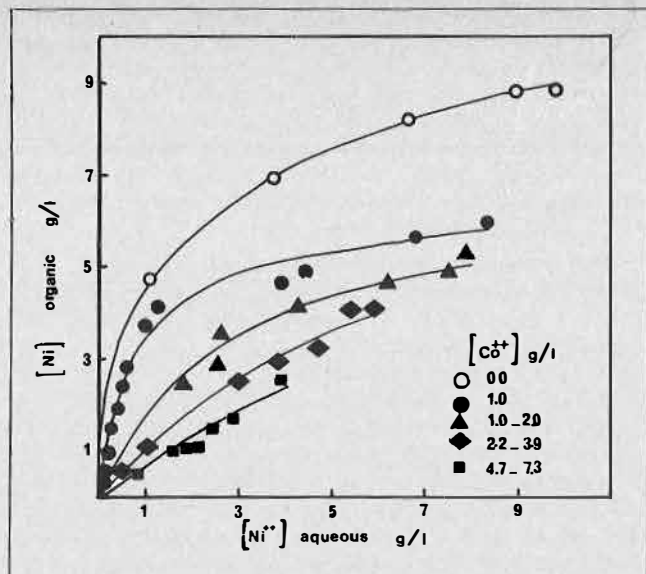
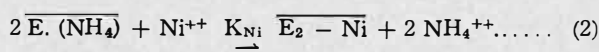
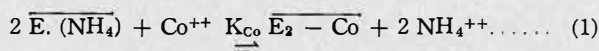


FIGURE 1. Effect of nickel on the extraction of cobalt in 10% D2EHPA.

the maximum value observed was 0.69. This high metal to extractant ratio could be due to the presence of tri n-butyl phosphate which is itself an extractant⁽¹⁾. It also appears to suggest that the extracted species may exist as a polymeric complex with the alkyl phosphoric group acting as a bridging ligand. The existence of polymeric structure for divalent cobalt and nickel complexes with D2EHPA was previously reported⁽⁶⁾.

The competitive cation exchange process could be described by the following equilibria:



It is difficult to calculate the individual equilibrium constants for each metal due to the presence of excess ammonia in the organic phase and the distribution of this species in the two phases is unknown. However, the ratio of the two equilibrium constants K_{Co} and K_{Ni} could be expressed as,

$$K_{\text{Ni}}^{\text{Co}} = \frac{\overline{E}_2 - \overline{\text{Co}} [\text{Ni}^{++}]}{\overline{E}_2 - \overline{\text{Ni}} [\text{Co}^{++}]} \dots \dots (3)$$

where

- $K_{\text{Ni}}^{\text{Co}}$ is the separation factor of the Co-Ni pair,
- $\overline{E}_2 - \overline{\text{Co}}$ is the concentration of cobalt species in the organic phase,
- $\overline{E}_2 - \overline{\text{Ni}}$ is the concentration of nickel species in the organic phase,
- $[\text{Co}^{++}]$ is the concentration of cobalt ions in the aqueous phase, and
- $[\text{Ni}^{++}]$ is the concentration of nickel ions in the aqueous phase.

Applying material balance for both metals, the concentrations in the organic phase could be written as

$$\overline{E}_o - \overline{\text{Co}} = \frac{V_a}{V_o} ([\text{Co}_i] - [\text{Co}^{++}]) \dots \dots (4)$$

$$\overline{E}_o - \overline{\text{Ni}} = \frac{V_a}{V_o} ([\text{Ni}_i] - [\text{Ni}^{++}]) \dots \dots (5)$$

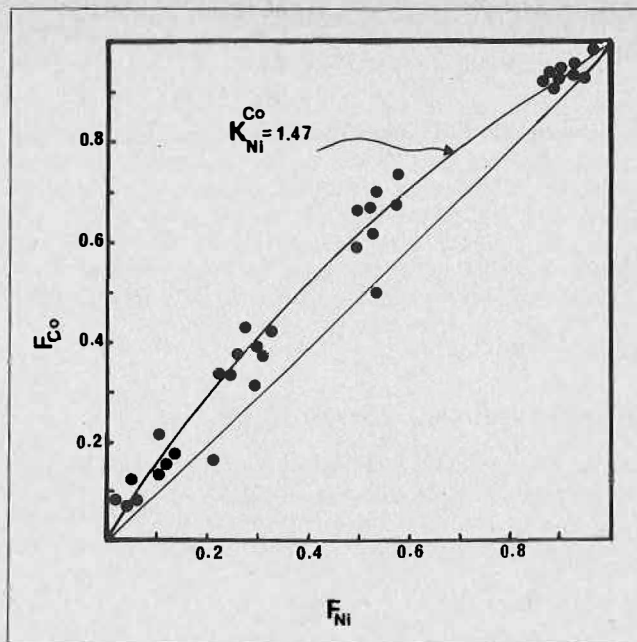


FIGURE 3. Relative extraction of cobalt and nickel.

where V_a and V_o are the volumes of the aqueous and organic phase, respectively.

$[\text{Co}_i]$ and $[\text{Ni}_i]$ are the initial concentration of cobalt and nickel, respectively.

$$K_{\text{Ni}}^{\text{Co}} = \frac{1}{F_{\text{Ni}}} - 1 / \frac{1}{F_{\text{Co}}} - 1 \dots \dots (6)$$

F_{Co} and F_{Ni} are the fractions removed from the aqueous phase of cobalt and nickel, respectively.

Treatment of the data in Table 1 according to equation 6, provides a value for the separation factor $K_{\text{Ni}}^{\text{Co}}$ of 1.47 ± 0.427 . Ritcey and Ashbrook reported a value of 1.6 for the separation factor using the same extractant⁽⁶⁾.

It is worthwhile mentioning that another set of shake-out tests were carried out whereby the initial concentration of one metal was fixed and variable initial concentrations of the other metal were used such that the total initial metal ion concentration was varied from 5-15 g/l. In this set of experiments more scatter in the data was observed and the equilibrium values were rather different, possibly due to the variations in the ionic strength in the system. The value of the separation factor obtained in this case, however, was 1.560 ± 0.37 which is within the estimated value at constant total metal ion concentration. It appears that the value of the separation factor is not affected by the metal concentration. A value of 0.56 for the separation factor of cobalt and nickel was reported to be constant for various concentrations using fatty acids as extractant⁽⁹⁾. Figure 3 shows the fraction of cobalt removed from the aqueous phase vs. that of nickel. The curve indicates the value of F_{Co} corresponding to a separation factor of 1.47.

The effect of temperature on the extraction isotherms is shown in Figure 4 for the pure metals at 25°C and 50°C. It was found that the extraction of metal decreased with increase in temperature. It can be seen that there is a difference between the pure metal isotherms for cobalt. This may be an effect of ionic strength as in Figure 1 metal concentration was 10 g/l while for Figure 4 the initial concentration was 5 g/l.

Mass Transfer Studies

Introduction

In the extraction and separation of cobalt and nickel using D2EHPA there are three distinct areas of interest, (1) the co-extraction of cobalt and nickel, (2) the scrubbing as cobalt preferentially concentrates in the organic phase and (3) during the acid stripping of the organic phase. This work was carried out to determine mass transfer coefficients under each of these conditions and provide information which could assist in design of liquid-liquid extraction equipment for separation of cobalt and nickel.

Equipment and Procedures

The mass transfer runs were carried out in a unit cell of the Lewis⁽¹⁰⁾ type. The cell was made up of two pieces of glass pipe 15.24 cm internal diameter, cut such that the volume of the upper cell was 1,010 ml and the lower cell

1,730 ml. The upper and lower cells were separated by a stainless steel partition plate and mounted between two stainless steel plates as shown in Figure 5. The contacting area was 30.5 cm² and the two phases were mixed by turbine, twin blade stirrers. The stirrers were mounted independently and were driven by Zero Max Model E-1 variable speed motors, 0 - 50 rpm range. The range of Reynolds numbers was 0 - 5,000 in the aqueous phase and 0 - 3,200 in the organic phase.

The extraction runs were carried out using 10% D2EHPA in kerosene solvent with 5% tri-butyl phosphate as the organic phase. The solution was equilibrated with ammonia, 5% excess, before starting the runs. In the extraction runs the aqueous feed contained 5 g/l nickel and 2 g/l cobalt, while in the scrubbing runs the aqueous cobalt concentration was 5 g/l. The stripping runs were carried out using 25% nitric acid. Each experimental run was carried out over a time period of three to four hours with samples taken from both phases at frequent intervals. The liquid level was maintained constant in the middle of the partition ring by addition or removal of one of the phases as required. Full details of the apparatus and procedures are given in reference (11).

Results and Discussion

Concentration Curves

Typical curves for the co-extraction of the two metals are shown in Figures 6 and 7 with curves obtained for scrubbing and stripping shown in Figures 8 and 9. The extraction curves showed that there was a continuous co-extraction of both metals from the aqueous phase into the organic phase. Some runs indicated the possibility of a

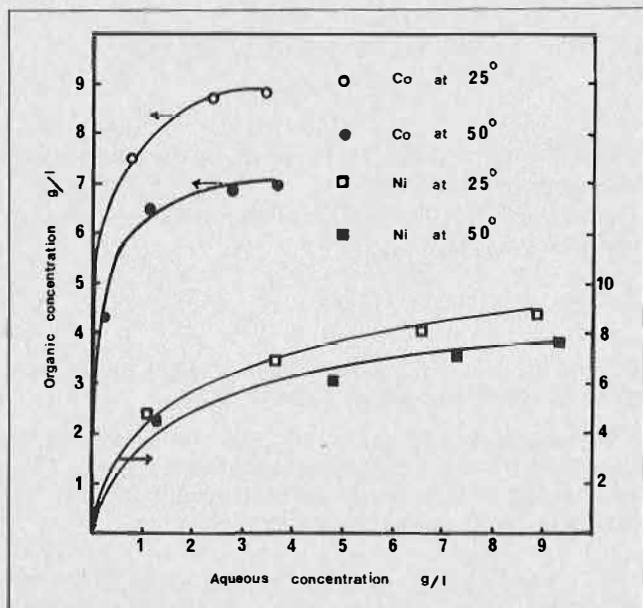


FIGURE 4. Effect of temperature of extraction.

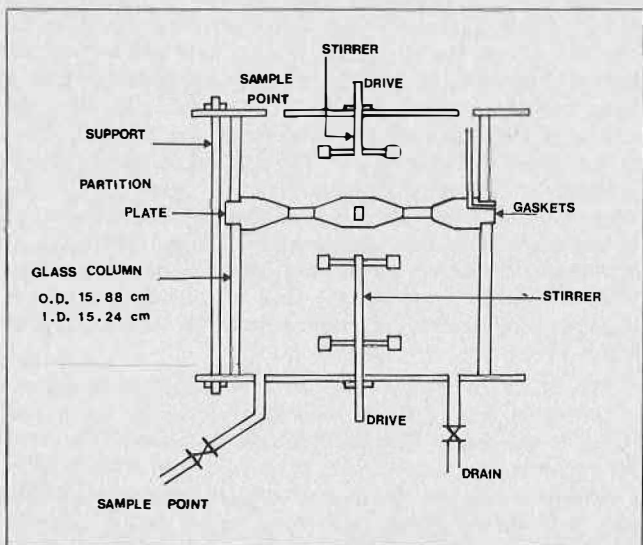


FIGURE 5. Extraction cell.

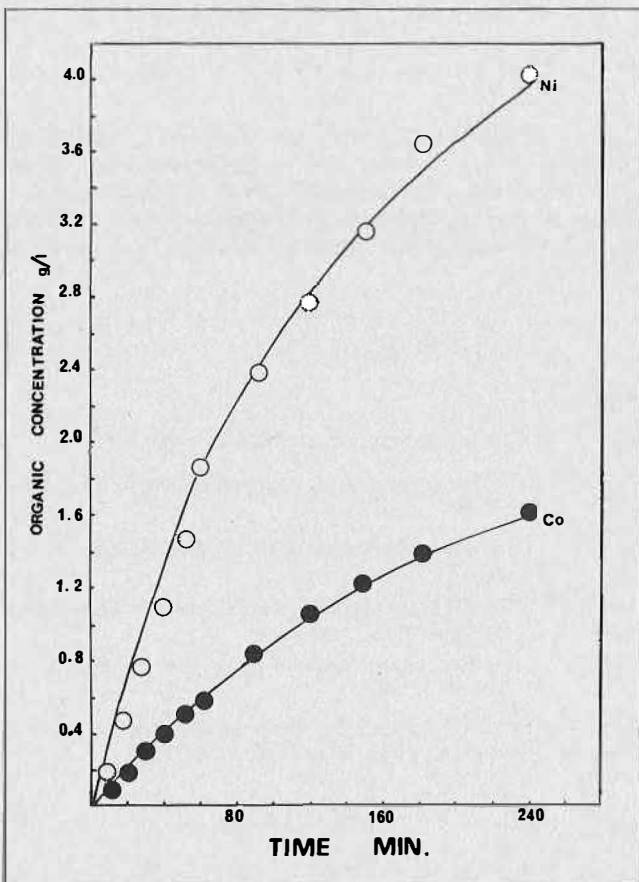


FIGURE 6. Extraction curves for cobalt and nickel.

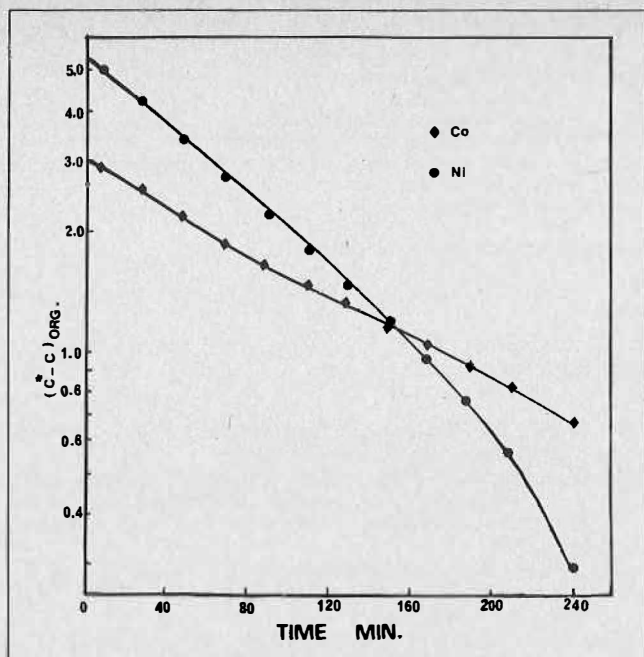


FIGURE 7. Log $(C^* - C)$ vs. t for the extraction of cobalt and nickel.

rapid initial uptake of cobalt and this is to be studied further. The extractions showed that mass transfer increased with increase in Reynold's number of each phase. The curves obtained for contacting the loaded organic with the aqueous cobalt solutions showed the shift in the organic phase equilibrium concentration (Figure 8). The stripping runs with 25% HNO_3 showed the removal of the extracted metal from the D2EHPA solution, into the aqueous phase (Figure 9).

Mass Transfer Coefficients

Mass transfer coefficients were evaluated over any interval, Δt , on the basis of the following equation:

$$\bar{K}_{org} = \frac{V_o}{\Delta t A_s} C_o(t) \int \frac{C_o(t + \Delta t)}{C_o^* - C_o} dt \dots \dots \dots (1)$$

where \bar{K}_{org} refers to the average overall organic phase mass transfer coefficient, V_o organic phase volume, A_s the interfacial area, C_o the concentration of metal in the organic phase and C_o^* the equilibrium concentration. The integral in equation (1) was evaluated numerically from plots of $\ln(C_o^* - C_o)$ versus contact time, t (as in Figure 7). Organic phase mass transfer coefficients for the extraction of cobalt and nickel are given in Table 3. The mass transfer coefficients are in general higher for nickel than for cobalt. Increase in Reynolds number resulted in an increase in the value of the mass transfer coefficients for both metals. It is not possible at the moment to fully explain the change in the mass transfer coefficient values with the contact time. The plot of $\log C_o^* - C_o$ vs. t (Figure 7) shows reasonable linearity except at long periods of contact time for nickel. This could be due to some uncertainty in the equilibrium values at this concentration range. It is not inconceivable, however, that the mass transfer coefficient values are dependent on the metal concentration in one or both phases. The metal salt, being an electrolyte, is expected to have considerable effect on the interfacial tension in the system. The effect of metal concentration on the mass transfer coefficient values is being studied in detail.

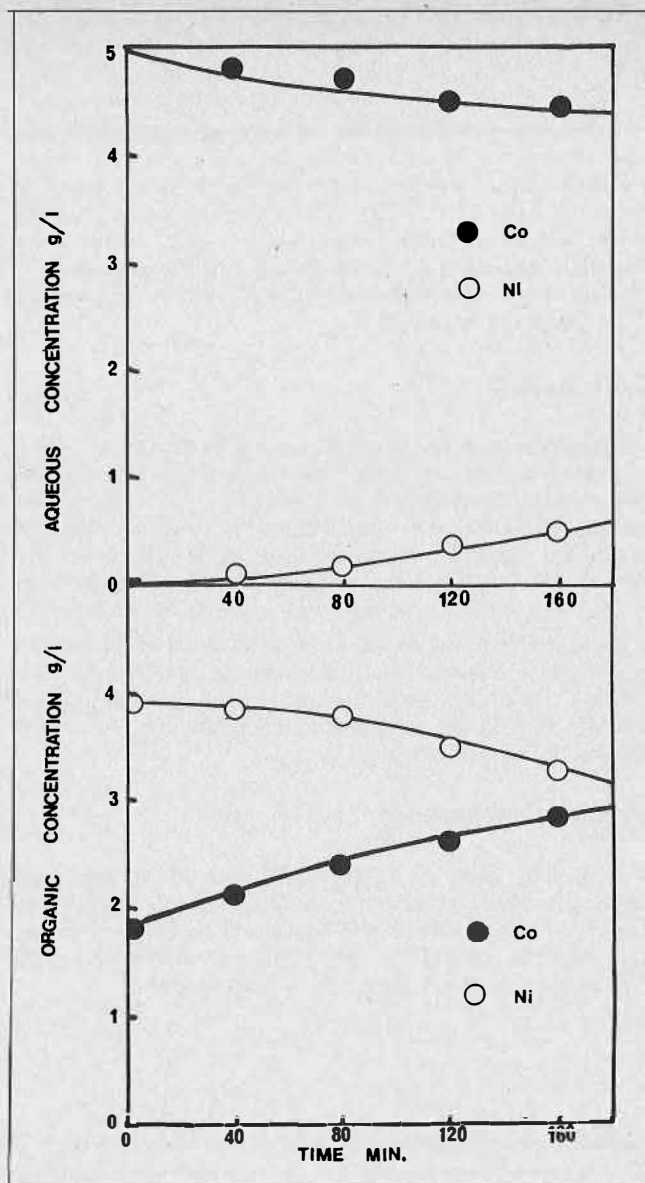


FIGURE 8. Extraction curve for cobalt scrubbing.

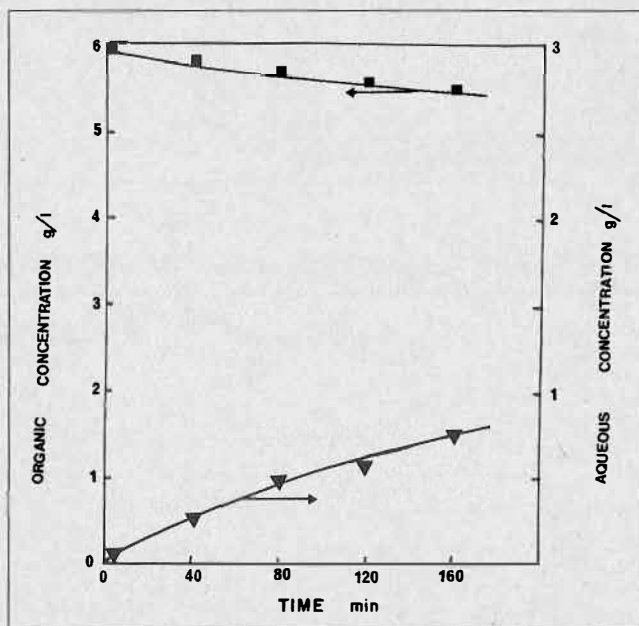


FIGURE 9. Extraction curve for cobalt stripping.

In the scrubbing and stripping runs, mass transfer coefficient values were lower than during extraction (see Table 4). Further work is being carried out on the effect of Reynold's number on mass transfer coefficient values.

A run was carried out on the extraction of acetic acid from benzene; aqueous phase Re 1,500 organic phase Re 1,000. Mass transfer coefficient values were found to lie in the 3.0×10^{-3} to 7.1×10^{-3} cm/s depending on the extraction time. These values indicate that, in the mass transfer, operations involved in the extraction separation and recovery of cobalt using D2EHPA can be assumed to be diffusion-controlled.

Conclusion

Equilibrium studies have shown that in the co-extraction of cobalt and nickel there is an interaction between the two metals which influences the amount of each of the metals extracted. The equilibrium data were used to evaluate a value for the separation factor consistent with that reported in the literature. The amount of metals extracted was found to decrease with increase in temperature.

Mass transfer was found to be diffusion-controlled with higher mass transfer coefficients being obtained for extraction than for scrubbing or stripping. This would indicate that larger size contacting equipment is needed for scrubbing and stripping.

Acknowledgments

S. Fouda and V. Saleh would like to acknowledge financial assistance from National Research Council of Canada. Appreciation is also expressed to Denison Mines Ltd. for the D2EHPA. The valuable discussions with Dr. M.H.I. Baird are gratefully acknowledged.

NOTATION

A_s	= interfacial area, cm^2
C	= concentration, g/l
C^*	= equilibrium concentration g/l
k	= extraction equilibrium constant
K_{org}	= overall organic phase mass transfer coefficient, cm/s
t	= contacting time, min
V	= cell volume, l

subscript o refers to organic phase

REFERENCES

- (1) Bailes, P.J., Hanson, C. and Hughes, M.A., Chemical Engineering, August 30th, 1976, 86.
- (2) Hummelstedt, L., Sand, H.E., Karoluolo, J., Berts, L.O., and Nyman, B.G., Proceedings of International Solvent Extraction Conference - ISEC '74 I, 829 (Soc. Chem. Ind. 1974).
- (3) Nyman, B.G. and Hummelstedt, L., Proceedings of International Solvent Extraction Conference - ISEC '74 I, 699 (Soc. Chem. Ind. 1974).
- (4) Ritcey, G.M. and Ashbrook, A.W., Trans. Inst. of Mining and Metallurgy 1969, C 78, No. 751, 57.
- (5) Ritcey, G.M., Ashbrook, A.W. and Lucas, B.H., C.I.M., Bulletin 1075, 68 (753), 111.
- (6) Ritcey, G.M., Ashbrook, A.W., U.S. Patent 3,438,768, April 1969.
- (7) Berger, S.A., J. Inorg. Nuclear Chem. 1973, 35, 4300.
- (8) Sato, T. and Ueda, M., Proceedings of International Solvent Extraction Conference - ISEC '74 I, 871 (Soc. Chem. Ind. 1974).
- (9) Bobikov, P.I. and Gindin, L.M., International Chem. Eng. 1963, 3, 133-38.
- (10) Lewis, J.B., Chem. Eng. Sci. 3, 248 (1954).
- (11) Saleh, V., M.A.Sc. Thesis, University of Ottawa, 1977.

TABLE 3. Average Overall Organic Phase Mass Transfer Coefficients

Time Interval min	Reynolds Number*		Overall Mass Transfer Coeff. $\times 10^3$ cm/s		Reynolds Number*		Overall Mass Transfer Coeff. $\times 10^3$ cm/sec		Reynolds Number*		Overall Mass Transfer Coeff. $\times 10^3$ cm/sec	
	Aqueous Phase	Organic Phase	Nickel	Cobalt	Aqueous Phase	Organic Phase	Nickel	Cobalt	Aqueous Phase	Organic Phase	Nickel	Cobalt
0-40	1,500	1,000	2.34	1.92	1,500	2,000	4.70	3.29	3,000	1,000	4.30	3.12
40-80	"	"	2.59	2.03	"	"	6.36	4.67	"	"	4.41	3.08
80-100	"	"	2.41	2.08	"	"	5.30	3.14	"	"	4.67	3.12
120-160	"	"	2.24	1.94	"	"	5.64	3.28	"	"	5.42	3.35
160-200	"	"	2.16	1.67	"	"	7.11	3.31	"	"	7.7	3.97

*Characteristic length is impeller diameter.

TABLE 4. Average Overall Organic Phase Coefficients for Cobalt

Time Interval min	SCRUBBING			Mass Transfer Coefficient cm/s	STRIPPING		Mass Transfer Coefficient cm/s
	Reynolds Number*	Aqueous Phase	Organic Phase		Reynolds Number*	Organic Phase	
0-30	1,500	1,000		1.19×10^{-3}	1,500	1,500	0.47×10^{-3}
30-60	"	"		0.78×10^{-3}	"	"	0.92×10^{-3}
60-90	"	"		0.63×10^{-3}	"	"	0.63×10^{-3}
90-120	"	"		0.51×10^{-3}	"	"	0.47×10^{-3}
120-150	"	"		0.58×10^{-3}	"	"	0.41×10^{-3}
150-180	"	"		0.60×10^{-3}	"	"	0.35×10^{-3}

*Characteristic length is impeller diameter.

DISCUSSION

P. Chiang: Did you determine the oxidation state of cobalt in the organic phase or did you use an inert-atmosphere blanket in your mixer? I am wondering if the higher extractability you obtained for cobalt over nickel is caused, at least partly, by the preferential extraction of Co(III).

S. Fouda: We did not take precautions to prevent any possible oxidation of Co(II) to Co(III). The preferential extraction of Co in this system was previously reported, however (reference 6). It is to be noted also that higher extractability for cobalt was observed in some runs where determinations were made after less than two minutes of shaking in which case the oxidation to Co(III), if any, could be neglected.

MASS TRANSFER

Electrostatic Extraction for Metals and Non-metals

P. J. Bailes,
Schools of Chemical Engineering,
University of Bradford,
Bradford, England.

ABSTRACT

The mass transfer performance of charged droplets in a d.c. field has been studied for three different electrode geometries. Measurements on droplets formed at a single nozzle in a divergent electric field were restricted to the extraction of metal species from an aqueous droplet phase and results are reported for the Nickel-D2EHPA and Copper-LIX 64N systems. Published data^(1,2) for heptane transfer into single droplets of furfuraldehyde in a uniform field have been newly interpreted to allow some comparison with theory. An organic solute has also been used to test a novel electrostatic contactor. The electric field proved beneficial in each case.

Introduction

PARTS I⁽¹⁾ AND II⁽²⁾ OF THIS STUDY have shown that charged droplets moving through a continuous liquid phase under the influence of an electric field possess properties which are attractive from an extraction standpoint. The results were confined to a parallel plate electrode geometry with either single or multiple nozzles incorporated into the upper electrode. The application of a dc potential difference across the plates modified the size of droplets leaving the charging nozzle and affected their movement between the plates, which were submerged in the continuous phase. In order to ascertain dispersed phase film coefficients by means of the Colburn and Welsh⁽³⁾ technique, the mass transfer measurements were made on a low interfacial tension partially miscible system n-heptane-furfuraldehyde. The choice of system is limited by electrical considerations⁽⁴⁾ since it is necessary for the dispersed phase to be a conducting liquid and the continuous phase to be an electrical insulator. Nevertheless, a number of suitable binary systems are available which satisfy both the mass transfer and electrical restrictions⁽⁵⁾.

The main difficulty in interpreting measurements made on charged droplets in a parallel plate electrode geometry is that the nominal field strength given by the quotient of the applied potential difference and the electrode separation bears little relation to that actually experienced by the droplet. In fact the voltage gradient between the electrodes is non-linear, being greatest in the vicinity of the electrodes where the space charge concentration is largest.

If the space charge were uniformly distributed between the electrodes the potential distribution would obey Poisson's relation: —

$$\nabla^2 \psi = - \rho / \epsilon \dots \dots \dots (1)$$

But the electric field concentrates the distributed charge at the electrodes and so the distributed charge, ρ per unit volume, varies with position in an unknown way and consequently equation (1) cannot be solved to give the potential distribution between the electrodes. In the absence of this information it is impossible to predict the charge induced on the forming droplet or the droplet velocity from purely fundamental considerations and a semi-empirical approach must be adopted.

A dimensional analysis based on the theoretical equations which describe charged droplet formation at a nozzle has been presented by Thornton⁽⁶⁾ and shown to give the following result: —

$$\frac{d_e}{D_N} = f \left[\left(\frac{Q^2}{\epsilon \epsilon_0 D_N^3 \gamma} \right), \left(\frac{D_N^2 \Delta \rho g}{\gamma} \right) \right] \dots \dots (2)$$

The three dimensionless groups were evaluated for slowly formed charged water droplets falling through n-heptane, and mixtures of n-heptane with carbon tetrachloride, and presented as a graphical correlation. These results indicate a unique relationship between the size of a droplet and its charge for a particular nozzle diameter and a given liquid-liquid system. The advantage of the correlation is that the electrostatic force on the detaching droplet is expressed solely in terms of the induced charge which is a quantity that is readily measured.

The problems involved in correlating data on the velocity of charged droplets are basically the same as those encountered in the prediction of droplet size. Once again it is impossible to relate the field in the vicinity of the droplet to the nominal field and as a consequence velocity measurements cannot be interpreted in terms of the nominal field. In addition since the field strength is a function of position, the droplet is unlikely to attain a true steady-state terminal velocity. Despite these difficulties it can be seen from Figure 1⁽⁷⁾ that a reasonable correlation exists between droplet charge and velocity for oscillating droplets in a number of different liquid-liquid systems. In fact dimensional analysis can be used⁽⁷⁾ to show that the

charge group $\frac{Q^2}{\epsilon \epsilon_0 D_N^3 \gamma}$ represents the contribution which the electric field makes towards enhancing the velocity of oscillating droplets.

Thus, the effect of the electric field on both droplet formation and velocity is described by the same dimensionless group. This finding gives an insight into the way in which mass transfer data may be analysed to give film coefficients for charged droplets.

In the present work a treatment is proposed for the mass transfer data on single charged droplets already presented in the earlier parts of this investigation. In addition to this fundamental study, hitherto unpublished results obtained with larger scale tests using a three component non-metal system are presented. The possibility of using electrostatic extraction for metals has also been investigated and results are given for the nickel-di-2-ethylhexyl phosphoric acid and copper-LIX 64N systems.

Non-Metal Systems

Dispersed Phase Film Coefficient

The determination of mass transfer coefficients on an area free basis requires an accurate knowledge of the interfacial area across which solute transfer is occurring. For this reason experiments were conducted on discrete droplets formed at a single charging nozzle. Droplets of pure furfuraldehyde were introduced into a column containing n-heptane saturated with furfuraldehyde and subsequently collected for analysis for their n-heptane content after falling through the continuous phase under the influence of an applied electric field. With this approach the droplet area during the fall period could be measured with reasonable accuracy, however, the area available for solute transfer during the formation, release and later coalescence stages was not so readily assessed. Some allowance for these "end effects" must be made before a mass transfer coefficient can be evaluated for the detached droplet.

In conventional uncharged systems a successful method^(8,9) of circumventing this problem is to vary the time of fall of the droplets by conducting experiments on several different lengths of column. The difference in exit

droplet concentration between a short column and any longer column being ascribed solely to the extra distance travelled by the droplet. This subtraction of data is only valid if the coalescence end effect is reduced to a minimum, by keeping the interfacial area of the coalesced layer very small, and if the conditions during droplet formation are maintained constant. The single droplet investigation described in detail in Part I was undertaken with the expectation that this method would be applicable to charged droplets. Droplet size, velocity and mass transfer data were reported^(1,2) for electrode separations of 4, 6, 8, 10 and 12 cm. using a range of applied potential differences. Unfortunately the non-linear potential distribution between the electrodes resulted in variable droplet formation conditions for applied field strengths which were nominally the same. This prevented the straightforward application of the column length subtraction method and finally the measurements were interpreted in terms of a mean droplet mass transfer coefficient based on a time averaged droplet area which included the formation stage.

Thorton's⁽⁶⁾ later observations on the charge carried by a droplet and its size reveal that, for a parallel electrode geometry and a fixed nozzle diameter, droplets of the same size carry an equivalent charge irrespective of the nominal applied field strength. It may be deduced from this that droplets of the same size have identical formation conditions although the nominal field strengths at which the droplets were produced may be different. In theory this means that a method based on different fall times may be used for charged droplets of the same size.

The first step in this approach was to arbitrarily select several droplet sizes and interpolate applied voltages and column lengths at which these would occur by using the data shown in Figure 2. These parameters could then be used in a reverse manner with the information given in Parts I and II to estimate the value of $(NTU)_{\infty}$ and velocity for the particular droplet size in question. Since

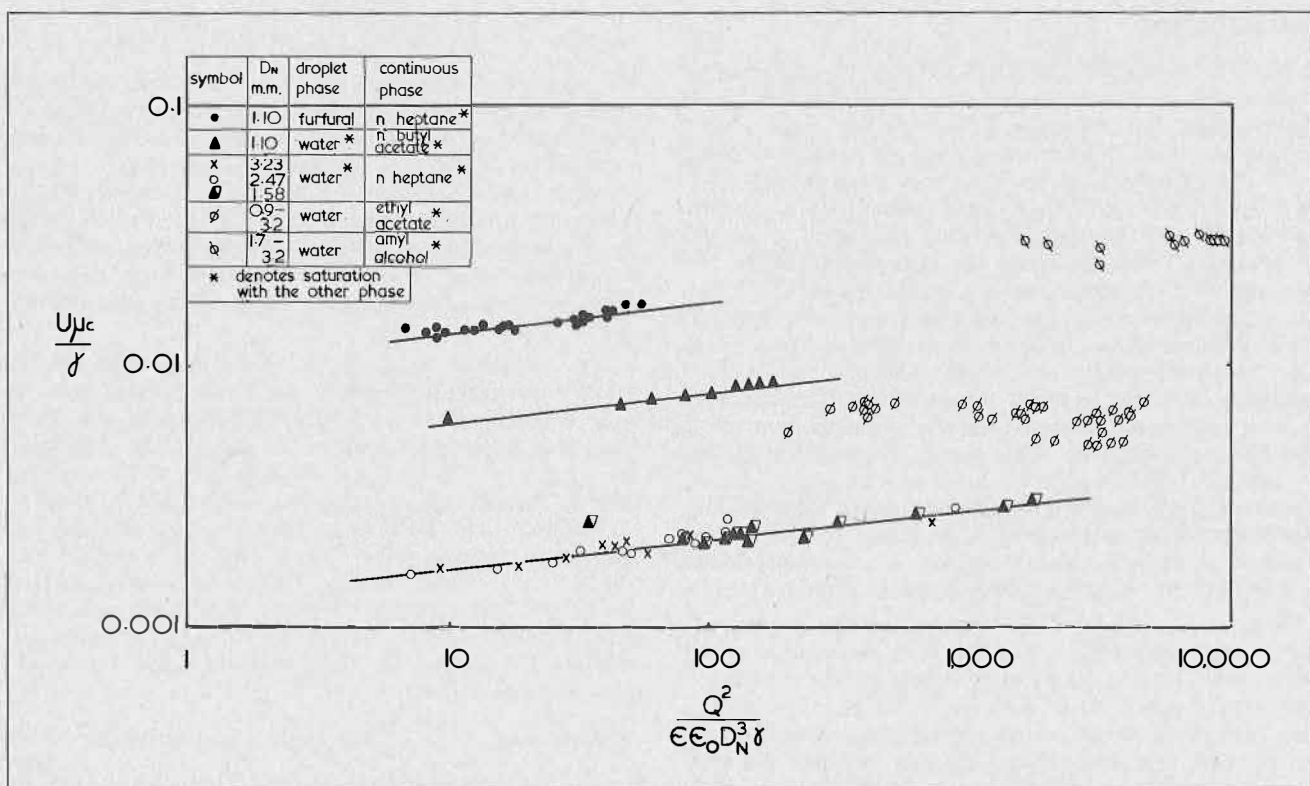


FIGURE 1. Relationship between dimensionless charge and velocity groups.

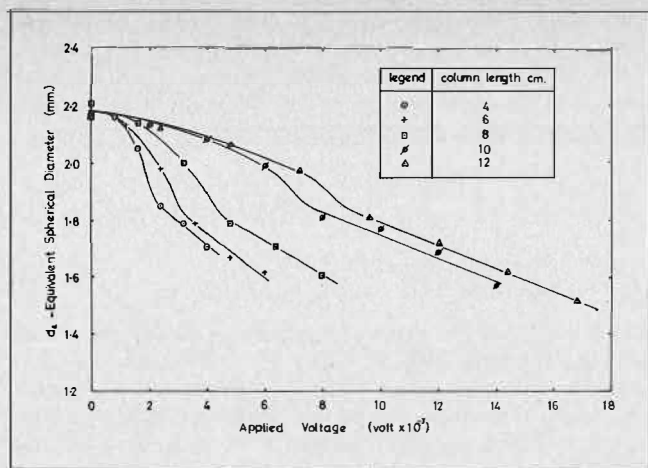


FIGURE 2. Effects of applied voltage on the single droplet size for different column lengths.

the droplets achieved their terminal velocities in a distance of less than twice their diameter it was assumed that only a very small error resulted from calculating the fall time directly from the column length and the droplet velocity.

Figure 3 shows the result of treating the data in this manner for droplet sizes ranging from 2.17 mm to 1.70 mm for a single nozzle 1.10 mm internal diameter. The justification for this type of plot has been explained by Johnson et al.⁽¹⁰⁾ who showed that a fractional approach to equilibrium could be assigned to each stage in the droplet's history such that the extraction efficiency during free fall is as follows:

$$E_M = \frac{E_T - E_{FC}}{1 - E_{FC}} \quad (3)$$

The formation and coalescence end effects are combined in the term E_{FC} which is independent of the fall time, t . Rearranging equation (3) and differentiating yields the result:—

$$\frac{d \ln(1 - E_T)}{dt} = \frac{d \ln(1 - E_M)}{dt} \quad (4)$$

where $(NTU)_{do} = -\ln(1 - E_T)$ (5)

Thus the slope of a graph based on the measured total or overall extraction efficiency should be the same as that which would be obtained if purely free fall efficiencies could be plotted. Furthermore, if the dispersed phase film coefficient is assumed constant during the period of droplet fall, it can be shown that:—

$$k_d = -\frac{d_e}{6t} \ln(1 - E_m) = -\frac{d_e}{6} \frac{d \ln(1 - E_T)}{dt} \quad (6)$$

The points in Figure 3 are in fact well represented by a family of straight lines indicating that k_d is relatively constant over the fall times studied. The values of the film coefficient calculated from the slopes of these lines are shown plotted against droplet diameter in Figure 4.

It is apparent that the film coefficient increases with decreasing droplet size. In electrical terms this means that the dispersed phase film coefficient increases with field strength by virtue of the effect which this has on the droplet size and charge. All the droplets considered in the investigation underwent oscillation and it seems probable that the higher film coefficients evaluated for the smaller

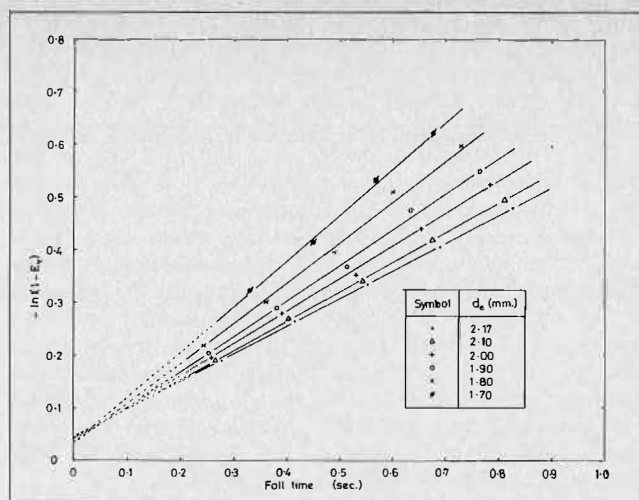


FIGURE 3. Interpolated mass-transfer data from measurements at different column lengths.

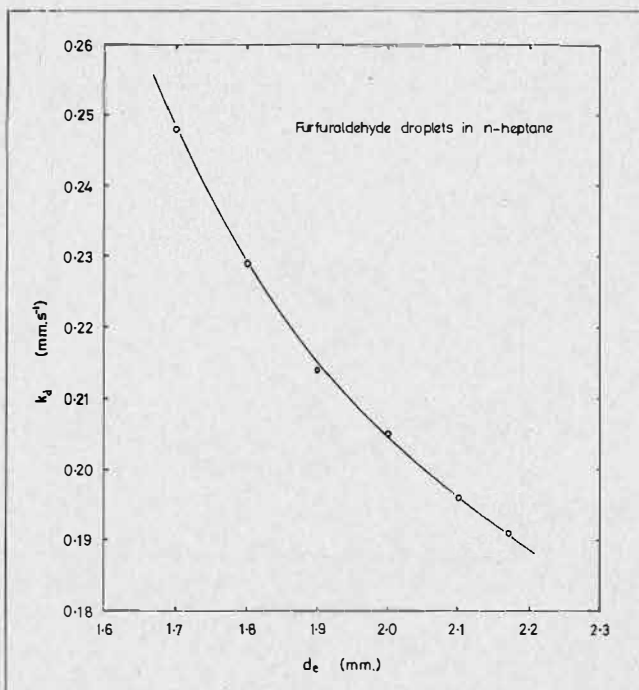


FIGURE 4. Dispersed phase film mass-transfer coefficient for a single falling charged droplet plotted against equivalent spherical droplet diameter.

charged droplets are linked to a similar trend in oscillation frequency with droplet size. Certainly for uncharged droplets it has been suggested by Rose and Kintner⁽¹¹⁾ and Angelo, Lightfoot and Howard⁽¹²⁾ that increases in oscillation frequency can give rise to an enhancement in the dispersed phase film coefficient.

In the present work, data on the amplitude and frequency of oscillation of the charged droplets were available⁽¹³⁾ from the high speed cine film which was taken during each experiment. This information used in conjunction with the mass transfer models of Rose and Kintner and Angelo et al. allowed an extraction efficiency to be calculated for the droplet fall period. These predicted efficiencies are shown compared with the experimental values in Figures 5a and 5b. For this purpose the experimental detached droplet extraction efficiency has been calculated for each observed droplet diameter using interpolated values of the film coefficient from Figure 4.

A regression analysis and subsequent examination of the residuals showed that the "observed versus calculated" data were less scattered than those presented by the authors of the models. Nevertheless, both models consistently underestimate the extraction efficiency for this system. The trend with droplet size and fall time is predicted, however, and this supports the view that the improvement under field conditions is achieved primarily through a modification in droplet size which itself causes an increase in the droplet oscillation frequency. A factor which is probably of secondary importance is the influence of the charge at the droplet interface on the interfacial tension. Theoretically, an isolated charged droplet has a reduced effective interfacial tension and oscillation frequency. In practice, however, the droplets exist between two electrodes and Stewart⁽¹⁴⁾ has shown that the additional field induced charge on the droplet virtually nullifies any free charge effects at the interface.

The Angelo and Kintner models both have the disadvantage that they require a knowledge of droplet deformation and oscillation frequency before they can be implemented. It was found, however, that the empirical

correlation of Skelland and Wellek⁽¹⁵⁾ for dispersed phase film coefficients in oscillating droplets gave good agreement with the experimental data and was much easier to use. A slight modification in the dimensionless constant in this correlation gave the relationship: —

$$\frac{k_a d_e}{D} = 0.42 \left[\frac{d_e U \rho_c}{\mu_c} \right]^{0.68} \left[\frac{\gamma^3 \rho_c^2}{8\mu_c^4 \Delta \rho} \right]^{0.1} \left[\frac{4 D t}{d_e^2} \right]^{-0.14} \quad (7)$$

which predicted the experimental extraction efficiencies of charged droplets with an error of $\pm 7\%$. Superficially, equation (7) appears to take no account of the droplet oscillation frequency, but in fact the dimensionless groups contain all the variables necessary to fully describe this phenomenon.

Multidroplet Studies with a Three Component System

Single droplet work with a partially miscible binary system provides fundamental information on the hydrodynamics and mass transfer characteristics of charged droplets but larger scale tests are essential to establish the viability of electrostatic extraction. Limited results have been reported⁽¹⁶⁾ for a small extractor based on a parallel electrode geometry. In this work, the dispersed phase entered the cell through a large number of holes drilled in the upper electrode and tests were conducted on the ternary system toluene-benzoic acid-water. These showed an almost threefold improvement in the rate of benzoic acid extraction from toluene using charged water droplets when the nominal field strength was 3.25 kV/cm. Furthermore, this was achieved with a power consumption of only a few watts since the current flowing in the contactor was small.

The operation of this type of equipment, however, is limited to systems where the continuous phase is a good electrical insulator, ($\epsilon < 4$), and the hold-up of dispersed phase is sufficiently small to avoid the risk of a conduction path forming between the electrodes. One solution

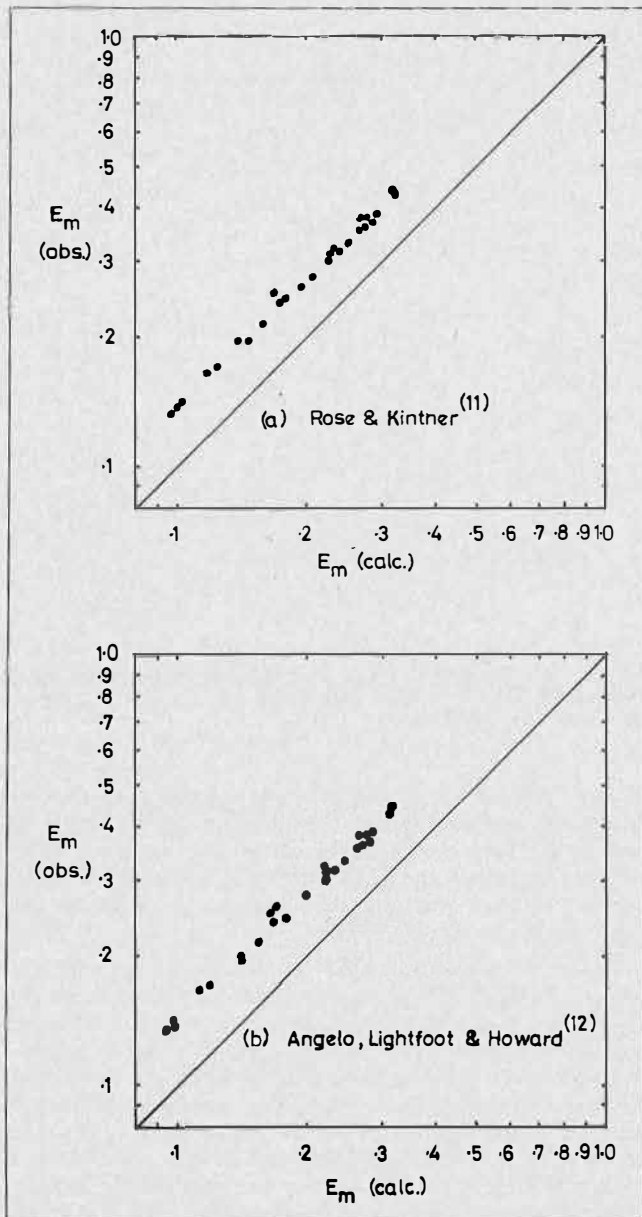


FIGURE 5. Comparison of observed and predicted extraction efficiencies.

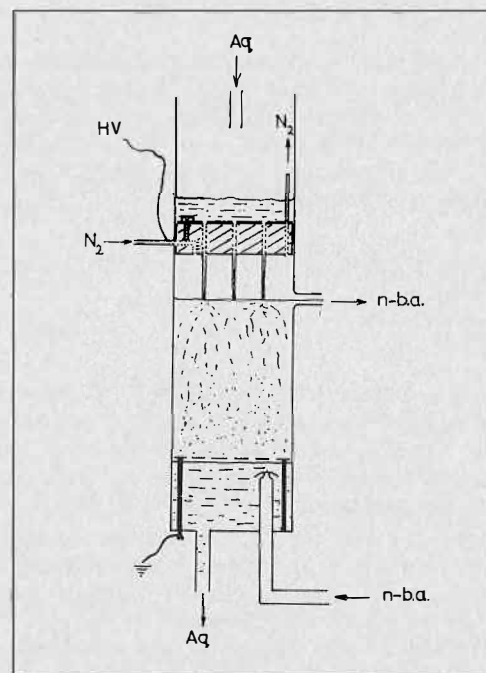


FIGURE 6. Three phase electrostatic extractor.

TABLE 1. Mass Transfer Performance of Single Stage Electrostatic Extractor

Applied Voltage kV.	Flowrates dm ³ /hr		Conc. of acetone g/dm ³			Temp. °C	E _c %	Material Balance Error %
	Aq.	n-b.a.	Exit Aq. Stream	Inlet n-b.a. Stream	Exit n-b.a. Stream			
0.0	11.7	11.0	19.7	53.7	34.5	22.5	51.0	3.4
8.0	10.5	11.0	19.5	56.0	40.6	24.5	39.0	6.3
15.0	11.0	11.0	21.5	55.4	33.9	23.5	57.5	0.6
20.0	12.2	11.0	22.4	55.4	31.3	24.0	66.4	2.0
23.0	11.8	11.0	24.6	56.6	30.7	23.0	71.4	0.7
25.5	12.4	11.0	22.7	52.2	29.0	25.5	70.3	4.5
28.0	10.9	11.0	22.7	44.7	23.8	20.0	78.3	3.4
37.5	10.2	11.0	27.5	54.2	30.2	21.0	76.4	2.9
40.0	12.1	11.0	24.6	49.3	23.8	22.5	88.2	3.3
45.0	12.0	11.0	25.6	52.8	27.0	25.0	83.2	4.3
45.0	10.3	11.0	29.6	56.8	31.9	22.5	77.5	4.9
48.0	10.6	11.0	31.0	58.0	30.7	21.5	85.3	4.8

Gap between surface of continuous phase and tip electrode:— 3.8 cm
 Depth of continuous phase:— 14.6 cm.

to these problems is to lift the upper nozzle plate of the usual parallel electrode geometry out of the continuous phase, then to maintain a gap (purged with nitrogen) between the electrode and the surface of the continuous phase. Preliminary experiments with a single nozzle revealed that the best dispersion with this arrangement was achieved when a continuous ribbon of liquid was allowed to flow from the nozzle to the surface of the continuous phase. The application of a potential gradient between the nozzle and another electrode submerged beneath the continuous phase had the effect of breaking the liquid jet on contact with the continuous phase into small droplets (approximately 1 mm in diameter). This behaviour is attributable to the strongly divergent electrical force field which exists in the continuous phase at the point where the conducting liquid jet meets the liquid surface.

Following the initial tests with a single nozzle it was possible to design the single stage extractor shown diagrammatically in Figure 6. The nozzle electrode consisted of a thin sheet of aluminum fixed to the upper surface of a disc of Tufnol which in turn was sealed with asbestos string into a precision bore glass column 0.1 m i.d. Three holes (1.59 mm i.d.) bored equidistant from each other in the upper electrode served as nozzles. The lower electrode was simply a perforated sheet of brass supported by a stainless steel plate which incorporated the dispersed phase exit and continuous phase inlet and was fitted by means of flanges to the end of the glass column. This electrode was maintained at earth potential.

The liquid-liquid system used for testing the extractor was n-butyl acetate-water, with acetone as solute. The electrical properties of the ester ($\epsilon = 5.1$) are such that it can be regarded as a semi-conducting liquid but this did not prohibit its use as the continuous phase in the new contactor. The phases were mutually saturated with respect to one another and then solute was added to the n-butyl acetate phase immediately before an experiment was started. Typically, the acetone concentration of the inlet continuous phase was arranged to be approximately 6% by weight and samples of this and the two exit streams were analysed for acetone. In all cases the inlet dispersed phase contained no solute and so a knowledge of the flow-rates allowed material balances to be worked out for each run. Experiments with a discrepancy of greater than $\pm 7\%$ based on the total amount of solute entering the column were regarded as invalid. The method chosen for the determination of acetone in both phases was the same as that described by Pratt and Glover⁽¹⁷⁾.

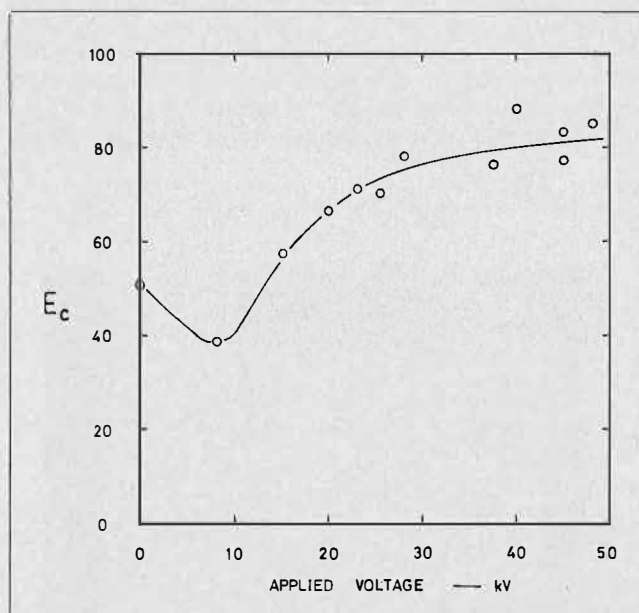


FIGURE 7. Effects of applied voltage on stage efficiency.

Mass transfer measurements were made over a range of applied voltages for a combined phase throughput of 22.3 dm³/hr and a phase ratio of approximately unity. The results shown in Table 1 were expressed in terms of Murphree stage efficiencies based on the continuous phase and calculated using published⁽¹⁸⁾ equilibrium data for the liquid system.

It seems from graphical presentation of the results (Figure 7) that an increase in the upper electrode voltage at constant electrode separation may cause initially a decrease in extraction stage efficiency, followed by a rapid improvement in efficiency with further increases in applied voltage. As expected from the preliminary results obtained with a single nozzle the effect of the electric field is to disperse the aqueous phase thereby providing a large interfacial surface for solute transfer. This increase in contact area between the phases is probably responsible for the enhancement in stage efficiency which is observed at higher voltages, however, it does not account for the apparent reduction in stage efficiency recorded at 8 kV. An explanation for this initial behaviour may be that the voltage causes a transition from large amorphous droplets undergoing distortion and presumably considerable

internal turbulence to smaller more rigid droplets. Alternatively, the depression in stage efficiency may be the result of backmixing in the continuous phase.

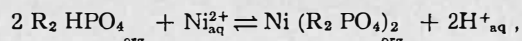
The test data obtained on this single stage three-phase cell confirm that improved performance is possible even under high hold-up conditions in a semi-conducting continuous phase. In addition, the enhanced settling of the droplets in the electric force field and the coalescence induced between the charged droplets and the bulk phase interface meant that for this system there were no phase separation problems. In any practical situation the cells would be arranged in cascades to give multistage contact. Figure 8 shows two such cells in operation; the upper electrode is negative in polarity, the middle electrode is positive and the lowest is at earth potential.

Metal Systems

Nickel — D2EHPA

Experimental work on electrostatic extraction has so far been confined to liquid-liquid systems where the solute undergoes a purely physical interaction with the solvent. In contrast, the solvent extraction of metals generally involves a specific reaction between the organic extractant and the metal of interest. In the extraction of nickel ions from an aqueous solution using di-2-ethylhexyl phosphoric

acid (D2EHPA) as the extractant the overall reaction is as follows:—



where R = 2-ethylhexyl. Maximum nickel extraction requires a pH in the region of 5 to 6 and therefore the hydrogen ions liberated into the aqueous phase must be removed if the reaction is to proceed to the right. In the present work this was achieved by treating the D2EHPA with sodium carbonate⁽¹⁹⁾ so that the aqueous phase was buffered during the extraction.

The organic phase adopted for the electrostatic tests consisted of a mixture of D2EHPA and its sodium salt in a mole ratio of 75:23.8 dissolved in a toluene diluent to give an overall concentration of 19.8% D2EHPA by volume. This composition was chosen after reference to a recent study by Durrani, Hanson and Hughes⁽²⁰⁾. The aqueous phase used in the investigation contained 14.37 g/dm³ of nickel as nickel sulphate. Both phases were presaturated with all solutes other than those undergoing mass transfer. In all cases nickel was transferred out of the droplets into the continuous phase.

The extraction cell comprised a glass column 6 cm i.d. and 35 cm in length with a fixed lower plate electrode and an adjustable upper point electrode. The latter was a glass tube drawn at the end to form a nozzle 1.0 mm internal diameter. Charging of the aqueous dispersed phase was achieved via the conducting path which existed once the delivery system contained the aqueous phase. The high voltage connection was made directly into the aqueous phase through a pin inserted immediately above the nozzle. The lower electrode was constructed in stainless steel and consisted of a small cup surrounded by an annulus ring. This design ensured that all the droplets could be collected for analysis after falling a distance of 30 cm between the electrodes. A schematic diagram of the electrode arrangement is given in Figure 9.

The aqueous phase flowrate to the nozzle was maintained at 0.022 cm³/s for each experiment and the drop size was estimated from the formation frequency. The space between the electrodes was filled with the stationary organic phase in accordance with the requirement that the continuous phase must be an electrical insulator. Fresh, unloaded solvent was used for each voltage setting in order to keep the condition of the extractant used in each run as

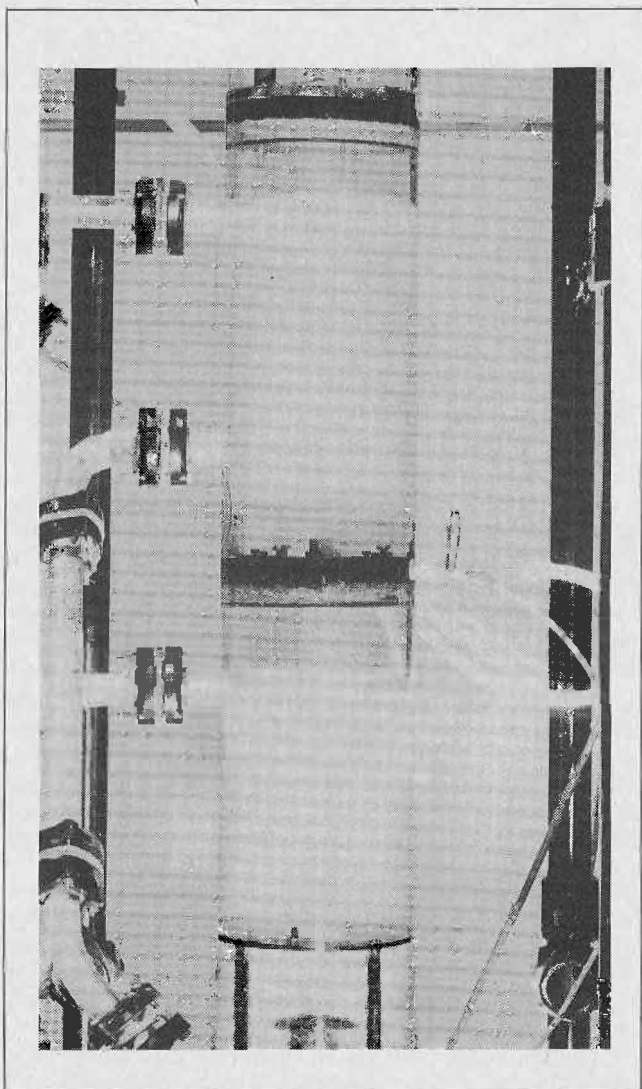


FIGURE 8. Cells in operation.

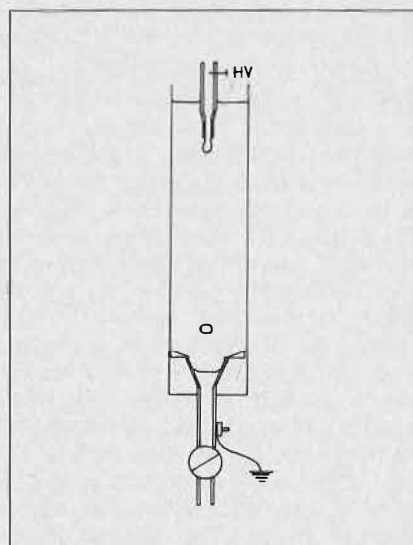


FIGURE 9. Electrode arrangement used for the extraction of nickel and copper from aqueous sulphate media.

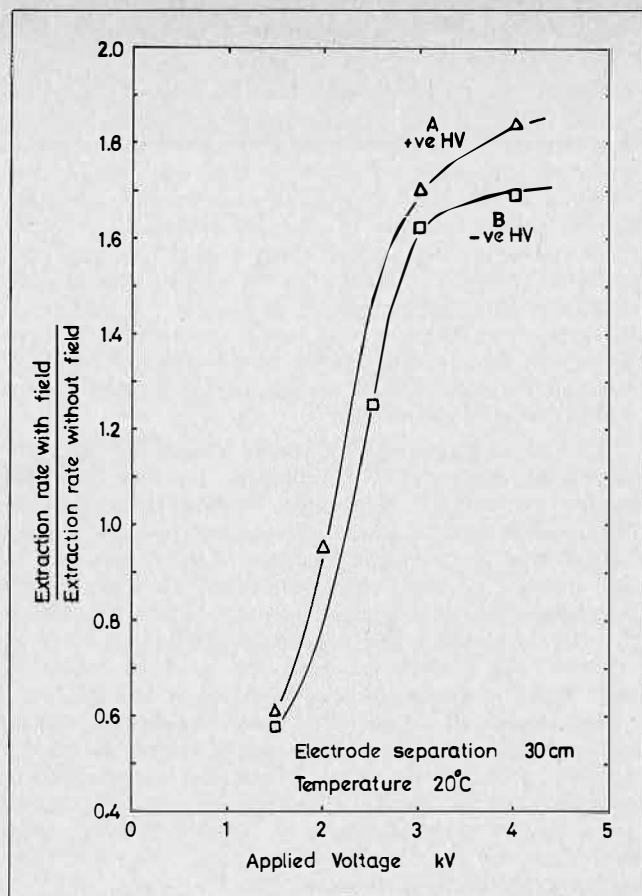


FIGURE 10. Effect of applied potential on the extraction of nickel into a mixture of D2EHPA and its sodium salt in a toluene diluent.

constant as possible. For comparative purposes an experiment under zero field conditions was carried out immediately after every high voltage run with the organic phase used in the experiment being the same as that used in the preceding high voltage experiment. Analysis was restricted to a determination of the nickel concentration in the exit aqueous phase using murexide indicator and titration with EDTA⁽²¹⁾.

The mass transfer data were normalised using the zero field information and are expressed in Figure 10 as relative extraction rates. The rate of extraction was calculated from the dispersed phase flowrate and the difference between the inlet and exit nickel concentrations in the aqueous phase; Table 2 gives the absolute values used for curve A.

It is apparent from Figure 10 that both positive and negative potentials with reference to the lower earthed electrode have a similar influence on the rate of nickel extraction from the droplets. The curves have the same form as Figure 7 and, as before, the trends can be explained in terms of droplet hydrodynamics; with a definite correspondence between droplet size and extraction rate. Careful observation of the droplets revealed the initial small change in droplet size with applied field to be associated with a marked decrease in droplet oscillation. This is perhaps responsible for the decrease in the relative extraction rate which is only terminated when the large interfacial area associated with small droplets more than compensates for the reduced turbulence which such droplets exhibit.

Voltages in excess of + 2.1 kV and - 2.5 kV caused a fine spray of droplets from the nozzle and it was under

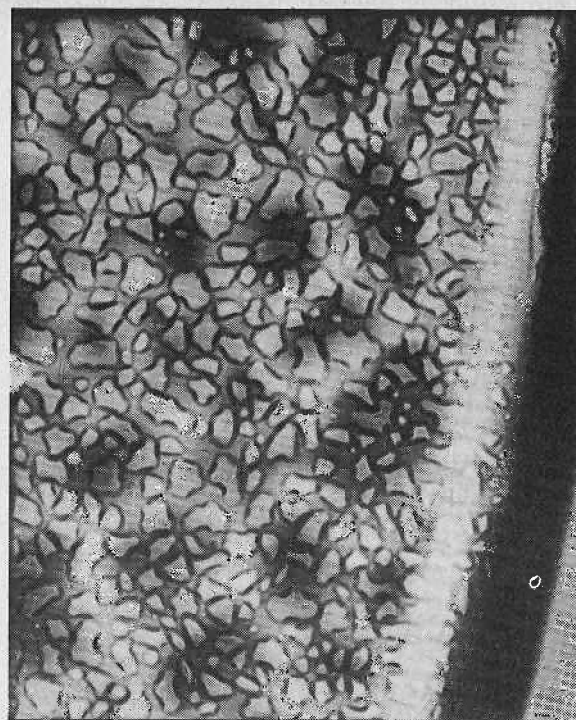


FIGURE 11. Product film at the aqueous-organic interface⁽²³⁾.

TABLE 2. Nickel-D2EHPA Results for Positive Nozzle Potentials and an Electrode Separation of 30 cm

Applied potential kV	Nominal field strength kV/cm	Equivalent droplet diameter cm	Change in aqueous phase nickel conc. g/dm ³
1.5	0.05	0.335	2.99
0	0	0.374	4.80
2.0	0.07	0.308	4.54
0	0	0.374	4.78
3.0	0.10	—	8.04
0	0	0.374	4.72
4.0	0.13	—	8.44
0	0	0.374	4.61

these conditions that the maximum enhancement in extraction rate was measured. Prolonged operation in the electrostatic spray regime⁽²²⁾ caused the organic phase to become turbid and eventually to emulsify. This behaviour was probably the result of minute droplets becoming entrained in a stationary organic phase rich in the highly surface active sodium salt (D2EHPA Na). Whilst the water content in the continuous phase must change the potential distribution between the electrodes this is not the only explanation for the limit to enhancement which is apparent at the highest voltages.

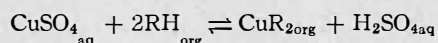
A study⁽²³⁾ of this system using uncharged droplets has indicated the existence of a physical interfacial resistance to mass transfer in the form of a viscous film made up of the nickel-organic product complex. Close-up photographs of the interface such as the one depicted in Figure 11 support this theory. In the present work it is probably some such interfacial barrier which limits the extent to which the electric field can be used to improve the extraction rate since relatively little new interface is generated once the droplets leave the nozzle. In fact the largest

droplets observed under spray conditions were approximately 1 mm in diameter and presumably these would lack sufficient turbulence to counter the effect of the interfacial resistance.

Copper — LIX 64N

The electrode arrangement used in this work was the same as that described for nickel extraction except that the glass nozzle was 2 mm i.d. and the electrode separation was reduced to 5 cm. As before, the aqueous phase was dispersed in the bulk organic and the direction of mass transfer was out of the droplets. The continuous phase was 20% LIX 64N in Escaid 100 whilst the aqueous feed to the nozzle contained 4 g/dm³ copper as copper sulphate and 0.5 mmol/dm³ sulphuric acid flowing at a rate of 1.55 cm³/min.

The exit droplet copper concentration was deduced from the change in sulphuric acid concentration in accordance with the reaction: —



where RH represents the extractant. The acid concentration in the aqueous phase was determined by extrapolation

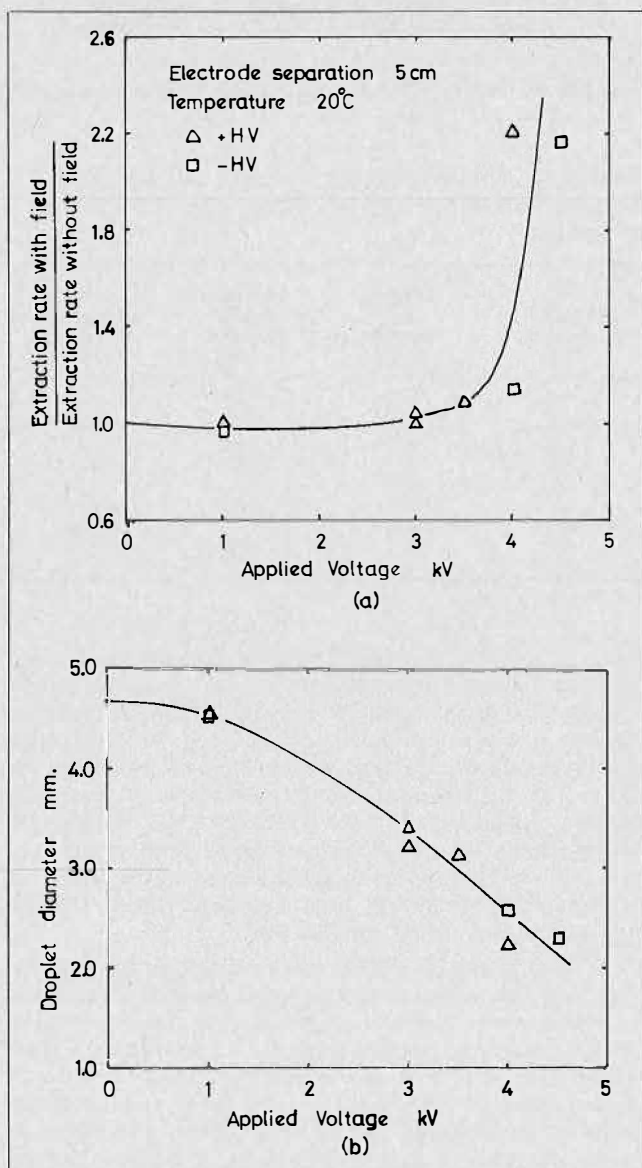


FIGURE 12. Effect of applied potential on extraction and droplet size for the copper-LIX system.

tion⁽²⁴⁾ of data obtained by potentiometric titration with sodium hydroxide.

Figure 12a shows the effect of positive and negative applied potentials on the relative extraction rate and it can be seen that considerable enhancement is possible at potentials in excess of 4 kV.⁽²⁵⁾ In fact, this improvement seems to be associated with the onset of droplet disintegration which was observed at -4.5 kV and +4 kV. Under these conditions the surface charge on the droplets was sufficient to cause instability of the droplet interface immediately after detachment. This electrical stress caused the droplets to split and form two or more daughter droplets which then moved directly to the collector cup. The effect of the applied field strength on the average droplet size is shown in Figure 12b.

Voltages in excess of 5 kV caused an electrostatic spray of minute droplets (~0.1 mm) to emanate from the nozzle and work is in progress to fully investigate the effect which this has on mass transfer. Preliminary results indicate that much greater increases in the relative extraction rate are possible when working in the spray regime but the situation is complicated by the uncertain residence time of the droplets between the electrodes due to recirculation. No coalescence problems or haze formation were apparent during the tests in the spray regime.

The absence of a guard ring round the charging nozzle means that the droplets were formed in a divergent electric field and a comparatively lower potential was required to achieve a given reduction in droplet size. Nevertheless there may be some advantage in working with a parallel plate geometry since this has been found⁽²⁶⁾ to have rather different performance characteristics.

Conclusion

Single droplet studies have shown that an applied d.c. field can be used to enhance the rate of extraction of both organic and metal species provided that the dispersed phase is an electrical conductor and the continuous phase is an electrical insulator. In the case of the organic solute this improvement has been explained in terms of droplet hydrodynamics and the experimental results have been compared with theoretical mass transfer models.

Larger scale applications of electrostatic extraction may give rise to an electrical short circuit between the electrodes and a contactor which solves this problem has been designed and tested.

Acknowledgment

The author is indebted to the Science Research Council for financial support during the course of this work, and to Mr. I. Wade and Mr. V.K. Chee for performing some of the experimental work.

NOTATION

d_e	= equivalent spherical droplet diameter
D	= molecular diffusivity
D_N	= nozzle diameter
E_C	= Murphree stage efficiency based on the continuous phase
E_{FC}, E_M, E_T	= extraction efficiencies, end effects, free fall and total, respectively.
g	= acceleration due to gravity
k_d	= dispersed phase film mass transfer coefficient
$(NTU)_{d_0}$	= number of dispersed phase transfer units based on droplet formation and free fall
Q	= droplet charge
t	= droplet fall time
U	= charged droplet velocity
γ	= interfacial tension
ϵ	= dielectric constant
ϵ_0	= permittivity of free space
μ_0	= viscosity of the continuous phase

- ρ_c = density of continuous phase (distributed charge per unit volume in equation 1)
 $\Delta \rho$ = density difference
 ψ = voltage

REFERENCES

- (1) Bailes, P.J. and Thornton, J.D., Proc. Int. Solvnt Extraction Conference, April 1971, 1431.
- (2) Bailes, P.J. and Thornton, J.D., Proc. Int. Solvent Extraction Conference, September 1974, 1101.
- (3) Colburn, A.P. and Welsh, D.B., Trans. Am. I. Chem. E. 1942, 38, 179.
- (4) Stewart, G. and Thornton, J.D. "Liquid-Liquid Extraction", Instn. of Chem. Engrs. (London) Symposium Series No. 26, 1967, 29.
- (5) Iyer, P.V.R. and Sawistowski, H., Proc. Int. Solvent Extraction Conference, September 1974, 1029.
- (6) Thornton, J.D., Birmingham University Chemical Engineering Journal (U.K.), 1976.
- (7) Bailes, P.J., Symposium on Solvent Extraction, University of Newcastle-upon-Tyne (U.K.), September, 1976.
- (8) Whewell, R.J., Hughes, M.A. and Hanson, C., J. Inorg. Nucl. Chem. 1975, 37, 2303.
- (9) Yamaguchi, M., Fujimoto, T. and Katayama, T., J. of Chem. Eng. Japan 1975, 8, 361.
- (10) Johnson, A.I., Hamielec, A.E., Ward, D. and Golding, J.A., Can. J. Chem. Eng. 1958, 7, 221.
- (11) Rose, P.M. and Kintner, R.C., A.I.Ch.E.J. 1966, 12, 530.
- (12) Angelo, J.B., Lightfoot, E.N. and Howard, D.W., A.I. Ch.E.J. 1966, 12, 751.
- (13) Bailes, P.J., Ph.D. Thesis, University of Newcastle-upon-Tyne, U.K. 1972.
- (14) Stewart, G., Ph.D. Thesis, University of Newcastle-upon-Tyne, U.K. 1970.
- (16) Skelland, A.H.P. and Wellek, R.M., A.I.Ch.E.J. 1964, 10, 491.
- (16) Thornton, J.D., Rev. Pure and Appl. Chem. 1968, 18, 197.
- (17) Pratt, H.R.C. and Glover, S.T., Trans. I. Chem. E. 1946, 24, 54.
- (18) Thornton, J.D. and Pratt, H.R.C., Trans. I. Chem. E. 1953, 31, 289.
- (19) Madigan, D.C., Aust. J. Chem. 1960, 13, 58.
- (20) Durrani, K., Hanson, C. and Hughes, M.A., Metallurgical Transactions, March 1977, 8B, 169.
- (21) Vogel, A.I., Textbook of Quantitative Inorganic Analysis, 3rd edit., Longmans, London, 1961.
- (22) Hendricks, C.D., Carson, R.S., Hogan, J.J. and Schneider, J.M., A.I.A.A.J. 1964, 2, 733.
- (23) Hughes, M.A., Paper presented at the University of Birmingham (U.K.), July 1977.
- (24) Gran, G., Analyst 1952, 77, 661.
- (25) Bailes, P.J. and Guymer, P., U.K. Patent Application No. 1737/76.
- (26) Bailes, P.J. and Wad, I., to be published.

DISCUSSION

G.M. Roberts: Have you investigated what happens with mixes of ions: you stated that Cu & Ni behave differently, but what about Cu & Fe, Ni & Co etc.? What are the possibilities for using the method to enhance separation, not just as envisaged to enhance the degree of extraction?

P.E. Bailes: The difference in the form of the curves obtained for copper and nickel may be due to the differing electrode separations or the kinetics of the two systems: whether improved separation could be achieved between similar metals such as cobalt and nickel using electrostatic extraction is therefore uncertain at this stage. We are at present engaged, however, on experimental work with the Cobalt-Nickel-D2EHPA system to establish whether charged aqueous droplets offer any advantage in the separation of the two metals.

R.F. Dalton: In the extraction of copper in the presence of an electrostatic field, can you give any explanation for the plateau in the rate up to 3kV followed by a great increase in rate at higher voltage?

P.E. Bailes: The increase in extraction rate observed at the higher potentials certainly corresponds to the onset of electrical instability at the nozzle which itself causes droplet dispersion and therefore large interfacial area. Experiments not reported in this study show that under very severe spraying conditions even greater enhancement of the extraction rate is possible. Whether the charge on the droplets also serves to modify the kinetics of the extraction reaction is unknown at this time. An explanation for the initial plateau to which you refer may simply be that the slight increase in interfacial area accorded at this stage is countered by a reduction in turbulence within the droplets. Alternatively it may be that in this short column the mass transfer at the nozzle dominates the result and the turbulence at the nozzle only changes significantly at the high voltages. Work is continuing to establish the significance of the extraction at the nozzle.

On Axial Mixing and the Design of Packed Extraction Columns from First Principles

H.R.C. Pratt and W.J. Anderson,
University of Melbourne, Victoria, Australia.

ABSTRACT

Existing individual phase mass-transfer data for ethyl acetate-water in packed columns, obtained by the Colburn-Welsh method, have been reassessed using the diffusional backmixing model. Using an improved relation for the effective interfacial area at high hold up, the individual area coefficients have been obtained and correlated as follows:

$$\frac{k_j}{\bar{v}_o} = c_j \left(\frac{d^o \text{ vs } \bar{v}_o}{D_j} \right)^{-0.6}$$

Values of the "true" H_{o_0} for acetone transfer from water into three solvents have been predicted from these results and compared with existing experimental data. The predicted values were found to be some 40% below the measured values for chlorex, and much closer for the other two solvents used. The discrepancy is explained in terms of interfacial activity for the binary unsaturated systems used in the Colburn-Welsh method, and values of C_j in the above expression are tentatively recommended for design purposes.

Introduction

A MAJOR PROGRAMME OF WORK was initiated some two and a half decades ago at the Atomic Energy Research Establishment, Harwell, by one of the present authors (HRCP) with the aim of obtaining an improved understanding of the factors controlling the performance of liquid-liquid extraction columns, and, if possible, putting the design of these on a rational basis. The question of design involves, in fact, two separate problems, namely the prediction of the column cross-section required to accommodate the desired flows, and the height required to achieve the specified performance. Of these, the former has proved the more tractable by far, since it is determined purely by hydrodynamic considerations and satisfactory correlations of upper transition and flooding rates are available for packed columns^(1,2,3).

The subject of performance is much more complex, and it was pointed out by Gayler and Pratt^(4,5) that up to six factors are operative, viz (i) the effective interfacial area of contact of the phases; (ii) and (iii) the two individual phase mass transfer coefficients; (iv) the interfacial resistance, if any; (v) axial mixing and "maldistribution" of the phases; and (vi) interfacial turbulence, etc., resulting from interfacial tension gradients (Marangoni effect).

A method was proposed⁽⁶⁾ for determining the interfacial area in packed columns based on a combination of the mean droplet size^(7,8) with the dispersed phase hold-up^(4,9). Values thus obtained were used by Gayler and Pratt^(9,10) to interpret their individual phase mass transfer coefficient data for the system ethyl acetate-water, obtained by the Colburn-Welsh method⁽¹¹⁾, on an area basis.

The results showed that it was necessary to incorporate a surface effectiveness correction to allow for loss of useful surface due to the proximity of the droplets to one another and to the packing ("shielding" effect); they also gave indirect confirmation that considerable axial mixing occurs in the continuous, but not the dispersed phase. A crude axial mixing correction in the form of a plot of a "maldistribution factor", F_m , was devised and the resulting corrected coefficients were combined for comparison with measured overall coefficient data obtained for both acetone⁽¹²⁾ and uranyl nitrate⁽¹³⁾ transfer. However, the experimental values for the organic solute, in particular, were considerably in excess of the predicted values.

Since then, considerable attention has been devoted to backmixing in liquid-liquid contactors, and work by various investigators⁽¹⁴⁻¹⁷⁾ has led to the formulation of two theoretical models, applicable, respectively, to stagewise and to differential contactors. However, the resulting analytical solutions, restricted to a linear equilibrium relationship, are complex and cannot be solved in closed form for the number of stages or height. As a result, simple empirical approximations were devised by a number of workers^(15,18,19), but a more satisfactory approach based on the solution to the differential model, applicable when $F \sim 1.0$, was later proposed by Hartland and Mecklenburgh⁽²⁰⁾. Rod⁽²¹⁾ devised a stepwise graphical method of solution which, however, involves trial and error when backmixing occurs in both phases. These methods have been reviewed by Misek and Rod (ref. 22, Chap. 7). More recently, simplified approximate solutions to both differential and stagewise models, of adequate accuracy for design purposes, have been described by Pratt⁽²³⁾.

In order to use these models for design purposes it is first necessary to obtain values of the backmixing coefficients and mass transfer rates. Values of the former can be determined relatively easily by tracer methods (see below), but mass transfer data are much more difficult to come by. Hennico et al⁽²⁴⁾ measured solute concentration profiles for a packed column and estimated H.T.U. values which, in conjunction with separately determined values of Peclet number, led to reasonable agreement with profiles calculated from the diffusional model. Hartland and Mecklenburgh⁽²⁰⁾ have described how both Peclet numbers and H.T.U. can be obtained by graphical integration using experimental dispersed and continuous phase profiles; however, the determination of accurate profiles is extremely difficult, especially for packed columns where concentration variations can occur over the cross-section.

Smoot and Babb⁽²⁵⁾ attempted to obtain values of the true H.T.U. for a pulsed plate column by iterative calculation from measured profiles using the diffusional model. However, in many of the runs the true H.T.U. was less than the piston flow value, whereas if backmixing occurs it can only be greater. Korchinsky⁽²⁶⁾ attempted to predict the performance of packed and other columns using available correlations of the various parameters involved, but concluded that there are glaring deficiencies in the available data, particularly for mass transfer.

The literature on mass transfer to droplets is fairly ex-

tensive, as shown by the review of Heertjes and de Nie (ref. 22, Chap. 10). However, the controlling factors are complex, particularly for droplet swarms in commercial extractors, where extensive coalescence and breakdown occur. The present approach therefore is to recorrelate the original Harwell individual area coefficient data (*loc cit*) using the diffusional backmixing model, and to relate these to the true overall coefficients obtained from the Harwell acetone transfer data.

Axial Dispersion

Measurement Techniques

Disregarding the use of measured solute profiles⁽²⁰⁾, two methods have been used to determine axial mixing coefficients, both of which employ tracers soluble only in the phase under consideration (ref. 22, Chap 8). In the first method tracer is injected continuously into the column and its concentration is monitored upstream of the point of injection. The second method employs a dynamic technique in which tracer is introduced as a pulse (delta function) step or occasionally as a sinusoidal input and the concentration variation is monitored downstream.

Application to Continuous Phase

The first method, by its nature, gives a measure of the true backmixing, i.e. with reference to fixed coordinates. The second method, on the other hand, determines the residence time distribution, which may be related to the total axial dispersion. Thus, in single phase flow of continuous phase through an empty tube or a packing there is a complete spectrum of flow rates from zero up to maximum, and elements moving more slowly than the mean are back-mixed with reference to coordinates moving at the velocity of the mean flow. Similarly, forward mixing occurs with the elements moving faster than the mean flow. At very low velocities radial diffusion may serve to average out the flow variations (Taylor⁽²⁷⁾). When dispersed phase droplets are present a circulatory backflow of continuous phase is set up as a result of entrainment and dissipation of potential energy by the droplets^(28,29).

Results obtained by the dynamic method are in effect "force fitted" to the unsteady state backmixing equation. The resulting backmixing coefficients E_c are normally higher (i.e. P_c values are lower) than those obtained by the backmixing method, but for mechanically stirred (e.g. rotary disc) columns they approach the latter at high rotor speeds⁽³⁰⁾; for non-mechanical columns they may similarly be expected to approach at high dispersed phase flows. The use of such P_c values is probably sound over most of the column. However, the boundary condition which determines the concentration "jump" at the phase inlet involves only the true backmixing component of the axial dispersion, and consequently the inclusion of the forward mixing component of the dynamic P_c values might be expected to lead to error in the inlet region.

Unfortunately, the available data on axial mixing for solvent-water systems in packed columns is limited to a single investigation, that of Vermeulen et al,^(24,31) who employed the dynamic method. The results were presented in a graphical form which permitted data for packings of spheres, Raschig rings and saddles to be correlated by a single line which converged asymptotically upon the single phase values of P_c . Data for both 0.5 and 0.75 inch rings were included, but those for the smaller size deviated appreciably from the correlation line, and it was therefore decided to recorrelate the ring data alone, omitting the shape factor (i.e. sphericity) term. This led to the fol-

lowing expression, which represented the data for both ring sizes with improved accuracy.

$$\epsilon P_c = \epsilon \left(\frac{d_e U_c}{E_c} \right) = 0.00786 \left(\frac{d_e U_c}{v_c} \right)^{0.47} \left(\frac{U_c}{U_d} \right)^{0.43} \left(\frac{d_e}{d_{vs}} \right)^{1.0} \dots \dots \dots (1)$$

In eq. (1) d_e is the equivalent diameter of the packing, and d_{vs} is given by the expression⁽⁸⁾.

$$d_{vs} = d^{0_{vs}} \left(\frac{\bar{v}_o \epsilon f}{U_d} \right) = 0.92 \left(\frac{\gamma}{\Delta \rho g} \right)^{0.50} \left(\frac{\bar{v}_o \epsilon f}{U_d} \right) \dots \dots \dots (2)$$

Axial Mixing of Dispersed Phase

The situation for a dispersed phase present as droplets is quite different due to the absence of regular flow profiles. Whilst bulk flow of mixed phases can occur in both directions with some types of contactor, e.g. rotary disc and pulsed columns, careful observation shows that droplet backflow does not occur to any appreciable degree in spray or unpulsed packed columns. This was confirmed by Gayler and Pratt⁽¹⁰⁾ in their study of individual area coefficients where it was found that the continuous, but not the dispersed phase showed clear evidence of the effect of backmixing.

There is no doubt, however, that forward mixing of a type described by Rod⁽³²⁾ does occur, due to differing droplet velocities in a multidisperse system. On the other hand Lewis *et al*⁽⁷⁾ showed that the mean droplet size in a packed column results from a balance between inertia forces, which cause breakdown, and surface forces which cause coalescence; it was also evident that coalescence is a relatively rapid process. This has been confirmed by preliminary experiments in this laboratory using methyl isobutyl ketone droplets coloured blue and yellow with organic-soluble dyes, which were brought close to their equilibrium size distribution in separate packed sections before being allowed to mingle and enter a further section packed with 10 mm Raschig rings. Colour photographs indicated that coalescence and redispersion of 40-90% of the droplets, depending upon the flowrates, had occurred over a height of 30 cm, with formation of green droplets.

Direct measurement of axial mixing in the dispersed phase were made by Vermeulen et al⁽³¹⁾, using the dynamic method. Although some degree of dispersion was reported, the work was conducted with the aqueous phase dispersed which would be expected to result (except possibly in one series using carbon rings) in the formation of films instead of droplets. This would lead to an increase in axial dispersion, so that the validity of the results is in doubt. In the present work, therefore, backmixing is assumed not to occur in the dispersed phase, but it is recognised that this matter requires further study.

Individual Mass Transfer Coefficients

Allowance for Axial Dispersion

In the present study the individual coefficient data of Gayler and Pratt^(9,10) were reprocessed. These were obtained by the Colburn-Welsh method⁽¹¹⁾, i.e. measuring the approach to saturation in each phase. Two columns were employed, one of 4 in. (10.2 cm) diameter packed with 12.5 mm ceramic Raschig rings to heights of 0.5, 1.0, 2.0 and 3.0 ft, and the other 6 in. (15.2 cm) diameter packed with 25 mm rings to heights of 1.2, 2.2 and 3.0 ft.

For such systems the backmixing in the continuous (i.e. aqueous) phase is described by a single second order differential equation with the solution⁽²⁴⁾.

$$N_{o,P} = \ln \frac{N_c (e^{-b_2} - e^{-b_1}) + b_1 e^{-b_2} - b_2 e^{-b_1}}{P_c B (1 + 4r)^{1/2}} \dots (3)$$

where

$$b_1, b_2 = \frac{1}{2} P_c B [1 \pm (1 + 4r)^{1/2}] \dots (4)$$

$$r = N_c / P_c B \dots (5)$$

Values of N_c , the number of "true" transfer units, were computed from the reported values of $N_{c,P}$, the number of piston flow transfer units, by an iterative procedure using values of P_c calculated from eq. (1) and (2), taking $d^o_{vs} = 4.5$ mm (ref. 8). In all, 116 sets of data were processed. The resulting N_c values were cross-plotted against height and the gradients used to estimate the reciprocals of H_c , the true heights of transfer unit corrected for end effects. The data for 2 ft of packing in the 3 in. diam. column did not fall into line with those for the other heights used, and were omitted. The results are included in Table 2 together with the corresponding data for the dispersed phase.

TABLE 1. Estimate of Exponent n in Equation 7

Column diam. cm	U_c mh ⁻¹	Basis	n	Correlation coefficient
15	10.8	(N_c/L)	0.66	0.998
"	"	(N_d/L)	0.67	0.980
10	7.62	(N_c/L)	0.66	0.990
"	"	(N_d/L)	0.45	0.998

Individual Area Coefficients

In the original work⁽⁹⁾ the gross interfacial area a_t was calculated from the following relation using experimentally determined values of d^o_{vs} and \bar{v}_o .

$$a_t = \frac{6 U_d}{d^o_{vs} \bar{v}_o} \dots (6)$$

This was later modified by incorporating a power function of the holdup⁽¹⁰⁾, i.e. f^m , to correct for droplet "shielding". In the present work it was found to be more satisfactory to express the correction in terms of a power function of the dimensionless group U_d/\bar{v}_o , which on combination with eq. (6) gives the effective surface, a_e , as follows:

$$a_e = \frac{M}{d^o_{vs}} \left(\frac{U_d}{\bar{v}_o} \right)^n \dots (7)$$

To evaluate the exponent n, the value of a_e from eq. (7) was substituted into the transfer unit relations, viz

$$Z = \frac{U_c N_c}{k_c a_e} = \frac{U_d N_d}{k_d a_e} \dots (8)$$

These were then rearranged in the following forms suited to simple regression analysis

$$\log (N_c/L) = \log \left[\frac{k_c M}{U_c d^o_{vs} \bar{v}_o^n} \right] + n \log U_d \dots (9a)$$

$$\log (N_d/L) = \log \left[\frac{k_d M}{d^o_{vs} \bar{v}_o^n} \right] + (n-1) \log U_d \dots (9b)$$

Using the data of Table 2, the results of the regressions of (N_c/L) and (N_d/L) on U_d are given in Table 1. The values of the exponent n are highly significant and consistent with

TABLE 2. Derived Individual Mass Transfer Coefficient Data

(a) Column diam. (b) Packing size	U_c mh ⁻¹	U_d mh ⁻¹	Hold-up	$H_{o,P}$ m	H_c m	H_d m	k_c mh ⁻¹	k_d mh ⁻¹
(a) 10.2 cm	3.04	11.2	0.12	0.27	0.13	0.27	0.28	0.50
(b) 12.5 mm	6.08	"	0.13	0.32	0.21	"	0.35	"
($\bar{v}_o = 144.8$ mh ⁻¹)	9.14	"	0.14	0.43	0.29	"	0.38	"
	12.2	"	0.15	0.56	0.42	"	0.36	"
	15.2	"	0.16	0.65	0.63	"	0.30	"
	18.3	"	0.17	0.80	0.77	"	0.29	"
	21.3	"	0.18	0.87	0.91	"	0.29	"
	7.62	3.04	0.032	0.68	0.48	0.14	0.46	0.62
	"	6.08	0.067	0.45	0.32	0.19	0.43	0.58
	"	9.12	0.11	0.37	0.25	0.25	0.42	0.51
	"	12.2	0.15	0.33	0.20	0.29	0.45	0.50
	"	15.2	0.20	0.30	0.17	0.33	0.45	0.45
	"	18.3	0.27	0.29	0.15	0.37	0.45	0.43
	"	21.3	0.41	0.28	0.14	0.40	0.45	0.43
						Mean =	0.383	0.501
(a) 15.2 cm	6.10	15.0	0.12	0.35	0.23	0.30	0.33	0.60
(b) 25 mm	9.14	"	0.12	0.48	0.33	0.29	0.33	0.62
($\bar{v}_o = 194.8$ mh ⁻¹)	12.2	"	0.12	0.55	0.43	0.29	0.34	0.64
	15.2	"	0.13	0.61	0.53	0.27	0.35	0.68
	18.2	"	0.13	0.68	0.61	0.26	0.37	0.70
	21.3	"	0.14	0.76	0.71	0.26	0.36	0.70
	24.4	"	0.14	0.82	0.83	0.26	0.36	0.70
	10.8	6.10	0.044	0.95	0.71	0.20	0.33	0.66
	"	9.14	0.068	0.73	0.59	0.26	0.31	0.60
	"	12.2	0.095	0.64	0.47	0.26	0.33	0.67
	"	15.8	0.12	0.58	0.40	0.29	0.33	0.63
	"	18.3	0.16	0.53	0.37	0.32	0.32	0.61
	"	21.3	0.19	0.48	0.33	0.33	0.32	0.62
	"	24.4	0.25	0.45	0.29	0.34	0.33	0.63
						Mean =	0.336	0.647

each other at $n = 0.66$, with the exception of the value based on N_d/L for the 10 cm diameter column. The value of 0.66 has therefore been adopted for the present analysis.

The value of M could not be obtained from the results of the regression since k_c and k_d are still unknown. To obtain this, therefore, use was made of the observation by Puranik and Sharma⁽³³⁾ that eq. (6) accurately represents their measured values of a_e in the pre-loading regime, i.e. where holdup is directly proportional to dispersed phase flow; these a_e values were obtained by a chemical method utilising the hydrolysis of formate esters. In order for eq. (7) to apply approximately to the preloading regime where eq. (6) is valid, M has been estimated at the intersection of eq. (6) and (7) at a suitable point within the preloading regime, taken as that for which the holdup is 7.0%. The use of U_a values from Table 2 corresponding to this holdup gave $M \approx 2.0$, so that eq. (7) becomes

$$a_e = \frac{2.0}{d_{vs}^0} \left(\frac{U_d}{v_o} \right)^{0.66} \quad (10)$$

Values of a_e from eq. (10) were used to calculate the k_c and k_d values listed in Table 2. With the exception of the k_c values for the 10 cm diameter column, the coefficients appear to vary in a random manner and have therefore been averaged. The resulting values were then expressed as follows:

$$\left(\frac{k_j}{v_o} \right) = C_j \left(\frac{d_{vs}^0 v_o}{v_j} \right)^{-0.5} \left(\frac{v_j}{D_j} \right)^{-0.5} \\ = C_j \left(\frac{d_{vs}^0 v_o}{D_j} \right)^{-0.5} \quad (11)$$

Using diffusivity values of 10.0×10^{-6} and 32.0×10^{-6} cm^2/sec for continuous and dispersed phases respectively⁽³⁴⁾, C_j was found to have values of 0.993 and 0.870. The incorporation of the Schmidt group in eq. (11) is justified by recent work by Bulicka and Prochazka⁽³⁵⁾ which showed that the penetration theory is applicable to mass transfer at a free interface. A comparison of the present k_c and k_d values with those calculated from published correlations of single droplet data is given in Table 3.

Acetone Transfer Data

Miyachi and Vermeulen⁽¹⁵⁾ have given the solution to the diffusional model for $P_y B = \infty$, i.e. no backmixing in the extractant phase (their Case 2a). On putting $Z = 0$, the exit solvent phase composition in dimensionless units, Y^o , is obtained thus:

$$Y^o = \frac{e^{\lambda^3} (a_3 \lambda_2 - a_2 \lambda_3) + a_2 \lambda_3 e^{(\lambda_3 - \lambda_2)} - a_3 \lambda_2}{e^{\lambda^3} (a_3 \lambda_2 - a_2 \lambda_3) + \lambda_3 e^{(\lambda_3 - \lambda_2)}} \quad (12) \\ \left(1 - \frac{\lambda_2}{P_c B} \right) - \lambda_2 \left(1 - \frac{\lambda_3}{P_c B} \right)$$

with λ_2 and λ_3 and the corresponding a_i given as follows, taking the positive sign for λ_2

$$\lambda_i = \frac{P_c B + F N_{oc}}{2} \pm \left[\left(\frac{P_c B + F N_{oc}}{2} \right)^2 + (1-F) N_{oc} P_c B \right]^{1/2} \quad (13)$$

$$a_i = F \left(1 - \frac{\lambda_i}{P_c B} \right) \quad (14)$$

TABLE 3. Comparison of Present Data with Single Droplet Values

Column Diam.	Present work	$k_c - \text{mh}^{-1}$		$k_d - \text{mh}^{-1}$	
		Ref. 36 ^a	Ref. 37 ^b	Present work	Ref. 38 ^c
10.2 cm	0.38 ₃	0.25 ₅	0.31 ₉	0.50 ₁	0.34 ₄
15.2 cm	0.33 ₆	0.29 ₅	0.38 ₁	0.64 ₇	0.39 ₆

(a) Eq. 10 of ref. 36

(b) Eq. 7 of ref. 37

(c) Eq. 9 of ref. 38 (non-oscillating droplets), using the mean of $(4D_d t_c / d_{vs}^0)^{-0.338}$, where $t_c = L/v_o$.

TABLE 4. Physical Properties of Ternary Systems Used

Dispersed phase (A)	Continuous phase (B)	$D \times 10^6, \text{cm}^2/\text{sec}$ for acetone in		d_{vs}^* mm	\bar{v}_o^\dagger mh^{-1}	m^\ddagger
		A	B			
Chlorex	Water	8.8	11.6	2.61	128.9	0.794
Ethyl acetate	"	31.8	"	2.62	111.6	0.800
Butyl acetate	"	26.6	"	3.11	111.3	1.20

*Predicted values.

†For 12.7 mm Raschig ring packing (experimental values)

‡From least squares fit to equation: $c_x^* = mc_y + \text{constant}$.

The Series A acetone data of Gayler and Pratt⁽¹²⁾ were obtained for four solvents, viz ethyl acetate, butyl acetate, toluene and chlorex* in 4 in. (10.2 cm) diameter columns packed with 12.5 mm Raschig rings to heights of 2.0, 4.0 — 4.2, and 8.2 or 10.0 ft. Only those runs were considered in which the transfer took place from aqueous into solvent phase since interfacial (Marangoni) effects leading to droplet growth occurred with transfer in the opposite direction. Values of the true N_{oc} were obtained for these runs by iterative solution of eq. (12) using the experimental values of exit solvent concentration, c_y^o , together with P_c values calculated from eq. (1) and (2).

The resulting values of N_{oc} were cross-plotted as before against packing height to eliminate end effects and values of H_{oc} were obtained from the gradients. The results for the system chlorex-water are summarised in Table 5, together with $H_{oc,P}$ values from the original data.

In order to predict values of H_{oc} from the ethyl acetate-water data, k_c and k_d were first calculated from eq. (11) using values of D_j , v_o and d_{vs}^0 summarized in Table 4. The overall coefficient, k_{oc} , was then obtained from the relation

$$k_{oc} = \left[\frac{1}{k_c} + \frac{m}{k_d} \right]^{-1} \quad (15)$$

Finally, H_{oc} values were computed from the following expression using values of a_e given by eq. (10)

$$H_{oc} = \frac{U_o}{k_{oc} a_e} \quad (16)$$

The results for the chlorex-water system are included in Table 5, where it is seen that the predicted values deviate from the experimental values by -13 to -62%, with a mean deviation of -42%.

* $\beta\beta'$ dichlorodiethyl ether.

Similar calculations for the other three solvents gave N_{oc} values which were subject to greater scatter, particularly for the 10 ft packing height. This is attributed to the close approach of the true operating lines to the equilibrium curves at the continuous phase inlet where the concentration "jump" occurs, so that small errors in analysis of the exit phase led to much greater errors in the computed values of N_{oc} . However, results for ethyl and butyl acetate based on the two shorter packing heights only are summarised in Table 6; the data for toluene were quite unsatisfactory, probably due to the packing size being too close to the critical for this solvent.

The reduced scatter of the chlorex data appeared to be due to two causes. Firstly, the diffusivity of acetone in this solvent is only about one-quarter of that for the other solvents so that the approach to equilibrium at the continuous phase inlet was not so close. Secondly, the maximum height of packing used was only 2.5 m, compared with 3.05 m for the other solvents.

Discussion

The low H_{oc} values (i.e. high coefficients) predicted for the chlorex-water system at all but the highest continuous phase flows requires explanation, especially as the discrepancy was less marked for the other two systems. For this purpose it is necessary to consider the effect of unsaturation in the Colburn-Welsh method.

Droplet size measurements for unsaturated systems⁽⁸⁾ show clear evidence of an increase in d°_{vs} as compared

with saturated (and otherwise equilibrated) systems. For ethyl acetate this increase was from 2.6 to about 4.5 mm; further, the individual coefficient experiments showed an increase in v_o , e.g. from 111 to 145 mh^{-1} for 12.5 mm rings⁽⁹⁾. Such a simultaneous increase in both d°_{vs} and v_o is clear evidence of interfacial activity for solute-containing systems, which Lewis⁽⁹⁹⁾ showed to lead to enhanced mass transfer rates, and this almost certainly applies also to unsaturated systems. Since the chlorex-acetone-water system does not exhibit interfacial activity⁽⁹⁹⁾, this would explain the high performance predicted for this system from the binary data. The closer agreement at high values of U_c may result from an overcorrection for surface effectiveness in this region.

On the other hand, ethyl acetate-acetone-water differs from the chlorex system in that it exhibits interfacial turbulence⁽⁹⁹⁾, so that the predicted and experimental performance should show closer agreement, as in fact is the case. The situation in regard to the butyl acetate system is less clear, however.

In view of these results it is tentatively proposed that individual coefficients should be predicted from eq. (11) using values of C_j reduced by 40%, i.e. to 0.58 and 0.50 for continuous and dispersed phases respectively. This should give a satisfactory design for systems exhibiting no interfacial activity, and an "overdesign" for those which do. On this basis the design is easily accomplished by first calculating H_{oc} from eq. (16) using (11) and (15) to obtain the overall coefficient and (10) for a_c . The value of P_c is then obtained from eq. (1), after which the required height of packing is calculated using the methods of ref. 23(a) or (b). The accuracy of such a calculation will be affected by possible errors in predicting d°_{vs} and v_o , and due allowance should be made for these if experimental values are not available.

There is an undoubted need for further studies of a_c at high hold up. For this purpose the use of a direct method such as that of Puranik and Sharma⁽³³⁾ would be desirable, provided that this does not introduce interfacial activity. However, the greatest need is for improved axial dispersion and mass transfer data. As far as axial mixing in the continuous phase is concerned, both the continuous injection and dynamic methods should be used, and should not present undue difficulty, but the question of dispersion and coalescence in the dispersed phase also requires study. However, mass transfer represents the most difficult problem in view of uncertainties with the Colburn-Welsh method. Overall coefficients can certainly be obtained from overall column performance data by means of eq. (12), preferably using P_c values obtained with the same column, but this requires extreme accuracy in analysis of the exit phases. The problem would still remain, however, of obtaining values of the individual coefficients.

TABLE 5. Comparison of Experimental and Predicted H_{oc} Values for the Chlorex-Water-Acetone System

Column Diameter Packing	10.2 cm	*Corrected for end effects				% error in prediction
	12.5 mm Raschig rings	N_{oc}/L^*	$H_{oc, P}$ m	$H_{oc, m}$ (exp'tal)	$H_{oc, m}$ (predicted)	
	7.2	3.0	1.0	1.17	1.00	-48
	"	6.0	1.3	0.83	0.77	-57
	"	9.0	1.6	0.66	0.63	-60
	"	12.0	2.1	0.56	0.48	-56
	"	15.0	2.5	0.52	0.40	-55
	"	18.0	2.9	0.49	0.34	-53
	6.0	11.3	2.6	0.48	0.38	-53
	9.0	"	2.4	0.59	0.42	-60
	12.0	"	2.2	0.62	0.45	-20
	15.0	"	1.9	0.68	0.53	-15
	18.0	"	1.6	0.71	0.63	-14
	21.0	"	1.4	0.75	0.71	-13
					Mean	-42

TABLE 6. Summary of Results for Acetone Systems

Solvent	U_c mh^{-1}	U_d mh^{-1}	Range of Values		% error
			H_{oc} (experimental) m	H_{oc} (predicted) m	
Chlorex	7.2	3.0 — 18.0	1.00 — 0.34	0.52 — 0.16	-60 to -48
	6.0 — 21.0	11.3	0.38 — 0.71	0.18 — 0.63	-60 to -13
Ethyl acetate	7.3	3.0 — 15.0	0.59 — 0.13	0.38 — 0.13	-36 to 0
	6.0 — 21.0	11.3	0.15 — 0.40	0.13 — 0.46	-13 to +22
Butyl acetate	7.2	3.0 — 12.0	0.67 — 0.24	0.60 — 0.24	-10 to 0
	6.0 — 12.0	11.3	0.23 — 0.38	0.21 — 0.41	-9 to +8

Acknowledgment

The work on droplet coalescence using dyes was carried out by P. Bierwirth and B. McCurry, as a final year project in the Chemical Engineering Department of the University of Melbourne.

NOTATION

a	= superficial area of packing, L^{-1}
a_i	= defined by eq. (14)
a_e, a_t	= effective, respectively total interfacial area of contact per unit volume, L^{-1}
B	= L/d
c_j	= concentration of solute in j th phase, ML^{-3} or (mole) L^{-3}
D_j	= molecular diffusion coefficient in j th phase, L^2T^{-1}
d	= characteristic length (e.g. d_p or d_c), L
d_e	= $4\epsilon/a$, equivalent diameter of packing, L
d_p	= nominal size of packing, L
d_{vs}	= Sauter mean diameter of droplets; d_{vs}^0 refers to the characteristic value ⁸ , L
E_j	= effective backmixing diffusion coefficient in j th phase
F	= stripping factor, mU_c/U_d
f	= fractional holdup of dispersed phase
g	= acceleration due to gravity, LT^{-2}
H_{oc}	= height of true overall transfer unit based on continuous phase, L
$H_{oc,P}$	= height of overall piston flow transfer unit based on continuous phase, L
k_j	= mass transfer coefficient for j th phase, LT^{-1}
k_{oc}	= overall mass transfer coefficient based on continuous phase, LT^{-1}
L	= height of packing, L
m	= slope of equilibrium line, dc_x/dc_y
N_j	= number of true transfer units for j th phase
N_{oc}	= number of true overall transfer units based on the continuous phase
$N_{oc,P}$	= number of overall piston flow transfer units based on continuous phase
P_j	= $U_j d/E_j$, backmixing Peclet number for j th phase
\bar{U}_j	= superficial velocity of j th phase, LT^{-1}
\bar{v}_o	= characteristic velocity of droplets in packing, LT^{-1}
Y^o	= dimensionless exit concentration of extractant phase (see ref. 23a for definition)
ϵ	= fractional voidage of packing
γ	= interfacial tension, dynes/cm, MT^{-2}
λ_i	= defined by eq. (13)
ν_j	= kinematic viscosity of j th phase, L^2T^{-1}
$\Delta\rho$	= density difference, $ \rho_c - \rho_d $, ML^{-3}

Subscripts

c	= continuous phase
a	= dispersed phase
i	= continuous or dispersed phase
x	= feed phase (continuous phase in present paper)
y	= extractant phase (dispersed phase in present paper)

REFERENCES

- Dell, F.R. and Pratt, H.R.C., *Trans. Inst. Chem. Eng.* 1951, 29, 87, 270.
- Watson, J.S., McNeese, L.E., Day, J. and Carrood, P.A., *A.I.Ch.E.J.* 1975, 21, 1080.
- Gayler, P., Roberts, N.W. and Pratt, H.R.C., *Trans. Inst. Chem. Eng.* 1953, 31, 57.
- Gayler, R. and Pratt, H.R.C., *Trans. Inst. Chem. Eng.* 1951, 29, 110.
- Pratt, H.R.C., *Ind. Chem.*, October 1955, 505.
- Pratt, H.R.C. and White, A.S., *Chem. and Ind.* 1952, 358.
- Lewis, J.B., Jones, I. and Pratt, H.R.C., *Trans. Inst. Chem. Eng.* 1951, 29, 126.
- Gayler, R. and Pratt, H.R.C., *Trans. Inst. Chem. Eng.* 1953, 31, 69.
- Gayler, R. and Pratt, H.R.C., *Trans. Inst. Chem. Eng.* 1953, 31, 78.
- Gayler, R. and Pratt, H.R.C., *Trans. Inst. Chem. Eng.* 1957, 35, 267.

- Colburn, A.P. and Welsh, D.G., *Trans. Amer. Inst. Chem. Eng.* 1942, 38, 199.
- Gayler, R. and Pratt, H.R.C., *Trans. Inst. Chem. Eng.* 1957, 35, 273.
- Smith, L.E., Thornton, J.D. and Pratt, H.R.C., *Trans. Inst. Chem. Eng.* 1957, 35, 292.
- Eguchi, W. and Nagata, S., *Chem. Eng. Jap.* 1958, 22, 218.
- Miyauchi, T. and Vermeulen, T., *I.E.C. Fundam.* 1963, 2, 113, 304.
- Sleicher, C.A., *A.I.Ch.E.J.* 1959, 5, 145; 1960, 6, 529.
- Hartland, S. and Mecklenburgh, J.C., *Chem. Eng. Sci.* 1966, 21, 1209.
- Stemerding, S. and Zuiderweg, F.J., *Chem. Eng. (London)*, May 1963, C.E. 156.
- Watson, J.S. and Cochrane, H.D., *I.E.C. Proc. Des. Develop.* 1971, 10, 83.
- Hartland, S., and Mecklenburgh, J.C., *I. Chem. E., Symp. Series No. 26*, 1967, 115.
- Rod, V., *Coll. Czech. Chem. Commun.* 1965, 30, 3822; *Brit. Chem. Eng.* 1964, 9, 300.
- Hanson, C. (Editor), "Recent Advances in Liquid-Liquid Extraction", Pergamon Press, 1971.
- Pratt, H.R.C., *I.E.C., Proc. Des. and Develop.* (a) 1975, 14, 74; (b) 1976, 15, 34; (c) 1976, 15, 544.
- Hennico, A., Jacques, G.L., Moon, J.S. and Vermeulen, T., *Univ. Cal. Rad. Lab. Rpt. No. U.C.R.L.-10696* (1964).
- Smoot, L.D. and Babb, A.L., *I.E.C. Fund.* 1962, 1, 93.
- Korchinsky, W.J., *Can. J. Chem. Eng.* 1974, 72, 468.
- Taylor, G.I., *Proc. Roy. Soc (London)* 1953, A219, 186; 1954, A223, 446.
- Wyffels, J.-B. and Rietema, K., *Trans. Inst. Chem. Eng.* 1972, 50, 224.
- Anderson, W.J. and Pratt, H.R.C. (to be published).
- Westerterp, K.R. and Landsman, P., *Chem. Eng. Sci.* 1962, 17, 363; Westerterp, K.R. and Meyberg, W.H., *idem*, 373.
- Moon, J.S., Hennico, A. and Vermeulen, T., *Univ. Cal. Rad. Lab. Rpt. No. U.C.R.L.-10928* (1963).
- Rod, V., *Brit. Chem. Eng.* 1966, 11, 483.
- Puranik, S.A. and Sharma, M.M., *Chem. Eng. Sci.* 1970, 25, 257.
- Lewis, J.B., *J. appl. Chem.* 1955, 5, 228.
- Bulicka, J. and Prochazka, J., *Chem. Eng. Sc.* 1976, 31, 137.
- Garner, F.H., Foord, A. and Tayeban, M., *J. appl. Chem.* 1959, 9, 315.
- Weber, M.E., *I.E.C. Fundam.* 1975, 14, 366.
- Skelland, A.H.P. and Wellek, R.M., *A.I.Ch.E.Jnl.* 1964, 10, 491.
- Lewis, J.B., *Chem. Eng. Sci.* 1954, 3, 260.

DISCUSSION

T.C. Lo: Can your model or correlation be used for prediction of HETS or HTU for a pulsed packed column?

H.R.C. Pratt: In principle the method should be applicable to pulsed packed columns although it would almost certainly be necessary to take into account backmixing in the dispersed phase also. It would therefore be necessary to employ the equation for backmixing in both phases.

However, unfortunately no droplet size data are available for pulsed packed columns to the best of my knowledge, and it is not known whether the area mass transfer coefficient is affected by pulsation. Until such data become available, therefore, it will be necessary to base design on pilot scale data. For this purpose performance data from the latter would be used in conjunction with backmixing data to obtain the "true" values of H_{ox} by iteration on the exact or approximate solution of the differential backmixing model and these would be used as the basis for design of the full-scale column.

Internal Sampling of Liquid-Liquid Spray Columns at Steady State

II. Application to Mass Transfer Experiments

C.J. Lim, J.E. Henton*, G. Bergeron*, and S.D. Cavers†, Department of Chemical Engineering, The University of British Columbia, Vancouver, B.C., Canada.

ABSTRACT

Hypodermic needles and a hook probe each have been used in a liquid-liquid extraction spray column to provide continuous-phase samples. A newly-designed plastic-cup probe, and a funnel probe have been used for dispersed-phase sampling. Results reported include the effect of rate of sampling on the concentration of solute in the samples obtained with each of the sampling devices except the hypodermic needles, and a comparison of the concentration in samples of each phase taken with the two different sampling devices available for use in that phase. Sampling rate has little effect on the measured concentrations. Agreement between hypodermic-needle and hook-probe results, and between plastic-cup and funnel-probe results was good. The hypodermic needles, and the plastic-cup probe are preferred over the other two samplers.

Introduction

IN A PREVIOUS PAPER⁽¹⁾, methods of sampling liquid-liquid spray columns were reviewed and various sampling devices were described. These included a hook probe and hypodermic needles for sampling the continuous phase, and a funnel probe for the dispersed phase. In the earlier work emphasis was on the sampling of the continuous phase in order to measure the concentration of a sodium tracer, insoluble in the dispersed phase.

In the work now to be described the operation of these sampling devices was studied under conditions of mass transfer of a solute between the two phases. In addition, a new plastic-cup sampler has been designed for obtaining dispersed-phase samples.

Experimental

Spray Column

A 38-mm i.d. spray column of Elgin design was used for the experiments. Figure 1 shows a schematic diagram of a typical column arrangement. Acetic acid was transferred from a continuous aqueous phase to a dispersed 4-methyl-2-pentanone (4M2P) phase in direct runs, or in the opposite direction in reverse runs. The water used was distilled or deionized; the 4M2P was technical grade. The continuous phase was saturated with 4M2P, and the dispersed phase with water. The operating conditions used were generally similar to those described before⁽¹⁾.

*J. E. Henton now is with Imperial Chemical Industries, Ltd., and G. Bergeron with the Aluminum Co. of Canada Ltd.

†To whom correspondence should be addressed.

Sample Probes

The hook probe and the hypodermic-needle samplers were used for sampling the continuous phase; the funnel probe and plastic-cup probes were used for the dispersed phase. (See Figures 2a and 2b). Table 1 is a summary of the operating conditions for each probe. Because of the internal volumes of the hook, the funnel, and the lines connecting them to the sample bottles, comparatively long purge times are required. Reference 1 provides more details of the form and operation of all the sampling devices except for the plastic-cup probes. However, a printing error was made in the description of the hypodermic-needle samplers. A correction has been provided here in the Appendix.

The plastic-cup probe consists of a 3-in. long, 22-gauge hypodermic needle inserted into a 6.4-mm o.d., and 5.1-mm high Teflon cup as shown in Figure 2b. As with the hypodermic needles used for sampling the continuous phase, the plastic-cup probes for sampling the dispersed phase were inserted through the polyethylene gaskets situated between successive sections of the Pyrex column. One plastic-cup probe was used at a time, with the cup facing downward at the centre line of the column. The other plastic-cup probes were withdrawn as close as possible to the column wall, and the hook probe and the funnel probe to a position above the interface at the top of the column. In addition, all the continuous-phase hypodermic-needle samplers were withdrawn so that their ends also were at the column wall. Analysis was by titration as described

TABLE 1. Operating Conditions for the Sample Probes

Sampler	Material	V_c/V_d in sample	Remarks re following columns	Purge time (min)	Flow rate* (ml/min)
hook	stainless steel	∞ ($V_d=0$)	approx. range of purge times required comparison with needles	24-60	2
				3-5	45
				23	5
funnel	stainless steel	approx. 0 to 1*	approx. range of purge times required comparison with plastic cup	18-60	2
				3-4	45
				17-11	7-11
needles	stainless steel	∞ ($V_d=0$)	all runs	1.5	1
plastic cup	Teflon	0	sampling — rate studies other direct runs reverse runs	15-1	0.5-12
				2	1
				6	0.3

*Depends on sampling rate, dispersed-phase superficial velocity, and other factors not well understood (including wetting behaviour of probe). Infrequently the value of 1 given above is exceeded.

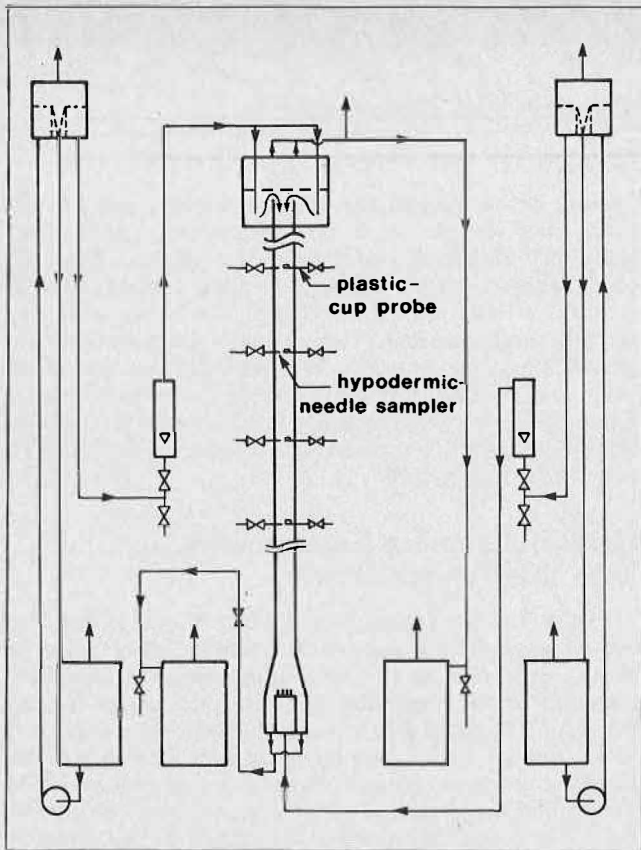


FIGURE 1. Schematic flow diagram.

previously⁽¹⁾. In changing from one method of sampling to another, appropriate time was allowed for the column to return to steady state.

Scope of Experiments

Measurements were made on the effect of rate of sampling on the concentration of acetic acid in the samples obtained with each of the sampling devices except for the hypodermic needles. Thus, the effect of rate of sampling was determined using the hook probe for the continuous phase, and the funnel probe and the plastic-cup probes for the dispersed phase. In addition, the effect was studied of substituting one sampling device for another. Continuous-phase concentrations obtained by sampling with hypodermic needles were compared with those obtained by sampling with the hook probe. Similar comparisons were made for dispersed-phase concentrations obtained from funnel-probe and plastic-cup probe samples.

Problems in the Interpretation of Results

As outlined in the earlier paper⁽¹⁾, samples withdrawn by the funnel-probe sampler ordinarily contain continuous as well as dispersed phase. Mass transfer between phases continues after the sample is taken, and before the analysis can be carried out. The dispersed-phase concentration at the time of sampling (C_{di}) is calculated from the dispersed-phase concentration at the time of analysis (C_{df}) by means of a material balance⁽¹⁾:

$$C_{di} = C_{df} + \frac{V_c}{V_d} (C_{cf} - C_{ci}) \dots \dots \dots (1)$$

To use this it is necessary to know V_c and V_d , the volumes of the respective phases in the funnel-probe sample and

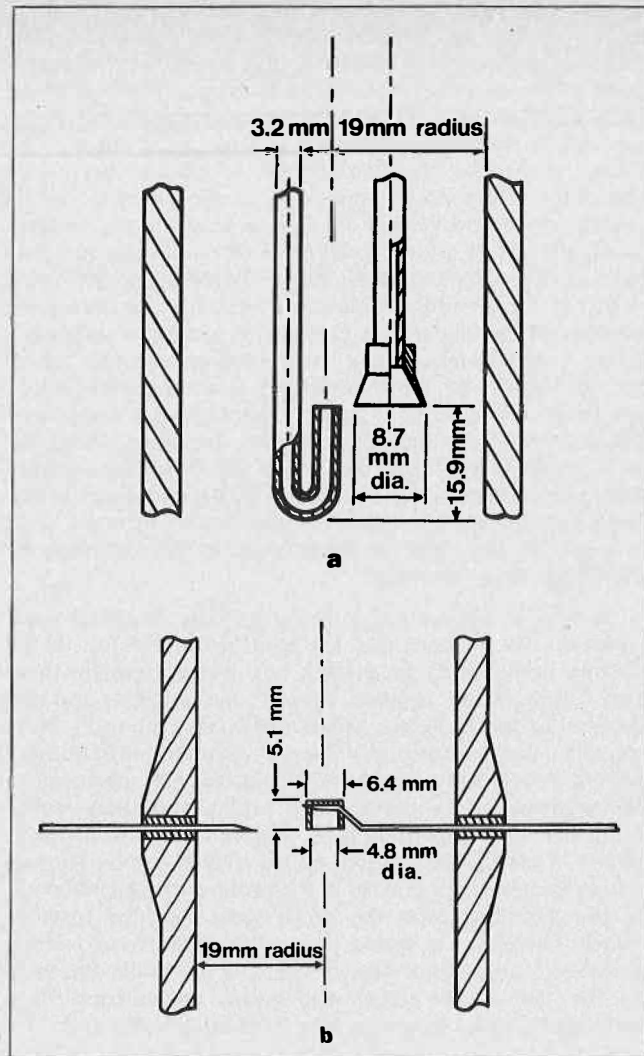


FIGURE 2. (a) Hook probe, and funnel probe; (b) Hypodermic-needle sampler, and plastic-cup probe.

C_{ci} , the concentration of continuous phase taken into the funnel probe along with the drops. Fortunately, neither hook-probe nor hypodermic-needle samples contained dispersed phase.

However, one difficulty anticipated as a result of the need for C_{ci} for use in Equation 1 was that the continuous-phase samplers might not give samples representative of the continuous phase entering the funnel, because continuous phase near drops, in wakes⁽²⁾ for example, should be of different concentration from that of the main body of the continuous phase. This situation arises because of mass transfer between continuous phase and drops, and because of the drops backmixing continuous phase from lower elevations in the column. It may be that both the hook probe and the hypodermic needles tend to sample preferentially from the main body of the continuous phase. The rate-of-sampling experiments with the hook probe were undertaken to see whether sample concentrations would be different at higher rates when, presumably, the samples would contain increased amounts of continuous phase from regions near the drops.

For the funnel-probe sampler, it was known that increasing the sampling rate increases the volume of continuous phase relative to dispersed phase in the sample. If, whenever a drop enters the funnel probe, it is accompanied by the continuous phase that has been close to it

immediately prior to its entry, then the increased volume of continuous phase in the samples at higher sampling rates would include a relatively large proportion of main-body continuous phase. On the other hand, at low sampling rates the flow of continuous phase near the funnel probe perhaps could strip away from a drop, as it entered the funnel probe, the continuous phase which had been near the drop during its last moments in the column. If this description is correct, the continuous phase in the samples would consist of a large proportion of main-body material even at low sampling rates. Rate-of-sampling experiments with the funnel probe were done primarily to determine whether or not significant changes in measured dispersed-phase concentration would arise in circumstances where the hook-probe or the hypodermic-needle samplers might not be providing samples representative of the continuous phase entering the funnel probe with the drops. However, it was considered that the results of these experiments would be influenced by an effect which could occur at the funnel-probe inlet, and at the plastic-cup inlets as well, and which also was of importance in the problem of dispersed-phase sampling.

By way of illustration, it is known that, in direct runs, drops do not coalesce into the interface at the top of the column immediately on arrival, but, instead, remain there for a time being agitated against one another and the column interface before coalescence takes place⁽³⁾. Mass transfer occurs during this interval. Similar mass transfer effects conceivably might occur during any coalescence taking place at the mouth of a probe, and these would influence the dispersed-phase concentration results obtained. Careful observation of the funnel probe showed no coalescence taking place at the probe entrance, although at low sampling rates the drops were crowded together there. Therefore it seems that coalescence time is long compared to residence time of drops at the probe entrance. In the case of the plastic-cup probe, coalescence times were short, and a meniscus was visible below the cup.

However, whatever the mechanism of mass transfer might be at the entrance of either type of dispersed-phase probe, it was considered that the rate of sampling would have to be high enough to reduce the residence time of the dispersed phase there to a small value in order to make such mass transfer negligible. On the other hand, the lower the rate of sampling, the less the disturbance of the steady operation of the column. Therefore, an intermediate rate of sampling would seem desirable.

Rate-of-sampling experiments with the plastic-cup probe were done in order to see if the residence-time effect would be observed, and in the light of the results, to find an optimum rate of sampling.

Although it is possible to obtain continuous-phase-free samples with the funnel probe by sampling at rates below about 2 ml/min, a long purge time (Table 1) is required for removing from the lines material of an earlier sample. Under these conditions supplies of feed for the column would run out before a sufficient number of samples could be taken in an experimental run. Therefore, higher sampling rates must be used for viable operation of the funnel probe, and the difficulty of having two phases in the sample results. It seemed advisable, therefore, to attempt to design a probe which would permit the withdrawing of samples containing only dispersed phase, and which, like a hypodermic-needle sampler, would have only a small volume so that the purge time could be short. The plastic-cup probe was the result.

As mentioned above, the residence-time effects would be expected to be coupled with continuous-phase concentration effects in the case of the funnel probe. When the

plastic-cup probe was used such coupling was avoided, and the results could therefore be interpreted more easily.

Results and Discussion

Design of the Plastic-Cup Probe

Initially it was thought that the organophilic polyethylene bead (ring) sampler of Letan and Kehat⁽⁴⁾ might withdraw only dispersed phase from the column. However, contamination with continuous phase could not be avoided, at least with the forms of the device used, and for the conditions under which these were tested in the present study. Nevertheless, by closing off one end of the ring, and making it into an inverted cup as shown in Figure 2b, a successful design was achieved in Teflon. The resulting sampler resembles that of Smoot and Babb⁽⁵⁾ who used polyethylene.

Rate-of-sampling Experiments With the Funnel Probe

Figure 3 shows results for the effect of rate of sampling on concentrations measured in samples taken with the plastic-cup probes in a direct run in which the superficial velocities of the continuous and dispersed phases (L_c and L_d) were 5.1 and 5.8 mm/s, respectively. (A second run at 4.1 and 3.1 mm/s gave similar results.) At each of the sampling positions shown, a value was calculated for C_d^* , the equilibrium dispersed-phase concentration corresponding to the continuous phase concentration at that sampling position. The value of C_d^* then was used to calculate the percent departure from equilibrium at each sampling position according to Equation 2.

$$\text{Dispersed phase, \% departure from equilibrium} = \frac{C_d - C_d^*}{C_d^*} (100) \dots \dots \dots (2)$$

For the conditions which applied in Figure 3, the dispersed phase was 20% away from equilibrium at sampling position 1, and 16% at position 7. Hence mass transfer would be possible during residence of dispersed phase in the cup. As Figure 3 shows, at sampling rates below about 1 ml/min slightly higher concentrations are observed than at higher sampling rates. Above about 1 ml/min relatively flat concentration curves are obtained. The final point on each of the curves in Figure 3 is one for which the sampling rate was sufficiently high that continuous phase (but only a small amount) was taken into the probe along with drop material. For each of these last points the concentration of the dispersed phase was calculated by means of Equation 1. The value used for C_{ei} was that provided by a hypodermic-needle sampler at the respective sampling position. As Figure 3 shows, the final point on each curve agrees with the points obtained at lower sampling rates, when only dispersed phase was present in the sample. The appearance of two phases in samples tended to occur at somewhat lower sampling rates as a probe "aged". The problem was overcome by replacing the Teflon cups after the probes had been in use for a few months.

In the run shown in Figure 3, transfer was from the continuous phase to the dispersed phase. Therefore the somewhat higher results at lower sampling rates may be due to the effects of residence time of dispersed phase at the probe entrance. It appears that a sampling rate of approximately 1 ml/min is appropriate in direct runs. The complications of having to apply Equation 1 are avoided, and the disturbance of the steady-state concentration within the column because of sampling is kept as small as possible without problems arising due to residence time.

TABLE 2. Rate of Sampling Experiments with the Hook Probe and the Funnel Probe

Run ¹	Probe	Superficial velocity of phases (mm/s)		Number of sampling rates studied	Range of sampling rates ² (ml/min)		Range of measured concentration (kg mole/m ³)		Average concentration	Percent departure from equilibrium by	
		L _c	L _d		from	to	from	to		Eqn. 2	Eqn. 3 ^a
1D	hook	4.6	5.7	3	12	34	0.764	0.767	0.766		8
11	hook	5.1	5.8	7	2	34	0.478	0.480	0.478 ^b		2
11	funnel	5.1	5.8	8	4	43	0.226 ^c	0.235 ^c	0.232 ^d	3	
5G	funnel	4.6	6.2	7	8	20	0.202 ^e	0.218 ^e	0.028	28	
12	funnel	3.8	5.8	5	6	33	0.256 ^f	0.266 ^f	0.262 ^g	14	

1All runs were direct runs.

2In the case of the funnel probe the rate is based on the total volume of 4M2P and water phase in the sample.

^aEqn. 3 is: % departure from equilibrium = $\frac{C_c - C_c^*}{C_c^*} (100\%) (3)$

^bAt the same location, average of 2 hypodermic-needle results = 0.477 kg mole/m³

^cCalculated from Equation 1 using result of footnote b.

^dAt the same location, average of 2 plastic-cup results = 0.234 kg mole/m³

^eCalculated from Equation 1 using average of 2 hook-probe results obtained from samples taken at 9 ml/min

^fCalculated from Equation 1 using a hypodermic-needle result = 0.594 kg mole/m³

^gA single plastic-cup result at the same location = 0.266 kg mole/m³

Complete experiments, of the sort described above for direct runs, were not made for reverse runs because it was found that the sampling rate had to be limited to 0.3 ml/min for it to be possible to withdraw dispersed-phase samples uncontaminated with continuous phase. This different behaviour in reverse runs arises perhaps from the difference in Marangoni effects for the two cases⁽⁶⁾. It was assumed that the use of 0.3 ml/min would give accurate dispersed-phase results for reverse runs on the basis that residence-time effects might still be about as shown in Figure 3. In any case reverse runs are of less practical interest than direct, because coalescence of drops within the column takes place⁽⁶⁾, and consequent or associated effects such as reduced interfacial area, changes in any interfacial turbulence, and changes in axial mixing cause net reductions in the overall capacity coefficient⁽³⁾. The rate-of-sampling experiments reported in subsequent sections of this paper for the hook probe, and for the funnel probe, all were done during direct runs.

Rate-of-sampling Experiments: Continuous phase

Studies have not been made of the effect of rate of sampling on the concentrations of solute measured in continuous-phase samples taken with hypodermic needles under conditions of mass transfer. However, as reported earlier⁽¹⁾, changing the sampling rate over the range from 0.25 to 2.0 ml/min produced no significant changes in the measured concentration of a sodium chloride tracer present only in the continuous phase. In the present work a sampling rate of 1 ml/min has been used, and, as will be seen from the data reported later in this paper, this rate seems to give accurate results.

Results of sampling-rate studies with the hook probe are shown in Table 2. In the case of Run 1D, interpretation of original data was necessary because of improper purging of the sample probes. For this run, and for Run 11, the measured water-phase concentration at each rate was within 0.3% of the average value. Therefore sampling rate appears not to affect the results. The importance of the figures for "Percent departure from equilibrium" is that there will be concentration differences between the main continuous phase and that near the drops due to mass transfer only when the phases are not at equilibrium. In Run 11 the phases were only about 2% away from equilibrium. However, in this case there probably would

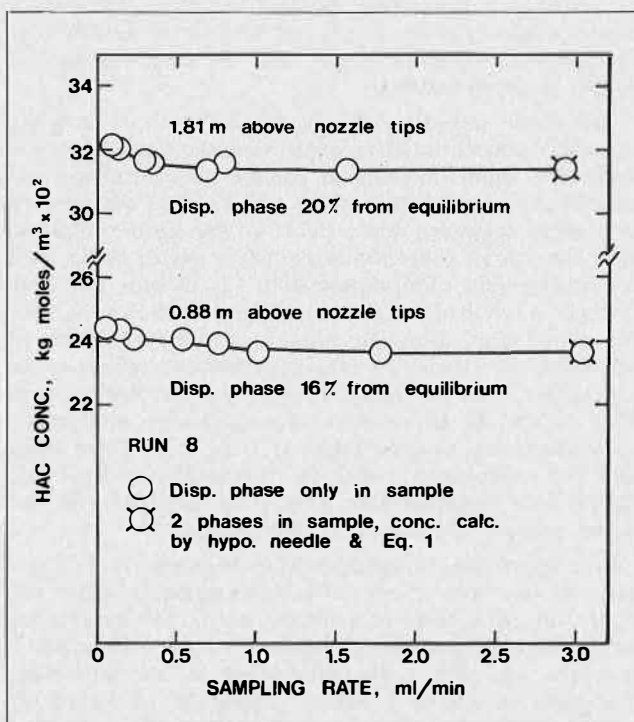


FIGURE 3. Effect of sampling rate on concentration in samples obtained with the plastic-cup probes (direct run).

be some concentration gradient toward the drops because of backmixing. Thus, in this run the concentration of the continuous phase leaving the column (1.81 m below the point of sampling used in Run 11) was 0.321 kg mole/m³, well below the Run 11 average of 0.478 kg mole/m³. Perhaps some low-concentration material was present in the drop wakes at the location where the samples were taken in Run 11, this material having been backmixed from locations nearer the bottom of the column.

It would seem likely that only at high rates of sampling would there be significant contributions to a sample of continuous phase from regions near drops. No definite conclusion can be drawn from the results of this work as to whether or not such material is indeed entering the hook probe along with liquid from the main body of the continuous phase. The results suggest either that, contrary to original expectations, varying the sampling rate does

not change the relative contributions of wake and of main-body liquid to the sample, or that little concentration difference exists between the two regions of the continuous phase (a hypothesis at variance with the deduction made earlier⁽¹⁾ based on assuming equal volumes of drop and wake).

Rate-of-sampling Experiments With the Funnel Probe

Table 2 shows the results of rate-of-sampling experiments done with the funnel probe. In Runs 11 and 12 a trend was noticed toward slightly lower measured concentrations at higher sampling rates. (See Figure 4 for Run 12.) In Run 5G the results appeared to be randomly distributed. As can be seen from Table 2, the spread of the individual results, expressed as a percentage of the average value, was 4, 8, and 4% for Runs 11, 5G, and 12, respectively. The figures for percent departure from equilibrium (especially in Runs 5G and 12) indicate that mass transfer would be possible if the drops remained for a time at or near the cup entrance. Also, concentration differences would be expected between the main body of the continuous phase very close to the drops, because of mass transfer into the drops, and because of backmixing. Therefore it seems important that the continuous-phase sample be representative.

The results indicate that any effect of rate of sampling on sample concentration is small when the funnel probe is used. The slight decrease in sample concentration with sampling rate noted in Runs 11 and 12 does not seem to be due to residence-time effects at the probe entrance, since the fall in concentration appears not to begin until a sampling rate of approximately 12 ml/min has been reached: a relatively large value. Figure 3 shows that, for the plastic cup, sampling rates had to be an order of magnitude less than this for residence-time effects to be noticeable. Also, the funnel-probe results at low rates in Runs 11 and 12 are in substantial agreement with results from plastic-cup samples taken at 1 ml/min. These facts, plus the randomness noted for the results of Run 5G, suggest that residence-time effects are negligible for the funnel probe at the rates of sampling studied.

It is interesting to consider what happens when Equation 1 is used with a series of samples taken at higher and higher sampling rates in a direct run. It will be remembered that at higher sampling rates, V_c/V_d in Equation 1 increases, and that it was anticipated, as one possibility, that there would be a higher proportion of main-body continuous phase in the samples. In this situation, C_{ef} and

C_{df} would be expected to increase. (However, no very clear pattern of this kind is evident when a detailed examination of the data is made.) Now only a single continuous-phase concentration, C_{ci} is used in applying Equation 1 to each series of samples, and, if the continuous-phase sampler which provides this value removes main-body continuous phase preferentially, the C_{ci} used would be a little too high for all the Equation-1 calculations of the series. However, the value would be more nearly correct, for the possibility envisaged above, at higher sampling rates. Then, in Equation 1 (rewritten below for the sake of convenience) the first two terms to the right of the equal sign increase

$$C_{di} = C_{df} + \frac{V_c}{V_d} C_{ef} - \frac{V_c}{V_d} C_{ci} \dots \dots \dots (1)$$

with sampling rate. This increase, however, is opposed by the increase of V_c/V_d in the negative third term, and experimentally C_{di} is found to remain more or less constant. Now, although C_{ci} may be a more appropriate value at higher sampling rates, changes in all the other factors in the equation operate to obscure the effect of such a situation in the series of calculated C_{di} values. Therefore, it is difficult to interpret the way in which C_{di} behaves, as sampling rate increases, as any indication of the appropriateness of the C_{ci} value used. Physically, of course, the reason that this difficulty arises is that, for the situation discussed, C_{ci} becomes more appropriate at higher sampling rates simply because V_c/V_d (and therefore C_{ef} and C_{df} as well) are higher. In short, rate-of-sampling experiments are probably not a satisfactory way of obtaining information about possible concentration differences between the main body of the continuous phase and that near to drops, and about the effect of such differences on funnel-probe results.

In Figure 4 (Run 12) the ratio of V_c to V_d in the funnel-probe samples ranged from 0.09 at the lowest sampling rate to 0.6 at the highest. Agreement with the plastic-cup result was best at low sampling rates, and therefore at low ratios of V_c to V_d in the samples. (Run 11 showed similar behaviour.) These matters are discussed further below.

Consideration of Possible Interaction Between Hook and Funnel Probes

In Run 11 the hook probe and the funnel probe were operated at the same time at various combinations of rates. Record was not kept of the relative rates of sampling with the two probes; however it probably was roughly true that a low rate with one probe corresponded to a low rate with the other, and similarly for other rates. Subject to the limitations implied by this situation, the fact that the sample concentrations remained almost constant for each probe is consistent with there being no effect on the results obtained with one probe, of the rate used with the other. There is a small amount of evidence from Run 5G to support the conclusion that rate of sampling with the funnel probe does not affect the hook-probe results. Two hook-probe samples were taken, each at a rate of 9 ml/min. One showed a concentration of 0.567 and the other of 0.572 mole/m³ when funnel-probe samples were taken concurrently at sampling rates of 14 and 20 ml/min respectively.

Comparison of Hook-probe and Hypodermic-needle, and of Funnel-probe and Plastic-Cup Probe Results

Several runs were made in which axial concentration profiles were measured over a part of the column height.

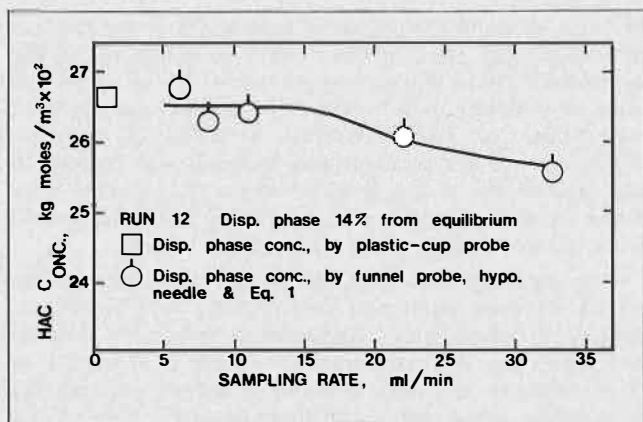


FIGURE 4. Effect of sampling rate on concentration in samples obtained with the funnel probe (direct run).

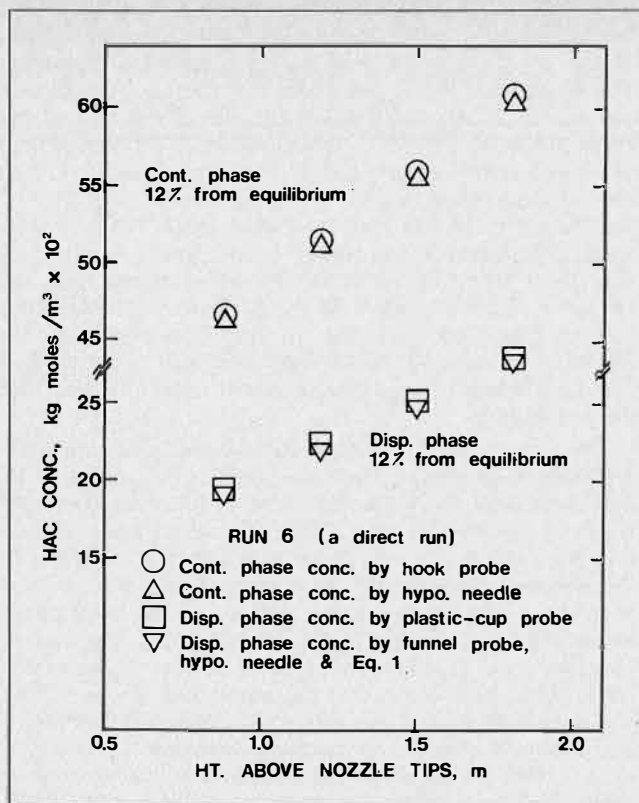


FIGURE 5. Comparison of results from hook-probe and hypodermic-needle samples, and from funnel-probe and plastic-cup samples (direct run).

At each elevation studied, a sample of continuous phase was withdrawn by means of the hook probe, and another by means of a hypodermic needle. A dispersed-phase sample was obtained with the funnel probe, and another with the plastic-cup probe. In applying Equation 1 to calculate C_{di} for each funnel-probe sample, the value C_{ci} used was that obtained from the hypodermic-needle sample. Typical results are shown in Figure 5 for a direct run and in Figure 6 for a reverse run. For these studies L_c ranged from 3.8 mm/s to 7.7 mm/s in direct runs and from 3.8 to 4.4 mm/s in reverse runs. These are fairly typical of the rates used in experiments in spray columns, where however, the ranges are wider⁽³⁾. In any case it is considered that there should be no effect of this order of L_c on sampling. Values of L_a were near 6 mm/s throughout, toward the higher end of the range used in typical spray-column experiments⁽³⁾. Obviously, in the limit of very low L_a , no dispersed-phase sample probe would be operable because it would sample only continuous phase. The funnel probe has been used with values of L_a down to 1.5 mm/s, and the plastic cup to 3.1 mm/s, but without taking samples with the other probe for comparison.

In this present work the value of the ratio of V_c to V_a in the funnel-probe samples averaged 0.08 (with both direct and reverse runs included). The range of individual values was from 0.05 to 0.11. In earlier work much higher values were sometimes obtained (Table 1), e.g. at lower values of L_a . Thus, in Run 39 of Ewanchyna⁽³⁾, with L_a of 1.5 mm/s, V_c/V_a averaged 0.7. However, in Run 23⁽³⁾ V_c/V_a averaged only 0.04 for L_a of 3.0 mm/s. Other factors in addition to L_a must be important here.

Figures 5 and 6 show, for each phase, almost identical results independent of which of the two appropriate sampling techniques was used. For direct runs the continuous-phase concentrations resulting from analysis of

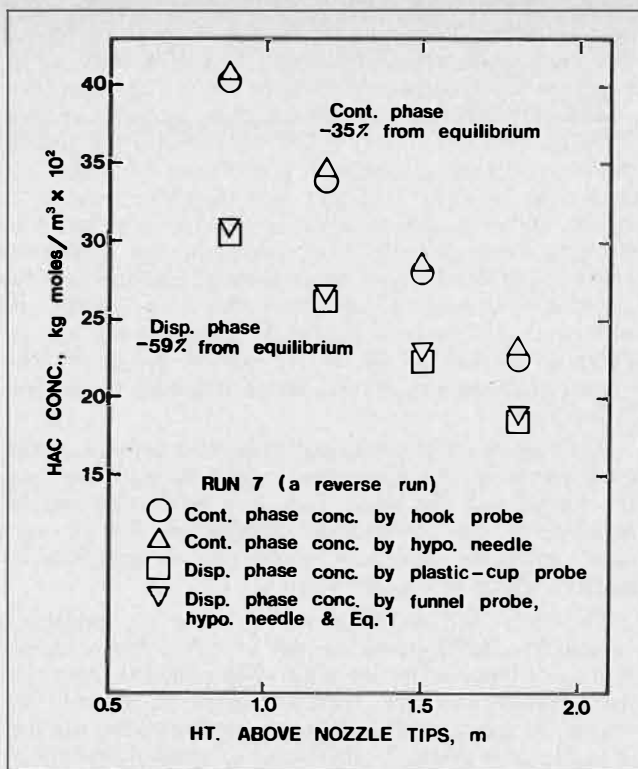


FIGURE 6. Comparison of results from hook-probe and hypodermic-needle samples, and from funnel-probe and plastic-cup samples (reverse run).

hook-probe samples were slightly higher than those from hypodermic-needle samples. The dispersed-phase concentrations obtained by means of the plastic-cup probes were slightly higher than those resulting from the use of the funnel probe. For each phase the percentage difference in results was about 1%. For reverse runs, the agreement between different sampling techniques was not quite as good; the percentage difference for all the results averaged about 2.5%. Also, instead of being slightly higher than the hypodermic-needle results, the hook-probe results lay slightly below. Similarly the plastic-cup results were slightly lower than those obtained by means of the funnel probe instead of slightly higher as in direct runs.

Plastic-cup results are believed to be correct for two main reasons. First, the samples on which these results are based were taken at rates sufficiently large that residence time of drops at the probe entrance did not affect the results. (This is true for direct runs, but is a little less certain for reverse runs as is indicated later.) Second, no correction is required for entrained continuous phase. The good agreement of the funnel-probe results, e.g. in Figures 5 and 6, with those from the plastic cups indicates that the funnel-probe results are too low by about 1% for direct runs, and too high by about 2% for reverse runs, at least where the V_c to V_a ratio in the funnel-probe samples is near 0.08. At higher V_c to V_a ratios, of the order of 0.6 to 0.9 (the latter figure coming from Run 11), the funnel-probe results for direct runs seem to be low by about 4%. (See Table 2, Figure 4, and Rate of Sampling Experiments (above). However, if the V_c to V_a ratio is the governing factor, the values of this ratio observed over many experiments indicate that the majority of funnel-probe results would be low by only about 2% or less in direct runs. (It would, nevertheless, be interesting to make in the future a further comparison of funnel-probe and plastic-cup sampling at a V_c to V_a ratio in the funnel samples of about 0.7.)

Since for Figures 4, 5, and 6 the funnel-probe results were calculated using hypodermic-needle results, it appears that the hypodermic-needle samplers provide values of C_{ei} which are sufficiently representative for use in Equation 1.

The two continuous-phase samplers, because of their different physical forms, might be expected to provide samples containing different proportions of wake and main-body material. The fact that they give samples of almost the same concentration is at least consistent with the hypothesis that the two regions of the continuous phase are of nearly equal concentration. Furthermore, the agreement supports a conclusion that both needles and hook are satisfactory samplers for present purposes; for example, the hook (as well as the needles) gives sufficiently representative samples for use in obtaining C_{ei} for use in Equation 1.

Although there is substantial agreement between results from the hook and the needles, and between those from the funnel and the plastic cup, it is interesting and instructive to look at possible explanations for the very small systematic deviations which exist between the respective results of Figures 5 and 6.

The fact that reversing the direction of extraction caused the funnel-probe results to move from slightly below to slightly above the plastic-cup results suggests that the hypodermic-needle samplers (used to provide C_{ei} values) do not provide **completely** representative samples of continuous phase. If they tend to remove main-body continuous phase preferentially to wake material, and this would seem likely, then the continuous phase concentrations used in Equation 1 would be too high for direct runs. Because the contribution of C_{ei} in Equation 1 is negative, it would be expected that the funnel-probe values of C_{ei} would be too low. For reverse runs, on the other hand, the value of C_{ei} would be too low. Too small an amount being subtracted when Equation 1 was applied would cause the calculated C_{ei} value to be too high. Thus, with the plastic-cup results taken as being correct, in going from direct to reverse runs the funnel-probe results should move from below to above the plastic-cup results, just as observed. With the amount of continuous phase in funnel-probe samples small (V_c/V_d averaged 0.08 for Figure 5 and 0.1 for Figure 6), the correction to C_{ei} applied by means of Equation 1 was small, especially so since a difference between concentrations: $(C_{ei} - C_{ei})$ is present as a factor in the correction term. The result is that the funnel-probe and plastic-cup results were almost the same.

The fact that the hook-probe results were a little higher for direct runs, and a little lower for reverse runs, than the hypodermic-needle results is an indication that the hypodermic needles remove a slightly larger proportion of continuous phase from near the drops than does the hook probe. Now, consider as an example the direct run shown in Figure 5. If the hook-probe results were used instead of the hypodermic-needle results in applying Equation 1 to find C_{ei} for the funnel-probe samples, the funnel-probe results would fall somewhat further below the plastic-cup results than they do in Figure 5. Indeed, a lower C_{ei} value is needed to improve the agreement. Including a higher proportion of continuous phase from near drops will produce this effect. Therefore, the hypodermic needles provide slightly more representative samples of the continuous phase than does the hook probe for use in Equation 1. (This fact is of small significance when this equation is used for calculating funnel-probe results, but does matter for piston results^(1,7).)

Although more representative sampling by the hypodermic needles seems a very likely reason for the slight lack of agreement between hypodermic-needle and hook-probe results, two other explanations also have been con-

sidered. The first of these is that, because of its **geometry**, the hook probe tends to suck in material from an elevation higher up the column than its actual position. However, this suggestion seems not attractive on the grounds that the use of a horizontal extension tube at the end of the hook probe (to provide a horizontal inlet for that probe) produced results which agreed with those obtained with the hook-probe of Figure 2a. Furthermore, the rate of sampling experiments with the hook probe (Table 2) were done at linear velocities (based on the inside diameter of the hook) which, even at the lowest sampling rate, exceeded L_c in the column. If the hook were sucking continuous phase as suggested, it would be expected that changing the sampling rate through the wide ranges studied (Table 2) would change the measured concentration. This did not happen.

The second additional explanation considered is that the relatively large size of the hook-probe causes drops to be deflected away from the region of continuous phase immediately above the hook. Then, for direct runs, extraction from the continuous phase would be less complete in the neighbourhood of the hook inlet than it would have been if the probe were smaller in size, and the hook probe would provide a slightly high result. Similarly, for reverse runs, the partial exclusion of drops from the region of the hook inlet would mean that the continuous phase in that volume would receive less solute than normal from drops, and a sample slightly low in solute would be obtained. It may be that the small difference between the hook-probe results and the hypodermic-needle results is due to a combination of this last effect with a tendency of the hypodermic needles to remove a slightly higher proportion of material from near drops than does the hook probe.

In the case of reverse runs, for example, as in Figure 6, the accuracy of the plastic-cup results may be a little less certain than for direct runs, since the plastic-cup results could be a little low because of the use of the rather low sampling rate of 0.3 ml/min to avoid having two phases in the sample. Perhaps in such runs there may be a little extraction of solute from the drops as they enter the cup. Indeed, it may be that the correct results for reverse runs lie between those for the funnel probe and those for the plastic cup. Remember, however, that what is being considered in Figure 6 is a correction of the order of only about 1% of the concentration.

Conclusion

The sampling devices described all provide satisfactory samples. However, the hypodermic needles are preferred to the hook probe because of the much shorter purge time required, and because of the indications that they provide samples of the continuous phase which are a little more representative than those obtained with the hook. In addition, the hypodermic needles do not disturb the steady operation of the column to the same degree. This advantage arises because of the relatively low rate of flow through the needles. One other advantage of a needle is that it occupies a smaller volume than does the hook. The advantage of small physical size is less for a plastic-cup probe, simply because it includes a cup in addition to a needle. However, a cup is of smaller volume than the funnel. A comparison of the volume occupied by plastic cups with that occupied by the funnel and its supporting tube depends on the number of cup probes in use, and on how far down the column the funnel probe is positioned. However in most cases the volume displaced is smaller for the plastic cups. A possible disadvantage of the cups is that, being organophilic, these may have some influence (presently unknown, but probably small) on drop-size distribution. The plastic-cup probes are preferred to the

funnel probe for three important reasons: the purge-time is very much smaller for a plastic cup, the samples obtained with it are free of continuous phase at suitable rates of sampling, and the flow rate used is very much lower than that used with the hook so that disturbance of steady operation is much less.

Results of sampling studies with the piston described previously⁽¹⁾, used in conjunction with some of the devices considered here, will be given in a future paper.

Acknowledgments

Financial support from the National Research Council of Canada, and from the Dean's Committee on Research, Faculty of Graduate Studies, The University of British Columbia, is gratefully acknowledged. J.S. Forsyth provided many helpful suggestions.

REFERENCES

- (1) Henton, J.E., Hawrelak, R.A., Forsyth, J.S. and Cavers, S.D., Proc. Int. Solvent Extraction Conference, 1971, *II*, 1302.
- (2) Kehat, E. and Letan, R., A.I.Ch.E. J. 1971, *17*, 984.
- (3) Cavers, S.D. and Ewanchyna, J.E., Can. J. Chem. Engng. 1957, *35*, 113.
- (4) Letan, R. and Kehat, E., Chem. Engng. Sci. 1965, *20*, 856.
- (5) Smoot, L.D. and Babb, A.L., Engng. Chem. Fundamentals 1962, *1*, 93.
- (6) Smith, A.R., Caswell, J.E., Larson, P.P. and Cavers, S.D., Can. J. Chem. Engng. 1963, *41*, 150.
- (7) Henton, J.E., Ph.D. thesis, The University of British Columbia, 1967.

DISCUSSION

T.C. Lo: What are your comments on how your method for measurement of column concentration profiles compares with that of Treybal (Ind. Engng. Chem. 1955, *47*, 2435)? Treybal proposed the removal of sidestream samples from the column. The two phases in a sample are brought to equilibrium, and the phases analysed. From the known relative volumes of the phases in the sample, equilibrium information, and the location of the operating line (or point), the composition of each of the phases as they existed in the column can be determined.

S.D. Cavers: The method referred to by Dr. Lo assumes that the phases flow in plug flow without axial mixing. However, it is now recognized that axial mixing takes place in spray columns, and, in addition, that there is an end effect where the drops coalesce at the column interface (See Reference 3 of the paper). One is in the position of having to take internal samples in order to determine the detailed position of the operating line, or alternately, axial mixing co-efficients must be available so that the position of the line can be computed.

However, the question of Dr. Lo suggested to us that, if two funnel-probe samples were withdrawn from the same position in a column, but with different V_c/V_d ratios, the composition of each phase in the column could be determined by writing Equation 1 for each sample, and solving the resulting two equations simultaneously. The value of C_{ci} would correspond to the continuous phase

SYMBOLS

C	= Concentration
C_c^*	= Concentration in a continuous phase in equilibrium with the dispersed phase of concentration C_d
C_d^*	= Concentration in a dispersed phase in equilibrium with the continuous phase of concentration C_c
L	= Superficial velocity of a phase
V	= Volume

Superscript

* = At equilibrium

Subscript

c	= Continuous phase
d	= Dispersed phase
f	= Final value, at time of analysis
i	= Initial value, at time of sampling

APPENDIX

Correction of printing error in Reference 1

Although correct in the galley proofs, the description of the hypodermic-needle samplers in Reference 1 is incorrect. The final sentences under the subheading "Hypodermic needle samplers" should have read:

"After appropriate purging, samples were taken at about 1 ml min⁻¹, often through two needles concurrently, which were not less than 10 in. apart. The other needles, not in use, were withdrawn so that their ends did not protrude into the column. Samples contained only continuous phase."

actually entering the funnel probe. This result could then be compared with the result from the hypodermic-needle sampler (or the hook probe) to determine whether or not it removes representative samples for use in Equation 1.

This approach was attempted for Runs 11 and 12, in each of which a series of funnel-probe samples was available, each sample having a different V_c/V_d ratio. (See paper, and Figure 4 for Run 12). Two simultaneous solutions were carried out for Run 11, and two for Run 12. The values of C_{ci} obtained ranged from 10.3% below to 9.6% above the result obtained from the hypodermic-needle sample. Agreement was better between the values of C_{di} from solving the simultaneous equations, and the corresponding values of C_{di} from the plastic-cup samples. The simultaneous-solution results ranged from 3.5% below to 2.4% above the plastic-cup figures. However, Figure 5 shows generally better overall agreement between funnel-probe and plastic-cup results.

Lack of accuracy seems to arise with the simultaneous-equation method because of the subtraction of two quantities of very roughly the same size when the equations are being solved. A loss of significant figures results. It seems likely that this is what lies behind the calculated value of C_{ci} being **above** the needle value. For direct runs (as these were), with concentration gradients towards the drops, one would expect C_{ci} from the simultaneous solution to be below the result from the needle sample.

It is concluded that the experimental methods described in the paper probably are preferable to the proposed simultaneous-solution approach.

The Retardation of Mass Transfer in a Modified Lewis Cell by Interfacially Active Copolymers

B.J.R. Scholtens⁽¹⁾, S. Bruin⁽²⁾ and B. H. Bijsterbosch⁽³⁾

- (1) Lab. for Physical and Colloid Chemistry, Agricultural University, De Dreijen 6, Wageningen, The Netherlands; present address: Central Laboratory DSM, Fundamental Polymer Research, P.O. Box 18, Geleen, The Netherlands.
- (2) Dept. of Food Process Engineering, Agricultural University, De Dreijen 12, Wageningen, The Netherlands.
- (3) Lab. for Physical and Colloid Chemistry, Agricultural University, De Dreijen 6, Wageningen, The Netherlands.

ABSTRACT

We have investigated the possibility of studying interfacial properties of copolymers spread at a liquid-liquid interface by means of mass transfer measurements between the two liquid phases. The main difficulty appears to be the interpretation of the observed effects: either hydrodynamic or physico-chemical factors may play a part in this process. A requisite for the proper analysis of the retarding effect is a well-defined hydrodynamic profile near the interface, so that model calculations are possible. Fulfilment of these conditions enabled us to interpret the maximum retardation quantitatively in terms of the influence of copolymers on the hydrodynamics near the interface.

Introduction

ALTHOUGH IN CHEMICAL ENGINEERING one is usually interested in increasing mass transfer rates during liquid-liquid extraction, it is also of importance to know which materials are able to retard this process, and by what mechanism. It is our purpose to analyse the retardation of mass transfer between two liquid phases by the presence of surface-active copolymers. Recently⁽¹⁾, one of us has indicated that these measurements may elucidate dynamic interfacial properties of these copolymers.

Usually⁽²⁾, the resistance to transfer of substance A from phase 1 to phase 2 may be described by a series of three separate resistances:

$$R_2^A = r_1^A m_{21}^A + r_{12}^A m_{21}^A + r_2^A \dots \dots \dots (1)$$

where R_2^A (s.m⁻¹) is the overall resistance with respect to phase 2 and r_1^A and r_2^A are the partial liquid phase resistances; r_{12}^A represents the resistance to passing through the interface from phase 1 to 2, and m_{21}^A is the distribution coefficient of A between phase 2 and 1. In fact, these resistances are defined to be equal to the ratios of the relevant concentration differences of A to its resulting mass flux.

Very frequently, the contribution of r_{12}^A is neglected in chemical engineering, whereas it is assumed to be the main factor in some biophysical and colloid-chemical reports⁽³⁾.

In principle, both liquid phase resistances can be estimated from the solution of the equation of continuity of A, provided the hydrodynamics near the interface are known. The presence and relative significance of any

interfacial resistance follows directly from a comparison of the experimental value of R_2^A and the theoretical values of r_1^A , m_{21}^A and r_2^A .

Surface-active molecules may influence mass transfer in several different ways. First, if no equilibrium exists between both phases, the rate may be increased by interfacial instabilities induced by transfer of the surfactant. Second, the adsorption layer may either interfere with the flow patterns near the interface or with A itself (by a chemical interaction); in addition, the interface may be partly blocked, all mechanisms resulting in a decrease of the transfer rate.

In each case, the mechanism depends primarily on the rate-determining step of the transfer process: diffusion to or from the interface is mainly changed by a variation in the hydrodynamics, whereas passage through the interface may be retarded by chemical interactions or blocking. The crucial question about the rate-determining step in the transfer process can only be decided upon when r_1^A and r_2^A can be calculated theoretically. Only when the resistance to transfer across the interface is at least comparable in magnitude to both diffusional resistances, will the retardation be possibly related directly to interfacial properties of the retarding agent. The hydrodynamic effects also find their origin in adsorption of the agent, but the information drawn from this can only be indirect. The boundary conditions of the interfacial flow may change as a result of a (partial) rigidity of the interface. In that case, these measurements may provide more knowledge on dynamic interfacial properties which are not readily amenable to other experimental methods.

Experimental

In order to be able to derive approximate theoretical values for the liquid phase resistances, we developed a transport vessel ("Lewis cell"), rather similar to the one used by Nitsch et al.⁽⁴⁾, with a simple laminar flow profile along the interface. The experimental conditions have been extensively described elsewhere⁽¹⁾, so that we confine ourselves here to a sketch of the vessel (Figure 1) and to some general remarks.

The propellers were always counterrotating, pumping the liquid in an inward radial direction along the interface, which was flat and usually without significant waves; this ensured a laminar, mainly radial flow near the interface. To achieve "comparable" hydrodynamic conditions at both sides of the interface, we chose the rotation speeds in such a way that Re was equal for both phases ($N_b/N_w = v_b/v_w = 2.78$).

The mass transfer rate of KC1 from water (0.1 mol.l⁻¹) to 1-butanol (always mutually saturated with the relevant component) was determined from the time-dependent KC1-concentration in the 1-butanol phase, which was measured conductometrically (at 25°C). We thoroughly checked that

Marangoni or interfacial instabilities were absent in this system. By applying moderate stirring speeds ($40 \leq N_b \leq 90 \text{ min}^{-1}$), a laminar velocity profile was maintained near the interface, with $500 < Re_w = Re_b < 1150$. In order to obtain the most reproducible results, the position of all parts that could influence the velocity profiles in both phases were controlled before each measurement with a cathetometer.

Using a micrometer syringe, the surface-active material, a polyvinyl alcohol-acetate copolymer⁽¹⁾ (B4) was always spread carefully at the interface from a solution containing water, 1-propanol and 1-butanol.

Theory

A fundamental requirement for establishing the relative contributions of the three resistances to the mass transfer process is to determine the liquid phase resistances theoretically. By approximating the real flow situations in the vicinity of the interface by two simple but realistic models, we were able to solve the equation of conservation of mass for the transferring component.

Let us consider an axially symmetric, flat liquid-liquid interface at $z = 0$, extending between r_0 and r_1 ($r_0 > r_1$), with a laminar boundary layer for $z \geq 0$. If we assume that the flow is stationary ($\partial/\partial t = 0$), that the density in the boundary layer is constant, and that only a radial velocity component is present near the interface ($\partial/\partial \theta = \partial/\partial z = 0$), the equation of continuity for the liquid in cylindrical coordinates (e.g. Bird et al.⁽⁵⁾ p. 83) can readily be integrated to:

$$rv_r = \text{constant} \dots \dots \dots (2)$$

In the experimental set-up, V_r is pointing to $r = 0$; thus, we shall only consider negative constants. It is evident that a clean liquid-liquid interface cannot resist any tangential shear stress, so it will be set into motion. This results in a plug-flow along the interface:

$$v_r = -b/r, \dots \dots \dots (3)$$

where $b(\text{m}^2 \cdot \text{s}^{-1})$ is a constant > 0 .

The ultimate case of zero interfacial velocity of the complete interface may be induced by the presence of an adsorption layer. In that case, both tangential shear stresses at the interface are (just) cancelled by the interfacial pressure gradient induced by the flow. In the innermost part of such a laminar boundary layer, the following then holds for the radial velocity:

$$v_r = -az/r, \dots \dots \dots (4)$$

where $a(\text{m} \cdot \text{s}^{-1})$ is a constant > 0 .

For the diffusion of A out of the interface into these laminar boundary layers, the equation of continuity of A must hold. This equation, also in cylindrical coordinates (Bird et al.⁽⁵⁾ p. 559) can be approximated for this configuration by:

$$v_r \frac{\partial c^A}{\partial r} = D \frac{\partial^2 c^A}{\partial z^2}, \dots \dots \dots (5)$$

provided a pseudo steady-state approximation is allowed ($\partial c/\partial t = 0$). In addition, we have assumed that the velocity profile is not affected by the transfer process, and we have neglected radial diffusion with respect to convective transport in that direction.

The boundary conditions for the transfer process read:

$$\left. \begin{aligned} c^A &= c_0^A \text{ at } z > 0 \text{ and } r = r_0 \\ c^A &= c_0^A \text{ at } z = 0 \text{ and } r_1 \leq r \leq r_0 \\ c^A &= c_0^A \text{ at } z = \infty \text{ and } r_1 \leq r \leq r_0 \end{aligned} \right\} \dots \dots \dots (6)$$

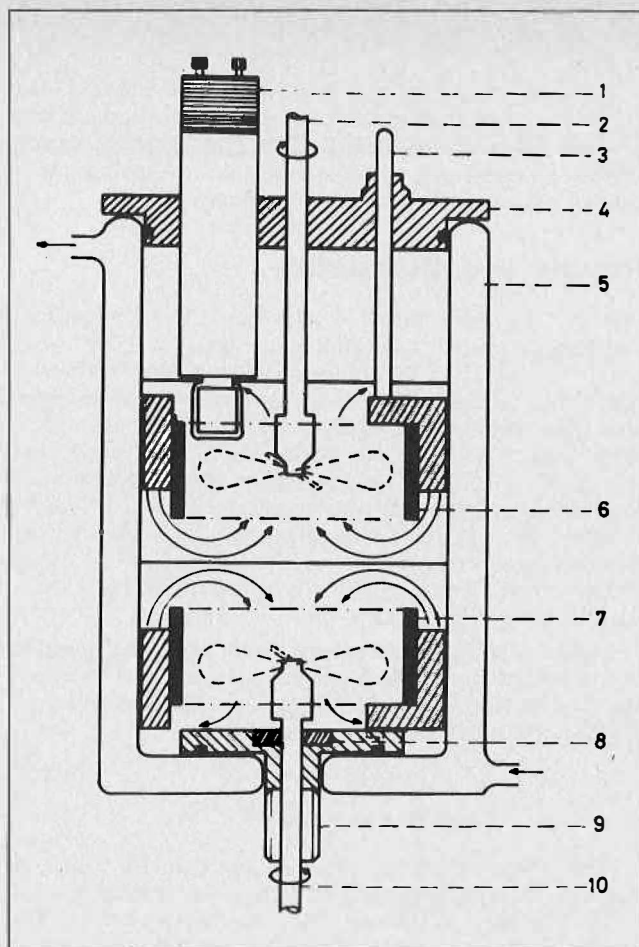


FIGURE 1. Vertical cross section of a transport vessel, with: (1) conductance cell for measuring the KCl concentration; (2) upper stirring shaft ($\varnothing = 0.6 \text{ cm}$) with a three-blade right-hand propeller ($\varnothing 5.1 \text{ cm}$, 2.7 cm above the interface), both stainless steel; (3) stainless steel shaft connected to a baffle of the draft tube; (4) PVC cover with O-ring (butyl rubber); (5) thermostatted double-walled Pyrex glass vessel (inside $\varnothing = 8.08 \pm 0.02 \text{ cm}$); (6) upper draft tube (inside $\varnothing = 5.9 \text{ cm}$, outside $\varnothing = 6.4 \text{ cm}$, height = 2.5 cm) with six baffles ($2.6 \times 0.8 \text{ cm}^2$), the lower edge 1.2 cm above the interface; (7) identical lower draft tube with six baffles; (8) butyl rubber gasket ring; (9) stainless steel plug ($\varnothing = 5.8$ and 1.5 cm , height = 0.6 and 3.4 cm) with butyl rubber O-ring, fixed by a PVC nut; (10) lower stirring shaft, identical to 2); Both propellers and draft tubes are situated symmetrically with respect to the interface.

The solution of (5) under these boundary conditions with either (3) or (4) provides the concentration profile, which enables us to determine the flux through the interface. From the concentration gradient and this flux, we obtained⁽²⁾, ultimately, an expression for the liquid phase resistance. This expression, averaged over the area between r_0 and r_1 , reads for plug flow along the interface:

$$r^A = \frac{\Gamma \left(\frac{1}{3} \right) (r_0^2 - r_1^2)^{1/3}}{2(2b DA)^{1/3}}, \dots \dots \dots (7)$$

while for a linear velocity profile near the interface r_A is given by:

$$r^A = \frac{2\Gamma \left(\frac{1}{3} \right) (r_0^2 - r_1^2)^{1/3}}{3(6a (DA)^2)^{1/3}} \dots \dots \dots (8)$$

The r -function has been tabulated, e.g. by Abramowitz et al.⁽⁹⁾

Provided we can estimate the values of D^A , b , a , r_0 and r_1 , we can thus calculate the liquid phase resistances with (7) and (8), and analyse separately the presence of any interfacial resistance and the influence of surface-active copolymers on the mass transfer process.

Results and Discussion

Since the distribution coefficient of KCl between mutually saturated 1-butanol and water is low⁽¹⁾ (1.72×10^{-2}) and D^{KC1} in 1-butanol is much lower than in water, and because the hydrodynamic conditions in water and 1-butanol are kept similar, it follows from (1) and (7) or (8) that $r_w^{KC1} m_b^{KC1} \ll r_b^{KC1}$ (calculations lead to less than $0.01 \times r_b^{KC1}$), so that we can neglect the first term of (1). From the limiting molar conductance of KCl in 1-butanol ($2.36 \text{ m}^2 \cdot \Omega^{-1} \cdot \text{kmol}^{-1}$), we estimated from the Nernst-Einstein equation that $D_b^{KC1} = 3 \times 10^{-10} \text{ m}^2 \cdot \text{s}^{-1}$. It can be shown⁽¹⁾ that D_b^{KC1} is practically constant in the relevant concentration region ($0.2 \leq c_b^{KC1} \leq 1.3 \text{ mmol} \cdot \text{l}^{-1}$).

Liquid-velocity measurements (with suspended particles in a confined part of both phases near the interface) as a function of N_b (min^{-1}) yielded average radial velocities for $r = 2.5 \times 10^{-2} \text{ m}$ and $|z| = 6 \times 10^{-3} \text{ m}$:

$$\begin{aligned} v_{wr} &= -2.3 \times 10^{-5} N_b^{1.4} \text{ (m} \cdot \text{s}^{-1}\text{)} \\ v_{br} &= -6.3 \times 10^{-5} N_b^{1.4} \text{ (m} \cdot \text{s}^{-1}\text{)} \end{aligned} \quad (9)$$

From these values, we obtained approximate values for a and b . The radial velocity of a clean interface at $r = 2.5 \times 10^{-2} \text{ m}$ can be derived from an expression for two parallel laminar streams given by Lock⁽⁶⁾, resulting in $v_{\sigma r} = -12 \times 10^{-7} N_b^{1.4}/r$ and thus $b_{\sigma} = 12 \times 10^{-7} N_b^{1.4} \text{ (m}^2 \cdot \text{s}^{-1}\text{)}$.

For a rigid interface, the flow near the periphery (at $r = r_0$) can be compared to the flow in the vicinity of a stagnation point. From the known solution of this problem (e.g. Schlichting⁽⁷⁾ p. 88) it followed that $a = 0.025 \times 0.227 |v_r|^{3/2} / \{0.2 (v \times 0.015)^{1/2}\} \text{ (m} \cdot \text{s}^{-1}\text{)}$, where v_r is the velocity at $r = 2.5 \times 10^{-2} \text{ m}$ and $|z| = 6 \times 10^{-3} \text{ m}$. In Table 1 we have collected the relevant hydrodynamic characteristics determined in this way.

Experimental overall resistances for KCl transfer from water to 1-butanol (determined with respect to the latter phase) are collected in column 2 of Table 2. The theoretical values for r_b^{KC1} as calculated with (7), using $r_0 = 4 \times 10^{-2} \text{ m}$ and $r_1 = 0 \text{ m}$, can be found in column 3, and the ratio of $R_b^{\text{exp}}/r_b^{\text{theor}}$ in column 4. Although in the derivation of (7) plug flow was assumed, this was, of course, not the actual velocity profile, since $v_{wr} \neq v_{br}$. But application of (7) will not introduce any serious error, because⁽⁸⁾ $a_b^2 D_b^{KC1} / r v_{\sigma r}^3 \ll 1$. Taking into account the approximate nature of the model and of the values of D_b^{KC1} and b_{σ} , the agreement between R_b^{exp} and r_b^{theor} is good. Although $R_b^{\text{exp}} >$

r_b^{theor} for all stirring speeds, this does not necessarily mean that there is an interfacial resistance: the largest deviations occur at the lowest N_b , just contrary to what would be expected if any interfacial resistance was present. From theory we find that $r_b^{\text{theor}} \propto N_b^{0.7}$, while $R_b^{\text{exp}} \propto N_b^{-0.84}$. Since any appreciable interfacial resistance will always yield a power smaller than the theoretical one (see equation 1), we must again conclude that its presence is highly improbable.

The deviations between R_b^{exp} and r_b^{theor} , especially at low N_b , are ascribed to a less well developed flow at the periphery and in the centre of the interface than assumed in our model. This causes a larger R_b at lower N_b , and also a higher negative slope for the $\log R_b - \log N_b$ plot. Qualitatively, we could indeed observe, with several different flow visualization experiments⁽¹⁾, that the flow along the interface was less effective for $r \lesssim 3.5 \times 10^{-2} \text{ m}$ and in particular for $r \lesssim 2 \times 10^{-2} \text{ m}$ than for the region in between.

In Figure 2, we have plotted for different N_b the retarding effect of B4 (being the ratio of the overall resistance with and without copolymer present), as a function of the amount of B4 spread.

As a consequence of our conclusion that r_b^{KC1} is the rate-determining resistance, it is obvious that the retardation must be ascribed to a change in r_b^{KC1} . This change is brought about by the presence of an adsorption layer of B4, causing a change in the concentration profile of KCl in the 1-butanol phase either due to a change in D_b^{KC1} or to a modified flow profile along the interface. We could reason⁽¹⁾ that the first cause is very improbable, and thus the retardation is mainly caused by a change in hydrodynamics in the diffusion boundary layer in 1-butanol, although B4 is insoluble in that phase. In addition, it was shown that this system does not exhibit any detectable excess interfacial shear viscosity⁽¹⁾.

Combining these facts and considerations, it seems very probable that only the boundary conditions for the flow along the interface are affected by the adsorption layer: dynamic interactions between both shear stresses and the (partly) compressed copolymer layer result in a non-homogeneous layer at the interface where these stresses are just cancelled by the interfacial pressure gradient induced, so that $v_{\sigma r} = 0$ in that region. The ultimate situation is a completely immobilized interface, so that the tangential flow may be represented by (4), and the liquid resistance by (8). This picture explains both the differences in retardation at different N_b for constant amount of B4 and the maximum possible retardation, that seems to become independent of N_b ultimately, as shown below.

The higher the rotation speed the higher the shear stresses and thus the more compressed the copolymer layer, the smaller the area of a completely immobilized interface and the smaller the retardation. This effect decreases at larger amounts of adsorbed copolymer since not

TABLE 1. Approximate Values for the Hydrodynamic Parameters in the Vicinity of the Interface

N_b min^{-1}	$10^4 b_{\sigma}$ $\text{m}^2 \cdot \text{s}^{-1}$	a_b $\text{m} \cdot \text{s}^{-1}$	a_w $\text{m} \cdot \text{s}^{-1}$
40	2.1	0.15	0.06
50	2.9	0.24	0.09
60	3.7	0.34	0.13
70	4.7	0.47	0.17
80	5.6	0.63	0.23
90	6.6	0.80	0.29

TABLE 2. Comparison of Experimental and Theoretical Mass Transfer Resistances for an Uncovered Interface.

N_b min^{-1}	$R_b^{\text{exp}}/10^5$ $\text{s} \cdot \text{m}^{-1}$	$r_b^{\text{theor}}/10^5$ $\text{s} \cdot \text{m}^{-1}$	$R_b^{\text{exp}}/r_b^{\text{theor}}$
40	11.6	10.0	1.16
50	9.5	8.5	1.11
60	8.3	7.6	1.09
70	7.3	6.8	1.08
80	6.4	6.2	1.05
90	5.9	5.7	1.04

the absolute value of the interfacial pressure but only the induced gradient is important in this mechanism.

Theoretically, we can predict the maximum effect of immobilization on r_b^{KC1} by determining the ratio of (8) and (7). This ratio appears to be independent of N_b (since $a \sim v^{3/2}$ and $b \sim v$) and to amount to 4.9. Although this theoretical value is about 20% lower than found experimentally, at high adsorption the first prediction seems to be confirmed by experiment (see Figure 2).

We think that the higher experimental retardation must be explained by the imperfection of the actual flow along the interface: its inner and outer parts are not directly reached by the flow, but only indirectly, because the intermediate part flows to the centre. This indirect flow mechanism will not be so effective for an immobilized interface because of viscous effects. Therefore, the maximum retardation will be larger than predicted theoretically.

The likelihood of the proposed mechanism could be demonstrated with talc particles at the interface: they were directed very quickly to the centre of a clean interface, but when 2 mg.m⁻² B4 was spread, they did not move at all at $N_b = 40$ and only at the periphery at $N_b = 90$ min⁻¹. When 100 mg.m⁻² was spread they did not even move at $N_b = 80$ min⁻¹.

The existing flow is too imperfect to allow quantitative conclusions as to which part of the interface is covered in those situations where the retardation is smaller than the maximum possible. But provided we knew the exact flow profile, we would be able to determine from the experimental retardation how the copolymers are distributed over the interface⁽¹⁾. This may provide a new technique to study adsorption layers under variable dynamic conditions.

NOTATION

c	= molar concentration (kmol.m ⁻³)
D	= diffusion coefficient (m ² .s ⁻¹)
m ₁₂	= distribution coefficient (= c ₁ /c ₂)
N	= rotation speed (min ⁻¹)
R	= overall mass transfer resistance (s.m. ⁻¹)
r	= partial mass transfer resistance (s.m. ⁻¹)
t	= time
v	= velocity (m.s ⁻¹)
r, z	= cylindrical coordinates (m)
ν	= kinematic viscosity (m ² .s ⁻¹)
b	= refers to the 1-butanol phase

In general, the super- end subscripts refer to the quantity or substance mentioned; the following abbreviations are used:

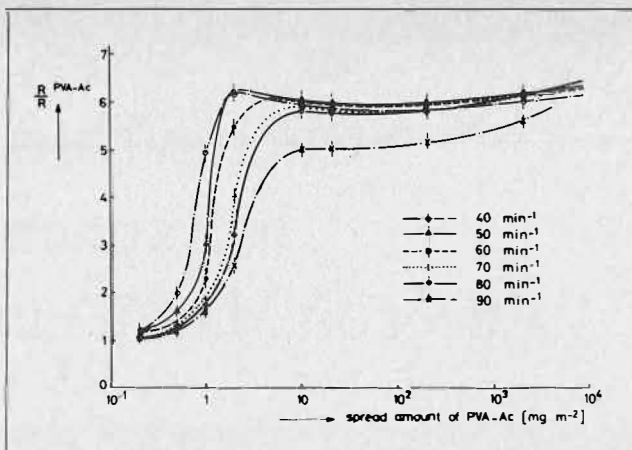


FIGURE 2. The retardation at different stirring speeds ($\approx N_b = 2.78 N_w$) as a function of the spread amount of PVA-Ac.

bw = refers to the 1-butanol — water equilibrium system
 r = radial
 w = refers to the water phase
 σ = refers to the interface
 Re = Reynolds number.

REFERENCES

- (1) Scholtens, B.J.R., Ph.D. thesis, Agricultural University, Wageningen, The Netherlands; *Communic. Agric. Univ. Wageningen* 1977, 77-7*.
- (2) Davies, J.T. and Rideal, E.K., "Interfacial Phenomena" 1961, Academic Press, New York, Ch. 7.
- (3) This controversy was first noted by Scholtens, B.J.R., and Bijsterbosch, B.H., *FEBS Lett.* 1976, 62, 233-5.
- (4) Nitsch, W. and Hillekamp, K., *Chem. Zeit.* 1972, 96, 254-61. Nitsch, W., Raab, M. and Wiedholz, R., *Chem. Ing. Tech.* 1973, 45, 1026-32.
- (5) Bird, R.B., Stewart, W.E. and Lightfoot, E.N., "Transport Phenomena" 1960, J. Wiley and Sons Inc., New York.
- (6) Lock, R.C., *Q.J. Mech. Appl. Math.* 1951, 4, 42-63.
- (7) Schlichting, H., "Boundary Layer Theory" 1968, McGraw-Hill, New York.
- (8) Beek, W.J. and Bakker, C.A.P., *Appl. Sci. Res.* 1961, A-10, 241-52.
- (9) Abramowitz, M. and Stegun, A., "Handbook of Mathematical Functions" 1968, Dover Publ. Inc., New York.
- (*) A reprint of this publication can be obtained from Dr. B.H. Bijsterbosch, Lab. for Physical and Colloid Chemistry, De Dreijen 6, Wageningen, The Netherlands.

Structural Mechanical Barriers in Extraction Systems. Effect on Mass Transfer and Coalescence

G.A. Yagodin, V.V. Tarasov, A.V. Fomin and S. Yu. Ivakhno,
The Mendeleev Institute of Chemical Technology,
Moscow, USSR.

The Mass Transfer Kinetics Research Method

ABSTRACT

Condensed interfacial films are shown to form in extraction systems with zirconium (also hafnium, titanium). It has been determined that these films can act as structural mechanical barriers and slow down mass transfer, drop coalescence and emulsion separation. Relative rheological properties of the barriers have been measured. Film formation is believed to be caused by adsorption and association of hydrolyzed forms of metals at the interface. This phenomenon is likely to be common for all extraction systems containing compounds of polyvalent metals exposed to hydrolysis and hydrolytic polymerization in solution.

Introduction

THE PROPERTIES OF STRUCTURAL mechanical barriers (SBM) at liquid-liquid interfaces have been studied using mainly water-oil systems with different organic surfactants.⁽¹⁾ Extraction systems have not been investigated from this point of view. Although the concept of mechanical barriers has been suggested several times^(2,3), the confirmation of this concept for extraction systems encountered great difficulties. Frequently, observed decreases of mass transfer coefficients could be accounted for in terms of the depression of convection at the interface rather than the additional resistance.

Recently the possibility of the existence of mechanical barriers has been proved experimentally in the case of zirconium and some other metals in their extraction by alkylphosphoric acids^(4,5) Taking into consideration the surface tension data, Flett⁽⁶⁾ has also concluded that the anomalously low rate of nickel extraction by a mixture of α -oxyoxime and lauric acid may be accounted for by the presence of SMB.

The specific SMB seems to be the result of association processes at the interface. Such barriers can slow down mass transfer and emulsion separation, thus reducing the efficiency of extraction equipment.

In this report the experimental data on this interesting phenomenon are summarized.

Experimental

The presence of SMB in some extraction systems was postulated at first^(4,5) on the basis of indirect data on the kinetics of mass transfer through the renewed and "unrenewed" interface as well as by means of life-time determination of a single drop at a plane interface and the rate of emulsion separation.

Diffusion cells with stirring (Lewis cells) were used for the investigation of mass transfer kinetics through the "unrenewed" interface. In such a cell the organic and aqueous phases were placed one under the other, the interface being in a narrow annulus. Each phase was stirred with its own stirrer, the interface being quiet in the range of the stirrer rate of 0-300 rpm. Thus we were able to determine the interfacial area and to calculate the mass transfer coefficients per unit area. The calculation was done according to following equations:

$$\frac{dm}{d\tau} = -kS(c_{eq} - c_{\tau}); m = c_{\tau}v; a = \frac{S}{V}; J = \frac{c_{\tau}}{c_{eq}};$$

$$\int_0^{c_{\tau}} \frac{dc_{\tau}}{c_{eq} - c_{\tau}} = - \int_0^{\tau} ka d\tau$$

$$\ln(1 - J) = -ka\tau$$

The distribution coefficient for Zr and Hf being much more than 100, the equilibrium concentration of these elements in the organic phase was actually equal to their original concentration in aqueous phase of the same volume. To compare the rates of mass transfer in different experiments, we used also the slope values ($\text{tg}\alpha$) of the function $\ln(1 - J) = f(\tau)$ that are proportional to the mass transfer coefficients ($\text{tg}\alpha = ka$).

The Drop Coalescence and Emulsion Separation Technique

The coalescence kinetics investigation technique has been described in detail in a monograph.⁽¹⁾ The drops of organic phase (about 3 mm in diameter) were formed at a capillary tip passing through the bottom of a wide cylindrical vessel at 5 cm distance from the interface. After separation from the capillary, the drop floated to the interface. The time interval between this moment and the coalescence is the drop life time.

The coalescence rate has been characterized by the average life time of the drops determined by over 100 experiments. The exception was the investigation on kinetics of film durability (or viscosity) stabilization. In these cases the average coalescence time has been calculated on the basis of 10 consequent measurements within each time interval.

A similar device with an upper capillary arrangement was used for the drops of aqueous phase.

The rate of emulsion separation has been estimated by the time of half-clearing of a fixed emulsion volume (100 cm³).

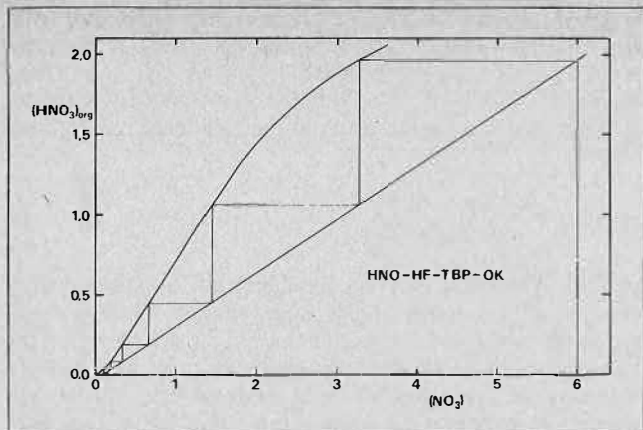


FIGURE 4. McCabe-Thiele diagram for the operating line shown in Figures 2 and 3.

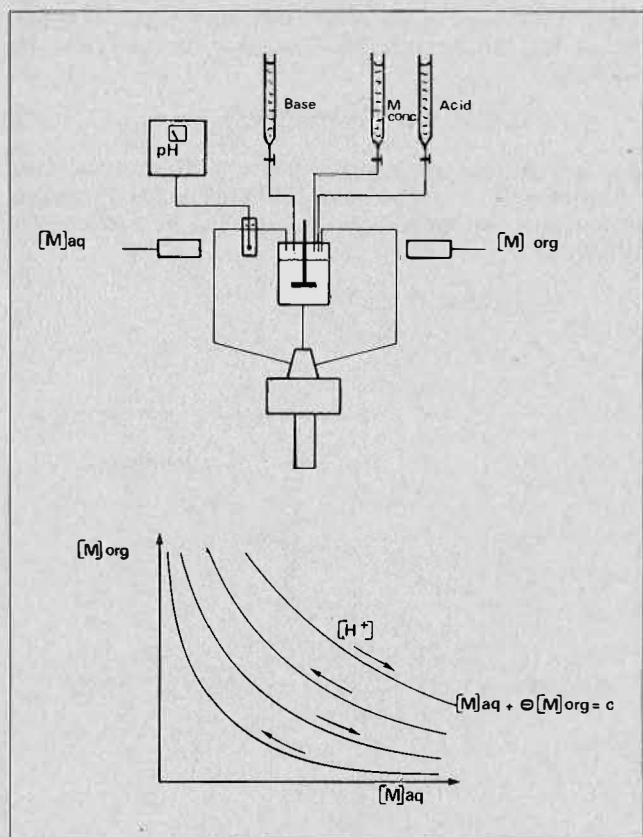


FIGURE 5. AKUFVE setup for the determination of arbitrary parts of the equilibrium surface at constant extractant concentration using the addition method. The addition of base to the system is limited by ionic strength consideration. However, the base can be generated in situ by electrolysis.

The Determination of Equilibrium Surfaces with the AKUFVE Equipment

To illustrate the different ways the AKUFVE can be used to obtain the experimental data needed to define the shape and position of equilibrium surfaces, a simple extraction mechanism, defined by reaction 2 above, will be assumed. All other complicated reactions are neglected.

Figure 5 shows the most widely used setup with the AKUFVE^(2,9). The metal concentration in both phases and the acidity are measured on-line with suitable detectors. Within certain limits it is possible to make random changes in the concentrations of interest by adding

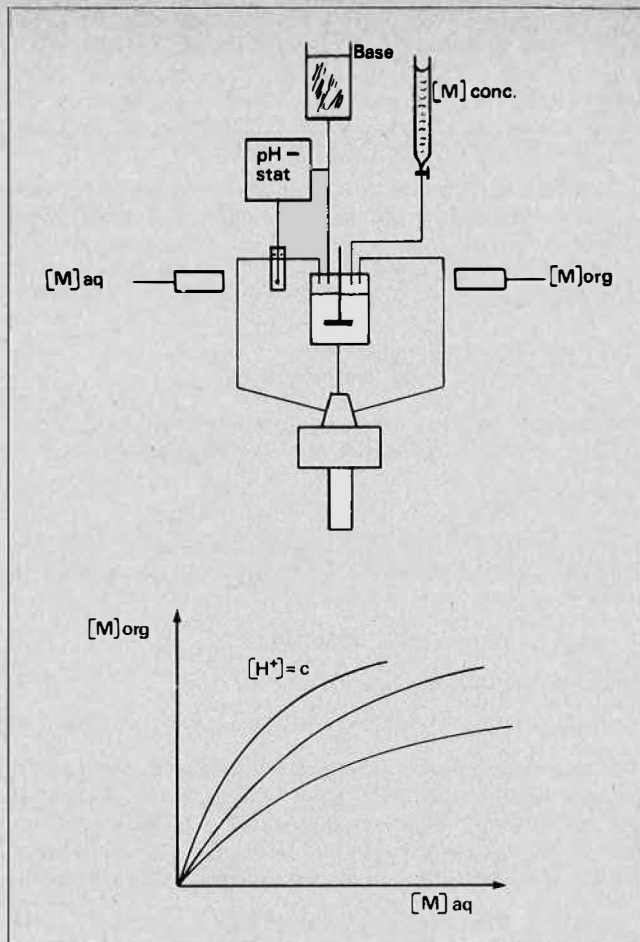


FIGURE 6. AKUFVE setup for measurements at constant acidity using the addition method.

stock solutions of acid, base, metal, organic diluent and extractant. Thus, it is possible to investigate a large part of the equilibrium surface in one experiment. The equilibrium surface can then be constructed from these data. This is best done by fitting a suitable chemical model to the data. Some experiments have been reported where, e.g. the pH was not recorded⁽⁹⁾. The metal stock solution can sometimes be a saturated extract.

Figure 6 shows a setup where a pH-stat is used to keep the acidity constant. This was first used by Cox and Flett⁽⁴⁾ in an investigation of metal extraction by mixtures of LIX63 and carboxylic acids. In this mode of operation the metal concentration in each phase is recorded for an increasing total amount of metal in the system. The curves obtained, \bar{M} vs $[M]$ at $[H^+] = \text{const.}$, correspond to cuts through the equilibrium surface parallel to the \bar{M} - $[M]$ plane. These data can then be easily used to construct the iso- $[M]$ curves in a diagram similar to Figure 2.

In the setups shown in Figures 7 and 8, a metal concentration controller is used on-line to keep either $[M]$ or \bar{M} constant. The data from the second of these methods corresponds directly to the iso- \bar{M} curves in a $[H^+]$ - $[M]$ diagram. Neither of these last two methods has however, been used so far.

A Possible Shortcut to the Equilibrium Curve

In analogy with the batch technique, varying phase volume ratios, θ , can be used to obtain \bar{M} vs $[M]$ for

varying θ (see Figure 9). It is obvious that this procedure needs some justification as it, with the AKUFVE, might involve partial removal of the aqueous or organic phase followed by replacement with "fresh" solution. In the extreme case, one of the phases slowly flows continuously through the AKUFVE system and out.

Consider a two-stage counter-current extraction process as shown in Figure 10a and the single AKUFVE stage shown in Figure 10b. Here a bar over the concentration symbol denotes the organic phase. The phase flow ratio, θ , is defined as,

$$\theta = \frac{\text{Organic phase flow rate}}{\text{Aqueous phase flow rate}} \quad (4)$$

Assume the existence of an equilibrium function, f , which is single valued and depends only on $[M]$, defined as,

$$[\bar{M}]_n = f([M]_{n-1}) \quad (5)$$

where n denotes the stage number in Figure 10a. The material balance over the first stage can be written as follows,

$$[M]_1 = [M]_0 - \theta[\bar{M}]_0 + \theta f([M]_0) \quad (6)$$

and over the second stage as,

$$[M]_2 = [M]_1 - \theta f([M]_0) + \theta f([M]_1) \quad (7)$$

These equations can then be compared with the material balance for the AKUFVE stage in Figure 10b. This stage has an effective phase volume ratio, θ_{eff} , which we are free to give any positive value. Using the nomenclature in Figure 10b, the material balance over this stage is given by

$$[M]_2 = [M]_1 - \theta_{\text{eff}}[\bar{M}]_0 + \theta_{\text{eff}}f([M]_1) \quad (8)$$

where the same indices have been used for the feed and

effluent streams as for the second stage in Figure 10a, and θ_{eff} is the ratio of the organic and aqueous flow ratio needed to give the same conditions in an extraction stage as in the AKUFVE. The requirement that these concentrations should be equal leads to the following requirement on θ_{eff} ,

$$\theta_{\text{eff}} = \frac{f([M]_1) - f([M]_0)}{f([M]_1) - [M]_0} \cdot \theta \quad (9)$$

This discussion can be extended to any stage in a counter-current battery with many stages. Thus, as long as we have only one extracted species or a case when the concentrations of all the other species can be expressed in terms of the concentration of a single species, it is always possible to measure the equilibrium curve for a given feed composition directly. This often corresponds to a large saving in experimental and computational effort. The actual values of θ_{eff} need not be known.

As an example, consider the extraction mechanism defined by reaction 2. The total concentration in the organic phase, C_R , of the extractant is given by the following equation,

$$C_R = m[(\bar{H}R)_m] + mx[MH_{m-x-z}R_{m-x}] \quad (10)$$

At the same time, the charge balance in the aqueous phase given by eqn. 3 above must be fulfilled. Let us further assume that an equilibrium constant, k_{ex} , for reaction 2 is defined as

$$k_{\text{ex}} = \frac{[MH_{m-x-z}R_{m-x}][H^+]_z}{[M^{z+}][(\bar{H}R)_m]^z} \quad (11)$$

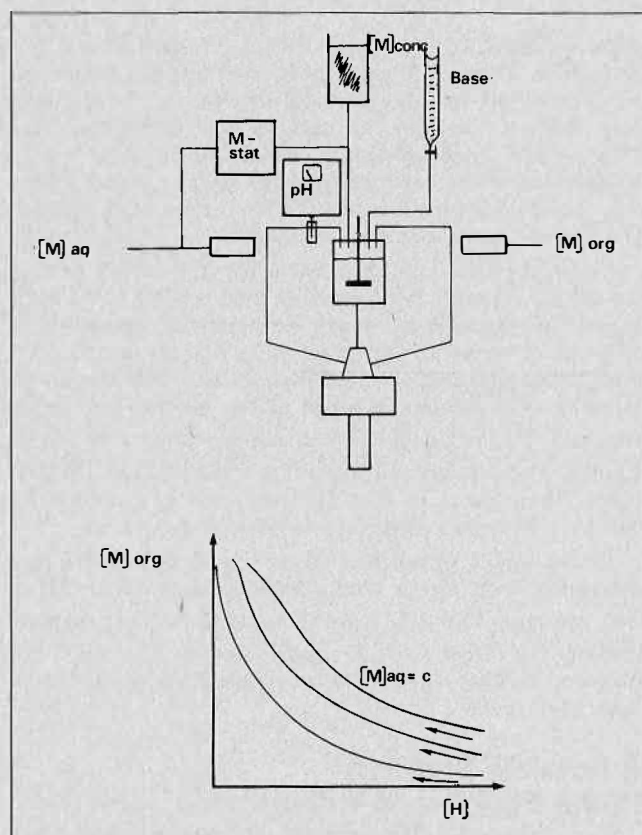


FIGURE 7. AKUFVE setup for measurements at constant aqueous metal concentration using the addition method.

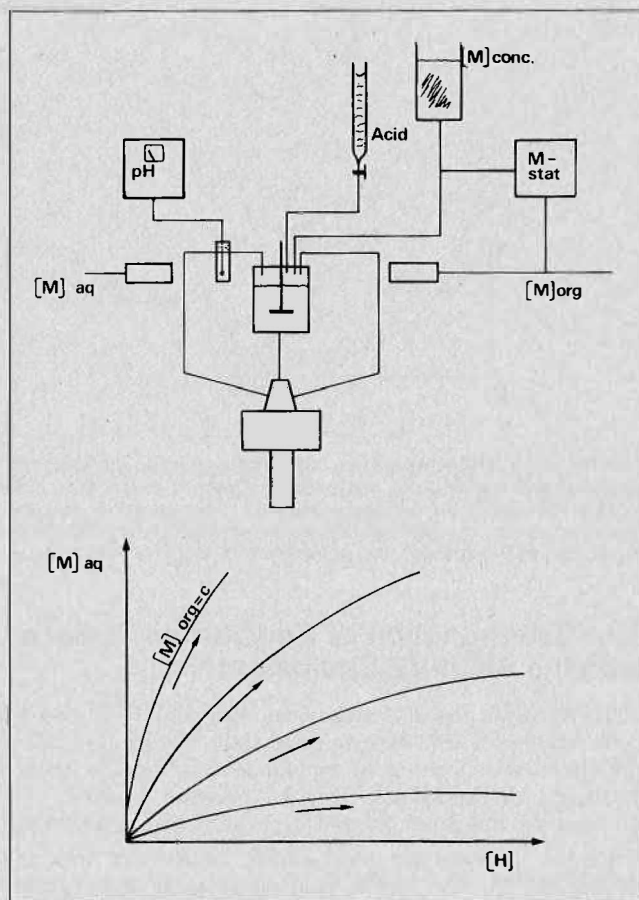


FIGURE 8. AKUFVE setup for direct measurement of the equilibrium surface in the form of metal iso-concentration curves for the organic phase using the addition method.

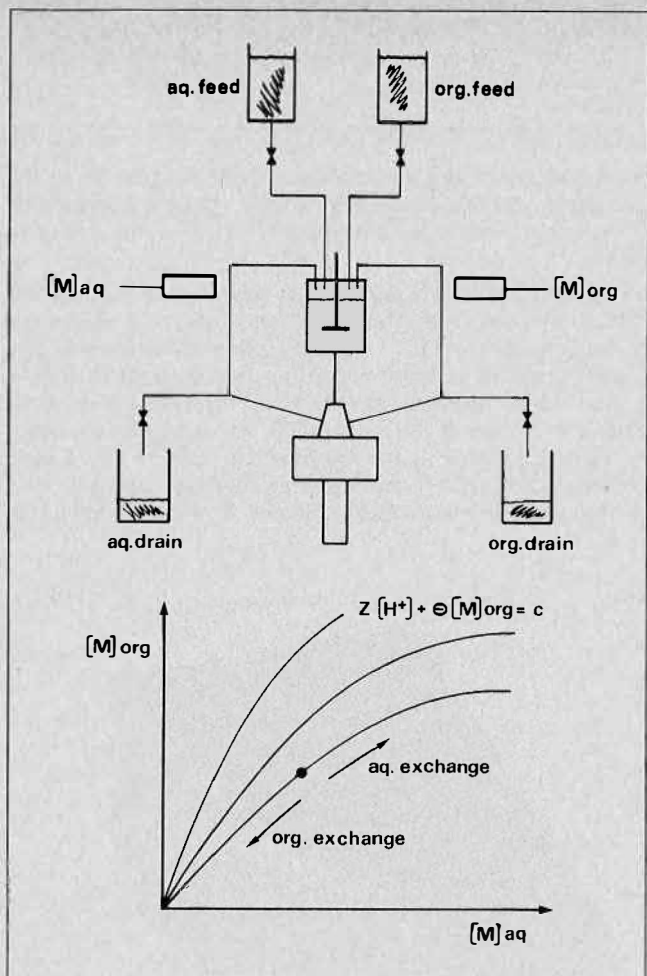


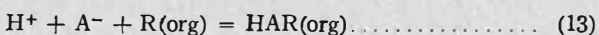
FIGURE 9. AKUFVE setup for direct measurement of the equilibrium curve for a counter current extraction battery. The method used is called the substitution method or the θ_{eff} -method.

A combination of equation 3, 10 and 11 gives the following expression for the metal concentration in the organic phase,

$$[\overline{MH}_{m-x-z}R_{mx}] = [\overline{M}] = k_{ex}[M^{z+}] \left(\frac{1}{m} \cdot C_R - x[\overline{M}] \right)^x (F - z[M^{z+}]^{-z}) \dots (12)$$

It is evident that $[\overline{M}]$ can be expressed as a function of $[M]$ only and thus the requirement on the function, f , (eqn. 5) is fulfilled in this case and the θ_{eff} method can be used.

Similarly it can be shown that, for the extraction of an acid by a solvating reagent, R, according to the reaction mechanism



with an equilibrium constant k_{ex} , the concentration of A in the organic phase, $[\overline{HAR}]$, is given by the following equation

$$[\overline{HAR}] = k_{ex}[A^-] (C_R - [\overline{HAR}]) (F + [A^-]) \dots (14)$$

and thus the θ_{eff} method should work also in this case.

To reach the high and low concentration parts of the equilibrium curve, very low and very high θ_{eff} values, respectively, are needed. This poses no practical problem when using a continuous phase replacement in the AKUFVE. However, when discrete replacement operations are performed, it can be shown that, using equal

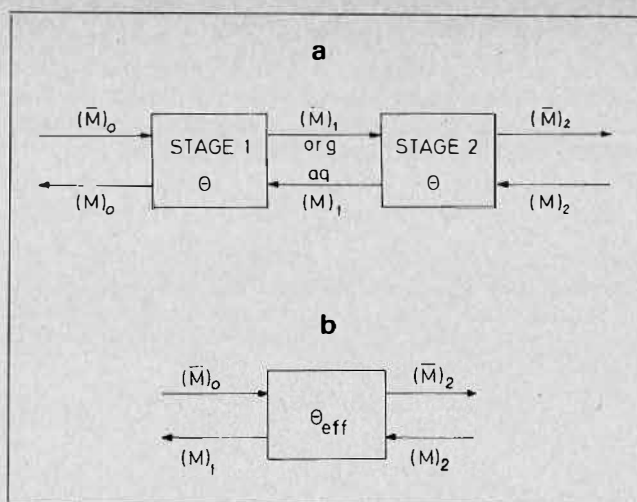


FIGURE 10. Comparison between a two stage counter current extraction battery with organic to aqueous flow ratio θ and a single extraction stage with the same feed and effluent concentrations but a different flow ratio, θ_{eff} .

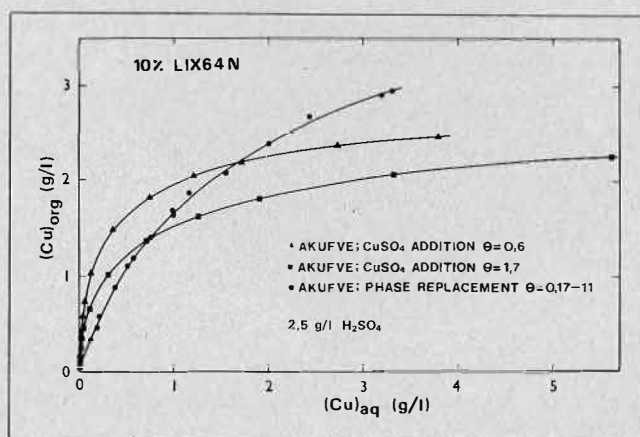


FIGURE 11. Equilibrium curves obtained with the AKUFVE using the addition and substitution methods. Initial aqueous phase contained 2.5 g/l sulphuric acid.

phase volumes in the AKUFVE, draining and replacing a fraction α of one phase n times lead to θ_{eff} values between the following limits for any distribution ratio,

$$(1 - \alpha)^n \leq \theta_{eff} \leq (1 + n\alpha)^{-1} \text{ aqueous phase exchange} \dots (15a)$$

$$(1 + n\alpha) \leq \theta_{eff} \leq (1 - \alpha)^{-n} \text{ organic phase exchange} \dots (15b)$$

where the added organic phase was assumed to be free from the extracted species.

Extraction of Copper with LIX64N

The AKUFVE equipment has, among other things, been used to investigate the H_2SO_4 -Cu-LIX64N-organic diluent system by several investigators^(10,11). Figure 11 shows the results from three different experiments, two using the method of Figure 5 and one using the method of Figure 9. The difference between the curves stems from the fact that they correspond to different cuts through the equilibrium surface. By pooling all the data kindly supplied by MX-Processor AB, the following simple model could be evaluated. The extraction of copper by LIX64N, HR, was assumed to proceed according to the following reaction,

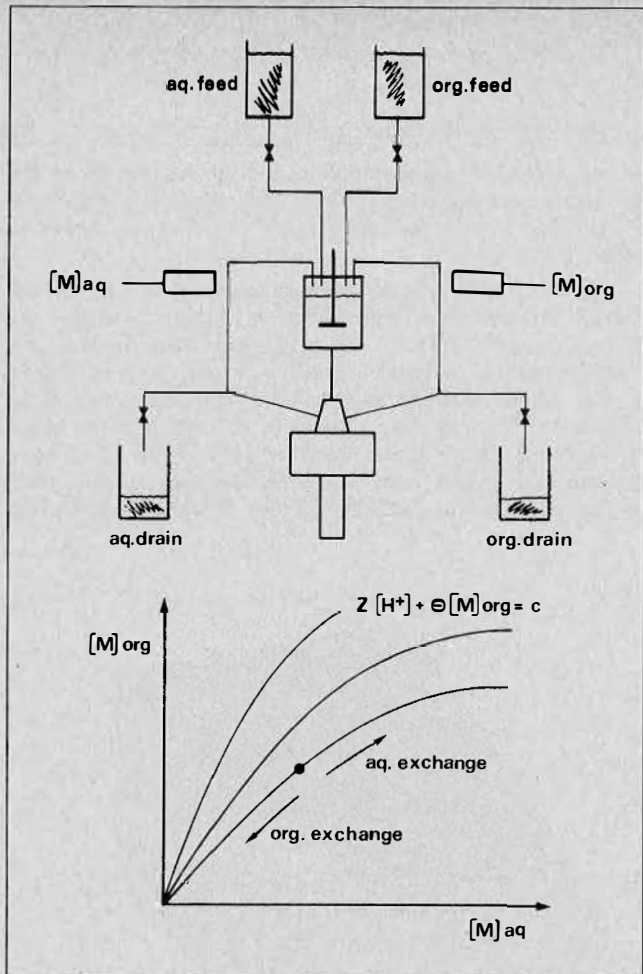


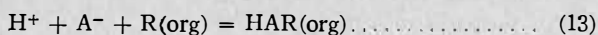
FIGURE 9. AKUFVE setup for direct measurement of the equilibrium curve for a counter current extraction battery. The method used is called the substitution method or the θ_{eff} -method.

A combination of equation 3, 10 and 11 gives the following expression for the metal concentration in the organic phase,

$$\overline{[MH_{m-x-z}R_{mx}]} = \overline{[M]} = k_{ex}[M^{z+}] \left(\frac{1}{m} \cdot C_R - x\overline{[M]} \right)^x (F - z[M^{z+}])^{-z} \quad (12)$$

It is evident that $\overline{[M]}$ can be expressed as a function of $[M]$ only and thus the requirement on the function, f , (eqn. 5) is fulfilled in this case and the θ_{eff} method can be used.

Similarly it can be shown that, for the extraction of an acid by a solvating reagent, R , according to the reaction mechanism



with an equilibrium constant k_{ex} , the concentration of A in the organic phase, $\overline{[HAR]}$, is given by the following equation

$$\overline{[HAR]} = k_{ex}[A^-] (C_R - \overline{[HAR]}) (F + [A^-]) \quad (14)$$

and thus the θ_{eff} method should work also in this case.

To reach the high and low concentration parts of the equilibrium curve, very low and very high θ_{eff} values, respectively, are needed. This poses no practical problem when using a continuous phase replacement in the AKUFVE. However, when discrete replacement operations are performed, it can be shown that, using equal

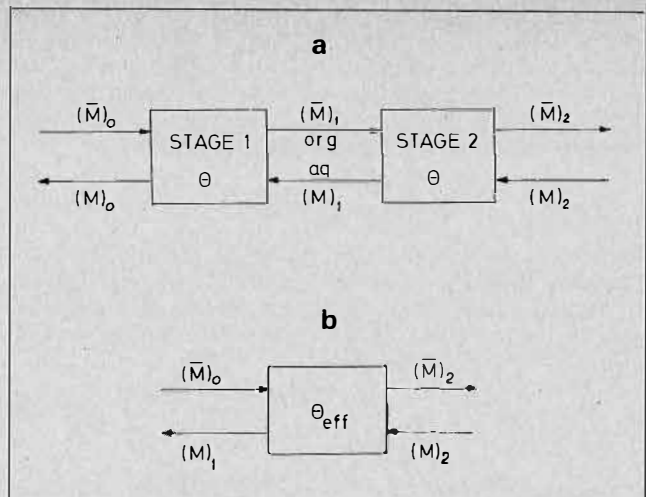


FIGURE 10. Comparison between a two stage counter current extraction battery with organic to aqueous flow ratio θ and a single extraction stage with the same feed and effluent concentrations but a different flow ratio, θ_{eff} .

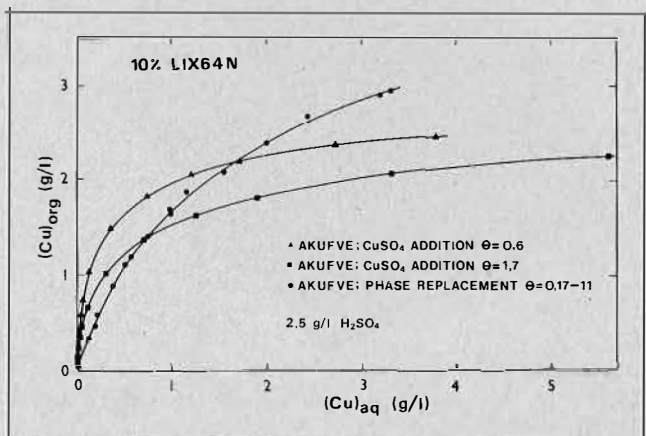


FIGURE 11. Equilibrium curves obtained with the AKUFVE using the addition and substitution methods. Initial aqueous phase contained 2.5 g/l sulphuric acid.

phase volumes in the AKUFVE, draining and replacing a fraction α of one phase n times lead to θ_{eff} values between the following limits for any distribution ratio,

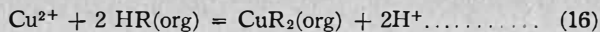
$$(1 - \alpha)^n \leq \theta_{eff} \leq (1 + n\alpha)^{-1} \quad \text{aqueous phase exchange} \quad (15a)$$

$$(1 + n\alpha) \leq \theta_{eff} \leq (1 - \alpha)^{-n} \quad \text{organic phase exchange} \quad (15b)$$

where the added organic phase was assumed to be free from the extracted species.

Extraction of Copper with LIX64N

The AKUFVE equipment has, among other things, been used to investigate the H_2SO_4 -Cu-LIX64N-organic diluent system by several investigators^(10,11). Figure 11 shows the results from three different experiments, two using the method of Figure 5 and one using the method of Figure 9. The difference between the curves stems from the fact that they correspond to different cuts through the equilibrium surface. By pooling all the data kindly supplied by MX-Processor AB, the following simple model could be evaluated. The extraction of copper by LIX64N, HR, was assumed to proceed according to the following reaction,



with an extraction constant, k_{ex} , whose magnitude varies with the LIX64N concentration. From the regular solution theory it can be shown that k_{ex} is expected to vary with the composition of the organic phase as follows:

$$\log k_{\text{ex}} = \log k_{\text{ex}}^{\circ} + a \varphi_{\text{LIX}} + b \varphi_{\text{LIX}}^2 \dots \dots \dots (17)$$

where k_{ex}° is the value of k_{ex} at infinite dilution, a and b are constants, and φ_{LIX} is the volume fraction of LIX64N in the organic phase. Eqn. 17 can be crudely approximated for a limited range of LIX64N concentrations (5% - 40% LIX64N) by the expression

$$k_{\text{ex}} = k'_{\text{ex}}/P \dots \dots \dots (18)$$

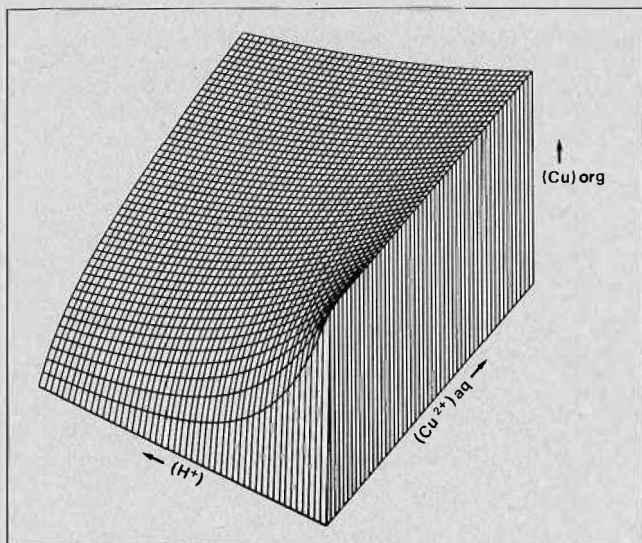


FIGURE 12. The equilibrium surface in the H_2SO_4 -Cu-10% LIX64N-OK system.

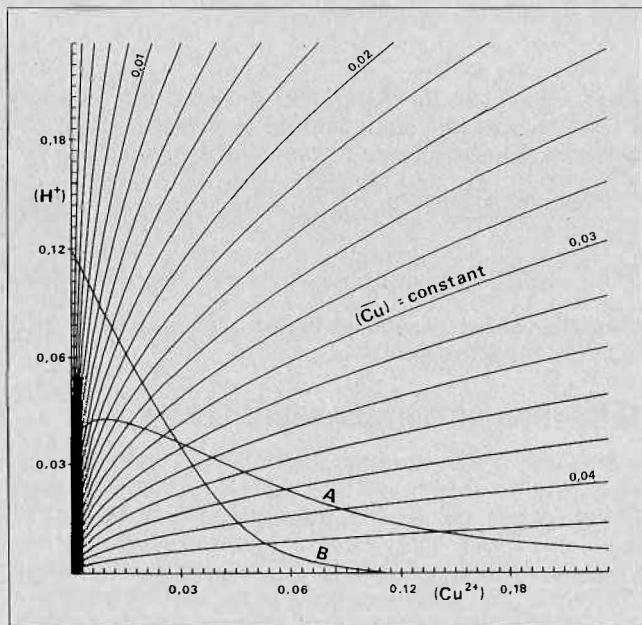


FIGURE 13. Iso- $[\text{Cu}]$ representation of the equilibrium surface shown in Figure 12. Curve A represents the working curve for the AKUFVE addition method without acidity control. Curve B represents the working curve for the AKUFVE substitution method and for a counter current extraction battery. Concentrations are in moles/l.

where P is the concentration (%) of LIX64N in OK.

The buffering action of the sulphate-bisulphate system is given by the reaction



No evidence for the dimerization of the reagent or of the formation of solvates was found. This result disagrees with some other reports on this system^(12,13). k'_{ex} was found to be 20.3.

Figure 12 shows a perspective view of the equilibrium surface obtained from this model and Figure 13 shows the projection on the $[\text{H}^+] - [\text{Cu}^{2+}]$ plane. When using the CuSO_4 addition method, according to the setup in Figure 5, the added sulphate ions lead to working curve A in Figure 13, whereas the θ_{eff} -method, according to the setup in Figure 9, leads to the working curve B in the Figure corresponding to a constant total sulphate concentration in the aqueous phase. Curve B also would correspond to

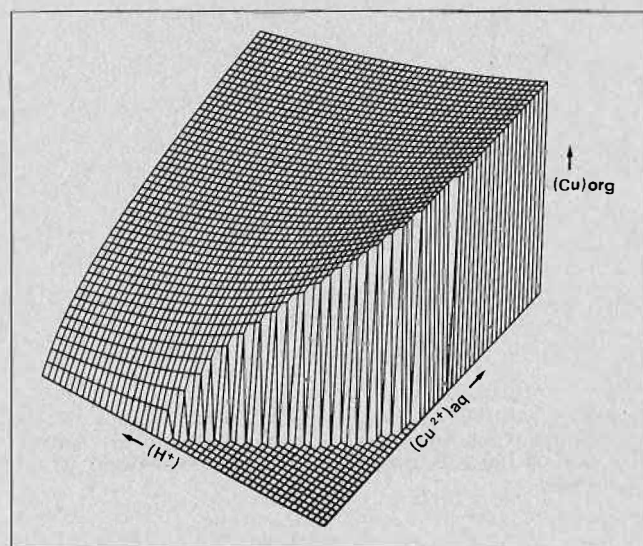


FIGURE 14. Perspective view of the cut between curve B in Figure 13 and the equilibrium surface for the H_2SO_4 -Cu-LIX64N-OK (10% LIX) system.

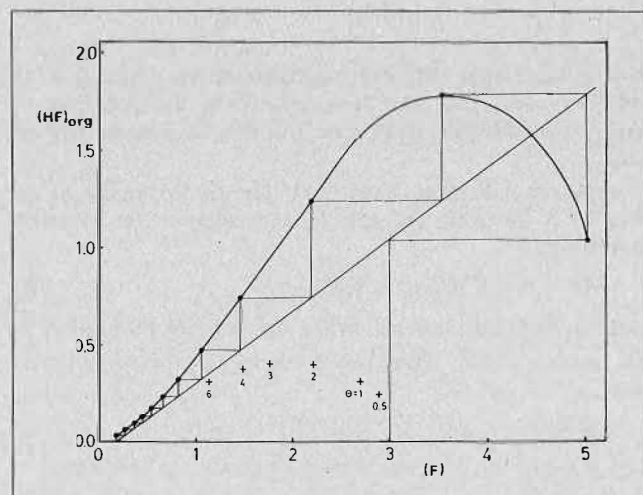


FIGURE 15. The strongly bent equilibrium curve for the extraction of HF by TBP in OK from $\text{HF-HNO}_3\text{-H}_2\text{SO}_4$ containing pickling liquor and the corresponding stage concentrations. The crosses indicate where measurement by the θ_{eff} -methods fall. The number by each cross gives the corresponding θ_{eff} value. Concentrations are in moles/l.

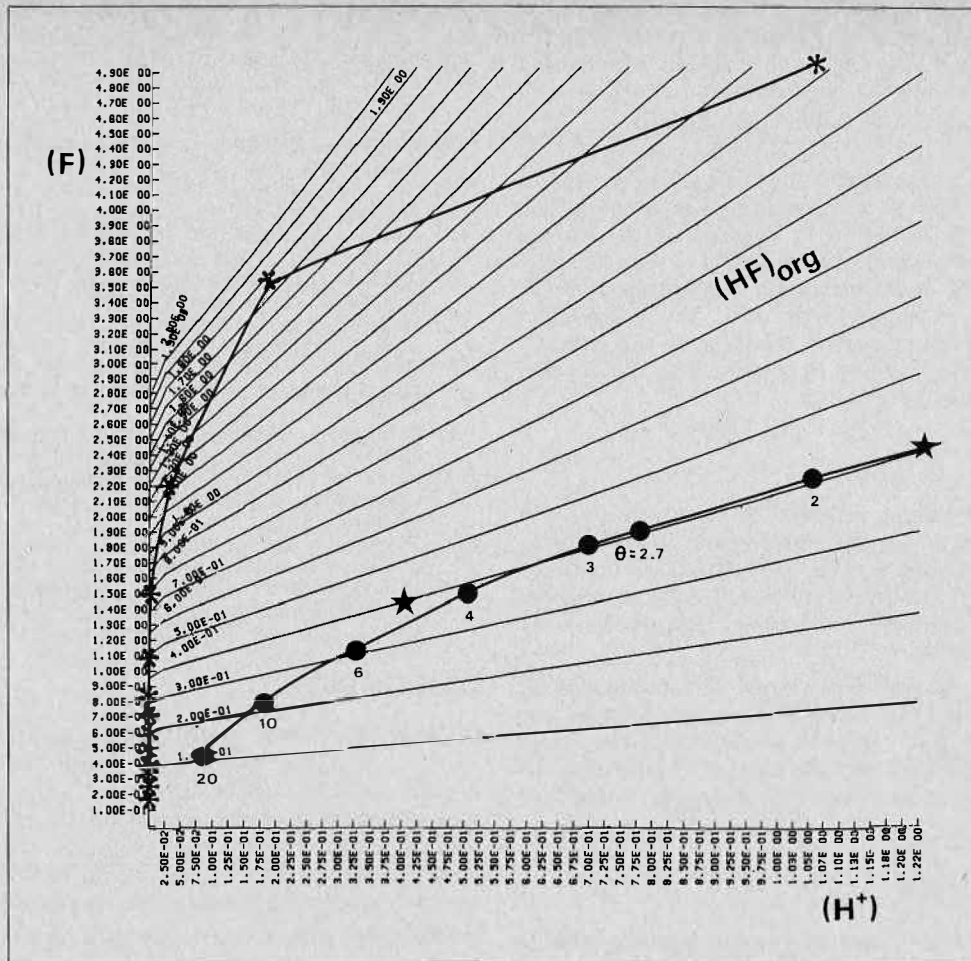


FIGURE 16. Iso-concentration diagram for the HF-TBP-system in the presence of HNO₃, H₂SO₄ and metal salts.* Actual stage effluent concentrations. ● and ★ AKUFVE experiments using the θ_{eff} -method. Concentrations are in moles/l.

the “operating line” in a counter-current extraction battery with the same feed solution. The occurrence of the equilibrium curve as a cut between the bent operating curve B (Figure 13) and the equilibrium surface is shown in Figure 14. Thus, the concept of an equilibrium surface is very illustrative in this case, which otherwise could easily have looked confusing.

The Determination of Equilibrium Surfaces and Equilibrium Lines in Multi-Component Systems

The systems discussed so far have been simple with either only one extractable component, eg. HA, or with all concentrations of the extractable components present expressible in terms of one of them. In many industrial systems it is common to have more than one extractable species present. Can then the θ_{eff} method also be used to reduce the experimental and computational work for these systems?

Using the symbolism of Figure 10 and defining two functions f and g to describe the concentration of the two components A and B in the organic phase we obtain

$$[\bar{A}]_n = f([A]_{n-1}, [B]_{n-1}) \dots \dots \dots (20a)$$

$$[\bar{B}]_n = g([A]_{n-1}, [B]_{n-1}) \dots \dots \dots (20b)$$

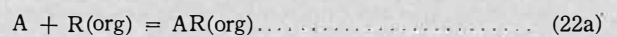
For the equivalence of a single stage and the second counter-current stage one obtains the following equations for θ_{eff} , one when considering component A and one when considering component B.

$$(\theta_{eff})_A = \frac{f([A]_1, [B]_1) - f([A]_0, [B]_0)}{f([A]_1, [B]_1) - [\bar{A}]_0} \dots \dots \dots (21a)$$

$$(\theta_{eff})_B = \frac{g([A]_1, [B]_1) - g([A]_0, [B]_0)}{g([A]_1, [B]_1) - [\bar{B}]_0} \dots \dots \dots (21b)$$

As f and g normally represent different functions, both θ_{eff} values can not always be the same and thus we can not in this case emulate the counter-current battery with the AKUFVE. It is important to find the conditions when f and g are both dependent on A and B simultaneously as this normally represents a case where the full equilibrium surfaces have to be determined.

The simplest case is when A and B both compete for the same reagent according to the following reactions.



with the equilibrium constants k_A and k_B . The material balance for R gives,

$$C_R = [\bar{R}] + [\bar{AR}] + [\bar{BR}] \dots \dots \dots (23)$$

Combining eqns. 22a, 22b and 23 we obtain

$$[\bar{A}] = k_A[A](C_R - [\bar{A}] - [\bar{B}]) = f([A], [B]) \dots \dots \dots (29a)$$

$$[\bar{B}] = k_B[B](C_R - [\bar{A}] - [\bar{B}]) = g([A], [B]) \dots \dots \dots (29b)$$

It is evident from this example that the θ_{eff} method is invalid when appreciable loading of the organic phase occurs and more than one component is extracted.

This might occur quite often. Even when one of the components, or both, occurs in small concentrations in the feed, a bent shape of the extraction isotherm (equilibrium curve) can lead to internal circulation and hence to considerable loading effects in some of the stages.

Figure 15 shows an actual equilibrium curve, as observed in the AX-process, for the extraction of hydrofluoric acid with TBP in the presence of nitric acid. The apparent ambiguity in Figure 15 depends on the various amounts of nitric acid present. Figure 16 shows clearly the strong bending of the operating curve caused by the simultaneous extraction of nitric acid. The θ_{eff} method also gives bent operating curves, but these do not coincide with the real operating curve in contrast with the copper-LIX64N system discussed earlier.

Conclusions

For extraction systems with one extracted species, it is always possible to reduce the experimental work by using the θ_{eff} method shown in Figure 9. This also holds for such multicomponent systems where all aqueous concentrations can be expressed in terms of one of the component's concentration.

It is generally **not** possible to avoid a determination of the complete equilibrium surfaces in multicomponent systems for a given feed, except at negligible loading. Here the use of the AKUFVE technique helps to obtain all the data needed within a reasonable time and with the required precision.

Acknowledgment

This research was sponsored by the Swedish Atomic Research Council and by the Board of Technical Development. The author is indebted to Dr. S. Wingefors, Dr. S.O. Andersson and Professor J. Rydberg for many helpful discussions during the various phases of this work and to Dr. H. Reinhardt for supplying data on the Cu-LIX64N system.

NOTATION

A	= extractable species
A ⁻	= anion
a	= constant in eqn. 17
B	= extractable species
b	= constant in eqn. 17
C _R	= total extractant concentration in the organic phase, (moles/l)
F	= function defining the direction of the operating curve, (moles/l)
f	= distribution function defined by eqns 5 or 20a
g	= distribution function defined by eqn. 20b
k _A	= extraction constant for A
k _B	= extraction constant for B
k _{ex}	= extraction constant
k _{ex} [∞]	= extraction constant at infinite dilution of extractant
k _{ex} ^{1%}	= extraction constant at 1% LIX64N
M	= metal
M ^{r+}	= metal ion
m	= mean aggregation number of extractant
n	= stage number in counter-current extraction battery or phase replacements in eqns. 15a and b
org	= organic phase
P	= LIX64N concentration, (% v/v)
R	= organic extractant
x	= number of extractant aggregates per metal
z	= charge of metal ion
α	= volume fraction of a phase
φ _{LIX}	= volume fraction of LIX64N
θ	= phase flow ratio defined by eqn. 4 or phase volume ratio
θ _{eff}	= effective phase flow ratio
[x]	= concentration of x in the aqueous phase, (moles/l)
[x] _{feed}	= concentration of x in the aqueous feed, (moles/l)
[x]	= concentration of x in the organic phase, (moles/l)

REFERENCES

- (1) Rydberg, J., Acta Chem. Scand. 1969, 23, 647.
- (2) Andersson, C., Andersson, S.O., Liljenzin, J.O., Reinhardt, H. and Rydberg, J., Acta Chem. Scand. 1969, 23, 2781.
- (3) Liljenzin, J.O., Stary, J. and Rydberg, J., "Solvent Extraction Research", Wiley, N.Y. 1969, 21.
- (4) Cox, M. and Flett, D.S., Proc. Int. Solv. Extr. Conf., London 1971, 204.
- (5) Rydberg, J., Reinhardt, H., Lunden, B. and Haglund, P., AIME Symp. Hydrometallurgy, Chicago, 1973, 589.
- (6) Liljenzin, J.O., Reinhardt, H. and Rydberg, J., Sw. pat. no. 364187, U.K. pat. no. 1367988 etc.
- (7) Hughes, M.A., Andersson, S.O. and Forrest, C., Int. J. Mineral Processing 1975, 2, 267.
- (8) Liljenzin, J.O., Introducing lecture at 4. Int. symp. "Reinstoffe in Wissenschaft und Technik" Dresden 1975.
- (9) Rydberg, J., Reinhardt, H. and Liljenzin, J.O., Ion Exchange and Solvent Extraction 1973, 3, 111.
- (10) Reinhardt, H., personal communications.
- (11) Okuhara, D., Solvent extraction of Cu(II), Thesis, Univ. Waterloo, 1971.
- (12) Robinson, C.G. and Paynter, J.C., Proc. ISEC 71, Society of Chemical Industry, London 1971, 1416.
- (13) Hummelstedt, L., Tammi, T., Paatero, E., Andréén, H. and Karjaluoto, J., Proc. 4th Int. Congr. in Scand. on Chem., Eng., Part B, Copenhagen 1977, 123.

DISCUSSION

H. Pratt: To obtain equilibria for systems with two distributed components using the AKUFVE or similar methods, would it not be more economical in effort to recirculate the organic phase, and to pass fresh aqueous phase continuously through the apparatus in order to bring the organic phase to equilibrium with aqueous phase of predetermined composition?

O. Liljenzin: If you know beforehand what the aqueous composition will be, one way of obtaining the distribution data is the continuous recirculation of the organic phase. However, for a counter-current process, normally none of the aqueous phases in the stages have the same composition as the aqueous feed. In this case the experiment can only be done in the way you suggest when the result is already known.

G. Petrich: If I understand your lecture correctly, then you are saying that the distribution ratios measured in the AKUFVE equipment can be applied to other counter-current extractors. Would it not be essential for such a transfer of results to know the absolute values of phase volume ratios and other hydrodynamic parameters for the extractors under consideration?

A. Naylor: I am interested in the correlation of the data from the AKUFVE equipment to the continuous mixer-settler or column extraction conditions. Where extraction systems are dependent on diffusion as well as chemical reaction rate steps, how do you interpret the AKUFVE conditions to the physical parameters and changes in the counter-current full-scale equipment?

O. Liljenzin: Both questions are very nearly the same and I would like to answer them together as follows:

My paper deals with equilibrium conditions and it is well known that these are to be regarded as a limiting case for actual counter-current extractors. The deviations between equilibrium performance and actual performance shows to which extent the equipment is running under such conditions that kinetic effects are important, etc. It is also well known that phase volume ratios or flow-rates do not change the equilibrium distribution data in systems with one extractable component. One of my points in the paper was to stress that this is not necessarily so for systems with several extractable components.

Modelling a Fluid Ion Exchange System

C.G. Brown, J.C. Agarwal, N. Beecher, W.C. Henderson and G.L. Hubred
 Kennecott Copper Corporation, Lexington, Mass., U.S.A.

process model allows optimization of the organic circulation rate to minimize the ammonia co-extraction problem.

ABSTRACT

A fluid ion exchange, FIX, process has been developed for the recovery of copper and nickel from an ammoniacal-ammonium carbonate leach liquor of deep ocean nodules. The process includes a co-extraction of copper and nickel with 40 volume percent LIX64N at 40°C from the ammoniacal solution. A model of the extraction equilibrium process was developed in several steps. First, a model of the aqueous phase was created which calculates the solution pH and amine complex speciation, given the solution concentration of total ammonia, carbon dioxide, and metals. Concentrations of up to 10 g/l of each metal and total ammoniacal concentrations up to 120 g/l are considered. Then the interaction of the aqueous phase species with LIX64N was modelled. This step provided some insight into the extraction stoichiometry of amine complexes. A complicated interaction exists between the metals and ammonia. Evidence is presented of both a competition between metals and ammonia for the oxime reagent and for a nickel amine complex extraction where ammonia extraction is enhanced by nickel extraction. The equilibrium models are incorporated into a multiple-stage countercurrent process model. This overall model then allows a description of the sharp decrease of metals extraction with increasing ammonia strength in the pregnant liquor and has allowed substantial process optimization with respect to pregnant liquor concentrations and flow rates. Ammonia co-extraction with copper and nickel presents a processing problem in the metals stripping section of the FIX process. Therefore, ammonia extraction must be minimized and extracted ammonia must be scrubbed from the metal loaded organic prior to metal stripping. The

Introduction

AN AMMONIACAL-AMMONIUM CARBONATE LEACH of ocean manganese nodules has been developed by the Ledgemont Laboratory of Kennecott Copper Corporation. The process includes recovery of copper, nickel, cobalt, molybdenum and zinc⁽¹⁾. After leaching and liquid-solid separation, copper and nickel are co-extracted from the pregnant liquor using multistage countercurrent fluid ion exchange, FIX⁽²⁾, and using an oxime reagent LIX64N (Figure 1).

The multiple-stage FIX of even a single cation involves subtle complications not encountered with the diffusion of a single species between two phases. Therefore, graphical representation of the process is difficult or impossible. Other authors have discussed this problem in detail for acid-FIX systems^(3,4).

The problem is that in FIX at least two ions are being transferred in opposite directions, and their equilibrium cannot be represented on a two-dimensional graphical solution such as a McCabe-Thiele plot. The problem is compounded for multi-component extractions such as the present case of copper, nickel and ammonia co-extraction.

Multicomponent extraction from an ammoniacal solution demands a computerized mathematical model because of the higher order non-linear dependence of metal amine complexation upon the free ammonia in solution.

The dramatic effect of ammonia upon metal complexing and therefore upon metals extraction is a second reason for creating a model of the extraction system. The effect is stronger for nickel than for copper presumably because nickel is more highly coordinated by ammonia than is copper (Figure 2).

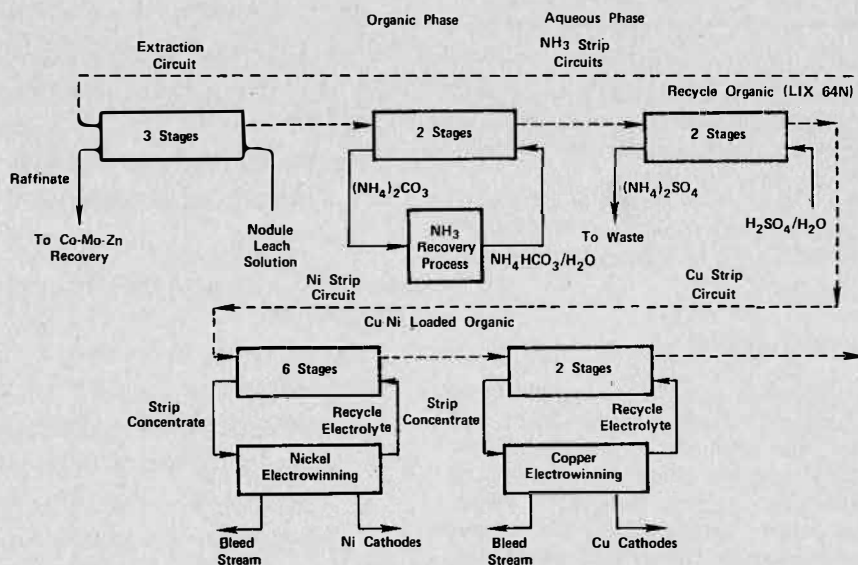


FIGURE 1. Schematic flow diagram of coextraction/selective stripping process.

Definition of the Problem and Approach

In order to narrow the problem, the following limitations were made.

All of the work was done with 40 volume percent LIX64N in Napoleum 470 kerosene at 40°C. LIX64N was the only suitable reagent available at the onset of this development and it was desired to make use of already measured equilibrium data. It is recognized that other suitable reagents, such as Shell SME 529 now exist⁽⁵⁾. In an ammoniacal system there is considerable incentive to use as high a reagent concentration as is compatible with settling characteristics, metal chelate solvency, and demonstrated use because there is no acid release problem comparable to that in extraction from acid solutions⁽⁶⁾. This is because the released hydrogen ion is immediately bound by free ammonia to form ammonium ion and does not inhibit the extraction. There was no difficulty with settling or metal chelate insolubility in 40% LIX solution at the 40°C operating temperature used in this system. If a different LIX concentration were used, it is expected that the model could be easily adapted. Napoleum 470 is a low aromatic-content kerosene of controlled purity with considerable history of successful application with LIX64N.

The modeling effort was limited to extraction from ammoniacal liquors because the conditions for copper and nickel stripping were limited by the respective electro-winning conditions to narrow ranges. Only the ammonium carbonate system has been studied, but the results of present work could easily be expanded to include ammonium sulfate solutions provided any metal sulfate complexing could be ignored.

The range of solution concentrations for which the model is known to converge is provided in Table 1. These should be sufficient to cover oxide ore leaching liquors.

TABLE 1. Range of Conditions to which Model Applies

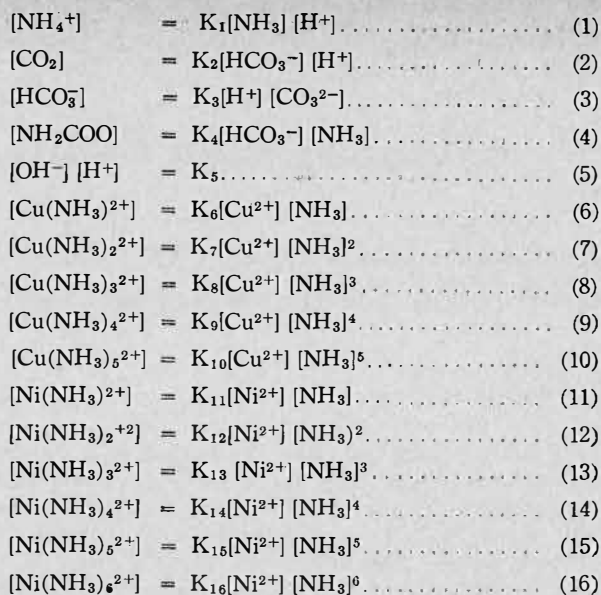
Ammonia	25 gpl — 140 gpl
Carbon dioxide	5 gpl — 40 gpl
Copper	1 ppm — 20 gpl
Nickel	1 ppm — 20 gpl
pH	8.5 — 11.5
Temperature	35°C — 45°C
Organic to aqueous flow ratio	0.05:1 — 20:1
Number of stages	1 — 10

The model was constructed on a theoretical foundation to allow some extrapolation beyond the range of data, Table I, used to fit the model. Empirical-fit constants were added to model deviations from the theory.

The model was developed in three steps: (1) simulation of aqueous phase equilibrium, (2) simulation of LIX64N — aqueous phase equilibrium, (3) simulation of multiple-stage countercurrent operation.

Aqueous Phase Equilibria

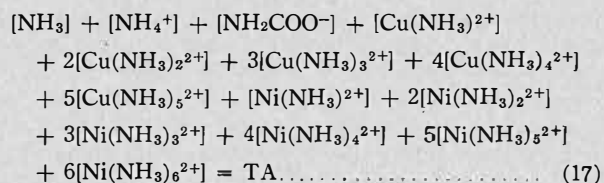
The first program developed models the equilibria in aqueous solutions of ammonia, ammonium carbonate, and copper and nickel ions. Free ammonia, average metal coordination numbers, hydrogen ion concentration and the concentrations of ammonium cation, carbamate, bicarbonate, and carbonate anions are predicted from input data on ammonia, carbon dioxide, copper and nickel concentrations and temperature and pressure. Equilibria considered were as follows:



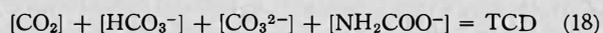
The equilibrium constants K_1 - K_{16} are known because values for these have been published in the literature⁽⁷⁻¹¹⁾.

In equations 1-16 there are 21 unknowns with 16 equations which means that the equations cannot yet be solved. Five further equations can be written from mass balance requirements, i.e., an ammonia balance, a carbon dioxide balance, a copper balance, a nickel balance, and an ionic balance.

Ammonia balance:

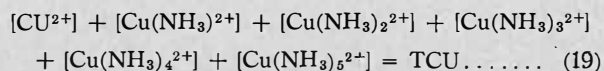


where TA is total ammonia concentration in moles/liter. Carbon dioxide balance:



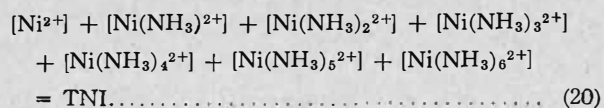
where TCD is total carbon dioxide concentration in moles/liter.

Copper balance:



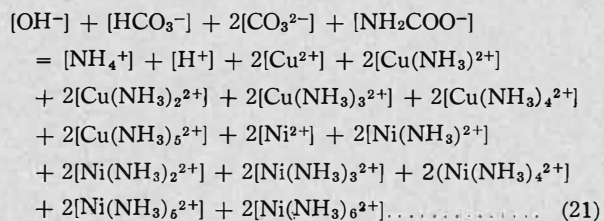
where TCU is total copper concentration in g. atom/liter.

Nickel balance:



where TNI is total nickel concentration in g. atom/liter.

Ionic balance:



The way in which these equations can be simplified for solution will now be described.

Simplifying Assumptions

To simplify this set of equations for solution, the following assumptions were made:

1. Concentrations were substituted for activities.
2. The concentrations of hydrogen and hydroxyl ions were neglected. This gives an immeasurably small error in the case of hydrogen ion because its concentration is so low in the pH range of interest, 8.5 to 11.5. With hydroxyl ion, the error is about 5% maximum at pH 11.5.
3. Dissolved, *un-ionized* carbon dioxide concentration was neglected. At pH 8.5, the error is about 0.6% and decreases rapidly at higher pH.

With these simplifications, the set of 21 equations can be solved by linear approximation procedures.

Equilibrium Constants

Equilibrium data were taken from the literature and a table of the values used in our computations is given in the Appendix.

Description of Equilibrium Program

The program has three parts:

1. Input — input data required are total ammonia, total carbon dioxide, total copper and total nickel. Zero values of copper or nickel are acceptable.
2. Iterative computation which solves the set of equations as discussed.
3. Output — prints the following items:
 - a. Average coordination number, copper and nickel,
 - b. Fractional distribution of amines, copper and nickel,
 - c. Percentage ammonia complexed by metal,
 - d. Distribution of ammonia, ammonium, amine, carbamate, carbonate, and bicarbonate species,
 - e. Predicted pH and $[H^+]$.

Prediction of pH

The prediction of pH, or more significantly, the prediction of aqueous hydrogen ion concentration is an essential step towards being able to calculate the extraction of copper and nickel by LIX64N. Unlike prediction of free ammonia, computations using mass balance and equilibrium equations lead to substantial differences between the calculated hydrogen ion concentration and the measured value obtained from pH determinations. The problem then arises as to which value should be used for hydrogen ion concentration in the prediction of copper and nickel extraction. The approach taken in the present work has been to use the hydrogen ion concentration (assuming an activity of 1 for hydrogen ion) obtained from experimental values of pH in developing the distribution correlations and correcting the calculated values from the program for the purposes of prediction.

A simple relationship between experimental values (HEXP) and calculated values (HCAL) was found:

$$HEXP = 0.3888 \times HCAL$$

The statistical T-value was high (70.95) indicating that HEXP and HCAL were highly correlated. This was supported by the correlation coefficient (95.1%) which was also very high. The standard error was $0.517 \times 10^{-10}M$ (the error in predicting HEXP would be $\pm 7\%$ of the average of the range covered by the data at the 95% confidence level).

The reason for the existence of a relationship between experimentally determined hydrogen ion concentration and calculated hydrogen ion concentration is not clear,

TABLE 2. Measured pH Versus Predicted pH in Ammonia-Ammonium Carbonate Solutions Containing Copper and Nickel

Total Ammonia (g/l)	Total Carbon Dioxide (g/l)	Nickel (g/l)	Copper (g/l)	Predicted Free Ammonia (g/l)	Predicted pH (at 40°C)	Measured pH (at 40°C)
121.0	23.5	—	0.00171	103.5	10.26	10.40
128.0	23.0	—	15.0	101.3	10.93	10.97
39.1	21.5	—	0.00066	24.4	9.63	9.59
39.9	22.1	—	9.65	19.7	9.93	9.77
126.0	35.6	—	5.97	95.7	10.16	10.35
127.0	10.4	—	5.95	115.4	11.11	11.21
61.9	10.1	—	6.01	51.0	10.80	10.58
117.0	21.3	1.95	—	99.0	10.35	10.45
118.0	17.9	10.7	—	92.9	10.96	11.01
28.7	21.4	1.96	—	13.4	9.48	9.36
93.0	33.5	5.69	—	62.4	10.02	10.17
111.0	20.1	2.93	8.99	87.2	10.83	10.87
28.1	19.8	2.97	9.09	8.70	9.93	9.62
118.0	18.6	8.93	2.99	92.5	11.00	11.09

but it appears to hold over a range of conditions (pH:9-11, CO₂: 7-60 gpl, NH₃: 30-120 gpl). This relationship was used to translate the calculated values of hydrogen ion concentration into a predicted measured value.

Comparison between predicted and experimental pH values (Table 2) shows an error somewhat higher than desired. However, virtually all of this error (0.1-0.15) pH units) is attributable to error in chemical analysis of the various ions affecting pH.

The ability to predict free ammonia and hydrogen ion concentration and other parameters such as average coordination numbers for copper and nickel, ammonium ion concentration and carbamate, bicarbonate and carbonate concentrations has enabled distribution expressions to be derived which describe the extraction of copper and nickel by LIX64N in kerosene. These are described below. These distribution expressions together with ANALAQ.F4 form the basis of two computer design models which describe single-stage and multistage extraction of copper and nickel from ammonia-ammonium carbonate solution by LIX64N in kerosene.

LIX-Aqueous Phase Equilibria

Measurement of Distribution Coefficients

Distribution coefficients were measured by shake-up in jacketed separatory funnels at an organic to aqueous phase ratio of 1:1 at 40°C. The range of components of the aqueous solutions were:

Total ammonia.....	30-130 gpl
Carbon dioxide.....	7- 36 gpl
Copper.....	1- 20 gpl
Nickel.....	2- 15 gpl

Analysis of Data

Expressions were then derived by linear regression techniques for the dependence of nickel, copper and ammonia extraction upon the major variables, e.g., free ammonia, metal coordination number, hydrogen ion concentration; and concentration of free LIX64N.

The following expressions were developed:

$$D_{Cu} = x_1 \cdot \left(\frac{[RH]^2}{[NH_3]^n [H]^2} \right)^{1.13}$$

$$D_{Ni} = y_1 \cdot \frac{[RH]^{2.1}}{[NH_3]^n [H]^2} + y_2 \cdot \frac{[RH]^{2.1} [NH_3]^2}{[NH_3]^n [H]^2}$$

$$\overline{[NH_3]} = z_1 + z_2 \cdot \overline{[RH]} [NH_3] + z_3 \cdot \frac{\overline{[Ni]} \cdot [NH_3]^2}{1 + \overline{[NH_3]}}$$

where:

- $D_{Cu \text{ or } Ni}$ = distribution coefficient between organic and aqueous phase
 $\overline{[RH]}$ = Free LIX64N concentration, (m/l)
 $\overline{[NH_3]}$ = Aqueous free ammonia concentration, (m/l)
 (NH_3) = Organic ammonia concentration, (m/l)
 $\overline{[Ni]}$ = Organic nickel concentration, (m/l)
 c = Average coordination number for copper
 n = Average coordination number for nickel
 $x(i), y(i), z(i)$ = Various empirical coefficients.

Expressions of this same form were developed on the basis of chemical theory and, thus, confirmed the empirically developed expressions. Predicted results were compared with experimental and average errors of $\pm 10-15\%$ were obtained with random distribution. (Table 3 presents examples) This was deemed acceptable in view of the large number of chemical analyses involved in the experimental results and the resulting error in these values.

Multistage Model

The LIX-aqueous phase equilibria are incorporated into the multistage countercurrent contact model, aqueous feed to stage 1, recycled solvent to stage N, as follows:

1. The total quantities of copper, nickel and ammonia in stage 1 (required for mass balance calculation) are calculated from aqueous feed to stage 1 and the organic stream from stage 2. (The contribution from the organic stream is initially zero.)
2. The equilibrium concentrations of the streams leaving stage 1 are calculated.
3. The total quantities of copper, nickel and ammonia in stage 2 are calculated from the composition of the aqueous stream leaving stage 1 and the organic stream from stage 3.
4. The equilibrium concentrations of the streams leaving stage 2 are calculated.
5. Steps 3 and 4 are repeated for stages 3 to N-1 where N is the number of stages.
6. The total quantities of copper, nickel and ammonia in the final stage (stage N) are calculated from the composition of the aqueous stream leaving stage N-1 and the composition of recycled solvent.
7. The compositions of aqueous and organic streams leaving stage N are calculated.
8. The concentrations of ammonia in the organic extract leaving stage 1 and the aqueous raffinate leaving stage N are tested for convergence. Steps 1 to 8 are repeated until convergence is achieved.

The procedure described above is approximately equivalent to feeding nodule process liquors to a liquid ion exchange plant filled initially with just water and recycled solvent. The plant achieves steady state as the solutes are carried into the plant. The logic executed by the computer as it proceeds through steps 1-8 effectively carries out an integration to achieve the steady-state condition. The greater the number of stages, the greater the number of iterations required. In the current version of the program, N, the maximum number of stages, is set at 10.

Application of the Model Flowsheet Optimization

The greatest practical value of the model has been to allow optimization of the processing circuit with respect to the total ammonia concentration. The concentration of free ammonia has a dramatic effect on the equilibrium of copper and even more on the loading of nickel, as is apparent from the form of equilibrium equation as shown in Figure 2 for nickel. In general, the lower the amount of free ammonia in the pregnant liquor, the better the loading of the two metals. In the leaching portion of the process, higher ammonia has a beneficial effect. Therefore, an economic trade-off is established to determine the optimum ammonia level for leaching, and the amount of ammonia which must be stripped from the pregnant liquor prior to the FIX plant. The model is now used as a routine tool in the design of FIX plants⁽⁶⁾.

Crowding

One aspect of the optimization procedure facilitated by the model is the minimization of the organic circulation rate. In the nodule FIX system all of the steps except extraction are proportional in size to the organic circulation. Therefore, capital costs, as well as organic inventory costs can be decreased by minimizing this rate. Ammonia extraction is decreased by minimizing this rate also because the available organic will be used by copper and then nickel so that extracted ammonia is crowded off. As the organic circulation is decreased, the extraction of nickel is decreased slightly but this may be significant. Residual nickel in the raffinate sharply decreases the cobalt to nickel ratio in this stream and may necessitate a nickel removal step in the cobalt recovery process.

Sensitivity to Flow Rate

LIX64N is extremely efficient at extracting copper and nickel from even dilute ammoniacal solution so that there is little loss of metal recovery if the pregnant liquor is made more dilute. The size of the extraction equipment is proportional to the pregnant liquor flow rate and the rest of the FIX system is sized by the organic circulation. The stripping steps of ammonia, nickel and copper require

TABLE 3. Comparison of Predicted Data and Actual Copper and Nickel Coextraction Data.

Exp. #	(Experimental Data are in Parentheses)			Aqueous Phase			pH
	Copper (g/l)	Organic Phase Nickel (g/l)	Ammonia (g/l)	Copper (g/l)	Nickel (g/l)	Ammonia (g/l)	
8-1	7.36 (7.09)	3.05 (2.42)	1.16 (1.41)	0.28 (0.15)	6.06 (6.48)	96.6 (93.7)	9.51
1-3	0.51 (0.51)	0.61 (0.59)	1.58 (1.74)	0.00016 (0.0003)	0.0079 (0.0097)	78.8 (67.4)	9.26
15-1	11.9 (11.7)	0.41 (0.21)	0.59 (0.53)	7.05 (6.98)	9.08 (9.04)	96.6 (93.2)	9.57
25-1	10.9 (11.0)	0.41 (0.73)	0.59 (0.68)	2.22 (0.191)	8.61 (8.81)	96.2 (95.0)	9.54
24-1	2.54 (2.43)	2.85 (2.75)	1.83 (2.67)	0.0077 (0.0074)	0.55 (0.45)	91.1 (88.9)	9.46

TABLE 4. Effect of Number of Stages on Percent Nickel Extraction

Pregnant Liquor (g/l); Ni = 10, NH ₃ = 70, CO ₂ = 25 Phase Ratio: 1.2	
Number of Stages	% Ni extraction
1	98.7%
2	99.9%
3	99.98%

TABLE 5. Effect of Phase Ratio on Crowding of Ammonia

Pregnant Liquor (g/l): NH ₃ = 100, CO ₂ = 50, Cu = 10, 2 stages					
Phase Ratio:	organic aqueous	vol.	% Copper extraction	% NH ₃ extraction	NH ₃ on Loaded organic g/l
.8			88%	.5%	.58
.9			97.5%	.5%	.60
1.0			99.95%	.8%	.78
1.1			99.98%	1 %	.97

nine stages so that the total FIX costs of the nodules process are much less sensitive to pregnant liquor dilution than would be the case for a simple copper extraction system. Therefore, there is an incentive to use more wash water in the liquid-solid separation, diluting the pregnant liquor and increasing metal recovery.

Examples of some of the uses of the model are presented in Tables 4, 5 and 6. In Table 4 the effect of increasing the number of stages for a given solution composition and phase ratio is shown. The effect of staging can be of considerable interest for the consideration of selective extraction from ammoniacal solutions separating copper and nickel. Table 5 shows the effect of phase ratio on ammonia loading during a copper extraction. Increases in phase ratio above 0.9 give some increase in copper extraction, but at a considerable penalty in increased ammonia extraction. Extracted ammonia must be scrubbed and recycled at considerable expense. The dramatic effect of ammonia on nickel extraction mentioned earlier is shown again in Table 6. Here it can be seen that nickel extraction can be raised from 91 to 99.9% by cutting the ammonia level from 100 gpl to 70 gpl for a 2-stage system.

REFERENCES

- (1) Agarwal, J.C. et al. "Kennecott process for recovery of copper, nickel, cobalt and molybdenum from ocean nodules". To be published.
- (2) Agarwal, J.C. et al, E/MJ, Dec. 1976, 74.
- (3) Robinson, C.G. and Paynter, J.C., "Optimization of the design of a counter current liquid - liquid extraction plant using LIX 64N", ISEC 1971, p. 1416.
- (4) Forest, C. and Hughes, M.A. "The modelling of equilibrium data for the liquid - liquid extraction of metals", Part I, (Part II) Hydrometallurgy, Vol. 1, No. 1, (2), p. 25, (139).
- (5) Van der Zeeuw, A.J. "Selective copper extractants of the 5-alkyl - 2 - hydroxyphenyl alkyl ketone oxime". I. Chem. E. Symp. Ser. No. 42.
- (6) Barner, H.E. et al. "Engineering parameters for solvent extraction processes". ISEC 1977.
- (7) Helgeson, H.C., J. Phys. Chem. 1967, 71 (10), 3121.

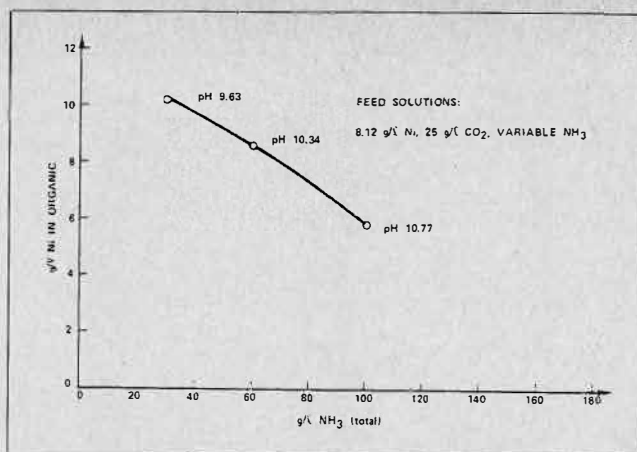


FIGURE 2. Effect of ammonia concentration in aqueous upon organic loading of nickel.

TABLE 6. Effect of Ammonia on Nickel Extraction

Pregnant Liquor (g/l): CO ₂ = 25, Ni = 10, 2 stages phase ratio 1.2	
Ammonia (g/l)	% Nickel extraction
100	91
90	95
80	97.5
70	99.9

- (8) "Stability Constants of Metal-Ion Complexes", Special Publication No. 17, The Chemical Society, London, 1964.
- (9) "Stability Constants of Metal-Ion Complexes", Supplement No. 1, Special Publication No. 25, The Chemical Society, London, 1971.
- (10) Osseo-Asare, K.A. Dissertation, Univ. of California, 1974.
- (11) VanKrevelen, D.W. et al. Recueil 1949, 68, 191.

APPENDIX

Equilibrium Constant Data

The LIX process for nodule liquors is designed to operate at 40°C and thus it is necessary to have values of stability constants for that temperature. Fortunately, fairly reliable data are available from the literature for most of the equilibrium reactions considered in the present work.

The equilibrium constants for the dissociation of ammonium hydroxide, bicarbonate and water at 40°C according to Helgeson⁽⁷⁾ are provided in Table A-1. Data on the stability constants of copper amines (K₆-K₁₀) and nickel amines (K₁₁-K₁₆) are less satisfactory because no determinations of these stability constants have been measured at this temperature. Complete sets measured at room temperature are available. However, the variation of the stability constants with temperature has been estimated at 10 using a method based on a model developed by Helgeson⁽⁷⁾. The stability constants (based on zero ionic strength) decrease with temperature. The stability constants at 40°C used in the equilibrium program are provided in Table A-1.

Automatic Control of a Multiple-Mixer Solvent Extraction Column

W.L. Wilkinson and C.R. McDonald,
Schools of Chemical Engineering,
University of Bradford, U.K.

ABSTRACT

A theoretical model of a multiple-mixer column has been used to investigate a number of possible control strategies designed to maintain the raffinate concentration constant, in spite of concentration disturbances in the feed concentration, by regulating the feed flow rate. These have included simple feedback control, feedforward control and combinations of the two. The work has shown that single loop control is not ideal, and that the combination of feedforward and feedback control is to be preferred. The theoretical predictions have been compared with the results of experiments on a pilot plant column using the system nitric acid/water/TBP, and the agreement is satisfactory.

Introduction

THE APPLICATION OF SOLVENT EXTRACTION as a method of separation is increasing rapidly in the process industries, notably for the purification of metals. However, whereas the steady-state design of solvent extraction contactors has received considerable attention for many years, little attention has been given to their behaviour under transient conditions or to the design of suitable control systems. In some cases this is now becoming an important problem and interest in the dynamic characteristics and control of solvent extraction processes is increasing. Industrial solvent extraction contactors vary greatly in both type and size but two main categories can be identified, namely mixer-settlers and columns. The mean residence time for the two phases in column plants is usually very much less than that in mixer-settlers, which have comparatively large hold-ups in both the mixing and settling compartments. Columns, therefore, show a faster response to load changes and disturbances than do mixer-settlers and the control problems for the two types of plant are different.

The theoretical models which have been developed to describe the dynamic characteristics of solvent extraction processes can be divided into those dealing with differential processes such as pulsed, packed or spray columns, and those dealing with stage-wise processes such as mixer-settlers or multiple-mixer columns. A review of previous work in this field is presented elsewhere⁽¹⁾.

This paper is concerned with a study of the control of a stage-wise process, viz., a multiple-mixer column as shown in Figure 1. The work is based on previous studies on this type of column which have included the development of a mathematical model for the prediction of the open-loop response to concentration and flow rate disturbances^(2,3) and also a theoretical study of the behaviour of a feedback control system⁽⁴⁾. In this work these control studies are extended to include feedforward as well as feedback control. The theoretical predictions are compared with the results of an experimental programme on a 23-stage column, 15 cm in diameter, using the system nitric acid/water/TBP.

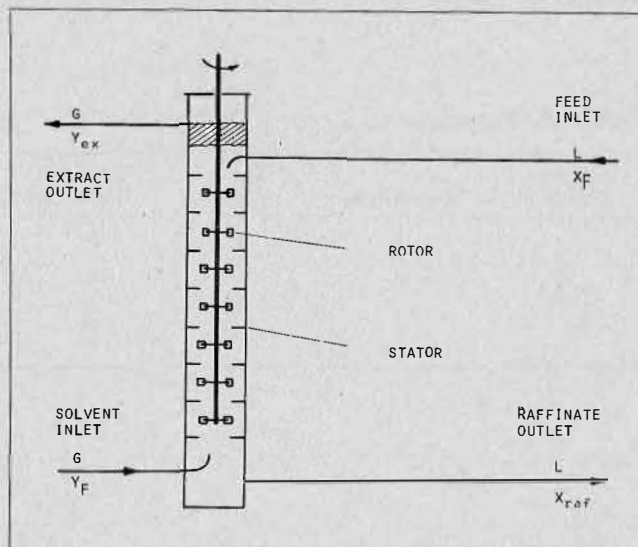


FIGURE 1. Diagram of the multiple mixer column.

Review of Control Strategies

The application of automatic control to a process normally has increased operational efficiency as its primary objective (although safety considerations could also be important). In the case of solvent extraction plants the efficiency is usually defined in terms of fixed exit streams.

The common situation involves the extraction of a component from an aqueous stream by an organic solvent. The criterion for satisfactory operation could then be defined in terms of a maximum raffinate concentration, above which the process would be uneconomic. Alternatively, it could be necessary to maintain the extract concentration above some minimum value in order to reduce subsequent stripping costs or to improve the product purity. In some cases it may be necessary to satisfy both of these criteria simultaneously.

The main disturbances which affect solvent extraction processes are variations in feed flows and concentrations. Consider a multiple-mixer column for the extraction of nitric acid from an aqueous solution by 30% TBP in kerosene. For a given set of experimental conditions the open-loop raffinate concentration responses to step changes, sufficient to cause an increase in raffinate concentration of 10%, have been calculated using the model considered later in this paper and are shown in Figure 2. The response to a change in the feed concentration, x_F , is seen to be delayed by about 1000 seconds which is the time taken for the disturbance to be transmitted through the column to the raffinate end. As a result, the raffinate response to x_F is the slowest and the most difficult to control. The responses to disturbances in the flow rates, L and G , begin immediately and are almost identical to each other. The response to a disturbance in y_F is the fastest one would expect.

Similar profiles could be derived for the responses of the extract concentration y_{ex} . In this case the shape of the profiles due to disturbances in x_F and y_F would be interchanged. The response to flow-rate changes would be much the same as for x_{raf} .

The various possible control parameters are indicated in Table 1.

An inlet flow rate is normally chosen as the control action and the aqueous feed is usually preferred. This is because the extract rate, which forms the feed to down-

stream operations, is then constant while the raffinate can often be discharged as an effluent stream.

There are many possible combinations of control objective, disturbance and measured variable. In this work, by way of example, it was decided to select the raffinate concentration, x_{raf} , as the controlled variable which has to be maintained at its desired value in spite of disturbances in the feed concentration, x_F , by regulating the feed flow rate, L . However, the model used in this work is flexible and other controlled variables, control actions and disturbances could equally well be studied, although the one investigated here is perhaps the most important.

The most straightforward approach would be to use a single feedback loop with the raffinate concentration, x_{raf} , itself as the measured variable, as illustrated in Figure 3, and employing the feed rate L as the control action. With proportional control, an error in x_{raf} due to any disturbance, in particular to changes in feed concentration, x_F , could be reduced and with integral action it could be eliminated in principle.

It could be argued, however, that the response of such a system would be slow and unsatisfactory since a disturbance in x_F would have to be transmitted through the whole column before an error in x_{raf} could be detected and the concentration profile would be disturbed everywhere before any corrective action could be applied. One method of overcoming this is to locate the measuring element at some point within the column, as in Figure 4, which would reduce the lag between the point of introduction of the disturbance and the measuring element. However, with this type of control, errors in x_{raf} would inevitably persist and this type of control has been considered previously⁽⁴⁾.

In order to correct for these errors a secondary feedback controller could be introduced as in Figure 5. In the extreme case, the primary control loop would incorporate the measuring element in the feed stream itself as in Figure 6 and a disturbance in x_F would then be detected before it entered the column and the appropriate compensation in the feed rate L could then be made. This is feedforward control. Intermediate cases, with the primary measuring element positioned within the column, would involve elements of both feedback and feedforward control. The nearer the control point is to the top of the column (where the disturbance enters in this case) the faster the response but the greater is the potential error in x_{raf} unless the secondary feedback loop is incorporated.

TABLE 1. Response to Control Parameters

Control Objectives	Disturbances	Control Actions	Measured Variables
x_{raf} y_{ex}	x_F	L	x_F
	y_F	G	x_n
	L		x_{raf}
	G		y_F y_{ex}

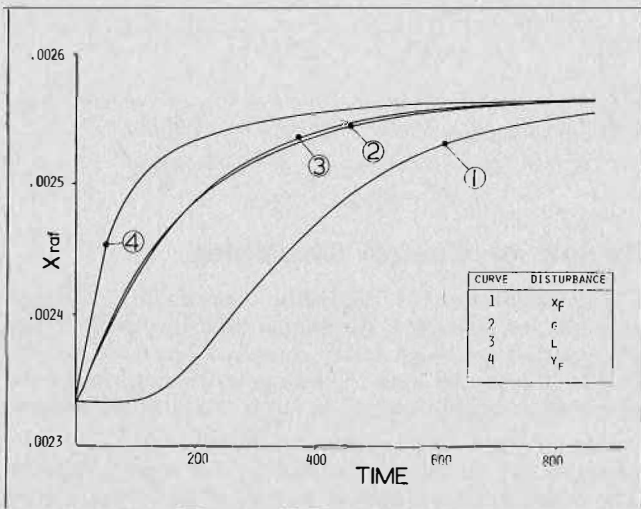


FIGURE 2. Raffinate responses to step changes in L , G , y_F and x_F .

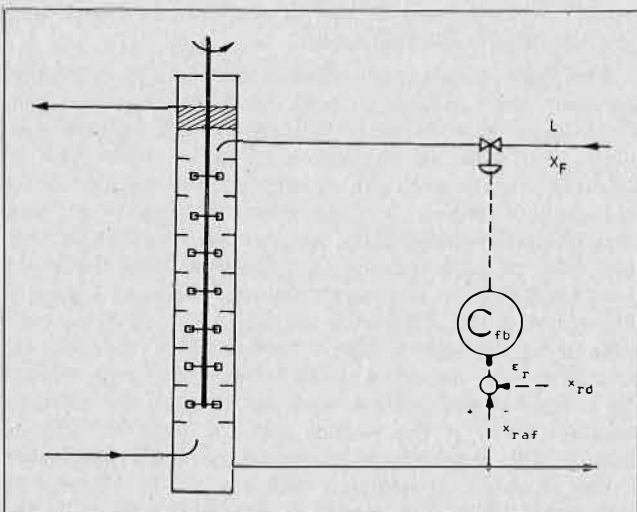


FIGURE 3. Simple feedback control system.

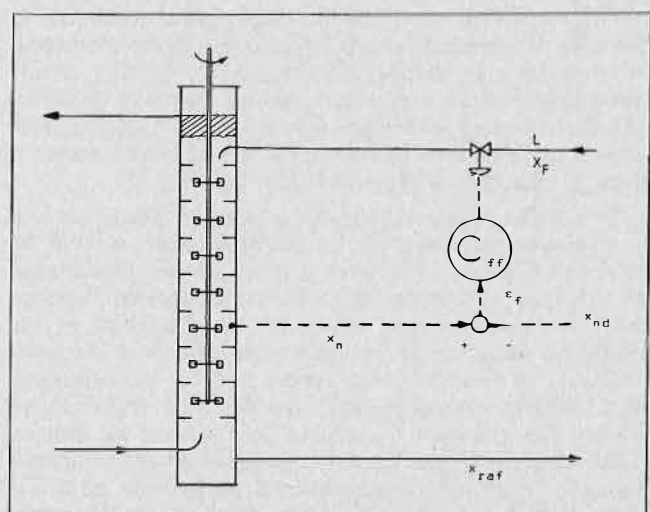


FIGURE 4. Quasi-feedforward control system.

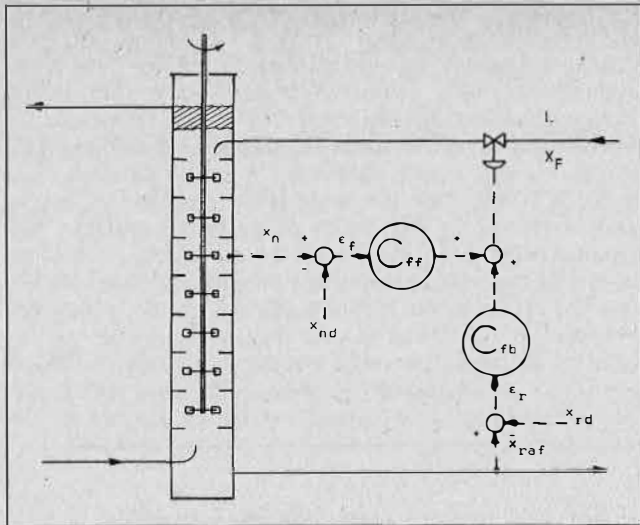


FIGURE 5. Feedback/feedforward control system 1.

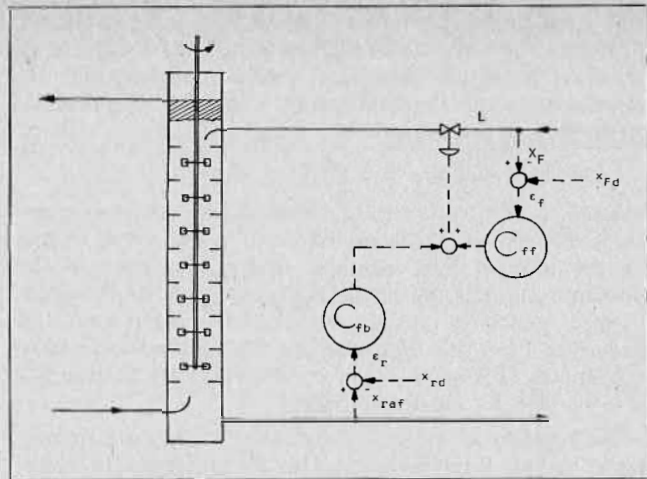


FIGURE 6. Feedback/feedforward control system 2.

In this work all the control systems discussed above have been studied theoretically and, in addition, the simple feedback system (Figure 3) and the feedback/feedforward system (Figure 6) have been investigated experimentally.

The Mathematical Model

The model to be used here is essentially that which was derived previously^(2,3) for open-loop studies on a multiple-mixer column. It allows for backmixing in both phases by the inclusion of backmixing factors and the stages are not assumed to be at equilibrium. It is assumed that a single solute is being transferred and the rate of transfer per unit interfacial area in a typical stage n is given by

$$Q_n = k (x_n - x_n^*), \dots \dots \dots (1)$$

where k is the mass transfer coefficient and x_n^* is the concentration of solute in the heavy phase which would be in equilibrium with the local light phase concentration, y_n . These are assumed to be related by a linear equilibrium relationship of the form,

$$y_n = mx_n^* + b \dots \dots \dots (2)$$

The stages are assumed to be perfectly mixed and hydraulic lags are neglected. The model is illustrated in Figure 7.

A solute balance on the heavy phase around stage n gives

$$L(1 + e_L)x_{n-1} - L(1 + 2e_L)x_n + L e_L x_{n+1} - Q_n aH = Hh_L \frac{dx_n}{dt}, \dots \dots \dots (3)$$

where a is the interfacial area per unit volume and H is the height of a stage.

Likewise, a solute balance on the organic phase around stage n gives

$$G(1 + e_L)y_{n+1} - G(1 + 2e_G)y_n + G e_G y_{n-1} + Q_n aH = Hh_g \frac{dy_n}{dt} \dots \dots \dots (4)$$

Suitable boundary conditions can be similarly derived by assuming that there is negligible mass transfer in the end sections of the column and these have been discussed in detail elsewhere^(2,3).

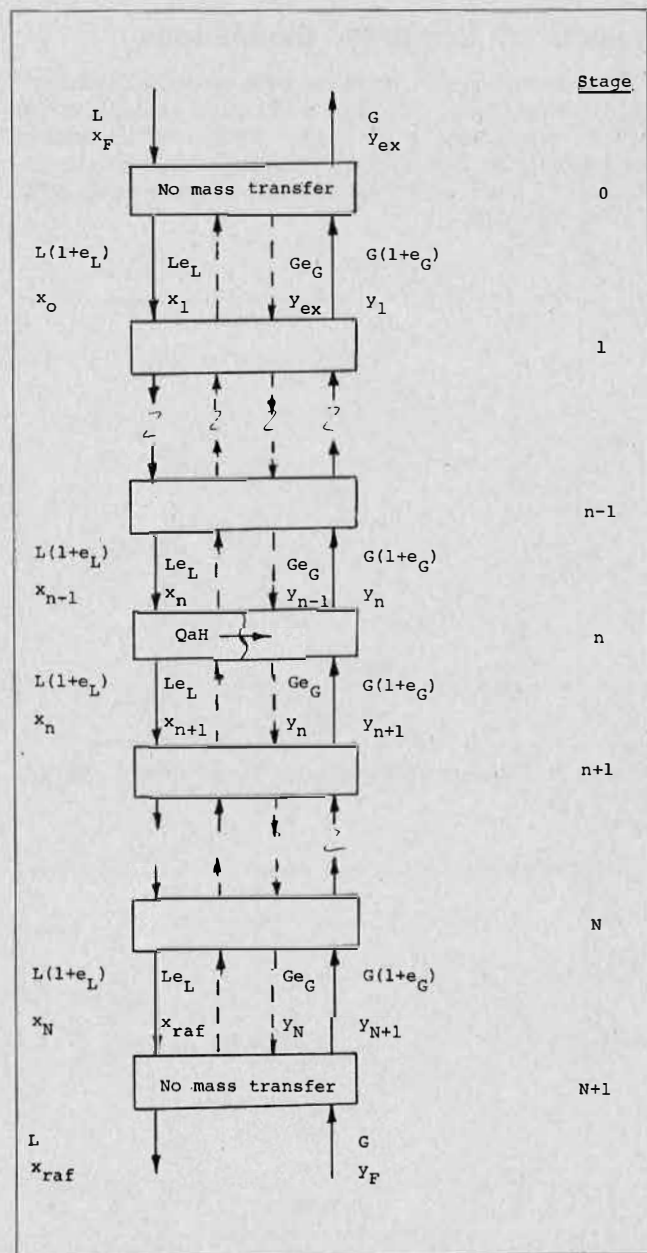


FIGURE 7. Basis for the mathematical model.

The mathematical representation of the most general feedback/feedforward control system shown in Figure 5, when the feedback controller has proportional plus integral actions and the feedforward controller proportional action only, is as follows,

$$L = L_o + K_{pr} \epsilon_r + K_{ir} \int \epsilon_r dt + K_{pf} \epsilon_f, \dots \dots \dots (5)$$

where L is the feed rate, L_o the feed rate for zero error, K_{pr} is the gain of the feedback loop, ϵ_r the error in x_{raf} , K_{ir} the integral term constant, and ϵ_f the error in the measured variable, x_n or x_f . K_{pf} is the gain of the feedforward controller. All the other control algorithms can be derived from this. For example, the simple feedforward loop shown in Figure 3 can be described by putting $K_{pr} = 0$. x_{nd} and x_{rd} are desired values.

The solution of the model has been carried out numerically in the time domain. This is preferred to semi-analytical solutions which rely on linearisation. A number of methods of solution were investigated and the linear multi-step methods, notably that of Gear, were found to be preferable to the explicit Runge-Kutta methods. Details of the solution procedure are to be found elsewhere^(1,4).

Results of Computer Simulations

The various control strategies were investigated theoretically using input data for a 23-stage multiple-mixed column which were in the range which could be realised subsequently in the experimental programme on the extraction of nitric acid from aqueous solution using 30% TBP in kerosene.

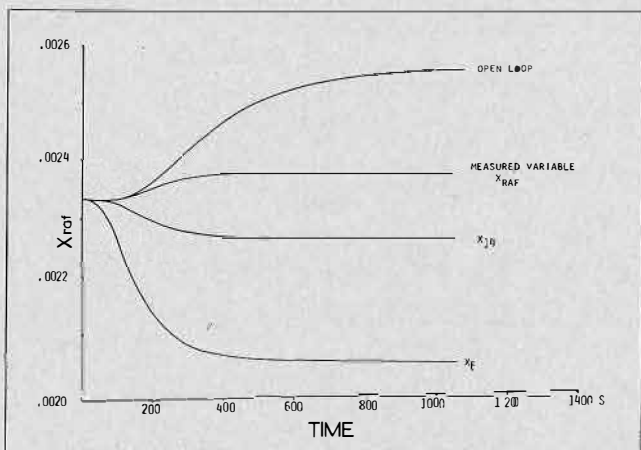


FIGURE 8. Raffinate responses for single loop P control; gain = 10.

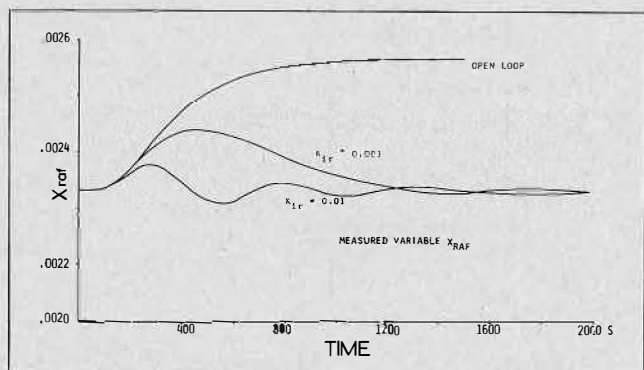


FIGURE 9. Raffinate responses for P + I feedback control; gain = 1.0.

Single-loop Proportional-Only Control

Some results are shown in Figure 8 for the single-loop proportional - only control corresponding to the control systems illustrated in Figures 3 and 4. The responses to step changes in x_f for different measured variables, viz., x_{raf} , x_{14} , x_6 and x_f are shown for a controller gain, K_{pr} , of 10. It is seen that the form of the response of x_{raf} is greatly affected by the choice of measured variable, the response being faster the nearer the measuring point is to the top of the column where the disturbance enters. However, the off-set is also affected and can in fact be positive or negative. The off-set is also greatly dependent on the value of the controller gain and by a suitable choice of gain it can be eliminated for measuring points within the column. However, this particular value of the gain would be difficult to predict accurately for a given situation.

Feedback Loop with Proportional and Integral Control

The response of raffinate concentration where x_{raf} is itself the measured variable, as illustrated in Figure 3, is shown in Figure 9 for $K_{pr} = 1$ for two values of K_{ir} , the higher one causing an oscillatory response. Integral action eliminates off-set in x_{raf} .

Feedforward/feedback Control

The performance of the feedforward/feedback control system illustrated in Figure 6 is shown in Figure 10 for a feedback gain, K_{pr} , of 1 and a range of values of the feedforward gain, K_{pf} . The beneficial effects of the feedback loop are apparent. If K_{pf} is well chosen, the off-set and the integral square error will be smaller and equilibrium conditions attained faster. This is shown quantitatively in Table 2.

The off-set and the integral square error are both reduced significantly by increasing the feedback gain, K_{pr} , for a given value of the feedforward gain, K_{pf} . This shows the value of the feedback loop when the feedforward gain is not correctly chosen to eliminate off-set.

Feedforward Control

The object of feedforward control is to allow a control action to be taken immediately following the detec-

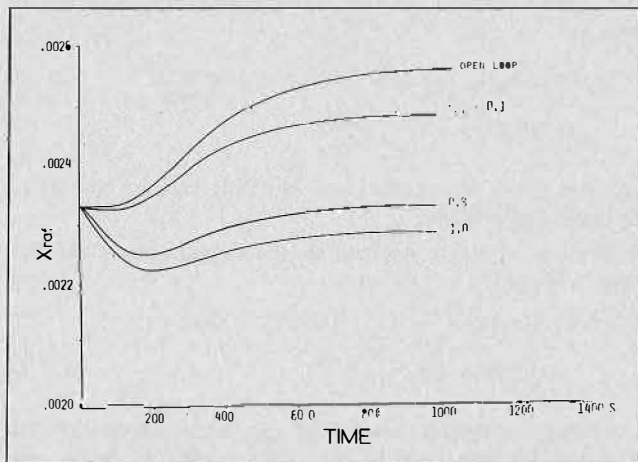


FIGURE 10. Raffinate responses for feedback/feedforward control; $K_{pr} = 1.0$.

TABLE 2. Effect of Choice of Feedforward/Feedback Values

K_{pr}	K_{pf}	Off-set conc. (g/g) $\times 10^3$	Integral square error ($\times 10^3$)
0	0	2.33	15.73
1	0	1.70	7.31
1	1	-0.44	1.00
10	0	0.48	0.44
10	1	-0.13	0.23

tion of the disturbance. If an adequate dynamic model is available it can be used to calculate the necessary control action to nullify the effects of the disturbance, the computer acting as the controller. If only a steady-state model is available, this can be used to calculate the magnitude of the corrective action, which is then immediately applied with no dynamic compensation. This form of control is termed steady-state feedforward compensation.

Ideally, for computer-aided control of this nature, all the disturbances should be monitored but only feed concentration disturbances have been considered here.

Some typical results are shown in Figure 11 for steady-state feedforward compensation alone and in conjunction with a subsidiary control loop based on a measured value of x_n at stage 14. Without the subsidiary loop there is the typical initial downward response of control schemes which act prematurely. The addition of proportional action in the subsidiary loop improves control but integral action can lead to undesirable oscillations.

Comparison of the Various Control Systems

From the results of the simulations it has been concluded that control loops based on x_{raf} as the measured variable are to be preferred for solvent extraction columns if the objective is to maintain x_{raf} constant following disturbances in the feed concentration. If the measuring point is moved up the column to allow the disturbance to be detected sooner, this only results in a premature application of the control action, in this case the feed flow rate, L.

The best control system for the process investigated here is therefore the feedforward/feedback arrangement shown in Figures 5 and 6. Steady-state feedforward compensation together with a subsidiary loop can also be satisfactory and for some applications the added complexity may well be justified.

Experimental Investigation

The equipment and techniques used in the experimental investigation have been described elsewhere⁽¹⁾. Two columns were used with the system nitric acid/water/30% TBP in kerosene. The 23-stage multiple-mixer column was used for extraction of nitric acid into the TBP solvent and the control systems were applied to this column. The second column which was used for stripping was controlled manually. The concentration of nitric acid in the aqueous raffinate was measured by an in-line conductivity instrument.

The coefficients in the equations describing the model have to be determined before these can be solved and this involves the estimation of the backmixing coefficients, the hold-up terms in both the column and the end-sections,

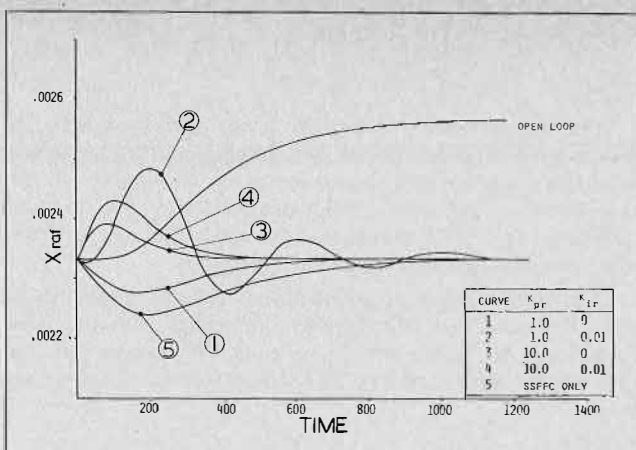


FIGURE 11. Steady state feed forward compensation with P + I control of Stage 14.

TABLE 3. Parameter Values for Experimental Transient Runs

Run	L	G	x_F	K_{pr}	K_{ir}	K_{pf}
1	0.18 → 0.12	0.14	0.066	0	0	0
2	0.12 → 0.18	0.14	0.066	0	0	0
3	0.067	0.16	0.094 → 0.055	1.0	0	0
4	0.067	0.16	0.094 → 0.055	0	0	0
5	0.067	0.16	0.094 → 0.055	1.0	0	0
6	0.067	0.16	0.094 → 0.055	2.5	0	0
7	0.067	0.16	0.094 → 0.055	1.0	0.0028	0
8	0.067	0.16	0.094 → 0.055	1.0	0.0024	0
9	0.067	0.16	0.094 → 0.055	0	0	0
10	0.067	0.16	0.094 → 0.055	1.0	0.0021	0
11	0.067	0.16	0.082 → 0.055	1.25	0	2.58
12	0.067	0.16	0.082 → 0.055	0	0	0
13	0.067	0.16	0.082 → 0.055	1.25	0	2.58
14	0.067	0.16	0.082 → 0.055	1.25	0	5.2
15	0.067	0.16	0.082 → 0.055	1.25	0	0

In Run 13 the control action was delayed by 1000 seconds.

and the product of the mass transfer coefficient and the interfacial area. The backmixing coefficients were found using the correlations presented by Ingham⁽⁵⁾ for a multiple-mixer column of the same geometry. The solvent hold-up in the column was found over a range of operating conditions by suddenly stopping the flow and measuring the increase in the solvent inventory. The value of the mass transfer coefficient was found by measuring the steady-state concentration profile in the column and then finding the value which gave the best fit between the predicted and measured profiles according to a minimum square error criterion.

Open-loop Results

The open-loop response of the controlled variable, x_{raf} , following step changes in the feed concentration, x_F , and feed flow rate, L, have been determined experimentally and these are compared with the corresponding theoretical predictions. Figure 12 shows the response of x_{raf} to downward and upward steps of equal magnitude in L. The agreement is reasonable but the experimental response is slower than that predicted because the hydrodynamic effects have been neglected. Figure 13 shows the response to step changes in x_F . The agreement is better than that for flow rate changes which is to be expected since the linearity assumption is now valid.

Closed-Loop Results

Single Feedback Loop

The system shown in Figure 3 was examined with proportional and proportional plus integral controller actions and the experimental results are given in Figure 14. The variation in the initial concentrations was due to slight changes in the TBP content of the solvent but nevertheless the results exhibit the expected behaviour.

The introduction of proportional control improves the raffinate response considerably compared with the open-loop case but some off-set remains. Increasing the gain, not shown here, reduces this off-set until instability sets

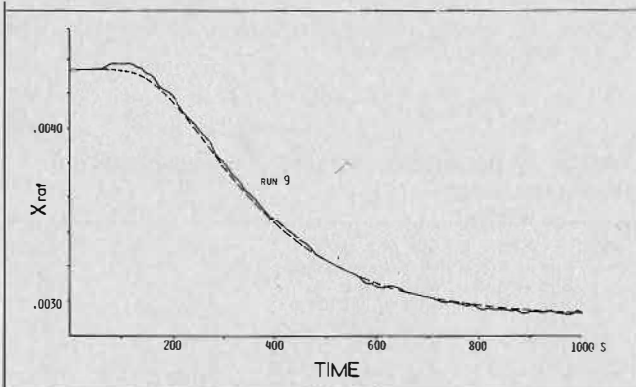


FIGURE 12. Open loop response to step changes in feed rate.

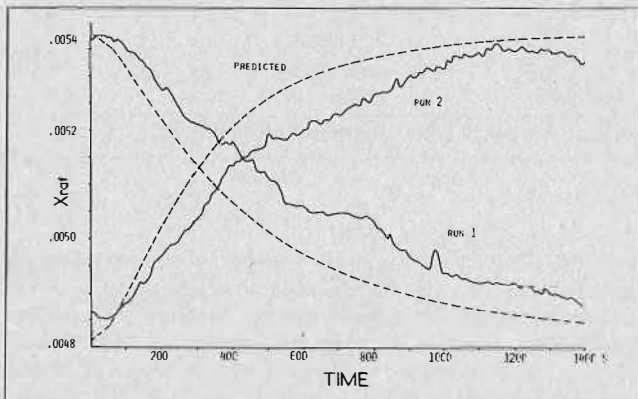


FIGURE 13. Open loop response to step change in feed concentration.

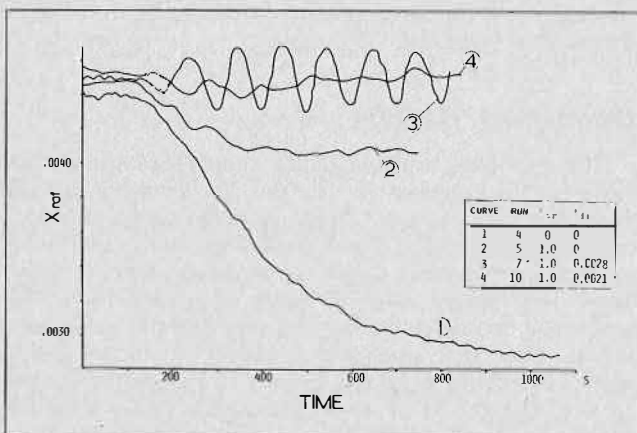


FIGURE 14. Results of P and P + I feedback control.

in. A small amount of integral action eliminates off-set as expected but the response becomes slightly less stable. Increasing integral action eventually worsens the control by causing oscillations.

Typical examples of comparisons between experimental and predicted responses are given in Figure 15 for proportional only control and also for proportional plus integral control. In the case of proportional control the time-delay and the approach to steady state is well predicted but the predicted off-set was somewhat lower than that found experimentally. With proportional plus integral control the zero off-set and the initial time delay are satisfactorily predicted but the oscillatory nature of the experimental response is not predicted as this is due to hydrodynamic factors which have been neglected in the model. However, this effect is of secondary significance and could be eliminated by a suitably designed interface level controller.

Feedback/Feedforward Control

Figure 16 shows the results of a sequence of tests comparing an open-loop response with the corresponding feedback only and feedback/feedforward controlled results. The addition of a feedforward component to the control scheme has the unexpected effect of increasing x_{raf} , at least initially. The response eventually peaks and the expected downward trend is introduced. For $K_{pt} = 2.6$ the response passes through an oscillatory period before settling down at a steady-state value very near to the zero off-set point. This is a fortuitous result, the size of the feedforward action being just sufficient to overcome the inherent off-set at this particular value of the feedback controller gain. For $K_{pt} = 5.2$, the peak is higher and the final steady state settles at a negative off-set value. The response is fully damped.

The reason for this behaviour lies in the difference in response times for L and x_F responses. The downward step in x_F is detected even before it enters the column and corrective action is applied immediately through a corresponding upward step in L , the size of which depends upon the feedforward controller gain. This upward step has the immediate effect of increasing x_{raf} and this continues until the effects of the step in x_F itself have had the time to pass down the column and into the raffinate stream. At this point the raffinate concentration begins to fall towards the final steady state, governed by the combined effects of the feedforward and feedback control actions. The severity of the control due to the feedforward element is sufficient to induce instability, as can be seen for $K_{pt} = 2.6$. The instability would have been more

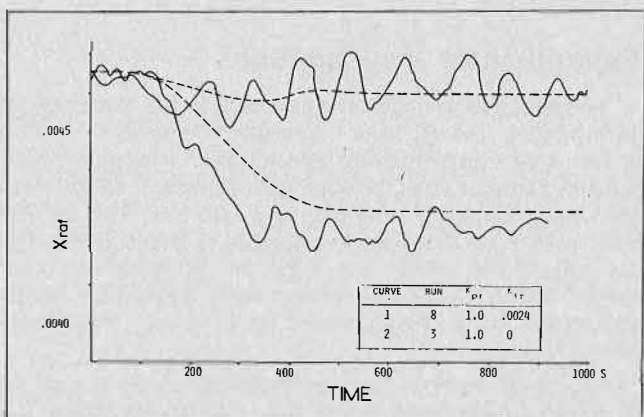


FIGURE 15. Comparison of experimental and predicted results for feedback control.

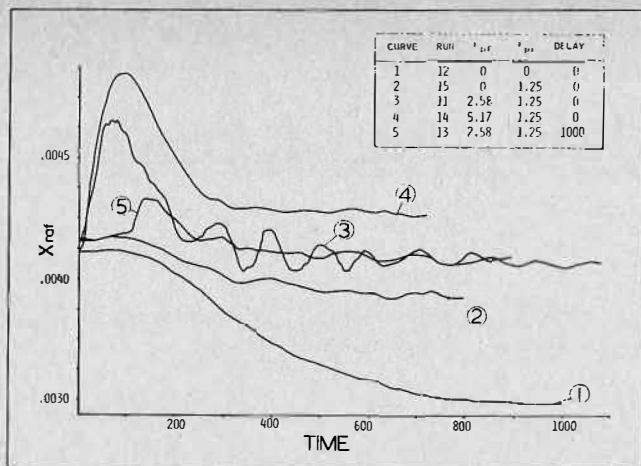


FIGURE 16. Results of open loop feedback and feedback/feedforward control.

marked for the higher value of K_{pf} had not the increase in L been sufficiently large to saturate the control system.

Since this unexpected behaviour is due to the feedforward control action being implemented before the disturbance has reached the raffinate stream, an experiment was carried out in which the feedforward element of the control was delayed for 1000 seconds, an approximation to the dead time associated with the disturbances in x_F . This run was carried out for $K_{pf} = 2.6$ and since the final value of L was the same as for the equivalent run without a delay, then the final values of x_{raf} were also identical. However, by delaying the implementation of the feedforward control, the magnitude of the peak was greatly reduced. Furthermore, by minimising the transient off-set in x_{raf} the oscillations caused to the corrective efforts of the feedback system can be avoided, giving a more stable overall response.

The simulation of the feedforward results was hampered by the inability to correctly simulate the raffinate response due to variations in L . Since, in this case, L varies in a step-wise manner, this effect is even more noticeable. Figure 17 shows a typical result. The failure to correct for the rapid increase in L following feedforward control action resulted in the high experimental peak value, while the difference in the final steady-state values is similar to that noted for feedback only control.

It can be seen from these results that, rather than preventing the development of erroneous intermediate concentration profiles during the early part of the run, the simple forms of feedforward control used here actually induces this behaviour. However, this form of control could be improved by suitable dynamic compensation.

Conclusions

Feedforward and feedback control schemes, as well as combinations of the two, have been investigated for the control of solvent extraction columns.

In the case of pure feedforward control, the application of the control action, L , occurs simultaneously with the detection of the disturbance in x_F . Due to the speed of the response of the controlled variable, x_{raf} , to the control action, feedforward control in this case causes an immediate change in x_{raf} . This undesirable transient is only counteracted when the effect of the original disturbance in x_F is ultimately felt at the raffinate outlet end of the column.

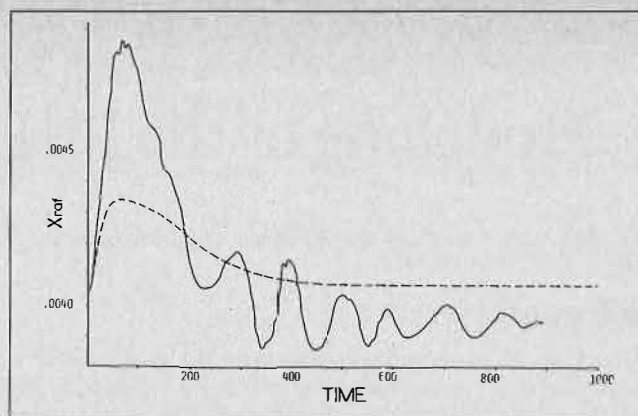


FIGURE 17. Comparison of experimental and predicted results for feedback/feedforward control (Run 11).

A time delay in the feedforward loop, which is a simple form of dynamic compensation, improves the control considerably and this could be optimised if necessary. Partial feedforward control, in which the time delay is effectively achieved by the transit time of the disturbance down the column, achieves a similar result.

With feedback control, changes in the control action, L , occur only as a result of errors in x_{raf} but, due to the speed of the response to the control action, the error in x_{raf} can be rapidly eliminated. This is the preferred control system for the column. A further advantage of feedback control in this system is that, due to the relatively slow rate of application of the control action, undesirable hydrodynamic effects are not excited.

Although this work has been concerned with a multiple-mixer column it is suggested that the conclusions will be relevant to other solvent extraction columns, in particular to pulsed columns, in so far as the results will be qualitatively similar.

NOTATIONS

- a = specific interfacial area
- b = intercept of linear equilibrium relationship, Equation 2.
- e_G = backmixing coefficient in G phase
- e_L = backmixing coefficient in L phase
- G = light phase flow rate
- h_G = hold up of G phase per unit height
- h_L = hold up of L phase per unit height
- H = height of a stage
- k = mass transfer coefficient
- K_{pr} = feedback proportional gain, Equation 5
- K_{ir} = feedback integral constant, Equation 5
- K_{pf} = feedforward proportional gain, Equation 5
- L = heavy phase flow rate
- L_o = midrange constant, Equation 5
- m = gradient of linear equilibrium relationship
- Q = rate of solute interphase mass transfer per unit area
- t = time
- x_n = solute concentration in the heavy phase at stage n
- x_F = feed concentration
- x_{raf} = raffinate concentration
- y_n = solute concentration in the light phase at stage n
- y^* = equilibrium light phase concentration

REFERENCES

- (1) McDonald, C.R., PhD Thesis, University of Bradford, U.K., 1976.
- (2) Jones, D.A. and Wilkinson, W.L., Chem. Eng. Sci. 1973, 28, 537.
- (3) Jones, D.A. and Wilkinson, W.L., Chem. Eng. Sci. 1973, 28, 1577.
- (4) McDonald, C.R. and Wilkinson, W.L., Proc. I.S.E.C. Lyon, 1975, p. 2608.
- (5) Ingham, J., Tran. Inst. Chem. Eng. 1972, 50, 372.

Modelling of the IMI $MgBr_2$ - $MgCl_2$ Process

J.E. Gai, IMI — Institute for Research and Development,
P.O.B. 313, Haifa, Israel

ABSTRACT

Modelling of two countercurrent batteries is described in which recovery and separation are made of $MgCl_2$ and $MgBr_2$, contained in a butanol extract. There are strong interactions between chloride, bromide and water, leading to equilibrium correlations of an unusual form. A fairly simple algorithm was used for calculating the batteries, taking into account that constant flowrates could not be assumed. The system itself is interesting because of the novel results which can be obtained when making full use of the strong influence that chloride has on the distribution of bromide.

Introduction

THE IMI $MgBr_2$ - $MgCl_2$ PROCESS⁽¹⁾ was developed for the recovery of these two components, by means of liquid-liquid extraction, from a brine also containing halides of Ca, Na and K. The solvent chosen for this purpose is n-butanol. One remarkable feature of the process is the ten- to twenty-fold increase in bromide concentration of the $MgBr_2$ product solution, despite the fact that only solvation mechanisms are involved. This is the result of complex interactions between chloride and bromide, and particularly of a strong effect of the former on increasing the distribution coefficients of the latter.

The model discussed here deals with simulation of the steady-state conditions in two of the six countercurrent extraction batteries of the process. It was worked out after the process flowsheet had been developed and after the chloride-bromide interactions, and the remarkable effects they produce, had been discovered but were known only qualitatively. The initial challenge was that of simulating this behaviour, and then of seeing how it behaved under changing conditions.

The main points of interest in the model are:

1. The system is one which is very remote from ideal behaviour and, on the other hand, no defined chemical reactions are involved. Thus, correlation of the equilibrium relationships is rather complex and is of an unusual form.
2. Contrary to widespread practice in other steady-state models, in the present case it cannot be assumed that the flowrates of aqueous and solvent phases are constant from stage to stage within a battery. The strong interactions between the solutes is an additional complicating factor. Nevertheless, a fairly simple algorithm was developed which required convergence on only 3 variables.
3. The system itself is interesting with respect to the unusual results possible because of the interactions between the solutes.

The IMI $MgBr_2$ $MgCl_2$ Process

The following brief description is intended only to provide sufficient background for appreciation of the place of the model in the process.

The essential feature of the solvent is its ability to extract halides of magnesium and calcium while almost com-

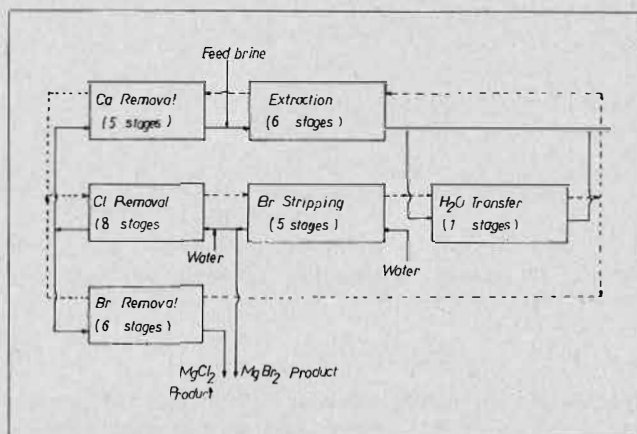


FIGURE 1. IMI $MgBr_2$ - $MgCl_2$ process.

pletely rejecting the alkali halides. Bromide is better extracted than chloride and magnesium better than calcium.

The process contains six batteries as illustrated schematically in Figure 1. The number of mixer-settler stages indicated in Figure 1 for the various batteries are for a typical application, but will vary according to the objectives set for the application. A typical composition of feed brine available is: Mg — 92 g/l, Ca — 32 g/l, Na — 4 g/l, K — 6 g/l, Cl — 316 g/l, Br — 11 g/l.

The functions of the batteries are as follows:

Extraction Battery: Magnesium and calcium halides are extracted into the solvent. In the strongly chloride medium, the extraction of bromide is about 75% complete. The alkali metal ions essentially all remain in the raffinate.

Calcium Removal: Utilizing the higher selectivity of the solvent for magnesium, the extract is backwashed with $MgCl_2$ solution in order to remove nearly all the calcium (which ultimately reports to the raffinate).

Chloride Removal: The extract entering this battery now contains essentially only $MgCl_2$ and $MgBr_2$ (and water). A separation is made so as to retain only $MgBr_2$ in the solvent while chloride, together with some bromide, is "removed" into the aqueous phase. The aqueous feed to this battery is a solution of $MgBr_2$, obtained by refluxing back most of the aqueous exit from Bromide Stripping, but diluted with some water. The effect of the chloride-bromide interaction is most evident in this battery and leads to the formation of a peak bromide concentration which, in the solvent, is easily ten times larger than that in the entering extract.

Bromide Stripping: This is a simple back-extraction of $MgBr_2$ with water. A small part of the exiting aqueous phase constitutes the product, which contains 100 to 200 g/l of bromide, i.e. some ten to twenty times the concentration in the feed brine.

Water Transfer: The aqueous raffinate from the Extraction battery has considerable dehydrating power and some of it is used to reduce the water content of the washed solvent (from 19 down to 11%). This permits retaining higher concentration levels in the whole system.

Very little transfer of other solutes occurs in this operation.

Bromide Removal: Washed solvent (after water transfer) is used to back-extract $MgBr_2$ from the $MgCl_2$ product, and the extract is recycled back to Chloride Stripping. The $MgCl_2$ product typically contains about 320 g/l of $MgCl_2$ with small concentrations of calcium and bromide.

Butanol has to be recovered from all 3 aqueous streams leaving the system. The two batteries which were modelled are the Chloride Removal and Bromide Stripping. As already stated, the salts in these batteries are limited essentially to $MgCl_2$ and $BgBr_2$, and the model neglects traces of calcium which may be present. The same model can also be applied to Bromide Removal.

Equilibrium Correlations

All the relationships presented in this section are for data obtained at temperatures of 22 to 25°C. The algorithm was constructed using weight fractions, x_k and y_k — of species k in the aqueous and organic phases, respectively — but the practical units used in the development work were g/l. Density (g/ml) correlations, needed to connect between the two, were straightforward linear correlations:

$$\text{Density (aqueous)} = 0.99 + 1.35(x_1) + 1.26(x_2) \dots (1)$$

$$\text{Density (solvent)} = 0.81 + 0.95(y_1) + 1.10(y_2) + 0.184(y_5) \dots (2)$$

In this x_k, y_k notation, k has the values 1, 2, and 5 representing bromide, chloride and water, respectively. The equations generally reproduce the measured values with deviations of less than 0.5%, and up to twice this figure in a few extreme cases. The effect of these errors in the model is small, and they largely cancel out in the final results.

Correlation of the chloride and bromide distributions is much more complex. After considerable testing of various empirical functions with but limited success, it was found that much better correlations could be obtained in terms of a function F , which was named the "salinity factor" (of the aqueous phase), defined by

$$F = \frac{1.828(x_1) + 2.866(x_2)}{1 - [2.239(x_1) + 3.482(x_2)]} \dots (3)$$

The choice of this function has a semi-theoretical basis, deriving from observations that the distribution coefficients are strongly dependent on the salinity of the aqueous phase, and that the species transferred are most certainly hydrated. This leads to a distinction between "bound" water and "free" water, i.e. water strongly coordinated to the ions, and that outside of the coordination spheres, respectively. In the above expression, the coefficients in the numerator — 1.828 for bromide and 2.866 for chloride — were arbitrarily chosen to convert each X^- to its magnesium hexahydrate, $MgX_2 \cdot 6H_2O$. The coefficients in the denominator resulted from regression analysis, that for bromide from data on $MgBr_2$ only, and for chloride from all 4 coefficients could probably be further optimized.

Defining distribution coefficients, D_k , as

$$D_k = \frac{y_k}{x_k} \dots (4)$$

it was found that the distribution coefficients for bromide and chloride, each taken in separate systems, could be represented by

$$D_1 = 0.225F + 0.013 \quad (MgBr_2 \text{ only}) \dots (5)$$

$$D_2 = 0.100F - 0.0039F^2 - 0.013 \quad (MgCl_2 \text{ only}) \dots (6)$$

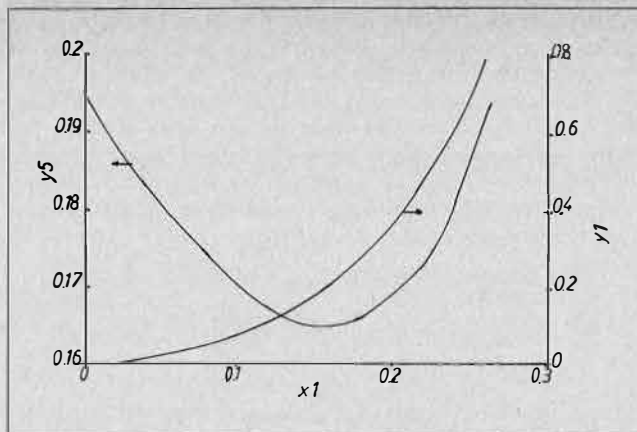


FIGURE 2. Water and bromide distributions in $MgBr_2-H_2O-BuOH$ system.

For systems containing the two salts together, the coefficients of terms in F change somewhat but, more important, interaction terms are also necessary.

For chloride, the expression found was

$$D_2 = 0.146F - 0.0159F^2 + 0.119(x_1) - 0.022 \dots (7)$$

For bromide it was found necessary to divide the correlations into two regions. At moderate to high salinities, the expression obtained was

$$D_1 = 0.214F - 0.0229F^2 + 1.25(x_2) + 0.027 \dots (8)$$

In both pairs of equations — 5 and 6, and 7 and 8 — it can be seen that the coefficients of F are significantly higher for bromide than for chloride on a weight basis, but are more or less equivalent when taken on a basis of equivalent weights. However, when present together, the effect of chloride on the distribution of bromide (the coefficient of 1.25 for x_2 in equation 8) is an order of magnitude higher than the effect of bromide on chloride distribution.

At lower salinities the effect of chloride on bromide distribution falls off. This decrease was not fully quantified; in the model the coefficient (1.25) of x_2 in equation 8 was arbitrarily reduced by a factor of $(F/1.1)^3$ for values of F less than 1.1. (Amongst others, one reason for this choice is the necessity of having a continuity of values over the whole range, without step changes.)

Solvent phase concentrations of the salts are generally reproduced to within 1% by the above expressions. For the sake of completion, it should be mentioned that safeguards had to be artificially introduced in the algorithm in order to accommodate the fact that, during computation, iterations sometimes caused the calculations to go through points outside of the range of validity of the correlations. (The final results were always within range.) The reference is to extremely high (non-existent) salinities which, algebraically, first cause D_1 and D_2 to go through maxima (see eqns 7 and 8) and then cause F to become discontinuous as the denominator of eqn 3 becomes zero and then negative. The safeguard was that at values of F greater than that corresponding to the maximum value of D , this latter maximum was retained.

Since there is considerable transport of water in different parts of the extraction system, correlations were also needed for the water contents of the solvent phases. When plotted against the salt concentration in the aqueous phases, it is found that the water content of the solvent initially drops and then rises again. An example is given in Figure 2 for $MgBr_2$ only, which is qualitatively re-

representative of all these systems. This behaviour is again explained in terms of free and bound water. As the salinity increases, the dehydrating power of the aqueous phase also increases*, so reducing the free water in the solvent. Initially, the extraction of hydrated ion pairs is small but as this increases, at some point the bound water which is coextracted exceeds the reduction in free water concentration. This hypothesis suggests the form of the correlations which were found:

$$y_5 = 0.412(y_1) + 2.239(y_2) - 0.0489(x_1) - 0.788(x_2) + 0.195 \quad (F \geq 1.3) \quad (9)$$

$$y_5 = 1.035(y_1) + 2.239(y_2) - 0.322(x_1) - 0.788(x_2) + 0.195 \quad (F < 1.3) \quad (10)$$

Eqn 9 applies at high salinities and eqn 10 at lower salinities. The difference between the two is only in the coefficients of bromide and relates to the previously made observation of decreasing influence of the chloride on bromide extraction at lower salinities.

The regression analysis was performed with the constant term fixed in advance so as to give the correct result for the solubility of water in the solvent in the absence of salts. The correlations reproduced the experimental results to within $\pm 2\%$. However, since these two equations will normally give a discontinuity of values at $F = 1.3$, eqn. 10 was artificially modified and used in the following form:

$$y_5 = (1.035 - F^5/5.9598)(y_1) + 2.239(y_2) - (0.322 - F^5/16.419)(x_1) - 0.788(x_2) + 0.195 \quad (F < 1.3) \quad (11)$$

This makes eqns. 9 and 11 give a continuous set of values and still leaves the results essentially correct at lower salinities.

One assumption which was left in the model was that the solubility of alcohol in the aqueous phases was neglected. Since the solubility is generally under 2% and does not vary much, the error is relatively small.

Computation Method

The method used is basically an extension of that described by Goto⁽²⁾. Consider the representation of a countercurrent battery shown in Figure 3. It is assumed that $S(N+1)$ and $y_i(N+1)$, i.e. the solvent feed, and $W(0)$ and $x_i(0)$, i.e. the aqueous feed, are given. Trial values are assumed for $W(N)$, $x_1(N)$ and $x_2(N)$, i.e. the aqueous

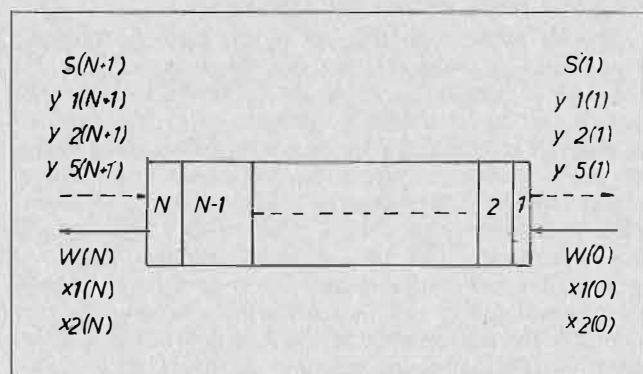


FIGURE 3. Schematic representation of a countercurrent battery.

*More rigorously, the activity of the water decreases. It may be noted that the operation of the Water Transfer stage (Figure 1) is based on this characteristic, the conditions there being chosen so as to be close to the minimum solvent water concentration, as exemplified in Figure 2.

phase leaving the battery, and then a stage-by stage calculation is made over the length of the battery. This supplies the weight and composition of the solvent leaving the battery. By means of material balances, the latter values together with the feed values are used to calculate back the aqueous phase leaving the battery. By means of the convergence procedure described later, a new set of trial values is taken and the procedure repeated until the iterations converge. Insertion of the bleed of bromide product and the water feed between the Chloride Removal and Bromide Stripping (Figure 1) is a matter of simple arithmetic, provided that the weight of $MgBr_2$ product is put in as a feed parameter. (This latter parameter is convenient for computation, but is not a realistic approach to process operation.)

For the calculation of any stage, the solvent entering it and the aqueous phase leaving it are given. For calculating the solvent leaving (4 items) and the aqueous phase entering (3 items), the following 7 relationships are used:

- 3 sets of equilibrium correlations for chloride, bromide and water in the solvent.
- 4 material balance relationships for the chloride, bromide, water and overall weight.

Each of the 4 streams must, of course, also be normalized in that the sum of all the weight fractions (after conversion of Br^- and Cl^- to $MgBr_2$ and $MgCl_2$, resp.) equals unity. Since non-linear equations are involved, an iterative procedure was used. Assuming the solvent leaving the stage to be in equilibrium with the aqueous phase leaving it, the composition of the former is determined from the equilibrium correlations — first the chloride and bromide, and then the water. A trial value is then taken for the weight of solvent leaving the stage. Using material balance equations for chloride, bromide and overall weight, the entering aqueous phase is calculated. The water balance is used to calculate back the weight of solvent leaving the stage, and this is the parameter which is tested for convergence. For convergence of this calculation, the Wegstein procedure⁽³⁾ was used. In most cases only one iteration was needed because a good estimate of the solvent weight could be made, based on the assumption of constant weight of solute-free alcohol in the solvent. Only where the bromide and/or chloride concentrations dropped to zero were iterations needed, up to a maximum of about 5 iterations. This occurs where the material balance calculations made the bromide and/or chloride negative in the entering aqueous phase, and this negative value is changed to zero. This leads to an insignificantly small change in the weight of solute-free alcohol leaving the stage.

Convergence of the iterations over the battery as a whole proved to be a more difficult task. Because of the strong interactions between bromide, chloride and water, no reliable procedure could be found which would simultaneously correct all 3 trial values. The method adopted is perhaps not so efficient, but is completely reliable. It consists of a series of unidirectional searches. At the end of the first iteration, the variable having the largest relative deviation between trial and calculated values is singled out for correction. For the two concentrations, the direction of this correction is known absolutely. For example, if the trial values for weight and for chloride concentration are kept constant, a low trial value of bromide always gives a calculated value which is too high, and vice versa. The beginning of the search procedure is then as illustrated in Figure 4. Successively larger corrections are made to the trial values until such time as the sign of $(c_j - t_j)$ changes compared to that of the previous iteration; in the example of the figure, this occurred on the 4th iteration. Thereafter, the interval between t_3 and t_4 is successively reduced by a half in the appropriate direction, until the relative devia-

TABLE 1. Comparison of Simulation with Pilot Unit Results

Chloride Removal — 8 stages; Bromide Stripping — 5 stages.					
Parameters		I		II	
Solvent to C1 Removal					
Flowrate (1/hr)		5.0		4.88	
Br ⁻ content (g/l)		4.3		5.0	
Cl ⁻ content (g/l)		56		52	
H ₂ O content (%)		15.3		15.2	
H ₂ O to Br Stripping (1/hr)		0.425		0.415	
H ₂ O to Cl Removal (1/hr)		0.575		0.585	
Weight of Br-Aq-out bled off as product (g)		52		52	

Results	Simulation	Pilot	Simulation	Pilot
Flowrates (1/hr)				
C1-S-out	4.90	4.71	4.82	4.69
C1-Aq-out	0.99	1.04	0.95	1.03
Br-Aq-out	0.31	0.19	0.31	0.21
Br-S-out	5.01	4.80	4.92	4.80
Concentrations				
C1-S-out: Cl ⁻ (g/l)	0.85	0.5	0.31	0.3
Br ⁻ (g/l)	10.0	6.2	9.7	5.2
H ₂ O (%)	15.7	13.2	16.3	13.0
C1-Aq-out: Cl ⁻ (g/l)	282	283	267	260
Br ⁻ (g/l)	9.5	12	14.8	17.7
Br-S-out: Br ⁻ (g/l)	1.18	0.4	0.75	0.1
H ₂ O (%)	18.3	16.9	18.6	17.3
Br-Aq-out: Br ⁻ (g/l)	141	140	139	115
Cl ⁻ (g/l)	13.4	13	4.8	7.1

Designation of streams:
 C1-S-out = Solvent leaving Chloride Removal
 C1-Aq-out = Aqueous phase leaving Chloride Removal
 Br-S-out = Solvent leaving Bromide Stripping
 Br-Aq-out = Aqueous phase leaving Bromide Stripping.

tion between trial and calculated values is satisfactorily small. Although calculated values can come out negative, trial values are always kept positive (or zero)*.

At this point, the variable now having the largest relative deviation receives the same treatment and iterations are continued until the sum of the absolute values of the 3 relative deviations falls below a predetermined value (0.005 in the present calculations). Concerning the weight variable, its behaviour is generally similar but occasionally it "loses direction", i.e. a high value, for example, gives a still higher value, eventually leading to very small corrections in the weight at a wrong point. The situation is remedied by re-starting the search procedure if the relative difference between two successive trial values on the weight falls below a certain value, e.g. one part per million.

The number of iterations required over the two batteries depends, of course, on how good are the initial trial values. In extreme cases about 400 iterations were required, whereas on the average about 150 sufficed. Much of the testing was done in BASIC on a Wang 2200 S Processor having an 8 K memory. This is a relatively slow machine and required several hours in the extreme cases, but its interactive nature and tracing capability made it very useful for debugging and program development. When performed in FORTRAN on an IBM 370, less than 2 seconds were needed.

It may be remarked that the same method has been tested on some other extraction flowsheets and in some cases the iterations could not be made to converge. This happens when there is a large change in one particular stage of a battery, usually an end stage. For example, if an extract comes from a battery in which there is a strong dehydrating effect of the aqueous phase and is introduced into another battery where there is very little such

*In the more general case, not applying here, suitable safeguards must be inserted to identify a correct solution equal to zero.

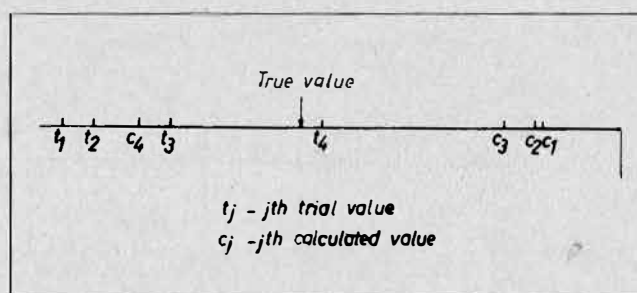


FIGURE 4. Example of search procedure.

effect, a large transfer of water occurs in the end stage where the extract is introduced. For such cases, different methods have to be used.

Results and Discussion

Agreement with Experimental Results

At two different times, continuous bench-scale units were run to test the process. On the first occasion more emphasis was placed on the MgBr₂ product and more stages were included in the Extraction and Chloride Removal batteries than indicated in Figure 1. This led to higher bromide concentrations in the MgBr₂ product than are referred to in the results discussed here, up to 200 g/l of Br⁻.

Of the numerous data available, only a few have been selected so as to high-light interesting aspects, and they all refer to conditions which existed in the second pilot plant run. Table 1 shows a comparison between simulations and two sets of operating conditions which existed. For convenience, the flowrates of the pilot unit have been scaled down to a common basis of 1 1/hr total water fed to the two batteries. On making the comparison, it should be noted that the pilot plant results are average results. In actual fact, during the period of 24-36 hours for which the results are given, there were always fluctuations so

that a truly stable steady state was not achieved. Also, some of the data, e.g. the weight of $MgBr_2$ product bled off, were not actually measured but were calculated by material balances.

Comparison of calculated and pilot results shows a fairly good fit, but far from perfect. The following points may be singled out:

1. Agreement of 3 of the flowrates is relatively good ($\pm 6\%$), but the differences on the Br — Aq — out stream are relatively much larger.
2. Water concentrations in the solvent are always higher in the simulated values than in the pilot plant results.
3. Most of the other concentrations show reasonable agreement, the largest single deviation being for the bromide in the Cl — S — out stream.

There are two main causes for the discrepancies. The first is that the pilot unit was operated at temperatures $10-15^\circ$ higher than those at which the equilibrium data were measured. It is known that this difference hardly influences the distribution of chloride and bromide, but it has a significant effect on the water distribution because of the effect of temperature on hydrogen bonding. The direction of this effect is that at lower temperatures the solvent has higher water contents, and hence the result mentioned in the second remark above.

The other main cause for discrepancy is the use of

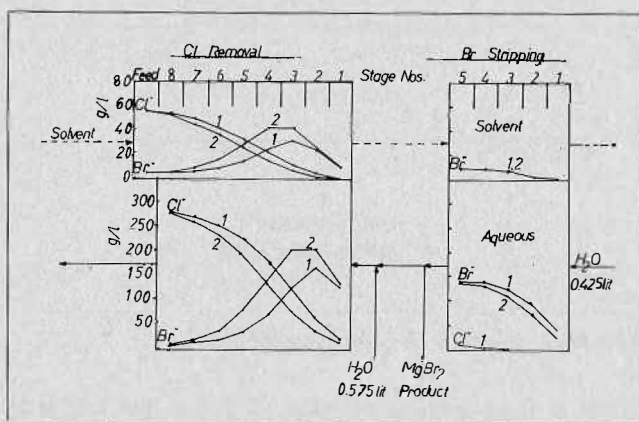


FIGURE 5. Concentration profiles in countercurrent batteries. Solvent flowrates 1 — 5.0 l, 2 — 4.8 l.

average values for representing the pilot plant results. In order to test the extent to which variation in operating conditions could influence the results, a number of calculations were performed with small variations. A few examples are given in Table 2 with variations of 5 — 10% in flowrates, and 20% in the weight of $MgBr_2$ product bled off (but the extra 10 g of product represents only 3% of the aqueous phase exiting from the Bromide Stripping). As can be seen, each variation leads to improvement in the agreement of some of the calculated with experimental results, but different ones in the different cases. For the reason given previously, the water contents of the solvent cannot be improved.

The general conclusion is that the discrepancies can be explained and that the model is reliable for the temperature at which the equilibrium data were measured.

Concentration profiles in the batteries

The most interesting feature of the system itself is the concentration profiles existing within the batteries, but more particularly in the Chloride Removal. Two examples of the profiles are given in Figure 5. Qualitatively, the profiles of chloride in the Chloride Removal and of both solutes in the Bromide Stripping are as to be expected, with monotonic decreases in the direction of solvent flow. However, the bromide concentration in the Chloride Removal is altogether different, showing a strong increase up to a maximum value and then decreasing. Such maxima are known, but the magnitude of the increase is striking. Thus, at the maximum, the aqueous phase bromide concentration can be as much as 20 times that in the exiting aqueous phase, and the solvent maximum can be 10 times that in the extract fed to the battery.

In the light of the correlations previously given, the build-up of the maximum concentration can be explained as follows. The aqueous phase moving from one stage to the next introduces bromide into ambients containing successively higher levels of chloride which increase the bromide distribution coefficients considerably beyond those expected on the basis of salinity alone. This "extra" bromide is carried by the solvent against the direction of the aqueous flow. Some of it is released back again into the aqueous phase in an earlier stage where the chloride level has dropped. Thus, a large amount of bromide recycles internally in the Chloride Stripping and, of course, also between the two batteries. The release of

TABLE 2. Effects of Small Variations in Operating Parameters

(Reference Conditions: Case I of Table 1)						
Parameter Changed	None (Pilot)	None (Simulation)	Water to Cl Removal	Water to Br Stripping	Solvent Feed Flow	Weight of $MgBr_2$ Product
Reference value			0.575	0.425	5.0	52
New value			0.600	0.465	4.8	62
Results						
Flowrates						
Cl-S-out	4.71	4.90	4.91	4.91	4.72	4.89
Cl-Aq-out	1.04	0.99	1.01	1.01	0.97	0.99
Br-Aq-out	0.19	0.31	0.32	0.35	0.32	0.31
Br-S-out	4.80	5.01	5.01	5.03	4.83	4.89
Concentrations						
Cl-S-out:						
Cl ⁻	0.5	0.85	0.40	0.42	0.41	0.96
Br ⁻	6.2	10.0	9.5	10.6	10.0	9.7
H ₂ O	13.2	15.7	16.2	16.1	16.1	15.6
Cl-Aq-out:						
Cl ⁻	283	282	278	278	278	283
Br ⁻	12	9.5	11.5	12.2	11.7	9.2
Br-S-out:						
Br ⁻	0.4	1.18	0.72	0.50	0.61	1.10
H ₂ O	16.9	18.3	18.6	18.8	18.7	18.3
Br-Aq-out:						
Br ⁻	140	141	137	143	140	137
Cl ⁻	13	13.4	6.5	6.1	6.2	15.4

Designation of streams and units as in Table 1.

bromide into aqueous phases containing less chloride also explains why the peak bromide concentration in the aqueous phase is displaced one stage away from the solvent peak concentration.

If conditions change such that significant amounts of chloride "break through" to the Bromide Stripping, small peaks can also build up there. Case 1 of Figure 5 is borderline, and by increasing the solvent flowrate slightly such a peak would form. The phenomenon was observed experimentally in the pilot plant operation.

It is found that the main parameter affecting the magnitude of the peak concentration is the solvent/aqueous ratio for the Chloride Removal. Thus, in Figure 5, the weight ratios for Cases 1 and 2 are, respectively, 5.14/1 and 4.90/1. This rather modest change leads to relatively large changes in the peak concentration, but the changes in the end conditions (details given in Table 2) are much milder.

An interesting fact, observed both experimentally and in the model, is that, as the solvent/aqueous ratio is decreased, the concentration of the chloride in the exiting aqueous phase decreases, as expected, but the bromide increases. This phenomenon occurs in the range of operating conditions of interest here but, of course, there is a limit. At sufficiently low ratios the bromide will eventually decrease, accompanied by a substantial reduction of the peak concentration.

Concerning the inapplicability of assuming constant flows, only one example will be cited. For Case 1 of Figure 5, the volume of water entering the Bromide Stripping is 0.425 l/hr (or 425 g/hr) but the aqueous phase leaving the battery is only 0.317 l/hr (368 g/hr). In this case the reduction is due to the fact that the water content of the solvent increases from 16.1 to 18.7%. Equally large variations occur in the Chloride Removal.

Applications

The value of a model is three-fold: it provides a better understanding of the process; it enables testing flowsheet variations which might be too expensive to test experimentally; and it is, of course, very important for control purposes. As already stated, the present model was constructed after the flowsheet had been developed, so that some of the discussion below is only academic at this stage.

Understanding of the Process

From the implementation of other integrated solvent extraction flowsheets, similar in complexity to the one described here, experience indicates that considerable time elapses before plant personnel become fully acquainted with the finer details of all the interactions involved. This can sometimes even lead to decisions made quite contrary to the principles used in designing the flowsheet. The availability of a steady-state model, particularly for executing simulated exercises, can be a very useful instrument in the training of personnel with respect to the physico-chemical interactions and the results they lead to. The Chloride Removal is a good example of how the results of changes are not always obvious.

Development of the correlations also provides the research chemist with deeper insight into the system. One example is the quantitative changes in the bromide and water correlations occurring at values of F of about 1.1 — 1.3. These indicate that a qualitative change occurs in the nature of the interactions at higher salinities. It would seem that, at the higher salinities, there are formed fairly structured aggregates of mixed ion pairs (i.e. Mg^{++} , Br^-

and Cl^- together) in which the coordinated water is less than expected for $MgCl_2$ or $MgBr_2$ taken separately.

Testing of Flowsheet Variations

Laboratory batchwise simulation of a countercurrent battery can be a tedious operation. This is particularly so for a battery such as the Chloride Removal with its huge bromide accumulation. On the other hand, continuous operation is often prohibitively expensive and only a few variations are tested. The point is obvious: a model can be very useful for both optimization (technological and economic) and for testing different flowsheet combinations. For example, referring to Case I of Table 1 (which is Case 1 of Figure 5), it is found that adding 1 stage to the Bromide Stripping hardly changes things; in particular, it reduces the loss of bromide exiting in the solvent by an almost insignificant amount.

Addition of stages to the Chloride Removal would normally be contemplated for improving the chloride-bromide separation. Simulation indicates that (for the same case) addition of three stages will completely eliminate transfer of chloride to the Bromide Stripping. In addition, the bromide concentration in the $MgBr_2$ product increases from 141 to 156 g/l.

Control Applications

For on-line control a dynamic model is required, but the steady-state model has its place in the design of the control system and in off-line control.

Concerning design, consider the Chloride Removal battery and assume that it is implemented by means of mixer-settlers, which have relatively long delays in their response to small changes, especially over a whole battery. From the curves in Figure 5, the points most sensitive to change are stages 3 and 4, if the aqueous phase is monitored, or 4 and 5 if the solvent is monitored. Comparing these changes to those produced at the ends of the battery (Table 2), it is obvious that monitoring at the ends is far less sensitive than monitoring in the middle, with respect to both chloride and bromide concentrations.

As regards off-line control, one of the problems an operator must consider is what to do if the feedstock changes. In the present example, this will have repercussions throughout the system, affecting throughputs, recoveries and concentrations of the products. No operator can be expected to analyze all these repercussions, although in practice that is what is expected of him. With a computerized model he can analyze numerous strategies within a matter of minutes and come to a better-based conclusion.

Concluding Remarks

This exercise illustrates the efficient use of limited data when the system itself is understood. Compared to most other reported solvent extraction models, the main points of novelty are the non-assumption of constant flowrates (which was mandatory here) and the equilibrium correlations. The form of the latter may possibly serve as a prototype in certain multicomponent systems.

The uses of a model, as described in the preceding section, need no further emphasis.

Acknowledgement

The author wishes to thank Dr. R. Blumberg for helpful discussions, and Dr. S. Wahrman for assistance in preparing the paper. Acknowledgement is also made to IMI, Institute for Research and Development, for permission to publish this work.

NOTATION

- c_j (Fig. 4) = Calculated result in the j th iteration
 D_k = Distribution coefficient of species k , defined by y_k/x_k
 F = Salinity factor, defined by eqn. 3.
 k = 1 for bromide
2 for chloride
5 for water
 t_j (Fig. 4) = Trial value in the j th iteration
 x_k = Aqueous phase weight fraction of species k
 $x_k(n)$ = x_k for aqueous phase leaving stage n

- y_k = Solvent phase weight fraction of species k
 $y_k(n)$ = y_k for solvent leaving stage n

REFERENCES

- (1) Baniel, A. and Blumberg, R., Israel Patent 23,760 (1968).
- (2) Goto, T., Proc. ISEC 1971, Soc. Chem. Ind., London (1971). Vol. II, p. 1011.
- (3) Franks, R.G.E., "Modelling and Simulation in Chemical Engineering", Willey-Interscience (1972), pp. 18 - 28.

DISCUSSION

J.O. Liljenzin: Would a small feed forward help to increase the outgoing $MgBr_2$ concentration?

J.E. Gai: I understand the term "feed forward" to mean an increase of the ratio of solvent feed to aqueous feed in the Chloride Removal battery. As explained in the paper, a small increase affects the peak bromide concentration but does not much affect the end concentration. Compared to the examples given in Table 1, a higher concentration of bromide, without increasing the chloride, could be obtained by an increase of solvent/ aqueous feeds coupled with more stages.

P.J. Lloyd: Would it be possible to use the model to study effects such as increasing recycles, or the number of stages, or introducing intra-stage recycle?

J.E. Gai: The model was indeed used to study the effects of inter-battery recycle and of the number of stages. Intra-stage recycle (e.g. recycle from settler back to mixer) has no effect on the steady state model since equilibrium is assumed in each stage.

Y. Marcus: Could your model be used for optimizing a system with respect to flows and number of stages in each unit, given the equilibrium and operating lines?

J.E. Gai: The way the model is constituted at present, it is an algorithm for solving each battery for a given number of stages with defined feeds (composition and flowrates). As such, an approach to optimization can be made by means of a parameter study, i.e., the flowrates and the number of stages can be changed in separate calculations and the results can then be evaluated by inspection. A more thorough solution would be to incorporate this algorithm as a subroutine in an optimization algorithm.

Chapter 7

Equipment

Peter Paige Memorial Session Session 6 — Mixer Settlers



Dr. J. Palley



J.B. Scuffham

Session Co-Chairmen

Session 8

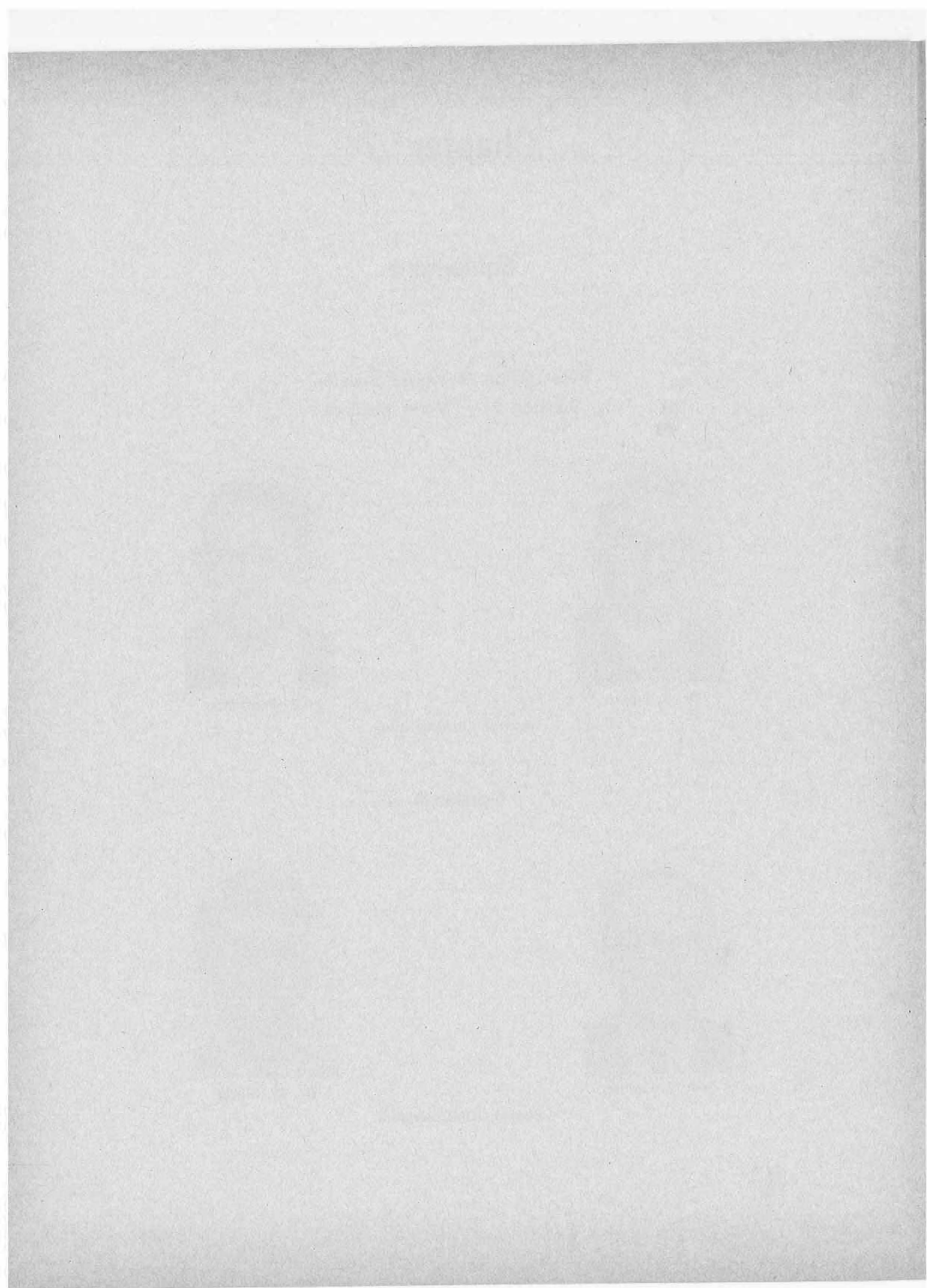


Prof. J. Landau



Dr. M. Slater

Session Co-Chairmen



Design of Mixer-Settlers to Achieve Low Entrainment Losses and Reduce Capital Costs

I.E. Lewis,
Conzinc Riotinto of Australia Limited,
Melbourne, Australia.

ABSTRACT

There is a considerable incentive to reduce the size and improve the operating performance of the large settlers in use in many mining operations around the world. The development of internal baffle systems for settlers is described and both laboratory and commercial plant trial results are reported. Entrainment losses have been reduced to very low levels and a baffled settler could be much smaller than a conventional unit. The first large scale commercial installations are in the final design stages and should be in operation by the end of 1978.

Introduction

THE LARGE FLOWS of low tenor liquors that have to be handled in the leaching of low grade ores in the mining industry has allowed little choice in the selection of solvent extraction equipment for metal recovery. The large mixer-settlers in use at so many operations around the world would appear to be here to stay for many years yet. However, in many leach SX-EW plants such as at Nchanga, etc., the mixer-settlers are required to treat large volumes of leach liquor. The capital cost of these large settlers is high and entrainment losses can lead to high operating and environmental costs.

The research section of Conzinc Riotinto of Australia Limited (C.R.A.), (80% owned by Rio Tinto Zinc of London), initiated a development programme in 1973, the aim of which was to improve operating efficiency and reduce capital cost of solvent extraction plants in the mining industry. The work has proceeded to the stage where new settler designs have been developed that can reduce entrainment losses by an order of magnitude if a conventionally sized settler is used. If normal entrainments can be tolerated, settler sizes can be reduced by possibly as much as 75%.

Experimental

Details of the mixer-settler used in the development work are shown in Figure 1. The mixer-settler was made with 316 stainless steel with a full glass wall on one side of the settler. Basis for design was the General Mills recommended mixer-settler design. The detail of the turbine used is shown in Figure 2. The size of the settler was such that for a flow of $5.87 \text{ m}^3/\text{hr}/\text{m}^2$ (2 Imp gpm per ft^2), the total flow was 250 litres/minute. The mixer was operated on the pump-mix principle and no external pumps were used in any of the laboratory or commercial tests. Flows were metered by either rotameters or orifice plates installed in the recycle lines and/or feed lines. In all laboratory tests the unit was operated with a 100% recycle of liquor from the overflow weirs back to the mixer. No surge tanks were used.

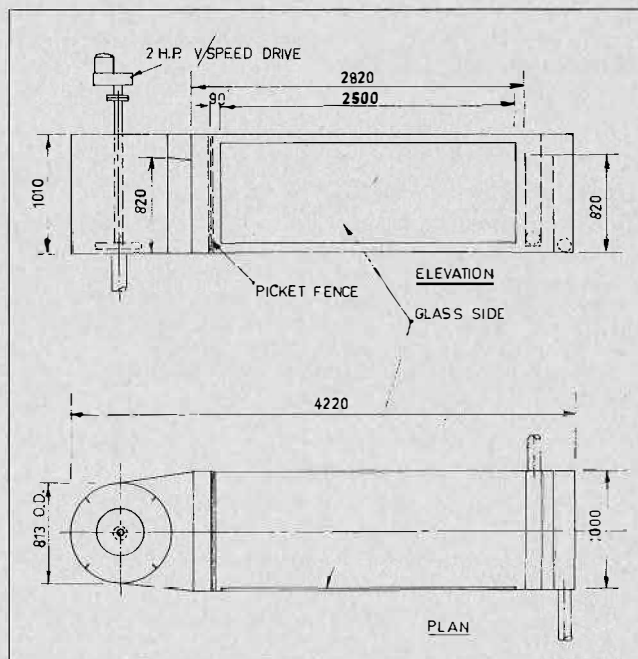


FIGURE 1. Experimental mixer settler.

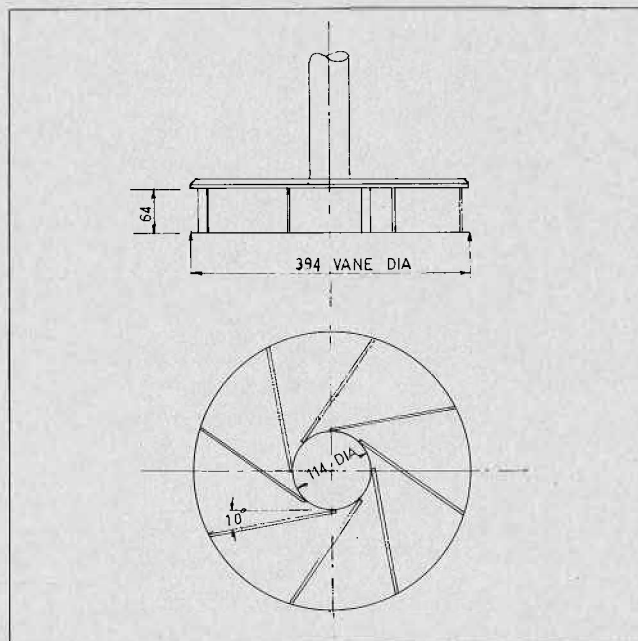


FIGURE 2. Mixer turbine.

The commercial tests were carried out with only the organic recycle necessary to duplicate the existing plant operating conditions. When the test unit was first operated without baffles in 1973 it was immediately observed that

high forward velocities were being achieved within the emulsion layer while liquid at the surface and the bottom of the settler was moving backwards towards the mixer.

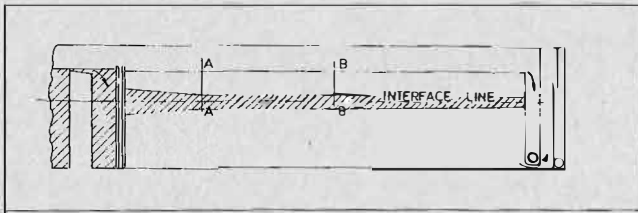


FIGURE 3. Unbaffled settler.

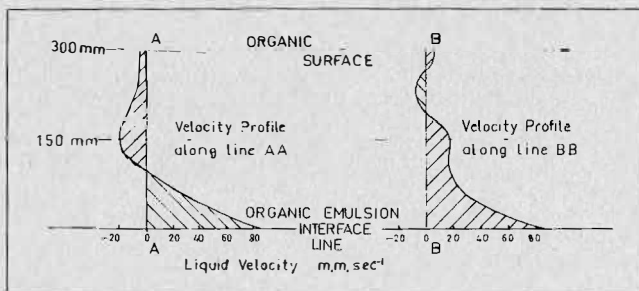
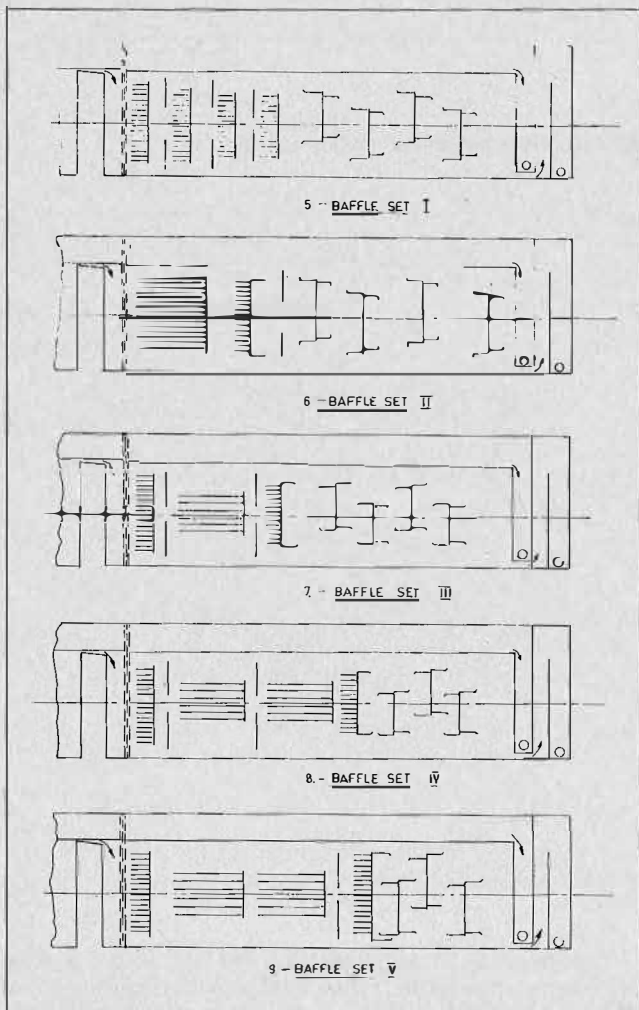


FIGURE 4. Unbaffled settler velocity profiles.



FIGURES 5, 6, 7, 8 and 9. Experimental baffle sets.

Typical velocity profiles, determined by tracer injection, along planes A-A and B-B in Figure 3, are shown in Figure 4. It was obvious that short circuiting of the settler was occurring and further tests confirmed that organic entering from the mixer as emulsion could pass right through the settler and over the overflow weir in 45 seconds. In addition, fine aqueous entrainment that was settling slowly from the back moving organic phase was being picked up in the fast moving liquid stream near the interface and carried out over the organic weir. Paige⁽¹⁾ and Taylor⁽²⁾ about the same time measured similar velocity profiles.

To improve settler performance it was decided to baffle the interface and to install baffles in the inlet end of the settler. These were fitted with horizontal attachments so that the area available for interfacial coalescence was greatly increased in comparison to an unbaffled settler. The aim was to completely coalesce all the emulsion in the first quarter to one-third of the settler length and to use the rest of the settler to re-entrain the organic and aqueous liquors.

While a number of different designs of baffles have been tested, the installation of any of the baffle systems resulted in a very substantial reduction in entrainments. In comparative tests with and without baffles, entrainments were reduced by a factor of 100 in some cases. Reduction of entrainment losses by a factor of 10 can be expected providing liquor viscosities are not so high as to make de-entraining very slow. In Figures 5 to 9 are shown five of the baffle layouts used in the test programmes in the C.R.A. research laboratories in Newcastle and in the commercial tests at a uranium SX plant. Details of the baffle construction are shown in Figure 10.

All baffle sets were hung from a metal frame that enabled the set to be quickly positioned in or out of the settler. This made it possible to carry out settler tests with a baffle set installed, followed immediately by a test with no baffles in the settler. The mixer-settler liquid flow conditions and temperature remained identical for both tests. This partially overcame the problem of variation of operating conditions, for comparison purposes. It was found that, providing the settler temperature was within the range from about 20°C to 32°C, results over a long period of time were fairly reproducible. In the test programme carried out in Newcastle, the mixer turbine power input was varied for various O:A ratios ranging from 3:1 to 1:3. The settler was heated to 30°C if the temperature dropped below 20°C.

Entrainment Determination

Settler performance was evaluated primarily by determination of entrainment in both organic and aqueous phases. Emulsion volume was also determined. The mixer-

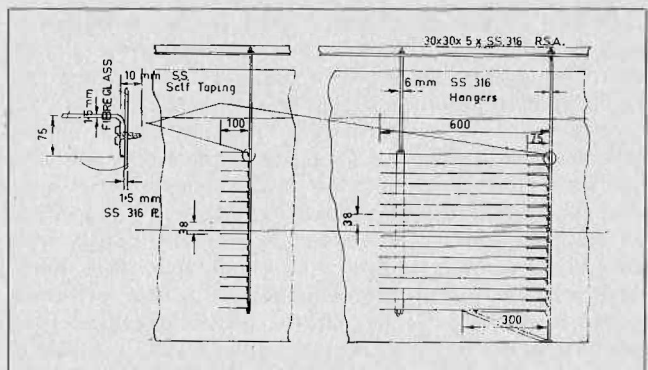


FIGURE 10. Baffle construction.

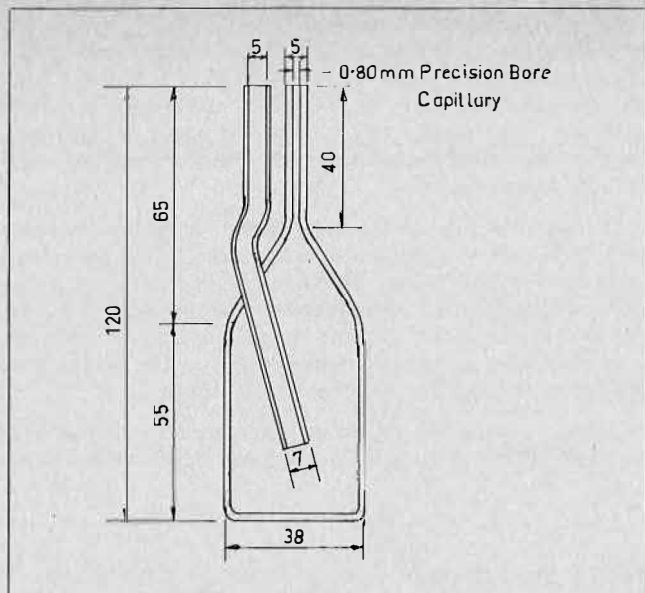


FIGURE 11. Entrainment bottle for determination of organic in aqueous phase.

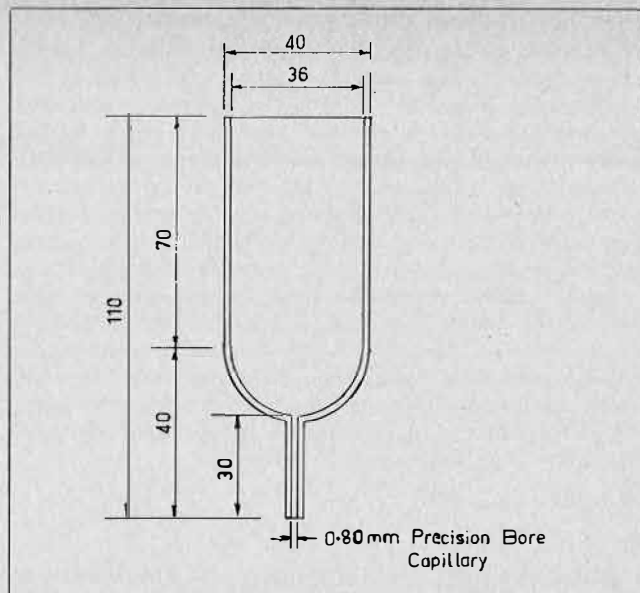


FIGURE 12. Entrainment bottle for determination of aqueous in organic phase.

settler was operated for at least 3 hours under any set of conditions before measurements were taken.

Very early in the test programme it became necessary to develop a rapid technique for determination of entrainments at the very low levels being encountered, commonly less than 1 ppm. A technique using glass bottles with sized capillaries was developed that allowed entrainment to be measured with an accuracy of approximately ± 2 ppm, down to a level of 1 ppm. The design of the entrainment bottles is shown in Figures 11 and 12. Sampling techniques had to be developed so that the results obtained were accurate and reproducible. After sampling, the bottles were placed in a high speed centrifuge for 30 minutes and the entrainment read directly from the height of either organic or aqueous phase in the capillary.

C.R.A. Research has found that entrainment in both organic and aqueous phases is very sensitive to problems that occur in SX plants, and in pilot plant evaluation of new SX solvents, entrainment determinations are considered essential for assessment of the circuit. Problems that would lead to major operating difficulties show up in increased entrainment readings long before actual physical plant problems occur. Some commercial plants have been supplied with entrainment bottles by C.R.A. Research and are now carrying out entrainment measurements as part of the routine daily sampling schedule.

Laboratory Mixer-Settler Test Results

The properties and composition of the aqueous and organic liquors used are shown in Table 1. These liquors were held in 1500 litre holding tanks when not being used in the settler tests. Four samples of liquor were taken for entrainment determinations and figures averaged to give the entrainment in that phase. Two samples were taken from near the side wall at the weir and two from near the centre of the settler at the weir. This was necessary because while entrainments were reproducible at any one point, there was a definite wall effect and entrainment varied, being higher near the side walls of the settler. It is unlikely this effect would be of any significance in large commercial settlers.

There was a significant effect from operating temperature, particularly on the volume of emulsion in the settler.

TABLE 1. Properties and Composition of Liquors Used in Test Work at C.R.A. Research Laboratories in Newcastle.

Organic Phase	
Deodorised kerosene supplied by Shell (Australia).	
Specific gravity	0.796
Flash point	38.8°C
I.B. point	145.5°C
50% distillation temperature	180°C
F.B. point	208.3°C
Aromatic content	16%
Viscosity	1.82 cp at 23.5°C
Kerosene-air surface tension	26.1 dynes/cm
Aqueous Phase	
Composition: 4 gpl. Cu as CuSO ₄ , 5 gpl. H ₂ SO ₄ .	
Specific gravity	1.002
Viscosity	1.1 cp at 24°C
Aqueous-Organic interfacial surface tension 16.2 dynes/cm.	

In Table 2A is shown a comparison of results with baffle set I (see Figure 5) installed at two operating temperatures. In Table 2B the effect of temperature with baffle set II is shown. It was found that operating in the range from about 20°C to 32°C, there was little temperature effect on entrainment. In winter, when liquor temperatures dropped to 16-17°C, the mixer-settler was heated to give an operating temperature of approximately 30°C.

In comparing the results in Tables 2A and 2B, it was evident that baffle set II, which was more successful in achieving rapid coalescing of the emulsion and thus lower emulsion volumes in the settler, did not also give lower entrainment. The turbulence occurring within the baffles in the coalescing region also tended to prevent any crud build-up within the baffle set, all crud tending to pass further down the settler to the quiescent zone near the exit end where it could be easily removed.

Table 3 shows the effect of the operating O:A ratio of the feed stream and variation in turbine power factor on emulsion volume and entrainment with and without baffles in the settler and equal volumes of aqueous and organic in the settler. The effect of operating with a baffled settler has been to greatly reduce entrainment losses under all conditions and, in some cases, the aqueous

entrainment has been reduced from very high levels to what might be regarded as a normal commercial plant operating level. The possibility of operating baffled settlers at much higher O:A and A:O ratios than the normal commercial practice is obvious. The ability of the baffled settler to reduce entrainment losses at the very high N^3D^2 turbine power factor of 204 is indicative of the performance improvement that might be possible on plants where high entrainment losses are a serious problem. The volume of emulsion was fairly constant in the baffled settler; this could be because the baffles bank the emulsion up quite high at the settler inlet end and there is a fairly large volume between the baffles where emulsion is virtually just held up with little coalescence occurring. Even with the highest emulsion volumes in the baffled settler the emulsion did not extend more than one third of the way down the settler.

Table 4 shows the results of the same set of tests as in Table 3 but with the aqueous depth equal to twice the organic depth. The results obtained in the baffled settler at the low turbine N^3D^2 of 44 have not been surpassed with any other baffle set, in fact the entrainments were so low that there was little room left for improvement with this liquor system.

In the unbaffled settler the organic entrainments were very high with this shallow organic layer, while there was little change in aqueous entrainment. In operating situations where organic entrainments must be kept low and the economics favour keeping organic inventory down by operating with a narrow organic layer in the settler, the baffled settler has a very obvious advantage.

Table 5 shows the results of a set of tests carried out at three different aqueous to organic depth ratios. It is

TABLE 2A. Effect of Temperature on Emulsion and Entrainments with Baffle Set I Installed

Total organic plus aqueous flow rate 250 litres/minute
Organic depth = Aqueous depth = 40 cm
Turbine N^3D^2 = 44

Temperature °C	O:A Ratio	Continuous Phase	Emulsion Volume m ³	Entrainment ppm	
				Organic in Aqueous.	Aqueous in Organic.
15	3:1	Organic	0.325	< 1	18
31	3:1	"	0.234	< 1	12
13	2:1	"	0.482	< 1	28
30	2:1	"	0.234	< 1	11
16	1:1	"	0.453	2	10
30	1:1	"	0.250	< 1	< 1
14	1:1	Aqueous	0.491	8	18
32	1:1	"	0.243	< 1	8
16	1:2	"	0.377	38	15
31	1:2	"	0.211	25	2
13	1:3	"	0.376	65	6
31	1:3	"	0.157	30	20

TABLE 2B. Effect of Temperature on Emulsion Volume and Entrainments with Baffle Set II Installed

Total organic plus aqueous flow rate 250 litres/minute
Organic depth = Aqueous depth = 40 cm
Turbine N^3D^2 = 44

Temperature °C	O:A Ratio	Continuous Phase	Emulsion Volume m ³	Entrainment ppm	
				Organic in Aqueous	Aqueous in Organic
17	3:1	Organic	0.271	< 1	127
30	3:1	"	0.041	< 1	140
16	2:1	"	0.244	2	45
31	2:1	"	0.122	< 1	8
16	1:1	"	0.203	5	15
30	1:1	"	0.122	< 1	5
17	1:1	Aqueous	0.163	10	32
30	1:1	"	0.122	2	15
14	1:2	"	0.183	28	8
30	1:2	"	0.081	8	9
14	1:3	"	0.203	140	28
31	1:3	"	0.054	70	18

TABLE 3. Effect of Change in O:A Ratio and Turbine Power Input on Emulsion Volume and Entrainments with Baffle Set I Installed.

Total organic plus aqueous flow rate 250 litres/minute
Organic depth = Aqueous depth = 40 cm

Turbine Power Factor N^3D^2	O:A. Ratio	Continuous Phase	Emulsion Volume m ³		Entrainment ppm			
			No Baffles in Settler	Baffle Set I in Settler	Organic in Aqueous No Baffles in Settler	Aqueous Baffle Set I in Settler	Organic No Baffles in Settler	Organic Baffle Set I in Settler
44	3:1	Organic	0.348	0.336	< 1	< 1	80	5
44	2:1	"	0.418	0.340	< 1	5	55	< 1
44	1:1	"	N.A.	0.329	N.A.	5	N.A.	< 1
44	1:1	Aqueous	0.139	0.379	200	5	35	< 1
44	1:2	"	0.104	0.302	350	5	20	< 1
44	1:3	"	0.104	0.271	880	45	40	< 1
91	3:1	Organic	0.452	0.325	< 1	5	90	10
91	2:1	"	0.380	0.418	< 1	5	65	20
91	1:1	"	N.A.	0.434	N.A.	5	N.A.	20
91	1:1	Aqueous	0.139	0.390	230	5	70	< 1
91	1:2	"	0.104	0.309	470	10	40	5
91	1:3	"	0.104	0.166	1500	50	60	< 1
204	3:1	Organic	0.313	0.379	< 1	10	90	50
204	2:1	"	0.348	0.453	< 1	5	65	30
204	1:1	"	N.A.	0.458	N.A.	10	N.A.	40
204	1:1	Aqueous	0.139	0.410	300	5	80	5
204	1:2	"	0.104	0.309	600	70	50	5
204	1:3	"	0.104	0.220	2000	110	60	< 1

TABLE 4. Effect of Change in O:A Ratio and Turbine Power Input on Emulsion Volume and Entrainments with Baffle Set I Installed

Total organic plus aqueous flow rate 250 litres/minute
Aqueous depth = twice Organic depth = 54 cm

Turbine Power Factor N ³ D ²	O:A Ratio	Continuous Phase	Emulsion Volume m ³		Entrainment ppm			
			No Baffles in Settler	Baffle Set I in Settler	Organic in Settler	Aqueous in Settler	No Baffles in Settler	Baffle Set I in Settler
44	3:1	Organic	0.592	0.190	5	< 1	550	5
44	2:1	"	0.122	0.371	10	< 1	350	5
44	1:1	"	0.383	0.472	10	< 1	190	< 1
44	1:1	Aqueous	0.313	0.383	110	< 1	25	< 1
44	1:2	"	0.174	0.255	530	< 1	90	< 1
44	1:3	"	0.105	0.174	850	15	10	< 1
91	3:1	Organic	0.592	0.213	10	10	800	5
91	2:1	"	0.453	0.434	10	5	550	10
91	1:1	"	0.383	0.430	10	< 1	290	10
91	1:1	Aqueous	0.383	0.418	130	< 1	100	5
91	1:2	"	0.174	0.290	750	5	110	< 1
91	1:3	"	0.105	0.182	1200	80	15	< 1
204	3:1	Organic	0.470	0.333	20	5	1150	20
204	2:1	"	0.383	0.399	10	5	750	15
204	1:1	"	0.209	0.460	15	< 1	590	20
204	1:1	Aqueous	0.314	0.418	150	< 1	130	30
204	1:2	"	0.105	0.271	1100	15	140	< 1
204	1:3	"	0.105	0.150	1700	80	20	< 1

TABLE 5. Effect of Aqueous to Organic Depth Ratio on Emulsion Volume and Entrainments with Baffle Set I Installed

Total organic plus aqueous flow rate 250 litres/minute
Turbine power factor N³D² = 44
Total liquor depth = 80 cm

Aqueous Depth: Organic Depth Ratio	O:A Ratio	Continuous Phase	Emulsion Volume m ³	Entrainment Organic in Aqueous	Entrainment Aqueous in Organic
1:2	1:1	Organic	0.410	< 1	< 1
1:1	1:1	"	0.329	5	< 1
2:1	1:1	"	0.472	< 1	< 1
1:2	2:1	"	0.314	5	5
1:1	2:1	"	0.341	5	< 1
2:1	2:1	"	0.372	< 1	5
1:2	3:1	"	0.236	< 1	< 1
1:1	3:1	"	0.337	< 1	5
2:1	3:1	"	0.190	< 1	5
1:2	1:1	Aqueous	0.379	5	< 1
1:1	1:1	"	0.205	10	< 1
2:1	1:1	"	0.383	< 1	< 1
1:2	1:2	"	0.302	5	< 1
1:1	1:2	"	0.236	15	< 1
2:1	1:2	"	0.255	< 1	< 1
1:2	1:3	"	0.271	45	< 1
1:1	1:3	"	0.135	85	< 1
2:1	1:3	"	0.174	15	< 1

interesting to see that in the baffled settler the height of the interface has had very little effect on the entrainment losses in both organic and aqueous phases. If a selection had to be made, there would be some small advantage in operating at an aqueous to organic depth ratio of 2:1. The variations in emulsion volumes with depth ratio did not appear to follow any distinct pattern.

A set of results obtained with baffle set III installed (see Figure 7) is shown in Table 6. While the temperature for these tests was low at 18°C, the entrainment results were still quite good. The emulsion volumes were high, but this could be a temperature effect. A similar set of results with baffle set IV installed (see Figure 8), is shown in Table 7. The entrainments with this set, still at the low temperature, were markedly higher than with baffle set III, Table 6, even though the emulsion volumes

TABLE 6. Emulsion Volumes and Entrainments with Baffle Set III Installed.

Total organic plus aqueous flow rate 250 litres/minute
Organic depth = Aqueous depth = 40 cm
Turbine power factor N³D² = 44
Liquor temperature 18°C.

O:A Ratio	Continuous Phase	Emulsion Volume m ³	Entrainment Organic in Aqueous	Entrainment Aqueous in Organic
3:1	Organic	0.529	< 1	50
2:1	"	0.500	< 1	10
1.5:1	"	0.470	5	10
1:1	"	0.619	10	10
1:1	Aqueous	0.386	10	10
1:2	"	0.305	10	< 1
1:3	"	0.477	70	< 1

TABLE 7. Emulsion Volumes and Entrainments with Baffle Set IV Installed

Total organic plus aqueous flow rate 250 litres/minute
Organic depth = Aqueous depth = 40 cm
Turbine power factor N³D² = 44
Liquor temperature 18°C.

O:A Ratio	Continuous Phase	Emulsion Volume m ³	Entrainment Organic in Aqueous	Entrainment Aqueous in Organic
3:1	Organic	0.356	5	30
2:1	"	0.323	5	20
1.5:1	"	0.371	5	15
1:1	"	0.366	5	5
1:1	Aqueous	0.388	10	15
1:2	"	0.230	40	10
1:3	"	0.210	180	10

were lower. In this case the emulsion layer extended two thirds of the way down the settler and there was not much settler volume available for effective de-entrainment.

Following the completion of these trials in Newcastle it was decided to test the baffled settler on actual commercial plant liquors and the unit was shipped to a commercial uranium solvent extraction plant for these further trials.

TABLE 8. Uranium Solvent Extraction Plant Operating Parameters. Extraction Circuit

Leach liquor feed rate:	2500 litres/minute	
Leach liquor composition:	U ₃ O ₈	0.5 - 0.8 gpl
	Fe ³⁺	1 - 2 "
	Fe ²⁺	1 - 2 "
	Mn	0.7 "
	Al	0.5 "
	Ca	0.7 "
	Total SiO ₂	2 - 3 "
	Rare Earth Oxides	2 "
	P ₂ O ₅	0.3 "
	Total SO ₄	15 - 20 "
Raffinate composition:	U ₃ O ₈	< 0.001 "
	H ₂ SO ₄	5 "
	pH	1.5
Mixer residence time:	22 seconds	
Turbine power factor:	Speed N	= 2.0 to 2.2 rps.
	Diam. D	= 2.896 ft
	N ³ D ²	= 67 - 89
O:A ratio of feed streams	1:5 to 1:7	
O:A in mixer by recycle of organic	to maintain organic continuous conditions 1.2:1 to 1.5:1	
Settler rate:	Aqueous	0.7 to 0.75 lmp g/min/ft ² (3.5. to 38 litres/min/m ²)
	Organic plus aqueous	1.65 to 1.75 lmp g/min/ft ² (83.6 to 88.6 litres/mln/m ²)
Residence time in settler:	Organic	~ 7 - 10 minutes
	Aqueous	~ 100 minutes
Organic depth	~ 450 mm.	
Aqueous depth	~ 3600 mm.	
Solvent	5% Adogen 364 3% Nonanol 92% Kerosene	
Adogen 364 (Supplied by Ashland Chemicals, U.S.A.)	Tertiary amine	95% min.
	Water	0.5% max.
	S.G. at 25°C	0.802
Nonanol (Supplied by I.C.I., Australia)	S. G.	0.827
Kerosene (Supplied by Ampol, Australia)	Flash point	65°C min. 68°C typical
	Boiling point	160 - 230°C
	S.G.	0.820
	Aromatics	15 - 20%
	Viscosity	1.15 to 1.80 cp.
	38°C	1.5 cp typical.

TABLE 9. Uranium Plant Trials — No Baffles in Settler

Total organic plus aqueous flow rate 250 litres/minute
Organic depth = Aqueous depth = 40 cm
Turbine power factor N³D² = 44
Liquor temperature 38°C - 40°C.
Unit operating in parallel to extraction stage E1.

O:A Ratio of Feed Streams	O:A Operating Ratio	Continuous Phase	Emulsion Volume m ³	Entrainment ppm Organic in Aqueous	
1:7.9	3:1	Organic	0.110	88	+480
1:6.5	2:1	"	0.095	56	+480
1:8	1.5:1	"	0.110	24	+480
1:7.9	1:1	"	0.095	40	+480
1:7.9	1:1	Aqueous	0.092	64	384
1:8	1:1.5	"	0.092	400	+480
1:8	1:2	"	0.092	500	+480
1:7.9	1:3	"	0.092	+800	+480

Uranium Solvent Extraction Plant Trials of the Baffled Settler

The uranium SX plant where the plant trials were carried out consists of four extraction stages, one wash stage and three strip stages. The basic operating parameters of the extraction section are given in Table 8. Because of the need for organic recycling, the piping on the baffled settler was modified and was set up as shown in Figure 13. The unit was set up to operate in parallel with extraction stage E1, which was the final organic loading stage and first aqueous extraction stage. For the baffled settler trials, the operating O:A ratio was varied from 3:1 to 1:3 and the unit was operated under both aqueous continuous and organic continuous conditions. The commercial plant has to operate with all extraction stages organic continuous because of the formation of very stable emulsions if the units are aqueous continuous. This was not a problem with the baffled settler during the trials.

The entrainment of organic in the aqueous phase from the extraction stages of the commercial plant was consistently very low and while ranging from about 2 to 90 ppm, typically averaged about 20 ppm. These very low figures were to be expected because of the very deep (~ 3600 mm) aqueous layer in the settlers, whereas entrainment of aqueous in organic was very high, typically in the range 800-1200 ppm but averaging about 1100 ppm. While organic entrainment was not a problem in this plant and the only plant requirement was to reduce organic losses in raffinate, the organic entrainments were important for comparison with the baffled settler performance.

The results at a series of O:A ratios without baffles installed in the settler are shown in Table 9. The entrainments in both phases when operating at the same O:A ratios as in the plant (i.e. 1.2:1 to 1.5:1) were very similar to the plant operating figures. Emulsion volumes were relatively low in all the tests and no coalescing troubles were experienced.

With baffle set I (see Figure 5) installed, the results are shown in Table 10. The emulsion volumes were all higher than without baffles but in no test did the emulsion extend more than 25% down the settler. Entrainment of organic in aqueous phase was consistently low under organic continuous conditions and was not excessively high even at O:A of 1:3. Entrainment of organic in aqueous under organic continuous conditions, while high at 100 ppm, was very much lower than in both the commercial plant (~ 1000 ppm) and the unbaffled settler

TABLE 10. Uranium Plant Trials — Emulsion Volumes and Entrainments with Baffle Set I Installed.

Total organic plus aqueous flow rate 250 litres/minute
Organic depth = Aqueous depth = 40 cm
Turbine power factor N³D² = 44
Liquor temperature 39°C - 43°C.
Unit operating in parallel to extraction stage E1.

O:A Ratio of Feed Streams	O:A Operating Ratio	Continuous Phase	Emulsion Volume m ³	Entrainment ppm Organic in Aqueous	
1:7.9	3:1	Organic	0.240	< 1	95
1:8	2:1	"	0.409	5	165
1:8	1.5:1	"	0.193	< 1	115
1:7.9	1:1	"	0.278	3	88
1:7.9	1:1	Aqueous	0.147	8	90
1:8	1:1.5	"	0.193	16	+480
1:8	1:2	"	0.201	28	280
1:7.9	1:3	"	0.116	40	+480

TABLE 11. Uranium Plant Trials — Emulsion Volumes and Entrainments with Baffle Set III Installed

Total organic plus aqueous flow rate 250 litres/minute
 Organic depth = Aqueous depth = 40 cm
 Turbine power factor $N^3D^2 = 44$
 Liquor temperature 38° - 43°C.
 Unit operating in parallel to extraction stage E1.

O:A Ratio of Feed Streams	O:A Operating Ratio	Continuous Phase	Emulsion Volume m ³	Entrainment ppm Organic in Aqueous in Aqueous Organic	
1:7.9	3:1	Organic	0.219	5	+480
1:6.5	2:1	"	0.219	5	250
1:8	1.5:1	"	0.271	3	40
1:7.9	1:1	"	0.242	5	360
1:7.9	1:1	Aqueous	0.155	5	360
1:8	1:1.5	"	0.210	10	470
1:8	1:2	"	0.170	150	220
1:7.9	1:3	"	0.186	160	320

(+ 480 ppm). Under aqueous continuous conditions the levels were higher than expected but this may have been the result of problems of stable emulsion formation when operating under these conditions. Crud did not build up in the horizontal baffle sets but tended to be carried further down the settler to settle out in the de-entraining zone where it could be easily removed if required. In this case, two of the vertical baffles with the horizontal attachments were not coming into contact with any emulsion and the unit had the obvious ability to handle higher flow rates. Note that at the operating flow rate used in these tests, i.e. 250 litres/minute total flow, the settler flow rate per unit of settler area was about 30% higher than the commercial plant settler E1 with which the test unit was operating in parallel.

With baffle set III (see Figure 7) installed, the emulsion volume and entrainment results are shown in Table 11. The results with this baffle set were not as good as for baffle set I, the aqueous in organic entrainments being markedly higher. When compared to the commercial plant and the un baffled settler, the results were still very good. Crud build-up within the baffle sets was not observed.

For comparison, the tests were also carried out with baffle set V (see Figure 9) and these results are shown in Table 12. While entrainments were at similar levels to those shown in Tables 10 and 11, the emulsion volumes were significantly higher. As two of the vertical baffles with the wide horizontal attachments were short, the emulsion tended to extend further down the settler, usually a little past the midway point to the third vertical baffle with the horizontal attachments, and this was probably the reason for the entrainments being a little higher. It was observed that the lower baffles lead to less turbulence within the emulsion layer, compared to the high coalescence rates per unit volume with the baffle set I, and this in turn could be the reason for the slower coalescence and higher emulsion volumes.

Following the series of tests at the settler flow of 5.87 m³/hr/m² (2 Imp gal./ft²/min.), there was still time to do a few tests at higher flow rates. The flows were set at 8.81 m³/hr/m² (3 Imp gal./ft²/min.), a total flow of 370 litres/minute. The results of these tests are given in Table 13. The flow rate used in these tests was nearly double the flow in the extraction plant settlers. The results for both organic in aqueous and aqueous in organic entrainment were similar to the commercial settler. There seemed to

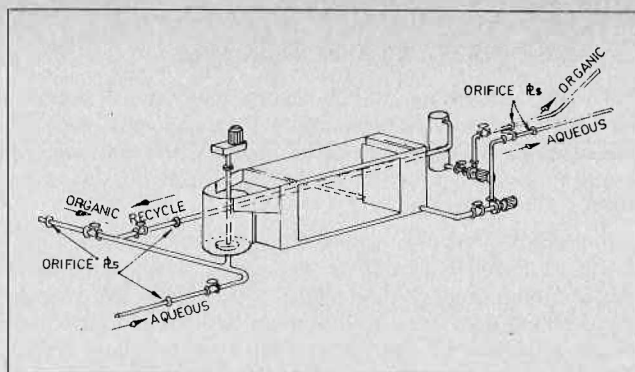


FIGURE 13. Piping arrangement for uranium SX plant trials.

TABLE 12. Uranium Plant Trials — Emulsion Volumes and Entrainments with Baffle Set V Installed

Total organic plus aqueous flow rate 250 litres/minute
 Organic depth = Aqueous depth = 40 cm
 Turbine power factor $N^3D^2 = 44$
 Liquor temperature 38°C - 40°C.
 Unit operating in parallel to extraction stage E1.

O:A Ratio of Feed Streams	O:A Operating Ratio	Continuous Phase	Emulsion Volume m ³	Entrainment ppm Organic in Aqueous in Aqueous Organic	
1:7.9	3:1	Organic	0.380	5	116
1:8	2:1	"	0.323	5	110
1:8	1.5:1	"	0.398	< 1	56
1:8	1:1	"	0.372	5	176
1:8	1:1	Aqueous	0.402	15	+480
1:8	1:1.5	"	0.416	30	+480
1:8	1:2	"	0.282	104	+480
1:7.9	1:3	"	0.275	180	+480

TABLE 13. Uranium Plant Trials — Emulsion Volumes and Entrainments at Higher Settler Flow Rates

Total organic plus aqueous flow rate 370 litres/minute (equivalent to 3 Imp. g./min./ft² settler area)
 Organic depth = Aqueous depth = 40 cm
 Turbine power factor $N^3D^2 = 44$
 Liquor temperature 36°C - 38°C.
 Unit operating in parallel to extraction stage E1.
 Continuous phase - organic

Baffle Set Installed	O:A Ratio of Feed Streams	O:A Operating Ratio	Emulsion Volume m ³	Entrainment ppm Organic in Aqueous in Aqueous Organic	
III	1:7.2	1:1	0.506	8	+480
III	1:8	1.5:1	0.482	16	382
III	1:8	2:1	0.399	24	+480
V	1:8	1:1	0.448	72	+480
V	1:8	1.5:1	0.432	15	+480
V	1:8	2:1	0.455	5	+480

be a requirement for deeper baffles to give better performance, but there was not time available to change the baffles over and do further tests. Deeper baffles would have maintained a deeper emulsion bed in the inlet end of the settler and allowed more settler length available for de-entraining. As it was, the emulsion extended about two-thirds of the way down the settler and the combination of higher flow rates and short settler length clear of emulsion did not lead to very satisfactory results with baffle sets III and V.

Future Programme for the Baffled Settler Test Unit

For the time being, the unit will remain at the uranium SX plant and will be available for further tests and demonstrations as required. Later in 1977 the unit will be tested at a rare earth SX plant. These trials are expected to take 2 - 3 months.

In 1978 the test unit will be returned to Newcastle where it will be installed as one of two strip stages on a 1000 tonne/annum copper SX plant. This plant will recover copper from lead dross by ammonia/ammonium carbonate leaching and the solvent to be used in the SX plant will be the new General Mills reagent XI-54. Copper will be recovered as copper sulphate for use in mineral flotation plants operated by C.R.A. group companies in Australia. In this particular SX plant, entrainment in both organic and aqueous phases from both strip and extraction stages must be kept as low as possible and all settlers will be baffled to maintain these low entrainment levels. The glass-sided settler will allow visual assessment of the baffles and will allow different baffle sets to be evaluated in a continuously operating commercial plant.

Wherever possible, all future testwork of the baffled settler concept will be on commercial SX plants.

Large Scale Installation of the Baffled Settler

It is planned to further develop the system by installation of the baffled settler concept in a proposed copper SX plant at Panguna in Papua-New Guinea for Bougainville Copper Limited. This plant will recover copper from low-grade ore dump leach liquors and the settlers will probably be the largest in the world. The size of the proposed settlers is 33 metres long and 14 metres wide and some details of the baffled settlers can be seen in Figure 14. Because of a large variation in leach liquor flow rates caused by the heavy rainfall (a monthly average of 390 mm/year) at Bougainville, the SX plant is being designed for a basic settler flow rate of just under $4.9 \text{ m}^3/\text{hr}/\text{m}^2$ (2 U.S. gal/ft²/min.) but with the capability of operating at twice the base rate. The use of the baffled settlers should keep entrainment losses very low under normal operating conditions and also allow operation at the high

flow rates without threat of settler flooding or high entrainment losses. If this proposed plant goes ahead on schedule, start up should be early in 1979.

PATENTS

Patents have been applied for in a number of countries.

REFERENCES

- (1) Paige, P.M., Paper presented at Annual Hydromet. Meeting of the Canadian Institute of Min. & Met., Oct. 7, 1975, Ontario, Canada.
- (2) Taylor, J.K. and Skelton, R.L., Paper presented at University of Newcastle-Upon-Tyne Sym. on S X, Sept. 7, 1976.

SYMBOLS

N = Turbine speed, rev/sec.
D = Turbine diameter, feet.

DISCUSSION

C. Hanson: May I confirm your observation that residence-time distribution studies show a wide divergence from plug flow in normal settlers. May I ask whether the particular design of baffle is important? Does it do more than back up the dispersion band as might be done, for example, with a number of picket fences? If the dispersion band depth/specific flowrate relation is linear, as found in our joint project with NCCM, increasing the band depth in the early part of the settler will increase settling rate per unit area. The end of the settler with no dispersion band should then reduce entrainment as little coalescence will be taking place and so there will not be the release of continuous phase at the interface to inhibit sedimentation of any fine droplets.

I.E. Lewis: The particular design of the baffles is important and they do considerably more than just back up the emulsion. The very high coalescence rates within a baffle set can only be achieved if the horizontal or near horizontal attachments are also present. This fast coalescence in the first part of the settler leaves much more settler area free of emulsion and available for de-entrainment purposes than if picket fences or vertical baffles alone were used.

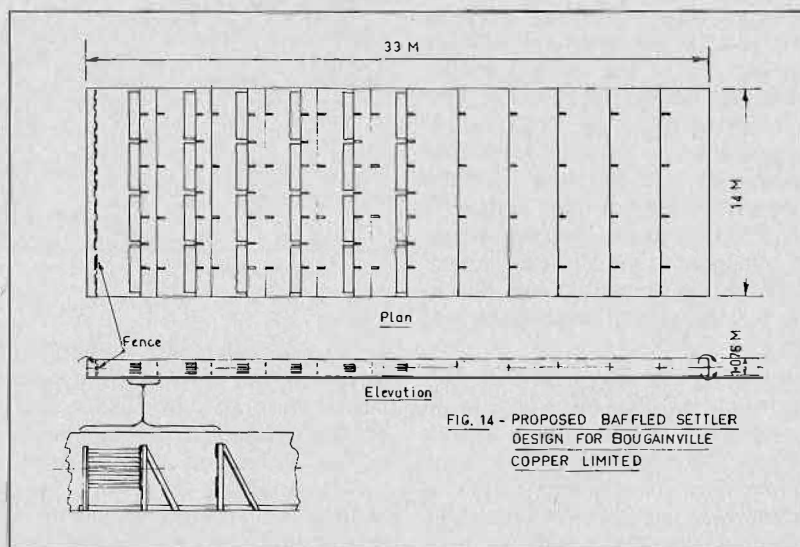


FIGURE 14. Proposed baffled settler design for Bougainville Copper Limited.

E. Barnea: The author had mentioned the development of a method for the accurate measurement of low levels of entrainment of the order of 1-5 ppm. Could he please give some details? The current practice is to measure the make-up required which, obviously, includes losses due to entrainment, solubility, evaporation and leakage and makes it difficult to split responsibility between contractor and plant operators.

While our own development of baffled settlers in IMI (the IMI Compact Settler) was originally aimed at the increase of settlers' capacity we did, more recently, look at its application for the reduction of entrainment as well. Pilot plant tests have shown that the entrainment is reduced exponentially with the number of free baffles between the dispersion band and the discharge port. Readers may be interested to learn that in a new plant that is now to be commissioned (the ERGO plant in South Africa), the last settler in the extraction battery was designed as a compact settler in order to minimize entrainment, instead of using an after-settler.

I.E. Lewis: The technique used for determining the physical entrainments in the organic and aqueous phases is described in the paper. This IMI approach to reduce entrainments and to do away with after-settlers is the same one being followed by C.R.A. Research in Australia.

J. Dollfus: The author seems to have considered only the entrainment reduction by means of introducing baffles in the settling chamber. From our experience, an important improvement can also be obtained by a special design of the impeller, particularly in lowering the amount of thin droplets which are very difficult to remove. Did the author envisage such possibility?

I.E. Lewis: C.R.A. has been financing a university research project where much effort has been put into characterizing the emulsion coming from a mixer and evaluating the effects of different impellers and power inputs. One thing that has become clear is that a baffled settler can very effectively remove even fine haze coming over in an emulsion and the actual mixer performance does not have such a significant effect on the entrainment levels in the liquors leaving the settler.

S. Andersson: How was the dispersion introduced into the settler in your experiments? What type and degree of clarification do you expect to require on the "river" feed stream in the full-scale copper plant?

I.E. Lewis: The dispersion overflowed the mixer and flowed into the settler behind a picket fence. The expected solids content in the feed stream for the full-scale copper SX plant to be installed in Bougainville is 5-10 ppm and no clarification is being planned at this stage.

EQUIPMENT

Cities Service Company's Solvent Extraction-Electrowinning Plant at Miami, Arizona

A.D. Kennedy and C.L. Pfalzgraff,
Cities Service Company

ABSTRACT

Cities Service's SX-EW plant started operation in April 1976. The plant is novel in that the "Low-Profile" concept was used for mixing, allowing construction of the mixer-settlers at ground level. Another unique feature is that the mixer-settlers do not have covers. Start-up problems were minimal, amounting mostly to learning about and tuning up the operation. Design capacity was soon achieved and product quality was outstanding from the initial production. Described are the features of the plant, the design and operating parameters, the product quality, the minor start-up problems, and the test programs for fine-tuning of the operation.

Introduction

THE MIAMI SOLVENT EXTRACTION-ELECTROWINNING PLANT was built to replace a copper precipitation plant in an existing leaching operation. The idea for changing to SX-EW was introduced in 1973 when alternative copper recovery systems were being studied for a proposed dump leaching operation associated with the new mine and concentrator at Cities Service Pinto Valley Operations. After looking at the possibilities, it was decided that solvent extraction-electrowinning was economically feasible for copper recovery at the Miami leaching operation.

History

The Miami orebody was mined by top slicing and block caving from 1910 to 1959. Mining was stopped when ore from the underground draw points no longer contained enough copper for profitable operation. However, the subsidence material above the draw points and the adjoining pillars contained copper values sufficient to encourage efforts to recover it by in-situ leaching. Actually small-scale leaching had been started above some worked out areas in 1941; these efforts were intensified in 1961 after mining had stopped, and the entire subsidence area of about 140 acres was brought under leach by 1963⁽¹⁾. The solution grade was over 2 gpl to start, but dropped to less than 1 gpl over a period of years.

In 1973-74 a core drilling program in the mine subsidence area was undertaken to prove the leaching ore reserves necessary to justify the SX-EW project. In addition, feasibility studies were made by Cities Service and outside engineering firms, and General Mills Chemicals Company conducted laboratory studies to determine if solvent extraction could be applied to the Miami leaching operation. The result of these studies was the decision to build the Miami SX-EW plant.

Plant Concepts and Design

As with all new plants, one objective for design was to build the best possible plant at minimum capital expense. This can be done by limiting the facilities to be

built and by incorporating new technology where appropriate. Both concepts were used for the Miami plant.

The first step taken to keep costs down was to minimize the number of mixer-settler stages in solvent extraction. Evaluation of test work by General Mills Chemical Company showed the optimum economic configuration to be three extraction and two stripping stages. The plant was built with two trains of this configuration, each handling half the feed.

Using new technology to reduce capital costs introduces a certain amount of risk. In this instance, the Holmes & Narver "low-profile" mixer⁽²⁾ was considered technically feasible and would result in a substantial saving by eliminating the support structure for the settlers as well as most catwalks, platforms, and handrails.

The low-profile concept is based on recognition that plug flow prevails in the mixer section. This means that after the initial mixing, the remainder of the mixer residence time is for organic-aqueous contact and that contact time can be achieved by horizontal flow in a channel as well as by vertical flow in a tank. One benefit of doing this is that there is less pumping function required of the pumping mixer which means less power input. While this power savings is not economically significant, the lower pumping energy input should result in lower entrainment losses, or additional low-shear mixing energy can be added downstream with no increase in entrainment losses⁽²⁾.

The mixer-settler units were built partly on cut and partly on fill. In order to minimize the chance of acid and organic leaks and spills, the mixer-settlers were built of concrete and lined with stainless steel. The stainless steel liner gave the greatest protection against costly spills at no extra cost over other liner materials considered. Figure 1 is a diagrammatic representation of the SX plant.

Mixing times were set at three minutes in each stage except the S-1's which were set at six minutes because of the greater copper transfer requirement in those mixers. The additional mixing time was achieved by doubling the length of the low-profile mixing channel. Each mixer section had one primary pumping mixer and a smaller secondary mixer for additional mixing energy input. The one exception to this was one E-3 which had three variable speed secondary mixers for test work.

A third step to decrease capital costs was a decision to omit roofs on the mixer-settlers. No technical reasons could be found to require the roofs, and investigation showed there should be little or no harmful effect from exposure to the weather. There was an added benefit to leaving the roofs off, which is that all areas of the mixers and settlers are open for visual inspection.

In the tankhouse, the primary consideration was to produce a high quality cathode at the lowest cost. By using a high current density for electrowinning, the size of the tankhouse could be decreased, resulting in a lower capital investment. With careful control, there should be no deterioration of cathode quality at the design current density of 21.2 amps per square foot.

The major significant contaminant in electrowon cathodes is lead from the anodes. In order to control this, the anodes selected were calcium-lead, and cobalt was added to the electrolyte at a concentration of 40 ppm before electro-winning was started. This combination resulted in very good quality cathodes from the start, eliminating the problem of what to do with off-grade cathodes produced during start-up.

Plant Construction and Start-up

The Miami SX-EW project was divided into seven phases which were⁽³⁾:

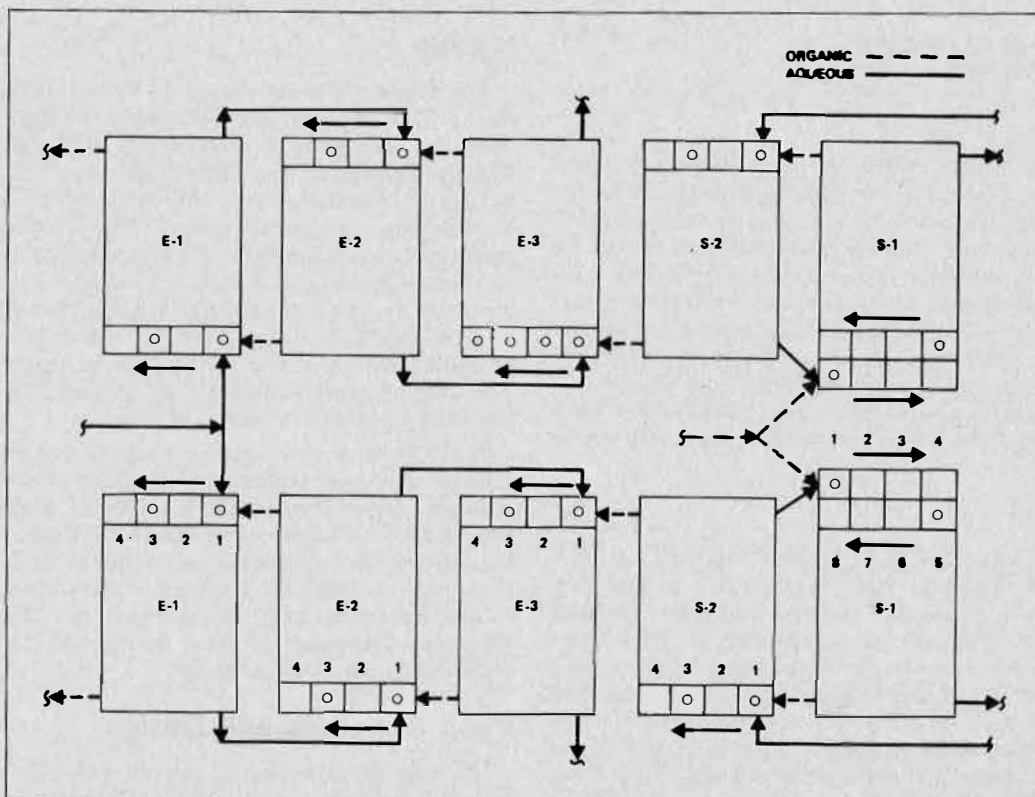


FIGURE 1. SX plant diagram.

1. Planning
2. Preliminary Engineering
3. Review
4. Detail Engineering
5. Detail Engineering/Construction Overlap
6. Construction
7. Start-up

In order to establish a time frame, certain milestones are listed below:

- September 1974 — Complete preliminary engineering and budget study
- November 1974 — Start detail engineering
- May 1975 — Start construction
- February 1976 — Start plant checkout
- March 1976 — Fill circuit with organic, electrolyte and leach solution
- April 29, 1976 — First cathode production
- July 1976 — Full production achieved

As Cities Service had no prior experience on this type of plant, special consideration was given to ensure satisfactory start-up and operation. First, a detailed start-up and operating manual was prepared. This served as a useful learning tool as well as a guide for start-up and early operation. Second, supervisory personnel visited operating SX-EW plants in Arizona (Cyprus Bagdad, Cyprus Johnson, and Ranchers Bluebird) in order to learn operating procedures and to better understand operating problems. Third, classroom sessions were held for supervisory personnel to explain the fundamentals of solvent extraction and electrowinning. Also at these sessions, there was discussion on unique features in the Miami plant and a trading of ideas and observations from the visits to operating plants. This program prepared our people to start the plant when it was completed, and was instrumental in achieving an unusually smooth start-up. Nevertheless, a few minor problems did arise.

There are always the little leaks which cannot be detected until a plant is placed under operating conditions. In the Miami plant, these leaks were detected when acid solutions and organic diluent were put into the pipelines and mixer-settlers. These facilities had been water, vacuum and dye tested and no leaks found, but operating conditions quickly pointed them out.

Another problem was that some of the stripper impellers fell off the shafts soon after the acid strength was build up in the electrolyte. It was found that not all of the impeller set screws were 316 stainless steel as specified; these screws had to be replaced.

Another situation which arose during start-up dealt with the mixer design. As originally conceived, the emulsion would move down the channel by overflowing and underflowing successive transverse baffles⁽²⁾. It was soon found that there was not enough freeboard to accommodate both the rise in head from the baffles and the mixing turbulence; some emulsion slopped over the sides of the mixing compartment. To prevent emulsion from slopping over, every other baffle was removed. This was a minor job, but it still leaves unanswered the question of how the mixers would perform as originally designed.

The most serious problem encountered during start-up was with the rectifier transformers in the tankhouse. There was no practical method to test this equipment until it was ready to be used under actual operating conditions and of course, this was the part of the plant which failed to work properly when needed. The problem was inadequate cooling, which caused the transformers to overheat and fail. Work by field crews and vendor representatives corrected the problem but not before it led to other complications. Solvent extraction was already in operation.

TABLE 1. Operating Parameters, Miami SX-EW Plant

	Design ⁽²⁾	Actual 1st Quarter 1977
Pregnant Leach Solution Flow	3000 gpm	3000 gpm
Pregnant Leach Solution Grade	0.95 gpl Cu	1.05 gpl Cu
Electrolyte Advance	125 gpm	140 gpm
O/A Ratio	1:1	1.1-1.2:1
Settler Area	1.85 gpm/sq ft	2.0 gpm/sq ft
LIX64N Concentration	4.5%	6.0-6.5%
Cathode Production	30,600 lb/day	33,000-34,000 lb/day
Electrowinning Current Density	21.2 amps/sq ft	25-30 amps/sq ft

When the rectifier transformers failed, there was an imbalance because copper was being extracted but was not being removed in the tankhouse. Some copper was extracted in the old cementation plant and some solution was bypassed, but these actions were not sufficient to prevent the copper concentration in the electrolyte from rising to the saturation point and precipitating copper sulfate in settlers, pipelines, and tanks. Some time was lost in redissolving copper sulfate in the smaller lines and re-establishing normal flows. After the problem with the rectifier transformers was solved, the plant was restarted and soon reached full production.

A problem associated with gaining experience in the plant presented itself when the iron concentration in the electrolyte became too high. This was the result of two mistakes: The LIX64N concentration in the organic was too high, which increased iron transfer to the electrolyte; and the iron bleed was not operated to maintain a safe level of iron in the electrolyte. The most serious effect of the high iron concentration was that, combined with high temperatures, it attacked the cathodes suspension loops and caused cathodes to drop in the electrowinning cells.

Even with these problems, it was considered a very smooth start-up for a new plant.

Plant Operation

There were changes in leaching operation between the time the plant was designed and the time the plant was built. These changes included using the exploratory drill holes in the subsidence area to inject part of the leach solution, and increasing the acid concentration of the leach solution. The result was a higher grade feed to solvent extraction than originally predicted. This was not a problem since solvent extraction was designed to handle a fixed flow, not a fixed grade. The situation was easily handled by increasing the LIX64N in the organic and increasing the current density in the tankhouse to correspond to the increase in copper.

A comparison of design and operating parameters is shown in Table 1. All of the changes, except the O/A ratio, were made because of the higher feed grade. The O/A ratio was determined by how to most easily run the plant and maintain the proper continuous phase in each mixer.

While results have been good, there is still room for improvement. The recovery in solvent extraction has been about 88-90%, but with improved mixing, a recovery of 93-94% should not be unrealistic.

The cathode quality has been very good from the start. Analyses of individual cathodes on September 7, 1976 and December 21, 1976 are shown in Table 2. These analyses are typical of the cathodes produced in the Miami tankhouse.

Another item of interest is the loss of organic. In the first few months there was a relatively high loss of the diluent, probably because of evaporation. There has also been some relatively small loss of organic to the ground because of spills. Total organic addition from startup to December 31, 1976 was equivalent to 108 ppm organic loss, with the losses having an apparent LIX concentration of 4% versus 6% actually in use. These losses include all spills, evaporation, and entrainment. Starting in August 1976, we have added make-up on the assumption of 50

ppm losses and have not been able to measure any change in our plant inventory. The information gathered during 1977 should give a much clearer picture since it will be continuous operation with less chance of interruptions or organic spills.

The very nature of solvent extraction and electrowinning presents certain problems. In solvent extraction, the most serious continuing problem is "gunk", the sludge layer that builds up at the interface in the settler. If gunk is not removed, it will eventually move with the organic from one mixer-settler to the next, carrying entrained aqueous. This can have a serious effect on the chemical balance of the circuit if the transfer of aqueous is significant.

In the Miami plant, the gunk collects primarily in the E-1's and the S-1's, and these are the settlers where most of the work has been done to remove it. Two methods have been used; one using a slotted collector pipe at the interface connected to a pump to transfer it to a holding tank for further processing, and the second using a screen basket attached to a crane to dip the gunk from the settlers. Neither of these methods is entirely satisfactory; the first requires very close attention to keep gunk, rather than organic or aqueous, going to the collector pipe, and the second method stirs up the gunk and causes it to move from one mixer-settler to another. After the gunk is removed from the circuit, it must be treated to recover the organic it contains. One common practice is to centrifuge the gunk to separate the solids and aqueous from the organic. This has been tried in the Miami plant, but to date a satisfactory separation has not been made between the solids and the organic.

One problem from not having settler roofs is wind, which causes a wave action on the organic surface and stirs up the gunk at the interface. Usually this is not serious, but it can increase the movement of gunk enough to affect recovery by carrying electrolyte from stripping to extraction.

There is some organic carried into the tankhouse with the electrolyte. This has been a decreasing problem since startup, but one which has had an interesting impact on plant operation. The pregnant electrolyte first passes through the starter cells where the combination of higher temperature and oxygen bubbles generated at the anode brings the organic to the surface. At this point, the organic can be skimmed from the electrolyte before it goes to the commercial cells. In February 1977, the emulsion in the S-1 mixers was changed from organic continuous to aqueous continuous to determine the effect of higher aqueous

TABLE 2. Cathode Analysis

	Sept. 7, 1976 Sample	Dec. 21, 1976 Sample
Cu%	99.98	99.98
Pb ppm	3.7	1.3
Fe ppm	2.8	3.2
Ni ppm	1.5	1.3
Sb ppm	1.6	1.3
As ppm	< 1	< 1
Se ppm	< 10	< 10
Te ppm	< 1	< 1
Bi ppm	< 0.1	< 0.1
Sn ppm	< 2	< 2
Au ppm	< 1	< 1
Ag ppm	< 1	< 1
O ₂ ppm	105	95
S ppm	11	31

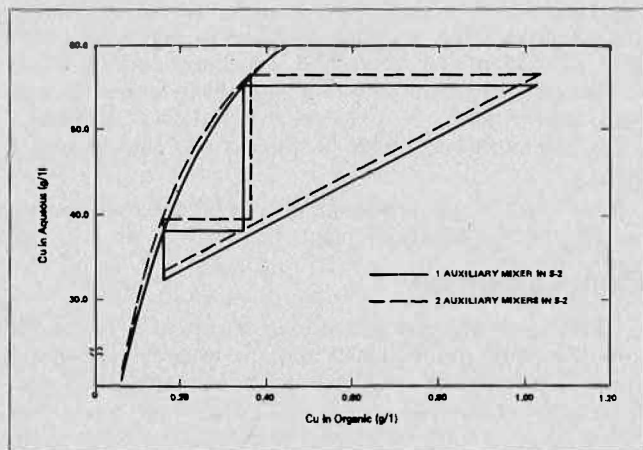


FIGURE 2. Stripping

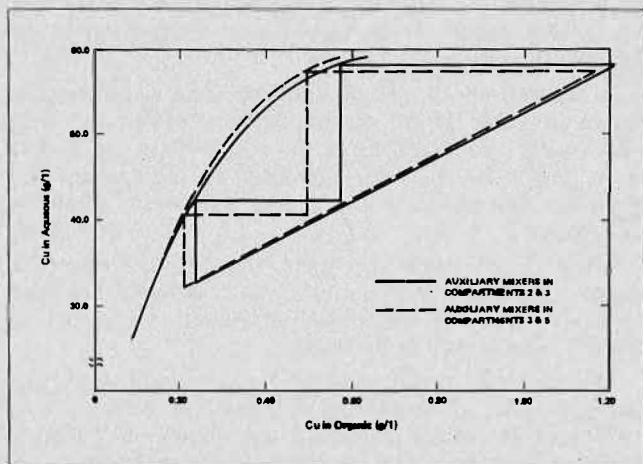


FIGURE 3. Mixer locations in S-1.

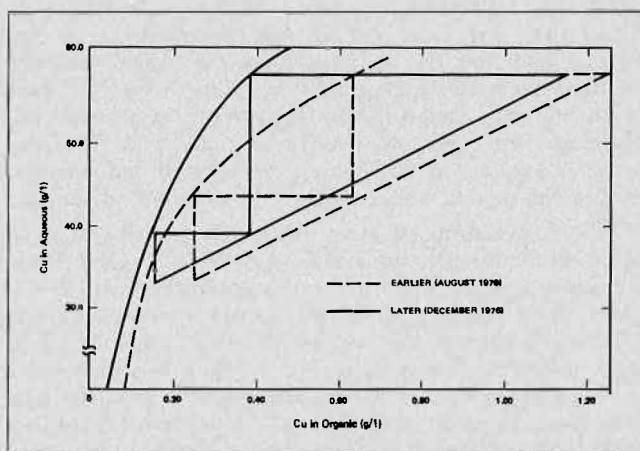


FIGURE 4. Stripping.

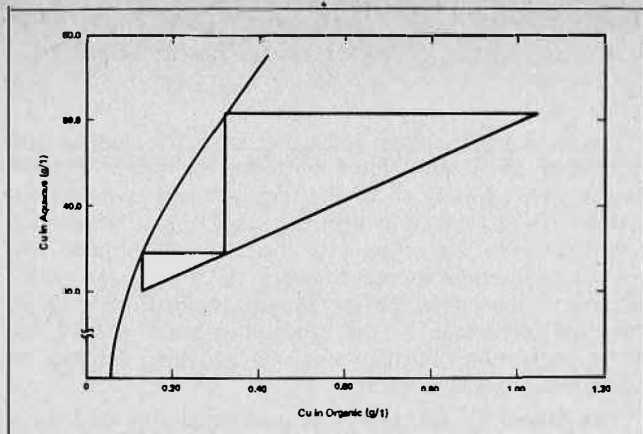


FIGURE 5. Stripping — March 1977.

ous recycle and the continuous phase on copper transfer. When this change was made, there was a noticeable decrease in the amount of organic entrainment going to the tankhouse. This finding is contrary to the idea that organic continuous mixing is necessary to produce a clean aqueous discharge at the weir. In this instance, there was both an increase in copper transfer, due to the higher recycle, and a decrease in organic entrainment in the electrolyte.

The most serious problem in the tankhouse has been corrosion due to the acid mist. Demisting balls are used on the commercial cells and removeable covers are used on the starter cells to control acid mist at a reasonable level. Repairs and changes on the tankhouse have been necessary because of concentrations of acid mist, especially around the ventilating fans. Another change has been to remove the solid floor around the cells and replace it with fiberglass grating to improve airflow at the tops of the electro-winning cells.

Test Work

After the startup problems have been solved, there is some fine tuning necessary in a new plant to achieve the desired efficiency. This is especially true in a plant using new technology as is the case with low-profile mixing in the Miami plant.

After a short period of operation, it was determined that the extraction portion of the plant was doing a very good job with the stripped organic which was being produced. However, the stripping section was not doing its job well enough to give the desired overall results. The problem was insufficient mixing to maintain an emulsion throughout the mixing compartments. In order to correct this situation, it was necessary to move auxiliary mixers from extraction to stripping. After starting this program, it was obvious that some routine procedure to measure progress would be needed. For that reason, a sampling procedure was established to obtain a complete copper profile of each train every day. The reason for taking a complete profile was that all parts of the plant are interconnected and a change in one mixer affects the performance of other mixers.

While working with the auxiliary mixers, several important parameters became readily apparent. These were:

1. Number of mixers in the mixing channel,
2. Location of mixers in the mixing channel,
3. Liquid depth to the impellers, and
4. Mixer speed.

Items 3 and 4 were mainly limiting conditions. Locating the impeller higher in the channel and running at faster

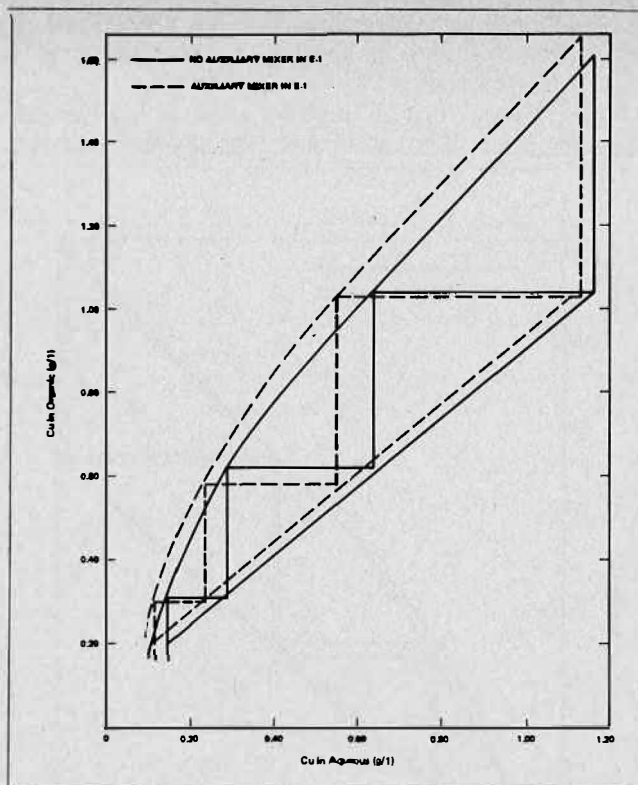


FIGURE 6.

speed produced better mixing but also caused vortexing and splashing. The controlling factors were the limiting speed for the mixer gear boxes and the minimum impeller liquid cover to prevent vortexing and splashing.

Figure 2 shows the effect of changing the number of auxiliary mixers in one of the S-2 mixers. In this case, the S-1 was doing such a good job of stripping the organic that there was little change observed in the results from the S-2 when comparing data while running one or two auxiliary mixers in the channel.

Figure 3 shows the effect of mixer location in the channel. In the first case (solid line) there were auxiliary mixers in the Nos. 2 and 3 compartments, and in the second case (dotted line), there were auxiliary mixers in the Nos. 3 and 5 compartments of the S-1. The second case shows much better copper transfer in the S-1, which resulted in lower stripped organic from the S-2. This was a good comparison of intense mixing near the feed end of the mixing channel (first case) and more uniform mixing throughout the length of the channel (second case). Later, a third auxiliary mixer was added to the S-1 which further improved stripping.

In order to demonstrate the progress made in stripping, Figure 4 shows typical stripping isotherms from plant data in August and December, 1976. Figure 5 shows the stripping isotherm for March, 1977 at different operating conditions. Two observations can be made from these graphs: as work progressed, more of the stripping was being done in the S-1, and better mixing has resulted in a lower copper content in the stripped organic. The improved stripping did show up in extraction by decreasing the copper content of the raffinate.

In extraction, the improvement has not been nearly as dramatic as in stripping. Figure 6 shows the effect of adding an auxiliary mixer to the E-1. There is significant improvement in the copper transfer in E-1, but this is not carried through the E-2 and E-3 mixers. In fact, the

decrease in copper in the raffinate is just about equal to the decrease in copper in the feed for the data periods before and after putting the mixer in the E-1.

Figure 7 shows that an auxiliary mixer in E-2 has just about the same effect as in E-1. The changes here are

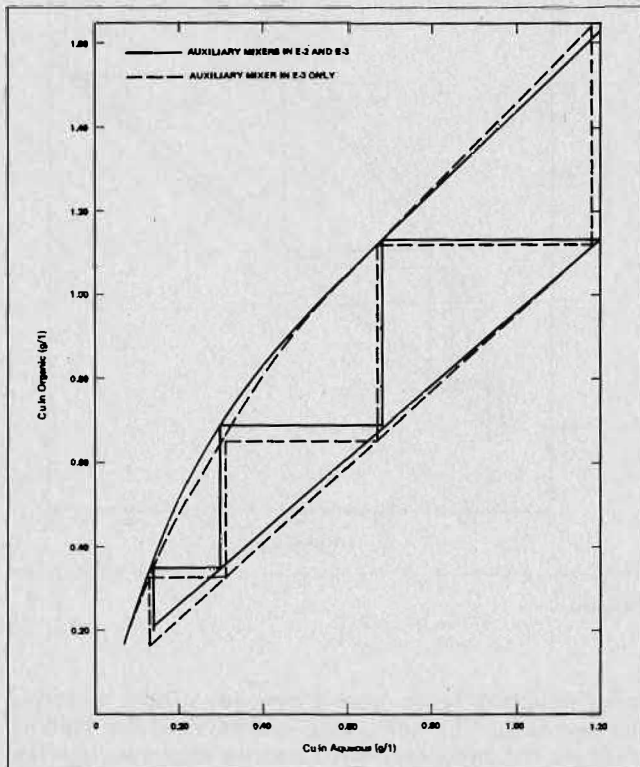


FIGURE 7.

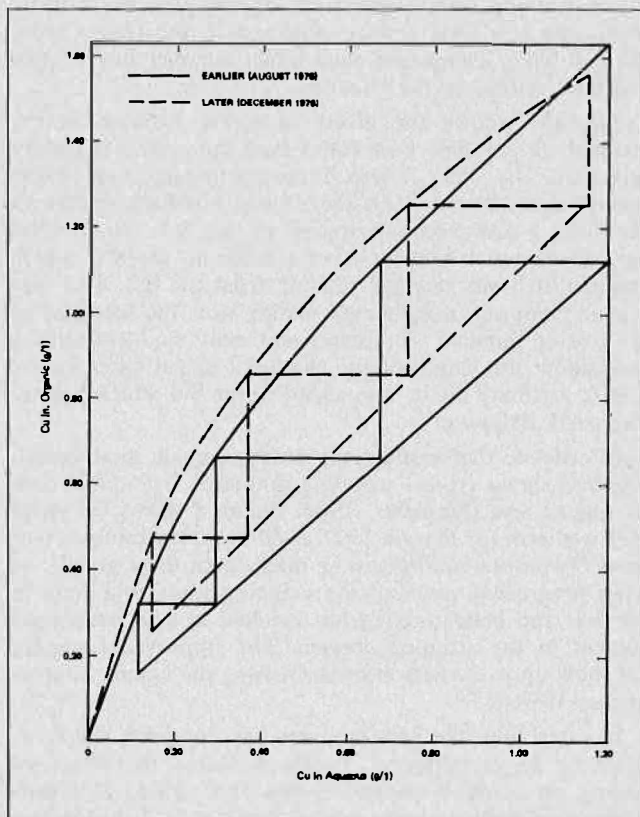


FIGURE 8. Extraction.

smaller because there is less copper transfer in E-2 than in E-1. The slope of the operating line is different for the two data periods because of a change in the O/A ratio.

Figure 8 shows plant extraction data for August and December 1976 and Figure 9 shows the same data for March 1977. Nearly all of the improvement in extraction is due to improvement in stripping since mixers were being removed from extraction. As the stripped organic improved, extraction started to work on a more favorable portion of the curve. Further improvement in mixing, to take full advantage of the stripped organic, should improve extraction. Further work is awaiting delivery of additional auxiliary mixers.

The Miami SX-EW plant has performed very well for a new facility. The low-profile mixing concept does work and results should improve as more information is gathered about mixing optimization.

Acknowledgement

The author wishes to acknowledge the cooperation of Cities Service Company's management in presenting this paper. Individuals participating in or rendering advice on the technical aspects of the studies include: Wayne Jensen and Brant Sudderth of General Mills Chemicals, Inc.; P. M. Paige of Holmes and Narver, Inc.; and N. B. Gillespie and B. M. Frazier of Cities Services Company.

REFERENCES

- (1) Fletcher, J.B., In-Place Leaching — Miami Mines, 1969.
- (2) Paige, P.M., Selected Equipment Modifications, Solvent Extraction and Electrowinning, Presented to the Annual Hydrometallurgical Meeting, Canadian Institute of Mining Metallurgy, October 7, 1975.
- (3) Bennett, W.A. and Kontny, V.L., The Cities Service SX-EW Project Story, Presented to the Arizona Conference of the American Institute of Mining Engineers, December 6, 1976.

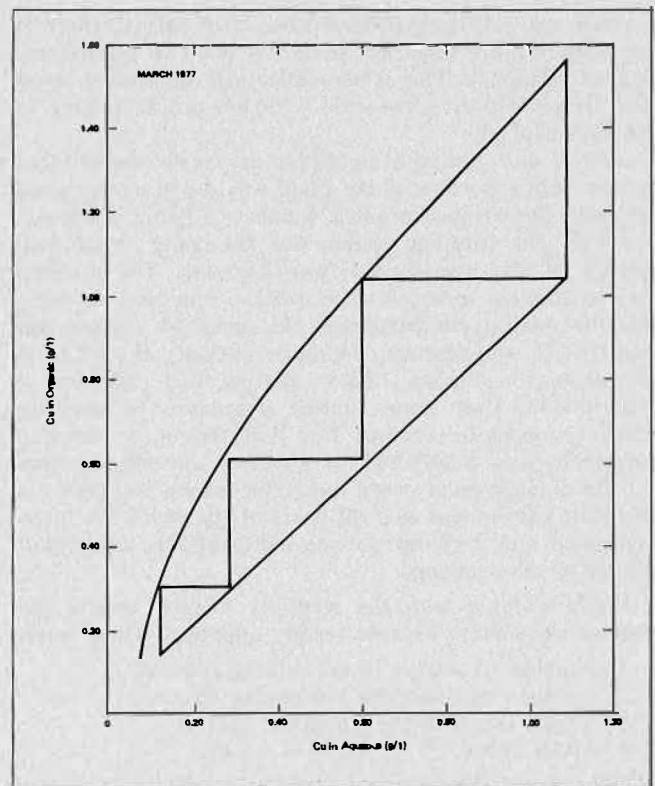


FIGURE 9. Extraction — March 1977.

DISCUSSION

J.R. Orjans: It has been suggested that one of the reasons why baffle arrangements in settlers reduce the entrainment is their flow straightening action. We in Zambia are concerned about dispersion distribution and eddies in our nearly quadratic settlers. Did you, during start-up when operating without LIX in the circuit and having the advantage of operating without roofs, observe the flow pattern in your settlers? If so, what was your flow pattern?

A.D. Kennedy: The flow pattern of the dispersion band, as observed before the addition of LIX, was perpendicular to the picket fence rather than parallel to the side walls. Since the picket fence is at a slight angle to the sidewalls, there is a slight eddy current. We considered putting in a second picket fence parallel to the sidewalls to straighten the flow, but decided the benefits were not worth the effort.

We believe the picket fence could be designed to straighten the flow. This would require the picket fence slots to have the edges perpendicular to the flow axis of the settler.

S. Andersson: What is your dispersion depth in the settlers and the height of clear organic phase?

A.D. Kennedy: At the picket fence or feed end of the settler, organic and dispersion band depths have been observed as follows:

	Depth, Inches	
	Clear Organic	Dispersion
No Auxiliary Mixers in Operation	7 to 8	2
With Auxiliary Mixers in Operation	7 to 8	6 to 7

Midway down the length of the settlers, the clear organic is 8 to 9 inches in depth and the dispersion band is zero to one inch in depth, regardless of auxiliary mixers. There is no dispersion band at the discharge weir, but a variable depth gunk layer is present.

R.J. Fiocco: In your summary you indicated that several methods to remove the sludge layer which builds up at the interface in the settler have been tried with little success to date. Please give more information on the methods tried, particularly the type and performance of the centrifuge technique used.

A.D. Kennedy: Sludge or "gunk" has been removed from the E-1's on a daily basis since May 1977 using the header pipes as installed. This is apparently enough to control the gunk generated by the very clean PLS feed in the Miami plant.

The centrifuge is a Dorr-Oliver Merco with three product streams: light phase, heavy phase, and nozzle separation of organic and solids, typically leaving 0.5-2.0% charge of solids. The centrifuge does not make a good solids in the organic returning to the circuit.

C.C. Lui: How is your organic loss, especially during the summer season for the extraction and stripping circuits?

A.D. Kennedy: Total organic loss is equivalent to approximately 50 ppm of the flowrate. There is insufficient data to determine seasonal variations, but they are not a significant factor in considering organic make-up. Other factors such as changes in feed grade are more important.

I. Noble: I would like to amplify Mr. Kennedy's statement on picket fence geometry. Wright Engineers have recently completed the start-up and commissioning of the Cerro Verde Plant in Peru. In the design of the SX Plant, we incorporated a second picket fence midway down the length of the settler. During the first month of operations, the dispersion band, which could be 1 to 1½ inches in width between the first and second fences, was almost non-existent between the second fence and the overflow weir. It may therefore be the case that complicated baffle systems are not necessary to reduce or eliminate the dispersion band in large-scale settlers.

A.D. Kennedy: Thank you for your comment. It reinforces our opinion that our plant has about twice as much settler area as is needed.

P.J. Lloyd: The height of the aqueous discharge weir is critically dependent on the relative depths of aqueous and organic phases. With large-area, open, shallow settlers such as you describe, it would be expected that wind action over the open settlers would affect the relative depths and the resultant coupling could lead to marked surging in flow over the aqueous weir, even to the point of discharging organic through that weir. Have you observed such a phenomenon, and would you recommend open settlers in general, under similar climatic conditions to your own?

A.D. Kennedy: Wind does cause some surging action, but these are very small changes when compared to total flow. The most serious problem due to wind is that the wave action stirs up the gunk layer and causes it to move. The result is usually lower total extraction until the gunk layer settles down. Lower extraction is caused by carryover of some electrolyte entrained in the gunk into the final stage of extraction.

We would recommend open settlers under climatic conditions similar to ours. However, we would recommend that the freeboard on the settlers be increased to about 16 or 18 inches.

The Design of Mixer-Settlers for the Zambian Copper Industry

J.R. Orjans, C.W. Notebaart,
Research and Development Nchanga Consolidated Copper
Mines Ltd., and Roan Consolidated Mines Ltd., Kitwe, Zambia.

J.C. Godfrey, C. Hanson, M.J. Slater,
Schools of Chemical Engineering, University of Bradford,
Bradford, West Yorkshire, England.

ABSTRACT

Experimental work has been conducted in laboratory, pilot plant, and commercial-size mixer-settlers with a view to improving existing operations in the Tailings Leach Plant in Chingola, and establishing a basis for design of an expansion of this plant. A number of general conclusions concerning mixer-settler design principles have been established. The design of the new mixer-settlers is discussed in the light of the testwork results.

Introduction

THE USE OF MIXER-SETTLERS in continuous liquid-liquid extraction processes dates back to the beginning of this century. A two-stage mixer-settler unit, which maintained gravity flow of both phases by level differences was used by Barstow; the Holley unit had additional control of interstage flows by valves. These and other types, used to about 1950, are reviewed by Morello⁽¹⁾. In a later design, the Windscale contactor, used in the uranium purification process⁽²⁾, flows also depend on gravity. In order to overcome the disadvantage of large organic depths, required in gravity flow mixer-settlers, various types of pumping arrangements, either internal or external, have been introduced for interstage transfer of the phases. The "pump-mix" mixer-settler was developed by Coplan et al⁽³⁾ in 1954. Large-scale mixer-settlers were first employed for the recovery of uranium from leach solutions in the early 1950's. In these plants both pump-mix systems and external pumping were applied⁽⁴⁾. The settlers in these plants are generally of the conventional gravity type, either rectangular or circular in shape. Only recently, new settler designs have been developed and applied industrially by I.M.I.⁽⁵⁾ and Lurgi⁽⁶⁾. In these settlers various types of physical aids have been introduced to increase the capacity.

Extensive studies on the performance of the Windscale mixer-settler and scale-up procedures have been conducted by Lowes et al⁽²⁾. The classical study of scale-up procedures by Ryon and co-workers⁽⁷⁾, relating to uranium extraction from leach liquors, is still used as the basis for mixer-settler design.

The application of solvent extraction in the copper industry began with the development of the LIX extractants by General Mills Inc. The first commercial plant using LIX 64N was designed and built by Bechtel for Ranchers Corp. at Bagdad, Arizona⁽⁸⁾, and commenced operation in 1968. Davy Powergas Limited in conjunction

with NCCM Ltd. introduced new concepts in mixer design for the Tailings Leach Plant, Chingola, Zambia which was commissioned in 1974^(9,10). The most recent development in mixer-settler design for the copper industry is the Holmes and Narver Inc. low profile mixer-settler⁽¹¹⁾, used in the City Services plant in Arizona. The use of multi-compartment mixers in this design offers two advantages: firstly, conditions approaching plug flow are achieved in the mixer, and secondly, due to the reduced mixer depth, elevated settlers can be avoided.

During the two years of operation of the Chingola Tailings Leach Plant it became evident that, although overall performance was very satisfactory from an economic point of view, considerable scope existed for improvement. With a future expansion of the Tailings Leach Plant in mind and in view of the possibility of applying the leach-solvent extraction route also to the treatment of other oxide orebodies in Zambia, it was decided to continue operation of the solvent extraction pilot plant at Chingola⁽¹⁰⁾ to widen the general knowledge of copper solvent extraction and in particular to develop and improve mixer-settler design and scale-up procedures. Concurrently, NCCM Ltd initiated a co-operative research project with the University of Bradford, England, to study the chemistry of the LIX 64N system and mixer-settler design.

Design of the Tailings Leach Plant expansion, designated Stage III, is now in progress. An additional 700,000 tonnes of tailings per month, reclaimed from the existing dams, will be treated.

The proposed solvent extraction circuit consists of three streams, each treating a maximum of 0.28 m³/s (1000 m³/hr) of pregnant liquor. From experience gained in the operation of the Tailings Leach Plant, three major areas in mixer-settler design requiring further study were identified:

(i) Stage Efficiency

The stage efficiencies in the solvent extraction circuit are low, in the region of 80 - 90%, and significantly lower than those in the pilot plant, in spite of a 10°C higher operating temperature in the commercial plant. This necessitated a critical assessment of the scale-up criterion of constant tip speed used in the design of the Tailings Leach Plant.

(ii) Phase Stability

In order to minimize entrainment, it is necessary to operate with organic phase continuity and to ensure stability against phase inversion. During aqueous continuous operation, entrapped air tends to float dispersion fragments up into the organic phase, resulting in a high rate of carry-over of leach liquor impurities and solids from the dispersion band into the electrolyte circuit. This phenomenon has not been observed when operating in the organic continuous mode. Previously, it has been generally accepted

that mixer-settlers should operate with organic phase continuity in order to minimize organic in aqueous losses. It is interesting to note, however, that contrary to this belief, the organic in aqueous entrainment levels in pilot plant and full-scale operations are not higher for aqueous phase continuity than for organic phase continuity, and may in fact be somewhat lower.

Organic phase continuity has been found difficult to maintain in the Tailings Leach Plant mixers at a phase ratio of 1:1. It would be necessary to operate at phase ratios higher than 1.2:1 to prevent phase inversion to aqueous continuity. This, however, is difficult to achieve mainly due to pumping and piping restrictions. The presence of significant quantities of suspended solids (gangue minerals and gypsum) in the aqueous phase could be a contributing factor to the phase stability problems experienced.

(iii) Settler Capacity

Because of the difficulty in predicting operating temperature, and the uncertainty regarding the use of specific throughput as a scale-up criterion for settlers very much larger than any in operation at that time, the Tailings Leach Plant settler design was conservative. This resulted in considerable settler overcapacity and, as a consequence, dispersion bands are wedge shaped. When operating in the organic continuous mode the dispersion band in the extraction settlers extends only over approximately two thirds of the settler length. Under aqueous continuous conditions the dispersion band covers less than half of the extraction settler area.

Extraction and Mixing Studies

Having established the critical areas, the objectives for an extensive mixing and extraction study could be defined: (a) determination of maximum stage efficiencies compatible with acceptable entrainment levels, (b) establishing the requirements for maintaining organic phase continuity, and (c) a critical comparison of the two commonly used mixer scale-up criteria: constant tip speed and constant power input per unit volume.

Observation of small mixers suggested that phase inversion is initiated in areas of low intensity of agitation. It seemed therefore that configurations in which power is more evenly distributed throughout the mixer volume, than is the case in the existing pump-mixer designs, were to be preferred. As a consequence it was decided at an early stage to investigate a mixer configuration in which the mixing and pumping functions of the impeller were separated.

A turbine impeller with six flat blades was chosen for comparison with the single and double shrouded turbines, which have been employed in copper solvent extraction plants. This turbine, extensively studied by Rushton⁽¹²⁾, has been used in solvent extraction, although not in copper systems. The experimental work was conducted in tanks of square cross section with and without baffles. Four tank sizes were used:

- a 3.5 l laboratory mixer in which the effect of impeller size, baffle arrangement and phase inlet configuration on stage efficiency, entrainment and stability against phase inversion were studied.

- a 20 l and a 780 l mixer, operating in parallel on leach liquors from the pilot plant, in which power correlations were determined and scale-up criteria compared.

- an 8000 l mixer, in which power correlations and vortex formation were studied in the absence of mass transfer.

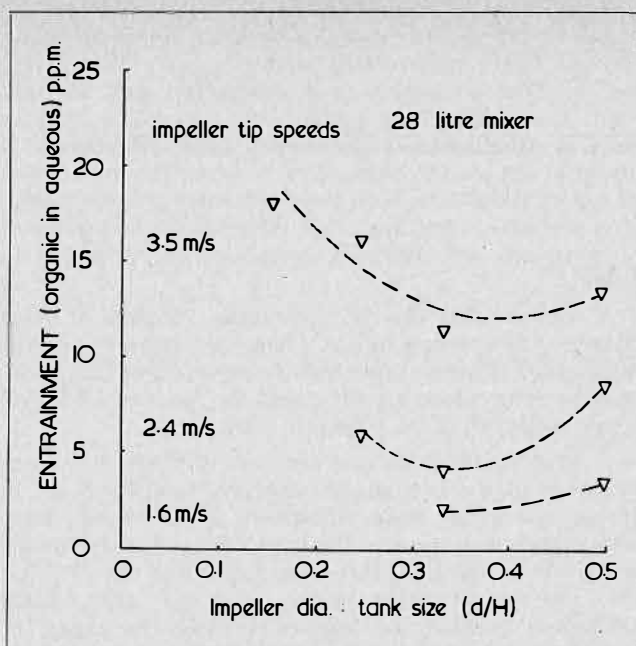


FIGURE 1. Entrainment and impeller: tank ratio.

TABLE 1. The Effect of Impeller Diameter on Extraction Efficiency

Impeller size (cm)	Impeller speed rpm	Stage efficiency* %
5.1	1250	87
7.6	833	85
10.2	625	85

In work involving mass transfer, copper was extracted from aqueous solutions containing sulphuric acid by a solvent comprising LIX 64N in Escaid 100, usually at a concentration of 20% by volume and at ambient temperature. The experiments were carried out under conditions of aqueous phase continuity and mostly at a phase ratio in the dispersion of 1:1. Measurements of entrainment and phase stability in the 3.5 l mixer were made in the absence of mass transfer using 20% LIX 64N and water containing 2 kg/m³ of sulphuric acid.

Extraction Characteristics

A series of batch extraction tests was conducted in the 3.5 l square tank, using a range of impeller sizes (5, 7.5, 10 cm) and impeller speeds; the findings were checked in continuous flow. It was found that at a constant tip speed the stage efficiency is independent of impeller size (Table 1). On the other hand organic in aqueous entrainment, at constant tip speed, varied with impeller diameter, showing a decrease with impeller size down to an impeller diameter/tank side ratio of 1:3 (Figure 1). A further decrease in impeller diameter gave increased entrainment levels. It is interesting, therefore, to note, that the generally accepted practice of employing an impeller diameter of one third of the tank diameter, seems to correspond with the optimum with respect to entrainment generation.

Scale-up criteria for extraction were examined by comparing the performance of the 20 l and 780 l mixers, operating in parallel on pilot plant liquor. Aqueous feed conditions varied over a wide range, which was partly due to deliberate changes in the leach circuit operating parameters, and partly due to normal operating variability.

In the first series of experiments, extraction performance of the two mixers was compared under conditions of equal power consumption per unit volume. Considering the variation in aqueous feed composition over an eight hour run, comparison should only be made between pairs of simultaneously determined stage efficiencies. A Student t-test on 136 pairs of such determinations showed no significant difference in stage efficiency at a confidence level of 95%. Average stage efficiencies for different power inputs and operating conditions are presented in Table 2.

A second series of tests comprising 74 pairs of stage efficiency determinations was conducted at two tip speeds. Again each of the runs extended over eight hours; the aqueous composition varied around the mean of 4.3 kg/m³ copper and 1.0 kg/m³ sulphuric acid.

A Student t-test showed that the difference in performance of the two mixers was very significant. In all except two cases, stage efficiencies in the small mixer were higher than those in the large mixer. Average results are given in Table 3. This data shows that for the flat-blade turbine, constant power input per unit volume adequately predicts the stage efficiencies in mixers of various sizes, and that at constant tip speed, lower stage efficiencies would be achieved in a large mixer than in the small experimental mixer.

As a conclusion of this testwork the following mixer design procedure is proposed:

- (i) the tip speed for the required stage efficiency is determined in a laboratory mixer.
- (ii) at this selected tip speed the optimum impeller/tank diameter ratio with respect to entrainment is determined

TABLE 2. Comparison of Stage Efficiencies at Equal Power Input

Phase Ratio D/A	Power input HP/m ³	Aqueous Composition		Stage Efficiencies*		Number of determinations averaged
		Cu kg/m ³	H ₂ SO ₄ kg/m ³	780 l mixer	20 l mixer	
1.0	1.0	3.8	3.2	88.9	86.6	14
1.0	0.7	3.5	3.8	82.7	80.9	8
1.0	0.7	2.5	4.1	83.4	83.2	9
1.0	0.3	3.6	2.7	77.8	76.2	23
1.5	1.0	0.99	8.0	76.6	76.3	7
1.5	0.7	0.75	7.9	75.2	76.9	7

TABLE 3. Comparison of Stage Efficiencies at Equal Tip Speed

Tip Speed m/s	Stage Efficiencies		Number of determinations averaged
	780 l mixer	20 l mixer	
1.667	83.0	89.8	17
2.000	88.9	93.1	20

$$\text{*Stage Efficiency} = \frac{C_F - C_O}{C_F - C_E} \times 100\%$$

where C_F = is the copper concentration in the aqueous feed stream
 C_O = is the copper concentration in the aqueous outlet stream
 C_E = is the appropriate equilibrium copper concentration

in the same vessel under continuous flow conditions.

- (iii) the scale-up from the laboratory mixer to commercial size is carried out using geometric similarity and equal power input per unit volume.

Mixing Characteristics

It is evident from the foregoing sections, that accurate power predictions for large-scale mixers is of prime importance to the designer. In view of this, studies of power correlation were conducted for all available mixer sizes.

The experiments showed that for a square mixer box, the power number changes with Reynolds number and therefore predictions of power consumption in large-scale mixers is difficult, if not impossible. With the addition of two baffles, however, the power number became independent of Reynolds number and of mixer size. Over the range in mixer volumes of 20 l to 8000 l a power number of 6.5 was determined. It is somewhat anomalous that a slightly lower power number (5.0) was found in the 3.5 l laboratory mixer, indicating that mixers below a certain size should not be used in scale-up experiments. Experiments with four vertical baffles showed no further changes in power characteristics, indicating that with two baffles, fully baffled conditions had already been reached. This is also illustrated by the elimination of vortex formation in the 8000 l mixer with the installation of two vertical baffles. Elimination of vortex formation was more difficult in the smaller tanks; in the 3.5 l laboratory mixer vortices and air entrainment could not be avoided without the use of a top baffle.

The instability against phase inversion in Tailings Leach Plant mixers has been difficult to reproduce in pilot plant and laboratory mixers.

The occurrences of phase instability in the smaller-scale mixers have however always coincided with high suspended solids or gypsum concentrations. Testwork has shown that other factors such as power input per unit volume and phase inlet configuration are important.

The power per unit volume in the Tailings Leach Plant mixers is considerably smaller than in the pilot plant mixers, since the design was based on constant tip speed. In addition, circulation in the lower part of the mixers is poor and segregation of the phases may take place. A tendency towards phase segregation in the 20 l and 780 l mixers has been observed at power inputs below 0.2 hp/m³. In order to investigate the effect of improved mixing conditions on phase stability it was decided to remove the draught tube, which conveys the two phases to the eye of the centrally located, double-shrouded impeller, from one of the Tailings Leach Plant mixers. This could conveniently be done in the last extraction stage. In this way the power input is utilised for mixing only and circulation in the lower part of the mixer is greatly improved. As a result of this modification it has been possible to operate with organic phase continuity for periods of several weeks, whereas for the same phase ratio (O/A = 1.1:1) it has not been possible to maintain organic phase continuity in a corresponding, unmodified mixer in one of the other streams. It is concluded from these results that the improved mixing tends to increase stability against phase inversion. The fact that the two phases are no longer introduced into the impeller eye, but at considerable distance from the high shear zone in the mixer, may also have contributed to the improvement in phase stability. The proposed mixer configuration, using a flat-blade turbine, will ensure adequate circulation and the scale-up criterion of constant power input per unit volume will provide an agitation intensity far exceeding that at which phase segregation has been observed.

Entrainment is also an important consideration in mixer design. In the pilot plant no significant differences in entrainment levels have been observed for different impeller types. However, information about entrainment at different scales of operations is currently very limited. Studies of entrainment characteristics in the 3.5 1 mixer showed a significant influence of inlet arrangement. In one case the aqueous phase (to be dispersed) was introduced by an extended inlet to the impeller region with the organic phase brought into a region distant from the impeller. With this inlet combination high levels of entrainment are observed. A high aqueous to organic ratio in the impeller eye region apparently causes high levels of organic entrainment. If, instead, the continuous phase is introduced into the eye of the impeller, or both phases are introduced separately at the base level of the mixer, the entrainments of organic (continuous) phase are significantly lower. It has also been observed that, during the tests which were conducted in the organic continuous mode of operation, any air entrainment was associated with high levels of organic entrainment.

Settler Characteristics

The two main considerations in settler design are:

(a) the functional relationship between dispersion band depth and throughput of dispersed phase per unit of horizontal settler area.

(b) the critical linear velocity in the clear organic phase above which aqueous entrainments increase sharply.

When generating design information, the difficulty experienced by the experimental worker is that the above two factors cannot be determined simultaneously in a laboratory-scale settler. It can be shown that, for equal specific flows and depths of clear organic phase, the ratio of linear velocities in the organic phase in settlers of different sizes equals the ratio of their lengths. Consequently, in order to obtain simultaneously similarity in velocities and specific flows, the lengths of the experimental and commercial settlers should be the same. To fulfill this requirement at least partially, an existing pilot plant settler (4.2 m² settling area) was converted into a 12.6 m long and 0.3 m wide channel by installing two length-wise baffles. Most of the design testwork was conducted in this settler. Comparative work was carried out in a laboratory settler and in one of the Tailings Leach Plant settlers, where facilities for varying the settling area by means of a moveable dam baffle had been installed.

Pilot Plant Studies

Most of the testwork was carried out in the channelled settler under conditions simulating the first extraction stage in the Tailings Leach Plant Stage III circuit. The composition of the leach liquor feed averaged 3 gpl copper and 1 gpl sulphuric acid. The extractant tenor was 23 v/v LIX 64N in Escald 100, and the operating temperature was 33°C in most experiments. Phase ratios (O/A) of 1.0:1 and 1.5:1 were investigated. To vary the settling area, dam baffles could be introduced at various positions along the settler length.

(i) The Relationship Between Dispersion Band Depth and Specific Settler Flow

In all pilot plant experiments the relationship between dispersion band depth and specific flow is distinctly linear within the range of determinations. However, individual determinations of this relationship showed marked variations in the slope of the line, representing data points, as is shown in Figure 2. It was not possible to relate these variations to measured changes in operating parameters and

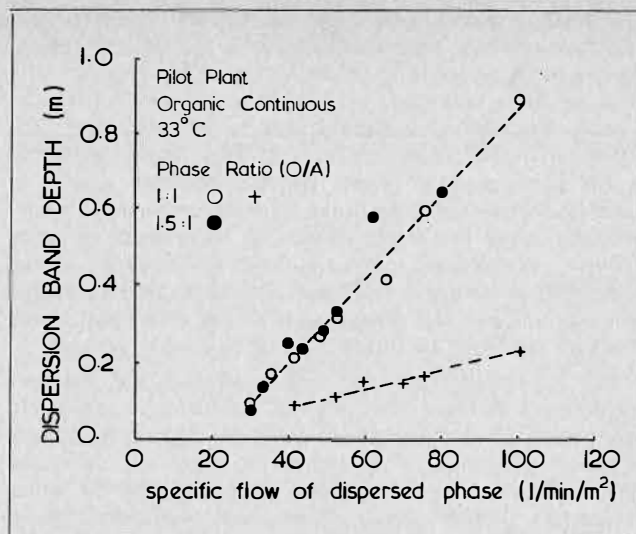


FIGURE 2. Dispersion band characteristics.

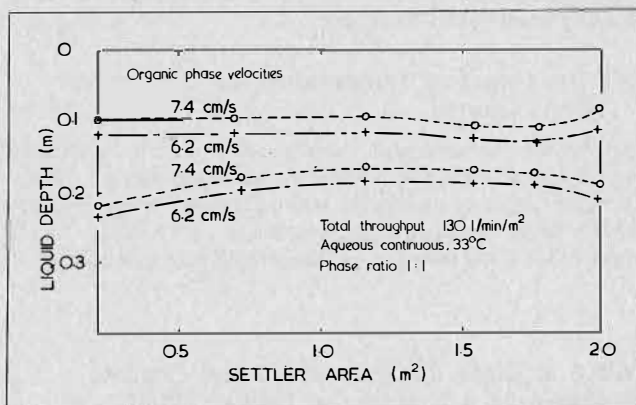


FIGURE 3. Dispersion band profile.

it is believed that factors such as changes in the nature of the suspended solids particles and possibly static electricity contribute to the phenomena observed.

The testwork also showed that the dispersion band depth is dependent only on the flow of dispersed phase per unit settler area and thus independent of the phase ratio.

It should be pointed out that in the laboratory experiments the functional relationship between dispersion band depth and specific settler flow was distinctly exponential (exponent generally greater than 2). The present pilot-scale and large-scale data, however, could only be described by either a linear relationship or an exponential relationship of lower exponent.

(ii) The Effect of Linear Velocity

In the unmodified settlers, at low specific flows the dispersion bands were generally of constant thickness throughout the settler length, whereas in the channelled settler operating at the same specific flows, wedged-shaped dispersion bands were observed. This difference can be explained by the high linear velocity of the dispersion in the channelled settler, the wedge providing the driving force for dispersion flow. At higher specific flows, where the dispersion band is thicker and the linear velocity of the incoming dispersion consequently lower, the wedge shape is less pronounced. At the dam baffle the profile of the dispersion band is influenced by the linear velocities of the clear phases. This effect becomes increasingly

Conclusions

Several hydrometallurgical applications of centrifugal extractors are feasible, particularly where advantage can be taken of their compactness and centrifugal force. This limits solvent inventory and provides better clarification of effluent streams. High dispersed/continuous phase can readily be maintained.

The kinetic loading rate for some liquid ion exchange systems may be too slow to be used in centrifugal extractors. However, the short contact time can be used to advantage to enhance selectivity between ions by discrimination in loading rates.

NOTATION

h	= holdup
k	= rate constant, sec^{-1}
K	= equilibrium constant
V	= superficial lineal velocity
ϕ	= phase ratio V_c/V_d
θ	= residence time

DISCUSSION

L. Steiner: Do you know any test systems which would show the superiority of centrifugal extractors against the gravitational ones?

D.B. Todd: Test systems which emphasize the superiority of centrifugal extractors are ones: (a) which have low density difference such as the water washing of certain polymer and plasticizer solutions, (b) where a very high phase ratio exists, such as the extraction of H_2O_2 from organic working solution with water (O/A from 30/1 to 70/1).

P.J. Lloyd: As I recall, in the installation at Mexican Hat, the problem arose that siliceous fines in the aqueous feed found their way, under the high pressures involved, into the rotating seals with a consequent short lifetime and the need to provide large surge capacity ahead of the extractor. Have the problems of wear of the seals been resolved in any way?

D.B. Todd: The problems with seals which occurred with the initial centrifugal uranium extraction installation some 20 years ago have been solved by: (a) selection of improved seal components; (b) arrangement of the process connections such that all seal faces are wetted with the solids-free organic phase, rather than with the acidic leach liquor. The installation of Mexican Hat closed down in 1965 because of termination of contract rather than mechanical problems. At the time of the last operation, 320 gpm of leach liquor was being extracted with 20 gpm of solvent (10% Alamine 336 in Diesel oil), producing a raffinate with 0.0025g U_3O_8 /liter for a 99.5% recovery.

E. Barnea: While the idea of basing separations on rate rather than equilibrium using short contact times is interesting from the theoretical point of view and may in principle allow separations that may not be otherwise possible, I would like to question its practical significance with special reference to the hydrometallurgical industry. Such a method is inherently sensitive to operational conditions and may hardly be considered for an industry characterized by inevitable fluctuations of conditions. For instance, feed rate may be significantly lower than nominal for extended periods of time which would result in the production of an off-grade product.

c	= continuous
d	= dispersed
f	= at flooding
s	= slip
t	= terminal

REFERENCES

- (1) Podbielniak, W.J., Kaiser, H.R. and Ziegenhorn, G.J., Chem. Engr. Progress Symposium Series No. 100, Chapter VI, 1970.
- (2) Todd, D.B. and Davies, G.R., Proceedings, International Solvent Extraction Conference, Lyon, 1974.
- (3) Todd, D.B., Chemical Engineering (1972) 79, No. 16, 152.
- (4) Banks, N.K., Mining Congress Journal 1959, 45, No. 1, 44.
- (5) Slater, M.J., Ritcey, G.M., and Pilgrim, R.F., Proceedings International Solvent Extraction Conference, Lyon, 1974.
- (6) Ritcey, G.M. and Lucas, B.H., (1976) I. Chem. Engr. Symposium Series No. 42, 12.1.
- (7) Ritcey, G.M. and Lucas, B.H. (1977) — private communication.
- (8) Todd, D.B. and Hopper, C.A., Chem. Engr. Progr. 1971, 67, No. 9, 60.

D.B. Todd: The ability of centrifugal extractors to operate with the high flow phase dispersed without deleterious backmixing means that even if the throughput is markedly reduced there is little change in the residence time of the dispersed phase drops. Thus, it is possible to take advantage of differential kinetics loading rates over a wide flowrate range.

J.F. Urstad: A question on operating costs — What is the power consumption of the centrifugal contactor, taken in units per unit volume of heated liquor, for example?

For treatment of highly corrosive liquors as in hydrometallurgy, e.g. chloride systems, is the unit available in construction materials other than alloyed steels, e.g. linings or plastics?

D.B. Todd: Steady-state power is essentially independent of throughput, but is dependent upon the size of the extractor. A 100 M^3/h centrifugal extractor runs with less than 20 kW. Centrifugal extractors are usually supplied in 316L stainless steel, but have been supplied in Hastelloy C and Alloy 20, and parts have been coated with Teflon and other plastics.

R.B. Akell: Please comment on the number of theoretical stages obtainable in the centrifugal extractor. How does the number of stages vary as the phase ratio is varied, especially with a ratio greatly different from unity?

D.B. Todd: The number of theoretical stages in a centrifugal extractor is dependent upon the internal design and the system. If there is a slow kinetic step, staging will not be good. Typical commercial centrifugal extractors have from 3 to 5 theoretical stages. One of the widest applications is a system where the dispersed phase/continuous phase ratio is about 50, and where there are between 3 and 4 theoretical stages.

G.G. Kusters: Can a centrifugal extractor also handle systems in which a large change in phase ratio occurs, e.g. in petroleum or petrochemical industry?

D.B. Todd: Changing flow ratios can be accommodated by design. In one application, 90% of the feed is extracted. There are many phenol-lube oil extraction plants wherein the aromatic constituents, up to half of the feed, are successfully extracted.

Determination of Actual Mass Transfer Rates in Extraction Columns

L. Steiner, M. Horvath and S. Hartland,
Swiss Federal Institute of Technology, (ETH),
Zürich, Switzerland

ABSTRACT

The main purpose of this investigation was to separate the actual mass transfer from the influence of the axial mixing, so that the rates would be applicable to columns of different sizes. Using the spray column as the simplest extractor type, the experiments have confirmed that the mass transfer rates are comparable to those calculated from the literature data for single drops and that the experimental concentration profiles may well be simulated using a modified backflow model with a relatively low number of hypothetical stages. The conclusions were further supported by successful recalculation of two sources of data from the literature and by our own measurements on single drops.

Introduction

THE PERFORMANCE OF THE COMMON TYPES of extractor may be predicted by numerical solution of the backmixing models. The computer time required is low and even small computers will deliver the desired accuracy. The procedures are not restricted to linear equilibrium relations or constant flows and densities of the phases, and more than one solute may be transferred. The procedure, therefore, has advantages compared with both the analytical solution of simplified backmixing models and the common HTU-NTU method. The principles of the method were presented at ISEC in Lyon⁽¹⁾, where the possibilities of the different backmixing models were enumerated. It was also stated that for successful computer work reliable data for the hydrodynamic parameters and the mass transfer rates in the column in question must be known, and a technique was developed for their measurement. It was assumed that the difficulties in scaling up the extractors are caused mostly by the hydrodynamics and that the actual mass transfer rates are more or less the same for different sizes of the same type of extractor.

These principles are now applied to the description and scaling up of the spray column. Admittedly, it is no new and efficient extractor. However, it is so simple that the experimental techniques are easily manageable and it may be used for comparison with more sophisticated types later. In this work, the back-flow model is modified to apply to the special conditions in the spray column, where the drops travel long distances without coalescing, and experimental data concerning drop diameter, hold-up of the dispersed phase, backmixing and mass transfer rates are presented. Finally, the concentration profiles along the column axis are simulated using the predicted values of the hydrodynamic parameters, and the agreement is found to be very good. The procedure is further confirmed by recalculation of earlier measurements of concentration profiles found in the literature and, here also, the results were good. Moreover, the mass transfer coefficients obtained in spray columns agreed roughly with

those measured on single drops, so that using the described procedure, the spray column may be designed from elementary data.

Theory

A successful model for the column performance must be sufficiently realistic to accurately reproduce the experimental data. However, this must not be achieved by a complicated procedure requiring large amounts of computer time if the model is not to remain of academic interest only. Bearing this in mind, the spray column is approximated by a series of hypothetical well mixed stages with backflow of the continuous phase as in the classical backflow model. The dispersed phase passes from stage to stage in drops which maintain their identity during their stay inside the column. In this way, the solute is accumulated in the drops (or depleted from them) and there is no mixing of the drops among themselves. It was confirmed by observation that the drops do not return long distances against the main flow direction and that there is no true backmixing in the dispersed phase comparable to that in the continuous phase. So if a tracer is injected at the outlet of the continuous phase, it will appear at the inlet after some time, while if marked drops are similarly introduced, they never appear at the other end of the column. Further, for successful performance of the spray column, the direction of mass transfer should be selected so that there is no coalescence between the drops, otherwise large drops are formed in a short distance from the distributor and interphase area decreases greatly. In this case other types of extractor which repeatedly disperse the coalesced drops should be used.

The full description of the model for both steady and unsteady-state operations will be published separately. Therefore, only a short review of the equations for steady-state operation is given here.

The instantaneous mass transfer rate for drops is defined as

$$r = \frac{dy}{dt} = \frac{6K_d}{\rho_a d} (y^* - y), \dots \dots \dots (1)$$

where y is the average mass fraction of the solute inside the drops and y^* corresponds to the concentration in equilibrium with the continuous phase, which is uniform within the well mixed hypothetical stages. For the parameter d , the mean volume-surface diameter is used in the case of ellipsoidal or otherwise distorted drops. The mean rate during the stay of the drop in a stage is then

$$\bar{r}_a = \frac{r_{no} v}{\delta} \left\{ 1 - \exp \left(- \frac{6K_d \delta}{\rho_a d v} \right) \right\}, \dots \dots \dots (2)$$

where r_{no} is the transfer rate at the time when a drop enters the section. The concentration inside a drop changes during its stay inside the stage to

$$y_n = y_{n-1} + \frac{\bar{r}_n \delta}{v}, \dots \dots \dots (3)$$

At the steady state, the material balance for a typical stage is

$$\frac{u}{\delta} \{ (1 + f) (x_{n+1} - x_n) + f (x_{n-1} - x_n) \} - \frac{\epsilon}{1 - \epsilon} \frac{\rho_d}{\rho_c} \bar{r}_n = 0 \dots \dots \dots (4)$$

where the backmixing is expressed by the backmixing coefficient *f* as in the usual backflow model. Numbering the stages from the entrance of the dispersed phase, there are deviations in the first stage where the drops are formed and in the last one where they coalesce. The first stage is therefore divided into formation and flow zones and the mass transfer coefficient for the drop formation is defined using the initial driving force ($y_1^* - y_1$) and the interfacial area of the formed drops. (These are the maximum values so that the coefficient is the smallest possible one).

The concentration inside the drops leaving the first stage is then;

$$y_1 = y_i + \bar{r}_1 \frac{\delta}{v} + r_1 t_f \dots \dots \dots (5)$$

where \bar{r}_1 is defined as in eq. (2) and the product $r_1 t_f$ is given by

$$r_1 t_f = \frac{\pi n_1 d^2 K_{df}}{L} (y_1^* - y_i) \dots \dots \dots (6)$$

The overall balance for the first stage is therefore

$$\frac{u}{\delta} (1 + f) (x_2 - x_1) - \frac{\epsilon}{1 - \epsilon} \frac{\rho_d}{\rho_c} \left(\bar{r}_1 + r_1 t_f \frac{v}{\delta} \right) = 0 \dots \dots \dots (7)$$

Similarly, the last stage *N* differs from the typical one, as the continuous phase is introduced here into a finite volume of mixed liquid, which causes a discontinuity on the concentration curve. At the same time there may be some additional mass transfer during the coalescence of the drops. This kind of mass transfer cannot be handled in a similar way to that at the drop inlet as it is not yet clear if it takes place during the time the drops are in the coalescence band or during film rupture and disappearance of the drop. Until more is known about the mechanism, this kind of mass transfer cannot be allowed for and the column must be designed as if there were no effect of this kind. The additional mass transfer provides a safety factor above that calculated. In any case, mass transfer during coalescence is often negligible. For evaluation of mass transfer coefficients from the concentration profiles, a correction may easily be made by reducing the inlet concentration of the continuous phase by the value which corresponds to the increase of the concentration in the dispersed phase in the coalescence band. This correction was introduced by Cavers and Ewanchyna⁽²⁾ who observed an effect due to coalescence in their measurements. Neglecting mass transfer during coalescence, the equation for the last stage is

$$\frac{u}{\delta} \{ x_1 + f x_{N-1} - (1 + f) x_N \} - \frac{\epsilon}{1 - \epsilon} \frac{\rho_c}{\rho_d} \bar{r}_N = 0 \dots \dots \dots (8)$$

Equations (7), (4) and (8) may be solved numerically to give the concentrations in both phases in all the hypothe-

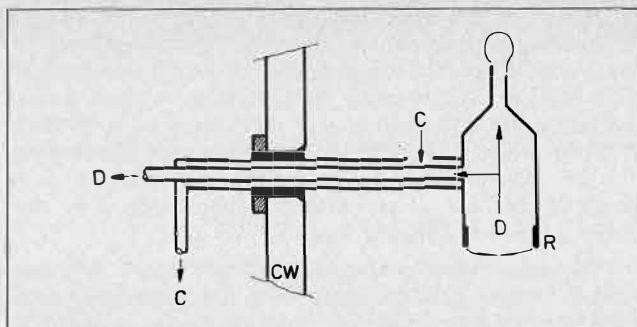


FIGURE 1. Sampling device for removing both phases from the column.
C — continuous phase, D — dispersed phase,
CW — column wall.
R — coalescence ring made of teflon.

tical stages, the number of which may be set arbitrarily. In this way, the concentration profiles may be simulated knowing the mass transfer rates, the mean drop diameter, hold-up of the dispersed phase and the backmixing coefficient in the continuous phase. Inversely, the true mass transfer rates may be calculated from the experimentally measured concentration profiles and the hydrodynamic parameters. For scaling up of the results from a laboratory column, the true mass transfer rates obtained on the small column may be used with new values of backmixing coefficient, hold-up and drop diameter to give the concentration profiles in the larger column using the same calculation procedure.

Experiment

To check the model, a spray column with a diameter of 0.1 m and a height of 2 m was built and equipped for simultaneous measurements of drop diameter, hold-up, backmixing in the continuous and the dispersed phases and the concentration profiles. The following methods were used for this purpose:

Concentration profiles: Using special funnels shown in Figure 1, inserted through holes drilled in the column walls, both phases were sampled continuously and analysed. For the accurate steady-state measurements as reported here the phases were collected in syringes without contacting air and analysed on a gas chromatograph. The funnels were also suitable for unsteady-state operation.

Backmixing in continuous phase: Saline solution was injected continuously close to the phase outlet and the salt concentration was measured conductometrically at four upstream positions along the column height.

Backmixing in dispersed phase: Since there is no actual backmixing as discussed in the last section, the only possibility was to use the unsteady-state injection method. Using a special distributor with two sets of syringe needles, coloured dispersed phase was introduced into the column for a short time interval with the same rate as, and instead of, the colourless one. The dye concentration was determined at the sampling points colorimetrically and the apparent dispersion coefficient was evaluated using an on-line computer. This measurement will be described later in a special publication.

Hold-up: The hydrostatic method was used with a membrane pressure transmitter connected to two different points along the column height. To see if the dynamic effects are of importance, the method was checked against the direct one when a part of the column was separated from the rest by two flat gate valves and the volume of the coalesced drops was directly measured.

Drop diameter: The drops were photographed at two points along the column and the mean volume-surface diameter was calculated based on about 200 measurements. Most of the measurements were done in a short period of steady-state operation so that there were no difficulties with evaluation caused by the dependence of the hold-up and the drop diameter on the solute concentration. This prevented the use of the unsteady-state method as presented at the last ISEC in Lyon⁽¹⁾.

The measurements were done with the water, o-xylene, acetone system, measurements with three further systems being in progress. Additional information was obtained by recalculating the published measurements of other authors. For the results of Gier and Hougen⁽²⁾ and Cavers and Ewanchyna⁽³⁾ a small model column was used to measure those parameters not found in the original papers.

Results

(a) Hydrodynamic Parameters:

The drop size, hold-up and the backmixing coefficient in the continuous phase were measured both with and without mass transfer. The resulting data were used to check the available relations found in the literature. The set of recommended equations is given in Appendix 1. It was found that the drop size in the region of slow formation (under jetting velocity) is best described by the equation (T-3) of de Chazal and Ryan⁽⁴⁾. In the jetting region no equation was found for the intermediate formation rates between the jetting and the critical velocities. An empirical equation (T-4) was therefore proposed which bridges the gap between the region of validity for de Chazal and Ryan's equation and those of Christiansen and Hixson⁽⁵⁾ which gives the critical drop diameter. Generally, it was found that the equations developed for formation of single drops may apply to spray columns if the distributor is constructed so that the drops do not touch each other and that it is made of a material which is not wetted by the dispersed phase. The only difference was observed for very low formation rates when the drops

are smaller than would correspond to the values of the Harkins-Brown factor as given by Scheele and Meister⁽⁶⁾. This may probably be explained by the fact that the release of one drop disturbs and releases neighbouring drops. However, this is not a region of interest for the actual performance of spray columns. For prediction of the hold-up of the dispersed phase and the actual slip velocity of the drops, the equation (T-9) derived by Pilhofer⁽⁷⁾ was found to give good results in the region of lower hold-ups (between 1 and 10%). An interesting observation was made for low hold-ups (under 2% in our case) when the rise velocity of the drops was higher than the velocity of single drop rising in a large quantity of undisturbed liquid. This may be explained by the circulation of the continuous phase which streams together with the drops in the central region of the column and returns to the distributor along the walls. Surprisingly, this region was well described by the Pilhofer equation which otherwise should be applicable for hold-ups higher than 6% only. The upper validity limit of about 60% as given by Pilhofer was not confirmed in our case and large deviations were found for hold-ups above 10%. The calculation of hold-ups from the flow rates of the phases is very sensitive mathematically and involves a numerical minimization. Backmixing in the continuous phase was found to be reasonably well described by the equation (T-11) of Zheleznyak and Landau⁽⁸⁾ which, in addition to our results, gave good correlation of the data of Perrut et al⁽⁹⁾ and Huplauf⁽¹⁰⁾. The difference between the experimental and theoretical values was about 30% and the accuracy is sufficient for both the simulation of the concentration profiles and for calculation of the mass transfer coefficients from the concentration profiles. Backmixing in the dispersed phase in the true sense of the word was never observed in our experiments and the drops never returned the full length of the column against the main stream. The shape of the response to a rectangular impulse as used in the unsteady-state method for backmixing determination may be reproduced if the different rise velocities of drops with slightly different diameters are considered.

(b) Mass Transfer Rates:

As mentioned in the theoretical part, there are two kinds of mass transfer in a spray column, occurring during formation of the drops and during the drop rise. No significant mass transfer was observed during the drop coalescence in our experiments. It is relatively easy to determine the mass transfer during the drop formation as the conditions in the close surroundings of the distributor are well defined, and at the steady state, the concentration in the continuous phase is constant. Furthermore, the formation time is short so that the change of concentration inside the drops is very small and the variation in the driving force may be neglected. For practical use, a coefficient based on the original concentration difference and the final drop surface was defined and measured using a sampling funnel placed close to the distributor. As the steady-state conditions need some time to be established, the unsteady period was incorporated into the drop formation time and the sampling funnel was placed 3 to 5 cm above the distributor. The coefficients were calculated from the measured exit concentration in the continuous phase and the concentration of the dispersed phase collected in the sampling funnel using the following formula:

$$K_{cf} = \frac{\dot{L} y_f}{\pi d^2 n_j x_{out}} \dots \dots \dots (9)$$

The coefficients obtained this way were correlated against

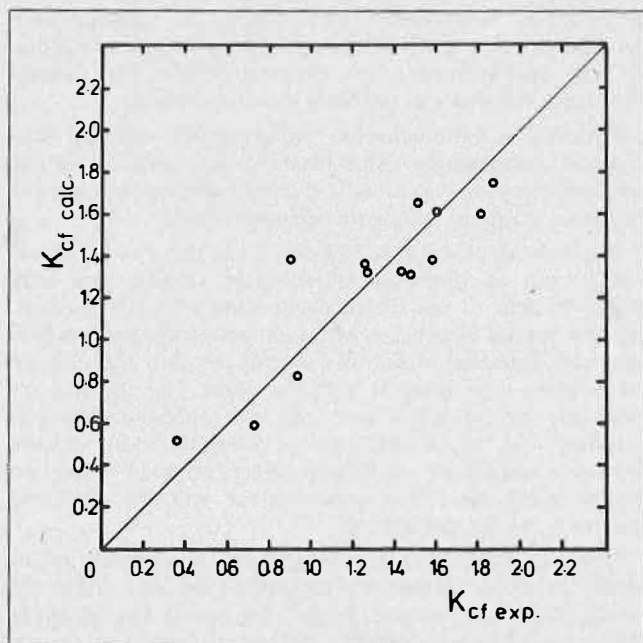


FIGURE 2. Mass transfer during drop formation. Correlation of the data by eq. (10). System water (C), o-xylene (D), acetone (C-D).

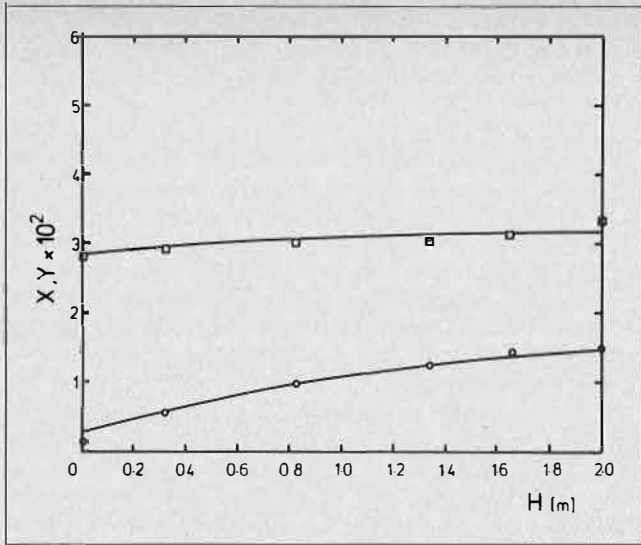


FIGURE 3. Comparison of measured concentration with simulated profiles. Figure 3: our measurements, system as in Fig. 2.

the nozzle velocity of the dispersed phase and the drop size as follows:

$$K_{ef} = 232.4 v_n^{1.67} d^{0.86} \dots \dots \dots (10)$$

The over-all fit may be seen from Figure 2. It should be emphasized that this coefficient is useful for simulation purposes only, as its value depends on the sampling position and the definition of the interfacial area.

The evaluation of the true mass transfer coefficients for moving drops is much more difficult as the influence of the backmixing must be eliminated. Two methods were developed for this purpose. The first approximated the middle part of the experimentally measured concentration profiles and calculated the coefficients analytically, using the dispersion model. The integrals and derivatives necessary for this purpose were obtained from the polynomial approximation. This method was not extremely accurate as it depended on subjective evaluation of the concentration profiles. A second method was therefore developed using a computer minimization routine to find the coefficient which gives the minimum sum of deviations of the simulated concentration profile from the experimental points. A program was developed for this purpose which, given the experimental values of the hydrodynamic parameters (drop size, hold-up, flow rates of both phases and backmixing coefficient), simulated the profiles from a given first estimation of the mass transfer coefficient, calculated the deviations in all positions where experimental measurements were available and minimized the sum of the squares of these deviations by varying the mass transfer coefficient. The model described here was used, employing a Newton-Raphson method for profile simulation, the minimization routine being based on Coggins' single parameter search⁽¹³⁾. This method eliminated the necessity of preliminary smoothing of the data and delivered very good results. The computer time required was reasonably low so that a large number of profiles could be recalculated. Some examples of the simulated profiles together with the experimental data are shown in Figures 3 to 5. Good agreement was obtained, the standard deviation being under 5% in most cases. It was found that the end effects have little influence on the mass transfer coefficient obtained from the profiles so that errors in the backmixing coefficient and in the estimate of the mass transfer rates during drop formation and coalescence are not too important.

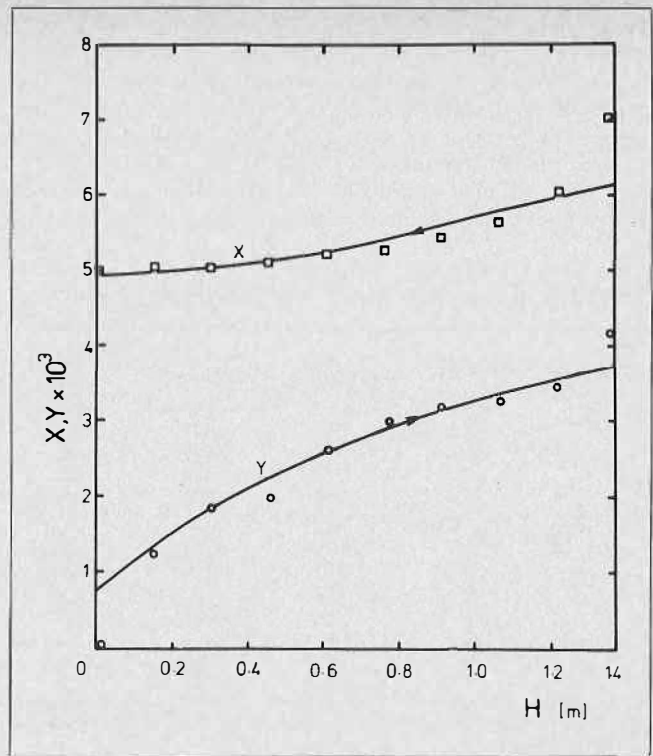


FIGURE 4. Comparison of measured concentration with simulated profiles. Gier and Hougen⁽²⁾, exp. No. 44.

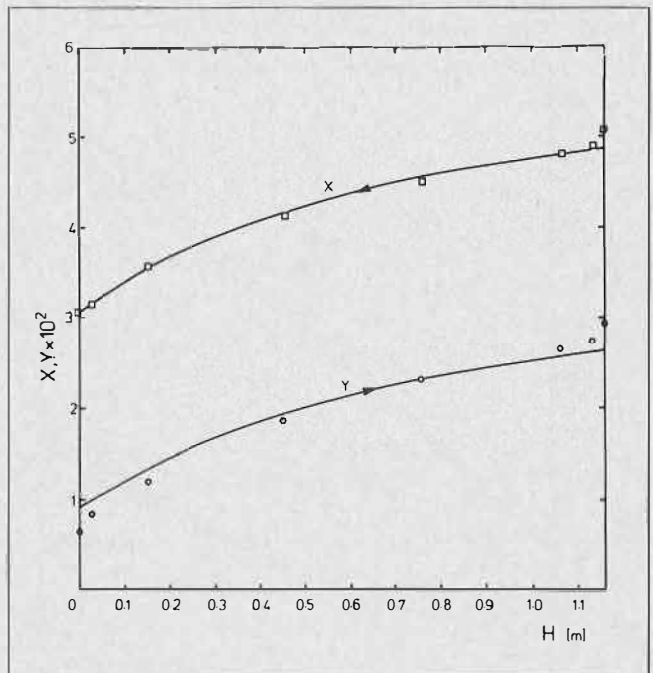


FIGURE 5. Comparison of measured concentration with simulated profiles. Cavers and Ewanchyna, exp. No. 41.

Two sets of data found in the literature were used to obtain further information about the mass transfer rates. Gier and Hougen⁽²⁾ published some concentration profiles obtained in a spray column with a diameter of 154 mm using a water, ethylether, adipic acid system. Using a model equipped with the same distributor as the original authors, the missing data about the drop diameter and the mass transfer rate during drop formation were meas-

ured and the true mass transfer coefficients were calculated as from our own profiles.

Cavers and Ewanchyna⁽³⁾ measured the profiles for water, methylisobutylketone and acetic acid in a column with a diameter of 38 mm. As the drop diameter is given in their work and the mass transfer during drop formation was directly calculable from the first experimental point above the column bottom, recalculation without

TABLE 1. Recalculation of the Literature Data

Reference	Run No.	K_{cpl} (kg/m ² s)	K_{copt}	S (%)
{2}	40	.0357	.0457	4.8
	41	.0287	.0444	5.9
	42	.0295	.0475	2.0
	43	.0216	.0425	5.1
	44	.0382	.0404	3.4
{3}	31	.0361	.0781	4.8
	33	.0382	.0784	4.6
	39	.0604	.0689	3.2
	23	.0539	.0798	2.3
	24	.0456	.0669	2.6
	27	.0367	.0612	3.0
	30	.049	.0650	2.9
	41	.0466	.0648	2.3

K_{cpl} is the coefficient calculated from the end concentrations assuming plug flow conditions.

K_{copt} is the true mass transfer coefficient obtained in this work by optimization from the concentration profiles.

S is one hundred times the mean absolute deviation divided by the mean concentration in the dispersed phase.

coalescence so the outlet dispersed phase concentration additional measurement was possible. In this case considerable mass transfer was observed during the drop and was not used for the minimization.

In both works cited here the drop size was constant in all experiments and so was the slip velocity of the drops, the effect of changes in the hold-up being small in the range used. This indicated that the mass transfer coefficients should be practically constant in all experiments which was confirmed since the coefficients obtained from the simulation did not change by more than 6% both for Gier and Hougen and for Cavers and Ewanchyna. Using the mean values, practically the same profiles as indicated in Figures 4 and 5 were obtained.

The backmixing coefficients used for recalculation of the mass transfer rates were those obtained from Zheleznyak's formula (T-11) for Gier and Hougen's work. For the work of Cavers and Ewanchyna these values were too high and a two-parameter optimization for the mass transfer and the backmixing coefficients was used. The resulting backmixing coefficients were about 2.4 times lower than those predicted by Zheleznyak. The direct evaluation from the concentration profiles of the backmixing coefficients is generally not possible as second order differences are involved and the experimental data practically never enables their calculation with meaningful accuracy. The results of the recalculations are given in Table 1.

Correlation

In general, the true mass transfer coefficients are up to three times higher than those calculated from the end concentrations under the assumption of plug flow. This is because the driving force is smaller than when plug-flow exists and the coefficient must therefore compensate for this. The differences may be seen in Table 1 for the data found in the literature.

In an attempt to correlate our own coefficients, different formulae for mass transfer from single drops found in the literature were tried. Obviously, the resistance to mass transfer may be on both sides of the phase boundary, and for both sides many different correlations exist, the most important ones being collected in Appendix 2. It was found that all relevant formulas for mass transfer on the side of the continuous liquid give similar results in the region used and the ones which give the lowest and the highest rates are shown in Figure 6. For the conditions inside the drops, two mechanisms are possible. Excluding the possibility that the drops behave like solid bodies, there may be either laminar circulation as described by Kronig and Brink⁽¹⁴⁾ or turbulent mixing which corresponds to the model of Handlos and Baron⁽¹⁵⁾. Plotting the data in terms of the Sherwood number against the Reynolds number gives the result shown in Figure 6, together with the lines for mass transfer from single drops. It may be seen that the data are in the region bounded by the theoretical curves for Kronig and Brink's and Handlos and Baron's models which indicates that all the measurements were made in the transient region before turbulence is fully developed. This explanation is supported by the fact that no clear dependence of the mass transfer coefficients on the hold-up was found and that the regions of validity of Kronig and Brink's and Handlos and Baron's equations are for Reynolds numbers under 10 and about 500, respectively. The best correlation for the overall coefficient appears to be the value calculated from a combination of Handlos and Baron's and Higbie's formulas multiplied by a correction factor of 0.57 for the water-xylene-acetone system. For the measurements of Cavers

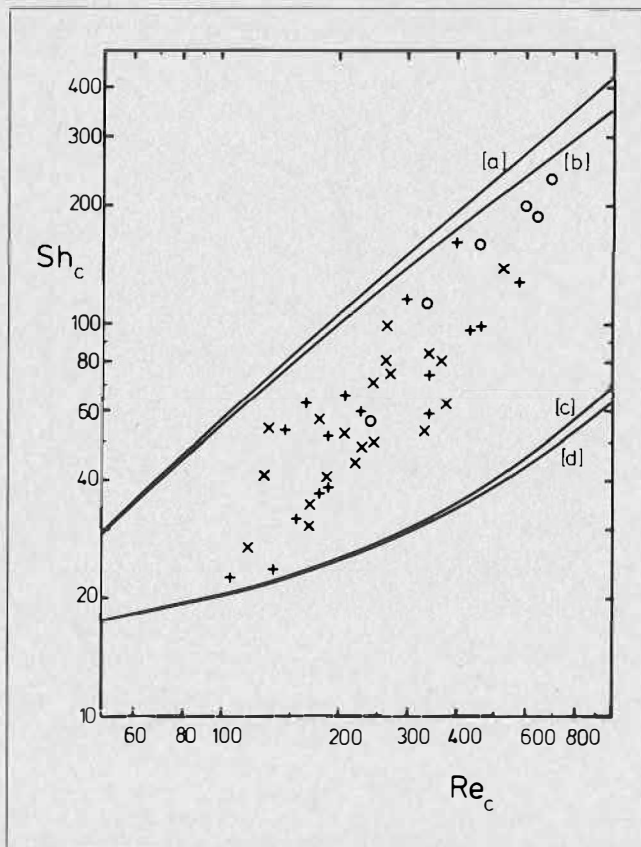


FIGURE 6. Comparison of the over-all mass transfer coefficients from our measurements with the predicted values for single drops. System as in Fig. 2, + column diameter 78 mm, x column diameter 100 mm, o single drop experiment. {a} Combination of Handlos-Baron with Higbie, {b} Handlos-Baron with Heertjes et al., {c} Kronig-Brink with Higbie, {d} Kronig-Brink with Heertjes et al.

and Ewanchyna, the coefficient roughly agrees with the one obtained on single drops. More measurements are now being performed on other systems which will allow extension of the working region and enable a final decision about the applicability of the single-drop formulas to be made.

Comparison to Mass Transfer from Single Drops

For the water-methyl isobutyl ketone-acetic acid system, the mass transfer rates from single drops were measured by Licht and Pansing⁽¹⁹⁾. Recalculating their results, the mass transfer coefficients defined as in our work may be obtained for comparison with the ones from the work of Cavers and Ewanchyna. The result is shown in Figure 7 where the mean coefficient for the Caver's profiles is also indicated. It may further be seen that the rates are enormous at the beginning of the drop movement and that a steady-state value is only reached after a considerable time. The agreement between the extraction rate for the single drop and in the spray column is very good.

To check the data measured in our laboratory, a few measurements with single drops were made, the results being given in Figure 6. The points indicated correspond to mass transfer coefficients measured between heights of 0.27 and 0.68 m and should therefore approximate the column measurements well. It may be seen that they are in the same region as the points obtained from the column and that the assumed transition from the Kronig-Brink to the Handlos and Baron's model may also be observed here. These measurements are preliminary; an apparatus for suspending stationary drops in a stream of continuous phase has been constructed and will enable the variation of mass transfer with time to be followed.

Discussion

As shown in this paper, the design and scaling up of spray columns may easily be done using the procedure described. Obviously, the prediction of the hydrodynamic parameters and the mass transfer rates from the generalized equations is less reliable than their measurement on a small model. However, even without measurements, prediction with quite good accuracy is possible. Among the hydrodynamic parameters, the drop size may be predicted safely using the equations from the literature as cited in Appendix 1. The hold-up is more difficult and much more should be done in this field, especially in the region of medium hold-ups between 0.1 and 0.3. Similarly, the backmixing in the continuous phase is not yet described theoretically and the formula suggested here is purely empirical. It gives good results in many cases, but it may fail completely as found in the recalculation of the Cavers and Ewanchyna's work.

For mass transfer rates it seems that the values measured on single drops are applicable for use in spray columns. However, some precaution is necessary due to the long period of unsteady state transfer at the beginning of the drop path. This was allowed for in the simulation by using an unsteady-state coefficient during the formation itself and the first half-second of the drop movements and the steady-state coefficient for the rest of the column. Comparison of the profiles with experimental points shows that this approximation is reasonable and that no time-dependent coefficient is necessary. Similarly, it was proved that the assumption of plug flow in the dispersed phase gives good results, and consideration of different drop velocities for not exactly uniform diameters was unnecessary. A refinement of the model in this aspect could be made, but it would not significantly improve the accuracy.

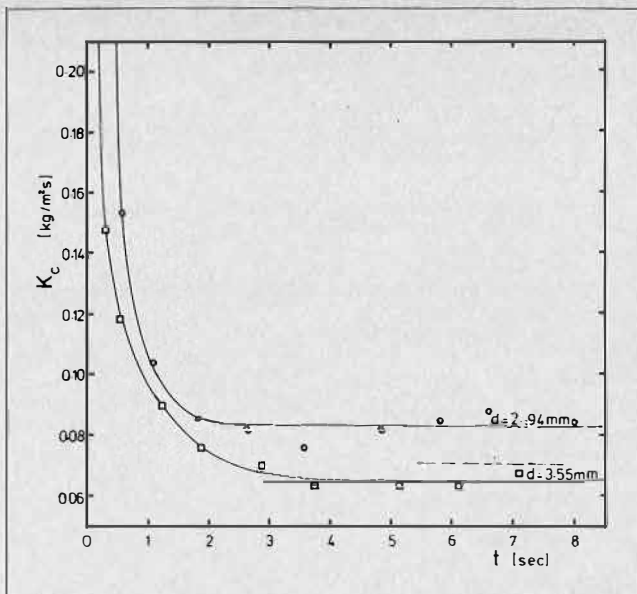


FIGURE 7. Mass transfer from single drops, data of Licht and Pansing (19). Broken line: mean coefficient recalculated from Cavers and Ewanchyna's work⁽³⁾, $d = 3.15$ mm.

Further work should collect available mass transfer data and measure the profiles for several other systems, e.g. those recommended by the Working Party for Extraction and Distillation⁽²⁰⁾. The principles described here will also be applied to other more complicated extractor types.

Conclusion

1. Concentration profiles in a spray column may be successfully simulated using a model based on the assumption of non-coalescing drops rising uniformly in strongly backmixed continuous phase.
2. True mass transfer coefficients may be calculated from experimentally measured concentration profiles. These coefficients are higher than those calculated from the end concentrations under the assumption of plug-flow conditions and similar to the coefficients obtained for single-drop mass transfer.
3. Preliminary results have shown that the combination of the Handlos and Baron's model for the inner side of the drops with the penetration theory for their outer side gives results which are about 50% higher than the experimental data for Re_c between 100 and 500.
4. Measurements on single drops have also shown that the mass transfer rates suggested by Handlos and Baron are not reached in the range of Re_c quoted which apparently represents the transient region between laminar circulation as described by Kronig and Brink and turbulent circulation as described by Handlos and Baron.

NOTATION

A	= column cross-sectional area
d	= drop diameter
D	= column diameter
E	= backmixing coefficient (dispersion model)
f	= backmixing coefficient in continuous phase (back-flow model)
g	= gravitational acceleration
H	= column height
\dot{H}	= mass flux of continuous phase
\dot{L}	= mass flux of dispersed phase

- K = over-all mass transfer coefficient
- k = individual mass transfer coefficient
- n_j = number of jets in distributor
- r = mass transfer rate
- s = percentage deviation
- t = time
- u = actual velocity of continuous phase $u = \dot{H}/A(1 - \epsilon)\rho_c$
- v = actual velocity of dispersed phase $v = \dot{L}/\rho_d A \epsilon$
- v_n = nozzle velocity of dispersed liquid
- v_s = slip velocity, $v_s = u + v$
- \bar{V} = drop volume
- y, x = mass fractions of dispersed and continuous phases respectively
- Y, X = relative mass fractions

Indices

- c = continuous phase
- d = disperse phase
- f = formation
- i = inlet
- n = typical stage
- N = last stage
- out = outlet

Greek letters

- ϵ = hold up of disperse phase
- δ = height of hypothetical stage
- ρ = density
- σ = surface tension
- μ = kinematic viscosity
- ν = dynamic viscosity
- ξ = diffusivity

Dimensionless groups

$Re = \frac{\rho d v}{\mu}$ Reynolds number

$Sc = \frac{\nu}{\xi}$ Schmidt number

$Sh = \frac{Kd}{\xi}$ Sherwood number

LITERATURE:

- (1) Steiner, L. and Hartland, S., Calculation of mass transfer coefficients in extraction columns under non-ideal flow conditions, Proc. I.S.E.C. Lyon, Soc. Chem. Ind. London, 1974.
- (2) Gier, T. and E. Hougen, J.O., Ind. & Eng. Chem. 1953, 45, 1362.
- (3) Cavers, S.D. and Ewanchyna, J.E., Can. J. Chem. Eng. 1957, p. 113.
- (4) De Chazal, L.E.M. and Ryan, J.T., A.I.Ch.E. Journal 1971, 17, 1226.
- (5) Christiansen, R.M. and Hixson, A.N., Ind. & Eng. Chem. 1957, 49, 1017.
- (6) Scheele, G.F. and Meister, B.J., A.I.Ch.E. Journal 1968, 14, 9.
- (7) Pilhofer, T., Chem. Ing. Tech. 1974, MS 133/74.
- (8) Zheleznyak, A.S. and Landau, A.M., Theor. Fund. Chem. Eng. 1973, 7, 525.
- (9) Perrut, M., Loutaty, R. and LeGoff, P., Chem. Eng. Sci. 1973, 28, 1541.
- (10) Huplauf, A., Lokaler Wärmeübergang and Rückvermischung in flüssig-flüssig Sprühkolonnen, Diss. ETH, No. 5093, 1973.
- (11) Hu, S. and Kinlner, R.C., A.I.Ch.E. Journal 1955, 1, 42.
- (12) Skelland, A.H.P. and Johnson, K.R., Can. J. Ch. Eng. 1974, 52, 732.
- (13) Non linear optimisation techniques, Monograph ICI No. 5, p. 13.
- (14) Kronig, R. and Brink, J.C., Appl. Sci. Res., A2, 1951, 142.
- (15) Handlos, A.E. and Baron, T., A.I.Ch.E. Journal 1957, 3, 127.
- (16) Higbie, R., Trans. A.I.Ch.E. 1935, 31, 365.
- (17) Garner, F.H., Foord, A. and Tayeban, M., J. appl. Chem. 1959, 9, 315.
- (18) Heertjes, P.M., Holve, W.A. and Talsma, H., Chem. Eng. Sci. 1954, 3, 122.
- (19) Licht, W. and Pansing, W.F., Ind. & Eng. Chem. 1953, 45, 1885.

(20) Recommended Systems for Liquid Extraction Studies. European Federation of Chemical Engineers, Working Party for Distillation, Absorption and Extraction, 1977.

APPENDIX 1 — Recommended equations for calculating the hydrodynamic parameters in spray columns

- a) Threshold nozzle velocities:
Jetting velocity {6}

$$v_{nj} = \left(\frac{3\sigma_i \left(1 - \frac{d_n}{d}\right)}{\rho_d d_n} \right)^{1/2} \dots \dots \dots (T1)$$

d_n is the nozzle diameter

σ_i is the interface tension

Critical velocity {12}

$$v_{nc} = 2.69 \left(\frac{d_{jc}}{d_n} \right)^2 \left[\frac{\sigma}{d_{jc} (0.514 \rho_d + 0.472 \rho_c)} \right]^{1/2} \dots \dots \dots (T2)$$

where $d_{jc} = d_n / (0.485K^2 + 1)$ for $K < 0.785$ and $d_{jc} = d_n / (1.51K + 0.12)$ for $K \geq 0.785$. The parameter K is defined as $K = d_n / (\sigma_i / \Delta \rho g)^{1/2}$

- b) Drop diameter:

b1) $v_n < v_{nj}$ {4}

$$V = \frac{\pi d_n \sigma}{\Delta \rho g} \left[\psi + 1.648 \frac{\Delta \rho d_n V^{1/3}}{2\sigma v_s} - \frac{\rho_d d_n v_n^2}{2\sigma} \right] (T3)$$

ψ is Harkins-Brown's correcting factor which may be found in Ref. {6}.

For v_s eq. (T7) or (T8) may be used. Iterative solution is required.

b2) $v_{nj} < v_n < v_{nc}$

$$\frac{d}{d_{jc}} = \frac{2.06}{v_n/v_{nc}} + 1.47 \ln \frac{v_n}{v_{nc}} \dots \dots \dots (T4)$$

b3) $v \geq v_c$ {5}

$$d = \frac{2.07 d_n}{0.487 E\ddot{o} + 1} \text{ for } E\ddot{o} = \frac{\Delta \rho g d_n^2}{\sigma} < 0.615 \dots (T5)$$

or

$$d = \frac{2.07 d_n}{1.51 E\ddot{o}^{1/2} + 0.12} \text{ for } E\ddot{o} \geq 0.615 \dots \dots \dots (T6)$$

- c) Free rise velocity of drops {11}:

$$v_{s\infty} = \frac{\mu_{cp}^{0.15}}{\rho_c d} (0.798 Y^{0.748} - 0.75) \quad 2 \leq Y \leq 70 (T7)$$

or

$$v_{s\infty} = \frac{\mu_{cp}^{0.15}}{\rho_c d} (3.701 Y^{0.422} - 0.75) \quad Y > 70 \dots (T8)$$

where $Y = 4 \Delta \rho d^2 g P^{0.15} / (3\sigma_i) \dots \dots \dots (T8a)$

and $P = \rho^2 \sigma_i^3 / (\mu_c^4 \Delta \rho g) \dots \dots \dots (T8b)$

σ_i is the interfacial tension

- d) Drop rise velocity in a swarm {7}

$$v_s = \frac{v_c}{d} \frac{3 z q^2 \epsilon}{c_i (1 - \epsilon)^3} \left[\left(\frac{c r q^3 A r (1 - \epsilon)^3}{54 (z q^2 \epsilon)^2} + 1 \right)^{1/2} - 1 \right] \dots \dots \dots (T9)$$

where

$$C_t = \frac{\Delta \rho d g}{6 \rho_c v_{s\infty}^2} - \frac{3\mu_c}{\rho_c d v_{s\infty}} \quad (T9a)$$

$$zq^2 = \frac{1-\epsilon}{\epsilon} \exp\left(\frac{\epsilon}{0.4 - 0.244\epsilon}\right) \quad (T9b)$$

$$q^3 = 5.0 \left(\frac{\epsilon}{1-\epsilon}\right) 0.45 \left\{1 - 0.31 \left(\frac{\mu_c}{\mu_d}\right) 0.39\right\} \quad (T9c)$$

e) Hold-up: The hold-up may be calculated by simultaneous solution of eq. (T9) with

$$v_s = \frac{\dot{H}}{\rho_c A (1-\epsilon)} + \frac{\dot{L}}{\rho_d A \epsilon} \quad (T10)$$

f) Backmixing in continuous phase {8}:

$$\frac{E_c}{v_c} = 6.5 \text{Re}^{0.987} \epsilon^{0.814} \bar{\mu}^{3.89} \quad (T11)$$

Re is based on hydraulic diameter defined as

$$\bar{d} = \frac{D(1-\epsilon)}{1.5\epsilon D/d + 1} \text{ and } \bar{\mu} = \frac{2}{3} \frac{\mu_c + \mu_d}{\mu_c + \mu_d}$$

APPENDIX 2 — Equations for calculations of mass transfer coefficients for single drops

Case (a) — Solid particle, (2) — liquid drop,

a) Inside the drops:

Laminar circulation {14}

$$k_d = 0.079 \frac{d}{t} + 17.66 \frac{\xi_d}{d} \quad (T12)$$

Turbulent mixing {15}:

$$k_d = 0.00375 \frac{v_s}{1 + \frac{\mu_d}{\mu_c}} \quad (T13)$$

b) In the continuous phase:

Penetration theory: {16}

$$Sh_c = 1.128 \text{Re}_c^{1/2} Sc_c^{1/2} \quad (T14)$$

Garner et al {17}:

$$Sh_c = -126 + 1.8 \text{Re}_c^{0.5} S^{0.42} \quad (T15)$$

Heertjes et al {18}:

$$Sh_c = 0.83 \text{Re}_c^{1/2} Sc_c^{1/2} \quad (T16)$$

DISCUSSION

E. Barnea: I would like to comment on the applicability of laminar circulation or turbulent-mixing-inside-the-drops models for a practical system. First, there was no convincing evidence that these models are any good even in the relatively sterile laboratory environment. The data may be interpreted as being not related at all to the predictions, rather as representing a transition process. But even if it would work for pure systems, the presence of surfactants and solids in an industrial system tend to retard motion inside the drops. The main means for mixing inside the drops is thus the coalescence-redispersion process, which plays a very important role in the mass transfer process if the main resistance lies in the dispersed phase. It is therefore suggested that a model based on penetration theory coupled with complete remixing at a frequency equal to the mean lifetime of the drop may be more promising.

L. Steiner: Dr. Barnea missed an important point in our lecture which emphasized that the model and all the experimental work were designed for non-coalescing drops. In the experimental work the mean drop diameter was measured close to both column ends and in all cases the result was identical. The mass transfer during the original drop formation on the distributor was measured from the first sampling point some 30 mm above the nozzles, so whatever change in concentration inside the drops was observed above this point was due to mass transfer into freely moving drops, without any coalescence and redistribution. It is well known that mass transfer to

rigid bodies is more than an order of magnitude slower than to circulating drops so the line for it in our Figure 6 would be nearly identical with the horizontal axis. The assumption of negligible mass transfer during drop movement would make any stagewise circulation very easy. Unfortunately, there is very little to prove that rigid drops with a diameter over 3 mm exist at all, especially outside sterile laboratory conditions.

D.H. Logsdail: Did you correct your concentration measurements in the dispersed phase to take account of mass transfer during the coalescence of the drops in the sampling device?

L. Steiner: Our sampling devices were designed to rapidly coalesce the dispersed phase on a teflon ring attached to the lower part of the funnel. The coalesced liquid then escaped as newly formed drops from the opening at the top of the device or was sampled for analysis. The coalescence on the ring was instantaneous, new drops being caught as soon as a part of the ring emerged from the coalesced layer. During the drop coalescence at the top of the column the drops formed a close-packed dispersion up to 10 cm thick and the time the drops spent in this dispersion was many times longer than in the sampling funnels. However, even in this case we did not observe any mass transfer so that we assume that the error caused by coalescence in the sampling funnels was negligible. A new sampler is being developed to check the performance of the existing samplers, with drops going through a layer of equilibrium liquid before coalescence. If any significant mass transfer is observed, the results will be corrected accordingly.

The Effects of a Packed-Bed Diffuser-Precoalescer on the Capacity of Simple Gravity Settlers and Compact Settlers

E. Barnea and J. Mizrahi*,
IMI-Institute for Research and Development, Haifa, Israel

ABSTRACT

General concepts in the design of more efficient liquid-liquid gravity separators are analysed and discussed. The results of experiments on the effects of a packed-bed diffuser-precoalescer, composed of a thin layer of standard packing elements, 6 to 10 mm in diameter, on the capacity of simple gravity settlers and IMI compact settlers are given and discussed. The effects of the thickness of the bed, interstitial velocity and particle diameter in four different phase systems were included in the investigation. The combinations of IMI compact settlers with packed-bed diffuser-precoalescers appear to be especially attractive since they have a higher capacity than that which may be obtained by each method separately, and retain the maximum value of the individual contributions of both effects.

Introduction

THE PENETRATION OF SOLVENT EXTRACTION technology to the large-scale heavy inorganic and hydro-metallurgical industries has created motives for the development of compact and efficient liquid-liquid separators that will minimize the problems associated with giant-size equipment, solvent inventory, equipment cost, and floor area.

Several types of improved gravity settlers appeared on the market and found industrial applications during the last decade. IMI was amongst the pioneers in the field with its compact settler^(1,2) based on racks of flat or corrugated partitions having alternating inclination to create "chimneys" through which the separated light and heavy phases flowed up and down respectively to common "manifold" layers. The IMI compact settler is already operating on an industrial scale in several plants, of which the actual industrial-scale capacity is 3 to 8 times the capacity of a simple gravity settler operating with the same phase system.

A new version of the IMI compact settler was developed recently by IMI. This settler incorporates a thin layer of comparatively large (¼ in. to ½ in.) conventional packing elements (rings, saddles, etc.) placed between the double-perforated or slotted plates of the diffuser⁽³⁾. This additional element has features that are comparable to those of the basic elements of the compact settler, namely, simplicity, flexibility, availability, relatively low cost, and operability with dispersions containing small proportions of finely divided solids on the interface, such as those encountered in most industrial solvent-extraction plants.

The new element has a dual function, acting both as an

improved diffuser for more efficient distribution of the dispersion and restraining of turbulence, and as a pre-coalescer to cause an increase of the mean diameter of the drops of feed. This results in an additional 30 to 70% increase of the capacity of the compact settler. The combination of compact settler with packed-bed diffuser, thus, has a capacity range of 5 to 12 times the capacity of simple gravity settler operated with the same phase system.

Some experimental results on the effects of the packed-bed diffuser-precoalescer will be given and discussed in this paper.

General Concepts in The Design of More Efficient Liquid-Liquid Separators

A comprehensive investigation into the mechanism of separation in deep-layer gravity settlers was described recently in a series of papers⁽⁴⁻⁷⁾. It was shown that the dispersion band in a deep-layer gravity settler is composed of two main sublayers, namely, the "dense" layer and the "even-concentration" layer. The "dense" layer is characterized and controlled by the following: the steep gradient of increasing concentration of drops towards the coalescence front, drop to drop coalescence, transmission of hydrostatic pressure, which facilitates "squeezing" of the film of continuous phase, and coalescence of drops with the interface on the coalescence front. The "even-concentration" layer is characterized and controlled by the following: liquid-liquid fluidized bed, hindered settling of droplets, drop to drop collision-coalescence process, and a concentration of drops slightly lower than the concentration of feed dispersion, with a mild gradient of concentration that decreases towards the settling front.

Generally, with the exception of dispersions that exhibit a tendency towards "creaming" (which are generally avoided in industrial solvent-extraction practice), the "even-concentration" layer dominates, fills most of the dispersion band, and controls the continuous-settling characteristic.

Thus, for increased capacity of settlers operating with this most commonly encountered category of liquid-liquid dispersions, the processes taking place in the "even-concentration" layer must be enhanced.

Although the following explanation may present a picture that is clear, but perhaps somewhat oversimplified, it may be useful to describe the thickness of the "even-concentration" sublayer as being adjusted so that sufficient residence time is provided for droplets to grow by drop-to-drop collision-coalescence mechanism to a size that will promote their hindered settling counter-current to the stream of draining continuous phase.

With this model, the capacity of the settler may be increased by one of the following general methods, or a combination thereof:

(a) increasing of the drop size available, and

*Present address, Miles Israel Ltd., P.O. Box 288, Haifa, Israel.

(b) decreasing of the drop size required.

The first goal may be achieved with one of the following methods. The feed for the settler could consist of a dispersion composed of larger droplets having a small variation in size. This method would eliminate the "tail" of small droplets that is generally present, by the employment of a suitable device producing dispersion. Unfortunately, to date, no such device (having also a reasonable rate of mass transfer) has been developed. Alternatively, a dispersion closer to the desired character may be produced from a dispersion discharged by a conventional mixer by treatment of the dispersion with a suitable pre-coalescing device installed, in effect, between the mixer and settler, even though, mechanically, it may be a part of either the settler or the mixer, or, actually, a separate item of equipment. Acceleration of the rate of drop-to-drop coalescence within the dispersion band would produce droplets greater than the critical size within a shorter residence time. A method falling within this category was developed successfully by the addition of suitable inert, finely divided, solid particles⁽⁸⁾, which increased the capacity of the settler by a factor of 2 to 3. The fraction of smallest droplets from the settler could be recycled back to the mixer.

The second goal may be achieved as follows. The velocity of the countercurrent of the draining continuous phase could be decreased. This method is actually the basis for the successful operation of the IMI compact settler^(1,2). If the feed dispersion is divided into n nearly horizontal compartments built up one upon the other, the velocity against which the droplets have to settle is reduced by a factor of n . The separated phases are delivered through separated "chimneys" to common upper and lower manifolds. In the "chimneys", the velocity of the continuous phase is obviously much higher than that in a simple gravity settler, but, ideally, no dispersed-phase droplets should be trapped in the continuous-phase "chimney".

The hindered-settling velocity of the droplets could be increased by the application of non-gravitational fields. It is known that electrostatic fields are used by the petrochemical industry, but these fields cannot be considered for general use, since the continuous phase must have very low conductivity. Centrifugal fields are used in centrifugal separators, which are efficient but expensive, and are used in special cases generally characterized by relatively low throughputs. Therefore, the use of centrifugal fields is not suited to the heavy inorganic and hydrometallurgical industries. The use of magnetic fields was suggested recently⁽⁹⁾.

Most of the methods currently applied in industry are based on the decrease in particle size required for separation to be achieved in a given residence time. In fact, for gravity separators the principle of lowering of the effective countercurrent flow of the continuous phase against the drops is utilized, whether intentionally or not. Thus, these settlers are close in concept to the IMI compact settler, incorporating the use of various partitions or trays of a certain shape and configuration, Lurgi's tray settler being one example⁽¹⁰⁾.

Packed beds, fibrous beds, and porous media of various kinds are well known aids to coalescence, and have been well discussed in the literature and widely applied on the industrial scale for increasing of drop diameter. However, the application of these aids is generally limited to the separation of dispersions characterized by low concentrations of droplets (usually less than 1%), such as the secondary haze remaining in the effluent of settlers after the primary break has been completed, and certain "natural" fine dispersions, e.g., the removal of water traces from jet fuels.

For such purposes, beds of very fine particles or closely packed fine fibres are in general use, resulting in a considerable pressure drop and frequent plugging of the bed with fine particles of solids, which are unfortunately nearly always present in recirculated liquid-liquid systems in industrial plants. The rate at which such secondary dispersions are "filtered" through these coalescence aids is generally lower (in volume rate of dispersion per unit area basis) than the order of magnitude of the capacity of settlers separating primary dispersions.

These features, especially the high pressure drop and the need for periodical washing-out of solid particles, has limited the industrial interest to secondary dispersions, which require a prohibitively long separation time.

For the separation of primary dispersions, especially when the absolute size of the settler is relatively small, the problem faced by the designer is of an entirely different nature. If the separation can be carried out easily in a simple gravity settler, the possible advantage to be gained by the use of coalescence aid is merely a certain reduction of the size of settler required which, for the most part, does not justify excessive liquid pumping head and maintenance. For this reason, the application of packed-bed coalescers in the heavy inorganic and hydrometallurgical industries used to be limited to the function of a post-separation polishing device mainly to remove tiny entrained solvent droplets from aqueous effluent streams.

Recent trends in the development of solvent-extraction processes for heavy chemicals led to the design and construction of plants having very large settlers and, consequently, large inventories of expensive solvent. These trends have resulted in a certain change of perspective, and the possible use of coalescence aids for the separation of primary dispersions, as well as any other potential means by which settler efficiency can be increased, are being reconsidered.

KnitMesh recently publicized the use of a low-pressure drop-knitted element for the separation of primary dispersions, claiming a reduction of the required settler area by a factor of about 2. This element includes either homogeneous mesh fabric or the specially designed D.C. Packing, a mixed fabric of hydrophilic and hydrophobic fibres, claimed to have the advantages of inducing the separation of both o/w and w/o dispersions, and extra efficiency as the result of a "junction effect".

The object of the study reported in this paper was the determination of whether a similar increase in the efficiency of separation of primary dispersions can be obtained by the simpler and less expensive conventional packed bed, in view of the general availability of standard packings of various sizes, shapes and construction materials, the negligible pressure drop and no problems resulting from plugging with eventual solid particles.

Flexibility in the application of the packed bed is another important factor. A special double-perforated or slotted diffuser-cage, having merits of its own, may be included in the original design, and may be fully or partially filled with suitable packing in case there are eventual problems in phase separation. The size and amount (and therefore the costs) of the packing may then be adjusted to cope with actual needs. With such a potential remedy for eventual malfunctioning, safety factors may be cut down considerably.

Of special interest is the possible hybrid separator, consisting of a packed-bed diffuser-precoalescer and an IMI compact settler with which it is hoped that a higher degree of efficiency will be achieved than that obtainable separately with each method.

Whereas, in principle, any of the general methods al-

ready mentioned may be combined for increased settler efficiency, a combination of methods falling within the same general category does not appear to be promising. The methods aimed at the increase of drop size are limited, since there is a certain maximum size of drop. The bigger the drop, the more difficult it is to effect further growth and the higher the probability of spontaneous breakdown due to turbulence or impingement. Thus, it is not expected that the combination of two methods for increase of drop size will allow the contribution by each method, used separately, to have its full effect, e.g., the combination of a specially designed contacting device producing large drops with a packed-bed precoalescer, or the combination of a packed-bed precoalescer with the addition of suitable finely divided solids to induce the coalescence of drops in the settler, do not appear to be very promising.

On the other hand, the combination of an available, efficient, and simple method for increase of drop size with yet another efficient and simple method for decrease of the drop size required for the accomplishment of separation within a given residence time appear to be mutually complementary.

Thus, the possible combination of the IMI compact settler with a simple packed-bed diffuser-precoalescer is, potentially, a fully complementary combination to which each of the individual methods would be expected to contribute nearly its full individual effect, i.e., under similar conditions, the combined improvement ratio is expected to equal nearly the product of the individual improvement ratios.

It was a further object of the present experimental study to check this assumption.

Previous Work

As has already been mentioned, most of the relevant literature deals with the separation of secondary dispersions in beds of very fine particles or fibres. Therefore, the results of such studies are not necessarily directly relevant to a coarse-bed precoalescer for primary dispersion. However, a short recapitulation of the results of these studies regarding the effect of some important parameters on the performance of the coalescers will be given here.

There seems to be general agreement that increase of the interstitial velocity of the dispersion through the coalescer would result in a decreased efficiency of separation. Some authors report a continuous effect⁽¹¹⁻¹³⁾, while others claim that separation occurred only below a certain critical velocity⁽¹⁴⁻¹⁶⁾. Some authors claim that the velocity, also, must be above a certain minimum for good performance to be achieved^(11,14).

Increased efficiency of separation due to the use of thicker beds⁽¹¹⁾ and finer particles⁽¹⁶⁾ has been reported, while other authors claim that both these parameters may be unified and that the total efficiency of separation grows with the total surface of the beds^(12,14). Gudesen *et al.*^(15,16) report an optimum thickness for the beds, their explanation for this phenomenon being based upon the assumption that, in excessively thick beds, redispersion overrides coalescence effects.

In most of the literature it is claimed that the particles in the bed should be preferentially wetted by the dispersed phase⁽¹⁷⁾, but several authors^(15,16,18) have indicated that this is not universally true. Davies and Jeffreys⁽¹⁹⁾ claim that, for separations of primary dispersions, the packing must be preferentially wetted by the dispersed phase. However, for secondary hazes, they postulate that "the droplets do not coalesce on the packing and the wettability of

the material is no longer the dominant design factor, rather that these very tiny drops adhere to points of roughness on the surface of the fibres for sufficient time to allow other droplets to coalesce on them by an impact mechanism. In this way droplets grow on the surface until such time as the viscous forces overcome the force of adhesion between the drop and fibre and then the droplet detaches from the surface and flows through the bed." Voyutskii *et al.*⁽¹⁴⁾ observed that an intermediate wettability gave the most effective separation, and concluded that, for best performance, the filter should be sufficiently well wetted by the dispersed phase for coalescence, but not wetted to the extent that excessive clogging by accumulation of the dispersed phase is produced. Later, these authors reported that a mixture of hydrophilic and hydrophobic fibres was advantageous⁽²⁰⁾. Davies and Jeffreys corroborate this observation, claiming that, for primary dispersions, a bed composed of mixed hydrophilic and hydrophobic fibres results in a better separation than beds of either pure hydrophilic or pure hydrophobic fibres, of both w/o and o/w dispersions as the result of a so-called "junction effect".

Experiments and Results

Set Up, Procedure, and Phase System

The work was carried out on a continuous, closed cycle, thermostatically controlled mixer-settler set up, a schematic flow sheet and description of which ("set up A") have been given in a previous paper⁽⁴⁾. The general experimental procedure has also been described⁽⁷⁾, and need not be repeated. The settler was a side-feed rectangular cross-section box of transparent PVC, and had a length (including diffuser chamber) of 50cm, a width of 18cm, a height of 100 cm, and a total cross-section area of 0.090 m². The first 7 cm of its length, close to the entrance for the feed, are separated from the main settler by a slotted vertical partition extending over the whole width (the diffuser) to form a diffuser chamber.

During experiments with simple gravity settling, the diffuser consisted of a single slotted partition for restraining feed turbulence. For experiments with the packed-bed diffuser-precoalescer, special cages of various dimensions were prepared. Each cage was in the shape of a rectangular box, two parallel sides of which had slots 0.3cm in width, and was filled with packing elements. The cage was inserted in the diffuser chamber of the settler in such a way that one of its slotted sides replaced the diffuser. The cage extended entirely within the diffuser chamber (Figure 1). Only for experiments with packed beds having thicknesses of 12cm was the cage extended 6cm within the diffuser chamber and 6cm to the main body of the settler. For simulation of compact-settler performance, a partition rack was inserted into the main body of the settler. The partition rack has 16 x 42cm parallel corrugated partitions that are 2.5cm apart vertically and have a slope of 10% towards the width. Although this configuration is not claimed to represent the optimum configuration for the phase system being studied, no other rack configuration for the compact settler was included in this study. During experiments on the combined effect of the compact settler with a fixed-bed diffuser-precoalescer, both the partition rack and the special cage containing the packed bed were inserted into the settler.

Two packing elements were investigated, namely, 6mm glass Raschig rings made by the cutting of 6mm glass pipes with a diamond saw, and 10mm glass Raschig rings (standard).

The experimental work was carried out on samples of phases obtained from the potassium nitrate solvent extrac-

tion plant of "Haifa Chemicals" in which the IMI KNO_3 process is implemented. It is essentially an acidic water and short-chain alcohol system. Two sets of conjugated phase systems representing the plant's extraction and washing batteries were studied. In both these phase systems, glass is preferentially wetted by the aqueous phase. All the experimental programme was carried out at $20 \pm 0.5^\circ C$. For each combination of "phase system — phase ratio-dispersion type-settler configuration" the continuous-settling characteristic (i.e., the graph of specific throughput versus the thickness of the dispersion band) was measured in accordance with the procedure described elsewhere⁽⁷⁾.

Experimental Results

Four different phase systems were investigated, as follows.

- A. Washing-battery phases, O:W ratio = 2.5 w/o dispersion.
- B. Washing-battery phases, O:W ratio = 2.5, o/w dispersion.
- C. Extraction-battery phases, O:W ratio = 1.5, w/o dispersion.
- D. Extraction-battery phases, O:W ratio = 1, o/w dispersion.

The effects of the following parameters on the thickness of the dispersion band versus specific throughput (dispersion throughput per unit cross-section area of the settler) continuous settling characteristics were studied: bed thicknesses for the packed-bed diffuser-precoalescer of 3, 6 and 12cm, particle sizes of 0.6 and 1.0cm Raschig rings, and residence time of dispersion in the bed. This residence time was changed, without affecting the thickness of the bed, by a change in the height of the bed. Bed heights of

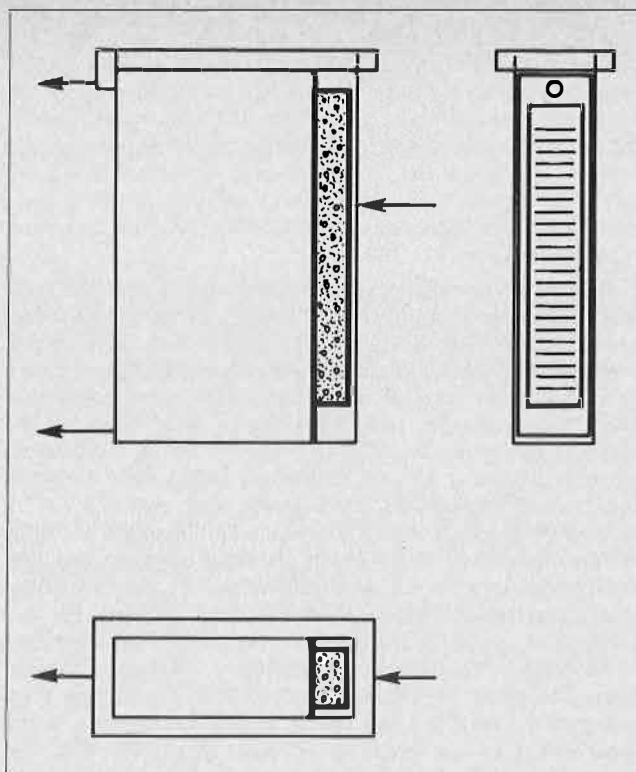


FIGURE 1. Schematic sketch of the packed-bed precoalescer cage installed in the diffuser chamber of the settlers.

15, 30 and 66cm were studied. In a single case (Run 7), the width of the bed was also changed (from 14cm in all other runs) to 7cm.

TABLE 1. Experimental results

Run no.	Dispersion type	Phase ratio O:W	Partition rack	Packing material (glass) (Raschig) mm	Cage			Capacity* [m ³ /h.m ²]	Improvement* ratio	Velocity through the packing* [m ³ /h.m ²]	Mean residence time in the packed-bed diffuser [s]
					Thickness [cm]	Width [cm]	Height [cm]				
Washing — Phase System											
1	w/o	2.5	No	No	—	—	—	11.4	1.00	—	—
2	"	"	No	6	6	14	66	17.8	1.56	17.5	12.3
3	"	"	Yes	No	—	—	—	32.0	2.79	—	—
4	"	"	Yes	6	6	14	66	43.4	3.81	39.8	5.4
5	"	"	No	6	6	14	30	15.2	1.33	32.6	6.6
6	"	"	"	6	6	14	15	14.9	1.31	63.8	3.4
7	"	"	"	6	6	7	30	15.6	1.37	66.8	3.2
8	"	"	"	6	3	14	66	13.9	1.22	13.4	8.0
9	"	"	"	6	12	14	66	19.8	1.74	19.3	22.3
10	"	"	"	10	6	14	66	15.4	1.35	15.0	14.3
Extraction — Phase System											
11	w/o	1.5	No	No	—	—	—	26.8	1.00	—	—
12	"	"	"	6	3	14	66	33.6	1.25	32.7	3.3
13	"	"	"	6	6	14	66	44.2	1.65	43.1	5.0
14	"	"	"	6	12	14	66	42.1	1.57	41.0	10.5
15	"	"	"	6	6	14	30	34.5	1.29	73.9	2.9
16	"	"	"	6	6	14	15	33.2	1.24	142.2	1.5
17	"	"	"	10	6	14	66	30.6	1.14	29.7	7.2
18	"	"	"	10	12	14	66	34.7	1.30	33.8	12.8
19	o/w	1	No	No	—	—	—	32.0	1.00	—	—
20	"	"	"	6	3	14	66	35.0	1.09	34.1	3.3
21	"	"	"	6	6	14	66	41.0	1.28	39.9	5.4
22	"	"	"	6	12	14	66	37.8	1.18	36.8	11.8
23	w/o	1.5	Yes	No	—	—	—	80.0**	3.2**	—	—
24	w/o	1.5	Yes	6	3	14	66	100.0**	4.0**	97.4	1.1
25	o/w	1	Yes	No	—	—	—	73.5**	2.45**	—	—
26	o/w	1	Yes	6	6	14	66	94.5**	3.15**	91.8	2.4

*Based on dispersion band thickness of 70 cm.

**These measurements and improvement ratios are based on a dispersion-band thickness of 50 cm, since, because of the high capacity, it was impossible to increase the loading of the settler so as to yield a dispersion band having a thickness of 70 cm with the existing arrangement.

In addition, in phase systems A, C, and D, the combined effect of partition racks with packed-bed diffuser-precoalescer were determined and compared with the individual effects of the partition rack (compact settler) and the packed-bed diffuser. Obviously, for each phase system, the continuous-settling characteristic of the simple gravity settler, having neither a packed-bed precoalescer-diffuser nor a partitions rack, was also measured for use as a reference. The experimental results for 26 runs are summarized in Table 1.

Improvement ratio was arbitrarily defined as the ratio of the loading of sophisticated settler, either CS (compact settler) or PBDP (settler with packed-bed diffuser-precoalescer) or combination of both (CS + PBDP), resulting in a 70 cm thickness of dispersion band (corresponding to about the maximum obtainable in the setup used) to the settler loading in case of simple gravity settler experiment carried out under similar conditions that would result in the same dispersion band thickness. For runs 23 to 26, very high loadings were achieved, and dispersion bands thicker than 40cm could not be obtained with the throughputs available with the experimental setup. So that excessive error due to extrapolation could be avoided, the improvement ratios for those runs were calculated according to dispersion-band thickness of 50cm. The improvement ratio according to 70cm is expected to be higher by a factor of 1.2 to 1.4. (The higher figure corresponds to the ideal effect of the compact settler). Note also that, for compact settlers, the improvement ratio increases with increase of the thickness of the dispersion band, and considerably higher values are expected for dispersion bands having thicknesses of say, 100cm.

As the cage dimensions were not changed in the course of an individual run, whereas the loading is variable, the

specific velocity of the feed through the packed bed, as well as the mean residence time, vary with the loading. In this context, it should be noted that, at relatively low loadings, when the thickness of the dispersion band is low, not all the packed bed available is effective. Although the thickness of dispersion band in the diffuser chamber may be significantly higher than in the settler, it is still lower than the packing height, so that part of the packing is not filled with dispersion.

The individual continuous-settling characteristics are shown on logarithmic coordinates in Figures 2 to 11.

Discussion

General

The present study is not extensive enough for a quantitative correlation of the effects of the various parameters involved to be made, so that, in the main, only general qualitative trends can be pointed out.

The maximum PBDP improvement ratios in Table 2 were actually measured for the various phase systems studied.

TABLE 2. Maximum PBDP Improvement Ratios

Phase system	Drops phase	Maximum PBDP improvement ratio, actually measured	Reference
A	Aqueous	1.74	Run 9
B	Organic	1.02	Fig. 11
C	Aqueous	1.65	Run 13
D	Organic	1.28	Run 21

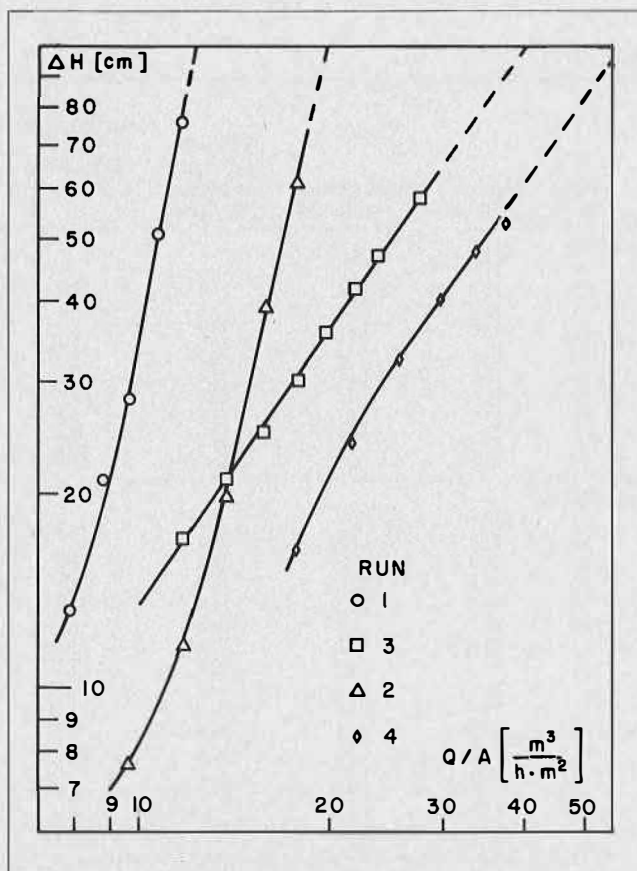


FIGURE 2. Continuous-settling characteristics — phase-system A. PBDP, CS, and PBDP + CS effects.

Clearly, the improvement in separation due to the PBDP effect is much more significant with w/o dispersions as compared with organic dispersed systems, most probably because of the preferential wetting effect. If it is taken into account that no attempt was made to fully optimize the PBDP effect, it may be assumed that, with packing of suitable surface properties, an increase of 90 or even 100% capacity of the settlers (Figure 12) may be obtained with particles having diameters of 0.6 to 1.0cm, and bed thickness of 8 to 10cm. This effect is rather significant for such a simple and relatively inexpensive installation, and is accompanied by no significant penalty either of pressure drop or plugging with eventual finely divided solids present in the dispersion.

For organic dispersed systems, the improvement in separation gained by packing elements of glass is rather poor, but still significant (an increase of 28% was actually obtained with phase-system D). For phase-system B, it seems that the effect was depressed as the result of the combination of two factors, namely, the unfavourable wetting characteristic and the very high natural rate of separation of this phase system resulting in high velocity of the dispersion through the packing. At relatively low loadings of the settler, a significant improvement was demonstrated even with this phase-system (Figure 11), but, with the increase in specific throughput, the effect diminished, and, by extrapolation, it appears to be nearly nullified with a dispersion band having a thickness of 70cm, which was chosen as the basis for calculation. This decrease is shown in Figure 11, since the PBDP characteristics are steeper than the simple gravity-settler characteristics approaching it at $\Delta H \approx 70$ cm.

Generally, the PBDP effect results in relatively minor changes in the slope of the continuous-settling characteristics. The main effect appears to be a nearly parallel shift

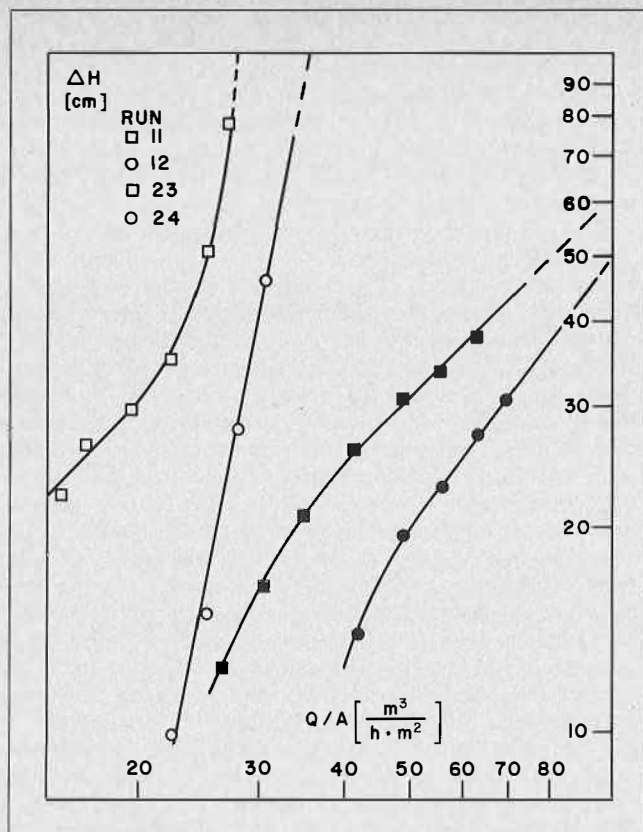


FIGURE 3. Continuous-settling characteristics — phase-system C. PBDP, CS, and PBDP + CS effects.

of the settling characteristics to the right, indicating a relatively mild dependence of the improvement ratio on the loading of the settlers. When the PBDP affects the slope of the characteristics, it may influence it in both directions.

On the other hand, the main CS effect is depression of the slope of the settling characteristics from its typical value of 2.5 to 5 towards a theoretical ideal slope of 1.0⁽²⁾. Thus, the improvement ratio tends to increase rapidly with the settler loading becoming significant for a thickness of the dispersion band of about 10 times the vertical distance between the plates, while the full effect is realized at a thickness of about 30 to 50 times this distance.

With the combined CS + PBDP effects, the continuous-settling characteristics are both shifted to the right (as a result of the PBDP effect) and depressed in slope (as a result of the CS effect), the characteristics being generally nearly parallel to the CS characteristics.

The Combination of CS with PBDP

The settling characteristics of the simple gravity settler, and the PBDP, CS, and PBDP + CS are given in Figures 2, 3, and 4 for phase-systems A, C, and D respectively. As demonstrated by these figures, the PBDP characteristics are nearly parallel to those for the simple gravity settler, and the PBDP + CS characteristics are nearly parallel to those for CS settlers, the shift to the right being similar in both cases. These results mean that the addition of PBDP increases the capacity of simple gravity settlers and of CS settlers by about the same factor, as shown in Table 3.

As can be seen, from these results, the product of the individual improvement ratios of PBDP and CS is equal

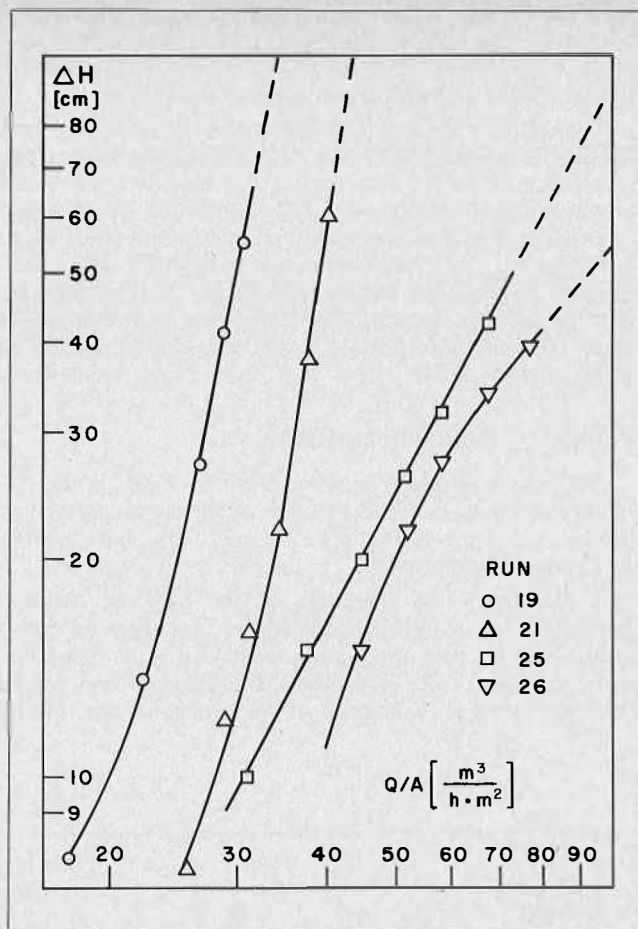


FIGURE 4. Continuous-settling characteristics — phase-system D. PBDP, CS, and PBDP + CS effects.

TABLE 3. Comparison of Improvement Ratios of PBDP, CS, and PBDP + CS Settlers

Phase System	PBDP		CS		PBDP + CS	
	Run no.	Improvement ratio	Run no.	Improvement ratio	Run no.	Improvement ratio
A	2	1.56	3	2.79	4	3.81
C	12	1.25	23	3.20	24	4.00
D	21	1.28	25	2.45	26	3.15

to, or only slightly higher than, the improvement ratio of the PBDP + CS combination. When a difference exists, it may be attributed to the change in interstitial velocity of the dispersion through the packed bed. This point is demonstrated for the case where the highest deviation is evidenced, namely, phase-system A, as follows. For Run 3 (CS) an improvement ratio of 2.79 was obtained. Upon the addition of a PBDP cage (6x14x66cm) having 0.6cm Raschig rings, the improvement ratio was raised to 3.81 (Run 4), i.e., by a factor of 1.32. The individual effect of the same PBDP results in an improvement ratio of 1.56, and, therefore, an improvement ratio as high as 4.35 could be expected, whereas an actual value of 3.81 was obtained. However, when such a comparison is being made, it should be borne in mind that, because of the increased capacity of PBDP + CS combination, the superficial velocity of the dispersion through the packing is increased from 17.5 m³/h.m² (Run 2) to 39.8 m³/h.m² (Run 4). Thus, the contribution of the PBDP of 3.81:2.79 = 1.32 to the improvement ratio should be compared with that

for Run 5, where packing of the same size of Raschig rings in a 6x14x30cm cage was used, resulting in a calculated superficial velocity of $32.6 \text{ m}^3/\text{h}\cdot\text{m}^2$ for the dispersion, and an improvement ratio of 1.33.

Thus, it may be concluded that the improvement ratio obtainable by the PBDP + CS combination is approximately equal to the product of the improvement ratios obtainable individually from CS and PBDP, on the basis of equal geometrical parameters of the CS and equal packing elements, bed thickness, and interstitial dispersion-velocity through the PBDP. The PBDP + CS combination appears to be especially promising, possible settler capacities being significantly higher than those experienced with compact settlers.

Effect of Bed Thickness

Continuous-settling characteristics for PBDP with different thicknesses of the bed, all other parameters being similar, are shown in Figures 5, 6, and 7 for phase-systems A, C, and D respectively.

A change in the thickness of the bed for constant throughput of the dispersions means a change in mean residence time with no simultaneous change in the interstitial velocity of the dispersions. In Figures 5 and 7, and less in Figure 6, a change in the slope of the settling

characteristics with change of the thickness of the bed is clearly indicated. In all cases, bed thicknesses of 3, 6, and 12cm are compared (5, 10, and 20 packing element diameters). With a bed thickness of 3cm, the characteristics slope appears to be steeper than that for the simple gravity settler; with a thickness of 6cm, it appears to be nearly parallel to that of the simple gravity settler; and with a thickness of 12cm it appears to be steeper again.

The phenomenon deserves a reasonable explanation, and, although this study is not extensive enough for a model to be tested fully, a possible explanation will be attempted. Assume that the pre-coalescence effect increases with residence time, but decreases with interstitial velocity, whereas the redispersion effect increases with both residence time and interstitial velocity. Furthermore, assume that the marginal contribution to pre-coalescence diminishes with residence time, so that no significant further increase is gained above a certain residence time, and that the redispersion effects increase sharply with interstitial velocity, and are not significant below a certain critical velocity. For thin beds having relatively low interstitial velocity, redispersion effects are negligible in comparison to pre-coalescence effects, and the latter are strongly dependent on residence time. The decrease in residence time, upon increase of the specific throughput, is reflected by a decrease in pre-coalescence effect, and results in a steeper characteristic. For optimum thickness, pre-coalescence is only mildly affected by residence time, and the improvement ratio tends to be the same over a relatively wide range of specific throughputs, resulting in a nearly parallel characteristic. Upon further increase of bed thickness, the

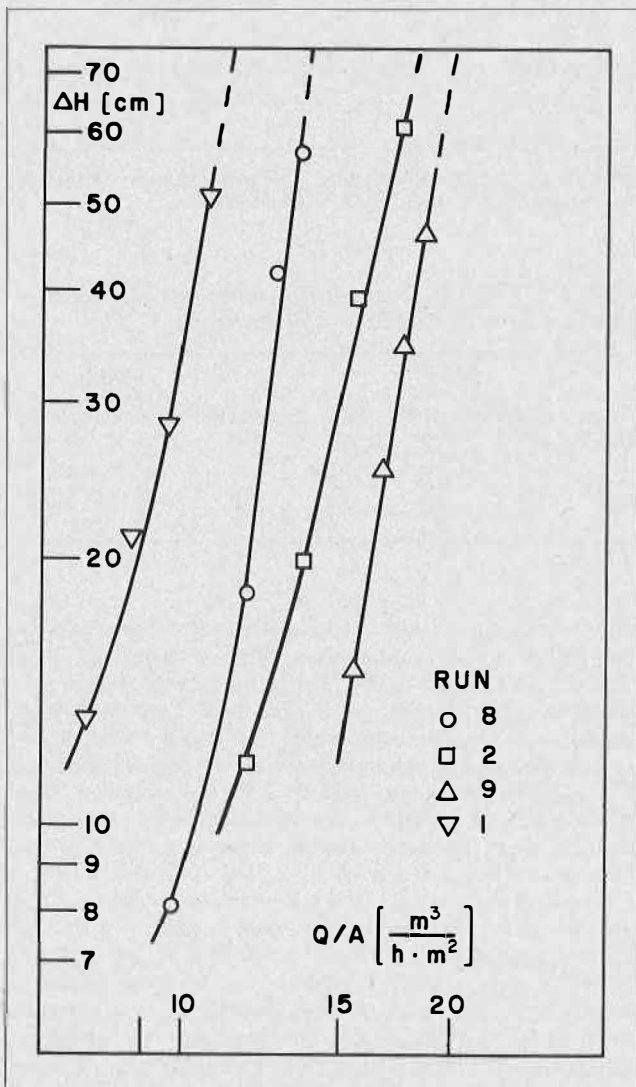


FIGURE 5. Continuous-settling characteristics — phase-system A. Effect of bed thickness.

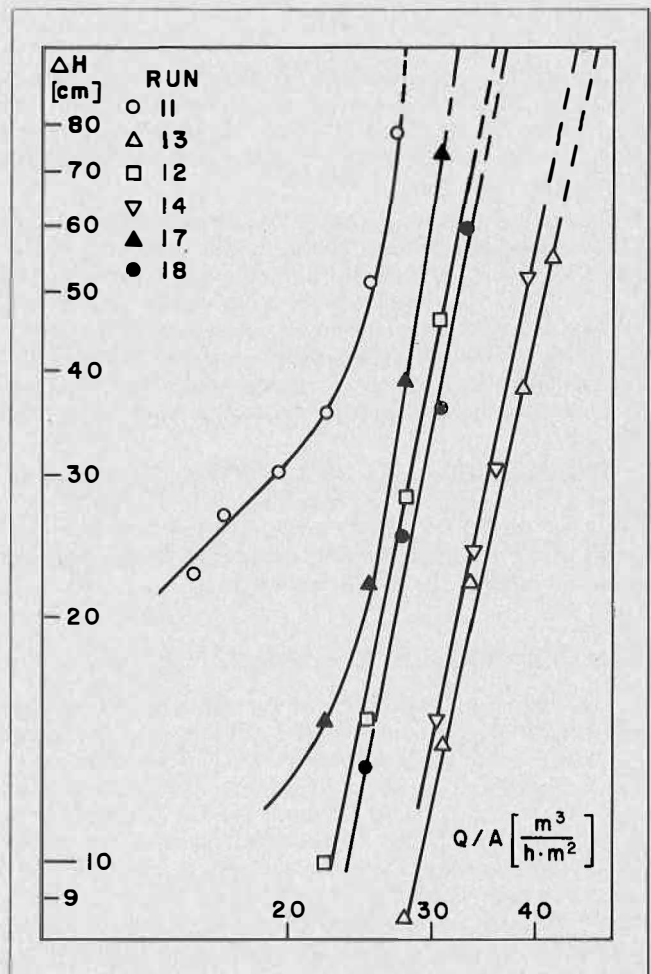


FIGURE 6. Continuous-settling characteristics — phase-system C. Effect of bed thickness and particle size.

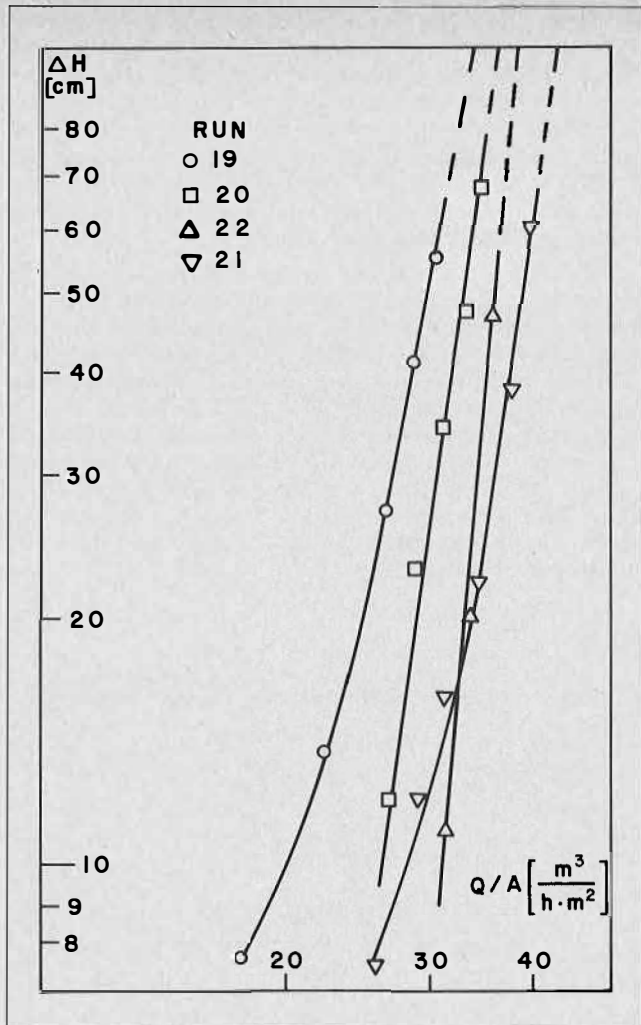


FIGURE 7. Continuous-settling characteristics — phase-system D. Effect of bed thickness.

increase of residence time may affect still more strongly the precoalescence effects for low specific throughputs, but, in the higher range of specific throughput, the effect of residence time on redispersion is dominant, and the net overall effect tends to diminish with specific throughput, resulting in a steeper settling characteristic once again. Hence, an optimum bed thickness must exist. In Figure 5 it can be seen that the performance of the 12cm bed is still better than that of the 6cm bed over the whole range studied. However, the characteristics of the 12cm are steeper than those of the 6cm bed, which implies that a bed thickness of 12cm may already be greater than the optimum thickness, and the optimum thickness may lie at an intermediate point. Figure 6 shows clearly that the 6cm bed is superior to the 12cm bed over the whole range studied (for 6mm Raschig rings) so that, obviously, the 12cm bed is already excessively thick. The graphs shown in Figure 7 are of special interest. In the low loading range, the 12cm bed still shows a superior performance over the 6cm bed, as a result of the beneficial effect of residence time on precoalescence, but, at higher loading, the detrimental effect of residence time on redispersion apparently becomes predominant, so that the characteristics intersect. The settling characteristics of the PBDP having 1.0cm Raschig rings and 6 and 12cm thickness of the bed (also given in Figure 6) imply that, with larger bed particles, the optimum thickness of the bed is shifted up, and is probably better defined in terms of number of packing element diameters.

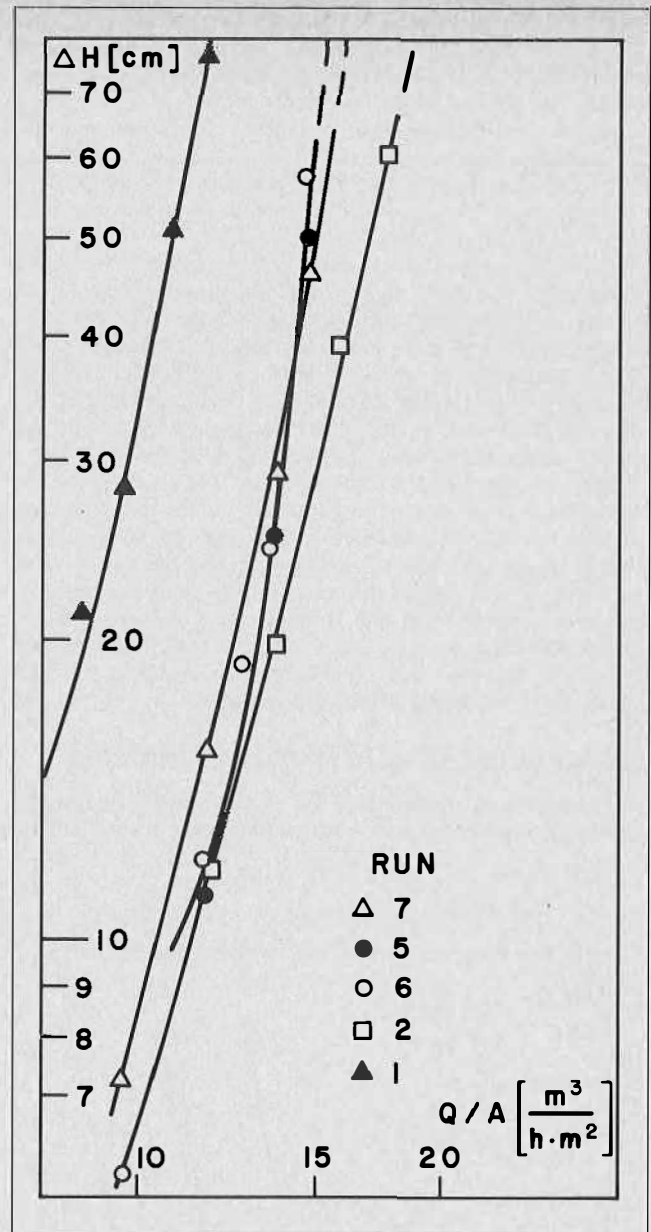


FIGURE 8 Continuous-settling characteristics — phase-system A. Effect of mean residence time in precoalescer.

With this model in mind, Figure 12 was constructed, and the graphs for the improvement ratio versus-bed thickness are apparently close to the dashed curves. However, there are no points, determined experimentally, with which to complete these parts of the curves and to prove this assumption. It appears that, for the phase system studied, the optimum thickness of the bed for 0.6cm Raschig rings is about 8 to 10cm. However, this is by no means a universal value, since, obviously, it depends on the nature of the phase system and the packing elements, and may also change with the scale-up if the basis for scale-up is other than constant interstitial velocity.

Effect of Interstitial Velocity

In Figures 8 and 9, settling characteristics for beds of different cross-section perpendicular to the direction of flow of the dispersion are given for phase-systems A and C respectively. The change in the cross-section area of the beds has been affected by changing of the height of the beds, and, in a single case (Run 7), also the width of the beds.

It should be noted that, for constant specific throughput of the dispersions, a change in the cross-section area of the beds perpendicular to the direction of flow simultaneously affects both the interstitial velocity and the residence time. A decrease in cross-section area results in an increase of interstitial velocity and decrease of residence time. In accordance with the proposed model, both effects will influence the pre-coalescence rate in the same direction, but may have an antagonistic effect on redispersion. Improvement ratio versus superficial velocity is plotted in Figure 13. In view of possible antagonistic effects, the results are not sufficiently extensive, and the picture revealed by Figures 8, 9, and 13 is not clear enough. It can be claimed only, as will obviously be anticipated, that the increase of interstitial velocity is never beneficial, and often detrimental, to the pre-coalescence effect. The different effect of a change in the height of the beds and a change in the width of the beds at low loadings of the settler is explained by the fact that, at low loadings, the diffuser chamber is not filled with dispersion, so that a bed of full width but reduced height may give the same results as a bed of full height, whereas a change in the width of the bed is effective at any loading. At full loading of the settler this difference vanishes, and the result of a proportional decrease in either the height or width of the beds is the same for equal cross-section areas.

Effect of the Size of Packing Elements

The effect of particle size for phase-systems A and C is shown in Figures 10 and 6 respectively. Only two packing

elements, i.e., those having diameters of 0.6 and 1.0cm, were included in the study, which represents the full range that is of practical interest in the opinion of the authors. The lower limit is determined by the following: availability of standard packing elements (1/4"), packing and installation costs, pressure drop, and plugging of the bed with finely divided solids. The upper limit is set by the maximum size that can still produce an effect of any significance for industrial application.

However, a study having such a limited range is insufficient from the scientific point of view if full insight of the phenomena is to be gained. Obviously, if all other parameters are kept constant, the pre-coalescence effect decreases with increased particle size. If the effect should be directly proportional to surface area, then packing of a different size should result in the same improvement ratio based on equal value of bed thickness divided by the particle diameter. Thus, a 12cm bed packed with 1.0cm rings should be equivalent to a 7.2cm bed packed with 0.6cm rings, 6cm bed of 1.0 cm rings is equivalent to a 3.6cm bed of 0.6cm rings.

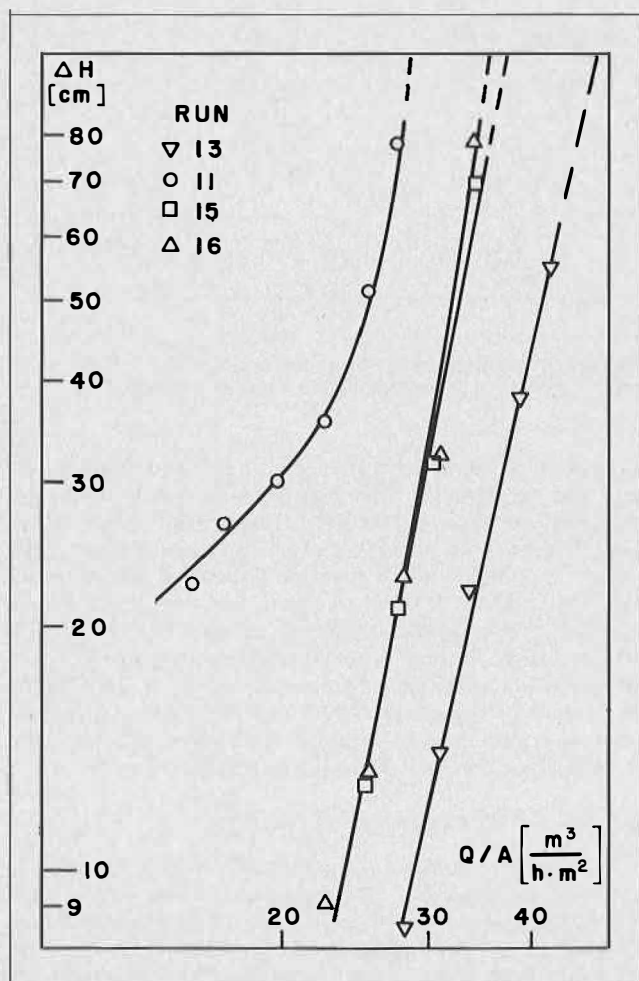


FIGURE 9. Continuous-settling characteristics — phase-system C. Effect of mean residence time in pre-coalescer.

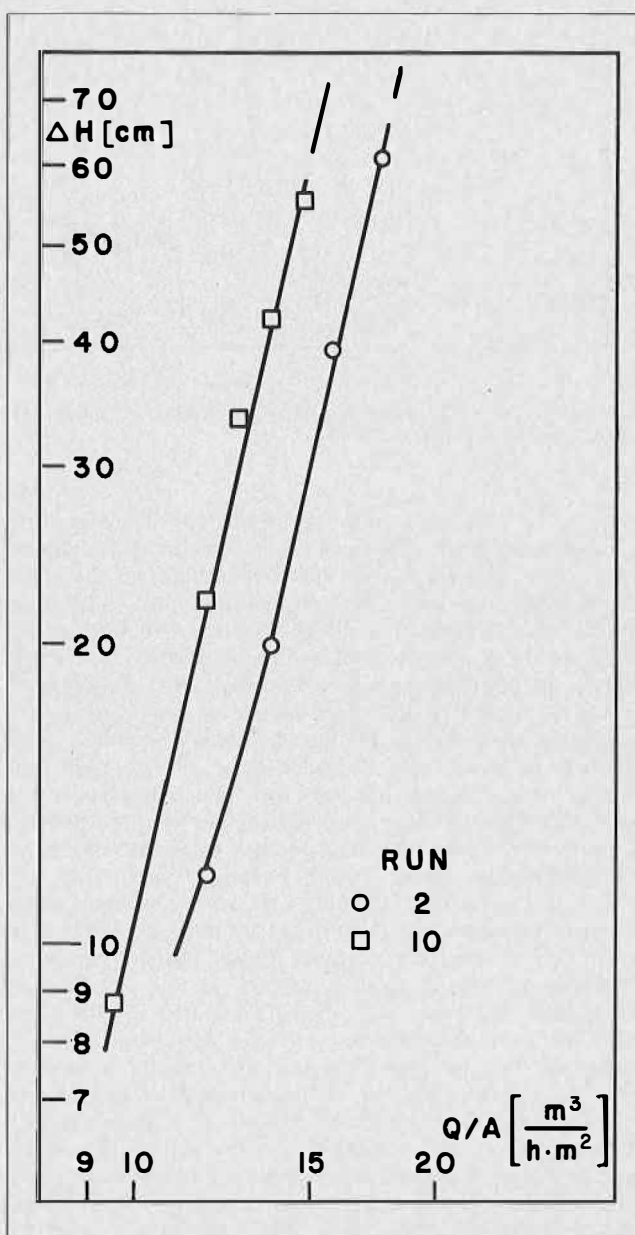


FIGURE 10. Continuous-settling characteristics — phase-system A. Effect of particle size.

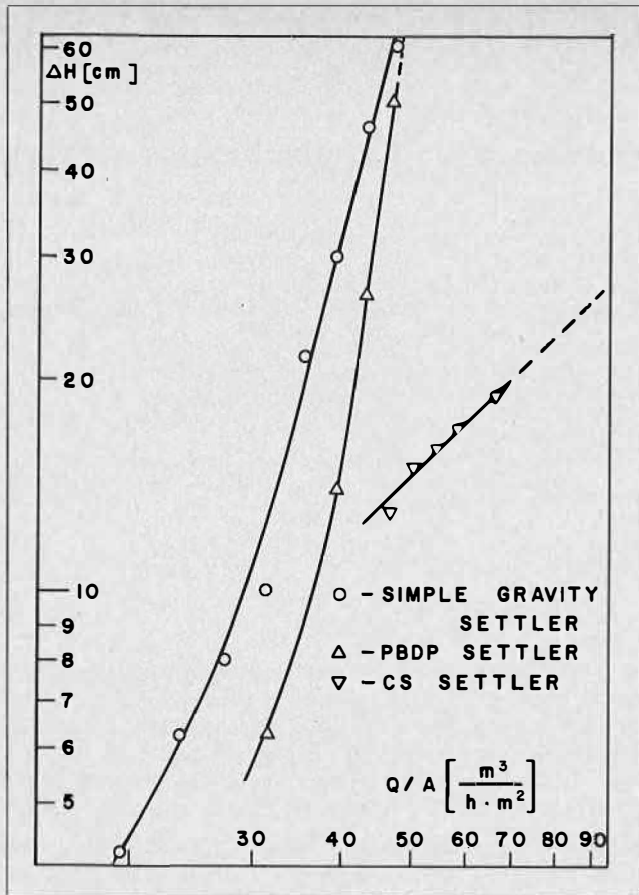


FIGURE 11. Continuous-settling characteristics — phase-system B. PBDP and CS effects.

Plotting of the results with 1.0cm rings according to this equivalent thickness in Figure 12 reveals that the point for phase-system A falls close to the improvement-ratio versus bed-thickness curve for this phase system, thus supporting this assumption. However, both points for phase-system C fall rather low.

Conclusion

It has been experimentally demonstrated that the capacity of a gravity settler may be significantly increased by means of a simple, and relatively inexpensive, thin-layer packed-bed diffuser-precoalescer with the use of available standard packing elements. With a bed having a thickness as low as 8 to 10cm and packing elements having diameters in the range of 6 to 10mm the capacity of the settler can be doubled, provided that the packing elements have suitable surface properties. It was found that there is an optimum thickness for the bed. For beds having packings consisting of 6mm Raschig rings this optimum thickness was found to be in the range of 8 to 10cm for the systems studied, but probably depends on the nature of the phase system, the size and type of packing, and the interstitial velocity of the dispersion through the packing. The optimum bed thickness is assumed to be the result of a balance between precoalescence and redispersion effects. Increase of either the interstitial velocity or the diameter of the packing element was found to decrease the efficiency of precoalescence.

The combinations of packed-bed diffuser-precoalescer with lamella compact-settler elements appear to be especially promising, since they have a higher capacity than that which may be obtained by each method separately, and

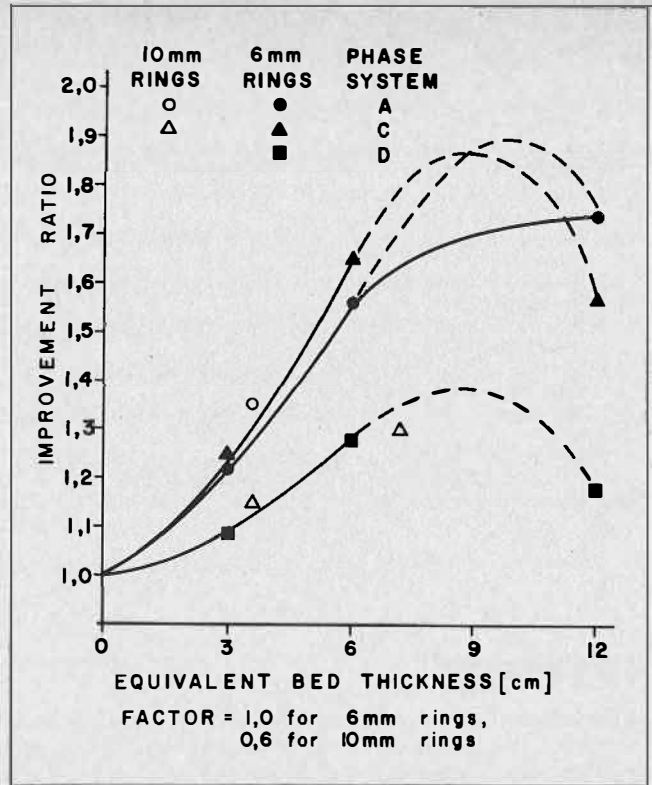


FIGURE 12. The effect of bed thickness on the improvement ratio.

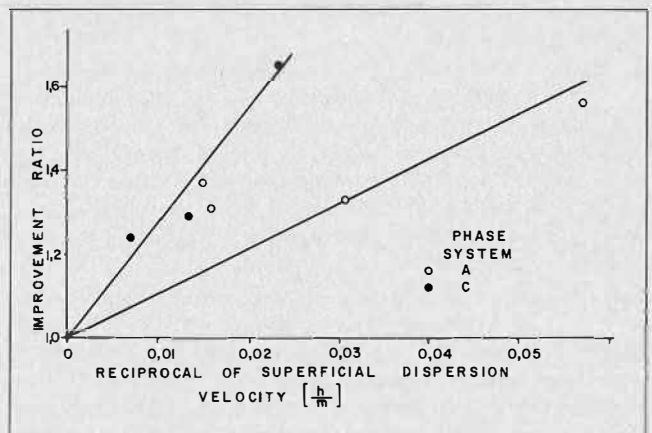


FIGURE 13. The effect of superficial dispersion velocity on the improvement ratio.

retain the maximum value of both individual effects, so that the improvement ratio for the combination is equal to the product of the individual improvement ratios.

Acknowledgement

This paper is published by permission of the Managing Director of IMI Institute for Research and Development, Haifa. Mr. A. Shpak assisted in the experimental work.

The paper was prepared while one of the authors (E. Barnea) was on sabbatical leave in South-Africa, first with the National Institute for Metallurgy, Johannesburg (NIM) and later with Edward L. Bateman Ltd. Boksburg (ELB). This author wishes to thank NIM and ELB for allowing him time for the preparation of the paper, and is indebted to NIM for help with the editing and preparation of the manuscript.

The Interaction of Droplets, Gas Bubbles and Solid Particles

W. Rushton*, G.A. Rowden† and G.A. Davies*

ABSTRACT

The problem of the interaction of a pair of droplets, a drop and gas bubble or a drop and a solid particle is considered and the solutions for quasi steady flow developed. The solutions are applied to the flocculation or hindered settling of a dispersion towards a phase boundary where the transport and surface properties of the phases control the settling velocities of the droplets. Interaction between the dispersed phase droplets may result in motion contrary to the operating density gradient. Conditions under which entrainment of one of the droplets against the density gradient forces are assessed in terms of the significant process parameters. Critical interdroplet separation distances at which entrainment is possible are predicted. These results are related to the dispersed phase hold-ups for a postulated packing structure. These enable the necessary criteria for entrainment in terms of the relevant system parameters to be produced.

As an application, a copper solvent extraction plant is discussed, in which these conditions of entrainment may be evident in decantation, solvent extraction and flotation. The importance of entrainment in the solvent extraction step of the overall copper process has been considered for a typical large copper plant operating on an acid leach system. In the operation of such a process entrainment of dispersed phase from settlers constitutes a significant solvent loss. Solid particles can be entrained, against the density gradient, in both the solution purification plant and in settlers. In the latter case this is a contributory reason for crud formation. These are considered and an economic evaluation presented. The importance of loss from crud removal is evident.

Part I. Introduction and Theory

Introduction

IN ANY TWO OR THREE-PHASE SYSTEM the possibility of entrainment of one of the phases exists. By this is meant that on attempting to separate the phases (for example by gravity settling utilising the density difference between the continuous and discontinuous phases), one phase may be entrained at least partially with another. This is no less true in hydrometallurgical processes than in other applications; indeed in hydrometallurgical processes, entrainment of solids in feed liquids, as for example in leaching and decantation, and entrainment of liquids in

solvent extraction give problems both to design engineers and to operations staff. There is, therefore, a need to be able to predict when entrainment will take place and to design equipment both to overcome entrainment and to provide better phase separation. This paper is an attempt to predict when entrainment is likely in particle settling processes, in counter-current decantation equipment, in settlers in solvent extraction processes and in air-sparging flotation equipment. The results are then applied to a problem of solids — crud — entrainment in a commercial copper extraction plant. Finally the effects of entrainment on the economics of typical large-scale commercial copper plants using a leaching, solvent extraction and electro-winning process route are discussed.

The processes referred to above, in which separation takes place under gravity by reason of the density difference between the phases, are all characterised by low particle-translational Reynolds numbers. In many applications, conditions of Stokes flow, $Re < 1$, can often be assumed. This is frequently used in design to establish the residence time required in settling flow for separation of particles of given size, since the settling velocity can be estimated. Thus, for a given flow condition in the vessel (usually assumed to be plug flow), the vertical dimension of the vessel can be calculated at a particular volumetric flowrate. This is a classic case in which single particle data are used to predict the performance of dispersions. In some cases correction factors are used, (a) to account for modified settling characteristics in the multiple particle situation (these are largely empirical), (b) to allow for variations in settling due to the fluidity of the particle — droplets (based on Hadamard-Rybczynski solution for translation of a single droplet)⁽¹⁾. This approach suffers the major disadvantage that in three-phase systems the interaction between particles which can lead to entrainment of one phase cannot be anticipated, let alone quantified. In two-phase systems the simple theory based on Stokes' law is inadequate in that interaction between the particles is ignored. This becomes important at high dispersed phase hold-up or in practical cases where a distribution in particle sizes exists. An attempt to describe dispersions of solid particles was made by Kynch⁽²⁾ who provided a series solution for the settling velocity of the particles. This allows for interaction between solid particles at large separations.

The problems involved in modelling dispersions are considerable and progress in this field has been slow. The minimum number of particles in a system for which interaction forces both exist and can become dominant (depending on the interparticle separation distance) is two. Thus, some progress could perhaps be made by investigating systems of doublets thoroughly. This will be the object of the theoretical section of the present paper. Equations will be derived from which conditions for large interactions leading to entrainment can be determined.

The problem will be considered in a general way so that all three phases (two dispersed phases and the continuous fluid phase) may be different. Furthermore, the dispersed phases can be any combinations of solid, liquid or gas.

*Department of Chemical Engineering UMIST, University of Manchester, Manchester 1, England.

†Davy Powergas Ltd., Research and Development Division, Stockton-on-Tees, Cleveland, England.

In this way all of the binary interactions can be studied. It is known for example that the presence of solid particles, usually as particulate contamination, can interfere with dispersion separation. Indeed, this will be considered from an economic standpoint in Part II of this paper. In such cases the interaction effects are deleterious to the process. In other cases they are an advantage, for example in air flotation. Thus, a better understanding may ultimately help in design and operation of separation equipment.

Theoretical Development

If we now consider the motion of two particles in a viscous liquid the orientation of the particles will clearly be important. Two limiting cases exist from which a solution for any particular configuration can be determined by proper linear combination of the limiting cases: — (a) motion of particles along their line of centres and (b) parallel motion of particles perpendicular to their line of centres. Kynch was one of the first to recognise this fact; he obtained a solution for settling of solid particles which was valid providing the velocities satisfied Laplace's equation, $\nabla^2 u_i = 0$, such that the solution could be written in the form $u_i = v_i + x_i p$ where $\nabla^2 v_i = 0$. Whilst this approach is useful the solution is valid only if the distance of separation of the particles $\epsilon > 3(r_i + r_j)$.

In the present context, since the prime interest is to assess the interaction between particles, this will be maximum when the particles are translating along their line of centres. Therefore, only this branch of the overall solution will be considered.

It is important to define precisely the conditions for a solution. Consider the general case that all three phases ($i = 1, 2, 3$) are fluids. Three flow regions can be defined therefore, and if we limit discussions to incompressible Newtonian fluids, then the flow in each region is defined by the Navier Stokes equations of motion: —

$$\frac{\partial \bar{u}_i}{\partial t} + \bar{u}_i \nabla \bar{u}_i + \frac{1}{\rho_i} \nabla p_i = \nu_i \nabla^2 \bar{u}_i \dots \dots \dots (1)$$

and

$$\nabla \cdot \bar{u}_i = 0 \dots \dots \dots (2)$$

where u_i and p_i are the local fluid velocity and pressure respectively.

In most gravity separation systems the translational Reynolds number of the particles is small $Re \approx O(1)$ and thus the non-linear inertial terms in (1) are small with respect to the viscous terms and the problem reduces to unsteady creeping flow. Even with this simplification, the solution of equation (1) for this problem has not been obtained; such a solution only exists for a single solid sphere.

Under certain conditions a further simplification is possible — the unsteady state terms can be shown to be small with respect to the viscous terms. To establish these conditions, define a characteristic velocity U (this could be the translational settling velocity of one particle) and a characteristic distance parallel to the flow ϵ which is defined as the minimum distance of separation of the particles. Then dimensionless quantities may be defined thus: —

$$\bar{u}_i^* = \frac{\bar{u}_i}{U}; t^* = \frac{tU}{\epsilon}; \nabla^* = r_i \nabla \cdot$$

Using these definitions in equation (1) the terms can be compared with the viscous terms.

$$\frac{\bar{u}_i \cdot \nabla \bar{u}_i}{\nu_i \nabla^2 \bar{u}_i} = \left[\frac{Ur_i}{\nu_i} \right] \frac{\nabla \bar{u}_i^*}{\nabla^2 \bar{u}_i^*} \dots \dots \dots (3i)$$

and

$$\frac{\partial \bar{u}_i / \partial t}{\nu_i \nabla^2 \bar{u}_i} = \left[\frac{Ur_i^2}{\nu \epsilon} \right] \frac{\partial \bar{u}_i^* / \partial t^*}{\nabla^2 \bar{u}_i^*} \dots \dots \dots (3ii)$$

Therefore (3i) shows that the inertial terms can be neglected compared to the viscous terms, providing the translation Reynolds number $(Ur_i/\nu_i) = O(1)$ and (3ii) shows that the unsteady terms can be neglected and providing the dimensionless group $\left[\frac{Ur_i^2}{\nu \epsilon} \right]$ is small $\{O(1)\}$. This is important to emphasize; the choice of ϵ as the characteristic dimension in the direction parallel to flow signifies the pertinent contribution of the time dependent terms. Other workers, studying the approach of a droplet or solid particle towards a flat plane (which is a limiting solution to the problem of motion of two particles along their line of centre), have specified the distance between the centre of the particle and plane ($\epsilon + r_i$) as the characteristic distance (Bart⁽³⁾, Wacholder and Weihs⁽⁴⁾). This is not a sufficient condition since the two separate physical conditions would be satisfied simultaneously for small values of the translational Reynolds number.

If both dimensionless groups (Ur/ν) and $(Ur^2/\nu\epsilon)$ are small, equation (1) may be simplified. Furthermore, because the motion is axisymmetric the problem may be formulated in terms of the Stokes' stream function, ψ_i . Thus

$$E^4 \psi_i = 0, \text{ where } E^2 = \frac{\partial^2}{\partial z^2} + R \frac{\partial}{\partial R} \left(\frac{1}{R} \frac{\partial}{\partial R} \right) \dots \dots \dots (4)$$

The equations cannot be conveniently solved for two spherical particles in polar co-ordinates because of the difficulty of representing the surface of one of the particles. This can be overcome by transforming the problem into a bipolar co-ordinate system (see Happel and Brenner⁽¹¹⁾), (ξ, π, Φ) . In this system two particles external to each other, travelling in the z direction, correspond to the surfaces $\xi = \xi_1 (> 0)$ and $\xi = \xi_2 (< 0)$. ξ_1 and ξ_2 are related to the particle radii, r_j , and distance from the centre of the particle to the plane $\epsilon = 0$, h_j , by: —

$$\xi_j = \cosh^{-1} \left(\frac{h_j}{r_j} \right) \quad (j = 1, 2) \dots \dots \dots (5)$$

The general solution for the stream function, ψ_i , has been obtained and explained elsewhere⁽⁵⁾. Only the material required for the present discussion will be presented here. Thus: —

$$\psi_i = (\cosh \xi - s)^{-3/2} \sum_{n=0}^{\infty} U_{ni}(\xi) C_{n+1/2}^{-1/2}(s) \dots \dots \dots (6)$$

where $s = \cos \eta$

$$\text{and } U_{ni}(\xi) = a_{ni} \cosh(n - 1/2)\xi + b_{ni} \sinh(n - 1/2)\xi + c_{ni} \cosh(n + 3/2)\xi + d_{ni} \sinh(n + 3/2)\xi \cdot$$

$C_{n+1/2}^{-1/2}$ is a Gegenbauer polynomial of order $(n + 1)$ and degree $-1/2$. The twelve constants a_{ni} , b_{ni} , c_{ni} and d_{ni} ($i = 1, 2, 3$) have to be obtained from the boundary conditions. At each interface the tangential velocity components and shear stresses must be continuous and, providing the surface tension forces are larger compared with the deforming viscous forces, i.e. $\frac{\mu_3 U_j}{\sigma_j} \cdot \frac{r_j}{\epsilon} \ll 1$ ($j = 1, 2$), the discontinuity in the normal stresses is balanced by the surface tension forces, σ_j/r_j . Using these conditions with the additional requirement that the velocity components at the centre of the particles must remain finite, the twelve constants can be obtained and

expressions for the drag force F_j ($j = 1, 2$) opposing the motion of each particle obtained⁽⁶⁾. The equations for the drag forces are:—

$$F_j = 6\pi\mu_3 r_j \sum_k a_{jk} U_k \quad (k = 1, 2) \dots \dots \dots (7)$$

$$(j = 1, 2)$$

where the a_{ki} 's ($k, i = 1, 2$) are functions of the inter-particle distances expressed through ξ_1 and ξ_2 ($\xi_j = \cosh h_j/r_j$), $\mu_1/\mu_3 = \bar{\mu}_1$ and $\mu_2/\mu_3 = \bar{\mu}_2$.

In gravity settling the drag force is balanced by the gravitational force acting on the particle. Thus: —

$$\frac{4}{3} \pi r_j^3 (\rho_j - \rho_3)g = 6\pi \mu_3 r_j \sum_k a_{jk} U_k \quad (k, j = 1, 2) \quad (8)$$

From this solution we can immediately see that the buoyancy force on each particle is related to the translation velocities of both particles and thus expressions for the interaction between particles can be obtained.

For gravity settling, the ratio of the settling velocities of the particles (U_2/U_1) can be obtained from equation (9):

$$\frac{U_2}{U_1} = \frac{a_{11} - a_{12}(r_1/r_2)^3 \Delta\rho}{a_{22} (r_1/r_2)^2 \Delta\rho - a_{12}} \dots \dots \dots (9)$$

where

$$\Delta\rho = \frac{\rho_1 - \rho_3}{\rho_2 - \rho_3}, \text{ is a dimensionless density ratio.}$$

From equation (9) the magnitude of the particle interactions can be assessed. They depend on the values of the cross coefficients a_{kj} ($k \neq j$); $k, j = 1, 2$. As the distance between the particles increases, $h_1 + h_2 \gg r_1 + r_2$ then $a_{kj} \rightarrow 0$, ($k \neq j$), and the ratio of the settling velocities, equation (9) becomes: —

$$\frac{U_2}{U_1} \Big|_{h_1+h_2 \gg r_1+r_2} \rightarrow \frac{a_{11}}{a_{22}} \{ (r_1/r_2)^2 \Delta\rho \}^{-1} \dots \dots (10)$$

The coefficients a_{11} , a_{22} are determined by the properties of the phases 1 and 2. If the particles are solid particles $a_{11} = a_{22} = 1$ and the solution tends to Stokes' solution whereas if phases 1 and 2 are fluids with viscosities μ_1 and μ_2 then

$$a_{11} = \frac{3\mu_1 + 2\mu_3}{3(\mu_1 + \mu_3)} \text{ and } a_{22} = \frac{3\mu_2 + 2\mu_3}{3(\mu_2 + \mu_3)}$$

and the solution tends to the Hadamard-Rybczynski solution.

Tabulated data are provided for a_{kj} ($k, j = 1, 2$) for all the binary cases for three phases systems⁽⁶⁾; generally the net result is that $U_j > \sum_k a_{jk} U_k$, that is that the presence of a second particle reduces the settling velocity.

If, in the design of equipment, settling velocities are based on calculations for single particles, the results will always be greater than the values for dispersions. The deviation will get larger as the number of particles in the system increases but will tend to a limiting value. It would perhaps seem that empirical correction factors could be applied. To examine this possibility, consider the single particle solutions for droplets — the Hadamard-Rybczynski solution. If we apply this to two droplets 1 and 2 the ratio of the settling velocities is: —

$$\left(\frac{U_2}{U_1} \right)_\infty = \left(\frac{3\mu_1 + 2\mu_3}{3\mu_2 + 2\mu_3} \right) \cdot \left(\frac{\mu_2 + \mu_3}{\mu_1 + \mu_3} \right) \frac{1}{(r_1/r_2)^2 \Delta\rho} \dots \dots \dots (11)$$

This is of course identical to Equation (10). The subscript ∞ is to indicate that the solution is for a single particle — or two particles at an infinite separation.

$$\left(\frac{U_2}{U_1} \right) = f_1(\Delta\rho, \bar{\mu}_1, \bar{\mu}_2, r_2/r_1) \dots \dots \dots (12)$$

If one particle is a solid then either μ_1 or $\mu_2 \rightarrow \infty$. Now $\bar{\mu}_1$ and $\bar{\mu}_2 > 0$ and $r_2/r_1 > 0$ therefore the sign of $(U_2/U_1)_\infty$ depends on $\Delta\rho$ and no other factor. Therefore, i) $U_2/U_1 < 0$ which will result in the particles separating a correction factor, U_2/U_1 will always have the same sign, either positive or negative. This would mean, for example, that if a gravity settler was used to separate a liquid dispersion and that, if the dispersion contained some particulate solids such that the drop phase 1 and solid phase 2 had properties $\rho_1 < \rho_3 < \rho_2$, the single particle data would always predict separation of the liquid dispersed phase and solid phase from the field phase 3. Apart from the fact that the settling velocities calculated may be greater (negatively), it is this type of situation where entrainment is found to be particularly prevalent in equipment and can only be understood by looking at a multiple particle situation.

Returning to the general solution, from equation (9)

$$\frac{U_2}{U_1} = f_2(\Delta\rho, \bar{\mu}_1, \bar{\mu}_2, \xi_1, \xi_2) \dots \dots \dots (13)$$

Now comparing equations (12) and (13), the solution for the doublet depends on the particle separation since $\xi_j = \cosh^{-1}(h_j/r_j)$. Furthermore, careful examination of the formal solution⁽⁶⁾ reveals that U_2/U_1 in equation (13) can take on positive and negative values depending on h_j 's. Thus the solution does not necessarily predict that the particles will always separate. This will have considerable repercussions on entrainment.

In the solution three regions will exist: —

- i) $U_2/U_1 < 0$ which will result in the particles separating or approaching
- ii) $U_2/U_1 = 0$ when $U_1 \neq 0$ or U_2 becomes stationary or apparently neutrally buoyant
- iii) $U_2/U_1 = 0$ when entrainment of one phase takes place

Solution for Motion of Two Particles

The full mathematical solution for drag coefficients has been presented elsewhere^(6,6). We are interested here in using this to interpret those cases when particle entrainment will become of major importance. These cases cannot be even anticipated from single particle theory. It is convenient to compute from equation (9) the relative settling velocities against particle separation. In order to define a dimensionless separation parameter which is significant with respect to the basic restrictions placed on the solution (3i and 3ii), $x = \epsilon/h_1 + h_2$ are chosen. x will take the range $0 \leq x \leq 1$. Equation (9) can be used for any system properties μ_i , $\Delta\rho$ or particle parameters r_j . In order to illustrate the regions of the solution graphically consider the case where $r_1 = r_2 = r$.

The results are shown graphically, U_2/U_1 vs. ϵ/r in Figure 1. This is for a system of a fluid droplet, viscosity $\mu_1 = 1.0$ and a solid particle $\mu_2 \rightarrow \infty$. The parameter on the graph is the dimensionless density, $\Delta\rho$. To understand the solution, consider the sketch shown in Figure 2. Here, two branches to the solution are clearly shown. The lower branch, $U_2/U_1 < 0$, will result in particle separation and would coincide with the conditions predicted from equation (11). Indeed the curve in this branch must asymptote to the value given by equation (11) as $\epsilon/r \rightarrow \infty$. As ϵ/r decreases the deviation from equation (11) increases until

expressions for the drag force F_j ($j = 1, 2$) opposing the motion of each particle obtained⁽⁵⁾. The equations for the drag forces are:—

$$F_j = 6\pi\mu_3 r_j \sum_k a_{jk} U_k \quad \begin{matrix} (k = 1, 2) \\ (j = 1, 2) \end{matrix} \dots\dots\dots (7)$$

where the a_{ki} 's ($k, i = 1, 2$) are functions of the inter-particle distances expressed through ξ_1 and ξ_2 ($\xi_1 = \cosh h_j/r_j$), $\mu_1/\mu_3 = \bar{\mu}_1$ and $\mu_2/\mu_3 = \bar{\mu}_2$.

In gravity settling the drag force is balanced by the gravitational force acting on the particle. Thus: —

$$\frac{4}{3} \pi r_j^3 (\rho_j - \rho_3)g = 6\pi \mu_3 r_j \sum_k a_{jk} U_k \quad (k, j = 1, 2) \quad (8)$$

From this solution we can immediately see that the buoyancy force on each particle is related to the translation velocities of both particles and thus expressions for the interaction between particles can be obtained.

For gravity settling, the ratio of the settling velocities of the particles (U_2/U_1) can be obtained from equation (9):

$$\frac{U_2}{U_1} = \frac{a_{11} - a_{12}(r_1/r_2)^3 \Delta\rho}{a_{22} (r_1/r_2)^2 \Delta\rho - a_{12}} \dots\dots\dots (9)$$

where

$$\Delta\rho = \frac{\rho_1 - \rho_3}{\rho_2 - \rho_3}, \text{ is a dimensionless density ratio.}$$

From equation (9) the magnitude of the particle interactions can be assessed. They depend on the values of the cross coefficients a_{kj} ($k \neq j$); $k, j = 1, 2$. As the distance between the particles increases, $h_1 + h_2 \gg r_1 + r_2$ then $a_{kj} \rightarrow 0$, ($k \neq j$), and the ratio of the settling velocities, equation (9) becomes: —

$$\frac{U_2}{U_1} \Big|_{h_1+h_2 \gg r_1+r_2} \rightarrow \frac{a_{11}}{a_{22}} \{(r_1/r_2)^2 \Delta\rho\}^{-1} \dots\dots (10)$$

The coefficients a_{11} , a_{22} are determined by the properties of the phases 1 and 2. If the particles are solid particles $a_{11} = a_{22} = 1$ and the solution tends to Stokes' solution whereas if phases 1 and 2 are fluids with viscosities μ_1 and μ_2 then

$$a_{11} = \frac{3\mu_1 + 2\mu_3}{3(\mu_1 + \mu_3)} \text{ and } a_{22} = \frac{3\mu_2 + 2\mu_3}{3(\mu_2 + \mu_3)}$$

and the solution tends to the Hadamard-Rybczynski solution.

Tabulated data are provided for a_{kj} ($k, j = 1, 2$) for all the binary cases for three phases systems⁽⁶⁾; generally the net result is that $U_j > \sum_k a_{jk} U_k$, that is that the presence of a second particle reduces the settling velocity.

If, in the design of equipment, settling velocities are based on calculations for single particles, the results will always be greater than the values for dispersions. The deviation will get larger as the number of particles in the system increases but will tend to a limiting value. It would perhaps seem that empirical correction factors could be applied. To examine this possibility, consider the single particle solutions for droplets — the Hadamard-Rybczynski solution. If we apply this to two droplets 1 and 2 the ratio of the settling velocities is: —

$$\left(\frac{U_2}{U_1}\right)_\infty = \left(\frac{3\mu_1 + 2\mu_3}{3\mu_2 + 2\mu_3}\right) \cdot \left(\frac{\mu_2 + \mu_3}{\mu_1 + \mu_3}\right) \frac{1}{(r_1/r_2)^2 \Delta\rho} \dots\dots\dots (11)$$

This is of course identical to Equation (10). The subscript ∞ is to indicate that the solution is for a single particle — or two particles at an infinite separation.

$$\left(\frac{U_2}{U_1}\right) = f_1(\Delta\rho, \bar{\mu}_1, \bar{\mu}_2, r_2/r_1) \dots\dots\dots (12)$$

If one particle is a solid then either μ_1 or $\mu_2 \rightarrow \infty$. Now $\bar{\mu}_1$ and $\bar{\mu}_2 > 0$ and $r_2/r_1 > 0$ therefore the sign of $(U_2/U_1)_\infty$ depends on $\Delta\rho$ and no other factor. Therefore, i) $U_2/U_1 < 0$ which will result in the particles separating a correction factor, U_2/U_1 will always have the same sign, either positive or negative. This would mean, for example, that if a gravity settler was used to separate a liquid dispersion and that, if the dispersion contained some particulate solids such that the drop phase 1 and solid phase 2 had properties $\rho_1 < \rho_3 < \rho_2$, the single particle data would always predict separation of the liquid dispersed phase and solid phase from the field phase 3. Apart from the fact that the settling velocities calculated may be greater (negatively), it is this type of situation where entrainment is found to be particularly prevalent in equipment and can only be understood by looking at a multiple particle situation.

Returning to the general solution, from equation (9)

$$\frac{U_2}{U_1} = f_2(\Delta\rho, \bar{\mu}_1, \bar{\mu}_2, \xi_1, \xi_2) \dots\dots\dots (13)$$

Now comparing equations (12) and (13), the solution for the doublet depends on the particle separation since $\xi_j = \cosh^{-1}(h_j/r_j)$. Furthermore, careful examination of the formal solution⁽⁵⁾ reveals that U_2/U_1 in equation (13) can take on positive and negative values depending on h_j 's. Thus the solution does not necessarily predict that the particles will always separate. This will have considerable repercussions on entrainment.

In the solution three regions will exist: —

- i) $U_2/U_1 < 0$ which will result in the particles separating or approaching
- ii) $U_2/U_1 = 0$ when $U_1 \neq 0$ or U_2 becomes stationary or apparently neutrally buoyant
- iii) $U_2/U_1 = 0$ when entrainment of one phase takes place

Solution for Motion of Two Particles

The full mathematical solution for drag coefficients has been presented elsewhere^(5,6). We are interested here in using this to interpret those cases when particle entrainment will become of major importance. These cases cannot be even anticipated from single particle theory. It is convenient to compute from equation (9) the relative settling velocities against particle separation. In order to define a dimensionless separation parameter which is significant with respect to the basic restrictions placed on the solution (3i and 3ii), $x = \epsilon/(h_1 + h_2)$ are chosen. x will take the range $0 \leq x \leq 1$. Equation (9) can be used for any system properties μ_i , $\Delta\rho$ or particle parameters r_j . In order to illustrate the regions of the solution graphically consider the case where $r_1 = r_2 = r$.

The results are shown graphically, U_2/U_1 vs. ϵ/r in Figure 1. This is for a system of a fluid droplet, viscosity $\mu_1 = 1.0$ and a solid particle $\mu_2 \rightarrow \infty$. The parameter on the graph is the dimensionless density, $\Delta\rho$. To understand the solution, consider the sketch shown in Figure 2. Here, two branches to the solution are clearly shown. The lower branch, $U_2/U_1 < 0$, will result in particle separation and would coincide with the conditions predicted from equation (11). Indeed the curve in this branch must asymptote to the value given by equation (11) as $\epsilon/r \rightarrow \infty$. As ϵ/r decreases the deviation from equation (11) increases until

the asymptotes tend to a minimum value of ϵ/r , ϵ_{crit} . At separation distances less than ϵ_{crit} $U_2/U_1 > 0$ and the droplet will be entrained with the solid particle. This results since $\Delta\rho < 0$ ($\rho_1 < \rho_3 < \rho_2$); entrainment will depend on the value of $\Delta\rho$. Cases will exist where the solid particle will be entrained upwards with the liquid drop. The limiting condition on entrainment will be given by ϵ_{crit} where the liquid droplet is neutrally buoyant in the liquid continuous phase. The upper branch of the curve asymptotes to infinity at this point, that is $U_1 = 0$. Returning to Figure 1, solutions for various values of $\Delta\rho$ are given. If $\Delta\rho > 0$, the solutions will lie in the envelope between $\Delta\rho = 0$ and $\Delta\rho = \infty$ and, as expected, entrainment would always take place. Apart from the numerical value of U_2/U_1 the results would be in accord with qualitative predictions from equation (11). The interesting cases affecting entrainment are when $\Delta\rho < 0$ and results are contrary to the qualitative predictions of equation (11). Similar curves can be generated for gas bubble-liquid droplet and gas bubble-solid particle interactions, both of which have practical significance. Three immiscible liquid phases can also be treated but from the practical standpoint these have only marginal relevance.

Although these results have indicated the pitfalls which await if single particle data are applied to heterogeneous dispersions, the data format of Figure 1 is of little use in application. A more useful format would be to present in graphical form the limiting conditions where the ratio of the settling velocities becomes zero or infinite, as shown in Figures 3 - 5. Conditions for entrainment or separation would then lie on either side of the curve.

The cases for a) solid particle — liquid drop interaction, b) solid particle — gas bubble interaction, and c) liquid drop — gas bubble interaction are considered. In each

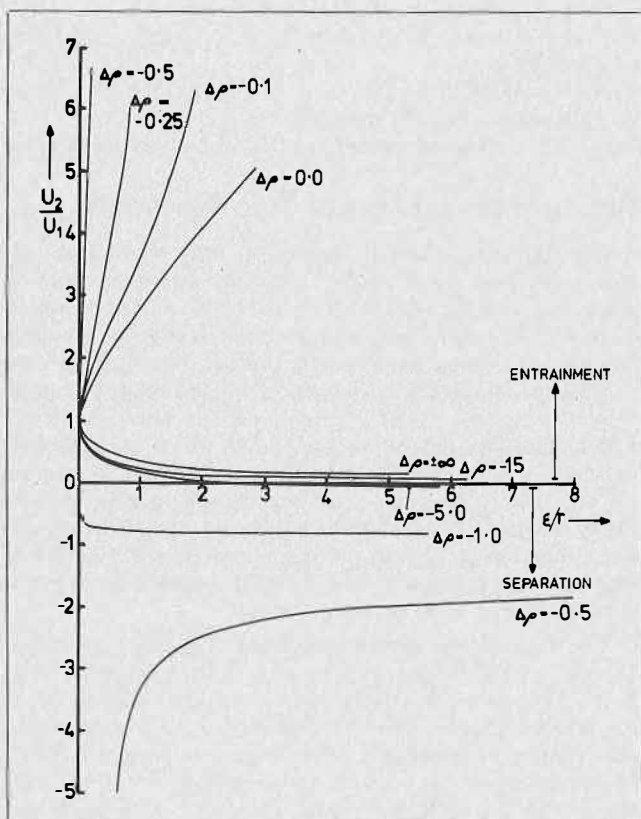


FIGURE 1. Settling velocity ratio U_2/U_1 as a function of geometric separation ϵ/r for equi-sized droplet — solid particle system ($r_1 = r_2 = r$, $\mu_1 = 1.0$, $\mu_2 \rightarrow \infty$) and various density ratios $\Delta\rho$.

case it is possible to locate a region where $U_2/U_1 = 0$ and $U_2/U_1 = \infty$. For case (a), that is for a solid particle to be entrained with a liquid droplet and for a liquid droplet to be entrained with a gas bubble. For (a) both conditions have practical significance but for (b) and (c) only one case $U_2/U_1 = 0$ will be considered. The limiting condition is shown as a function of $\Delta\rho$ and χ .

Case (a) — Solid particle, (2) liquid drop,
 (1) $0 < \mu_1 < \infty$, $\mu_2 = \infty$, $\rho_1 < \rho_3 < \rho_2$.

This case is met in practice where solid particles, more dense than the continuous phase, are present in a droplet dispersion. These normally settle out to form a residue on the settler floor. The problem to consider is: what are the conditions when interaction between the dispersed fluid and solid phases could reduce settling of the fluid phase or worsen entrainment downwards through the continuous phase? A corollary also exists, i.e., entrainment of solid particles upwards with the dispersed phase. This is also met in practice. In gravity settlers in solvent extraction plants it usually causes some problems in the close packed dispersion band and gives rise to substantial quantities of 'rag' and reduces coalescence rates in this zone. In decantation equipment this form of entrainment can reduce the efficiency of solid separation — the converse problem to that in solvent extraction. Both problems $U_2/U_1 = 0$ and $U_2/U_1 \rightarrow \infty$ are therefore of interest. These conditions are shown in Figures 3 and 4. In each case a series of curves are computed for different particle radii, r_1/r_2 .

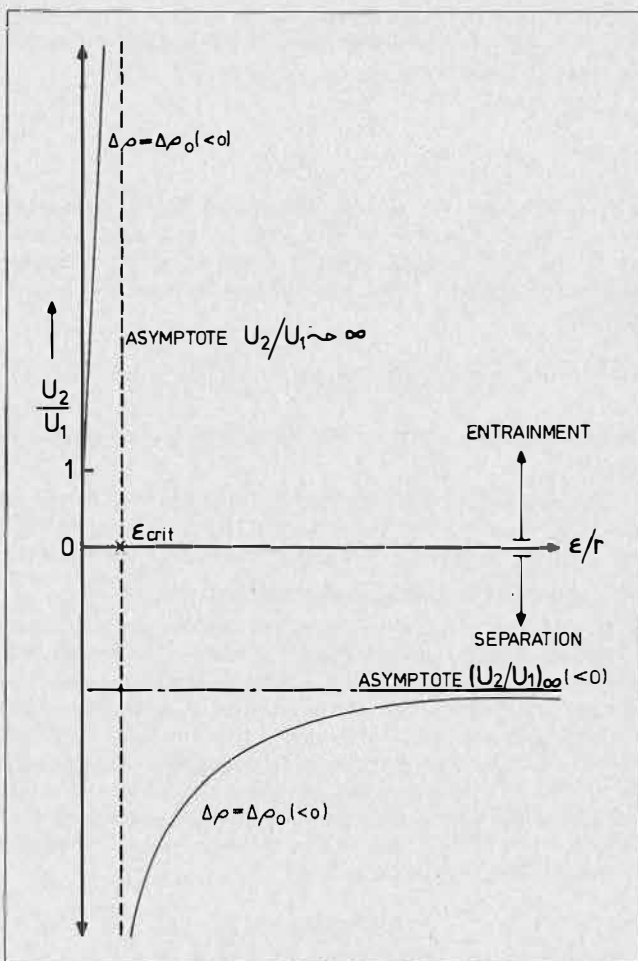


FIGURE 2. Settling velocity ratio U_2/U_1 dependence on ϵ/r for equi-sized droplet-particle system ($r_1 = r_2 = r$, $\mu_2 \rightarrow \infty$, $\Delta\rho < 0$).

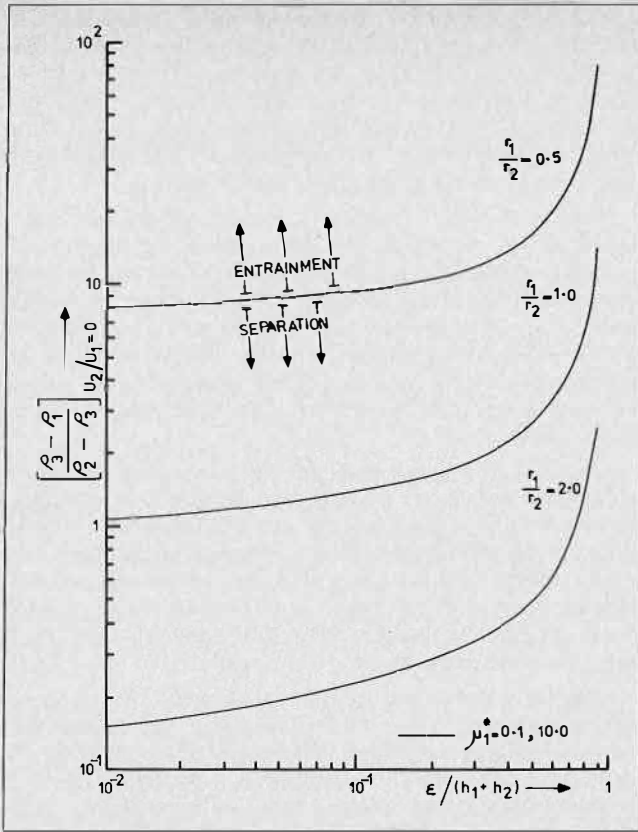


FIGURE 3. Regions for solid particle entrainment by droplet. Density ratio, $(-\Delta\rho)_{U_2/U_1=0}$ as a function of geometric separation $\epsilon/(h_1+h_2)$, droplet size, r_1/r_2 , for viscosity ratios $\mu_1 = 0.1, 10.0$ and $\mu_2 \rightarrow \infty$.

Consider Figure 3: the curve for a particle ratio of particle radii and dispersed phase 1 viscosity represents the condition for neutral buoyancy of the liquid droplet. If the operating condition, $\Delta\rho'$ and ϵ , lies below this curve, i.e. if the particles approach a distance $\epsilon/(h_1+h_2)$ less than that on the curve at a particular value of $\Delta\rho'$, when the liquid droplet would be entrained with the settling solid particle and flocculation leading to coalescence in the settler would not take place. Conversely, providing the separation distance between the particles is greater than this value of $\epsilon/(h_1+h_2)$ the liquid droplet will settle out, albeit the settling velocity will be less than that predicted by equation (12). This then allows the limiting conditions to be determined. The effect of the ratio of radii r_1/r_2 can be easily seen. As would be expected, a larger particle has more effect on a smaller particle. At a given particle separation $\Delta\rho'_{crit}$ increases. Similarly, as the viscosity of the droplet phase 1 increases $\Delta\rho'_{crit}$ increases. This again is as expected when one considers the effect of the droplet fluidity in reducing the drag coefficient. Compare, for example, the simple case of a single solid particle with that of a liquid drop and decreasing the viscosity of the drop — Stokes' law vs. Hadamard-Rybczynski equation.

The second case of a solid-drop interaction is that when the solid is entrained. Again, a neutral buoyancy curve can be obtained from solution of equation (13). In this case $U_2 = 0$ at neutral buoyancy so that, in order to keep the ratio of velocities finite U_2/U_1 is used. The results are shown in Figure 4. A similar pattern emerges; in this case, however, entrainment takes place for conditions above the curve and separation for conditions below the curve. The same conclusions can again be made with respect to both relative particle sizes and liquid phase 1 viscosity.

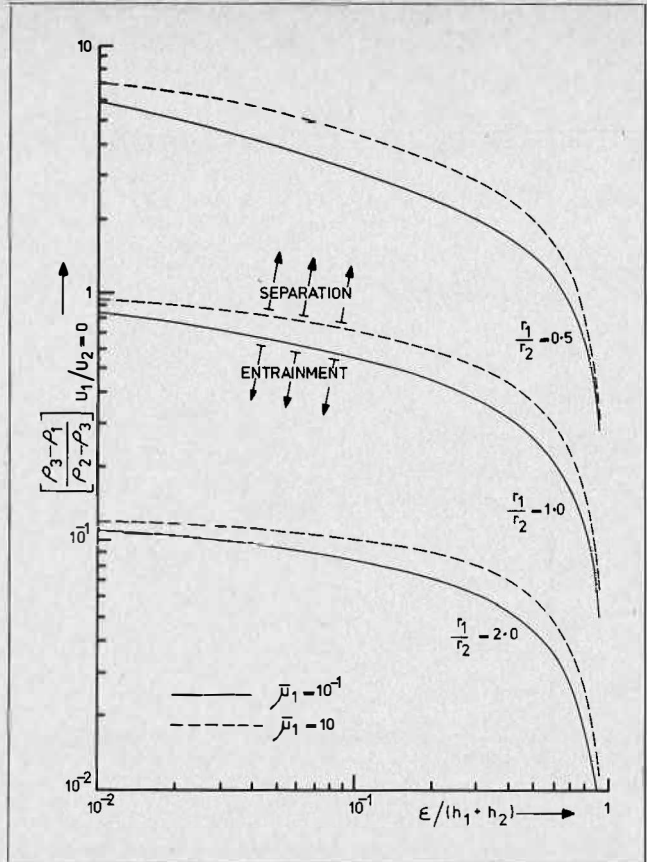


FIGURE 4. Regions for droplet entrainment by solid particle. Density ratio, $(-\Delta\rho)_{U_1/U_2=0}$ as a function of geometric separation $\epsilon/(h_1+h_2)$, droplet size, r_1/r_2 , for viscosity ratios $\mu_1 = 0.1, 10.0$ and $\mu_2 \rightarrow \infty$.

Case (b) Liquid drop, (2) — gas bubble (1)
 $\mu_1 \rightarrow 0, 0 < \bar{\mu}_2 < \infty, \rho_1 < \rho_3 < \rho_2$.

In practice air is frequently used to promote separation of droplets when $\rho_2 < \rho_3$. However, droplets more dense than the field phase can be separated by entrainment with air. The conditions are illustrated in Figure 5. Using the nomenclature given and considering the requirement of phase 2 entrainment the conditions are analogous to those for the case of solid particle entrainment with a droplet (Figure 4). Indeed Figure 5 is a limited case of the condition in Figure 4. Thus the same conclusions versus r_1/r_2 and μ_2 apply.

Case (c) Solid particle, (2) — gas bubble (1)
 $\mu_1 \rightarrow 0, \mu_2 = \rho_1 < \rho_3 < \rho_2$.

The last practical case of interest, that of solid particle entrainment by a gas bubble, has some application to ore flotation. This case can be treated and analysed in a similar manner to case b).

Part II — Application of the Theory and the Implications of Entrainment in Commercial Solvent Extraction Plants

Introduction

In Part I interactions between particles of dissimilar phases, 1 and 2, were considered from the standpoint of creeping flow conditions. In this section the theory will be considered in relation to practical entrainment problems. It would not be expected that a theory based on binary in-

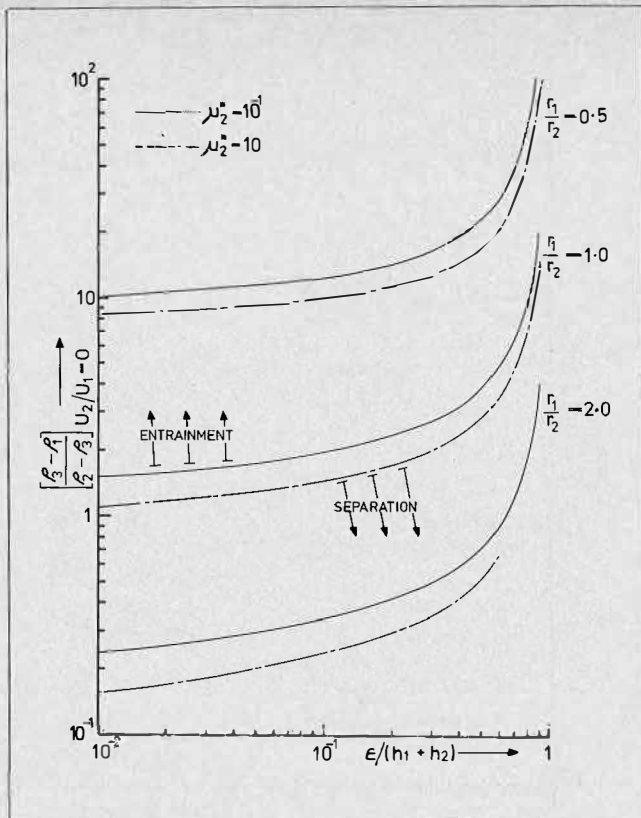


FIGURE 5. Regions for gas bubble entrainment by a droplet. Density ratio $(-\Delta\rho)u_2/u_1 = 0$ as a function of separation $\epsilon/(h_1 + h_2)$, droplet size r_1/r_2 , for viscosity ratios $\mu_1 = 0, \mu_2 = 0, 1, 10, 0$.

teractions could be used as a basis for a general solution. Nor is it presently possible to relate dispersion characteristics in terms of these interactions (problems exist relating to defining the distance apart of particles such that interaction forces can be calculated from available data). However, information can be obtained which is not available from presently used single particle theory.

As an example of application to an important industrial process, consider the extraction of copper by acid leaching of oxide ore followed by solvent extraction and electrowinning. This process contains some interesting solid-liquid, solid-liquid-liquid, liquid-liquid, and gas-liquid (or solid)-liquid separation problems. Dispersed phase entrainment provides serious process problems and, as will be seen later, can contribute significantly to operating plant costs.

Consider the process from the standpoint of phase separation problems: a simplified flowsheet is illustrated in Figure 6. Five process steps can be identified: — (i) ore preparation, (ii) leaching, (iii) solution purification, (iv) solvent extraction, (v) electrowinning. In the present work problems relating to phase disengagement and entrainment can be restricted to steps (iii) and (iv). Thus, consider these in more detail.

The leachate should contain principally the solute (if acid leaching of oxide ore is considered then the desired solute is copper sulphate). Other metal ions will also be present notably Fe^{+++} as well as unreacted sulphuric acid and undissolved solid particles. In the solution purification stage, the undissolved-entrained-solids must be removed down to some designed level to prevent problems in the subsequent processing equipment. This is done using continuous counter-current thickeners; the underflow from the thickeners is washed with the raffinate from the

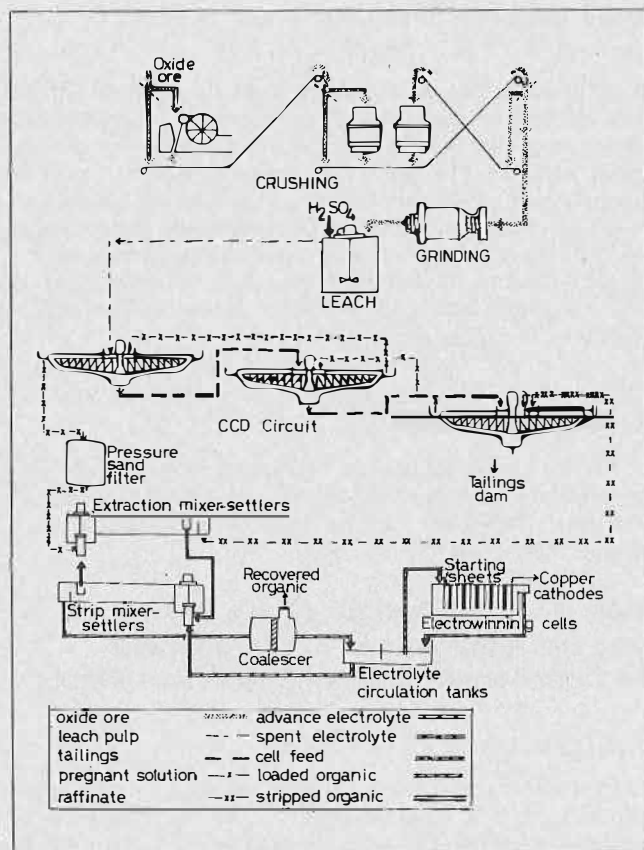


FIGURE 6. Flowsheet for a plant to produce copper from an oxide ore.

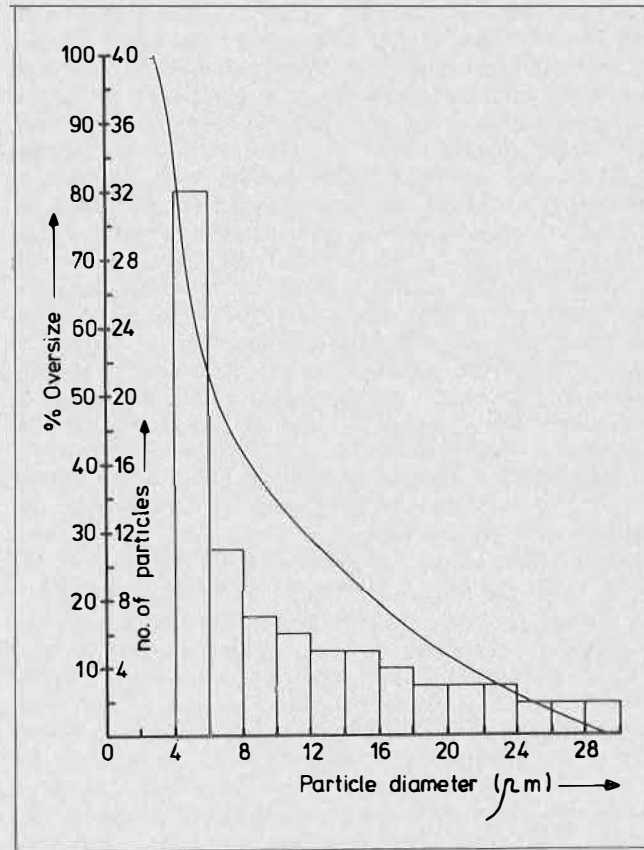


FIGURE 7. Particle size distribution in a sample of crud from a commercial copper solvent extraction plant.

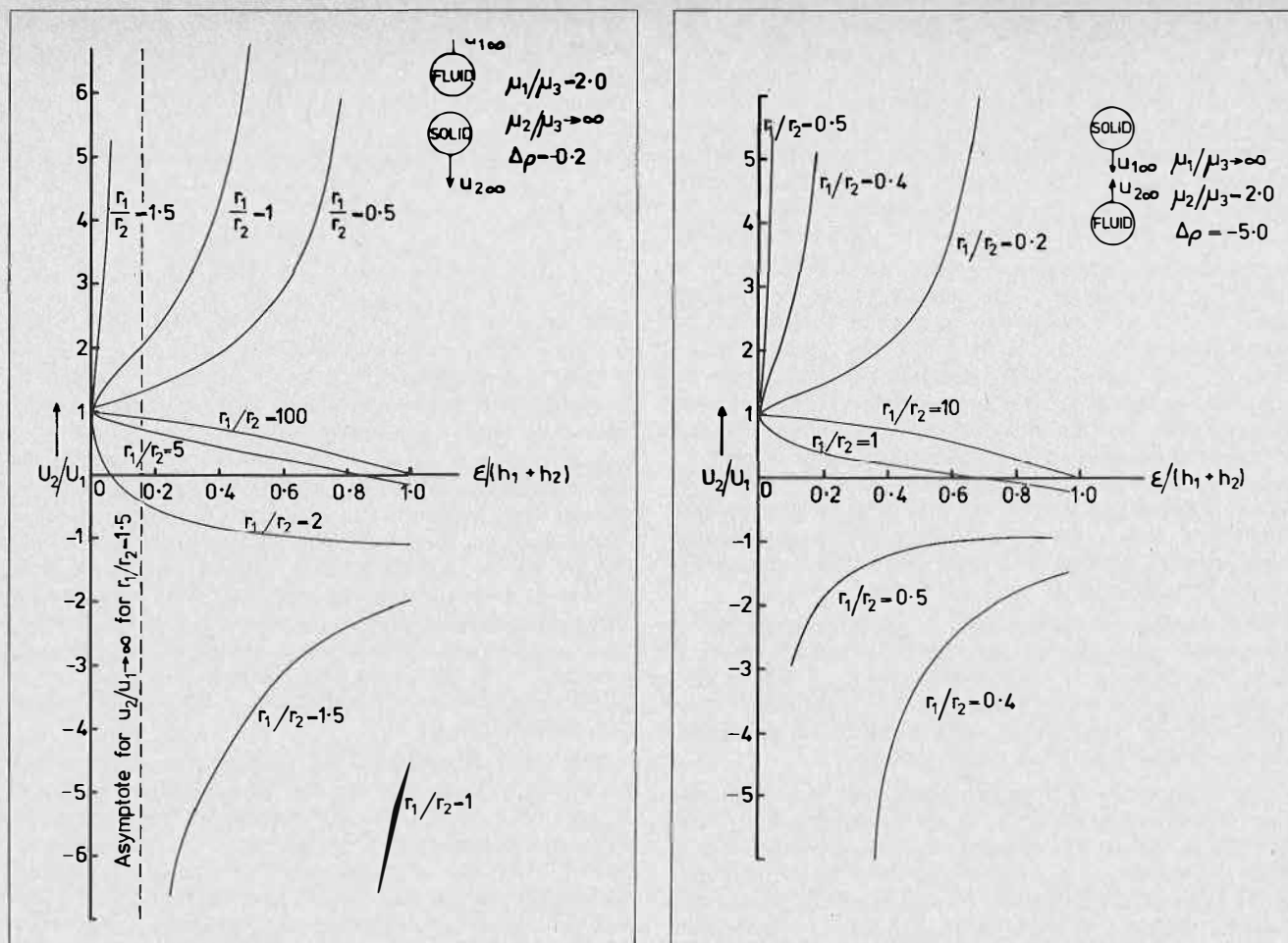


FIGURE 8. Ratio of the settling velocities predicted as a function of r_1/r_2 and separation $\epsilon/(h_1 + h_2)$ for Crud System.

solvent extraction process and the final overflow is fed back to the leaching stage or raffinate dam. A flotation or filtration stage may be used between the solution purification stage and solvent extraction to remove solids passing through the thickeners.

Solvent extraction is a two-stage operation — selective extraction of the solute into an organic solution, followed by a stripping operation where the direction of mass transfer is reversed and the solute is transferred back into an acid solution, giving an overall effective increase in concentration such that copper can be produced from the solution by direct electrowinning.

Steps (iii) and (iv) are therefore inter-related with recycle streams. Where therefore do problems of entrainment exist?

It is perhaps convenient to consider solvent extraction first. In the extraction stage(s) after settling of the primary dispersion, entrainment is experienced both of the organic phase in the aqueous raffinate and of aqueous phase in the organic extract. Both are examples of liquid-liquid entrainment and are not directly related to the three-phase problems being considered. However, in solution purification, it is not possible to remove all of the entrained solids and these will enter the extraction circuit. Entrained solids constitute part of the so-called crud problem in extraction circuits (crud — Chalk River unidentified deposit). Crud interferes with flocculation and coalescence of the dispersion in gravity settlers and reduces the efficiency of settlers. Crud tends to be neutrally buoyant collecting at the interface of the settlers where it can build up to form a substantial layer. This layer may

have to be removed periodically. It is usually associated with organic solvent and its removal with solvent phase can constitute a loss of organic inventory. The operating costs and reagent losses involved will be reviewed later. It has been suggested that this crud is adsorbed at the liquid-liquid interface and is carried by the dispersion into the dispersion band in the settler. An alternative mechanism is possible whereby the solid particles making up the deposit interact with the flocculating dispersion and, if the less dense phase is dispersed in the mixer-settler, when the droplets flocculate to the phase boundary, the solid particles rather than settling out are entrained into the dispersion band where they form a liquid-solid matrix. To investigate this, crud from an industrial copper plant was analysed and the particle size distribution of the solids and the density of the solid phase determined. The results are shown in Figure 7.

The theory developed in Part I may be used to investigate this proposed entrainment. It will be necessary to predict what size of droplet could entrain a solid of given size and density, and what is the critical particle-particle separation required for this to be achieved. If crud formation in the dispersion band takes place by way of entrainment then, if the dispersion is inverted when the more dense phase is dispersed, both the solid particles and dispersed droplets naturally settle in the same direction and the solid particles would reach the dispersion band. The settling velocities would of course be different from that predicted by single particle theory. It is only for organic dispersions that entrainment into the band can take place by interactions resulting in a reversal of the direction of settling of the solid particles.

Quantitative Analysis of Entrainment

Results computed from the equations developed in Part I for the interaction of organic phase droplets and crud particles are shown in Figure 8. The two branches of the solution are illustrated; the limiting condition for entrainment is again given when $U_2/U_1 = 0$. The branches of the curves are presented for various ratios of the particle radii to illustrate the effect of particle dimensions.

The limiting conditions are better shown in Figure 9. Curve (a), the solid line, represents the locus of points at which $U_2/U_1 = 0$, when the solid crud particle will be expected, as the ratio r_1/r_2 increases, the critical distance of separation of solid particles will take place in this system. As expected, as the ratio r_1/r_2 increases the critical distance of separation for entrainment increases, indicating that entrainment becomes more probable. The range of particles size, r_1/r_2 , found in the extraction process studied is shown on Figure 9 by the bar line. This is seen to span the critical region for separations, $\epsilon/(h_1 + h_2)$ between 0.075 to 0.95; again at the higher end of the scale entrainment will be possible.

The solution can also be used to predict entrainment of the organic dispersion by solid particles and is shown as curve (b) on Figure 9. Conditions for entrainment correspond to the region to the left of the curve. Under these conditions the presence of solid particles in the settler would interfere with liquid/liquid settling.

The main problem of applying this work is to relate the mean inter-particle distances in the dispersion (and therefore get a measurement of ϵ) to some property that is easily measurable. In practice this reduces to relating ϵ to the hold-up of each phase, H_1 and H_2 . To illustrate this, consider the case when $H_1 = H_2$ and $r_1 = r_2$, a situation that is unlikely in the practical application discussed here. This condition does, however, allow an analytical solu-

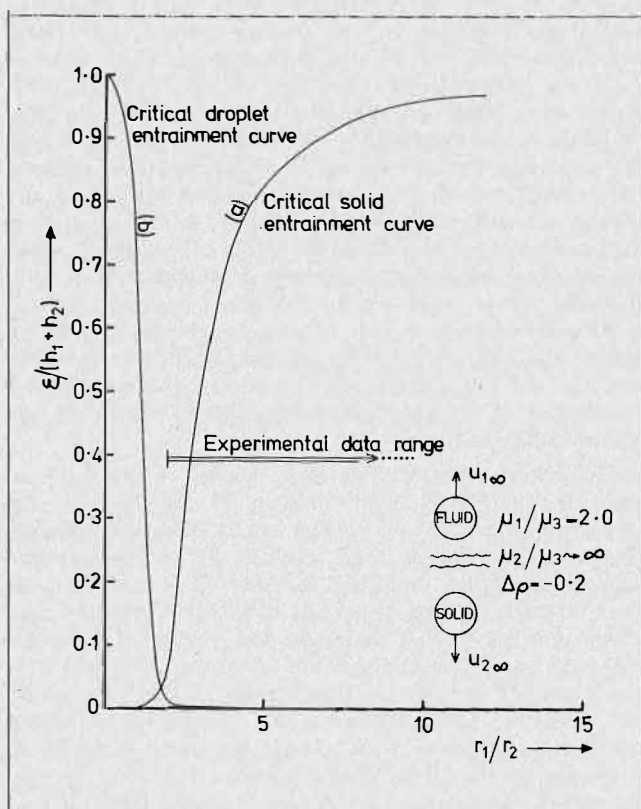


FIGURE 9. Critical distance of separation as a function of the ratio of particle radii (Crud System).

tion to be obtained. If a cubic packing structure is assumed then the volumetric hold-up for both dispersed phases, H , is related to the distance between particle centres, $h_1 + h_2 = 2h$,

$$H = \frac{4}{3} \pi \left(\frac{r}{2h} \right)^3 \dots \dots \dots (2.1)$$

Thus

$$\frac{\epsilon}{2h} = 1 - \left(\frac{r}{h} \right) = 1 - \left(\frac{6H}{\pi} \right)^{1/3} \dots \dots \dots (2.2)$$

Thus equation (2.2) can be used to determine $\epsilon/(h_1 + h_2)$ and the limiting condition for entrainment can be assessed. An alternate approach could be to determine the hold-up at which entrainment would take place in a given system since, as was demonstrated in Part I, $(U_2/U_1) = f(\Delta\rho, \mu_1, \mu_2, r_1, r_2, \epsilon)$. Then if the solution is presented for entrainment/separation in terms of $\Delta\rho_{crit}$. Figures 3 - 5, and the hold-up curve also displayed, the critical hold-up can be deduced. Thus on Figure 10, $\Delta\rho$ can be determined for the system and the critical solution conditions determined from curve 1. From this, step onto the hold-up-particle separation curve 2 and locate the critical hold-up when entrainment will take place. If the operating hold-up is greater than this value, then entrainment may be expected whereas below this separation solid sedimentation will be dominant.

The major difficulty, as was stated earlier, is to ascribe a value to ϵ . Since the particles of both dispersed phases are not uniformly distributed throughout the system, the more useful approach is to calculate the probability of finding a particle of the dissimilar phase (1, 2) within a critical distance so that entrainment takes place. Entrainment is a function of particle radii, separation and system physical properties. A procedure would be thus: —

- (a) A design limit would be set on the maximum acceptable solid particle size which will be entrained. This will set d_{max} .
- (b) For the physical properties of the system $\Delta\rho', \mu_i$ ($i = 1, 2, 3$) use the theoretical solution for binary interactions to determine the diameter of a droplet, d_1 , required to cause entrainment. Then check to determine whether d_1 lies within the the range of droplets in the system.
- (c) If d_1 calculated, lies within the practical distribution range then consider a cylindrical control volume of diameter d_1 and length $d_1 + d_2 + \epsilon_{crit}$. ϵ_{crit} is obtained from the solution produced in b).
- (d) Calculate the probability of finding a particle of size d_1 (phase 1) within this volume, P_{11} .

$$P_{11} = \frac{n_1}{\sum n_1} w_1 w_{12}$$

w_1 and w_{12} are weighting factors to correct for volume size and hold-up.

- (e) Calculate the probability of finding a particle of size d_2 in this volume, P_{22}

$$P_{22} = \frac{n_2}{\sum n_2} w_2 w_{21}$$

- (f) The probability of finding particles 1 and 2 simultaneously in the control volume, P_{12} , with correct orientation is then

$$P_{12} = P_{11} P_{22} \int_0^{\pi/2} \cos \theta d\theta$$

The weighting factor is related to particle size and hold-up.

$$w_1 = H_1 \int_{d_1}^{\infty} n dd$$

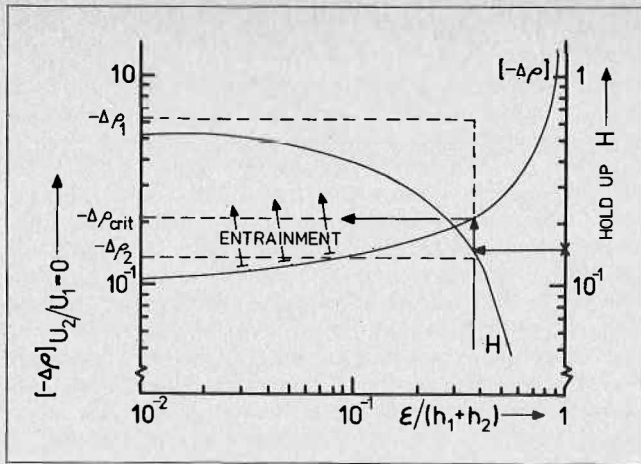


FIGURE 10. Entrainment of a solid particle with a fluid droplet.

The integral is determined by the distribution function for the dispersed phase 1. Thus, the probability for interaction of particles diameter i phase 1 with particles diameter j phase 2 is: —

$$P_{12} = \frac{n_{i1}}{\sum n_{i1}} \frac{n_{j2}}{\sum n_{j2}} H_1 H_2 \int_{d_{i1}}^{\infty} n_{j2} dd \int_{d_{j2}}^{\infty} n_{i1} dd \int_0^{\pi} \cos \theta d\theta$$

This may be used to calculate the probability for entrainment. If P_{12} is too high then since $\Delta\rho'$ and d_{i1}, μ_i are fixed the design variable to change is the size of particle which can be entrained.

In the problems involving the interaction between droplets and solid particles, if the droplet dispersion is inverted so that the aqueous phase is dispersed, then $\rho_2 > \rho_1 > \rho_3$. In the problem of crud formation the solid particle will either (i) flocculate to collect in the dispersion band, (ii) flocculate and settle out on the settler floor or (iii) entrain dispersed droplets towards the settler floor away from the dispersion band and thereby reduce the coalescence rate and potentially increase entrainment. All of these conditions can be studied from the solution in Part I. The solution for the critical conditions is outlined in Figure 11 and may be directly compared for the inverted case shown in Figure 9. The format adopted in Figure 11 is identical to that in Figure 9; both cases of droplet entrainment and solid entrainment are considered. The relative positions of these curves are now reversed to correspond with the reversal of the system. Apart from this the discussion is similar.

The second unit process involved in the flowsheet in which a three-phase problem, potentially leading to entrainment of one or both of the dispersed phases, exists is counter-current thickening or decantation, CCD. It was stated the raffinate from solvent extraction may be used to wash the underflow from the thickeners so that the recovery of copper sulphate from the leach is improved. The raffinate from solvent extraction will contain entrained organic phase. This not only constitutes an operating loss in that the overall solvent inventory in the plant has to be maintained but also the presence of this O/A dispersion can interfere with the CCD operation and may result in poor efficiency or the need to over-design the decanting thickeners to counteract this. The problem is all related to interaction during settling of the solids in the aqueous underflows with the organic dispersion in the wash liquors. The organic droplets will, under certain conditions, reduce the

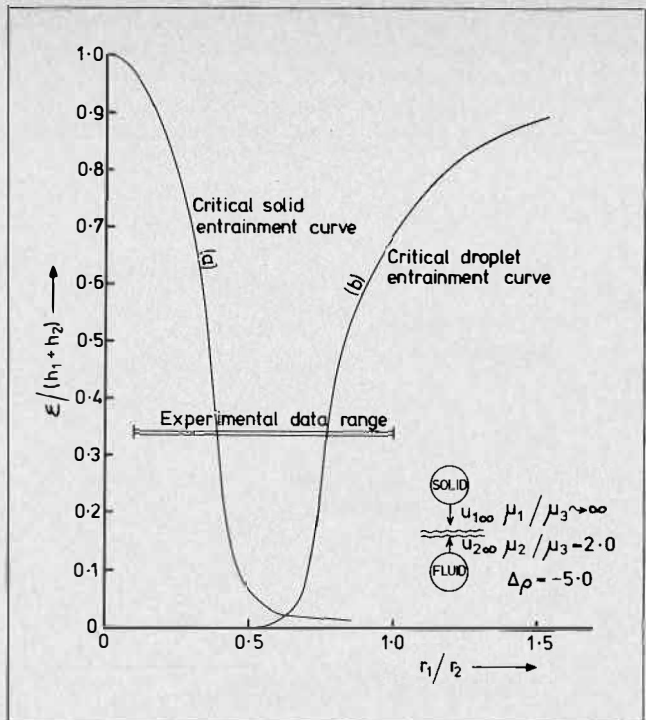


FIGURE 11. Critical distance of separation as a function of the ratio of particle radii (Crud System).

settling rate of the solids (hence the need to over design the thickeners) or may even prevent settling and cause entrainment of solid backwards through the CCD circuit. The counter possibility also exists, that of the organic droplets being entrained with the solid particles into the underflow of the CCD circuit.

The results from Part 1 for these cases are summarised on Figures 12 and 13. These may be used to assess the probability for entrainment for given droplet and solid particle sizes. In this case, providing the settlers in the solvent extraction plant have been correctly designed, only secondary dispersions, droplets less than $50 \mu\text{m}$ diameter, should be involved. This applies to gravity settlers; improvements in phase separation are possible by using other more advanced forms of settler or by inserting coalescers in the aqueous line after the final extraction settler.

The conditions for solid entrainment are most important and are given by curve (a) on Figures 12 and 13. These correspond to the two limiting cases. Entrainment will take place for conditions corresponding to the regions to the left and right of these curves respectively. Again it is evident that the experimental values of r_1/r_2 measured cover regions where entrainment is probable particularly when the hold-up of the phases increases when ϵ will decrease.

In the two cases discussed interaction of two dissimilar dispersed phases (liquid and solid) have resulted (or could result) in undesirable entrainment of one phase. There are, however, cases when entrainment is desirable and is a basis of a separation method. In the present example of copper extraction, examples may be cited as flotation of liquid entrained droplets (in raffinate streams) and of undissolved solids, using air. In part, this process depends on particle interactions. The case using air flotation to remove organic entrainment is considered in Figures 14 and 15 which give the two limiting conditions. (These figures are analogous to 12 and 13). It may be noted that in order to preserve a finite negative value for $\Delta\rho$, the dimensionless density difference, phases 1 and 3, in the basic defini-

tions, are interchanged in this case. The condition of major importance is droplet entrainment by air bubbles to promote efficient separation of the entrained organic liquid. The critical conditions for this case are given by curves a) on Figures 14 and 15. Again, entrainment takes place

in the regions to the left and right of these curves respectively.

In considering the interaction between gas bubbles and liquid droplets in solvent extraction, there is an example where this interaction is deleterious to the process. If air is entrained into the system (usually by ingress in the mixer or via splashing at the weirs), then when this air engages in the settler it may interfere with flocculation of the droplet dispersion and reduce the settling rate. The conditions for this correspond to curve (a) on Figure 15. Clearly the solution to the problem is to prevent air ingress. In some cases, however, this may be difficult to achieve. For the case of ammonia leaching of copper ores, free ammonia may be liberated in the solvent extraction circuit, for example by temperature changes, and as the gas comes out of solution it may affect settling in gravity systems.

Thus far we have considered examples of entrainment in three-phase systems; the question is how important are these? Consider first the crud problem and organic entrainment. Normally organic entrainment is considered in terms of the composition of the aqueous raffinate in the extraction circuit and of the advanced electrolyte after stripping. Both are normally thought to be primarily responsible for organic loss from extraction plant. In the case of the stripping circuit this entrainment has another possibly more serious result in affecting the electrolysis process and results in production of off-standard copper due to organic burn. Another major source of organic loss is, however, in crud removal. It is interesting to compare direct entrainment losses from extraction circuits with loss via crud formation and removal. A number of factors influence these direct costs. In the case of entrainment, the organic phase loss in ppm and the organic phase composition (reagent/diluent ratio) are most important. For crud removal, the growth rate of crud in the system and the composition of the liquid associated with it are important.

Consider as a base case a plant treating 50 m³/min of aqueous solution containing 2 gpl Cu²⁺, the aqueous flows leaving the plant are 50 m³/min raffinate plus 10 m³/min

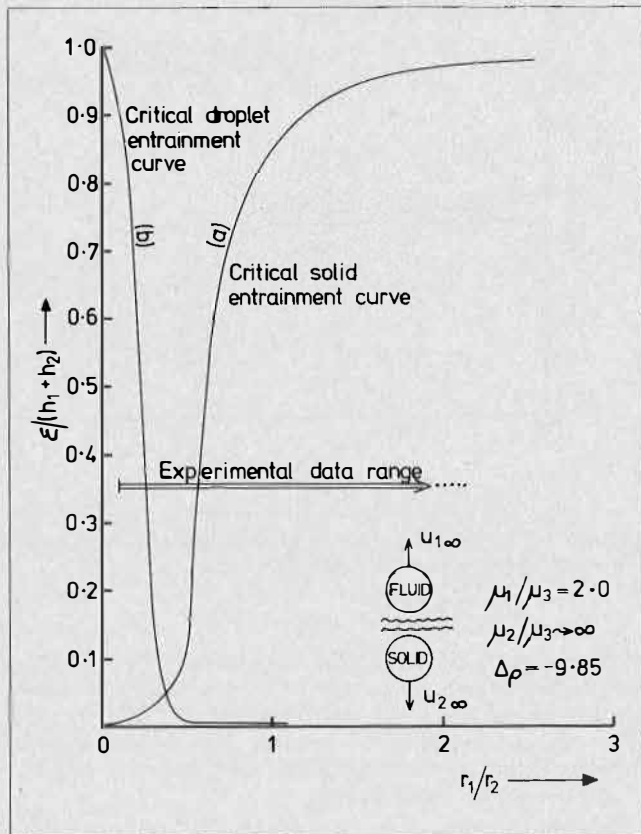


FIGURE 12. Critical distance of separation as a function of the ratio of particle radii (CCD System).

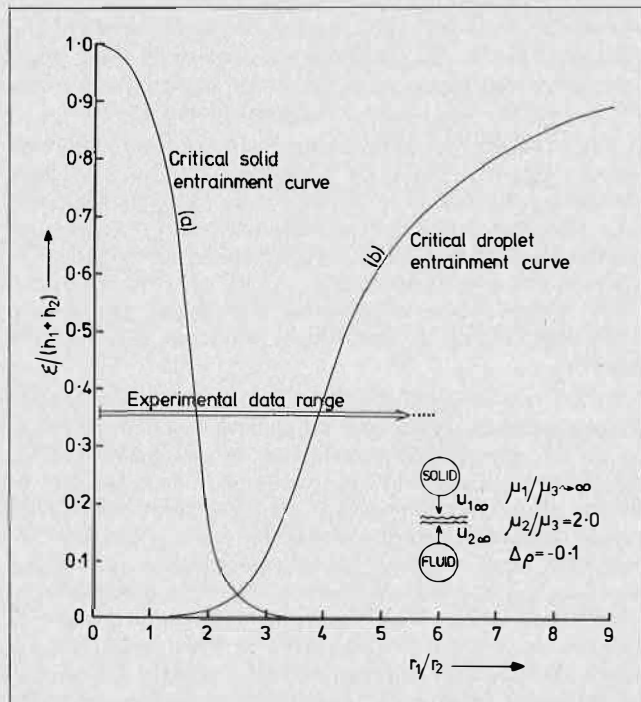


FIGURE 13. Critical distance of separation as a function of the ratio of particle radii (CCD System).

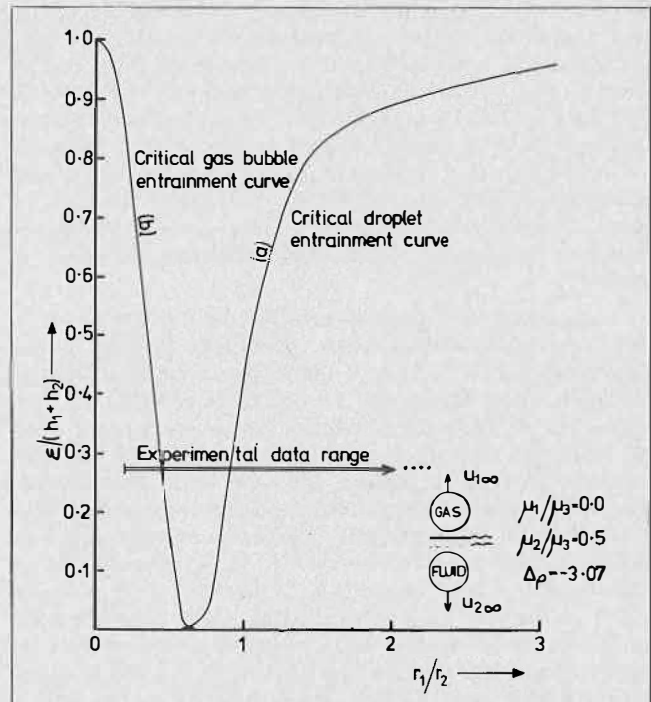


FIGURE 14. Critical distance of separation as a function of the ratio of particle radii (Flotation System).

TABLE 1. Source of Organic Phase Loss

Entrainment						
Entrainment level in raffinate p.p.m.	Entrainment level in advanced electrolyte p.p.m.	Total loss/year, m ³		Cost of LIX64N make up \$ US × 1000/yr	Cost of Diluent make up \$ US × 1000/yr	Cost cents/lb Cu produced
		Reagent	Diluent			
10	25	32.4	291.4	178.7	27.0	0.22
20	50	64.8	583.2	357.5	54.0	0.43
30	75	97.8	874.8	536.2	81.0	0.65
50	125	162.0	1458.0	893.6	134.9	1.08

Crud formation						
Crud growth rate 1/m ³ of aqueous feed	Total loss/year, m ³		Make-up costs \$ US × 1000/yr		Cost cents/lb Cu produced	
	Reagent	Diluent	Reagent	Diluent		
0.2	216	1944	1191.5	179.8	1.44	
0.4	432	3888	2383	359.7	2.88	
0.6	648	5832	3574	539.4	4.32	
0.8	864	7776	4765.5	719.3	5.76	
1.0	1080	9720	5957	899.1	7.20	

advanced electrolyte. This latter figure assumes a tankhouse copper drop of 10 gpl. Assume plant operation of 7200 hr/year to produce 43,200 tpa of copper. The organic phase is 10% v/v reagent (say LIX64N, cost \$2.78/lb), 90% diluent (cost 35 cent/U.S. gal). Organic phase make-up costs can now be compared for losses due to entrainment and via crud formation. The figures are shown in Table 1. In this table typical entrainment losses and crud/formation rates are considered.

The comparisons illustrate the importance of crud formation. Clearly if the crud growth rate can be suppressed by more efficient particle separation upstream in the CCD circuit or by using some form of filter (sand filters are applied but are not always efficient in operation), this will help to reduce these direct costs. In some cases where large amounts of solid are produced in the extraction circuit by precipitation from solution, this approach on its own would not be effective. Clearly more attention must be paid to improving pretreatment of the leach solution before solvent extraction.

A similar comparison may be made with respect to aqueous entrainment versus crud formation in the stripping circuit. Aqueous entrainment results in losses of advanced electrolyte containing a high concentration of copper and acid. Following on this base case assuming an electrolyte composition of 25 gpl Cu²⁺, 150 gpl free H₂SO₄ a comparison of losses via entrainment and crud are shown in Table 2.

The figures again indicate the importance of crud formation which may be attributed to two-phase interaction. They also indicate the economic importance of both pre-treating the liquors to remove as much of the solid phase as possible and to have an efficient crud removal and treatment system to recover as much as possible of the material.

For the case discussed above, organic entrained dispersion in the raffinate from solvent extraction affecting settling of solids in the CCD equipment shows up in the capital cost of the equipment. As was stated, if organic dispersion reduces the solids settling rate, then the size of the thickeners must be increased to counteract this. In a large copper plant treating 50 m³/min of leach solution

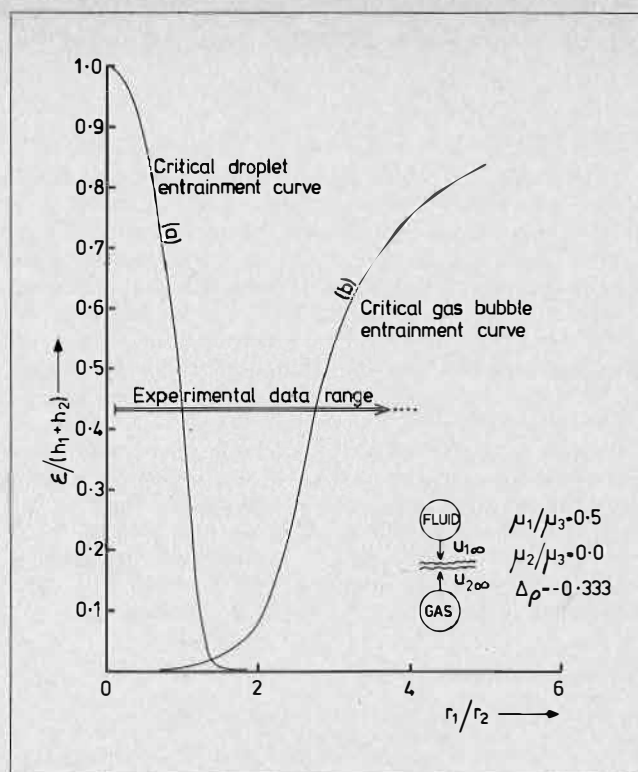


FIGURE 15. Critical distance of separation as a function of the ratio of particle radii (Flotation System)

TABLE 2. Source of Aqueous Phase Loss in Stripping

Entrainment			
Aqueous Entrainment ppm	Losses from Tankhouse tpa tonnes		
	Cu	H ₂ SO ₄	
100	10.8	64.8	
250	27.0	162	
500	54.0	324	
1000	108	648	

Crud formation			
Crud growth rate 1/m ³ of aqueous	Losses/yr tonnes		
	Cu	H ₂ SO ₄	
0.2	64.8	307.8	
0.4	129.6	615.6	
0.6	194.4	923.4	
0.8	259.2	1231.2	
1.0	324.0	1539.0	

derived from oxide ore via the typical flowsheet shown in Figure 6, the CCD equipment (as designed assuming no interaction and reduction of settling rates of entrained organic phase) can represent approximately 20% of the total plant capital cost. In reviewing the effect of organic phase we have considered a limiting situation where settling of solids could be prevented. This will not, of course, happen but a significant reduction in settling rate can be anticipated. If this was assumed to be 10% then the CCD cost would increase, increasing the total plant cost and increasing the CCD contribution to approximately 24%. Thus the total plant cost is sensitive to this unit process and the effects of organic entrainment must be considered.

In reviewing the consequences of entrainment on plant costs there are many other factors to consider. In partic-

ular, materials of construction may have to change to use more costly passive materials. This has not been considered.

Conclusion

In conclusion, problems relating to entrainment in three-phase systems have been considered and conditions of a simplified system of two dissimilar particles translating in a third liquid phase have been analysed. The solutions have been used to outline conditions where entrainment of one dispersed phase by the other can be expected. As an example, a copper solvent extraction plant has been discussed in which these conditions of entrainment may be found in decantation (thickening), solvent extraction and flotation to remove entrained droplets from solvent extraction or to remove entrained solids after decantation. The importance of entrainment in the solvent extraction step of the overall copper process has been considered for a typical large copper plant operating on an acid leach system. Here relative costs of liquid-liquid entrainment and liquid-solid entrainment (crud) are compared. The importance of loss from crud removal is evident.

NOMENCLATURE: Part I

$a_{ni}, b_{ni}, c_{ni}, d_{ni}$	= constants of integration, equation (6)
a_{jk}	= constants, equation (7)
$C_{n+1}^{-1/2}$	= Gegenbauer polynomial of order $(n + 1)$ and degree $-1/2$ with argument s .
E	= differential operator
F_j	= drag force on particle, $\xi = \xi_j$
h_j	= distance of centre of particle $\xi = \xi_j$ from $z = 0$
n	= summation index
p	= pressure
r	= characteristic radius
r_j	= radius of particle, $\xi = \xi_j$
s	= $\cos \eta$
t	= time
t^*	= dimensionless time, tU/ϵ
\underline{u}	= vector fluid velocity
\bar{u}^*	= dimensionless vector fluid velocity, \bar{u}/U
U	= characteristic velocity

U_j	= settling velocity of particle, $\xi = \xi_j$
U_{ni}	= mathematical function, equation 6.
z, R, ϕ	= cylindrical co-ordinates
∇^2	= Laplacian operator
$\Delta \rho$	= dimensionless density $(\rho_1 - \rho_3)/(\rho_2 - \rho_3)$
$\Delta \rho'$	= $-\Delta \rho$
ϵ	= minimum distance of separation of particles, $\xi = \xi_1, \xi = \xi_2$
ϵ_{crit}	= minimum distance of separation of particles when U_1 or $U_2 = 0$
μ_1	= viscosity phase i
μ_j	= μ_j/μ_3
ξ, η, ϕ	= bi-polar co-ordinates
ξ_j	= defines boundary of particle regime j
ρ_i	= density of phase i
ν_i	= kinematic viscosity of phase i
σ_j	= interfacial tension phase $j, 3$
ψ_i	= stream function, phase i
z	= $\epsilon/(h_1 + h_2)$

Subscripts

i	= denotes fluid phase i ($i = 1, 2, 3$)
j	= denotes fluid boundary ($j = 1, 2$)
∞	= denotes conditions associated with a single particle problem

Part II

d_j	= solid particle size, phase j
\bar{H}_j	= volumetric hold-up of dispersed phase j in continuous phase
H	= total volumetric hold-up of dispersed phases
n	= number of droplets
P	= probability
w	= weighting factor

REFERENCES

- (1) Happel, J. and Brenner, H. "Low Reynolds number hydrodynamics", Prentice-Hall Book Co. N.Y. (1965).
- (2) Kynch, G.J. J. Fluid. Mech. 1958, 5, 193.
- (3) Bart, E., Chem. Eng. Sci. 1968, 23, 193.
- (4) Wacholder, E. and Weihs, D., Chem. Eng. Sci. 1972, 27, 1817.
- (5) Rushton, E. and Davies, G.A., Appl. Sci. Res. 1973, 28, 37.
- (6) Rushton, E., Ph.D. Thesis Univ. Manchester, (1974).

The Relationship Between Batch and Continuous Phase — Disengagement

A.M.S. Vieler, D. Glasser* and A.W. Bryson,
 Department of Chemical Engineering, University of the
 Witwatersrand, Johannesburg, South Africa.

ABSTRACT

An internal age-distribution model is derived to relate a batch settler with a completely mixed continuous steady-state settler. If the internal phase-disengagement rate is a function of age as well as other properties this leads to a non-uniqueness in going from batch to continuous experiments. Continuous and batch runs were performed on the same feed and the results interpreted in the light of the above model. There was reasonable agreement between the two although the problem of the non-uniqueness could not be resolved on the experimental results available.

Introduction

THE ADVANTAGES OF BEING ABLE to design a continuous settler from batch experiments are so obvious that they have engaged the efforts of many workers but one can say with only a limited amount of success. It is firstly the intention of this work to examine the problem from a fundamental level and to suggest some of the reasons for the lack of success. This is based on a residence-time model for the process which will be derived and then applied to results which have been obtained for this purpose.

It is not the intention to review the previous literature as this has only recently been done in a review article⁽¹⁾. The presentation will begin with the development of a model for the relationship between the batch and continuous phase-disengagement. (This term deliberately is used to be non-specific about the actual mechanism of the process.) This model will highlight some of the difficulties which can be encountered in experimental work and will suggest the type of experiments that are needed.

The second part will concern itself with the experimental apparatus and the results will be presented. Finally the results will be discussed in the light of the model.

Mathematical Model

In view of the fact that we have a drop-size distribution and distributions of coalescence times, even for similar drops, it is sensible to use a statistical type of model. The model we use here is a residence-time distribution model similar to that used for chemical reactors but, in fact, a generalization of that model. This model is similar to one proposed by Valentas and Amundson⁽²⁾ for liquid-liquid mixing.

Suppose in such a system we define $\psi(t)dt$ as the volume of the dispersion in the settler of age between t and $t+dt$ where age is defined as the time since the volume element entered the system. In a more complex model this could be a function of position, etc., but for the purposes of this paper we restrict ourselves to this definition.

Associated with this volume element, we define a phase-disengagement rate $g(x,t)$ which is the fraction of volume disengaging per unit time when the age is t and the properties of the system are x . Examples of such properties might be the phase ratio and the total dispersion band thickness. In terms of these two quantities a material balance over a differential age interval leads to the equation

$$\frac{d\psi(t)}{dt} = -g(\underline{x}, t)\psi(t) \dots \dots \dots (1.1)$$

The major assumption in the derivation of this equation is that we can, in fact, define such a property as g which is a property of the system. Furthermore it will be necessary to assume we can relate the value of g from the batch and continuous experiments.

Batch Separation

As all the dispersion in a batch experiment is of the same age we can let $v(t)$ be the volume of the dispersion at time (age) t

$$v(t) = \psi(t)dt \dots \dots \dots (1.2)$$

and so equation (1.1) becomes

$$\frac{dv(t)}{dt} = -g(\underline{x}, t)v(t) \dots \dots \dots (1.3a)$$

For constant cross-sectional area let $h(t)$ be the height of the dispersion band

$$\frac{dh(t)}{dt} = -g(\underline{x}, t)h(t) \dots \dots \dots (1.3b)$$

$$\frac{d \ln(h(t))}{dt} = -g(\underline{x}, t) \dots \dots \dots (1.3c)$$

In principle it seems possible to obtain $g(x,t)$ from a batch experiment. However, if any of the, say, local properties x , are time dependent, $x_1 = x_1(t)$, it is easy to see that we cannot from a simple batch experiment separate the effects of the variation of $x_1(t)$ and t itself.

To clarify the position let us be more specific. Suppose the only local property on which g depends is the height of the dispersion, i.e.

$$g = g(h, t) \dots \dots \dots (1.4)$$

Then for the batch run

$$\frac{d \ln(h(t))}{dt} = -g(h(t), t) \dots \dots \dots (1.5)$$

where at time $t = 0$, $h(0) = h_0$. The result of the batch experiment will be a curve

$$h = h(h_0, t) \dots \dots \dots (1.6)$$

From this curve we are not able to separate the effects on g of h and t and therefore cannot uniquely determine the

form of g from simple experiments only. One could separate the effects of h and t doing, say, a batch experiment in which the cross-sectional area changed with time, keeping the overall height constant. If, say, $g = g(h)$ only, this experiment would give a constant rate while any effect of t would cause a change with time. If on the other hand $g = g(t)$ only the result would be the same as the ordinary batch experiment.

The important conclusion is that if there is any age-dependent phenomena associated with g then it is not possible to evaluate g from a simple batch experiment alone. Or more relevantly to this paper, there will be a non-uniqueness in going from the batch experiment to the continuous experiment. This important conclusion will be highlighted later when the experimental results are analysed.

Continuous Settling

Define $G(X\tau)$ for the continuous perfectly mixed steady-state settler in exact analogy to $g(x,t)$ for the batch (to avoid later confusion between the two). We may now integrate equation (1.1) with χ as independent of age as the system is at steady-state

$$\psi(\tau) = \frac{V \exp(-\int_0^\tau G(\underline{X}, \tau') d\tau')}{\int_0^\infty \exp(-\int_0^\tau G(\underline{X}, \tau') d\tau') d\tau} \dots (1.7)$$

Where V is the volume of the dispersion.

Now if Q is the total volumetric flowrate of the dispersion, from steady-state considerations

$$Q = \int_0^\infty G(\underline{X}, \tau) \psi(\tau) d\tau \dots (1.8a)$$

$$= \psi(0) - \psi(\infty)$$

$$= \psi(0) \dots (1.8b)$$

as $\psi(\infty)$ must be zero for steady-state. We may therefore obtain the result

$$\frac{V}{Q} = \int_0^\infty \exp(-\int_0^\tau G(\underline{X}, \tau') d\tau') d\tau \dots (1.9)$$

where $\frac{V}{Q}$ is the mean residence time of the dispersion in the settler and

$$V = AH \dots (1.10)$$

A is the cross-sectional area of the settler and H is the height of the dispersion band.

Examining the form of the equation one may very easily draw one important conclusion. Any volume element with a small value of G will have a large contribution towards the mean residence time or more specifically any slowly disengaging particles will tend to build up in the continuous settler and make a large contribution to the volume of the dispersion, while the rapidly disengaging section will make a small contribution. Thus, it is the slowly disengaging material from the batch experiment which will tend to dominate the operation of the continuous settler.

Relationship Between Batch and Continuous Settling

The difficulty of interpreting simple batch experiments has already been highlighted and this will have a profound effect in trying to determine a settling rate which we can use for predicting continuous results. However, it is instructive to examine a few limiting cases.

(1) Suppose the properties of the continuous and batch systems are the same i.e. $X = x$ and $t = \tau$ and furthermore from the batch $x \neq x(t)$ then we may write

$$G(\underline{X}, \tau) = g(\underline{x}, t) \dots (1.11)$$

Under these conditions we obtain

$$\ln \frac{h}{h_0} = - \int_0^{\tau'} G(\underline{X}, \tau) d\tau \dots (1.12)$$

and

$$\frac{V}{Q} = \int_0^\infty \frac{h(t)}{h_0} dt \dots (1.13)$$

where $h_0 = H$.

(2) Suppose the fractional settling rates G and g are not functions of time i.e.

$$G = G(\underline{X}) \text{ only} \dots (1.14)$$

This is directly analogous to the chemical reactor where the rate of reaction is a function of concentration only.

In this case for the continuous settler

$$\frac{V}{Q} = \frac{1}{G(\underline{X})} \dots (1.15)$$

where the X refers to the properties in the settler. For the batch settler we would get

$$\frac{d \ln h}{dt} = -g(\underline{x}) \dots (1.16)$$

and we could get the continuous mean residence time from a knowledge of the settling rate in the batch system under the same conditions i.e. $x = X$. This corresponds to the basic design procedure used by many workers.

In general to perform the integration required in Equation (1.9) we have to separate the effects of x and τ in our batch experiments and may in fact need to perform many types of batch experiments and under a wide variety of conditions to either obtain all the values of G we require either as a model or as experimental values. These points will be clarified during the discussion of the experiments.

Experimental Work

Experimental Equipment

Settler

A box settler was designed, which would allow variation of the depth, position and horizontal area of the dispersion band in continuous settling. To achieve this, a deep settler was designed for a maximum liquid depth of ninety centimetres and a dispersion width of seventy-five centimetres, which consequently minimizes any wall effects. It was decided to use a movable dam to vary the settler length and hence the horizontal settler area, while maintaining the same flowrates and mixing conditions. Thus, a perspex box of length 1.80 m, width 0.75 m, and height 1.00 m was constructed (see Figure 1).

At one end forty-five centimetres from the floor, a full width slot five centimetres high was cut to serve as the dispersion entrance to the settler. Into this tank was placed a perspex separation box, which could be moved the entire length of the settler and consisted of two chambers, one overflow chamber for the organic phase and an underflow full width slot for the aqueous phase (see Figure 1). This box was sealed around its edges by means of silicon rubber strips, once in position in the settler. The separated

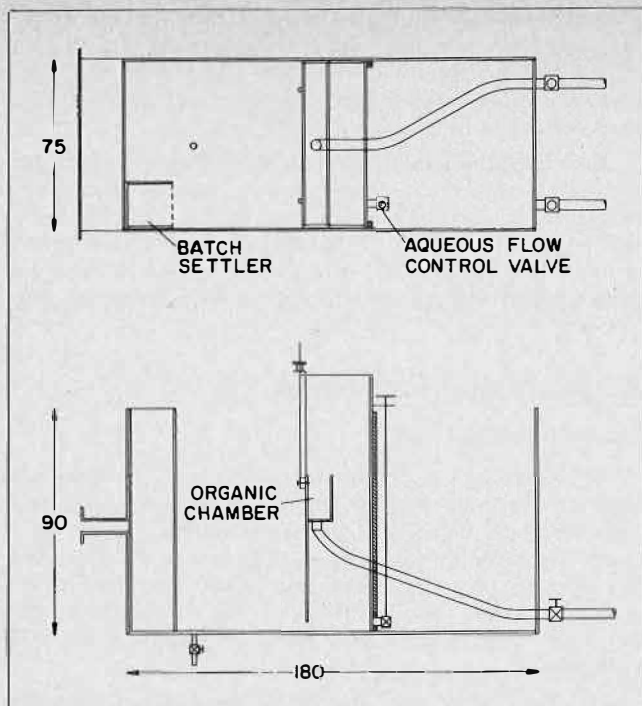


FIGURE 1. The Continuous Horizontal Gravity Settler (Dimensions in cm.)

organic phase was led away from the overflow chamber through a flexible pipe to a flow control valve outside the main settler box and returned to the bulk light phase circulation system. The underflow flowrate from the separating box was controlled by a valve, which was used to control the position of the dispersion band in the settler. The overflow weir height could be varied from sixty to ninety centimetres. Following general trends, the overflow and underflow weirs were all designed to be the full width of the settler to reduce uneven circulation and dead spots in the settler.

Phase Mixing

A reasonably conventional paddle mixer system was designed and constructed. This consisted of a rectangular base perspex box of base size sixty by thirty centimetres and a minimum liquid depth of forty-five centimetres which depends on the depth of the liquid in the settler.

Two impeller shafts were positioned symmetrically in the base fifteen centimetres from the walls. Each shaft carried one four-bladed impeller of diameter fifteen centimetres and one two-bladed impeller of the same diameter positioned as in Figure 2. The blades of each impeller were twisted to forty-five degrees to give a slight pumping effect and improve the general uniformity of the dispersion in the mixer. The second impeller on each shaft was added after finding that one impeller on each shaft provided insufficient mixing unless rotated at high speeds, which subsequently caused secondary haze problems. The impeller shafts, which were made of brass, were connected by pulleys and vee belts to a variable speed half-horsepower direct current motor with speeds varying between one hundred and fifty and fifteen hundred revolutions per minute.

A tee piece was placed in the base of the mixer box to serve as an initial phase mixer and inlet section for the two phases entering the mixer-settler unit. A horizontal plate of size eight by twenty centimetres was placed three centimetres above the mixer box inlet to ensure even

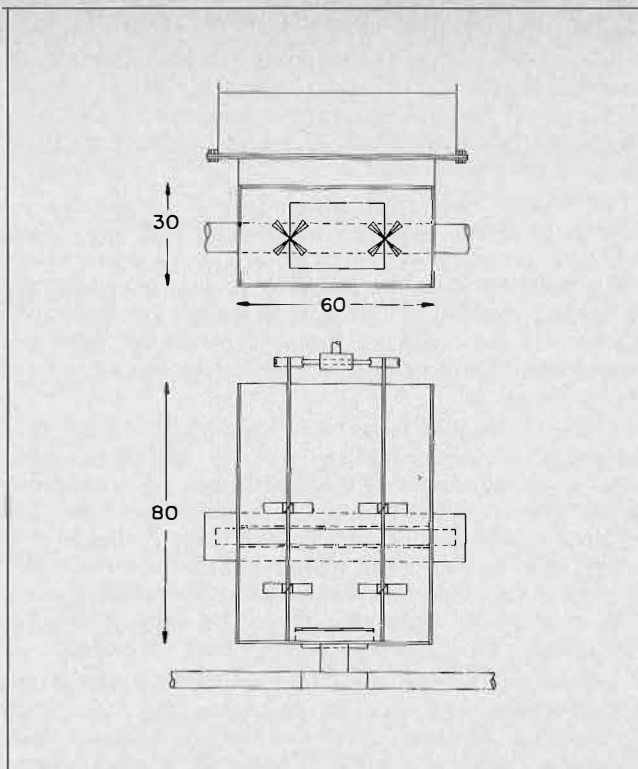


FIGURE 2. The Phase Mixing Chamber (Dimensions in cm.)

spreading of the incoming liquid through the mixer, thus improving the overall uniformity of the dispersion entering the settler. The mixer was connected to the settler inlet via a five centimetre deep channel, which widened to the settler width. As some circulation was caused in the settler by the stirring in the mixer, several vanes of perspex were placed in the settler inlet channel to damp out these disturbances.

Phase System

As it is immaterial to the phase separation model what phase system is used, since no physical parameters enter the model, the system of kerosene and water was chosen. Kerosene does not require any special storage or pumping system in the experimental equipment designed and does not attack perspex, unless it contains aromatic hydrocarbon compounds. Additionally it is not as volatile or toxic as other suitable organic liquids such as toluene or xylene, for example. A further reason for this choice was the possibility of using full-scale settler data from a uranium extraction plant, which uses a kerosene-water system.

Since the size of the mixer-settler necessitated large flowrates, it was found that at least two cubic metres of each phase would be needed for the experimental runs. This bulk of liquid eliminated possibilities of maintaining constant purity levels of the phases. Contamination of the liquids by dust, bacteria and fungus was unavoidable and the effects and growth were minimized by small concentrations of formalin and reasonably lengthy settling and filtration periods between experimental runs. It was generally found that a week was sufficient time to clear the two phases with removal of sedimented dirt by filtration and suction. After cleaning the system in this manner, it was possible to maintain reasonably reproducible batch settling for eight to nine hours continuous settling, which proved sufficient time for one complete experimental run.

Pumping, Circulation and Storage

Comparative work in mixer-settler equipment led to conclusion that, for the settler designed, dispersion flow rates of up to nine litres per second (about 120 gpm) would be required to allow complete flexibility in the phase separation work.

A constant circulation system for each phase was designed to reduce pumping fluctuations and allow more efficient pumping with a draw off to the mixer-settler from each system. The variation in flow rates of each phase delivered by the centrifugal pumps directly to the mixer was not noticeable during experimental runs, and any fluctuations present were damped by the size of the mixer-settler.

Since reasonably heavy duty centrifugal pumps were employed, it was decided to use five centimetre piping and, since little detail of material design for a kerosene-water system could be found in the published work, galvanized mild steel piping was chosen. Since the design flow rates were large, it was found that at least two cubic metres of each phase should be stored. To facilitate cleaning, two smaller tanks of capacity 1.1 cubic metres for each phase rather than a single large tank were chosen.

After initial experimental runs, extensive bacterial and fungal growth occurred at the phase interface. This caused considerable corrosion particularly in the aqueous phase circulation system as well as blinding the dispersion interfaces and seriously disrupting phase separation. After attempts at control using fungicides, formalin in concentrations of about two hundred parts per million was found to contain the growth problem. However, separation problems continued until it was established that the galvanizing, particularly in the aqueous phase system, was oxidizing off the piping and forming a microfine suspension in the liquid. This caused secondary haze and phase separation instability.

Consequently a new aqueous circulation system was designed with a very much larger storage capacity (eight to nine cubic metres), a PVC lined storage tank and five centimetre PVC piping. The original mild steel pump was retained. It was found that the larger capacity storage

allowed further settling of dirt and organic phase carried into the bulk aqueous phase in the mixer-settler. The organic phase circulation was not changed as the solids contamination levels dropped considerably and remained at controllable levels with the alterations.

All control valves in the circulation system were five centimetre gate valves. The flow rates into the mixer were measured by orifice meters, one and a half inches in diameter. These were calibrated during initial experimental runs and checked throughout the experimental test period. Very little change occurred over the seven-week period.

Experimental Procedure

Continuous Settling

At the start of a continuous settling test the separation box was fixed in position and the settler half filled with aqueous phase before the mixer was started and the kerosene introduced into the system. The settler was filled and the aqueous phase exit flow rate adjusted to position the dispersion band at the level of the settler dispersion entrance. This position was found to minimize the inlet turbulence.

Generally after start up the settler reached a steady-state condition within twenty minutes and the first batch test could be completed. After the disruption of the dispersion flow and a batch test, the continuous settler regained its steady state and a further batch test could be taken. The continuous dispersion band thickness was measured. For most runs it was possible to do at least four batch tests before stopping and changing the settler area. Valve settings for a continuous run over a day were fixed and flow readings taken at least twice during each area run. Temperatures of the liquids during a day run varied very slightly and batch tests over a day were reasonably reproducible.

Batch Settling

The phase separation model requires that the same dispersion should be used in the batch and continuous tests for one run. The easiest method of sampling the dispersion at the settler entrance is to place a batch settler inside the main settler and fill it with the dispersion entering the continuous settler.

To do this, a box of the same height as the continuous settler with a square base of twenty centimetre sides was constructed (see Figure 3). This had three fixed sides, one containing an entrance slot forty-five centimetres from the bottom and a fourth side which could be removed entirely. This side was designed in segments so that the initial dispersion height in the batch settling tests could be varied from fifteen to eighty centimetres. It was subsequently found that this range was reduced to twenty to about sixty centimetres by the general hydrostatics of the dispersion bands in and outside the batch settler.

This batch settler was placed in one corner of the settler and for continuous runs was left with the entrance open and the fourth side removed. It was found to have very little effect on the continuous settling in this position. To execute a batch test, the fourth side, with segments chosen to give an initial batch height, was inserted and the batch settler filled with incoming dispersion from the mixer by closing the rest of the entrance of the continuous settler. Once a steady flow of dispersion was achieved through the batch settler, the entrance port was closed and the height of the batch dispersion was measured photographically at various time intervals until the first clear break point at the interface was observed.

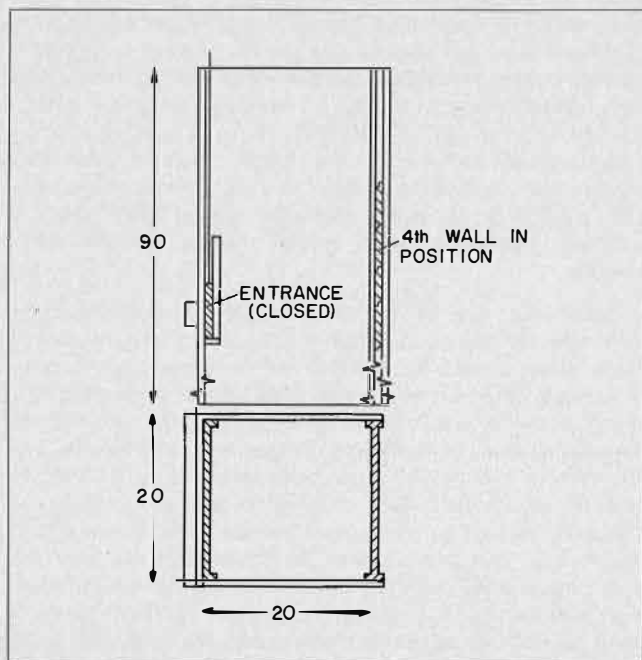


FIGURE 3. The Batch Settler (Dimensions in cm.)

TABLE 1. Conditions for Runs

Run No.	Water Flow Rate litres/sec.	Kerosene Flow Rate litres/sec.	Mixer Speed rpm
1	2.30	2.55	200
2	2.50	2.93	200
3	2.13	2.30	200
4	1.12	1.44	240
5	1.63	1.00	250
6	1.12	1.00	225

For each continuous settler area a set of three or four batch tests was taken. This procedure was chosen to reflect any general change in the settling characteristics of the dispersion during a full run and to provide a large number of batch tests for the purpose of evaluating $g(x, t)$.

Results and Discussion

A series of runs were done, each with a fixed flow rate of each component and fixed stirrer speed. The appropriate conditions for each run are given in Table I. For each run batch experiments were interspersed with continuous runs where the settler cross-sectional area was changed. The batch experiments also covered a wide range of initial heights. It is important to remember that these runs, as near as reasonably possible, represent the same feed to the batch as to the continuous settlers and were done in equipment sufficiently large for edge effects to be minimized. The batch experiments were also interspersed with the continuous runs so that if there were any changes in the settling characteristics with time, these would have been apparent in both the continuous and the batch runs. In this way it was hoped to overcome many of the shortcomings in previous work.

Batch Results

As the reproducibility of runs for a batch experiment was not very good and there were of the order of about 20-30 per run it was decided to break them up into sets which covered an initial height $\pm 2-4$ cm. By taking the average of these runs it was easier to compare the effect of initial conditions. Typical curves are given in Figure 4 for Run 1 where $\ln \frac{h}{h_0}$ is plotted vs time for each of the mean curves. It is immediately obvious that, in fact, there is quite a large effect of initial conditions on the shape of the curves, the higher the initial height the slower the normalized settling. This result was paralleled for the other runs which are given in Vieler⁽³⁾. However, by plotting these same curves so that they each are shifted along the time axis to be more or less on top of each other a much better fit is obtained as in Figure 5. The significance of this will be discussed later, but again this is paralleled in all the six runs.

Continuous Results

These can conveniently be summarized in a Graph of $\frac{V}{Q}$ vs H and are given in Figure 6. One may immediately note that the mean residence time increases with H in a linear fashion but does not approach zero at $H \rightarrow 0$

$$\frac{V}{Q} = aH + b \dots \dots \dots (3.0)$$

where a and b are positive constants. It can be seen that runs 1-3 form one set and runs 4-6 another; the latter, having been more thoroughly mixed, have slower settling characteristics.

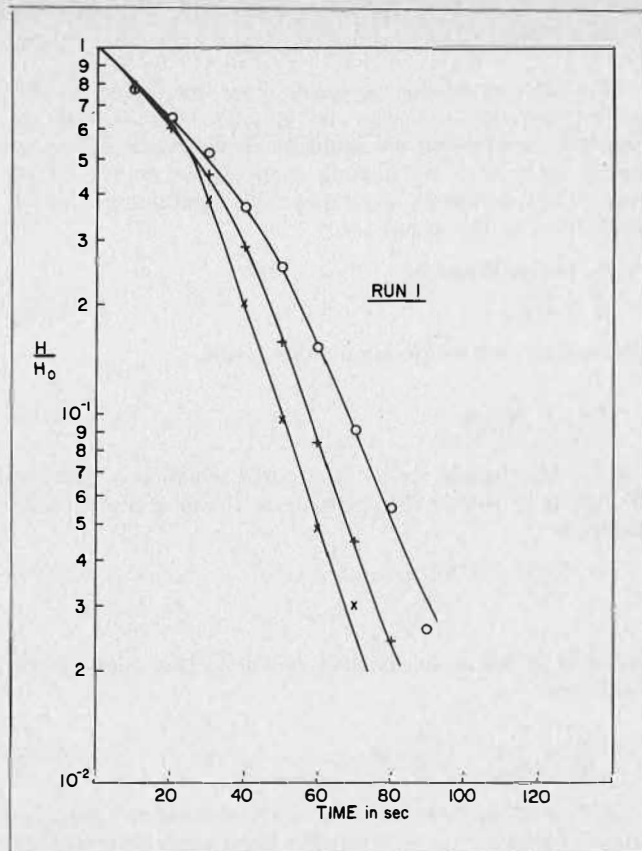


FIGURE 4. Height over initial height against time for a range of initial heights.
 × 18.2 cm.
 + 27.9 cm.
 ○ 35.1 cm.

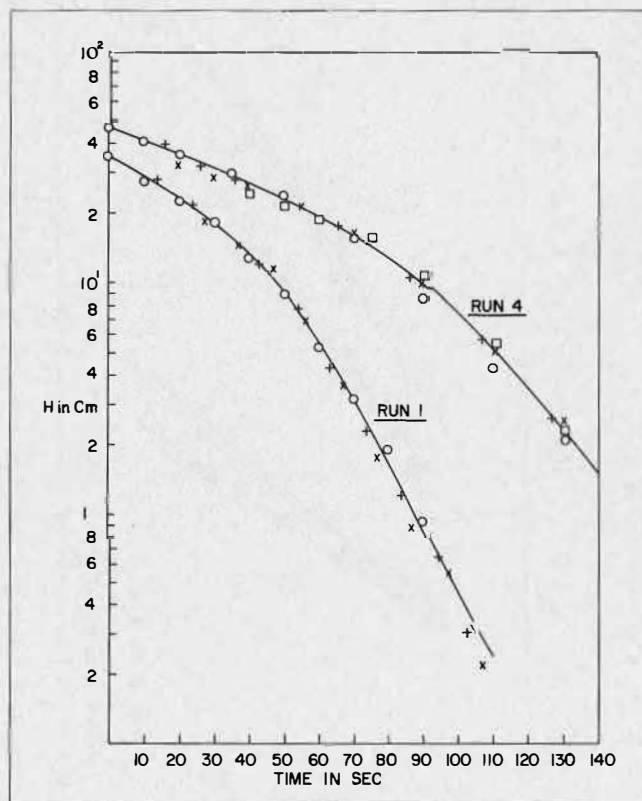


FIGURE 5. Height on a Logarithmic scale versus time where each of the curves for different initial heights has been shifted by a constant amount on the time axis.

$$\text{i.e. } \frac{dn(h)}{dt} = -k \dots \dots \dots (3.6)$$

but we would not be able to fit the constant C from batch results.

The form of the equation (3.5) has been used by Stöner and Wöhler⁽⁴⁾ to correlate these results and as can be seen from Figure 6 the results of this paper are also well-fitted by this model. Similar plots for the results of Thomas⁽⁶⁾, Allak and Jeffreys⁽⁶⁾, and Barnea and Mizrahi⁽⁷⁾ show this to fit their results as well.

Up until this point we have avoided being specific about the details of the process particularly as the model could prove useful for any type of phase-disengagement, such as crystallization and thickening as well as settling. However, at this stage it might prove useful to discuss what we mean by time (age) dependent phenomena. In particular the one that appears most commonly is an induction period. For many processes there appears to be a specific time at the beginning of the experiment during which rates are different from those which might be expected just from the properties of the system. This we call the induction period. For settling, this period might be a time for internal turbulence to die down or an internal rearrangement time to achieve a more stable initial configuration. In any event it can be seen from our discussion that these phenomena can lead to difficulties which might not be immediately apparent.

In defining a single disengagement rate g we have, of course, vastly oversimplified the settling process as we know we actually have at least the two separate processes of drainage and coalescence and either one or neither might be rate limiting in a particular situation. In the initial stages of introducing the model it seemed to be complicating matters unnecessarily to try to introduce both effects. In principle, however, the model could be rewritten taking into account both rate effects and the rate of movement of both interfaces could be observed separately for the batch system.

Conclusions

This paper has attempted to explain the difficulty in going from batch to continuous experiments. In so doing an internal age distribution model has been derived and it has been shown in what way there might be a non-uniqueness in going from the one experiment to the other. However, the awareness of the difficulty suggests ways of overcoming the problem.

An experimental apparatus was built and extensive batch and continuous data were taken. Using various assumptions to overcome the non-uniqueness, the two sets of experiments were found to correlate reasonably well, particularly considering the poor reproducibility of the batch experiments and the fact that there are no free parameters to be used to help to fit the results.

The internal age distribution model also highlights the fact that for accurate correlation between the two types of experiments, exactly the same feed must be used on both. Further experimentation may, however, allow one to be better able to predict the change in settling properties with the change in mixing conditions. Another important factor to be investigated is the phase ratio of the two components.

The model and results presented in this paper have by no means solved the problem of predicting continuous from batch results but have attempted to clarify the problem and lay down the guidelines for both the experimental and theoretical solution of the problem.

Acknowledgment

One of us (A.M.S.V.) would like to thank the national Institute for Metallurgy for a bursary.

NOMENCLATURE

A	= cross-sectional area of settler
a	= constant
b	= constant
C	= constant
g	= fractional volumetric disengaging rate in batch settler
G	= fractional volumetric disengaging rate in continuous settler
h	= height of dispersion zone in batch settler
H	= height of dispersion zone in continuous settler
H	= Heaviside step function
\bar{k}	= constant
Q	= volumetric flow rate of dispersion in continuous settler
r	= function of time
t	= age or time in batch settler
τ	= age of dispersion element in continuous settler
v	= volume of dispersion in batch settler
V	= volume of dispersion in continuous settler
\bar{x}	= vector of properties in batch settler
\bar{X}	= vector of properties in continuous settler
$\psi(t)$	= internal age density function

REFERENCES

- (1) Glasser, D., Arnold, D.R., Bryson, A.W. and Vieler, A.M.S., *Minerals Sci. Engng.* 1976, 8, 23.
- (2) Valentas, K.J. and Amundson, N.R., *I.E.C. Fund.* 1968, 7, 66.
- (3) Vieler, A.M.S., M.Sc. Dissertation, University of the Witwatersrand, Johannesburg, South Africa 1977.
- (4) Stöner, H.M. and Wöhler, F., *Inst. Chem. E. Symp. series No. 42 (Hydrometallurgy)* April 1975, p. 14.1.
- (5) Thomas, W.W., M.Sc. Thesis, University of Cape Town, Cape Town, South Africa 1974.
- (6) Allak, A.M.A. and Jeffreys, G.V., *A.I.Ch.E.J.* 1974, 20, 564.
- (7) Barnea, E. and Mizrahi, J., *Trans. Inst. Chem. Eng.* 1975, 53 (2), 83.

DISCUSSION

E. Barnea: What is the physical meaning of the statement that the rate of disengagement of an element is a function of its life time? What is the mechanism by which the element "knows" its age? The answer must be the particle size distribution which provides the linkage with the time scale through its continuous change as result of drop to drop coalescence processes.

Hence, for the proposed model to predict continuous settler behaviour based on batch data, it is required to assume the same coalescence probabilities under the same conditions in batch and continuous separations. The question is, thus, can we really expect the same conditions in batch and continuous separations? In my opinion the answer is negative. In a continuous settler we find a counter-current flow of droplets of different sizes in a fluidized and very "lively" situation while in batch-settling, stratification takes place and coalescence is mainly between droplets of similar size flowing concurrently. With this in mind I would tend to question the validity of such a model.

D. Glasser: This model essentially states that each element of dispersion is unaware of whether it is in a continuous or batch system but knows only of its local environment. Its local phase disengagement rate depends only on these properties which are designated by the x . These properties alone in certain circumstances may not be sufficient. For instance, a high degree of turbulence

on entering a settler may alter the value of g even though all other x are the same. This turbulence may require time to be dissipated and the value of g for the same x will in this sense be a function of time.

Thus if we know all the local properties in our settler and can relate these to g , we can, by doing a wide enough series of experiments, evaluate g for all x and t . Once we have done this, in principle the behaviour of any other settler will be a weighted average over the correct values of the independent variables. What this paper does is to show what form this correct average takes.

We have not directly indicated what the important local properties, x , are, but any one with some experience in the field will certainly be able to identify many of them. Thus Dr. Barnea's question of whether we can expect the same conditions in the continuous and the batch settlers is precisely the one to which this paper presents itself. That is, given that batch and continuous are not the same, we may still use the information from the one to predict the other if we recognize that each element of the dispersion only knows its local environment and not the total system, and so by averaging correctly over all the local environments we may produce the desired relationships in each kind of settler and thus relate the different types of settler.

H.M. Stoenner: By plotting total disengagement time (T) as the main variable measured in *batch* settling tests over initial dispersion heights (H_i) we found empirically a linear function: $T = T_0 + m.H_i$. By plotting hold-up time (T) of *continuous* settler feed (Q) in dispersion volume (V_D) over dispersion band thickness (ΔH) using the method proposed by Warner⁽¹⁾ (i.e., changing settler

(1) Windscale.

area (A) only), we found a similar linearity: $T = V_D/Q = T_{0c} + M_c.\Delta H$. Replacing V_D by $A.\Delta H$ we derived the hyperbolic function for specific flow rate: $Q/A = \Delta H/(T_{0c} + m_c.\Delta H)$. The parameters depend on: system, phase ratio, inlet turbulence, temperature, etc. and cannot be measured directly, but could be interpreted as follows:

- (1) (T_{0c}) as settling time of smallest dispersion band (one drop at interface)
- (2) (T/m_c) as (limiting) settling rate (Q/A) at infinite dispersion band thickness ($\Delta H = \infty$). (T/m_c) is the asymptote to the hyperbolic function.

It would be useful, if a method could be found, to derive the parameters (T_{0c} , m_c) for the continuous settler from the parameters (T_0 , m) measured in batch settling tests. Is there any work in this direction?

I consider the presented paper as a breakthrough in the field of modeling batch and continuous phase disengagement.

D. Glasser: It is our intention to continue the work and study the effect of various parameters such as the drop-size distributions, additives and phase ratios. As well as this, the model is oversimplified at the moment and there are various refinements that can be incorporated when the experimental results warrant this. Moreover, various other batch-type experiments are envisaged to try to resolve the non-uniqueness in the results discussed in the paper. Whether the final model will be in the form as suggested by you and supported by your preliminary results, however, still remain to be seen. If this does prove to be the case, our results should throw light on the parameters in the model.

DISPERSION AND COALESCENCE

The Interpretation of Batch Separation Tests for Liquid-Liquid Mixer-Settler Design

J.C. Godfrey, D.K. Chang-Kakoti, M.J. Slater and S. Tharmalingam, Schools of Chemical Engineering, University of Bradford, Bradford, West Yorkshire.

SYNOPSIS

The rate of separation of liquid-liquid dispersions in rectangular tanks has been studied with a view to finding a method of predicting the performance of flow settlers. Data for both batch and continuously operated mixers have been obtained. A procedure for predicting the performance of a flow settler is proposed and it is shown that, whereas data from a flow mixer can be used with confidence, batch interpretations may be invalid. The two conditions of operation affected the rate of separation very markedly; it was found that the presence of haze in batch tests was associated with a faster coalescence rate than that experienced in the flow mixer. Haze produced during start-up of the mixer in a flow system was gradually washed out and the coalescence rate in the mixer on shut-down and in the settler slowed down in consequence.

Introduction

THE USE OF MIXER-SETTLER equipment for solvent extraction processes is widespread and recent years have seen the development of very large-scale apparatus particularly for the extraction of copper and uranium from clarified leach liquors⁽¹⁾.

The development of more sophisticated design procedures is warranted since the solvent inventory in both mixer and settler has a high capital cost and this should be minimized. However, progress in understanding has been hindered by complexities due to the effects of contaminants, reaction or diffusion rates of solutes, and design has been carried out on the basis of pilot plant results using real solutions and the application of various scale-up procedures^(2,3).

A number of workers have tried to reduce the scale of pilot work and the cost involved by attempting to relate observations of batch to continuous settler performance^(4,5). This paper demonstrates a practical procedure for settler design and shows that batch data cannot generally be used without risk of serious under-design.

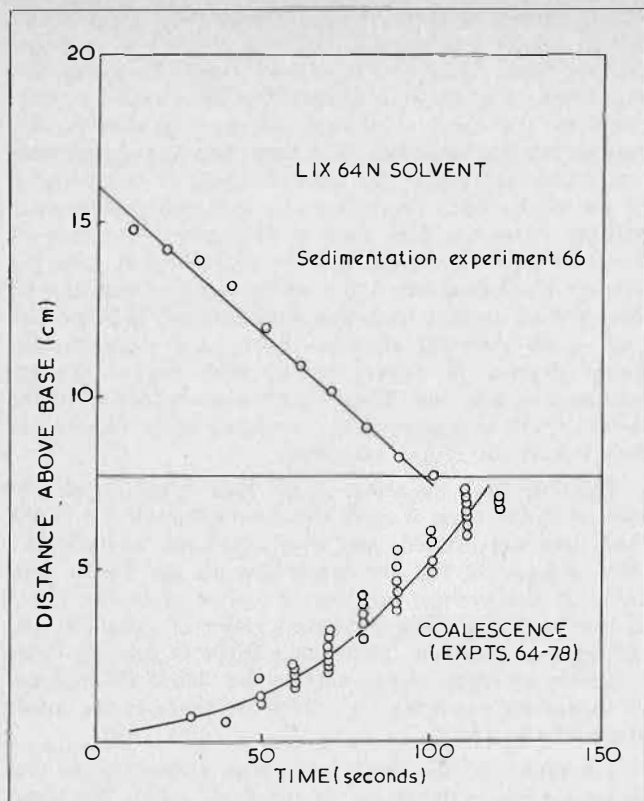


FIGURE 1. Batch separation data.

Experimental Work

Batch experiments were carried out in perspex rectangular tanks of 6 inches and 12 inches square cross-section. The tanks were filled with volumes of solvent and aqueous phases such that the total liquid height was approximately equal to the tank width. Six-bladed Rushton turbine impellers of 2 inches, 3 inches and 4 inches diameter were used, placed at the interface level between aqueous and solvent phases.

The two phases were agitated for various times, using various impellers at several speeds. The start-up procedure required that the phase to be dispersed is added to the agitated continuous phase or alternatively that the impeller was located in the continuous phase before agitation was commenced. The stirrer motor was switched off after a given time and the dispersion produced was allowed to collapse by sedimentation and coalescence processes. With the systems used, two clear demarcation lines were seen at the level of the sedimenting front and at the coalescence front where drops were coalescing with bulk separated liquid. The levels of these two fronts were recorded as a function of time until the dispersion had completely separated. The movement of the fronts of the dispersion bands was sufficiently slow to be followed by eyes. Typical data are shown in Figure 1.

This basic batch separation test has been discussed by other workers⁽⁶⁾. The present authors have previously studied the determination of drop sizes using the relationship between the velocity of the sedimenting front and the hold-up of dispersed phase⁽⁹⁾. This paper investigates the relevance of the batch velocity measurements to the performance of the settler in a flow system.

The solvent used in all cases was initially unloaded 20% LIX® 64N*/Escaid 100⁺ or kerosene and the aqueous phase was one of the following: — (1) 3 gm Cu/1, 2 gm H₂SO₄/1; (2) 2 gm H₂SO₄/1; or (3) water.

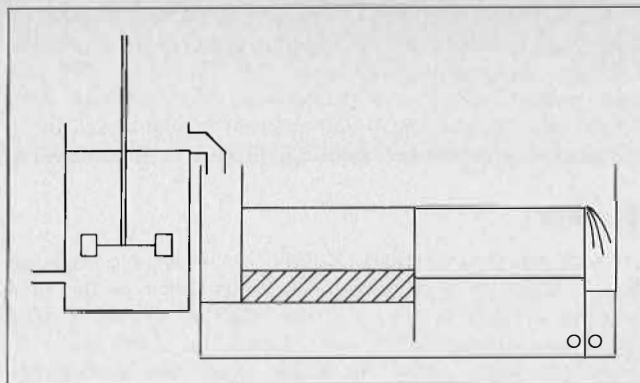


FIGURE 2. Mixer-settler construction.

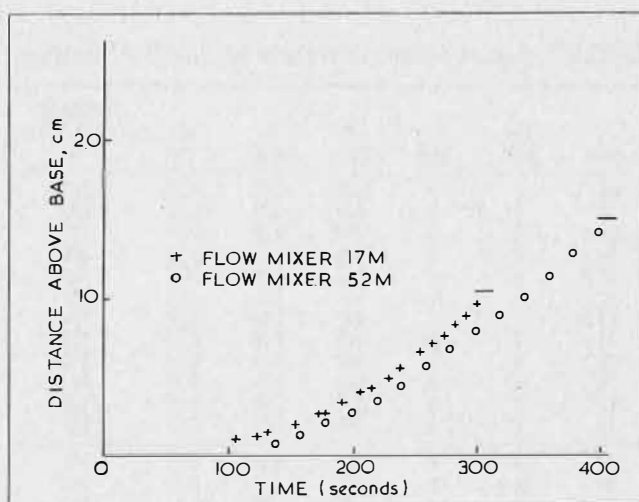


FIGURE 3. Separation data for 6 in. and 12 in. mixers on shutdown.

Sedimentation and coalescence measurements were made for aqueous drops dispersed in a LIX 64N/Escaid 100 continuum. The dispersed phase hold-up was varied from 0.31 to 0.59; at low hold-up the sedimentation front is diffuse and difficult to observe. Kerosene was dispersed with water as the continuous phase in a study of the behaviour of organic drops.

The same vessel and impeller geometries were used for both batch and continuous tests; LIX 64N and kerosene were used. Flows of solvent and aqueous were pumped in through separate pipes in one tank side near the base; the impeller was relocated after start-up at half the total liquid depth and the dispersion overflowed at the top of the mixer via a distributor into a settler (Figure 2). The length of the settler could be varied by moving a baffle. After operating the flow system for a time long enough for steady-state to be achieved, the dispersion band thickness in the settler was measured. Then the settler baffle was moved and another steady-state band thickness recorded. This was done for as many baffle positions as possible. The band was normally of constant thickness along its length. The pumps and the impeller motor were then switched off, inlet and outlet flows were stopped, and the dispersions in both mixer and settler were allowed to separate. Observations of the movement of the sedimenting and coalescing fronts in the mixer were made as in the batch experiments (Figure 3).

As described below, measurements of the degree of organic entrainment in the aqueous phase were made for a limited number of conditions for flow tests. Samples were treated with Freon (Arklone P) in a ratio of 1:10 Freon/aqueous and the Freon solution was analysed using infra-red to measure the carbon-hydrogen bond stretching.

Results

The batch tests for the LIX 64N solvent were considered first in terms of a primary break time, taken as the time for clear patches to appear at the interface (Table 1). The break-time appeared to vary irregularly. Two types of behaviour were noted: in most cases the coalescence velocity (the slope of the line relating position of the coalescence front to time) increased up to the time of appearance of clear patches at the interface. In some cases, after a period of increasing coalescence velocity a

falling coalescence velocity was found for the condition of a thin layer of dispersion (one centimetre or so) and primary break times were then much longer. It is suggested that different levels of contamination or amounts of haze could be the cause. However, Barnea⁽⁶⁾ proposes other reasons for this behaviour. The time used to compare tests was therefore taken as the value obtained by extrapolation of the coalescence line using the maximum coalescence velocity observed. This time is obviously a function of depth of liquid involved. For the 6-inch batch tank the average break-time was 128 s with a standard deviation of 14 s for all results, including variations of impeller size and speed, different aqueous phases and therefore different degrees of solvent-loading with copper. Twelve tests were carried out. These observations were for mixing times of 110 s, typical of the residence times required in flow mixers for copper extraction.

The data from the mixer in the flow system were considered in the same way. It was found that all the 6-inch tank data were similar and overlapped the 12-inch tank data (Figure 3), but the break-time in the 6-inch flow tank, on the average, was 323 s compared to the 128 s in the batch tests. No significant effect of agitation conditions was indicated. These data apply to running times sufficient to reach steady-state in the settler (20 minutes or longer for example) with residence times in the mixer from 40 s to 180 s.

The object of the batch separation measurements was to predict the performance of the flow settler. The usual design procedure is to obtain a plot of dispersion band thickness in a flow settler against dispersed phase flow rate per unit horizontal area of settler for various flow ratios and agitation conditions^(3,6). Most previously published data appear to have been obtained in apparatus with fixed settler area. In order to generate data, previous workers have changed flow rates. Consequently, residence times in the mixer have been varied with possible changes⁽⁷⁾ in drop size produced, which may affect the settler. The data for the flow system have been obtained in this work with both fixed area settler and varying flow rates and varying area settler and fixed flow rates. No significant difference was obtained but this observation may not apply to all systems. In the present case no major effects of phase ratio, agitation conditions or aqueous phase composition were found for the LIX 64N solvent system.

TABLE 1. Batch Separation Data for LIX 64N Solvent

Run	D _T inch	d _i inch	N rpm.	V _s mm/s	d mm	Primary break time, s
31	6	2	1260	0.83	0.20	160
32	6	2	840	0.91	0.21	140
64 b	6	2	900	0.98	0.22	120
65 b	6	2	900	0.98	0.22	120
66 b	6	2	687	1.00	0.22	120
67 b	6	2	687	1.06	0.23	120
68 b	5	2	495	1.06	0.23	112
71 b	6	2	346	1.18	0.24	115
73 b	6	2	567	1.14	0.24	120
76	6	2	900	1.01	0.22	125
77	6	3	687	1.02	0.22	130
78	6	3	495	1.01	0.22	120
<hr/>						
84 b	12	4	563	2.10	0.36	105
90	12	4	225	1.40	0.27	140
91	12	4	450	1.45	0.27	140
93	12	4	563	1.37	0.27	140
86 b	12	4	450	1.70	0.31	140
88 b	12	4	225	1.39	0.27	130

b Two side baffles, width 0.1 D_T
Phase ratio 1/1, aqueous dispersed

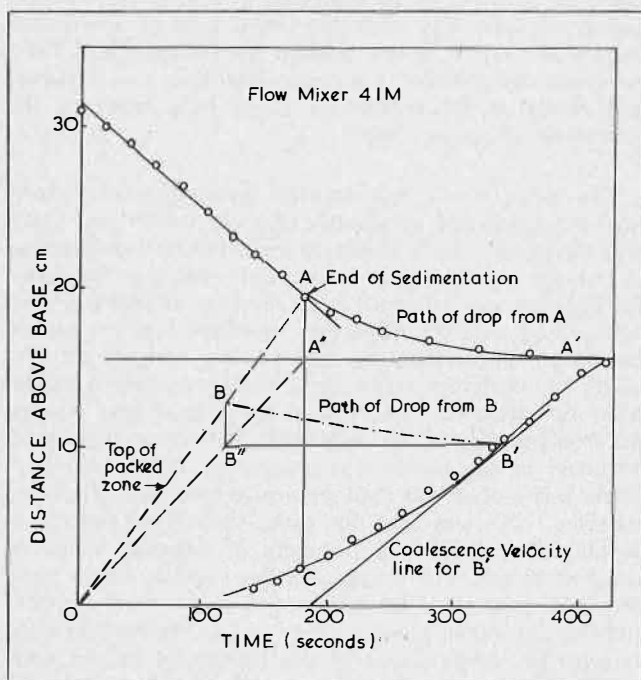


FIGURE 4. Graphical interpretation of separation data.

Interpretation of Results

During separation in a batch test it is considered that drops sediment and begin to form a packed bed of drops which coalesce with each other to form a quantity of bulk separated phase. Depending on the arrival rate of drops by sedimentation and the loss rate by coalescence with the bulk phase a packed bed will build up in thickness and then decrease in thickness when sedimentation has ceased⁽⁸⁾. Drops arriving at the surface of the packed zone travel through the dispersion, growing by interdroplet coalescence to a particular size at the coalescence front, which gives a certain coalescence velocity. The nature of the interdroplet coalescence process during this period or at the interface need not be defined.

It is assumed that sedimentation ends when the observed sedimentation velocity (the slope of the sedimentation lines) begins to decrease and that a packed zone builds up before substantial coalescence at the coalescence front occurs. In the absence of any substantial interface coalescence the height of the packed zone would increase linearly with time from zero thickness to a maximum when sedimentation ends. The height of the packed bed at any time is taken

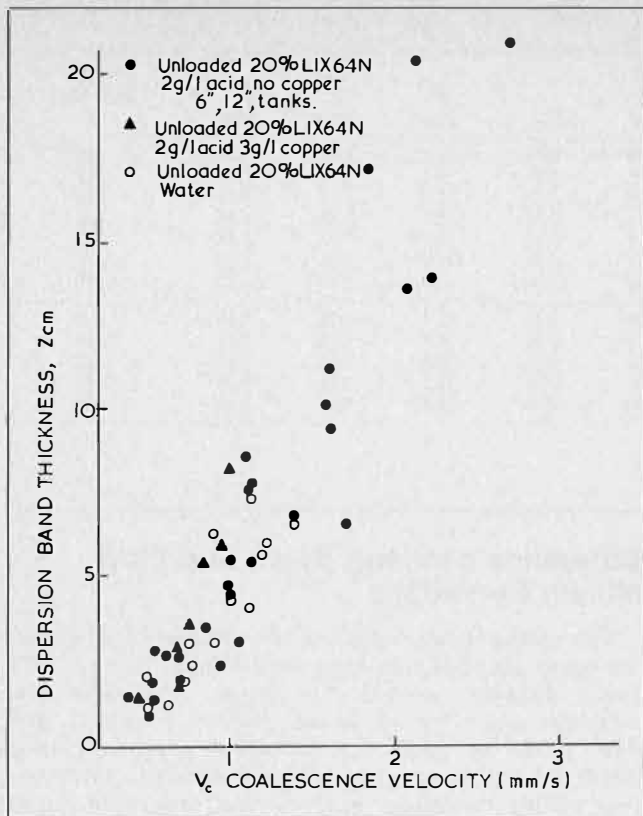


FIGURE 5. Settler performance predicted from batch data.

from the line joining the origin to the point on the sedimentation curve corresponding to the end of sedimentation.

The last drops to arrive at the top of the packed zone are assumed to be the last drops to arrive at the coalescence front. The average residence time of these drops in the packed zone is therefore taken to be the time difference given by the separation of points A (top of packed bed) and A' (coalescence front) shown in Figure 4. At any time the total volume of the packed zone will be larger than the volume of aqueous drops by an amount equal to the volume of organic phase held between drops. At the end of sedimentation the volume of packed bed present is given approximately by the point A but the volume of aqueous phase by the point A''. At any time before that corresponding to A'', the volume of aqueous phase in the packed bed may be estimated from the line joining the origin and A''. Thus for a drop at any point B, there will be a certain amount of downward movement, corresponding to the release of organic phase during the coalescence process, and the drop will move from level B to level B'' to meet the coalescence interface. During this process the coalescence interface rises to meet the drop at level B''. The time taken for the drop to move from point B on the top of the packed bed to point B'' at the coalescence interface is given by the time difference between B and B'. The coalescence velocity at B', V_c , can be related to this drop residence time, t_c .

In a dispersion band in a flow system the throughput of dispersed phase per unit horizontal area may be taken as the coalescence velocity V_c if the dispersion band is of even thickness. The residence time of drops in the band must be given by:

$$t_c = Zh_p/V_c$$

where Z is the band thickness and h_p is the average volume fraction of dispersed phase in the band. The true velocity

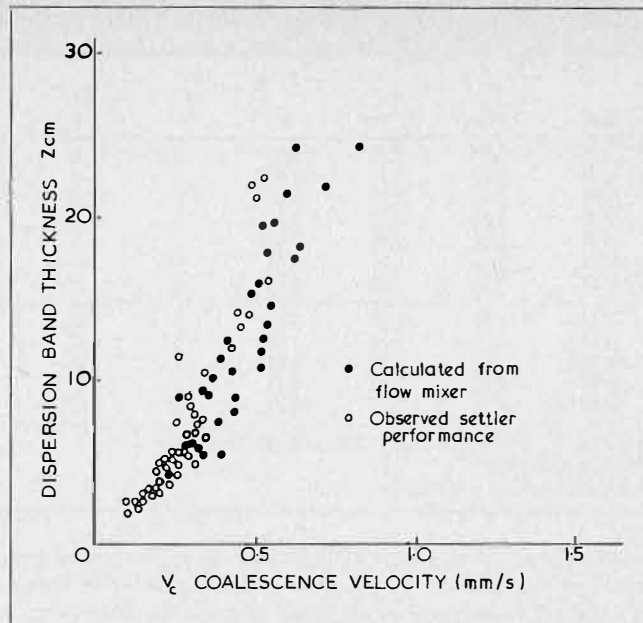


FIGURE 6. Settler performance predicted from flow data.

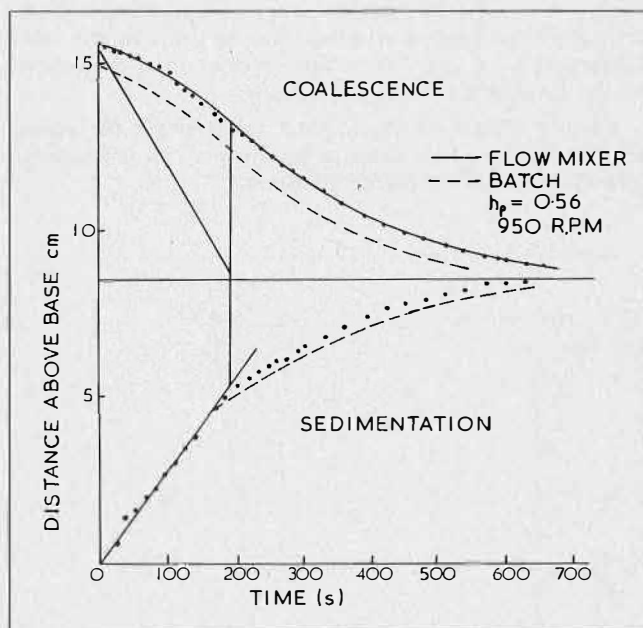


FIGURE 7. Separation data for kerosene/water.

of drops through the bed must be V_c/h_p at all levels for the sake of continuity of flow.

At any time during a batch separation test, the average volume fraction of dispersed phase in the dispersion band is easily calculated knowing the initial and separated volumes of each phase. Assuming that the dispersion band in the flow system is essentially in a packed state, calculation of the average hold-up from a batch test when sedimentation has just finished should furnish a reasonable estimate of h_p . In fact values of h_p calculated from batch data vary little after sedimentation has finished until complete separation has been achieved. On Figure 4 h_p is given by the ratio CA''/CA .

Using values of t_c , v_c and h_p from a batch test, values of Z may be calculated and plotted against V_c for comparison

TABLE 2. Flow Separation Data for LIX 64N Solvent

Run	F_e 1/min	F_A 1/min	h_A	d_i in	D_T in	N rpm	h_p	z mm	V_s mm/s	d mm	Primary break time s
17 M	0.45	0.45	0.59	2	6	660	0.74	19.4	0.68	0.25	300
19 M	0.45	0.45	0.50	2	6	660	0.88	19.8	1.09	0.23	360
21 M	0.56	0.56	0.50	2	6	840	0.72	20.0	0.62	0.17	280
27 M	0.78	0.33	0.31	2	6	840	0.71	19.4	1.12	0.14	360
29 M	0.66	0.46	0.45	2	6	840	0.68	19.5	0.91	0.18	349
36 M	0.66	0.46	0.45	2	6	840	0.69	19.0	0.94	0.18	328
37 M	0.50	0.50	0.50	2	6	840	0.77	17.0	0.71	0.18	285
40 M b	1.12	1.12	0.45	4	12	300	0.72	31.0	0.84	0.18	460
41 M b	0.70	0.70	0.50	4	12	300	0.78	30.8	0.69	0.18	412
46 M b	0.70	0.70	0.54	4	12	300	0.78	30.6	0.69	0.21	426
58 M b	1.20	1.20	0.48	4	12	300	0.75	30.9	0.71	0.18	480
52 M b	1.15	1.15	0.44	4	12	400	0.68	30.3	0.65	0.15	410

3 g/1 Cu, 2 g/1 H₂SO₄, unloaded 20% LIX 64N/Escaid 100
 Aqueous dispersed
 b Two side baffles, width 0.1 D_T

with data from the flow system. This procedure was carried out for the batch tank data and the plot of Z versus V_c shows consistency of the data (Figure 5). However, a very large discrepancy between the predicted and observed flow settler data is apparent by comparing with Figure 6. The procedure applied to mixer data from the flow system, in contrast, gives excellent agreement with the settler data (Figure 6). A limited number of tests with kerosene/water confirmed the method of calculation; in this case the batch separation time was only a little shorter than that shown by the flow mixer (Figures 7 and 8).

Further tests were carried out to ascertain the reason for the differing behaviour of the mixers run under batch and flow conditions before shut-down.

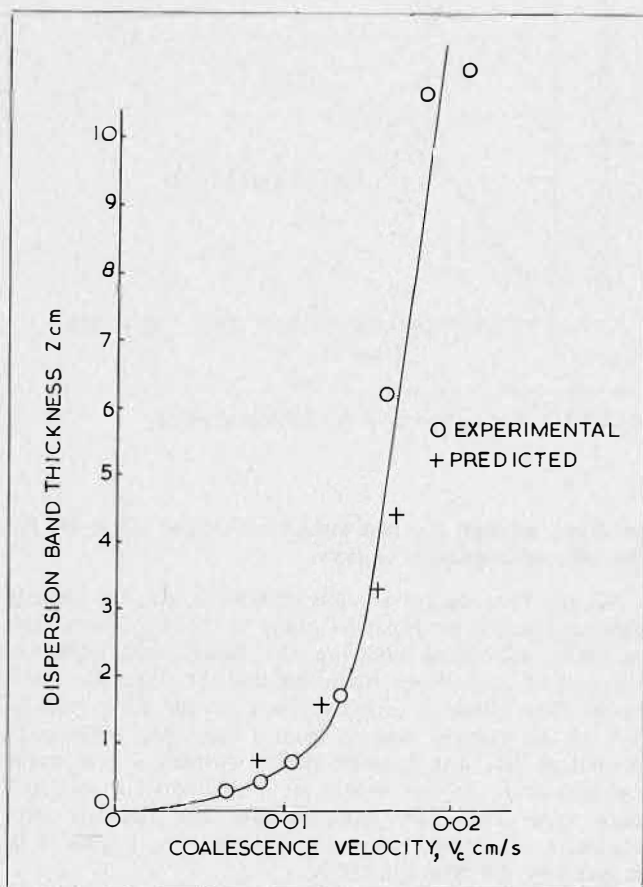


FIGURE 8. Settler performance prediction for kerosene/water.

Difference between Batch and Flow Mixing Conditions

The sedimentation velocities in separation tests carried out under all conditions were very similar. Using a technique described elsewhere⁽⁹⁾ average drop sizes were estimated and were all similar (Tables 1 and 2). Differences did not seem large enough to explain the large differences in coalescence velocities between batch and flow mixing conditions. The following tests were carried out:

- (a) the batch mixer was run for times from 0.5 to 40 minutes before shut-down with only small effect on sedimentation and coalescence velocities. Therefore, drops were probably not getting smaller with time, a possibility that might give longer break-times;
- (b) the flow system was operated with very low flow rates to simulate the non-flow batch mixer; mixer residence times of about 4 minutes were used but the running time before shut-down was much longer. No major effect on break-time was observed;
- (c) the flow system was operated for short times down to 1.0 minute before shut-down. In this case the coalescence process in the mixer was much faster at shorter times, approaching the results for a batch mixer, (Figure 9).

The conclusion from these tests is that the drop population produced during the first minute or so during batch and flow tests is different to that produced in the flow mixer over much longer running times.

Attention was turned then to the amount of haze produced in the phases after separation in the mixers. During batch tests with LIX 64N in Escaid 100 both phases were very cloudy on separation, regardless of the clarity of the phases initially. During flow tests, on shut-down after long periods of operation to reach a steady state in the settler, both phases were very clear on separation. However for short periods of operation haziness was substantial. For kerosene/water the water phase was always cloudy in both types of tests.

It therefore seems that the starting-up process of dispersing one bulk phase into the other produces haze which is associated with a rapid coalescence rate. In a batch process the haze does not escape the system and coalescence velocities remain high. In a flow system haze is generated during the start-up procedure but may be washed out of the mixer during the time required to reach steady conditions in the settler. The absence of haze is associated with a low coalescence velocity. Gel'perin⁽⁹⁾ has also noted this link.

It is conceivable that, if an increase in impeller speed leads to higher levels of entrainment, dispersion band thicknesses in a flow system may begin to decrease. Similarly, predictions of dispersion band characteristics from the fundamental principles of coalescence are unlikely to be successful if entrainment is present. Measurements of solvent haze content of the aqueous phase in the mixer after shut-down were carried out for different operating times in the flow system (Figure 10) and it is evident that this explanation is correct.

Although materials of construction were the same in all apparatus, the effect of wetting of the bottom surface of a 6-inch batch tank by aqueous drops was assessed briefly. No marked effect on break-time was found with Perspex, aluminium, mild-steel or stainless steel bottom plates wetted first with aqueous phase during tank filling.

In order, therefore, to obtain valid data from a simple apparatus for purposes of predicting dispersion band thickness as a function of flow rate and other operating conditions the following system is suggested. A mixing tank is required with an overflow system as proposed for a flow system. Storage tanks for the two phases holding a volume to give flow for ten residence times in the mixer are required. The flows from each storage tank should pass through rotameters to the mixer. The mixer is started up with the appropriate flows from the storage tanks and after several residence times of liquid in the mixer, the flows are shut off and the impeller stopped. The sedimentation and coalescence velocity data obtained can then be used to predict the behaviour of a settler. The same apparatus can be used for obtaining kinetic data valid for a flow system.

Conclusions

Separation tests conducted in batch mixing tanks are not generally valid in predicting the performance of a settler in a flow system because of differences in the amount of haze of very small drops in both phases between batch and flow conditions.

A simple method of interpretation of data from a mixer operated with flows through it, then shut-down, has been described and shown to be valid for the system tested in predicting the performance of a flow settler. Savings in time and test equipment costs can therefore be made.

Acknowledgements

This work was carried out as part of a contract with Nchanga Consolidated Copper Mines Ltd., Zambia, under the directorship of Professor C. Hanson. Mr. K. Rowley assisted with some of the experimental work.

NOMENCLATURE

d	= drop diameter mm
d_i	= impeller diameter inches
D_T	= tank size inches
F_A	= aqueous flow rate 1/min
F_s	= solvent flow rate 1/min
h_A	= aqueous hold-up
h_p	= volume fraction of dispersed phase in packed zone
N	= impeller speed rpm
t_c	= residence time of drops in the dispersion band s
V_c	= coalescence velocity mm/s
V_s	= sedimentation velocity mm/s
Z	= dispersion band thickness in a flow settler cm

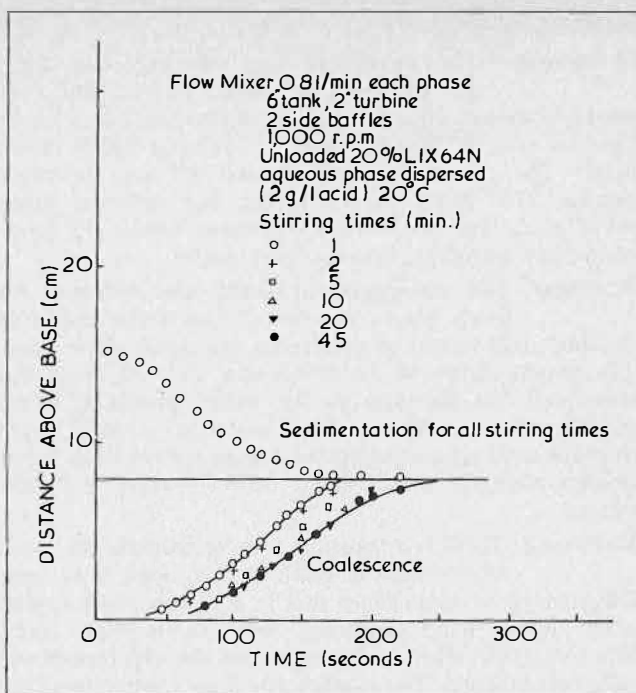


FIGURE 9. Effect of stirring time on coalescence rate.

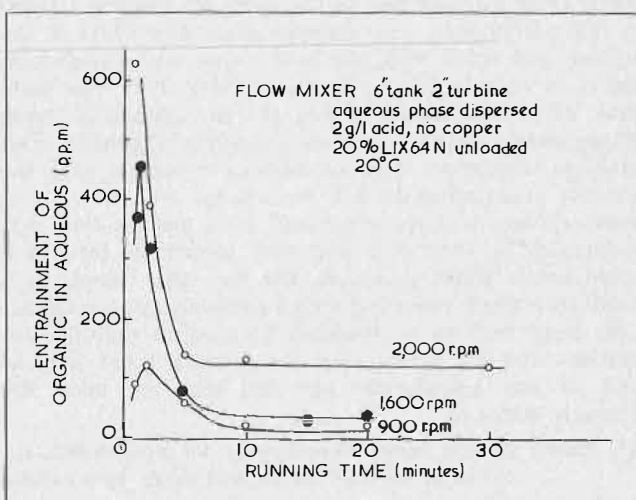


FIGURE 10. Entrainment levels as a function of operating time and impeller speed in the flow mixer.

REFERENCES

- (1) Holmes, J.A., Deuchar, A.D., Stewart, L.N. and Parker, J.D., "Extracting Metallurgy of Copper", Chapter 46, p. 907, A.I.M.E. Symp. Las Vegas, February 1976.
- (2) Ryon, A., Daley, F. and Lowrie, R., USAEC Report 2951 (1960).
- (3) Sweeney, W. and Wilke, C., UCRL Report 11182, (1964).
- (4) Stonner, H.M. and Wohler, F., I. Chem. E. Symp. Ser. No. 42, Manchester, April 1975, P. 14.1.
- (5) Holmes and Narver, Inc., "Some Ideas on Solvent Extraction", 1974.
- (6) Barnea, E. and Mizrahi, J., Tr. Inst. Chem. Eng. 1975, 53, (1), 61.
- (7) Godfrey, J.C. and Grilc, V., Second European Conference on Mixing, BHRA, March 1977, paper C1.
- (8) Assenov, A. and Slater M.J., Hydrometallurgy 1976, 2, 157.
- (9) Gel'perin, N.I., Pebalk, V.L. and Mishev, V.M., J. App. Chem. (USSR) 1972, 4, 58.

DISCUSSION

H. Stoenner: You mentioned that disengagement times are different for batch mixers and flow mixers after the halt of mixing (and flow) (3 times longer for flow mixers). Was this done on the same height conditions? The compared slides showed different interface heights. This could be interpreted that different phase ratios occur due to the flow conditions versus the batch conditions, assuming constant total height.

M. Slater: The disengagement times are different for batch mixers and flow mixers when compared at equal total height of dispersion and equal phase ratio. The graphs shown at the Conference did not show this adequately but the data in the Tables provided in the paper give more evidence. Small variations in total height or phase ratio have an effect on disengagement times much smaller than the effect noted between batch and flow mixers.

E. Barnea: There is a tendency to over-estimate the speed of processes in batch mixing. Some years ago, I discovered by coincidence that in a certain phase system under certain fixed conditions, spontaneous phase inversion took place after ± 20 minutes and the experiment was fully reproducible. This implies that it may sometimes take a very long time to establish a full equilibrium in batch mixing. The difference between batch and flow systems stems from the fact that in the latter the dispersed phase is fed continuously into existing dispersion while in the former, one starts with two bulk phases and a dispersion has to be established. At least for a very short time there may be a competition between the two dispersion types giving rise to the formation of a multiple dispersion. This multiple dispersion may be stable, in which case the amount of entrainment will not change with time or in other systems it may be released by a process that may sometimes be very slow and may sometimes lead to a spontaneous phase inversion. On the other hand, in a small flow mixer operating with a relatively large residence time there may be no tendency to produce multiple dispersions and the phases after the primary break may be free of any entrainment provided that the inlets are properly designed.

M. Slater: In our batch experiments we determined the effect of stirring for various times up to about

40 minutes and found that the amount of haze present did not change with mixing time nor did the sedimentation and coalescence characteristics. We have never observed a phase inversion after long stirring times. Our paper emphasizes the different nature of the dispersions produced in batch and flow experiments in terms of the haze generated by creation of multiple dispersions or otherwise, and shows the large effect of the presence of haze on coalescence rates.

D. Glasser: In your paper you compare two situations: one where the batch correlates well with a continuous settler; the other not. I suggest that this may be due to the fact that the mixing for the batch and that for the continuous situations were not necessarily comparable. If the steady-state drop-size distribution is rapidly attained, the output from the mixer will be the same for the batch and continuous settlers. If not, the feed to the batch will be a transient distribution of drop-sizes which could be very different from the steady-state fed to the continuous settler. In this latter case one would expect no simple correlation between the two situations. If one is to compare the batch with the continuous settler one must be sure that both have the same feed or make allowance for the fact that they do not.

M. Slater: Despite mixing in the batch tank for various times up to 40 minutes, we never created a batch dispersion which showed the low concentrations of haze observed in the flow mixer after shut-down. We were never able to create conditions in the batch mixer which gave long collapse times similar to those observed in the flow mixer except in the case of kerosine/water for which conditions in the flow mixer were always hazy, and for LIX64N at very short flow mixer running times. Particularly, we did not find clear liquids in our batch mixer on shut-down in any operating condition tried.

We feel, therefore, that our batch mixer had reached steady state and the problem was that the tiny droplets comprising the haze did not disappear by coalescence during batch mixing even at long times. In the flow mixer, haze created at start-up is swept out of the system. Since batch mixers cannot "a priori" be guaranteed to produce a dispersion similar to that experienced in a flow mixer because of the haze problem, then they should not be used to give data for prediction of flow settler performance.

Efficiency of Stabilized and Regenerated Fibrous Glass Coalescers

W.M. Langdon, T. Sumpatchalit, V. Sampath and D.T. Wasan,
Department of Chemical Engineering, Illinois Institute of
Technology, Chicago, U.S.A.

ABSTRACT

The performance of coalescers using fine fiber glass coalescer beds was studied with emulsions of kerosene and Mobil Oil Stock No. 141 dispersed in Chicago city water. The fibrous medium was $3.2 \mu\text{M}$ diameter fibers, treated under compression with isobutyl methacrylate resin, to form a rigid and stable structure. During coalescence of both oils a small percentage of the oil gradually collects in the fiber bed. After 3-5 hours over 5 ppm of secondary emulsion appears in the effluent. This spent coalescer can be repeatedly regenerated by steam treatment. The separation efficiency of individual sized drops showed a decrease at intermediate diameters between $2 \mu\text{M}$ to $8 \mu\text{M}$ at all cycle times for both kerosene and Mobil Oil. This efficiency continually decreases with increasing cycle time. Mobil Oil shows the greatest effect and after the 5 ppm break-through period the efficiency decreases substantially, showing that the coalescer is generating these intermediate sized drops.

Introduction

SECONDARY EMULSIONS are encountered in many industrial operations involving solvent extraction and recycle of process and cooling water. Environmental concerns have developed with respect to oil in ballast water from tankers and other ships. Rivers and lakes are often contaminated by accidental spills, leaks, and run-off water, not to mention the intentional dumping of waste material such as spent crank-case oil. When the dispersed phase consists of small drops, $10 \mu\text{M}$ or smaller, these can often be removed most economically and effectively by a fibrous bed coalescer.

Modern coalescers date from the filter/separators developed in the 1950's to remove water from aviation gas and jet fuel. Bitten⁽¹⁾, Sherony et al.⁽²⁾, and Langdon and Wasan⁽³⁾ have reviewed the literature to 1969, 1974 and 1976 respectively. The mechanism of the coalescer process has been modelled by numerous investigators^(4,5,6,7,8,9,10). These models are detailed by Sherony et al.⁽²⁾ They usually treat coalescence as a steady-state process. This is effectively true for water in jet fuel, where coalescer element life is usually limited by the pressure drop buildup due to dirt. These separators rarely see any water and then only for minutes. However, it has been observed⁽¹¹⁾ that recycling several per cent water in kerosene through a fiber glass coalescer for several months will result in a steady rise of the pressure drop of several psi. The element will usually start blowing "grapes", that is, drops of oil encased in a film of water and floating in the continuous oil phase. These "grapes" continually burst and put fine drops of water back in the effluent. The elements can be regenerated⁽¹¹⁾ by treatment with anhydrous methanol, care being taken to maintain the element flooded with liquid at all times.

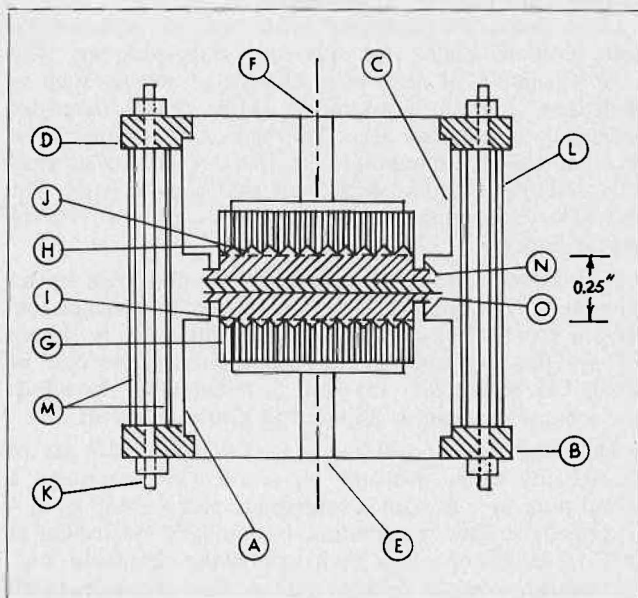


FIGURE 1. Coalescer cell by Sampath

- A End plate.
- B Clamping nuts.
- C End plate.
- D Clamping nuts.
- E Inlet or Outlet port.
- F Inlet or Outlet port.
- G Support plates, corrugated and drilled through.
- H Support plates, corrugated and drilled through.
- I Perforated brass plates, 30% open area.
- J Perforated brass plates, 30% open area.
- K Clamping rod.
- L Spacing collars.
- M Spacing collars.
- N Sealing lips.
- O Sealing lips.

Langdon et al.⁽¹²⁾ have reported on the pressure-drop increase over fibrous bed coalescers operating on oil and kerosene dispersed in water which is some hundredfold more pronounced than the case of water in oil. Shah et al.⁽¹³⁾ recently described the dependence of cycle life, the time when 5 ppm appears in the effluent, and the pressure-drop variation with velocity and time for fibrous bed coalescers operating on kerosene/water systems. Since these high-efficiency coalescers have such a limited life, techniques for stabilizing and regenerating the coalescer media after the breakthrough period were developed by Langdon et al.⁽¹⁴⁾ and Shah et al.⁽¹³⁾

Experimental

The coalescer cell used in this work is shown in Figure 1. It employs three layers of coarse/fine/coarse commercially available fiber glass which are compressed 18 times by means of filter press construction. The entrance and exit layers are each formed from 2 in. of (uncompressed) coarse glass, Owens-Corning "Aerocor" insulation PF3340,

nominal diameter 10.1 μm . The coalescing layer is formed from $\frac{1}{2}$ in. of (uncompressed) Owens-Corning grade FM-004, nominal diameter 3.2 μm . These 3 layers are compressed to an overall length of $\frac{1}{4}$ in. between support screens with an open area of at least 35%. The screens are supported on corrugated or grooved disks provided with drain holes. This cell differs from small coalescers used by previous investigators in that it does not employ precision-cut glass disks. The method of assembly, by allowing edge leakage to the outside, eliminates the possibility of leakage from the inlet to the outlet.

Glass fibers are stabilized with isobutyl methacrylate resin (DuPont Lucite 45). The fine glass pad, wet with a 10% solution of resin in a chlorinated solvent such as methylene chloride, is assembled in the cell as described above for unstabilized glass. However, excess liquid must be eliminated by discarding the first set of coarse glass pads and reassembling with fresh coarse glass pads. The resin is set by heating the assembly in an oven at 100°C for several hours.

A used coalescer with stabilized fiber glass can be regenerated by treatment with dry steam. The steam, expanded from 60 psi to atmospheric pressure, is passed through the cell assembly for 30 minutes in the case of Mobil Oil Stock No. 141 and 5 minutes for kerosene. The volume of steam is adjusted to give a plume of 2 ft.

The feed emulsion is made by circulating 50 gal of filtered city water, with 19 ml of oil added, through a stirred tank by means of a centrifugal pump (3450 rpm, 4 in. impeller). The temperature is manually controlled at 25°C by means of a heat exchanger in the circulation line. The emulsion passes through a 6 in. glass tee (presettler),

a flow meter, 2 back pressure regulators, and then through the coalescer cell. The pressure drop across the cell is measured by a mercury manometer every 15 minutes. The inlet differential volume per cent and differential ppm distribution is shown in Figure 2. for kerosene and Mobil Oil. The kerosene feed contains 36.8 ppm out of 90 entering with diameters under 10 μm and the differential curve peaks at 7 μm . Mobil Oil has 13.5 ppm out of 100 entering below 10 μm and the differential curve peaks at some diameter above 10 μm .

The samples, withdrawn before and after the cell, are allowed to stand 5 minutes and then removed from below the surface of the standing liquid. The turbidity measurement requires that the inlet sample be diluted 10 times. Both inlet and outlet samples in the amount of 1 liter are dispersed in a Waring blender for 5 minutes. The dispersed samples are allowed to stand 5 minutes during which time the temperature is adjusted to $25 \pm 1^\circ\text{C}$, and the turbidity measured in a Hach 2100A turbidity meter. A blank for the turbidity of the makeup water is subtracted from the preceding reading. The calibrations are for kerosene, 0 to 30 ppm, v/v,

$$C_T = (3.0) (\text{FTU}) \dots \dots \dots (1)$$

and for Mobil Oil, 0 to 10 ppm, v/v.

$$C_T = (1.7) (\text{FTU}) \dots \dots \dots (2)$$

where

C_I, C_O — Inlet and Outlet concentration, ppm (v/v)

FTU — Florizin turbidity unit.

The efficiency of separation for individual drop sizes is determined with a Coulter Counter, Model TA II. Using 150 ml of Isoton, a standard electrolyte solution obtained from the Coulter Co., after running a blank a count is taken of an added 5 ml sample of either inlet (undiluted) or outlet liquid which has stood for 5 minutes as described above for the turbidity measurement. The count is made on a volume of 0.05 ml in either time or manometer mode on the diameters 1 to 10 μm using the orifice with 32 μm diameter.

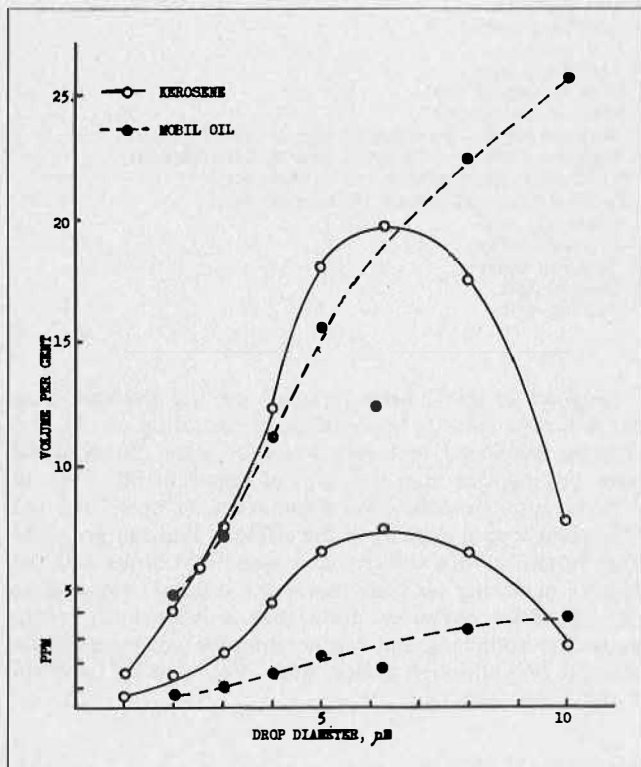


FIGURE 2. Inlet Feed Emulsions

$$\text{Kerosene } \sum_1^{10} C_i = 36.8 \text{ ppm, } C_T = 100 \text{ ppm}$$

$$\text{Mobil Oil } \sum_1^{10} C_i = 1.49 \text{ ppm, } C_T = 100 \text{ ppm}$$

TABLE 1. Specifications of Materials

Kerosene	(Government specification VVK-220)	
	Density	0.82 g/cm ³
	Viscosity	0.22 CP at 25°C
Mobil Oil	(Stock No. 141, solvent refined, paraffinic, neutral)	
	Density	0.86 g/cm ³
	Viscosity	26. CP at 25°C
Fine Fiber Glass	(Owens-Corning FM-004)	
	Mean fiber diameter	3.2 μm
	Commercial batts	
	Thickness	1/2 in.
	Weight	0.025 lb/ft ²
	Density	0.60 lb/ft ³
	Cell material (1 batt)	
	Compression	18X
	Length	0.028 in., 0.07/cm
	Void fraction, unstabilized	0.92
	Void fraction, stabilized	0.85
Coarse Fiber Glass	(Owens-Corning "Aerocor")	insulation, PF 3340
	Mean fiber diameter	10.1 μm
	Commercial batts	
	Thickness	1 in.
	Weight	0.025 lb/ft ²
	Density	0.60 lb/ft ³
	Cell material (4 batts, 2 front and back)	
	Compression	18X
	Overall length, including fine glass layer	0.25 in.

TABLE 2. Kerosene-Water System at Standard Run Conditions

Item	Type	C _{OT} at t _b /2 ppm	t _c Min	t _r t _c /300	ΔP, psi		Δ ² P / (Δt)(V) psi/ft		B _o × 10 ⁺⁹ cm ²		
					at t _o	at t _b	m _o (at t = 0)	m _c (at t _c)			
1a	UF	3.5	150	0.50	1.9	7.0	0.068	0.017	2.4		
2a	UF	2.5	165	0.55	0.29	6.6	0.039	0.023	16.2		
3a	UF	2	225	0.75	0.77	4.3	0.015	0.088	6.1		
4b	UF	3	110	0.37	1.3	8.2			0.032	0.088	3.7
5b	UF	1	110	0.37	0.84	7.9			0.040	0.090	5.6
				0.51					6.8		
6a	SF	3.5	330	1.10	0.83	5.9	0.019	0.008	5.6		
7b	SF	3	140	0.47	0.50	7.4	0.076	0.030	9.4		
8b	SF	3	140	0.47	1.46	9.1	0.080	0.030	3.2		
				0.68					6.1		
9a	SR1	3.5	315	1.05	0.96	8.0	0.027		4.9		
10a	SR2	2	(150)	(0.50)	1.54	7.2	(0.032)		3.1		
11a	SR3	3	300	1.0	1.16	5.5	0.015		4.0		
12a	SR4	2	315	1.05	1.5	7.2	0.016		3.1		
		2.6	310	1.03			0.019		3.8		

(a) Sampath⁽¹⁵⁾ (b) Sumpatchalit⁽¹⁶⁾

TABLE 3. Kerosene-Water System at Different Velocities

Item	Type	V ft/min	t _c min	t _r (t _c V) 300	ΔP psi		Δ ² P (Δt)(V) psi/ft at t _c	B _o × 10 ⁺⁹ cm ²
					at t _o	at t _b		
1a**	SR2	1.5	225	1.13	1.25	6.0	0.015	5.6
2a	SR1-4	1.0	310	1.03	—	—	0.019	3.8
3a	SF	0.45	588*	0.88	0.54	—	0.022	3.9
4a	SR1	0.45	601*	0.90	0.48	—	0.024	4.4
5a	SR5	0.22	1103*	0.81	0.23	—	0.028	4.5
6a	SR6	0.22	1060*	0.78	0.24	—		4.3
				0.93			0.022	4.4

*Extrapolated by a least squares straight line.

**Sampath¹⁵

Discussion of Results

The performance of coalescers using fine fiber glass was studied with kerosene and with Mobil Oil dispersed in Chicago city water. The fiber glass used was commercially available (UF, unstabilized fresh), and glass treated with isobutyl methacrylate resin (SF, stabilized fresh, and SR, stabilized and steam regenerated). The tests were made at 25°C with a nominal inlet concentration of 100 ppm (v/v) at superficial velocities for standard run conditions of 1 ft/min and some tests at 0.22, 0.45 and 1.5 ft/min. Representative inlet mass distribution curves for kerosene and Mobil Oil are shown in Figure 2. The measurements included the pressure drop across the bed and inlet and outlet oil concentrations both by turbidity and by the Coulter Counter, all as a function of run time. (Tables 2, 3 and 4). The separation efficiency of individual sizes as a function of diameter and cycle time are shown in Figures 3, and 4.

The cycle time is tabulated as, t_c, the breakthrough time where the effluent concentration reaches 5 ppm. The relative breakthrough time, t_r, is defined as:

$$t_r = t_c V/300, \dots \dots \dots (3)$$

where

- t_c = breakthrough time, min
- V = superficial velocity, ft/min
- 300 = nominal standard cycle time for stabilized glass at 1 ft/min velocity, min

The value of t_r for the kerosene/water system (Table 2) varied from 0.37 to 1.2. The average values at 1 ft/min for UF glass were 0.51 (Table 2 Nos. 1-5) and for SR glass 1.03 (Table 2 Nos. 5-8). The system, Mobil Oil/water, gave an average t_r of 0.875 for velocities of 1 ft/min (Table 4) and one run with UF glass gave the high value of 1.10. The wide variation in t_r for UF glass must be due to variations in the surface coating applied to the commercial glass. The stabilizing resin generally improves the coalescing performance of the glass. The lower t_r value with SR glass for Mobil Oil, 0.88, compared to that for kerosene, 1.03, may be due to either differences in the glass batches or the technique used in stabilizing the glass.

Tests with kerosene/water with both SR and SF glass at velocities varying from 0.22 to 1.4 ft/min gave an average value of 0.93 for t_r (Table 3). The relative breakthrough time appears to vary with the velocity to the 0.8 power.

The relative rate of pressure drop change, m, is defined as

$$m = \Delta^2P/\Delta t \dots \dots \dots (4)$$

where

- m_o, m_c = relative rate at time 0 and t_c, psi/ft
- ΔP = Pressure drop vs time at start and break-through, psi/min
- Δt = time increment, min
- V = superficial velocity, ft/min

The more important value is the slope, m_c , at the breakthrough time, t_c . It is seen that the overall average for m_c is close to 0.02 psi/ft for all of the runs (Tables 2, 3 and 4). Both kerosene and Mobil Oil show almost the same variation for the runs with t_c close to unity, namely 0.008 to 0.027 psi/ft for kerosene (Table 2 Nos. 6,9,11,12; Table 3 Nos. 1,2) and for Mobil Oil 0.016 to 0.030 (Table 4, Nos. 1,3,10). It should be noted that the lowest value for kerosene, 0.008, is approximately 1/2 the lowest values for Mobil Oil, 0.016 and 0.014. The value of 0.008 was previously reported by Shah et al.⁽¹³⁾ for both UF and SF glass with the kerosene/water system. In this work the UF glass with the same system does show the widest variations and the runs with the low t_c of 0.37 had the largest m_c , 0.09 psi/ft (Table 2 Nos. 4,5)

The initial slope, m_0 , for kerosene/water shows no consistency, being the same, larger, or smaller than m_c . However, except for the first run with UF glass, all runs with Mobil Oil/water shows an initial slope of 0.055 psi/ft.

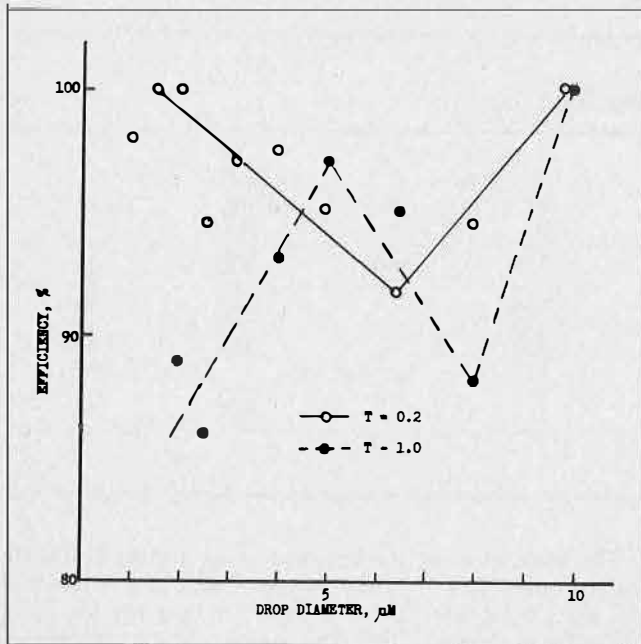


FIGURE 3. Kerosene-water. Particle size efficiency at $T = 0.2$ and 1.0.

This latter phenomena is what would be expected. The rate of oil accumulation, which is responsible for the change in pressure drop, should decrease as the amount of oil holdup increases.

The permeability of the fiber bed at the start of the run before the bed is contacted with oil, by Darcy's law, is

$$B_0 = \frac{X\mu_c}{\frac{\Delta P_0}{V}} \dots \dots \dots (5)$$

where

- B_0 = permeability, cm^2
- X = bed length, 0.71 cm
- μ_c = viscosity of continuous phase, 0.009 g/cm-sec
- ΔP_0 = pressure drop at zero time, dynes/cm²
- V = superficial velocity, cm/sec

The values of B_0 average near $4 \times 10^{-9} \text{ cm}^2$ but show wide variations from 1.2 to $16.2 \times 10^{-9} \text{ cm}^2$. The permeability values do not appear to be significant since values of 2.4 and 16.2×10^{-9} for UF glass with kerosene/water (Table 2 Nos. 1,2) gave approximately the same breakthrough times, 150 and 165 min, respectively. The variations may be partly due to the difficulty of eliminating oil from the system in the start-up period.

The separation efficiency for an individual drop size is defined as

$$E_i = \left(1 - \frac{n_i''}{n_i'} \right) 100 \dots \dots \dots (6)$$

where

- E_i = Efficiency of separation of drop size, D_i , per cent
- n_i', n_i'' = Number of drop size, D_i , in inlet and outlet respectively, per given volume

The results for kerosene and Mobil Oil are shown in Figures 3 and 4. Both systems show high efficiencies at drop sizes around $2 \mu\text{M}$ and over $8 \mu\text{M}$. For drop sizes below $1 \mu\text{M}$, noise in the Coulter Counter prevented definitive measurements. The decrease in efficiency for intermediate sized particles has been often noted in aerosol filtration. Kapoor⁽¹⁷⁾ summarizes this data and shows curves similar to Figure 3. Langmuir⁽¹⁸⁾ in 1942 postulated

TABLE 4. Mobil Oil-Water System at Standard Run Conditions

Item	Type	C_{OT} at $t_b/2$ ppm	t_c min	$\frac{t_c}{T_c V}$ 300	Δ psi		$\frac{\Delta^2 P}{\Delta t}$ (psi/ft)		$B_0 \times 10^9$ cm^2
					at t_c	at t_b	m_0 (at $t=0$)	m_c (at t_c)	
1c*	UF	0.5	330	1.10	1.25	11.3	0.030		3.7
2b**	SF	4	258	0.86	0.50	7.3	0.050	0.024	4.5
3b	SF	2	299	1.00	1.46	9.1	0.056	0.024	5.4
4b	SF	2	227	0.76	0.84	8.6	0.058	0.024	2.1
5b	SF	2.5	268	0.89	1.04	9.1	0.058	0.027	3.8
			263	0.88			0.055	0.024	4.0
Stop/start operation									
6b	SR1	3	270	0.90	0.87	6.6	0.053	0.021	1.3
7	SR2	3	220	0.73	3.5	11.0	0.057	0.027	1.2
8	SR1	2	235	0.78	3.76	12.1	0.056	0.024	1.3
9	SR1	3	235	0.78	2.22	11.3	0.058	0.027	1.7
10	SR2	2.5	320	1.06	3.47	10.9	0.052	0.016	1.6
11	SR3	2	280	0.93	1.22	12.1	0.052	0.014	1.6
			260	0.87			0.055	0.022	1.5

*c refers to special project, summer of 1976 at IIT by John McNamara
 **Sumpatchalit¹⁶

that the intermediate particles should show a lower separation efficiency than smaller sizes when their size interferes with the attraction or diffusion mechanism which prevails for the smaller sizes. Additionally, their intermediate size interferes with the sieving action which prevails for the larger sizes. The curve of efficiency vs particle diameter for kerosene shows several dips between 2 and 4 μM for which there is no obvious explanation. The curves for Mobil Oil show only one dip in efficiency above 2 μM . The efficiency decreases for Mobil Oil are also manifold-greater than those for kerosene, and the decrease becomes more pronounced as the cycle time approaches and passes the breakthrough point. When T equals 1.32, the efficiency values dip to -254% indicating that the coalescer is generating small particles. It is probable that the dips at low cycle times are also due to particle generation rather than inefficient coalescence. Bitten⁽¹⁾ has shown for the system, water/jet fuel, that the concentration of dispersed phase at the inlet face of the coalescer bed rapidly reaches 70% saturation or more. Calculated distances⁽³⁾ for this saturation are in the order of 4 μM . Consequently, due to the high local velocities, small particles can be torn from coalesced films. It is equally possible that the drops being forced through the small clearance undergo some degree of rupture.

Conclusions

The relative breakthrough time for stabilized fiber glass with kerosene/water was 1.03 and with Mobil Oil/water was 0.88. The stabilizing resin generally improves the performance of the fiber glass. The relative breakthrough time appears to vary with the velocity to the 0.8 power.

The relative rate of pressure drop change at the breakthrough time averaged 0.02 psi/ft for both kerosene and Mobil Oil systems. However, the lowest value for runs with t_r near 1 for kerosene was half of the lowest value for Mobil Oil. The initial permeability of the fiber bed shows wide variations and does not seem to be related to the rate of pressure drop change or breakthrough time.

The efficiency of separation of individual sized drop usually showed a decrease at intermediate diameters between 2 to 8 μM at all cycle times for both kerosene and Mobil Oil and the efficiency decreases with increasing time. With Mobil Oil past the breakthrough, the efficiency goes from -150 to -240% showing that the coalescer is generating the intermediate sized drops.

NOTATION

B_0	= Permeability of bed for single phase flow at zero time, Eq. 5, m^2/cm^2
C	= Concentration of dispersed phase, C^i inlet, C^o outlet, C_T by turbidity, C_c by Coulter Counter, ppm, v/v
cp	= Viscosity unit, centipoise, 0.01 g/cm-sec
D	= Drop size, μM
E_i	= Efficiency of separation of individual drops with diameter, D_i , %
m	= Relative rate of pressure drop change, m_0 at zero time, m_b at breakthrough, psi/ft
n_i	= Number of drops with diameter, D_i , in 1 cm^3 of undiluted sample, count times 600, cm^{-3}
ΔP	= Pressure drop across cell, in Eq. 4, psi, in Eq. 5, dynes/ cm^2
ppm	= Concentration unit, parts per million, volume/volume
psi	= Pressure unit, pounds (force)/ in^2
SF	= Stabilized fresh fiber glass
SR	= Stabilized and steam regenerated fiber glass
t	= Elapsed cycle time, t_c , and t_b at breakthrough, min; t_r relative breakthrough time, Eqn. 3.
Δt	= Time increment, Eq. 4, min
T	= Fraction time to breakthrough, t_c/t_b
UF	= Unstabilized fresh fiber glass
V	= Superficial velocity through cell, ft/min, in Eq. 5, cm/sec .

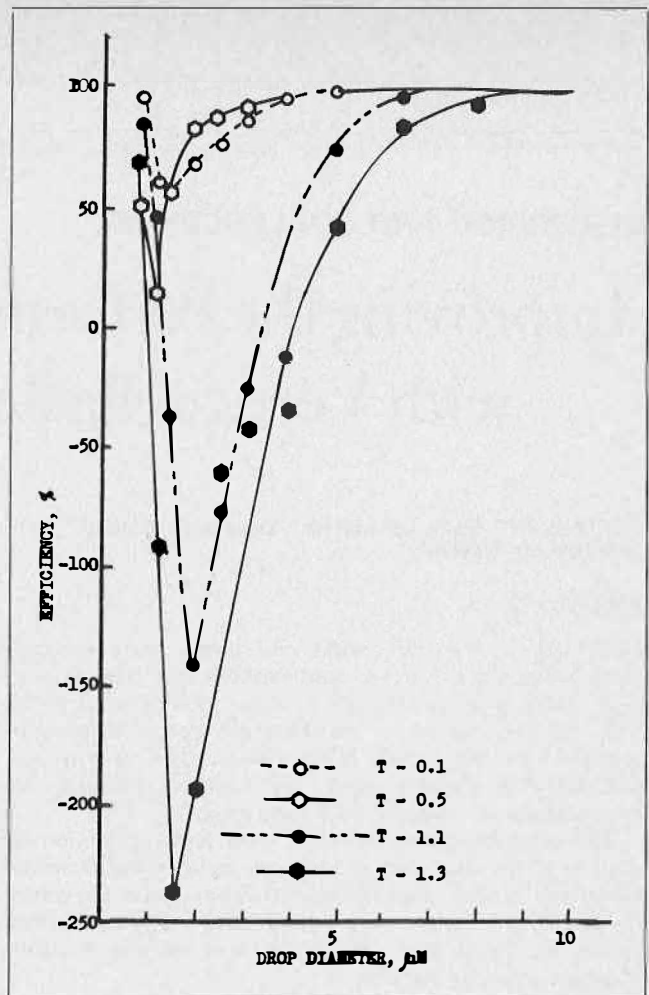


FIGURE 4. Mobil Oil-water. Particle size efficiency at $T = 0.11$ to 1.32.

- x = Length of fine glass coalescing bed, 0.028 in., in Eq. 5' 0.071 cm.
 μ = Viscosity, in Eq. 5 for water at 25°C, 0.009 g/cm-sec length
 μM = Micron, 10^{-6}M

REFERENCES

- (1) Bitten, J.F. and Fochtman, E.G., *J. of Colloid Interface Sci.* 1971, 37, 312.
- (2) Sherony, D.F., Kintner, R.C. and Wasan, D.T., *Surface and Colloid Science*, in press, Plenum Press, 1977.
- (3) Langdon, W.M. and Wasan, D.T., *Recent Developments in Separation Science*, Volume IV, CRC Press, in press (1977).
- (4) Farley, R. and Valentin, F.H.H., *Advances in Separation Science A.I.Ch.E. — I.Ch.E. Symp. Series No. 1*, (London Inst. Chem. Eng.) 1 (1965).
- (5) Vinson, C.G. Jr and Churchill, S.W., *Chem. Eng. J.* 1970, 1, 110.
- (6) Spielman, L.A. and Goren, S.L., *Environ. Sci. Tech.* 1968, 2, 279.
- (7) Davies, G.A. and Jeffries, G.V., *Filt. and Sep.* 1969, 6, 349.
- (8) Hazlett, R.N., *Ind. Eng. Chem. Fund.* 1969, 8, 625.
- (9) Sherony, D.F. and Kintner, R.C., *Can. J. Chem. Eng.* 1971, 49, 314.
- (10) Rosenfeld, J.I. and Wasan, D.T., *Can. J. Chem. Eng.* 1974, 3, 19 Feb.
- (11) Langdon, W.M., Report No. ARF (now IIT research Inst.) 3169-11 Jan. (1961).
- (12) Langdon, W.M., Naik, P.P. and Wasan, D.T., *Environ., Sci. Tech.* 1972, 6, 905.
- (13) Shah, B.S., Langdon, W.M. and Wasan, D.T., *Environ. Sci. Tech.* 1977, 11, 167.

- (14) Langdon, W.M., Naik, B.S. and Wasan, D.T., Water Pollution Control Research Series, 12050 EPA Report, Nov. 1971.
- (15) Sampath, V., M.S. Thesis, Illinois Institute of Technology, May 1976.
- (16) Sumpatchalit, T., M.S. Thesis, Illinois Institute of Technology, May 1977.
- (17) Kapoor, J.C., Subramanian, K.G and Khan, A.A., Filt. and Sep. 1977, 14, 133.
- (18) Langmuir, I., OSRD-865, 1942.

DISPERSION AND COALESCENCE

Improving the Performance of Gravity Settlers with Vertical Baffles and Picket Fences

John Roberts*, Keith Lyne-Smith*, Douglas E. Collier**, and Jennifer McGee***

ABSTRACT

Picket fences, vertical baffles and plane gauze internals were compared in various combinations and relative positions within a small laboratory settler by measuring emulsion volume and phase entrainments, for a number of specific flow rates and N^3D^2 values. The system was ESCAID-100, disperse phase, and aqueous acidified copper sulphate, at constant O/A ratio of 1:1.

The most important internals were picket fence arrays directly at the inlet and at least one vertical baffle within the settler length. Further improvement could be gained by installing a single or a tiered compartmental vertical baffle, the latter with through-the-wall orifices to allow drainage of separated phases.

Batch-mix runs show inter-related cyclic variation in primary break time, crud growth and spectroscopic absorption of the ESCAID.

Introduction

ALTHOUGH DESIGN INFORMATION for pump-mix mixer-settlers is now becoming available through international publications^(1,2,3), it is still necessary to carry out pilot plant evaluation and testing for new solvent-diluent extraction processes⁽⁴⁾. Recent investigations into mixer inlet configurations and impeller geometry has to some extent shifted the "unknown" elements in design-scale-up from the mixer to the settler⁽⁵⁾.

As many publications note, the throughput limitation in the settler is usually imposed by the rate of coalescence of the dispersed phase. In large pilot plants units and full-scale operating plants, the dispersed phase flows into the settler as an emulsion band approximately a rectangular prism in shape and not a wedge as used in small research type investigations^(1,3,4). This band covers the whole of the active region within the confined coalescing volume.

It is the thickness of this emulsion band which then characterizes and controls the flow rates of both phases into and out of the settler. The emulsion band should be relatively thick to collect and aid coalescence of tiny secondary droplets, but not too deep to cause emulsion over-

flow problems if process conditions are changed.

With capital cost incentives towards more compact designs, higher throughputs in terms of flow capacity per unit active interface area are now being contemplated⁽⁶⁾. However, for a given settler and internals, the thickness of the band increases approximately exponentially with increase in flow rate^(7,8,9). This results in a maximum flow capacity above which quite small changes lead to flooding.

A factor of safety and/or increase in throughput can be achieved by some practical means of enhancing droplet coalescence rate and liquid drainage out of the emulsion band.

Picket fences⁽¹⁰⁾ or baffles at the inlet to the settler reduce entry disturbance⁽²⁾, while short vertical, horizontal baffle or mesh bundle assemblies spaced along the settler length are thought to promote coalescence and reduce turbulent eddies⁽³⁾. These combined internals tend to maintain laminar velocities along the settler and help to minimise entrainment of tiny droplets⁽¹¹⁾.

Settler Inlet Arrangements

Little detailed information is available on the real cause-and-effect of particular inlet configurations. The oldest types of mixer-settlers had antechambers and simple port inlets at approximately the static interface level. American and U.K. Atomic Energy Authorities followed this design and included vertical curved louvres placed across an inlet rectangular slot⁽¹²⁾. In some large full-scale hydrometallurgical extraction plants, the inlet distribution has become a diverging rectangular duct⁽¹³⁾ leading into a picket fence diffuser. Smaller semi-commercial mixer-settlers have followed these design principles but included an impingement baffle⁽¹⁴⁾ immediately after entry to the settler to reduce jetting of the incoming emulsion stream into the coalescing region.

Israeli research has been quite specific in detailing the location of the settler inlet in stating that this should be at the boundary between the dense and even concentration layers in the emulsion band⁽¹⁵⁾.

Coalescent Aids Within the Settler

Over the past few years a variety of patents have been awarded for promoting or enhancing coalescence within the settler. Examples are: — vertical baffles with attachments⁽¹⁶⁾, vertical baffles with horizontal slots⁽¹⁷⁾, horizontal or inclined tray assemblies⁽¹⁾, suspended cages of random packing⁽⁸⁾, or wire gauze bundles⁽¹⁾. Each of these basically has a primary function, the development of a deep

*Senior Lecturer in Chemical Engineering, University of Newcastle, N.S.W. Australia.

**Metallurgist, King Island Scheelite, Tasmania, Australia.

***Technical Officer in Chemical Engineering, University of Newcastle, N.S.W. Australia.

shortlength emulsion bed and provision for favourable conditions for coalescence and drainage. Coupled with this gain is considerably increased throughput.

This greater settler compactness is to be offset against any operational difficulty in cleaning "third-phase" build-up from within the assembly. Increased entrainment resulting from secondary droplet formation produced by the rapid coalescence at preferentially wetted surfaces⁽¹⁸⁾ or carryover of tiny droplets and emulsion within up-or-down flowing homophase drainage holes is a severe limitation. The Israelis⁽¹⁹⁾ again have led the research into measurements of density profiles^(20,21) throughout the emulsion volume and in highlighting performance characteristics of compartmental baffles.

A realisation and subsequent determination of velocity profiles^(3,7) along the settler has led to the introduction of patented baffle attachment configurations^(16,17). These appendages are said to reduce (a) shear and, therefore, some secondary droplet formation at the upper and lower emulsion band boundaries and (b) turbulent eddies which would otherwise promote entrainment.

In summary then, there have been only a few publications in which the authors have quantitatively compared changes in emulsion bed volume with alterations of settler internals, especially compartmental baffles^(1,13,16,17).

This study has attempted to assess the effect of combinations of picket fences, vertical baffles and baffles with simple attachments on emulsion volume, density and entrainments. These measurements have generally been made for a number of equal phase flowrates and impeller speed (N^3D^2).

Experimental

The Apparatus

The mixer-settler equipment is shown in Figure 1. The cylindrical mixing tank and rectangular settling tank were constructed from transparent acrylic, and the single stage was close-circuited by rigid PVC piping. The dimensions of the equipment components are given in the figure.

The mixer was fitted with four standard tank wall baffles at regular 90° spacings around the inside of the tank. The two phases were introduced into the mixer via a common t-section draught tube directly beneath the eye of the impeller. The impeller had the dual function of both pump and mixer and was a top-shrouded low-shear turbine agitator with the blades inclined back from the radial position. It was operated with a low clearance from the tank bottom to prevent recirculation within the mixing tank.

The agitator shaft was driven by a 0.19 kW variable speed motor via v-belt driven pulleys to give the desired range of power inputs to the mixer. A photocell tachometer was sighted on the agitator shaft pulley, and the impeller speed displayed on a Hewlett Packard universal counter display. The mixer was operated at a power input represented by an N^3D^2 in the range 6-90, where N = rotational speed of impeller (sec^{-1}), D = impeller diameter (ft).

A value of 30 for N^3D^2 is close to a practical value where mass transfer is attained without severe secondary haze formation, and corresponds to a Reynolds number of 1.17×10^5 , which is greater than the recommended minimum value of 10^4 for 'complete' mixing.

The emulsion overflowed from the mixer across a diverging rectangular duct into the settler. The picket fences used extended the full depth of the settler. The level of the O/A interface in the settler was controlled at 250 mm by means of an adjustable overflow aqueous weir. The organic

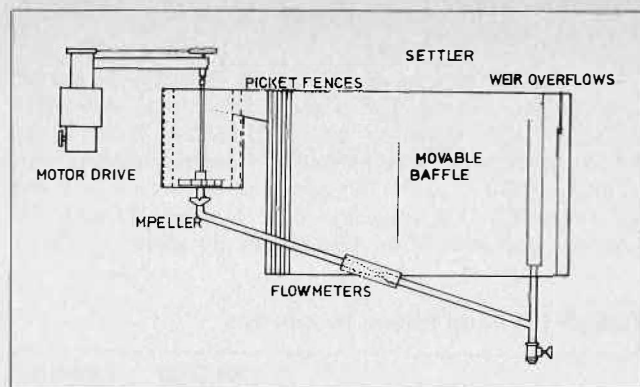


FIGURE 1. Pump-mix mixer settler apparatus.

Apparatus dimensions

Mixer Tank: i.d. 265 mm, height: 245 mm to overflow lip, 26 mm tank wall baffles with 10 mm gap between baffle and tank wall.

Pump-mix impeller: o.d. 150 mm, clearance ~ 2 mm from bottom of tank.

Settler: 853 mm length corresp. to total available settling area of 0.216 m^2 (2.32 ft^2).

575 mm height to top of organic phase overflow weir. 253 mm width.

Picket fence baffles: Each set comprises 3 rows of 50 mm wide x 6 mm thick slats spaced at 10 mm. Each row is spaced 6 mm from next row and slats are staggered from row to row.

Vertical dam baffle: 400 mm deep flat perspex sheet.

Heating device: Two Electrothermal Red Rod 0.5 kw immersion heaters, thermostatically controlled to maintain temperature of aqueous phase at $25 \pm 0.5^\circ\text{C}$.

Cooling device: 3.65 m long 15 mm o.d. copper coil, with water from thermostatically controlled water bath circulating through it. Ice is added to the bath when necessary. Insufficient ice was available on very hot days.

phase flowed over a fixed outlet weir. Measurements were usually made over one square foot (0.093 m^2) of settling area by inserting a vertical dam baffle 370 mm from the entrance to the settler. The baffle was loose-fitting and allowed some crud drainage between the baffle and the tank walls into the quiescent area of the settler. The range of flow rates used was from 6-18 l/min in each phase which corresponded to specific settling rates of from 1.3 to 4.0 $\text{gal}(\text{imp})/\text{ft}^2\cdot\text{min}$ (3.8 to $11.7 \text{ m}^3/\text{m}^2\cdot\text{h}$). A practical value for LIX/Cu systems is 2 $\text{gal}(\text{U.S.})/\text{ft}^2\cdot\text{min}$ ($4.9 \text{ m}^3/\text{m}^2\cdot\text{h}$) total. The O/A ratio was kept constant at (1:1) throughout the entire investigation. The flow rates were controlled by Asahi ball valves to within $\pm 1\%$. They were measured using calibrated venturi meters formed from epoxy resin, and pressure tapings connected to open-ended manometers. Venturis were chosen as they offer least resistance to the pumping head developed by the mixer impeller.

A constant temperature of 25°C was chosen as most practicable, in order to eliminate temperature as a variable. If the ambient was less than 25°C , the system was maintained at temperature by thermostatically controlling the temperature of the aqueous phase using immersion heaters in the aqueous phase weir box. If the ambient was greater than 25°C , the system temperature was maintained by means of a copper coil heat exchanger located in the organic phase weir box. On very hot days (ambient $\geq 34^\circ\text{C}$) insufficient cooling was available for the system. The system took 1-2 hr to reach a steady temperature, depending on the ambient. The temperature was monitored in the mixer, and near the organic overflow weir.

The System

The equipment was operated with 70% each of organic and aqueous phases. The organic phase used was ESSO ESCAID 100. Available specifications are listed below. The aqueous phase was an acidified copper sulphate solution (2g CuSO₄/l or ~ 780 ppm Cu in towns water) with pH adjusted to 1.5 using 0.15% V/V sulphuric acid. The physical properties of the two phases are given in Table 1.

TABLE 1. Liquid Phase Properties

	ESCAID 100	AQUEOUS
Density g/cm ³ (25°C)	0.790	1.004
Viscosity cp (25°C)	1.52	0.96
Surface Tension dyne/cm (25°C) (after equilibration)	22.3	61.2
Flash point	76 C	
Initial boiling point	191 C	
50% Recovery point	203 C	
Dry point	225 C	

Standard component analysis: 56.6% paraffins, 23.4% naphthenes, 20% aromatics.

Run Procedure

The experiments were made with an oil-in-water emulsion, since much deeper dispersion beds were obtained with this type of emulsion. The phase ratio was kept constant at 1:1. Starting up with both phases going into the mixer produced a stable O/W dispersion. To obtain a W/O dispersion, start-up procedure was to allow only kerosene in the mixer, and then gradually build up the aqueous phase flow. The W/O emulsion showed no sign of inversion over short periods.

Equilibrium was reached in about 4 hours, and while the emulsion bed height changed over a period of time, in any one day's operation, after equilibrium had been reached the bed height would only fluctuate by about 5-10 mm.

The formation of crud in the system appeared to be a continuous process, but when working over one square foot of surface, the end dam baffle allowed continuous leakage of the crud (and a very small amount of emulsion) into the static interface of the tank. The crud was periodically removed from this region by syphoning.

Results of Various Internals Combinations

Initial experiments were carried out on the mixer-settler to evaluate the effect of different types of baffling arrangements on the coalescence rate and carry-over of tiny droplets. A qualitative picture was developed of the improvements that can be made using flat vertical baffles, picket fences, or a plane gauze in the system.

The different types of baffling arrangements used to contact and contain the emulsion band were:

- (1) Unbaffled tank: Emulsion flows across full width of settler, if necessary to end of settler. Settler is flooded if emulsion overflows into offtake ports.
- (2) Baffle at inlet to settler: With depth $\frac{2}{3}$ down from top surface: affects distribution into settler.
- (3) Flat baffles: Submerged depth $\frac{1}{2}$ of total, centred about the static interface; contains emulsion within a certain length of tank.
- (4) Knife-edge baffle: Similar depth to flat baffle; more

surface contact with emulsion than flat baffle: contains emulsion in certain length of tank.

(5) Picket fence baffles: Covers whole depth of tank; distributes flow of emulsion across tank; constrains flow of emulsion through set spaces, hence affects movement of emulsion: more flat surface contact.

(6) Wire gauze insert: larger emulsion-bulk phase surface area: flow distribution across tank.

From this it was possible to see the effect on the emulsion band of:

(i) Picket fences — one, two or three (a) close packed (b) spaced — different spacing between fences compared with (a) unbaffled tank (b) spaced flat baffles.

(ii) Knife-edge baffle compared with a single flat baffle at same distance from inlet.

(iii) Baffle at inlet to settler (a) flat baffle directly at inlet (b) picket fence directly at inlet compared with — no baffle directly at settler inlet.

Entrainment measurements on the unbaffled tank were made and these figures were compared with results for flat vertical baffles, or a series of picket fences at the settler inlet and then an added flat vertical baffle spaced after the picket fences. In all these cases an initial fence was placed at the settler inlet. The measurements were also carried out at two different pH's, pH 1.5 and pH 7.

A few runs were carried out using a plane wire gauze insert with 2 mm square holes, after the initial picket fence, and with or without a flat vertical baffle in the system.

For runs observing emulsion volume only, the power input corresponded to $N^3D^2 = 19$ (1.8) for flows 6l/min each of organic and aqueous phases, corresponding to a specific settling rate of 1 gal/ft².min (2.93 m³/m².h). ESCAID was the dispersed phase. The second set of runs compared emulsion volumes and entrainments at pH 1.5 and pH 7.0. Specific settling rates were 1.5 — 2 gal/ft².min (4.4-5.9 m³/m².h) and power inputs corresponding to N^3D^2 6, 19, 46, 90, (0.56, 1.8, 4.3, 8.4). Entrainment in the organic phase was generally less than 5-10 ppm.

The findings from these preliminary investigations are summarised below and in Table 2. One or a number of picket fences, immediately at the inlet distribution generally gives less emulsion volume and with increase in number of fence arrays, reduced entrainment.

Particular Settler Internals and Entrainment in Aqueous Phase (pH 1.5 and 2.0 gal/ft² min flow rates each phase.)

Code in Table 2.

A	1 picket fence at inlet	... 440-450 ppm
B	2 picket fences close packed at inlet	... 300-350 ppm
C	3 equally spaced picket fences along length of settler	
D	As C... with a flat baffle at inlet down to $\frac{3}{4}$ depth	... 275-325 ppm
E	1 picket fence at inlet and 2 fences equally spaced along active length of settler (N.E.)	
F	3 fences at inlet ... 2.5 cm apart (N.E.)	
G	3 fences at inlet close packed	... 175-225 ppm
H	1 picket fence at inlet and a knife-edged vertical baffle (N.E.)	
I	1 picket fence and a wire gauze baffle	... 175-225 ppm
J	No internals	... 500-700 ppm
K	2 vertical baffles equally spaced along active length of settler	... 150-250 ppm

Note: The flow of combined phases is considered to be contained within one square foot of active emulsion volume held between inlet and last baffle prior to the settler exit weirs.

Entrainment samples were siphoned from 2 cm. above or below the last vertical baffle. Samples were centrifuged for 15 minutes at 3500 rpm in a Clements GS100 laboratory centrifuge. The length of phase slug in the sample bottle capillary directly gave entrainment concentration.

TABLE 2. Comparison of Particular Internals with 1 or 2 Picket Fence Arrays

Code	Factor Reduction in Emulsion Volume or Entrainment			
	In comparison with 1 picket fence		2 picket fences	
	Bed Volume	Entrainment	Bed Volume	Entrainment
B	0.83	0.77	—	—
C	1.2	—	1.5	—
D	1.1	0.71	1.4	0.91
E	0.91	—	1.1	—
F	0.77	—	0.91	—
G	0.63	0.48	0.77	0.63
H	0.91	—	1.0	—
I	0.40	0.48	0.48	0.63
J	9.1	1.4	10	1.5
K	2.5	0.48	3.0	0.63

Note: Factors less than unity are decreased emulsion volume and decreased entrainment.

The only improvement upon picket fence arrays may be a knife-edged vertical exit baffle or a plane wire gauze exit baffle. If the first picket fence is placed at any location other than immediately after the inlet distributor (i) greatly pronounced turbulent eddies result, (ii) considerable recirculation velocities develop in both phases, and (iii) gross entrainment of secondary droplets occur in both phases.

A general variation of emulsion volume and entrainment with change in numbers of picket fence arrays, N^3D^2 and flow rates is shown in Figures 2 and 3, with arrays close-packed at inlet.

One flat vertical baffle placed immediately after the inlet distributor forces all emulsion to flow downwards. In theory, emulsion then moves into the centre band region of the coalescing dispersion. However, at flow rates greater than about 1.5 gal/ft² min (4.4 m³/m².h) turbulent recirculating eddies are produced in the volume below the aqueous boundary of the dispersion. Emulsion bursts down through the band, violently disturbing the lower boundary, causing enhanced organic entrainment and a short-circuiting velocity along the bottom of the settler.

There is some justification for a number of short vertical baffles placed so that no underflow from any one occurs, and spaced equally or otherwise along the settler length to completely contain the emulsion volume. These short baffles stop the direct forward motion of stratified velocity streams and helps to reduce turbulent eddies within the emulsion volume. Coalescence of the disperse phase is thought to be enhanced together with reduced entrainment in both organic and aqueous phases.

Wire gauze promotes coalescence and greatly reduces emulsion volume. One plane gauze baffle can allow a settler to operate at about 1½ times the flow rates of one without any other coalescence aids or baffles. However, at higher flow rates, many tiny secondary droplets are generated with considerably greater entrainment in the organic phase at the gauze interface. These are swept out the overflow weir.

Effect of pH7 on Emulsion Volume and Entrainment

The aqueous phase was milky to opaque and it was impossible to identify the lower boundary of emulsion. It would seem though, that the total emulsion volume contained within the settler was at least as much for any baffle or picket fence arrangement when operating at pH 1.5. With one picket fence or other simple baffle

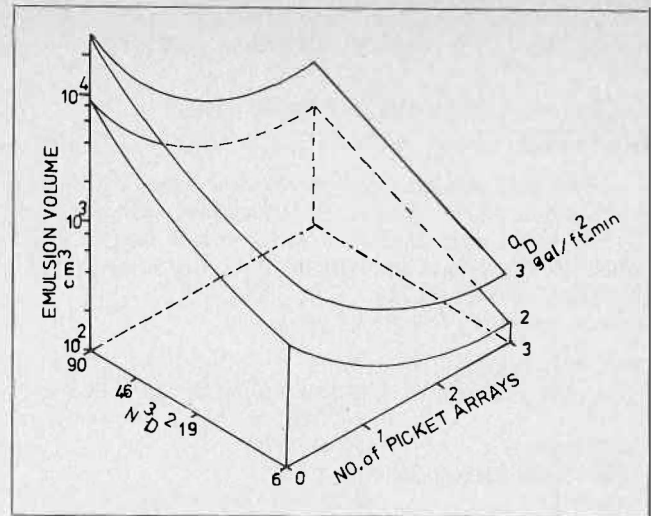


FIGURE 2. Emulsion volume variation.

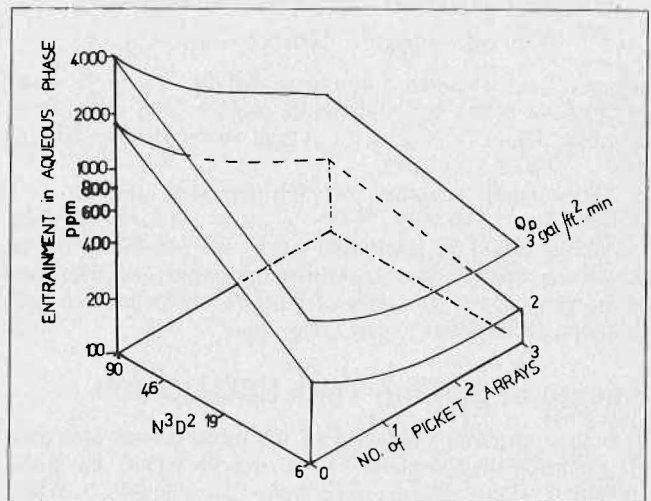


FIGURE 3. Aqueous entrainment variation.

configurations, entrainments were as high as 10,000 ppm. By having three picket fence arrays, entrainment was reduced to about 1500 ppm. Any increase in N^3D^2 or flow rates made (i) the aqueous phase more opaque, (ii) considerably increased emulsion volume, (iii) caused recirculation of haze and therefore build-up of entrainment with time.

Effect of Sulphate Ion Concentration on Emulsion Volume and Entrainment

Near neutral pH mixer-settler performance was most disappointing. To experimentally verify the effect of a theoretical zeta potential as a contributing cause of large emulsion volume and gross entrainment, sulphate ions were added (as sodium sulphate) to the system. The quantity added was approximately equivalent to that of sulphuric acid to yield pH 1.5. In this experiment, though, pH was about 8, thereby confirming the Schulze-Hardy and Derjaguin's rules of emulsion stability. The lower section of the emulsion band originally consisted of a distinct layer of tiny droplets. A dramatic decrease in emulsion volume occurred followed by a considerable reduction in entrainment. Tiny droplets in the lower emulsion band and in the aqueous phase disappeared. Once steady state was

reached, emulsion volume and entrainments were slightly greater than when operating the system at pH 1.5.

Effect of Flowrate, Temperature and N^3D^2

The unit was operated for several months with one combination picket fence at the distributor entry and one vertical baffle positioned to give one square foot of active settler plane surface area. In all runs, the organic liquid was the dispersed phase.

Process operating conditions were: —

O/A ratio constant at (1:1)
 Flow rate each phase . . . 1.3 to 4.0 gal/ft². min (3.8 to 11.7 m³/m².h)
 Temperature 20 to 37°C
 Power input corresponding to N^3D^2 6 to 90 (0.56 to 8.4)

Emulsion volume (or height) was measured once steady-state was assumed to have been reached for each of the flow rate — N^3D^2 — temperature combinations.

A multiple regression analysis of results yielded

$$Z \propto Q_b^2/T^2 \cdot (N^3D^2)^{2/3}$$

where Z = Emulsion Volume or height, Q_b = flowrate of disperse phase per unit active surface area T = Temperature degrees Celsius with overall correlation coefficient of $r = 0.87$ for 46 data.

The standard deviation of each exponent was $Q \pm 0.25$, $T \pm 0.39$, $N^3D^2 \pm 0.13$. Some of the variability could be accounted for by the sensitivity of the system to ageing, slow drift in temperature and dispersed phase ratio if the flowrates of both constituents were not matched throughout a particular run.

Ageing of Settling Tank ESCAID 100

Semi-continuous operation of the mixer-settler unit over 12 months with complete recycle of both phases has highlighted a slow change in diluent characteristics. While viscosity has changed little, interfacial tension has shown a downward drift of approximately 0.5 dynes/cm per month. This can be explained to some extent by the accumulation of surfactant material leached from the PVC piping and from organic microbiological cell disintegration of "crud". Standard ASTM distillations of stored and recycled ESCAID indicated that 20 percent of the most volatile components with bp less than 200°C had been lost, probably due to evaporation from the open assembly.

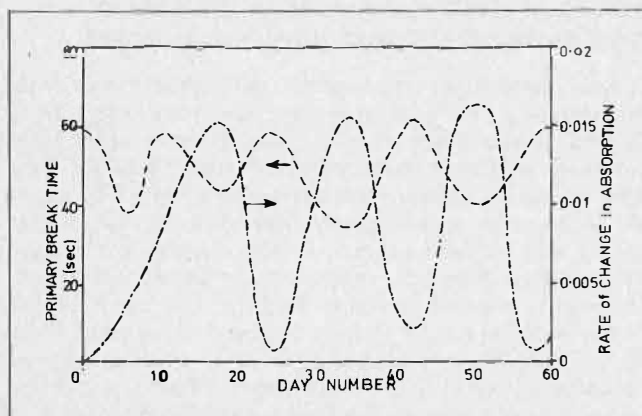


FIGURE 4. ESCAID 100 batch mix variations.

The other simple method of monitoring change in ESCAID with time has been visible region spectrophotometry. By using stored ESCAID as the reference, there has been a consistent steady increase in relative absorption in the 350-500 m μ region. One possible explanation is a build-up of degradation products from "crud" production.

Crud at The Interface

This topic has been discussed by several authors^(4,20,21) when referring to pilot plants which have been operating with kerosene-water systems, such as copper sulphate solutions and LIX64N in kerosene. The presence of *Cladosporium resiniae* in this type of system using ESCAID 100 and copper sulphate solution alone has been recognised as the principle bacteria involved in the production of "crud". It is common to find that species of *Pseudomonas*, *Aureobasidium* and *Cladosporium* are present. These are primary hydrocarbon degrading organisms⁽²²⁾. These bacteria survive well in refined kerosene such as ESCAID, but spore germination does not take place unless free water is present. The specific micro-organism present in our system is *Aureobasidium Pullulans*.

Successful identification has occurred of growth and death phases in batch-mix tests conducted over a 4 month period using ESCAID 100 & 110 with copper sulphate solution at pH 1.5.

Otherwise uncontaminated stored ESCAID and acidified copper sulphate solutions were batch-mixed continuously, using turbine agitation at $N^3D^2 = 30$ (2.8). Twice a week (sometimes more frequently) the primary break times and spectrophotometric absorption (between 350 — 600 m μ) were determined. Visual observations were also noted when agitation was stopped for primary break times. In the early stages of "crud" growth, spidery cobweb-like material spread across the static interface (when stationary). At some later stages it disappeared, but light absorption had increased, indicating that cellular debris has been dispersed into solution. Figure 4 shows the variation of primary break time and rate of change of light absorption with day number. Both ESCAIDs showed the same behaviour. There can be no doubt that this diagram is illustrating growth and death cycles — typical of bacterial ecospheres.

Causal Effects of Crud in the Settling Tank

The continual growth of micro-organisms in the dispersion band is perhaps the major contribution to the ageing effect of this "sensitive" system. Over many months of visual observations, the following causal effects can be stated:

- 1) Growth of crud prior to reaching steady-state balance in the dispersion bed volume, reduces bed depth.
- 2) Crud causes localised rapid coalescence in its immediate vicinity together with localised turbulence. This effect then promotes higher entrainment rates of tiny secondary droplets.
- 3) Crud accumulates on walls and "dead" regions such as corners where there is no flow movement.
- 4) Any leakage of phases past or through the vertical baffle assists in removal of crud from the dispersion volume. In the second section of the settler where the interface is plane, micro-organisms and dead cells accumulate. The collapse of coalescing droplets can be pictured as in Figure 5.
- 5) Removal of accumulated bacteria at the static interface results in a new growth phase within the dispersion. This situation reverts to (1) above.

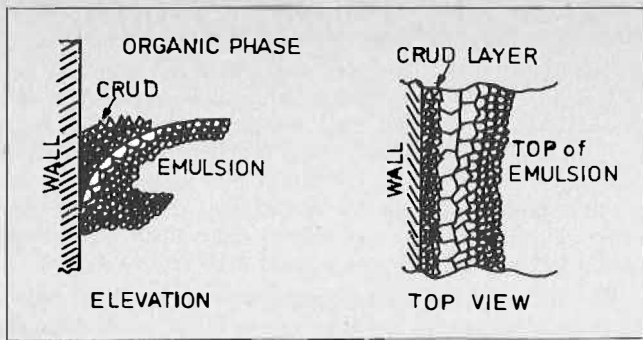


FIGURE 5. Effect of crud on emulsion.

6) Mass transfer of bacteria must be occurring out of the droplets into the water and accelerating coalescence, continuously shifting equilibrium towards larger droplets and smaller interfacial area.

Emulsion Bed Hold-up Profiles

In order to obtain density and organic phase hold-up profiles through the deep dispersion bands a differential pressure technique as described in Appendix A has been used rather than sample withdrawal techniques^(19,20) which are more likely to disturb the system.

Density profiles were determined at three locations along the length of the dispersion band. The first profile was made directly after the picket fence (at approximately 10 mm from the picket fence). This enabled the bed density to be determined at the feed inlet region of the dispersion band. The second profile was made midway between the picket fence and the vertical baffle. The third profile was 10 mm from the vertical baffle. All profiles were made approximately centrally between the two side walls of the tank.

For a power input of $N^3D^2 = 90$ (8.4) the emulsion density ρ_E profile gives an integrated average bed density of 0.943. This is considerably higher than was thought would be the case. A homogeneous emulsion of aqueous to organic ratio of $(A/O) = 1$ would have a density of $\rho_E = 0.897$. The holdup of kerosene obtained from the profile was $\Phi_D = 0.285$ rather than a theoretical value of 0.50.

The density and dispersed phase holdups were similarly obtained for the other two profile locations. The results for comparison are as follows:

Location of Profile	$\bar{\rho}_E$	$\bar{\Phi}_D$
Near picket fence	0.943	0.285
Centre of bed	0.947	0.266
Near vertical baffle	0.956	0.224

The phase profiles for the three locations are given in Figure 6. Together with visual observation these profiles substantiate the above trend of increasing holdup of aqueous phase on going from the picket fence to the vertical baffle. At the vertical baffle a layer of kerosene-coated aqueous droplets is very well defined, occupying the bottom 40 percent of the total bed depth. The profiles are of the same form as those obtained by Mizrahi and Barnea who used another measuring technique⁽¹⁹⁾. As these writers observed, there is an "even concentration layer" in which the dispersed phase holdup, ϕ_n , is approximately equal to (or slightly less than) the holdup in the feed emulsion to the settler. As such, this layer represents the "natural" level at which to introduce feed emulsion. The

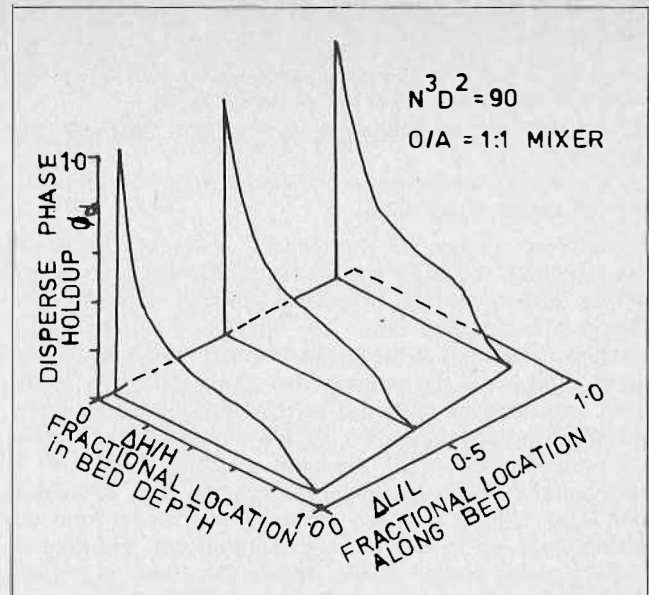


FIGURE 6. Disperse phase holdup — high power input.

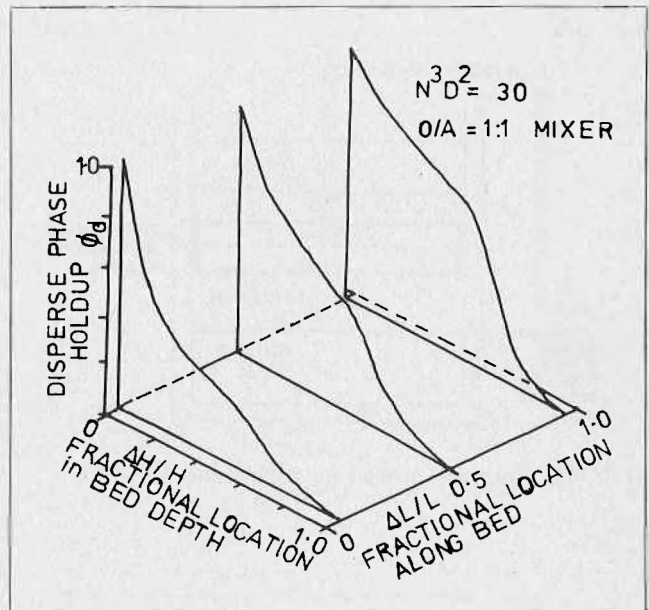


FIGURE 7. Disperse phase holdup — low power input.

layer represents 30 to 40 percent of the bed. Above this layer, the kerosene droplets are densely packed and approach a foamlike structure at the active interface. In this lower region up to 40 percent of the emulsion bed is occupied by a layer of kerosene-coated aqueous phase droplets. These drops are much larger than the droplets in the two upper sublayers. This layer which is primarily aqueous phase (with thin films of kerosene) is not described by other writers.

Profiles were obtained while operating at a power input of $N^3D^2 = 30$ (2.8). These are shown in Figure 7. The dispersed phase holdup in the emulsion bed for power input of $N^3D^2 = 30$ is as follows:

Location of Profile	$\bar{\rho}_E$	$\bar{\Phi}_D$
Near picket fence	0.941	0.295
Centre of bed	0.955	0.230
Near Vertical baffle	0.891	0.526

Except for the profile at the centre of the emulsion bed these results indicate,

- (a) a higher holdup of organic phase in the emulsion bed than was obtained for the higher power input,
- (b) an increase in holdup as the vertical baffle is approached, and
- (c) a much greater variation in holdup than was obtained for the higher power input.

Different holdups are expected for differences in power input because the latter are normally reflected in a change of the dispersed phase drop size which is a determining factor of coalescence rates. An explanation for the higher holdups could be that the larger drop size in the low power input emulsion is packing together more efficiently in the even concentration layer due to the larger buoyancy force, giving higher holdup values in this sublayer which makes up a major portion of the total emulsion bed. This is substantiated by the profiles in which the even concentration layer holdup increases from 0.2 just away from the picket fence, up to 0.4 half way along the bed and then up to 0.75 at the vertical baffle. Beside this, there is visually a much less significant band of kerosene-coated aqueous phase droplets along the bottom of the emulsion bed. This

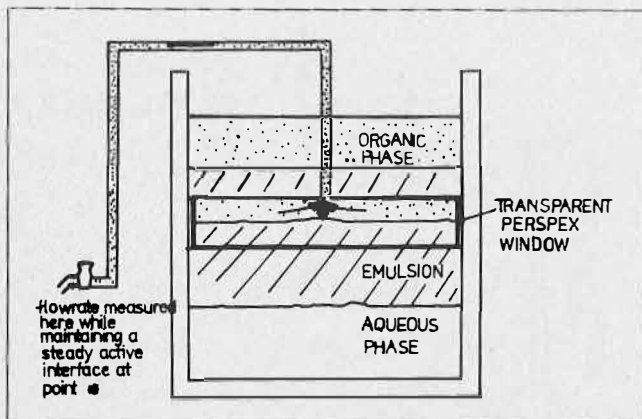


FIGURE 8. Kerosene siphon for compartmental baffle.

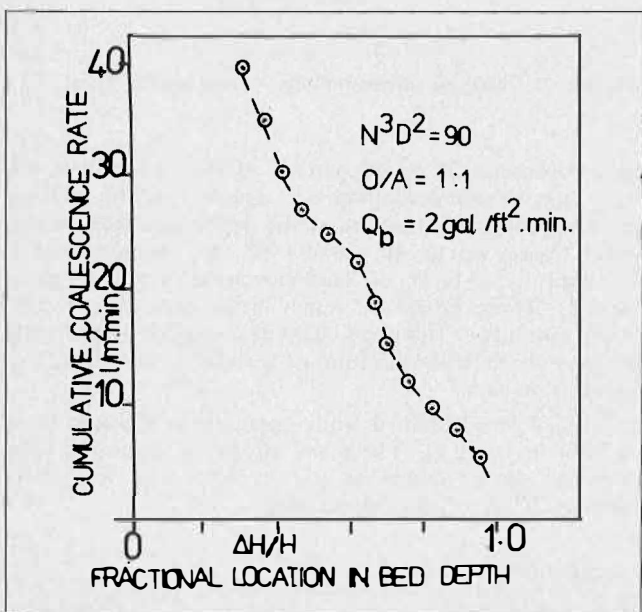


FIGURE 9. Coalescence from 0.5 ft² compartmental baffle — high power input.

band is shown to a major extent to reduce the overall hold-up levels in the higher power input emulsion beds.

The drainage of continuous phase from the emulsion bed is apparently occurring faster than coalescence of the dispersed phase as it flows from the picket fence. This is to be expected from the increased drainage rate associated with larger droplets. For the higher power input the trend is the opposite although not as extreme. Here, the coalescence rate is occurring just slightly faster than continuous phase drainage resulting in a small drop in bed holdup.

The fact that the film-coated droplet layer is so much more pronounced for the high power input case (although the flowrates remain the same) suggests that the film-coated droplets are a product of the mixer rather than, for instance, the settler feeding technique such as impingement against the picket fence.

Shallow Vertical Baffle with Horizontal Appendages

Instead of using several vertical baffles, with side height $\frac{1}{4}$ to $\frac{2}{3}$ of the total static two-phase depth, to contain the emulsion, a one or two-tiered compartmental shallow baffle with horizontal face and side walls was substituted.

Initial evaluations and comparisons were carried out on single and two-tiered baffles with 37 mm horizontal projections and 13 mm sidewalls. The plane surface areas of these assemblies were 0.1 and 0.02 ft² (0.0093, 0.0186 m²), respectively. Coalesced phase drainage was allowed through a 2 mm gap against the settler wall. These baffles were located at various depths in the emulsion bed, positioned midway between the picket fence array and vertical baffle, allowing one square foot of emulsion surface area.

For both assemblies, it was observed that either drainage of aqueous phase or coalescing organic phase near their respective homophases, increased entrainment in that homophase. This was particularly the case with regard to increased entrainment of fine kerosene droplets in the aqueous phase. Vigorous disturbance at the passive interface was always observed on those occasions. It was obvious that the two phase streams issuing from the tiered baffle should be kept separate and away from the emulsion volume. Otherwise, flow patterns develop which carry smaller droplets further into the bed and generally disturb the natural progressive increase in droplet size as the active interface is approached. Copious water-filmed kerosene droplets were observed to be present in the active interface region. Any localised turbulence ejects these droplets out into the organic homophase. While these baffle arrangements improved coalescence and aided drainage, there was no significant decrease in emulsion volume.

To reduce the deficiencies of these shallow baffles, a larger baffle with 185 mm horizontal face and 20 or 40 mm sidewall (0.50 square feet plane area) (0.047 m²) was constructed to fit neatly across the settler width.

Single Horizontal Compartmental Baffle with Separate Organic Phase Take-off

An 0.5 ft² horizontal compartment was made to extend across the full width of the settler, with one vertical baffle behind this providing one square foot of plane active area. Coalesced organic phase is siphoned off as shown in Figure 8, from an outlet point located in the centre of the baffle. The active interface below the baffle is maintained at approximately 10 mm below the outlet point, while the siphoning rate, i.e. coalescence rate, is measured with a one-litre measuring-cylinder and stopwatch. The

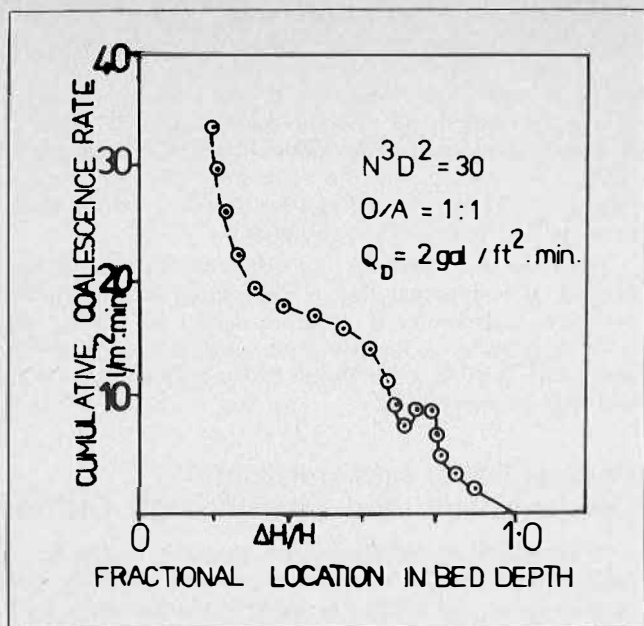


FIGURE 10. Coalescence from 0.5 ft² compartmental baffle — lower-power input.

emulsion band depth was measured while operating the baffle. The baffle location was varied through the emulsion band. Two baffles were needed. One with a depth of 20 mm could be employed near the settling interface since this does not interfere with flow of emulsion to the quiet area directly beneath the baffle. As the active interface is approached, however, the coalescence rate increases and a camber forms in the active interface below the baffle with a tendency for emulsion to be sucked along with the coalesced kerosene stream. In this case a deeper 40 mm baffle is used, otherwise the baffle becomes flooded and coalesced kerosene escapes around the edges of the baffle as indicated by movement of the droplets on the active interface beneath the baffle. Near the top of the bed (active interface) it is necessary to keep the meniscus (or camber of the active interface beneath the baffle) close to the coalesced kerosene outlet port in order to prevent this. As the baffle approaches the top of the bed the remaining emulsion above the baffle may coalesce and perhaps form a wedge on top of the baffle.

In practice, the baffles should probably be sloped slightly (1 to 2°) in the lateral direction of the settler. This should be such as to direct separated draining aqueous phase to the upstream end of the baffle and allow any fine droplets to be carried into the quiescent zone beneath the baffle where they have better chance of settling.

For all subsequent runs, one flow rate of 2 gal/min (0.55 m³/hr) in each phase was used. Figure 9 represents the data obtained while operating at a power input of $N^3D^2 = 90$ cumulatively up through the dispersion band from the passive to the active interface ($\Delta H/H = 1.0$ to 0.0).

Data obtained when the power input was at the lower value of $N^3D^2 = 30$ provides cumulative coalescence rate up through the dispersion band as shown in Figure 10. A distinct plateau and peak appear in the curve. These features were checked by repeated runs. These data indicate that dividing the emulsion bed into a number of equally deep layers of emulsion using a band of horizontal baffles may not give anything like a constant flowrate of kerosene from each compartment, but gives a widely fluctuating distribution of flowrates.

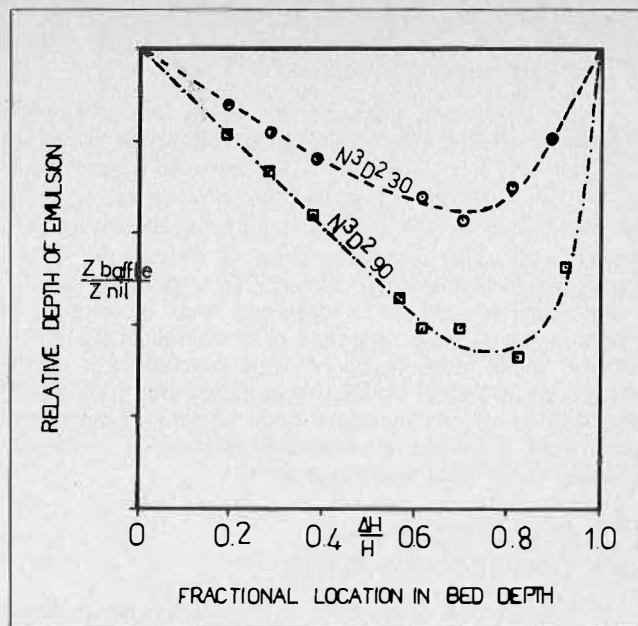


FIGURE 11. Variation of emulsion depth with horizontal baffle position.

Although the calculated and measured maximum coalescence rates beneath the baffle are not equal, the experimental results do verify that more than 50 percent of the kerosene has coalesced by the time the emulsion is fed into the emulsion band.

Another aspect of technical interest arising from the accumulated data for both power inputs is shown in Figure 11. It strongly suggests that baffle location nearer to the passive interface has a greater effect on bed depth than does location near the active interface.

Compartmental Vertical Baffle with Flow-Through Orifices

The baffle described in the previous section, while entirely successful in improving performance, was impractical. A slightly inclined horizontal compartmental baffle with flow-through orifices was then designed and tested to demonstrate (a) that the data obtained from previous sections on bed density and phase holdup can be used to design such a baffle and (b) that suitable orifices can be incorporated in the rear vertical wall to allow flow of separated liquids into their respective homophases without contacting or disturbing emulsion volume.

This novel compartmental baffle, shown in Figure 12, had an horizontal attachment area of 0.5 square feet with the assembly placed to provide one square foot of plane active area. Total coalescence area available was then 1.5 square feet (0.140 m²) with flowrate as previously, 2 gal/min (0.55 m³/hr)-each phase. For $N^3D^2 = 30$ and 90 (2.8 and 8.4), emulsion bed volume decreased by 15 and 33 percent respectively. Aqueous entrainment in the organic phase did not change from approximately 20 ppm. Organic entrainment into the aqueous increased from about 8 to 28 ppm due to localised turbulence of the passive interface below the discharging aqueous orifice. Although there was negligible emulsion draw-off from the lower orifice, a small proportion of the organic phase issuing from the top orifice was emulsion. This emulsion stream collapsed very quickly into the quiet organic phase and did not appear to cause any secondary haze.

DISCUSSION

The Role of the Picket Fence

In the equipment used, the divergent tray inlet from the mixer causes the emulsion to flow at a Reynolds Number (N_{Re}) ≈ 3200 (at 2 gal/min each phase (0.55 m³/h)) on entry to the settler. On flowing through the picket fence arrays, $N_{Re} \approx 1250$, allowing the emulsion to quietly enter the coalescing band at its natural hydrostatic level. From visual observations and the density profiles determined, it is apparent that a fraction of emulsion has already separated prior to and in the picket fences. While there may be some coalescence in the arrays, the principal function is in aiding and maintaining distribution of the emulsion and allowing upward and downward drainage of separated phases at minimum turbulence by ensuring laminar flow.

Phase Holdup Profiles and Coalescence Rates

If drop-to-drop coalescence is a predominant mode of coalescence in the emulsion bed being studied and drop-drop coalescence rates fluctuate through the depth of the bed as suggested by the data, then it would not be possible to design compartmental baffles solely from holdup data. This data only shows the relative amounts of phases present. Varying probability of coalescence may result in emulsion moving into different compartments at different rates determined by the different overall coalescence (drop-drop plus drop-interface) rates inside those compartments.

The difference in data obtained for beds resulting from the two power inputs may result from a basic difference in modes of coalescence. There is other evidence, in comparing the nature of the active interface. The active interface of the deeper bed obtained at the higher power input is relatively quiet and flat with even coalescence over the whole surface. The smaller, lower power input bed however, behaves completely differently. Large areas of emulsion instantaneously coalesce leaving long irregular valleys (up to 10 mm deep) running across the top of emul-

sion bed. It can be explained in terms of the critical film thickness of continuous phase between droplets which must be reached before coalescence occurs. In this system (it could depend on such factors as the level of surfactant or crud present in the system) the critical film thickness is reduced to some smaller value at which rupture occurs with such violence that the resultant shock waves cause large numbers of surrounding films to also rupture thereby causing local collapse of the droplets.

Whatever the cause for the difference in the two sets of data, it is apparent that a close study of a particular emulsion is necessary if accurate design of settling aids is to be possible. A linearly increasing cumulative coalescence rate through an emulsion bed is only an assumption and may be a poor one.

Vertical Baffle with Horizontal Compartments and Flow-through Orifices

A horizontal baffle attachment slope of 5 degrees, as used by the Israelis⁽¹⁾, was used here but is probably more than required; the higher the slope the larger the velocity of separated phase film flowing towards the orifice end of the horizontal baffle. This causes shear between the separated phase and emulsion, and may contribute to entrainment into the separated phase. A small slope is probably desirable to prevent build-up of excessive volume of separated phase. The slope would lead to a reservoir near the orifice with an overflow such that an excessive amount of separated stream could overflow back into the emulsion bed but could do so without being highly localised.

Improved performance is expected from vertical baffles with horizontal attachment incorporating orifices because, as is observed, the emulsion is very quiet inside the baffle compartments compared to that in the bulk emulsion. The very bottom passive interface below the compartmental baffle is very quiet and therefore ideal for settling tiny droplets.

Besides the uncertainty of how the baffle would perform because of restricted density profile data during design, there appeared two other sources of uncertainty. These were (a) the buildup of the kerosene film-coated water droplet layer at the bottom of the dispersion bed and (b) the possibility that emulsion would not move into compartments at the same flowrate because of variation of the probability of coalescence of the different emulsion structures located at different levels in the bed.

The general performance of this baffle is good. The separated phase streams of the two phases flow on opposite sides of the settling tank to their respective homophases. Even with large amounts of emulsion flowing through the orifices with the separated phase streams, this does not appear to be a problem as this emulsion appears to coalesce quickly. In practice it would be safe to slightly underdesign the orifice size and allow some separated phase to drain back through the emulsion bed. Separated phase streams do not jet into the settler downstream from the baffle, but fall directly to the settled interface. The orifices allow most of the crud to move past the baffle but some crud does collect in quiet areas inside the compartments and can cause vigorous localised coalescence in these areas. The lower horizontal baffle and its associated active interface appears to particularly assist the coalescence of the film-coated droplets.

Conclusions

Initial and preliminary investigations showed that zeta potential as applied to emulsion stability was important.

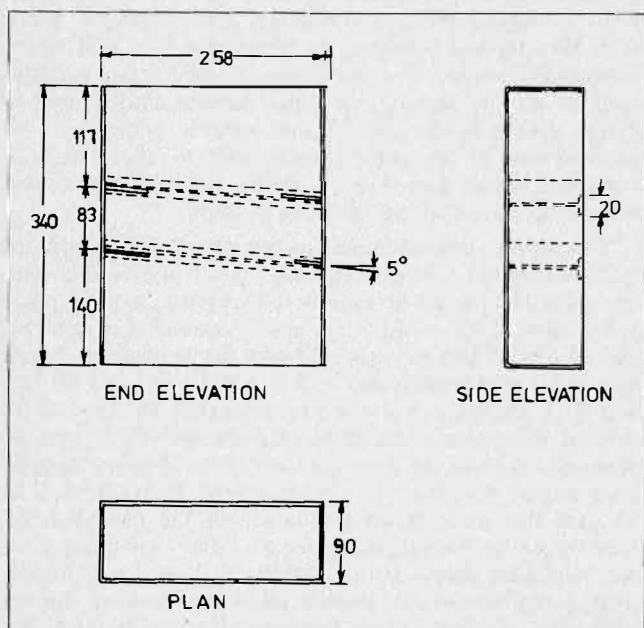


FIGURE 12. Compartmental baffle with orifices in the end wall.

This potential of the droplets could be counteracted by lowering the pH or adding sulphate ions (in this study) to the aqueous phase.

Throughout the investigation, crud growth was a persistent problem and complication, in that long equilibration times were necessary. In parallel with the settler research, extensive batch mix runs on the same system clearly showed inter-related cyclic variation of about 17 days in primary break time, visible growth of crud and increase in spectroscopic absorption of ESCAID-100 and 110 at 400 m μ . This particular crud micro-organism has been identified as *Aureobasidium Pullulans*. Visual observations note that the film of crud aids coalescence at the settler walls and in the emulsion volume. The extent of coalescence promotion is unknown because of the variable quantity present at any instant.

Picket fence arrays, vertical baffles and plane gauze internals were evaluated. A number of picket fences, directed at the distributor inlet in conjunction with at least one vertical baffle to contain the whole emulsion volume along the settler length, proved best. Ranking criteria used were reduction in emulsion volume, entrainments and minimising turbulence. The accumulated data suggest that picket fence assemblies primarily assist separation and drainage of both phases entering the settler.

A general regression analysis of the independent variables affecting emulsion volume contained within the settler internals gave: —

$$\text{Emulsion volume} \propto Q_D^2/T^2 \cdot (N^3D^2)^{2/3},$$

where N^3D^2 = power input per unit volume, Q_D = specific flow rate of disperse phase, T = temperature ($^{\circ}\text{C}$).

Density (and from this dispersed phase holdup) data were obtained from sensitive pressure difference measurements. Holdup profiles at three positions in the settler indicate that: —

(i) Although phase flow rates to the mixer were 1:1, $\phi_D \approx 0.30$ after passing through the picket fence arrays, independent of N^3D^2 . Therefore, about 40 percent of the emulsion had coalesced prior to entering the settler.

(ii) The structure of emulsion beds produced from N^3D^2 30, 90 (2.8, 8.4) were quite different. At the lower N^3D^2 , continuous phase drainage occurred faster than coalescence as the vertical baffle was approached. Overall bed holdup consequently increased towards the exit weirs. In the case of higher N^3D^2 however, drainage and coalescence rates are approximately the same, with overall bed holdup decreasing slightly along the settler.

(iii) Organic phase film-coated aqueous droplets formed a considerable lower wedge volume of emulsion at the higher N^3D^2 , but was not significant at the lower power input. This suggests that complex droplet formation originates in the pump-mixer.

The testing of several simple horizontal baffle attachments within the emulsion volume indicate that: —

(i) Separated phase flow in the emulsion bed near its homophase results in turbulence and increased entrainment in that phase.

(ii) Separated phases leaving a compartment must be kept apart within the emulsion; otherwise severe internal turbulence develops disrupting the packing of coalescing droplets.

A large baffle with horizontal compartment incorporating organic phase withdrawal also highlighted the difference between the emulsion volumes produced at the two N^3D^2 . Coalesced organic phase flowrate withdrawal could be interpreted as coalescence rates and showed steeper peaks and troughs for the lower N^3D^2 . Analysis of the total data indicated that drop-drop coalescence is the

preferred mechanism at the lower input while drop-interface coalescence is more important at the higher N^3D^2 .

Using the whole of the previous information, a novel two-compartment baffle with through-the-baffle orifices was designed. This configuration allowed coalesced organic and aqueous phases to flow quietly into their respective homophases. Both these simple special baffles reduced emulsion volumes by up to 50 percent and maintained entrainments at low levels.

NOMENCLATURE

N_{RE}	= Reynolds Number (—)
Q_D	= Dispersed phase specific flow rate gal/ft ² . min
T	= Temperature $^{\circ}\text{C}$
Z	= Emulsion Volume or depth cm ³ or cm
ϕ_D	= Dispersed phase volume fraction or holdup (—)
ρ_A	= Aqueous phase density
ρ_E	= Emulsion density g/cm ³
ρ_o	= organic phase density

Note: Units in brackets after Imperial units throughout the text are equivalent S.I. units.

Acknowledgements

The experimental phases of this work were conducted in 1974-1977 with major support from a Conzinc Riotinto Australia grant.

REFERENCES

- (1) Mizrahi, J. and Barnea, E., Proc. Engng. 1973, Jan, 60.
- (2) Bailes, R.J., Hanson, C. and Hughes, M.A., Chem. Engng. 83, 86.
- (3) Taylor, J.K. and Skelton, R.L., Symp. on Solvent Extraction, Univ. of Newcastle-on-Tyne, Sept., 1976.
- (4) Warwick, G.C.I., Scuffham, J.B. and Lott, J.B., Proc. I.S.E.C., 1971, Paper 85.
- (5) Godfrey, J.C. and Grile, V., Symp. on Solvent Extraction, Univ. Newcastle-on-Tyne, Sept., 1976.
- (6) Glasser, D., Arnold, D.R., Bryson, A.W. and Vieler, A.M.S., Min.Sc.Engng. 1976, 8, 23.
- (7) Ryon, A.D., Daley, F.L. and Lowrie, R.S., USAEC Report ORNL-2951: 1960.
- (8) Ryon, A.D. and Lowrie, R.S., U.S.A.E.C. Report ORNL-3381: 1963.
- (9) Ryon, A.D., Daley, F.L. and Lowrie, R.S., Chem. Eng. Prog. 1959, 55, Oct., 70.
- (10) Royston, D. and Buxwell, A., A.A.E.C. Report E274: 1973.
- (11) Conzinc Riotinto Australia — Patent (Aust.) PB-6624: 1974.
- (12) Davis, M. and Vermuelen, T., Chem. Eng. Prog. 1954, 50, 188.
- (13) Davies, G.A., Jeffreys, G.V. and Ali, F., Chem. Engr. 1970, 243, 379.
- (14) Brown, A.H. and Hanson, C., Brit. Chem. Engng. 1966, 11, 695.
- (15) Barnea, E. and Mizrahi, J., Trans. Instn. Chem. Engrs. 1975, 53, 70.
- (16) Conzinc Riotinto Australia — Patent (U.S.A.) PC0039 and PC1830: 1974.
- (17) Paige, P.M., Solvent Extraction and Electrowinning Annual Meet., Can. Instit. Min. and Met., Sudbury, Oct. 1975.
- (18) Jackson, I.D., Scuffham, J.B., Warrick, G.C.I. and Davies, G.A., Proc. I.S.E.C., 1974, 1, 567.
- (19) Barnea, E. and Mizrahi, J., Trans. Instn. Chem. Engrs. 1975, 53, 61.
- (20) Sweeney, W.F. and Wilke, C.R., U.S.A.E.C. Report UCRL-11182: 1964.
- (21) Pike, F.P. and Wanhawan, S.C., Proc. I.S.E.C., 1971, Paper 163.
- (22) Hill, E.C., Evans, D.A. and Davies, I. J. Inst. Petrol. 1967, 53, 280.

APPENDIX A

The Pressure Differential Probe

The apparatus is used to obtain emulsion density (ρ_E) profiles and therefore dispersed phase holdup (ϕ_D) profiles through emulsion beds. Such data helps in understanding the behaviour of picket fences and various baffle arrangements in settlers with deep emulsion beds.

The probe detects the pressure difference between two levels which are 1 cm apart. The apparatus consists of two

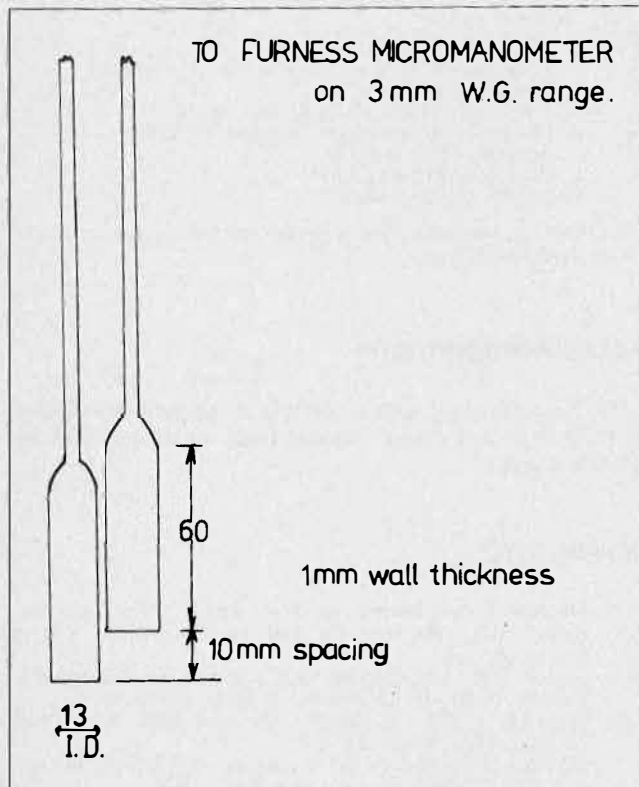


FIGURE A1. Approximate dimensions of glass bells for density probe.

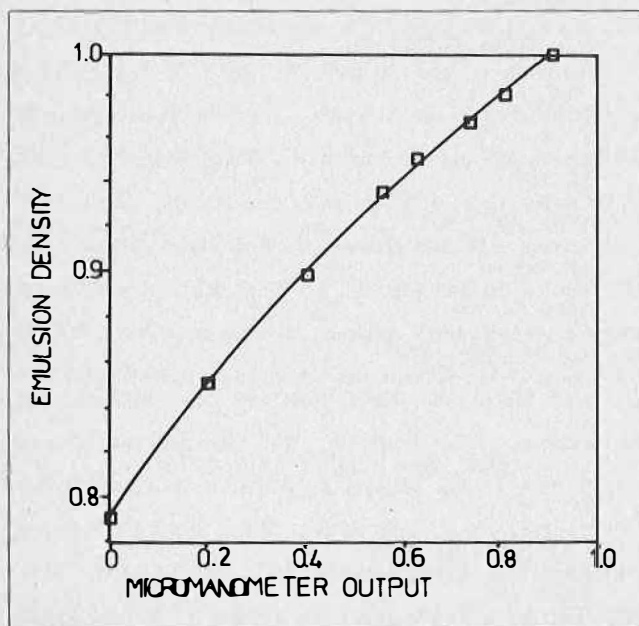


FIGURE A2. Calibration curve for density probe.

glass bells (see Figure A1) connected by equal lengths of small-diameter tubing to a Furness micromanometer. The micromanometer, using a transducer to sense a diaphragm movement, measures the differential pressure. It is operated on an 0-3 mm water gauge range with 20 scale divisions.

The glass bells are lowered into the organic layer in the settler and the manometer is adjusted to zero to remove the pressure difference due to the 1 cm difference in static pressure. The 0-3 mm scale is used as the reading for the pure aqueous phase is then also on scale. The intermediate readings vary approximately linearly with emulsion density although more accurate density values were obtained by calibration of the apparatus using aqueous solutions of ethanol. The calibration curve for the probe is shown in Figure A2.

The volume fraction of organic in the emulsion or the holdup ϕ_D is given by

$$\phi_D = \frac{\rho_A - \rho_E}{\rho_A - \rho_o}$$

There are two major contributors to spurious results from the probe. These are:

- 1) The expansion of air in the plastic lines to the micromanometer. This causes bubble formation at the glass bells which then results in a sudden drop in micromanometer reading. If the bubble is dislodged without removing the bells from solution the subsequent results may be erroneous. Minimising the length and internal diameter of the plastic lines will help to prevent this.
- 2) Excessive turbulence in the emulsion bed. This can make interpretation of a fluctuating output very difficult. It may be acceptable to take readings at some distance away from the turbulent region.

The density reading at a particular location should be taken over a period of at least one hour to ensure that the reading is steady. Occasional zeroing will also help to eliminate spurious results.

DISCUSSION

H. Kimmels: The authors have found that the use of picket fences, etc. — along with a flush inlet to the settler — considerably reduces phase entrainment from the settler. However, as a design engineer, I would not use such a flush inlet but rather a wedge-shaped diffuser-type inlet with its exit away from the direction of flow in the settler. This should give a much better flow distribution at the settler inlet and as a consequence, a better separation performance of the settler. I should be interested in the authors' comments on this point.

J. Roberts: As indicated in the full paper, an overflow divergent tray outlet directs dispersion from the mixer into the settler. In common with Holmes and Narver, U.S.A. liquid-liquid separation practice (by analogy) and the worldwide approach to raw-water-treatment inlet geometry of rectangular sedimentation tanks, the initial direction of flow is parallel to the gross flow movement along the tank length.

Incorporation of pickets or multiple slots at tray discharge to the settler ensures smooth transition of liquids into the dispersion band with minimum turbulence.

If, as suggested by the Questioner, inlet flow direction is not forward — parallel to the general flow pattern, recirculating turbulent eddies develop which contribute to gross entrainments produced by extensive shear across the active interfaces.

Study of Dispersion in a Pulsed Perforated-Plate Column

V. Khemangkorn*, G. Muratet and H. Angelino,
Institut du Génie Chimique, Laboratoire Associé C.N.R.S.,
Toulouse, France

ABSTRACT

Drop size and hold-up were investigated in a pulsed perforated-plate extraction column using the ternary system water-iodine-carbon tetrachloride. Drop size distribution was compared with various statistical distributions namely: normal, log-normal, root-normal, Gamma, Weibull, Gal-Or, Mugele-Evans and Rosin-Rammler. Influences of amplitude, frequency, dispersed phase flow rate and direction of mass transfer on drop size and hold-up were also determined. Correlations for interfacial area were also derived.

Introduction

IN A LIQUID-LIQUID EXTRACTION PROCESS, one of the methods of enhancing the rate of mass transfer is to increase the area of contact between the two immiscible liquids. This is done by increasing the degree of agitation within the extractor. In a pulsed perforated-plate column the liquids are pulsed through small holes in fixed plates and a dispersion is formed in which continuous breakup and coalescence of dispersed phase droplets occurs. Drop size and its distribution will depend on the intensity of pulsation and physical properties of the liquids. It is well known that interfacial area increases with intensity of pulsation as a result of a decrease in drop size and an increase in hold-up of the dispersed phase. In order to achieve a useful analysis of extraction data, it is commonly assumed that drops are spherical and uniformly dispersed. However, distribution of drop size is always observed in reality and despite the fact that drop size distribution plays an important role in the mass transfer process, not much work with this type of extractor has been done so far⁽¹⁻⁴⁾ due chiefly to time-consuming task required in analysing the data.

The purpose of this paper is to present some information on drop size and its distribution as related to experimental conditions such as amplitude, frequency, dispersed phase flow rate and direction of mass transfer. Correlations of dispersed phase hold-up and interfacial area are also included here since these two quantities have close relations with drop size.

Drop Size

If an isotropical turbulent flow field is established in the apparatus, the drop diameter at equilibrium will be a function of energy dissipation in the system and the physical properties of the liquids according to the relation^(6,7)

$$D_{32} = K \left(\frac{\sigma}{\rho_c} \right)^{0.6} E^{-0.4} \dots \dots \dots (1)$$

In the case of a pulsed perforated-plate column, mean energy dissipation is given by⁽¹⁾

$$E = \frac{\gamma_c}{\beta_c} \frac{(Af)^3}{h_c} \dots \dots \dots (2)$$

where

$$\gamma_c = \frac{5\pi^2}{6\sqrt{2}} \cdot \frac{1 + h_c/L}{C_o}$$

and

$$\beta_c = m^2 / [(1 - m)(1 - m^2)]$$

Substitution of (2) in (1) gives

$$D_{32} \sim \left(\frac{\sigma}{\rho_c} \right)^{0.6} \left(\frac{\gamma_c}{h_c \beta_c} \right)^{-0.4} (Af)^{-1.2} \dots \dots \dots (3)$$

For a given system of liquids and fixed geometry of the column the first two terms on the right hand side of (3) are constant, and

$$D_{32} \sim (Af)^{-1.2} \dots \dots \dots (4)$$

If dynamic equilibrium is attained within the system, drop size distribution according to Chen and Middleman's analysis⁽⁸⁾ can be written in the form:

$$P(D) = f \left[\left(\frac{\rho_c}{\sigma} \right)^{0.6} E^{0.4} D \right] \dots \dots \dots (5)$$

where $P(D)$ is the probability that droplet of size D will exist in the dispersion.

In the case of pulsed column with fixed geometry and with a given system of liquids equation (5) becomes

$$P(D) = f [(Af)^{1.2} D] \dots \dots \dots (6)$$

If the drop size distribution is known a test of the validity of equation (6) can be made. From (6), D_{32} can be calculated by applying the relation:

$$D_{32}^* = \int_0^{+\infty} D^3 P(D) dD / \int_0^{+\infty} D^2 P(D) dD \dots \dots \dots (7)$$

Experimental Work

Apparatus

A schematic diagram of the apparatus is shown in Figure 1, with principal characteristics given in Table 1. The cylindrical glass column was fitted with 20 stainless steel perforated plates equally spaced along the height of the column. Pulsation was generated by means of flexible PTFE bellows connected to a crank-shaft and a motor. The light and heavy phases flowed countercurrently and were introduced into the column by means of constant-level feed vessels. The interface position was fixed by a level-leg connected with the heavy phase outlet.

The ternary system employed was water-iodine-carbon tetrachloride, with the organic phase dispersed. The two directions of solute transfer were studied, i.e. iodine from water (continuous phase) to CCl_4 (dispersed phase) or "c \rightarrow d", and iodine from CCl_4 to water or "d \rightarrow c".

*Department of Chemical Technology, Faculty of Sciences, Chulalongkorn University, Bangkok (Thaïlande).

Physical properties of liquids and experimental conditions were summarized in Table 2.

Drop Size Measurement

Drop size was determined photographically for each run at 5 different positions corresponding to the 3rd, 6th, 10th, 14th and 18th compartment, with the dispersed phase entering in the first. Two to six photographs were taken at each position, depending on the density of drop-population in the column. 250 to 500 drops were measured from the negative films enlarged about 20 times on a translucent

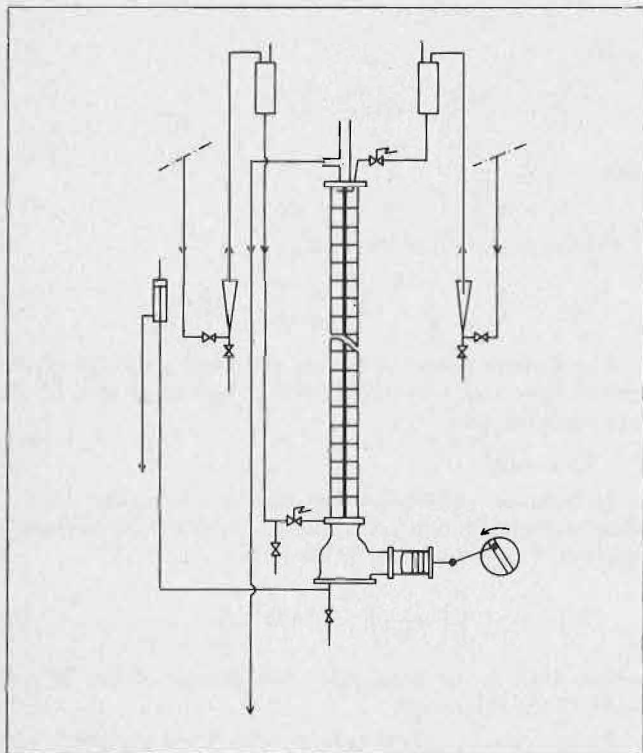


FIGURE 1. Diagram of experimental apparatus.

TABLE 1. Dimensions of Pulsed Perforated-Plate Column

Inside diameter of column	50 mm
Effective height of column	1000 mm
Compartment height	50 mm
Hole diameter of plate	2 mm
Number of holes	111
Plate thickness	1 mm
Free area of plate	18.8 %
Number of plates	20

TABLE 2. Experimental Conditions and Liquid Properties

Flow rate: water (continuous phase)	40 l/h
CCl ₄ (dispersed phase)	1 and 2 l/h
Amplitude	1 - 4 cm
Frequency	60 - 180 (cycles/min)
Density: continuous phase	1.00 g/cm ³
dispersed phase	1.59 g/cm ³
Interfacial tension	45.0 dyne/cm
Partition coefficient	89.6
Solute concentration at inlets	Iodine (mg/l)
Direction "c → d": continuous phase	180
Dispersed phase	0
Direction "d → c": continuous phase	0
Dispersed phase	5500

screen. They were classified into intervals of about 500 microns.

Hold-up Measurement

Hold-up was determined by emptying the extraction section of the column after closing a butterfly valve and stopping the flows of the two phases simultaneously.

Results and Discussion

Drop Size

Mean drop size taken as the Sauter diameter was calculated according to the usual expression:

$$D_{32} = \frac{\sum n_i D_i^3}{\sum n_i D_i^2} \dots \dots \dots (8)$$

D_{32} was found to decrease with an increase in amplitude, frequency and the distance from the dispersed phase inlet expressed as the number of compartment N . Figure 2 shows an example of variations of drop size with amplitude and number of compartment for the direction of transfer "c → d". For the system studied with the experimental conditions employed, drop size was found to be relatively smaller (about 7%) when mass transfer took place from drops to the continuous phase or in the direction "d → c". The influence of the dispersed phase flow rate however was very small. Figure 3 shows the influence of direction of mass transfer and dispersed phase flow rate on drop size as the latter was plotted as a function of frequency of pulsation.

It is generally observed^(9,10) with other ternary systems that coalescence of dispersed phase droplets is enhanced

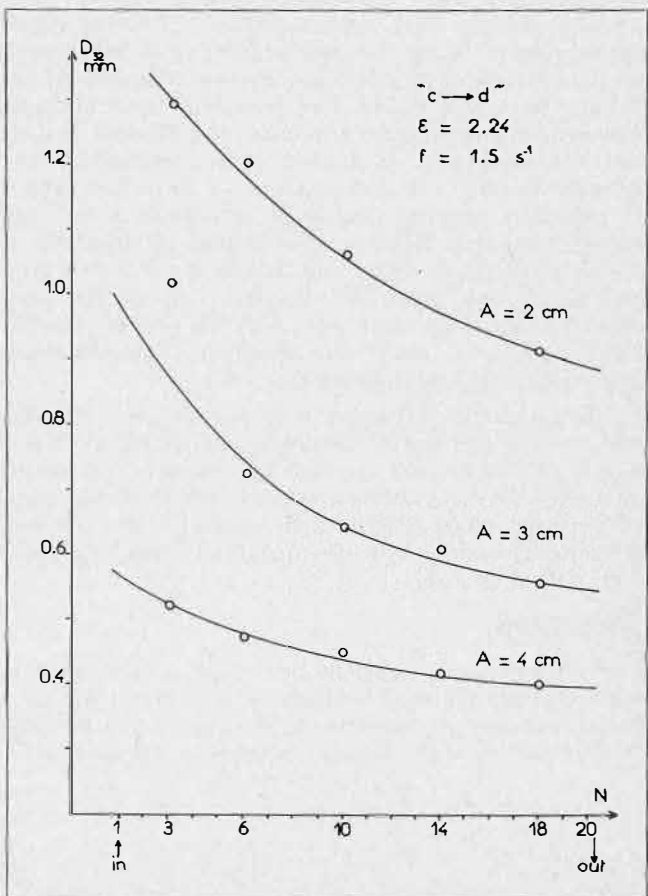


FIGURE 2. Sauter diameter along the column.

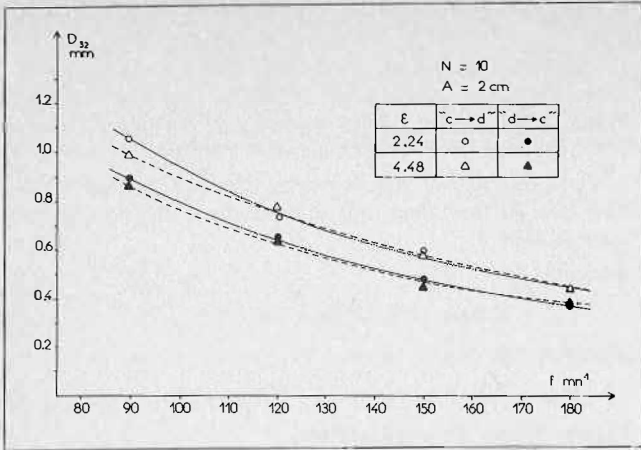


FIGURE 3. Variation of Sauter diameter with pulsation.

if mass transfer is from droplets to the continuous phase, and this would make drop size bigger than that in the opposite direction of transfer. However, our experimental results contradict this general observation. This contradiction led us to carry out a cinematographical verification by filming the dispersion with a high-speed movie camera (3000 images/sec), and it was found that no coalescence of droplets took place in both directions of mass transfer. This may be due to small hold-up (0.3 to 5%) and high interfacial tension of the system studied (45 dynes/cm).

Overall influence of A, f and N were determined using a formula of the form:

$$D_{32} = C_1 A c^2 f c^3 N c^4 \dots \dots \dots (9)$$

The constants C_1 to C_4 were determined by the Gauss-Newton's optimisation method and the following relation was found for both directions of mass transfer:

$$D_{32} = C_1 A^{-1.0} f^{-1.24} N^{-0.21} \dots \dots \dots (10)$$

and at a given position:

$$D_{32} \sim A^{-1.0} f^{-1.24} \dots \dots \dots (11)$$

The constant C_1 was found to depend on the direction of transfer and was very slightly affected by the dispersed phase flow rate. In the direction "c → d", C_1 was 0.54 and 0.51 for 1 l/h and 2 l/h of dispersed phase flow rate respectively. In the other direction "d → c", the value was 0.49 for the two dispersed phase flow rates.

Figure 4 shows a plot of D_{32} as a function of $(A^{-1.0} f^{-1.24} N^{-0.21})$ on a log-log scale, where the slope was found to be unity and the intercept 0.49. Experimental points lie within the limit of $\pm 20\%$.

Considering the D_{32} values measured at the middle of the column as a good mean value of the Sauter diameter, experimental results were used to evaluate the constant K in equation (1). A comparison of this value with the results of three other studies is presented in Table 3. It shows that our result is very close to the value obtained by Miyauchi and Oya⁽¹⁾ in a similar column. However, with other types of equipment, different values of K are obtained; indicating that, for a given power input per unit volume, various drop sizes are obtained in different types of column. Experimental mean Sauter diameters are plotted in Figure 5 versus the Af product. The following equation may be used:

$$\bar{D}_{32} = 0.37 (Af)^{-1.2} \dots \dots \dots (12)$$

but it should be noted that experimental points for smaller amplitudes lie under this straight line.

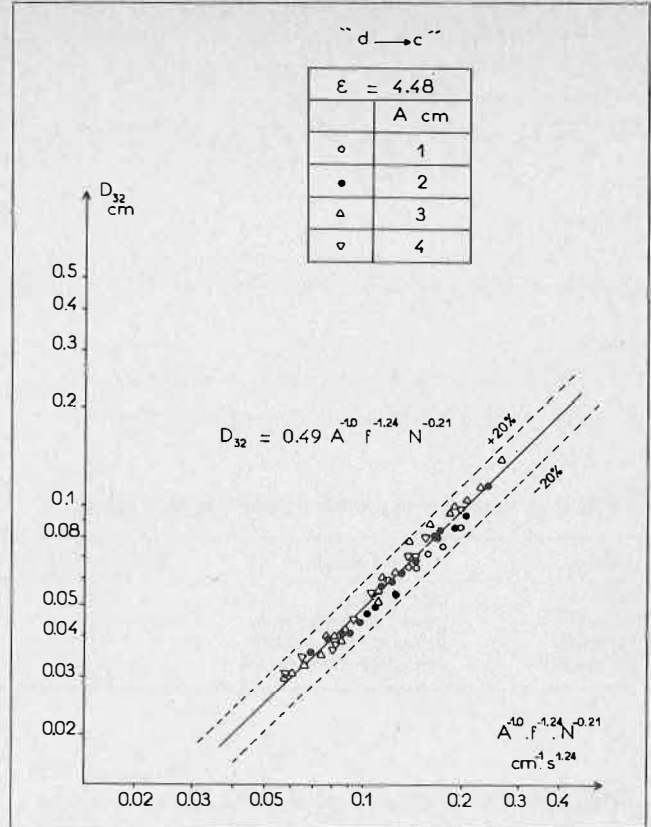


FIGURE 4. Correlation of Sauter diameters.

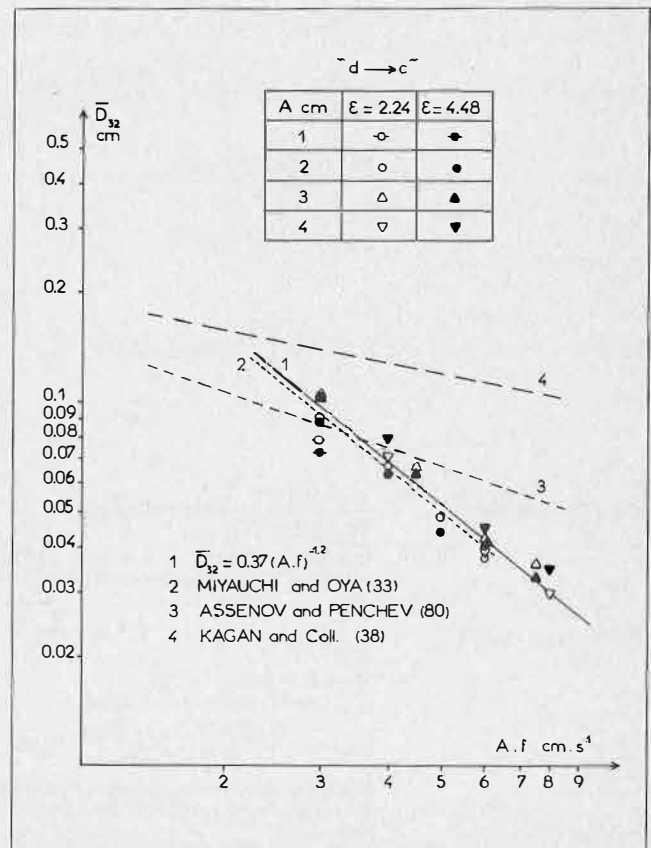


FIGURE 5. Comparison of various correlations of Sauter diameter.

Assenov and Penchev⁽⁴⁾ and Kagan et al⁽³⁾ have proposed correlations for drop size in this type of column. Their relations are:

Assenov and Penchev,

$$D_{32} = 10^{-2} \left(\frac{\sigma}{\Delta \rho_g} \right)^{0.5} \left(\frac{Af \mu}{\sigma} \right)^{0.5} N^{-0.1} \dots \dots \dots (13)$$

Kagan et al,

$$D_{32} = 0.92 \left(\frac{\sigma}{\rho_g} \right)^{0.5} Re^{-0.1} Fr^{-0.1} N^{-0.11} \dots \dots \dots (14)$$

where

$$Re = \text{Reynolds number of drop} = Af D_{32} \rho / \mu$$

$$Fr = \text{Froude number of drop} = (Af)^2 / g D_{32}$$

N = compartment number, equal to 10 at mid section of the column.

These two equations (13, 14) are also shown in Figure 5. It should be noted, however, that the two equations were found in the region of low intensity of pulsation, with the "Af" product between 0.5 and 2.5 cm/sec.

The influence of the dispersed phase flow rate on drop size was further determined, and the following relations were obtained:

direction "c → d",

$$D_{32} = 0.38 A^{-1.0} f^{-1.24} N^{-0.21} F_d^{-0.083} \dots \dots \dots (15)$$

direction "d → c",

$$D_{32} = 0.49 A^{-1.0} f^{-1.24} N^{-0.21} F_d^{-0.0002} \dots \dots \dots (16)$$

Drop Size Distribution

Examples of drop size distribution curves are shown in Figure 6. At low pulsation (Figure 6b) drop sizes spread over a very wide range and the curves show a number of peaks. As pulsation increases the spread becomes narrower, and at high pulsation only one maximum was generally observed (Figure 6a). For the same pulsing intensity, the spread is also less when the number of compartment increases.

TABLE 3. Comparison of Experimental Results

Authors	Column	K in equation (1)
Baird ⁽¹⁴⁾	Karr column	0.357
Miyauchi ⁽¹⁾	pulsed perforated plate	0.17
This study	pulsed perforated plate	0.18
Miyamami ⁽¹³⁾	multistage vibrating disk	0.12

TABLE 4. Descriptions of Various Distributions

Distribution	Probability density function P(D)	Calculation of parameters
Normal	$\frac{1}{\sqrt{2\pi}\sigma} \exp \left\{ -\frac{1}{2} \left(\frac{D - \bar{D}}{\sigma} \right)^2 \right\}$	$\bar{D} = \sum n_i D_i / N$ $\sigma^2 = \sum (D_i - \bar{D})^2 / (N - 1)$
Log-normal	$\frac{1}{\sqrt{2\pi}\sigma_L} \exp \left\{ -\frac{1}{2} \left(\frac{\ln D - \bar{D}_L}{\sigma_L} \right)^2 \right\}$	$\bar{D}_L = \sum n_i \ln D_i / N$ $\sigma_L^2 = \sum (\ln D_i - \bar{D}_L)^2 / (N - 1)$
Root-normal	$\frac{1}{\sqrt{2\pi}\sigma_R} \exp \left\{ -\frac{1}{2} \left(\frac{\sqrt{D} - \bar{D}_R}{\sigma_R} \right)^2 \right\}$	$\bar{D}_R = \sum n_i \sqrt{D_i} / N$ $\sigma_R^2 = \sum (\sqrt{D_i} - \bar{D}_R)^2 / (N - 1)$
Gamma	$\frac{\beta^{\alpha+1} D^\alpha \exp(-\beta D)}{\Gamma(\alpha+1)}$	$\bar{D} = (\alpha+1)/\beta$ $\sigma^2 = (\alpha+1)/\beta^2$
Weibull	$\zeta \omega D^{\zeta-1} \exp(-\omega D^\zeta)$	$\bar{D} = \omega^{-1/\zeta} \Gamma(1/\zeta + 1)$ $\sigma^2 = \omega^{-2/\zeta} \{ \Gamma(2/\zeta + 1) - \Gamma^2(1/\zeta + 1) \}$
Gal-Or	$8 \left(\frac{\delta^3}{\pi} \right)^{\frac{1}{3}} D^2 \exp(-\delta D^2)$	$\delta = \left(\frac{4}{\sqrt{\pi} D_v^3} \right)^{2/3}$ $D_v = \left(\frac{\sum n_i D_i^3}{N} \right)^{1/3}$
Rosin-Rammler (Ref. 5)	$\frac{\gamma D^{\gamma-4}}{\bar{D}_{RR}^{\gamma-3} (1 - 3/\gamma)} \exp(-D/\bar{D}_{RR})^\gamma$ or in volumetric form $1 - v = \exp(-D/\bar{D}_{RR})$, v_i is the volumetric fraction of drops having diameters less than D	Plot of $\ln \ln \left(\frac{1}{1 - v_i} \right)$ v.s. $\ln D_i$ gives a straight line with slope = γ and intercept = $(-\gamma \ln \bar{D}_{RR})$
Mugele-Evans (Ref. 5)	$\frac{1}{\sqrt{2\pi}} \sigma_M \exp \left\{ -\frac{1}{2} \left(\frac{\ln U - \bar{D}_M}{\sigma_M} \right)^2 \right\}$ where $U = D/(D_{max} - D)$ D_{max} can be calculated according to $D_{max} = \frac{D_{50}(D_{90} + D_{10}) - 2D_{90}D_{10}}{D_{50}^2 - D_{90}D_{10}} D_{50}$ where D_{10} , D_{50} and D_{90} are drop's diameters under which correspond 10, 50 and 90% of the population of drops respectively	$\bar{D}_M = \sum n_i \ln U_i / N_2$ $\sigma_M^2 = \sum (\ln n_i - \bar{D}_M)^2 / (N - 1)$

N.B. Γ denotes a gamma function whose expression is $\Gamma(c) = \int_0^{+\infty} U^{c-1} \exp(-U) dU$ where c represent any number, real or integer.

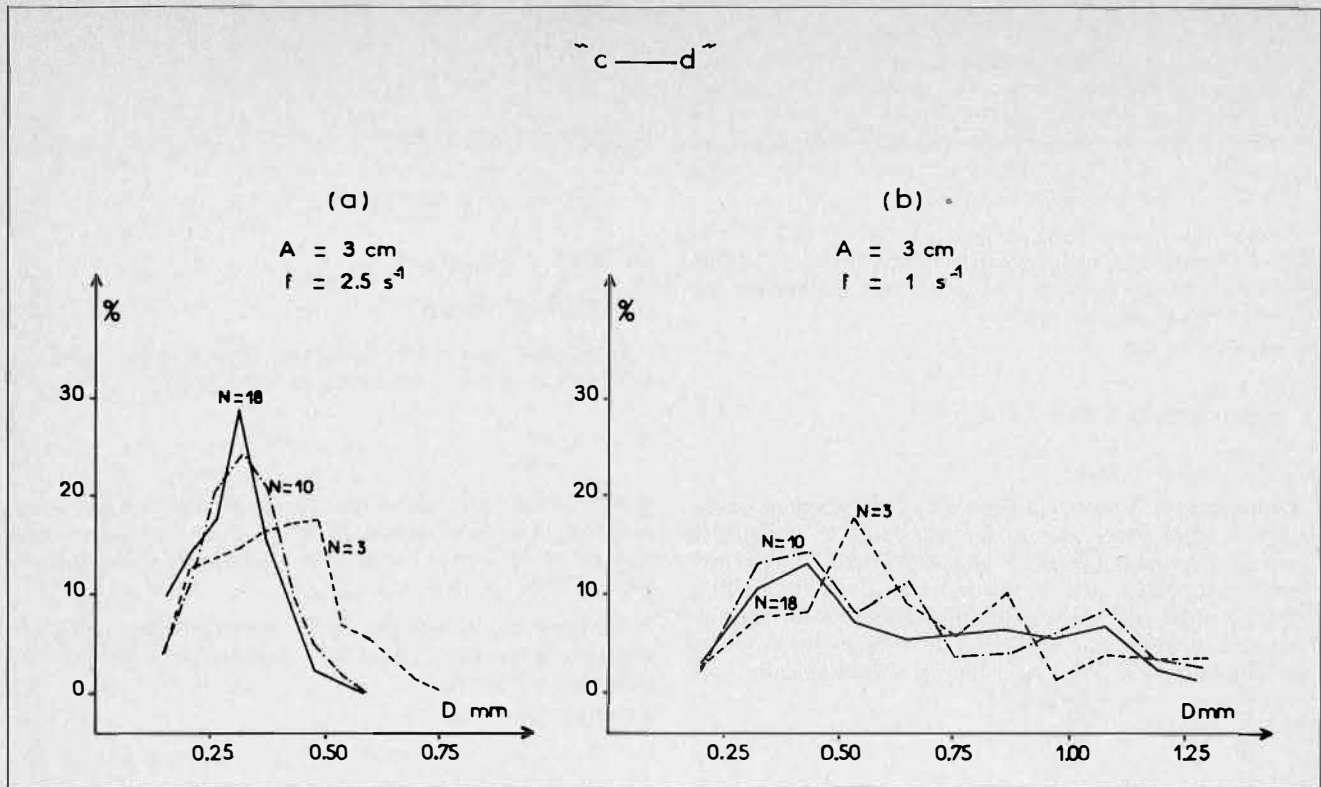


FIGURE 6. Experimental diameters distributions.

The break-up process of drops increases with intensity of agitation as well as with an increase in residence time of drops in the column. This results in a decrease of the portion of larger drops and in an increase of the portion of smaller drops. Various statistical distributions had been proposed in the past to represent drop size distribution in an extractor. In order to find the best distribution to fit the experimental data, a chi-square test was performed by comparing the experimental distributions with eight theoretical distributions namely: "normal", "log-normal", "root-normal", "gamma", "Weibull", "Gal-Or", "Rosin-Rammler" and "Mugele-Evans". Descriptions of these distributions are given in Table 4.

Chi-square, χ^2 was calculated according to the expression:

$$\chi^2 = \sum_i \frac{(n_i - n_i^*)^2}{n_i^*} \dots \dots \dots (17)$$

Another test of the validity of these distributions was also carried out comparing the experimental Sauter diameters D_{32} defined by equation (8) with the calculated values D_{32}^* obtained from each distribution by the expression (7), where $P(D)$ is the corresponding probability density function. Expressions for D_{32}^* after integration of (7) are given in Table 5.

From the results of these two tests it was found that Weibull distribution was the most appropriate. However, Gamma and Mugele-Evans distributions were also found very satisfactory. Figure 7 shows an example of plots of experimental results on a Weibull distribution paper for various operating conditions. Comparison between experimental D_{32} and D_{32}^* obtained from Weibull distribution showed an agreement better than 97%.

According to Chen and Middleman, drop size distribution at equilibrium can be characterized by the group

TABLE 5. Expressions for Sauter Diameters after Integration of Equation (7)

Distribution	$D_{32}^* = \frac{\int_0^{+\infty} D^3 P(D) dD}{\int_0^{+\infty} D^2 P(D) dD}$
Normal	$(\bar{D}^3 + 3 \bar{D} \sigma^2) / (\bar{D}^2 + \sigma^2)$.*
Log-Normal	$\text{Exp}(\bar{D}_L + 2.5 \sigma_L^2)$. * $(225 \sigma_R^6 + 135 \sigma_R^4 \bar{D}_R^2 + 15 \sigma_R^2 \bar{D}_R^4 + \bar{D}_R^6) / (9 \sigma_R^4 + 6 \sigma_R^2 \bar{D}_R^2 + \bar{D}_R^4)$.*
Gamma	$(\alpha + 3) / \beta$.*
Weibull	$\omega^{-1} \zeta \Gamma(3/\zeta + 1) / \Gamma(2/\zeta + 1)$.*
Gal-Or	$1,148 D_v$.*
Rosin-Rammler	$\bar{D}_{RR} / \Gamma(1 - 1/\gamma)$, Ref. (5)
Mugele-Evans	$D_{\max} / \{1 + B \exp(1/4 \lambda^2)\}$. Ref. (5) with $\lambda = 0.394 / \log(U_{90}/U_{50})$ $U_{50} = D_{50} / (D_{\max} - D_{50})$ $U_{90} = D_{90} / (D_{\max} - D_{90})$ $B = 1/U_{50}$

*Moment generating functions were employed for the evaluations, these functions can be found in Johnson and Kotz⁽¹²⁾

$(Af)^{1.2} D$ (Cf equation (6)) and D_{32} will be proportional to $(Af)^{1.2}$. However, experimental results for our system and operating conditions showed different influences of "A" and "f", and also dependence of drop size on "N".

Equation 10 suggested that the characteristic group for our distribution of drop size was proportional to $(D \cdot A \cdot f^{1.24} N^{0.21})$. Figure 8 shows an example of a plot of the group on a Weibull distribution paper with the same experimental conditions as those in Figure 7. Scattering of data due to differences in "A", "f" and "N" observed in Figure 7 is considerably reduced here, where experimental points distribute more closely around a single straight line.

Hold-up

Hold-up ϕ was found to increase with both amplitude and frequency. Under the same experimental conditions, ϕ for the direction of transfer "d \rightarrow c" was found to be greater than that for the opposite direction. This confirms our results on drop size which was found to be smaller in this direction of transfer "d \rightarrow c".

As was the case with drop size, the group $(Af^{1.24})$ was found to be more satisfactory in relating hold-up data than the usual pulsing velocity "Af". At high pulsations the following equation was found:

direction "c \rightarrow d",

$$\frac{\phi}{F_d^{2/3}} = 5.40 \times 10^{-4} (Af^{1.24})^{2.91} \dots \dots \dots (18)$$

for $Af^{1.24} \geq 5.5 \text{ cm} \cdot \text{sec}^{-1.24}$

Equation (18) is shown in Figure 9. The influence of the dispersed phase flow rate under the form $F_d^{2/3}$ was also found by Miyauchi and Oka⁽¹⁾ and Arthayukti⁽¹¹⁾. However Figure 9 shows also that, at low pulsations, the term $F_d^{2/3}$ is no longer applicable since experimental points for the two flow rates separate into two different straight lines. Under these conditions, it was found that ϕ varied linearly with F_d according to the relation:

direction "c \rightarrow d",

$$\frac{\phi}{F_d} = 3.04 \times 10^{-2} (Af^{1.24})^{1.26} \dots \dots \dots (19)$$

for $Af^{1.24} < 5.5 \text{ cm} \cdot \text{sec}^{-1.24}$.

Similar relations were found for the other direction of transfer:

direction "d \rightarrow c",

$$\frac{\phi}{F_d^{2/3}} = 2.30 \times 10^{-4} (Af^{1.24})^{3.45} \dots \dots \dots (20)$$

for $Af^{1.24} \geq 5.2 \text{ cm} \cdot \text{sec}^{-1.24}$.

$$\frac{\phi}{F_d} = 2.66 \times 10^{-2} (Af^{1.24})^{1.38} \dots \dots \dots (21)$$

for $Af^{1.24} < 5.2 \text{ cm} \cdot \text{sec}^{-1.24}$.

Interfacial Area

Interfacial area S was calculated from the experimental values of ϕ and D_{32} according to the equation:

$$S = \frac{6\phi}{\bar{D}_{32}} \dots \dots \dots (22)$$

S was found to increase rapidly as intensity of pulsation increases. The value about $20 \text{ m}^2/\text{m}^3$ at low pulsation, was as high as $750 \text{ m}^2/\text{m}^3$ at high pulsation with the dispersed phase flow rate as low as 2 l/h.

By replacing ϕ and \bar{D}_{32} by the corresponding empirical relations obtained, S could be calculated according to the following equations:

direction "c \rightarrow d",

$$S = 1.38 \times 10^{-2} (Af^{1.24})^{3.91} F_d^{0.75} ; Af^{1.24} \geq 5.5 \dots (23)$$

$$S = 0.779 (Af^{1.24})^{2.26} F_d^{1.083} ; Af^{1.24} < 5.5 \dots \dots \dots (24)$$

direction "d \rightarrow c",

$$S = 0.457 \times 10^{-2} (Af^{1.24})^{4.46} F_d^{2/3} ; Af^{1.24} \geq 5.2 \dots (25)$$

$$S = 0.528 (Af^{1.24})^{2.38} F_d ; Af^{1.24} < 5.2 \dots \dots \dots (26)$$

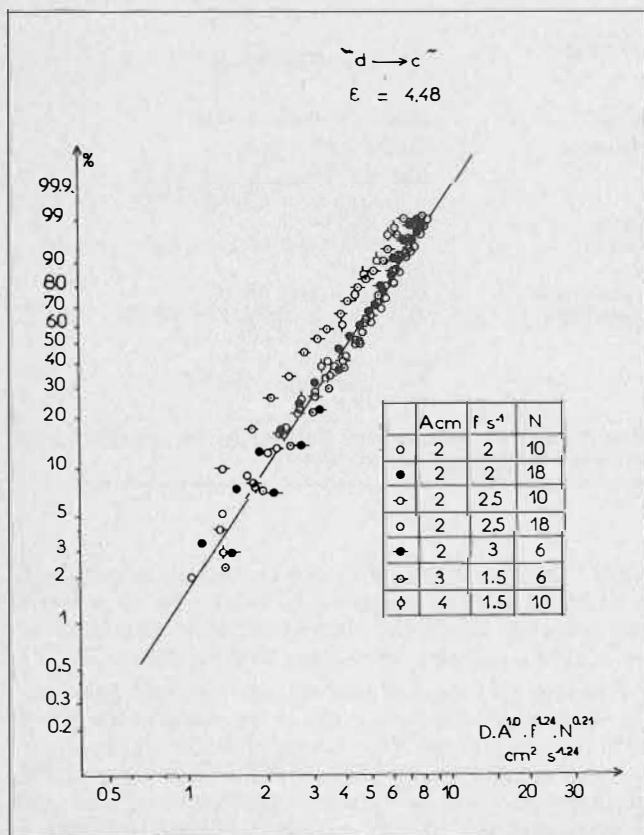


FIGURE 8. Modified diameters distribution on Weibull distribution paper.

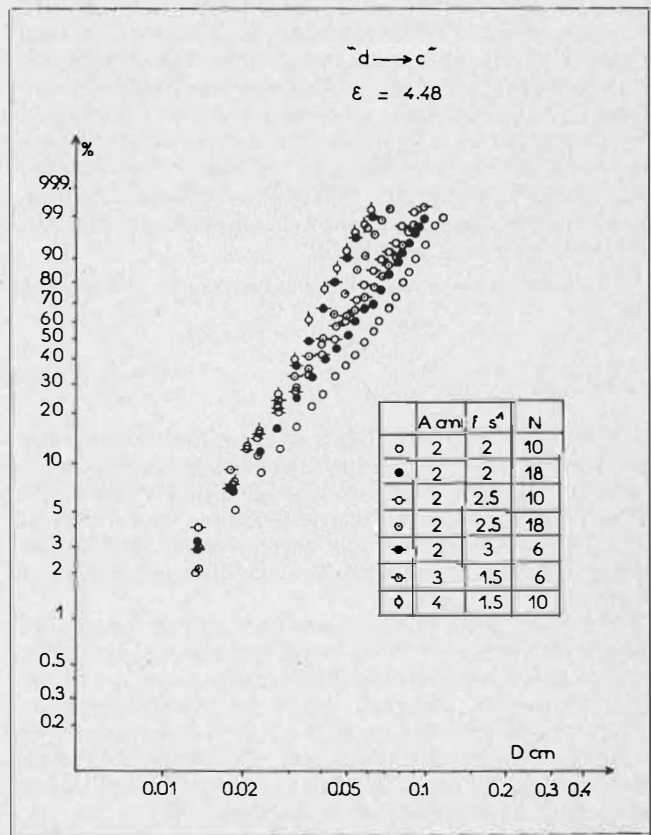


FIGURE 7. Diameters distribution on Weibull distribution paper.

Comparison between the experimental values, obtained by direct substitution of individual values of ϕ and D_{32} , and those obtained from equations (23-26) give agreement within the limit of $\pm 30\%$.

Conclusions

1. — Amplitude and frequency were found to have different influences on drop size, hold-up and interfacial area. The group $(Af)^{2.91}$ was found to relate these data more satisfactorily than the usual "Af" product.
2. — Assumptions of isotropical turbulence, though impossible to be realized in practice, was found to give an approximation for drop size.
3. — Drop size distribution was best represented by the Weibull distribution.
4. — Hold-up was found to be greater while drop size was found to be smaller when mass transfer was from the dispersed phase to the continuous phase.
5. — No coalescence of dispersed phase droplets was found in both directions of mass transfer under the experimental conditions studied.

REFERENCES

- (1) Miyauchi, T. and Oya, H., A.I.Ch.E. Journal 1965, 11, 395.
- (2) Elenkov, D., Boyadzhien, L., Kyuchoukov, G. and Naplatonova, M., paper n^o I.4.4., CHISA (1975).
- (3) Kagan, S.Z., Aerov, M.E., Lonik, V. and Volvoka, T.S., Int. Chem. Eng. 1965, 5(4), 656.
- (4) Assenov, A. and Penchev, I., Compte Rendu de l'Académie Bulgare des Sciences 1971, 24, (10), 1381.
- (5) Mugele, R.A. and Evans, H.D., Ind. Engng. Chem. 1951, 43, (6), 1317.
- (6) Hinze, J.O., A.I.Ch.E. Journal 1955, 1, 289.
- (7) Church, J.M. and Shinnar, R., Ind. Engng. Chem. 1961, 53, 479.
- (8) Chen, H. and Middleman, S., A.I.Ch.E. Journal 1967, 13, 989.
- (9) Thornton, J.D., Trans Instn. Chem. Engrs. 1957, 35, 316.
- (10) Thornton, J.D. and Pratt, H.R.C., Trans. Instn. Chem. Engrs. 1953, 31, 289.
- (11) Arthayukti, W., Thèse de Docteur-Ingénieur, Université de Paul-Sabatier, Toulouse (1975).
- (12) Johnson, N.I. and Kotz, S., "Continuous univariate distributions", Houghton Mifflin Company (1970).
- (13) Miyayami, K., Tojo, K., Yano, T., Miyaji, K. and Minami, I., Chem. Engng. Sci. 1975, 30, 1415.
- (14) Baird, M.H.I. and Lane, S.J., Chem. Engng. Sci. 1973, 28, 947.

NOTATION

A	= amplitude of pulsation, cm
$C_1 - C_5$	= constants
C_o	= constant of orifice
D	= drop's diameter, cm
D_{max}	= maximum drop's diameter, cm
D_{32}	= Sauter diameter, cm
D_{32}	= Sauter diameter calculated by equation (7), cm
\bar{D}_{32}	= mean Sauter diameter, cm
\bar{D}	= arithmetic mean diameter
D_v	= volumetric diameter (Gal-Or distribution), cm
$\bar{D}_L, \bar{D}_R, \bar{D}_M, \bar{D}_{RR}$	= parameter in various probability density function
F_d	= superficial velocity of the dispersed phase

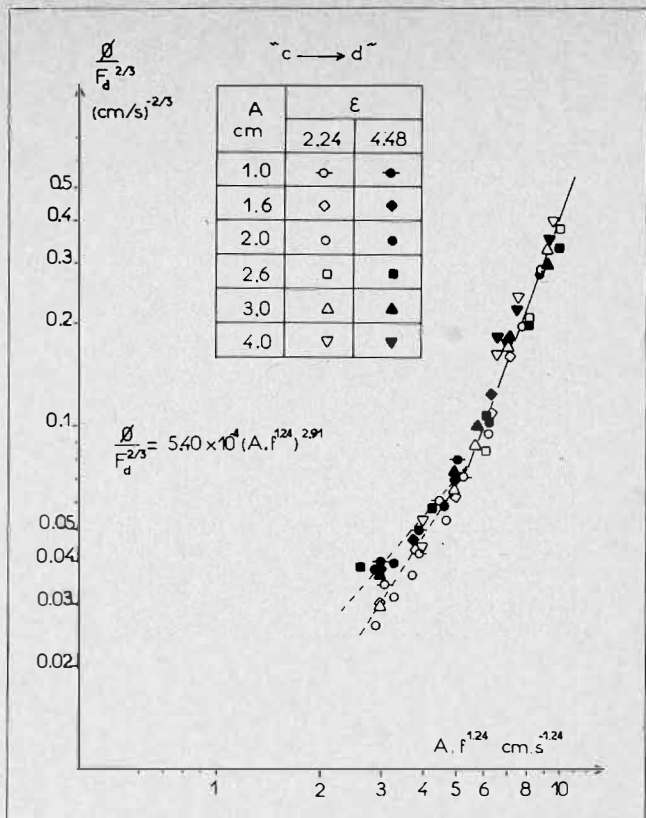


FIGURE 9. Correlation of holdup with pulsation.

f	= frequency of pulsation, pulsation per second
g	= gravitational acceleration, m/sec ²
h_c	= height of a compartment, cm
L	= effective column length, cm
m	= fraction of total free hole area,
N	= total number of drops or compartment number
n_i	= number of drops in the i th interval
n_i^*	= theoretical number of drops in the i th interval
S	= interfacial area per unit volume of reactor, cm ² /cm ³

GREEK SYMBOLS

α, β	= parameters in Gamma distribution
γ	= parameter in Rosin-Rammler distribution
δ	= parameter in Gal-Or distribution
ϵ	= extraction factor
χ^2	= chi-square
ϕ	= hold up, fraction
μ	= viscosity, g/cm.sec
ρ	= density, g/cm ³
$\Delta\rho$	= density difference, g/cm ³
σ	= interfacial tension, g/sec ²
$\sigma_L, \sigma_R, \sigma_M$	= parameters in various probability density functions
ω, ζ	= parameters in Weibull distribution

SUBSCRIPTS

c	= continuous phase
d	= dispersed phase

